$\mathcal{P}$art I

Molecular Components of Cells

All life depends on water; all organisms are aqueous chemical systems. (Waves in Oahu, Hawaii, Brad Lewis/Liaison International)

*C*hapter 1

Chemistry Is the Logic of Biological Phenomena

"Swamp Animals and Birds on the River Gambia," c. 1912 by Harry Hamilton Johnston (1858–1927). (Royal Geographical Society, London/The Bridgeman Art Library.)

Molecules are lifeless. Yet, in appropriate complexity and number, molecules compose living things. These living systems are distinct from the inanimate world because they have certain extraordinary properties. They can grow, move, perform the incredible chemistry of metabolism, respond to stimuli from the environment, and, most significantly, replicate themselves with exceptional fidelity. The complex structure and behavior of living organisms veil the basic truth that their molecular constitution can be described and understood. The chemistry of the living cell resembles the chemistry of organic reactions.

2

Indeed, cellular constituents or **biomolecules** must conform to the chemical and physical principles that govern all matter. Despite the spectacular diversity of life, the intricacy of biological structures, and the complexity of vital mechanisms, life functions are ultimately interpretable in chemical terms. *Chemistry is the logic of biological phenomena.*

logic • a system of reasoning, using principles of valid inference

1.1 • Distinctive Properties of Living Systems

The most obvious quality of **living organisms** is that they are *complicated and highly organized* (Figure 1.1). For example, organisms large enough to be seen with the naked eye are composed of many **cells,** typically of many types. In turn, these cells possess subcellular structures or **organelles,** which are complex assemblies of very large polymeric molecules or **macromolecules.** These macromolecules themselves show an exquisite degree of organization in their intricate three-dimensional architecture, even though they are composed of simple sets of chemical building blocks, such as sugars and amino acids. Indeed, the complex three-dimensional structure of a macromolecule, known as its **conformation,** is a consequence of interactions between the monomeric units, according to their individual chemical properties.

Biological structures serve functional purposes. That is, biological structures have a role in terms of the organism's existence. From parts of organisms, such as limbs and organs, down to the chemical agents of metabolism, such as enzymes and metabolic intermediates, a biological purpose can be given for each component. Indeed, it is this functional characteristic of biological structures that separates the science of biology from studies of the inanimate world such as chemistry, physics, and geology. In biology, it is always meaningful to seek the purpose of observed structures, organizations, or patterns, that is, to ask what functional role they serve within the organism.

Living systems are actively engaged in energy transformations. The maintenance of the highly organized structure and activity of living systems depends upon their ability to extract energy from the environment. The ultimate source of energy is the sun. Solar energy flows from *photosynthetic organisms* (those organisms able to capture light energy by the process of photosynthesis) through

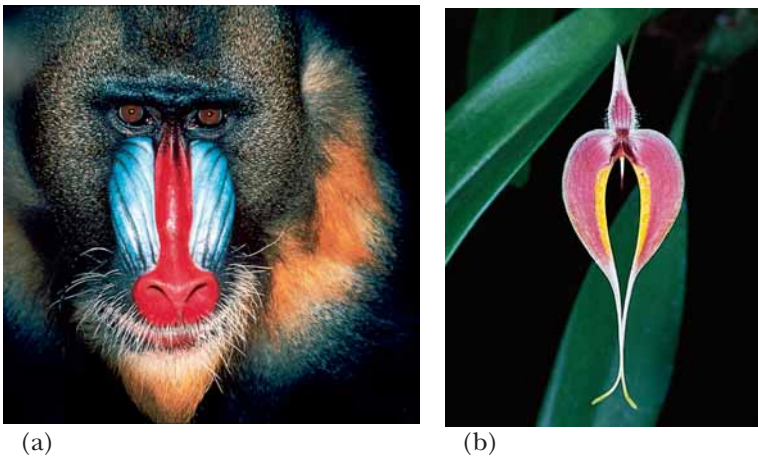(a)   (b)

FIGURE 1.1 • (a) Mandrill (*Mandrillus sphinx*), a baboon native to West Africa. (b) Tropical orchid (*Bulbophyllum blumei*), New Guinea. (*a, Tony Angermayer/Photo Researchers, Inc.; b, Thomas C. Boydon/Marie Selby Botanical Gardens*)
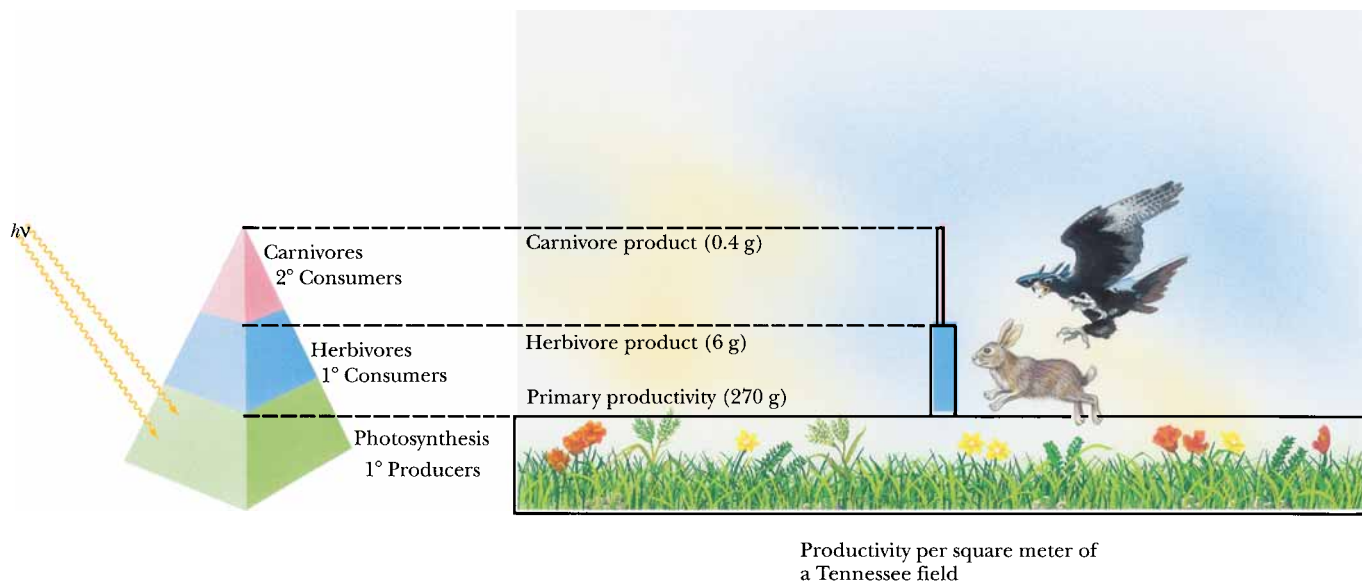
FIGURE 1.2 • The food pyramid. Photosynthetic organisms at the base capture light energy. Herbivores and carnivores derive their energy ultimately from these primary producers.

food chains to herbivores and ultimately to carnivorous predators at the apex of the food pyramid (Figure 1.2). The biosphere is thus a system through which energy flows. Organisms capture some of this energy, be it from photosynthesis or the metabolism of food, by forming special energized biomolecules, of which **ATP** and **NADPH** are the two most prominent examples (Figure 1.3). (Commonly used abbreviations such as ATP and NADPH are defined on the inside back cover of this book.) ATP and NADPH are energized biomolecules because they represent chemically useful forms of stored energy. We explore the chemical basis of this stored energy in subsequent chapters. For now, suffice it to say that when these molecules react with other molecules in the cell, the energy released can be used to drive unfavorable processes. That is, ATP, NADPH, and related compounds are the power sources that drive the energy-requiring activities of the cell, including biosynthesis, movement, osmotic work against concentration gradients, and, in special instances, light emission (bioluminescence). Only upon death does an organism reach equilibrium with its inanimate environment. *The living state is characterized by the flow of energy through the organism.* At the expense of this energy flow, the organism can maintain its
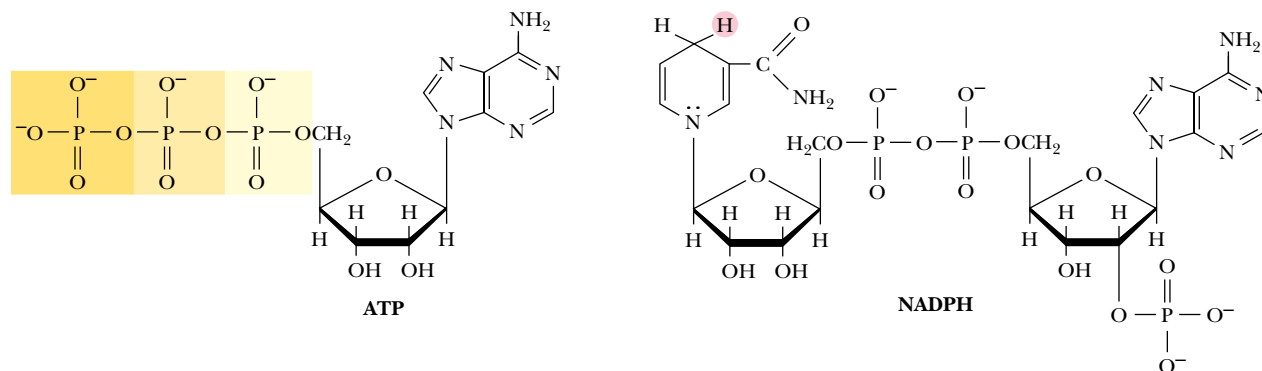

FIGURE 1.3 • ATP and NADPH, two biochemically important energy-rich compounds.

intricate order and activity far removed from equilibrium with its surroundings, yet exist in a state of apparent constancy over time. This state of apparent constancy, or so-called **steady-state,** is actually a very dynamic condition: energy and material are consumed by the organism and used to maintain its stability and order. In contrast, inanimate matter, as exemplified by the universe in totality, is moving to a condition of increasing disorder or, in thermodynamic terms, maximum entropy.

Living systems have a remarkable capacity for self-replication. Generation after generation, organisms reproduce virtually identical copies of themselves. This self-replication can proceed by a variety of mechanisms, ranging from simple division in bacteria to sexual reproduction in plants and animals, but in every case, it is characterized by an astounding degree of fidelity (Figure 1.4). Indeed, if the accuracy of self-replication were significantly greater, the evolution of organisms would be hampered. This is so because evolution depends upon natural selection operating on individual organisms that vary slightly in their fitness for the environment. The fidelity of self-replication resides ultimately in the chemical nature of the genetic material. This substance consists of polymeric chains of deoxyribonucleic acid, or **DNA,** which are structurally complementary to one another (Figure 1.5). These molecules can generate new copies of themselves in a rigorously executed polymerization process that ensures a faithful reproduction of the original DNA strands. In contrast, the

(a)

(b)

(c)

FIGURE 1.4 • Organisms resemble their parents. (a) Reg Garrett with sons Robert, Jeffrey, Randal, and grandson Jackson. (b) Orangutan with infant. (c) The Grishams: Andrew, Rosemary, Charles, Emily, and David. (*a, William W. Garrett, II; b, Randal Harrison Garrett; c, Charles Y. Sipe*)
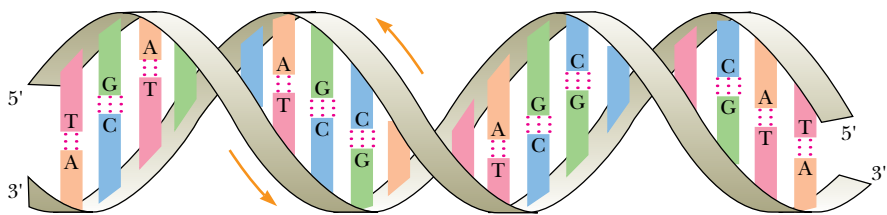
FIGURE 1.5 • The DNA double helix. Two complementary polynucleotide chains running in opposite directions can pair through hydrogen bonding between their nitrogenous bases. Their complementary nucleotide sequences give rise to structural complementarity.

complementary • completing, making whole or perfect by combining or filling a deficiency

molecules of the inanimate world lack this capacity to replicate. A crude mechanism of replication, or specification of unique chemical structure according to some blueprint, must have existed at life's origin. This primordial system no doubt shared the property of **structural complementarity** (see later section) with the highly evolved patterns of replication prevailing today.

1.2 • Biomolecules: The Molecules of Life

The elemental composition of living matter differs markedly from the relative abundance of elements in the earth's crust (Table 1.1). Hydrogen, oxygen, carbon, and nitrogen constitute more than 99% of the atoms in the human body, with most of the H and O occurring as H_2O. Oxygen, silicon, aluminum, and iron are the most abundant atoms in the earth's crust, with hydrogen, carbon, and nitrogen being relatively rare (less than 0.2% each). Nitrogen as dinitrogen (N_2) is the predominant gas in the atmosphere, and carbon dioxide (CO_2) is present at a level of 0.05%, a small but critical amount. Oxygen is also abundant in the atmosphere and in the oceans. What property unites H, O, C, and

Table 1.1

Composition of the Earth's Crust, Seawater, and the Human Body*

Earth's Crust		Seawater		Human Body[†]	
Element	%	Compound	mM	Element	%
O	47	Cl^-	548	H	63
Si	28	Na^+	470	O	25.5
Al	7.9	Mg^{2+}	54	C	9.5
Fe	4.5	SO_4^{2-}	28	N	1.4
Ca	3.5	Ca^{2+}	10	Ca	0.31
Na	2.5	K^+	10	P	0.22
K	2.5	HCO_3^-	2.3	Cl	0.08
Mg	2.2	NO_3^-	0.01	K	0.06
Ti	0.46	HPO_4^{2-}	<0.001	S	0.05
H	0.22			Na	0.03
C	0.19			Mg	0.01

*Figures for the earth's crust and the human body are presented as percentages of the total number of atoms; seawater data are millimoles per liter. Figures for the earth's crust do *not* include water, whereas figures for the human body do.
[†]Trace elements found in the human body serving essential biological functions include Mn, Fe, Co, Cu, Zn, Mo, I, Ni, and Se.

N and renders these atoms so suitable to the chemistry of life? It is their ability to form covalent bonds by electron-pair sharing. Furthermore, H, C, N, and O are among the lightest elements of the periodic table capable of forming such bonds (Figure 1.6). Because the strength of covalent bonds is inversely proportional to the atomic weights of the atoms involved, H, C, N, and O form the strongest covalent bonds. Two other covalent bond-forming elements, phosphorus (as phosphate $-OPO_3^{2-}$ derivatives) and sulfur, also play important roles in biomolecules.

Biomolecules Are Carbon Compounds

All biomolecules contain carbon. The prevalence of C is due to its unparalleled versatility in forming stable covalent bonds by electron-pair sharing. Carbon can form as many as four such bonds by sharing each of the four electrons in its outer shell with electrons contributed by other atoms. Atoms commonly found in covalent linkage to C are C itself, H, O, and N. Hydrogen can form one such bond by contributing its single electron to formation of an electron pair. Oxygen, with two unpaired electrons in its outer shell, can participate in two covalent bonds, and nitrogen, which has three unshared electrons, can form three such covalent bonds. Furthermore, C, N, and O can share two electron pairs to form double bonds with one another within biomolecules, a property that enhances their chemical versatility. Carbon and nitrogen can even share three electron pairs to form triple bonds.

Atoms	e⁻ pairing	Covalent bond	Bond energy (kJ/mol)
H· + H· ⟶ H:H		H—H	436
·C· + H· ⟶ ·C:H		−C—H	414
·C· + ·C· ⟶ ·C:C·		−C—C−	343
·C· + ·N: ⟶ ·C:N:		−C—N⟨	292
·C· + ·O: ⟶ ·C:O:		−C—O−	351
·C· + ·C· ⟶ C::C		⟩C=C⟨	615
·C· + ·N: ⟶ C::N:		⟩C=N−	615
·C· + ·O: ⟶ C::O:		⟩C=O	686
·O: + ·O: ⟶ ·O:O·		−O—O−	142
·O: + ·O: ⟶ O::O		O=O	402
·N: + ·N: ⟶ :N:::N:		N≡N	946
·N: + H· ⟶ :N:H		⟩N—H	393
·O: + H· ⟶ ·O:H		−O—H	460

FIGURE 1.6 • Covalent bond formation by e⁻ pair sharing.

FIGURE 1.7 • Examples of the versatility of C—C bonds in building complex structures: linear aliphatic, cyclic, branched, and planar.
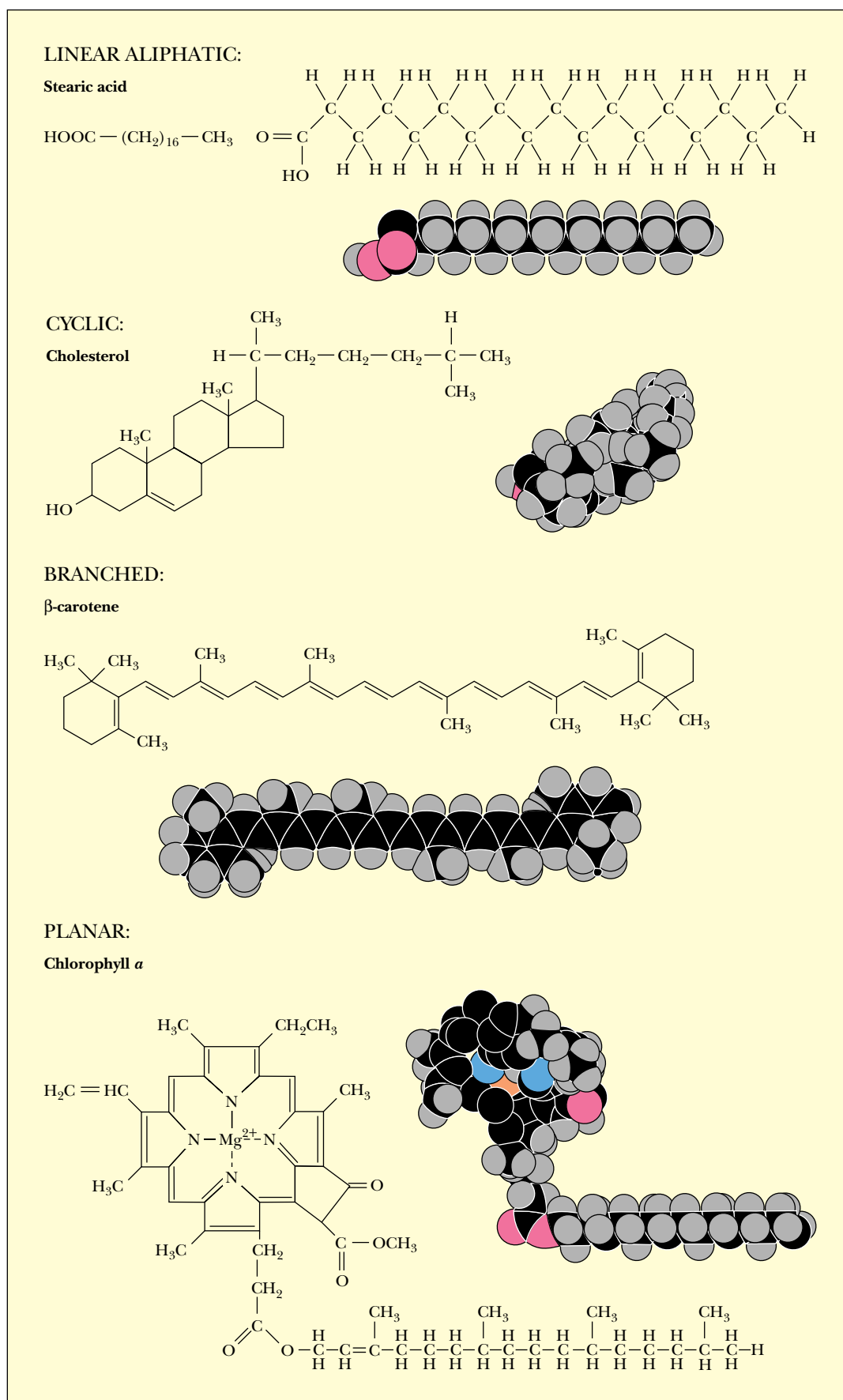
Two properties of carbon covalent bonds merit particular attention. One is the ability of carbon to form covalent bonds with itself. The other is the tetrahedral nature of the four covalent bonds when carbon atoms form only single bonds. Together these properties hold the potential for an incredible variety of linear, branched, and cyclic compounds of C. This diversity is multiplied further by the possibilities for including N, O, and H atoms in these compounds (Figure 1.7). We can therefore envision the ability of C to generate complex structures in three dimensions. These structures, by virtue of appropriately included N, O, and H atoms, can display unique chemistries suitable to the living state. Thus, we may ask, is there any pattern or underlying organization that brings order to this astounding potentiality?

1.3 • A Biomolecular Hierarchy: Simple Molecules Are the Units for Building Complex Structures

Examination of the chemical composition of cells reveals a dazzling variety of organic compounds covering a wide range of molecular dimensions (Table 1.2). As this complexity is sorted out and biomolecules are classified according to the similarities in size and chemical properties, an organizational pat-

Table 1.2

Biomolecular Dimensions

The dimensions of mass* and length for biomolecules are given typically in daltons and nanometers,[†] respectively. One dalton (D) is the mass of one hydrogen atom, 1.67×10^{-24} g. One nanometer (nm) is 10^{-9} m, or 10 Å (angstroms).

| | | Mass | |
| | Length (long dimension, nm) | Daltons | Picograms |
Biomolecule			
Water	0.3	18	
Alanine	0.5	89	
Glucose	0.7	180	
Phospholipid	3.5	750	
Ribonuclease (a small protein)	4	12,600	
Immunoglobulin G (IgG)	14	150,000	
Myosin (a large muscle protein)	160	470,000	
Ribosome (bacteria)	18	2,520,000	
Bacteriophage ϕX174 (a very small bacterial virus)	25	4,700,000	
Pyruvate dehydrogenase complex (a multienzyme complex)	60	7,000,000	
Tobacco mosaic virus (a plant virus)	300	40,000,000	6.68×10^{-5}
Mitochondrion (liver)	1,500		1.5
Escherichia coli cell	2,000		2
Chloroplast (spinach leaf)	8,000		60
Liver cell	20,000		8,000

*Molecular mass is expressed in units of daltons (D) or kilodaltons (kD) in this book; alternatively, the dimensionless term *molecular weight*, symbolized by Mr, and defined as the ratio of the mass of a molecule to 1 dalton of mass, is used.

[†]Prefixes used for powers of 10 are

10^6	mega M	10^{-3}	milli m
10^3	kilo k	10^{-6}	micro μ
10^{-1}	deci d	10^{-9}	nano n
10^{-2}	centi c	10^{-12}	pico p
		10^{-15}	femto f

tern emerges. The molecular constituents of living matter do not reflect randomly the infinite possibilities for combining C, H, O, and N atoms. Instead, only a limited set of the many possibilities is found, and these collections share certain properties essential to the establishment and maintenance of the living state. The most prominent aspect of biomolecular organization is that macromolecular structures are constructed from simple molecules according to a hierarchy of increasing structural complexity. What properties do these biomolecules possess that make them so appropriate for the condition of life?

Metabolites and Macromolecules

The major precursors for the formation of biomolecules are water, carbon dioxide, and three inorganic nitrogen compounds—ammonium (NH_4^+), nitrate (NO_3^-), and dinitrogen (N_2). Metabolic processes assimilate and transform these inorganic precursors through ever more complex levels of biomolecular order (Figure 1.8). In the first step, precursors are converted to **metabolites,** simple organic compounds that are intermediates in cellular energy transformation and in the biosynthesis of various sets of **building blocks:** amino acids, sugars, nucleotides, fatty acids, and glycerol. By covalent linkage of these building blocks, the **macromolecules** are constructed: proteins, polysaccharides, polynucleotides (DNA and RNA), and lipids. (Strictly speaking, lipids contain relatively few building blocks and are therefore not really polymeric like other macromolecules; however, lipids are important contributors to higher levels of complexity.) Interactions among macromolecules lead to the next level of structural organization, **supramolecular complexes.** Here, various members of one or more of the classes of macromolecules come together to form specific assemblies serving important subcellular functions. Examples of these supramolecular assemblies are multifunctional enzyme complexes, ribosomes, chromosomes, and cytoskeletal elements. For example, a eukaryotic ribosome contains four different RNA molecules and at least 70 unique proteins. These supramolecular assemblies are an interesting contrast to their components because their structural integrity is maintained by noncovalent forces, not by covalent bonds. These noncovalent forces include hydrogen bonds, ionic attractions, van der Waals forces, and hydrophobic interactions between macromolecules. Such forces maintain these supramolecular assemblies in a highly ordered functional state. Although noncovalent forces are weak (less than 40 kJ/mol), they are numerous in these assemblies and thus can collectively maintain the essential architecture of the supramolecular complex under conditions of temperature, pH, and ionic strength that are consistent with cell life.

Organelles

The next higher rung in the hierarchical ladder is occupied by the **organelles,** entities of considerable dimensions compared to the cell itself. Organelles are found only in **eukaryotic cells,** that is, the cells of "higher" organisms (eukaryotic cells are described in Section 1.5). Several kinds, such as mitochondria and chloroplasts, evolved from bacteria that gained entry to the cytoplasm of early eukaryotic cells. Organelles share two attributes: they are cellular inclusions, usually membrane bounded, and are dedicated to important cellular tasks. Organelles include the nucleus, mitochondria, chloroplasts, endoplasmic reticulum, Golgi apparatus, and vacuoles as well as other relatively small cellular inclusions, such as peroxisomes, lysosomes, and chromoplasts. The **nucleus** is the repository of genetic information as contained within the linear sequences of nucleotides in the DNA of chromosomes. **Mitochondria** are the

The inorganic precursors:
(18–64 daltons)
Carbon dioxide, Water, Ammonia,
Nitrogen (N_2), Nitrate (NO_3^-)

Carbon dioxide

Metabolites:
(50–250 daltons)
Pyruvate, Citrate, Succinate,
Glyceraldehyde-3-phosphate,
Fructose-1,6-bisphosphate,
3-Phosphoglyceric acid

Pyruvate

Building blocks:
(100–350 daltons)
Amino acids, Nucleotides,
Monosaccharides, Fatty acids,
Glycerol

Alanine (an amino acid)

Macromolecules:
$(10^3–10^9$ daltons)
Proteins, Nucleic acids,
Polysaccharides, Lipids

Protein

Supramolecular complexes:
$(10^6–10^9$ daltons)
Ribosomes, Cytoskeleton,
Multi-enzyme complexes

Organelles:
Nucleus, Mitochondria,
Chloroplasts, Endoplasmic
reticulum, Golgi apparatus,
Vacuole

The cell

FIGURE 1.8 • Molecular organization in the cell is a hierarchy.

"power plants" of cells by virtue of their ability to carry out the energy-releasing aerobic metabolism of carbohydrates and fatty acids, capturing the energy in metabolically useful forms such as ATP. **Chloroplasts** endow cells with the ability to carry out photosynthesis. They are the biological agents for harvesting light energy and transforming it into metabolically useful chemical forms.

Membranes

Membranes define the boundaries of cells and organelles. As such, they are not easily classified as supramolecular assemblies or organelles, although they share the properties of both. Membranes resemble supramolecular complexes in their construction because they are complexes of proteins and lipids maintained by noncovalent forces. **Hydrophobic interactions** are particularly important in maintaining membrane structure. Hydrophobic interactions arise because water molecules prefer to interact with each other rather than with nonpolar substances. The presence of nonpolar molecules lessens the range of opportunities for water–water interaction by forcing the water molecules into ordered arrays around the nonpolar groups. Such ordering can be minimized if the individual nonpolar molecules redistribute from a dispersed state in the water into an aggregated organic phase surrounded by water. The spontaneous assembly of membranes in the aqueous environment where life arose and exists is the natural result of the hydrophobic ("water-fearing") character of their lipids and proteins. Hydrophobic interactions are the creative means of membrane formation and the driving force that presumably established the boundary of the first cell. The membranes of organelles, such as nuclei, mitochondria, and chloroplasts, differ from one another, with each having a characteristic protein and lipid composition suited to the organelle's function. Furthermore, the creation of discrete volumes or **compartments** within cells is not only an inevitable consequence of the presence of membranes but usually an essential condition for proper organellar function.

The Unit of Life Is the Cell

The **cell** is characterized as the unit of life, the smallest entity capable of displaying the attributes associated uniquely with the living state: growth, metabolism, stimulus response, and replication. In the previous discussions, we explicitly narrowed the infinity of chemical complexity potentially available to organic life, and we previewed an organizational arrangement, moving from simple to complex, that provides interesting insights into the functional and structural plan of the cell. Nevertheless, we find no obvious explanation within these features for the living characteristics of cells. Can we find other themes represented within biomolecules that are explicitly chemical yet anticipate or illuminate the living condition?

1.4 • Properties of Biomolecules Reflect Their Fitness to the Living Condition

If we consider what attributes of biomolecules render them so fit as components of growing, replicating systems, several biologically relevant themes of structure and organization emerge. Furthermore, as we study biochemistry, we will see that these themes serve as principles of biochemistry. Prominent among them is *the necessity for information and energy in the maintenance of the living state.* Some biomolecules must have the capacity to contain the information or "recipe" of life. Other biomolecules must have the capacity to translate this information so that the blueprint is transformed into the functional, organized structures essential to life. Interactions between these structures *are* the processes of life. An orderly mechanism for abstracting energy from the environment must also exist in order to obtain the energy needed to drive these processes. What properties of biomolecules endow them with the potential for such remarkable qualities?

Biological Macromolecules and Their Building Blocks Have a "Sense" or Directionality

The macromolecules of cells are built of units—amino acids in proteins, nucleotides in nucleic acids, and carbohydrates in polysaccharides—that have **structural polarity.** That is, these molecules are not symmetrical, and so they can be thought of as having a "head" and a "tail." Polymerization of these units to form macromolecules occurs by head-to-tail linear connections. Because of this, the polymer also has a head and a tail, and hence, the macromolecule has a "sense" or direction to its structure (Figure 1.9).
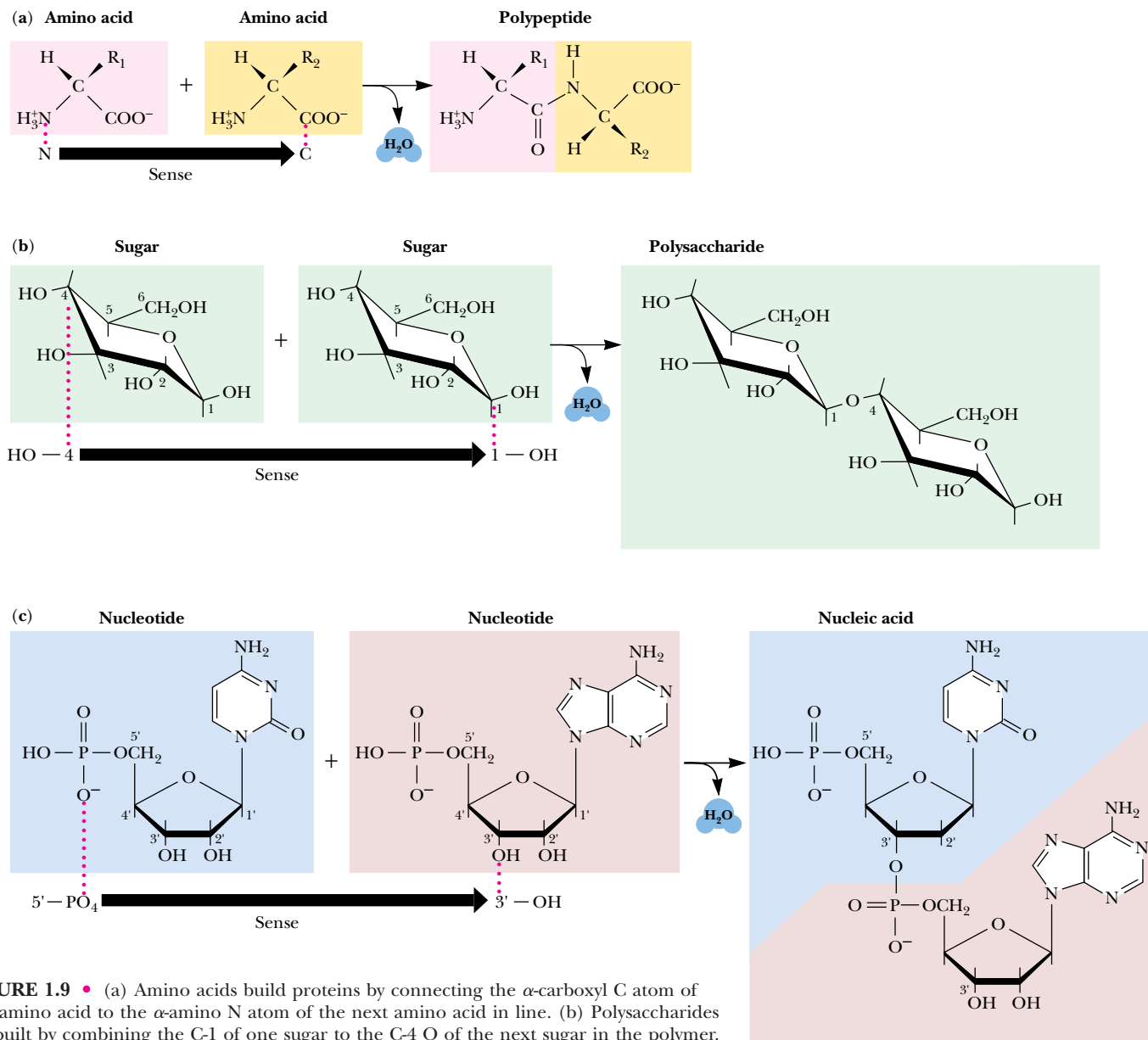
FIGURE 1.9 • (a) Amino acids build proteins by connecting the α-carboxyl C atom of one amino acid to the α-amino N atom of the next amino acid in line. (b) Polysaccharides are built by combining the C-1 of one sugar to the C-4 O of the next sugar in the polymer. (c) Nucleic acids are polymers of nucleotides linked by bonds between the 3′-OH of the ribose ring of one nucleotide to the 5′-PO_4 of its neighboring nucleotide. All three of these polymerization processes involve bond formations accompanied by the elimination of water (dehydration synthesis reactions).

FIGURE 1.10 • The sequence of monomeric units in a biological polymer has the potential to contain information if the diversity and order of the units are not overly simple or repetitive. Nucleic acids and proteins are information-rich molecules; polysaccharides are not.

A strand of DNA

5' T A C G A C G G T C A G C C A T A G A G T C T A 3'

A polypeptide segment

Phe Ser Asn Lys Gly Pro Thr Glu

A polysaccharide chain

Glc Glc Glc Glc Glc Glc Glc Glc Glc
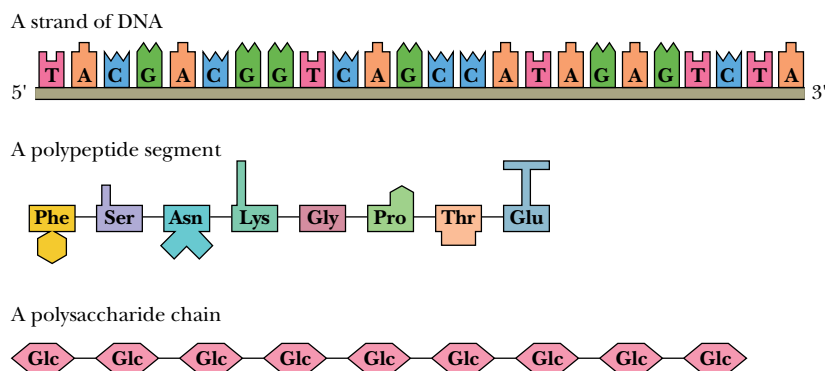
Biological Macromolecules Are Informational

Because biological macromolecules have a sense to their structure, the sequential order of their component building blocks, when read along the length of the molecule, has the capacity to specify information in the same manner that the letters of the alphabet can form words when arranged in a linear sequence (Figure 1.10). Not all biological macromolecules are rich in information. Polysaccharides are often composed of the same sugar unit repeated over and over, as in cellulose or starch, which are homopolymers of many glucose units. On the other hand, proteins and polynucleotides are typically composed of building blocks arranged in no obvious repetitive way; that is, their sequences are unique, akin to the letters and punctuation that form this descriptive sentence. In these unique sequences lies meaning. To discern the meaning, however, requires some mechanism for recognition.

Biomolecules Have Characteristic Three-Dimensional Architecture

The structure of any molecule is a unique and specific aspect of its identity. Molecular structure reaches its pinnacle in the intricate complexity of biological macromolecules, particularly the proteins. Although proteins are linear sequences of covalently linked amino acids, the course of the protein chain can turn, fold, and coil in the three dimensions of space to establish a specific, highly ordered architecture that is an identifying characteristic of the given protein molecule (Figure 1.11).

Weak Forces Maintain Biological Structure and Determine Biomolecular Interactions

Covalent bonds hold atoms together so that molecules are formed. In contrast, **weak chemical forces** or **noncovalent bonds,** (hydrogen bonds, van der Waals forces, ionic interactions, and hydrophobic interactions) are intramolecular or intermolecular attractions between atoms. None of these forces, which typically range from 4 to 30 kJ/mol, are strong enough to bind free atoms together (Table 1.3). The average kinetic energy of molecules at 25°C is 2.5 kJ/mol, so the energy of weak forces is only several times greater than the dissociating tendency due to thermal motion of molecules. Thus, these weak forces create interactions that are constantly forming and breaking at physiological temperature, unless by cumulative number they impart stability to the structures generated by their collective action. These weak forces merit further discussion because their attributes profoundly influence the nature of the biological structures they build.
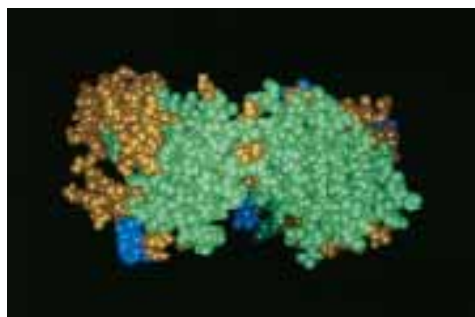

FIGURE 1.11 • Three-dimensional space-filling representation of part of a protein molecule, the antigen-binding domain of immunoglobulin G (IgG). Immunoglobulin G is a major type of circulating antibody. Each of the spheres represents an atom in the structure.

Table 1.3

| Weak Chemical Forces and Their Relative Strengths and Distances			
Force	Strength (kJ/mol)	Distance (nm)	Description
Van der Waals interactions	0.4–4.0	0.2	Strength depends on the relative size of the atoms or molecules and the distance between them. The size factor determines the area of contact between two molecules: The greater the area, the stronger the interaction.
Hydrogen bonds	12–30	0.3	Relative strength is proportional to the polarity of the H bond donor and H bond acceptor. More polar atoms form stronger H bonds.
Ionic interactions	20	0.25	Strength also depends on the relative polarity of the interacting charged species. Some ionic interactions are also H bonds: $-NH_3^+ \ldots {}^-OOC-$
Hydrophobic interactions	<40	—	Force is a complex phenomenon determined by the degree to which the structure of water is disordered as discrete hydrophobic molecules or molecular regions coalesce.

Van der Waals Attractive Forces

Van der Waals forces are the result of induced electrical interactions between closely approaching atoms or molecules as their negatively-charged electron clouds fluctuate instantaneously in time. These fluctuations allow attractions to occur between the positively charged nuclei and the electrons of nearby atoms. Van der Waals interactions include dipole–dipole interactions, whose interaction energies decrease as $1/r^3$; dipole-induced dipole interactions, which fall off as $1/r^5$; and induced dipole-induced dipole interactions, often called **dispersion** or **London dispersion forces,** which diminish as $1/r^6$. Dispersion forces contribute to the attractive intermolecular forces between all molecules, even those without permanent dipoles, and are thus generally more important than dipole–dipole attractions. Van der Waals attractions operate only over a limited interatomic distance and are an effective bonding interaction at physiological temperatures only when a number of atoms in a molecule can interact with several atoms in a neighboring molecule. For this to occur, the atoms on interacting molecules must pack together neatly. That is, their molecular surfaces must possess a degree of structural complementarity (Figure 1.12).

At best, van der Waals interactions are weak and individually contribute 0.4 to 4.0 kJ/mol of stabilization energy. However, the sum of many such interactions within a macromolecule or between macromolecules can be substantial. For example, model studies of heats of sublimation show that each methylene group in a crystalline hydrocarbon accounts for 8 kJ, and each C—H group in a benzene crystal contributes 7 kJ of van der Waals energy per mole. Calculations indicate that the attractive van der Waals energy between the enzyme lysozyme and a sugar substrate that it binds is about 60 kJ/mol.

(a)

(b)

Phe 91
Trp 92
Tyr 32
Tyr 101
Gln 121

FIGURE 1.12 • Van der Waals packing is enhanced in molecules that are structurally complementary. Gln[121] represents a surface protuberance on the protein lysozyme. This protuberance fits nicely within a pocket (formed by Tyr[101], Tyr[32], Phe[91], and Trp[92]) in the antigen-binding domain of an antibody raised against lysozyme. (See also Figure 1.16.) (a) A space-filling representation. (b) A ball-and-stick model. (*From* Science **233**:751 (1986), *figure 5.*)
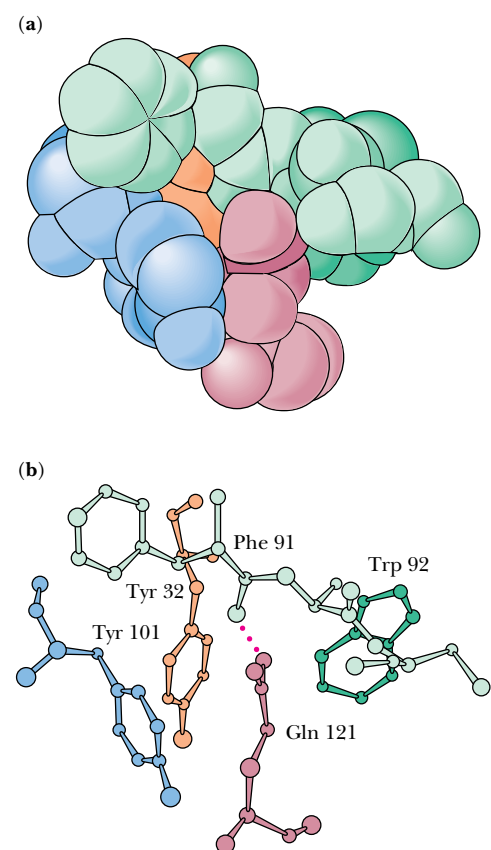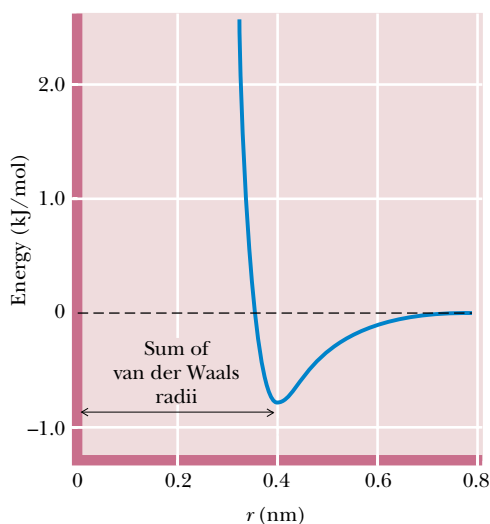
FIGURE 1.13 • The van der Waals interaction energy profile as a function of the distance, r, between the centers of two atoms. The energy was calculated using the empirical equation $U = B/r^{12} - A/r^6$. (Values for the parameters $B = 11.5 \times 10^{-6}$ kJnm^{12}/mol and $A = 5.96 \times 10^{-3}$ kJnm^6/mol for the interaction between two carbon atoms are from Levitt, M., 1974, *Journal of Molecular Biology* **82:**393–420.)

When two atoms approach each other so closely that their electron clouds interpenetrate, strong repulsion occurs. Such *repulsive* van der Waals forces follow an inverse 12th-power dependence on r ($1/r^{12}$), as shown in Figure 1.13. Between the repulsive and attractive domains lies a low point in the potential curve. This low point defines the distance known as the **van der Waals contact distance,** which is the interatomic distance that results if only van der Waals forces hold two atoms together. The limit of approach of two atoms is determined by the sum of their van der Waals radii (Table 1.4).

Hydrogen Bonds

Hydrogen bonds form between a hydrogen atom covalently bonded to an electronegative atom (such as oxygen or nitrogen) and a second electronegative atom that serves as the hydrogen bond acceptor. Several important biological examples are given in Figure 1.14. Hydrogen bonds, at a strength of 12 to 30 kJ/mol, are stronger than van der Waals forces and have an additional property: H bonds tend to be highly directional, forming straight bonds between donor, hydrogen, and acceptor atoms. Hydrogen bonds are also more specific than van der Waals interactions because they require the presence of complementary hydrogen donor and acceptor groups.

Ionic Interactions

Ionic interactions are the result of attractive forces between oppositely charged polar functions, such as negative carboxyl groups and positive amino groups (Figure 1.15). These electrostatic forces average about 20 kJ/mol in aqueous solutions. Typically, the electrical charge is radially distributed, and so these interactions may lack the directionality of hydrogen bonds or the precise fit of van der Waals interactions. Nevertheless, because the opposite charges are restricted to sterically defined positions, ionic interactions can impart a high degree of structural specificity.

The strength of electrostatic interactions is highly dependent on the nature of the interacting species and the distance, r, between them. Electrostatic interactions may involve **ions** (species possessing discrete charges), **permanent dipoles** (having a permanent separation of positive and negative charge), and **induced dipoles** (having a temporary separation of positive and negative charge induced by the environment). Between two ions, the energy falls off as $1/r$. The interaction energy between permanent dipoles falls off as $1/r^3$, whereas the energy between an ion and an induced dipole falls off as $1/r^4$.

Bonded atoms	Approximate bond length*
O—H---O	0.27 nm
O—H---O⁻	0.26 nm
O—H---N	0.29 nm
N—H---O	0.30 nm
N⁺—H---O	0.29 nm
N—H---N	0.31 nm
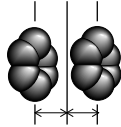
*Lengths given are distances from the atom covalently linked to the H to the atom H-bonded to the hydrogen:

O—H---O
|←0.27 nm→|

Functional groups which are important H bond donors and acceptors:

Donors   **Acceptors**

FIGURE 1.14 • Some of the biologically important H bonds and functional groups that serve as H bond donors and acceptors.

Table 1.4

Radii of the Common Atoms of Biomolecules

Atom	Van der Waals radius, nm	Covalent radius, nm	Atom represented to scale
H	0.1	0.037	
C	0.17	0.077	
N	0.15	0.070	
O	0.14	0.066	
P	0.19	0.096	
S	0.185	0.104	
Half-thickness of an aromatic ring	0.17	—	
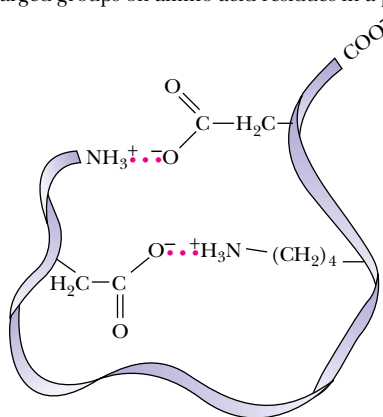
FIGURE 1.15 • Ionic bonds in biological molecules.

Hydrophobic Interactions

Hydrophobic interactions are due to the strong tendency of water to exclude nonpolar groups or molecules (see Chapter 2). Hydrophobic interactions arise not so much because of any intrinsic affinity of nonpolar substances for one another (although van der Waals forces do promote the weak bonding of nonpolar substances), but because water molecules prefer the stronger interactions that they share with one another, compared to their interaction with nonpolar molecules. Hydrogen-bonding interactions between polar water molecules can be more varied and numerous if nonpolar molecules coalesce to form a distinct organic phase. This phase separation raises the entropy of water because fewer water molecules are arranged in orderly arrays around individual nonpolar molecules. It is these preferential interactions between water molecul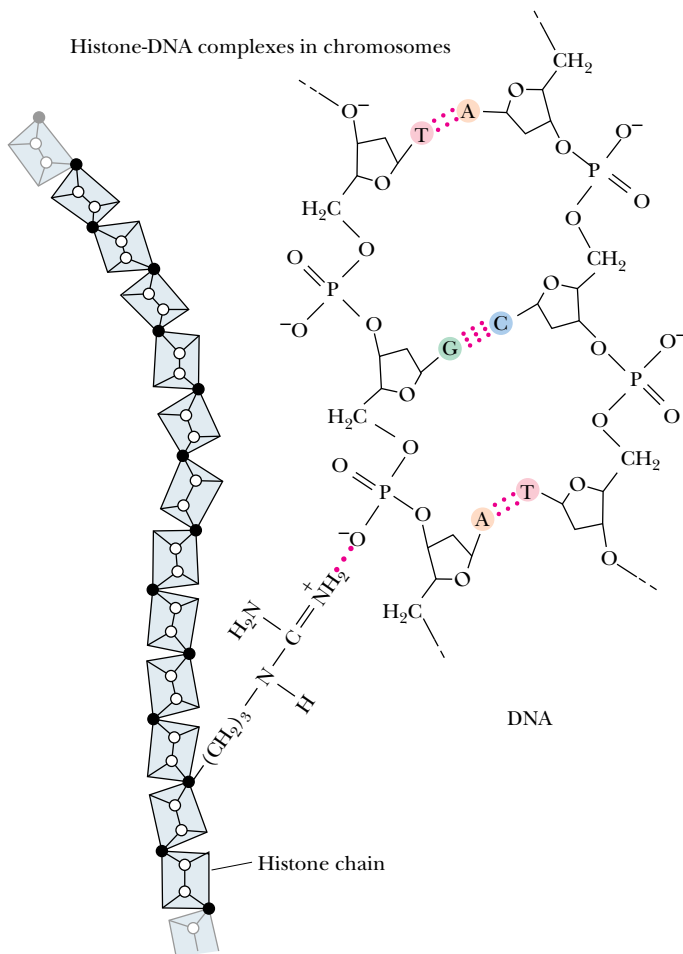es that "exclude" hydrophobic substances from aqueous solution and drive the tendency of nonpolar molecules to cluster together. Thus, nonpolar regions of biological macromolecules are often buried in the molecule's interior to exclude them from the aqueous milieu. The formation of oil droplets as hydrophobic nonpolar lipid molecules coalesce in the presence of water is an approximation of this phenomenon. These tendencies have important consequences in the creation and maintenance of the macromolecular structures and supramolecular assemblies of living cells.

milieu • the environment or surroundings; from the French *mi* meaning "middle" and *lieu* meaning "place"

## Structural Complementarity Determines Biomolecular Interactions

Structural complementarity is the means of recognition in biomolecular interactions. The complicated and highly organized patterns of life depend upon the ability of biomolecules to recognize and interact with one another in very specific ways. Such interactions are fundamental to metabolism, growth, replication, and other vital processes. The interaction of one molecule with another, a protein with a metabolite, for example, can be most precise if the structure of one is complementary to the structure of the other, as in two connecting pieces of a puzzle or, in the more popular analogy for macromolecules and their **ligands,** a lock and its key (Figure 1.16). This principle of **structural complementarity** is the very essence of biomolecular recognition. *Structural complementarity is the significant clue to understanding the functional properties of biological systems.* Biological systems from the macromolecular level to the cellular level operate via specific molecular recognition mechanisms based on structural complementarity: a protein recognizes its specific metabolite, a strand of DNA recognizes its complementary strand, sperm recognize an egg. All these interactions involve structural complementarity between molecules.

ligand • something that binds; a molecule that is bound to another molecule; from the Latin *ligare,* meaning "to bind"

Biomolecular Recognition Is Mediated by Weak Chemical Forces

The biomolecular recognition events that occur through structural complementarity are mediated by the weak chemical forces previously discussed. It is important to realize that, because these interactions are sufficiently weak, they are readily reversible. Consequently, biomolecular interactions tend to be transient; rigid, static lattices of biomolecules that might paralyze cellular activities are not formed. Instead, a dynamic interplay occurs between metabolites and macromolecules, hormones and receptors, and all the other participants instrumental to life processes. This interplay is initiated upon specific recognition between complementary molecules and ultimately culminates in unique physiological activities. *Biological function is achieved through mechanisms based on structural complementarity and weak chemical interactions.*

Puzzle   Lock and key
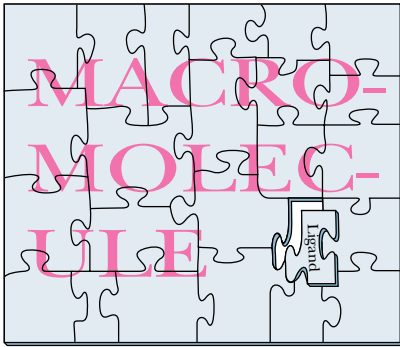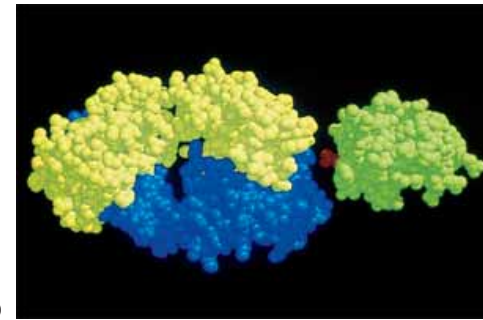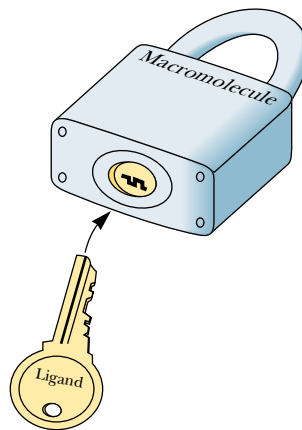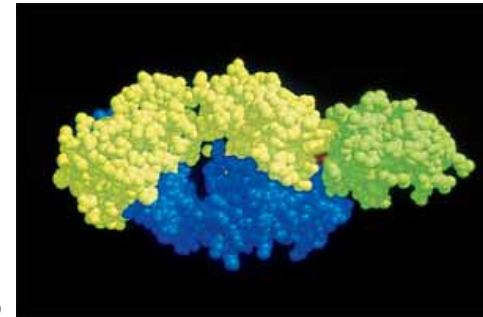
FIGURE 1.16 • Structural complementarity: the pieces of a puzzle, the lock and its key, a biological macromolecule and its ligand—an antigen–antibody complex. (a) The antigen on the right (green) is a small protein, lysozyme, from hen egg white. The part of the antibody molecule (IgG) shown on the left in blue and yellow includes the antigen-binding domain. (b) This domain has a pocket that is structurally complementary to a surface protuberance (Gln[121], shown in red between antigen and antigen-binding domain) on the antigen. (See also Figure 1.12.) (*photos, courtesy of Professor Simon E. V. Philips*)

This principle of structural complementarity extends to higher interactions essential to the establishment of the living condition. For example, the formation of supramolecular complexes occurs because of recognition and interaction between their various macromolecular components, as governed by the weak forces formed between them. If a sufficient number of weak bonds can be formed, as in macromolecules complementary in structure to one another, larger structures assemble spontaneously. The tendency for nonpolar molecules and parts of molecules to come together through hydrophobic interactions also promotes the formation of supramolecular assemblies. Very complex subcellular structures are actually spontaneously formed in an assembly process that is driven by weak forces accumulated through structural complementarity.

Weak Forces Restrict Organisms to a Narrow Range of Environmental Conditions

The central role of weak forces in biomolecular interactions restricts living systems to a narrow range of physical conditions. Biological macromolecules are functionally active only within a narrow range of environmental conditions, such as temperature, ionic strength, and relative acidity. Extremes of these conditions disrupt the weak forces essential to maintaining the intricate structure of macromolecules. The loss of structural order in these complex macromolecules, so-called **denaturation,** is accompanied by loss of function (Figure 1.17). As a consequence, cells cannot tolerate reactions in which large amounts of energy are released. Nor can they generate a large energy burst to drive energy-requiring processes. Instead, such transformations take place via sequential series of chemical reactions whose overall effect achieves dramatic energy changes, even though any given reaction in the series proceeds with only mod-

FIGURE 1.17 • Denaturation and renaturation of the intricate structure of a protein.

Native   Denatured
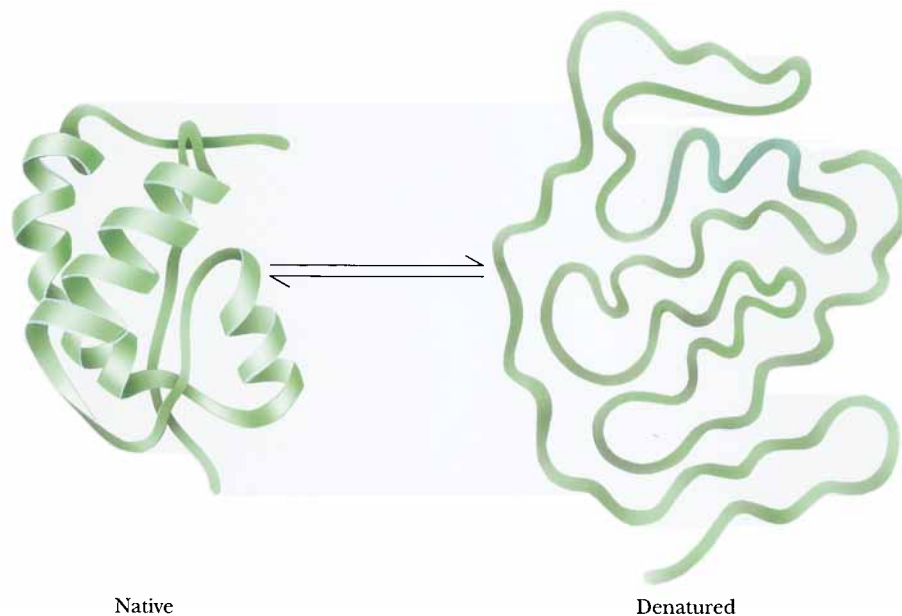
The combustion of glucose: $C_6H_{12}O_6 + 6O_2 \longrightarrow 6CO_2 + 6H_2O + 2{,}870$ kJ energy

(a) In an aerobic cell

Glucose

Glycolysis

2 Pyruvate

Citric acid cycle and oxidative phosphorylation

$6CO_2 + 6H_2O$

30–38 ATP

(b) In a bomb calorimeter

Glucose

2,870 kJ energy as heat

$6CO_2 + 6H_2O$
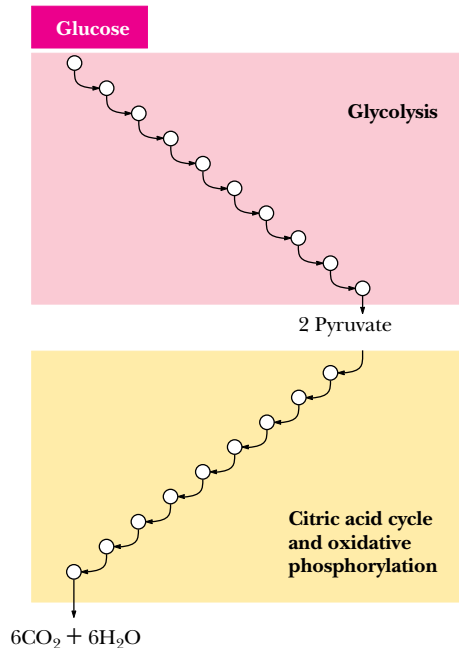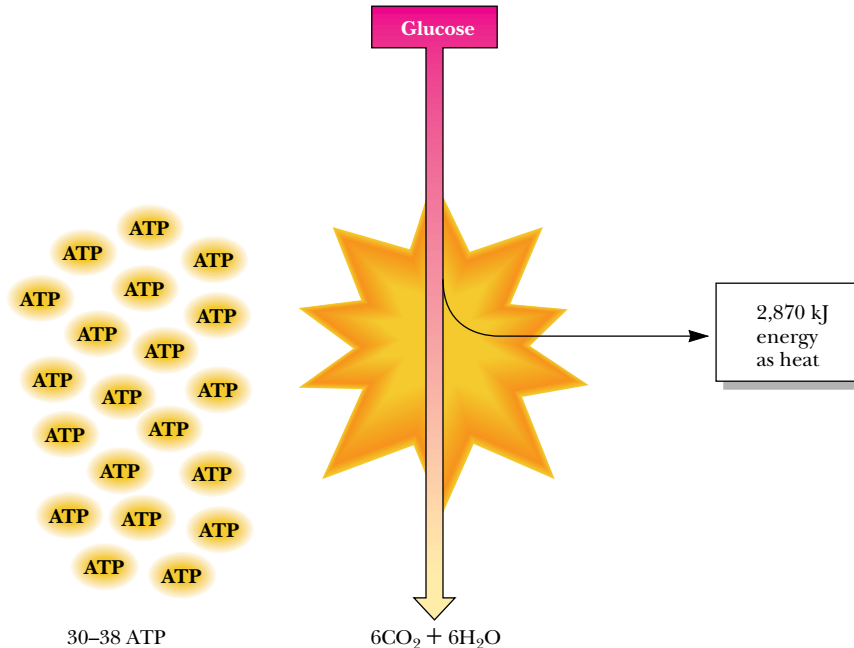
FIGURE 1.18 • Metabolism is the organized release or capture of small amounts of energy in processes whose overall change in energy is large. (a) For example, the combustion of glucose by cells is a major pathway of energy production, with the energy captured appearing as 30 to 38 equivalents of ATP, the principal energy-rich chemical of cells. The ten reactions of glycolysis, the nine reactions of the citric acid cycle, and the successive linked reactions of oxidative phosphorylation release the energy of glucose in a stepwise fashion and the small "packets" of energy appear in ATP. (b) Combustion of glucose in a bomb calorimeter results in an uncontrolled, explosive release of energy in its least useful form, heat.

est input or release of energy (Figure 1.18). These sequences of reactions are organized to provide for the release of useful energy to the cell from the breakdown of food or to take such energy and use it to drive the synthesis of biomolecules essential to the living state. Collectively, these reaction sequences constitute cellular **metabolism**—the ordered reaction pathways by which cellular chemistry proceeds and biological energy transformations are accomplished.

Enzymes

The sensitivity of cellular constituents to environmental extremes places another constraint on the reactions of metabolism. The rate at which cellular reactions proceed is a very important factor in maintenance of the living state. However, the common ways chemists accelerate reactions are not available to cells; the temperature cannot be raised, acid or base cannot be added, the pressure cannot be elevated, and concentrations cannot be dramatically increased. Instead, biomolecular catalysts mediate cellular reactions. These catalysts, called **enzymes,** accelerate the reaction rates many orders of magnitude and, by selecting the substances undergoing reaction, determine the specific reaction taking place. Virtually every metabolic reaction is served by an enzyme whose sole biological purpose is to catalyze its specific reaction (Figure 1.19).

Metabolic Regulation Is Achieved by Controlling the Activity of Enzymes

Thousands of reactions mediated by an equal number of enzymes are occurring at any given instant within the cell. Metabolism has many branch points, cycles, and interconnections, as a glance at a metabolic pathway map reveals
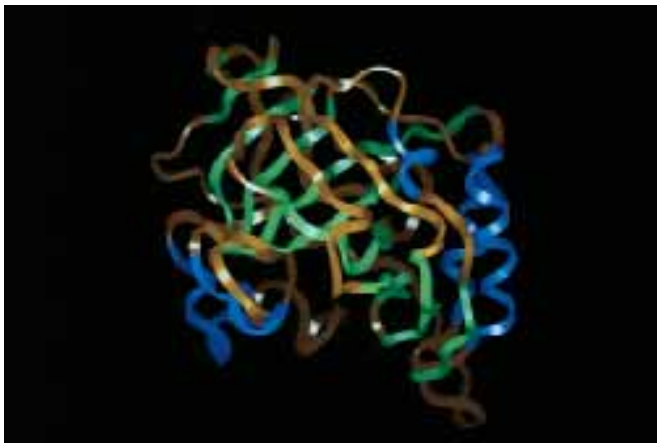
FIGURE 1.19 • Carbonic anhydrase, a representative enzyme, and the reaction that it catalyzes. Dissolved carbon dioxide is slowly hydrated by water to form bicarbonate ion and H^+:

$$CO_2 + H_2O \rightleftharpoons HCO_3^- + H^+$$
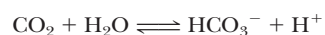
At 20°C, the rate constant for this uncatalyzed reaction, k_{uncat}, is 0.03/sec. In the presence of the enzyme carbonic anhydrase, the rate constant for this reaction, k_{cat}, is 10^6/sec. Thus carbonic anhydrase accelerates the rate of this reaction 3.3×10^7 times. Carbonic anhydrase is a 29-kD protein.

Biochemical Pathways — Metabolic Map
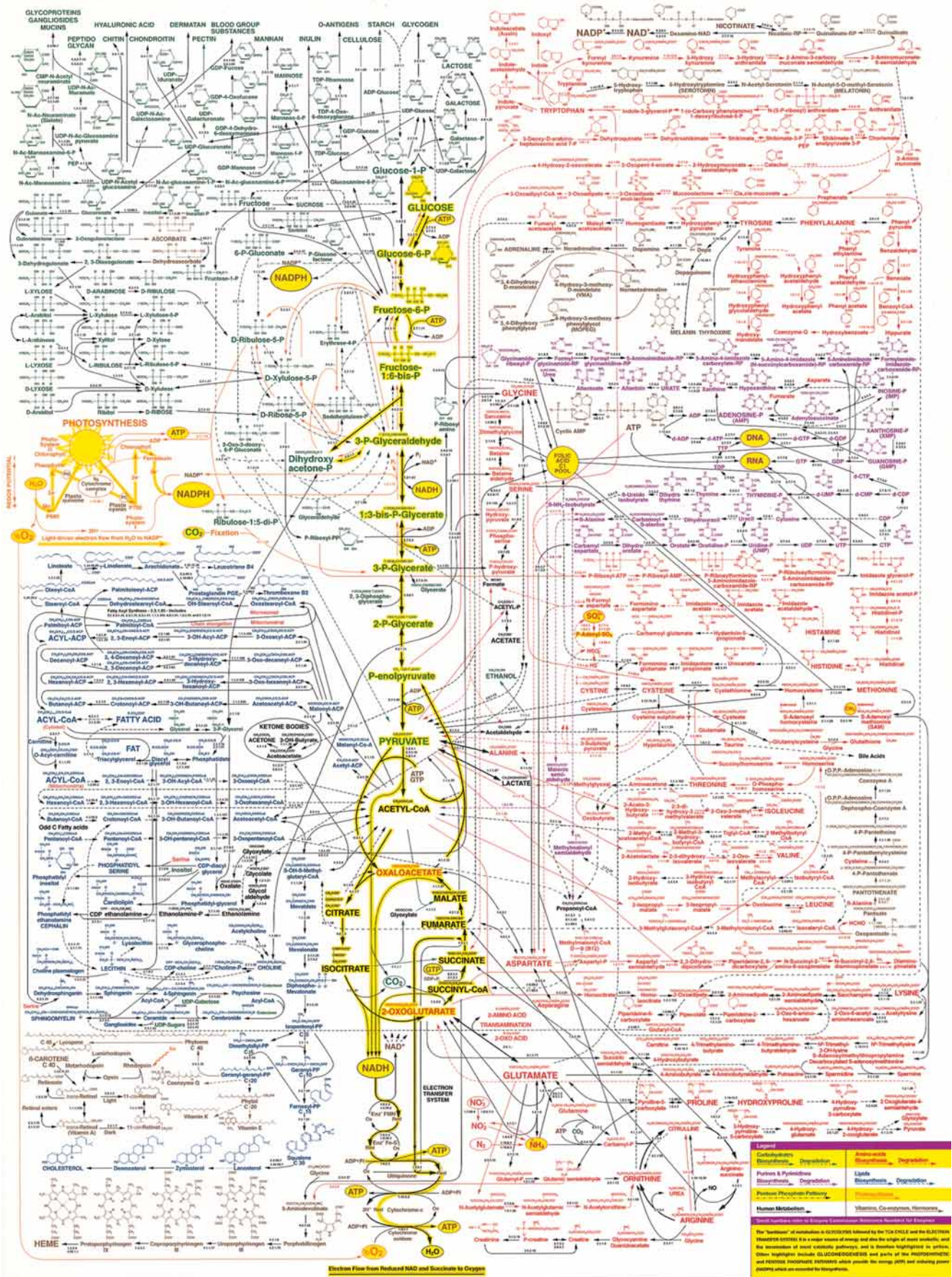
◀ **FIGURE 1.20** • Reproduction of a metabolic map. *(Courtesy of D. E. Nicholson, University of Leeds and Sigma Chemical Co., St. Louis, MO.)*

(Figure 1.20). All of these reactions, many of which are at apparent cross-purposes in the cell, must be fine-tuned and integrated so that metabolism and life proceed harmoniously. The need for metabolic regulation is obvious. This metabolic regulation is achieved through controls on enzyme activity so that the rates of cellular reactions are appropriate to cellular requirements.

Despite the organized pattern of metabolism and the thousands of enzymes required, cellular reactions nevertheless conform to the same thermodynamic principles that govern any chemical reaction. Enzymes have no influence over energy changes (the thermodynamic component) in their reactions. Enzymes only influence reaction rates. Thus, cells are systems that take in food, release waste, and carry out complex degradative and biosynthetic reactions essential to their survival while operating under conditions of essentially constant temperature and pressure and maintaining a constant internal environment **(homeostasis)** with no outwardly apparent changes. *Cells are open thermodynamic systems exchanging matter and energy with their environment and functioning as highly regulated isothermal chemical engines.*

1.5 • Organization and Structure of Cells

All living cells fall into one of two broad categories—**prokaryotic** and **eukaryotic.** The distinction is based on whether or not the cell has a nucleus. Prokaryotes are single-celled organisms that lack nuclei and other organelles; the word is derived from *pro* meaning "prior to" and *karyote* meaning "nucleus." In conventional biological classification schemes, prokaryotes are grouped together as members of the kingdom Monera, represented by bacteria and cyanobacteria (formerly called blue-green algae). The other four living kingdoms are all eukaryotes—the single-celled Protists, such as amoebae, and all multicellular life forms, including the Fungi, Plant, and Animal kingdoms. Eukaryotic cells have true nuclei and other organelles such as mitochondria, with the prefix *eu* meaning "true."

Early Evolution of Cells

Until recently, most biologists accepted the idea that eukaryotes evolved from the simpler prokaryotes in some linear progression from simple to complex over the course of geological time. Contemporary evidence favors the view that present-day organisms are better grouped into three classes or lineages: eukaryotes and two prokaryotic groups, the **eubacteria** and the **archaea** (formerly designated as **archaebacteria**). All are believed to have evolved approximately 3.5 billion years ago from a common ancestral form called the **progenote.** It is now understood that eukaryotic cells are, in reality, composite cells derived from various prokaryotic contributions. Thus, the dichotomy between prokaryotic cells and eukaryotic cells, although convenient, is an artificial distinction.

Despite the great diversity in form and function, cells and organisms share a common biochemistry. This commonality, although long established, has received further validation through **whole genome sequencing,** or the determination of the complete nucleotide sequence within the DNA of an organism. For example, the recently sequenced genome of the archaeon *Methanococcus*

jannaschii shows 44% similarity to known genes in eubacteria and eukaryotes, yet 56% of its genes are new to science. Whole genome sequencing is revolutionizing biochemistry as the protein-coding sequences of newly revealed genes outpace our understanding of what the proteins are and what they do.

Structural Organization of Prokaryotic Cells

Among prokaryotes (the simplest cells), most known species are eubacteria and they form a widely spread group. Certain of them are pathogenic to humans. The archaea are remarkable because they can be found in unusual environments where other cells cannot survive. Archaea include the **thermoacidophiles** (heat- and acid-loving bacteria) of hot springs, the **halophiles** (salt-loving bacteria) of salt lakes and ponds, and the **methanogens** (bacteria that generate methane from CO_2 and H_2). Prokaryotes are typically very small, on the order of several microns in length, and are usually surrounded by a rigid **cell wall** that protects the cell and gives it its shape. The characteristic structural organization of a prokaryotic cell is depicted in Figure 1.21.

Prokaryotic cells have only a single membrane, the **plasma membrane** or **cell membrane.** Because they have no other membranes, prokaryotic cells contain no nucleus or organelles. Nevertheless, they possess a distinct **nuclear area** where a single circular chromosome is localized, and some have an internal membranous structure called a **mesosome** that is derived from and continuous with the cell membrane. Reactions of cellular respiration are localized on these membranes. In photosynthetic prokaryotes such as the **cyanobacteria,**

E. *coli* bacteria

A BACTERIAL CELL

Ribosomes

Nucleoid (DNA)

Capsule

Flagella
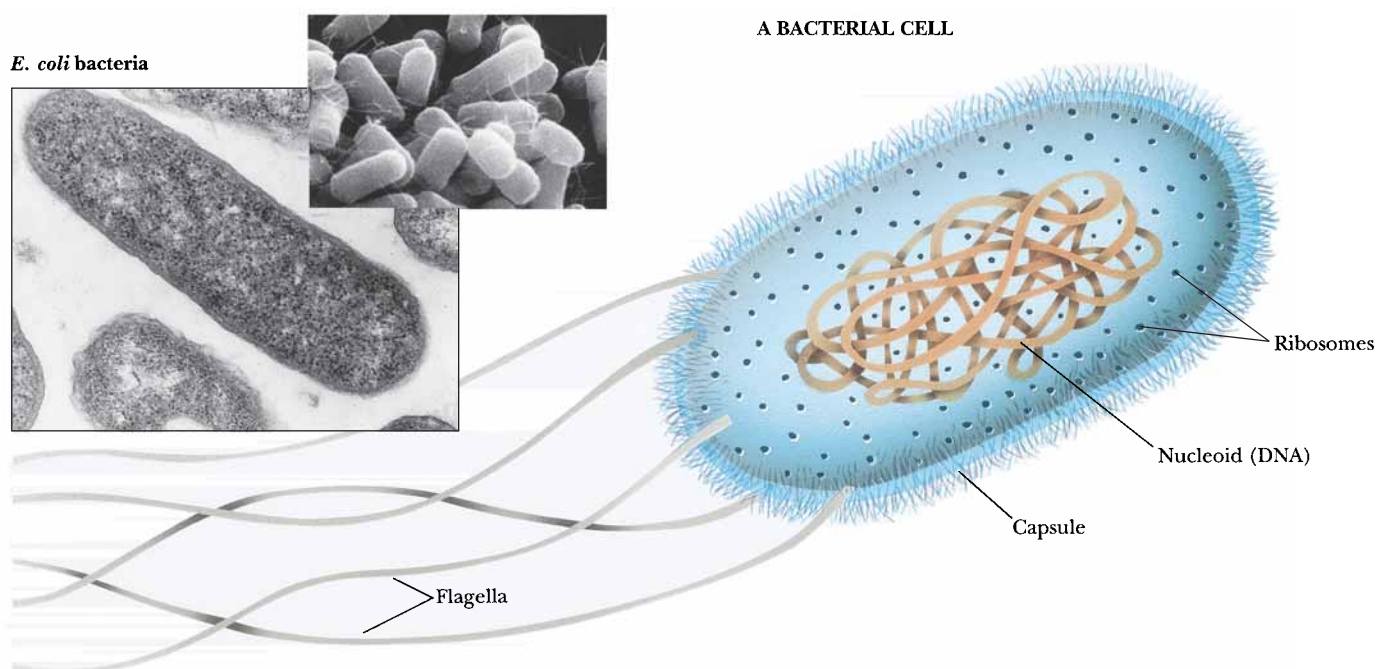
FIGURE 1.21 • This bacterium is *Escherichia coli,* a member of the coliform group of bacteria that colonize the intestinal tract of humans. *E. coli* organisms have rather simple nutritional requirements. They grow and multiply quite well if provided with a simple carbohydrate source of energy (such as glucose), ammonium ions as a source of nitrogen, and a few mineral salts. The simple nutrition of this "lower" organism means that its biosynthetic capacities must be quite advanced. When growing at 37°C on a rich organic medium, *E. coli* cells divide every 20 minutes. Subcellular features include the cell wall, plasma membrane, nuclear region, ribosomes, storage granules, and cytosol (Table 1.5). (*photo, Martin Rotker/Phototake, Inc.; inset photo, David M. Phillips/The Population Council/Science Source/Photo Researchers, Inc.*)

Table 1.5

| Major Features of Prokaryotic Cells		
Structure	**Molecular Composition**	**Function**
Cell wall	Peptidoglycan: a rigid framework of polysaccharide cross-linked by short peptide chains. Some bacteria possess a lipopolysaccharide- and protein-rich outer membrane.	Mechanical support, shape, and protection against swelling in hypotonic media. The cell wall is a porous nonselective barrier that allows most small molecules to pass.
Cell membrane	The cell membrane is composed of about 45% lipid and 55% protein. The lipids form a bilayer that is a continuous nonpolar hydrophobic phase in which the proteins are embedded.	The cell membrane is a highly selective permeability barrier that controls the entry of most substances into the cell. Important enzymes in the generation of cellular energy are located in the membrane.
Nuclear area or nucleoid	The genetic material is a single tightly coiled DNA molecule 2 nm in diameter but over 1 mm in length (molecular mass of *E. coli* DNA is 3×10^9 daltons; 4.64×10^6 nucleotide pairs).	DNA is the blueprint of the cell, the repository of the cell's genetic information. During cell division, each strand of the double-stranded DNA molecule is replicated to yield two double-helical daughter molecules. Messenger RNA (mRNA) is transcribed from DNA to direct the synthesis of cellular proteins.
Ribosomes	Bacterial cells contain about 15,000 ribosomes. Each is composed of a small (30S) subunit and a large (50S) subunit. The mass of a single ribosome is 2.3×10^6 daltons. It consists of 65% RNA and 35% protein.	Ribosomes are the sites of protein synthesis. The mRNA binds to ribosomes, and the mRNA nucleotide sequence specifies the protein that is synthesized.
Storage granules	Bacteria contain granules that represent storage forms of polymerized metabolites such as sugars or β-hydroxybutyric acid.	When needed as metabolic fuel, the monomeric units of the polymer are liberated and degraded by energy-yielding pathways in the cell.
Cytosol	Despite its amorphous appearance, the cytosol is now recognized to be an organized gelatinous compartment that is 20% protein by weight and rich in the organic molecules that are the intermediates in metabolism.	The cytosol is the site of intermediary metabolism, the interconnecting sets of chemical reactions by which cells generate energy and form the precursors necessary for biosynthesis of macromolecules essential to cell growth and function.

flat, sheetlike membranous structures called **lamellae** are formed from cell membrane infoldings. These lamellae are the sites of photosynthetic activity, but in prokaryotes, they are not contained within **plastids,** the organelles of photosynthesis found in higher plant cells. Prokaryotic cells also lack a cytoskeleton; the cell wall maintains their structure. Some bacteria have **flagella,** single, long filaments used for motility. Prokaryotes largely reproduce by asexual division, although sexual exchanges can occur. Table 1.5 lists the major features of prokaryotic cells.

Structural Organization of Eukaryotic Cells

In comparison to prokaryotic cells, eukaryotic cells are much greater in size, typically having cell volumes 10^3 to 10^4 times larger. Also, they are much more complex. These two features require that eukaryotic cells partition their diverse

Rough endoplasmic reticulum (plant and animal)
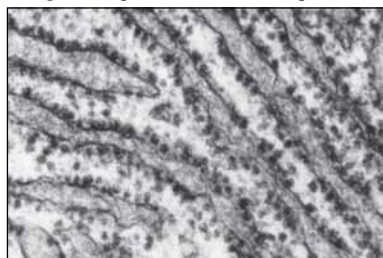
Smooth endoplasmic reticulum (plant and animal)
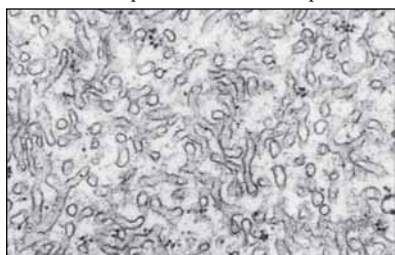
Mitochondrion (plant and animal)

AN ANIMAL CELL

Smooth endoplasmic reticulum

Nuclear membrane

Rough endoplasmic reticulum

Nucleolus

Lysosome

Nucleus

Plasma
membrane

Mitochondrion

Golgi body

Cytoplasm

Filamentous cytoskeleton
(microtubules)
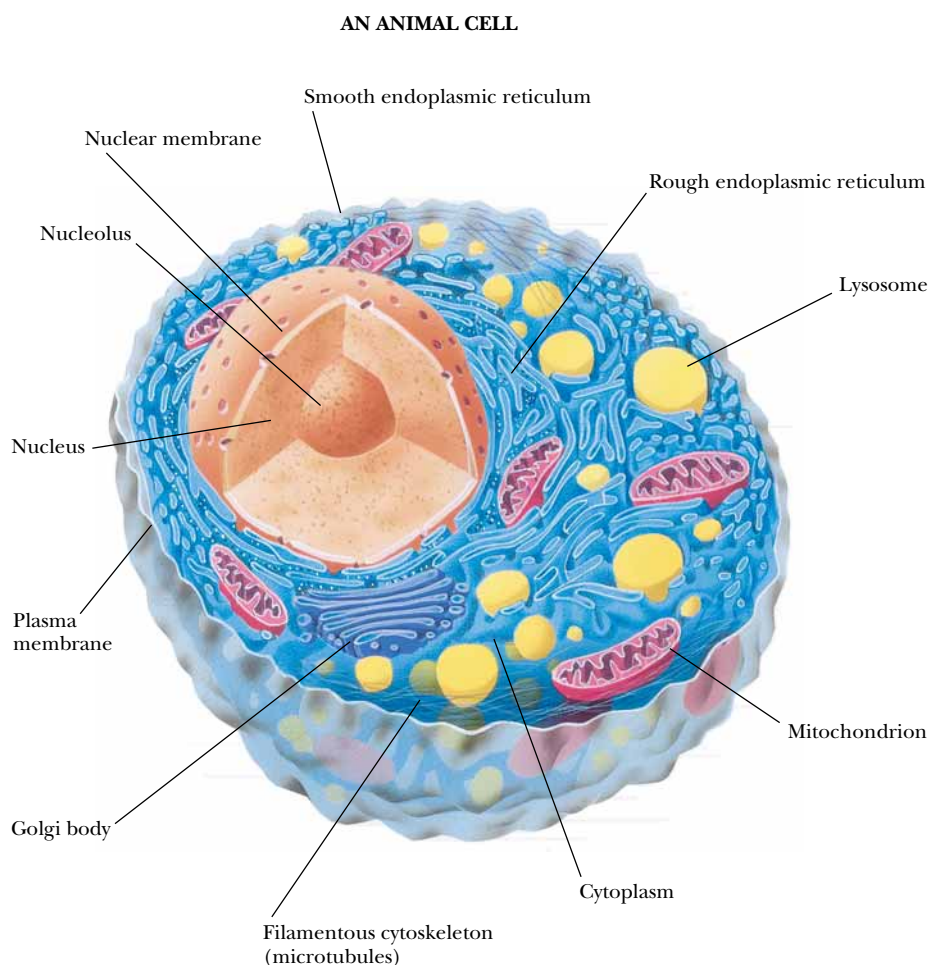
FIGURE 1.22 • This figure diagrams a rat liver cell, a typical higher animal cell in which the characteristic features of animal cells are evident, such as a nucleus, nucleolus, mitochondria, Golgi bodies, lysosomes, and endoplasmic reticulum (ER). Microtubules and the network of filaments constituting the cytoskeleton are also depicted. (*photos, top, Dwight R. Kuhn/Visuals Unlimited; middle, D.W. Fawcett/Visuals Unlimited; bottom, Keith Porter/Photo Researchers, Inc.*)

metabolic processes into organized compartments, with each compartment dedicated to a particular function. A system of internal membranes accomplishes this partitioning. A typical animal cell is shown in Figure 1.22; a typical plant cell in Figure 1.23. Tables 1.6 and 1.7 list the major features of a typical animal cell and a higher plant cell, respectively.

Eukaryotic cells possess a discrete, membrane-bounded **nucleus,** the repository of the cell's genetic material, which is distributed among a few or many **chromosomes.** During cell division, equivalent copies of this genetic material must be passed to both daughter cells through duplication and orderly partitioning of the chromosomes by the process known as **mitosis.** Like prokaryotic

Table 1.6

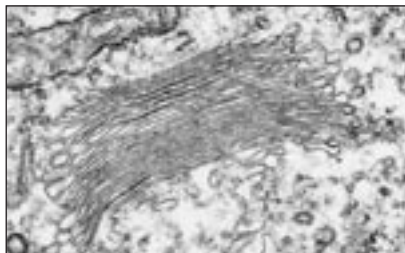| Major Features of a Typical Animal Cell		
Structure	**Molecular Composition**	**Function**
Extracellular matrix	The surfaces of animal cells are covered with a flexible and sticky layer of complex carbohydrates, proteins, and lipids.	This complex coating is cell-specific, serves in cell–cell recognition and communication, creates cell adhesion, and provides a protective outer layer.
Cell membrane (plasma membrane)	Roughly 50:50 lipid:protein as a 5-nm-thick continuous sheet of lipid bilayer in which a variety of proteins are embedded.	The plasma membrane is a selectively permeable outer boundary of the cell, containing specific systems—pumps, channels, transporters—for the exchange of nutrients and other materials with the environment. Important enzymes are also located here.
Nucleus	The nucleus is separated from the cytosol by a double membrane, the nuclear envelope. The DNA is complexed with basic proteins (histones) to form chromatin fibers, the material from which chromosomes are made. A distinct RNA-rich region, the nucleolus, is the site of ribosome assembly.	The nucleus is the repository of genetic information encoded in DNA and organized into chromosomes. During mitosis, the chromosomes are replicated and transmitted to the daughter cells. The genetic information of DNA is transcribed into RNA in the nucleus and passes into the cytosol where it is translated into protein by ribosomes.
Mitochondria	Mitochondria are organelles surrounded by two membranes that differ markedly in their protein and lipid composition. The inner membrane and its interior volume, the matrix, contain many important enzymes of energy metabolism. Mitochondria are about the size of bacteria, ≈ 1 μm. Cells contain hundreds of mitochondria, which collectively occupy about one-fifth of the cell volume.	Mitochondria are the power plants of eukaryotic cells where carbohydrates, fats, and amino acids are oxidized to CO_2 and H_2O. The energy released is trapped as high-energy phosphate bonds in ATP.
Golgi apparatus	A system of flattened membrane-bounded vesicles often stacked into a complex. Numerous small vesicles are found peripheral to the Golgi and contain secretory material packaged by the Golgi.	Involved in the packaging and processing of macromolecules for secretion and for delivery to other cellular compartments.
Endoplasmic reticulum (ER) and ribosomes	Flattened sacs, tubes, and sheets of internal membrane extending throughout the cytoplasm of the cell and enclosing a large interconnecting series of volumes called *cisternae*. The ER membrane is continuous with the outer membrane of the nuclear envelope. Portions of the sheetlike areas of the ER are studded with ribosomes, giving rise to *rough ER*. Eukaryotic ribosomes are larger than prokaryotic ribosomes.	The endoplasmic reticulum is a labyrinthine organelle where both membrane proteins and lipids are synthesized. Proteins made by the ribosomes of the rough ER pass through the outer ER membrane into the cisternae and can be transported via the Golgi to the periphery of the cell. Other ribosomes unassociated with the ER carry on protein synthesis in the cytosol.
Lysosomes	Lysosomes are vesicles 0.2–0.5 μm in diameter, bounded by a single membrane. They contain hydrolytic enzymes such as proteases and nucleases which, if set free, could degrade essential cell constituents. They are formed by budding from the Golgi apparatus.	Lysosomes function in intracellular digestion of materials entering the cell via phagocytosis or pinocytosis. They also function in the controlled degradation of cellular components.
Peroxisomes	Like lysosomes, peroxisomes are 0.2–0.5 μm single-membrane–bounded vesicles. They contain a variety of oxidative enzymes that use molecular oxygen and generate peroxides. They are formed by budding from the smooth ER.	Peroxisomes act to oxidize certain nutrients, such as amino acids. In doing so, they form potentially toxic hydrogen peroxide, H_2O_2, and then decompose it to H_2O and O_2 by way of the peroxide-cleaving enzyme catalase.
Cytoskeleton	The cytoskeleton is composed of a network of protein filaments: actin filaments (or microfilaments), 7 nm in diameter; intermediate filaments, 8–10 nm; and microtubules, 25 nm. These filaments interact in establishing the structure and functions of the cytoskeleton. This interacting network of protein filaments gives structure and organization to the cytoplasm.	The cytoskeleton determines the shape of the cell and gives it its ability to move. It also mediates the internal movements that occur in the cytoplasm, such as the migration of organelles and mitotic movements of chromosomes. The propulsion instruments of cells—cilia and flagella—are constructed of microtubules.

Chloroplast (plant cell only)

Golgi body (plant and animal)

Nucleus (plant and animal)

A PLANT CELL

Smooth endoplasmic reticulum

Nuclear membrane

Lysosome

Nucleolus

Mitochondrion

Nucleus

Vacuole

Rough endoplasmic reticulum

Chloroplast

Golgi body

Plasma membrane

Cellulose wall   } Cell wall

Pectin
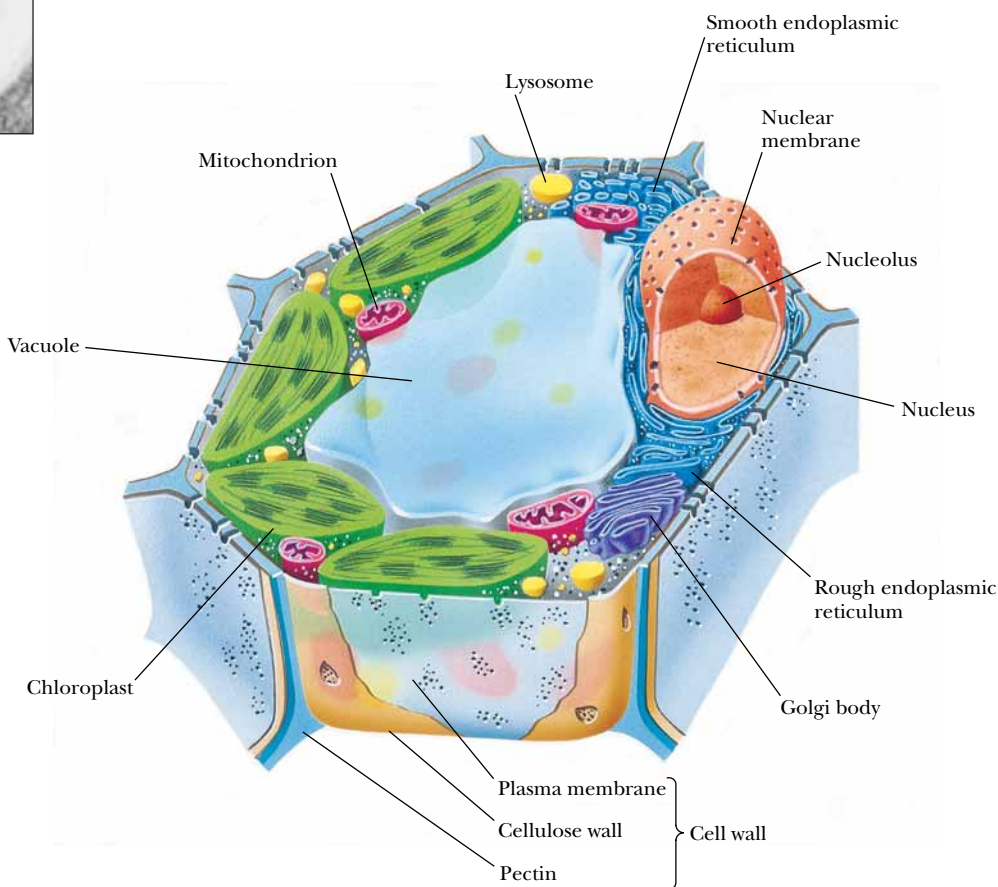
FIGURE 1.23 • This figure diagrams a cell in the leaf of a higher plant. The cell wall, membrane, nucleus, chloroplasts, mitochondria, vacuole, ER, and other characteristic features are shown. (*photos, top, middle, Dr. Dennis Kunkel/Phototake, NYC; bottom, Biophoto Associates*)

cells, eukaryotic cells are surrounded by a plasma membrane. Unlike prokaryotic cells, eukaryotic cells are rich in internal membranes that are differentiated into specialized structures such as the **endoplasmic reticulum (ER)** and the **Golgi apparatus.** Membranes also surround certain organelles (**mitochondria** and **chloroplasts,** for example) and various vesicles, including **vacuoles, lysosomes,** and **peroxisomes.** The common purpose of these membranous partitionings is the creation of cellular compartments that have specific, organized metabolic functions, such as the mitochondrion's role as the principal site of cellular energy production. Eukaryotic cells also have a **cytoskeleton** composed of arrays of filaments that give the cell its shape and its capacity to move. Some eukaryotic cells also have long projections on their surface—cilia or flagella—which provide propulsion.

Table 1.7

Major Features of a Higher Plant Cell: A Photosynthetic Leaf Cell		
Structure	**Molecular Composition**	**Function**
Cell wall	Cellulose fibers embedded in a polysaccharide/protein matrix; it is thick (>0.1 μm), rigid, and porous to small molecules.	Protection against osmotic or mechanical rupture. The walls of neighboring cells interact in cementing the cells together to form the plant. Channels for fluid circulation and for cell–cell communication pass through the walls. The structural material confers form and strength on plant tissue.
Cell membrane	Plant cell membranes are similar in overall structure and organization to animal cell membranes but differ in lipid and protein composition.	The plasma membrane of plant cells is selectively permeable, containing transport systems for the uptake of essential nutrients and inorganic ions. A number of important enzymes are localized here.
Nucleus	The nucleus, nucleolus, and nuclear envelope of plant cells are like those of animal cells.	Chromosomal organization, DNA replication, transcription, ribosome synthesis, and mitosis in plant cells are grossly similar to the analogous features in animals.
Chloroplasts	Plant cells contain a unique family of organelles, the plastids, of which the chloroplast is the prominent example. Chloroplasts have a double membrane envelope, an inner volume called the **stroma,** and an internal membrane system rich in thylakoid membranes, which enclose a third compartment, the thylakoid **lumen.** Chloroplasts are significantly larger than mitochondria. Other plastids are found in specialized structures such as fruits, flower petals, and roots and have specialized roles.	Chloroplasts are the site of photosynthesis, the reactions by which light energy is converted to metabolically useful chemical energy in the form of ATP. These reactions occur on the thylakoid membranes. The formation of carbohydrate from CO_2 takes place in the stroma. Oxygen is evolved during photosynthesis. Chloroplasts are the primary source of energy in the light.
Mitochondria	Plant cell mitochondria resemble the mitochondria of other eukaryotes in form and function.	Plant mitochondria are the main source of energy generation in photosynthetic cells in the dark and in nonphotosynthetic cells under all conditions.
Vacuole	The vacuole is usually the most obvious compartment in plant cells. It is a very large vesicle enclosed by a single membrane called the **tonoplast.** Vacuoles tend to be smaller in young cells, but in mature cells, they may occupy more than 50% of the cell's volume. Vacuoles occupy the center of the cell, with the cytoplasm being located peripherally around it. They resemble the lysosomes of animal cells.	Vacuoles function in transport and storage of nutrients and cellular waste products. By accumulating water, the vacuole allows the plant cell to grow dramatically in size with no increase in cytoplasmic volume.
Golgi apparatus, endoplasmic reticulum, ribosomes, lysosomes, peroxisomes, and cytoskeleton	Plant cells also contain all of these characteristic eukaryotic organelles, essentially in the form described for animal cells.	These organelles serve the same purposes in plant cells that they do in animal cells.

1.6 • Viruses Are Supramolecular Assemblies Acting as Cell Parasites

Viruses are supramolecular complexes of nucleic acid, either DNA or RNA, encapsulated in a protein coat and, in some instances, surrounded by a membrane envelope (Figure 1.24). The bits of nucleic acid in viruses are, in reality, mobile elements of genetic information. The protein coat serves to protect the nucleic acid and allows it to gain entry to the cells that are its specific hosts. Viruses unique for all types of cells are known. Viruses infecting bacteria are called **bacteriophages** ("bacteria eaters"); different viruses infect animal cells and plant cells. Once the nucleic acid of a virus gains access to its specific host, it typically takes over the metabolic machinery of the host cell, diverting it to the production of virus particles. The host metabolic functions are subjugated to the synthesis of viral nucleic acid and proteins. Mature virus particles arise by encapsulating the nucleic acid within a protein coat called the **capsid.** Viruses are thus supramolecular assemblies that act as parasites of cells (Figure 1.25).

(a)   (b)

(c)
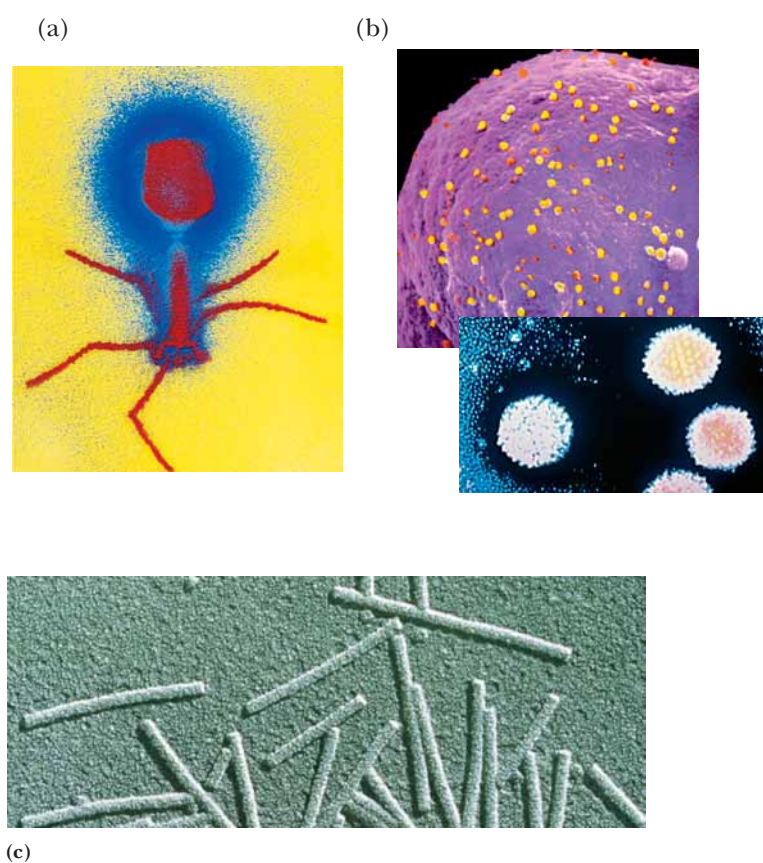
FIGURE 1.24 • Viruses are genetic elements enclosed in a protein coat. Viruses are not free-living and can only reproduce within cells. Viruses show an almost absolute specificity for their particular host cells, infecting and multiplying only within those cells. Viruses are known for virtually every kind of cell. Shown here are examples of (a) a bacterial virus, bacteriophage T_4; (b) an animal virus, adenovirus (inset at greater magnification); and (c) a plant virus, tobacco mosaic virus. (*a, M. Wurtz/Biozeentrum/University of Basel/SPL/Photo Researchers, Inc.; b, Dr. Thomas Broker/Phototake, NYC; inset, CNRI/SPL/Photo Researchers, Inc.; c, Biology Media/Photo Researchers, Inc.*)

Often, viruses cause the lysis of the cells they infect. It is their cytolytic properties that are the basis of viral disease. In certain circumstances, the viral genetic elements may integrate into the host chromosome and become quiescent. Such a state is termed **lysogeny.** Typically, damage to the host cell activates the replicative capacities of the quiescent viral nucleic acid, leading to viral propagation and release. Some viruses are implicated in transforming cells into a cancerous state, that is, in converting their hosts to an unregulated state of cell division and proliferation. Because all viruses are heavily dependent on their host for the production of viral progeny, viruses must have arisen after cells were established in the course of evolution. Presumably, the first viruses were fragments of nucleic acid that developed the ability to replicate independently of the chromosome and then acquired the necessary genes enabling protection, autonomy, and transfer between cells.
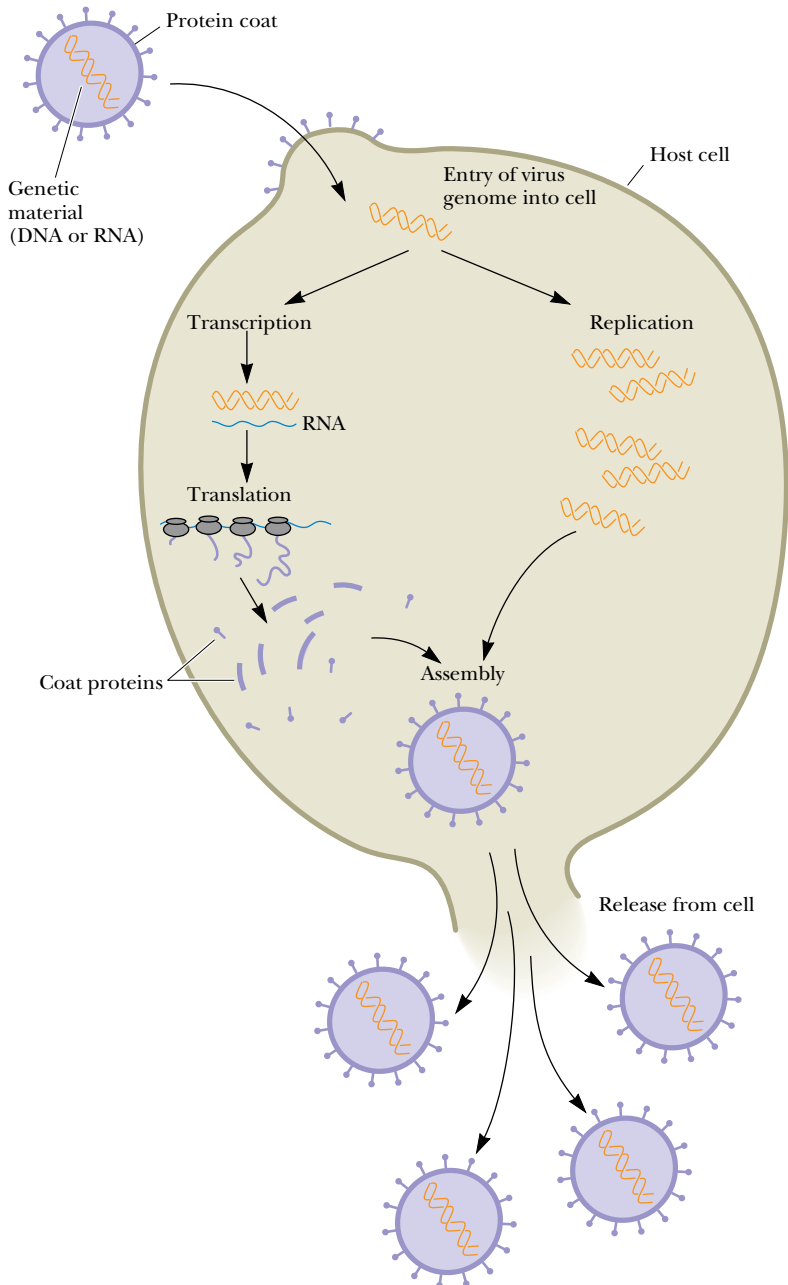
FIGURE 1.25 • The virus life cycle. Viruses are mobile bits of genetic information encapsulated in a protein coat. The genetic material can be either DNA or RNA. Once this genetic material gains entry to its host cell, it takes over the host machinery for macromolecular synthesis and subverts it to the synthesis of viral-specific nucleic acids and proteins. These virus components are then assembled into mature virus particles that are released from the cell. Often, this parasitic cycle of virus infection leads to cell death and disease.

PROBLEMS

1. The nutritional requirements of *Escherichia coli* cells are far simpler than those of humans, yet the macromolecules found in bacteria are about as complex as those of animals. Since bacteria can make all their essential biomolecules while subsisting on a simpler diet, do you think bacteria may have more biosynthetic capacity and hence more metabolic complexity than animals? Organize your thoughts on this question, pro and con, into a rational argument.

2. Without consulting chapter figures, sketch the characteristic prokaryotic and eukaryotic cell types and label their pertinent organelle and membrane systems.

3. *Escherichia coli* cells are about 2 μm (microns) long and 0.8 μm in diameter.

a. How many *E. coli* cells laid end to end would fit across the diameter of a pin head? (Assume a pinhead diameter of 0.5 mm.)

b. What is the volume of an *E. coli* cell? (Assume it is a cylinder, with the volume of a cylinder given by $V = \pi r^2 h$, where $\pi = 3.14$.)

c. What is the surface area of an *E. coli* cell? What is the surface-to-volume ratio of an *E. coli* cell?

d. Glucose, a major energy-yielding nutrient, is present in bacterial cells at a concentration of about 1 mM. How many glucose molecules are contained in a typical *E. coli* cell? (Recall that Avogadro's number $= 6.023 \times 10^{23}$.)

e. A number of regulatory proteins are present in *E. coli* at only one or two molecules per cell. If we assume that an *E. coli* cell contains just one molecule of a particular protein, what is the molar concentration of this protein in the cell?

f. An *E. coli* cell contains about 15,000 ribosomes, which carry out protein synthesis. Assuming ribosomes are spherical and have a diameter of 20 nm (nanometers), what fraction of the *E. coli* cell volume is occupied by ribosomes?

g. The *E. coli* chromosome is a single DNA molecule whose mass is about 3×10^9 daltons. This macromolecule is actually a linear array of nucleotide pairs. The average molecular weight of a nucleotide pair is 660, and each pair imparts 0.34 nm to the length of the DNA molecule. What is the total length of the *E. coli* chromosome? How does this length compare with the overall dimensions of an *E. coli* cell? How many nucleotide pairs does this DNA contain? The average *E. coli* protein is a linear chain of 360 amino acids. If three nucleotide pairs in a gene encode one amino acid in a protein, how many different proteins can the *E. coli* chromosome encode? (The answer to this question is a reasonable approximation of the maximum number of different kinds of proteins that can be expected in bacteria.)

4. Assume that mitochondria are cylinders 1.5 μm in length and 0.6 μm in diameter.

a. What is the volume of a single mitochondrion?

b. Oxaloacetate is an intermediate in the citric acid cycle, an important metabolic pathway localized in the mitochondria of eukaryotic cells. The concentration of oxaloacetate in mitochondria is about 0.03 μM. How many molecules of oxaloacetate are in a single mitochondrion?

5. Assume that liver cells are cuboidal in shape, 20 μm on a side.

a. How many liver cells laid end to end would fit across the diameter of a pin head? (Assume a pinhead diameter of 0.5 mm.)

b. What is the volume of a liver cell? (Assume it is a cube.)

c. What is the surface area of a liver cell? What is the surface-to-volume ratio of a liver cell? How does this compare to the surface-to-volume ratio of an *E. coli* cell (compare this answer to that of problem 3c)? What problems must cells with low surface-to-volume ratios confront that do not occur in cells with high surface-to-volume ratios?

d. A human liver cell contains two sets of 23 chromosomes, each set being roughly equivalent in information content. The total mass of DNA contained in these 46 enormous DNA molecules is 4×10^{12} daltons. Since each nucleotide pair contributes 660 daltons to the mass of DNA and 0.34 nm to the length of DNA, what is the total number of nucleotide pairs and the complete length of the DNA in a liver cell? How does this length compare with the overall dimensions of a liver cell? The maximal information in each set of liver cell chromosomes should be related to the number of nucleotide pairs in the chromosome set's DNA. This number can be obtained by dividing the total number of nucleotide pairs calculated above by 2. What is this value? If this information is expressed in proteins that average 400 amino acids in length and three nucleotide pairs encode one amino acid in a protein, how many different kinds of proteins might a liver cell be able to produce? (In reality, liver cells express at most about 30,000 different proteins. Thus, a large discrepancy exists between the theoretical information content of DNA in liver cells and the amount of information actually expressed.)

6. Biomolecules interact with one another through molecular surfaces that are structurally complementary. How can various proteins interact with molecules as different as simple ions, hydrophobic lipids, polar but uncharged carbohydrates, and even nucleic acids?

7. What structural features allow biological polymers to be informational macromolecules? Is it possible for polysaccharides to be informational macromolecules?

8. Why is it important that weak forces, not strong forces, mediate biomolecular recognition?

9. Why does the central role of weak forces in biomolecular interactions restrict living systems to a narrow range of environmental conditions?

10. Describe what is meant by the phrase "cells are steady-state systems."

FURTHER READING

Alberts, B., Bray, D., Lewis, J., et al., 1989. *Molecular Biology of the Cell,* 2nd ed. New York: Garland Press.

Goodsell, D. S., 1991. Inside a living cell. *Trends in Biochemical Sciences* **16:**203–206.

Koonin, E. V., et al., 1996. Sequencing and analysis of bacterial genomes. *Current Biology* **6:**404–416.

Lloyd, C., ed., 1986. Cell organization. *Trends in Biochemical Sciences* **11:**437–485.

Loewy, A. G., Siekevitz, P., Menninger, J. R., Gallant, J. A. N., 1991. *Cell Structure and Function.* Philadelphia: Saunders College Publishing.

Pace, N. R., 1996. New perspective on the natural microbial world: Molecular microbial ecology. *ASM News* **62:**463–470.

Service, R. F., 1997. Microbiologists explore life's rich, hidden kingdoms. *Science* **275:**1740–1742.

Solomon, E. P., Berg, L. R., Martin, D. W., and Villee, C., 1999. *Biology,* 5th ed. Philadelphia: Saunders College Publishing.

Wald, G., 1964. The origins of life. *Proceedings of the National Academy of Science, U.S.A.* **52:**595–611.

Watson, J. D., Hopkins, N.H., Roberts, J. W., et al., 1987. *Molecular Biology of the Gene,* 4th ed. Menlo Park, CA: Benjamin/Cummings Publishing Co.

Woese, C. R., 1996. Phylogenetic trees: Whither microbiology? *Current Biology* **6:**1060–1063.

Chapter 2

Water, pH, and Ionic Equilibria

Some of the magic: Students and teacher view a coral crab in Graham's Harbour, San Salvador Island, the Bahamas. (Lara Call)

Water is a major chemical component of the earth's surface. It is indispensable to life. Indeed, it is the only liquid that most organisms ever encounter. We alternately take it for granted because of its ubiquity and bland nature or marvel at its many unusual and fascinating properties. At the center of this fascination is the role of water as the medium of life. Life originated, evolved, and thrives in the seas. Organisms invaded and occupied terrestrial and aerial niches, but none gained true independence from water. Typically, organisms are constituted of 70 to 90% water. Indeed, normal metabolic activity can occur only when cells are at least 65% H_2O. This dependency of life on water is not a simple matter, but it can be grasped through a consideration of the unusual chemical and physical properties of H_2O. Subsequent chapters establish that water and its ionization products, hydrogen ions and hydroxide ions, are crit-

ical determinants of the structure and function of proteins, nucleic acids, and membranes. In yet another essential role, water is an indirect participant—a difference in the concentration of hydrogen ions on opposite sides of a membrane represents an energized condition essential to biological mechanisms of energy transformation. First, let's review the remarkable properties of water.

2.1 • Properties of Water

Unusual Properties

In comparison with chemical compounds of similar atomic organization and molecular size, water displays unexpected properties. For example, compare water, the hydride of oxygen, with hydrides of oxygen's nearest neighbors in the periodic table, namely, ammonia (NH_3) and hydrogen fluoride (HF), or with the hydride of its nearest congener, sulfur (H_2S). Water has a substantially higher boiling point, melting point, heat of vaporization, and surface tension. Indeed, all of these physical properties are anomalously high for a substance of this molecular weight that is neither metallic nor ionic. These properties suggest that intermolecular forces of attraction between H_2O molecules are high. Thus, the internal cohesion of this substance is high. Furthermore, water has an unusually high dielectric constant, its maximum density is found in the liquid (not the solid) state, and it has a negative volume of melting (that is, the solid form, ice, occupies more space than does the liquid form, water). It is truly remarkable that so many eccentric properties should occur together in a single substance. As chemists, we expect to find an explanation for these apparent anomalies in the structure of water. The key to its intermolecular attractions must lie in its atomic constitution. Indeed, *the unrivaled ability to form hydrogen bonds is the crucial fact to understanding its properties.*

Structure of Water

The two hydrogen atoms of water are linked covalently to oxygen, each sharing an electron pair, to give a nonlinear arrangement (Figure 2.1). This "bent" structure of the H_2O molecule is of enormous significance to its properties. If H_2O were linear, it would be a nonpolar substance. In the bent configuration, however, the electronegative O atom and the two H atoms form a dipole that renders the molecule distinctly polar. Furthermore, this structure is ideally suited to H-bond formation. Water can serve as both an H donor and an H acceptor in H-bond formation. The potential to form four H bonds per water molecule is the source of the strong intermolecular attractions that endow this substance with its anomalously high boiling point, melting point, heat of vaporization, and surface tension. In ordinary ice, the common crystalline form of water, each H_2O molecule has four nearest neighbors to which it is hydrogen bonded: each H atom donates an H bond to the O of a neighbor, while the O atom serves as an H-bond acceptor from H atoms bound to two different water molecules (Figure 2.2). A local tetrahedral symmetry results.

Hydrogen bonding in water is cooperative. That is, an H-bonded water molecule serving as an acceptor is a better H-bond donor than an unbonded molecule (and an H_2O molecule serving as an H-bond donor becomes a better H-bond acceptor). Thus, participation in H bonding by H_2O molecules is a phenomenon of mutual reinforcement. The H bonds between neighboring molecules are weak (23 kJ/mol each) relative to the H—O covalent bonds (420 kJ/mol). As a consequence, the hydrogen atoms are situated asymmetrically
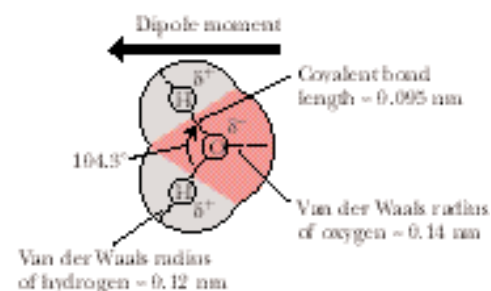

FIGURE 2.1 • The structure of water. Two lobes of negative charge formed by the lone-pair electrons of the oxygen atom lie above and below the plane of the diagram. This electron density contributes substantially to the large dipole moment and polarizability of the water molecule. The dipole moment of water corresponds to the O—H bonds having 33% ionic character. Note that the H—O—H angle is 104.3°, *not* 109°, the angular value found in molecules with tetrahedral symmetry, such as CH_4. Many of the important properties of water derive from this angular value, such as the decreased density of its crystalline state, ice. (The dipole moment in this figure points in the direction from negative to positive, the convention used by physicists and physical chemists; organic chemists draw it pointing in the opposite direction.)
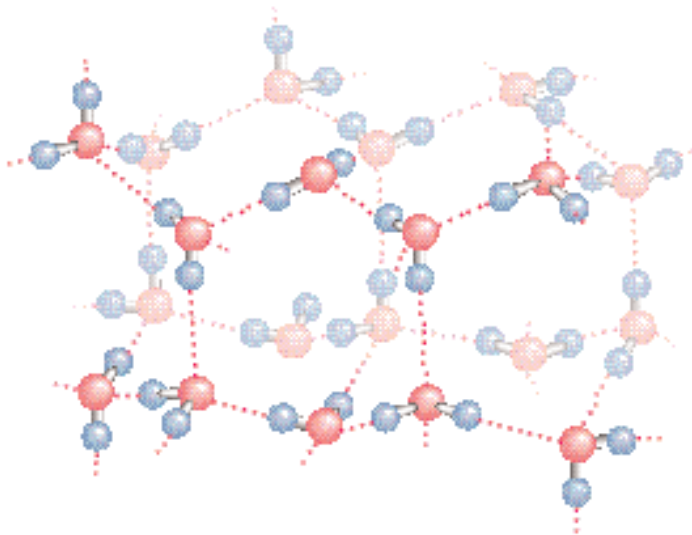
FIGURE 2.2 • The structure of normal ice. The hydrogen bonds in ice form a three-dimensional network. The smallest number of H_2O molecules in any closed circuit of H-bonded molecules is six, so that this structure bears the name *hexagonal ice*. Covalent bonds are represented as solid lines, whereas hydrogen bonds are shown as dashed lines. The directional preference of H bonds leads to a rather open lattice structure for crystalline water and, consequently, a low density for the solid state. The distance between neighboring oxygen atoms linked by a hydrogen bond is 0.274 nm. Because the covalent H—O bond is 0.995 nm, the H—O hydrogen bond length in ice is 0.18 nm.

between the two oxygen atoms along the O—O axis. There is never any ambiguity about which O atom the H atom is chemically bound to, nor to which O it is H-bonded.

Structure of Ice

In ice, the hydrogen bonds form a space-filling, three-dimensional network. These bonds are directional and straight; that is, the H atom lies on a direct line between the two O atoms. This linearity and directionality mean that the resultant H bonds are strong. In addition, the directional preference of the H bonds leads to an open lattice structure. For example, if the water molecules are approximated as rigid spheres centered at the positions of the O atoms in the lattice, then the observed density of ice is actually only 57% of that expected for a tightly packed arrangement of such spheres. The H bonds in ice hold the water molecules apart. Melting involves breaking some of the H bonds that maintain the crystal structure of ice so that the molecules of water (now liquid) can actually pack closer together. Thus, the density of ice is slightly less than the density of water. Ice floats, a property of great importance to aquatic organisms in cold climates.

In liquid water, the rigidity of ice is replaced by fluidity, and the crystalline periodicity of ice gives way to spatial homogeneity. The H_2O molecules in liquid water form a random, H-bonded network with each molecule having an average of 4.4 close neighbors situated within a center-to-center distance of 0.284 nm (2.84 Å). At least half of the hydrogen bonds have nonideal orientations (that is, they are not perfectly straight); consequently, liquid H_2O lacks the regular latticelike structure of ice. The space about an O atom is not defined by the presence of four hydrogens, but can be occupied by other water mole-

cules randomly oriented so that the local environment, over time, is essentially uniform. Nevertheless, the heat of melting for ice is but a small fraction (13%) of the heat of sublimation for ice (the energy needed to go from the solid to the vapor state). This fact indicates that the majority of H bonds between H_2O molecules survive the transition from solid to liquid. At 10°C, 2.3 H bonds per H_2O molecule remain, and the tetrahedral bond order persists even though substantial disorder is now present.

Molecular Interactions in Liquid Water

The present interpretation of water structure is that water molecules are connected by uninterrupted H bond paths running in every direction, spanning the whole sample. The participation of each water molecule in an average state of H bonding to its neighbors means that each molecule is connected to every other in a fluid network of H bonds. The average lifetime of an H-bonded connection between two H_2O molecules in water is 9.5 psec (picoseconds, where 1 psec = 10^{-12} sec). Thus, about every 10 psec, the average H_2O molecule moves, reorients, and interacts with new neighbors, as illustrated in Figure 2.3.

In summary, pure liquid water consists of H_2O molecules held in a random, three-dimensional network that has a local preference for tetrahedral geometry but contains a large number of strained or broken hydrogen bonds. The presence of strain creates a kinetic situation in which H_2O molecules can switch H-bond allegiances; fluidity ensues.

Solvent Properties

Because of its highly polar nature, water is an excellent solvent for ionic substances such as salts; nonionic but polar substances such as sugars, simple alcohols, and amines; and carbonyl-containing molecules such as aldehydes and ketones. Although the electrostatic attractions between the positive and negative ions in the crystal lattice of a salt are very strong, water readily dissolves salts. For example, sodium chloride is dissolved because dipolar water molecules participate in strong electrostatic interactions with the Na^+ and Cl^- ions, leading to the formation of **hydration shells** surrounding these ions (Figure 2.4). Although hydration shells are stable structures, they are also dynamic. Each water molecule in the inner hydration shell around a Na^+ ion is replaced on average every 2 to 4 nsec (nanoseconds, where 1 nsec = 10^{-9} sec) by another H_2O. Consequently, a water molecule is trapped only several hundred times longer by the electrostatic force field of an ion than it is by the H-bonded network of water. (Recall that the average lifetime of H bonds between water molecules is about 10 psec.)

Water Has a High Dielectric Constant

The attractions between the water molecules interacting with, or **hydrating,** ions are much greater than the tendency of oppositely charged ions to attract one another. The ability of water to surround ions in dipole interactions and

FIGURE 2.3 • The fluid network of H bonds linking water molecules in the liquid state. It is revealing to note that, in 10 psec, a photon of light (which travels at 3×10^8 m/sec) would move a distance of only 0.003 m.
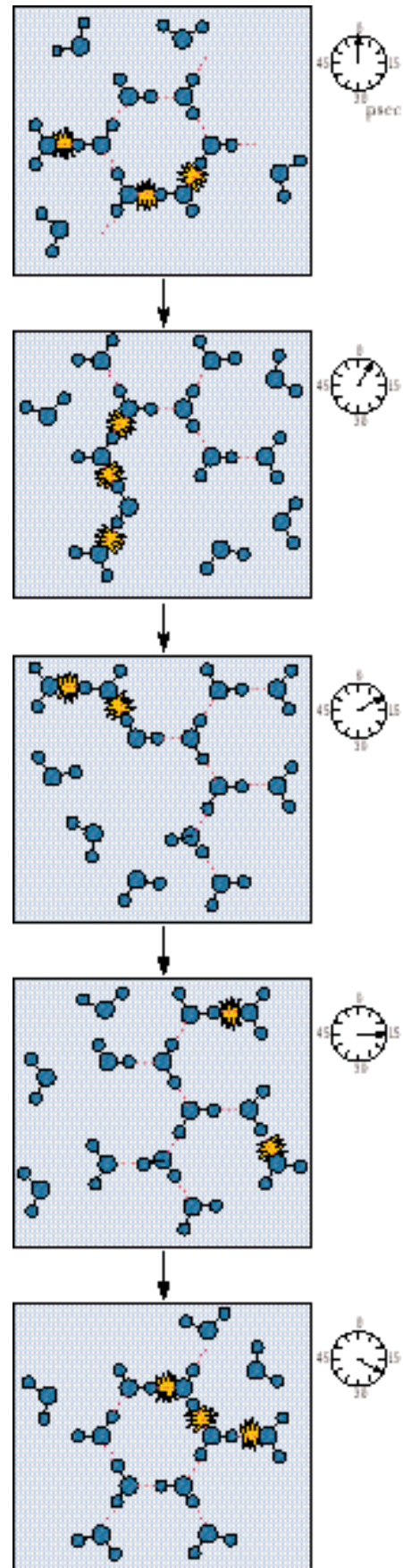
FIGURE 2.4 • Hydration shells surrounding ions in solution. Water molecules orient so that the electrical charge on the ion is sequestered by the water dipole. For positive ions (cations), the partially negative oxygen atom of H_2O is toward the ion in solution. Negatively charged ions (anions) attract the partially positive hydrogen atoms of water in creating their hydration shells.
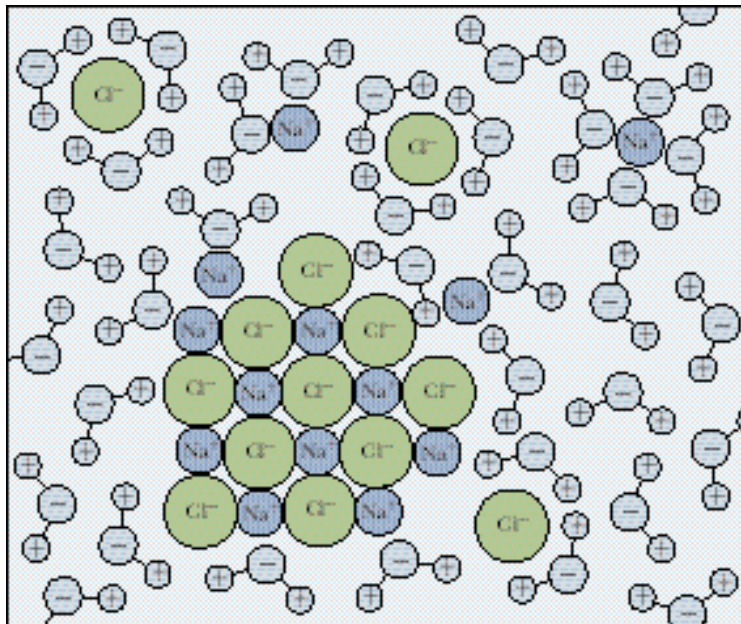
diminish their attraction for one another is a measure of its **dielectric constant, *D*.** Indeed, ionization in solution depends on the dielectric constant of the solvent; otherwise the strongly attracted positive and negative ions would unite to form neutral molecules. The strength of the dielectric constant is related to the force, *F*, experienced between two ions of opposite charge separated by a distance, *r*, as given in the relationship

$$F = e_1 e_2 / Dr^2$$

where e_1 and e_2 are the charges on the two ions. Table 2.1 lists the dielectric constants of some common liquids. Note that the dielectric constant for water is more than twice that of methanol and more than 40 times that of hexane.

Water Forms H Bonds with Polar Solutes

In the case of nonionic but polar compounds such as sugars, the excellent solvent properties of water stem from its ability to readily form hydrogen bonds with the polar functional groups on these compounds, such as hydroxyls, amines, and carbonyls. These polar interactions between solvent and solute are stronger than the intermolecular attractions between solute molecules caused by van der Waals forces and weaker hydrogen bonding. Thus, the solute molecules readily dissolve in water.

Hydrophobic Interactions

The behavior of water toward nonpolar solutes is different from the interactions just discussed. Nonpolar solutes (or nonpolar functional groups on biological macromolecules) do not readily H bond to H_2O, and, as a result, such compounds tend to be only sparingly soluble in water. The process of dissolving such substances is accompanied by significant reorganization of the water surrounding the solute so that the response of the solvent water to such solutes can be equated to "structure making." Because nonpolar solutes must occupy space, the random H-bond network of water must reorganize to accommodate them. At the same time, the water molecules participate in as many H-bonded

Table 2.1

Dielectric Constants* of Some Common Solvents at 25°C

Solvent	Dielectric Constant (*D*)
Water	78.5
Methyl alcohol	32.6
Ethyl alcohol	24.3
Acetone	20.7
Acetic acid	6.2
Chloroform	5.0
Benzene	2.3
Hexane	1.9

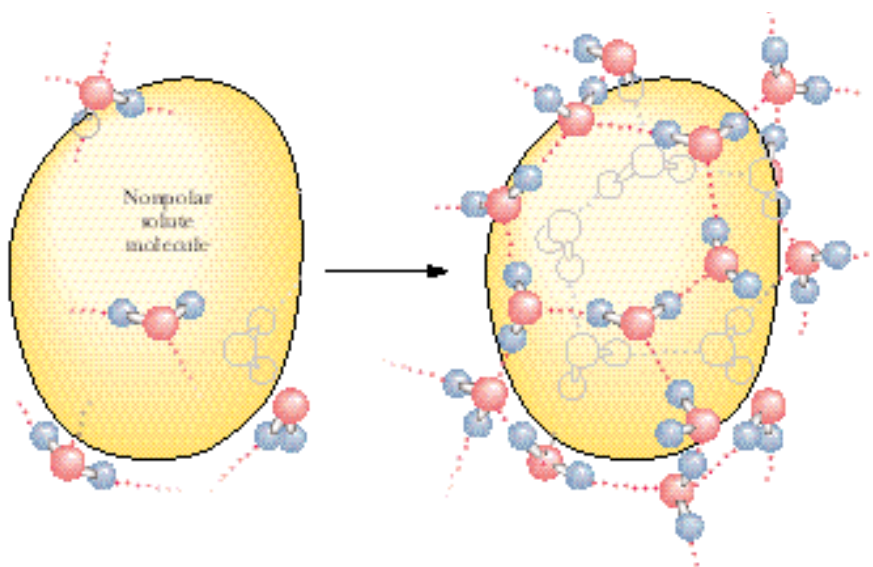*The dielectric constant is also referred to as *relative permittivity* by physical chemists.

interactions with one another as the temperature permits. Consequently, the H-bonded water network rearranges toward formation of a local cagelike **(clathrate)** structure surrounding each solute molecule (Figure 2.5). This fixed orientation of water molecules around a hydrophobic "solute" molecule results in a hydration shell. A major consequence of this rearrangement is that the molecules of H_2O participating in the cage layer have markedly reduced orientational options. Water molecules tend to straddle the nonpolar solute such that two or three tetrahedral directions (H-bonding vectors) are tangential to the space occupied by the inert solute. This "straddling" means that no water H-bonding capacity is lost because no H-bond donor or acceptor of the H_2O is directed toward the caged solute. The water molecules forming these clathrates are involved in highly ordered structures. That is, clathrate formation is accompanied by significant ordering of structure or negative entropy.

Under these conditions, nonpolar solute molecules experience a net attraction for one another that is called **hydrophobic interaction.** The basis of this interaction is that when two nonpolar molecules meet, their joint solvation cage involves less surface area and less overall ordering of the water molecules than in their separate cages. The "attraction" between nonpolar solutes is an entropy-driven process due to a net decrease in order among the H_2O molecules. To be specific, hydrophobic interactions between nonpolar molecules are maintained not so much by direct interactions between the inert solutes themselves as by the increase in entropy when the water cages coalesce and reorganize. Because interactions between nonpolar solute molecules and the water surrounding them are of uncertain stoichiometry and do not share the equality of atom-to-atom participation implicit in chemical bonding, the term *hydrophobic interaction* is more correct than the misleading expression *hydrophobic bond.*

Amphiphilic Molecules

Compounds containing both strongly polar and strongly nonpolar groups are called **amphiphilic molecules** (from the Greek *amphi* meaning "both," and *philos* meaning "loving"), also referred to as **amphipathic molecules** (from the Greek *pathos* meaning "passion"). Salts of fatty acids are a typical example that

amphiphilic molecules, amphipathic molecules • compounds containing both strongly polar and strongly nonpolar groups

FIGURE 2.6 • An amphiphilic molecule: sodium palmitate. Amphiphilic molecules are frequently symbolized by a ball and zig-zag line structure, ⬤〰〰, where the ball represents the hydrophilic polar head and the zig-zag represents the nonpolar hydrophobic hydrocarbon tail.

The sodium salt of palmitic acid   Sodium palmitate
$(Na^+ {}^-OOC(CH_2)_{14}CH_3)$

Polar head
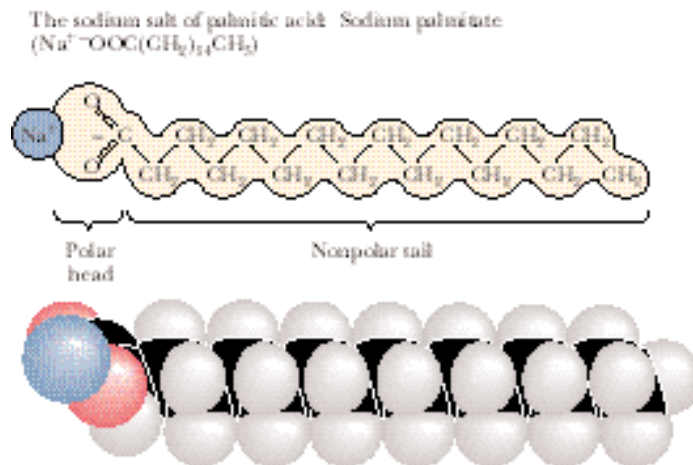
Nonpolar tail

has biological relevance. They have a long nonpolar hydrocarbon tail and a strongly polar carboxyl head group, as in the sodium salt of palmitic acid (Figure 2.6). Their behavior in aqueous solution reflects the combination of the contrasting polar and nonpolar nature of these substances. The ionic carboxylate function hydrates readily, whereas the long hydrophobic tail is intrinsically insoluble. Nevertheless, sodium palmitate and other amphiphilic molecules readily disperse in water because the hydrocarbon tails of these substances are joined together in hydrophobic interactions as their polar carboxylate functions are hydrated in typical hydrophilic fashion. Such clusters of amphipathic molecules are termed **micelles;** Figure 2.7 depicts their structure. Of enormous biological significance is the contrasting solute behavior of the two ends of amphipathic molecules upon introduction into aqueous solutions. The polar ends express their hydrophilicity in ionic interactions with the solvent, whereas their nonpolar counterparts are excluded from the water into a hydrophobic domain constituted from the hydrocarbon tails of many like molecules. It is this behavior that accounts for the formation of membranes, the structures that define the limits and compartments of cells (see Chapter 9).
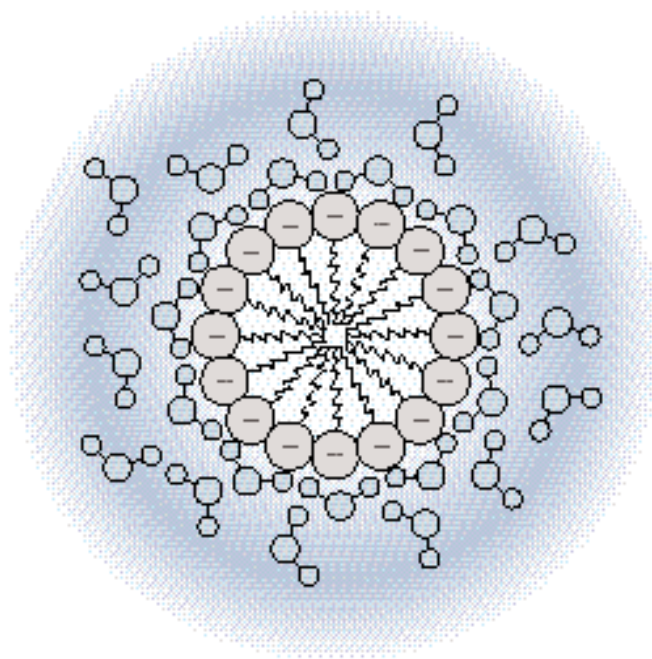
FIGURE 2.7 • Micelle formation by amphiphilic molecules in aqueous solution. Negatively charged carboxylate head groups orient to the micelle surface and interact with the polar H_2O molecules via H bonding. The nonpolar hydrocarbon tails cluster in the interior of the spherical micelle, driven by hydrophobic exclusion from the solvent and the formation of favorable van der Waals interactions. Because of their negatively charged surfaces, neighboring micelles repel one another and thereby maintain a relative stability in solution.

Influence of Solutes on Water Properties

The presence of dissolved substances disturbs the structure of liquid water so that its properties change. The dynamic hydrogen-bonding pattern of water must now accommodate the intruding substance. The net effect is that solutes, regardless of whether they are polar or nonpolar, fix nearby water molecules in a more ordered array. Ions, by the establishment of hydration shells through interactions with the water dipoles, create local order. Hydrophobic effects, for different reasons, make structures within water. To put it another way, by limiting the orientations that neighboring water molecules can assume, solutes give order to the solvent and diminish the dynamic interplay among H_2O molecules that occurs in pure water.

Colligative Properties

This influence of the solute on water is reflected in a set of characteristic changes in behavior that are termed **colligative properties,** or properties related by a common principle. These alterations in solvent properties are related in that they all depend only on the number of solute particles per unit volume of solvent and not on the chemical nature of the solute. These effects include freezing point depression, boiling point elevation, vapor pressure lowering, and osmotic pressure effects. For example, 1 mol of an ideal solute dissolved in 1000 g of water (a 1 m, or molal, solution) at 1 atm pressure depresses the freezing point by 1.86°C, raises the boiling point by 0.543°C, lowers the vapor pressure in a temperature-dependent manner, and yields a solution whose osmotic pressure relative to pure water is 22.4 atm. In effect, by imposing local order on the water molecules, solutes make it more difficult for water to assume its crystalline lattice (freeze) or escape into the atmosphere (boil or vaporize). Furthermore, when a solution (such as the 1 m solution discussed here) is separated from a volume of pure water by a semipermeable membrane, the solution draws water molecules across this barrier. The water molecules are moving from a region of higher effective concentration (pure H_2O) to a region of lower effective concentration (the solution). This movement of water into the solution dilutes the effects of the solute that is present. The osmotic force exerted by each mole of solute is so strong that it requires the imposition of 22.4 atm of pressure to be negated (Figure 2.8).

Osmotic pressure from high concentrations of dissolved solutes is a serious problem for cells. Bacterial and plant cells have strong, rigid cell walls to contain these pressures. In contrast, animal cells are bathed in extracellular fluids of comparable osmolarity, so no net osmotic gradient exists. Also, to minimize the osmotic pressure created by the contents of their cytosol, cells tend
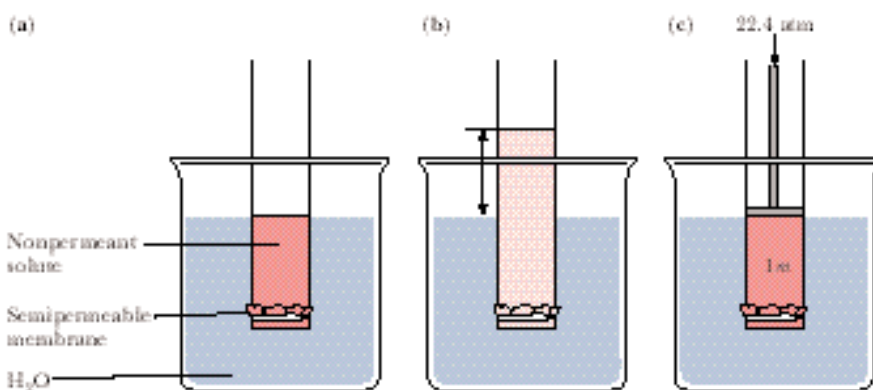
FIGURE 2.8 • The osmotic pressure of a 1 molal (m) solution is equal to 22.4 atmospheres of pressure. (a) If a nonpermeant solute is separated from pure water by a semipermeable membrane through which H_2O passes freely, (b) water molecules enter the solution (osmosis) and the height of the solution column in the tube rises. The pressure necessary to push water back through the membrane at a rate exactly equaled by the water influx is the osmotic pressure of the solution. (c) For a 1 m solution, this force is equal to 22.4 atm of pressure. Osmotic pressure is directly proportional to the concentration of the nonpermeant solute.

FIGURE 2.9 • The ionization of water.

to store substances such as amino acids and sugars in polymeric form. For example, a molecule of glycogen or starch containing 1000 glucose units exerts only 1/1000 the osmotic pressure that 1000 free glucose molecules would.
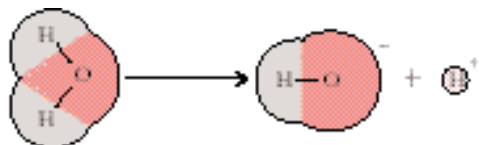
Ionization of Water

Water shows a small but finite tendency to form ions. This tendency is demonstrated by the electrical conductivity of pure water, a property that clearly establishes the presence of charged species (ions). Water ionizes because the larger, strongly electronegative oxygen atom strips the electron from one of its hydrogen atoms, leaving the proton to dissociate (Figure 2.9):

$$H-O-H \longrightarrow H^+ + OH^-$$

Two ions are thus formed: protons or **hydrogen ions,** H^+, and **hydroxyl ions,** OH^-. Free protons are immediately hydrated to form **hydronium ions,** H_3O^+:

$$H^+ + H_2O \longrightarrow H_3O^+$$

Indeed, because most hydrogen atoms in liquid water are hydrogen-bonded to a neighboring water molecule, this protonic hydration is an instantaneous process and the ion products of water are H_3O^+ and OH^-:

The amount of H_3O^+ or OH^- in 1 L (liter) of pure water at 25°C is 1×10^{-7} mol; the concentrations are equal because the dissociation is stoichiometric.

Although it is important to keep in mind that the hydronium ion, or hydrated hydrogen ion, represents the true state in solution, the convention is to speak of hydrogen ion concentrations in aqueous solution, even though "naked" protons are virtually nonexistent. Indeed, H_3O^+ itself attracts a hydration shell by H bonding to adjacent water molecules to form an $H_9O_4^+$ species (Figure 2.10) and even more highly hydrated forms. Similarly, the hydroxyl ion, like all other highly charged species, is also hydrated.
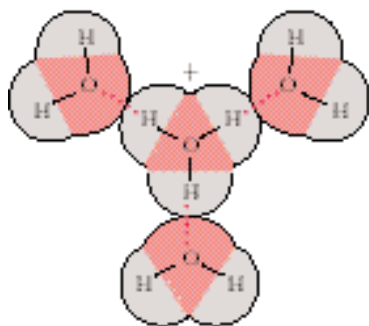
FIGURE 2.10 • The hydration of H_3O^+. Solid lines denote covalent bonds; dashed lines represent the H bonds formed between the hydronium ion and its waters of hydration.

Proton Jumping

Because of the high degree of hydrogen bonding in water, H^+ ions show an apparent rate of migration in an electrical field that is vastly greater than other univalent cations in aqueous solution, such as Na^+ and K^+. In effect, the net transfer of a proton from molecule to molecule throughout the H-bonded network accounts for this apparent rapidity of migration (Figure 2.11).

FIGURE 2.11 • Proton jumping via the hydrogen-bonded network of water molecules.

That is, the H-bonded network provides a natural route for rapid H^+ transport. This phenomenon of **proton jumping** thus occurs with little actual movement of the water molecules themselves. Ice has an electrical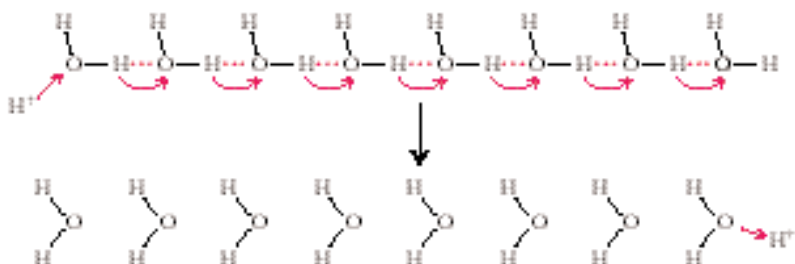 conductivity close to that of water because such proton jumps also readily occur even when the water molecules are fixed in a crystal lattice. Such conduction of protons via H-bonded networks has been offered as an explanation for a number of rapid proton transfers of biological significance.

K_w, the Ion Product of Water

The dissociation of water into hydrogen ions and hydroxyl ions occurs to the extent that 10^{-7} mol of H^+ and 10^{-7} mol of OH^- are present at equilibrium in 1 L of water at 25°C.

$$H_2O \longrightarrow H^+ + OH^-$$
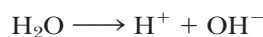
The equilibrium constant for this process is

$$K_{eq} = \frac{[H^+][OH^-]}{[H_2O]}$$

where brackets denote concentrations in moles per liter. Because the concentration of H_2O in 1 L of pure water is equal to the number of grams in a liter divided by the gram molecular weight of H_2O, or 1000/18, the molar concentration of H_2O in pure water is 55.5 M (molar). The decrease in H_2O concentration as a result of ion formation ($[H^+]$, $[OH^-] = 10^{-7}$ M) is negligible in comparison, and thus its influence on the overall concentration of H_2O can be ignored. Thus,

$$K_{eq} = \frac{(10^{-7})(10^{-7})}{55.5} = 1.8 \times 10^{-16}$$

Because the concentration of H_2O in pure water is essentially constant, a new constant, K_w, the **ion product of water,** can be written as

$$K_w = 55.5\ K_{eq} = 10^{-14} = [H^+][OH^-]$$

The equation has the virtue of revealing the reciprocal relationship between H^+ and OH^- concentrations of aqueous solutions. If a solution is acidic, that is, of significant $[H^+]$, then the ion product of water dictates that the OH^- concentration is correspondingly less. For example, if $[H^+]$ is 10^{-2} M, $[OH^-]$ must be 10^{-12} M ($K_w = 10^{-14} = [10^{-2}][OH^-]$; $[OH^-] = 10^{-12}$ M). Similarly, in an alkaline, or basic, solution in which $[OH^-]$ is great, $[H^+]$ is low.

2.2 • pH

To avoid the cumbersome use of negative exponents to express concentrations that range over 14 orders of magnitude, Sørensen, a Danish biochemist, devised the **pH scale** by defining **pH** as *the negative logarithm of the hydrogen ion concentration*[1]:

$$pH = -\log_{10} [H^+]$$

---

[1]To be precise in physical chemical terms, the *activities* of the various components, *not* their molar concentrations, should be used in these equations. The activity (a) of a solute component is defined as the product of its molar concentration, c, and an *activity coefficient*, γ: $a = [c]\gamma$. Most biochemical work involves dilute solutions, and the use of activities instead of molar concentrations is usually neglected. However, the concentration of certain solutes may be very high in living cells.

Table 2.2

pH Scale

The hydrogen ion and hydroxyl ion concentrations are given in moles per liter at 25°C.

pH	$[H^+]$		$[OH^-]$	
0	(10^0)	1.0	0.00000000000001	(10^{-14})
1	(10^{-1})	0.1	0.0000000000001	(10^{-13})
2	(10^{-2})	0.01	0.000000000001	(10^{-12})
3	(10^{-3})	0.001	0.00000000001	(10^{-11})
4	(10^{-4})	0.0001	0.0000000001	(10^{-10})
5	(10^{-5})	0.00001	0.000000001	(10^{-9})
6	(10^{-6})	0.000001	0.00000001	(10^{-8})
7	$\mathbf{(10^{-7})}$	**0.0000001**	**0.0000001**	$\mathbf{(10^{-7})}$
8	(10^{-8})	0.00000001	0.000001	(10^{-6})
9	(10^{-9})	0.000000001	0.00001	(10^{-5})
10	(10^{-10})	0.0000000001	0.0001	(10^{-4})
11	(10^{-11})	0.00000000001	0.001	(10^{-3})
12	(10^{-12})	0.000000000001	0.01	(10^{-2})
13	(10^{-13})	0.0000000000001	0.1	(10^{-1})
14	(10^{-14})	0.00000000000001	1.0	(10^0)

Table 2.3

The pH of Various Common Fluids

Fluid	pH
Household lye	13.6
Bleach	12.6
Household ammonia	11.4
Milk of magnesia	10.3
Baking soda	8.4
Seawater	8.0
Pancreatic fluid	7.8–8.0
Blood plasma	7.4
Intracellular fluids	
Liver	6.9
Muscle	6.1
Saliva	6.6
Urine	5–8
Boric acid	5.0
Beer	4.5
Orange juice	4.3
Grapefruit juice	3.2
Vinegar	2.9
Soft drinks	2.8
Lemon juice	2.3
Gastric juice	1.2–3.0
Battery acid	0.35

Table 2.2 gives the pH scale. Note again the reciprocal relationship between $[H^+]$ and $[OH^-]$. Also, because the pH scale is based on negative logarithms, low pH values represent the highest H^+ concentrations (and the lowest OH^- concentrations, as K_w specifies). Note also that

$$pK_w = pH + pOH = 14$$

The pH scale is widely used in biological applications because hydrogen ion concentrations in biological fluids are very low, about 10^{-7} *M* or 0.0000001 *M,* a value more easily represented as pH 7. The pH of blood plasma, for example, is 7.4 or 0.00000004 *M* H^+. Certain disease conditions may lower the plasma pH level to 6.8 or less, a situation that may result in death. At pH 6.8, the H^+ concentration is 0.00000016 *M,* four times greater than at pH 7.4.

At pH 7, $[H^+] = [OH^-]$; that is, there is no excess acidity or basicity. The point of **neutrality** is at pH 7, and solutions having a pH of 7 are said to be at **neutral pH.** The pH values of various fluids of biological origin or relevance are given in Table 2.3. Because the pH scale is a logarithmic scale, two solutions whose pH values differ by one pH unit have a 10-fold difference in $[H^+]$. For example, grapefruit juice at pH 3.2 contains more than 12 times as much H^+ as orange juice at pH 4.3.

Dissociation of Strong Electrolytes

Substances that are almost completely dissociated to form ions in solution are called **strong electrolytes.** The term **electrolyte** describes substances capable of generating ions in solution and thereby causing an increase in the electrical conductivity of the solution. Many salts (such as NaCl and K_2SO_4) fit this category, as do strong acids (such as HCl) and strong bases (such as NaOH). Recall from general chemistry that acids are proton donors and bases are pro-

ton acceptors. In effect, the dissociation of a strong acid such as HCl in water can be treated as a proton transfer reaction between the acid HCl and the base H_2O to give the **conjugate acid** H_3O^+ and the **conjugate base** Cl^-:

$$HCl + H_2O \longrightarrow H_3O^+ + Cl^-$$

The equilibrium constant for this reaction is

$$K = \frac{[H_3O^+][Cl^-]}{[H_2O][HCl]}$$

Customarily, because the term $[H_2O]$ is essentially constant in dilute aqueous solutions, it is incorporated into the equilibrium constant K to give a new term, K_a, the acid dissociation constant (where $K_a = K[H_2O]$). Also, the term $[H_3O^+]$ is often replaced by H^+, such that

$$K_a = \frac{[H^+][Cl^-]}{[HCl]}$$

For HCl, the value of K_a is exceedingly large because the concentration of HCl in aqueous solution is vanishingly small. Because this is so, the pH of HCl solutions is readily calculated from the amount of HCl used to make the solution:

$$[H^+] \text{ in solution} = [HCl] \text{ added to solution}$$

Thus, a 1 M solution of HCl has a pH of 0; a 1 mM HCl solution has a pH of 3. Similarly, a 0.1 M NaOH solution has a pH of 13. (Because $[OH^-] = 0.1$ M, $[H^+]$ must be 10^{-13} M.)

Viewing the dissociation of strong electrolytes another way, we see that the ions formed show little affinity for one another. For example, in HCl in water, Cl^- has very little affinity for H^+:

$$HCl \longrightarrow H^+ + Cl^-$$
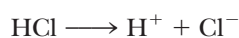
and in NaOH solutions, Na^+ has little affinity for OH^-. The dissociation of these substances in water is effectively complete.

Dissociation of Weak Electrolytes

Substances with only a slight tendency to dissociate to form ions in solution are called **weak electrolytes.** Acetic acid, CH_3COOH, is a good example:

$$CH_3COOH + H_2O \rightleftharpoons CH_3COO^- + H_3O^+$$

The acid dissociation constant K_a for acetic acid is 1.74×10^{-5}:

$$K_a = \frac{[H^+][CH_3COO^-]}{[CH_3COOH]} = 1.74 \times 10^{-5}$$

The term K_a is also called an **ionization constant** because it states the extent to which a substance forms ions in water. The relatively low value of K_a for acetic acid reveals that the un-ionized form, CH_3COOH, predominates over H^+ and CH_3COO^- in aqueous solutions of acetic acid. Viewed another way, CH_3COO^-, the acetate ion, has a high affinity for H^+.

EXAMPLE

What is the pH of a 0.1 M solution of acetic acid? Or, to restate the question, what is the final pH when 0.1 mol of acetic acid (HAc) is added to water and the volume of the solution is adjusted to equal 1 L?

ANSWER

The dissociation of HAc in water can be written simply as

$$HAc \rightleftharpoons H^+ + Ac^-$$
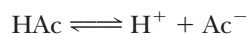
where Ac^- represents the acetate ion, CH_3COO^-. In solution, some amount x of HAc dissociates, generating x amount of Ac^- and an equal amount x of H^+. Ionic equilibria characteristically are established very rapidly. At equilibrium, the concentration of $HAc + Ac^-$ must equal 0.1 M. So, [HAc] can be represented as $(0.1 - x)$ M, and $[Ac^-]$ and $[H^+]$ then both equal x molar. From $1.74 \times 10^{-5} = ([H^+][Ac^-])/[HAc]$, we get $1.74 \times 10^{-5} = x^2/[0.1 - x]$. The solution to quadratic equations of this form $(ax^2 + bx + c = 0)$ is $x = (-b \pm \sqrt{b^2 - 4ac})/2a$. However, the calculation of x can be simplified by noting that, because K_a is quite small, $x \ll 0.1$ M. Therefore, K_a is essentially equal to $x^2/0.1$. This simplification yields $x^2 = 1.74 \times 10^{-6}$, or $x = 1.32 \times 10^{-3}$ M and pH = 2.88.

Henderson–Hasselbalch Equation

Consider the ionization of some weak acid, HA, occurring with an acid dissociation constant, K_a. Then,
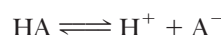
$$HA \rightleftharpoons H^+ + A^-$$

and

$$K_a = \frac{[H^+][A^-]}{[HA]}$$

Rearranging this expression in terms of the parameter of interest, $[H^+]$, we have

$$[H^+] = \frac{K_a[HA]}{[A^-]}$$

Taking the logarithm of both sides gives

$$\log\,[H^+] = \log\,K_a + \log_{10}\frac{[HA]}{[A^-]}$$

If we change the signs and define $pK_a = -\log\,K_a$, we have

$$pH = pK_a - \log_{10}\frac{[HA]}{[A^-]}$$

or

$$\mathbf{pH = p\mathit{K}_a + \log_{10}\frac{[A^-]}{[HA]}}$$

This relationship is known as the **Henderson–Hasselbalch equation.** Thus, the pH of a solution can be calculated, provided K_a and the concentrations of the weak acid HA and its conjugate base A^- are known. Note particularly that when $[HA] = [A^-]$, $pH = pK_a$. For example, if equal volumes of 0.1 M HAc and 0.1 M sodium acetate are mixed, then

$$pH = pK_a = 4.76$$

$$pK_a = -\log\,K_a = -\log_{10}\,(1.74 \times 10^{-5}) = 4.76$$

(Sodium acetate, the sodium salt of acetic acid, is a strong electrolyte and dissociates completely in water to yield Na^+ and Ac^-.)

Table 2.4

Acid Dissociation Constants and pK_a Values for Some Weak Electrolytes (at 25°C)

Acid	K_a (M)	pK_a
HCOOH (formic acid)	1.78×10^{-4}	3.75
CH_3COOH (acetic acid)	1.74×10^{-5}	4.76
CH_3CH_2COOH (propionic acid)	1.35×10^{-5}	4.87
$CH_3CHOHCOOH$ (lactic acid)	1.38×10^{-4}	3.86
$HOOCCH_2CH_2COOH$ (succinic acid) pK_1*	6.16×10^{-5}	4.21
$HOOCCH_2CH_2COO^-$ (succinic acid) pK_2	2.34×10^{-6}	5.63
H_3PO_4 (phosphoric acid) pK_1	7.08×10^{-3}	2.15
$H_2PO_4^-$ (phosphoric acid) pK_2	6.31×10^{-8}	7.20
HPO_4^{2-} (phosphoric acid) pK_3	3.98×10^{-13}	12.40
$C_3N_2H_5^+$ (imidazole)	1.02×10^{-7}	6.99
$C_6O_2N_3H_{11}^+$ (histidine–imidazole group) pK_R†	9.12×10^{-7}	6.04
H_2CO_3 (carbonic acid) pK_1	1.70×10^{-4}	3.77
HCO_3^- (bicarbonate) pK_2	5.75×10^{-11}	10.24
$(HOCH_2)_3CNH_3^+$ (*tris*-hydroxymethyl aminomethane)	8.32×10^{-9}	8.07
NH_4^+ (ammonium)	5.62×10^{-10}	9.25
$CH_3NH_3^+$ (methylammonium)	2.46×10^{-11}	10.62

*These pK values listed as pK_1, pK_2, or pK_3 are in actuality pK_a values for the respective disso-ciations. This simplification in notation is used throughout this book.
†pK_R refers to the imidazole ionization of histidine.

Data from *CRC Handbook of Biochemistry*, The Chemical Rubber Co., 1968.

The Henderson–Hasselbalch equation provides a general solution to the quantitative treatment of acid–base equilibria in biological systems. Table 2.4 gives the acid dissociation constants and pK_a values for some weak electrolytes of biochemical interest.

EXAMPLE

What is the pH when 100 mL of 0.1 N NaOH is added to 150 mL of 0.2 M HAc if pK_a for acetic acid = 4.76?

ANSWER

100 mL 0.1 N NaOH = 0.01 mol OH^-, which neutralizes 0.01 mol of HAc, giv-ing an equivalent amount of Ac^-:

$$OH^- + HAc \longrightarrow Ac^- + H_2O$$

0.02 mol of the original 0.03 mol of HAc remains essentially undissociated. The final volume is 250 mL.

$$pH = pK_a + \log_{10} \frac{[Ac^-]}{[HAc]} = 4.76 + \log\ (0.01\ \text{mol})/(0.02\ \text{mol})$$

$$pH = 4.76 - \log_{10} 2 = 4.46$$

If 150 mL of 0.2 M HAc had merely been diluted with 100 mL of water, this would leave 250 mL of a 0.12 M HAc solution. The pH would be given by:

$$K_a = \frac{[\text{H}^+][\text{Ac}^-]}{[\text{HAc}]} = \frac{x^2}{0.12\ M} = 1.74 \times 10^{-5}$$
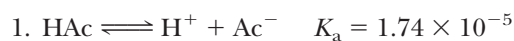
$$x = 1.44 \times 10^{-3} = [\text{H}^+]$$

$$\text{pH} = 2.84$$

Clearly, the presence of sodium hydroxide has mostly neutralized the acidity of the acetic acid through formation of acetate ion.

Titration Curves

Titration is the analytical method used to determine the amount of acid in a solution. A measured volume of the acid solution is titrated by slowly adding a solution of base, typically NaOH, of known concentration. As incremental amounts of NaOH are added, the pH of the solution is determined and a plot of the pH of the solution versus the amount of OH^- added yields a **titration curve.** The titration curve for acetic acid is shown in Figure 2.12. In considering the progress of this titration, keep in mind two important equilibria:

1. $\text{HAc} \rightleftharpoons \text{H}^+ + \text{Ac}^- \qquad K_a = 1.74 \times 10^{-5}$

2. $\text{H}^+ + \text{OH}^- \longrightarrow \text{H}_2\text{O} \qquad K = \dfrac{[\text{H}_2\text{O}]}{K_w} = 5.55 \times 10^{15}$

As the titration begins, mostly HAc is present, plus some H^+ and Ac^- in amounts that can be calculated (see the Example on page 45). Addition of a solution of NaOH allows hydroxide ions to neutralize any H^+ present. Note that reaction (2) as written is strongly favored; its apparent equilibrium constant is greater than 10^{15}! As H^+ is neutralized, more HAc dissociates to H^+ and Ac^-. As further NaOH is added, the pH gradually increases as Ac^- accumulates at the expense of diminishing HAc and the neutralization of H^+. At the point where half of the HAc has been neutralized, that is, where 0.5 equivalent of OH^- has been added, the concentrations of HAc and Ac^- are equal and pH $=$ pK_a for HAc. Thus, we have an experimental method for determining the pK_a values of weak electrolytes. These pK_a values lie at the midpoint of their respective titration curves. After all of the acid has been neutralized (that is, when one equivalent of base has been added), the pH rises exponentially.

The shapes of the titration curves of weak electrolytes are identical, as Figure 2.13 reveals. Note, however, that the midpoints of the different curves vary in a way that characterizes the particular electrolytes. The pK_a for acetic acid is 4.76, the pK_a for imidazole is 6.99, and that for ammonium is 9.25. These pK_a values are directly related to the dissociation constants of these substances, or, viewed the other way, to the relative affinities of the conjugate bases for protons. NH_3 has a high affinity for protons compared to Ac^-; NH_4^+ is a poor acid compared to HAc.

Phosphoric Acid Has Three Dissociable H^+

Figure 2.14 shows the titration curve for phosphoric acid, H_3PO_4. This substance is a *polyprotic acid,* meaning it has more than one dissociable proton. Indeed, it has three, and thus three equivalents of OH^- are required to neutralize it, as Figure 2.14 shows. Note that the three dissociable H^+ are lost in discrete steps, each dissociation showing a characteristic pK_a. Note that pK_1 occurs at pH $= 2.15$, and the concentrations of the acid H_3PO_4 and the conjugate base H_2PO_4^- are equal. As the next dissociation is approached, H_2PO_4^-
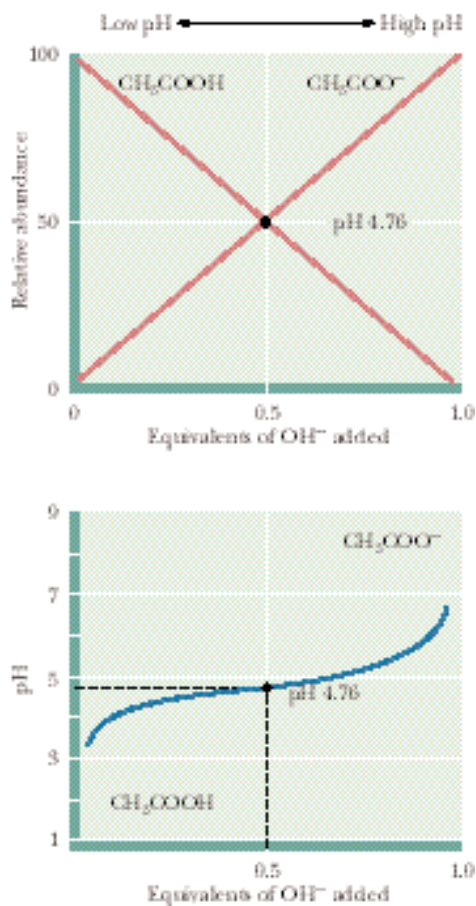

FIGURE 2.12 • The titration curve for acetic acid. Note that the titration curve is relatively flat at pH values near the pK_a; in other words, the pH changes relatively little as OH^- is added in this region of the titration curve.
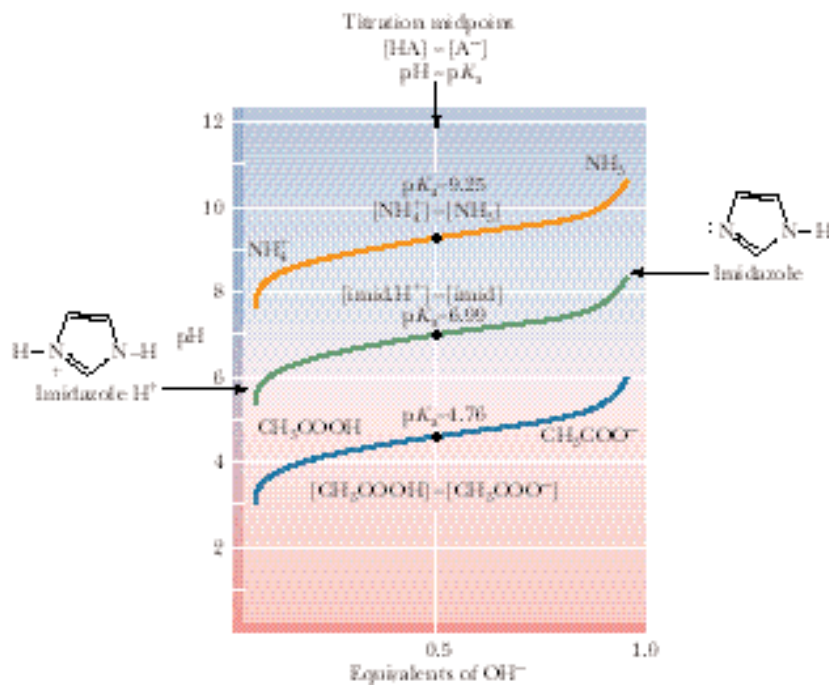
is treated as the acid and HPO_4^{2-} is its conjugate base. Their concentrations are equal at pH 7.20, so $pK_2 = 7.20$. (Note that at this point, 1.5 equivalents of OH^- have been added.) As more OH^- is added, the last dissociable hydrogen is titrated, and pK_3 occurs at pH = 12.4, where $[HPO_4^{2-}] = [PO_4^{3-}]$.

A biologically important point is revealed by the basic shape of the titration curves of weak electrolytes: in the region of the pK_a, pH remains relatively unaffected as increments of OH^- (or H^+) are added. The weak acid and its conjugate base are acting as a buffer.
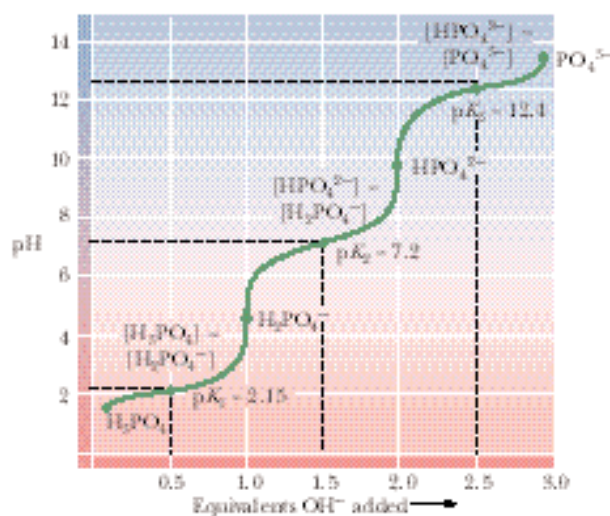

FIGURE 2.14 • The titration curve for phosphoric acid. The chemical formulas show the prevailing ionic species present at various pH values. Phosphoric acid (H_3PO_4) has three titratable hydrogens and therefore three midpoints are seen: at pH 2.15 (pK_1), pH 7.20 (pK_2), and pH 12.4 (pK_3).
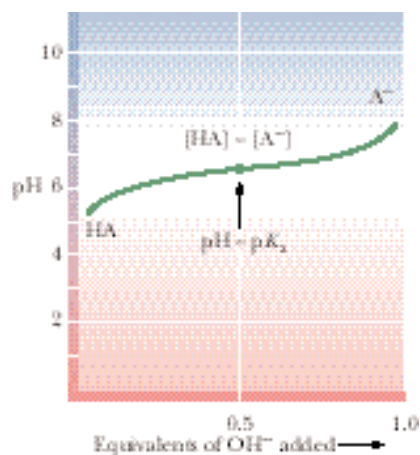
FIGURE 2.15 • A buffer system consists of a weak acid, HA, and its conjugate base, A^-. The pH varies only slightly in the region of the titration curve where $[HA] = [A^-]$. The unshaded box denotes this area of greatest buffering capacity. Buffer action: when HA and A^- are both available in sufficient concentration, the solution can absorb input of either H^+ or OH^-, and pH is maintained essentially constant.

2.3 • Buffers

Buffers are solutions that tend to resist changes in their pH as acid or base is added. Typically, a buffer system is composed of a weak acid *and* its conjugate base. A solution of a weak acid that has a pH nearly equal to its pK_a by definition contains an amount of the conjugate base nearly equivalent to the weak acid. Note that in this region, the titration curve is relatively flat (Figure 2.15). Addition of H^+ then has little effect because it is absorbed by the following reaction:

$$H^+ + A^- \longrightarrow HA$$
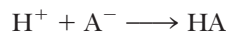
Similarly, added OH^- is consumed by the process

$$OH^- + HA \longrightarrow A^- + H_2O$$

The pH then remains relatively constant. The components of a buffer system are chosen such that the pK_a of the weak acid is close to the pH of interest. It is at the pK_a that the buffer system shows its greatest buffering capacity. At pH values more than one pH unit from the pK_a, buffer systems become ineffective because the concentration of one of the components is too low to absorb the influx of H^+ or OH^-. The molarity of a buffer is defined as the *sum* of the concentrations of the acid and conjugate base forms.

Maintenance of pH is vital to all cells. Cellular processes such as metabolism are dependent on the activities of enzymes, and in turn, enzyme activity is markedly influenced by pH, as the graphs in Figure 2.16 show. Consequently, changes in pH would be very disruptive to metabolism for reasons that become apparent in later chapters. Organisms have a variety of mechanisms to keep the pH of their intra- and extracellular fluids essentially constant, but the primary protection against harmful pH changes is provided by buffer systems. The buffer systems selected reflect both the need for a pK_a value near pH 7 and the compatibility of the buffer components with the metabolic machinery of cells. Two buffer systems act to maintain intracellular pH essentially constant—the phosphate ($HPO_4^{2-}/H_2PO_4^-$) system and the histidine system. The pH of the extracellular fluid that bathes the cells and tissues of animals is maintained by the bicarbonate/carbonic acid (HCO_3^-/H_2CO_3) system.

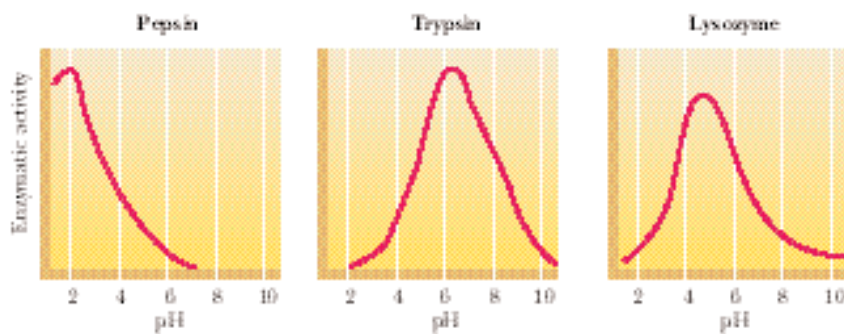FIGURE 2.16 • pH versus enzymatic activity. The activity of enzymes is very sensitive to pH. The pH optimum of an enzyme is one of its most important characteristics. Pepsin is a protein-digesting enzyme active in the gastric fluid. Trypsin is also a proteolytic enzyme, but it acts in the more alkaline milieu of the small intestine. Lysozyme digests the cell walls of bacteria; it is found in tears.

Phosphate System

The **phosphate system** serves to buffer the intracellular fluid of cells at physiological pH because pK_2 lies near this pH value. The intracellular pH of most cells is maintained in the range between 6.9 and 7.4. Phosphate is an abundant anion in cells, both in inorganic form and as an important functional group on organic molecules that serve as metabolites or macromolecular precursors. In both organic and inorganic forms, its characteristic pK_2 means that the ionic species present at physiological pH are sufficient to donate or accept hydrogen ions to buffer any changes in pH, as the titration curve for H_3PO_4 in Figure 2.14 reveals. For example, if the total cellular concentration of phosphate is 20 mM (millimolar) and the pH is 7.4, the distribution of the major phosphate species is given by

$$pH = pK_2 + \log_{10} \frac{[HPO_4{}^{2-}]}{[H_2PO_4{}^-]}$$

$$7.4 = 7.20 + \log_{10} \frac{[HPO_4{}^{2-}]}{[H_2PO_4{}^-]}$$

$$\frac{[HPO_4{}^{2-}]}{[H_2PO_4{}^-]} = 1.58$$

Thus, if $[HPO_4{}^{2-}] + [H_2PO_4{}^-] = 20$ mM, then

$$[HPO_4{}^{2-}] = 12.25 \text{ m}M \quad \text{and} \quad [H_2PO_4{}^-] = 7.75 \text{ m}M$$

Histidine System

Histidine is one of the 20 naturally occurring amino acids commonly found in proteins (see Chapter 4). It possesses as part of its structure an imidazole group, a five-membered heterocyclic ring possessing two nitrogen atoms. The pK_a for dissociation of the imidazole hydrogen of histidine is 6.04.

In cells, histidine occurs as the free amino acid, as a constituent of proteins, and as part of dipeptides in combination with other amino acids. Because the concentration of free histidine is low and its imidazole pK_a is more than 1 pH unit removed from prevailing intracellular pH, its role in intracellular buffering is minor. However, protein-bound and dipeptide histidine may be the dominant buffering system in some cells. In combination with other amino acids, as in proteins or dipeptides, the imidazole pK_a may increase substantially. For example, the imidazole pK_a is 7.04 in **anserine,** a dipeptide containing β-alanine and histidine (Figure 2.17). Thus, this pK_a is near physiological pH, and some histidine peptides are well suited for buffering at physiological pH.
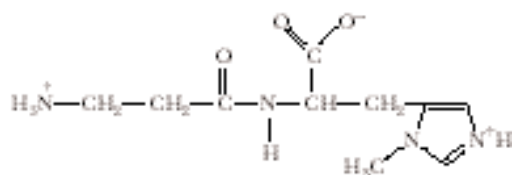

FIGURE 2.17 • Anserine (N-β-alanyl-3-methyl-L-histidine) is an important dipeptide buffer in the maintenance of intracellular pH in some tissues. The structure shown is the predominant ionic species at pH 7. pK_1 (COOH) = 2.64; pK_2 (imidazole–N$^+$H) = 7.04; pK_3 (NH$_3{}^+$) = 9.49.

The Bicarbonate Buffer System of Blood Plasma

The important buffer system of blood plasma is the bicarbonate/carbonic acid couple:

$$H_2CO_3 \rightleftharpoons H^+ + HCO_3^-$$

The relevant pK_a, pK_1 for carbonic acid, has a value far removed from the normal pH of blood plasma (pH 7.4). (The pK_1 for H_2CO_3 at 25°C is 3.77 (Table 2.4), but at 37°C, pK_1 is 3.57.) At pH 7.4, the concentration of H_2CO_3 is a minuscule fraction of the HCO_3^- concentration, and thus the plasma appears to be poorly protected against an influx of OH^- ions.

$$pH = 7.4 = 3.57 + \log_{10} \frac{[HCO_3^-]}{[H_2CO_3]}$$

$$\frac{[HCO_3^-]}{[H_2CO_3]} = 6761$$

For example, if $[HCO_3^-] = 24$ mM, then $[H_2CO_3]$ is only 3.55 μM (3.55 $\times 10^{-6}$ M), and an equivalent amount of OH^- (its usual concentration in plasma) would swamp the buffer system, causing a dangerous rise in the plasma pH. How, then, can this bicarbonate system function effectively? The bicarbonate buffer system works well because the critical concentration of H_2CO_3 is maintained relatively constant through equilibrium with dissolved CO_2 produced in the tissues and available as a gaseous CO_2 reservoir in the lungs.[2]

"Good" Buffers

Not many common substances have pK_a values in the range from 6 to 8. Consequently, biochemists conducting *in vitro* experiments were limited in their choice of buffers effective at or near physiological pH. In 1966, N.E. Good devised a set of synthetic buffers to remedy this problem, and over the years the list has expanded so that a "good" selection is available (Figure 2.18).
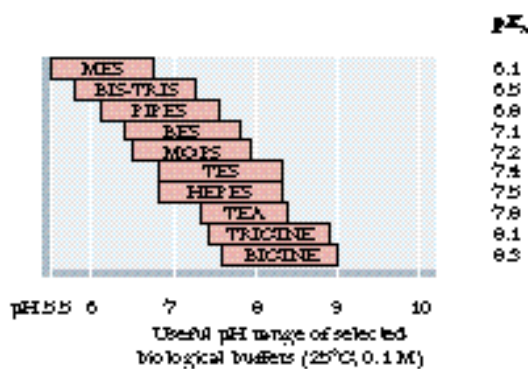

FIGURE 2.18 • The pK_a values and pH range of some "good" buffers.

[2]Well-fed human adults exhale about 1 kg of CO_2 daily. Imagine the excretory problem if CO_2 were not a volatile gas!


## $\mathcal{A}$ D E E P E R   L O O K

How the Bicarbonate Buffer System Works

Gaseous carbon dioxide from the lungs and tissues is dissolved in the blood plasma, symbolized as $CO_2(d)$, and hydrated to form H_2CO_3:

$$CO_2(g) \rightleftharpoons CO_2(d)$$
$$CO_2(d) + H_2O \rightleftharpoons H_2CO_3$$
$$H_2CO_3 \rightleftharpoons H^+ + HCO_3^-$$
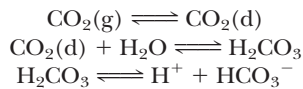
Thus, the concentration of H_2CO_3 is itself buffered by the available pools of CO_2. The hydration of CO_2 is actually mediated by an enzyme, *carbonic anhydrase,* which facilitates the equilibrium by rapidly catalyzing the reaction

$$H_2O + CO_2(d) \rightleftharpoons H_2CO_3$$
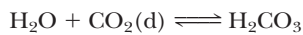
Under the conditions of temperature and ionic strength prevailing in mammalian body fluids, the equilibrium for this reaction lies far to the left, such that about 500 CO_2 molecules are present in solution for every molecule of H_2CO_3. Because dissolved CO_2 and H_2CO_3 are in equilibrium, the proper expression for H_2CO_3 availability is $[CO_2(d)] + [H_2CO_3]$, the so-called total carbonic acid pool, consisting primarily of $CO_2(d)$. The overall equilibrium for the bicarbonate buffer system then is

$$CO_2(d) + H_2O \xrightarrow{K_h} H_2CO_3$$

$$H_2CO_3 \xrightarrow{K_a} H^+ + HCO_3^-$$
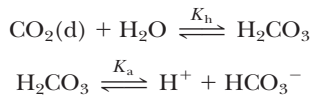
An expression for the ionization of H_2CO_3 under such conditions (that is, in the presence of dissolved CO_2) can be obtained from K_h, the equilibrium constant for the hydration of CO_2, and from K_a, the first acid dissociation constant for H_2CO_3:

$$K_h = \frac{[H_2CO_3]}{[CO_2(d)]}$$

Thus,

$$[H_2CO_3] = K_h[CO_2(d)]$$

Putting this value for $[H_2CO_3]$ into the expression for the first dissociation of H_2CO_3 gives

$$K_a = \frac{[H^+][HCO_3^-]}{[H_2CO_3]}$$

$$= \frac{[H^+][HCO_3^-]}{K_h[CO_2(d)]}$$

Therefore, the overall equilibrium constant for the ionization of H_2CO_3 in equilibrium with $CO_2(d)$ is given by

$$K_aK_h = \frac{[H^+][HCO_3^-]}{[CO_2(d)]}$$

and K_aK_h, the product of two constants, can be defined as a new equilibrium constant, $\boldsymbol{K_{overall}}$. The value of K_h is 0.003 at 37°C and K_a, the ionization constant for H_2CO_3, is $10^{-3.57} = 0.000269$. Therefore,

$$K_{overall} = (0.000269)(0.003)$$
$$= 8.07 \times 10^{-7}$$
$$pK_{overall} = 6.1$$

which yields the following Henderson–Hasselbalch relationship:

$$pH = pK_{overall} + \log_{10}\frac{[HCO_3^-]}{[CO_2(d)]}$$

Although the prevailing blood pH of 7.4 is more than 1 pH unit away from $pK_{overall}$, the bicarbonate system is still an effective buffer. That is, at blood pH, the concentration of the acid component of the buffer is less than 10% of the conjugate base component. One might imagine that this buffer component could be overwhelmed by relatively small amounts of alkali, with consequent disastrous rises in blood pH. However, the acid component is the total carbonic acid pool, that is, $[CO_2(d)] + [H_2CO_3]$, which is stabilized by its equilibrium with $CO_2(g)$. The gaseous CO_2 buffers any losses from the total carbonic acid pool by entering solution as $CO_2(d)$, and blood pH is effectively maintained. Thus, the bicarbonate buffer system is an *open system*. The natural presence of CO_2 gas at a partial pressure of 40 mm Hg in the alveoli of the lungs and the equilibrium

$$CO_2(g) \rightleftharpoons CO_2(d)$$

keep the concentration of $CO_2(d)$ (the principal component of the total carbonic acid pool in blood plasma) in the neighborhood of 1.2 mM. Plasma $[HCO_3^-]$ is about 24 mM under such conditions.

2.4 • Water's Unique Role in the Fitness of the Environment

The remarkable properties of water render it particularly suitable to its unique role in living processes and the environment, and its presence in abundance favors the existence of life. Let's examine water's physical and chemical properties to see the extent to which they provide conditions that are advantageous to organisms.

As a *solvent,* water is powerful yet innocuous. No other chemically inert solvent compares with water for the substances it can dissolve. Also, it is very impor-

Blood pH and Respiration

Hyperventilation, defined as a breathing rate more rapid than necessary for normal CO_2 elimination from the body, can result in an inappropriately low $[CO_2(g)]$ in the blood. Central nervous system disorders such as meningitis, encephalitis, or cerebral hemorrhage, as well as a number of drug- or hormone-induced physiological changes, can lead to hyperventilation. As $[CO_2(g)]$ drops due to excessive exhalation, $[H_2CO_3]$ in the blood plasma falls, followed by decline in $[H^+]$ and $[HCO_3^-]$ in the blood plasma. Blood pH rises within 20 sec of the onset of hyperventilation, becoming maximal within 15 min. $[H^+]$ can change from its normal value of 40 nM (pH = 7.4) to 18 nM (pH = 7.74). This rise in plasma pH (increase in alkalinity) is termed **respiratory alkalosis.**

Hypoventilation is the opposite of hyperventilation and is characterized by an inability to excrete CO_2 rapidly enough to meet physiological needs. Hypoventilation can be caused by narcotics, sedatives, anesthetics, and depressant drugs; diseases of the lung also lead to hypoventilation. Hypoventilation results in **respiratory acidosis,** as $CO_2(g)$ accumulates, giving rise to H_2CO_3, which dissociates to form H^+ and HCO_3^-.

tant to life that water is a "poor" solvent for nonpolar substances. Thus, through hydrophobic interactions, lipids coalesce, membranes form, boundaries are created delimiting compartments, and the cellular nature of life is established. Because of its very high dielectric constant, water is a medium for ionization. Ions enrich the living environment in that they enhance the variety of chemical species and introduce an important class of chemical reactions. They provide electrical properties to solutions and therefore to organisms. Aqueous solutions are the prime source of ions.

The *thermal properties* of water are especially relevant to its environmental fitness. It has great power as a buffer resisting thermal (temperature) change. Its heat capacity, or specific heat (4.1840 J/g°C), is remarkably high; it is ten times greater than iron, five times greater than quartz or salt, and twice as great as hexane. Its heat of fusion is 335 J/g. Thus, at 0°C, it takes a loss of 335 J to change the state of 1 g of H_2O from liquid to solid. Its heat of vaporization, 2.24 kJ/g, is exceptionally high. These thermal properties mean that it takes substantial changes in heat content to alter the temperature and especially the *state* of water. Water's thermal properties allow it to buffer the climate through such processes as condensation, evaporation, melting, and freezing. Furthermore, these properties allow effective temperature regulation in living organisms. For example, heat generated within an organism as a result of metabolism can be efficiently eliminated by evaporation or conduction. The thermal conductivity of water is very high in comparison with other liquids. The anomalous expansion of water as it cools to temperatures near its freezing point is a unique attribute of great significance to its natural fitness. As water cools, H bonding increases because the thermal motions of the molecules are lessened. Hydrogen bonding tends to separate the water molecules (Figure 2.2), and thus the density of water decreases. These changes in density mean that, at temperatures below 4°C, cool water rises and, most importantly, ice freezes on the surface of bodies of water, forming an insulating layer protecting the liquid water underneath.

Water has the highest *surface tension* (75 dyne/cm) of all common liquids (except mercury). Together, surface tension and density determine how high a liquid rises in a capillary system. Capillary movement of water plays a prominent role in the life of plants. Lastly, consider *osmosis,* the bulk movement of water in the direction from a dilute aqueous solution to a more concentrated one across a semipermeable boundary. Such bulk movements determine the shape and form of living things.

Water is truly a crucial determinant of the fitness of the environment. In a very real sense, organisms are aqueous systems in a watery world.

PROBLEMS

1. Calculate the pH of the following.
a. 5×10^{-4} M HCl
b. 7×10^{-5} M NaOH
c. 2 μM HCl
d. 3×10^{-2} M KOH
e. 0.04 mM HCl
f. 6×10^{-9} M HCl

2. Calculate the following from the pH values given in Table 2.3.
a. $[H^+]$ in vinegar
b. $[H^+]$ in saliva
c. $[H^+]$ in household ammonia
d. $[OH^-]$ in milk of magnesia
e. $[OH^-]$ in beer
f. $[H^+]$ inside a liver cell

3. The pH of a 0.02 M solution of an acid was measured at 4.6.
a. What is the $[H^+]$ in this solution?
b. Calculate the acid dissociation constant K_a and pK_a for this acid.

4. The K_a for formic acid is 1.78×10^{-4} M.
a. What is the pH of a 0.1 M solution of formic acid?
b. 150 mL of 0.1 M NaOH is added to 200 mL of 0.1 M formic acid, and water is added to give a final volume of 1 L. What is the pH of the final solution?

5. Given 0.1 M solutions of acetic acid and sodium acetate, describe the preparation of 1 L of 0.1 M acetate buffer at a pH of 5.4.

6. If the internal pH of a muscle cell is 6.8, what is the $[HPO_4{}^{2-}]/[H_2PO_4{}^-]$ ratio in this cell?

7. Given 0.1 M solutions of Na_3PO_4 and H_3PO_4, describe the preparation of 1 L of a phosphate buffer at a pH of 7.5. What are the molar concentrations of the ions in the final buffer solution, including Na^+ and H^+?
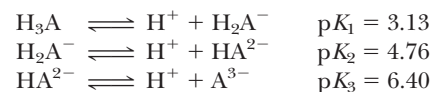
8. BICINE is a compound containing a tertiary amino group whose relevant pK_a is 8.3 (Figure 2.18). Given 1 L of 0.05 M BICINE with its tertiary amino group in the unprotonated form, how much 0.1 N HCl must be added to have a BICINE buffer solution of pH 7.5? What is the molarity of BICINE in the final buffer?

9. What are the approximate fractional concentrations of the following phosphate species at pH values of 0, 2, 4, 6, 8, 10, and 12?
a. H_3PO_4
b. $H_2PO_4{}^-$
c. $HPO_4{}^{2-}$
d. $PO_4{}^{3-}$

10. Citric acid, a tricarboxylic acid important in intermediary metabolism, can be symbolized as H_3A. Its dissociation reactions are

$$
\begin{array}{lll}
H_3A & \rightleftharpoons H^+ + H_2A^- & pK_1 = 3.13 \\
H_2A^- & \rightleftharpoons H^+ + HA^{2-} & pK_2 = 4.76 \\
HA^{2-} & \rightleftharpoons H^+ + A^{3-} & pK_3 = 6.40
\end{array}
$$

If the *total* concentration of the acid *and* its anion forms is 0.02 M, what are the individual concentrations of H_3A, H_2A^-, HA^{2-}, and A^{3-} at pH 5.2?

11. a. If 50 mL of 0.01 M HCl is added to 100 mL of 0.05 M phosphate buffer at pH 7.2, what is the resultant pH? What are the concentrations of $H_2PO_4{}^-$ and $HPO_4{}^{2-}$ in the final solution?
b. If 50 mL of 0.01 M NaOH is added to 100 mL of 0.05 M phosphate buffer at pH 7.2, what is the resultant pH? What are the concentrations of $H_2PO_4{}^-$ and $HPO_4{}^{2-}$ in this final solution?

12. If the plasma pH is 7.4 and the plasma concentration of $HCO_3{}^-$ is 15 mM, what is the plasma concentration of H_2CO_3? What is the plasma concentration of $CO_{2(\text{dissolved})}$? If metabolic activity changes the concentration of $CO_{2(\text{dissolved})}$ to 3 mM, and $[HCO_3{}^-]$ remains at 15 mM, what is the pH of the plasma?

FURTHER READING

Beynon, R. J., and Easterby, J. S., 1996. *Buffer Solutions: The Basics.* New York: IRL Press: Oxford University Press.

Cooper, T. G., 1977. *The Tools of Biochemistry,* Chap. 1. New York: John Wiley & Sons.

Darvey, I. G., and Ralston, G. B., 1993. Titration curves—misshapen or mislabeled? *Trends in Biochemical Sciences* **18:**69–71.

Edsall, J. T., and Wyman, J., 1958. Carbon dioxide and carbonic acid, in *Biophysical Chemistry,* Vol. 1, Chap. 10. New York: Academic Press.

Franks, F., ed., 1982. *The Biophysics of Water.* New York: John Wiley & Sons.

Henderson, L. J., 1913. *The Fitness of the Environment.* New York: Macmillan Co. (Republished 1970. Gloucester, MA: P. Smith).

Hille, B., 1992. *Ionic Channels of Excitable Membranes,* 2nd ed., Chap. 10. Sunderland, MA: Sinauer Associates.

Masoro, E. J., and Siegel, P. D., 1971. *Acid–Base Regulation: Its Physiology and Pathophysiology.* Philadelphia: W.B. Saunders Co.

Perrin, D. D., 1982. *Ionization Constants of Inorganic Acids and Bases in Aqueous Solution.* New York: Pergamon Press.

Rose, B. D., 1994. *Clinical Physiology of Acid–Base and Electrolyte Disorders,* 4th ed., New York: McGraw–Hill, Inc.

Segel, I. H., 1976. *Biochemical Calculations,* 2nd ed., Chap. 1. New York: John Wiley & Sons.

Stillinger, F. H., 1980. Water revisited. *Science* **209:**451–457.

A theory is the more impressive the greater is the simplicity of its premises, the more different are the kinds of things it relates and the more extended is its range of applicability. Therefore, the deep impression which classical thermodynamics made upon me. It is the only physical theory of universal content which I am convinced, that within the framework of applicability of its basic concepts, will never be overthrown.

ALBERT EINSTEIN

$\mathcal{C}$hapter 3

Thermodynamics of Biological Systems

Sun emblem of Louis XIV on a gate at Versailles. The sun is the prime source of energy for life, and thermodynamics is the gateway to understanding metabolism. (Giraudon/Art Research, New York)

The activities of living things require energy. Movement, growth, synthesis of biomolecules, and the transport of ions and molecules across membranes all demand energy input. All organisms must acquire energy from their surroundings and must utilize that energy efficiently to carry out life processes. To study such bioenergetic phenomena requires familiarity with **thermodynamics,** a collection of laws and principles describing the flows and interchanges of heat, energy, and matter in systems of interest. Thermodynamics also allows us to determine whether or not chemical processes and reactions occur spontaneously. The student should appreciate the power and practical

value of thermodynamic reasoning and realize that this is well worth the effort needed to understand it.

Even the most complicated aspects of thermodynamics are based ultimately on three rather simple and straightforward laws. These laws and their extensions sometimes run counter to our intuition. However, once truly understood, the basic principles of thermodynamics become powerful devices for sorting out complicated chemical and biochemical problems. At this milestone in our scientific development, thermodynamic thinking becomes an enjoyable and satisfying activity.

Several basic thermodynamic principles are presented in this chapter, including the analysis of heat flow, entropy production, and free energy functions and the relationship between entropy and information. In addition, some ancillary concepts are considered, including the concept of standard states, the effect of pH on standard-state free energies, the effect of concentration on the net free energy change of a reaction, and the importance of coupled processes in living things. The chapter concludes with a discussion of ATP and other energy-rich compounds.

3.1 • Basic Thermodynamic Concepts

In any consideration of thermodynamics, a distinction must be made between the system and the surroundings. The **system** is that portion of the *universe* with which we are concerned, whereas the **surroundings** include everything else in the universe (Figure 3.1). The nature of the system must also be specified. There are three basic systems: isolated, closed, and open. An **isolated system** cannot exchange matter or energy with its surroundings. A **closed system** may exchange energy, but not matter, with the surroundings. An **open system** may exchange matter, energy, or both with the surroundings. Living things are typically open systems that exchange matter (nutrients and waste products) and heat (from metabolism, for example) with their surroundings.

The First Law: Heat, Work, and Other Forms of Energy

It was realized early in the development of thermodynamics that heat could be converted into other forms of energy, and moreover that all forms of energy could ultimately be converted to some other form. The **first law of thermodynamics** states that *the total energy of an isolated system is conserved.* Thermodynamicists have formulated a mathematical function for keeping track of heat transfers and work expenditures in thermodynamic systems. This function is called the **internal energy,** commonly designated E or U. The internal energy depends only on the present state of a system and hence is referred to as a **state function.** The internal energy does not depend on how the system got there and is thus **independent of path.** An extension of this thinking is that we can manipulate the system through any possible pathway of changes, and as long as the system returns to the original state, the internal energy, E, will not have been changed by these manipulations.

The internal energy, E, of any system can change only if energy flows in or out of the system in the form of heat or work. For any process that converts one state (state 1) into another (state 2), the change in internal energy, ΔE, is given as

$$\Delta E = E_2 - E_1 = q + w \tag{3.1}$$

where the quantity q is the *heat absorbed by the system from the surroundings,* and w is the *work done on the system by the surroundings.* **Mechanical work** is defined

Isolated system

No exchange of matter or heat
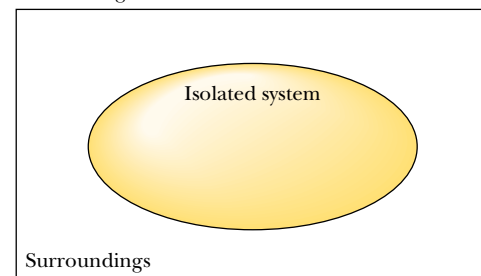
Closed system

Heat exchange may occur
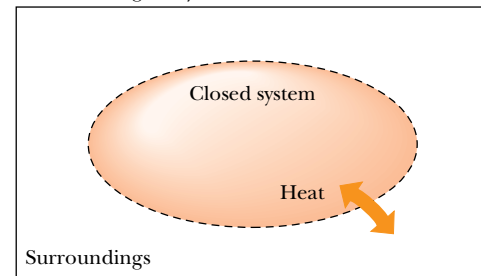
Open system

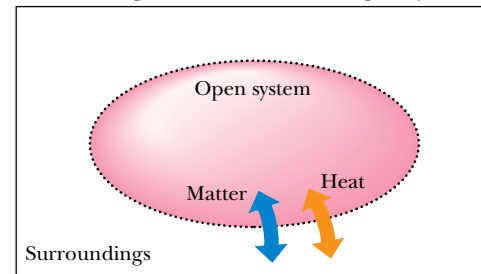Heat exchange and/or matter exchange may occur

FIGURE 3.1 • The characteristics of isolated, closed, and open systems. Isolated systems exchange neither matter nor energy with their surroundings. Closed systems may exchange energy, but not matter, with their surroundings. Open systems may exchange either matter or energy with the surroundings.

as *movement through some distance caused by the application of a force.* Both of these must occur for work to have occurred. For example, if a person strains to lift a heavy weight but fails to move the weight at all, then, in the thermodynamic sense, no work has been done. (The energy expended in the muscles of the would-be weight lifter is given off in the form of heat.) In chemical and biochemical systems, work is often concerned with the pressure and volume of the system under study. The mechanical work done on the system is defined as $w = -P\Delta V$, where P is the pressure and ΔV is the volume change and is equal to $V_2 - V_1$. When work is defined in this way, the sign on the right side of Equation (3.1) is positive. (Sometimes w is defined as work done *by* the system; in this case, the equation is $\Delta E = q - w$.) Work may occur in many forms, such as mechanical, electrical, magnetic, and chemical. ΔE, q, and w must all have the same units. The **calorie,** abbreviated **cal,** and **kilocalorie (kcal),** have been traditional choices of chemists and biochemists, but the SI unit, the **joule,** is now recommended.

Enthalpy: A More Useful Function for Biological Systems

If the definition of work is limited to mechanical work, an interesting simplification is possible. In this case, ΔE is merely the *heat exchanged at constant volume.* This is so because if the volume is constant, no mechanical work can be done on or by the system. Then $\Delta E = q$. Thus ΔE is a very useful quantity in constant volume processes. However, chemical and especially biochemical processes and reactions are much more likely to be carried out at constant pressure. In constant pressure processes, ΔE is not necessarily equal to the heat transferred. For this reason, chemists and biochemists have defined a function that is especially suitable for constant pressure processes. It is called the **enthalpy, H,** and it is defined as

$$H = E + PV \qquad (3.2)$$

The clever nature of this definition is not immediately apparent. However, if the pressure is constant, then we have

$$\Delta H = \Delta E + P\Delta V = q + w + P\Delta V = q - P\Delta V + P\Delta V = q \qquad (3.3)$$

Clearly, ΔH is equal to the heat transferred in a constant pressure process. Often, because biochemical reactions normally occur in liquids or solids rather than in gases, volume changes are small and *enthalpy and internal energy are often essentially equal.*

In order to compare the thermodynamic parameters of different reactions, it is convenient to define a *standard state.* For solutes in a solution, the standard state is normally unit activity (often simplified to 1 M concentration). Enthalpy, internal energy, and other thermodynamic quantities are often given or determined for standard-state conditions and are then denoted by a superscript degree sign ("°"), as in $\Delta H°$, $\Delta E°$, and so on.

Enthalpy changes for biochemical processes can be determined experimentally by measuring the heat absorbed (or given off) by the process in a *calorimeter* (Figure 3.2). Alternatively, for any process $A \rightleftharpoons B$ at equilibrium, the standard-state enthalpy change for the process can be determined from the temperature dependence of the equilibrium constant:

Chamber thermometer

Ignition electrodes

Jacket thermometer

Chamber

Jacket

Water bath in calorimeter chamber
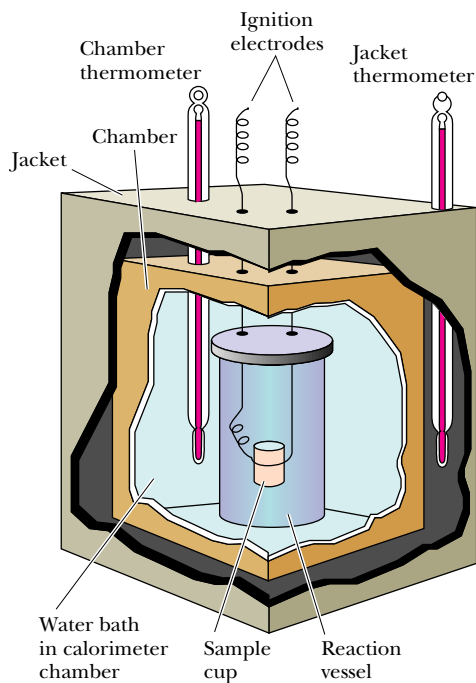
Sample cup

Reaction vessel

FIGURE 3.2 • Diagram of a calorimeter. The reaction vessel is completely submerged in a water bath. The heat evolved by a reaction is determined by measuring the rise in temperature of the water bath.

$$\Delta H^\circ = -R\frac{d(\ln K_{eq})}{d(1/T)} \tag{3.4}$$

Here R is the *gas constant,* defined as $R = 8.314$ J/mol·K. A plot of $R(\ln K_{eq})$ versus $1/T$ is called a **van't Hoff plot.**

EXAMPLE

In a study[1] of the temperature-induced reversible denaturation of the protein chymotrypsinogen,

$$\text{Native state (N)} \rightleftharpoons \text{denatured state (D)}$$
$$K_{eq} = [D]/[N]$$
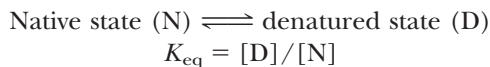
John F. Brandts measured the equilibrium constants for the denaturation over a range of pH and temperatures. The data for pH 3:

T(K):	324.4	326.1	327.5	329.0	330.7	332.0	333.8
K_{eq}:	0.041	0.12	0.27	0.68	1.9	5.0	21

A plot of $R(\ln K_{eq})$ versus $1/T$ (a van't Hoff plot) is shown in Figure 3.3. ΔH° for the denaturation process at any temperature is the negative of the slope of the plot at that temperature. As shown, ΔH° at 54.5°C (327.5 K) is

$$\Delta H^\circ = -[-3.2 - (-17.6)]/[(3.04 - 3.067) \times 10^{-3}] = +533 \text{ kJ/mol}$$

What does this value of ΔH° mean for the unfolding of the protein? Positive values of ΔH° would be expected for the breaking of hydrogen bonds as well as for the exposure of hydrophobic groups from the interior of the native, folded protein during the unfolding process. Such events would raise the energy of the protein–water solution. The magnitude of this enthalpy change (533 kJ/mol) at 54.5°C is large, compared to similar values of ΔH° for other proteins and for this same protein at 25°C (Table 3.1). If we consider only this positive enthalpy change for the unfolding process, the native, folded state is strongly favored. As we shall see, however, other parameters must be taken into account.

FIGURE 3.3 • The enthalpy change, ΔH°, for a reaction can be determined from the slope of a plot of $R \ln K_{eq}$ versus $1/T$. To illustrate the method, the values of the data points on either side of the 327.5 K (54.5°C) data point have been used to calculate ΔH° at 54.5°C. Regression analysis would normally be preferable. *(Adapted from Brandts, J. F., 1964. The thermodynamics of protein denaturation. I. The denaturation of chymotrypsinogen. Journal of the American Chemical Society 86:4291–4301.)*

Table 3.1

Thermodynamic Parameters for Protein Denaturation				
Protein **(and conditions)**	**ΔH°** **kJ/mol**	**ΔS°** **kJ/mol · K**	**ΔG°** **kJ/mol**	**ΔC_p** **kJ/mol · K**
Chymotrypsinogen (pH 3, 25°C)	164	0.440	31	10.9
β-Lactoglobulin (5 *M* urea, pH 3, 25°C)	−88	−0.300	2.5	9.0
Myoglobin (pH 9, 25°C)	180	0.400	57	5.9
Ribonuclease (pH 2.5, 30°C)	240	0.780	3.8	8.4

Adapted from Cantor, C., and Schimmel, P., 1980. *Biophysical Chemistry.* San Francisco: W.H. Freeman, and Tanford, C., 1968. Protein denaturation. *Advances in Protein Chemistry* **23:**121–282.
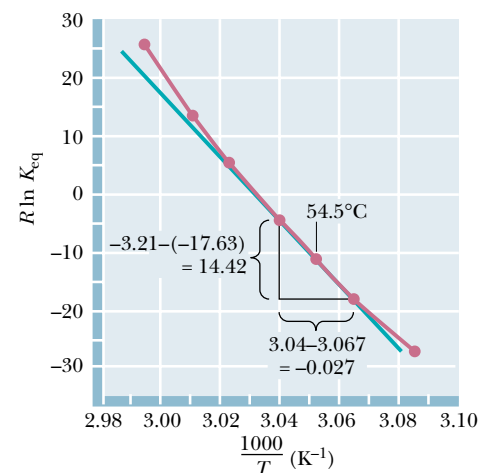
---

[1]Brandts, J. F., 1964. The thermodynamics of protein denaturation. I. The denaturation of chymotrypsinogen. *Journal of the American Chemical Society* **86:**4291–4301.

A DEEPER LOOK

Entropy, Information, and the Importance of "Negentropy"

When a thermodynamic system undergoes an increase in entropy, it becomes more disordered. On the other hand, a decrease in entropy reflects an increase in order. A more ordered system is more highly organized and possesses a greater information content. To appreciate the implications of decreasing the entropy of a system, consider the random collection of letters in the figure. This disorganized array of letters possesses no inherent information content, and nothing can be learned by its perusal. On the other hand, this particular array of letters can be systematically arranged to construct the first sentence of the Einstein quotation that opened this chapter: "A theory is the more impressive the greater is the simplicity of its premises, the more different are the kinds of things it relates and the more extended is its range of applicability."

Arranged in this way, this same collection of 151 letters possesses enormous information content—the profound words of a great scientist. Just as it would have required significant effort to rearrange these 151 letters in this way, so large amounts of energy are required to construct and maintain living organisms. Energy input is required to produce information-rich, organized structures such as proteins and nucleic acids. Information content can be thought of as *negative entropy*. In 1945 Erwin Schrödinger took time out from his studies of quantum mechanics to publish a delightful book entitled *What is Life?* In it, Schrödinger coined the term *negentropy* to describe the negative entropy changes that confer organization and information content to living organisms. Schrödinger pointed out that organisms must "acquire negentropy" to sustain life.

The Second Law and Entropy: An Orderly Way of Thinking About Disorder

The **second law of thermodynamics** has been described and expressed in many different ways, including the following.

1. Systems tend to proceed from *ordered* (*low entropy* or low probability) states to *disordered* (*high entropy* or *high probability*) states.

2. The *entropy* of the system plus surroundings is unchanged by *reversible processes;* the entropy of the system plus surroundings increases for *irreversible processes.*

3. All naturally occurring processes proceed toward **equilibrium,** that is, to a state of minimum potential energy.

Several of these statements of the second law invoke the concept of **entropy,** which is a measure of disorder and randomness in the system (or the surroundings). An organized or ordered state is a low-entropy state, whereas a disordered state is a high-entropy state. All else being equal, reactions involving large, positive entropy changes, ΔS, are more likely to occur than reactions for which ΔS is not large and positive.

Entropy can be defined in several quantitative ways. If W is the number of ways to arrange the components of a system without changing the internal

energy or enthalpy (that is, the number of microscopic states at a given temperature, pressure, and amount of material), then the entropy is given by

$$S = k \ln W \qquad (3.5)$$

where k is Boltzmann's constant ($k = 1.38 \times 10^{-23}$ J/K). This definition is useful for statistical calculations (it is in fact a foundation of *statistical thermodynamics*), but a more common form relates entropy to the heat transferred in a process:

$$dS_{\text{reversible}} = \frac{dq}{T} \qquad (3.6)$$

where $dS_{\text{reversible}}$ is the entropy change of the system in a reversible[2] process, q is the heat transferred, and T is the temperature at which the heat transfer occurs.

The Third Law: Why Is "Absolute Zero" So Important?

The **third law of thermodynamics** states that the entropy of any crystalline, perfectly ordered substance must approach zero as the temperature approaches 0 K, and at $T = 0$ K *entropy is exactly zero.* Based on this, it is possible to establish a quantitative, absolute entropy scale for any substance as

$$S = \int_0^T C_P d \ln T \qquad (3.7)$$

where C_P is the *heat capacity* at constant pressure. The heat capacity of any substance is the amount of heat one mole of it can store as the temperature of that substance is raised by one degree. For a constant pressure process, this is described mathematically as

$$C_P = \frac{dH}{dT} \qquad (3.8)$$

If the heat capacity can be evaluated at all temperatures between 0 K and the temperature of interest, an absolute entropy can be calculated. For biological processes, *entropy changes* are more useful than absolute entropies. The entropy change for a process can be calculated if the enthalpy change and *free energy change* are known.

Free Energy: A Hypothetical but Useful Device

An important question for chemists, and particularly for biochemists, is, "Will the reaction proceed in the direction written?" J. Willard Gibbs, one of the founders of thermodynamics, realized that the answer to this question lay in a comparison of the enthalpy change and the entropy change for a reaction at a given temperature. The **Gibbs free energy, *G*,** is defined as

$$G = H - TS \qquad (3.9)$$

For any process A $\rightleftharpoons$ B at constant pressure and temperature, the *free energy change* is given by

$$\Delta G = \Delta H - T\Delta S \qquad (3.10)$$

---

[2]A reversible process is one that can be reversed by an infinitesimal modification of a variable.

If ΔG is equal to 0, the process is at *equilibrium,* and there is no net flow either in the forward or reverse direction. When $\Delta G = 0$, $\Delta S = \Delta H/T$, and the enthalpic and entropic changes are exactly balanced. Any process with a nonzero ΔG proceeds spontaneously to a final state of lower free energy. If ΔG is negative, the process proceeds spontaneously in the direction written. If ΔG is positive, the reaction or process proceeds spontaneously in the reverse direction. (The sign and value of ΔG do not allow us to determine *how fast* the process will go.) If the process has a negative ΔG, it is said to be **exergonic,** whereas processes with positive ΔG values are **endergonic.**

The Standard-State Free Energy Change

The free energy change, ΔG, for any reaction depends upon the nature of the reactants and products, but it is also affected by the conditions of the reaction, including temperature, pressure, pH, and the concentrations of the reactants and products. As explained earlier, it is useful to define a standard state for such processes. If the free energy change for a reaction is sensitive to solution conditions, what is the particular significance of the standard-state free energy change? To answer this question, consider a reaction between two reactants A and B to produce the products C and D.

$$A + B \rightleftharpoons C + D \tag{3.11}$$

The free energy change for non–standard-state concentrations is given by

$$\Delta G = \Delta G^\circ + RT \ln \frac{[C][D]}{[A][B]} \tag{3.12}$$

At equilibrium, $\Delta G = 0$ and $[C][D]/[A][B] = K_{eq}$. We then have

$$\Delta G^\circ = -RT \ln K_{eq} \tag{3.13}$$

or, in base 10 logarithms,

$$\Delta G^\circ = -2.3RT \log_{10} K_{eq} \tag{3.14}$$

This can be rearranged to

$$K_{eq} = 10^{-\Delta G^\circ/2.3RT} \tag{3.15}$$

In any of these forms, this relationship allows the standard-state free energy change for any process to be determined if the equilibrium constant is known. More importantly, it states that *the equilibrium established for a reaction in solution is a function of the standard-state free energy change for the process.* That is, ΔG° is another way of writing an equilibrium constant.

EXAMPLE

The equilibrium constants determined by Brandts at several temperatures for the denaturation of chymotrypsinogen (see previous Example) can be used to calculate the free energy changes for the denaturation process. For example, the equilibrium constant at 54.5°C is 0.27, so

$$\Delta G^\circ = -(8.314 \text{ J/mol} \cdot \text{K})(327.5 \text{ K}) \ln (0.27)$$

$$\Delta G^\circ = -(2.72 \text{ kJ/mol}) \ln (0.27)$$

$$\Delta G^\circ = 3.56 \text{ kJ/mol}$$

The positive sign of ΔG° means that the unfolding process is unfavorable; that is, the stable form of the protein at 54.5°C is the folded form. On the other hand, the relatively small magnitude of ΔG° means that the folded form is only slightly favored. Figure 3.4 shows the dependence of ΔG° on temperature for

the denaturation data at pH 3 (from the data given in the Example on page 59).

Having calculated both $\Delta H°$ and $\Delta G°$ for the denaturation of chymotrypsinogen, we can also calculate $\Delta S°$, using Equation (3.10):

$$\Delta S° = -\frac{(\Delta G° - \Delta H°)}{T} \tag{3.16}$$

At 54.5°C (327.5 K),

$$\Delta S° = -(3560 - 533{,}000 \text{ J/mol})/327.5 \text{ K}$$

$$\Delta S° = 1{,}620 \text{ J/mol·K}$$

Figure 3.5 presents the dependence of $\Delta S°$ on temperature for chymotrypsinogen denaturation at pH 3. A positive $\Delta S°$ indicates that the protein solution has become more disordered as the protein unfolds. Comparison of the value of 1.62 kJ/mol·K with the values of $\Delta S°$ in Table 3.1 shows that the present value (for chymotrypsinogen at 54.5°C) is quite large. The physical significance of the thermodynamic parameters for the unfolding of chymotrypsinogen becomes clear in the next section.

FIGURE 3.4 • The dependence of $\Delta G°$ on temperature for the denaturation of chymotrypsinogen. *(Adapted from Brandts, J. F., 1964. The thermodynamics of protein denaturation. I. The denaturation of chymotrypsinogen.* Journal of the American Chemical Society **86:***4291–4301.)*

3.2 • The Physical Significance of Thermodynamic Properties

What can thermodynamic parameters tell us about biochemical events? The best answer to this question is that a single parameter (ΔH or ΔS, for example) is not very meaningful. A positive $\Delta H°$ for the unfolding of a protein might reflect *either* the breaking of hydrogen bonds within the protein or the exposure of hydrophobic groups to water (Figure 3.6). However, *comparison of several thermodynamic parameters can provide meaningful insights about a process.* For example, the transfer of Na^+ and Cl^- ions from the gas phase to aqueous solution involves a very large negative $\Delta H°$ (thus a very favorable stabilization of the ions) and a comparatively small $\Delta S°$ (Table 3.2). The negative entropy term reflects the ordering of water molecules in the hydration shells of the Na^+ and Cl^- ions. This unfavorable effect is more than offset by the large heat of hydration, which makes the hydration of ions a very favorable process overall. The negative entropy change for the dissociation of acetic acid in water also reflects the ordering of water molecules in the ion hydration shells. In this case, however, the enthalpy change is much smaller in magnitude. As a result, $\Delta G°$ for
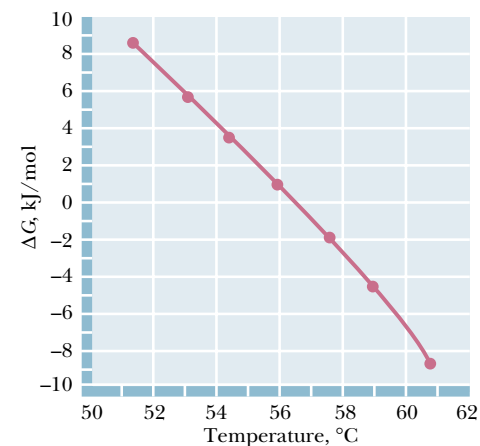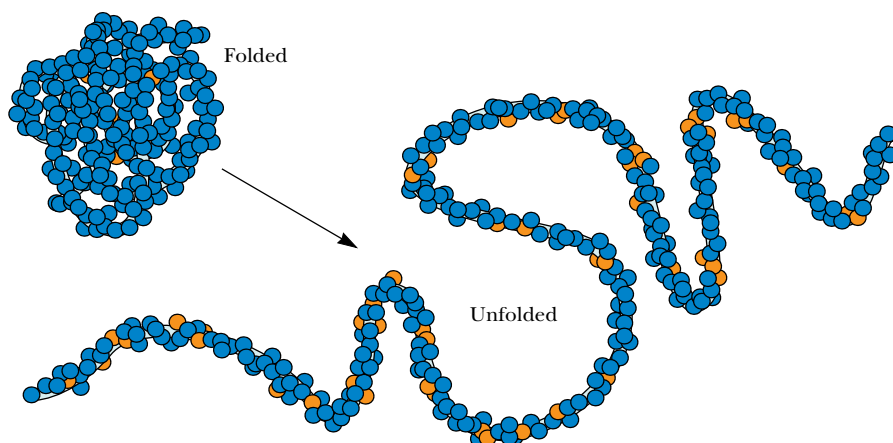

FIGURE 3.5 • The dependence of $\Delta S°$ on temperature for the denaturation of chymotrypsinogen. *(Adapted from Brandts, J. F., 1964. The thermodynamics of protein denaturation. I. The denaturation of chymotrypsinogen.* Journal of the American Chemical Society **86:***4291– 4301.)*
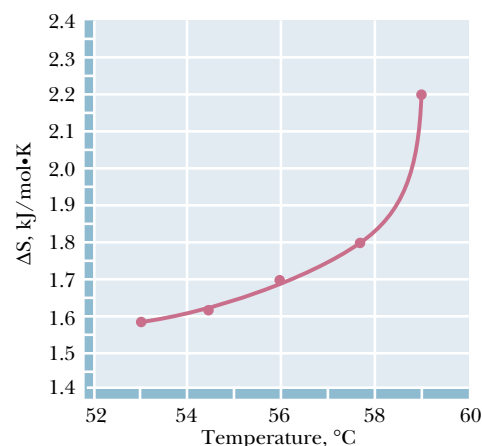

FIGURE 3.6 • Unfolding of a soluble protein exposes significant numbers of nonpolar groups to water, forcing order on the solvent and resulting in a negative $\Delta S°$ for the unfolding process. Yellow spheres represent nonpolar groups; blue spheres are polar and/or charged groups.

Table 3.2

Thermodynamic Parameters for Several Simple Processes*				
Process	$\Delta H°$ **kJ/mol**	$\Delta S°$ **kJ/mol·K**	$\Delta G°$ **kJ/mol**	ΔC_P **kJ/mol·K**
Hydration of ions[†] $Na^+(g) + Cl^-(g) \longrightarrow Na^+(aq) + Cl^-(aq)$	-760.0	-0.185	-705.0	
Dissociation of ions in solution[‡] $H_2O + CH_3COOH \longrightarrow H_3O^+ + CH_3COO^-$	-10.3	-0.126	27.26	-0.143
Transfer of hydrocarbon from pure liquid to water[‡] Toluene (in pure toluene) $\longrightarrow$ toluene (aqueous)	1.72	-0.071	22.7	0.265

*All data collected for 25°C.
[†]Berry, R. S., Rice, S. A., and Ross, J., 1980. *Physical Chemistry.* New York: John Wiley.
[‡]Tanford, C., 1980. *The Hydrophobic Effect.* New York: John Wiley.

dissociation of acetic acid in water is positive, and acetic acid is thus a weak (largely undissociated) acid.

The transfer of a nonpolar hydrocarbon molecule from its pure liquid to water is an appropriate model for the exposure of protein hydrophobic groups to solvent when a protein unfolds. The transfer of toluene from liquid toluene to water involves a negative $\Delta S°$, a positive $\Delta G°$, and a $\Delta H°$ that is small compared to $\Delta G°$ (a pattern similar to that observed for the dissociation of acetic acid). *What distinguishes these two very different processes is the change in heat capacity* (Table 3.2). A positive heat capacity change for a process indicates that the molecules have acquired new ways to move (and thus to store heat energy). A negative ΔC_P means that the process has resulted in less freedom of motion for the molecules involved. ΔC_P is negative for the dissociation of acetic acid and positive for the transfer of toluene to water. The explanation is that polar and nonpolar molecules *both* induce organization of nearby water molecules, *but in different ways*. The water molecules near a nonpolar solute are *organized but labile*. Hydrogen bonds formed by water molecules near nonpolar solutes rearrange more rapidly than the hydrogen bonds of pure water. On the other hand, the hydrogen bonds formed between water molecules near an ion are less labile (rearrange more slowly) than they would be in pure water. This means that ΔC_P should be negative for the dissociation of ions in solution, as observed for acetic acid (Table 3.2).

3.3 • The Effect of pH on Standard-State Free Energies

For biochemical reactions in which hydrogen ions (H^+) are consumed or produced, the usual definition of the standard state is awkward. Standard state for the H^+ ion is 1 *M*, which corresponds to pH 0. At this pH, nearly all enzymes would be denatured, and biological reactions could not occur. It makes more sense to use free energies and equilibrium constants determined at pH 7. Biochemists have thus adopted a modified standard state, designated with prime (′) symbols, as in $\Delta G°′$, K'_{eq}, $\Delta H°′$, and so on. For values determined in this way, a standard state of 10^{-7} *M* H^+ and unit activity (1 *M* for solutions, 1 atm for gases and pure solids defined as unit activity) for all other components (in the ionic forms that exist at pH 7) is assumed. The two standard states can be related easily. For a reaction in which H^+ is produced,

$$A \longrightarrow B^- + H^+ \tag{3.17}$$

the relation of the equilibrium constants for the two standard states is

$$K_{eq}' = K_{eq}[H^+] \tag{3.18}$$

and $\Delta G^{\circ\prime}$ is given by

$$\Delta G^{\circ\prime} = \Delta G^{\circ} + RT \ln [H^+] \tag{3.19}$$

For a reaction in which H^+ is consumed,

$$A^- + H^+ \longrightarrow B \tag{3.20}$$

the equilibrium constants are related by

$$K_{eq}' = \frac{K_{eq}}{[H^+]} \tag{3.21}$$

and $\Delta G^{\circ\prime}$ is given by

$$\Delta G^{\circ\prime} = \Delta G^{\circ} + RT \ln \left(\frac{1}{[H^+]}\right) = \Delta G^{\circ} - RT \ln [H^+] \tag{3.22}$$

3.4 • The Important Effect of Concentration on Net Free Energy Changes

Equation (3.12) shows that the free energy change for a reaction can be very different from the standard-state value if the concentrations of reactants and products differ significantly from unit activity (1 *M* for solutions). The effects can often be dramatic. Consider the hydrolysis of phosphocreatine:

$$\text{Phosphocreatine} + H_2O \longrightarrow \text{creatine} + P_i \tag{3.23}$$
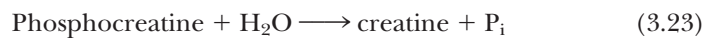
This reaction is strongly exergonic and ΔG° at 37°C is -42.8 kJ/mol. Physiological concentrations of phosphocreatine, creatine, and inorganic phosphate are normally between 1 m*M* and 10 m*M*. Assuming 1 m*M* concentrations and using Equation (3.12), the ΔG for the hydrolysis of phosphocreatine is

$$\Delta G = -42.8 \text{ kJ/mol} + (8.314 \text{ J/mol} \cdot \text{K})(310 \text{ K}) \ln \left(\frac{[0.001][0.001]}{[0.001]}\right) \tag{3.24}$$

$$\Delta G = -60.5 \text{ kJ/mol} \tag{3.25}$$

At 37°C, the difference between standard-state and 1 m*M* concentrations for such a reaction is thus approximately -17.7 kJ/mol.

3.5 • The Importance of Coupled Processes in Living Things

Many of the reactions necessary to keep cells and organisms alive must run against their **thermodynamic potential,** that is, in the direction of positive ΔG. Among these are the synthesis of adenosine triphosphate and other high-energy molecules and the creation of ion gradients in all mammalian cells. These processes are driven in the thermodynamically unfavorable direction via *coupling* with highly favorable processes. Many such *coupled processes* are discussed later in this text. They are crucially important in intermediary metabolism, oxidative phosphorylation, and membrane transport, as we shall see.

We can predict whether pairs of coupled reactions will proceed spontaneously by simply summing the free energy changes for each reaction. For example, consider the reaction from glycolysis (discussed in Chapter 19)
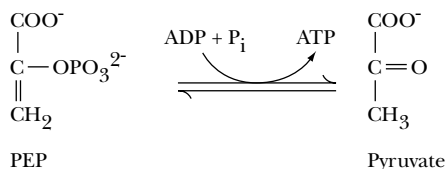
$$
\begin{array}{c}
\text{COO}^- \\
| \\
\text{C}-\text{OPO}_3{}^{2-} \\
\| \\
\text{CH}_2
\end{array}
\quad
\xrightarrow[]{\text{ADP} + \text{P}_i \qquad \text{ATP}}
\quad
\begin{array}{c}
\text{COO}^- \\
| \\
\text{C}=\text{O} \\
| \\
\text{CH}_3
\end{array}
$$

PEP   Pyruvate

FIGURE 3.7 • The pyruvate kinase reaction.

involving the conversion of phospho(enol)pyruvate (PEP) to pyruvate (Figure 3.7). The hydrolysis of PEP is energetically very favorable, and it is used to drive phosphorylation of ADP to form ATP, a process that is energetically unfavorable. Using values of ΔG that would be typical for a human erythrocyte:

$$\text{PEP} + \text{H}_2\text{O} \longrightarrow \text{pyruvate} + \text{P}_i \qquad \Delta G = -78 \text{ kJ/mol} \tag{3.26}$$

$$\text{ADP} + \text{P}_i \longrightarrow \text{ATP} + \text{H}_2\text{O} \qquad \Delta G = +55 \text{ kJ/mol} \tag{3.27}$$

$$\text{PEP} + \text{ADP} \longrightarrow \text{pyruvate} + \text{ATP} \qquad \text{Total } \Delta G = -23 \text{ kJ/mol} \tag{3.28}$$

The net reaction catalyzed by this enzyme depends upon coupling between the two reactions shown in Equations (3.26) and (3.27) to produce the net reaction shown in Equation (3.28) with a net negative $\Delta G^{\circ\prime}$. Many other examples of coupled reactions are considered in our discussions of intermediary metabolism (Part III). In addition, many of the complex biochemical systems discussed in the later chapters of this text involve reactions and processes with positive $\Delta G^{\circ\prime}$ values that are driven forward by coupling to reactions with a negative $\Delta G^{\circ\prime}$.
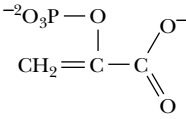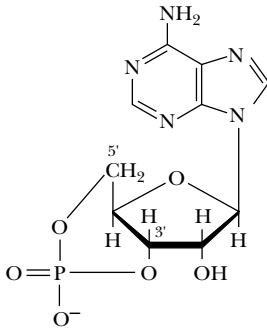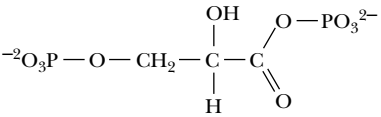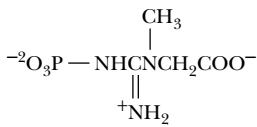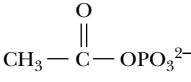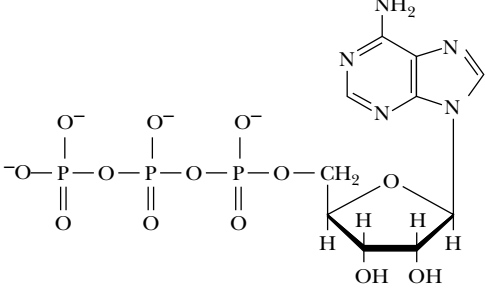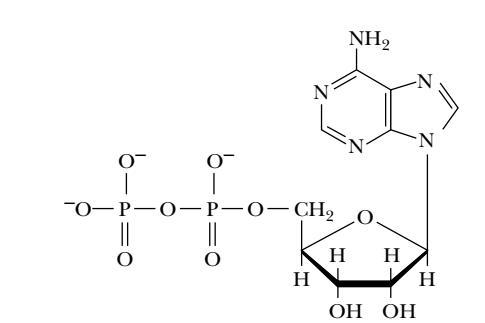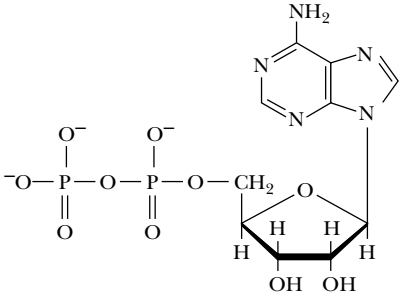
3.6 • The High-Energy Biomolecules

Virtually all life on earth depends on energy from the sun. Among life forms, there is a hierarchy of energetics: certain organisms capture solar energy directly, whereas others derive their energy from this group in subsequent processes. Organisms that absorb light energy directly are called **phototrophic organisms.** These organisms store solar energy in the form of various organic molecules. Organisms that feed on these latter molecules, releasing the stored energy in a series of oxidative reactions, are called **chemotrophic organisms.** Despite these differences, both types of organisms share common mechanisms for generating a useful form of chemical energy. Once captured in chemical form, energy can be released in controlled exergonic reactions to drive a variety of life processes (which require energy). A small family of universal biomolecules mediates the flow of energy from exergonic reactions to the energy-requiring processes of life. These molecules are the *reduced coenzymes* and the *high-energy phosphate compounds.* Phosphate compounds are considered high energy if they exhibit large negative free energies of hydrolysis (that is, if $\Delta G^{\circ\prime}$ is more negative than -25 kJ/mol).

    Table 3.3 lists the most important members of the high-energy phosphate compounds. Such molecules include *phosphoric anhydrides* (ATP, ADP), an *enol phosphate* (PEP), an *acyl phosphate* (acetyl phosphate), and a *guanidino phosphate* (creatine phosphate). Also included are thioesters, such as acetyl-CoA, which do not contain phosphorus, but which have a high free energy of hydrolysis. As noted earlier in this chapter, the exact amount of chemical free energy available from the hydrolysis of such compounds depends on concentration, pH, temperature, and so on, but the $\Delta G^{\circ\prime}$ values for hydrolysis of these substances are substantially more negative than for most other metabolic species. Two important points: first, high-energy phosphate compounds are not long-term energy storage substances. They are transient forms of stored energy, meant to carry energy from point to point, from one enzyme system to another, in the minute-to-minute existence of the cell. (As we shall see in subsequent chapters, other molecules bear the responsibility for long-term storage of energy

Table 3.3

Free Energies of Hydrolysis of Some High-Energy Compounds*

Compound (and Hydrolysis Product)	$\Delta G°'$ (kJ/mol)	Structure
Phosphoenolpyruvate (pyruvate + P_i)	−62.2	
3′,5′-Cyclic adenosine monophosphate (5′-AMP)	−50.4	
1,3-Bisphosphoglycerate (3-phosphoglycerate + P_i)	−49.6	
Creatine phosphate (creatine + P_i)	−43.3	
Acetyl phosphate (acetate + P_i)	−43.3	
Adenosine-5′-triphosphate (ADP + P_i)	−35.7[†]	
Adenosine-5′-triphosphate (ADP + P_i), excess Mg^{2+}	**−30.5**	
Adenosine-5′-diphosphate (AMP + P_i)	−35.7	
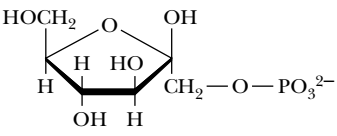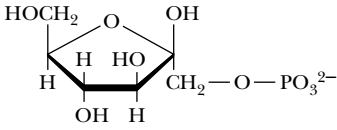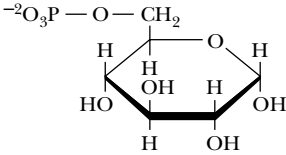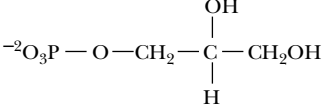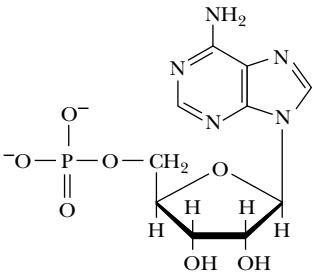
Table 3.3

Continued

Compound (and Hydrolysis Product)	$\Delta G°'$ (kJ/mol)	Structure
Pyrophosphate $(P_i + P_i)$ in 5 mM Mg^{2+}	−33.6	
Adenosine-5′-triphosphate $(AMP + PP_i)$, excess Mg^{2+}	−32.3	(See ATP structure on previous page)
Uridine diphosphoglucose (UDP + glucose)	−31.9	
Acetyl-coenzyme A (acetate + CoA)	−31.5	
S-adenosylmethionine (methionine + adenosine)	−25.6‡	

supplies.) Second, the term *high-energy compound* should not be construed to imply that these molecules are unstable and hydrolyze or decompose unpredictably. ATP, for example, is quite a stable molecule. A substantial activation energy must be delivered to ATP to hydrolyze the terminal, or γ, phosphate group. In fact, as shown in Figure 3.8, the *activation energy* that must be absorbed by the molecule to break the O—P$_\gamma$ bond is normally 200 to 400 kJ/mol, which is substantially larger than the net 30.5 kJ/mol released in the hydrolysis reaction. Biochemists are much more concerned with the *net release* of 30.5 kJ/mol

Compound (and Hydrolysis Product)	$\Delta G°'$ (kJ/mol)	Structure
Lower-Energy Phosphate Compounds		
Glucose-1-P (glucose + P_i)	−21.0	
Fructose-1-P (fructose + P_i)	−16.0	
Glucose-6-P (glucose + P_i)	−13.9	
sn-Glycerol-3-P (glycerol + P_i)	−9.2	
Adenosine-5′-monophosphate (adenosine + P_i)	−9.2	

*Adapted primarily from *Handbook of Biochemistry and Molecular Biology*, 1976, 3rd ed. In *Physical and Chemical Data*, G. Fasman, ed., Vol. 1, pp. 296–304. Boca Raton, FL: CRC Press.

†From Gwynn, R. W., and Veech, R. L., 1973. The equilibrium constants of the adenosine triphosphate hydrolysis and the adenosine triphosphate-citrate lyase reactions. *Journal of Biological Chemistry* **248:**6966–6972.

‡From Mudd, H., and Mann, J., 1963. Activation of methionine for transmethylation. *Journal of Biological Chemistry* **238:**2164–2170.

than with the activation energy for the reaction (because suitable enzymes cope with the latter). The net release of large quantities of free energy distinguishes the high-energy phosphoric anhydrides from their "low-energy" ester cousins, such as glycerol-3-phosphate (Table 3.3). The next section provides a quantitative framework for understanding these comparisons.
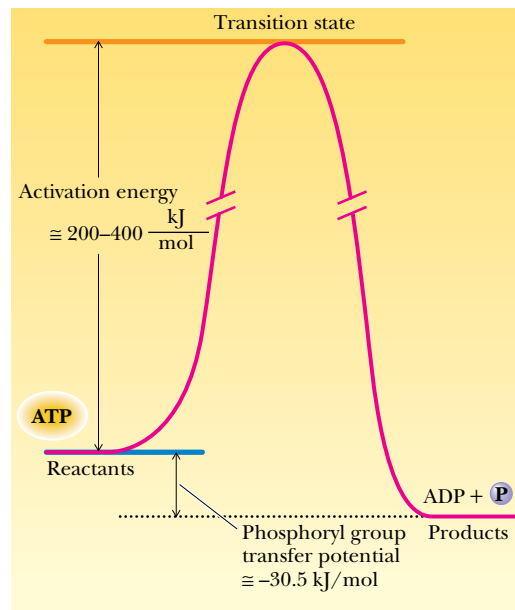
FIGURE 3.8 • The activation energies for phosphoryl group-transfer reactions (200 to 400 kJ/mol) are substantially larger than the free energy of hydrolysis of ATP (-30.5 kJ/mol).

ATP Is an Intermediate Energy-Shuttle Molecule

One last point about Table 3.3 deserves mention. Given the central importance of ATP as a high-energy phosphate in biology, students are sometimes surprised to find that ATP holds an intermediate place in the rank of high-energy phosphates. PEP, cyclic AMP, 1,3-BPG, phosphocreatine, acetyl phosphate, and pyrophosphate all exhibit higher values of $\Delta G°'$. This is not a biological anomaly. ATP is uniquely situated between the very high energy phosphates synthesized in the breakdown of fuel molecules and the numerous lower-energy acceptor molecules that are phosphorylated in the course of further metabolic reactions. ADP can accept both phosphates and energy from the higher-energy phosphates, and the ATP thus formed can donate both phosphates and energy to the lower-energy molecules of metabolism. The ATP/ADP pair is an intermediately placed acceptor/donor system among high-energy phosphates. In this context, ATP functions as a very versatile but intermediate energy-shuttle device that interacts with many different energy-coupling enzymes of metabolism.

Group Transfer Potential

Many reactions in biochemistry involve the transfer of a functional group from a donor molecule to a specific receptor molecule or to water. The concept of **group transfer potential** explains the tendency for such reactions to occur. Biochemists define the group transfer potential as the free energy change that occurs upon hydrolysis, that is, upon transfer of the particular group to water. This concept and its terminology are preferable to the more qualitative notion of *high-energy bonds*.

The concept of group transfer potential is not particularly novel. Other kinds of transfer (of hydrogen ions and electrons, for example) are commonly

Table 3.4

Types of Transfer Potential

	Proton Transfer Potential (Acidity)	Standard Reduction Potential (Electron Transfer Potential)	Group Transfer Potential (High-Energy Bond)
Simple equation	$AH \rightleftharpoons A^- + H^+$	$A \rightleftharpoons A^+ + e^-$	$A \sim P \rightleftharpoons A + P_i$
Equation including acceptor	$AH + H_2O \rightleftharpoons$ $A^- + H_3O^+$	$A + H^+ \rightleftharpoons$ $A^+ + \frac{1}{2} H_2$	$A \sim PO_4{}^{2-} + H_2O \rightleftharpoons$ $A{-}OH + HPO_4{}^{2-}$
Measure of transfer potential	$pK_a = \dfrac{\Delta G^\circ}{2.303\,RT}$	$\Delta \mathscr{E}_o = \dfrac{-\Delta G^\circ}{n\mathscr{F}}$	$\ln K_{eq} = \dfrac{-\Delta G^\circ}{RT}$
Free energy change of transfer is given by:	ΔG° per mole of H^+ transferred	ΔG° per mole of e^- transferred	ΔG° per mole of phosphate transferred

Adapted from: Klotz, I. M., 1986. *Introduction to Biomolecular Energetics.* New York: Academic Press.

characterized in terms of appropriate measures of transfer potential (pK_a and reduction potential, $\mathscr{E}_o$, respectively). As shown in Table 3.4, the notion of group transfer is fully analogous to those of ionization potential and reduction potential. The similarity is anything but coincidental, because all of these are really specific instances of free energy changes. If we write

$$AH \longrightarrow A^- + H^+ \tag{3.29a}$$

we really don't mean that a proton has literally been removed from the acid AH. In the gas phase at least, this would require the input of approximately 1200 kJ/mol! What we really mean is that the proton has been *transferred* to a suitable acceptor molecule, usually water:

$$AH + H_2O \longrightarrow A^- + H_3O^+ \tag{3.29b}$$

The appropriate free energy relationship is of course

$$pK_a = \frac{\Delta G^\circ}{2.303\,RT} \tag{3.30}$$

Similarly, in the case of an oxidation-reduction reaction

$$A \longrightarrow A^+ + e^- \tag{3.31a}$$
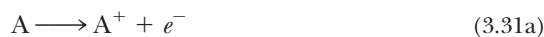
we don't really mean that A oxidizes independently. What we really mean (and what is much more likely in biochemical systems) is that the electron is transferred to a suitable acceptor:

$$A + H^+ \longrightarrow A^+ + \tfrac{1}{2} H_2 \tag{3.31b}$$

and the relevant free energy relationship is

$$\Delta \mathscr{E}_o = \frac{-\Delta G^\circ}{n\mathscr{F}} \tag{3.32}$$

where n is the number of equivalents of electrons transferred, and $\mathscr{F}$ is **Faraday's constant.**

Similarly, the release of free energy that occurs upon the hydrolysis of ATP and other "high-energy phosphates" can be treated quantitatively in terms of *group transfer*. It is common to write for the hydrolysis of ATP

$$ATP + H_2O \longrightarrow ADP + P_i \tag{3.33}$$
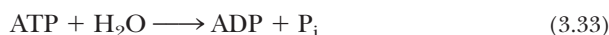
The free energy change, which we henceforth call the *group transfer potential,* is given by

$$\Delta G^\circ = -RT \ln K_{eq} \tag{3.34}$$

where K_{eq} is the equilibrium constant for the group transfer, which is normally written as

$$K_{eq} = \frac{[\text{ADP}][\text{P}_i]}{[\text{ATP}][\text{H}_2\text{O}]} \tag{3.35}$$

Even this set of equations represents an approximation, because ATP, ADP, and P_i all exist in solutions as a mixture of ionic species. This problem is discussed in a later section. For now, it is enough to note that the free energy changes listed in Table 3.3 are the group transfer potentials observed for transfers to water.

Phosphoric Acid Anhydrides

ATP contains two *pyrophosphoryl* or *phosphoric acid anhydride* linkages, as shown in Figure 3.9. Other common biomolecules possessing phosphoric acid anhydride linkages include ADP, GTP, GDP and the other nucleoside triphosphates, sugar nucleotides such as UDP-glucose, and inorganic pyrophosphate itself. All exhibit large negative free energies of hydrolysis, as shown in Table 3.3. The chemical reasons for the large negative $\Delta G^{\circ\prime}$ values for the hydrolysis reactions include destabilization of the reactant due to bond strain caused by electrostatic repulsion, stabilization of the products by ionization and resonance, and entropy factors due to hydrolysis and subsequent ionization.

Destabilization Due to Electrostatic Repulsion

Electrostatic repulsion in the reactants is best understood by comparing these phosphoric anhydrides with other reactive anhydrides, such as acetic anhydride. As shown in Figure 3.10a, the electronegative carbonyl oxygen atoms withdraw electrons from the C=O bonds, producing partial negative charges on the oxygens and partial positive charges on the carbonyl carbons. Each of
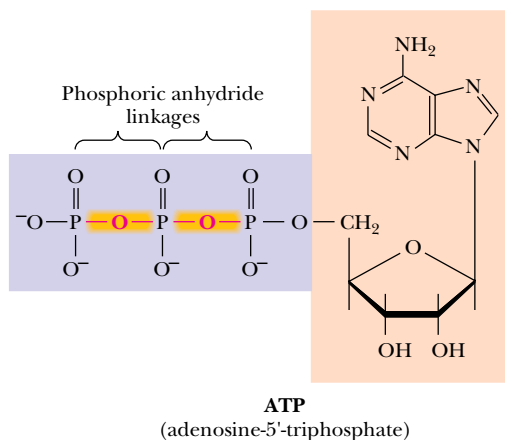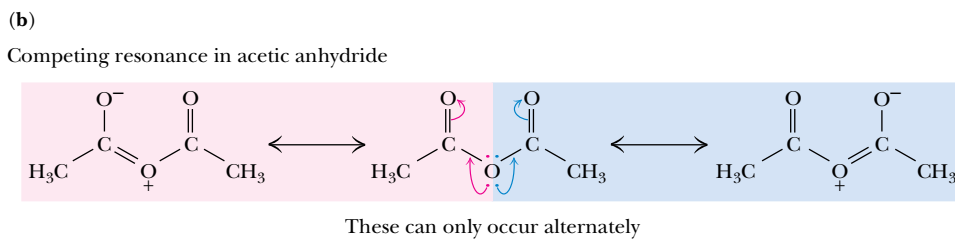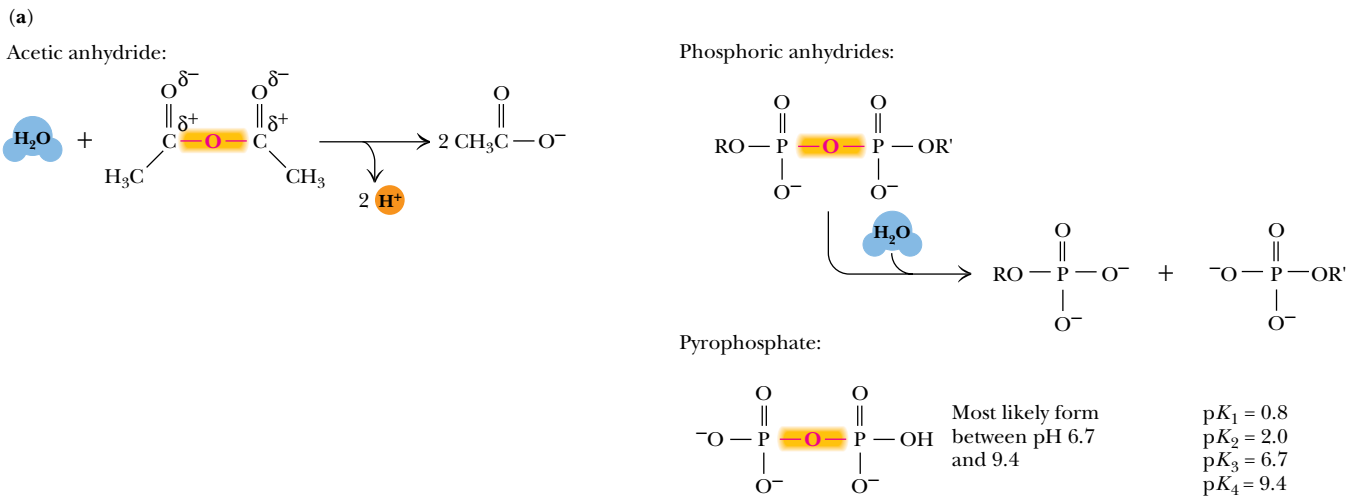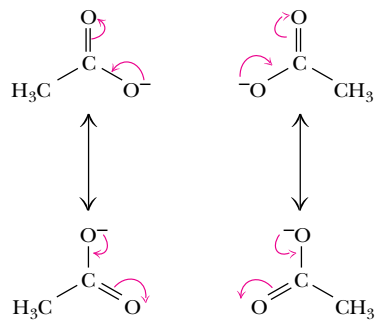

ATP
(adenosine-5'-triphosphate)

FIGURE 3.9 • The triphosphate chain of ATP contains two pyrophosphate linkages, both of which release large amounts of energy upon hydrolysis.

(a)

Acetic anhydride:

Phosphoric anhydrides:

Pyrophosphate:

Most likely form between pH 6.7 and 9.4	$pK_1 = 0.8$ $pK_2 = 2.0$ $pK_3 = 6.7$ $pK_4 = 9.4$

(b)

Competing resonance in acetic anhydride

These can only occur alternately

Simultaneous resonance in the hydrolysis products

These resonances can occur simultaneously

FIGURE 3.10 • (a) Electrostatic repulsion between adjacent partial positive charges (on carbon and phosphorus, respectively) is relieved upon hydrolysis of the anhydride bonds of acetic anhydride and phosphoric anhydrides. The predominant form of pyrophosphate at pH values between 6.7 and 9.4 is shown. (b) The competing resonances of acetic anhydride and the simultaneous resonance forms of the hydrolysis product, acetate.

these electrophilic carbonyl carbons is further destabilized by the other acetyl group, which is also electron-withdrawing in nature. As a result, acetic anhydride is unstable with respect to the products of hydrolysis.

The situation with phosphoric anhydrides is similar. The phosphorus atoms of the pyrophosphate anion are electron-withdrawing and destabilize PP_i with respect to its hydrolysis products. Furthermore, the reverse reaction, reformation of the anhydride bond from the two anionic products, requires that the electrostatic repulsion between these anions be overcome (see following).

Stabilization of Hydrolysis Products by Ionization and Resonance

The pyrophosphate moiety possesses three negative charges at pH values above 7.5 or so (note the pK_a values, Figure 3.10a). The hydrolysis products, two mole-

cules of inorganic phosphate, both carry about two negative charges, at pH values above 7.2. The increased ionization of the hydrolysis products helps to stabilize the electrophilic phosphorus nuclei.

Resonance stabilization in the products is best illustrated by the reactant anhydrides (Figure 3.10b). The unpaired electrons of the bridging oxygen atoms in acetic anhydride (and phosphoric anhydride) cannot participate in resonance structures with both electrophilic centers at once. This **competing resonance** situation is relieved in the product acetate or phosphate molecules.

Entropy Factors Arising from Hydrolysis and Ionization

For the phosphoric anhydrides, and for most of the high-energy compounds discussed here, there is an additional "entropic" contribution to the free energy of hydrolysis. Most of the hydrolysis reactions of Table 3.3 result in an increase in the number of molecules in solution. As shown in Figure 3.11, the hydrolysis of ATP (as pH values above 7) creates three species—ADP, inorganic phosphate (P_i), and a hydrogen ion—from only two reactants (ATP and H_2O). The entropy of the solution increases because the more particles, the more disordered the system.[3] (This effect is ionization-dependent because, at low pH, the

FIGURE 3.11 • Hydrolysis of ATP to ADP (and/or of ADP to AMP) leads to relief of electrostatic repulsion.
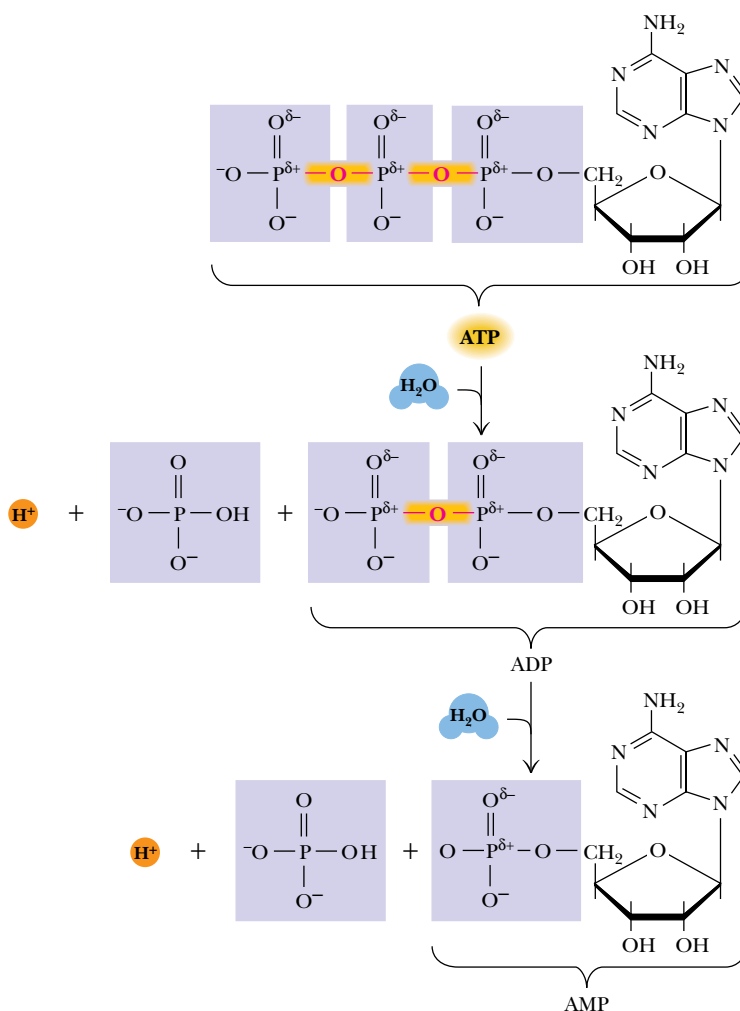
[3] Imagine the "disorder" created by hitting a crystal with a hammer and breaking it into many small pieces.

hydrogen ion created in many of these reactions simply protonates one of the phosphate oxygens, and one fewer "particle" results from the hydrolysis.)

A Comparison of the Free Energy of Hydrolysis of ATP, ADP, and AMP

The concepts of destabilization of reactants and stabilization of products described for pyrophosphate also apply for ATP and other phosphoric anhydrides (Figure 3.11). ATP and ADP are destabilized relative to the hydrolysis products by electrostatic repulsion, competing resonance, and entropy. AMP, on the other hand, is a phosphate ester (not an anhydride) possessing only a single phosphoryl group and is not markedly different from the product inorganic phosphate in terms of electrostatic repulsion and resonance stabilization. Thus, the $\Delta G°'$ for hydrolysis of AMP is much smaller than the corresponding values for ATP and ADP.

Phosphoric–Carboxylic Anhydrides

The mixed anhydrides of phosphoric and carboxylic acids, frequently called acyl phosphates, are also energy-rich. Two biologically important acyl phosphates are acetyl phosphate and 1,3-bisphosphoglycerate. Hydrolysis of these species yields acetate and 3-phosphoglycerate, respectively, in addition to inorganic phosphate (Figure 3.12). Once again, the large $\Delta G°'$ values indicate that the reactants are destabilized relative to products. This arises from bond strain, which can be traced to the partial positive charges on the carbonyl carbon and phosphorus atoms of these structures. The energy stored in the mixed anhydride bond (which is required to overcome the charge–charge repulsion) is released upon hydrolysis. Increased resonance possibilities in the products relative to the reactants also contribute to the large negative $\Delta G°'$ values. The
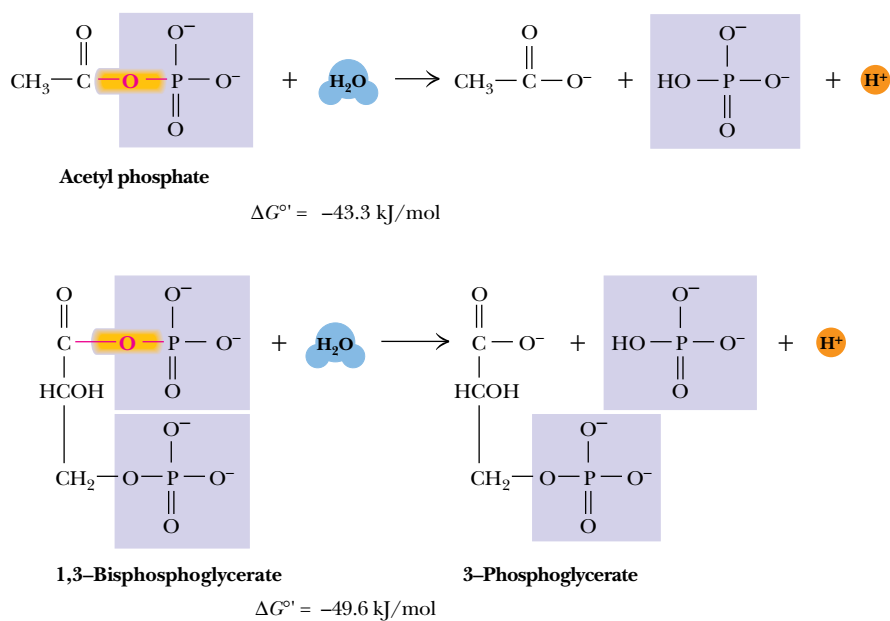

FIGURE 3.12 • The hydrolysis reactions of acetyl phosphate and 1,3-bisphosphoglycerate.
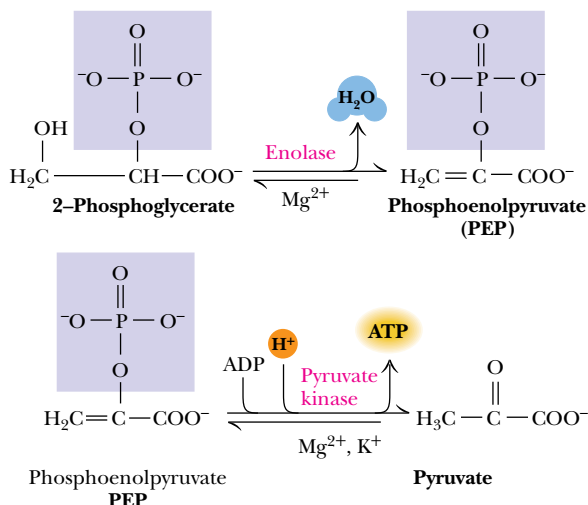
FIGURE 3.13 • Phosphoenolpyruvate (PEP) is produced by the enolase reaction (in glycolysis; see Chapter 19) and in turn drives the phosphorylation of ADP to form ATP in the pyruvate kinase reaction.

value of $\Delta G°'$ depends on the pK_a values of the starting anhydride and the product phosphoric and carboxylic acids, and of course also on the pH of the medium.

Enol Phosphates

The largest value of $\Delta G°'$ in Table 3.3 belongs to *phosphoenolpyruvate* or *PEP*, an example of an enolic phosphate. This molecule is an important intermediate in carbohydrate metabolism and, due to its large negative $\Delta G°'$, it is a potent phosphorylating agent. PEP is formed via dehydration of 2-phosphoglycerate by enolase during fermentation and glycolysis. PEP is subsequently transformed into pyruvate upon transfer of its phosphate to ADP by pyruvate kinase (Figure 3.13). The very large negative value of $\Delta G°'$ for the latter reaction is to a large extent the result of a secondary reaction of the *enol* form of pyruvate. Upon hydrolysis, the unstable enolic form of pyruvate immediately converts to the keto form with a resulting large negative $\Delta G°'$ (Figure 3.14). Together, the hydrolysis and subsequent *tautomerization* result in an overall $\Delta G°'$ of -62.2 kJ/mol.
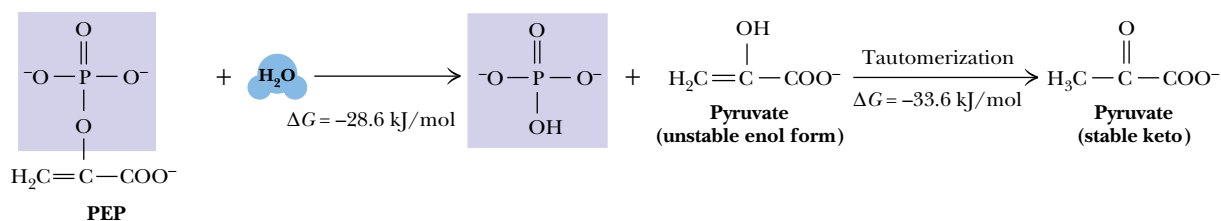

FIGURE 3.14 • Hydrolysis and the subsequent tautomerization account for the very large $\Delta G°'$ of PEP.
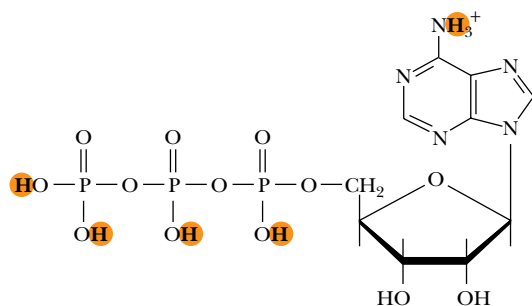
FIGURE 3.15 • Adenosine 5′-triphosphate (ATP).

Color indicates the locations of the five dissociable protons of ATP.

3.7 • Complex Equilibria Involved in ATP Hydrolysis

So far, as in Equation (3.33), the hydrolyses of ATP and other high-energy phosphates have been portrayed as simple processes. The situation in a real biological system is far more complex, owing to the operation of several ionic equilibria. First, ATP, ADP, and the other species in Table 3.3 can exist in several different ionization states that must be accounted for in any quantitative analysis. Second, phosphate compounds bind a variety of divalent and monovalent cations with substantial affinity, and the various metal complexes must also be considered in such analyses. Consideration of these special cases makes the quantitative analysis far more realistic. The importance of these multiple equilibria in group transfer reactions is illustrated for the hydrolysis of ATP, but the principles and methods presented are general and can be applied to any similar hydrolysis reaction.

The Multiple Ionization States of ATP and the pH Dependence of $\Delta G°'$

ATP has five dissociable protons, as indicated in Figure 3.15. Three of the protons on the triphosphate chain dissociate at very low pH. The adenine ring amino group exhibits a pK_a of 4.06, whereas the last proton to dissociate from the triphosphate chain possesses a pK_a of 6.95. At higher pH values, ATP is completely deprotonated. ADP and phosphoric acid also undergo multiple ionizations. These multiple ionizations make the equilibrium constant for ATP hydrolysis more complicated than the simple expression in Equation (3.35). Multiple ionizations must also be taken into account when the pH dependence of $\Delta G°$ is considered. The calculations are beyond the scope of this text, but Figure 3.16 shows the variation of $\Delta G°$ as a function of pH. The free energy of hydrolysis is nearly constant from pH 4 to pH 6. At higher values of pH, $\Delta G°$ varies linearly with pH, becoming more negative by 5.7 kJ/mol for every pH unit of increase at 37°C. Because the pH of most biological tissues and fluids is near neutrality, the effect on $\Delta G°$ is relatively small, but it must be taken into account in certain situations.

The Effect of Metal Ions on the Free Energy of Hydrolysis of ATP

Most biological environments contain substantial amounts of divalent and monovalent metal ions, including Mg^{2+}, Ca^{2+}, Na^+, K^+, and so on. What effect do metal ions have on the equilibrium constant for ATP hydrolysis and the
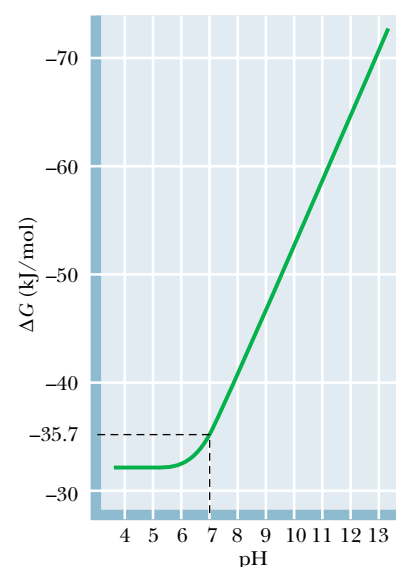

FIGURE 3.16 • The pH dependence of the free energy of hydrolysis of ATP. Because pH varies only slightly in biological environments, the effect on ΔG is usually small.
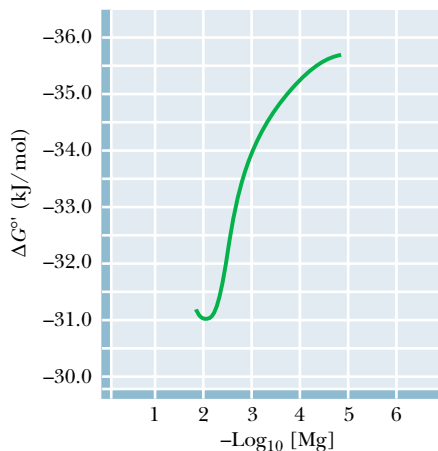
FIGURE 3.17 • The free energy of hydrolysis of ATP as a function of total Mg^{2+} ion concentration at 38°C and pH 7.0. *(Adapted from Gwynn, R. W., and Veech, R. L., 1973. The equilibrium constants of the adenosine triphosphate hydrolysis and the adenosine triphosphate-citrate lyase reactions.* Journal of Biological Chemistry **248:***6966–6972.)*

associated free energy change? Figure 3.17 shows the change in $\Delta G^{\circ\prime}$ with pMg (that is, $-\log_{10}[Mg^{2+}]$) at pH 7.0 and 38°C. The free energy of hydrolysis of ATP at zero Mg^{2+} is -35.7 kJ/mol, and at 5 mM free Mg^{2+} (the minimum in the plot) the $\Delta G_{obs}{}^{\circ}$ is approximately -31 kJ/mol. Thus, in most real biological environments (with pH near 7 and Mg^{2+} concentrations of 5 mM or more) the free energy of hydrolysis of ATP is altered more by metal ions than by protons. A widely used "consensus value" for $\Delta G^{\circ\prime}$ of ATP in biological systems is **−30.5 kJ/mol** (Table 3.3). This value, cited in the 1976 *Handbook of Biochemistry and Molecular Biology* (3rd ed., *Physical and Chemical Data*, Vol. 1, pp. 296–304, Boca Raton, FL: CRC Press), was determined in the presence of "excess Mg^{2+}." *This is the value we use for metabolic calculations in the balance of this text.*

The Effect of Concentration on the Free Energy of Hydrolysis of ATP

Through all these calculations of the effect of pH and metal ions on the ATP hydrolysis equilibrium, we have assumed "standard conditions" with respect to concentrations of all species except for protons. The levels of ATP, ADP, and other high-energy metabolites never even begin to approach the standard state of 1 M. In most cells, the concentrations of these species are more typically 1 to 5 mM or even less. Earlier, we described the effect of concentration on equilibrium constants and free energies in the form of Equation (3.12). For the present case, we can rewrite this as

$$\Delta G = \Delta G^{\circ} + RT \ln \frac{[\Sigma ADP][\Sigma P_i]}{[\Sigma ATP]} \tag{3.36}$$

where the terms in brackets represent the sum (Σ) of the concentrations of all the ionic forms of ATP, ADP, and P_i.

It is clear that changes in the concentrations of these species can have large effects on ΔG. The concentrations of ATP, ADP, and P_i may, of course, vary rather independently in real biological environments, but if, for the sake of some model calculations, we assume that all three concentrations are equal, then the effect of concentration on ΔG is as shown in Figure 3.18. The free energy of hydrolysis of ATP, which is -35.7 kJ/mol at 1 M, becomes -49.4 kJ/mol at 5 mM (that is, the concentration for which p$C = -2.3$ in Figure 3.18). At 1 mM ATP, ADP, and P_i, the free energy change becomes even more negative at -53.6 kJ/mol. *Clearly, the effects of concentration are much greater than the effects of protons or metal ions under physiological conditions.*

Does the "concentration effect" change ATP's position in the energy hierarchy (in Table 3.3)? Not really. All the other high- and low-energy phosphates experience roughly similar changes in concentration under physiological conditions and thus similar changes in their free energies of hydrolysis. The roles of the very high-energy phosphates (PEP, 1,3-bisphosphoglycerate, and creatine phosphate) in the synthesis and maintenance of ATP in the cell are considered in our discussions of metabolic pathways. In the meantime, several of the problems at the end of this chapter address some of the more interesting cases.

FIGURE 3.18 • The free energy of hydrolysis of ATP as a function of concentration at 38°C, pH 7.0. The plot follows the relationship described in Equation (3.36), with the concentrations [C] of ATP, ADP, and P_i assumed to be equal.

3.8 • The Daily Human Requirement for ATP

We can end this discussion of ATP and the other important high-energy compounds in biology by discussing the daily metabolic consumption of ATP by humans. An approximate calculation gives a somewhat surprising and impressive result. Assume that the average adult human consumes approximately
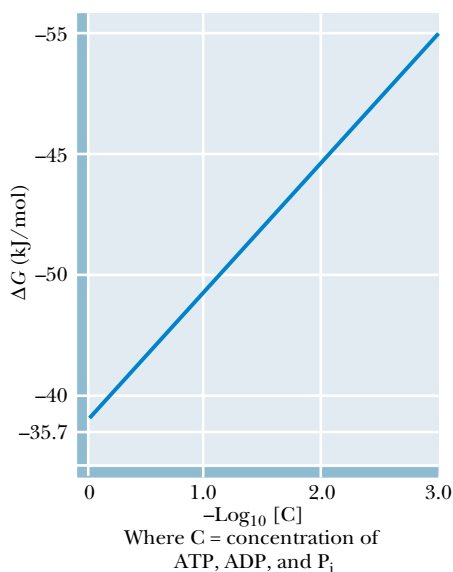
11,700 kJ (2800 kcal, that is, 2,800 Calories) per day. Assume also that the metabolic pathways leading to ATP synthesis operate at a thermodynamic efficiency of approximately 50%. Thus, of the 11,700 kJ a person consumes as food, about 5,860 kJ end up in the form of synthesized ATP. As indicated earlier, the hydrolysis of 1 mole of ATP yields approximately 50 kJ of free energy under cellular conditions. This means that the body cycles through $5860/50 = 117$ moles of ATP each day. The disodium salt of ATP has a molecular weight of 551 g/mol, so that an average person hydrolyzes about

$$(117 \text{ moles})\frac{551 \text{ g}}{\text{mole}} = 64,467 \text{ g of ATP per day}$$

The average adult human, with a typical weight of 70 kg or so, thus consumes approximately 65 kilograms of ATP per day, an amount nearly equal to his/her own body weight! Fortunately, we have a highly efficient recycling system for ATP/ADP utilization. The energy released from food is stored transiently in the form of ATP. Once ATP energy is used and ADP and phosphate are released, our bodies recycle it to ATP through intermediary metabolism, so that it may be reused. The typical 70-kg body contains only about 50 grams of ATP/ADP total. Therefore, each ATP molecule in our bodies must be recycled nearly 1300 times each day! Were it not for this fact, at current commercial prices of about $10 per gram, our ATP "habit" would cost approximately $650,000 per day! In these terms, the ability of biochemistry to sustain the marvelous activity and vigor of organisms gains our respect and fascination.

PROBLEMS

1. An enzymatic hydrolysis of fructose-1-P,

$$\text{Fructose-1-P} + H_2O \rightleftharpoons \text{fructose} + P_i$$

was allowed to proceed to equilibrium at 25°C. The original concentration of fructose-1-P was 0.2 M, but when the system had reached equilibrium the concentration of fructose-1-P was only 6.52×10^{-5} M. Calculate the equilibrium constant for this reaction and the free energy of hydrolysis of fructose-1-P.

2. The equilibrium constant for some process A $\rightleftharpoons$ B is 0.5 at 20°C and 10 at 30°C. Assuming that $\Delta H°$ is independent of temperature, calculate $\Delta H°$ for this reaction. Determine $\Delta G°$ and $\Delta S°$ at 20° and at 30°C. Why is it important in this problem to assume that $\Delta H°$ is independent of temperature?

3. The standard-state free energy of hydrolysis for acetyl phosphate is $\Delta G° = -42.3$ kJ/mol.

$$\text{Acetyl-P} + H_2O \longrightarrow \text{acetate} + P_i$$

Calculate the free energy change for acetyl phosphate hydrolysis in a solution of 2 mM acetate, 2 mM phosphate, and 3 nM acetyl phosphate.

4. Define a state function. Name three thermodynamic quantities that are state functions and three that are not.

5. ATP hydrolysis at pH 7.0 is accompanied by release of a hydrogen ion to the medium

$$\text{ATP}^{4-} + H_2O \rightleftharpoons \text{ADP}^{3-} + \text{HPO}_4^{2-} + H^+$$

If the $\Delta G°'$ for this reaction is -30.5 kJ/mol, what is $\Delta G°$ (that is, the free energy change for the same reaction with all components, including H^+, at a standard state of 1 M)?

6. For the process A $\rightleftharpoons$ B, $K_{eq}(AB)$ is 0.02 at 37°C. For the process B $\rightleftharpoons$ C, $K_{eq}(BC) = 1000$ at 37°C.

a. Determine $K_{eq}(AC)$, the equilibrium constant for the overall process A $\rightleftharpoons$ C, from $K_{eq}(AB)$ and $K_{eq}(BC)$.

b. Determine standard-state free energy changes for all three processes, and use $\Delta G°(AC)$ to determine $K_{eq}(AC)$. Make sure that this value agrees with that determined in part a of this problem.

7. Draw all possible resonance structures for creatine phosphate and discuss their possible effects on resonance stabilization of the molecule.
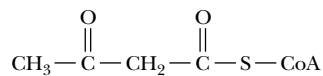
8. Write the equilibrium constant, K_{eq}, for the hydrolysis of creatine phosphate and calculate a value for K_{eq} at 25°C from the value of $\Delta G°'$ in Table 3.3.

9. Imagine that creatine phosphate, rather than ATP, is the universal energy carrier molecule in the human body. Repeat the calculation presented in Section 3.8, calculating the weight of creatine phosphate that would need to be consumed each day by a typical adult human if creatine phosphate could not be recycled. If recycling of creatine phosphate were possible, and if the typical adult human body contained 20 grams of creatine phosphate, how many times would each creatine phosphate molecule need to be turned over or recycled each day? Repeat the calculation assuming that glycerol-3-phosphate is the universal energy carrier, and that the body contains 20 grams of glycerol-3-phosphate.

10. Calculate the free energy of hydrolysis of ATP in a rat liver cell in which the ATP, ADP, and P_i concentrations are 3.4, 1.3, and 4.8 mM, respectively.

11. Hexokinase catalyzes the phosphorylation of glucose from ATP, yielding glucose-6-P and ADP. Using the values of Table 3.3, calculate the standard-state free energy change and equilibrium constant for the hexokinase reaction.

12. Would you expect the free energy of hydrolysis of aceto-acetyl-coenzyme A (see diagram) to be greater than, equal to, or less than that of acetyl-coenzyme A? Provide a chemical rationale for your answer.

$$CH_3 - \overset{\overset{\displaystyle O}{\|}}{C} - CH_2 - \overset{\overset{\displaystyle O}{\|}}{C} - S - CoA$$

13. Consider carbamoyl phosphate, a precursor in the biosynthesis of pyrimidines:

$$H_3\overset{+}{N} \diagup \overset{\overset{\displaystyle O}{\overset{\displaystyle \|}{C}}}{} \diagdown O - PO_3{}^{2-}$$
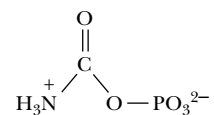
Based on the discussion of high-energy phosphates in this chapter, would you expect carbamoyl phosphate to possess a high free energy of hydrolysis? Provide a chemical rationale for your answer.

FURTHER READING

Alberty, R. A., 1968. Effect of pH and metal ion concentration on the equilibrium hydrolysis of adenosine triphosphate to adenosine diphosphate. *Journal of Biological Chemistry* **243:**1337–1343.

Alberty, R. A., 1969. Standard Gibbs free energy, enthalpy, and entropy changes as a function of pH and pMg for reactions involving adenosine phosphates. *Journal of Biological Chemistry* **244:**3290–3302.

Brandts, J. F., 1964. The thermodynamics of protein denaturation. I. The denaturation of chymotrypsinogen. *Journal of the American Chemical Society* **86:**4291–4301.

Cantor, C. R., and Schimmel, P. R., 1980. *Biophysical Chemistry.* San Francisco: W.H. Freeman.

Dickerson, R. E., 1969. *Molecular Thermodynamics.* New York: Benjamin Co.

Edsall, J. T., and Gutfreund, H., 1983. *Biothermodynamics: The Study of Biochemical Processes at Equilibrium.* New York: John Wiley.

Edsall, J. T., and Wyman, J., 1958. *Biophysical Chemistry.* New York: Academic Press.

Gwynn, R. W., and Veech, R. L., 1973. The equilibrium constants of the adenosine triphosphate hydrolysis and the adenosine triphosphate-citrate lyase reactions. *Journal of Biological Chemistry* **248:**6966–6972.

Klotz, I. M., 1967. *Energy Changes in Biochemical Reactions.* New York: Academic Press.

Lehninger, A. L., 1972. *Bioenergetics,* 2nd ed. New York: Benjamin Co.

Morris, J. G., 1968. *A Biologist's Physical Chemistry.* Reading, MA: Addison-Wesley.

Patton, A. R., 1965. *Biochemical Energetics and Kinetics.* Philadelphia: W.B. Saunders.

Schrödinger, E., 1945. *What Is Life?* New York: Macmillan.

Segel, I. H., 1976. *Biochemical Calculations,* 2nd ed. New York: John Wiley.

Tanford, C., 1980. *The Hydrophobic Effect,* 2nd ed. New York: John Wiley.

*C*hapter 4

Amino Acids

All objects have mirror images. Like many biomolecules, amino acids exist in mirror-image forms (stereoisomers) that are not superimposable. Only the L-isomers of amino acids commonly occur in nature. (The Mirror of Venus *(1898), Sir Edward Burne-Jones/Museu Calouste Gulbenkian Lisbon/The Bridgeman Art Library)*

Proteins are the indispensable agents of biological function, and **amino acids** are the building blocks of proteins. The stunning diversity of the thousands of proteins found in nature arises from the intrinsic properties of only 20 commonly occurring amino acids. These features include (1) the capacity to polymerize, (2) novel acid–base properties, (3) varied structure and chemical functionality in the amino acid side chains, and (4) chirality. This chapter describes each of these properties, laying a foundation for discussions of protein structure (Chapters 5 and 6), enzyme function (Chapters 14–16), and many other subjects in later chapters.

4.1 • Amino Acids: Building Blocks of Proteins

Structure of a Typical Amino Acid

The structure of a single typical amino acid is shown in Figure 4.1. Central to this structure is the tetrahedral alpha (α) carbon (C_α), which is covalently linked to both the amino group and the carboxyl group. Also bonded to this α-carbon is a hydrogen and a variable side chain. It is the side chain, the so-called R group, that gives each amino acid its identity. The detailed acid–base properties of amino acids are discussed in the following sections. It is sufficient for now to realize that, in neutral solution (pH 7), the carboxyl group exists as —COO^- and the amino group as —NH_3^+. Because the resulting amino acid contains one positive and one negative charge, it is a neutral molecule called a **zwitterion.** Amino acids are also *chiral* molecules. With four different groups attached to it, the α-carbon is said to be *asymmetric.* The two possible configurations for the α-carbon constitute nonidentical mirror image isomers or *enantiomers.* Details of amino acid stereochemistry are discussed in Section 4.4.

Amino Acids Can Join via Peptide Bonds

The crucial feature of amino acids that allows them to polymerize to form peptides and proteins is the existence of their two identifying chemical groups: the amino (—NH_3^+) and carboxyl (—COO^-) groups, as shown in Figure 4.2. The amino and carboxyl groups of amino acids can react in a head-to-tail fashion, eliminating a water molecule and forming a covalent amide linkage, which, in the case of peptides and proteins, is typically referred to as a **peptide bond.** The equilibrium for this reaction in aqueous solution favors peptide bond hydrolysis. For this reason, biological systems as well as peptide chemists in the laboratory must carry out peptide bond formation in an indirect manner or with energy input.

Iteration of the reaction shown in Figure 4.2 produces **polypeptides** and **proteins.** The remarkable properties of proteins, which we shall discover and come to appreciate in later chapters, all depend in one way or another on the unique properties and chemical diversity of the 20 common amino acids found in proteins.

Common Amino Acids

The structures and abbreviations for the 20 amino acids commonly found in proteins are shown in Figure 4.3. All the amino acids except proline have both free α-amino and free α-carboxyl groups (Figure 4.1). There are several ways to classify the common amino acids. The most useful of these classifications is based on the polarity of the side chains. Thus, the structures shown in Figure 4.3 are grouped into the following categories: (1) nonpolar or hydrophobic
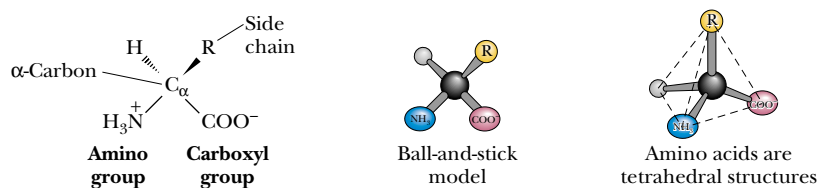

FIGURE 4.1 • Anatomy of an amino acid. Except for proline and its derivatives, all of the amino acids commonly found in proteins possess this type of structure.
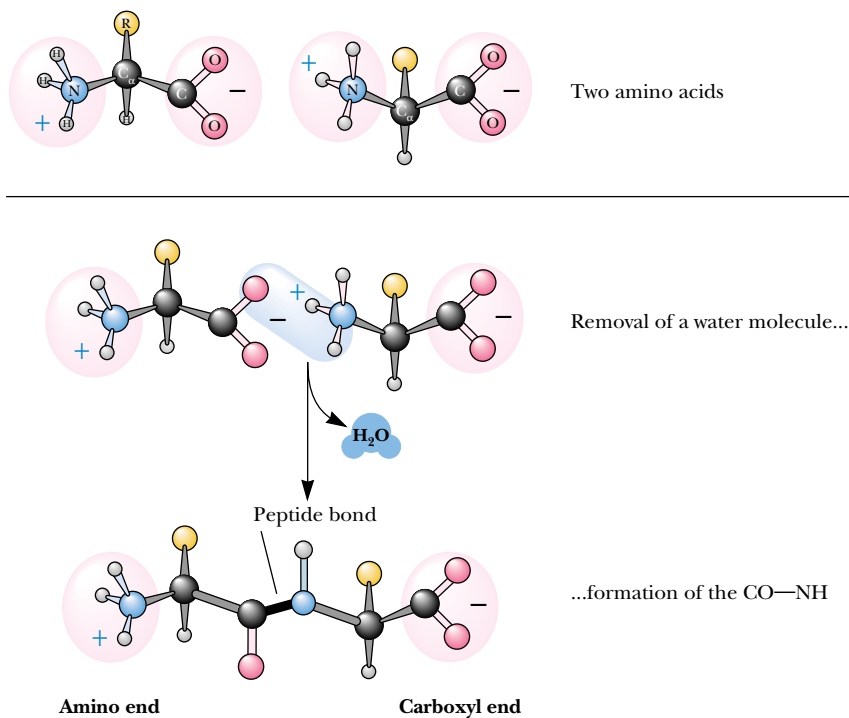
Two amino acids

Removal of a water molecule...

H_2O

Peptide bond

...formation of the CO—NH

Amino end **Carboxyl end**

FIGURE 4.2 • The α-COOH and α-NH$_3^+$ groups of two amino acids can react with the resulting loss of a water molecule to form a covalent amide bond. *(Irving Geis.)*

amino acids, (2) neutral (uncharged) but polar amino acids, (3) acidic amino acids (which have a net negative charge at pH 7.0), and (4) basic amino acids (which have a net positive charge at neutral pH). In later chapters, the importance of this classification system for predicting protein properties becomes clear. Also shown in Figure 4.3 are the three-letter and one-letter codes used to represent the amino acids. These codes are useful when displaying and comparing the sequences of proteins in shorthand form. (Note that several of the one-letter abbreviations are phonetic in origin: arginine = "Rginine" = R, phenylalanine = "Fenylalanine" = F, aspartic acid = "asparDic" = D.)

Nonpolar Amino Acids

The nonpolar amino acids (Figure 4.3a) include all those with alkyl chain R groups (alanine, valine, leucine, and isoleucine), as well as proline (with its unusual cyclic structure), methionine (one of the two sulfur-containing amino acids), and two aromatic amino acids, phenylalanine and tryptophan. Tryptophan is sometimes considered a borderline member of this group because it can interact favorably with water via the N–H moiety of the indole ring. Proline, strictly speaking, is not an amino acid but rather an α-imino acid.

Polar, Uncharged Amino Acids

The polar, uncharged amino acids (Figure 4.3b) except for glycine contain R groups that can form hydrogen bonds with water. Thus, these amino acids are usually more soluble in water than the nonpolar amino acids. Several exceptions should be noted. Tyrosine displays the lowest solubility in water of the 20 common amino acids (0.453 g/L at 25°C). Also, proline is very soluble in water, and alanine and valine are about as soluble as arginine and serine. The amide groups of asparagine and glutamine; the hydroxyl groups of tyrosine, threonine, and serine; and the sulfhydryl group of cysteine are all good hydrogen
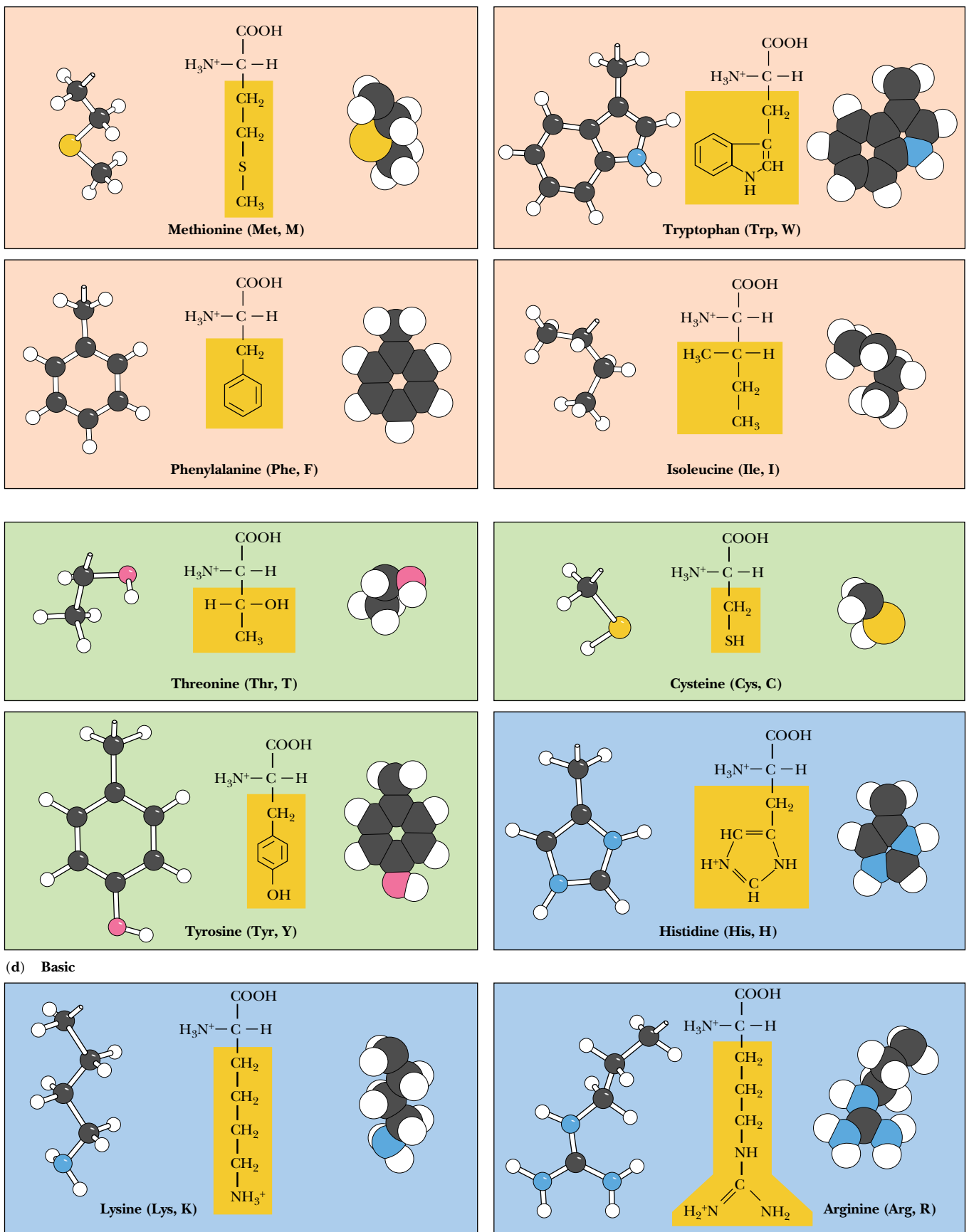
FIGURE 4.3 • The 20 amino acids that are the building blocks of most proteins can be classified as (a) nonpolar (hydrophobic), (b) polar, neutral, (c) acidic, or (d) basic.

(a) Nonpolar (hydrophobic)

Leucine (Leu, L)

Proline (Pro, P)

Alanine (Ala, A)

Valine (Val, V)

(b)   Polar, uncharged

Glycine (Gly, G)

Serine (Ser, S)

Asparagine (Asn, N)

Glutamine (Gln, Q)

(c)   Acidic

Aspartic acid (Asp, D)

Glutamic acid (Glu, E)
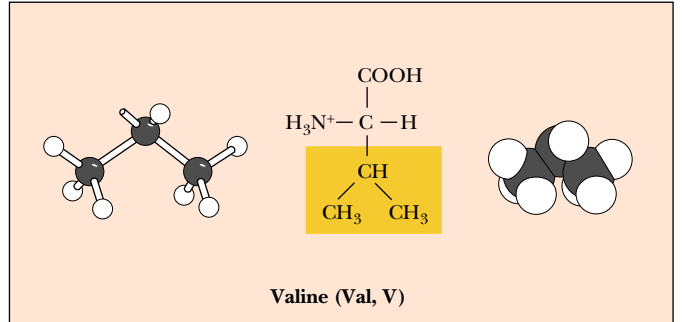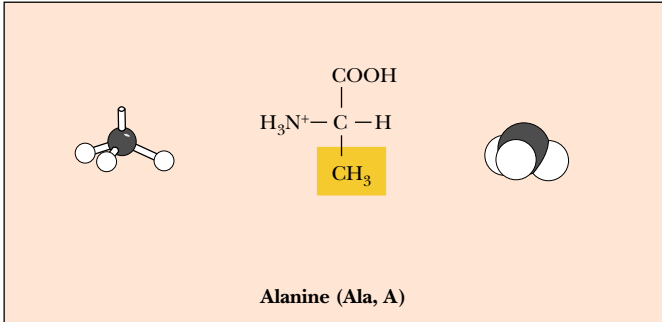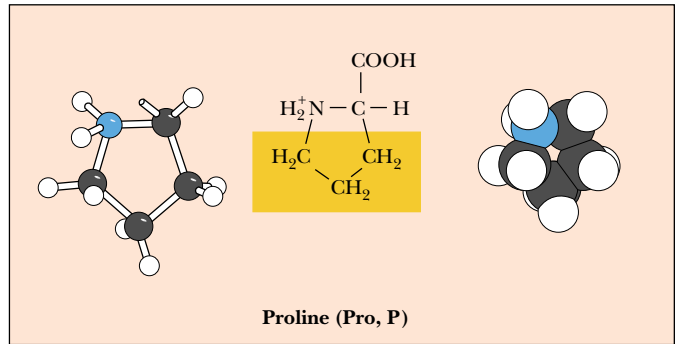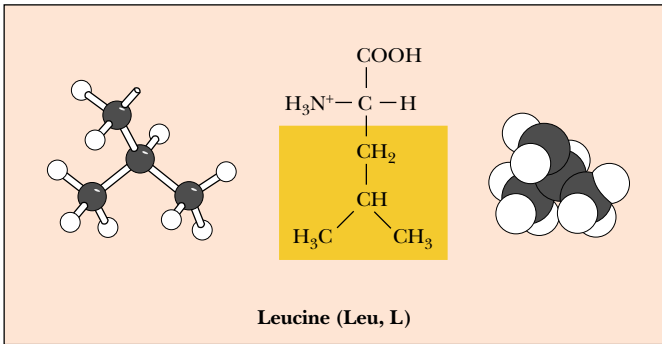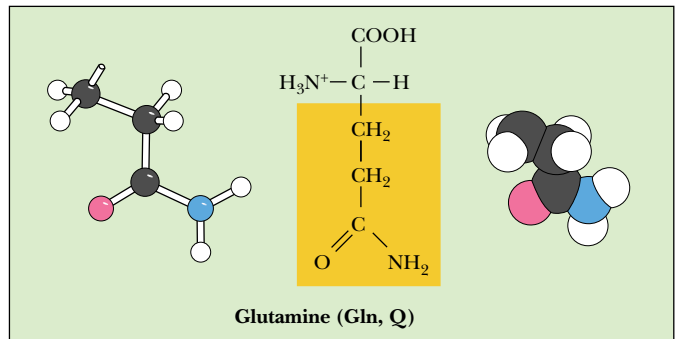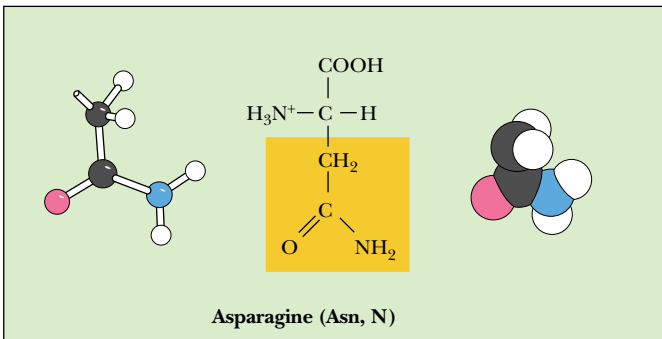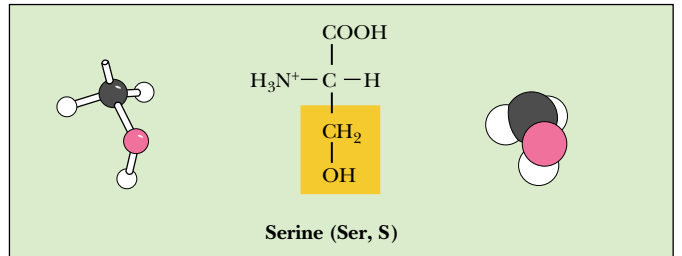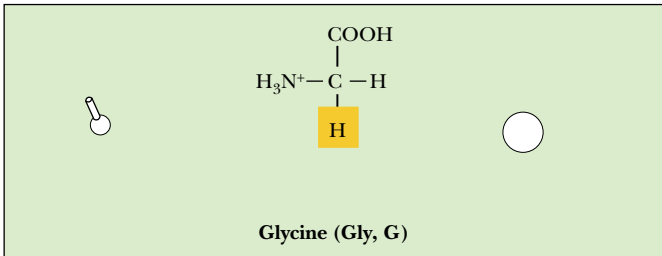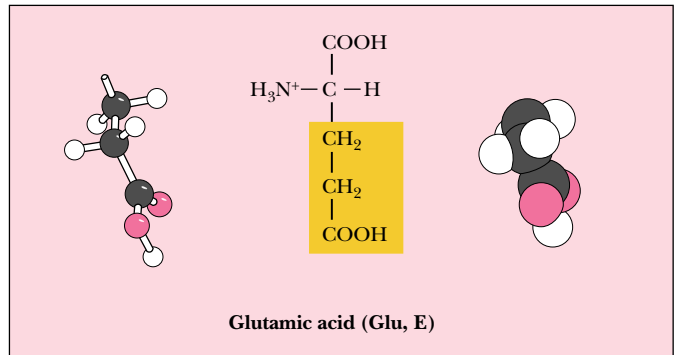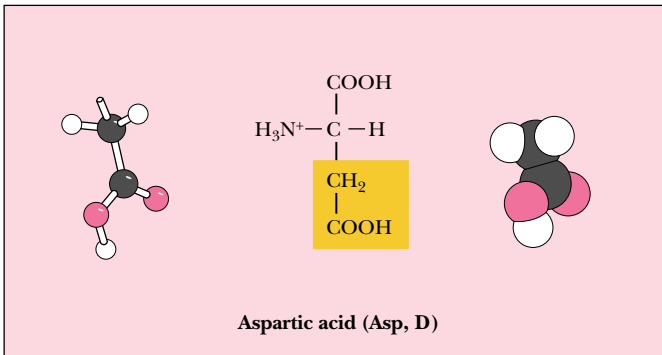
Also shown are the one-letter and three-letter codes used to denote amino acids. For each amino acid, the ball-and-stick *(left)* and space-filling *(right)* models show only the side chain. *(Irving Geis)*

bond–forming moieties. Glycine, the simplest amino acid, has only a single hydrogen for an R group, and this hydrogen is not a good hydrogen bond former. Glycine's solubility properties are mainly influenced by its polar amino and carboxyl groups, and thus glycine is best considered a member of the polar, uncharged group. It should be noted that tyrosine has significant nonpolar characteristics due to its aromatic ring and could arguably be placed in the nonpolar group (Figure 4.3a). However, with a pK_a of 10.1, tyrosine's phenolic hydroxyl is a charged, polar entity at high pH.

Acidic Amino Acids

There are two acidic amino acids—aspartic acid and glutamic acid—whose R groups contain a carboxyl group (Figure 4.3c). These side chain carboxyl groups are weaker acids than the α-COOH group, but are sufficiently acidic to exist as —COO$^-$ at neutral pH. Aspartic acid and glutamic acid thus have a net negative charge at pH 7. These negatively charged amino acids play several important roles in proteins. Many proteins that bind metal ions for structural or functional purposes possess metal binding sites containing one or more aspartate and glutamate side chains. Carboxyl groups may also act as nucleophiles in certain enzyme reactions and may participate in a variety of electrostatic bonding interactions. The acid–base chemistry of such groups is considered in detail in Section 4.2.

Basic Amino Acids

Three of the common amino acids have side chains with net positive charges at neutral pH: histidine, arginine, and lysine (Figure 4.3d). The ionized group of histidine is an imidazolium, that of arginine is a guanidinium, and lysine contains a protonated alkyl amino group. The side chains of the latter two amino acids are fully protonated at pH 7, but histidine, with a side chain pK_a of 6.0, is only 10% protonated at pH 7. With a pK_a near neutrality, histidine side chains play important roles as proton donors and acceptors in many enzyme reactions. Histidine-containing peptides are important biological buffers, as discussed in Chapter 2. Arginine and lysine side chains, which are protonated under physiological conditions, participate in electrostatic interactions in proteins.

Uncommon Amino Acids

Several amino acids occur only rarely in proteins (Figure 4.4). These include **hydroxylysine** and **hydroxyproline,** which are found mainly in the collagen and gelatin proteins, and **thyroxine** and **3,3′,5-triiodothyronine,** iodinated amino acids that are found only in thyroglobulin, a protein produced by the thyroid gland. (Thyroxine and 3,3′,5-triiodothyronine are produced by iodination of tyrosine residues in thyroglobulin in the thyroid gland. Degradation of thyroglobulin releases these two iodinated amino acids, which act as hormones to regulate growth and development.) Certain muscle proteins contain methylated amino acids, including **methylhistidine,** ϵ-**N-methyllysine,** and ϵ-**N,N, N-trimethyllysine** (Figure 4.4). γ-**Carboxyglutamic acid** is found in several proteins involved in blood clotting, and **pyroglutamic acid** is found in a unique light-driven proton-pumping protein called bacteriorhodopsin, which is discussed elsewhere in this book. Certain proteins involved in cell growth and regulation are reversibly phosphorylated on the —OH groups of serine, threonine, and tyrosine residues. **Aminoadipic acid** is found in proteins isolated from corn. Finally, *N*-**methylarginine** and *N*-**acetyllysine** are found in histone proteins associated with chromosomes.
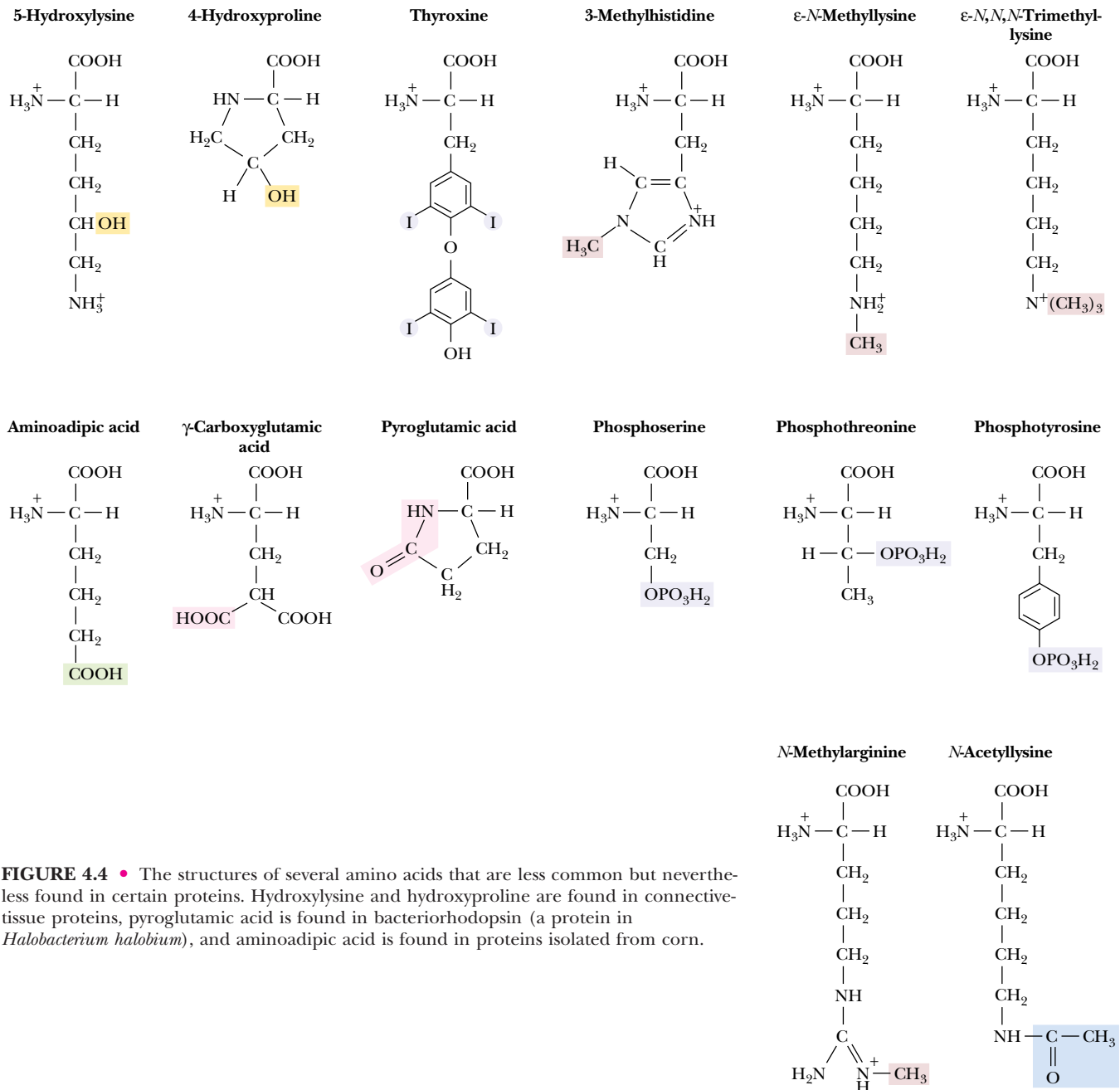
FIGURE 4.4 • The structures of several amino acids that are less common but nevertheless found in certain proteins. Hydroxylysine and hydroxyproline are found in connective-tissue proteins, pyroglutamic acid is found in bacteriorhodopsin (a protein in *Halobacterium halobium*), and aminoadipic acid is found in proteins isolated from corn.

Amino Acids Not Found in Proteins

Certain amino acids and their derivatives, although not found in proteins, nonetheless are biochemically important. A few of the more notable examples are shown in Figure 4.5. **γ-Aminobutyric acid,** or **GABA,** is produced by the decarboxylation of glutamic acid and is a potent neurotransmitter. **Histamine,** which is synthesized by decarboxylation of histidine, and **serotonin,** which is derived from tryptophan, similarly function as neurotransmitters and regulators. **β-Alanine** is found in nature in the peptides carnosine and anserine and is a component of pantothenic acid (a vitamin), which is a part of coenzyme A. **Epinephrine** (also known as **adrenaline**), derived from tyrosine, is an important hormone. **Penicillamine** is a constituent of the penicillin antibiotics. **Ornithine, betaine, homocysteine,** and **homoserine** are important metabolic intermediates. **Citrulline** is the immediate precursor of arginine.

Sarcosine
(*N*-methylglycine)

γ-Aminobutyric acid
(GABA)

Betaine
(*N*,*N*,*N*-trimethylglycine)

β-Alanine

Azaserine
O-diazoacetylserine

Homoserine

L-Lanthionine

Homocysteine

L-Phenylserine

L-Chloramphenicol

Cycloserine

Epinephrine

Histamine

Serotonin

Penicillamine

Ornithine

Citrulline
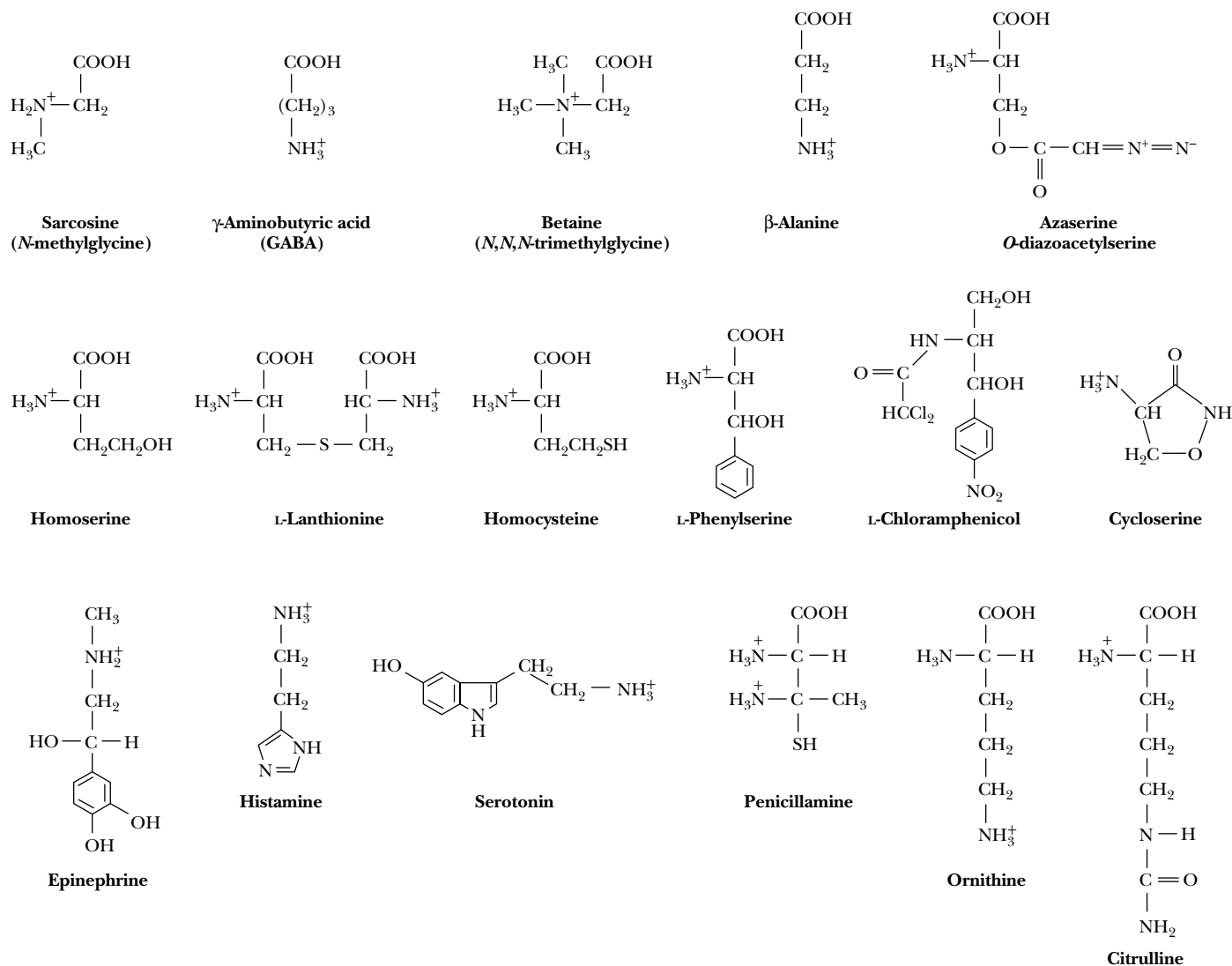
FIGURE 4.5 • The structures of some amino acids that are not normally found in proteins but that perform other important biological functions. Epinephrine, histamine, and serotonin, although not amino acids, are derived from and closely related to amino acids.

4.2 • Acid–Base Chemistry of Amino Acids

Amino Acids Are Weak Polyprotic Acids

From a chemical point of view, the common amino acids are all weak polyprotic acids. The ionizable groups are not strongly dissociating ones, and the degree of dissociation thus depends on the pH of the medium. All the amino acids contain at least two dissociable hydrogens.

Consider the acid–base behavior of glycine, the simplest amino acid. At low pH, both the amino and carboxyl groups are protonated and the molecule has a net positive charge. If the counterion in solution is a chloride ion, this form is referred to as **glycine hydrochloride.** If the pH is increased, the carboxyl group is the first to dissociate, yielding the neutral zwitterionic species Gly^0 (Figure 4.6). Further increase in pH eventually results in dissociation of the amino group to yield the negatively charged **glycinate.** If we denote these

pH 1 Net charge +1   pH 7 Net charge 0   pH 13 Net charge −1

Cationic form   **Zwitterion (neutral)**   **Anionic form**
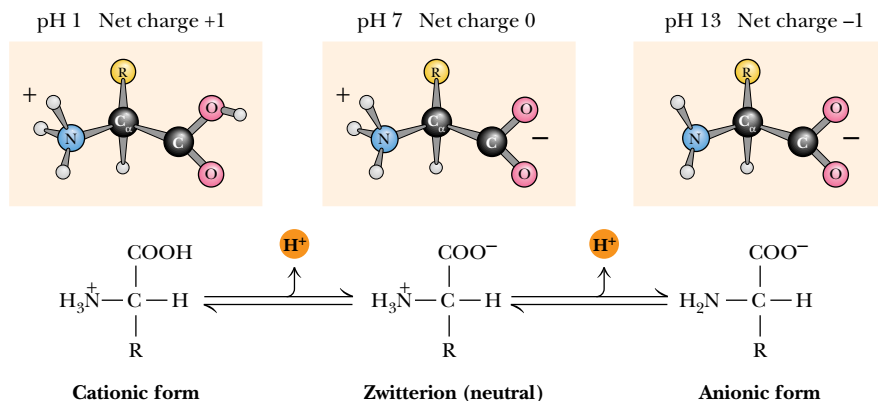
FIGURE 4.6 • The ionic forms of the amino acids, shown without consideration of any ionizations on the side chain. The cationic form is the low pH form, and the titration of the cationic species with base yields the zwitterion and finally the anionic form. (*Irving Geis*)

three forms as Gly^+, Gly^0, and Gly^-, we can write the first dissociation of Gly^+ as

$$Gly^+ + H_2O \rightleftharpoons Gly^0 + H_3O^+$$

and the dissociation constant K_1 as

$$K_1 = \frac{[Gly^0][H_3O^+]}{[Gly^+]}$$

Values for K_1 for the common amino acids are typically 0.4 to 1.0×10^{-2} M, so that typical values of pK_1 center on values of 2.0 to 2.4 (see Table 4.1). In a similar manner, we can write the second dissociation reaction as

$$Gly^0 + H_2O \rightleftharpoons Gly^- + H_3O^+$$
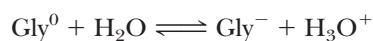
Table 4.1

pK_a Values of Common Amino Acids

Amino Acid	α-COOH pK_a	α-NH$_3^+$ pK_a	R group pK_a
Alanine	2.4	9.7	
Arginine	2.2	9.0	12.5
Asparagine	2.0	8.8	
Aspartic acid	2.1	9.8	3.9
Cysteine	1.7	10.8	8.3
Glutamic acid	2.2	9.7	4.3
Glutamine	2.2	9.1	
Glycine	2.3	9.6	
Histidine	1.8	9.2	6.0
Isoleucine	2.4	9.7	
Leucine	2.4	9.6	
Lysine	2.2	9.0	10.5
Methionine	2.3	9.2	
Phenylalanine	1.8	9.1	
Proline	2.1	10.6	
Serine	2.2	9.2	~13
Threonine	2.6	10.4	~13
Tryptophan	2.4	9.4	
Tyrosine	2.2	9.1	10.1
Valine	2.3	9.6	
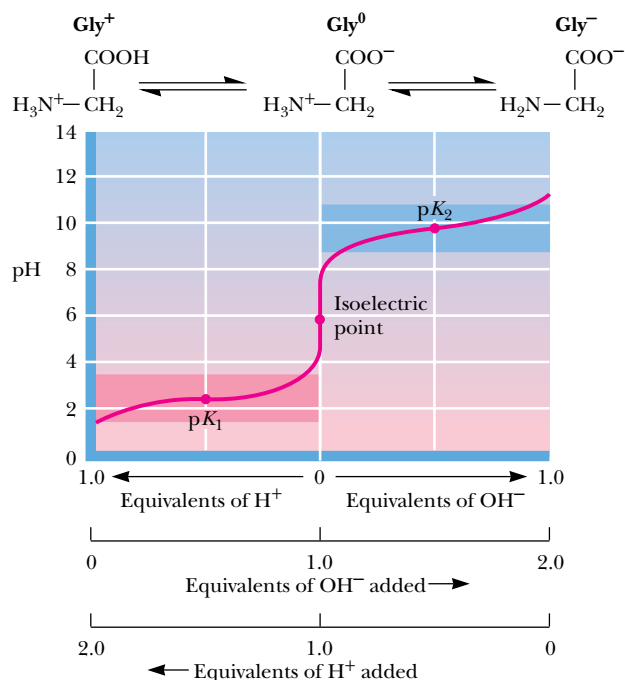
FIGURE 4.7 • Titration of glycine, a simple amino acid. The isoelectric point, pI, the pH where the molecule has a net charge of 0, is defined as $(pK_1 + pK_2)/2$.

and the dissociation constant K_2 as

$$K_2 = \frac{[Gly^-][H_3O^+]}{[Gly^0]}$$

Typical values for pK_2 are in the range of 9.0 to 9.8. At physiological pH, the α-carboxyl group of a simple amino acid (with no ionizable side chains) is completely dissociated, whereas the α-amino group has not really begun its dissociation. The titration curve for such an amino acid is shown in Figure 4.7.

EXAMPLE

What is the pH of a glycine solution in which the α-NH_3^+ group is one-third dissociated?

SOLUTION

The appropriate Henderson–Hasselbalch equation is

$$pH = pK_a + \log_{10}\frac{[Gly^-]}{[Gly^0]}$$

If the α-amino group is one-third dissociated, there is one part Gly^- for every two parts Gly^0. The important pK_a is the pK_a for the amino group. The glycine α-amino group has a pK_a of 9.6. The result is

$$pH = 9.6 + \log_{10}(1/2)$$
$$pH = 9.3$$

Note that the dissociation constants of both the α-carboxyl and α-amino groups are affected by the presence of the other group. The adjacent α-amino group makes the α-COOH group more acidic (that is, it lowers the pK_a) so

that it gives up a proton more readily than simple alkyl carboxylic acids. Thus, the pK_1 of 2.0 to 2.1 for α-carboxyl groups of amino acids is substantially lower than that of acetic acid ($pK_a = 4.76$), for example. What is the chemical basis for the low pK_a of the α-COOH group of amino acids? The α-NH$_3^+$ (ammonium) group is strongly electron-withdrawing, and the positive charge of the amino group exerts a strong field effect and stabilizes the carboxylate anion. (The effect of the α-COO$^-$ group on the pK_a of the α-NH$_3^+$ group is the basis for Problem 4 at the end of this chapter.)

Ionization of Side Chains

As we have seen, the side chains of several of the amino acids also contain dissociable groups. Thus, aspartic and glutamic acids contain an additional carboxyl function, and lysine possesses an aliphatic amino function. Histidine contains an ionizable imidazolium proton, and arginine carries a guanidinium function. Typical pK_a values of these groups are shown in Table 4.1. The β-carboxyl group of aspartic acid and the γ-carboxyl side chain of glutamic acid exhibit pK_a values intermediate to the α-COOH on the one hand and typical aliphatic carboxyl groups on the other hand. In a similar fashion, the ϵ-amino group of lysine exhibits a pK_a that is higher than the α-amino group but similar to that for a typical aliphatic amino group. These intermediate values for side-chain pK_a values reflect the slightly diminished effect of the α-carbon dissociable groups that lie several carbons removed from the side-chain functional groups. Figure 4.8 shows typical titration curves for glutamic acid and lysine, along with the ionic species that predominate at various points in the


FIGURE 4.8 • Titrations of glutamic acid and lysine.
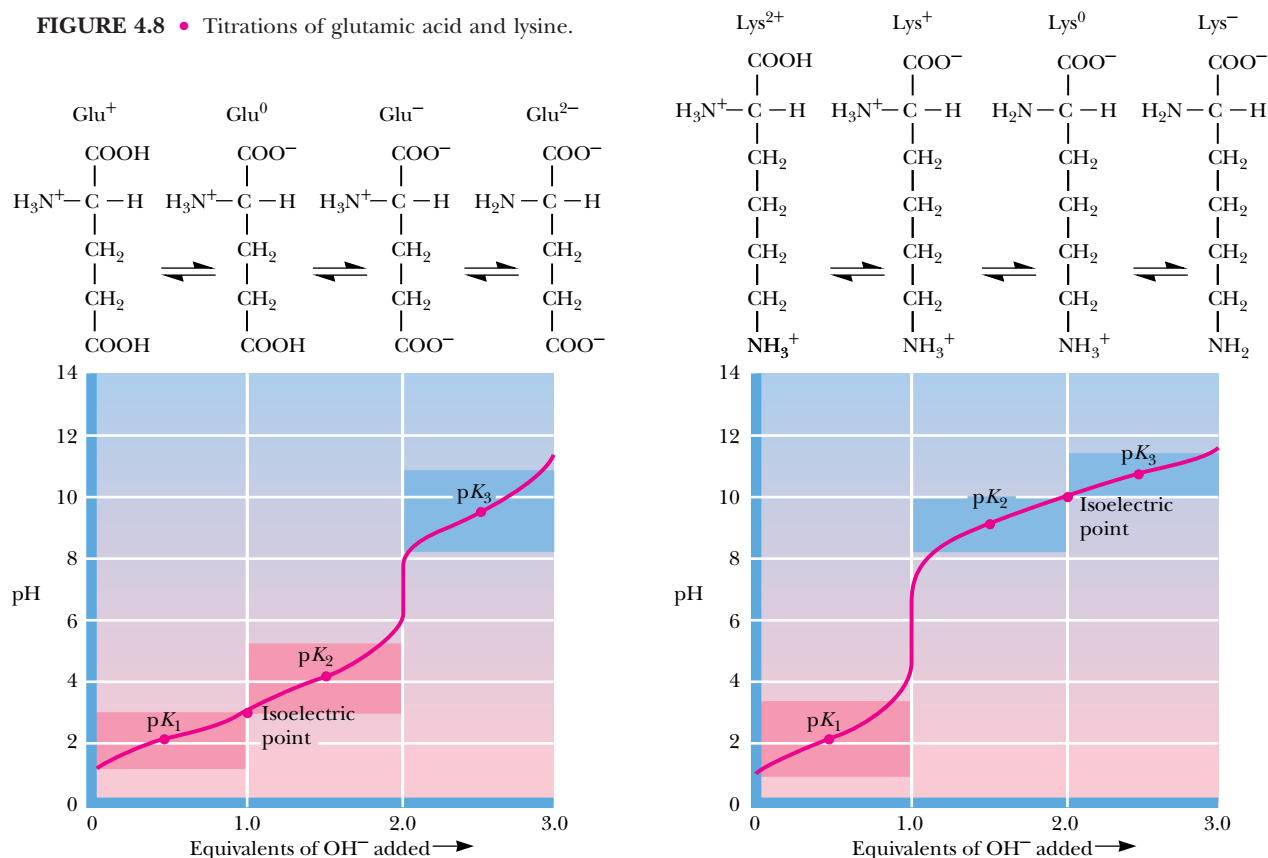
CRITICAL DEVELOPMENTS IN BIOCHEMISTRY

Green Fluorescent Protein—The "Light Fantastic" from Jellyfish to Gene Expression

Aquorea victoria, a species of jellyfish found in the northwest Pacific Ocean, contains a **green fluorescent protein (GFP)** that works together with another protein, **aequorin,** to provide a defense mechanism for the jellyfish. When the jellyfish is attacked or shaken, aequorin produces a blue light. This light energy is captured by GFP, which then emits a bright green flash that presumably blinds or startles the attacker. Remarkably, the fluorescence of GFP occurs without the assistance of a **prosthetic group**—a "helper molecule" that would mediate GFP's fluorescence. Instead, the light-transducing capability of GFP is the result of a reaction between three amino acids in the protein itself. As shown below, adjacent **serine, tyrosine,** and **glycine** in the sequence of the protein react to form the pigment complex—termed a **chromophore.** No enzymes are required; the reaction is autocatalytic.

Because the light-transducing talents of GFP depend only on the protein itself (upper photo, chromophore highlighted), GFP has quickly become a darling of genetic engineering laboratories. The promoter of any gene whose cellular expression is of interest can be fused to the DNA sequence coding for GFP. Telltale green fluorescence tells the researcher when this fused gene has been expressed (see lower photo and also Chapter 13).
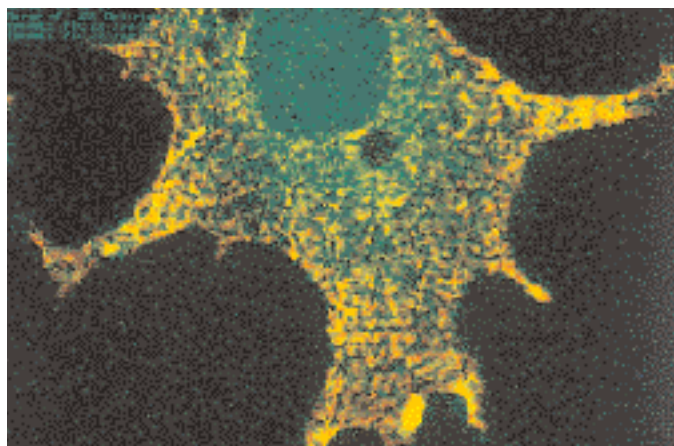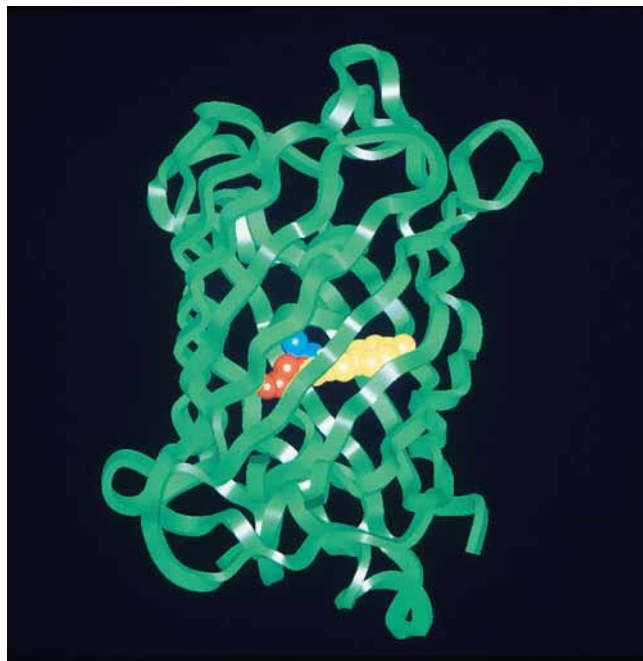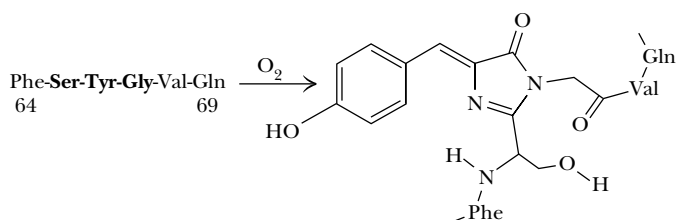
Autocatalytic oxidation of GFP amino acids leads to the chromophore shown on the left. The green fluorescence requires further interactions of the chromophore with other parts of the protein.

Boxer, S.G., 1997. Another green revolution. *Nature* **383:**484–485.

titration. The only other side-chain groups that exhibit any significant degree of dissociation are the *para*-OH group of tyrosine and the —SH group of cysteine. The pK_a of the cysteine sulfhydryl is 8.32, so that it is about 12% dissociated at pH 7. The tyrosine *para*-OH group is a very weakly acidic group, with a pK_a of about 10.1. This group is essentially fully protonated and uncharged at pH 7.

4.3 • Reactions of Amino Acids

Carboxyl and Amino Group Reactions

The α-carboxyl and α-amino groups of all amino acids exhibit similar chemical reactivity. The side chains, however, exhibit specific chemical reactivities, depending on the nature of the functional groups. Whereas all of these reactivities are important in the study and analysis of isolated amino acids, it is the characteristic behavior of the side chain that governs the reactivity of amino acids incorporated into proteins. There are three reasons to consider these reactivities. Proteins can be chemically modified in very specific ways by taking advantage of the chemical reactivity of certain amino acid side chains. The detection and quantification of amino acids and proteins often depend on reactions that are specific to one or more amino acids and that result in color, radioactivity, or some other quantity that can be easily measured. Finally and most importantly, the biological functions of proteins depend on the behavior and reactivity of specific R groups.

The carboxyl groups of amino acids undergo all the simple reactions common to this functional group. Reaction with ammonia and primary amines yields unsubstituted and substituted amides, respectively (Figure 4.9a,b). Esters

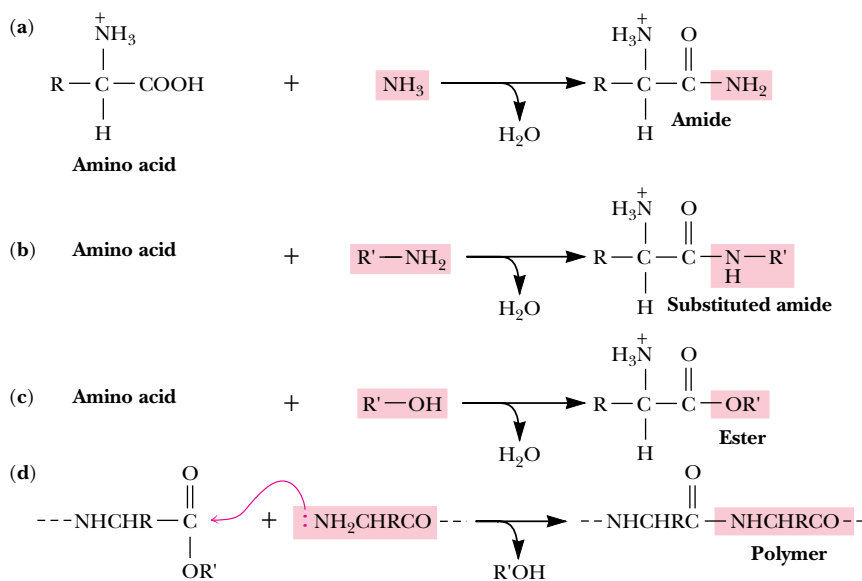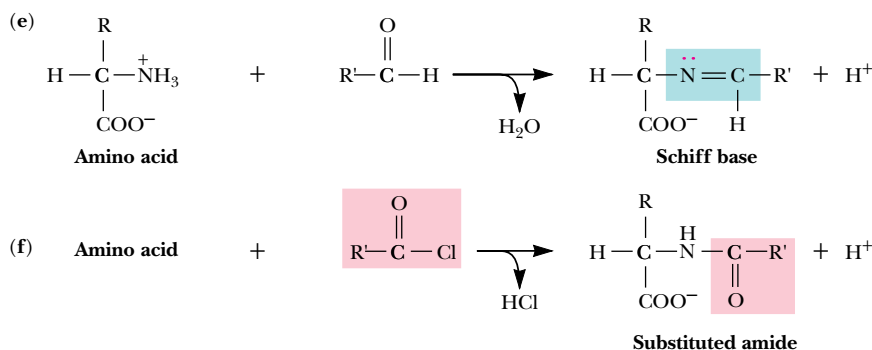**FIGURE 4.9** • Typical reactions of the common amino acids (see text for details).
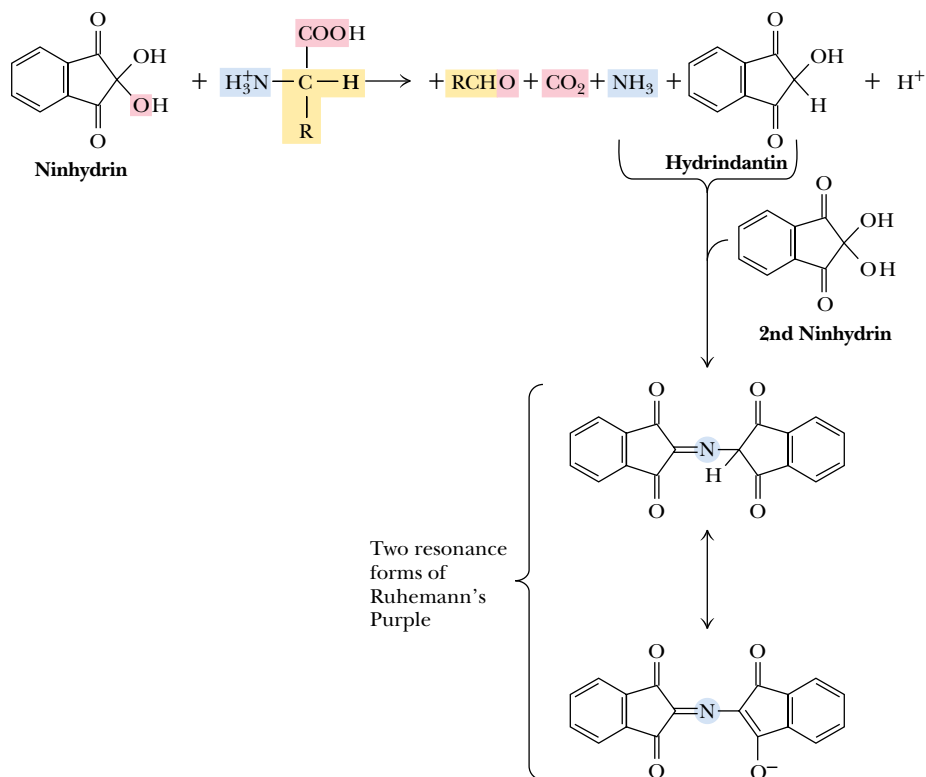
FIGURE 4.10 • The pathway of the ninhydrin reaction, which produces a colored product called "Ruhemann's Purple" that absorbs light at 570 nm. Note that the reaction involves and consumes two molecules of ninhydrin.

and acid chlorides are also readily formed. Esterification proceeds in the presence of the appropriate alcohol and a strong acid (Figure 4.9c). Polymerization can occur by repetition of the reaction shown in Figure 4.9d. Free amino groups may react with aldehydes to form Schiff bases (Figure 4.9e) and can be acylated with acid anhydrides and acid halides (Figure 4.9f).

The Ninhydrin Reaction

Amino acids can be readily detected and quantified by reaction with ninhydrin. As shown in Figure 4.10, *ninhydrin,* or triketohydrindene hydrate, is a strong oxidizing agent and causes the oxidative deamination of the α-amino function. The products of the reaction are the resulting aldehyde, ammonia, carbon dioxide, and hydrindantin, a reduced derivative of ninhydrin. The ammonia produced in this way can react with the hydrindantin and another molecule of ninhydrin to yield a purple product (Ruhemann's Purple) that can be quantified spectrophotometrically at 570 nm. The appearance of CO_2 can also be monitored. Indeed, CO_2 evolution is diagnostic of the presence of an α-amino acid. α-Imino acids, such as proline and hydroxyproline, give bright yellow ninhydrin products with absorption maxima at 440 nm, allowing these to be distinguished from the α-amino acids. Because amino acids are one of the components of human skin secretions, the ninhydrin reaction was once used extensively by law enforcement and forensic personnel for fingerprint detection. (Fingerprints as old as 15 years can be successfully identified using the ninhydrin reaction.) More sensitive fluorescent reagents are now used routinely for this purpose.

Specific Reactions of Amino Acid Side Chains

A number of reactions of amino acids have become important in recent years because they are essential to the degradation, sequencing, and chemical synthesis of peptides and proteins. These reactions are discussed in Chapter 5.

In recent years, biochemists have developed an arsenal of reactions that are relatively specific to the side chains of particular amino acids. These reactions can be used to identify functional amino acids at the active sites of enzymes or to label proteins with appropriate reagents for further study. Cysteine residues in proteins, for example, react with one another to form disulfide species and also react with a number of reagents, including maleimides (typically *N*-ethylmaleimide), as shown in Figure 4.11. Cysteines also react effectively

FIGURE 4.11 • Reactions of amino acid side-chain functional groups.

with iodoacetic acid to yield *S*-carboxymethyl cysteine derivatives. There are numerous other reactions involving specialized reagents specific for particular side chain functional groups. Figure 4.11 presents a representative list of these 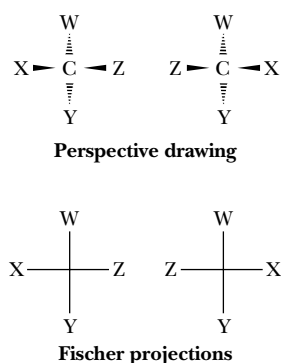reagents and the products that result. It is important to realize that few if any of these reactions are truly specific for one functional group; consequently, care must be exercised in their use.

Perspective drawing

Fischer projections

FIGURE 4.12 • Enantiomeric molecules based on a chiral carbon atom. Enantiomers are nonsuperimposable mirror images of each other.

4.4 • Optical Activity and Stereochemistry of Amino Acids

Amino Acids Are Chiral Molecules

Except for glycine, all of the amino acids isolated from proteins have four different groups attached to the α-carbon atom. In such a case, the α-carbon is said to be **asymmetric** or **chiral** (from the Greek *cheir,* meaning "hand"), and the two possible configurations for the α-carbon constitute nonsuperimposable mirror image isomers, or **enantiomers** (Figure 4.12). Enantiomeric molecules display a special property called **optical activity**—the ability to rotate the plane of polarization of plane-polarized light. Clockwise rotation of incident light is referred to as **dextrorotatory** behavior, and counterclockwise rotation is called **levorotatory** behavior. The magnitude and direction of the optical rotation depend on the nature of the amino acid side chain. The temperature, the wavelength of the light used in the measurement, the ionization state of the amino acid, and therefore the pH of the solution, can also affect optical rotation behavior. As shown in Table 4.2, some protein-derived amino acids at a given pH are dextrorotatory and others are levorotatory, even though all of them are of the L configuration. The direction of optical rotation can be specified in the name by using a (+) for dextrorotatory compounds and a (−) for levorotatory compounds, as in L(+)-leucine.

Nomenclature for Chiral Molecules

The discoveries of optical activity and enantiomeric structures (see the box, page 97) made it important to develop suitable nomenclature for chiral molecules. Two systems are in common use today: the so-called D,L system and the (*R,S*) system.

In the **D,L system** of nomenclature, the (+) and (−) isomers of glyceraldehyde are denoted as **D-glyceraldehyde** and **L-glyceraldehyde,** respectively (Figure 4.13). Absolute configurations of all other carbon-based molecules are referenced to D- and L-glyceraldehyde. When sufficient care is taken to avoid racemization of the amino acids during hydrolysis of proteins, it is found that all of the amino acids derived from natural proteins are of the L configuration. Amino acids of the D configuration are nonetheless found in nature, especially as components of certain peptide antibiotics, such as valinomycin, gramicidin, and actinomycin D, and in the cell walls of certain microorganisms.

In spite of its widespread acceptance, problems exist with the D,L system of nomenclature. For example, this system can be ambiguous for molecules with two or more chiral centers. To address such problems, the (*R,S*) **system** of nomenclature for chiral molecules was proposed in 1956 by Robert Cahn, Sir Christopher Ingold, and Vladimir Prelog. In this more versatile system, priorities are assigned to each of the groups attached to a chiral center on the basis of atomic number, atoms with higher atomic numbers having higher priorities (see the box, page 100).

The newer (*R,S*) system of nomenclature is superior to the older D,L system in one important way. The configuration of molecules with more than one

Table 4.2

Specific Rotations for Some Amino Acids

Amino Acid	Specific Rotation $[\alpha]_D^{25}$, Degrees
L-Alanine	+1.8
L-Arginine	+12.5
L-Aspartic acid	+5.0
L-Glutamic acid	+12.0
L-Histidine	−38.5
L-Isoleucine	+12.4
L-Leucine	−11.0
L-Lysine	+13.5
L-Methionine	−10.0
L-Phenylalanine	−34.5
L-Proline	−86.2
L-Serine	−7.5
L-Threonine	−28.5
L-Tryptophan	−33.7
L-Valine	+5.6

CRITICAL DEVELOPMENTS IN BIOCHEMISTRY

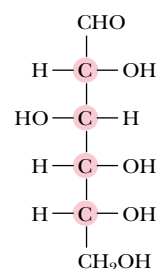## Discovery of Optically Active Molecules and Determination of Absolute Configuration

The optical activity of quartz and certain other materials was first discovered by Jean-Baptiste Biot in 1815 in France, and in 1848 a young chemist in Paris named Louis Pasteur made a related and remarkable discovery. Pasteur noticed that preparations of optically inactive sodium ammonium tartrate contained two visibly different kinds of crystals that were mirror images of each other. Pasteur carefully separated the two types of crystals, dissolved them each in water, and found that each solution was *optically active*. Even more intriguing, the specific rotations of these two solutions were equal in magnitude and of opposite sign. Because these differences in optical rotation were apparent properties of the dissolved molecules, Pasteur eventually proposed that the molecules themselves were mirror images of each other, just like their respective crystals. Based on this and other related evidence, in 1847 van't Hoff and LeBel proposed the tetrahedral arrangement of valence bonds to carbon.

In 1888, Emil Fischer decided that it should be possible to determine the *relative* configuration of (+)-glucose, a six-carbon sugar with four asymmetric centers (see figure). Because each of the four C could be either of two configurations, glucose conceivably could exist in any one of 16 possible isomeric structures. It took three years to complete the solution of an elaborate chemical and logical puzzle. By 1891, Fischer had reduced his puzzle to a choice between two enantiomeric structures. (Methods for determining *absolute* configuration were not yet available, so Fischer made a simple guess, selecting the structure shown in the figure.) For this remarkable feat, Fischer received the Nobel Prize in chemistry in 1902. Sadly, Fischer, a brilliant but troubled chemist, later committed suicide.

The absolute choice between Fischer's two enantiomeric possibilities would not be made for a long time. In 1951, J.M. Bijvoet in Utrecht, the Netherlands, used a new X-ray diffraction technique to determine the absolute configuration of (among other things) the sodium rubidium salt of (+)-tartaric acid. Because the tartaric acid configuration could be related to that of glyceraldehyde and because sugar and amino acid configurations could all be related to glyceraldehyde, it became possible to determine the absolute configuration of sugars and the common amino acids. The absolute configuration of tartaric acid determined by Bijvoet turned out to be the configuration that, up to then, had only been assumed. This meant that Emil Fischer's arbitrary guess 60 years earlier had been correct.
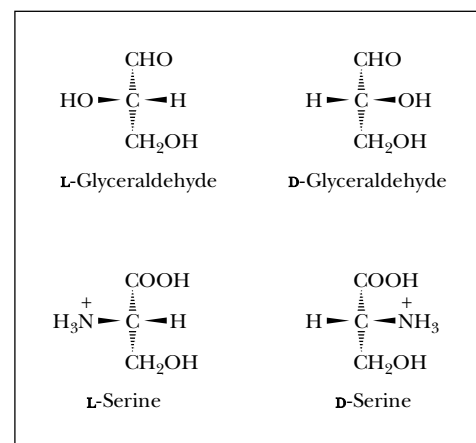
It was M.A. Rosanoff, a chemist and instructor at New York University, who first proposed (in 1906) that the isomers of glyceraldehyde be the standards for denoting the stereochemistry of sugars and other molecules. Later, when experiments showed that the configuration of (+)-glyceraldehyde was related to (+)-glucose, (+)-glyceraldehyde was given the designation D. Emil Fischer rejected the **Rosanoff convention,** but it was universally accepted. Ironically, this nomenclature system is often mistakenly referred to as the **Fischer convention.**

$$
\begin{array}{c}
\text{CHO} \\
\text{H}-\text{C}-\text{OH} \\
\text{HO}-\text{C}-\text{H} \\
\text{H}-\text{C}-\text{OH} \\
\text{H}-\text{C}-\text{OH} \\
\text{CH}_2\text{OH}
\end{array}
$$

The absolute configuration of (+)-glucose.

chiral center can be more easily, completely, and unambiguously described with (R,S) notation. Several amino acids, including isoleucine, threonine, hydroxyproline, and hydroxylysine, have two chiral centers. In the (R,S) system, L-threonine is (2S,3R)-threonine. A chemical compound with n chiral centers can exist in 2^n-isomeric structures, and the four amino acids just listed can thus each take on four different isomeric configurations. This amounts to two pairs of enantiomers. Isomers that differ in configuration at only one of the asymmetric centers are non–mirror image isomers or **diastereomers.** The four stereo-

FIGURE 4.13 • The configuration of the common L-amino acids can be related to the configuration of L(−)-glyceraldehyde as shown. These drawings are known as Fischer projections. The horizontal lines of the Fischer projections are meant to indicate bonds coming out of the page from the central carbon, and vertical lines represent bonds extending behind the page from the central carbon atom.

$$
\begin{array}{cc}
\begin{array}{c}
\text{CHO} \\
\text{HO}-\text{C}-\text{H} \\
\text{CH}_2\text{OH}
\end{array}
&
\begin{array}{c}
\text{CHO} \\
\text{H}-\text{C}-\text{OH} \\
\text{CH}_2\text{OH}
\end{array}
\\
\textbf{L}\text{-Glyceraldehyde} & \textbf{D}\text{-Glyceraldehyde}
\end{array}
$$

$$
\begin{array}{cc}
\begin{array}{c}
\text{COOH} \\
\text{H}_3\overset{+}{\text{N}}-\text{C}-\text{H} \\
\text{CH}_2\text{OH}
\end{array}
&
\begin{array}{c}
\text{COOH} \\
\text{H}-\text{C}-\overset{+}{\text{N}}\text{H}_3 \\
\text{CH}_2\text{OH}
\end{array}
\\
\textbf{L}\text{-Serine} & \textbf{D}\text{-Serine}
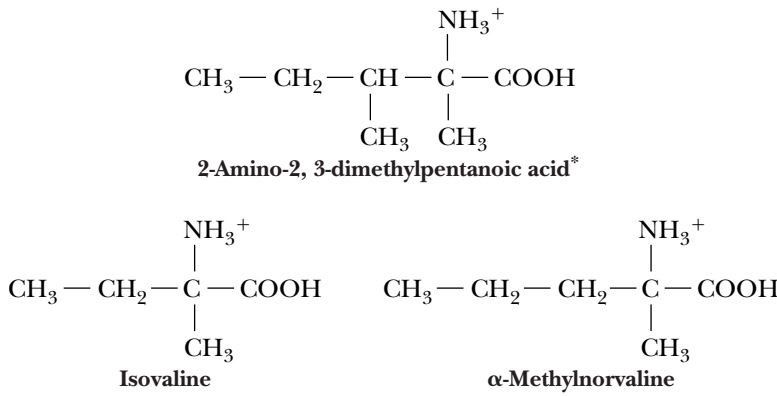\end{array}
$$

The Murchison Meteorite—Discovery of Extraterrestrial Handedness

The predominance of L-amino acids in biological systems is one of life's most intriguing features. Prebiotic syntheses of amino acids would be expected to produce equal amounts of L- and D-enantiomers. Some kind of enantiomeric selection process must have intervened to select L-amino acids over their D-counterparts as the constituents of proteins. Was it random chance that chose L- over D-isomers?

Analysis of carbon compounds—even amino acids—from extraterrestrial sources might provide deeper insights into this mystery. John Cronin and Sandra Pizzarello have examined the enantiomeric distribution of unusual amino acids obtained from the Murchison meteorite, which struck the earth on September 28, 1969, near Murchison, Australia. (By selecting unusual amino

acids for their studies, Cronin and Pizzarello ensured that they were examining materials that were native to the meteorite and not earth-derived contaminants.) Four α-dialkyl amino acids—α-methylisoleucine, α-methylalloisoleucine, α-methylnorvaline, and isovaline—were found to have an L-enantiomeric excess of 2 to 9%.

This may be the first demonstration that a natural L-enantiomer enrichment occurs in certain cosmological environments. Could these observations be relevant to the emergence of L-enantiomers as the dominant amino acids on the earth? And, if so, could there be life elsewhere in the universe that is based upon the same amino acid handedness?
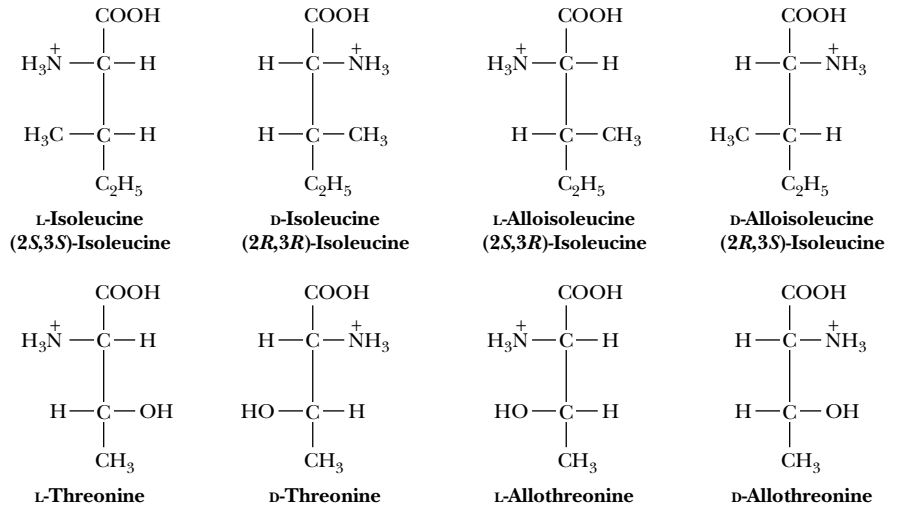
$$CH_3 \!-\! CH_2 \!-\! \overset{\displaystyle NH_3{}^+}{\underset{\displaystyle CH_3}{\overset{|}{CH}}} \!-\! \overset{|}{\underset{\displaystyle CH_3}{C}} \!-\! COOH$$

2-Amino-2, 3-dimethylpentanoic acid*

Amino acids found in the Murchison meteorite

$$CH_3 \!-\! CH_2 \!-\! \overset{\displaystyle NH_3{}^+}{\underset{\displaystyle CH_3}{\overset{|}{C}}} \!-\! COOH \qquad CH_3 \!-\! CH_2 \!-\! CH_2 \!-\! \overset{\displaystyle NH_3{}^+}{\underset{\displaystyle CH_3}{\overset{|}{C}}} \!-\! COOH$$

Isovaline   **α-Methylnorvaline**

The four stereoisomers of this amino acid include the D- and L-forms of α-methylisoleucine and α-methylalloisoleucine.
*Cronin, J.R., and Pizzarello, S., 1997. Enantiomeric excesses in meteoritic amino acids. Science **275**:951–955.*

isomers of isoleucine are shown in Figure 4.14. The isomer obtained from digests of natural proteins is arbitrarily designated L-isoleucine. In the (R,S) system, L-isoleucine is $(2S,3S)$-isoleucine. Its diastereomer is referred to as L-allo-isoleucine. The D-enantiomeric pair of isomers is named in a similar manner.

FIGURE 4.14 • The stereoisomers of isoleucine and threonine. The structures at the far left are the naturally occurring isomers.

|			
L-Isoleucine (2S,3S)-Isoleucine	D-Isoleucine (2R,3R)-Isoleucine	L-Alloisoleucine (2S,3R)-Isoleucine	D-Alloisoleucine (2R,3S)-Isoleucine
L-Threonine	D-Threonine	L-Allothreonine	D-Allothreonine

*C*RITICAL DEVELOPMENTS IN BIOCHEMISTRY

Rules for Description of Chiral Centers in the (R,S) *System*

Naming a chiral center in the (*R,S*) system is accomplished by viewing the molecule from the chiral center to the atom with the lowest priority. If the other three atoms facing the viewer then decrease in priority in a clockwise direction, the center is said to have the (*R*) configuration (where *R* is from the Latin *rectus* meaning "right"). If the three atoms in question decrease in priority in a counterclockwise fashion, the chiral center is of the (*S*) configuration (where *S* is from the Latin *sinistrus* meaning "left"). If two of the atoms coordinated to a chiral center are identical, the atoms bound to these two are considered for priorities. For such purposes, the priorities of certain functional groups found in amino acids and related molecules are in the following order:

$$SH > OH > NH_2 > COOH > CHO > CH_2OH > CH_3$$

From this, it is clear that ᴅ-glyceraldehyde is (*R*)-glyceraldehyde, and ʟ-alanine is (*S*)-alanine (see figure). Interestingly, the α-carbon configuration of all the ʟ-amino acids *except for cysteine* is (*S*). Cysteine, by virtue of its thiol group, is in fact (*R*)-cysteine.
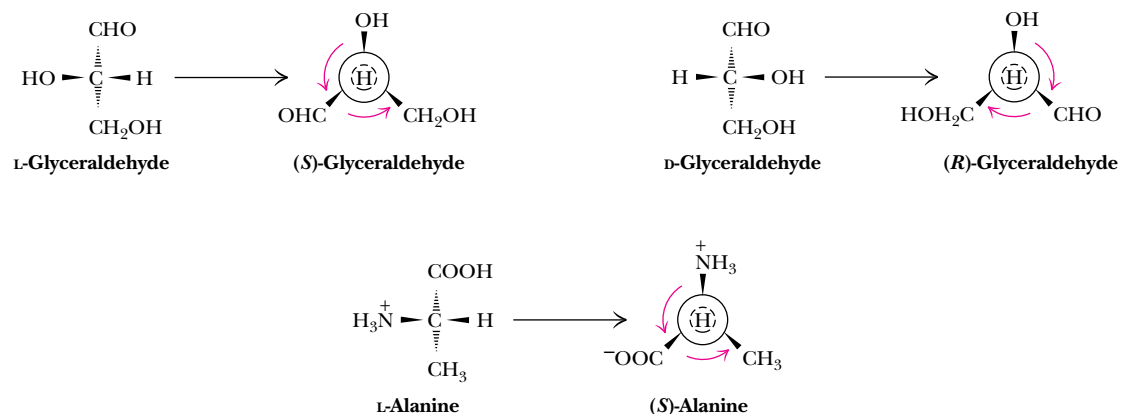
The assignment of (*R*) and (*S*) notation for glyceraldehyde and ʟ-alanine.

4.5 • Spectroscopic Properties of Amino Acids

One of the most important and exciting advances in modern biochemistry has been the application of **spectroscopic methods,** which measure the absorption and emission of energy of different frequencies by molecules and atoms. Spectroscopic studies of proteins, nucleic acids, and other biomolecules are providing many new insights into the structure and dynamic processes in these molecules.

Ultraviolet Spectra

Many details of the structure and chemistry of the amino acids have been elucidated or at least confirmed by spectroscopic measurements. None of the amino acids absorbs light in the visible region of the electromagnetic spectrum. Several of the amino acids, however, do absorb **ultraviolet** radiation, and all absorb in the **infrared** region. The absorption of energy by electrons as they rise to higher energy states occurs in the ultraviolet/visible region of the energy spectrum. Only the aromatic amino acids phenylalanine, tyrosine, and tryptophan exhibit significant ultraviolet absorption above 250 nm, as shown in Figure 4.15. These strong absorptions can be used for spectroscopic determinations of protein concentration. The aromatic amino acids also exhibit relatively weak fluorescence, and it has recently been shown that tryptophan can exhibit *phos-*
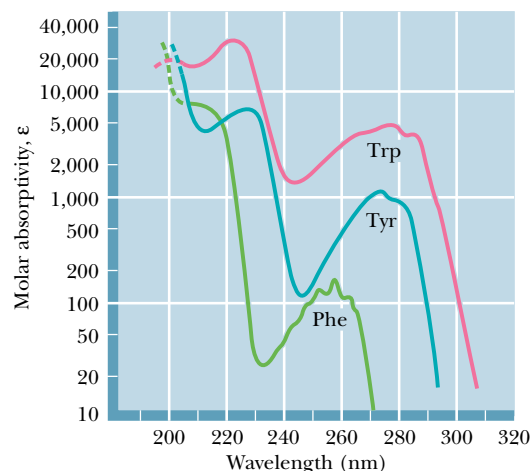
FIGURE 4.15 • The ultraviolet absorption spectra of the aromatic amino acids at pH 6.
(From Wetlaufer, D.B., 1962. Ultraviolet spectra of proteins and amino acids. Advances in Protein Chemistry **17:**303–390.)

phorescence—a relatively long-lived emission of light. These fluorescence and phosphorescence properties are especially useful in the study of protein structure and dynamics (see Chapter 6).

Nuclear Magnetic Resonance Spectra

The development in the 1950s of **nuclear magnetic resonance** (NMR), a spectroscopic technique that involves the absorption of radio frequency energy by certain nuclei in the presence of a magnetic field, played an important part in the chemical characterization of amino acids and proteins. Several important principles rapidly emerged from these studies. First, the **chemical shift**[1] of amino acid protons depends on their particular chemical environment and thus on the state of ionization of the amino acid. Second, the change in electron density during a titration is transmitted throughout the carbon chain in the aliphatic amino acids and the aliphatic portions of aromatic amino acids, as evidenced by changes in the chemical shifts of relevant protons. Finally, the magnitude of the **coupling constants** between protons on adjacent carbons depends in some cases on the ionization state of the amino acid. This apparently reflects differences in the preferred conformations in different ionization states. Proton NMR spectra of two amino acids are shown in Figure 4.16. Because they are highly sensitive to their environment, the chemical shifts of individual NMR signals can detect the pH-dependent ionizations of amino acids. Figure 4.17 shows the ^{13}C chemical shifts occurring in a titration of lysine. Note that the chemical shifts of the carboxyl C, C_α, and C_β carbons of lysine are sensitive to dissociation of the nearby α-COOH and α-NH$_3^+$ protons (with pK_a values of about 2 and 9, respectively), whereas the C_δ and C_ϵ carbons are sensitive to dissociation of the ϵ-NH$_3^+$ group. Such measurements have been very useful for studies of the ionization behavior of amino acid residues in pro-

---

[1]The chemical shift for any NMR signal is the difference in resonant frequency between the observed signal and a suitable reference signal. If two nuclei are magnetically coupled, the NMR signals of these nuclei split, and the separation between such split signals, known as the coupling constant, is likewise dependent on the structural relationship between the two nuclei.
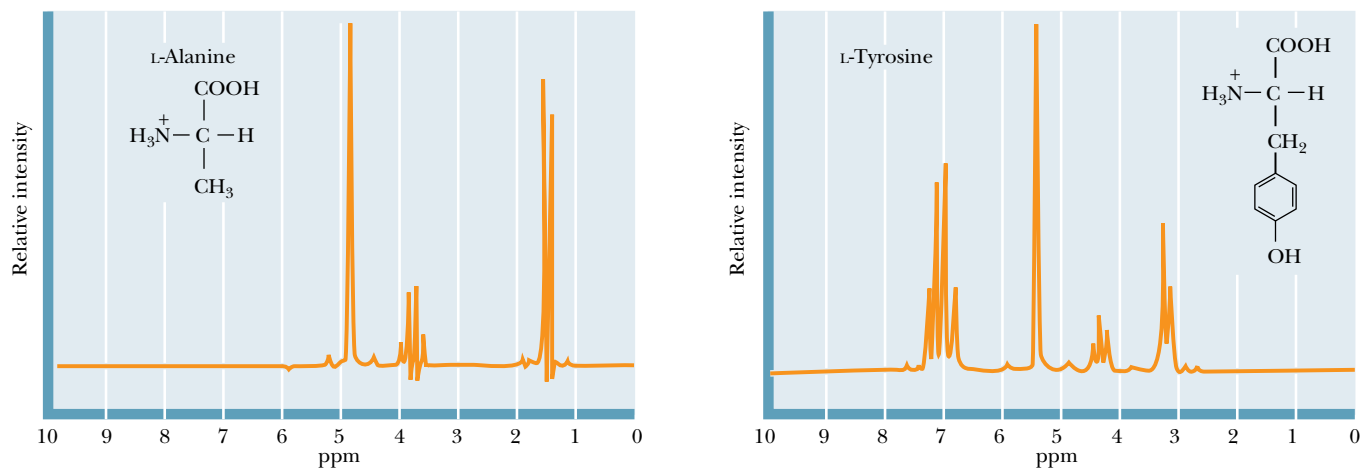
FIGURE 4.16 • Proton NMR spectra of several amino acids. Zero on the chemical shift scale is defined by the resonance of tetramethylsilane (TMS). (*Adapted from Aldrich Library of NMR Spectra.*)

teins. More sophisticated NMR measurements at very high magnetic fields are also used to determine the three-dimensional structures of peptides and even small proteins.

4.6 • Separation and Analysis of Amino Acid Mixtures

Chromatographic Methods

The purification and analysis of individual amino acids from complex mixtures was once a very difficult process. Today, however, the biochemist has a wide variety of methods available for the separation and analysis of amino acids, or for that matter, any of the other biological molecules and macromolecules we

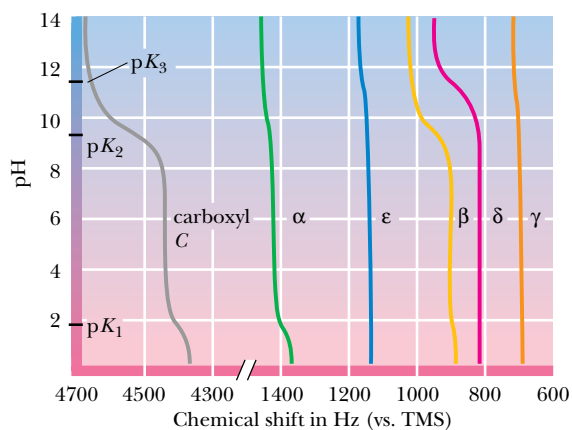**FIGURE 4.17** • A plot of chemical shifts versus pH for the carbons of lysine. Changes in chemical shift are most pronounced for atoms near the titrating groups. Note the correspondence between the pK_a values and the particular chemical shift changes. All chemical shifts are defined relative to tetramethylsilane (TMS). (*From Suprenant, H., et al., 1980. Journal of Magnetic Resonance* **40**:231–243.)

encounter. All of these methods take advantage of the relative differences in the physical and chemical characteristics of amino acids, particularly ionization behavior and solubility characteristics. The methods important for amino acids include separations based on **partition** properties (the tendency to associate with one solvent or phase over another) and separations based on **electrical charge.** In all of the partition methods discussed here, the molecules of interest are allowed (or forced) to flow through a medium consisting of two phases—solid–liquid, liquid–liquid, or gas–liquid. In all of these methods, the molecules must show a preference for associating with one or the other phase. In this manner, the molecules partition, or distribute themselves, between the two phases in a manner based on their particular properties. The ratio of the concentrations of the amino acid (or other species) in the two phases is designated the *partition coefficient*.
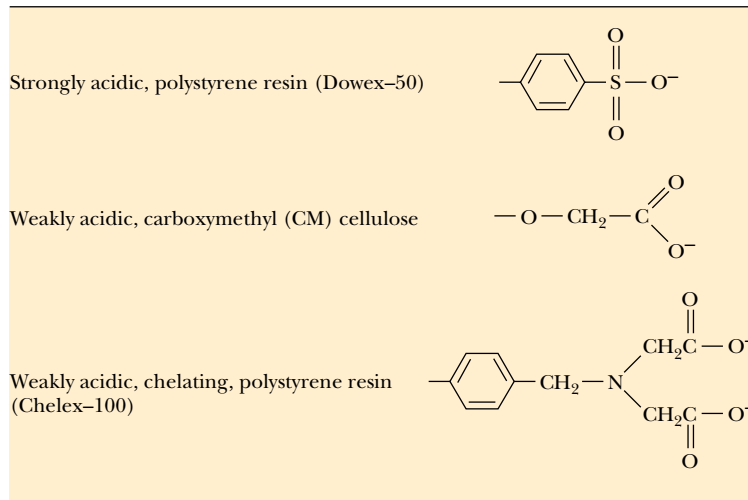
In 1903, a separation technique based on repeated partitioning between phases was developed by Mikhail Tswett for the separation of plant pigments (carotenes and chlorophylls). Tswett, a Russian botanist, poured solutions of the pigments through columns of finely divided alumina and other solid media, allowing the pigments to partition between the liquid solvent and the solid support. Owing to the colorful nature of the pigments thus separated, Tswett called his technique **chromatography.** This term is now applied to a wide variety of separation methods, regardless of whether the products are colored or not. The success of all chromatography techniques depends on the repeated microscopic partitioning of a solute mixture between the available phases. The more frequently this partitioning can be made to occur within a given time span or over a given volume, the more efficient is the resulting separation. Chromatographic methods have advanced rapidly in recent years, due in part to the development of sophisticated new solid-phase materials. Methods important for amino acid separations include ion exchange chromatography, gas chromatography (GC), and high-performance liquid chromatography (HPLC).

Ion Exchange Chromatography

The separation of amino acids and other solutes is often achieved by means of **ion exchange chromatography,** in which the molecule of interest is *exchanged* for another ion onto and off of a charged solid support. In a typical procedure, solutes in a liquid phase, usually water, are passed through columns filled with a porous solid phase, usually a bed of synthetic resin particles, containing charged groups. Resins containing positive charges attract negatively charged solutes and are referred to as *anion exchangers*. Solid supports possessing negative charges attract positively charged species and are referred to as *cation exchangers*. Several typical cation and anion exchange resins with different types of charged groups are shown in Figure 4.18. The strength of the acidity or basicity of these groups and their number per unit volume of resin determine the type and strength of binding of an exchanger. Fully ionized acidic groups such as sulfonic acids result in an exchanger with a negative charge which binds cations very strongly. Weakly acidic or basic groups yield resins whose charge (and binding capacity) depends on the pH of the eluting solvent. The choice of the appropriate resin depends on the strength of binding desired. The bare charges on such solid phases must be counterbalanced by oppositely charged ions in solution ("counterions"). Washing a cation exchange resin, such as Dowex-50, which has strongly acidic phenyl-SO_3^- groups, with a NaCl solution results in the formation of the so-called sodium form of the resin (see Figure 4.19). When the mixture whose separation is desired is added to the column, the positively charged solute molecules displace the Na^+ ions and bind to the

(a) Cation Exchange Media Structure

Strongly acidic, polystyrene resin (Dowex–50)

Weakly acidic, carboxymethyl (CM) cellulose

Weakly acidic, chelating, polystyrene resin (Chelex–100)

(b) Anion Exchange Media Structure

Strongly basic, polystyrene resin (Dowex–1)

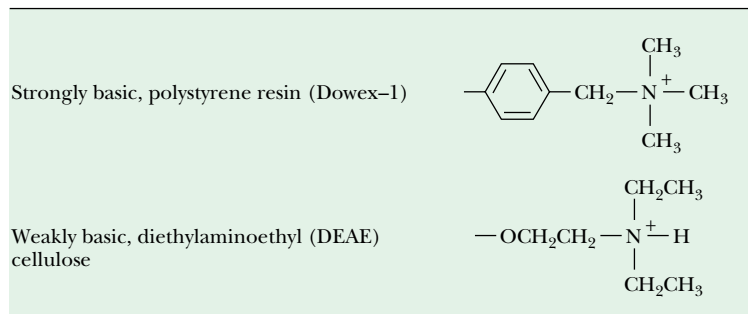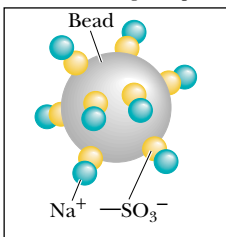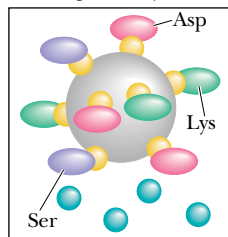Weakly basic, diethylaminoethyl (DEAE) cellulose

FIGURE 4.18 • Cation (a) and anion (b) exchange resins commonly used for biochemical separations.

Cation exchange bead before adding sample

Bead

Na^+ —SO_3^-

(a)

Add mixture of Asp, Ser, Lys

Asp

Lys

Ser

(b)

Add Na^+ (NaCl)
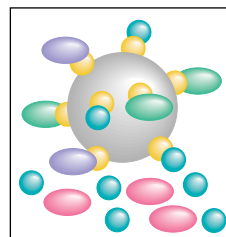
(c) Asp, the least positively charged amino acid, is eluted first

Increase $[Na^+]$
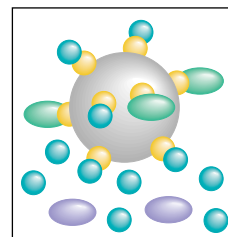
(d) Serine is eluted next

Increase $[Na^+]$
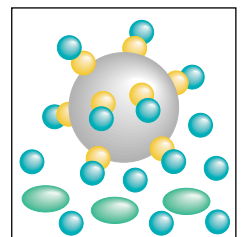
(e) Lysine, the most positively charged amino acid, is eluted last

FIGURE 4.19 • Operation of a cation exchange column, separating a mixture of Asp, Ser, and Lys. (a) The cation exchange resin in the beginning, Na^+ form. (b) A mixture of Asp, Ser, and Lys is added to the column containing the resin. (c) A gradient of the eluting salt (e.g., NaCl) is added to the column. Asp, the least positively charged amino acid, is eluted first. (d) As the salt concentration increases, Ser is eluted. (e) As the salt concentration is increased further, Lys, the most positively charged of the three amino acids, is eluted last.

resin. A gradient of an appropriate salt is then applied to the column, and the solute molecules are competitively (and sequentially) displaced (eluted) from the column by the rising concentration of cations in the gradient, in an order that is inversely related to their affinities for the column. The separation of a mixture of amino acids on such a column is shown in Figures 4.19 and 4.20. Figure 4.21, taken from a now-classic 1958 paper by Stanford Moore, Darrel Spackman, and William Stein, shows a typical separation of the common amino acids. The events occurring in this separation are essentially those depicted in Figures 4.19 and 4.20. The amino acids are applied to the column at low pH (4.25), under which conditions the acidic amino acids (aspartate and gluta-mate, among others) are weakly bound and the basic amino acids, such as argi-nine and lysine, are tightly bound. Sodium citrate solutions, at two different concentrations and three different values of pH, are used to elute the amino acids gradually from the column.

A typical HPLC chromatogram using precolumn derivatization of amino acids with *o*-phthaldialdehyde (OPA) is shown in Figure 4.22. HPLC has rapidly become the chromatographic technique of choice for most modern bio-chemists. The very high resolution, excellent sensitivity, and high speed of this technique usually outweigh the disadvantage of relatively low capacity.
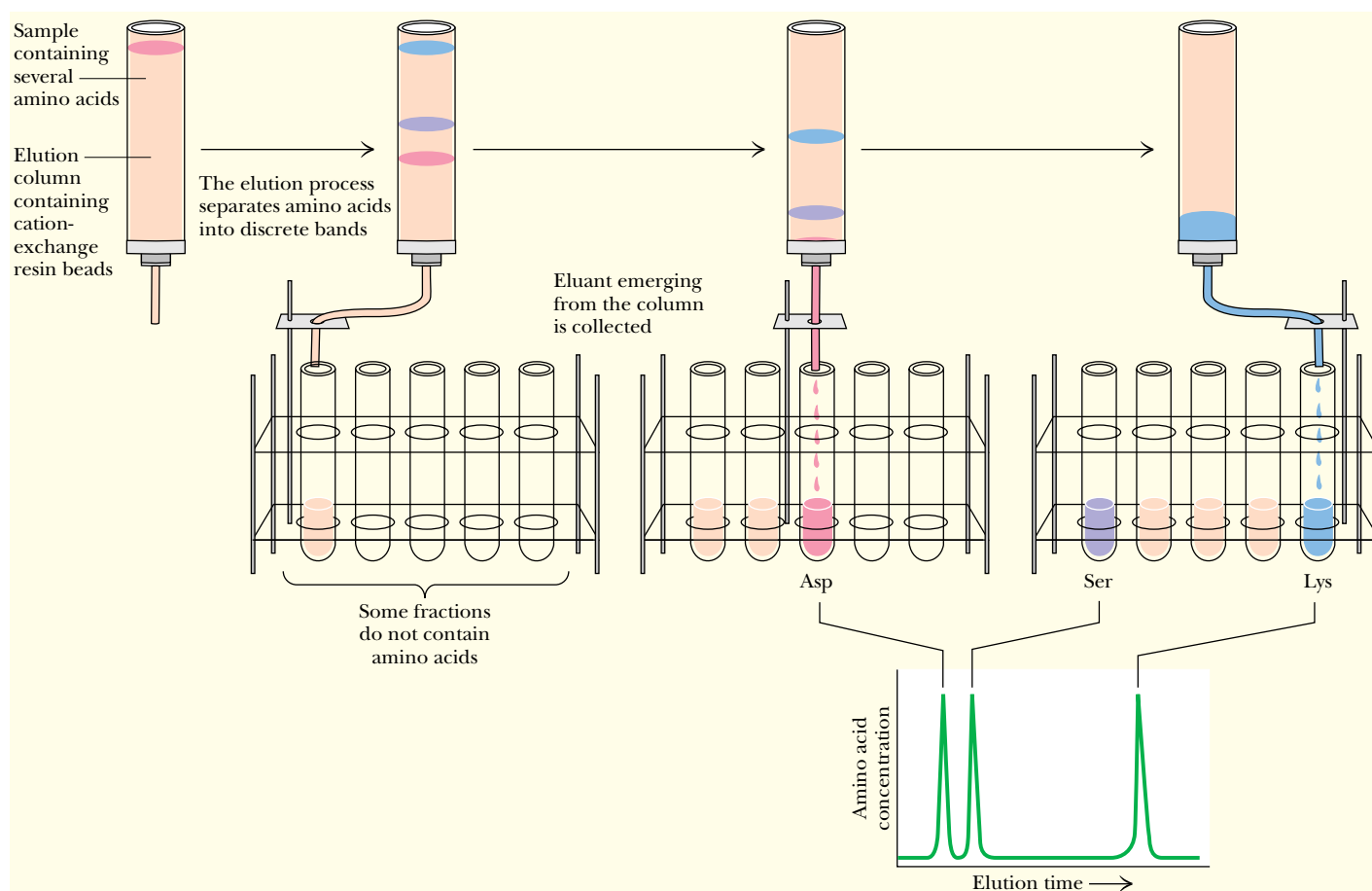
FIGURE 4.20 • The separation of amino acids on a cation exchange column.
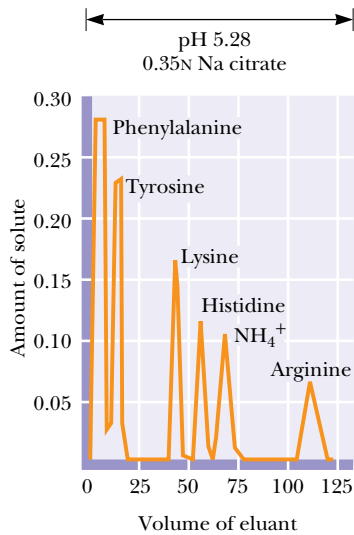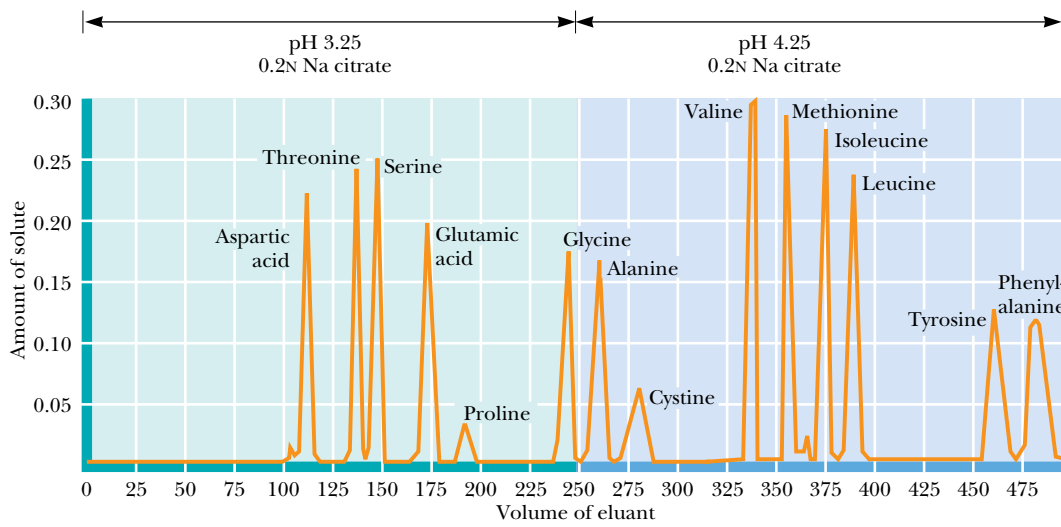
FIGURE 4.21 • Chromatographic fractionation of a synthetic mixture of amino acids on ion exchange columns using Amberlite IR-120, a sulfonated polystyrene resin similar to Dowex-50. A second column with different buffer conditions is used to resolve the basic amino acids. (*Adapted from Moore, S., Spackman, D., and Stein, W., 1958. Chromatography of amino acids on sulfonated polystyrene resins.* Analytical Chemistry **30:***1185–1190.)*
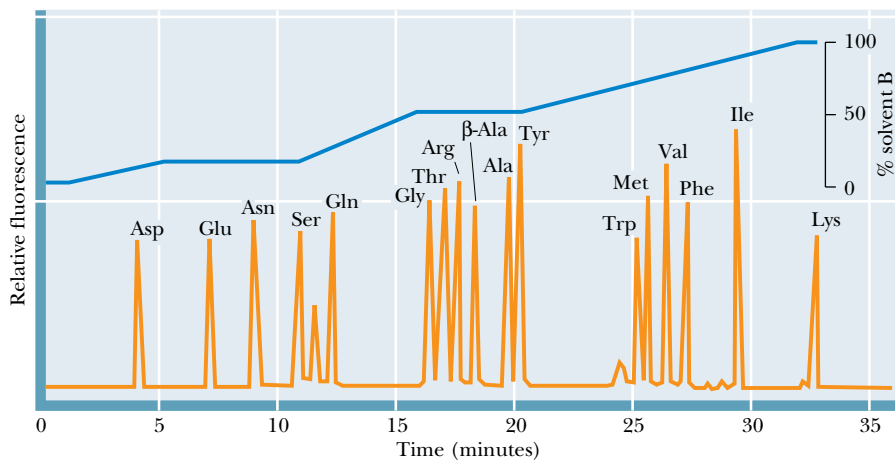
FIGURE 4.22 • HPLC chromatogram of amino acids employing precolumn derivatization with OPA. Chromatography was carried out on an Ultrasphere ODS column using a complex tetrahydrofuran:methanol:0.05 M sodium acetate (pH 5.9) 1:19:80 to methanol:0.05 M sodium acetate (pH 5.9) 4:1 gradient at a flow rate of 1.7 mL/min. *(Adapted from Jones, B. N., Pääbo, S., and Stein, S., 1981. Amino acid analysis and enzymic sequence determination of peptides by an improved o-phthaldialdehyde precolumn labeling procedure.* Journal of Liquid Chromatography **4:***56–586.)*

PROBLEMS

1. Without consulting chapter figures, draw Fischer projection formulas for glycine, aspartate, leucine, isoleucine, methionine, and threonine.

2. Without reference to the text, give the one-letter and three-letter abbreviations for asparagine, arginine, cysteine, lysine, proline, tyrosine, and tryptophan.

3. Write equations for the ionic dissociations of alanine, glutamate, histidine, lysine, and phenylalanine.

4. How is the pK_a of the α-NH_3^+ group affected by the presence on an amino acid of the α-COO^-?

5. Draw an appropriate titration curve for aspartic acid, labeling the axes and indicating the equivalence points and the pK_a values.

6. Calculate the concentrations of all ionic species in a 0.25 M solution of histidine at pH 2, pH 6.4, and pH 9.3.

7. Calculate the pH at which the γ-carboxyl group of glutamic acid is two-thirds dissociated.

8. Calculate the pH at which the ϵ-amino group of lysine is 20% dissociated.

9. Calculate the pH of a 0.3 M solution of (a) leucine hydrochloride, (b) sodium leucinate, and (c) isoelectric leucine.

10. Quantitative measurements of optical activity are usually expressed in terms of the specific rotation, $[\alpha]_D^{25}$, defined as

$$[\alpha]_D^{25} = \frac{\text{Measured rotation in degrees} \times 100}{(\text{Optical path in dm}) \times (\text{conc. in g/mL})}$$

For any measurement of optical rotation, the wavelength of the light used and the temperature must both be specified. In this case, D refers to the "D line" of sodium at 589 nm and 25 refers to a measurement temperature of 25°C. Calculate the concentration of a solution of L-arginine that rotates the incident light by 0.35° in an optical path length of 1 dm (decimeter).

11. Absolute configurations of the amino acids are referenced to D- and L-glyceraldehyde on the basis of chemical transformations that can convert the molecule of interest to either of these reference isomeric structures. In such reactions, the stereochemical consequences for the asymmetric centers must be understood for each reaction step. Propose a sequence of reactions that would demonstrate that L(−)-serine is stereochemically related to L(−)-glyceraldehyde.

12. Describe the stereochemical aspects of the structure of cystine, the structure that is a disulfide-linked pair of cysteines.

13. Draw a simple mechanism for the reaction of a cysteine sulfhydryl group with iodoacetamide.

14. Describe the expected elution pattern for a mixture of aspartate, histidine, isoleucine, valine, and arginine on a column of Dowex-50.

15. Assign (R,S) nomenclature to the threonine isomers of Figure 4.14.

FURTHER READING

Barker, R., 1971. *Organic Chemistry of Biological Compounds,* Chap. 4. Englewood Cliffs, NJ: Prentice-Hall.

Barrett, G. C., ed., 1985. *Chemistry and Biochemistry of the Amino Acids.* New York: Chapman and Hall.

Bovey, F. A., and Tiers, G. V. D., 1959. Proton N.S.R. spectroscopy. V. Studies of amino acids and peptides in trifluoroacetic acid. *Journal of the American Chemical Society* **81:**2870–2878.

Cahn, R. S., 1964. An introduction to the sequence rule. *Journal of Chemical Education* **41:**116–125.

Greenstein, J. P., and Winitz, M., 1961. *Chemistry of the Amino Acids.* New York: John Wiley & Sons.

Heiser, T., 1990. Amino acid chromatography: The "best" technique for student labs. *Journal of Chemical Education* **67:**964–966.

Herod, D. W., and Menzel, E. R., 1982. Laser detection of latent fingerprints: Ninhydrin. *Journal of Forensic Science* **27:**200–204.

Iizuka, E., and Yang, J. T., 1964. Optical rotatory dispersion of L-amino acids in acid solution. *Biochemistry* **3:**1519–1524.

Kauffman, G. B., and Priebe, P. M., 1990. The Emil Fischer–William Ramsey friendship. *Journal of Chemical Education* **67:**93–101.

Mabbott, G., 1990. Qualitative amino acid analysis of small peptides by GC/MS. *Journal of Chemical Education* **67:**441–445.

Meister, A., 1965. *Biochemistry of the Amino Acids,* 2nd ed., Vol. 1. New York: Academic Press.

Moore, S., Spackman, D., and Stein, W. H., 1958. Chromatography of amino acids on sulfonated polystyrene resins. *Analytical Chemistry* **30:**1185–1190.

Roberts, G. C. K., and Jardetzky, O., 1970. Nuclear magnetic resonance spectroscopy of amino acids, peptides and proteins. *Advances in Protein Chemistry* **24:**447–545.

Segel, I. H., 1976. *Biochemical Calculations,* 2nd ed. New York: John Wiley & Sons.

Suprenant, H. L., Sarneski, J. E., Key, R. R., Byrd, J. T., and Reilley, C. N., 1980. Carbon-13 NMR studies of amino acids: Chemical shifts, protonation shifts, microscopic protonation behavior. *Journal of Magnetic Resonance* **40:**231–243.

$\mathcal{C}$hapter 5

Proteins: Their Biological Functions and Primary Structure

Although helices are uncommon in manmade architecture, they are a common structural theme in biological macromolecules—proteins, nucleic acids, and even polysaccharides.
(Loretto Chapel, Santa Fe, NM/ © Sarbo)

Proteins are a diverse and abundant class of biomolecules, constituting more than 50% of the dry weight of cells. This diversity and abundance reflect the central role of proteins in virtually all aspects of cell structure and function. An extraordinary diversity of cellular activity is possible only because of the versatility inherent in proteins, each of which is specifically tailored to its biological role. The pattern by which each is tailored resides within the genetic information of cells, encoded in a specific sequence of nucleotide bases in DNA.

107

Each such segment of encoded information defines a gene, and expression of the gene leads to synthesis of the specific protein encoded by it, endowing the cell with the functions unique to that particular protein. Proteins are the agents of biological function; they are also the expressions of genetic information.

5.1 • Proteins Are Linear Polymers of Amino Acids

Chemically, proteins are unbranched polymers of amino acids linked head to tail, from carboxyl group to amino group, through formation of covalent **peptide bonds,** a type of amide linkage (Figure 5.1).

Peptide bond formation results in the release of H_2O. The peptide "backbone" of a protein consists of the repeated sequence —N—C_α—C—, where the N represents the amide nitrogen, the C_α is the α-carbon atom of an amino acid in the polymer chain, and the final C is the carbonyl carbon of the amino acid, which in turn is linked to the amide N of the next amino acid down the line. The geometry of the peptide backbone is shown in Figure 5.2. Note that the carbonyl oxygen and the amide hydrogen are *trans* to each other in this figure. This conformation is favored energetically because it results in less steric hindrance between nonbonded atoms in neighboring amino acids. Because the α-carbon atom of the amino acid is a chiral center (in all amino acids except glycine), the polypeptide chain is inherently asymmetric. Only L-amino acids are found in proteins.

The Peptide Bond Has Partial Double Bond Character

The peptide linkage is usually portrayed by a single bond between the carbonyl carbon and the amide nitrogen (Figure 5.3a). Therefore, in principle, rotation may occur about any covalent bond in the polypeptide backbone because all three kinds of bonds (N—C_α, C_α—C_o, and the C_o—N peptide bond) are single bonds. In this representation, the C and N atoms of the peptide grouping are both in planar sp^2 hybridization and the C and O atoms are linked by a π bond, leaving the nitrogen with a lone pair of electrons in a $2p$ orbital. However, another resonance form for the peptide bond is feasible in which the C and N atoms participate in a π bond, leaving a lone e^- pair on the oxygen (Figure 5.3b). This structure prevents free rotation about the C_o—N peptide bond because it becomes a double bond. The real nature of the peptide bond lies somewhere between these extremes; that is, it has partial double bond character, as represented by the intermediate form shown in Figure 5.3c.

Peptide bond resonance has several important consequences. First, it restricts free rotation around the peptide bond and leaves the peptide backbone with only two degrees of freedom per amino acid group: rotation around
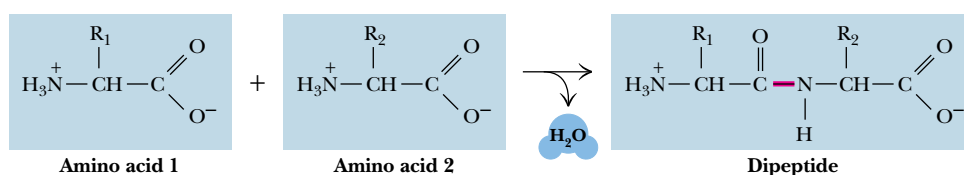

FIGURE 5.1 • Peptide formation is the creation of an amide bond between the carboxyl group of one amino acid and the amino group of another amino acid. R_1 and R_2 represent the R groups of two different amino acids.
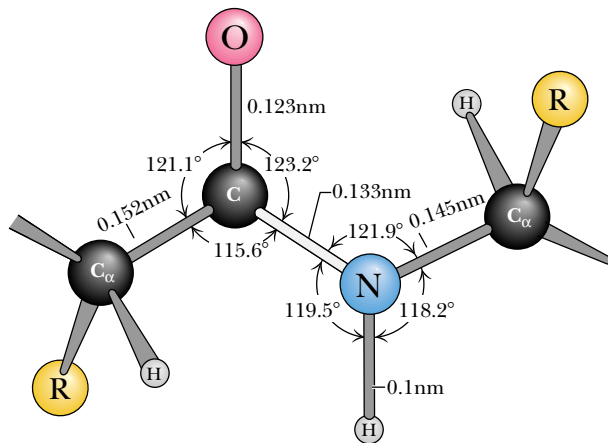
FIGURE 5.2 • The peptide bond is shown in its usual *trans* conformation of carbonyl O and amide H. The C_α atoms are the α-carbons of two adjacent amino acids joined in peptide linkage. The dimensions and angles are the average values observed by crystallographic analysis of amino acids and small peptides. The peptide bond is the light gray bond between C and N. (*Adapted from Ramachandran, G. N., et al., 1974. Biochimica Biophysica Acta* **359**:*298–302.*)

the $N—C_\alpha$ bond and rotation around the $C_\alpha—C_o$ bond.[1] Second, the six atoms composing the peptide bond group tend to be coplanar, forming the so-called **amide plane** of the polypeptide backbone (Figure 5.4). Third, the $C_o—N$ bond length is 0.133 nm, which is shorter than normal C—N bond lengths (for example, the $C_\alpha—N$ bond of 0.145 nm) but longer than typical C=N bonds (0.125 nm). The peptide bond is estimated to have 40% double-bond character.

(a)

A pure double bond between C and O would permit free rotation around the C —N bond.

(b)

The other extreme would prohibit C —N bond rotation but would place too great a charge on O and N.

(c) The true electron density is intermediate. The barrier to C —N bond rotation of about 88 kJ/mol is enough to keep the amide group planar.
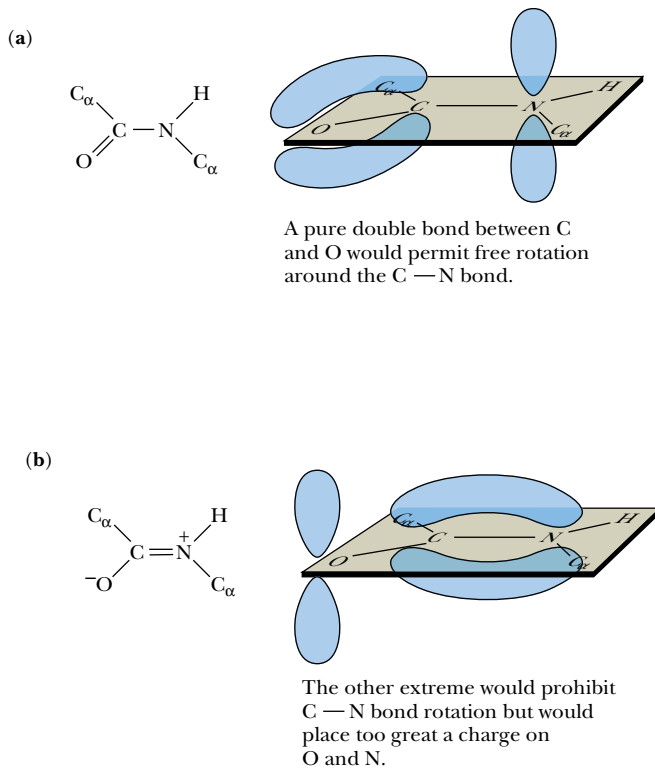
FIGURE 5.3 • The partial double bond character of the peptide bond. Resonance interactions among the carbon, oxygen, and nitrogen atoms of the peptide group can be represented by two resonance extremes (a and b). (a) The usual way the peptide atoms are drawn. (b) In an equally feasible form, the peptide bond is now a double bond; the amide N bears a positive charge and the carbonyl O has a negative charge. (c) The actual peptide bond is best described as a resonance hybrid of the forms in (a) and (b). Significantly, all of the atoms associated with the peptide group are coplanar, rotation about $C_o—N$ is restricted, and the peptide is distinctly polar. (*Irving Geis*)
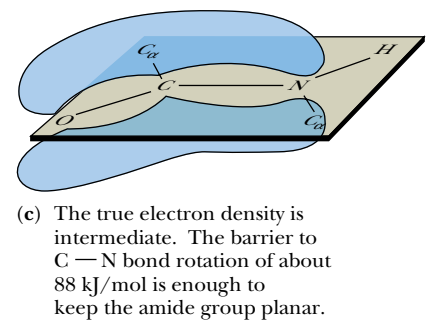
[1]The angle of rotation about the $N—C_\alpha$ bond is designated ϕ, phi, whereas the $C_\alpha—C_o$ angle of rotation is designated ψ, psi.

FIGURE 5.4 • The coplanar relationship of the atoms in the amide group is highlighted as an imaginary shaded plane lying between two successive α-carbon atoms in the peptide backbone.
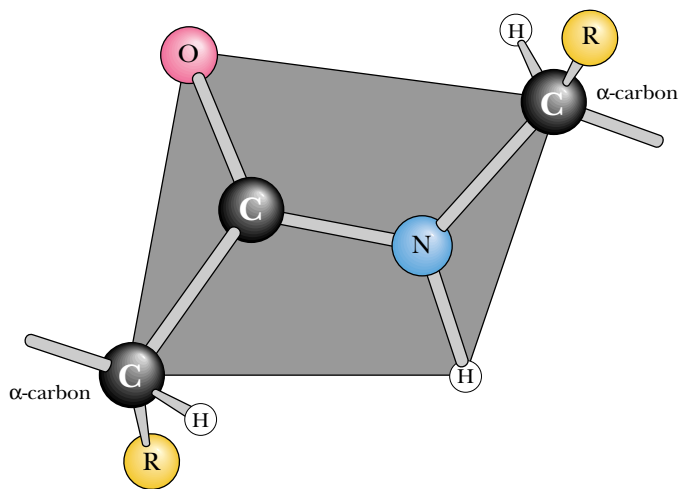
The Polypeptide Backbone Is Relatively Polar

Peptide bond resonance also causes the peptide backbone to be relatively polar. As shown in Figure 5.3b, the amide nitrogen represents a protonated or positively charged form, and the carbonyl oxygen becomes a negatively charged atom in the double-bonded resonance state. In actuality, the hybrid state of the partially double-bonded peptide arrangement gives a net positive charge of 0.28 on the amide N and an equivalent net negative charge of 0.28 on the carbonyl O. The presence of these partial charges means that the peptide bond has a permanent dipole. Nevertheless, the peptide backbone is relatively unreactive chemically, and protons are gained or lost by the peptide groups only at extreme pH conditions.

Peptide Classification

Peptide is the name assigned to short polymers of amino acids. Peptides are classified by the number of amino acid units in the chain. Each unit is called an **amino acid residue,** the word *residue* denoting what is left after the release of H_2O when an amino acid forms a peptide link upon joining the peptide chain. **Dipeptides** have two amino acid residues, tripeptides have three, tetrapeptides four, and so on. After about 12 residues, this terminology becomes cumbersome, so peptide chains of more than 12 and less than about 20 amino acid residues are usually referred to as **oligopeptides,** and, when the chain exceeds several dozen amino acids in length, the term **polypeptide** is used. The distinctions in this terminology are not precise.

Proteins Are Composed of One or More Polypeptide Chains

The terms *polypeptide* and *protein* are used interchangeably in discussing single polypeptide chains. The term **protein** broadly defines molecules composed of one or more polypeptide chains. Proteins having only one polypeptide chain are **monomeric proteins.** Proteins composed of more than one polypeptide chain are **multimeric proteins.** Multimeric proteins may contain only one kind of polypeptide, in which case they are **homomultimeric,** or they may be composed of several different kinds of polypeptide chains, in which instance they are **heteromultimeric.** Greek letters and subscripts are used to denote the polypeptide composition of multimeric proteins. Thus, an α_2-type protein is a dimer of identical polypeptide subunits, or a **homodimer.** Hemoglobin (Table 5.1) consists of four polypeptides of two different kinds; it is an $\alpha_2\beta_2$ heteromultimer.

Table 5.1

Size of Protein Molecules*			
Protein	**M_r**	**Number of Residues per Chain**	**Subunit Organization**
Insulin (bovine)	5,733	21 (A)	$\alpha\beta$
		30 (B)	
Cytochrome c (equine)	12,500	104	α_1
Ribonuclease A (bovine pancreas)	12,640	124	α_1
Lysozyme (egg white)	13,930	129	α_1
Myoglobin (horse)	16,980	153	α_1
Chymotrypsin (bovine pancreas)	22,600	13 (α)	$\alpha\beta\gamma$
		132 (β)	
		97 (γ)	
Hemoglobin (human)	64,500	141 (α)	$\alpha_2\beta_2$
		146 (β)	
Serum albumin (human)	68,500	550	α_1
Hexokinase (yeast)	96,000	200	α_4
γ-Globulin (horse)	149,900	214 (α)	$\alpha_2\beta_2$
		446 (β)	
Glutamate dehydrogenase (liver)	332,694	500	α_6
Myosin (rabbit)	470,000	1800 (heavy, h)	$h_2\alpha_1\alpha'_2\beta_2$
		190 (α)	
		149 (α')	
		160 (β)	
Ribulose bisphosphate carboxylase (spinach)	560,000	475 (α)	$\alpha_8\beta_8$
		123 (β)	
Glutamine synthetase (*E. coli*)	600,000	468	α_{12}

Insulin

Cytochrome c

Ribonuclease

Lysozyme

Myoglobin

Hemoglobin

Immunoglobulin

Glutamine synthetase
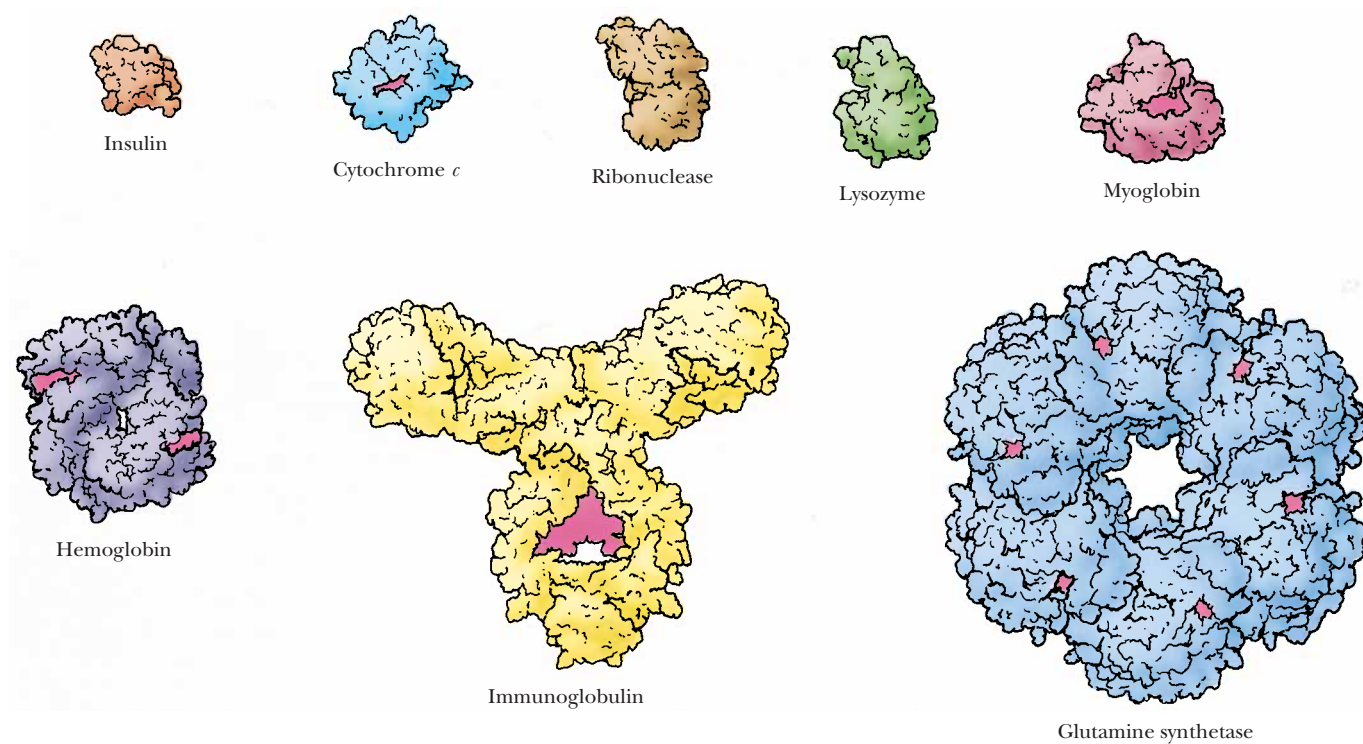
*Illustrations of selected proteins listed in Table 5.1 are drawn to constant scale.

Adapted from Goodsell and Olson, 1993. *Trends in Biochemical Sciences* **18:**65–68.

Polypeptide chains of proteins range in length from about 100 amino acids to 1800, the number found in each of the two polypeptide chains of myosin, the contractile protein of muscle. However, titin, another muscle protein, has nearly 27,000 amino acid residues and a molecular weight of 2.8×10^6. The average molecular weight of polypeptide chains in eukaryotic cells is about 31,700, corresponding to about 270 amino acid residues. Table 5.1 is a representative list of proteins according to size. The molecular weights (M_r) of proteins can be estimated by a number of physicochemical methods such as polyacrylamide gel electrophoresis or ultracentrifugation (see Chapter Appendix). Precise determinations of protein molecular masses are best obtained by simple calculations based on knowledge of their amino acid sequence. No simple generalizations correlate the size of proteins with their functions. For instance, the same function may be fulfilled in different cells by proteins of different molecular weight. The *Escherichia coli* enzyme responsible for glutamine synthesis (a protein known as *glutamine synthetase*) has a molecular weight of 600,000, whereas the analogous enzyme in brain tissue has a molecular weight of just 380,000.

Acid Hydrolysis of Proteins

Peptide bonds of proteins are hydrolyzed by either strong acid or strong base. Because acid hydrolysis proceeds without racemization and with less destruction of certain amino acids (Ser, Thr, Arg, and Cys) than alkaline treatment, it is the method of choice in analysis of the amino acid composition of proteins and polypeptides. Typically, samples of a protein are hydrolyzed with 6 *N* HCl at 110°C for 24, 48, and 72 hr in sealed glass vials. Tryptophan is destroyed by acid and must be estimated by other means to determine its contribution to the total amino acid composition. The OH-containing amino acids serine and threonine are slowly destroyed, but the data obtained for the three time points (24, 48, and 72 hr) allow extrapolation to zero time to estimate the original Ser and Thr content (Figure 5.5). In contrast, peptide bonds involving hydrophobic residues such as valine and isoleucine are only slowly hydrolyzed in acid. Another complication arises because the β- and γ-amide linkages in asparagine (Asn) and glutamine (Gln) are acid labile. The amino nitrogen is released as free ammonium, and all of the Asn and Gln residues of the protein become aspartic acid (Asp) and glutamic acid (Glu), respectively. The
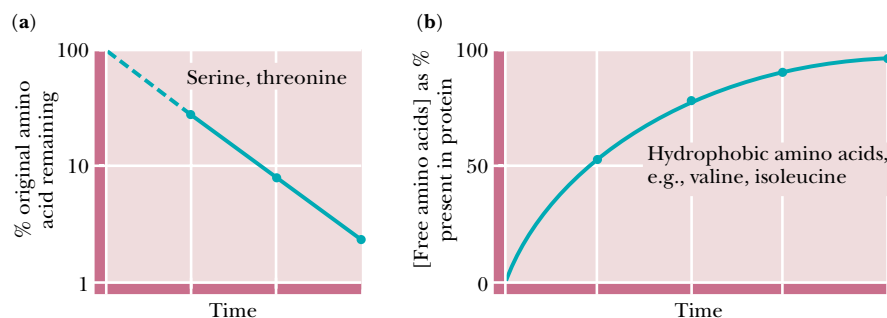
FIGURE 5.5 • (a) The hydroxy amino acids serine and threonine are slowly destroyed during the course of protein hydrolysis for amino acid composition analysis. Extrapolation of the data back to time zero allows an accurate estimation of the amount of these amino acids originally present in the protein sample. (b) Peptide bonds involving hydrophobic amino acid residues such as valine and isoleucine resist hydrolysis by HCl. With time, these amino acids are released and their free concentrations approach a limiting value that can be approximated with reliability.

amount of ammonium released during acid hydrolysis gives an estimate of the total number of Asn and Gln residues in the original protein, but not the amounts of either. Accordingly, the concentrations of Asp and Glu determined in amino acid analysis are expressed as Asx and Glx, respectively. Because the relative contributions of [Asn + Asp] or [Gln + Glu] cannot be derived from the data, this information must be obtained by alternative means.

Amino Acid Analysis of Proteins

The complex amino acid mixture in the hydrolysate obtained after digestion of a protein in 6 *N* HCl can be separated into the component amino acids by either ion exchange chromatography (see Chapter 4) or by reversed-phase high-pressure liquid chromatography (HPLC) (see Chapter Appendix). The amount of each amino acid can then be determined. In ion exchange chromatography, the amino acids are separated and then quantified following reaction with ninhydrin (so-called postcolumn derivatization). In HPLC, the amino acids are converted to phenylthiohydantoin (PTH) derivatives via reaction with Edman's reagent (see Figure 5.19) prior to chromatography (precolumn derivatization). Both of these methods of separation and analysis are fully automated in instruments called **amino acid analyzers.** Analysis of the amino acid composition of a 30-kD protein by these methods requires less than 1 hour and only 6 μg (0.2 nmol) of the protein.

Table 5.2 gives the amino acid composition of several selected proteins: ribonuclease A, alcohol dehydrogenase, myoglobin, histone H3, and collagen. Each of the 20 naturally occurring amino acids is usually represented at least once in a polypeptide chain. However, some small proteins may not have a representative of every amino acid. Note that ribonuclease (12.6 kD, 124 amino acid residues) does not contain any tryptophan. Amino acids almost never occur in equimolar ratios in proteins, indicating that proteins are not composed of repeating arrays of amino acids. There are a few exceptions to this rule. Collagen, for example, contains large proportions of glycine and proline, and much of its structure is composed of (Gly-*x*-Pro) repeating units, where *x* is any amino acid. Other proteins show unusual abundances of various amino acids. For example, histones are rich in positively charged amino acids such as arginine and lysine. Histones are a class of proteins found associated with the anionic phosphate groups of eukaryotic DNA.

Amino acid analysis itself does not directly give the number of residues of each amino acid in a polypeptide, but it does give amounts from which the percentages or ratios of the various amino acids can be obtained (Table 5.2). If the molecular weight *and* the exact amount of the protein analyzed are known (or the number of amino acid residues per molecule is known), the molar ratios of amino acids in the protein can be calculated. Amino acid analysis provides no information on the order or sequence of amino acid residues in the polypeptide chain. Because the polypeptide chain is unbranched, it has only two ends, an amino-terminal or **N-terminal end** and a carboxyl-terminal or **C-terminal end.**

The Sequence of Amino Acids in Proteins

The unique characteristic of each protein is the distinctive sequence of amino acid residues in its polypeptide chain(s). Indeed, it is the **amino acid sequence** of proteins that is encoded by the nucleotide sequence of DNA. This amino acid sequence, then, is a form of genetic information. By convention, the amino acid sequence is read from the N-terminal end of the polypeptide chain through to the C-terminal end. As an example, every molecule of ribonucle-

Table 5.2

Amino Acid Composition of Some Selected Proteins

Values expressed are percent representation of each amino acid.

Amino Acid	Proteins*				
	RNase	ADH	Mb	Histone H3	Collagen
Ala	6.9	7.5	9.8	13.3	11.7
Arg	3.7	3.2	1.7	13.3	4.9
Asn	7.6	2.1	2.0	0.7	1.0
Asp	4.1	4.5	5.0	3.0	3.0
Cys	6.7	3.7	0	1.5	0
Gln	6.5	2.1	3.5	5.9	2.6
Glu	4.2	5.6	8.7	5.2	4.5
Gly	3.7	10.2	9.0	5.2	32.7
His	3.7	1.9	7.0	1.5	0.3
Ile	3.1	6.4	5.1	5.2	0.8
Leu	1.7	6.7	11.6	8.9	2.1
Lys	7.7	8.0	13.0	9.6	3.6
Met	3.7	2.4	1.5	1.5	0.7
Phe	2.4	4.8	4.6	3.0	1.2
Pro	4.5	5.3	2.5	4.4	22.5
Ser	12.2	7.0	3.9	3.7	3.8
Thr	6.7	6.4	3.5	7.4	1.5
Trp	0	0.5	1.3	0	0
Tyr	4.0	1.1	1.3	2.2	0.5
Val	7.1	10.4	4.8	4.4	1.7
Acidic	8.4	10.2	13.7	8.1	7.5
Basic	15.0	13.1	21.8	24.4	8.8
Aromatic	6.4	6.4	7.2	5.2	1.7
Hydrophobic	18.0	30.7	27.6	23.0	6.5

*Proteins are as follows:
RNase: Bovine ribonuclease A, an enzyme; 124 amino acid residues. Note that RNase lacks tryptophan.
ADH: Horse liver alcohol dehydrogenase, an enzyme; dimer of identical 374 amino acid polypeptide chains. The amino acid composition of ADH is reasonably representative of the norm for water-soluble proteins.
Mb: Sperm whale myoglobin, an oxygen-binding protein; 153 amino acid residues. Note that Mb lacks cysteine.
Histone H3: Histones are DNA-binding proteins found in chromosomes; 135 amino acid residues. Note the very basic nature of this protein due to its abundance of Arg and Lys residues. It also lacks tryptophan.
Collagen: Collagen is an extracellular structural protein; 1052 amino acid residues. Collagen has an unusual amino acid composition; it is about one-third glycine and is rich in proline. Note that it also lacks Cys and Trp and is deficient in aromatic amino acid residues in general.

ase A from bovine pancreas has the same amino acid sequence, beginning with N-terminal lysine at position 1 and ending with C-terminal valine at position 124 (Figure 5.6). Given the possibility of any of the 20 amino acids at each position, the number of unique amino acid sequences is astronomically large. The astounding sequence variation possible within polypeptide chains provides
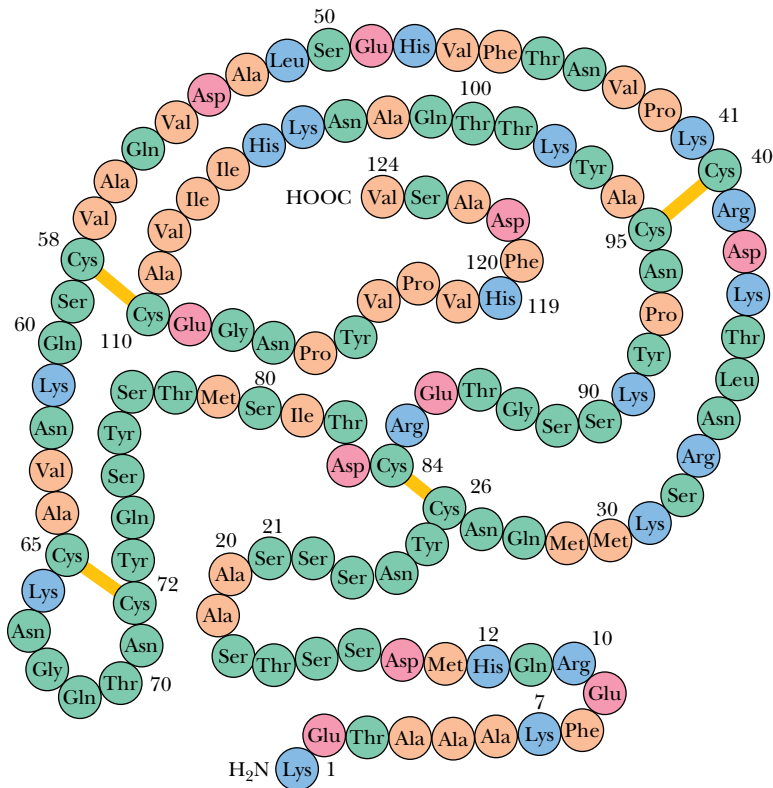
FIGURE 5.6 • Bovine pancreatic ribonuclease A contains 124 amino acid residues, none of which are tryptophan. Four intrachain disulfide bridges (S—S) form cross-links in this polypeptide between Cys[26] and Cys[84], Cys[40] and Cys[95], Cys[58] and Cys[110], and Cys[65] and Cys[72]. These disulfides are depicted by yellow bars.

a key insight into the incredible functional diversity of protein molecules in biological systems, which is discussed shortly.

5.2 • Architecture of Protein Molecules

Protein Shape

As a first approximation, proteins can be assigned to one of three global classes on the basis of shape and solubility: fibrous, globular, or membrane (Figure 5.7). **Fibrous proteins** tend to have relatively simple, regular linear structures. These proteins often serve structural roles in cells. Typically, they are insoluble in water or in dilute salt solutions. In contrast, **globular proteins** are roughly spherical in shape. The polypeptide chain is compactly folded so that hydrophobic amino acid side chains are in the interior of the molecule and the hydrophilic side chains are on the outside exposed to the solvent, water. Consequently, globular proteins are usually very soluble in aqueous solutions. Most soluble proteins of the cell, such as the cytosolic enzymes, are globular in shape. **Membrane proteins** are found in association with the various membrane systems of cells. For interaction with the nonpolar phase within membranes, membrane proteins have hydrophobic amino acid side chains oriented outward. As such, membrane proteins are insoluble in aqueous solutions but can be solubilized in solutions of detergents. Membrane proteins characteristically have fewer hydrophilic amino acids than cytosolic proteins.
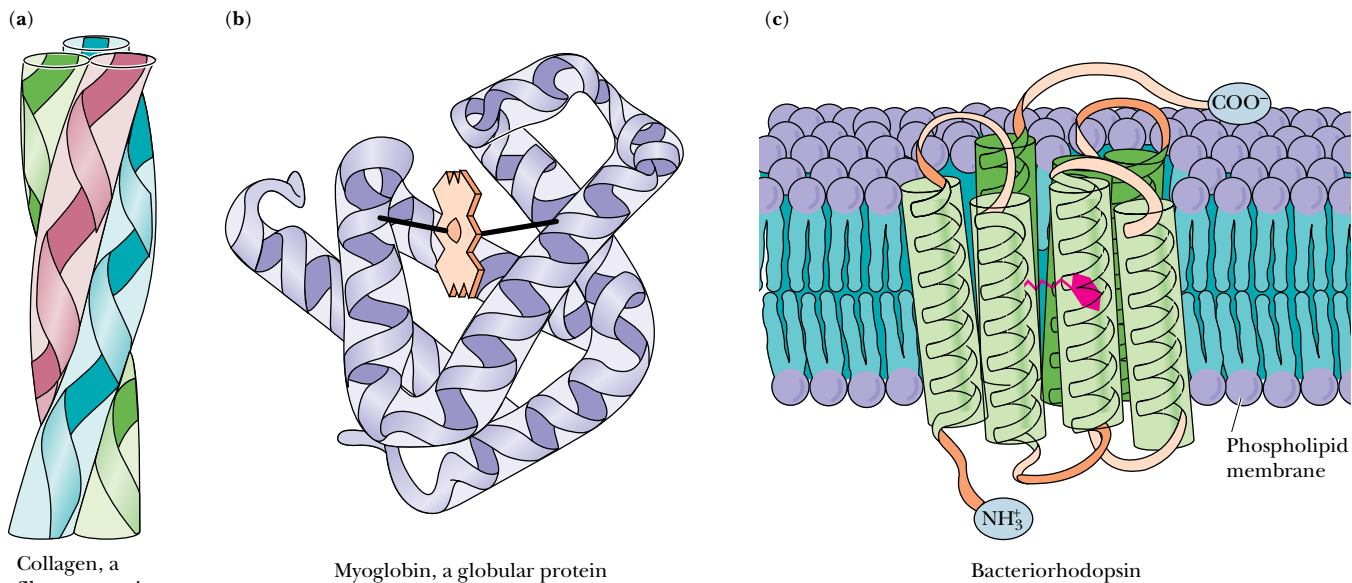
(a)

Collagen, a
fibrous protein

(b)

Myoglobin, a globular protein

(c)

Phospholipid
membrane

COO⁻

NH₃⁺

FIGURE 5.7 • (a) Proteins having structural roles in cells are typically fibrous and often water insoluble. Collagen is a good example. Collagen is composed of three polypeptide chains that intertwine. (b) Soluble proteins serving metabolic functions can be characterized as compactly folded globular molecules, such as myoglobin. The folding pattern puts hydrophilic amino acid side chains on the outside and buries hydrophobic side chains in the interior, making the protein highly water soluble. (c) Membrane proteins fold so that hydrophobic amino acid side chains are exposed in their membrane-associated regions. The portions of membrane proteins extending into or exposed at the aqueous environments are hydrophilic in character, like soluble proteins. Bacteriorhodopsin is a typical membrane protein; it binds the light-absorbing pigment, *cis*-retinal, shown here in red.
(*a, b, Irving Geis*)

𝒜 D E E P E R   L O O K

The Virtually Limitless Number of Different Amino Acid Sequences

Given 20 different amino acids, a polypeptide chain of n residues can have any one of 20^n possible sequence arrangements. To portray this, consider the number of tripeptides possible if there were only three different amino acids, A, B, and C (tripeptide $= 3 = n$; $n^3 = 3^3 = 27$):

AAA	BBB	CCC
AAB	BBA	CCA
AAC	BBC	CCB
ABA	BAB	CBC
ACA	BCB	CAC
ABC	BAA	CBA
ACB	BCC	CAB
ABB	BAC	CBB
ACC	BCA	CAA

For a polypeptide chain of 100 residues in length, a rather modest size, the number of possible sequences is 20^{100}, or because $20 = 10^{1.3}$, 10^{130} unique possibilities. These numbers are more than astronomical! Because an average protein molecule of 100 residues would have a mass of 13,800 daltons (average molecular mass of an amino acid residue = 138), 10^{130} such molecules would have a mass of 1.38×10^{134} daltons. The mass of the observable universe is estimated to be 10^{80} proton masses (about 10^{80} daltons). Thus, the universe lacks enough material to make just one molecule of each possible polypeptide sequence for a protein only 100 residues in length.

The Levels of Protein Structure

The architecture of protein molecules is quite complex. Nevertheless, this complexity can be resolved by defining various levels of structural organization.

Primary Structure

The amino acid sequence is the **primary (1°) structure** of a protein, such as that shown in Figure 5.6, for example.

Secondary Structure

Through hydrogen bonding interactions between adjacent amino acid residues (discussed in detail in Chapter 6), the polypeptide chain can arrange itself into characteristic helical or pleated segments. These segments constitute structural conformities, so-called **regular structures,** that extend along one dimension, like the coils of a spring. Such architectural features of a protein are designated **secondary (2°) structures** (Figure 5.8). Secondary structures are just one of the higher levels of structure that represent the three-dimensional arrangement of the polypeptide in space.
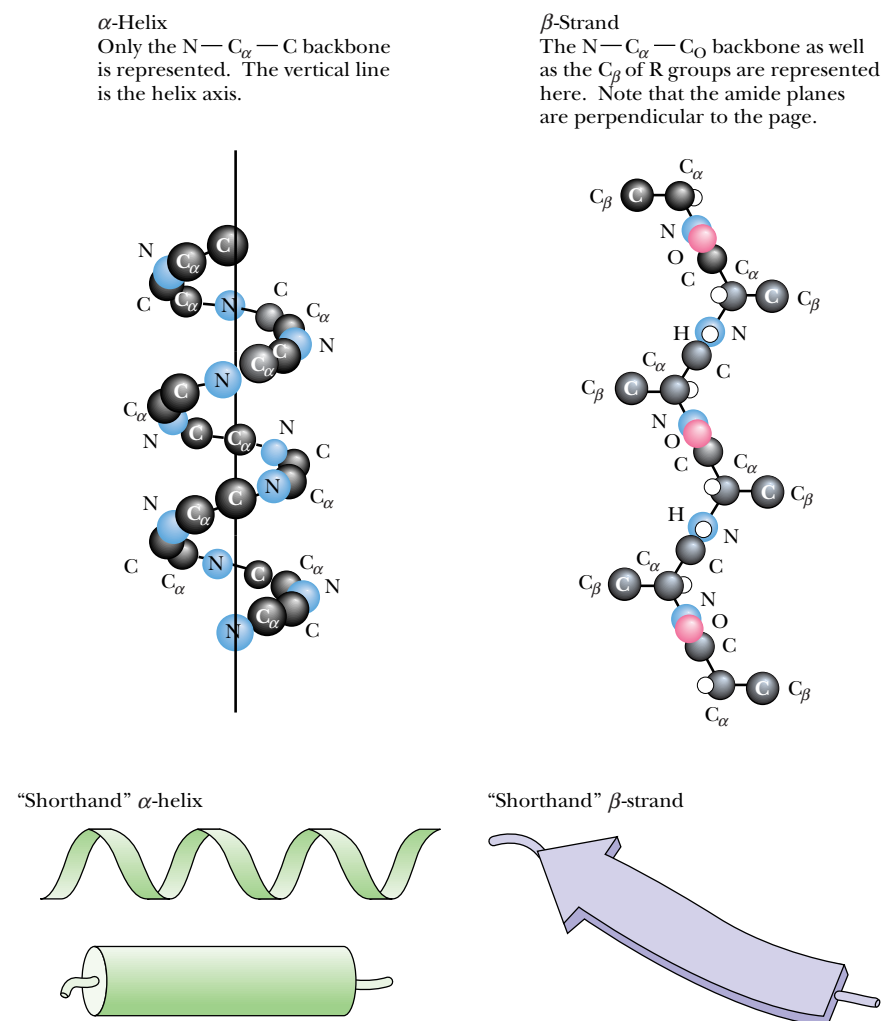
α-Helix
Only the N—C_α—C backbone is represented. The vertical line is the helix axis.

β-Strand
The N—C_α—C_O backbone as well as the C_β of R groups are represented here. Note that the amide planes are perpendicular to the page.

FIGURE 5.8 • Two structural motifs that arrange the primary structure of proteins into a higher level of organization predominate in proteins: the α-helix and the β-pleated strand. Atomic representations of these secondary structures are shown here, along with the symbols used by structural chemists to represent them: the flat, helical ribbon for the α-helix and the flat, wide arrow for β-structures. Both of these structures owe their stability to the formation of hydrogen bonds between N—H and O=C functions along the polypeptide backbone (see Chapter 6).

"Shorthand" α-helix

"Shorthand" β-strand

(a) Chymotrypsin primary structure

H$_2$N–CGVPAIQPVL$_{10}$SGL[SR]IVNGE$_{20}$EAVPGSWPWQ$_{30}$VSLQDKTGFH$_{40}$GGSLINEN$_{50}$WVVTAAHCGV$_{60}$TTSDVVVAGE$_{70}$FDQGSSSEKI$_{80}$QKLKIA
KVFK$_{90}$NSKYNSLTIN$_{100}$NDITLLKLST$_{110}$AASFSQTVSA$_{120}$VCLPSASDDF$_{130}$AAGTTCVTTG$_{140}$WGLTRY[TN]AN$_{150}$LPSDRLQQASL$_{160}$PLLSNTNCK
K$_{170}$YWGTKIKDAM$_{180}$ICAGASGVSS$_{190}$CMGDSGGPLV$_{200}$CKKNGAWTLV$_{210}$GIVSWGSSTC$_{220}$STSTPGVYAR$_{230}$VTALVNWVQQ$_{240}$TLAAN–COOH
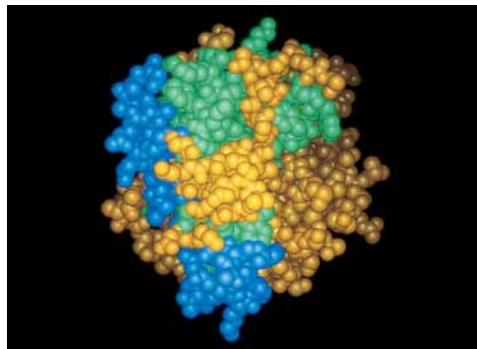
Chymotrypsin space-filling model
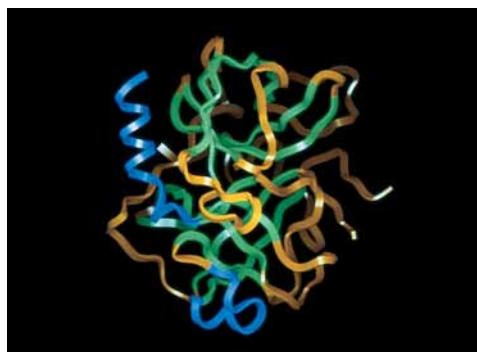
Chymotrypsin ribbon

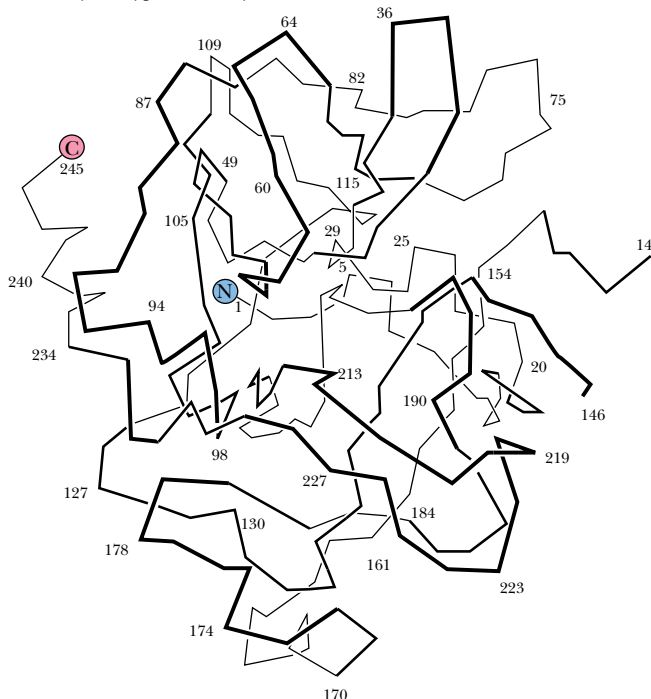**(b)** Chymotrypsin tertiary structure

FIGURE 5.9 • Folding of the polypeptide chain into a compact, roughly spherical conformation creates the tertiary level of protein structure. (a) The primary structure and (b) a representation of the tertiary structure of chymotrypsin, a proteolytic enzyme, are shown here. The tertiary representation in (b) shows the course of the chymotrypsin folding pattern by successive numbering of the amino acids in its sequence. (Residues 14 and 15 and 147 and 148 are missing because these residues are removed when chymotrypsin is formed from its larger precursor, chymotrypsinogen.) The ribbon diagram depicts the three-dimensional track of the polypeptide in space.

Tertiary Structure

When the polypeptide chains of protein molecules bend and fold in order to assume a more compact three-dimensional shape, a **tertiary (3°) level of structure** is generated (Figure 5.9). It is by virtue of their tertiary structure that proteins adopt a globular shape. A globular conformation gives the lowest surface-to-volume ratio, minimizing interaction of the protein with the surrounding environment.

Quaternary Structure

Many proteins consist of two or more interacting polypeptide chains of characteristic tertiary structure, each of which is commonly referred to as a **subunit** of the protein. Subunit organization constitutes another level in the hierarchy of protein structure, defined as the protein's **quaternary (4°) structure** (Figure 5.10). Questions of quaternary structure address the various kinds of subunits within a protein molecule, the number of each, and the ways in which they interact with one another.

Whereas the primary structure of a protein is determined by the covalently linked amino acid residues in the polypeptide backbone, secondary and higher

orders of structure are determined principally by noncovalent forces such as hydrogen bonds and ionic, van der Waals, and hydrophobic interactions. It is important to emphasize that *all the information necessary for a protein molecule to achieve its intricate architecture is contained within its 1° structure,* that is, within the amino acid sequence of its polypeptide chain(s). Chapter 6 presents a detailed discussion of the 2°, 3°, and 4° structure of protein molecules.

Protein Conformation

The overall three-dimensional architecture of a protein is generally referred to as its **conformation.** This term is not to be confused with **configuration,** which denotes the geometric possibilities for a particular set of atoms (Figure 5.11). In going from one configuration to another, covalent bonds must be broken and rearranged. In contrast, the conformational possibilities of a molecule are achieved without breaking any covalent bonds. In proteins, rotations about each of the single bonds along the peptide backbone have the potential to alter the course of the polypeptide chain in three-dimensional space. These rotational possibilities create many possible orientations for the protein chain, referred to as its *conformational possibilities.* Of the great number of theoretical conformations a given protein might adopt, only a very few are favored energetically under physiological conditions. At this time, the rules that direct the folding of protein chains into energetically favorable conformations are still not entirely clear; accordingly, they are the subject of intensive contemporary research.
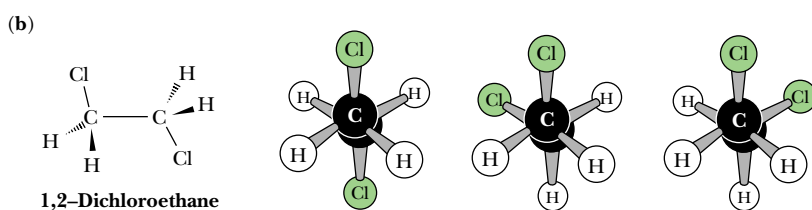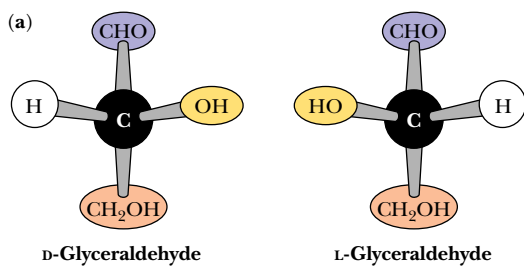

FIGURE 5.10 • Hemoglobin, which consists of two α and two β polypeptide chains, is an example of the quaternary level of protein structure. In this drawing, the β-chains are the two uppermost polypeptides and the two α-chains are the lower half of the molecule. The two closest chains (darkest colored) are the β₂-chain (*upper left*) and the α₁-chain (*lower right*). The heme groups of the four globin chains are represented by rectangles with spheres (the heme iron atom). Note the symmetry of this macromolecular arrangement. (*Irving Geis*)

FIGURE 5.11 • Configuration and conformation are *not* synonymous. (a) Rearrangements between configurational alternatives of a molecule can be achieved only by breaking and remaking bonds, as in the transformation between the D- and L-configurations of glyceraldehyde. No possible rotational reorientation of bonds linking the atoms of D-glyceraldehyde yields geometric identity with L-glyceraldehyde, even though they are mirror images of each other. (b) The intrinsic free rotation around single covalent bonds creates a great variety of three-dimensional conformations, even for relatively simple molecules. Consider 1,2-dichloroethane. Viewed end-on in a Newman projection, three principal rotational orientations or conformations predominate. Steric repulsion between eclipsed and partially eclipsed conformations keeps the possibilities at a reasonable number. (c) Imagine the conformational possibilities for a protein in which two of every three bonds along its backbone are freely rotating single bonds.
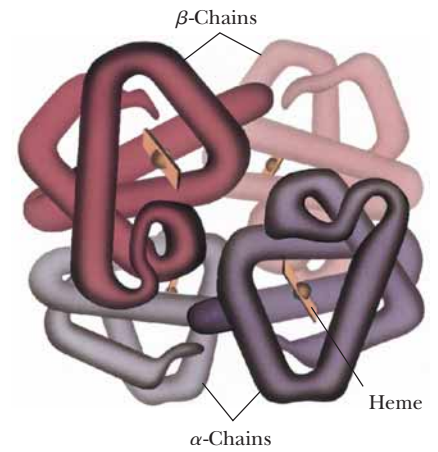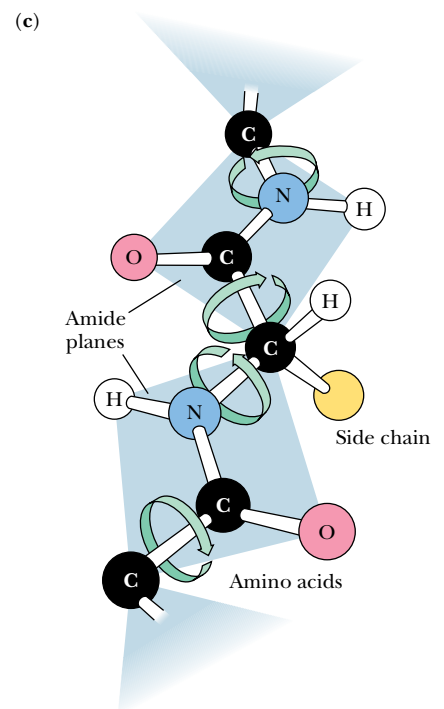
Later we return to an analysis of the 1° structure of proteins and the methodology used in determining the amino acid sequence of polypeptide chains, but let's first consider the extraordinary variety and functional diversity of these most interesting macromolecules.

5.3 • The Many Biological Functions of Proteins

Proteins are the agents of biological function. Virtually every cellular activity is dependent on one or more particular proteins. Thus, a convenient way to classify the enormous number of proteins is by the biological roles they fill. Table 5.3 summarizes the classification of proteins by function and gives examples of representative members of each class.

Enzymes

By far the largest class of proteins is enzymes. More than 3000 different enzymes are listed in *Enzyme Nomenclature,* the standard reference volume on enzyme classification. **Enzymes** are catalysts that accelerate the rates of biological reactions. Each enzyme is very specific in its function and acts only in a particular metabolic reaction. Virtually every step in metabolism is catalyzed by an enzyme. The catalytic power of enzymes far exceeds that of synthetic catalysts. Enzymes can enhance reaction rates in cells as much as 10^{16} times the uncatalyzed rate. Enzymes are systematically classified according to the nature of the reaction that they catalyze, such as the transfer of a phosphate group (*phosphotransferase*) or an oxidation–reduction (*oxidoreductase*). The formal names of enzymes come from the particular reaction within the class that they catalyze, as in ATP:D-fructose-6-phosphate 1-phosphotransferase and alcohol:NAD^+ oxidoreductase. Often, enzymes have common names in addition to their formal names. ATP:D-fructose-6-phosphate 1-phosphotransferase is more commonly known as *phosphofructokinase* (*kinase* is a common name given to ATP-dependent phosphotransferases). Similarly, alcohol:NAD^+ oxidoreductase is casually referred to as *alcohol dehydrogenase.* The reactions catalyzed by these two enzymes are shown in Figure 5.12. Other enzymes are known by trivial names that have historical roots, such as *catalase* (systematic name, hydrogen-peroxide:hydrogen-peroxide oxidoreductase), and sometimes these trivial names have descriptive connotations as well, as in *malic enzyme* (systematic name, L-malate:$NADP^+$ oxidoreductase).

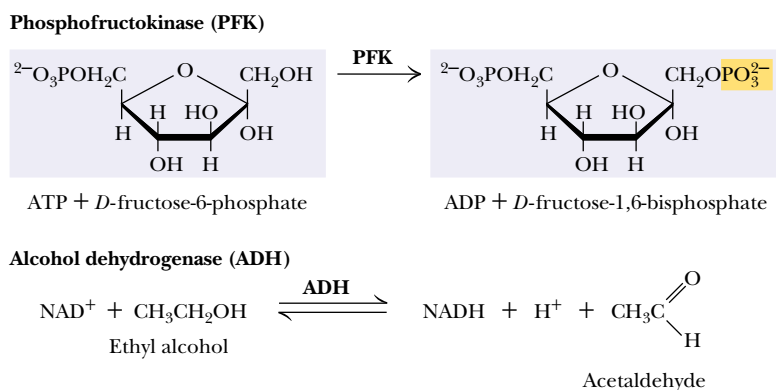**FIGURE 5.12** • Enzymes are classified according to the specific biological reaction that they catalyze. Cells contain thousands of different enzymes. Two common examples drawn from carbohydrate metabolism are phosphofructokinase (PFK), or, more precisely, ATP:D-fructose-6-phosphate 1-phosphotransferase, and alcohol dehydrogenase (ADH), or alcohol:NAD^+ oxidoreductase, which catalyze the reactions shown here.

Table 5.3

Biological Functions of Proteins and Some Representative Examples	
Functional Class	**Examples**
Enzymes	Ribonuclease
	Trypsin
	Phosphofructokinase
	Alcohol dehydrogenase
	Catalase
	"Malic" enzyme
Regulatory proteins	Insulin
	Somatotropin
	Thyrotropin
	lac repressor
	NF1 (nuclear factor 1)
	Catabolite activator protein (CAP)
	AP1
Transport proteins	Hemoglobin
	Serum albumin
	Glucose transporter
Storage proteins	Ovalbumin
	Casein
	Zein
	Phaseolin
	Ferritin
Contractile and motile proteins	Actin
	Myosin
	Tubulin
	Dynein
	Kinesin
Structural proteins	α-Keratin
	Collagen
	Elastin
	Fibroin
	Proteoglycans
Scaffold proteins	Grb 2
	crk
	shc
	stat
	IRS-1
Protective and exploitive proteins	Immunoglobulins
	Thrombin
	Fibrinogen
	Antifreeze proteins
	Snake and bee venom proteins
	Diphtheria toxin
	Ricin
Exotic proteins	Monellin
	Resilin
	Glue proteins

Regulatory Proteins

A number of proteins do not perform any obvious chemical transformation but nevertheless can regulate the ability of other proteins to carry out their physiological functions. Such proteins are referred to as **regulatory proteins.** A well-known example is *insulin,* the hormone regulating glucose metabolism in animals. Insulin is a relatively small protein (5.7 kD) and consists of two polypeptide chains held together by disulfide cross-bridges. Other hormones that are also proteins include pituitary *somatotropin* (21 kD) and *thyrotropin* (28 kD), which stimulates the thyroid gland. Another group of regulatory proteins is involved in the regulation of gene expression. These proteins characteristically act by binding to DNA sequences that are adjacent to coding regions of genes, either activating or inhibiting the transcription of genetic information into RNA. Examples include **repressors,** which, because they block transcription, are considered negative control elements.

A prokaryotic representative is *lac repressor* (37 kD), which controls expression of the enzyme system responsible for the metabolism of lactose (milk sugar); a mammalian example is *NF1* (*nuclear factor 1,* 60 kD), which inhibits transcription of the gene encoding the β-globin polypeptide chain of hemoglobin. Positively acting control elements are also known. For example, the *E. coli* catabolite gene activator protein (**CAP**) (44 kD), under appropriate metabolic conditions, can bind to specific sites along the *E. coli* chromosome and increase the rate of transcription of adjacent genes. The mammalian *AP1* is a heterodimeric transcription factor composed of one polypeptide from the *Jun* family of gene-regulatory proteins and one polypeptide from the *Fos* family of gene-regulatory proteins. AP1 activates expression of the β-globin gene. These various DNA-binding regulatory proteins often possess characteristic structural features, such as helix-turn-helix, leucine zipper, and zinc finger motifs (see Chapter 31).

Transport Proteins

A third class of proteins is the **transport proteins.** These proteins function to transport specific substances from one place to another. One type of transport is exemplified by the transport of oxygen from the lungs to the tissues by *hemoglobin* (Figure 5.13a) or by the transport of fatty acids from adipose tissue to various organs by the blood protein *serum albumin.* A very different type is the transport of metabolites across permeability barriers such as cell membranes, as mediated by specific membrane proteins. These *membrane transport proteins* take up metabolite molecules on one side of a membrane, transport them across the membrane, and release them on the other side. Examples include the transport proteins responsible for the uptake of essential nutrients into the cell, such as glucose or amino acids (Figure 5.13b). All naturally occurring membrane transport proteins studied thus far form channels in the membrane through which the transported substances are passed.

Storage Proteins

Proteins whose biological function is to provide a reservoir of an essential nutrient are called **storage proteins.** Because proteins are amino acid polymers and because nitrogen is commonly a limiting nutrient for growth, organisms have exploited proteins as a means to provide sufficient nitrogen in times of need. For example, *ovalbumin,* the protein of egg white, provides the developing bird embryo with a source of nitrogen during its isolation within the egg. *Casein* is the most abundant protein of milk and thus the major nitrogen source for
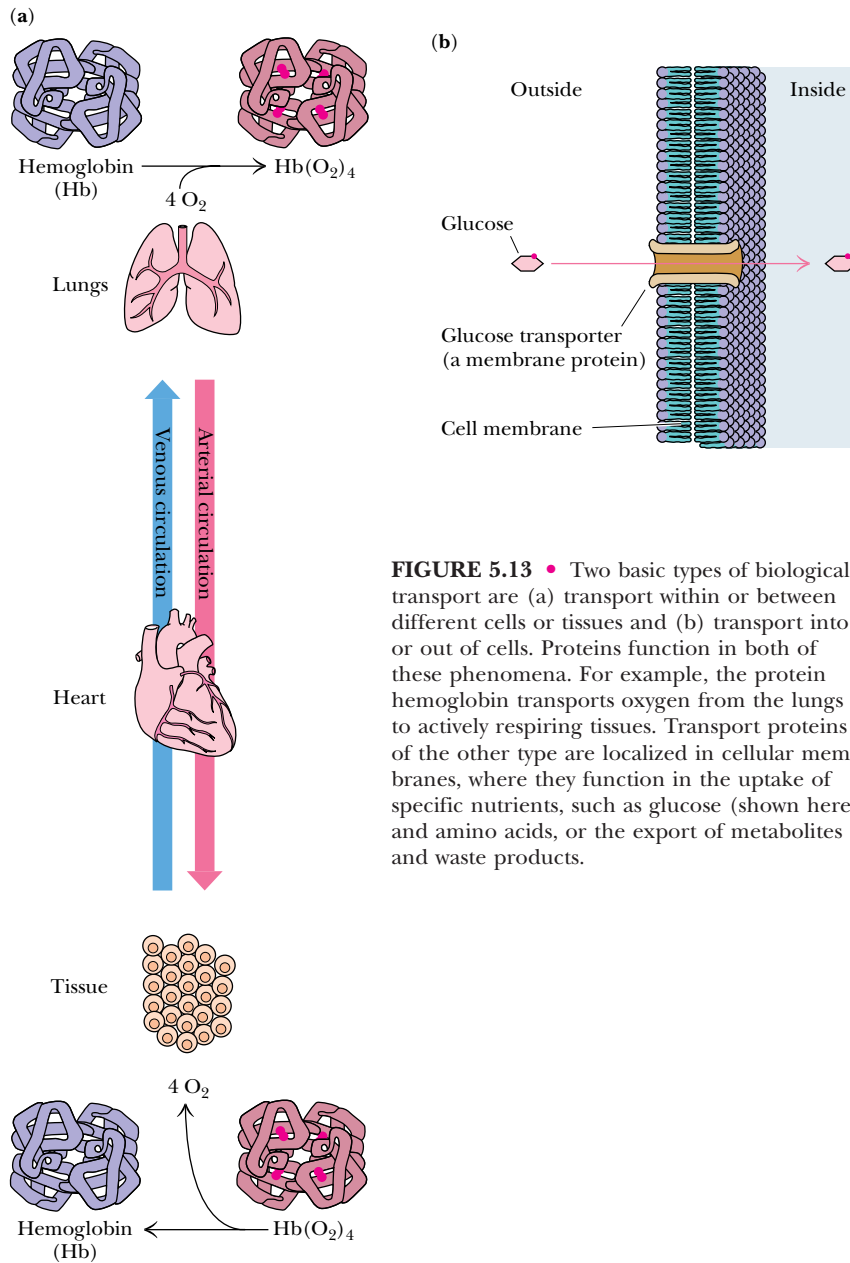
(a)

(b)

FIGURE 5.13 • Two basic types of biological transport are (a) transport within or between different cells or tissues and (b) transport into or out of cells. Proteins function in both of these phenomena. For example, the protein hemoglobin transports oxygen from the lungs to actively respiring tissues. Transport proteins of the other type are localized in cellular membranes, where they function in the uptake of specific nutrients, such as glucose (shown here) and amino acids, or the export of metabolites and waste products.

mammalian infants. The seeds of higher plants often contain as much as 60% storage protein to make the germinating seed nitrogen-sufficient during this crucial period of plant development. In corn (*Zea mays* or *maize*), a family of low molecular weight proteins in the kernel called *zeins* serve this purpose; peas (the seeds of *Phaseolus vulgaris*) contain a storage protein called *phaseolin*. The use of proteins as a reservoir of nitrogen is more efficient than storing an equivalent amount of amino acids. Not only is the osmotic pressure minimized, but the solvent capacity of the cell is taxed less in solvating one molecule of a polypeptide than in dissolving, for example, 100 molecules of free amino acids. Proteins can also serve to store nutrients other than the more obvious elements composing amino acids (N, C, H, O, and S). As an example, *ferritin* is a protein found in animal tissues that binds iron, retaining this essential metal so

that it is available for the synthesis of important iron-containing proteins such as hemoglobin. One molecule of ferritin (460 kD) binds as many as 4500 atoms of iron (35% by weight).

Contractile and Motile Proteins

Certain proteins endow cells with unique capabilities for movement. Cell division, muscle contraction, and cell motility represent some of the ways in which cells execute motion. The **contractile** and **motile proteins** underlying these motions share a common property: they are filamentous or polymerize to form filaments. Examples include *actin* and *myosin,* the filamentous proteins forming the contractile systems of cells, and *tubulin,* the major component of microtubules (the filaments involved in the mitotic spindle of cell division as well as in flagella and cilia). Another class of proteins involved in movement includes *dynein* and *kinesin,* so-called **motor proteins** that drive the movement of vesicles, granules, and organelles along microtubules serving as established cytoskeletal "tracks."

Structural Proteins

An apparently passive but very important role of proteins is their function in creating and maintaining biological structures. **Structural proteins** provide strength and protection to cells and tissues. Monomeric units of structural proteins typically polymerize to generate long fibers (as in hair) or protective sheets of fibrous arrays, as in cowhide (leather). *α-Keratins* are insoluble fibrous proteins making up hair, horns, and fingernails. *Collagen,* another insoluble fibrous protein, is found in bone, connective tissue, tendons, cartilage, and hide, where it forms inelastic fibrils of great strength. One-third of the total protein in a vertebrate animal is collagen. A structural protein having elastic properties is, appropriately, *elastin,* an important component of ligaments. Because of the way elastin monomers are cross-linked in forming polymers, elastin can stretch in two dimensions. Certain insects make a structurally useful protein, *fibroin* (a *β*-keratin), the major constituent of cocoons (silk) and spider webs. An important protective barrier for animal cells is the **extracellular matrix** containing *collagen* and *proteoglycans,* covalent protein–polysaccharide complexes that cushion and lubricate.

Scaffold Proteins (Adapter Proteins)

Some proteins play a recently discovered role in the complex pathways of cellular response to hormones and growth factors. These proteins, the **scaffold** or **adapter proteins,** have a modular organization in which specific parts (**modules**) of the protein's structure recognize and bind certain structural elements in other proteins through **protein–protein interactions.** For example, *SH2* modules bind to proteins in which a tyrosine residue has become phosphorylated on its phenolic —OH, and *SH3* modules bind to proteins having a characteristic grouping of proline residues. Others include *PH* modules, which bind to membranes, and *PDZ*-containing proteins, which bind specifically to the C-terminal amino acid of certain proteins. Because scaffold proteins typically possess several of these different kinds of modules, they can act as a scaffold onto which a set of different proteins is assembled into a multiprotein complex. Such assemblages are typically involved in coordinating and communicating the many intracellular responses to hormones or other signalling molecules (Figure 5.14). **Anchoring** (or **targeting**) **proteins** are proteins that bind other proteins, causing them to associate with other structures in the cell. A family of *anchoring proteins,* known as *AKAP* or *A kinase anchoring proteins,* exists in
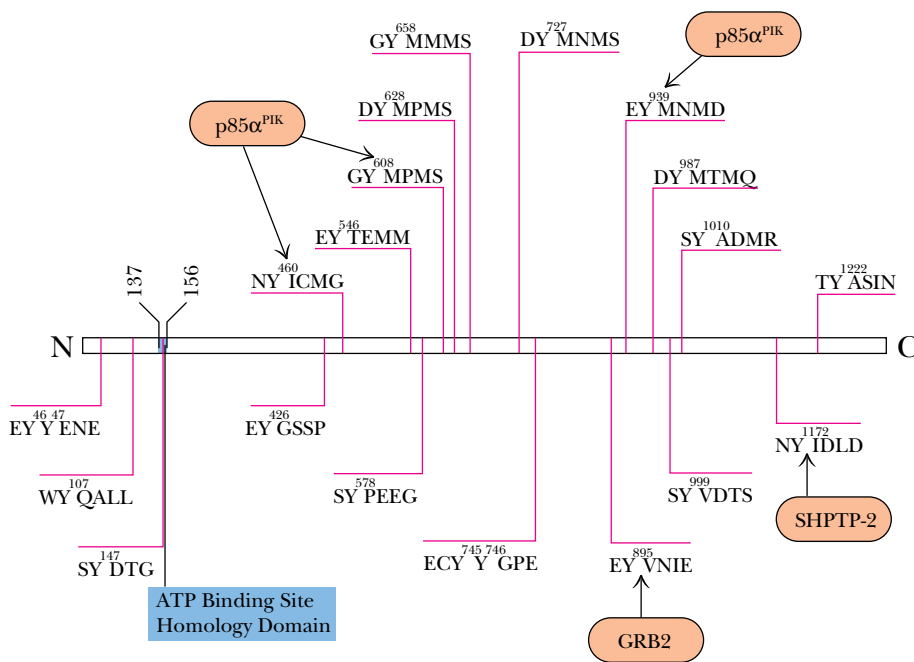
FIGURE 5.14 • Diagram of the N→C sequence organization of the adapter protein *insulin receptor substrate-1 (IRS-1)* showing the various amino acid sequences (in one-letter code) that contain tyrosine (Y) residues that are potential sites for phosphorylation. The other adapter proteins that recognize various of these sites are shown as *Grb2, SHPTP-2,* and *p85α^PIK^*. Insulin binding to the insulin receptor activates the enzymatic activity that phosphorylates these Tyr residues on IRS-1. (*Adapted from White, M. F., and Kahn, C. R., 1994.* Journal of Biological Chemistry **269:**1–4.)

which specific AKAP members bind the regulatory enzyme *protein kinase A* (PKA) to particular subcellular compartments. For example, AKAP100 targets PKA to the endoplasmic reticulum, whereas AKAP79 targets PKA to the plasma membrane.

Protective and Exploitive Proteins

In contrast to the passive protective nature of some structural proteins, another group can be more aptly classified as **protective** or **exploitive proteins** because of their biologically active role in cell defense, protection, or exploitation. Prominent among the protective proteins are the *immunoglobulins* or *antibodies* produced by the lymphocytes of vertebrates. Antibodies have the remarkable ability to "ignore" molecules that are an intrinsic part of the host organism, yet they can specifically recognize and neutralize "foreign" molecules resulting from the invasion of the organism by bacteria, viruses, or other infectious agents. Another group of protective proteins is the blood-clotting proteins, *thrombin* and *fibrinogen,* which prevent the loss of blood when the circulatory system is damaged. Arctic and Antarctic fishes have *antifreeze proteins* to protect their blood against freezing in the below-zero temperatures of high-latitude seas. In addition, various proteins serve defensive or exploitive roles for organisms, including the lytic and neurotoxic proteins of snake and bee venoms and toxic plant proteins, such as *ricin,* whose apparent purpose is to thwart predation by herbivores. Another class of exploitive proteins includes the toxins produced by bacteria, such as diphtheria toxin and cholera toxin.

Exotic Proteins

Some proteins display rather exotic functions that do not quite fit the previous classifications. *Monellin,* a protein found in an African plant, has a very sweet taste and is being considered as an artificial sweetener for human consumption. *Resilin,* a protein having exceptional elastic properties, is found in

the hinges of insect wings. Certain marine organisms such as mussels secrete *glue proteins,* allowing them to attach firmly to hard surfaces. It is worth repeating that the great diversity of function in proteins, as reflected in this survey, is attained using just 20 amino acids.

5.4 • Some Proteins Have Chemical Groups Other Than Amino Acids

Many proteins consist of only amino acids and contain no other chemical groups. The enzyme ribonuclease and the contractile protein actin are two such examples. Such proteins are called **simple proteins.** However, many other proteins contain various chemical constituents as an integral part of their structure. These proteins are termed **conjugated proteins** (Table 5.4). If the nonprotein part is crucial to the protein's function, it is referred to as a **prosthetic group.** If the nonprotein moiety is not covalently linked to the protein, it can usually be removed by denaturing the protein structure. However, if the conjugate is covalently joined to the protein, it may be necessary to carry out acid hydrolysis of the protein into its component amino acids in order to release it. Conjugated proteins are typically classified according to the chemical nature of their nonamino acid component; a representative selection of them is given here and in Table 5.4. (Note that comparisons of Tables 5.3 and 5.4 reveal two distinctly different ways of considering the nature of proteins—function versus chemistry.)

GLYCOPROTEINS. Glycoproteins are proteins that contain carbohydrate. Proteins destined for an extracellular location are characteristically glycoproteins. For example, fibronectin and proteoglycans are important components of the extracellular matrix that surrounds the cells of most tissues in animals. Immunoglobulin G molecules are the principal antibody species found circulating free in the blood plasma. Many membrane proteins are glycosylated on their extracellular segments.

LIPOPROTEINS. Blood plasma lipoproteins are prominent examples of the class of proteins conjugated with lipid. The plasma lipoproteins function primarily in the transport of lipids to sites of active membrane synthesis. Serum levels of *low density lipoproteins* (LDLs) are often used as a clinical index of susceptibility to vascular disease.

NUCLEOPROTEINS. Nucleoprotein conjugates have many roles in the storage and transmission of genetic information. Ribosomes are the sites of protein synthesis. Virus particles and even chromosomes are protein–nucleic acid complexes.

PHOSPHOPROTEINS. These proteins have phosphate groups esterified to the hydroxyls of serine, threonine, or tyrosine residues. Casein, the major protein of milk, contains many phosphates and serves to bring essential phosphorus to the growing infant. Many key steps in metabolism are regulated between states of activity or inactivity, depending on the presence or absence of phosphate groups on proteins, as we shall see in Chapter 15. Glycogen phosphorylase *a* is one well-studied example.

METALLOPROTEINS. Metalloproteins are either metal storage forms, as in the case of ferritin, or enzymes in which the metal atom participates in a catalytically important manner. We encounter many examples throughout this book of the vital metabolic functions served by metalloenzymes.

Table 5.4

Representative Conjugated Proteins		
Class	**Prosthetic Group**	**Percent by Weight (approx.)**
Glycoproteins contain carbohydrate		
Fibronectin		
γ-Globulin		
Proteoglycan		
Lipoproteins contain lipid		
Blood plasma lipoproteins:		
High density lipoprotein (HDL) (α-lipoprotein)	Triacylglycerols, phospholipids, cholesterol	75
Low density lipoprotein (LDL) (β-lipoprotein)	Triacylglycerols, phospholipids, cholesterol	67
Nucleoprotein complexes contain nucleic acid		
Ribosomes	RNA	60
Tobacco mosaic virus	RNA	5
Adenovirus	DNA	
HIV-1 (AIDS virus)	RNA	
Phosphoproteins contain phosphate		
Casein	Phosphate groups	
Glycogen phosphorylase *a*	Phosphate groups	
Metalloproteins contain metal atoms		
Ferritin	Iron	35
Alcohol dehydrogenase	Zinc	
Cytochrome oxidase	Copper and iron	
Nitrogenase	Molybdenum and iron	
Pyruvate carboxylase	Manganese	
Hemoproteins contain heme		
Hemoglobin		
Cytochrome *c*		
Catalase		
Nitrate reductase		
Ammonium oxidase		
Flavoproteins contain flavin		
Succinate dehydrogenase	FAD	
NADH dehydrogenase	FMN	
Dihydroorotate dehydrogenase	FAD and FMN	
Sulfite reductase	FAD and FMN	

HEMOPROTEINS. These proteins are actually a subclass of metalloproteins because their prosthetic group is **heme,** the name given to iron protoporphyrin IX (Figure 5.15). Because heme-containing proteins enjoy so many prominent biological functions, they are considered a class by themselves.

FLAVOPROTEINS. *Flavin* is an essential substance for the activity of a number of important oxidoreductases. We discuss the chemistry of flavin and its derivatives, FMN and FAD, in the chapter on electron transport and oxidative phosphorylation (Chapter 21).

FIGURE 5.15 • Heme consists of protopor-phyrin IX and an iron atom. Protoporphyrin, a highly conjugated system of double bonds, is composed of four 5-membered heterocyclic rings (pyrroles) fused together to form a tetrapyrrole macrocycle. The specific isomeric arrangement of methyl, vinyl, and propionate side chains shown is protoporphyrin IX. Coordination of an atom of ferrous iron (Fe^{2+}) by the four pyrrole nitrogen atoms yields heme.

Protoporphyrin IX

Heme
(Fe-protoporphyrin IX)
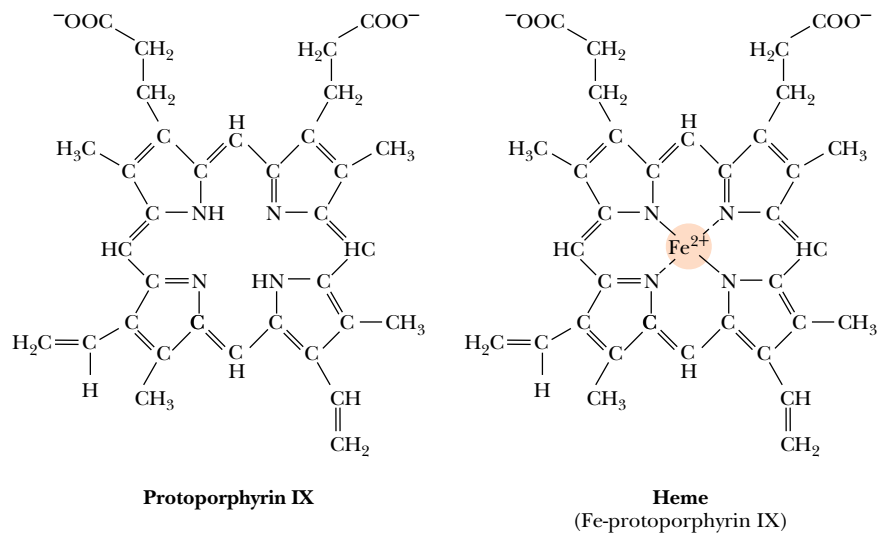
5.5 • Reactions of Peptides and Proteins

The chemical properties of peptides and proteins are most easily considered in terms of the chemistry of their component functional groups. That is, they possess reactive amino and carboxyl termini and they display reactions characteristic of the chemistry of the R groups of their component amino acids. These reactions are familiar to us from Chapter 4 and from the study of organic chemistry and need not be repeated here.

5.6 • Purification of Protein Mixtures

Cells contain thousands of different proteins. A major problem for protein chemists is to purify a chosen protein so that they can study its specific properties in the absence of other proteins. Proteins have been separated and purified on the basis of their two prominent physical properties: size and electrical charge. A more direct approach is to employ **affinity purification** strategies that take advantage of the biological function or similar specific recognition properties of a protein (see Table 5.5 and Chapter Appendix).

Separation Methods

Separation methods based on size include size exclusion chromatography, ultrafiltration, and ultracentrifugation (see Chapter Appendix). The ionic properties of peptides and proteins are determined principally by their complement of amino acid side chains. Furthermore, the ionization of these groups is pH-dependent.

A variety of procedures exploit electrical charge as a means of discriminating between proteins, including ion exchange chromatography (see Chapter 4), electrophoresis (see Chapter Appendix), and solubility. Proteins tend to be least soluble at their **isoelectric point,** the pH value at which the sum of their positive and negative electrical charges is zero. At this pH, electrostatic repulsion between protein molecules is minimal and they are more likely to coalesce and precipitate out of solution. Ionic strength also profoundly influences protein solubility. Most globular proteins tend to become increas-

Estimation of Protein Concentrations in Solutions of Biological Origin

Biochemists are often interested in knowing the protein concentration in various preparations of biological origin. Such quantitative analysis is not straightforward. Cell extracts are complex mixtures that typically contain protein molecules of many different molecular weights, so the results of protein estimations cannot be expressed on a molar basis. Also, aside from the rather unreactive repeating peptide backbone, little common chemical identity is seen among the many proteins found in cells that might be readily exploited for exact chemical analysis. Most of their chemical properties vary with their amino acid composition, for example, nitrogen or sulfur content or the presence of aromatic, hydroxyl, or other functional groups.

Lowry Procedure

A method that has been the standard of choice for many years is the **Lowry procedure.** This method uses Cu^{2+} ions along with *Folin–Ciocalteau reagent,* a combination of phosphomolybdic and phosphotungstic acid complexes that react with Cu^+. Cu^+ is generated from Cu^{2+} by readily oxidizable protein components, such as cysteine or the phenols and indoles of tyrosine and tryptophan. Although the precise chemistry of the Lowry method remains uncertain, the Cu^+ reaction with the Folin reagent gives intensely colored products measurable spectrophotometrically.

BCA Method

Recently, a reagent that reacts more efficiently with Cu^+ than Folin–Ciocalteau reagent has been developed for protein assays. *Bicinchoninic acid (BCA)* forms a purple complex with Cu^+ in alkaline solution.

Assays Based on Dye Binding

Several other protocols for protein estimation enjoy prevalent usage in biochemical laboratories. The **Bradford assay** is a rapid and reliable technique that uses a dye called *Coomassie Brilliant Blue G-250,* which undergoes a change in its color upon noncovalent binding to proteins. The binding is quantitative and less sensitive to variations in the protein's amino acid composition. The color change is easily measured by a spectrophotometer. A similar, very sensitive method capable of quantifying nanogram amounts of protein is based on the shift in color of colloidal gold upon binding to proteins.

$$Cu^+ + BCA \longrightarrow$$

BCA–Cu$^+$ complex
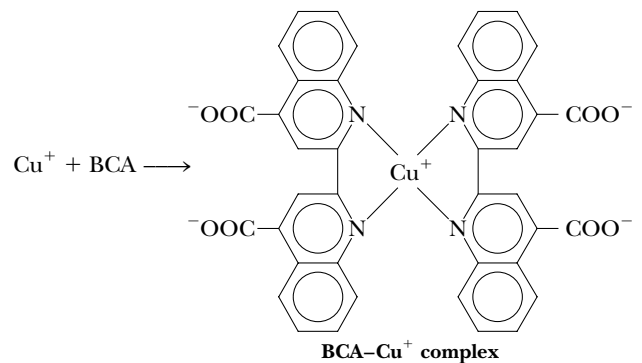
ingly soluble as the ionic strength is raised. This phenomenon, the salting-in of proteins, is attributed to the diminishment by the salt ions of electrostatic attractions between the protein molecules. Such electrostatic interactions would otherwise lead to precipitation. However, as the salt concentration reaches high levels (greater than 1 M), the effect may reverse so that the protein is salted out of solution. In such cases, the numerous salt ions begin to compete with the protein for waters of solvation, and, as they win out, the protein becomes insoluble. The solubility properties of a typical protein are shown in Figure 5.16.

Although the side chains of most nonpolar amino acids in soluble proteins are usually buried in the interior of the protein away from contact with the aqueous solvent, a portion of them is exposed at the protein's surface, giving
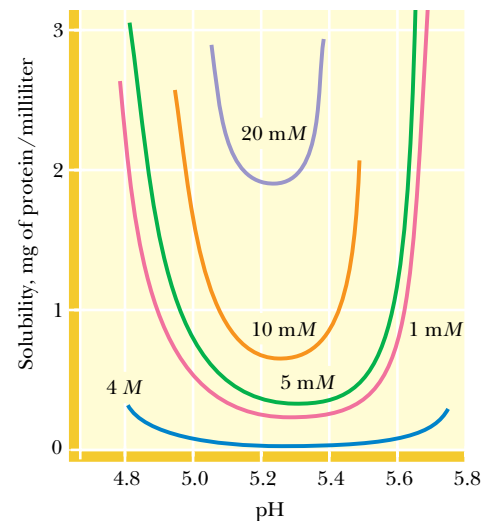
FIGURE 5.16 • The solubility of most globular proteins is markedly influenced by pH and ionic strength. This figure shows the solubility of a typical protein as a function of pH and various salt concentrations.

Table 5.5

Example of a Protein Purification Scheme: Purification of the Enzyme Xanthine Dehydrogenase from a Fungus

Fraction	Volume (mL)	Total Protein (mg)	Total Activity*	Specific Activity[†]	Percent Recovery[‡]
1. Crude extract	3,800	22,800	2,460	0.108	100
2. Salt precipitate	165	2,800	1,190	0.425	48
3. Ion exchange chromatography	65	100	720	7.2	29
4. Molecular sieve chromatography	40	14.5	555	38.3	23
5. Immunoaffinity chromatography[§]	6	1.8	275	152	11

*The relative enzymatic activity of each fraction in catalyzing the xanthine dehydrogenase reaction is cited as arbitrarily defined units.
[†]The specific activity is the total activity of the fraction divided by the total protein in the fraction. This value gives an indication of the increase in purity attained during the course of the purification as the samples become enriched for xanthine dehydrogenase protein.
[‡]The percent recovery of total activity is a measure of the yield of the desired product, xanthine dehydrogenase.
[§]The last step in the procedure is an affinity method in which antibodies specific for xanthine dehydrogenase are covalently coupled to a chromatography matrix and packed into a glass tube to make a chromatographic column through which fraction 4 is passed. The enzyme is bound by this immunoaffinity matrix while other proteins pass freely out. The enzyme is then recovered by passing a strong salt solution through the column, which dissociates the enzyme–antibody complex.

Adapted from Lyon, E. S., and Garrett, R. H., 1978. *Journal of Biological Chemistry.* **253:**2604–2614.

it a partially hydrophobic character. *Hydrophobic interaction chromatography* is a protein purification technique that exploits this hydrophobicity (see Chapter Appendix).

A Typical Protein Purification Scheme

Most purification procedures for a particular protein are developed in an empirical manner, the overriding principle being purification of the protein to a homogeneous state with acceptable yield. Table 5.5 presents a summary of a purification scheme for a selected protein. Note that the **specific activity** of the protein (the enzyme xanthine dehydrogenase) in the immuno-affinity purified fraction (fraction 5) has been increased 152/0.108, or 1407 times the specific activity in the crude extract (fraction 1). Thus, xanthine dehydrogenase in fraction 5 versus fraction 1 is enriched more than 1400-fold by the purification procedure.

5.7 • The Primary Structure of a Protein: Determining the Amino Acid Sequence

In 1953, Frederick Sanger of Cambridge University in England reported the amino acid sequences of the two polypeptide chains composing the protein insulin (Figure 5.17). Not only was this a remarkable achievement in analytical chemistry but it helped to demystify speculation about the chemical nature of proteins. Sanger's results clearly established that all of the molecules of a given protein have a fixed amino acid composition, a defined amino acid sequence, and therefore an invariant molecular weight. In short, proteins are well defined chemically. Today, the amino acid sequences of some 100,000 different proteins are known. Although many sequences have been determined from application of the principles first established by Sanger, most are now deduced from knowledge of the nucleotide sequence of the gene that encodes the protein.

Protein Sequencing Strategy

The usual strategy for determining the amino acid sequence of a protein involves eight basic steps:

1. If the protein contains more than one polypeptide chain, the chains are separated and purified.
2. Intrachain S—S (disulfide) cross-bridges between cysteine residues in the polypeptide chain are cleaved. (If these disulfides are interchain linkages, then step 2 precedes step 1.)
3. The amino acid composition of each polypeptide chain is determined.
4. The N-terminal and C-terminal residues are identified.
5. Each polypeptide chain is cleaved into smaller fragments, and the amino acid composition and sequence of each fragment are determined.
6. Step 5 is repeated, using a different cleavage procedure to generate a different and therefore overlapping set of peptide fragments.
7. The overall amino acid sequence of the protein is reconstructed from the sequences in overlapping fragments.
8. The positions of S—S cross-bridges formed between cysteine residues are located.

Each of these steps is discussed in greater detail in the following sections.

Step 1. Separation of Polypeptide Chains

If the protein of interest is a **heteromultimer** (composed of more than one type of polypeptide chain), then the protein must be dissociated and its component polypeptide subunits must be separated from one another and sequenced individually. Subunit associations in multimeric proteins are typically maintained solely by noncovalent forces, and therefore most multimeric proteins can usually be dissociated by exposure to pH extremes, 8 M urea, 6 M guanidinium hydrochloride, or high salt concentrations. (All of these treatments disrupt polar interactions such as hydrogen bonds both within the protein molecule and between the protein and the aqueous solvent.) Once dissociated, the individual polypeptides can be isolated from one another on the basis of differences in size and/or charge. Occasionally, heteromultimers are linked together by interchain S—S bridges. In such instances, these cross-links must be cleaved prior to dissociation and isolation of the individual chains. The methods described under step 2 are applicable for this purpose.

Step 2. Cleavage of Disulfide Bridges

A number of methods exist for cleaving disulfides (Figure 5.18). An important consideration is to carry out these cleavages so that the original or even new S—S links do not form. Oxidation of a disulfide by performic acid results in the formation of two equivalents of cysteic acid (Figure 5.18a). Because these cysteic acid side chains are ionized SO_3^- groups, electrostatic repulsion (as well as altered chemistry) prevents S—S recombination. Alternatively, sulfhydryl compounds such as 2-mercaptoethanol readily reduce S—S bridges to regenerate two cysteine—SH side chains (Figure 5.18b). However, these SH groups recombine to re-form either the original disulfide link or, if other free Cys—SHs are available, new disulfide links. To prevent this, S—S reduction must be followed by treatment with alkylating agents such as iodoacetate or 3-bromopropylamine, which modify the SH groups and block disulfide bridge formation (Figure 5.18a).
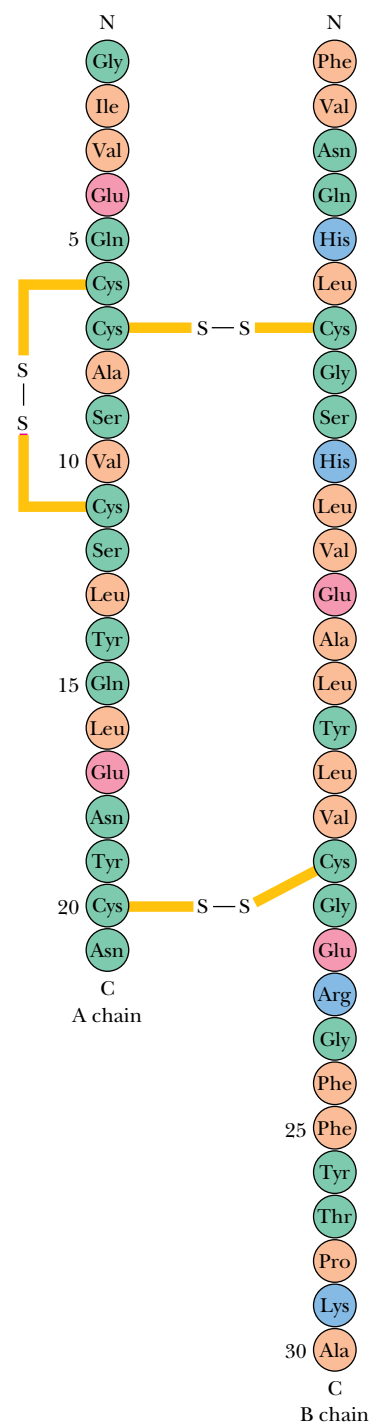

FIGURE 5.17 • The hormone insulin consists of two polypeptide chains, A and B, held together by two disulfide cross-bridges (S—S). The A chain has 21 amino acid residues and an intrachain disulfide; the B polypeptide contains 30 amino acids. The sequence shown is for bovine insulin.
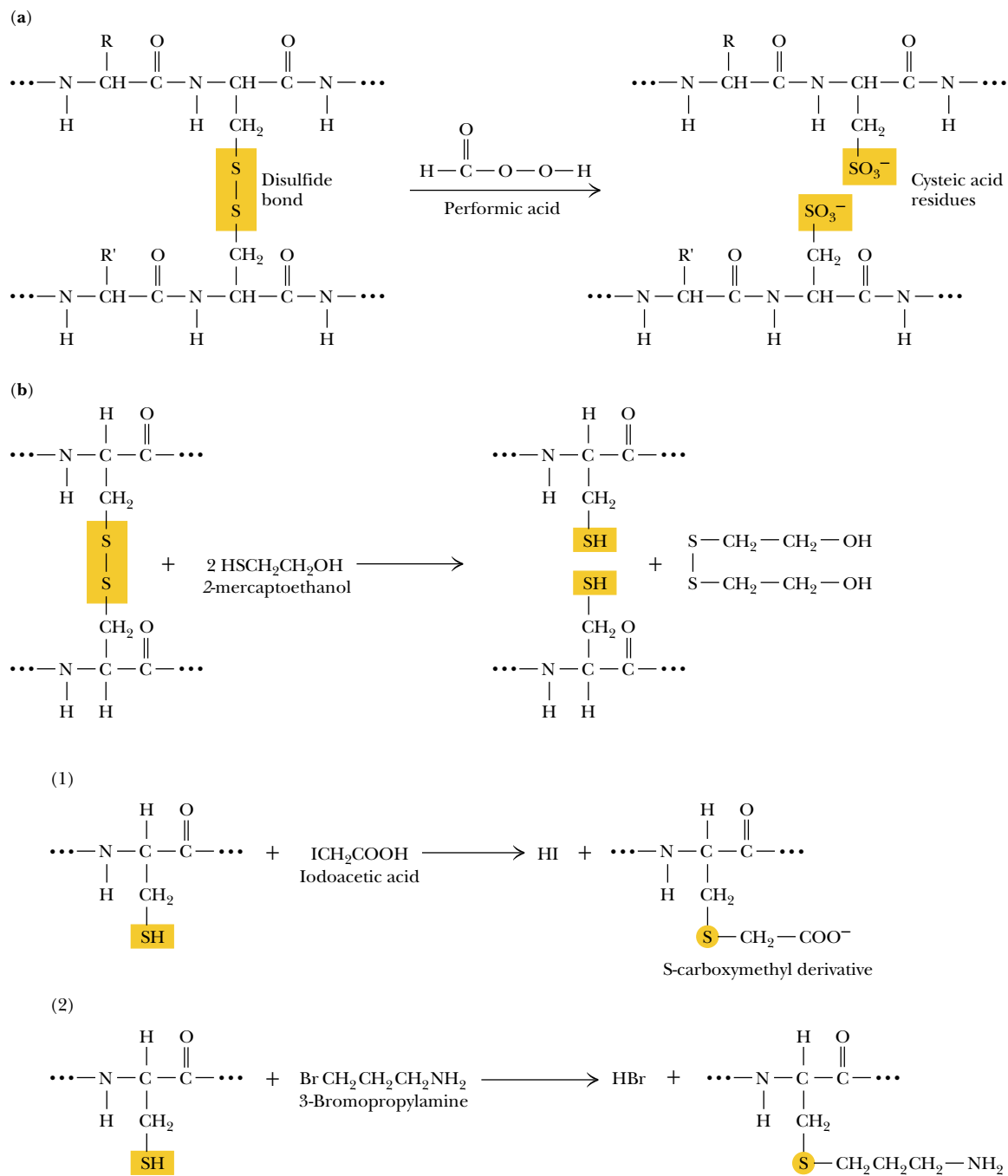
FIGURE 5.18 • Methods for cleavage of disulfide bonds in proteins. (a) Oxidative cleavage by reaction with performic acid. (b) Reductive cleavage with sulfhydryl compounds. Disulfide bridges can be broken by reduction of the S—S link with sulfhydryl agents such as 2-mercaptoethanol or dithiothreitol. Because reaction between the newly reduced —SH groups to re-establish disulfide bonds is a likelihood, S—S reduction must be followed by —SH modification: (1) alkylation with iodoacetate (ICH_2COOH) or (2) modification with 3-bromopropylamine (Br—$(CH_2)_3$—NH_2).

Step 3. Analysis of Amino Acid Composition

The standard protocol for analysis of the amino acid composition of proteins is discussed in Section 5.1. Results of such analyses allow the researcher to anticipate which methods of polypeptide fragmentation might be useful for the protein.

Step 4. Identification of the N- and C-Terminal Residues

End-group analysis reveals several things. First, it identifies the N- and C-terminal residues in the polypeptide chain. Second, it can be a clue to the number of ends in the protein. That is, if the protein consists of two or more different polypeptide chains, then more than one end group may be discovered, alerting the investigator to the presence of multiple polypeptides.

A. N-Terminal Analysis

The amino acid residing at the N-terminal end of a protein can be identified in a number of ways; one method, **Edman degradation,** has become the procedure of choice. This method is preferable because it allows the sequential identification of a series of residues beginning at the N-terminus (Figure 5.19). In weakly basic solutions, phenylisothiocyanate, or **Edman's reagent** (phenyl—N=C=S), combines with the free amino terminus of a protein (Figure 5.19), which can be excised from the end of the polypeptide chain and recovered as a phenylthiohydantoin (PTH) derivative. This PTH derivative can be identified by chromatographic methods. Importantly, in this procedure, the rest of the polypeptide chain remains intact and can be subjected to further rounds of Edman degradation to identify successive amino acid residues in the chain. Often, the carboxyl terminus of the polypeptide under analysis is coupled to an insoluble matrix, allowing the polypeptide to be easily recovered by filtration following each round of Edman reaction. Thus, Edman reaction not only identifies the N-terminus of proteins but can also reveal additional information regarding sequence. Automated instruments (so-called *Edman sequenators*) have been designed to carry out the reaction cycle of the Edman procedure. In practical terms, as many as 50 cycles of reaction can be accomplished
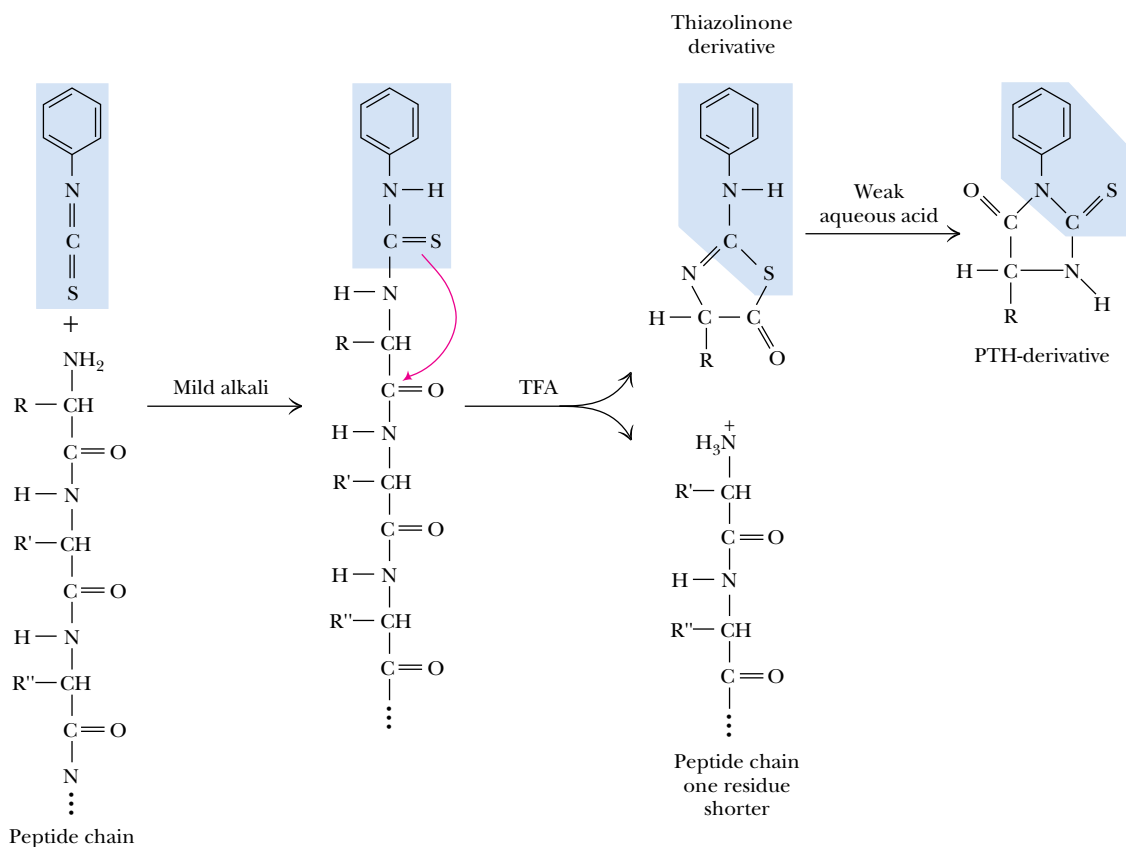

FIGURE 5.19 • N-Terminal analysis using Edman's reagent, phenylisothiocyanate. Phenylisothiocyanate combines with the N-terminus of a peptide under mildly alkaline conditions to form a phenylthiocarbamoyl substitution. Upon treatment with TFA (trifluoroacetic acid), this cyclizes to release the N-terminal amino acid residue as a thiazolinone derivative, but the other peptide bonds are not hydrolyzed. Organic extraction and treatment with aqueous acid yield the N-terminal amino acid as a phenylthiohydantoin (PTH) derivative.

on 50 pmol (about 0.1 μg) of a polypeptide 100 to 200 residues long, generating the sequential order of the first 50 amino acid residues in the protein. The efficiency with larger proteins is less; a typical 2000-amino acid protein provides only 10 to 20 cycles of reaction.

B. C-Terminal Analysis

For the identification of the C-terminal residue of polypeptides, an enzymatic approach is commonly used.

ENZYMATIC ANALYSIS WITH CARBOXYPEPTIDASES. Carboxypeptidases are enzymes that cleave amino acid residues from the C-termini of polypeptides in a successive fashion. Four carboxypeptidases are in general use: A, B, C, and Y. *Carboxypeptidase A* (from bovine pancreas) works well in hydrolyzing the C-terminal peptide bond of all residues except proline, arginine, and lysine. The analogous enzyme from hog pancreas, *carboxypeptidase B,* is effective only when Arg or Lys are the C-terminal residues. Thus, a mixture of carboxypeptidases A and B liberates any C-terminal amino acid except proline. *Carboxypeptidase C* from citrus leaves and *carboxypeptidase Y* from yeast act on any C-terminal residue. Because the nature of the amino acid residue at the end often determines the rate at which it is cleaved and because these enzymes remove residues successively, care must be taken in interpreting results. Carboxypeptidase Y cleavage has been adapted to an automated protocol analogous to that used in Edman sequenators.

Steps 5 and 6. Fragmentation of the Polypeptide Chain

The aim at this step is to produce fragments useful for sequence analysis. The cleavage methods employed are usually enzymatic, but proteins can also be fragmented by specific or nonspecific chemical means (such as partial acid hydrolysis). Proteolytic enzymes offer an advantage in that they may hydrolyze only specific peptide bonds, and this specificity immediately gives information about the peptide products. As a first approximation, fragments produced upon cleavage should be small enough to yield their sequences through end-group analysis and Edman degradation, yet not so small that an over-abundance of products must be resolved before analysis. However, the determination of total sequences for proteins predates the Edman procedure, and alternative approaches obviously exist.

A. Trypsin

The digestive enzyme *trypsin* is the most commonly used reagent for specific proteolysis. Trypsin is specific in hydrolyzing only peptide bonds in which the carbonyl function is contributed by an arginine or a lysine residue. That is, trypsin cleaves on the C-side of Arg or Lys, generating a set of peptide fragments having Arg or Lys at their C-termini. The number of smaller peptides resulting from trypsin action is equal to the total number of Arg and Lys residues in the protein *plus* one—the protein's C-terminal peptide fragment (Figure 5.20).

B. Chymotrypsin

Chymotrypsin shows a strong preference for hydrolyzing peptide bonds formed by the carboxyl groups of the aromatic amino acids, phenylalanine, tyrosine, and tryptophan. However, over time chymotrypsin also hydrolyzes amide bonds involving amino acids other than Phe, Tyr, or Trp. Peptide bonds having leucine-donated carboxyls become particularly susceptible. Thus, the specificity
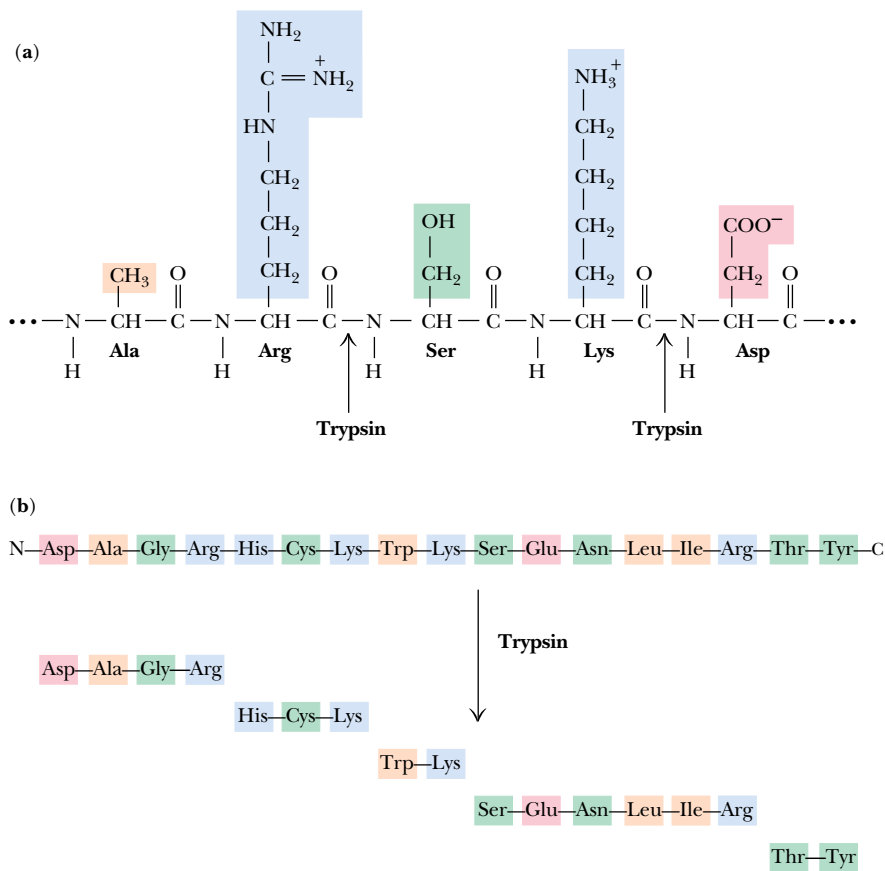
(a)

(b)

of chymotrypsin is only relative. Because chymotrypsin produces a very different set of products than trypsin, treatment of separate samples of a protein with these two enzymes generates fragments whose sequences overlap. Resolution of the order of amino acid residues in the fragments yields the amino acid sequence in the original protein.

C. Relatively Nonspecific Endopeptidases

A number of other *endopeptidases* (proteases that cleave peptide bonds within the interior of a polypeptide chain) are also used in sequence investigations. These include *clostripain,* which acts only at Arg residues, *endopeptidase Lys-C,* which cleaves only at Lys residues, and *staphylococcal protease,* which acts at the acidic residues, Asp and Glu. Other, relatively nonspecific endopeptidases are handy for digesting large tryptic or chymotryptic fragments. *Pepsin, papain, subtilisin, thermolysin,* and *elastase* are some examples. Papain is the active ingredient in meat tenderizer and in soft contact lens cleaner as well as in some laundry detergents. The abundance of papain in papaya, and a similar protease (bromelain) in pineapple, causes the hydrolysis of gelatin and prevents the preparation of Jell-O® containing either of these fresh fruits. Cooking these fruits thermally denatures their proteolytic enzymes so that they can be used in gelatin desserts.

D. Cyanogen Bromide

Several highly specific chemical methods of proteolysis are available, the most widely used being *cyanogen bromide (CNBr)* cleavage. CNBr acts upon methio-
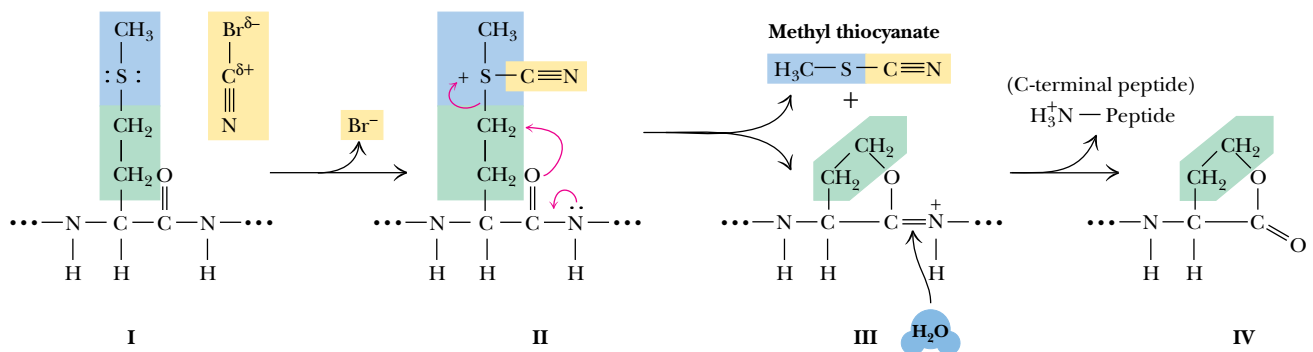
FIGURE 5.21 • Cyanogen bromide (CNBr) is a highly selective reagent for cleavage of peptides only at methionine residues. (I) The reaction occurs in 70% formic acid via nucleophilic attack of the Met S atom on the —C≡N carbon atom, with displacement of Br. (II) The cyano intermediate undergoes nucleophilic attack by the Met carbonyl oxygen atom on the R group, (III) resulting in formation of the cyclic derivative, which is unstable in aqueous solution. (IV) Hydrolysis ensues, producing cleavage of the Met peptide bond and release of peptide fragments, with C-terminal homoserine lactone residues where Met residues once were. One peptide does not have a C-terminal homoserine lactone: the original C-terminal end of the polypeptide.

OVERALL REACTION:
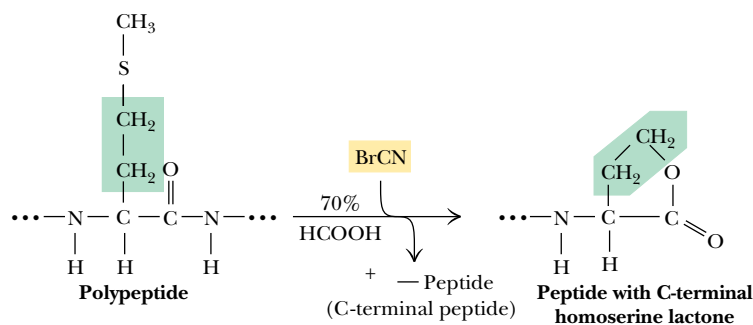
nine residues (Figure 5.21). The nucleophilic sulfur atom of Met reacts with CNBr, yielding a sulfonium ion that undergoes a rapid intramolecular rearrangement to form a cyclic iminolactone. Water readily hydrolyzes this iminolactone, cleaving the polypeptide and generating peptide fragments having C-terminal homoserine lactone residues at the former Met positions.

Other Methods of Fragmentation

A number of other chemical methods give specific fragmentation of polypeptides, including cleavage at asparagine–glycine bonds by hydroxylamine (NH_2OH) at pH 9 and selective hydrolysis at aspartyl–prolyl bonds under mildly acidic conditions. Table 5.6 summarizes the various procedures described here for polypeptide cleavage. These methods are only a partial list of the arsenal of reactions available to protein chemists. Cleavage products generated by these procedures must be isolated and individually analyzed with respect to amino acid composition, end-group identity, and amino acid sequence to accumulate the information necessary to reconstruct the protein's total amino acid sequence. In the past, sequence was often deduced from exhaustive study of the amino acid composition and end-group analysis of small, overlapping peptides. Peptide sequencing today is most commonly done by Edman degradation of relatively large peptides.

Sequence Determination by Mass Spectrometry (MS)

Mass spectrometers exploit the difference in the mass-to-charge (m/z) ratio of ionized atoms or molecules to separate them from each other. The m/z ratio of a molecule is also a highly characteristic property that can be used for determining chemical and structural information. Further, molecules can be fragmented in distinctive ways in mass spectrometers, and the fragments that arise also provide quite specific structural information about the molecule. The basic

Table 5.6

**Specificity of Representative Polypeptide Cleavage Procedures
Used in Sequence Analysis**

Method	Peptide Bond on Carboxyl (C) or Amino (N) Side of Susceptible Residue	Susceptible Residue(s)
Proteolytic enzymes		
Trypsin	C	Arg or Lys
Chymotrypsin	C	Phe, Trp, or Tyr; Leu
Clostripain	C	Arg
Staphylococcal protease	C	Asp or Glu
Chemical methods		
Cyanogen bromide	C	Met
NH_2OH	Asn-Gly bonds	
pH 2.5, 40°C	Asp-Pro bonds	

Table 5.7

Macromolecular Ionization Methods in Mass Spectrometry

Electrospray ionization (ESI-MS)	A solution of macromolecules is sprayed in the form of fine droplets from a glass capillary under the influence of a strong electrical field. The droplets pick up charge as they exit the capillary; evaporation of the solvent leaves highly charged molecules.
Fast-atom bombardment (FAB-MS)	A high-energy beam of inert gas molecules (argon or xenon) is directed at a solid sample, knocking molecules into the gas phase and ionizing them.
Laser ionization (LIMS)	A laser pulse is used to knock material from the surface of a solid sample; the laser pulse creates a microplasma that ionizes molecules in the sample.
Matrix-assisted desorption ionization (MALDI)	MALDI is a LIMS method capable of vaporizing and ionizing large biological molecules such as proteins or DNA. The biological molecules are dispersed in a solid matrix that serves as a carrier. Nicotinic acid is a commonly used matrix substance.

operation of a mass spectrometer is to (1) evaporate and ionize molecules in a vacuum, creating gas-phase ions, (2) separate the ions in space and/or time based on their *m/z* ratios, and (3) measure the amount of ions with specific *m/z* ratios. Because proteins (as well as nucleic acids and carbohydrates) decompose upon heating, rather than evaporating, attempts to ionize such molecules for MS analysis require innovative approaches (Table 5.7). Figure 5.22 illus-

FIGURE 5.22 • The three principal steps in electrospray mass spectrometry (ES-MS). (a) Small, highly charged droplets are formed by electrostatic dispersion of a protein solution through a glass capillary subjected to a high electric field; (b) protein ions are desorbed from the droplets into the gas phase (assisted by evaporation of the droplets in a stream of hot N_2 gas; and (c) analysis of the protein ions in a mass spectrometer. (*Adapted from Figure 1 in Mann, M., and Wilm, M., 1995.* Trends in Biochemical Sciences *20:219–224.*)

Counter-current

Glass capillary

Sample
solution

(a) High voltage

Mass spectrometer

(c)
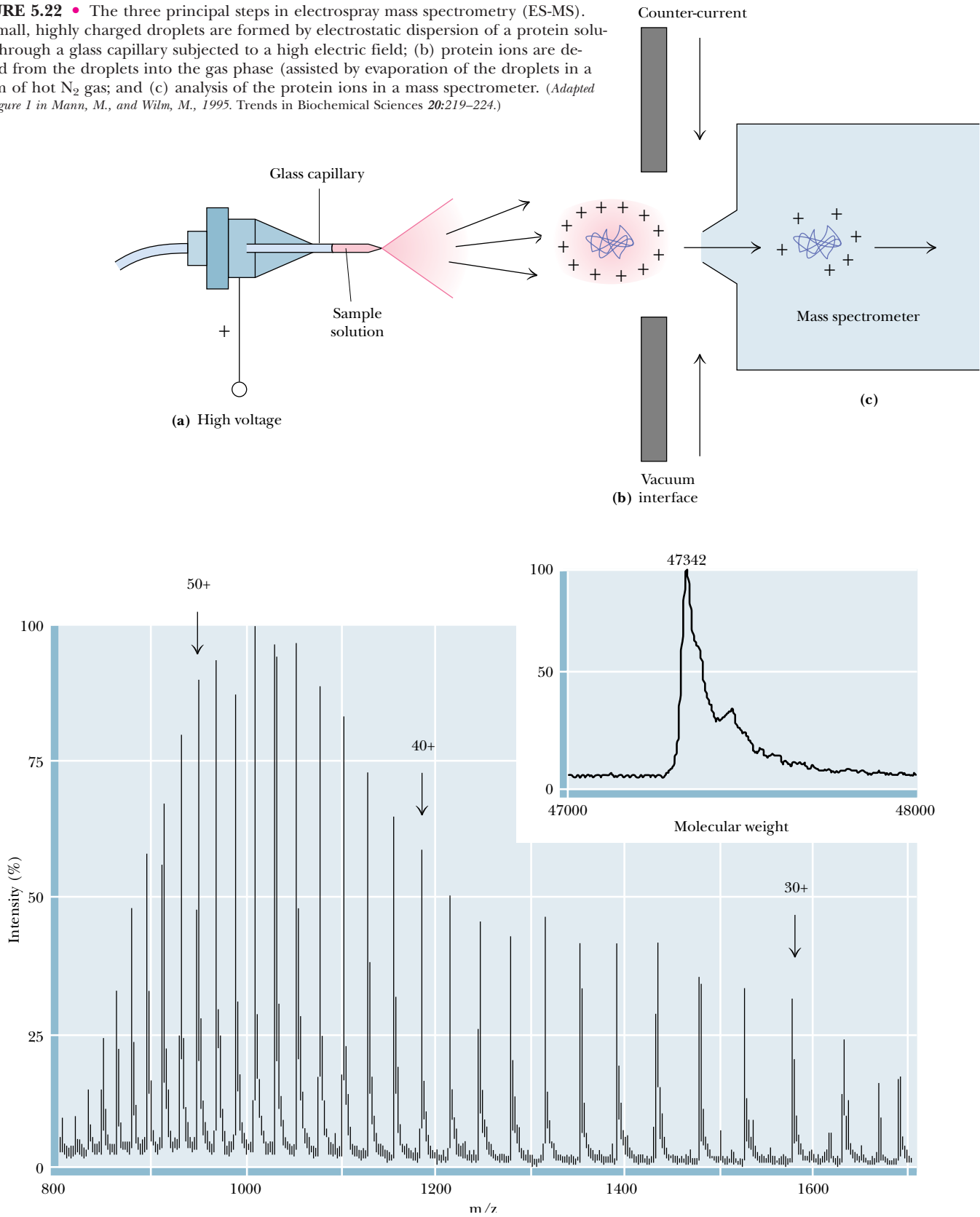
Vacuum
(b) interface

FIGURE 5.23 • Electrospray mass spectrum of the protein, aerolysin K. The attachment of many protons per protein molecule (from less than 30 to more than 50 here) leads to a series of *m/z* peaks for this single protein. The inset shows a computer analysis of the data from this series of peaks that generates a single peak at the correct molecular mass of the protein. (*Adapted from Figure 2 in Mann, M., and Wilm, M., 1995.* Trends in Biochemical Sciences *20:219–224.*)

trates the basic features of electrospray mass spectrometry (ES-MS). In this technique, proteins pick up, on average, about one positive charge (proton) per kilodalton, leading to the spectrum of m/z ratios for a single protein species (Figure 5.23). Computer algorithms can convert these data into a single spectrum having a peak at the correct protein mass (inset, Figure 5.23).

SEQUENCING BY TANDEM MASS SPECTROMETRY. *Tandem MS* (or *MS/MS*) allows sequencing of proteins by hooking two mass spectrometers in tandem. The first mass spectrometer is used to separate oligopeptides from a protein digest and then to select in turn each of these oligopeptides for further analysis. A selected ionized oligopeptide is directed toward the second mass spectrometer; on the way, this oligopeptide is fragmented by collision with helium or argon gas molecules, and the collection of fragments is analyzed by the second mass spectrometer (Figure 5.24). Fragmentation occurs primarily in the peptide bonds
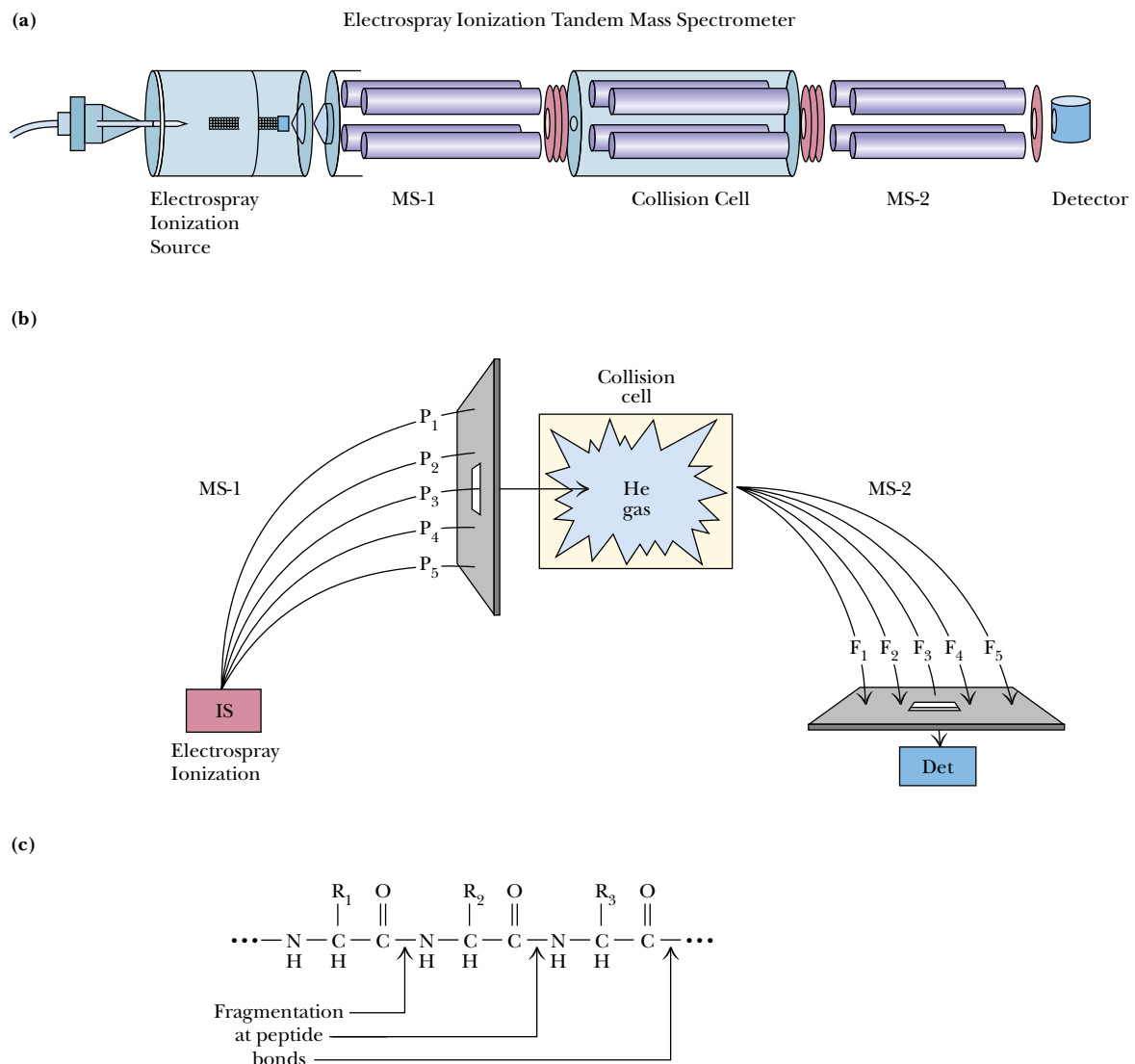
(a)   Electrospray Ionization Tandem Mass Spectrometer

Electrospray   MS-1   Collision Cell   MS-2   Detector
Ionization
Source

(b)

FIGURE 5.24 • Tandem mass spectrometry. (a) Configuration used in tandem MS. (b) Schematic description of tandem MS: tandem MS involves electrospray ionization of a protein digest (IS in this figure), followed by selection of a single peptide ion mass for collision with inert gas molecules (He) and mass analysis of the fragment ions resulting from the collisions. (c) Fragmentation usually occurs at peptide bonds, as indicated. (*I: Adapted from Yates, J. R., 1996.* Methods in Enzymology *271:351–376; II: Adapted from Gillece-Castro, B. L., and Stults, J. T., 1996.* Methods in Enzymology *271:427–447.*)

linking successive amino acids in the oligopeptide, so the fragments created represent a nested set of peptides that differ in size by one amino acid residue. The fragments differ in mass by 56 atomic mass units (the mass of the peptide backbone atoms (NH-CH-CO)) *plus* the mass of the R group at each position, which ranges from 1 atomic mass unit (Gly) to 130 (Trp). MS sequencing has the advantages of very high sensitivity, fast sample processing, and the ability to work with mixtures of proteins. Subpicomoles (less than 10^{-12} moles) of peptide can be analyzed. However, in practice, tandem MS is limited to rather short sequences (no longer than 15 or so amino acid residues). Nevertheless, capillary HPLC-separated peptide mixtures from trypsin digests of proteins can be directly loaded into the tandem MS spectrometer. Further, separation of a complex mixture of proteins from a whole-cell extract by two-dimensional gel electrophoresis (see Chapter Appendix), followed by trypsin digest of a specific protein spot on the gel and injection of the digest into the HPLC/tandem MS, gives sequence information that can be used to identify specific proteins. Often, by comparing the mass of tryptic peptides from a protein digest with a database of all possible masses for tryptic peptides (based on all known protein and DNA sequences), a protein of interest can be identified without actually sequencing it.

Step 7. Reconstruction of the Overall Amino Acid Sequence

The sequences obtained for the sets of fragments derived from two or more cleavage procedures are now compared, with the objective being to find overlaps that establish continuity of the overall amino acid sequence of the polypeptide chain. The strategy is illustrated by the example shown in Figure 5.25. Peptides generated from specific hydrolysis of the polypeptide can be aligned to reveal the overall amino acid sequence. Such comparisons are also useful in eliminating errors and validating the accuracy of the sequences determined for the individual fragments.
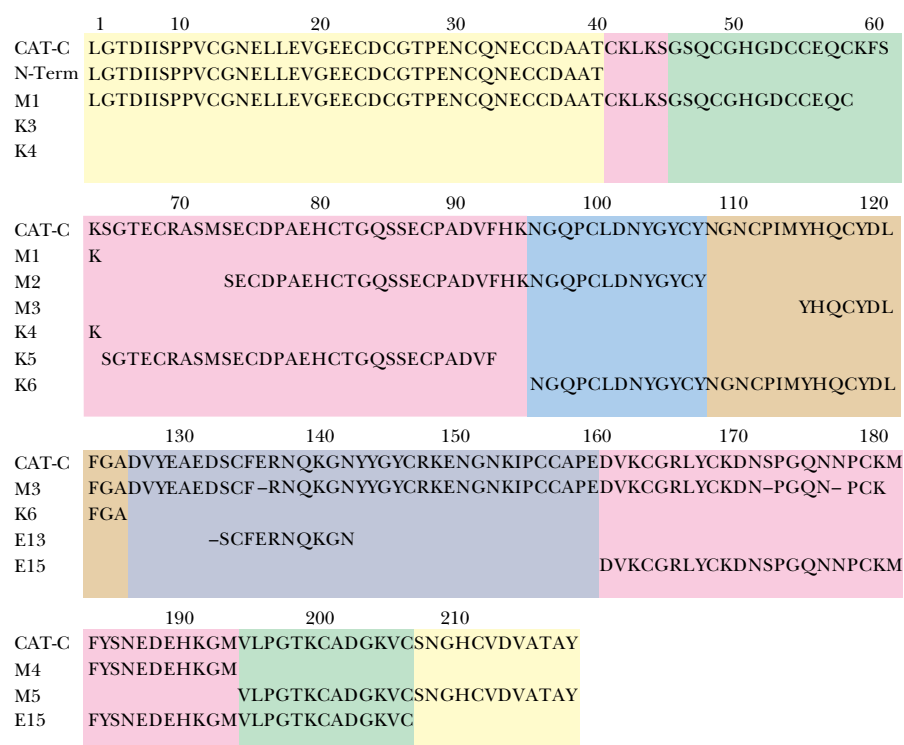

FIGURE 5.25 • Summary of the sequence analysis of catrocollastatin-C, a 23.6-kD protein found in the venom of the western diamond-back rattlesnake *Crotalus atrox*. Sequences shown are given in the one-letter amino acid code. The overall amino acid sequence (216 amino acid residues long) for catrocollastatin-C as deduced from the overlapping sequences of peptide fragments is shown on the lines headed **CAT-C.** The other lines report the various sequences used to obtain the overlaps. These sequences were obtained from (a) **N-term.**: Edman degradation of the intact protein in an automated Edman sequenator; (b) **M:** proteolytic fragments generated by CNBr cleavage, followed by Edman sequencing of the individual fragments (numbers denote fragments M1 through M5); (c) **K:** proteolytic fragments (K3 through K6) from endopeptidase Lys-C cleavage, followed by Edman sequencing; (d) **E:** proteolytic fragments from *Staphylococcus* protease (E13 through E15) digestion of catrocollastatin sequenced in the Edman sequenator. (*Adapted from Shimokawa, K., et al., 1997.* Archives of Biochemistry and Biophysics *343:35–43.*)

Step 8. Location of Disulfide Cross-Bridges

Strictly speaking, the disulfide bonds formed between cysteine residues in a protein are not a part of its primary structure. Nevertheless, information about their location can be obtained by procedures used in sequencing, provided the disulfides are not broken prior to cleaving the polypeptide chain. Because these covalent bonds are stable under most conditions used in the cleavage of polypeptides, intact disulfides link the peptide fragments containing their specific cysteinyl residues and thus these linked fragments can be isolated and identified within the protein digest.

An effective way to isolate these fragments is through **diagonal electrophoresis** (Figure 5.26) (the basic technique of *electrophoresis* is described in
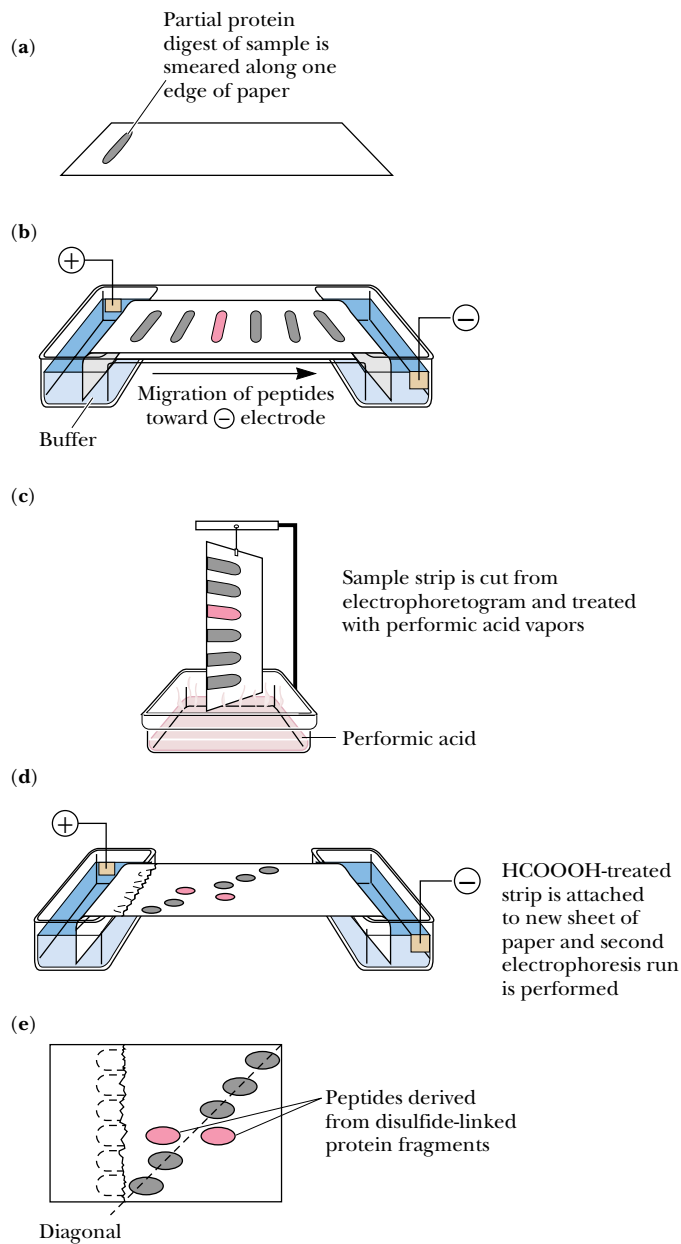

(a) Partial protein digest of sample is smeared along one edge of paper

(b)
+
−
Migration of peptides toward ⊖ electrode
Buffer

(c)
Sample strip is cut from electrophoretogram and treated with performic acid vapors
Performic acid

(d)
+
−
HCOOOH-treated strip is attached to new sheet of paper and second electrophoresis run is performed

(e)
Peptides derived from disulfide-linked protein fragments
Diagonal

FIGURE 5.26 • Disulfide bridges typically are cleaved prior to determining the primary structure of a polypeptide. Consequently, the positions of disulfide links are not obvious from the sequence data. To determine their location, a sample of the polypeptide with intact S—S bonds can be fragmented and the sites of any disulfides can be elucidated from fragments that remain linked. *Diagonal electrophoresis* is a technique for identifying such fragments. (a) A protein digest in which any disulfide bonds remain intact and link their respective Cys-containing peptides is streaked along the edge of a filter paper and (b) subjected to electrophoresis. (c) A strip cut from the edge of the paper is then exposed to performic acid fumes to oxidize any disulfide bridges. (d) Then the paper strip is attached to a new filter paper so that a second electrophoresis can be run in a direction perpendicular to the first. (e) Peptides devoid of disulfides experience no mobility change, and thus their pattern of migration defines a diagonal. Peptides that had disulfides migrate off this diagonal and can be easily identified, isolated, and sequenced to reveal the location of cysteic acid residues formerly involved in disulfide bridges.

the Chapter Appendix). Peptides that were originally linked by disulfides now migrate as distinct species following disulfide cleavage and are obvious by their location off the diagonal (Figure 5.26e). These cysteic acid–containing peptides are then isolated from the paper and sequenced. From this information, the positions of the disulfides in the protein can be stipulated.

Sequence Databases

A database of protein sequences collected by protein chemists can be found in the *Atlas of Protein Sequence and Structure*. However, most protein sequence information has been derived from translating the nucleotide sequences of genes into codons and, thus, amino acid sequences (see Chapter 13). Sequencing the order of nucleotides in cloned genes is a more rapid, efficient, and informative process than determining the amino acid sequences of proteins. A number of electronic databases containing continuously updated sequence information are readily accessible by personal computer. Prominent among these are PIR (Protein Identification Resource Protein Sequence Database), GenBank (Genetic Sequence Data Bank), and EMBL (European Molecular Biology Laboratory Data Library).

5.8 • Nature of Amino Acid Sequences

With a knowledge of the methodology in hand, let's review the results of amino acid composition and sequence studies on proteins. Table 5.8 lists the relative frequencies of the amino acids in various proteins. It is very unusual for a globular protein to have an amino acid composition that deviates substantially from these values. Apparently, these abundances reflect a distribution of amino acid polarities that is optimal for protein stability in an aqueous milieu. Membrane proteins have relatively more hydrophobic and fewer ionic amino acids, a condition consistent with their location. Fibrous proteins may show compositions that are atypical with respect to these norms, indicating an underlying relationship between the composition and the structure of these proteins.

Proteins have unique amino acid sequences, and it is this uniqueness of sequence that ultimately gives each protein its own particular personality. Because the number of possible amino acid sequences in a protein is astronomically large, the probability that two proteins will, by chance, have similar amino acid sequences is negligible. Consequently, sequence similarities between proteins imply evolutionary relatedness.

Homologous Proteins from Different Organisms Have Homologous Amino Acid Sequences

Proteins sharing a significant degree of sequence similarity are said to be **homologous.** Proteins that perform the same function in different organisms are also referred to as homologous. For example, the oxygen transport protein, hemoglobin, serves a similar role and has a similar structure in all vertebrates. The study of the amino acid sequences of homologous proteins from different organisms provides very strong evidence for their evolutionary origin within a common ancestor. Homologous proteins characteristically have polypeptide chains that are nearly identical in length, and their sequences share identity in direct correlation to the relatedness of the species from which they are derived.

Table 5.8

Frequency of Occurrence of Amino Acid Residues in Proteins

Amino Acid		M_r*	Occurrence in Proteins (%)[†]
Alanine	Ala A	71.1	9.0
Arginine	Arg R	156.2	4.7
Asparagine	Asn N	114.1	4.4
Aspartic acid	Asp D	115.1	5.5
Cysteine	Cys C	103.1	2.8
Glutamine	Gln Q	128.1	3.9
Glutamic acid	Glu E	129.1	6.2
Glycine	Gly G	57.1	7.5
Histidine	His H	137.2	2.1
Isoleucine	Ile I	113.2	4.6
Leucine	Leu L	113.2	7.5
Lysine	Lys K	128.2	7.0
Methionine	Met M	131.2	1.7
Phenylalanine	Phe F	147.2	3.5
Proline	Pro P	97.1	4.6
Serine	Ser S	87.1	7.1
Threonine	Thr T	101.1	6.0
Tryptophan	Trp W	186.2	1.1
Tyrosine	Tyr Y	163.2	3.5
Valine	Val V	99.1	6.9

*Molecular weight of amino acid *minus* that of water.
[†]Frequency of occurrence of each amino acid residue in the polypeptide chains of 207 unrelated proteins of known sequence.

Values from Klapper, M. H., 1977. *Biochemical and Biophysical Research Communications* **78:**1018–1024.

Cytochrome c

The electron transport protein, cytochrome *c,* found in the mitochondria of all eukaryotic organisms, provides the best-studied example of homology. The polypeptide chain of cytochrome *c* from most species contains slightly more than 100 amino acids and has a molecular weight of about 12.5 kD. Amino acid sequencing of cytochrome *c* from more than 40 different species has revealed that there are 28 positions in the polypeptide chain where the same amino acid residues are always found (Figure 5.27). These **invariant residues** apparently serve roles crucial to the biological function of this protein, and thus substitutions of other amino acids at these positions cannot be tolerated.

FIGURE 5.27 • Cytochrome *c* is a small protein consisting of a single polypeptide chain of 104 residues in terrestrial vertebrates, 103 or 104 in fishes, 107 in insects, 107 to 109 in fungi and yeasts, and 111 or 112 in green plants. Analysis of the sequence of cytochrome *c* from more than 40 different species reveals that 28 residues are invariant. These invariant residues are scattered irregularly along the polypeptide chain, except for a cluster between residues 70 and 80. All cytochrome *c* polypeptide chains have a cysteine residue at position 17, and all but one have another Cys at position 14. These Cys residues serve to link the heme prosthetic group of cytochrome *c* to the protein, a role explaining their invariable presence.
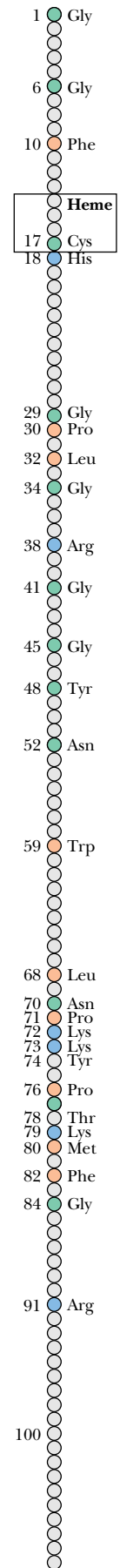
	Chimpanzee	Sheep	Rattlesnake	Carp	Snail	Moth	Yeast	Cauliflower	Parsnip
Human	0	10	14	18	29	31	44	44	43
Chimpanzee		10	14	18	29	31	44	44	43
Sheep			20	11	24	27	44	46	46
Rattlesnake				26	28	33	47	45	43
Carp					26	26	44	47	46
Garden snail						28	48	51	50
Tobacco hornworm moth							44	44	41
Baker's yeast (iso-1)								47	47
Cauliflower									13

FIGURE 5.28 • The number of amino acid differences among the cytochrome *c* sequences of various organisms can be compared. The numbers bear a direct relationship to the degree of relatedness between the organisms. Each of these species has a cytochrome *c* of at least 104 residues, so any given pair of species has more than half its residues in common. (*Adapted from Creighton, T. E., 1983.* Proteins: Structure and Molecular Properties. *San Francisco: W. H. Freeman and Co.*)

Furthermore, as shown in Figure 5.28, the number of amino acid differences between two cytochrome *c* sequences is proportional to the phylogenetic difference between the species from which they are derived. The cytochrome *c* in humans and in chimpanzees is identical; human and another mammalian (sheep) cytochrome *c* differ at 10 residues. The human cytochrome *c* sequence has 14 variant residues from a reptile sequence (rattlesnake), 18 from a fish (carp), 29 from a mollusc (snail), 31 from an insect (moth), and more than 40 from yeast or higher plants (cauliflower).

The Phylogenetic Tree for Cytochrome c

Figure 5.29 displays a **phylogenetic tree** (a diagram illustrating the evolutionary relationships among a group of organisms) constructed from the sequences of cytochrome *c*. The tips of the branches are occupied by contemporary species whose sequences have been determined. The tree has been deduced by computer analysis of these sequences to find the minimum number of mutational changes connecting the branches. Other computer methods can be used to infer potential ancestral sequences represented by *nodes,* or branch points, in the tree. Such analysis ultimately suggests a primordial cytochrome *c* sequence lying at the base of the tree. Evolutionary trees constructed in this manner, that is, solely on the basis of amino acid differences occurring in the primary sequence of one selected protein, show remarkable agreement with phylogenetic relationships derived from more classic approaches and have given rise to the field of *molecular evolution.*

FIGURE 5.29 • This phylogenetic tree depicts the evolutionary relationships among organisms as determined by the similarity of their cytochrome *c* amino acid sequences. The numbers along the branches give the amino acid changes between a species and a hypothetical progenitor. Note that extant species are located only at the tips of branches. Below, the sequence of human cytochrome *c* is compared with an inferred ancestral sequence represented by the base of the tree. Uncertainties are denoted by question marks. (*Adapted from Creighton, T. E., 1983.* Proteins: Structure and Molecular Properties. *San Francisco: W. H. Freeman and Co.*)
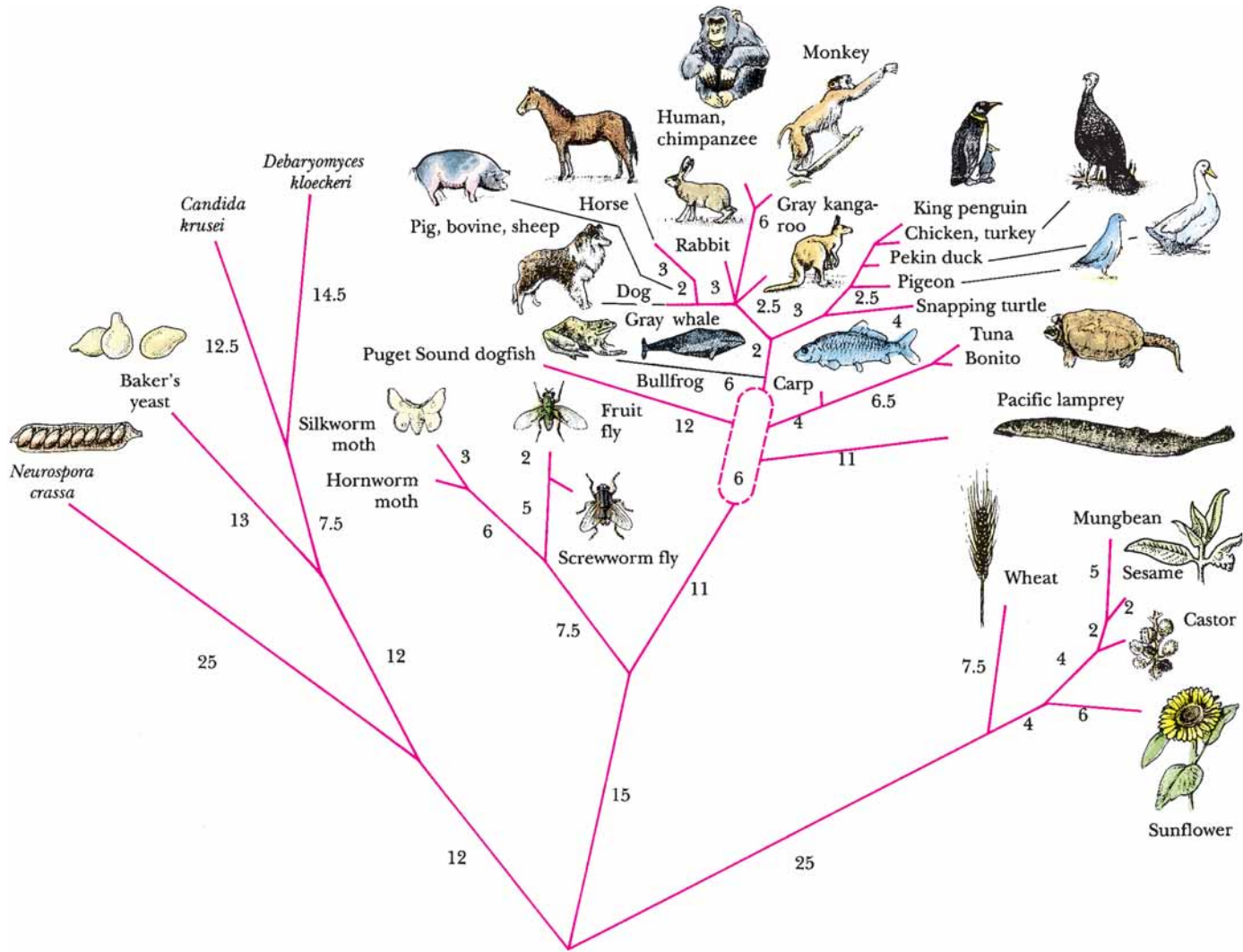
Ancestral
cytochrome *c*

| 1 | 10 | 20 |

−Pro−Ala−Gly−Asp− ? −Lys−Lys−Gly−Ala−Lys−Ile−Phe−Lys−Thr− ? −Cys−Ala−Gln−Cys−His−Thr−Val−Glu− ? − Gly−Gly− ? −

Human
cytochrome *c*

Gly−Asp−Val−Glu−Lys−Gly−Lys−Lys−Ile−Phe−Ile−Met−Lys−Cys−Ser−Gln−Cys−His−Thr−Val−Glu−Lys−Gly−Gly−Lys−

| 30 | 40 | 50 |

−His−Lys−Val−Gly−Pro−Asn−Leu−His−Gly−Leu−Phe−Gly−Arg−Lys− ? −Gly−Gln−Ala− ? −Gly−Tyr−Ser−Tyr−Thr−Asp−

−His−Lys−Thr−Gly−Pro−Asn−Leu−His−Gly−Leu−Phe−Gly−Arg−Lys−Thr−Gly−Gln−Ala−Pro−Gly−Tyr−Ser−Tyr−Thr−Ala−

| 60 | 70 |

−Ala−Asn−Lys−Asn−Lys−Gly− ? − ? −Trp− ? −Glu−Asn−Thr−Leu−Phe−Glu−Tyr−Leu−Glu−Asn−Pro−Lys−Lys−Tyr−Ile−

−Ala−Asn−Lys−Asn−Lys−Gly−Ile−Ile−Trp−Gly−Glu−Asp−Thr−Leu−Met−Gln−Tyr−Leu−Glu−Asn−Pro−Lys−Lys−Tyr−Pro−

| 80 | 90 | 100 |

−Pro−Gly−Thr−Lys−Met− ? −Phe− ? −Gly−Leu−Lys−Lys− ? − ? −Asp−Arg−Ala−Asp−Leu−Ile−Ala−Tyr−Leu−Lys− ? −

−Pro−Gly−Thr−Lys−Met−Ile−Phe−Val−Gly−Ile−Lys−Lys−Lys−Glu−Glu−Arg−Ala−Asp−Leu−Ile−Ala−Tyr−Leu−Lys−Lys−

−Ala−Thr−Ala

−Ala−Thr−Asn−Glu

Related Proteins Share a Common Evolutionary Origin

Amino acid sequence analysis reveals that proteins with related functions often show a high degree of sequence similarity. Such findings suggest a common ancestry for these proteins.

Oxygen-Binding Heme Proteins

The oxygen-binding heme protein of muscle, **myoglobin,** consists of a single polypeptide chain of 153 residues. **Hemoglobin,** the oxygen transport protein of erythrocytes, is a tetramer composed of two α-**chains** (141 residues each) and two β-**chains** (146 residues each). These globin polypeptides—myoglobin, α-globin, and β-globin—share a strong degree of sequence homology (Figure 5.30). Human myoglobin and the human α-globin chain show 38 amino acid

```
           1                             10                              20
Myoglobin  Gly— —-Leu—Ser—Asp—Gly—Glu—Trp—Gln—Leu—Val—Leu—Asn—Val—Trp—Gly—Lys—Val—Glu—Ala—Asp—Ile—Pro—Gly—His—Gly—Gln—Glu—Val—
        α  Val— —-Leu—Ser—Pro—Ala—Asp—Lys—Thr—Asn—Val—Lys—Ala—Ala—Trp—Gly—Lys—Val—Gly—Ala—His—Ala—Gly—Gln—Tyr—Gly—Ala—Glu—Ala—
        β  Val—His—Leu—Thr—Pro—Glu—Glu—Lys—Ser—Ala—Val—Thr—Ala—Leu—Trp—Gly—Lys—Val—Asn— — —-—Val—Asp—Glu—Val—Gly—Gly—Glu—Ala—

           30                            40                              50                               60
        —Leu—Ile—Arg—Leu—Phe—Lys—Gly—His—Pro—Glu—Thr—Leu—Glu—Lys—Phe—Asp—Lys—Phe—Lys—His—Leu—Lys—Ser—Glu—Asp—Glu—Met—Lys—Ala—Ser—Glu—
        —Leu—Glu—Arg—Met—Phe—Leu—Ser—Phe—Pro—Thr—Thr—Lys—Thr—Tyr—Phe—Pro—His—Phe— — —Asp—Leu—Ser—His— — — — — — — — —Gly—Ser—Ala—
        —Leu—Gly—Arg—Leu—Leu—Val—Val—Tyr—Pro—Trp—Thr—Gln—Arg—Phe—Phe—Glu—Ser—Phe—Gly—Asp—Leu—Ser—Thr—Pro—Asp—Ala—Val—Met—Gly—Asn—Pro—

                                         70                              80                               90
        —Asp—Leu—Lys—Lys—His—Gly—Ala—Thr—Val—Leu—Thr—Ala—Leu—Gly—Gly—Ile—Leu—Lys—Lys—Lys—Gly—His—His—Glu—Ala—Glu—Ile—Lys—Pro—Leu—Ala—
        —Gln—Val—Lys—Gly—His—Gly—Lys—Lys—Val—Ala—Asp—Ala—Leu—Thr—Asn—Ala—Val—Ala—His—Val—Asp—Asp—Met—Pro—Asn—Ala—Leu—Ser—Ala—Leu—Ser—
        —Lys—Val—Lys—Ala—His—Gly—Lys—Lys—Val—Leu—Gly—Ala—Phe—Ser—Asp—Gly—Leu—Ala—His—Leu—Asp—Asn—Leu—Lys—Gly—Thr—Phe—Ala—Thr—Leu—Ser—

                                         100                             110                              120
        —Gln—Ser—His—Ala—Thr—Lys—His—Lys—Ile—Pro—Val—Lys—Tyr—Leu—Glu—Phe—Ile—Ser—Glu—Cys—Ile—Ile—Gln—Val—Leu—Gln—Ser—Lys—His—Pro—Gly—
        —Asp—Leu—His—Ala—His—Lys—Leu—Arg—Val—Asp—Pro—Val—Asn—Phe—Lys—Leu—Leu—Ser—His—Cys—Leu—Leu—His—Thr—Leu—Ala—Ala—His—Leu—Pro—Ala—
        —Glu—Leu—His—Cys—Asp—Lys—Leu—His—Val—Asp—Pro—Glu—Asn—Phe—Arg—Leu—Leu—Gly—Asn—Val—Leu—Val—Asn—Val—Leu—Ala—His—His—Phe—Gly—Lys—

                                         130                             140                              150
        —Asp—Phe—Gly—Ala—Asp—Ala—Gln—Gly—Ala—Met—Asn—Lys—Ala—Leu—Glu—Leu—Phe—Arg—Lys—Asp—Met—Ala—Ser—Asn—Tyr—Lys—Glu—Leu—Gly—Phe—Gln—Gly
        —Glu—Phe—Thr—Pro—Ala—Val—His—Ala—Ser—Leu—Asp—Lys—Phe—Leu—Ala—Ser—Val—Ser—Thr—Val—Leu—Thr—Ser—Lys—Tyr—Arg—
        —Glu—Phe—Thr—Pro—Pro—Val—Gln—Ala—Ala—Tyr—Gln—Lys—Val—Val—Ala—Gly—Val—Ala—Asn—Ala—Leu—Ala—His—Lys—Tyr—His—
```


α–chain of horse methemoglobin

β–chain of horse methemoglobin

Sperm whale myoglobin

FIGURE 5.30 • Inspection of the amino acid sequences of the globin chains of human hemoglobin and myoglobin reveals a strong degree of homology. The α-globin and β-globin chains share 64 residues of their approximately 140 residues in common. Myoglobin and the α-globin chain have 38 amino acid sequence identities. This homology is further reflected in these proteins' tertiary structure. (*Irving Geis*)

identities, whereas human α-globin and human β-globin have 64 residues in common. The relatedness suggests an evolutionary sequence of events in which chance mutations led to amino acid substitutions and divergence in primary structure. The ancestral myoglobin gene diverged first, after duplication of a primordial globin gene had given rise to its progenitor and an ancestral hemoglobin gene (Figure 5.31). Subsequently, the ancestral hemoglobin gene duplicated to generate the progenitors of the present-day α-globin and β-globin genes. The ability to bind O_2 via a heme prosthetic group is retained by all three of these polypeptides.

Serine Proteases

Whereas the globins provide an example of gene duplication giving rise to a set of proteins in which the biological function has been highly conserved, other sets of proteins united by strong sequence homology show more divergent biological functions. **Trypsin**, **chymotrypsin** (see Section 5.7), and **elastase** are members of a class of proteolytic enzymes called **serine proteases** because of the central role played by specific serine residues in their catalytic activity. **Thrombin,** an essential enzyme in blood clotting, is also a serine protease. These enzymes show sufficient sequence homology to conclude that they arose via duplication of a progenitor serine protease gene, even though their substrate preferences are now quite different.

Apparently Different Proteins May Share a Common Ancestry

A more remarkable example of evolutionary relatedness is inferred from sequence homology between hen egg white **lysozyme** and human milk α-**lactalbumin,** proteins of quite different biological activity and origin. Lysozyme (129 residues) and α-lactalbumin (123 residues) are identical at 48 positions. Lysozyme hydrolyzes the polysaccharide wall of bacterial cells, whereas α-lactalbumin regulates milk sugar (lactose) synthesis in the mammary gland. Although both proteins act in reactions involving carbohydrates, their functions show little similarity otherwise. Nevertheless, their tertiary structures are strikingly similar (Figure 5.32). It is conceivable that many proteins are related in this way, but time and the course of evolutionary change erased most evidence of their common ancestry. In an interesting contrast to this case, the proteins *actin* and *hexokinase* share essentially no sequence homology, yet they have very similar three-dimensional structures, even though their biological roles and physical properties are quite different. Actin forms a filamentous polymer that is a principal component of the contractile apparatus in muscle; hexokinase is a cytosolic enzyme that catalyzes the first reaction in glucose catabolism.

Mutant Proteins

Given a large population of individuals, a considerable number of sequence variants can be found for a protein. These variants are a consequence of **mutations** in a gene (base substitutions in DNA) that have arisen naturally within the population. Gene mutations lead to mutant forms of the protein in which the amino acid sequence is altered at one or more positions. Many of these mutant forms are "neutral" in that the functional properties of the protein are unaffected by the amino acid substitution. Others may be nonfunctional (if loss of function is not lethal to the individual), and still others may display a range of aberrations between these two extremes. The severity of the effects on function depends on the nature of the amino acid substitution and its role in the protein. These conclusions are exemplified by the more than 300 human
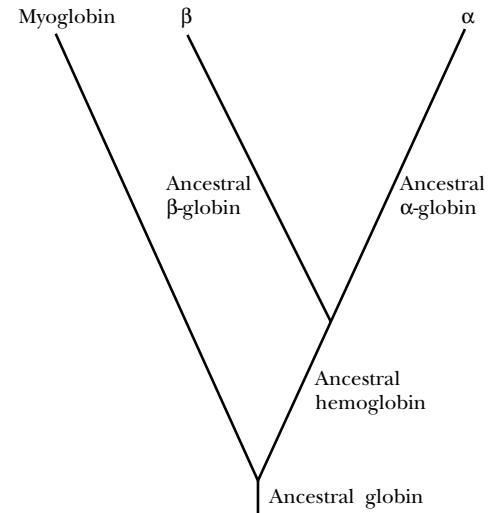
FIGURE 5.31 • This evolutionary tree is inferred from the homology between the amino acid sequences of the α-globin, β-globin, and myoglobin chains. Duplication of an ancestral globin gene allowed the divergence of the myoglobin and ancestral hemoglobin genes. Another gene duplication event subsequently gave rise to ancestral α and β forms, as indicated. Gene duplication is an important evolutionary force in creating diversity.

Human milk α-lactalbumin

Hen egg white lysozyme
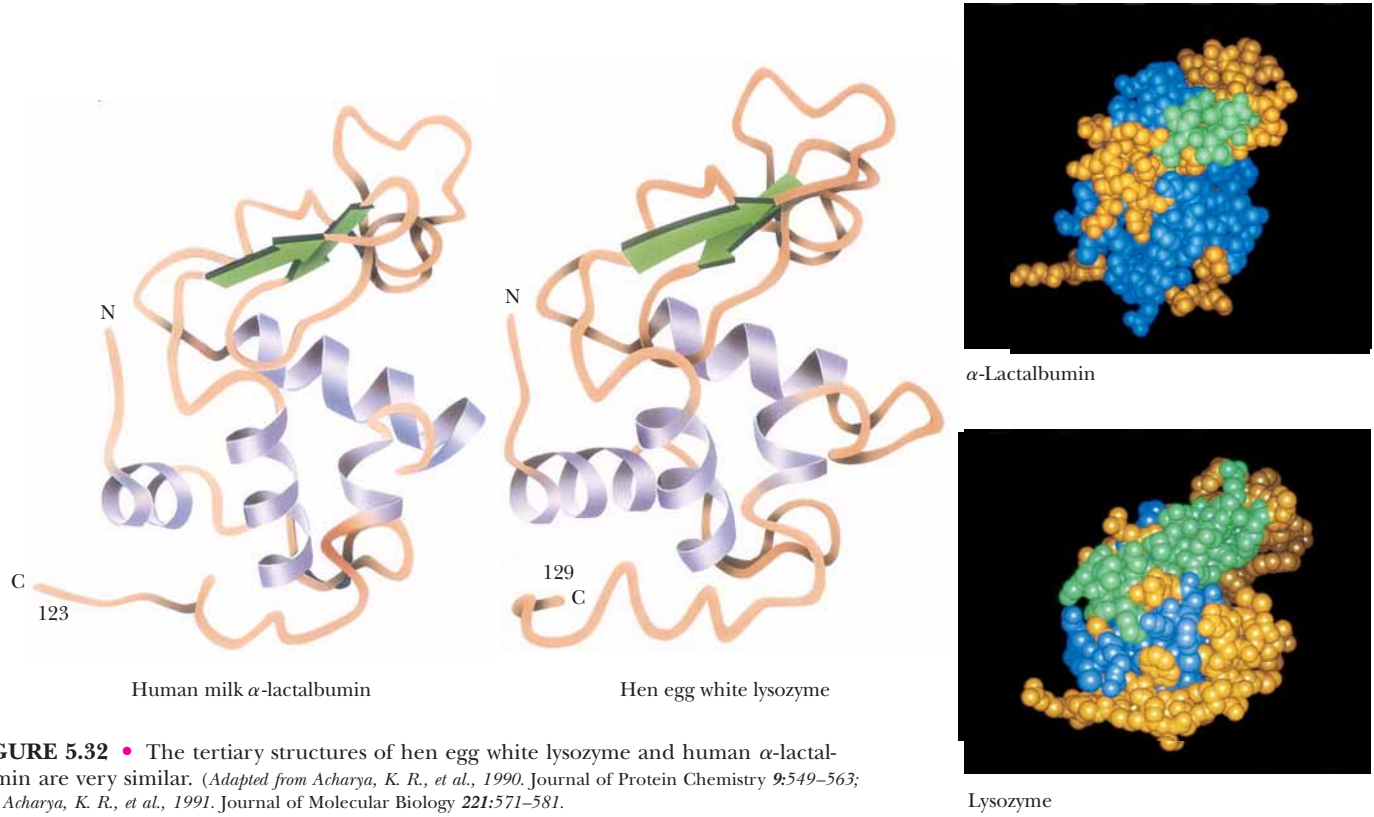
FIGURE 5.32 • The tertiary structures of hen egg white lysozyme and human α-lactalbumin are very similar. (*Adapted from Acharya, K. R., et al., 1990.* Journal of Protein Chemistry **9:**549–563; *and Acharya, K. R., et al., 1991.* Journal of Molecular Biology **221:**571–581.)

α-Lactalbumin

Lysozyme

Table 5.9

Some Pathological Sequence Variants of Human Hemoglobin

Abnormal Hemoglobin*	Normal Residue and Position	Substitution
Alpha chain		
Torino	Phenylalanine 43	Valine
M$_{Boston}$	Histidine 58	Tyrosine
Chesapeake	Arginine 92	Leucine
G$_{Georgia}$	Proline 95	Leucine
Tarrant	Aspartate 126	Asparagine
Suresnes	Arginine 141	Histidine
Beta chain		
S	Glutamate 6	Valine
Riverdale–Bronx	Glycine 24	Arginine
Genova	Leucine 28	Proline
Zurich	Histidine 63	Arginine
M$_{Milwaukee}$	Valine 67	Glutamate
M$_{Hyde\ Park}$	Histidine 92	Tyrosine
Yoshizuka	Asparagine 108	Aspartate
Hiroshima	Histidine 146	Aspartate

*Hemoglobin variants are often given the geographical name of their origin.

Adapted from Dickerson, R. E., and Geis, I., 1983. *Hemoglobin: Structure, Function, Evolution and Pathology.* Menlo Park, CA: Benjamin-Cummings Publishing Co.

hemoglobin variants that have been discovered to date. Some of these are listed in Table 5.9.

A variety of effects on the hemoglobin molecule are seen in these mutants, including alterations in oxygen affinity, heme affinity, stability, solubility, and subunit interactions between the α-globin and β-globin polypeptide chains. Some variants show no apparent changes, whereas others, such as HbS, sickle-cell hemoglobin (see Chapter 15), result in serious illness. This diversity of response indicates that some amino acid changes are relatively unimportant, whereas others drastically alter one or more functions of a protein.

5.9 • Synthesis of Polypeptides in the Laboratory

Chemical synthesis of peptides and polypeptides of defined sequence can be carried out in the laboratory. Formation of peptide bonds linking amino acids together is not a chemically complex process, but making a specific peptide can be challenging because various functional groups present on side chains of amino acids may also react under the conditions used to form peptide bonds. Furthermore, if correct sequences are to be synthesized, the α-COOH group of residue *x* must be linked to the α-NH$_2$ group of neighboring residue *y* in a way that prevents reaction of the amino group of *x* with the carboxyl group of *y*. Ingenious synthetic strategies are required to circumvent these technical problems. In essence, any functional groups to be excluded from reaction must be blocked while the desired coupling reactions proceed. Also, the blocking groups must be removable later under conditions in which the newly formed peptide bonds are stable. These limitations mean that addition of each amino acid requires several steps. Further, all reactions must proceed with high yield if peptide recoveries are to be acceptable. Peptide formation between amino and carboxyl groups is not spontaneous under normal conditions (see Chapter 4), so one or the other of these groups must be activated to facilitate the reaction. Despite these difficulties, biologically active peptides and polypeptides have been recreated by synthetic organic chemistry. Milestones include the pioneering synthesis of the nonapeptide posterior pituitary hormones oxytocin and vasopressin by du Vigneaud in 1953, and in later years, the blood pressure–regulating hormone bradykinin (9 residues), melanocyte-stimulating hormone (24 residues), adrenocorticotropin (39 residues), insulin (21 A-chain and 30 B-chain residues), and ribonuclease A (124 residues).

Solid Phase Peptide Synthesis

Bruce Merrifield and his collaborators found a clever solution to the problem of recovering intermediate products in the course of a synthesis. The carboxyl-terminal residues of synthesized peptide chains were covalently anchored to an insoluble resin particle large enough to be removed from reaction mixtures simply by filtration. After each new residue was added successively at the free amino-terminus, the elongated product was recovered by filtration and readied for the next synthetic step. Because the growing peptide chain was coupled to an insoluble resin bead, the method is called **solid phase synthesis.** The procedure is detailed in Figure 5.33. This cyclic process has been automated and computer controlled so that the reactions take place in a small cup with reagents being pumped in and removed as programmed. The 124-residue-long bovine pancreatic ribonuclease A sequence was synthesized, and the final product was enzymatically active as an RNase.
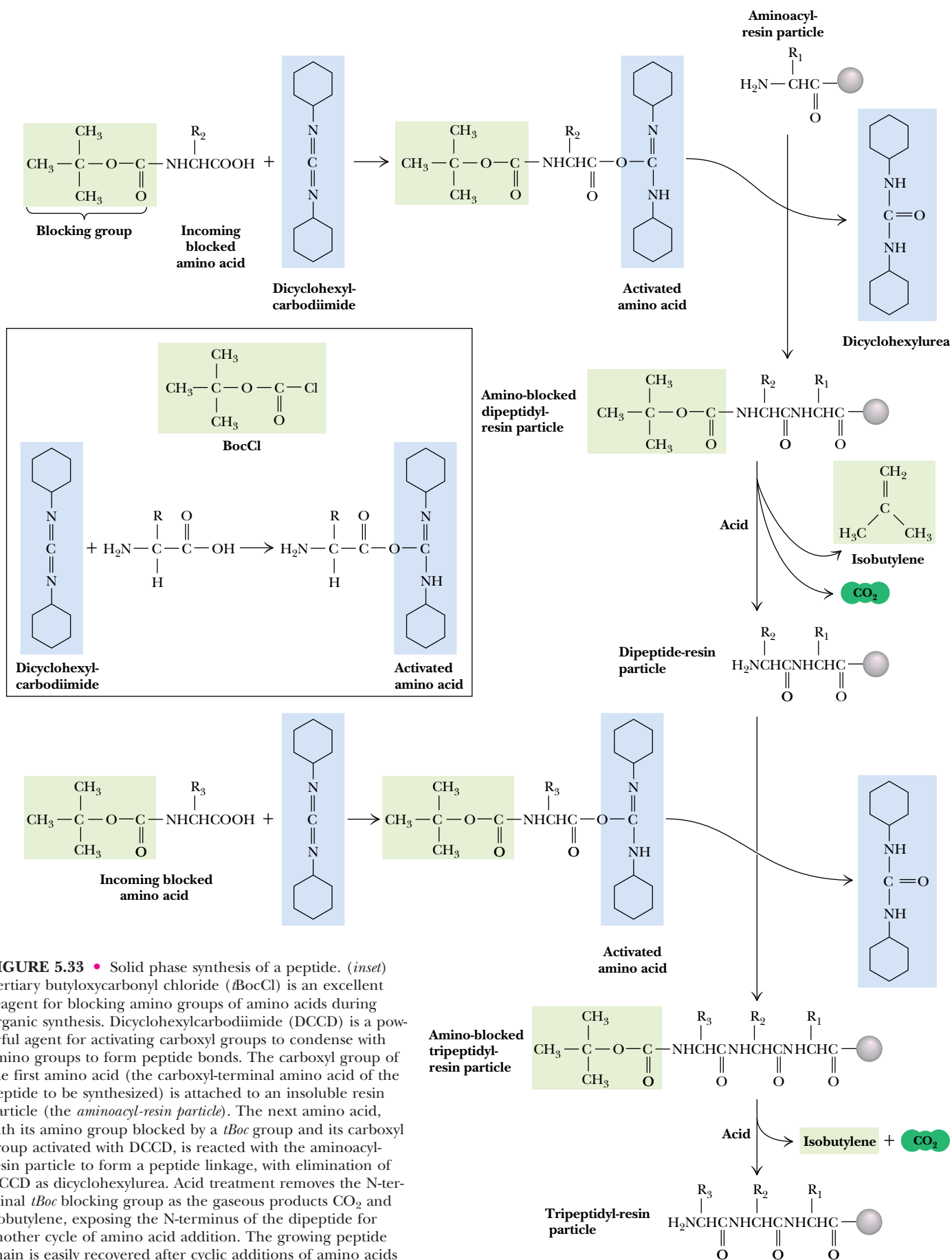
FIGURE 5.33 • Solid phase synthesis of a peptide. (*inset*) Tertiary butyloxycarbonyl chloride (*t*BocCl) is an excellent reagent for blocking amino groups of amino acids during organic synthesis. Dicyclohexylcarbodiimide (DCCD) is a powerful agent for activating carboxyl groups to condense with amino groups to form peptide bonds. The carboxyl group of the first amino acid (the carboxyl-terminal amino acid of the peptide to be synthesized) is attached to an insoluble resin particle (the *aminoacyl-resin particle*). The next amino acid, with its amino group blocked by a *t*Boc group and its carboxyl group activated with DCCD, is reacted with the aminoacyl-resin particle to form a peptide linkage, with elimination of DCCD as dicyclohexylurea. Acid treatment removes the N-terminal *t*Boc blocking group as the gaseous products CO_2 and isobutylene, exposing the N-terminus of the dipeptide for another cycle of amino acid addition. The growing peptide chain is easily recovered after cyclic additions of amino acids simply by filtering or centrifuging the reaction mixture.

PROBLEMS

1. The element molybdenum (atomic weight 95.95) constitutes 0.08% of the weight of nitrate reductase. If the molecular weight of nitrate reductase is 240,000, what is its likely quaternary structure?

2. Amino acid analysis of an oligopeptide seven residues long gave

Asp Leu Lys Met Phe Tyr

The following facts were observed:
a. Trypsin treatment had no apparent effect.
b. The phenylthiohydantoin released by Edman degradation was
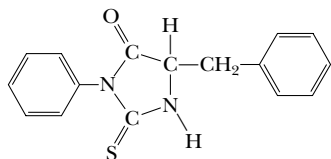
(phenylthiohydantoin structure with —CH₂—phenyl group)

c. Brief chymotrypsin treatment yielded several products, including a dipeptide and a tetrapeptide. The amino acid composition of the tetrapeptide was Leu, Lys, and Met.
d. Cyanogen bromide treatment yielded a dipeptide, a tetrapeptide, and free Lys.
What is the amino acid sequence of this heptapeptide?

3. Amino acid analysis of another heptapeptide gave

Asp Glu Leu Lys

Met Tyr Trp NH_4^+

The following facts were observed:
a. Trypsin had no effect.
b. The phenylthiohydantoin released by Edman degradation was
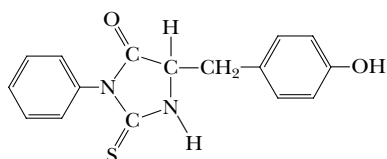
(phenylthiohydantoin structure with —CH₂—phenyl—OH group)

c. Brief chymotrypsin treatment yielded several products, including a dipeptide and a tetrapeptide. The amino acid composition of the tetrapeptide was Glx, Leu, Lys, and Met.
d. Cyanogen bromide treatment yielded a tetrapeptide that had a net positive charge at pH 7 and a tripeptide that had a zero net charge at pH 7.
What is the amino acid sequence of this heptapeptide?

4. Amino acid analysis of a decapeptide revealed the presence of the following products:

NH_4^+ Asp Glu Tyr Arg

Met Pro Lys Ser Phe

The following facts were observed:
a. Neither carboxypeptidase A or B treatment of the decapeptide had any effect.
b. Trypsin treatment yielded two tetrapeptides and free Lys.
c. Clostripain treatment yielded a tetrapeptide and a hexapeptide.
d. Cyanogen bromide treatment yielded an octapeptide and a dipeptide of sequence NP (using the one-letter codes).
e. Chymotrypsin treatment yielded two tripeptides and a tetrapeptide. The N-terminal chymotryptic peptide had a net charge of −1 at neutral pH and a net charge of −3 at pH 12.

f. One cycle of Edman degradation gave the PTH derivative

(phenylthiohydantoin structure with —CH₂OH group)
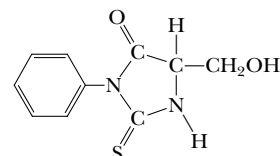
What is the amino acid sequence of this decapeptide?

5. Analysis of the blood of a catatonic football fan revealed large concentrations of a psychotoxic octapeptide. Amino acid analysis of this octapeptide gave the following results:

2 Ala 1 Arg 1 Asp 1 Met 2 Tyr 1 Val 1 NH_4^+

The following facts were observed:
a. Partial acid hydrolysis of the octapeptide yielded a dipeptide of the structure

(dipeptide structure showing $H_3^+N—C(H)(CH_3)—C(=O)—N(H)—C(H)(CH(CH_3)_2)—COOH$)
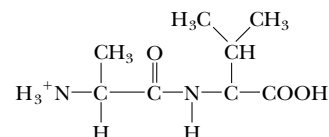
b. Chymotrypsin treatment of the octapeptide yielded two tetrapeptides, each containing an alanine residue.
c. Trypsin treatment of one of the tetrapeptides yielded two dipeptides.
d. Cyanogen bromide treatment of another sample of the same tetrapeptide yielded a tripeptide and free Tyr.
e. End-group analysis of the other tetrapeptide gave Asp.
What is the amino acid sequence of this octapeptide?

6. Amino acid analysis of an octapeptide revealed the following composition:

2 Arg 1 Gly 1 Met 1 Trp 1 Tyr 1 Phe 1 Lys

The following facts were observed:
a. Edman degradation gave

(phenylthiohydantoin structure with —H group)
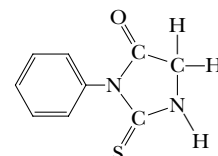
b. CNBr treatment yielded a pentapeptide and a tripeptide containing phenylalanine.
c. Chymotrypsin treatment yielded a tetrapeptide containing a C-terminal indole amino acid, and two dipeptides.
d. Trypsin treatment yielded a tetrapeptide, a dipeptide, and free Lys and Phe.
e. Clostripain yielded a pentapeptide, a dipeptide, and free Phe.
What is the amino acid sequence of this octapeptide?

7. Amino acid analysis of an octapeptide gave the following results:

1 Ala 1 Arg 1 Asp 1 Gly 3 Ile 1 Val 1 NH_4^+

The following facts were observed:
a. Trypsin treatment yielded a pentapeptide and a tripeptide.
b. Chemical reaction of the free α-COOH and subsequent acid hydrolysis yielded 2-aminopropanol.
c. Partial acid hydrolysis of the tryptic pentapeptide yielded,

among other products, two dipeptides, each of which contained C-terminal isoleucine. One of these dipeptides migrated as an anionic species upon electrophoresis at neutral pH.
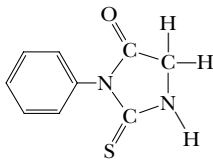
d. The tryptic tripeptide was degraded in an Edman sequenator, yielding first **A,** then **B:**

A.

B.
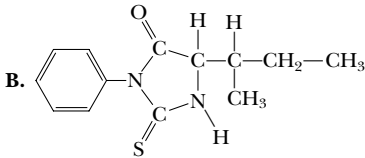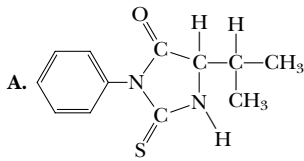
What is an amino acid sequence of the octapeptide? Four sequences are possible, but only one suits the authors. Why?

8. An octapeptide consisting of 2 Gly, 1 Lys, 1 Met, 1 Pro, 1 Arg, 1 Trp, and 1 Tyr was subjected to sequence studies. The following was found:

a. Edman degradation yielded

b. Upon treatment with carboxypeptidases A, B, and C, only carboxypeptidase C had any effect.

c. Trypsin treatment gave two tripeptides and a dipeptide.

d. Chymotrypsin treatment gave two tripeptides and a dipeptide. Acid hydrolysis of the dipeptide yielded only Gly.

e. Cyanogen bromide treatment yielded two tetrapeptides.

f. Clostripain treatment gave a pentapeptide and a tripeptide.

What is the amino acid sequence of this octapeptide?

9. Amino acid analysis of an oligopeptide containing nine residues revealed the presence of the following amino acids:

Arg Cys Gly Leu Met Pro Tyr Val

The following was found:

a. Carboxypeptidase A treatment yielded no free amino acid.

b. Edman analysis of the intact oligopeptide released
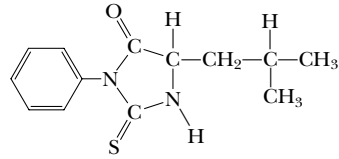
c. Neither trypsin nor chymotrypsin treatment of the nonapeptide released smaller fragments. However, combined trypsin and chymotrypsin treatment liberated free Arg.

d. CNBr treatment of the eight-residue fragment left after combined trypsin and chymotrypsin action yielded a six-residue fragment containing Cys, Gly, Pro, Tyr, and Val; and a dipeptide.

e. Treatment of the six-residue fragment with β-mercaptoethanol yielded two tripeptides. Brief Edman analysis of the tripeptide mixture yielded only PTH-Cys. (The sequence of each tripeptide, as read from the N-terminal end, is alphabetical if the one-letter designation for amino acids is used.)

What is the amino acid sequence of this nonapeptide?

10. Describe the synthesis of the dipeptide Lys-Ala by Merrifield's solid phase chemical method of peptide synthesis. What pitfalls might be encountered if you attempted to add a leucine residue to Lys-Ala to make a tripeptide?

FURTHER READING

Creighton, T. E., 1983. *Proteins: Structure and Molecular Properties.* San Francisco: W.H. Freeman and Co., 515 pp.

Creighton, T. E., ed., 1997. *Protein Function—A Practical Approach,* 2nd ed. Oxford: IRL Press at Oxford University Press.

Dayhoff, M. O., 1972–1978. *The Atlas of Protein Sequence and Structure,* Vols. 1–5. Washington, DC: National Medical Research Foundation.

Deutscher, M. P., ed., 1990. *Guide to Protein Purification.* Vol. 182, *Methods in Enzymology.* San Diego: Academic Press, 894 pp.

Goodsell, D. S., and Olson, A. J., 1993. Soluble proteins: Size, shape and function. *Trends in Biochemical Sciences* **18:**65–68.

Heijne, G. von, 1987. *Sequence Analysis in Molecular Biology: Treasure Trove or Trivial Pursuit?* San Diego: Academic Press.

Hill, R. L., 1965. Hydrolysis of proteins. *Advances in Protein Chemistry* **20:**37–107.

Hirs, C. H. W., ed., 1967. *Enzyme Structure.* Vol. XI, *Methods in Enzymology.* New York: Academic Press, 987 pp.

Hirs, C. H. W., and Timasheff, S. E., eds., 1977–1986. *Enzyme Structure,* Parts E–L. New York: Academic Press.

Hsieh, Y. L., et al., 1996. Automated analytical system for the examination of protein primary structure. *Analytical Chemistry* **68:**455–462. An analytical system is described in which a protein is purified by affinity chromatography, digested with trypsin, and its peptides separated by HPLC and analyzed by tandem MS in order to determine its amino acid sequence.

Hunt, D. F., et al., 1987. Tandem quadrupole Fourier transform mass spectrometry of oligopeptides and small proteins. *Proceedings of the National Academy of Sciences, U.S.A.* **84:**620–623.

Johnstone, R. A. W., and Rose, M. E., 1996. *Mass Spectrometry for Chemists and Biochemists,* 2nd ed. Cambridge, England: Cambridge University Press.

Karger, B. L., and Hancock, W. S., eds. 1996. *Methods in Enzymology* **271,** Section III: *Protein Structure Analysis by Mass Spectrometry,* J. R. Yates; *Peptide Characterization by Mass Spectrometry,* B. L. Gillece-Castro and J. T. Stults. New York: Academic Press.

Mann, M., and Wilm, M., 1995. Electrospray mass spectrometry for protein characterization. *Trends in Biochemical Sciences* **20:**219–224. A review of the basic application of mass spectrometric methods to the analysis of protein sequence and structure.

Merrifield, B., 1986. Solid phase synthesis. *Science* **232:**341–347.

Quadroni, M., et al., 1996. Analysis of global responses by protein and peptide fingerprinting of proteins isolated by two-dimensional electrophoresis. Application to sulfate-starvation response of *Escherichia coli. European Journal of Biochemistry* **239:**773–781. This paper describes the use of tandem MS in the analysis of proteins in cell extracts.

$\mathcal{A}$ppendix to Chapter 5

Protein Techniques[1]

Size Exclusion Chromatography

Size exclusion chromatography is also known as *gel filtration chromatography* or *molecular sieve chromatography.* In this method, fine, porous beads are packed into a chromatography column. The beads are composed of dextran polymers (*Sephadex*), agarose (*Sepharose*), or polyacrylamide (*Sephacryl* or *BioGel P*). The pore sizes of these beads approximate the dimensions of macromolecules. The total bed volume (Figure 5A.1) of the packed chromatography column, V_t, is equal to the volume outside the porous beads (V_o) plus the volume inside the beads (V_i) plus the volume actually occupied by the bead material (V_g): $V_t = V_o + V_i + V_g$. (V_g is typically less than 1% of V_t and can be conveniently ignored in most applications.)

(a) Small molecule / Large molecule / Porous gel beads / Elution column

(b) Protein concentration / Elution profile of a large macromolecule (excluded from pores) ($V_e \approx V_o$) / A smaller macromolecule / V_o / V_e / V_t / Volume (mL) →
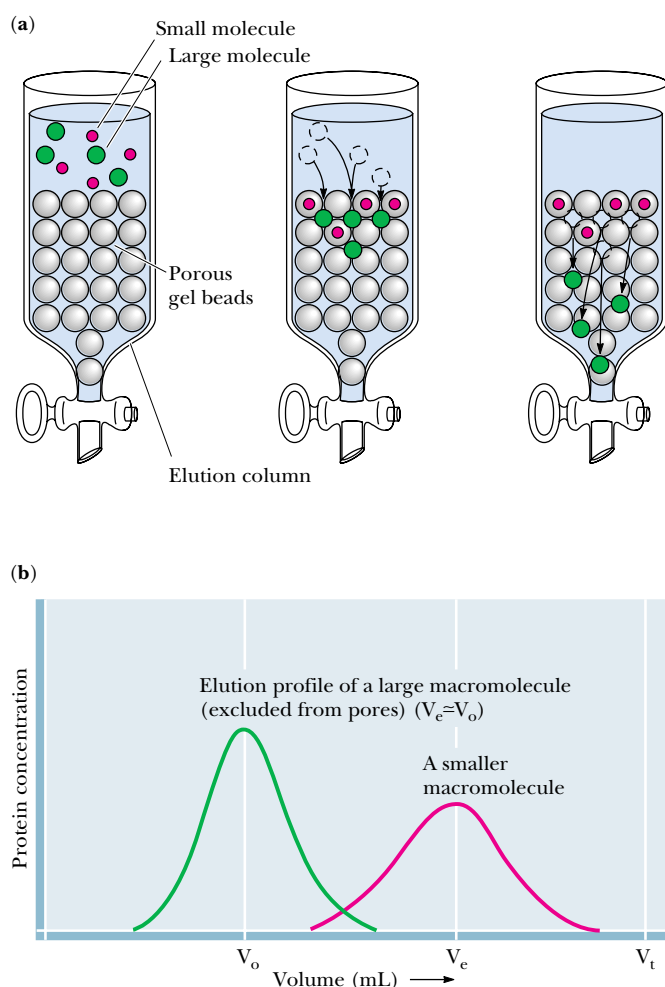
FIGURE 5A.1 • A gel filtration chromatography column. Larger molecules are excluded from the gel beads and emerge from the column sooner than smaller molecules, whose migration is retarded because they can enter the beads.

---

[1]Although this appendix is entitled *Protein Techniques,* these methods are also applicable to other macromolecules such as nucleic acids.

As a solution of molecules is passed through the column, the molecules passively distribute between V_o and V_i, depending on their ability to enter the pores (that is, their size). If a molecule is too large to enter at all, it is totally excluded from V_i and emerges first from the column at an elution volume, V_e, equal to V_o (Figure 5A.1). If a particular molecule can enter the pores in the gel, its distribution is given by the *distribution coefficient, K_D*:

$$K_D = (V_e - V_o)/V_i$$

where V_e is the molecule's characteristic elution volume (Figure 5A.1). The chromatography run is complete when a volume of solvent equal to V_t has passed through the column.

Dialysis and Ultrafiltration

If a solution of protein is separated from a bathing solution by a semipermeable membrane, small molecules and ions can pass through the semipermeable membrane to equilibrate between the protein solution and the bathing solution, called the *dialysis bath* or *dialysate* (Figure 5A.2). This method is useful for removing small molecules from macromolecular solutions or for altering the composition of the protein-containing solution.

Ultrafiltration is an improvement on the dialysis principle. Filters having pore sizes over the range of biomolecular dimensions are used to filter solutions to select for molecules in a particular size range. Because the pore sizes in these filters are microscopic, high pressures are often required to force the solution through the filter. This technique is useful for concentrating dilute solutions of macromolecules. The concentrated protein can then be diluted into the solution of choice.

Semipermeable bag containing protein solution

Dialysate

Stir bar

Magnetic stirrer for mixing
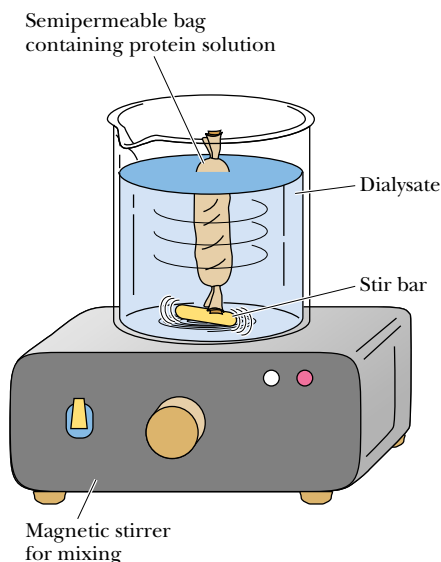
FIGURE 5A.2 • A dialysis experiment. The solution of macromolecules to be dialyzed is placed in a semipermeable membrane bag, and the bag is immersed in a bathing solution. A magnetic stirrer gently mixes the solution to facilitate equilibrium of diffusible solutes between the dialysate and the solution contained in the bag.

Electrophoresis

Electrophoretic techniques are based on the movement of ions in an electrical field. An ion of charge q experiences a force F given by $F = Eq/d$, where E is the voltage (or *electrical potential*) and d is the distance between the electrodes. In a vacuum, F would cause the molecule to accelerate. In solution, the molecule experiences *frictional drag, F_f*, due to the solvent:

$$F_f = 6\pi r \eta v$$

where r is the radius of the charged molecule, η is the viscosity of the solution, and v is the velocity at which the charged molecule is moving. So, the velocity of the charged molecule is proportional to its charge q and the voltage E, but inversely proportional to the viscosity of the medium η and d, the distance between the electrodes.

Generally, electrophoresis is carried out *not* in free solution but in a porous support matrix such as polyacrylamide or agarose, which retards the movement of molecules according to their dimensions relative to the size of the pores in the matrix.

SDS-Polyacrylamide Gel Electrophoresis (SDS-PAGE)

SDS is sodium dodecylsulfate (sodium lauryl sulfate) (Figure 5A.3). The hydrophobic tail of dodecylsulfate interacts strongly with polypeptide chains. The number of SDS molecules bound by a polypeptide is proportional to the length (number of amino acid residues) of the polypeptide. Each dodecylsulfate contributes two negative charges. Collectively, these charges overwhelm any intrinsic charge that the protein might have. SDS is also a detergent that

$$Na^+ \quad ^-O - \overset{\displaystyle O}{\underset{\displaystyle O^-}{\overset{\displaystyle \|}{\underset{\displaystyle |}{S}}}} - O \diagdown \underset{CH_2}{\diagup} CH_2 \underset{CH_2}{\diagup} CH_2 \underset{CH_2}{\diagup} CH_2 \underset{CH_2}{\diagup} CH_2 \underset{CH_2}{\diagup} CH_2 \diagup CH_3$$

$$Na^+$$
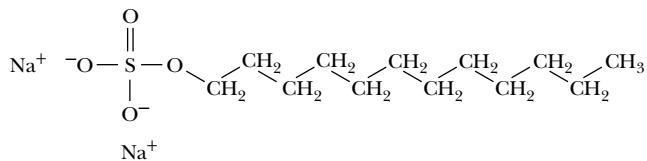
FIGURE 5A.3 • The structure of sodium dodecylsulfate (SDS).

disrupts protein folding (protein 3° structure). SDS-PAGE is usually run in the presence of sulfhydryl-reducing agents such as β-mercaptoethanol so that any disulfide links between polypeptide chains are broken. The electrophoretic mobility of proteins upon SDS-PAGE is inversely proportional to the logarithm of the protein's molecular weight (Figure 5A.4). SDS-PAGE is often used to determine the molecular weight of a protein.

Isoelectric Focusing

Isoelectric focusing is an electrophoretic technique for separating proteins according to their *isoelectric points* (pIs). A solution of *ampholytes* (amphoteric electrolytes) is first electrophoresed through a gel, usually contained in a small tube. The migration of these substances in an electric field establishes a pH gradient in the tube. Then a protein mixture is applied to the gel and electrophoresis is resumed. As the protein molecules move down the gel, they experience the pH gradient and migrate to a position corresponding to their respective pIs. At its pI, a protein has no net charge and thus moves no farther.

Two-Dimensional Gel Electrophoresis

This separation technique uses isoelectric focusing in one dimension and SDS-PAGE in the second dimension to resolve protein mixtures. The proteins in a mixture are first separated according to pI by isoelectric focusing in a polyacrylamide gel in a tube. The gel is then removed and laid along the top of an SDS-PAGE slab, and the proteins are electrophoresed into the SDS polyacrylamide gel, where they are separated according to size (Figure 5A.5). The gel slab can then be stained to reveal the locations of the individual proteins. Using this powerful technique, researchers have the potential to visualize and construct catalogs of virtually *all* the proteins present in particular cell types. The **ExPASy** Molecular Biology World Wide Web server of the University of Geneva (located at URL: http://expasy.hcuge.ch/) provides access to a two-dimensional polyacrylamide gel electrophoresis database named **SWISS-2DPAGE.** This database contains information on proteins, identified as spots on two-dimensional electrophoresis gels, from many different cell and tissue types.
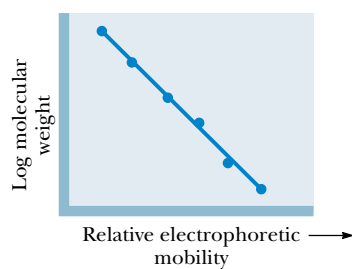
FIGURE 5A.4 • A plot of the relative electrophoretic mobility of proteins in SDS-PAGE versus the log of the molecular weights of the individual polypeptides.
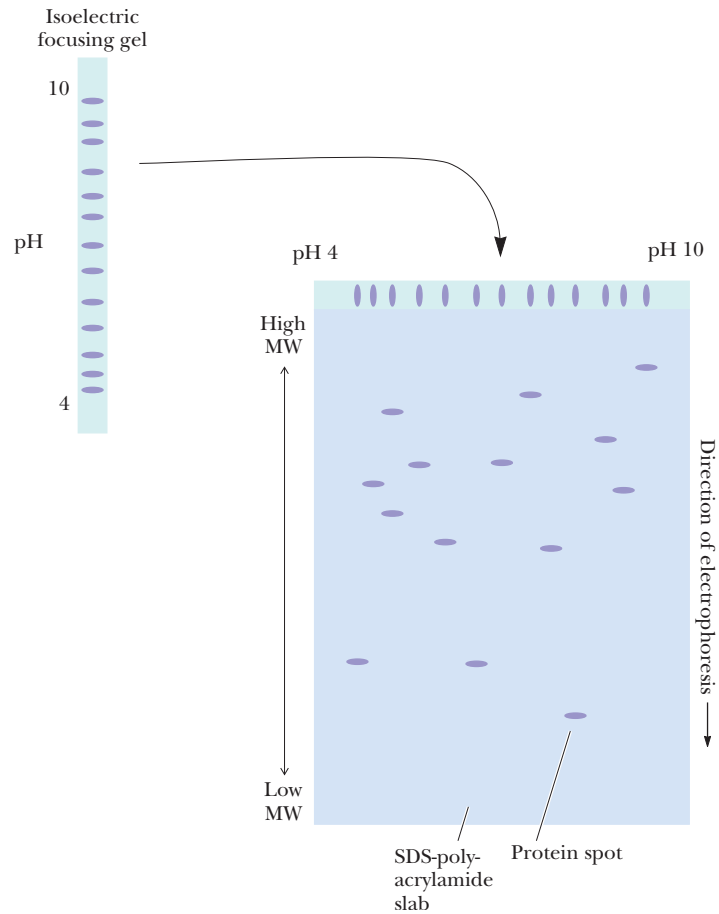
FIGURE 5A.5 • A two-dimensional electrophoresis separation. A mixture of macromolecules is first separated according to charge by isoelectric focusing in a tube gel. The gel containing separated molecules is then placed on top of an SDS-PAGE slab, and the molecules are electrophoresed into the SDS-PAGE gel, where they are separated according to size.

Affinity Chromatography

Recently, *affinity purification* strategies for proteins have been developed to exploit the biological function of the target protein. In most instances, proteins carry out their biological activity through binding or complex formation with specific small biomolecules, or *ligands,* as in the case of an enzyme binding its substrate. If this small molecule can be immobilized through covalent attachment to an insoluble matrix, such as a chromatographic medium like cellulose or polyacrylamide, then the protein of interest, in displaying affinity for its ligand, becomes bound and immobilized itself. It can then be removed from contaminating proteins in the mixture by simple means such as filtration and washing the matrix. Finally, the protein is dissociated or eluted from the matrix by the addition of high concentrations of the free ligand in solution. Figure 5A.6 depicts the protocol for such an *affinity chromatography* scheme. Because this method of purification relies on the biological specificity of the protein of interest, it is a very efficient procedure and proteins can be purified several thousandfold in a single step.
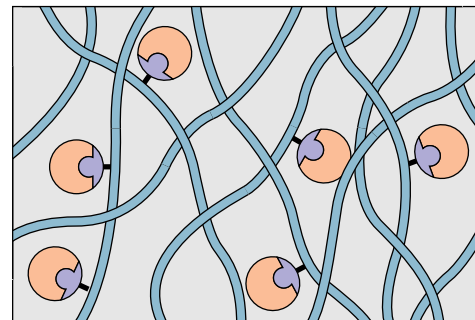
A protein interacts with a metabolite. The metabolite is thus a ligand which binds specifically to this protein

Protein   Metabolite

Hydrophobic Interaction Chromatography (HIC)

Hydrophobic interaction chromatography (*HIC*) exploits the hydrophobic nature of proteins in purifying them. Proteins are passed over a chromatographic column packed with a support matrix to which hydrophobic groups are covalently linked. *Phenyl Sepharose*®, an agarose support matrix to which phenyl groups are affixed, is a prime example of such material. In the presence of high salt concentrations, proteins bind to the phenyl groups by virtue of hydrophobic interactions. Proteins in a mixture can be differentially eluted from the phenyl groups by lowering the salt concentration or by adding solvents such as polyethylene glycol to the elution fluid.

The metabolite can be immobilized by covalently coupling it to an insoluble matrix such as an agarose polymer. Cell extracts containing many individual proteins may be passed through the matrix.

High-Performance Liquid Chromatography

The principles exploited in *high-performance* (or high-pressure) *liquid chromatography (HPLC)* are the same as those used in the common chromatographic methods such as ion exchange chromatography or size exclusion chromatography. Very high resolution separations can be achieved quickly and with high sensitivity in HPLC using automated instrumentation. *Reverse-phase HPLC* is a widely used chromatographic procedure for the separation of nonpolar solutes. In reverse-phase HPLC, a solution of nonpolar solutes is chromatographed on a column having a nonpolar liquid immobilized on an inert matrix; this nonpolar liquid serves as the *stationary phase*. A more polar liquid that serves as the *mobile phase* is passed over the matrix, and solute molecules are eluted in proportion to their solubility in this more polar liquid.

Specific protein binds to ligand. All other unbound material is washed out of the matrix.

Ultracentrifugation

Centrifugation methods separate macromolecules on the basis of their characteristic densities. Particles tend to "fall" through a solution if the density of the solution is less than the density of the particle. The velocity of the particle through the medium is proportional to the difference in density between the particle and the solution. The tendency of any particle to move through a solution under centrifugal force is given by the *sedimentation coefficient, S:*

$$S = (\rho_p - \rho_m)V/f$$

where ρ_p is the density of the particle or macromolecule, ρ_m is the density of the medium or solution, V is the volume of the particle, and f is the frictional coefficient, given by

$$f = F_f/v$$

where v is the velocity of the particle and F_f is the frictional drag. Nonspherical molecules have larger frictional coefficients and thus smaller sedimentation coefficients. The smaller the particle and the more its shape deviates from spherical, the more slowly that particle sediments in a centrifuge.

  Centrifugation can be used either as a preparative technique for separating and purifying macromolecules and cellular components or as an analytical technique to characterize the hydrodynamic properties of macromolecules such as proteins and nucleic acids.

Adding an excess of free metabolite that will compete for the bound protein dissociates the protein from the chromatographic matrix. The protein passes out of the column complexed with free metabolite.
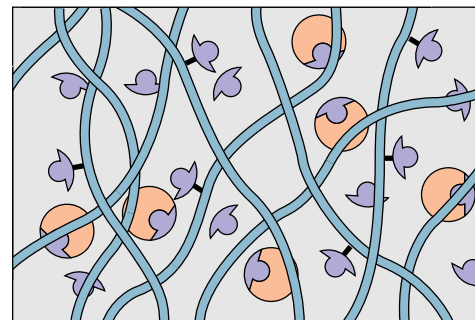
Purifications of proteins as much as 1000-fold or more are routinely achieved in a single affinity chromatographic step like this.

Growing in size and complexity

Living things, masses of atoms, DNA, protein

Dancing a pattern ever more intricate.

Out of the cradle onto the dry land

Here it is standing

Atoms with consciousness

Matter with curiosity.

Stands at the sea

Wonders at wondering

I

A universe of atoms

An atom in the universe.

RICHARD P. FEYNMAN (1918 – 1988)
From "*The Value of Science*" in Edward Hutchings, Jr. (ed.), *Frontiers of Science: A Survey.* New York: Basic Books, 1958.

*C*hapter 6

Proteins: Secondary, Tertiary, and Quaternary Structure

Like the Greek sea god Proteus, who could assume different forms, proteins act through changes in conformation. Proteins (from the Greek proteios, *meaning "primary") are the primary agents of biological function. ("Proteus, Old Man of the Sea, Roman period mosaic, from Thessalonika, 1st century A.D. National Archaeological Museum, Athens/Ancient Art and Architecture Collection Ltd./Bridgeman Art Library, London/New York.)*

Nearly all biological processes involve the specialized functions of one or more protein molecules. Proteins function to produce other proteins, control all aspects of cellular metabolism, regulate the movement of various molecular and ionic species across membranes, convert and store cellular energy, and carry out many other activities. Essentially all of the information required to initiate, conduct, and regulate each of these functions must be contained in

the structure of the protein itself. The previous chapter described the details of primary protein structure. However, proteins do not normally exist as fully extended polypeptide chains but rather as compact, folded structures, and the function of a given protein is rarely if ever dependent only on the amino acid sequence. Instead, the ability of a particular protein to carry out its function in nature is normally determined by its overall three-dimensional shape or *conformation*. This native, folded structure of the protein is dictated by several factors: (1) interactions with solvent molecules (normally water), (2) the pH and ionic composition of the solvent, and most important, (3) the sequence of the protein. The first two of these effects are intuitively reasonable, but the third, the role of the amino acid sequence, may not be. In ways that are just now beginning to be understood, the primary structure facilitates the development of short-range interactions among adjacent parts of the sequence and also long-range interactions among distant parts of the sequence. Although the resulting overall structure of the complete protein molecule may at first look like a disorganized and random arrangement, it is in nearly all cases a delicate and sophisticated balance of numerous forces that combine to determine the protein's unique conformation. This chapter considers the details of protein structure and the forces that maintain these structures.

6.1 • Forces Influencing Protein Structure

Several different kinds of noncovalent interactions are of vital importance in protein structure. Hydrogen bonds, hydrophobic interactions, electrostatic bonds, and van der Waals forces are all noncovalent in nature, yet are extremely important influences on protein conformations. The stabilization free energies afforded by each of these interactions may be highly dependent on the local environment within the protein, but certain generalizations can still be made.

Hydrogen Bonds

Hydrogen bonds are generally made wherever possible within a given protein structure. In most protein structures that have been examined to date, component atoms of the peptide backbone tend to form hydrogen bonds with one another. Furthermore, side chains capable of forming H bonds are usually located on the protein surface and form such bonds primarily with the water solvent. Although each hydrogen bond may contribute an average of only about 12 kJ/mol in stabilization energy for the protein structure, the number of H-bonds formed in the typical protein is very large. For example, in α-helices, the C$=$O and N—H groups of every residue participate in H bonds. The importance of H bonds in protein structure cannot be overstated.

Hydrophobic Interactions

Hydrophobic "bonds," or, more accurately, *interactions,* form because nonpolar side chains of amino acids and other nonpolar solutes prefer to cluster in a nonpolar environment rather than to intercalate in a polar solvent such as water. The forming of hydrophobic bonds minimizes the interaction of nonpolar residues with water and is therefore highly favorable. Such clustering is entropically driven. The side chains of the amino acids in the interior or core of the protein structure are almost exclusively hydrophobic. Polar amino acids are almost never found in the interior of a protein, but the protein surface may consist of both polar and nonpolar residues.

intercalate • to insert between

FIGURE 6.1 • An electrostatic interaction between the ϵ-amino group of a lysine and the γ-carboxyl group of a glutamate residue.
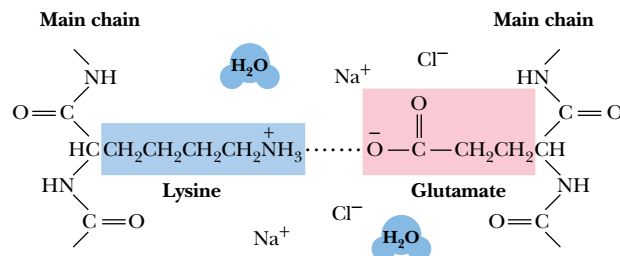
Electrostatic Interactions

Ionic interactions arise either as electrostatic attractions between opposite charges or repulsions between like charges. Chapter 4 discusses the ionization behavior of amino acids. Amino acid side chains can carry positive charges, as in the case of lysine, arginine, and histidine, or negative charges, as in aspartate and glutamate. In addition, the NH_2-terminal and COOH-terminal residues of a protein or peptide chain usually exist in ionized states and carry positive or negative charges, respectively. All of these may experience electrostatic interactions in a protein structure. Charged residues are normally located on the protein surface, where they may interact optimally with the water solvent. It is energetically unfavorable for an ionized residue to be located in the hydrophobic core of the protein. Electrostatic interactions between charged groups on a protein surface are often complicated by the presence of salts in the solution. For example, the ability of a positively charged lysine to attract a nearby negative glutamate may be weakened by dissolved NaCl (Figure 6.1). The Na^+ and Cl^- ions are highly mobile, compact units of charge, compared to the amino acid side chains, and thus compete effectively for charged sites on the protein. In this manner, electrostatic interactions among amino acid residues on protein surfaces may be damped out by high concentrations of salts. Nevertheless, these interactions are important for protein stability.

Van der Waals Interactions

Both attractive forces and repulsive forces are included in van der Waals interactions. The attractive forces are due primarily to instantaneous dipole-induced dipole interactions that arise because of fluctuations in the electron charge distributions of adjacent nonbonded atoms. Individual van der Waals interactions are weak ones (with stabilization energies of 4.0 to 1.2 kJ/mol), but many such interactions occur in a typical protein, and, by sheer force of numbers, they can represent a significant contribution to the stability of a protein. Peter Privalov and George Makhatadze have shown that, for pancreatic ribonuclease A, hen egg white lysozyme, horse heart cytochrome *c*, and sperm whale myoglobin, van der Waals interactions between tightly packed groups in the interior of the protein are a major contribution to protein stability.

6.2 • Role of the Amino Acid Sequence in Protein Structure

It can be inferred from the first section of this chapter that many different forces work together in a delicate balance to determine the overall three-dimensional structure of a protein. These forces operate both within the protein structure itself and between the protein and the water solvent. How, then, does nature dictate the manner of protein folding to generate the three-dimensional

structure that optimizes and balances these many forces? *All of the information necessary for folding the peptide chain into its "native" structure is contained in the amino acid sequence of the peptide.* This principle was first appreciated by C. B. Anfinsen and F. White, whose work in the early 1960s dealt with the chemical denaturation and subsequent renaturation of bovine pancreatic ribonuclease. Ribonuclease was first denatured with urea and mercaptoethanol, a treatment that cleaved the four covalent disulfide (S—S) cross-bridges in the protein. Subsequent air oxidation permitted random formation of disulfide cross-bridges, most of which were incorrect. Thus, the air-oxidized material showed little enzymatic activity. However, treatment of these inactive preparations with small amounts of mercaptoethanol allowed a reshuffling of the disulfide bonds and permitted formation of significant amounts of active native enzyme. In such experiments, the only road map for the protein, that is, the only "instructions" it has, are those directed by its primary structure, the linear sequence of its amino acid residues.

Just how proteins recognize and interpret the information that is stored in the polypeptide sequence is not well understood yet. It may be assumed that certain loci along the peptide chain act as nucleation points, which initiate folding processes that eventually lead to the correct structures. Regardless of how this process operates, it must take the protein correctly to the final native structure, without getting trapped in a local energy-minimum state which, although stable, may be different from the native state itself. A long-range goal of many researchers in the protein structure field is the prediction of three-dimensional conformation from the amino acid sequence. As the details of secondary and tertiary structure are described in this chapter, the complexity and immensity of such a prediction will be more fully appreciated. This area is perhaps the greatest uncharted frontier remaining in molecular biology.

6.3 • Secondary Structure in Proteins

Any discussion of protein folding and structure must begin with the *peptide bond,* the fundamental structural unit in all proteins. As we saw in Chapter 5, the resonance structures experienced by a peptide bond constrain the oxygen, carbon, nitrogen, and hydrogen atoms of the peptide group, as well as the adjacent α-carbons, to all lie in a plane. The resonance stabilization energy of this planar structure is approximately 88 kJ/mol, and substantial energy is required to twist the structure about the C—N bond. A twist of θ degrees involves a twist energy of $88 \sin^2\theta$ kJ/mol.

Consequences of the Amide Plane

The planarity of the peptide bond means that there are only two degrees of freedom per residue for the peptide chain. Rotation is allowed about the bond linking the α-carbon and the carbon of the peptide bond and also about the bond linking the nitrogen of the peptide bond and the adjacent α-carbon. As shown in Figure 6.2, each α-carbon is the joining point for two planes defined by peptide bonds. The angle about the C_α—N bond is denoted by the Greek letter ϕ (phi) and that about the C_α—C_o is denoted by ψ (psi). For either of these bond angles, a value of 0° corresponds to an orientation with the amide plane bisecting the H—C_α—R (sidechain) plane and a *cis* configuration of the main chain around the rotating bond in question (Figure 6.3). In any case, the entire path of the peptide backbone in a protein is known if the ϕ and ψ rotation angles are all specified. Some values of ϕ and ψ are not allowed due to steric interference between nonbonded atoms. As shown in Figure 6.4, values

$\phi = 180°, \psi = 180°$
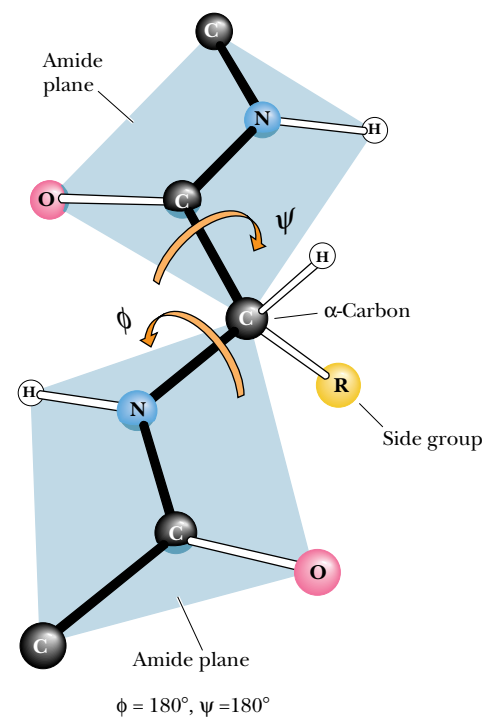
FIGURE 6.2 • The amide or peptide bond planes are joined by the tetrahedral bonds of the α-carbon. The rotation parameters are ϕ and ψ. The conformation shown corresponds to $\phi = 180°$ and $\psi = 180°$. Note that positive values of ϕ and ψ correspond to clockwise rotation as viewed from C_α. Starting from 0°, a rotation of 180° in the clockwise direction ($+180°$) is equivalent to a rotation of 180° in the counterclockwise direction ($-180°$). *(Irving Geis)*

Nonbonded
contact
radius

$\phi = 0°, \psi = 180°$

Nonbonded
contact
radius

$\phi = 180°, \psi = 0°$

$\phi = -60°, \psi = 180°$
A further ϕ rotation of 120°
removes the bulky carbonyl
group as far as possible
from the side chain

$\phi = 0°, \psi = 0°$
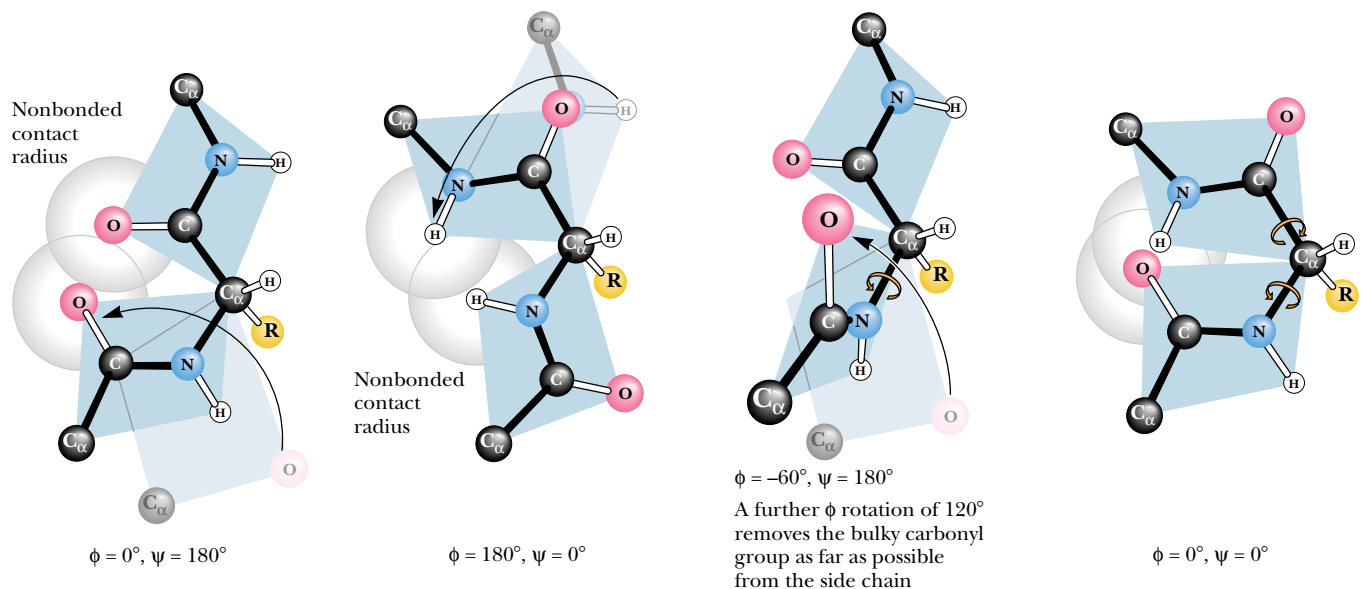
FIGURE 6.3 • Many of the possible conformations about an α-carbon between two peptide planes are forbidden because of steric crowding. Several noteworthy examples are shown here.
Note: The formal IUPAC-IUB Commission on Biochemical Nomenclature convention for the definition of the torsion angles ϕ and ψ in a polypeptide chain (*Biochemistry* **9:**3471–3479, 1970) is different from that used here, where the C_α atom serves as the point of reference for both rotations, but the result is the same. *(Irving Geis)*

of $\phi = 180°$ and $\psi = 0°$ are not allowed because of the forbidden overlap of the N—H hydrogens. Similarly, $\phi = 0°$ and $\psi = 180°$ are forbidden because of unfavorable overlap between the carbonyl oxygens.

G. N. Ramachandran and his coworkers in Madras, India, first showed that it was convenient to plot ϕ values against ψ values to show the distribution of allowed values in a protein or in a family of proteins. A typical **Ramachandran plot** is shown in Figure 6.4. Note the clustering of ϕ and ψ values in a few regions of the plot. Most combinations of ϕ and ψ are sterically forbidden, and the corresponding regions of the Ramachandran plot are sparsely populated. The combinations that are sterically allowed represent the subclasses of structure described in the remainder of this section.

The Alpha-Helix

The discussion of hydrogen bonding in Section 6.1 pointed out that the carbonyl oxygen and amide hydrogen of the peptide bond could participate in H bonds either with water molecules in the solvent or with other H-bonding groups in the peptide chain. In nearly all proteins, the carbonyl oxygens and the amide protons of many peptide bonds participate in H bonds that link one peptide group to another, as shown in Figure 6.5. These structures tend to form in cooperative fashion and involve substantial portions of the peptide chain. Structures resulting from these interactions constitute **secondary structure** for proteins (see Chapter 5). When a number of hydrogen bonds form between portions of the peptide chain in this manner, two basic types of structures can result: α-*helices* and β-*pleated sheets*.
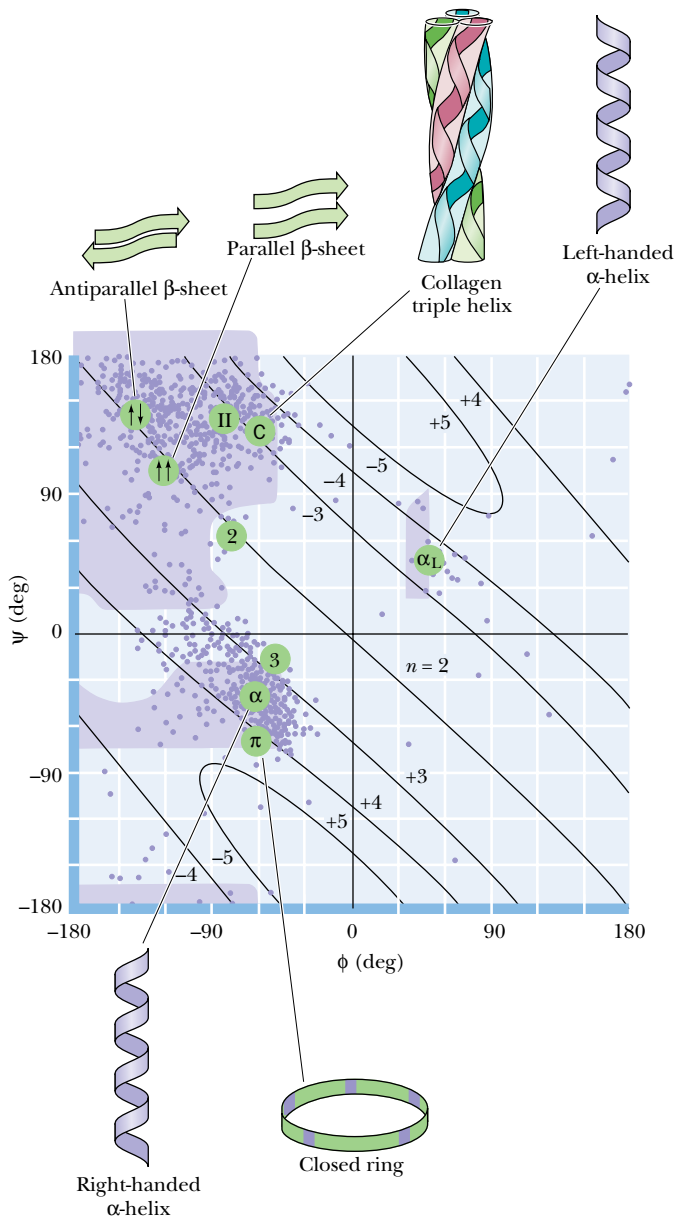
FIGURE 6.4 • A Ramachandran diagram showing the sterically reasonable values of the angles ϕ and ψ. The shaded regions indicate particularly favorable values of these angles. Dots in purple indicate actual angles measured for 1000 residues (excluding glycine, for which a wider range of angles is permitted) in eight proteins. The lines running across the diagram (numbered +5 through 2 and −5 through −3) signify the number of amino acid residues per turn of the helix; "+" means right-handed helices; "−" means left-handed helices. *(After Richardson, J. S., 1981, Advances in Protein Chemistry 34:167–339.)*

FIGURE 6.5 • A hydrogen bond between the amide proton and carbonyl oxygen of adjacent peptide groups.
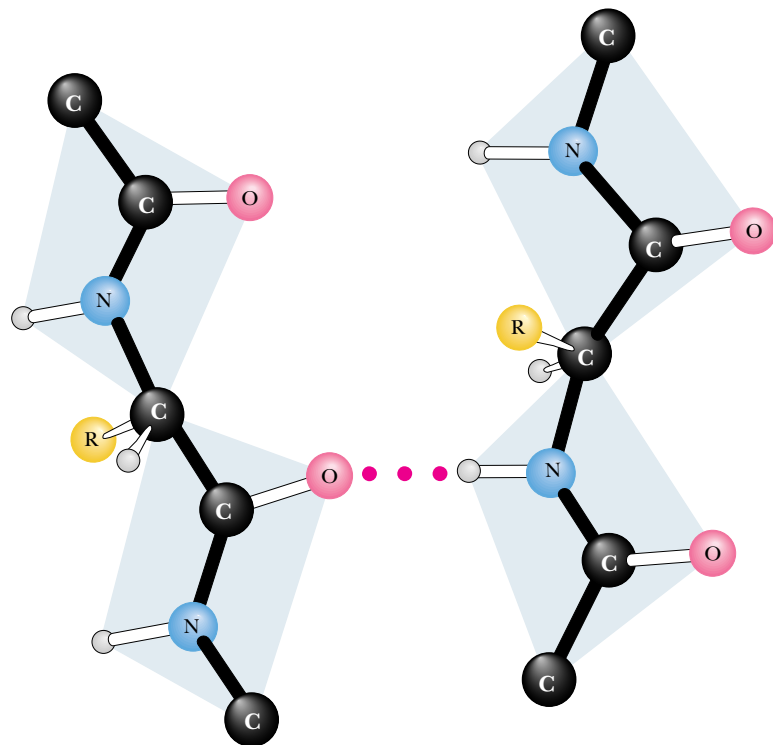
𝒜   **D E E P E R   L O O K**

Knowing What the Right Hand and Left Hand Are Doing

Certain conventions related to peptide bond angles and the "handedness" of biological structures are useful in any discussion of protein structure. To determine the ϕ and ψ angles between peptide planes, viewers should imagine themselves at the C_α carbon looking outward and should imagine starting from the $\phi = 0°$, $\psi = 0°$ conformation. From this perspective, positive values of ϕ correspond to clockwise rotations about the C_α—N bond of the plane that includes the adjacent N—H group. Similarly, positive values of ψ correspond to clockwise

rotations about the C_α—C bond of the plane that includes the adjacent C=O group.

Biological structures are often said to exhibit "right-hand" or "left-hand" twists. For all such structures, the sense of the twist can be ascertained by holding the structure in front of you and looking along the polymer backbone. If the twist is clockwise as one proceeds outward and through the structure, it is said to be right-handed. If the twist is counterclockwise, it is said to be left-handed.

Evidence for helical structures in proteins was first obtained in the 1930s in studies of fibrous proteins. However, there was little agreement at that time about the exact structure of these helices, primarily because there was also lack of agreement about interatomic distances and bond angles in peptides. In 1951, Linus Pauling, Robert Corey, and their colleagues at the California Institute of Technology summarized a large volume of crystallographic data in a set of dimensions for polypeptide chains. (A summary of data similar to what they reported is shown in Figure 5.2.) With these data in hand, Pauling, Corey, and their colleagues proposed a new model for a helical structure in proteins, which they called the **α-helix.** The report from Caltech was of particular interest to Max Perutz in Cambridge, England, a crystallographer who was also interested in protein structure. By taking into account a critical but previously ignored feature of the X-ray data, Perutz realized that the α-helix existed in keratin, a protein from hair, and also in several other proteins. Since then, the α-helix has proved to be a fundamentally important peptide structure. Several representations of the α-helix are shown in Figure 6.6. One turn of the helix represents 3.6 amino acid residues. (A single turn of the α-helix involves 13 atoms from the O to the H of the H bond. For this reason, the α-helix is sometimes referred to as the 3.6_{13} helix.) This is in fact the feature that most confused crystallographers before the Pauling and Corey α-helix model. Crystallographers were so accustomed to finding twofold, threefold, sixfold, and similar integral axes in simpler molecules that the notion of a nonintegral number of units per turn was never taken seriously before Pauling and Corey's work.

Each amino acid residue extends **1.5 Å (0.15 nm)** along the helix axis. With **3.6 residues per turn,** this amounts to 3.6×1.5 Å or **5.4 Å (0.54 nm)** of travel along the helix axis per turn. This is referred to as the translation distance or the **pitch** of the helix. If one ignores side chains, the helix is about 6 Å in diameter. The side chains, extending outward from the core structure of the helix, are removed from steric interference with the polypeptide backbone. As can be seen in Figure 6.6, *each peptide carbonyl is hydrogen bonded to the peptide N—H group four residues farther up the chain.* Note that all of the H bonds lie parallel to the helix axis and that all of the carbonyl groups are pointing in one direction along the helix axis while the N—H groups are pointing in the opposite direction. Recall that the entire path of the peptide backbone can be known if the ϕ and ψ twist angles are specified for each residue. The α-helix is formed if the values of ϕ are approximately $-60°$ and the values of ψ are in the range of -45 to $-50°$. Figure 6.7 shows the structures of two proteins that contain α-helical segments. The number of residues involved in a given α-helix

(a)
Hydrogen bonds stabilize
the helix structure.

(b)
The helix can be viewed
as a stacked array of
peptide planes hinged
at the α-carbons and
approximately parallel
to the helix.

α-Carbon

Side group

(c)

(d)
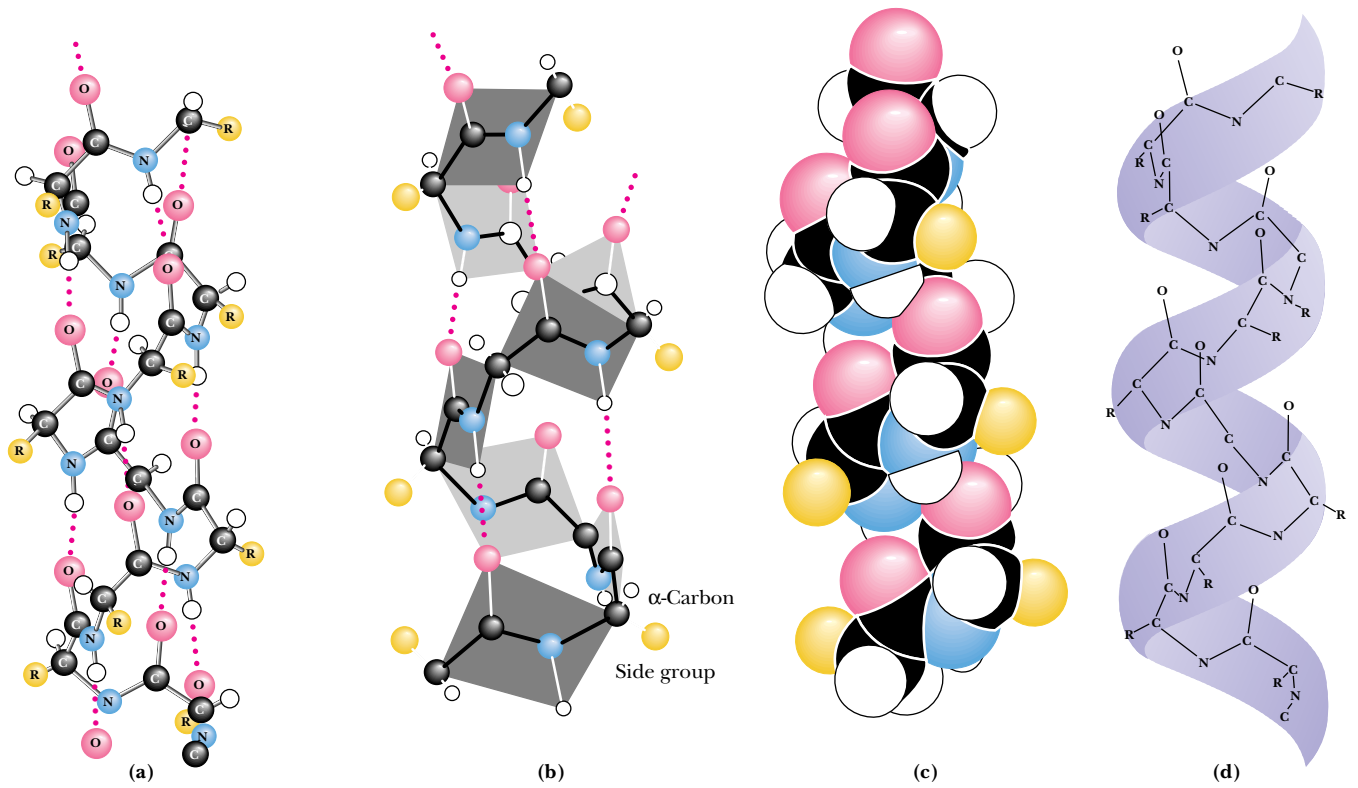
FIGURE 6.6 • Four different graphic representations of the α-helix. (a) As it originally appeared in Pauling's 1960 *The Nature of the Chemical Bond.* (b) Showing the arrangement of peptide planes in the helix. (c) A space-filling computer graphic presentation. (d) A "ribbon structure" with an inlaid stick figure, showing how the ribbon indicates the path of the polypeptide backbone. *(Irving Geis)*

β-Hemoglobin subunit
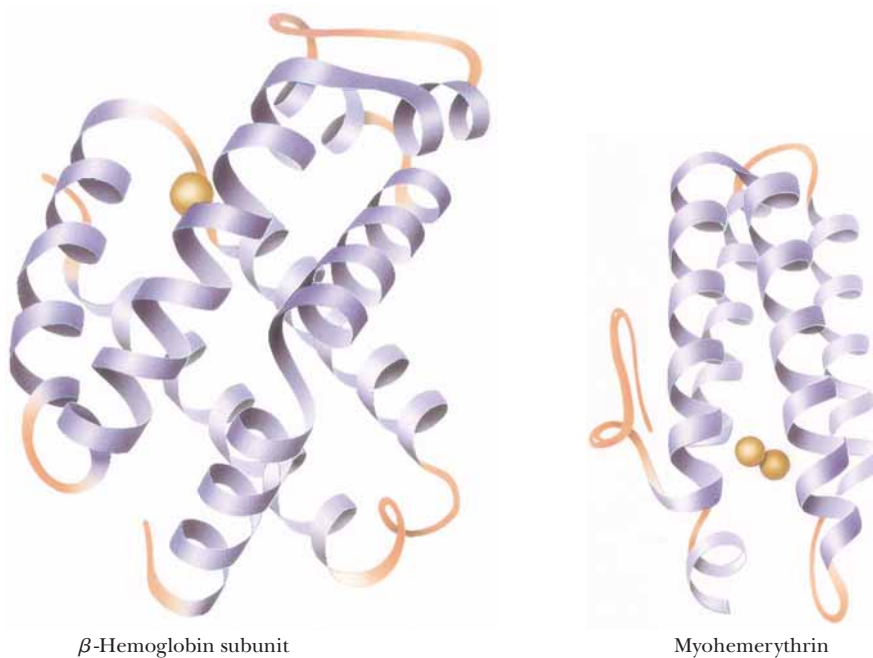
Myohemerythrin

FIGURE 6.7 • The three-dimensional structures of two proteins that contain substantial amounts of α-helix in their structures. The helices are represented by the regularly coiled sections of the ribbon drawings. Myohemerythrin is the oxygen-carrying protein in certain invertebrates, including *Sipunculids,* a phylum of marine worm. *(Jane Richardson)*

FIGURE 6.8 • The arrangement of N—H and C=O groups (each with an individual dipole moment) along the helix axis creates a large net dipole for the helix. Numbers indicate fractional charges on respective atoms.

(a)

(b)
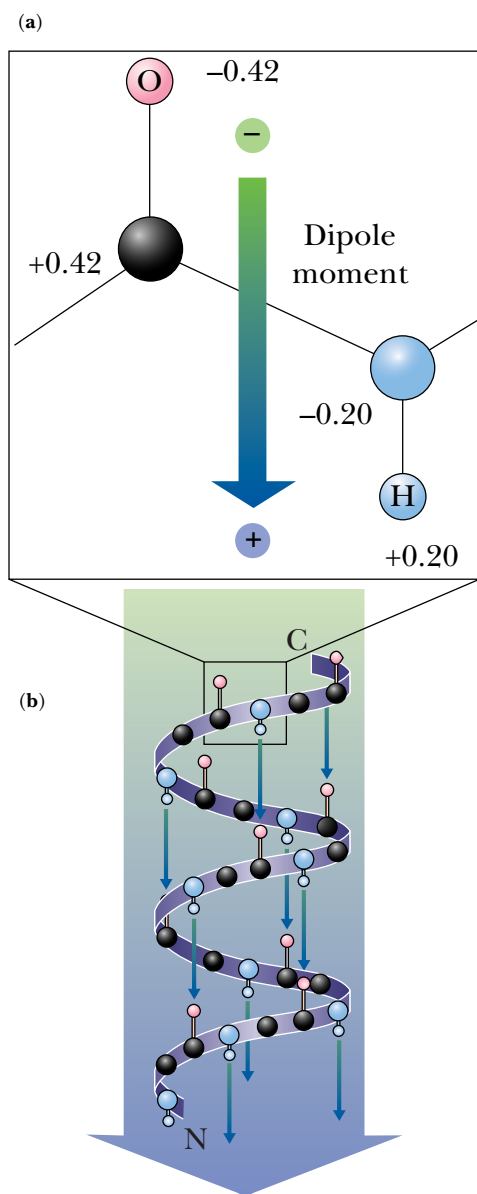
varies from helix to helix and from protein to protein. On average, there are about 10 residues per helix. Myoglobin, one of the first proteins in which α-helices were observed, has eight stretches of α-helix that form a box to contain the heme prosthetic group. The structures of the α and β subunits of hemoglobin are strikingly similar, with only a few differences at the C- and N-termini and on the surfaces of the structure that contact or interact with the other subunits of this multisubunit protein.

As shown in Figure 6.6, all of the hydrogen bonds point in the same direction along the α-helix axis. Each peptide bond posesses a dipole moment that arises from the polarities of the N—H and C=O groups, and, because these groups are all aligned along the helix axis, the helix itself has a substantial dipole moment, with a partial positive charge at the N-terminus and a partial negative charge at the C-terminus (Figure 6.8). Negatively charged ligands (e.g., phosphates) frequently bind to proteins near the N-terminus of an α-helix. By contrast, positively charged ligands are only rarely found to bind near the C-terminus of an α-helix.

In a typical α-helix of 12 (or n) residues, there are 8 (or $n - 4$) hydrogen bonds. As shown in Figure 6.9, the first 4 amide hydrogens and the last 4 carbonyl oxygens cannot participate in helix H-bonds. Also, nonpolar residues sit-
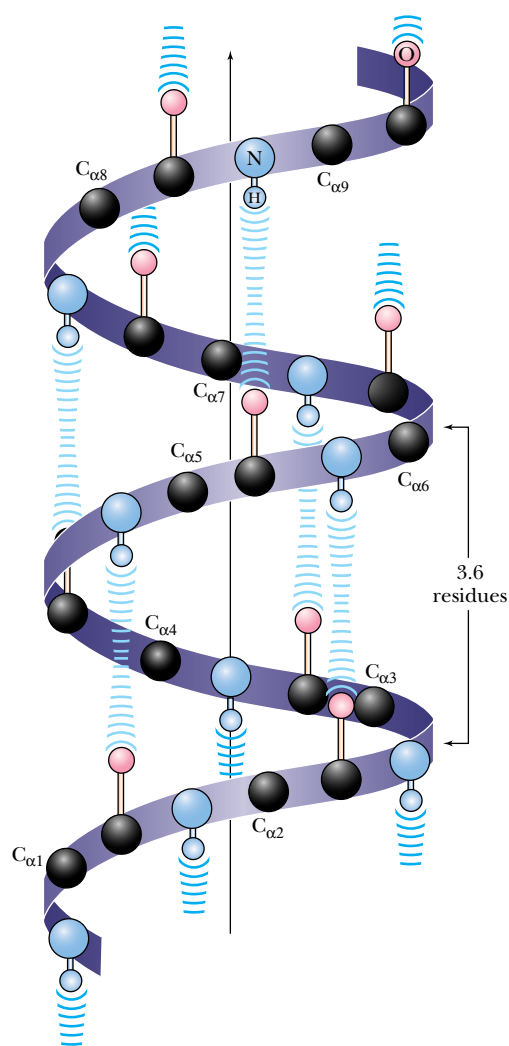
FIGURE 6.9 • Four N—H groups at the N-terminal end of an α-helix and four C=O groups at the C-terminal end cannot participate in hydrogen bonding. The formation of H-bonds with other nearby donor and acceptor groups is referred to as **helix capping.** Capping may also involve appropriate hydrophobic interactions that accomodate nonpolar side chains at the ends of helical segments.

uated near the helix termini can be exposed to solvent. Proteins frequently compensate for these problems by **helix capping—**providing H-bond partners for the otherwise bare N—H and C=O groups and folding other parts of the protein to foster hydrophobic contacts with exposed nonpolar residues at the helix termini.

Careful studies of the **polyamino acids,** polymers in which all the amino acids are identical, have shown that certain amino acids tend to occur in α-helices, whereas others are less likely to be found in them. Polyleucine and polyalanine, for example, readily form α-helical structures. In contrast, polyaspartic acid and polyglutamic acid, which are highly negatively charged at pH 7.0, form only random structures because of strong charge repulsion between the R groups along the peptide chain. At pH 1.5 to 2.5, however, where the side chains are protonated and thus uncharged, these latter species spontaneously form α-helical structures. In similar fashion, polylysine is a random coil at pH values below about 11, where repulsion of positive charges prevents helix formation. At pH 12, where polylysine is a neutral peptide chain, it readily forms an α-helix.

---

*C*RITICAL DEVELOPMENTS IN BIOCHEMISTRY

In Bed with a Cold, Pauling Stumbles onto the α-Helix and a Nobel Prize[1]

As high technology continues to transform the modern biochemical laboratory, it is interesting to reflect on Linus Pauling's discovery of the α-helix. It involved only a piece of paper, a pencil, scissors, and a sick Linus Pauling, who had tired of reading detective novels. The story is told in the excellent book *The Eighth Day of Creation* by Horace Freeland Judson:

> From the spring of 1948 through the spring of 1951 . . . rivalry sputtered and blazed between Pauling's lab and (Sir Lawrence) Bragg's — over protein. The prize was to propose and verify in nature a general three-dimensional structure for the polypeptide chain. Pauling was working up from the simpler structures of components. In January 1948, he went to Oxford as a visiting professor for two terms, to lecture on the chemical bond and on molecular structure and biological specificity. "In Oxford, it was April, I believe, I caught cold. I went to bed, and read detective stories for a day, and got bored, and thought why don't I have a crack at that problem of alpha keratin." Confined, and still fingering the polypeptide chain in his mind, Pauling called for paper, pencil, and straightedge and attempted to reduce the problem to an almost Euclidean purity. "I took a sheet of paper — I still have this sheet of paper — and drew, rather roughly, the way that I thought a polypeptide chain would look if it were spread out into a plane." The repetitious herringbone of the chain he could stretch across the paper as simply as this —
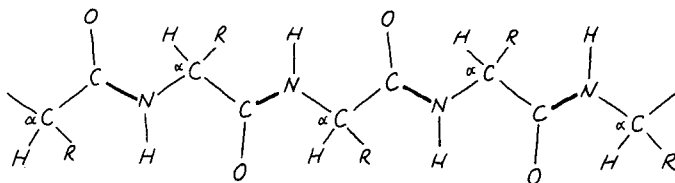
— putting in lengths and bond angles from memory. . . . He knew that the peptide bond, at the carbon-to-nitrogen link, was always rigid:
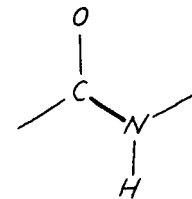
And this meant that the chain could turn corners only at the alpha carbons. . . . "I creased the paper in parallel creases through the alpha carbon atoms, so that I could bend it and make the bonds to the alpha carbons, along the chain, have tetrahedral value. And then I looked to see if I could form hydrogen bonds from one part of the chain to the next." He saw that if he folded the strip like a chain of paper dolls into a helix, and if he got the pitch of the screw right, hydrogen bonds could be shown to form, N—H···O—C, three or four knuckles apart along the backbone, holding the helix in shape. After several tries, changing the angle of the parallel creases in order to adjust the pitch of the helix, he found one where the hydrogen bonds would drop into place, connecting the turns, as straight lines of the right length. He had a model.

[1]The discovery of the α-helix structure was only one of many achievements that led to Pauling's Nobel Prize in chemistry in 1954. The official citation for the prize was "for his research into the nature of the chemical bond and its application to the elucidation of the structure of complex substances."

Table 6.1

Helix-Forming and Helix-Breaking Behavior of the Amino Acids

Amino Acid		Helix Behavior*	
A	Ala	H	(I)
C	Cys	Variable	
D	Asp	Variable	
E	Glu	H	
F	Phe	H	
G	Gly	I	(B)
H	His	H	(I)
I	Ile	H	(C)
K	Lys	Variable	
L	Leu	H	
M	Met	H	
N	Asn	C	(I)
P	Pro	B	
Q	Gln	H	(I)
R	Arg	H	(I)
S	Ser	C	(B)
T	Thr	Variable	
V	Val	Variable	
W	Trp	H	(C)
Y	Tyr	H	(C)

*H = helix former; I = indifferent; B = helix breaker; C = random coil; ( ) = secondary tendency.

The tendencies of the amino acids to stabilize or destabilize α-helices are different in typical proteins than in polyamino acids. The occurrence of the common amino acids in helices is summarized in Table 6.1. Notably, proline (and hydroxyproline) act as helix breakers due to their unique structure, which fixes the value of the C_α—N—C bond angle. Helices can be formed from either D- or L-amino acids, but a given helix must be composed entirely of amino acids of one configuration. α-Helices cannot be formed from a mixed copolymer of D- and L-amino acids. An α-helix composed of D-amino acids is left-handed.

Other Helical Structures

There are several other far less common types of helices found in proteins. The most common of these is the 3_{10} helix, which contains 3.0 residues per turn (with 10 atoms in the ring formed by making the hydrogen bond three residues up the chain). It normally extends over shorter stretches of sequence than the α-helix. Other helical structures include the 2_7 ribbon and the π-helix, which has 4.4 residues and 16 atoms per turn and is thus called the 4.4_{16} helix.

The Beta-Pleated Sheet

Another type of structure commonly observed in proteins also forms because of local, cooperative formation of hydrogen bonds. That is the pleated sheet, or β-structure, often called the **β-pleated sheet.** This structure was also first postulated by Pauling and Corey in 1951 and has now been observed in many natural proteins. A β-pleated sheet can be visualized by laying thin, pleated strips of paper side by side to make a "pleated sheet" of paper (Figure 6.10). Each strip of paper can then be pictured as a single peptide strand in which the peptide backbone makes a zigzag pattern along the strip, with the α-carbons lying at the folds of the pleats. The pleated sheet can exist in both par-
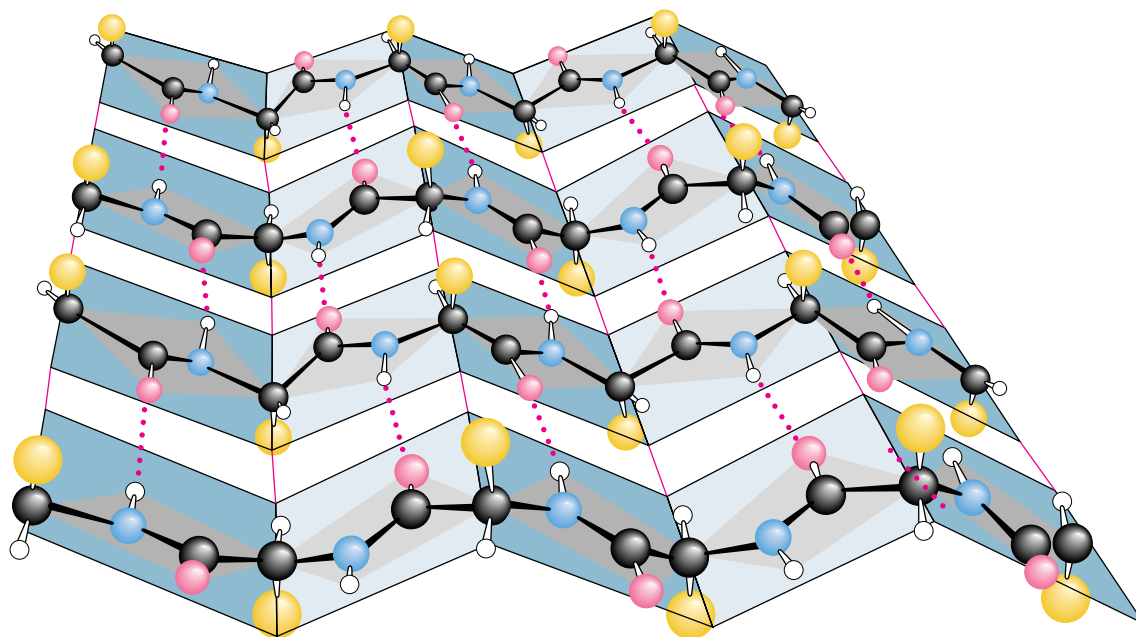
FIGURE 6.10 • A "pleated sheet" of paper with an antiparallel β-sheet drawn on it. *(Irving Geis)*

allel and antiparallel forms. In the **parallel β-pleated sheet,** adjacent chains run in the same direction (N → C or C → N). In the **antiparallel β-pleated sheet,** adjacent strands run in opposite directions.

Each single strand of the β-sheet structure can be pictured as a twofold helix, that is, a helix with two residues per turn. The arrangement of successive amide planes has a pleated appearance due to the tetrahedral nature of the C_α atom. It is important to note that the hydrogen bonds in this structure are essentially *inter*strand rather than *intra*strand. The peptide backbone in the β-sheet is in its most extended conformation (sometimes called the **ε-conformation**). The optimum formation of H bonds in the parallel pleated sheet results in a slightly less extended conformation than in the antiparallel sheet. The H bonds thus formed in the parallel β-sheet are bent significantly. The distance between residues is 0.347 nm for the antiparallel pleated sheet, but only 0.325 nm for the parallel pleated sheet. Figure 6.11 shows examples of both parallel and antiparallel β-pleated sheets. Note that the side chains in the pleated sheet are oriented perpendicular or normal to the plane of the sheet, extending out from the plane on alternating sides.

Parallel β-sheets tend to be more regular than antiparallel β-sheets. The range of ϕ and ψ angles for the peptide bonds in parallel sheets is much smaller than that for antiparallel sheets. Parallel sheets are typically large structures; those composed of less than five strands are rare. Antiparallel sheets, however, may consist of as few as two strands. Parallel sheets characteristically distribute
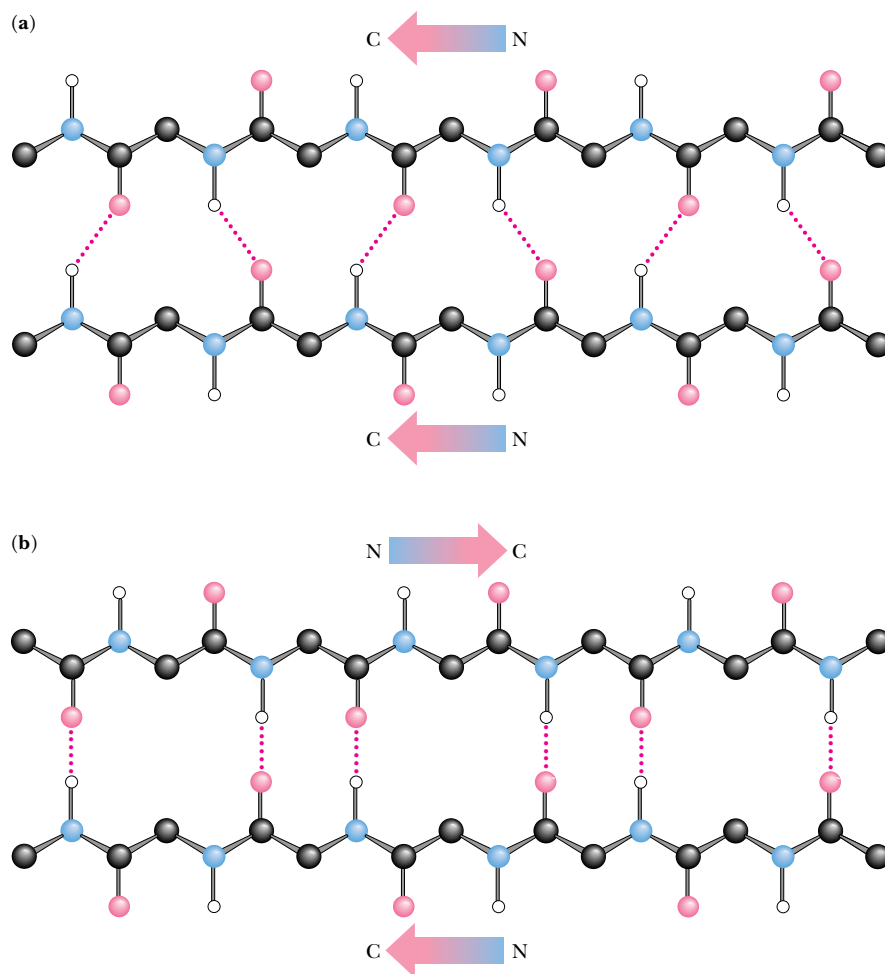
FIGURE 6.11 • The arrangement of hydrogen bonds in (a) parallel and (b) antiparallel β-pleated sheets.

hydrophobic side chains on both sides of the sheet, while antiparallel sheets are usually arranged with all their hydrophobic residues on one side of the sheet. This requires an alternation of hydrophilic and hydrophobic residues in the primary structure of peptides involved in antiparallel β-sheets because alternate side chains project to the same side of the sheet (see Figure 6.10).

Antiparallel pleated sheets are the fundamental structure found in silk, with the polypeptide chains forming the sheets running parallel to the silk fibers. The silk fibers thus formed have properties consistent with those of the β-sheets that form them. They are quite flexible but cannot be stretched or extended to any appreciable degree. Antiparallel structures are also observed in many other proteins, including immunoglobulin G, superoxide dismutase from bovine erythrocytes, and concanavalin A. Many proteins, including carbonic anhydrase, egg lysozyme, and glyceraldehyde phosphate dehydrogenase, possess both α-helices and β-pleated sheet structures within a single polypeptide chain.

The Beta-Turn

Most proteins are globular structures. The polypeptide chain must therefore possess the capacity to bend, turn, and reorient itself to produce the required compact, globular structures. A simple structure observed in many proteins is the **β-turn** (also known as the *tight turn* or *β-bend*), in which the peptide chain forms a tight loop with the carbonyl oxygen of one residue hydrogen-bonded with the amide proton of the residue three positions down the chain. This H bond makes the β-turn a relatively stable structure. As shown in Figure 6.12, the β-turn allows the protein to reverse the direction of its peptide chain. This figure shows the two major types of β-turns, but a number of less common types are also found in protein structures. Certain amino acids, such as proline and glycine, occur frequently in β-turn sequences, and the particular conformation of the β-turn sequence depends to some extent on the amino acids composing it. Due to the absence of a side chain, glycine is sterically the most adaptable of the amino acids, and it accommodates conveniently to other steric constraints in the β-turn. Proline, however, has a cyclic structure and a fixed ϕ angle, so, to some extent, it forces the formation of a β-turn, and in many cases this facilitates the turning of a polypeptide chain upon itself. Such bends promote formation of antiparallel β-pleated sheets.
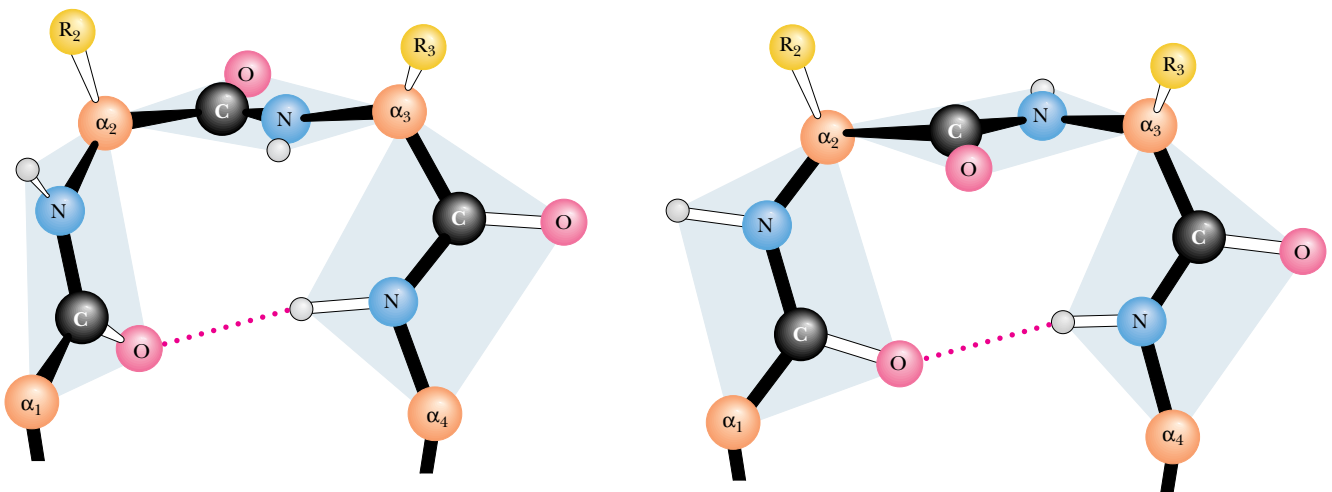
FIGURE 6.12 • The structures of two kinds of β-turns (also called tight turns or β-bends) *(Irving Geis)*

Classic bulge   G-1 bulge   Wide bulge
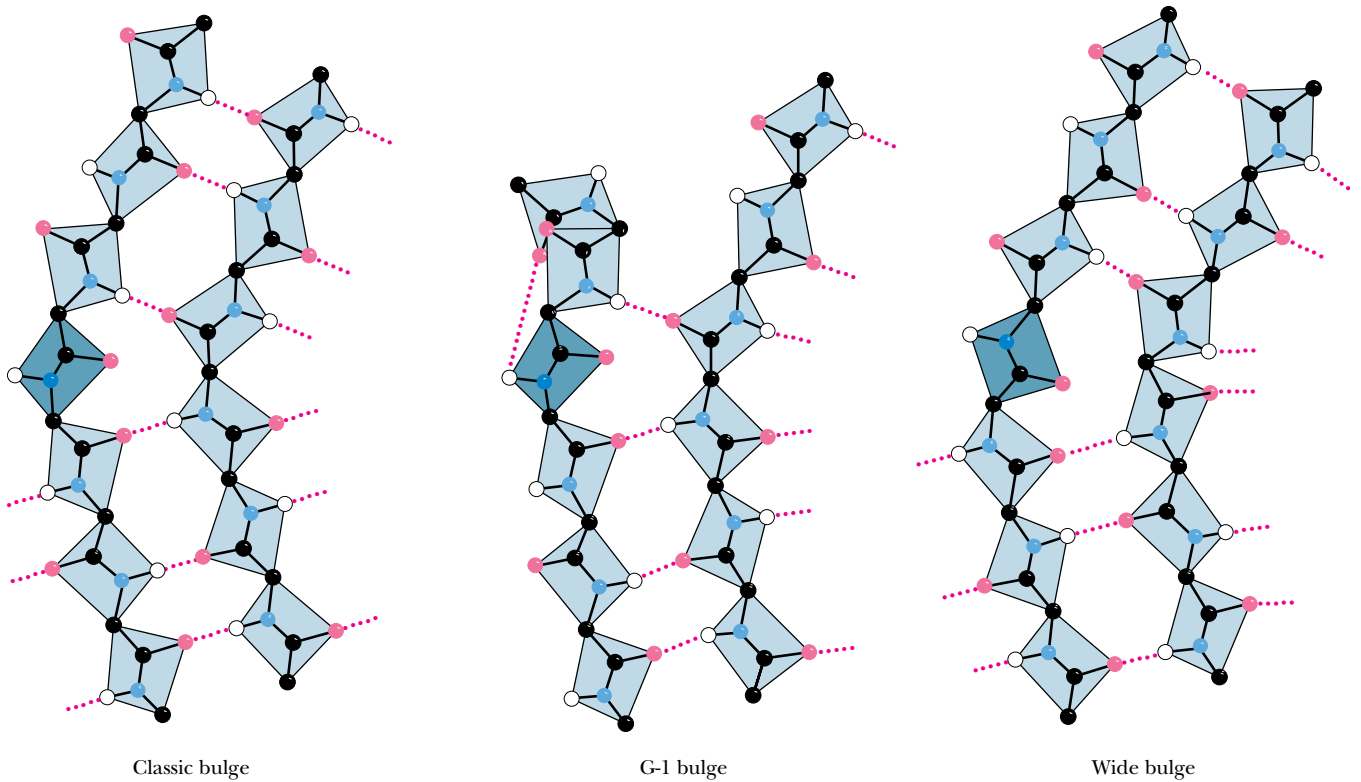
FIGURE 6.13 • Three different kinds of β-bulge structures involving a pair of adjacent polypeptide chains. *(Adapted from Richardson, J. S., 1981.* Advances in Protein Chemistry ***34***:167–339.)

The Beta-Bulge

One final secondary structure, the **β-bulge,** is a small piece of nonrepetitive structure that can occur by itself, but most often occurs as an irregularity in antiparallel β-structures. A β-bulge occurs between two normal β-structure hydrogen bonds and comprises two residues on one strand and one residue on the opposite strand. Figure 6.13 illustrates typical β-bulges. The extra residue on the longer side, which causes additional backbone length, is accommodated partially by creating a bulge in the longer strand and partially by forcing a slight bend in the β-sheet. Bulges thus cause changes in the direction of the polypeptide chain, but to a lesser degree than tight turns do. Over 100 examples of β-bulges are known in protein structures.

  The secondary structures we have described here are all found commonly in proteins in nature. In fact, it is hard to find proteins that do not contain one or more of these structures. The energetic (mostly H-bond) stabilization afforded by α-helices, β-pleated sheets, and β-turns is important to proteins, and they seize the opportunity to form such structures wherever possible.

6.4 • Protein Folding and Tertiary Structure

The folding of a single polypeptide chain in three-dimensional space is referred to as its **tertiary structure.** As discussed in Section 6.2, all of the information needed to fold the protein into its native tertiary structure is contained within the primary structure of the peptide chain itself. With this in mind, it was disappointing to the biochemists of the 1950s when the early protein structures did not reveal the governing principles in any particular detail. It soon became apparent that the proteins knew how they were supposed to fold into tertiary

shapes, even if the biochemists did not. Vigorous work in many laboratories has slowly brought important principles to light.

First, secondary structures—helices and sheets—form whenever possible as a consequence of the formation of large numbers of hydrogen bonds. Second, α-helices and β-sheets often associate and pack close together in the protein. No protein is stable as a single-layer structure, for reasons that become apparent later. There are a few common methods for such packing to occur. Third, because the peptide segments between secondary structures in the protein tend to be short and direct, the peptide does not execute complicated twists and knots as it moves from one region of a secondary structure to another. A consequence of these three principles is that protein chains are usually folded so that the secondary structures are arranged in one of a few common patterns. For this reason, there are families of proteins that have similar tertiary structure, with little apparent evolutionary or functional relationship among them. Finally, proteins generally fold so as to form the most stable structures possible. The stability of most proteins arises from (1) the formation of large numbers of intramolecular hydrogen bonds and (2) the reduction in the surface area accessible to solvent that occurs upon folding.

Fibrous Proteins

In Chapter 5, we saw that proteins can be grouped into three large classes based on their structure and solubility: *fibrous proteins, globular proteins,* and *membrane proteins.* Fibrous proteins contain polypeptide chains organized approximately parallel along a single axis, producing long fibers or large sheets. Such proteins tend to be mechanically strong and resistant to solubilization in water and dilute salt solutions. Fibrous proteins often play a structural role in nature (see Chapter 5).

α-Keratin

As their name suggests, the structure of the **α-keratins** is dominated by α-helical segments of polypeptide. The amino acid sequence of α-keratin subunits is composed of central α-helix–rich rod domains about 311 to 314 residues in length, flanked by nonhelical N- and C-terminal domains of varying size and composition (Figure 6.14a). The structure of the central rod domain of a typical α-keratin is shown in Figure 6.14b. It consists of four helical strands arranged as twisted pairs of two-stranded **coiled coils.** X-ray diffraction patterns show that these structures resemble α-helices, but with a pitch of 0.51 nm rather than the expected 0.54 nm. This is consistent with a tilt of the helix relative to the long axis of the fiber, as in the two-stranded "rope" in Figure 6.14.

The primary structure of the central rod segments of α-keratin consists of quasi-repeating seven-residue segments of the form $(a\text{-}b\text{-}c\text{-}d\text{-}e\text{-}f\text{-}g)_n$. These units are not true repeats, but residues a and d are usually nonpolar amino acids. In α-helices, with 3.6 residues per turn, these nonpolar residues are arranged in an inclined row or stripe that twists around the helix axis. These nonpolar residues would make the helix highly unstable if they were exposed to solvent, but the association of hydrophobic strips on two coiled coils to form the two-stranded rope effectively buries the hydrophobic residues and forms a highly stable structure (Figure 6.14). The helices clearly sacrifice some stability in assuming this twisted conformation, but they gain stabilization energy from the packing of side chains between the helices. In other forms of keratin, covalent disulfide bonds form between cysteine residues of adjacent molecules, making the overall structure rigid, inextensible, and insoluble—important properties for structures such as claws, fingernails, hair, and horns in animals. How and

(a)

		N-terminal domain		Rod domain							C-terminal domain		

Keratin type I H_3^+N—

*	*	35	11/14	101	16	19	8	121	*	*	—COO^-

Keratin type II H_3^+N—

*	*	36	35	12	101	17	19	8	121	20	*	20	—COO^-

(b)

α-Helix

Coiled coil of two α-helices

Protofilament (pair of coiled coils)

Filament (four right-hand twisted protofibrils)
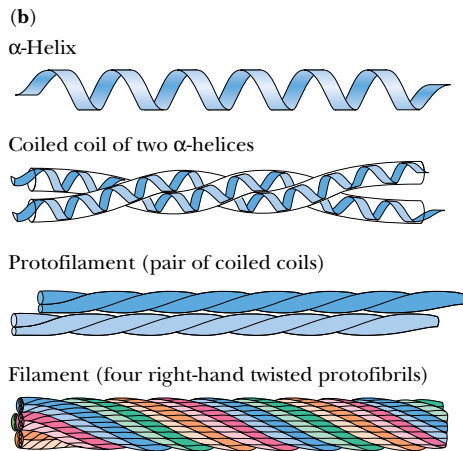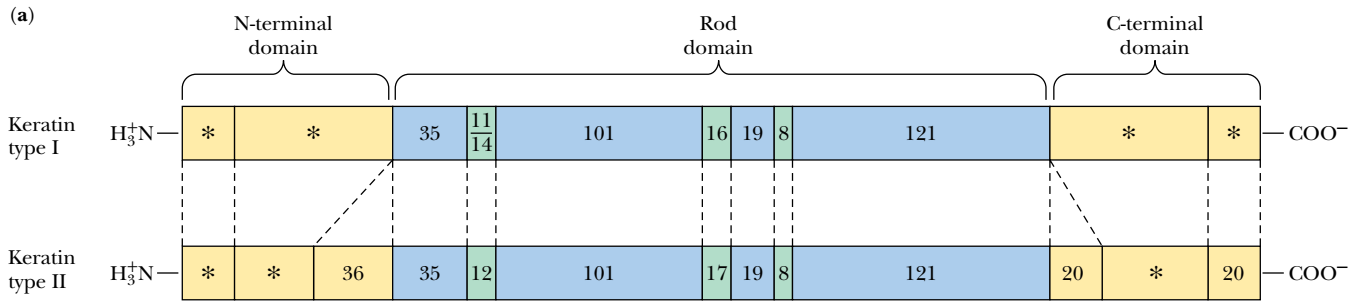
FIGURE 6.14 • (a) Both type I and type II α-keratin molecules have sequences consisting of long, central rod domains with terminal cap domains. The numbers of amino acid residues in each domain are indicated. Asterisks denote domains of variable length. (b) The rod domains form coiled coils consisting of intertwined right-handed α-helices. These coiled coils then wind around each other in a left-handed twist. Keratin filaments consist of twisted protofibrils (each a bundle of four coiled coils). *(Adapted from Steinert, P., and Parry, D., 1985.* Annual Review of Cell Biology *1:41–65; and Cohlberg, J., 1993.* Trends in Biochemical Sciences *18:360–362.)*

where these disulfides form determines the amount of curling in hair and wool fibers. When a hairstylist creates a permanent wave (simply called a "permanent") in a hair salon, disulfides in the hair are first reduced and cleaved, then reorganized and reoxidized to change the degree of curl or wave. In contrast, a "set" that is created by wetting the hair, setting it with curlers, and then drying it represents merely a rearrangement of the hydrogen bonds between helices and between fibers. (On humid or rainy days, the hydrogen bonds in curled hair may rearrange, and the hair becomes "frizzy.")

Fibroin and β-Keratin: β-Sheet Proteins

The **fibroin** proteins found in silk fibers represent another type of fibrous protein. These are composed of stacked antiparallel β-sheets, as shown in Figure 6.15. In the polypeptide sequence of silk proteins, there are large stretches in which every other residue is a glycine. As previously mentioned, the residues of a β-sheet extend alternately above and below the plane of the sheet. As a result, the glycines all end up on one side of the sheet and the other residues (mainly alanines and serines) compose the opposite surface of the sheet. Pairs of β-sheets can then pack snugly together (glycine surface to glycine surface or alanine–serine surface to alanine–serine surface). The β-keratins found in bird feathers are also made up of stacked β-sheets.

Collagen: A Triple Helix

Collagen is a rigid, inextensible fibrous protein that is a principal constituent of connective tissue in animals, including tendons, cartilage, bones, teeth, skin, and blood vessels. The high tensile strength of collagen fibers in these struc-
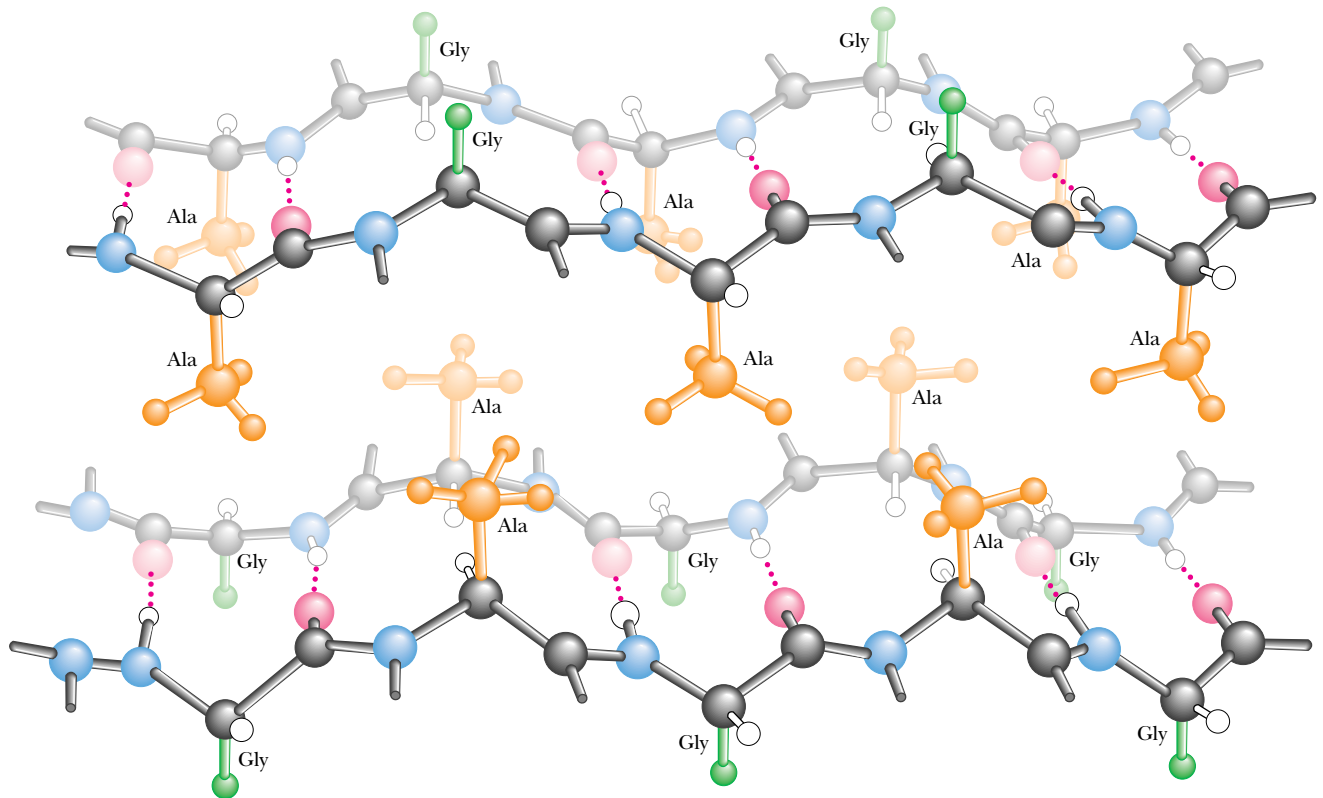
FIGURE 6.15 • Silk fibroin consists of a unique stacked array of β-sheets. The primary structure of fibroin molecules consists of long stretches of alternating glycine and alanine or serine residues. When the sheets stack, the more bulky alanine and serine residues on one side of a sheet interdigitate with similar residues on an adjoining sheet. Glycine hydrogens on the alternating faces interdigitate in a similar manner, but with a smaller intersheet spacing. *(Irving Geis)*

tures makes possible the various animal activities such as running and jumping that put severe stresses on joints and skeleton. Broken bones and tendon and cartilage injuries to knees, elbows, and other joints involve tears or hyperextensions of the collagen matrix in these tissues.

The basic structural unit of collagen is **tropocollagen,** which has a molecular weight of 285,000 and consists of three intertwined polypeptide chains, each about 1000 amino acids in length. Tropocollagen molecules are about 300 nm long and only about 1.4 nm in diameter. Several kinds of collagen have been identified. *Type I collagen,* which is the most common, consists of two identical peptide chains designated $\alpha 1(I)$ and one different chain designated $\alpha 2(I)$. Type I collagen predominates in bones, tendons, and skin. *Type II collagen,* found in cartilage, and *type III collagen,* found in blood vessels, consist of three identical polypeptide chains.

Collagen has an amino acid composition that is unique and is crucial to its three-dimensional structure and its characteristic physical properties. Nearly one residue out of three is a glycine, and the proline content is also unusually high. Three unusual modified amino acids are also found in collagen: 4-hydroxyproline (Hyp), 3-hydroxyproline, and 5-hydroxylysine (Hyl) (Figure 6.16). Proline and Hyp together compose up to 30% of the residues of collagen. Interestingly, these three amino acids are formed from normal proline and lysine *after* the collagen polypeptides are synthesized. The modifications are

A D E E P E R   L O O K

Charlotte's Web Revisited: Helix–Sheet Composites in Spider Dragline Silk

E. B. White's endearing story *Charlotte's Web* centers around the web-spinning feats of Charlotte the spider. Although the intricate designs of spiderwebs are eye- (and fly-) catching, it might be argued that the composition of web silk itself is even more remarkable. Spider silk is synthesized in special glands in the spider's abdomen. The silk strands produced by these glands are both strong and elastic. *Dragline silk* (that from which the spider hangs) has a tensile strength of 200,000 psi (pounds per square inch)—stronger than steel and similar to Kevlar, the synthetic material used in bulletproof vests! This same silk fiber is also flexible enough to withstand strong winds and other natural stresses.

This combination of strength and flexibility derives from the *composite nature* of spider silk. As keratin protein is extruded from the spider's glands, it endures shearing forces that break the H bonds stabilizing keratin α-helices. These regions then form microcrystalline arrays of β-sheets. These microcrystals are surrounded by the keratin strands, which adopt a highly disordered state composed of α-helices and random coil structures.

The β-sheet microcrystals contribute strength, and the disordered array of helix and coil make the silk strand flexible. The resulting silk strand resembles modern human-engineered composite materials. Certain tennis racquets, for example, consist of fiberglass polymers impregnated with microcrystalline graphite. The fiberglass provides flexibility, and the graphite crystals contribute strength. Modern high technology, for all its sophistication, is merely imitating nature—and Charlotte's web—after all.

(a) Spider web   **(b)** Radial strand

(c) Ordered β-sheets surrounded by disordered α-helices and β-bends.

(d) β-sheets impart strength and α-helices impart flexibility to the strand.

4-Hydroxyprolyl residue (Hyp)   **3-Hydroxyprolyl residue**   **5-Hydroxylysyl residue (Hyl)**
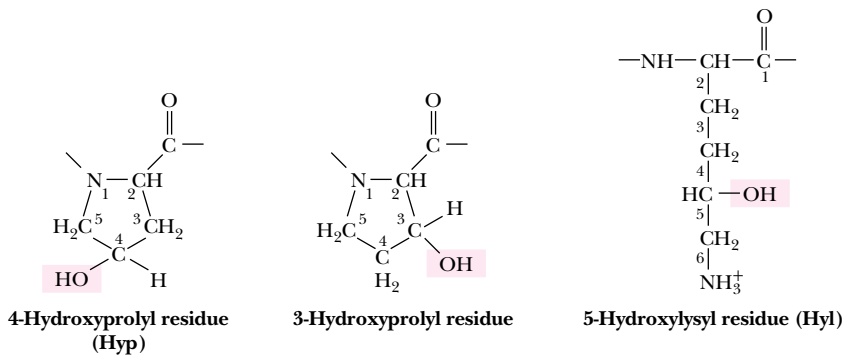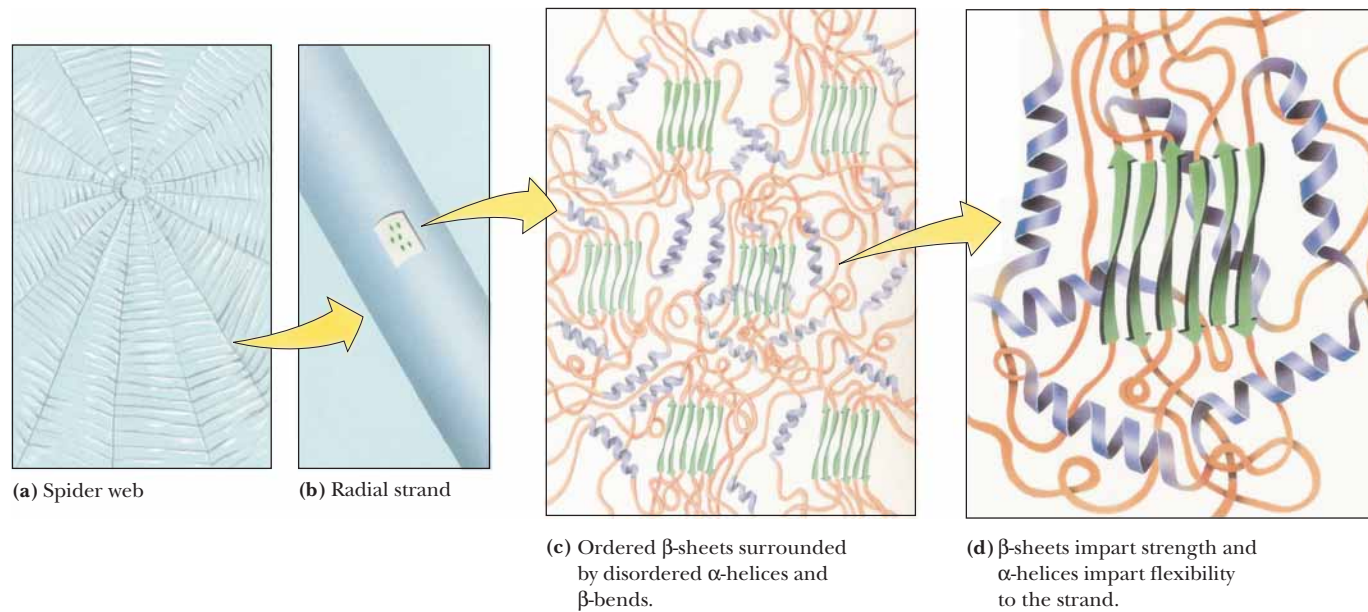
FIGURE 6.16 • The hydroxylated residues typically found in collagen.
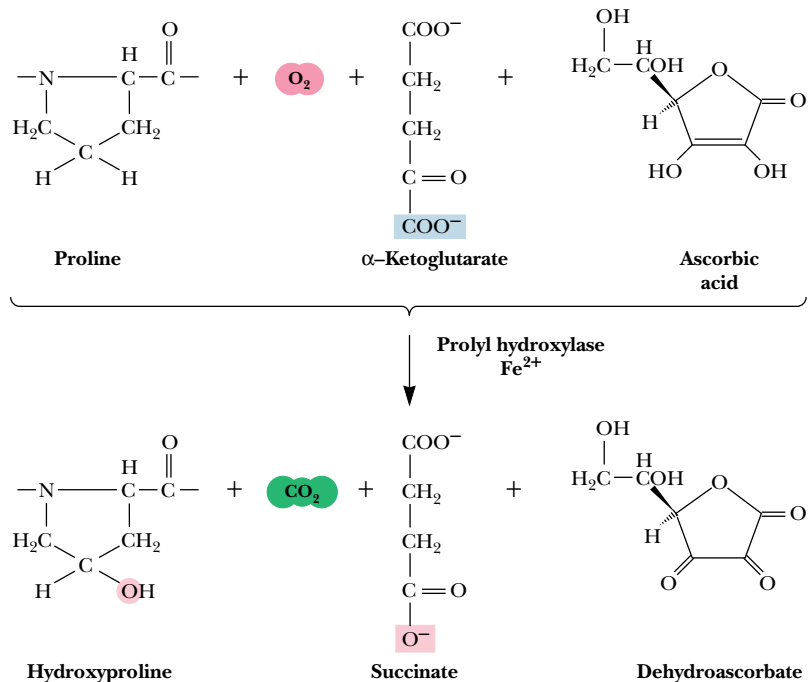
FIGURE 6.17 • Hydroxylation of proline residues is catalyzed by prolyl hydroxylase. The reaction requires α-ketoglutarate and ascorbic acid (vitamin C).
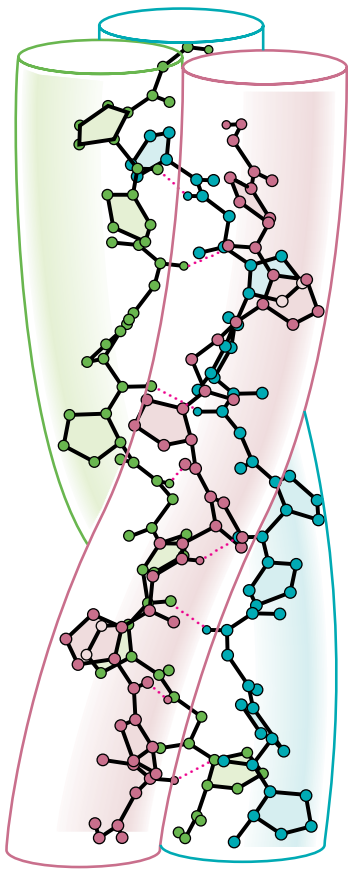
FIGURE 6.18 • Poly(Gly-Pro-Pro), a collagen-like right-handed triple helix composed of three left-handed helical chains. *(Adapted from Miller, M. H., and Scheraga, H. A., 1976, Calculation of the structures of collagen models. Role of interchain interactions in determining the triple-helical coiled-coil conformation. I. Poly(gly-cyl-prolyl-prolyl). Journal of Polymer Science Symposium 54:171–200.)*

effected by two enzymes: *prolyl hydroxylase* and *lysyl hydroxylase*. The prolyl hydroxylase reaction (Figure 6.17) requires molecular oxygen, α-ketoglutarate, and ascorbic acid (vitamin C) and is activated by Fe^{2+}. The hydroxylation of lysine is similar. These processes are referred to as **posttranslational modifications** because they occur after genetic information from DNA has been *translated* into newly formed protein.

Because of their high content of glycine, proline, and hydroxyproline, collagen fibers are incapable of forming traditional structures such as α-helices and β-sheets. Instead, collagen polypeptides intertwine to form a unique **triple helix,** with each of the three strands arranged in a helical fashion (Figure 6.18). Compared to the α-helix, the collagen helix is much more extended, with a rise per residue along the triple helix axis of 2.9 Å, compared to 1.5 Å for the α-helix. There are about 3.3 residues per turn of each of these helices. *The triple helix is a structure that forms to accommodate the unique composition and sequence of collagen.* Long stretches of the polypeptide sequence are repeats of a Gly-x-y motif, where x is frequently Pro and y is frequently Pro or Hyp. In the triple helix, every third residue faces or contacts the crowded center of the structure. This area is so crowded that only Gly can fit, and thus every third residue must be a Gly (as observed). Moreover, the triple helix is a *staggered* structure, such that Gly residues from the three strands stack along the center of the triple helix and the Gly from one strand lies adjacent to an x residue from the second strand and to a y from the third. This allows the N—H of each Gly residue to hydrogen bond with the C=O of the adjacent x residue. The triple helix structure is further stabilized and strengthened by the formation of interchain H bonds involving hydroxyproline.

Collagen types I, II, and III form strong, organized **fibrils,** consisting of staggered arrays of tropocollagen molecules (Figure 6.19). The periodic
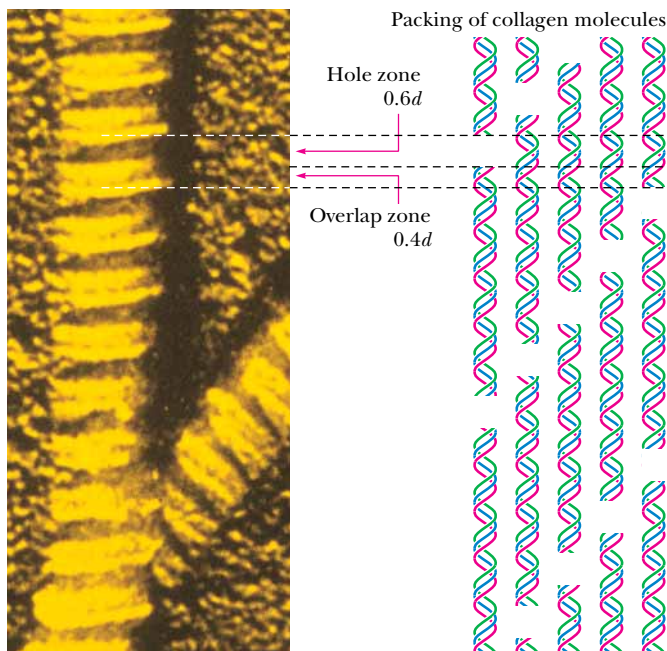
FIGURE 6.19 • In the electron microscope, collagen fibers exhibit alternating light and dark bands. The dark bands correspond to the 40-nm gaps or "holes" between pairs of aligned collagen triple helices. The repeat distance, *d,* for the light- and dark-banded pattern is 68 nm. The collagen molecule is 300 nm long, which corresponds to 4.41*d.* The molecular repeat pattern of five staggered collagen molecules corresponds to 5*d.* *(J. Gross, Biozentrum/Science Photo Library)*

arrangement of triple helices in a head-to-tail fashion results in banded patterns in electron micrographs. The banding pattern typically has a periodicity (repeat distance) of 68 nm. Because collagen triple helices are 300 nm long, 40-nm gaps occur between adjacent collagen molecules in a row along the long axis of the fibrils and the pattern repeats every five rows (5 × 68 nm = 340 nm). The 40-nm gaps are referred to as *hole regions,* and they are important in at least two ways. First, sugars are found covalently attached to 5-hydroxylysine residues in the hole regions of collagen (Figure 6.20). The occurrence of carbohydrate in the hole region has led to the proposal that it plays a role in organizing fibril assembly. Second, the hole regions may play a role in bone formation. Bone consists of microcrystals of **hydroxyapatite,** $Ca_5(PO_4)_3OH$, embedded in a matrix of collagen fibrils. When new bone tissue forms, the formation of new hydroxyapatite crystals occurs at intervals of 68 nm. The hole regions of collagen fibrils may be the sites of nucleation for the mineralization of bone.

The collagen fibrils are further strengthened and stabilized by the formation of both *intramolecular* (within a tropocollagen molecule) and *intermolecular* (between tropocollagen molecules in the fibril) cross-links. Intramolecular cross-links are formed between lysine residues in the (nonhelical) N-terminal region of tropocollagen in a unique pair of reactions shown in Figure 6.21. The enzyme *lysyl oxidase* catalyzes the formation of aldehyde groups at the lysine side chains in a copper-dependent reaction. The aldehyde groups of two such side chains then link covalently in a spontaneous nonenzymatic *aldol condensation.* The intermolecular cross-linking of tropocollagens involves the formation of a unique **hydroxypyridinium** structure from one lysine and two hydroxy-
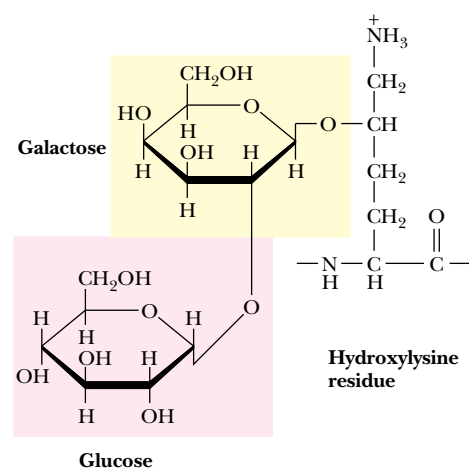
FIGURE 6.20 • A disaccharide of galactose and glucose is covalently linked to the 5-hydroxyl group of hydroxylysines in collagen by the combined action of the enzymes galactosyl transferase and glucosyl transferase.

$\mathcal{H}$UMAN BIOCHEMISTRY

Collagen-Related Diseases

Collagen provides an ideal case study of the molecular basis of physiology and disease. For example, the nature and extent of collagen cross-linking depends on the age and function of the tissue. Collagen from young animals is predominantly un-cross-linked and can be extracted in soluble form, whereas collagen from older animals is highly cross-linked and thus insoluble. The loss of flexibility of joints with aging is probably due in part to increased cross-linking of collagen.

Several serious and debilitating diseases involving collagen abnormalities are known. **Lathyrism** occurs in animals due to the regular consumption of seeds of *Lathyrus odoratus,* the sweet pea, and involves weakening and abnormalities in blood vessels, joints, and bones. These conditions are caused by **β-amino-propionitrile** (see figure), which covalently inactivates lysyl oxi-dase and leads to greatly reduced intramolecular cross-linking of collagen in affected animals (or humans).

$$N \equiv C - CH_2 - CH_2 - \overset{+}{N}H_3$$
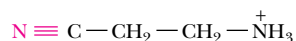
β-Aminopropionitrile (present in sweet peas) covalently inactivates lysyl oxidase, preventing intramolecular cross-linking of collagen and causing abnormalities in joints, bones, and blood vessels.

Scurvy results from a dietary vitamin C deficiency and involves the inability to form collagen fibrils properly. This is the result of reduced activity of prolyl hydroxylase, which is vitamin C–dependent, as previously noted. Scurvy leads to lesions in the skin and blood vessels, and, in its advanced stages, it can lead to grotesque disfiguration and eventual death. Although rare in the modern world, it was a disease well known to sea-faring explorers in earlier times who did not appreciate the importance of fresh fruits and vegetables in the diet.

A number of rare genetic diseases involve collagen abnormalities, including *Marfan's syndrome* and the *Ehlers–Danlos syndromes,* which result in hyperextensible joints and skin. The formation of *atherosclerotic plaques,* which cause arterial blockages in advanced stages, is due in part to the abnormal formation of collagenous structures in blood vessels.
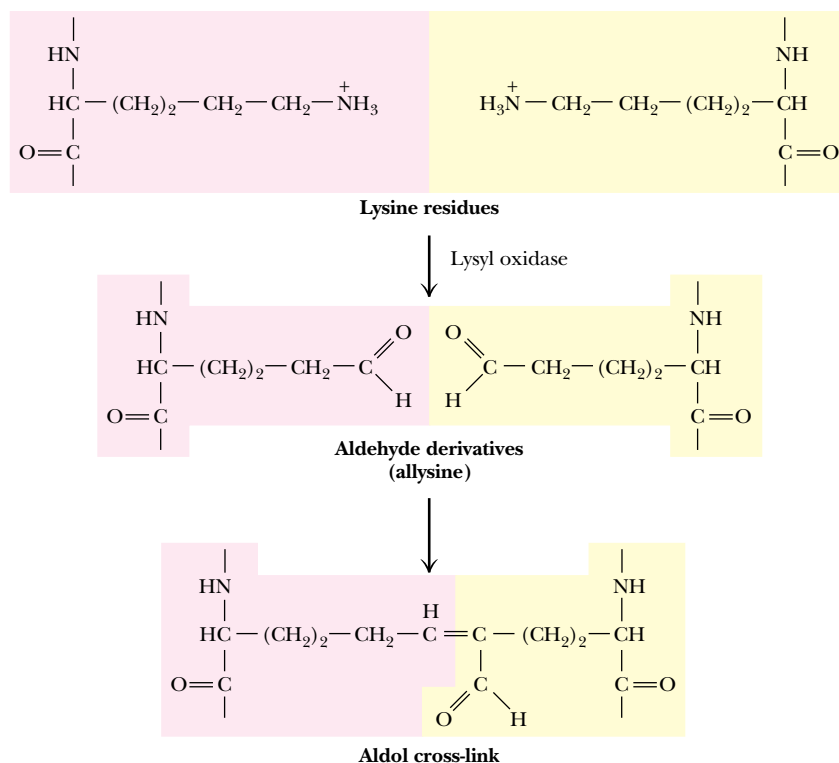
FIGURE 6.21 • Collagen fibers are stabilized and strengthened by Lys–Lys cross-links. Aldehyde moieties formed by lysyl oxidase react in a spontaneous nonenzymatic aldol reaction.

lysine residues (Figure 6.22). These cross-links form between the N-terminal region of one tropocollagen and the C-terminal region of an adjacent tropocollagen in the fibril.

Globular Proteins

Fibrous proteins, although interesting for their structural properties, represent only a small percentage of the proteins found in nature. **Globular proteins,** so named for their approximately spherical shape, are far more numerous.

Helices and Sheets in Globular Proteins

Globular proteins exist in an enormous variety of three-dimensional structures, but nearly all contain substantial amounts of the α-helices and β-sheets that form the basic structures of the simple fibrous proteins. For example, myoglobin, a small, globular, oxygen-carrying protein of muscle (17 kD, 153 amino acid residues), contains eight α-helical segments, each containing 7 to 26 amino acid residues. These are arranged in an apparently irregular (but invariant) fashion (see Figure 5.7). The space between the helices is filled efficiently and tightly with (mostly hydrophobic) amino acid side chains. Most of the polar side chains in myoglobin (and in most other globular proteins) face the outside of the protein structure and interact with solvent water. Myoglobin's structure is unusual because most globular proteins contain a relatively small amount of α-helix. A more typical globular protein (Figure 6.23) is *bovine ribonuclease* A, a small protein (14.6 kD, 129 residues) that contains a few short helices, a broad section of antiparallel β-sheet, a few β-turns, and several peptide segments without defined secondary structure.
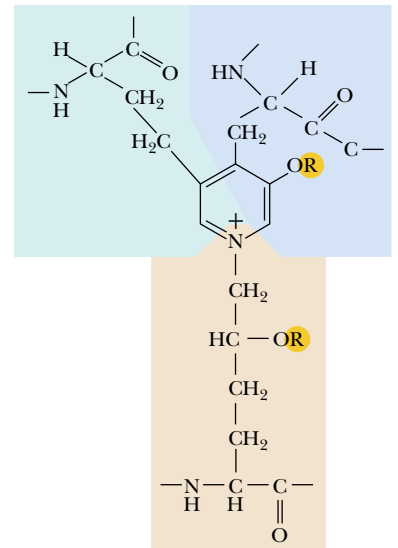
FIGURE 6.22 • The hydroxypyridinium structure formed by the cross-linking of a Lys and two hydroxy Lys residues.

(a)   (b)
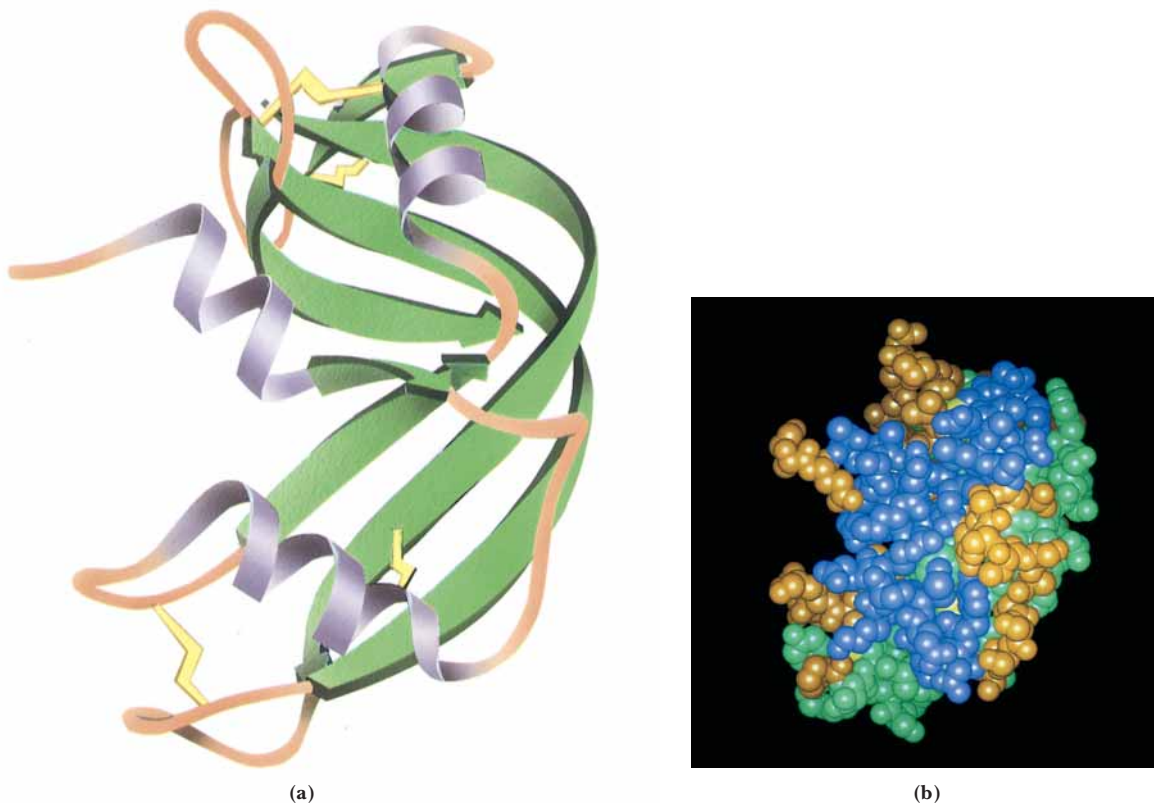
FIGURE 6.23 • The three-dimensional structure of bovine ribonuclease A, showing the α-helices as ribbons. *(Jane Richardson)*
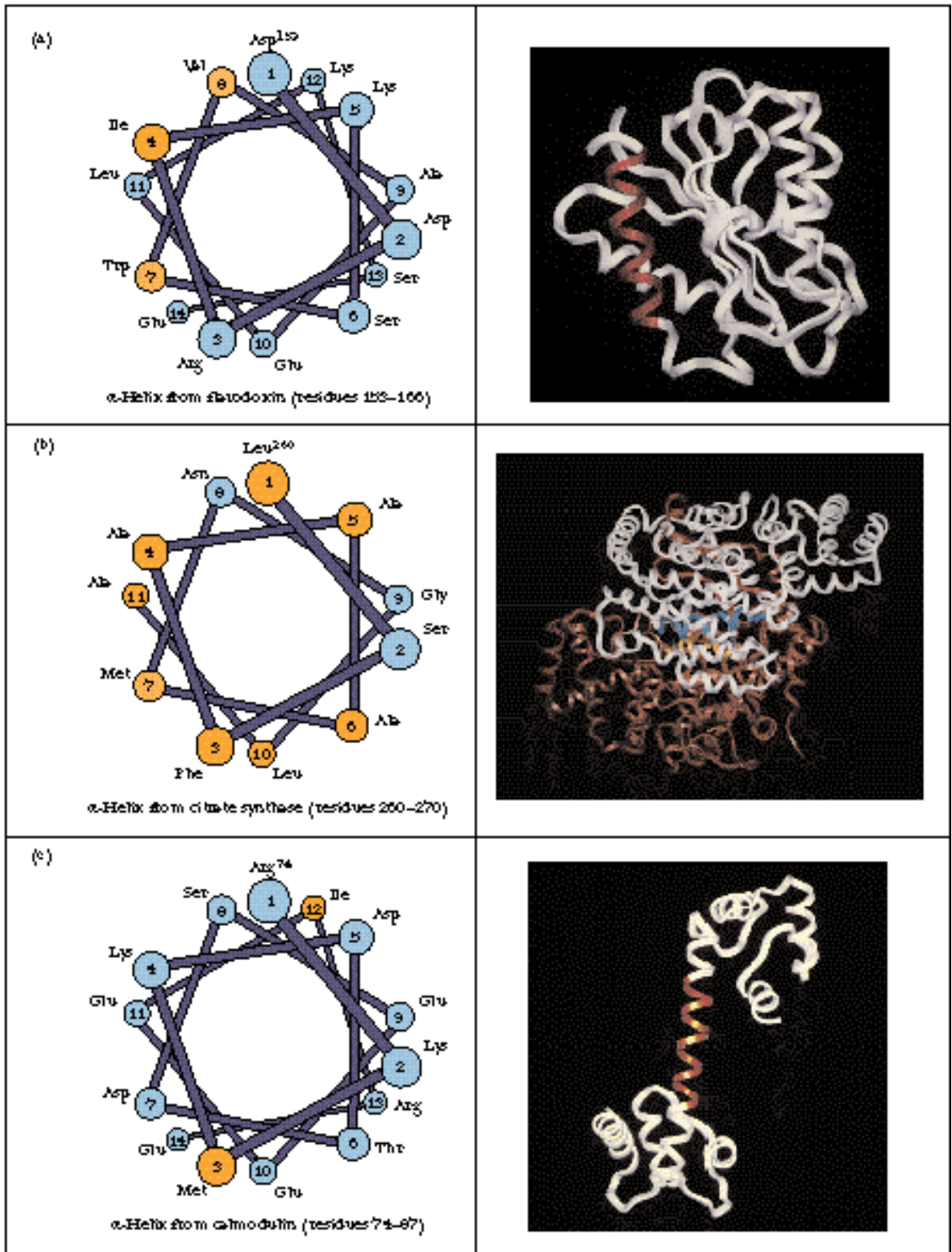
FIGURE 6.24 • (a) The alpha helix consisting of residues 153–166 (red) in flavodoxin from *Anabaena* is a surface helix and is amphipathic. (b) The two helices (yellow and blue) in the interior of the citrate synthase dimer (residues 260–270 in each monomer) are mostly hydrophobic. (c) The exposed helix (residues 74–87—red) of calmodulin is entirely accessible to solvent and consists mainly of polar and charged residues.

Why should the cores of most globular and membrane proteins consist almost entirely of α-helices and β-sheets? The reason is that the highly polar N—H and C=O moieties of the peptide backbone must be neutralized in the hydrophobic core of the protein. The extensively H-bonded nature of α-helices and β-sheets is ideal for this purpose, and these structures effectively stabilize the polar groups of the peptide backbone in the protein core.

In globular protein structures, it is common for one face of an α-helix to be exposed to the water solvent, with the other face toward the hydrophobic interior of the protein. The outward face of such an **amphiphilic helix** consists mainly of polar and charged residues, whereas the inward face contains mostly nonpolar, hydrophobic residues. A good example of such a surface helix is that of residues 153 to 166 of **flavodoxin** from *Anabaena* (Figure 6.24). Note that the **helical wheel presentation** of this helix readily shows that one face contains four hydrophobic residues and that the other is almost entirely polar and charged.

Less commonly, an α-helix can be completely buried in the protein interior or completely exposed to solvent. **Citrate synthase** is a dimeric protein in which α-helical segments form part of the subunit–subunit interface. As shown in Figure 6.24, one of these helices (residues 260 to 270) is highly hydrophobic and contains only two polar residues, as would befit a helix in the protein core. On the other hand, Figure 6.24 also shows the solvent-exposed helix (residues 74 to 87) of **calmodulin,** which consists of 10 charged residues, 2 polar residues, and only 2 nonpolar residues.

Packing Considerations

The secondary and tertiary structures of myoglobin and ribonuclease A illustrate the importance of packing in tertiary structures. Secondary structures pack closely to one another and also intercalate with (insert between) extended polypeptide chains. If the sum of the van der Waals volumes of a protein's constituent amino acids is divided by the volume occupied by the protein, packing densities of 0.72 to 0.77 are typically obtained. This means that, even with close packing, approximately 25% of the total volume of a protein is not occupied by protein atoms. Nearly all of this space is in the form of very small cavities. Cavities the size of water molecules or larger do occasionally occur, but they make up only a small fraction of the total protein volume. It is likely that such cavities provide flexibility for proteins and facilitate conformation changes and a wide range of protein dynamics (discussed later).

Ordered, Nonrepetitive Structures

In any protein structure, the segments of the polypeptide chain that cannot be classified as defined secondary structures, such as helices or sheets, have been traditionally referred to as *coil* or *random coil*. Both these terms are misleading. Most of these segments are neither coiled nor random, in any sense of the words. These structures are every bit as highly organized and stable as the defined secondary structures. They are just more variable and difficult to describe. These so-called coil structures are strongly influenced by side-chain interactions. Few of these interactions are well understood, but a number of interesting cases have been described. In his early studies of myoglobin structure, John Kendrew found that the —OH group of threonine or serine often forms a hydrogen bond with a backbone NH at the beginning of an α-helix. The same stabilization of an α-helix by a serine is observed in the three-dimensional structure of pancreatic trypsin inhibitor (Figure 6.25). Also in this same structure, an asparagine residue adjacent to a β-strand is found to form H bonds that stabilize the β-structure.

Pancreatic trypsin inhibitor
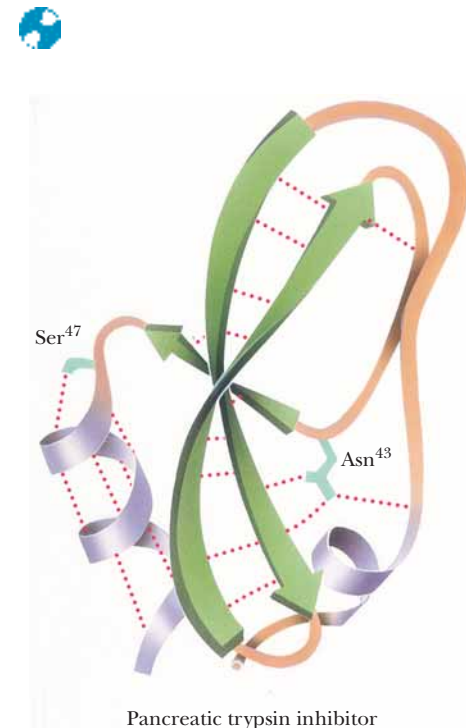
FIGURE 6.25 • The three-dimensional structure of bovine pancreatic trypsin inhibitor. Note the stabilization of the α-helix by a hydrogen bond to Ser[47] and the stabilization of the β-sheet by Asn[43].
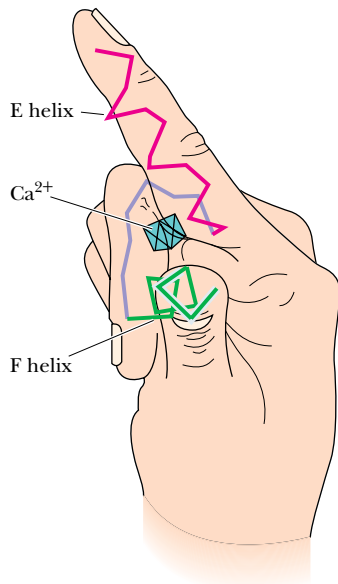
FIGURE 6.26 • A representation of the so-called E–F hand structure, which forms calcium-binding sites in a variety of proteins. The stick drawing shows the peptide backbone of the E–F hand motif. The "E" helix extends along the index finger, a loop traces the approximate arrangement of the curled middle finger, and the "F" helix extends outward along the thumb. A calcium ion (Ca^{2+}) snuggles into the pocket created by the two helices and the loop. Kretsinger and coworkers originally assigned letters alphabetically to the helices in parvalbumin, a protein from carp. The E–F hand derives its name from the letters assigned to the helices at one of the Ca^{2+}-binding sites.

Nonrepetitive but well-defined structures of this type form many important features of enzyme active sites. In some cases, a particular arrangement of "coil" structure providing a specific type of functional site recurs in several functionally related proteins. The peptide loop that binds iron–sulfur clusters in both ferredoxin and high potential iron protein is one example. Another is the central loop portion of the *E–F hand structure* that binds a calcium ion in several calcium-binding proteins, including calmodulin, carp parvalbumin, troponin C, and the intestinal calcium-binding protein. This loop, shown in Figure 6.26, connects two short α-helices. The calcium ion nestles into the pocket formed by this structure.

Flexible, Disordered Segments

In addition to nonrepetitive but well-defined structures, which exist in all proteins, genuinely disordered segments of polypeptide sequence also occur. These sequences either do not show up in electron density maps from X-ray crystallographic studies or give diffuse or ill-defined electron densities. These segments either undergo actual motion in the protein crystals themselves or take on many alternate conformations in different molecules within the protein crystal. Such behavior is quite common for long, charged side chains on the surface of many proteins. For example, 16 of the 19 lysine side chains in myoglobin have uncertain orientations beyond the δ-carbon, and five of these are disordered beyond the β-carbon. Similarly, a majority of the lysine residues are disordered in trypsin, rubredoxin, ribonuclease, and several other proteins. Arginine residues, however, are usually well ordered in protein structures. For the four proteins just mentioned, 70% of the arginine residues are highly ordered, compared to only 26% of the lysines.

Motion in Globular Proteins

Although we have distinguished between well-ordered and disordered segments of the polypeptide chain, it is important to realize that even well-ordered side chains in a protein undergo motion, sometimes quite rapid. These motions should be viewed as momentary oscillations about a single, highly stable conformation. *Proteins are thus best viewed as dynamic structures.* The allowed motions may be motions of individual atoms, groups of atoms, or even whole sections of the protein. Furthermore, they may arise from either thermal energy or specific, triggered conformational changes in the protein. **Atomic fluctuations** such as vibrations typically are random, very fast, and usually occur over small distances (less than 0.5 Å), as shown in Table 6.2. These motions arise from the kinetic energy within the protein and are a function of temperature. These very fast motions can be modeled by molecular dynamics calculations and studied by X-ray diffraction.

A class of slower motions, which may extend over larger distances, is **collective motions.** These are movements of groups of atoms covalently linked in such a way that the group moves as a unit. Such groups range in size from a few atoms to hundreds of atoms. Whole structural domains within a protein may be involved, as in the case of the flexible antigen-binding domains of immunoglobulins, which move as relatively rigid units to selectively bind separate antigen molecules. Such motions are of two types—(1) those that occur quickly but infrequently, such as tyrosine ring flips, and (2) those that occur slowly, such as *cis-trans* isomerizations of prolines. These collective motions also arise from thermal energies in the protein and operate on a time scale of 10^{-12} to 10^{-3} sec. These motions can be studied by nuclear magnetic resonance (NMR) and fluorescence spectroscopy.

Table 6.2

Motion and Fluctuations in Proteins			
Type of Motion	Spatial Displacement (Å)	Characteristic Time (sec)	Source of Energy
Atomic vibrations	0.01–1	10^{-15}–10^{-11}	Kinetic energy
Collective motions	0.01–5 or more	10^{-12}–10^{-3}	Kinetic energy
1. Fast: Tyr ring flips; methyl group rotations 2. Slow: hinge bending between domains			
Triggered conformation changes	0.5–10 or more	10^{-9}–10^{3}	Interactions with triggering agent

Adapted from Petsko and Ringe (1984).

Conformational changes involve motions of groups of atoms (individual side chains, for example) or even whole sections of proteins. These motions occur on a time scale of 10^{-9} to 10^{3} sec, and the distances covered can be as large as 1 nm. These motions may occur in response to specific stimuli or arise from specific interactions within the protein, such as hydrogen bonding, electrostatic interactions, and ligand binding. More will be said about conformational changes when enzyme catalysis and regulation are discussed (see Chapters 14 and 15).

Forces Driving the Folding of Globular Proteins

As already pointed out, the driving force for protein folding and the resulting formation of a tertiary structure is the formation of the most stable structure possible. Two forces are at work here. The peptide chain must both (1) satisfy the constraints inherent in its own structure and (2) fold so as to "bury" the hydrophobic side chains, minimizing their contact with solvent. The polypeptide itself does not usually form simple straight chains. Even in chain segments where helices and sheets are not formed, an extended peptide chain, being composed of L-amino acids, has a tendency to twist slightly in a right-handed direction. As shown in Figure 6.27, this tendency is apparently the basis for the formation of a variety of tertiary structures having a right-handed sense. Principal among these are the right-handed twists in arrays of β-sheets and right-handed cross-overs in parallel β-sheet arrays. Right-handed twisted β-sheets are found at the center of a number of proteins and provide an extended, highly stable structural core. Phosphoglycerate mutase, adenylate kinase, and carbonic anhydrase, among others, exist as smoothly twisted planes or saddle-shaped structures. Triose phosphate isomerase, soybean trypsin inhibitor, and domain 1 of pyruvate kinase contain right-handed twisted cylinders or barrel structures at their cores.

Connections between β-strands are of two types—hairpins and cross-overs. **Hairpins,** as shown in Figure 6.27, connect adjacent antiparallel β-strands. **Cross-overs** are necessary to connect adjacent (or nearly adjacent) parallel β-strands. Nearly all cross-over structures are right-handed. Only in subtilisin and phosphoglucoisomerase have isolated left-handed cross-overs been identi-

Antiparallel

Natural right-handed twist by polypeptide chain

Parallel, right-handed

Parallel, left-handed
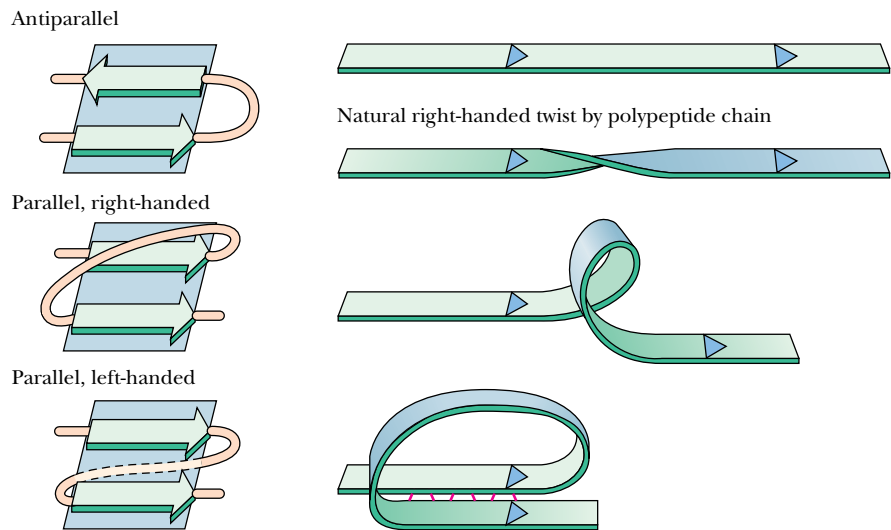
FIGURE 6.27 • The natural right-handed twist exhibited by polypeptide chains, and the variety of structures that arise from this twist.

fied. In many cross-over structures, the cross-over connection itself contains an α-helical segment. This is referred to as a **βαβ-loop.** As shown in Figure 6.27, the strong tendency in nature to form right-handed cross-overs, the wide occurrence of α-helices in the cross-over connection, and the right-handed twists of β-sheets can all be understood as arising from the tendency of an extended polypeptide chain of L-amino acids to adopt a right-handed twist structure. This is a chiral effect. Proteins composed of D-amino acids would tend to adopt left-handed twist structures.

The second driving force that affects the folding of polypeptide chains is the need to bury the hydrophobic residues of the chain, protecting them from solvent water. From a topological viewpoint, then, all globular proteins must have an "inside" where the hydrophobic core can be arranged and an "outside" toward which the hydrophilic groups must be directed. The sequestration of hydrophobic residues away from water is the dominant force in the arrangement of secondary structures and nonrepetitive peptide segments to form a given tertiary structure. Globular proteins can be classified mainly on the basis of the particular kind of core or backbone structure they use to accomplish this goal. The term *hydrophobic core,* as used here, refers to a region in which hydrophobic side chains cluster together, away from the solvent. *Backbone* refers to the polypeptide backbone itself, excluding the particular side chains. Globular proteins can be pictured as consisting of "layers" of backbone, with hydrophobic core regions between them. Over half the known globular protein structures have two layers of backbone (separated by one hydrophobic core). Roughly one-third of the known structures are composed of three backbone layers and two hydrophobic cores. There are also a few known four-layer structures and one known five-layer structure. A few structures are not easily classified in this way, but it is remarkable that most proteins fit into one of these classes. Examples of each are presented in Figure 6.28.

Classification of Globular Proteins

In addition to classification based on layer structure, proteins can be grouped according to the type and arrangement of secondary structure. There are four such broad groups: antiparallel α-helix, parallel or mixed β-sheet, antiparallel β-sheet, and the small metal- and disulfide-rich proteins.

Layer 1   Layer 2

Hydrophobic residues are
buried between layers

(a) Cytochrome c′

(b) Phosphoglycerate kinase
(Domain 2)

(c) Phosphorylase
(Domain 2)

FIGURE 6.28 • Examples of protein domains with different numbers of layers of backbone
structure. (a) Cytochrome c′ with two layers of α-helix. (b) Domain 2 of phosphoglycerate
kinase, composed of a β-sheet layer between two layers of helix, three layers overall. (c) An
unusual five-layer structure, domain 2 of glycogen phosphorylase, a β-sheet layer sandwiched
between four layers of α-helix. (d) The concentric "layers" of β-sheet (*inside*) and α-helix (*out-side*) in triose phosphate isomerase. Hydrophobic residues are buried between these concentric
layers in the same manner as in the planar layers of the other proteins. The hydrophobic layers
are shaded yellow. (*Jane Richardson*)

(d) Triose phosphate isomerase

It is important to note that the similarities of tertiary structure within these
groups do not necessarily reflect similar or even related functions. Instead,
functional homology usually depends on structural similarities on a smaller and
more intimate scale.

Antiparallel α-Helix Proteins

Antiparallel α-helix proteins are structures heavily dominated by α-helices. The
simplest way to pack helices is in an antiparallel manner, and most of the pro-
teins in this class consist of bundles of antiparallel helices. Many of these exhibit
a slight (15°) left-handed twist of the helix bundle. Figure 6.29 shows a repre-
sentative sample of antiparallel α-helix proteins. Many of these are regular, uni-
form structures, but in a few cases (uteroglobin, for example) one of the helices
is tilted away from the bundle. Tobacco mosaic virus protein has small, highly

Myohemerythrin

TMV protein

Influenza virus hemagglutinin HA2

Uteroglobin

Myohemerythrin

Uteroglobin
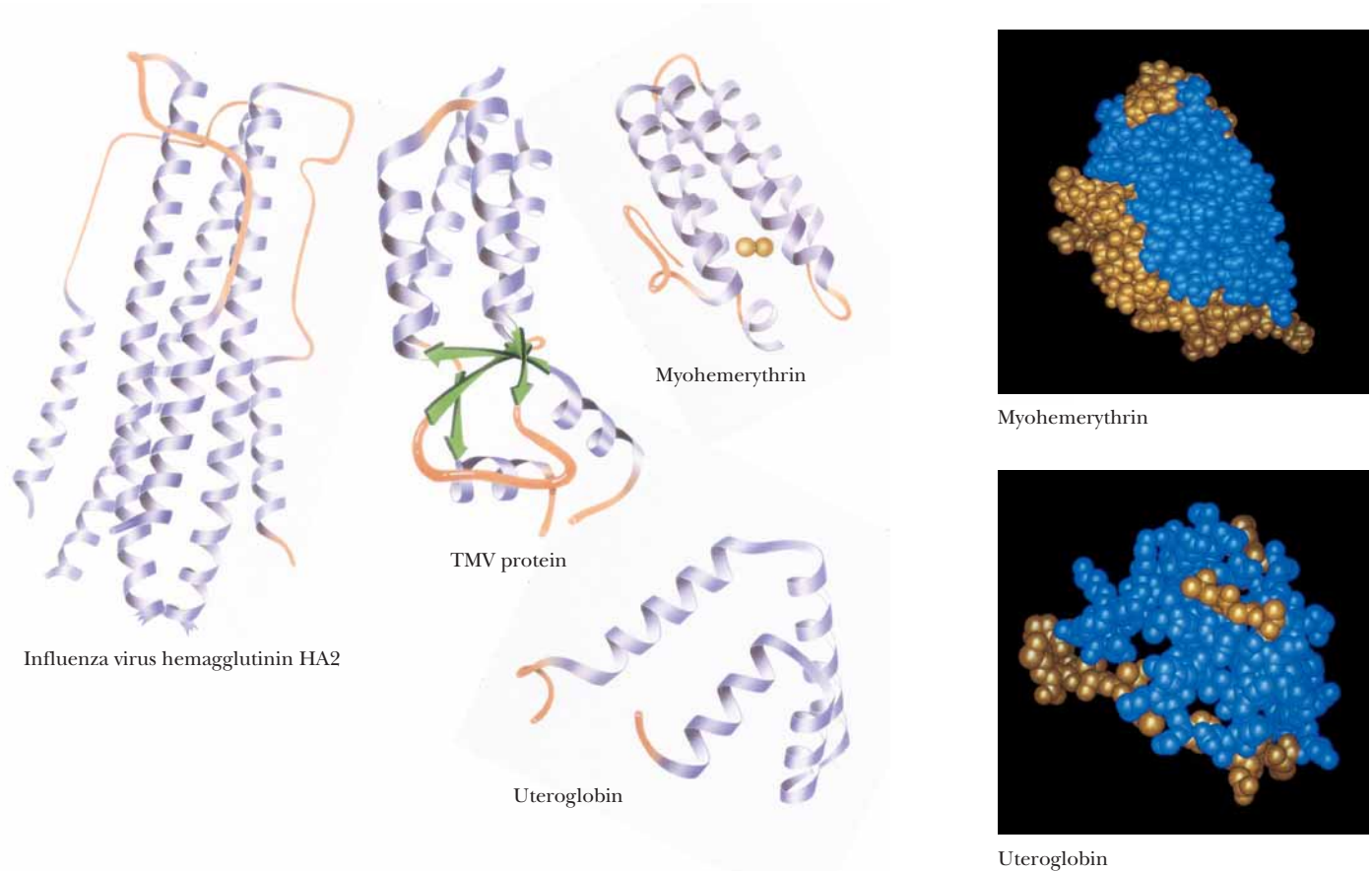
FIGURE 6.29 • Several examples of antiparallel α-proteins. *(Jane Richardson)*

twisted antiparallel β-sheets on one end of the helix bundle with two additional helices on the other side of the sheet. Notice in Figure 6.29 that most of the antiparallel α-helix proteins are made up of four-helix bundles.

The so-called globin proteins are an important group of α-helical proteins. These include hemoglobins and myoglobins from many species. The globin structure can be viewed as two layers of helices, with one of these layers perpendicular to the other and the polypeptide chain moving back and forth between the layers.

Parallel or Mixed β-Sheet Proteins

The second major class of protein structures contains structures based around **parallel** or **mixed β-sheets.** Parallel β-sheet arrays, as previously discussed, distribute hydrophobic side chains on both sides of the sheet. This means that neither side of parallel β-sheets can be exposed to solvent. Parallel β-sheets are thus typically found as core structures in proteins, with little access to solvent.

Another important parallel β-array is the eight-stranded **parallel β-barrel,** exemplified in the structures of triose phosphate isomerase and pyruvate kinase (Figure 6.30). Each β-strand in the barrel is flanked by an antiparallel α-helix. The α-helices thus form a larger cylinder of parallel helices concentric with the β-barrel. Both cylinders thus formed have a right-handed twist. Another parallel β-structure consists of an internal twisted wall of parallel or mixed β-sheet protected on both sides by helices or other substructures. This structure is called the **doubly wound parallel β-sheet** because the structure can be

(a)

Triose phosphate isomerase (side)

(b)

Triose phosphate isomerase (top)

(c)
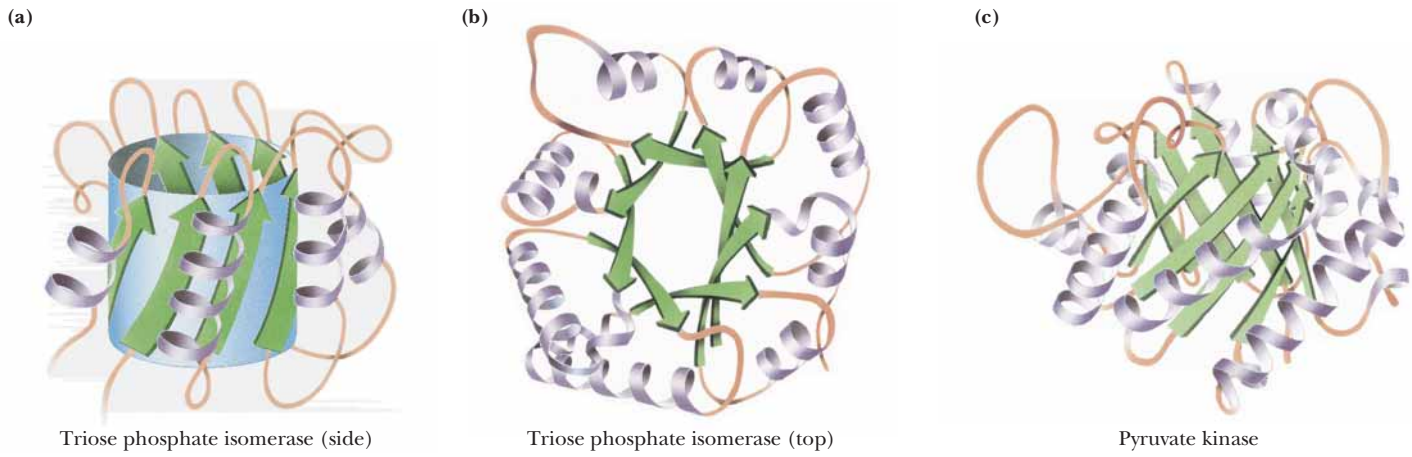
Pyruvate kinase

FIGURE 6.30 • Parallel β-array proteins—the eight-stranded β-barrels of triose phosphate isomerase (a, *side view*, and b, *top view*) and (c) pyruvate kinase. *(Jane Richardson)*

imagined to have been wound by strands beginning in the middle and going outward in opposite directions. The essence of this structure is shown in Figure 6.31. Whereas the barrel structures have four layers of backbone structure, the doubly wound sheet proteins have three major layers and thus two hydrophobic core regions.

Hexokinase domain 1

Flavodoxin

Flavodoxin

Phosphoglycerate mutase

Phosphoglycerate mutase
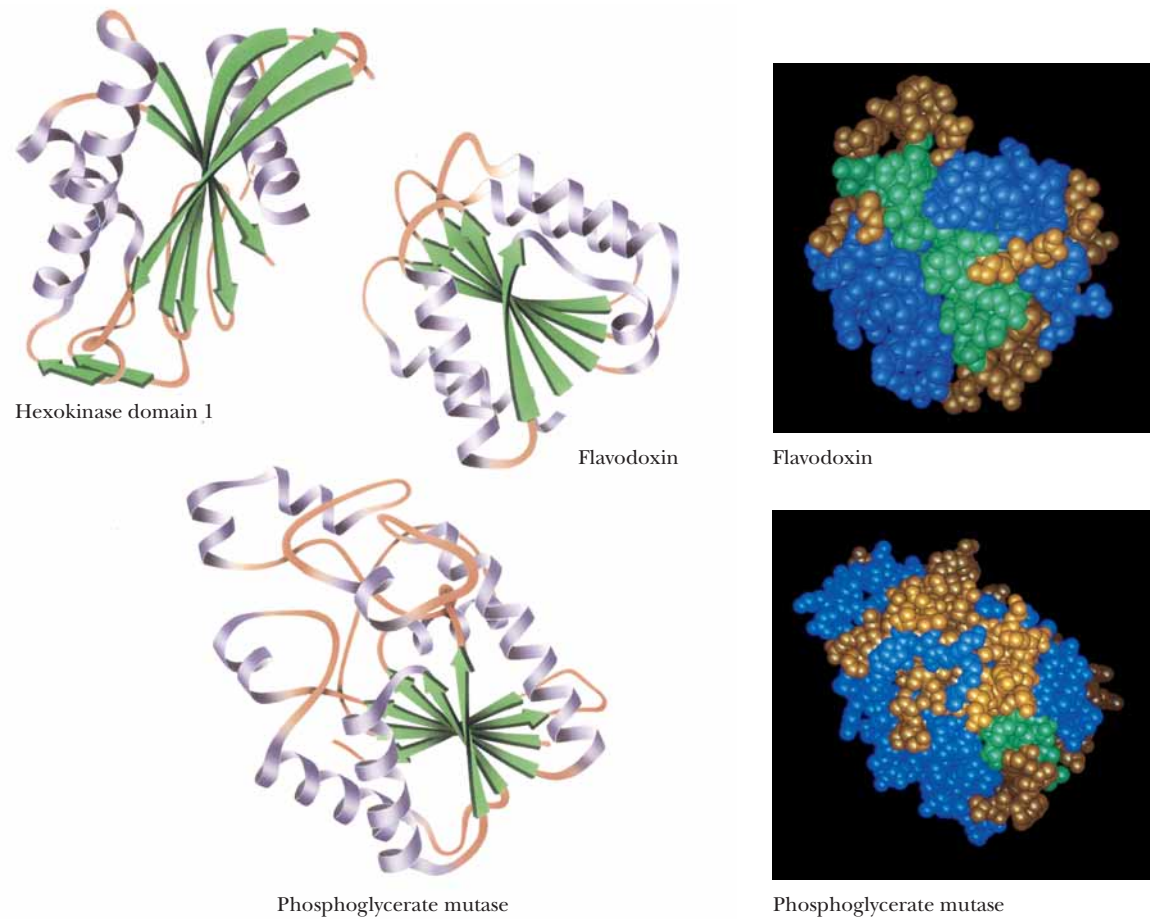
FIGURE 6.31 • Several typical doubly wound parallel β-sheet proteins. *(Jane Richardson)*

The Coiled Coil Motif in Proteins

The **coiled coil** motif was first identified in 1953 by Linus Pauling, Robert Corey, and Francis Crick as the main structural element of fibrous proteins such as keratin and myosin. Since that time, many proteins have been found to contain one or more coiled coil segments or domains. A coiled coil is a bundle of α-helices that are wound into a superhelix. Two, three, or four helical segments may be found in the bundle, and they may be arranged parallel or antiparallel to one another. Coiled coils are characterized by a distinctive and regular packing of side chains in the core of the bundle. This regular meshing of side chains requires that they occupy equivalent positions turn after turn. This is not possible for undistorted α-helices, which have 3.6 residues per turn. The positions of side chains on their surface shift continuously along the helix surface (see figure). However, giving the right-handed α-helix a left-handed twist reduces the number of residues per turn to 3.5, and, because 3.5 times 2 equals 7.0, the positions of the side chains repeat after two turns (seven residues). Thus, a **heptad repeat** pattern in the peptide sequence is diagnostic of a coiled coil structure. The figure shows a sampling of coiled coil structures (highlighted in color) in various proteins.

Pitch
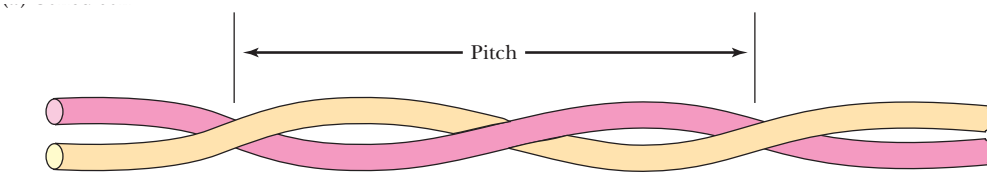
(b) Periodicity of hydrophobic residues

Undistorted   Supercoiled   Left-handed coiled coil

Helices with a heptad repeat
of hydrophobic residues
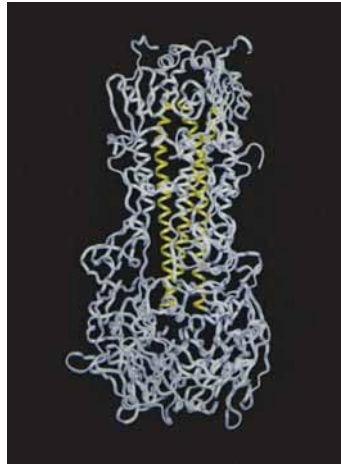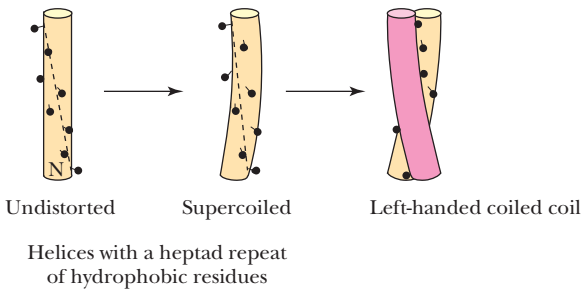
Influenza hemagglutinin
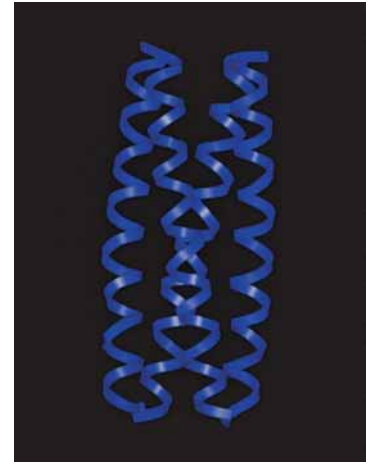
GCN4 leucine/isoleucine mutant
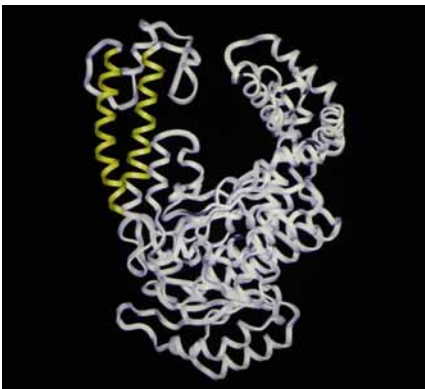
DNA polymerase

Seryl tRNA synthetase
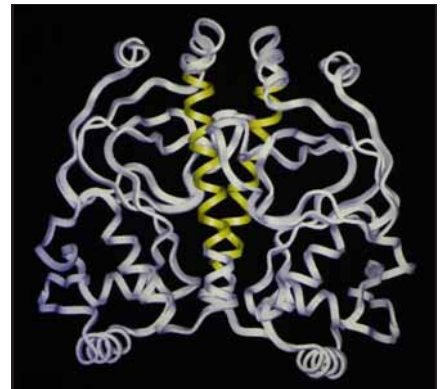
Catabolite activator protein

Antiparallel β-Sheet Proteins

Another important class of tertiary protein conformations is the **antiparallel β-sheet** structures. Antiparallel β-sheets, which usually arrange hydrophobic residues on just one side of the sheet, can exist with one side exposed to solvent. The minimal structure for an antiparallel β-sheet protein is thus a two-layered structure, with hydrophobic faces of the two sheets juxtaposed and the opposite faces exposed to solvent. Such domains consist of β-sheets arranged in a cylinder or barrel shape. These structures are usually less symmetric than the singly wound parallel barrels and are not as efficiently hydrogen bonded, but they occur much more frequently in nature. Barrel structures tend to be either all parallel or all antiparallel and usually consist of even numbers of β-strands. Good examples of antiparallel structures include soybean trypsin inhibitor, rubredoxin, and domain 2 of papain (Figure 6.32). Topology diagrams of antiparallel β-sheet barrels reveal that many of them arrange the polypeptide sequence in an interlocking pattern reminiscent of patterns found on ancient Greek vases (Figure 6.33) and are thus referred to as a *Greek key topology*. Several of these, including concanavalin A and γ-crystallin, contain an extra swirl in the Greek key pattern (see Figure 6.33). Antiparallel arrangements of β-strands can also form sheets as well as barrels. Glyceraldehyde-3-phosphate dehydrogenase, *Streptomyces* subtilisin inhibitor, and glutathione reductase are examples of single-sheet, double-layered topology (Figure 6.34).

Metal- and Disulfide-Rich Proteins

Other than the structural classes just described and a few miscellaneous structures that do not fit nicely into these categories, there is only one other major class of protein tertiary structures—the small metal-rich and disulfide-rich structures. These proteins or fragments of proteins are usually small (<100 residues), and their conformations are heavily influenced by their high content of either liganded metals or disulfide bonds. The structures of disulfide-rich proteins are unstable if their disulfide bonds are broken. Figure 6.35 shows several representative disulfide-rich proteins, including insulin, phospholipase A_2, and crambin (from the seeds of *Crambe abyssinica*), as well as several metal-rich proteins, including ferredoxin and high potential iron protein (HiPIP). The structures of some of these proteins bear a striking resemblance to structural classes that have already been discussed. For example, phospholipase A_2

| Soybean trypsin inhibitor | Rubredoxin | Papain domain 2 | Rubredoxin |
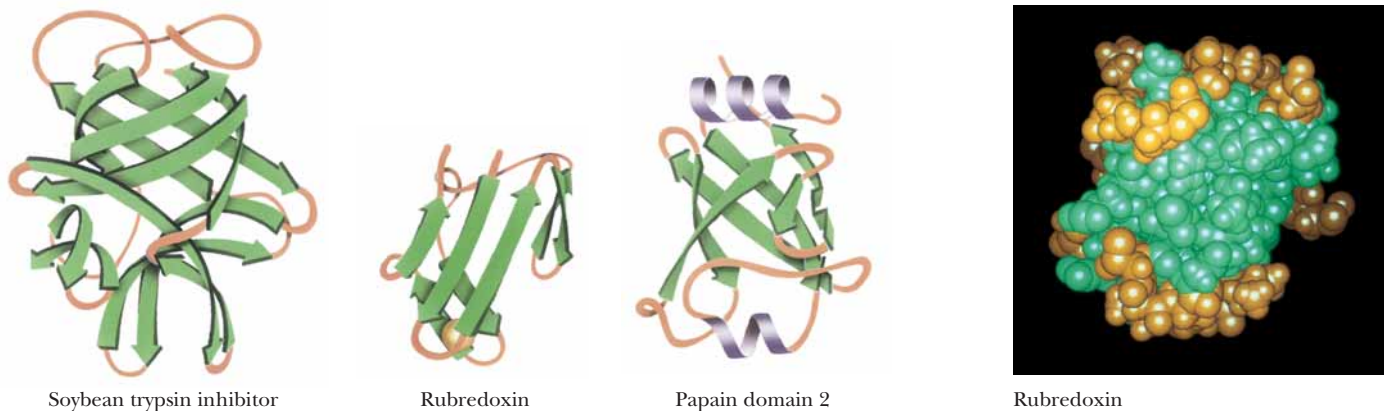
FIGURE 6.32 • Examples of antiparallel β-sheet structures in proteins. *(Jane Richardson)*

FIGURE 6.33 • Examples of the so-called Greek key antiparallel β-barrel structure in proteins.

"Greek key" topology

Concanavalin A

Concanavalin A

γ-Crystallin

γ-Crystallin

Streptomyces subtilisin inhibitor

(a) *Streptomyces* subtilisin inhibitor

(b) Glutathione reductase domain 3

(c) Glyceraldehyde-3-P dehydrogenase domain 2
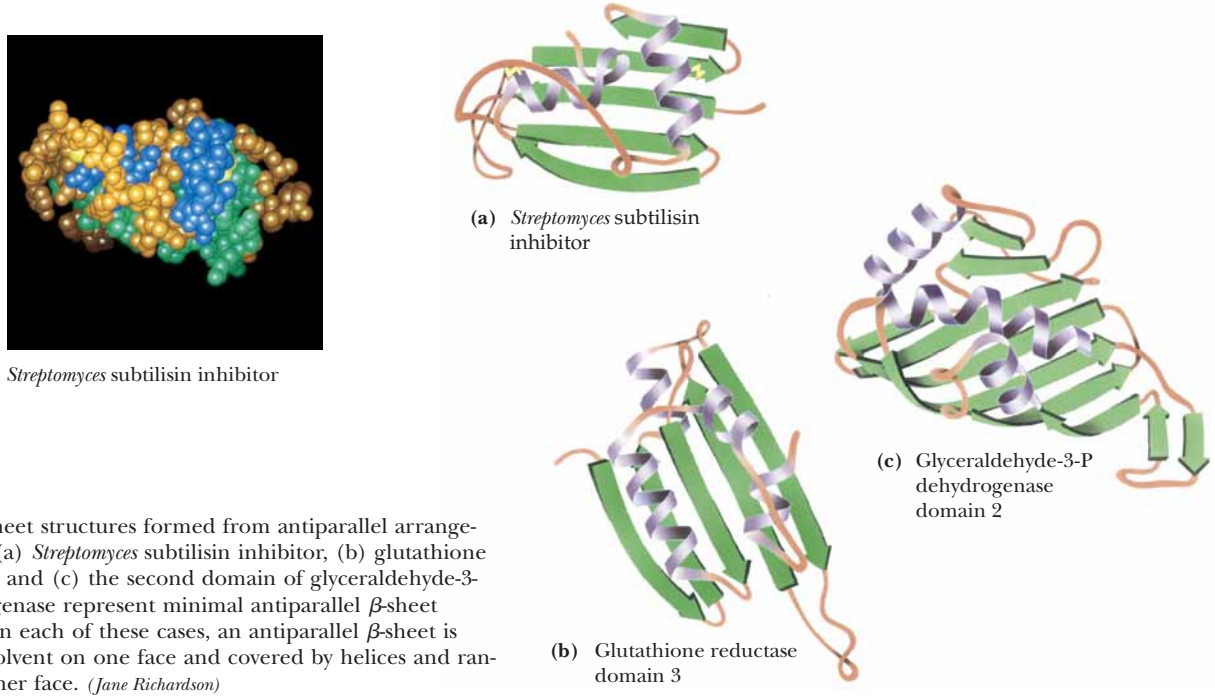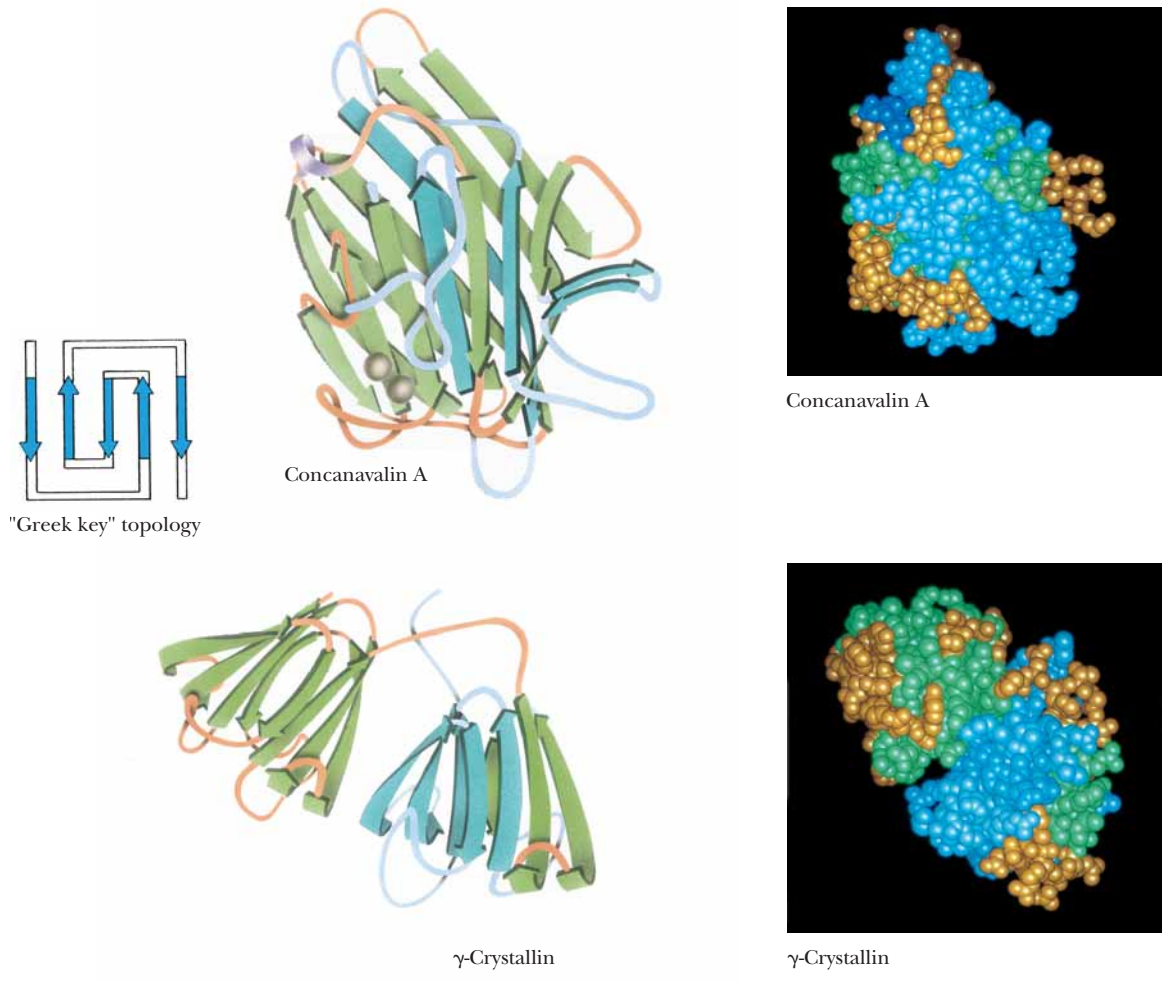
FIGURE 6.34 • Sheet structures formed from antiparallel arrangements of β-strands. (a) *Streptomyces* subtilisin inhibitor, (b) glutathione reductase domain 3, and (c) the second domain of glyceraldehyde-3-phosphate dehydrogenase represent minimal antiparallel β-sheet domain structures. In each of these cases, an antiparallel β-sheet is largely exposed to solvent on one face and covered by helices and random coils on the other face. *(Jane Richardson)*

FIGURE 6.35 • Examples of the (a) disulfide-rich and (b) metal-rich proteins. *(Jane Richardson)*

(a) Disulfide-rich proteins

Insulin   Crambin   Phospholipase A$_2$

(b) Metal-rich proteins

High-potential iron   Ferredoxin
protein
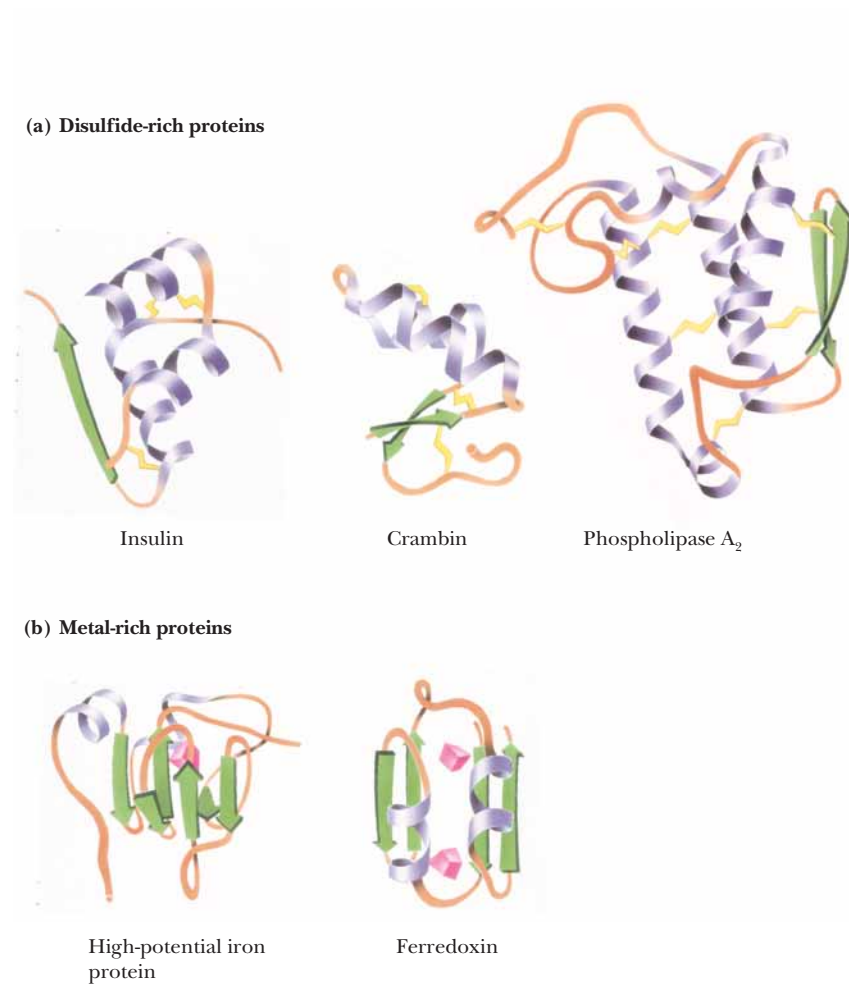
is a distorted α-helix cluster, whereas HiPIP is a distorted β-barrel structure. Others among this class (such as insulin and crambin), however, are not easily likened to any of the standard structure classes.

Molecular Chaperones: Proteins That Help Fold Globular Proteins

The landmark experiments by Christian Anfinsen on the refolding of ribonuclease clearly show that the refolding of a denatured protein *in vitro* can be a spontaneous process. As noted above, this refolding is driven by the small Gibbs free energy difference between the unfolded and folded states. It has also been generally assumed that all the information necessary for the correct folding of a polypeptide chain is contained in the primary structure and requires no additional molecular factors. However, the folding of proteins in the cell is a different matter. The highly concentrated protein matrix in the cell may adversely affect the folding process by causing aggregation of some unfolded or partially folded proteins. Also, it may be necessary to accelerate slow steps in the folding process or to suppress or reverse incorrect or premature folding. Recent studies have uncovered a family of proteins, known as **molecular chaperones,**
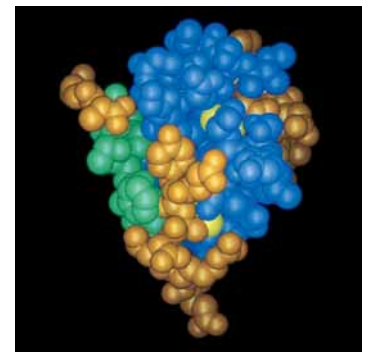
Insulin
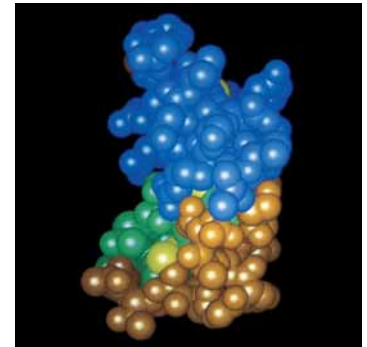
Crambin
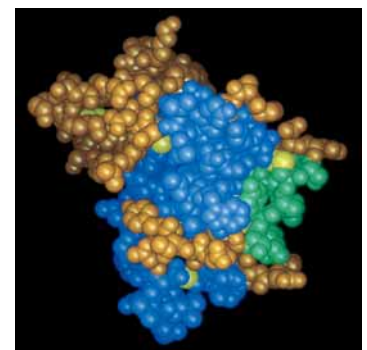
Phospholipase A$_2$

CRITICAL DEVELOPMENTS IN BIOCHEMISTRY

Thermodynamics of the Folding Process in Globular Proteins

Section 6.1 considered the noncovalent binding energies that stabilize a protein structure. However, the folding of a protein depends ultimately on the difference in Gibbs free energy (ΔG) between the folded (F) and unfolded (U) states at some temperature T:

$$\Delta G = G_F - G_U = \Delta H - T\Delta S$$
$$= (H_F - H_U) - T(S_F - S_U)$$

In the unfolded state, the peptide chain and its R groups interact with solvent water, and any measurement of the free energy change upon folding must consider contributions to the enthalpy change (ΔH) and the entropy change (ΔS) both for the polypeptide chain and for the solvent:

$$\Delta G_{total} = \Delta H_{chain} + \Delta H_{solvent}$$
$$- T\Delta S_{chain} - T\Delta S_{solvent}$$

If each of the four terms on the right side of this equation is understood, the thermodynamic basis for protein folding should be clear. A summary of the signs and magnitudes of these quantities for a typical protein is shown in the accompanying figure. The folded protein is a highly ordered structure compared to the unfolded state, so ΔS_{chain} is a negative number and thus $- T\Delta S_{chain}$ is a positive quantity in the equation. The other terms depend on the nature of the particular ensemble of R groups. The nature of ΔH_{chain} depends on both residue–residue interactions and residue–solvent interactions. Nonpolar groups in the folded protein interact mainly with one another via weak van der Waals forces. Interactions between nonpolar groups and water in the unfolded state are stronger because the polar water molecules induce dipoles in the nonpolar groups, producing a significant electrostatic interaction. As a result, ΔH_{chain} is positive for nonpolar groups and favors the unfolded state. $\Delta H_{solvent}$ for nonpolar groups, however, is negative and favors the folded state. This is because folding allows many water molecules to interact (favorably) with one another rather than (less favorably) with the nonpolar side chains. The magnitude of ΔH_{chain} is smaller than that of $\Delta H_{solvent}$, but both these terms are small and usually do not dominate the folding process. However, $\Delta S_{solvent}$ for nonpolar

groups is large and positive and strongly favors the folded state. This is because nonpolar groups force order upon the water solvent in the unfolded state.

For polar side chains, ΔH_{chain} is positive and $\Delta H_{solvent}$ is negative. Because solvent molecules are ordered to some extent around polar groups, $\Delta S_{solvent}$ is small and positive. As shown in the figure, ΔG_{total} for the polar groups of a protein is near zero. Comparison of all the terms considered here makes it clear that *the single largest contribution to the stability of a folded protein is $\Delta S_{solvent}$ for the nonpolar residues.*
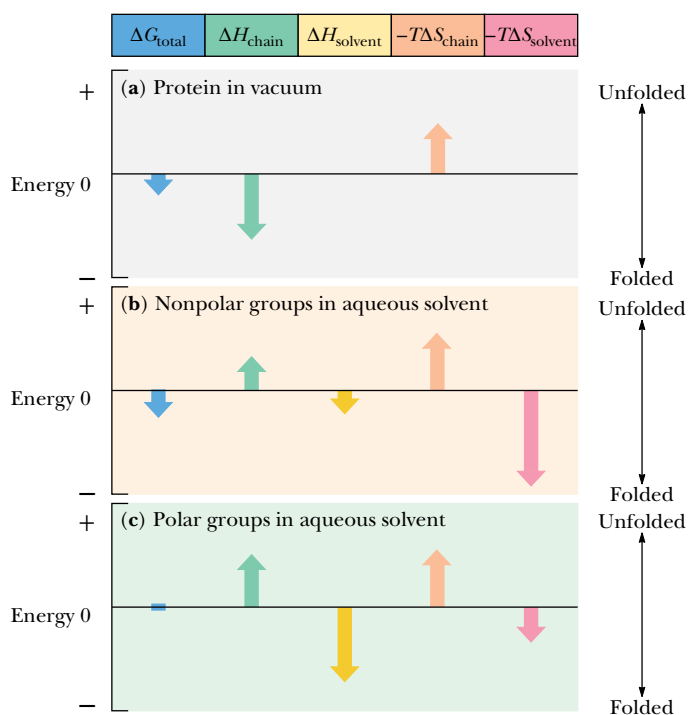
that appear to be essential for the correct folding of certain polypeptide chains *in vivo*, for their assembly into oligomers, and for preventing inappropriate liaisons with other proteins during their synthesis, folding, and transport. Many of these proteins were first identified as **heat shock proteins,** which are induced in cells by elevated temperature or other stress. The most thoroughly studied proteins are **hsp70,** a 70-kD heat shock protein, and the so-called **chaperonins,** also known as **cpn60s** or **hsp60s,** a class of 60-kD heat shock proteins. A well-characterized **hsp60** chaperonin is **GroEL,** an *E. coli* protein that has been shown to affect the folding of several proteins.

The way in which molecular chaperones interact with polypeptides during the folding process is not completely understood. What *is* clear is that chaperones bind effectively to the exposed hydrophobic regions of partially folded structures. These folding intermediates are less compact than the native folded proteins. They contain large amounts of secondary and even some tertiary

structure, but they undergo relatively large conformational fluctuations. It is possible that chaperone proteins recognize exposed helices or other secondary structure elements on their target proteins. This initial interaction may then allow the chaperone to guide or regulate the subsequent events of folding (Figure 6.36).

(1) The rapid and reversible formation of local secondary structures

(2) Formation of domains through the cooperative aggregation of folding nuclei

(3) "Molten globule" formation of the assembled domains

(4) An adjustment in the conformation of the domains

(5) Final protein monomer
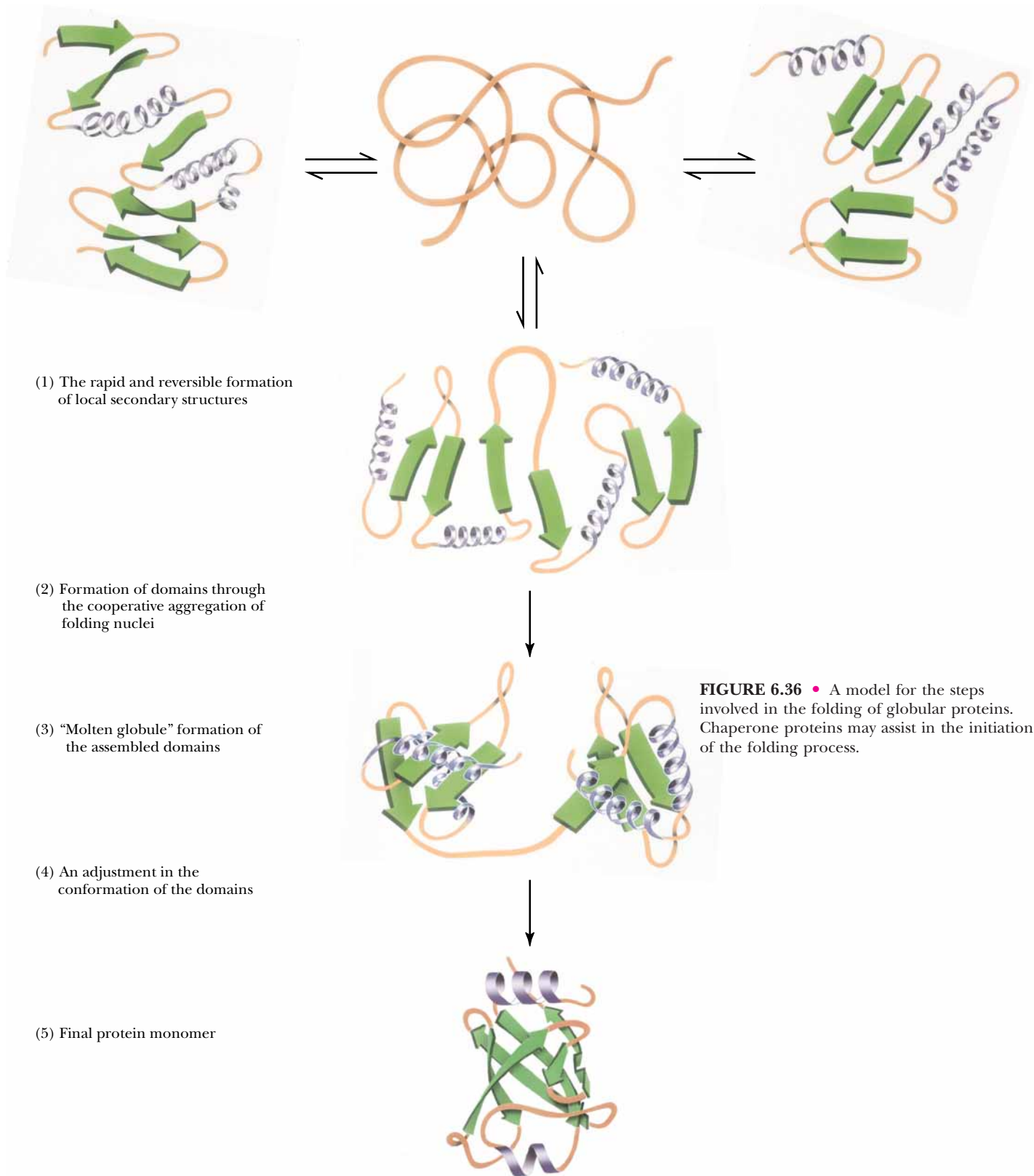
FIGURE 6.36 • A model for the steps involved in the folding of globular proteins. Chaperone proteins may assist in the initiation of the folding process.

$\mathcal{H}$ UMAN BIOCHEMISTRY

*A Mutant Protein That Folds Slowly Can Cause Emphysema
and Liver Damage*

Lungs enable animals to acquire oxygen from the air and to give off CO_2 produced in respiration. Exchange of oxygen and CO_2 occurs in the alveoli—air sacs surrounded by capillaries that connect the pulmonary veins and arteries. The walls of alveoli consist of the elastic protein **elastin.** Inhalation expands the alveoli and exhalation compresses them. A pair of human lungs contains 300 million alveoli, and the total area of the alveolar walls in contact with capillaries is about 70 m^2—an area about the size of a tennis court! White blood cells naturally secrete **elastase**—a serine protease—which can attack and break down the elastin of the alveolar walls. However, $\boldsymbol{\alpha_1}$**-antitrypsin**—a 52-kD protein belonging to the **serpin** (*ser*ine *p*rotease *in*hibitor) family—normally binds to elastase, preventing alveolar damage. The structural gene for α_1-antitrypsin is extremely polymorphic (i.e., occurs as many different sequence variants), and several versions of this gene encode a protein that is poorly secreted into the circulation. Deficiency of α_1-antitrypsin in the blood can lead to destruction of the alveolar walls by white cell elastase, resulting in **emphysema** —a condition in which the alveoli are destroyed, leaving large air sacs that cannot be compressed during exhalation.

α_1-Antitrypsin normally adopts a highly ordered tertiary structure composed of three β-sheets and eight α-helices (see figure). Elastase and other serine proteases interact with a reactive, inhibitory site involving two amino acids—Met^{358} and Ser^{359}— on the so-called **reactive-center loop.** Formation of a tight complex between elastase and α_1-antitrypsin renders the elastase inactive. The most common α_1-antitrypsin deficiency involves the so-called **Z-variant** of the protein, in which lysine is substituted for glutamate at position 342 ($Glu^{342}\rightarrow Lys$). Residue 342 lies at the amino-terminal base of the **reactive-center loop,** and glutamate at this position normally forms a crucial salt bridge with Lys^{290} on an adjacent strand of sheet A (see figure). In normal α_1-antitrypsin, the reactive-center loop is fully exposed and can interact readily with elastase. However, in the Z-variant, the $Glu^{342}\rightarrow Lys$ substitution destabilizes sheet A, separating the strands slightly and allowing the reactive-center loop of one molecule to insert into the β-sheet of another. Repetition of this anomalous association of α_1-antitrypsin molecules results in "loop-sheet" polymerization and the formation of large protein aggregates. α_1-Antitrypsin is synthesized in hepatocytes of the liver and is normally secreted into the circulation. Accumulation of Z-variant protein aggregates in the endoplasmic reticulum of liver cells leads to deficiency of circulating α_1-antitrypsin. In some cases, the accumulation of these protein aggregates can also cause liver damage.

Myeong-Hee Yu and coworkers at the Korea Institute of Science and Technology have studied the folding kinetics of normal and Z-variant α_1-antitrypsin and have found that the Z-variant of α_1-antitrypsin folds identically to—but much more slowly than—normal α_1-antitrypsin. Newly synthesized Z-variant protein, incubated for 5 hours at 30°C, eventually adopts a native and active conformation and can associate tightly with elastase. However, incubation of the Z-variant at 37°C results in loop-sheet polymerization and self-aggregation of the protein. These results imply that emphysema arising in individuals carrying the Z-variant of α_1-antitrypsin is due to the slow folding kinetics of the protein rather than the adoption of an altered three-dimensional structure.
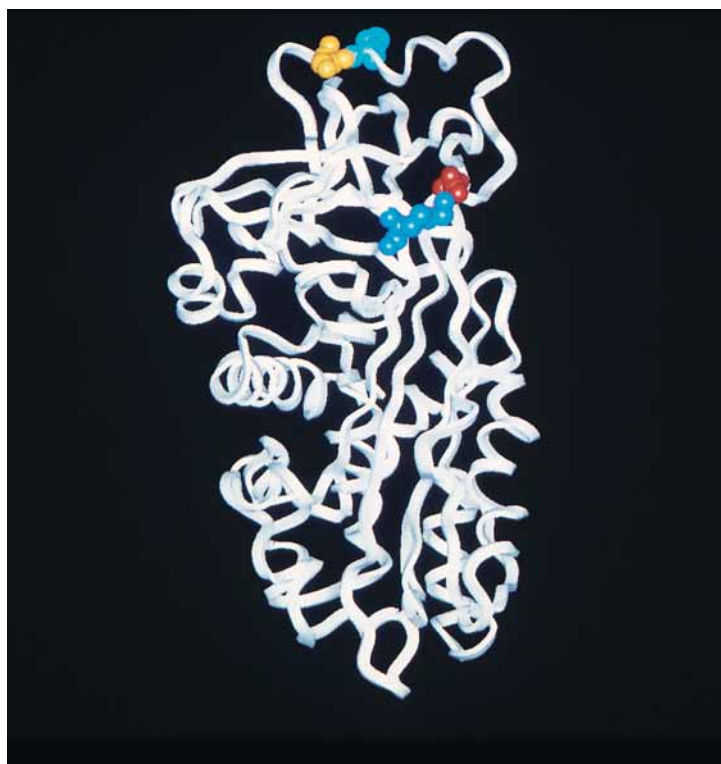
α_1-Antitrypsin. Note Met^{358} (blue) and Ser^{354} (yellow) at top, as well as Glu^{342} (red) and Lys^{290} (blue—upper right).

Protein Domains: Nature's Modular Strategy for Protein Design

Now that many thousands of proteins have been sequenced (more than 100,000 sequences are known), it has become obvious that certain protein sequences that give rise to distinct structural domains are used over and over again in modular fashion. These **protein modules** may occur in a wide variety of pro-
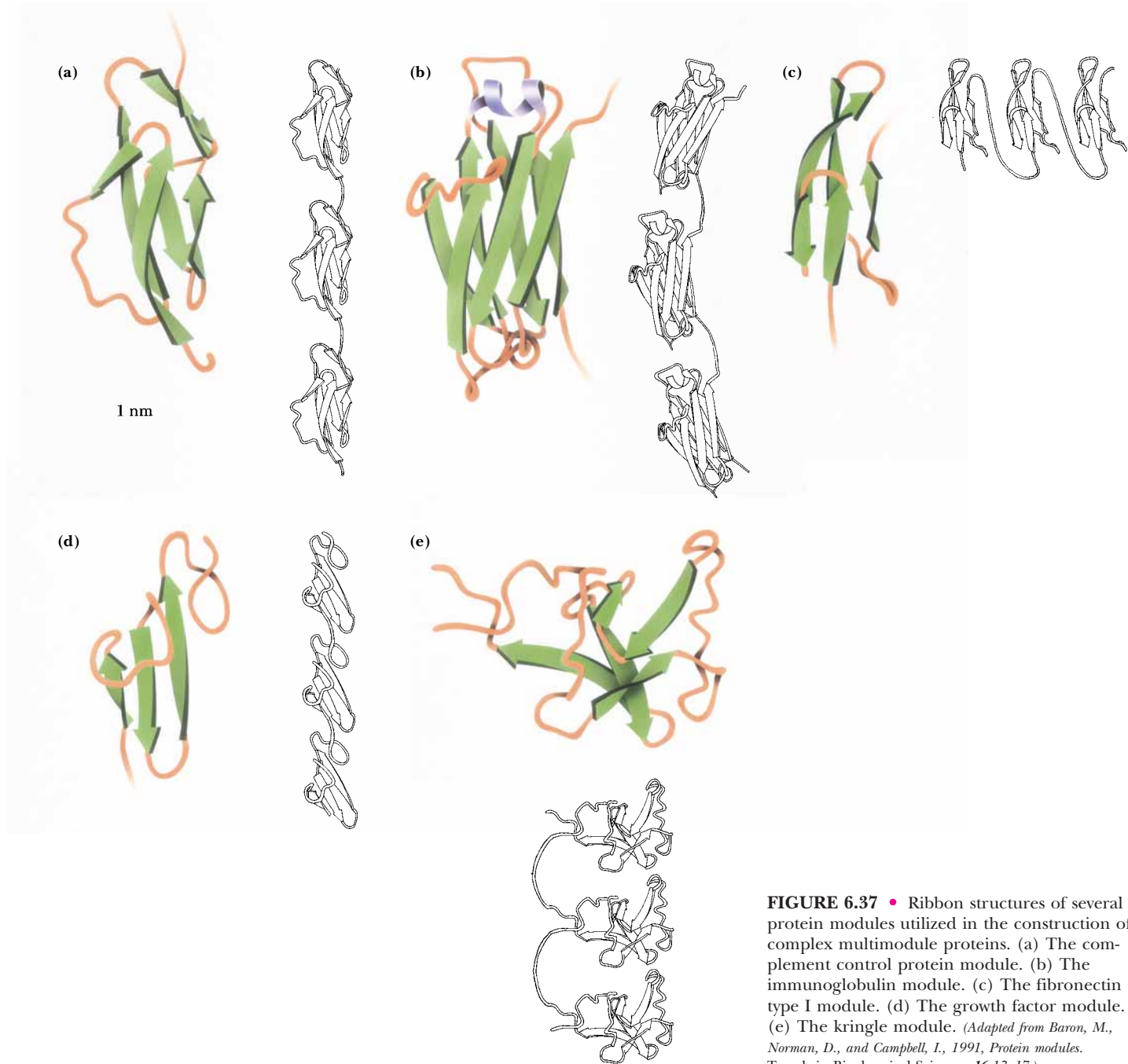
FIGURE 6.37 • Ribbon structures of several protein modules utilized in the construction of complex multimodule proteins. (a) The complement control protein module. (b) The immunoglobulin module. (c) The fibronectin type I module. (d) The growth factor module. (e) The kringle module. *(Adapted from Baron, M., Norman, D., and Campbell, I., 1991, Protein modules.* Trends in Biochemical Sciences *16:13–17.)*

teins, often being used for different purposes, or they may be used repeatedly in the same protein. Figure 6.37 shows the tertiary structures of five protein modules, and Figure 6.38 presents several proteins that contain versions of these modules. These modules typically contain about 40 to 100 amino acids and often adopt a stable tertiary structure when isolated from their parent protein. One of the best-known examples of a protein module is the **immunoglobulin module,** which has been found not only in immunoglobulins but also in a wide variety of cell surface proteins, including cell adhesion molecules and growth factor receptors, and even in *twitchin,* an intracellular protein found in muscle. It is likely that more protein modules will be identified. (The role of protein modules in signal transduction is discussed in Chapter 34.)

FIGURE 6.38 • A sampling of proteins that consist of mosaics of individual protein modules. The modules shown include γCG, a module containing γ-carboxyglutamate residues; G, an epidermal growth-factor–like module; K, the "kringle" domain, named for a Danish pastry; C, which is found in complement proteins; F1, F2, and F3, first found in fibronectin; I, the immunoglobulin superfamily domain; N, found in some growth factor receptors; E, a module homologous to the calcium-binding E–F hand domain; and LB, a lectin module found in some cell surface proteins. *(Adapted from Baron, M., Norman, D., and Campbell, I., 1991, Protein modules. Trends in Biochemical Sciences* **16:**13–17.)
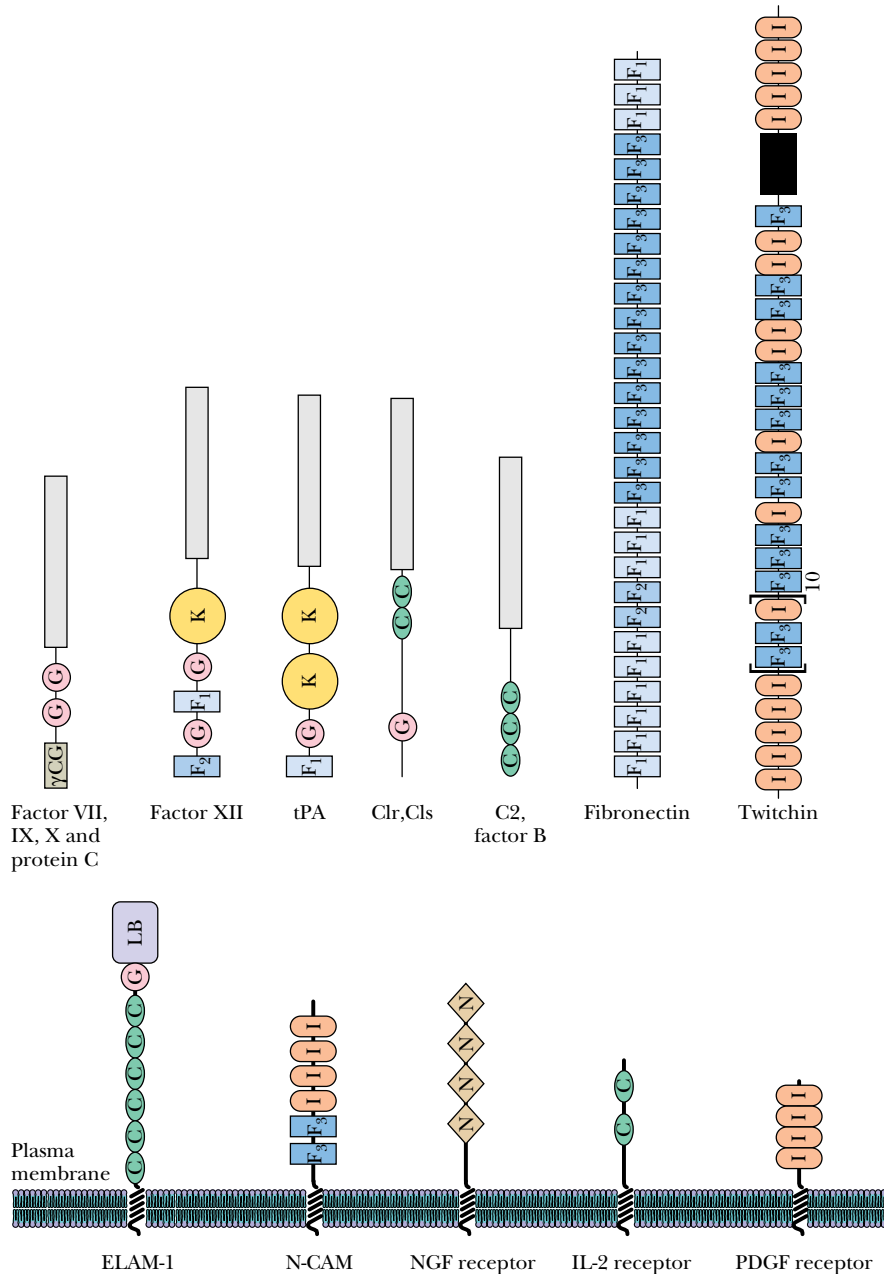
How Do Proteins Know How to Fold?

Christian Anfinsen's experiments demonstrated that proteins can fold reversibly. A corollary result of Anfinsen's work is that the native structures of at least some globular proteins are thermodynamically stable states. But the matter of how a given protein achieves such a stable state is a complex one. Cyrus Levinthal pointed out in 1968 that so many conformations are possible for a typical protein that the protein does not have sufficient time to reach its most stable conformational state by sampling all the possible conformations. This argument, termed "Levinthal's paradox," goes as follows: consider a protein of 100 amino acids. Assume that there are only two conformational possibilities per amino acid, or $2^{100} = 1.27 \times 10^{30}$ possibilities. Allow 10^{-13} sec for

the protein to test each conformational possibility in search of the overall energy minimum:

$$(10^{-13} \text{ sec})(1.27 \times 10^{30}) = 1.27 \times 10^{17} \text{ sec} = 4 \times 10^9 \text{ years}$$

Levinthal's paradox led protein chemists to hypothesize that proteins must fold by specific "folding pathways," and many research efforts have been devoted to the search for these pathways.

Implicit in the presumption of folding pathways is the existence of inter-mediate, partially folded conformational states. The notion of intermediate states on the pathway to a tertiary structure raises the possibility that segments of a protein might independently adopt local and well-defined secondary struc-tures (α-helices and β-sheets). The tendency of a peptide segment to prefer a particular secondary structure depends in turn on its amino acid composition and sequence.

Surveys of the frequency with which various residues appear in helices and sheets show that some residues, such as alanine, glutamate, and methionine, occur much more frequently in α-helices than do others. In contrast, glycine and proline are the least likely residues to be found in an α-helix. Likewise, certain residues, including valine, isoleucine, and the aromatic amino acids, are more likely to be found in β-sheets than other residues, and aspartate, glu-tamate, and proline are much less likely to be found in β-sheets.

Such observations have led to many efforts to predict the occurrence of secondary structure in proteins from knowledge of the peptide sequence. Such **predictive algorithms** consider the composition of short segments of a polypep-tide. If these segments are rich in residues that are found frequently in helices or sheets, then that segment is judged likely to adopt the corresponding sec-ondary structure. The predictive algorithm designed by Peter Chou and Gerald Fasman in 1974 used data like that in Figure 6.39 to classify the 20 amino acids for their α-helix–forming and β-sheet–forming **propensities, P_α and P_β** (Table 6.3). These residues are classified as strong helix formers (H_α), helix formers (h_α), weak helix formers (I_α), indifferent helix formers (i_α), helix breakers (b_α), and strong helix breakers (B_α). Similar classes were established by Chou
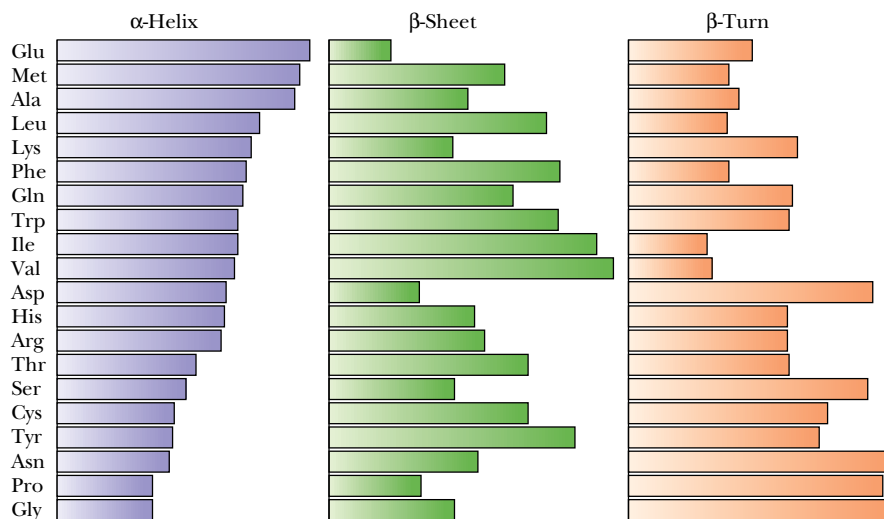
FIGURE 6.39 • Relative frequencies of occurrence of amino acid residues in α-helices, β-sheets, and β-turns in proteins of known structure. *(Adapted from Bell, J. E., and Bell, E. T., 1988, Proteins and Enzymes, Englewood Cliffs, NJ: Prentice-Hall.)*

Table 6.3

Chou–Fasman Helix and Sheet Propensities (P_α and P_β) of the Amino Acids

Amino Acid	P_α	Helix Classification	P_β	Sheet Classification
A Ala	1.42	H_α	0.83	i_β
C Cys	0.70	i_α	1.19	h_β
D Asp	1.01	I_α	0.54	B_β
E Glu	1.51	H_α	0.37	B_β
F Phe	1.13	h_α	1.38	h_β
G Gly	0.57	B_α	0.75	b_β
H His	1.00	I_α	0.87	h_β
I Ile	1.08	h_α	1.60	H_β
K Lys	1.16	h_α	0.74	b_β
L Leu	1.21	H_α	1.30	h_β
M Met	1.45	H_α	1.05	h_β
N Asn	0.67	b_α	0.89	i_β
P Pro	0.57	B_α	0.55	B_β
Q Gln	1.11	h_α	1.10	h_β
R Arg	0.98	i_α	0.93	i_β
S Ser	0.77	i_α	0.75	b_β
T Thr	0.83	i_α	1.19	h_β
V Val	1.06	h_α	1.70	H_β
W Trp	1.08	h_α	1.37	h_β
Y Tyr	0.69	b_α	1.47	H_β

Source: Chou, P. Y., and Fasman, G. D., 1978. *Annual Review of Biochemistry* **47:**258.

and Fasman for β-sheet–forming ability. Such algorithms are only modestly successful in predicting the occurrence of helices and sheets in proteins.

George Rose and Rajgopal Srinivasan at Johns Hopkins University have taken a different, and very successful, approach to the prediction of protein structures. They begin by assuming that protein folding is both *local* and *hierarchical*. "Local" in this context means that each amino acid's folding behavior is influenced by other residues nearby in the sequence. "Hierarchical" means that folded structures develop from the smallest structural units and work up to more and more complex entities. These and other assumptions are the basis for a computer program called **LINUS**—for Local Independently Nucleated Units of Structure—which Rose and Srinivasan have used to generate remarkably accurate predicted structures for a number of small proteins. LINUS considers groups of three amino acids in a sequence—for example, residues 2, 3, and 4 in a sequence of 50. The initial assumption is that this group of amino acids will (randomly) adopt one of four possible structures—helix, sheet, turn, or "loop" (any tertiary structure that is not helix, sheet, or turn). The program then asks whether this assumed "ministructure" is energetically suited to the six amino acids on either side. The program then moves on to the next set of three residues—amino acids 3, 4, and 5 in the present case—and randomly selects one of the four secondary structures for this unit, evaluates the energetic consequences in terms of the six residues on either side, and then continues in like manner to groups 4, 5, and 6, then 5, 6, and 7, and so on to the end of the protein. The program carries out this random selection and testing

routine a total of 5000 times for the entire protein. Once this is done, the program analyzes all the trials, looking for local groups of amino acids that seem to prefer one of the four conformations 70% of the time. Such groups are then held in those conformations while the program repeats the entire process, this time comparing energetic preferences with respect to 12 amino acids on either side of selected groups of three residues, then 18 amino acids on either side, 24, 32, and so on up to 48 residues. The results of calculations with LINUS on several proteins whose structures are known are shown in Figure 6.40.
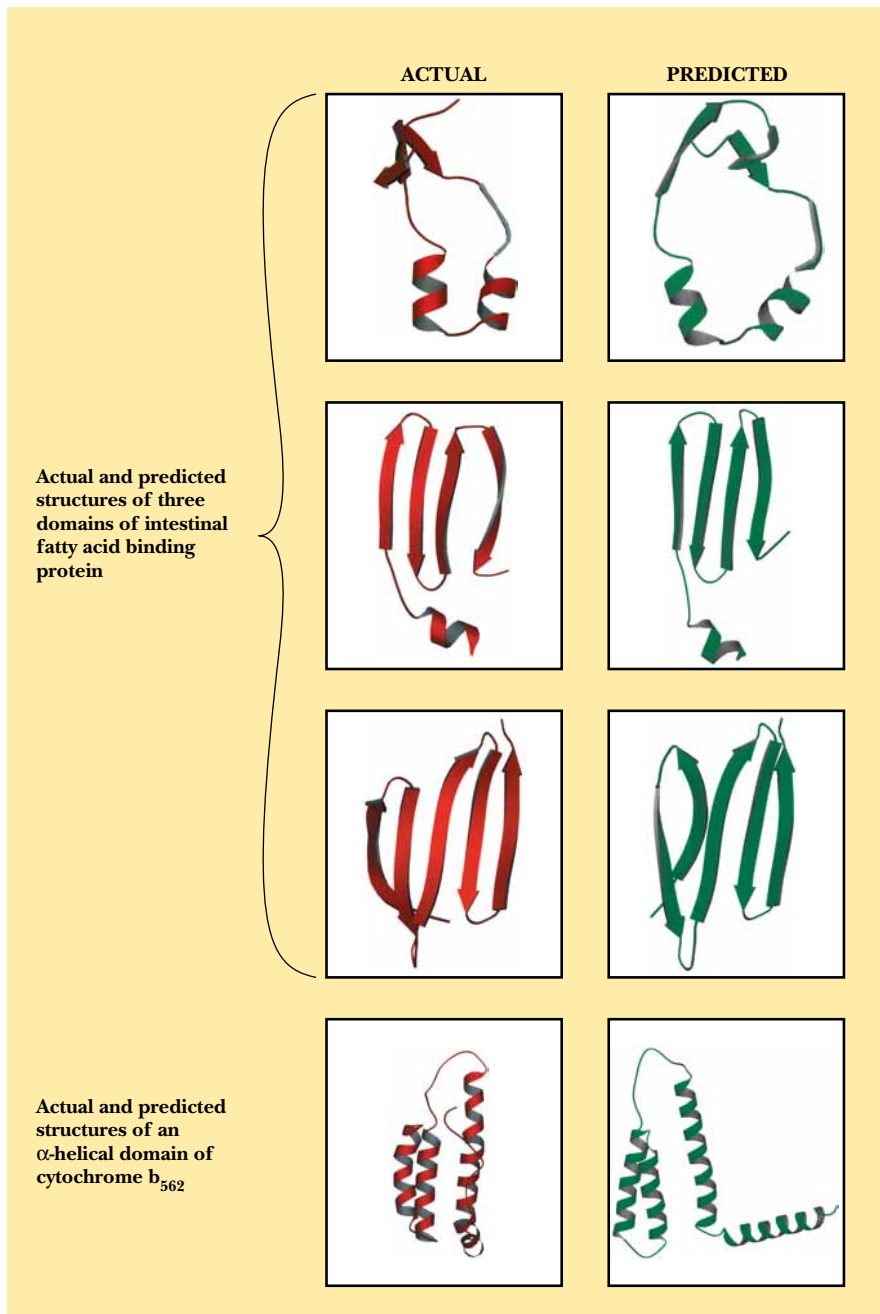
FIGURE 6.40 • A comparison of the structures of four protein domains and predictions of these structures by the program LINUS by Rose and Srinivasan. *(Professor George Rose/Johns Hopkins University)*

6.5 • Subunit Interactions and Quaternary Structure

Many proteins exist in nature as **oligomers,** complexes composed of (often symmetric) noncovalent assemblies of two or more monomer subunits. In fact, subunit association is a common feature of macromolecular organization in biology. Most intracellular enzymes are oligomeric and may be composed either of a single type of monomer subunit (*homomultimers*) or of several different kinds of subunits (*heteromultimers*). The simplest case is a protein composed of identical subunits. Liver alcohol dehydrogenase, shown in Figure 6.41, is such a protein. More complicated proteins may have several different subunits in one, two, or more copies. Hemoglobin, for example, contains two each of two different subunits and is referred to as an $\alpha_2\beta_2$-complex. An interesting counterpoint to these relatively simple cases is made by the proteins that form polymeric structures. Tubulin is an $\alpha\beta$-dimeric protein that polymerizes to form microtubules of the formula $(\alpha\beta)_n$. The way in which separate folded monomeric protein subunits associate to form the oligomeric protein constitutes the **quaternary structure** of that protein. Table 6.4 lists several proteins and their subunit compositions (see also Table 5.1). Clearly, proteins with two to four subunits dominate the list, but many cases of higher numbers exist.
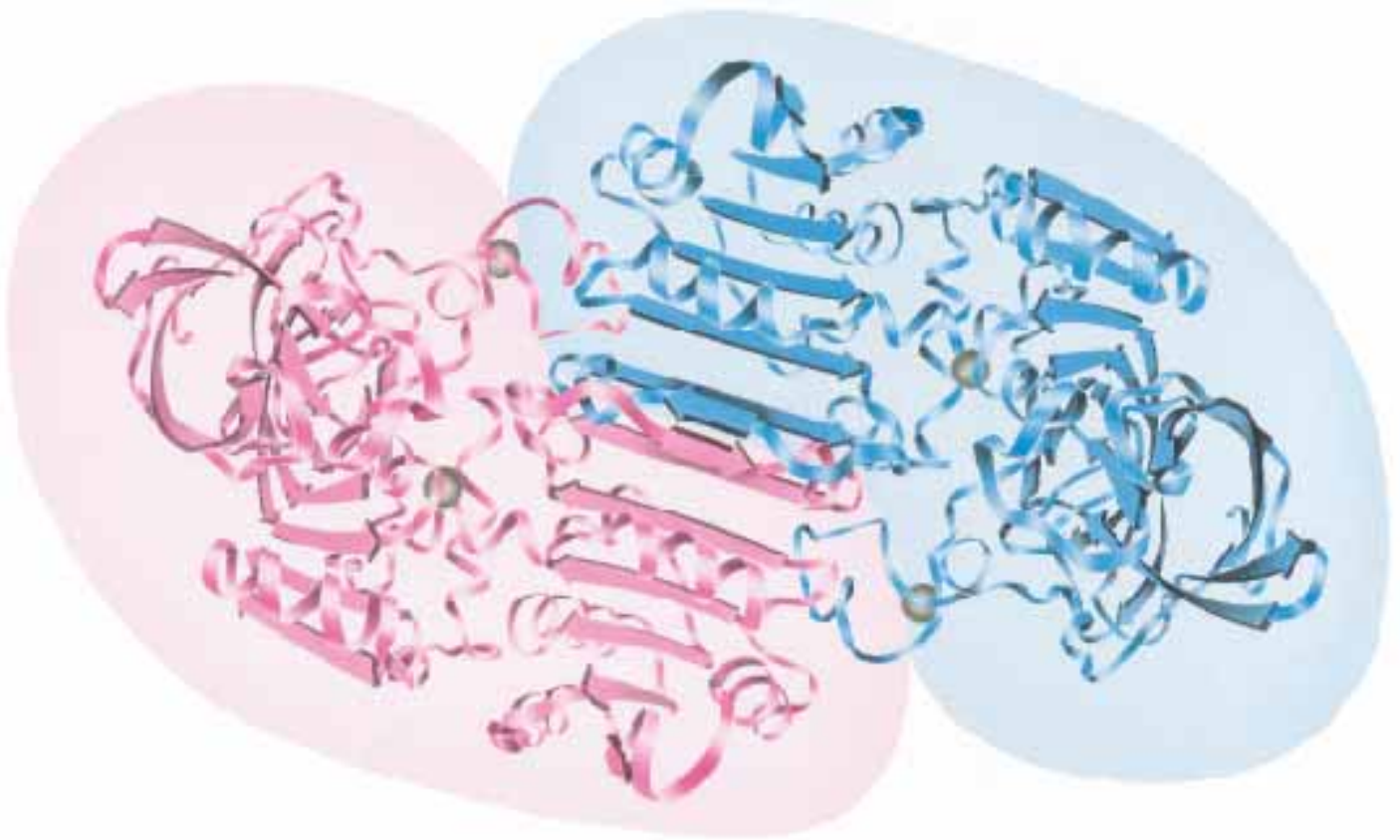
FIGURE 6.41 • The quaternary structure of liver alcohol dehydrogenase. Within each subunit is a six-stranded parallel sheet. Between the two subunits is a two-stranded antiparallel sheet. The point in the center is a C_2 symmetry axis. (*Jane Richardson*)

The subunits of an oligomeric protein typically fold into apparently independent globular conformations and then interact with other subunits. The particular surfaces at which protein subunits interact are similar in nature to the interiors of the individual subunits. These interfaces are closely packed and involve both polar and hydrophobic interactions. Interacting surfaces must therefore possess complementary arrangements of polar and hydrophobic groups.

Oligomeric associations of protein subunits can be divided into those between **identical** subunits and those between **nonidentical** subunits. Interactions among identical subunits can be further distinguished as either **isologous** or **heterologous.** In isologous interactions, the interacting surfaces are identical, and the resulting structure is necessarily dimeric and closed, with a twofold axis of symmetry (Figure 6.42). If any additional interactions occur to form a trimer or tetramer, these must use different interfaces on the protein's surface. Many proteins, including concanavalin and prealbumin, form tetramers by means of two sets of isologous interactions, one of which is shown in Figure 6.43. Such structures possess three different twofold axes of symmetry. In contrast, heterologous associations among subunits involve nonidentical interfaces. These surfaces must be complementary, but they are generally not symmetric. As shown in Figure 6.43, heterologous interactions are necessarily open-ended. This can give rise either to a closed cyclic structure, if geometric constraints exist, or to large polymeric assemblies. The closed cyclic structures are far more common and include the trimers of aspartate transcarbamoylase catalytic subunits and the tetramers of neuraminidase and hemerythrin.

Table 6.4

Aggregation Symmetries of Globular Proteins

Protein	Number of Subunits
Alcohol dehydrogenase	2
Immunoglobulin	4
Malate dehydrogenase	2
Superoxide dismutase	2
Triose phosphate isomerase	2
Glycogen phosphorylase	2
Alkaline phosphatase	2
6-Phosphogluconate dehydrogenase	2
Wheat germ agglutinin	2
Phosphoglucoisomerase	2
Tyrosyl-tRNA synthetase	2
Glutathione reductase	2
Aldolase	3
Bacteriochlorophyll protein	3
TMV protein disc	17
Concanavalin A	4
Glyceraldehyde-3-phosphate dehydrogenase	4
Lactate dehydrogenase	4
Prealbumin	4
Pyruvate kinase	4
Phosphoglycerate mutase	4
Hemoglobin	2 + 2
Insulin	6
Aspartate transcarbamoylase	6 + 6
Glutamine synthetase	12
Apoferritin	24
Coat of tomato bushy stunt virus	180

(c) Heterologous tetramer

(a) Isologous association

(b) Heterologous association

(d) Isologous tetramer

Symmetry axis

FIGURE 6.42 • Isologous and heterologous associations between protein subunits. (a) An isologous interaction between two subunits with a twofold axis of symmetry perpendicular to the plane of the page. (b) A heterologous interaction that could lead to the formation of a long polymer. (c) A heterologous interaction leading to a closed structure—a tetramer. (d) A tetramer formed by two sets of isologous interactions.

FIGURE 6.43 • The polypeptide backbone of the prealbumin dimer. The monomers associate in a manner that continues the β-sheets. A tetramer is formed by isologous inter-actions between the side chains extending outward from sheet D′A′G′H′HGAD in both dimers, which pack together nearly at right angles to one another. (*Jane Richardson*)

Symmetry of Quaternary Structures

One useful way to consider quaternary interactions in proteins involves the symmetry of these interactions. Globular protein subunits are always asymmetric objects. All of the polypeptide's α-carbons are asymmetric, and the polypeptide nearly always folds to form a low-symmetry structure. (The long helical arrays formed by some synthetic polypeptides are an exception.) Thus, protein subunits do not have mirror reflection planes, points, or axes of inversion. The only symmetry operation possible for protein subunits is a rotation. The most common symmetries observed for multisubunit proteins are cyclic symmetry and dihedral symmetry. In **cyclic symmetry,** the subunits are arranged around a single rotation axis, as shown in Figure 6.44. If there are two subunits, the axis is referred to as a *twofold rotation axis*. Rotating the quaternary structure 180° about this axis gives a structure identical to the original one. With three subunits arranged about a threefold rotation axis, a rotation of 120° about that axis gives an identical structure. **Dihedral symmetry** occurs when a structure possesses at least one twofold rotation axis perpendicular to another n-fold rotation axis. This type of subunit arrangement (Figure 6.44) occurs in concanavalin A (where $n = 2$) and in insulin (where $n = 3$). Higher symmetry groups, including the tetrahedral, octahedral, and icosahedral symmetries, are much less common among multisubunit proteins, partly because of the large number of asymmetric subunits required to assemble truly symmetric tetrahedra and other high symmetry groups. For example, a truly symmetric tetrahedral protein structure would require 12 identical monomers arranged in triangles, as shown in Figure 6.45. Simple four-subunit tetrahedra of protein monomers, which actually possess dihedral symmetry, are more common in biological systems.

(a) Cyclic symmetries

C_2

C_3

C_5

(b) Dihedral symmetries

D_2

D_4

D_3

(c) Tetrahedral symmetry

Octohedral (cubic) symmetry

Icosahedral symmetry

T

O

I
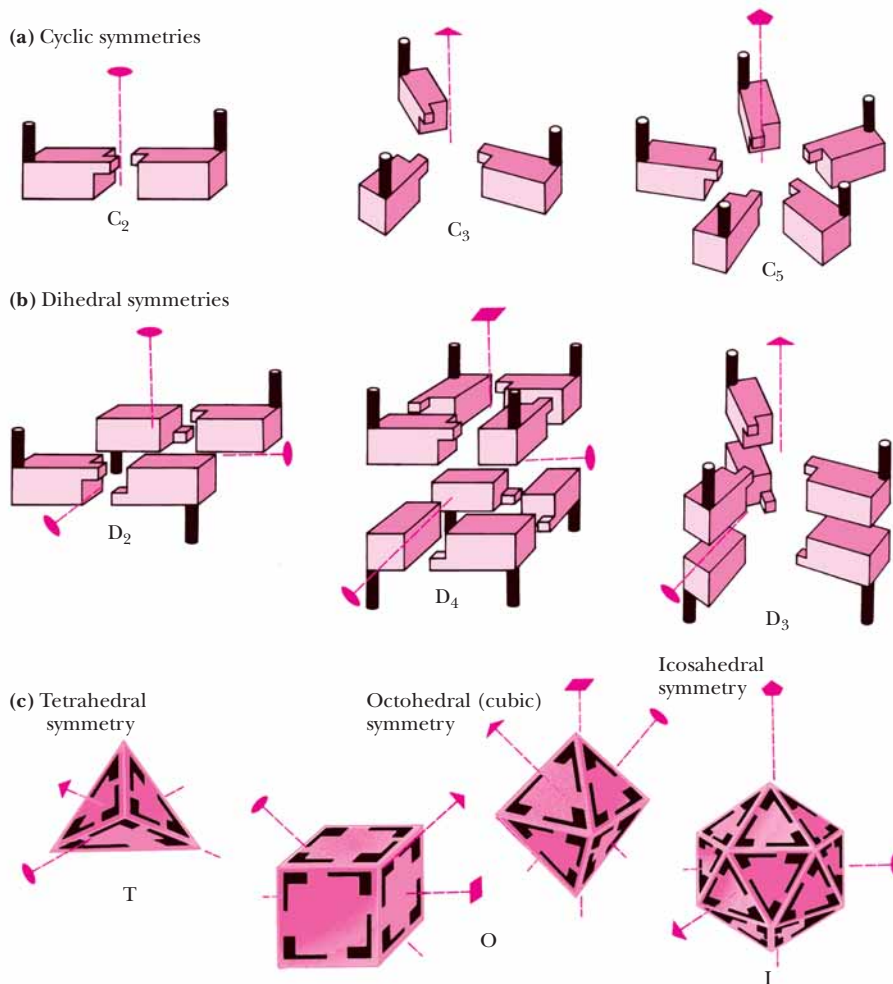
FIGURE 6.44 • Several possible symmetric arrays of identical protein subunits, including (a) cyclic symmetry, (b) dihedral symmetry, and (c) cubic symmetry, including examples of tetrahedral (T), octahedral (O), and icosahedral (I) symmetry. *(Irving Geis)*

Forces Driving Quaternary Association

The forces that stabilize quaternary structure have been evaluated for a few proteins. Typical dissociation constants for simple two-subunit associations range from 10^{-8} to 10^{-16} *M*. These values correspond to free energies of association of about 50 to 100 kJ/mol at 37°C. Dimerization of subunits is accompanied by both favorable and unfavorable energy changes. The favorable interactions include van der Waals interactions, hydrogen bonds, ionic bonds, and hydrophobic interactions. However, considerable entropy loss occurs when subunits interact. When two subunits move as one, three translational degrees of freedom are lost for one subunit because it is constrained to move with the other one. In addition, many peptide residues at the subunit interface, which were previously free to move on the protein surface, now have their movements restricted by the subunit association. This unfavorable energy of association is in the range of 80 to 120 kJ/mol for temperatures of 25 to 37°C. Thus, to achieve stability, the dimerization of two subunits must involve approximately 130 to 220 kJ/mol of favorable interactions.[1] Van der Waals interactions at protein interfaces are numerous, often running to several hundred for a typical monomer–monomer association. This would account for about 150 to 200

[1]For example, 130 kJ/mol of favorable interaction minus 80 kJ/mol of unfavorable interaction equals a net free energy of association of 50 kJ/mol.
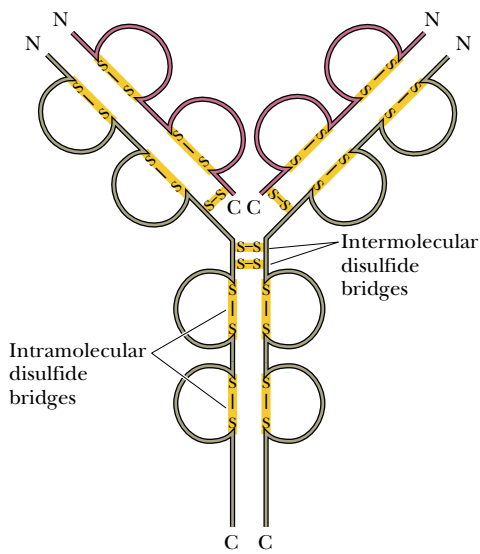
FIGURE 6.45 • Schematic drawing of an immunoglobulin molecule showing the intramolecular and intermolecular disulfide bridges. (A space-filling model of the same molecule is shown in Figure 1.11.)

kJ/mol of favorable free energy of association. However, when solvent is removed from the protein surface to form the subunit–subunit contacts, nearly as many van der Waals associations are lost as are made. One subunit is simply trading water molecules for peptide residues in the other subunit. As a result, the energy of subunit association due to van der Waals interactions actually contributes little to the stability of the dimer. Hydrophobic interactions, however, are generally very favorable. For many proteins, the subunit association process effectively buries as much as 20 nm^2 of surface area previously exposed to solvent, resulting in as much as 100 to 200 kJ/mol of favorable hydrophobic interactions. Together with whatever polar interactions occur at the protein–protein interface, this is sufficient to account for the observed stabilization that occurs when two protein subunits associate.

An additional and important factor contributing to the stability of subunit associations for some proteins is the formation of disulfide bonds between different subunits. All antibodies are $\alpha_2\beta_2$-tetramers composed of two heavy chains (53 to 75 kD) and two relatively light chains (23 kD). In addition to *intrasubunit* disulfide bonds (four per heavy chain, two per light chain), two *intersubunit* disulfide bridges hold the two heavy chains together and a disulfide bridge links each of the two light chains to a heavy chain (Figure 6.45).

Modes and Models for Quaternary Structures

When a protein is composed of only one kind of polypeptide chain, the manner in which the subunits interact and the arrangement of the subunits to produce the quaternary structure are usually simple matters. Sometimes, however, the same protein derived from several different species can exhibit different modes of quaternary interactions. Hemerythrin, the oxygen-carrying protein in certain species of marine invertebrates, is composed of a compact arrangement of four antiparallel α-helices. It is capable of forming dimers, trimers, tetramers, octamers, and even higher aggregates (Figure 6.46).

When two or more distinct peptide chains are involved, the nature of their interactions can be quite complicated. Multimeric proteins with more than one kind of subunit often display different affinities between different pairs of sub-

(a)

(b)

(c)

P1
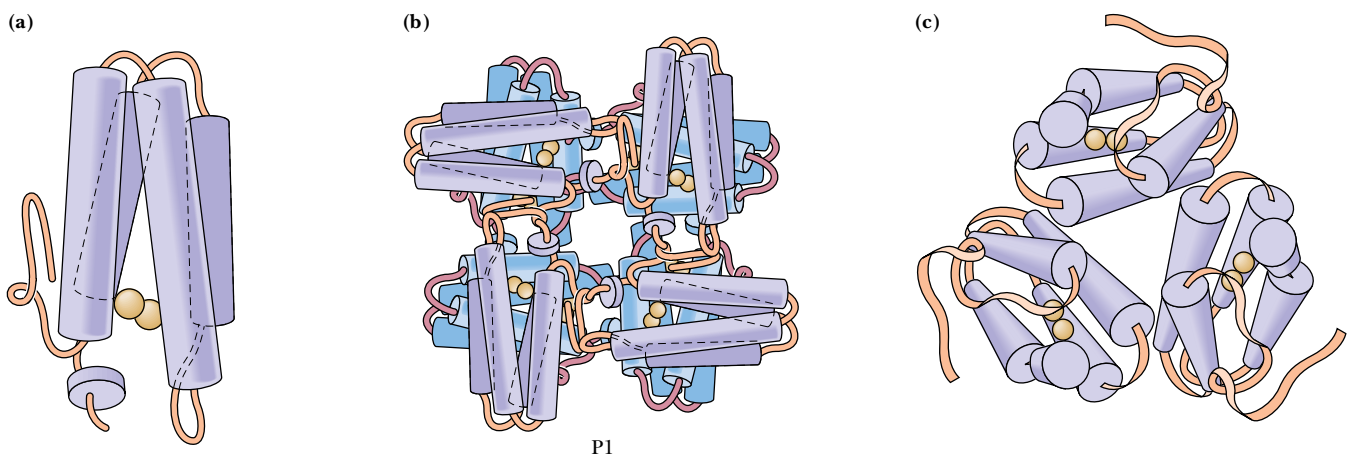
FIGURE 6.46 • The oligomeric states of hemerythrin in various marine worms. (a) The hemerythrin in *Thermiste zostericola* crystallized as a monomer; (b) the octameric hemerythrin crystallized from *Phascolopsis gouldii;* (c) the trimeric hemerythrin crystallized from *Siphonosoma* collected in mangrove swamps in Fiji.

A DEEPER LOOK

Immunoglobulins—All the Features of Protein Structure Brought Together

The immunoglobulin structure in Figure 6.45 represents the confluence of all the details of protein structure that have been thus far discussed. As for all proteins, the primary structure determines other aspects of structure. There are numerous elements of secondary structure, including β-sheets and tight turns. The tertiary structure consists of 12 distinct domains, and the protein adopts a heterotetrameric quaternary structure. To make matters more interesting, both intrasubunit and intersubunit disulfide linkages act to stabilize the discrete domains and to stabilize the tetramer itself.

One more level of sophistication awaits. As discussed in Chapter 29, the amino acid sequences of both light and heavy immunoglobulin chains are not constant! Instead, the primary structure of these chains is highly variable in the N-terminal regions (first 108 residues). Heterogeneity of amino acid sequence leads to variations in the conformation of these variable regions. This variation accounts for antibody diversity and the ability of antibodies to recognize and bind a virtually limitless range of antigens. This full potential of antibody:antigen recognition enables organisms to mount immunologic responses to almost any antigen that might challenge the organism.

units. Whereas strongly denaturing solvents may dissociate the protein entirely into monomers, more subtle denaturing conditions may dissociate the oligomeric structure in a carefully controlled stepwise manner. Hemoglobin is a good example. Strong denaturants dissociate hemoglobin into α- and β-monomers. Using mild denaturing conditions, however, it is possible to dissociate hemoglobin almost completely into αβ-dimers, with few or no free monomers occurring. In this sense, hemoglobin behaves functionally like a two-subunit protein, with each "subunit" composed of an αβ-dimer.

Open Quaternary Structures and Polymerization

All of the quaternary structures we have considered to this point have been **closed** structures, with a limited capacity to associate. Many proteins in nature associate to form **open** heterologous structures, which can polymerize more or less indefinitely, creating structures that are both esthetically attractive and functionally important to the cells or tissue in which they exist. One such protein is **tubulin,** the αβ-dimeric protein that polymerizes into long, tubular structures, which are the structural basis of cilia flagella and the cytoskeletal matrix. The *microtubule* thus formed (Figure 6.47) may be viewed as consisting of 13 parallel filaments arising from end-to-end aggregation of the tubulin dimers. Human immunodeficiency virus, HIV, the causative agent of AIDS (also discussed in Chapter 16), is enveloped by a spherical shell composed of hundreds of coat protein subunits, a large-scale quaternary association.

Structural and Functional Advantages of Quaternary Association

There are several important reasons for protein subunits to associate in oligomeric structures.

Stability

One general benefit of subunit association is a favorable reduction of the protein's surface-to-volume ratio. The surface-to-volume ratio becomes smaller as the radius of any particle or object becomes larger. (This is because surface area is a function of the radius squared and volume is a function of the radius cubed.) Because interactions within the protein usually tend to stabilize the protein energetically and because the interaction of the protein surface with
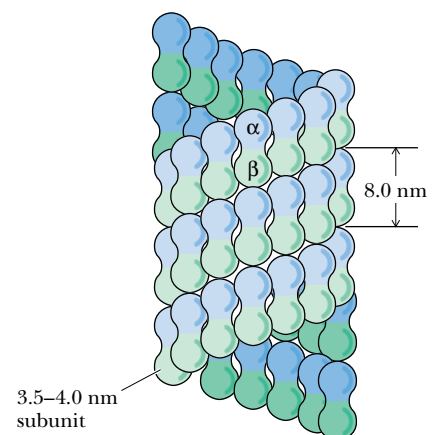
FIGURE 6.47 • The structure of a typical microtubule, showing the arrangement of the α- and β-monomers of the tubulin dimer.

solvent water is often energetically unfavorable, decreased surface-to-volume ratios usually result in more stable proteins. Subunit association may also serve to shield hydrophobic residues from solvent water. Subunits that recognize either themselves or other subunits avoid any errors arising in genetic translation by binding mutant forms of the subunits less tightly.

Genetic Economy and Efficiency

Oligomeric association of protein monomers is genetically economical for an organism. Less DNA is required to code for a monomer that assembles into a homomultimer than for a large polypeptide of the same molecular mass. Another way to look at this is to realize that virtually all of the information that determines oligomer assembly and subunit–subunit interaction is contained in the genetic material needed to code for the monomer. For example, HIV protease, an enzyme that is a dimer of identical subunits, performs a catalytic function similar to homologous cellular enzymes that are single polypeptide chains of twice the molecular mass (Chapter 16).

Bringing Catalytic Sites Together

Many enzymes (see Chapters 14 to 16) derive at least some of their catalytic power from oligomeric associations of monomer subunits. This can happen in several ways. The monomer may not constitute a complete enzyme active site. Formation of the oligomer may bring all the necessary catalytic groups together to form an active enzyme. For example, the active sites of bacterial glutamine synthetase are formed from pairs of adjacent subunits. The dissociated monomers are inactive.

Oligomeric enzymes may also carry out different but related reactions on different subunits. Thus, tryptophan synthase is a tetramer consisting of pairs of different subunits, $\alpha_2\beta_2$. Purified α-subunits catalyze the following reaction:

$$\text{Indoleglycerol phosphate} \rightleftharpoons \text{Indole} + \text{Glyceraldehyde-3-phosphate}$$

and the β-subunits catalyze this reaction:

$$\text{Indole} + \text{L-Serine} \rightleftharpoons \text{L-Tryptophan}$$
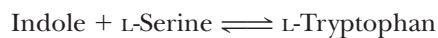
Indole, the product of the α-reaction and the reactant for the β-reaction, is passed directly from the α-subunit to the β-subunit and cannot be detected as a free intermediate.

Cooperativity

There is another, more important reason for monomer subunits to associate into oligomeric complexes. Most oligomeric enzymes regulate catalytic activity by means of subunit interactions, which may give rise to cooperative phenomena. Multisubunit proteins typically possess multiple binding sites for a given ligand. If the binding of ligand at one site changes the affinity of the protein for ligand at the other binding sites, the binding is said to be **cooperative.** Increases in affinity at subsequent sites represent positive cooperativity, whereas decreases in affinity correspond to negative cooperativity. The points of contact between protein subunits provide a mechanism for communication between the subunits. This in turn provides a way in which the binding of ligand to one subunit can influence the binding behavior at the other subunits. Such cooperative behavior, discussed in greater depth in Chapter 15, is the underlying mechanism for regulation of many biological processes.

Faster-Acting Insulin: Genetic Engineering Solves a Quaternary Structure Problem

Insulin is a peptide hormone, secreted by the pancreas, that regulates glucose metabolism in the body. Insufficient production of insulin or failure of insulin to stimulate target sites in liver, muscle, and adipose tissue leads to the serious metabolic disorder known as *diabetes mellitus*. Diabetes afflicts millions of people worldwide. Diabetic individuals typically exhibit high levels of glucose in the blood, but insulin injection therapy allows diabetic individuals to maintain normal levels of blood glucose.

Insulin is composed of two peptide chains covalently linked by disulfide bonds (Figures 5.17 and 6.35). This "monomer" of insulin is the active form that binds to receptors in target cells. However, in solution, insulin spontaneously forms dimers, which themselves aggregate to form hexamers. The surface of the insulin molecule that self-associates to form hexamers is also the surface that binds to insulin receptors in target cells. Thus, hexamers of insulin are inactive.

Insulin released from the pancreas is monomeric and acts rapidly at target tissues. However, when insulin is administered (by injection) to a diabetic patient, the insulin hexamers dissociate slowly, and the patient's blood glucose levels typically drop slowly (over a period of several hours).

In 1988, G. Dodson showed that insulin could be genetically engineered to prefer the monomeric (active) state. Dodson and his colleagues used recombinant DNA technology (discussed in Chapter 13) to produce insulin with an aspartate residue replacing a proline at the contact interface between adjacent subunits. The negative charge on the Asp side chain creates electrostatic repulsion between subunits and increases the dissociation constant for the hexamer $\rightleftarrows$ monomer equilibrium. Injection of this mutant insulin into test animals produced more rapid decreases in blood glucose than did ordinary insulin. The Danish pharmaceutical company Novo is conducting clinical trials of the mutant insulin, which may eventually replace ordinary insulin in treatment of diabetes.

PROBLEMS

1. The central rod domain of a keratin protein is approximately 312 residues in length. What is the length (in Å) of the keratin rod domain? If this same peptide segment were a true α-helix, how long would it be? If the same segment were a β-sheet, what would its length be?

2. A teenager can grow 4 inches in a year during a "growth spurt." Assuming that the increase in height is due to vertical growth of collagen fibers (in bone), calculate the number of collagen helix turns synthesized per minute.

3. Discuss the potential contributions to hydrophobic and van der Waals interactions and ionic and hydrogen bonds for the side chains of Asp, Leu, Tyr, and His in a protein.

4. Figure 6.40 shows that Pro is the amino acid least commonly found in α-helices but most commonly found in β-turns. Discuss the reasons for this behavior.

5. For flavodoxin in Figure 6.32, identify the right-handed crossovers and the left-handed cross-overs in the parallel β-sheet.

6. Choose any three regions in the Ramachandran plot and discuss the likelihood of observing that combination of ϕ and ψ in a peptide or protein. Defend your answer using suitable molecular models of a peptide.

7. A new protein of unknown structure has been purified. Gel filtration chromatography reveals that the native protein has a molecular weight of 240,000. Chromatography in the presence of 6 M guanidine hydrochloride yields only a peak for a protein of M_r 60,000. Chromatography in the presence of 6 M guanidine hydrochloride and 10 mM β-mercaptoethanol yields peaks for proteins of M_r 34,000 and 26,000. Explain what can be determined about the structure of this protein from these data.

8. Two polypeptides, A and B, have similar tertiary structures, but A normally exists as a monomer, whereas B exists as a tetramer, B_4. What differences might be expected in the amino acid composition of A versus B?

9. The hemagglutinin protein in influenza virus contains a remarkably long α-helix, with 53 residues.
a. How long is this α-helix (in nm)?
b. How many turns does this helix have?
c. Each residue in an α-helix is involved in two H bonds. How many H bonds are present in this helix?

FURTHER READING

Abeles, R., Frey, P., and Jencks, W., 1992. *Biochemistry*. Boston: Jones and Bartlett.

Aurora, R., Creamer, T., Srinivasan, R., and Rose, G. D., 1997. Local interactions in protein folding: Lessons from the α-helix. *The Journal of Biological Chemistry* **272:**1413–1416.

Branden, C., and Tooze, J., 1991. *Introduction to Protein Structure*. New York: Garland Publishing, Inc.

Cantor, C. R., and Schimmel, P. R., 1980. *Biophysical Chemistry*, Part I: The Conformation of Biological Macromolecules. New York: W. H. Freeman and Co.

Chothia, C., 1984. Principles that determine the structure of proteins. *Annual Review of Biochemistry* **53:**537–572.

Creighton, T. E., 1983. *Proteins: Structure and Molecular Properties*. New York: W. H. Freeman and Co.

Creighton, T. E., 1997. How important is the molten globule for correct protein folding? *Trends in Biochemical Sciences* **22:**6–11.

Dickerson, R. E., and Geis, I., 1969. *The Structure and Action of Proteins.* New York: Harper and Row.

Dill, K. A., and Chan, H. S., 1997. From Levinthal to pathways to funnels. *Nature Structural Biology* **4:**10–19.

Englander, S. W., and Mayne, L., 1992. Protein folding studied using hydrogen exchange labeling and two-dimensional NMR. *Annual Review of Biophysics and Biomolecular Structure* **21:**243–265.

Hardie, D. G., and Coggins, J. R., eds., 1986. *Multidomain Proteins: Structure and Evolution.* New York: Elsevier.

Harper, E., and Rose, G. D., 1993. Helix stop signals in proteins and peptides: The capping box. *Biochemistry* **32:**7605–7609.

Judson, H. F., 1979. *The Eighth Day of Creation.* New York: Simon and Schuster.

Klotz, I. M., 1996. Equilibrium constants and free energies in unfolding of proteins in urea solutions. *Proceedings of the National Academy of Sciences* **93:**14411–14415.

Klotz, I. M., Langerman, N. R., and Darnell, D. W., 1970. Quaternary structure of proteins. *Annual Review of Biochemistry* **39:**25–62.

Lupas, A., 1996. Coiled coils: New structures and new functions. *Trends in Biochemical Sciences* **21:**375–382.

Petsko, G. A., and Ringe, D., 1984. Fluctuations in protein structure from X-ray diffraction. *Annual Review of Biophysics and Bioengineering* **13:**331–371.

Privalov, P. L., and Makhatadze, G. I., 1993. Contributions of hydration to protein folding thermodynamics. II. The entropy and Gibbs energy of hydration. *Journal of Molecular Biology* **232:**660–679.

Raschke, T. M., and Marqusee, S., 1997. The kinetic folding intermediate of ribonuclease H resembles the acid molten globule and partially unfolded molecules detected under native conditions. *Nature Structural Biology* **4:**298–304.

Richardson, J. S., 1981. The anatomy and taxonomy of protein structure. *Advances in Protein Chemistry* **34:**167–339.

Richardson, J. S., and Richardson, D. C., 1988. Amino acid preferences for specific locations at the ends of α-helices. *Science* **240:**1648–1652.

Rossman, M. G., and Argos, P., 1981. Protein folding. *Annual Review of Biochemistry* **50:**497–532.

Salemme, F. R., 1983. Stuctural properties of protein β-sheets. *Progress in Biophysics and Molecular Biology* **42:**95–133.

Schulze, A. J., Huber, R., Bode, W., and Engh, R. A., 1994. Structural aspects of serpin inhibition. *FEBS Letters* **344:**117–124.

Sifers, R. M., 1995. Defective protein folding as a cause of disease. *Nature Structural Biology* **2:**355–367.

Srinivasan, R., and Rose, G. D., 1995. LINUS: A hierarchic procedure to predict the fold of a protein. *Proteins: Structure, Function and Genetics* **22:**81–99.

Stein, P. E., and Carrell, R. W., 1995. What do dysfunctional serpins tell us about molecular mobility and disease? *Nature Structural Biology* **2:**96–113.

Thomas, P. J., Qu, B.-H., and Pedersen, P. L., 1995. Defective protein folding as a basis of human disease. *Trends in Biochemical Sciences* **20:**456–459.

Torchia, D. A., 1984. Solid state NMR studies of protein internal dynamics. *Annual Review of Biophysics and Bioengineering* **13:**125–144.

Wagner, G., Hyberts, S., and Havel, T., 1992. NMR structure determination in solution: A critique and comparison with X-ray crystallography. *Annual Review of Biophysics and Biomolecular Structure* **21:**167–242.

Xiong, H., Buckwalter, B., Shieh, H.-M., and Hecht, M. H., 1995. Periodicity of polar and nonpolar amino acids is the major determinant of secondary structure in self-assembling oligomeric peptides. *Proceedings of the National Academy of Sciences* **92:**6349–6353.

$\mathcal{C}$hapter 7

Carbohydrates
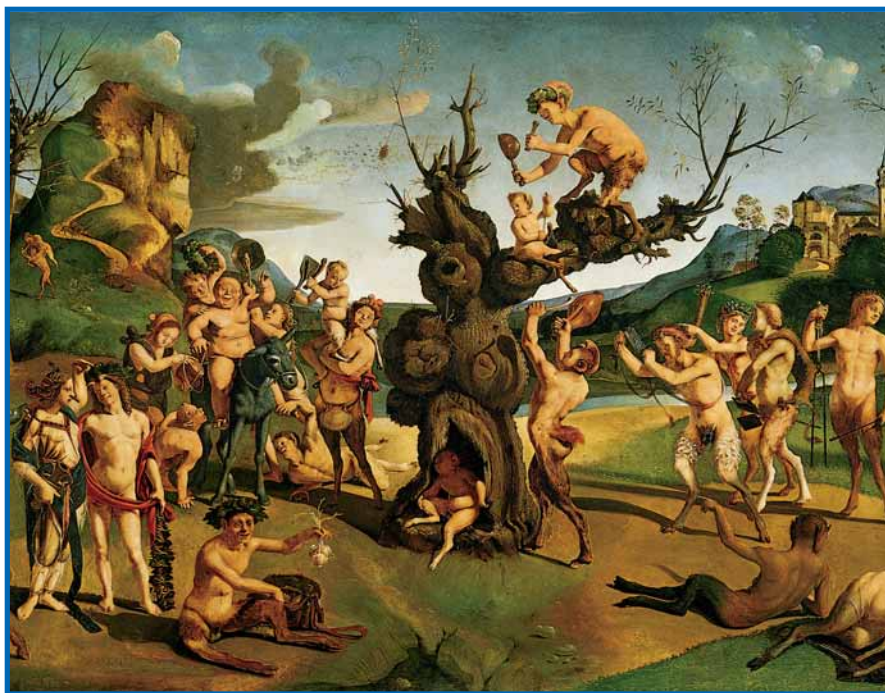
"The Discovery of Honey"—Piero di Cosimo (1462). (Courtesy of the Worcester Art Museum)

$\mathbf{C}$arbohydrates are the single most abundant class of organic molecules found in nature. The name *carbohydrate* arises from the basic molecular formula $(CH_2O)_n$, which can be rewritten $(C \cdot H_2O)_n$ to show that these substances are hydrates of carbon, where $n = 3$ or more. Carbohydrates constitute a versatile class of molecules. Energy from the sun captured by green plants, algae, and some bacteria during photosynthesis (see Chapter 22) is stored in the form of carbohydrates. In turn, carbohydrates are the metabolic precursors of virtually all other biomolecules. Breakdown of carbohydrates provides the energy that sustains animal life. In addition, carbohydrates are covalently linked with a variety of other molecules. Carbohydrates linked to lipid molecules, or **glycolipids,** are common components of biological membranes. Proteins that have covalently linked carbohydrates are called **glycoproteins.** These two classes of biomolecules, together called **glycoconjugates,** are important components of cell walls and extracellular structures in plants, animals, and bacteria. In addition to the structural roles such molecules play, they also serve in a variety of

209

processes involving *recognition* between cell types or recognition of cellular structures by other molecules. Recognition events are important in normal cell growth, fertilization, transformation of cells, and other processes.

All of these functions are made possible by the characteristic chemical features of carbohydrates: (1) the existence of at least one and often two or more asymmetric centers, (2) the ability to exist either in linear or ring structures, (3) the capacity to form polymeric structures via *glycosidic* bonds, and (4) the potential to form multiple hydrogen bonds with water or other molecules in their environment.

7.1 • Carbohydrate Nomenclature

Carbohydrates are generally classified into three groups: **monosaccharides** (and their derivatives), **oligosaccharides,** and **polysaccharides.** The monosaccharides are also called **simple sugars** and have the formula $(CH_2O)_n$. Monosaccharides cannot be broken down into smaller sugars under mild conditions. Oligosaccharides derive their name from the Greek word *oligo,* meaning "few," and consist of from two to ten simple sugar molecules. Disaccharides are common in nature, and trisaccharides also occur frequently. Four- to six-sugar-unit oligosaccharides are usually bound covalently to other molecules, including glycoproteins. As their name suggests, polysaccharides are polymers of the simple sugars and their derivatives. They may be either linear or branched polymers and may contain hundreds or even thousands of monosaccharide units. Their molecular weights range up to 1 million or more.

7.2 • Monosaccharides

Classification

Monosaccharides consist typically of three to seven carbon atoms and are described either as **aldoses** or **ketoses,** depending on whether the molecule contains an aldehyde function or a ketone group. The simplest aldose is glyceraldehyde, and the simplest ketose is dihydroxyacetone (Figure 7.1). These two simple sugars are termed **trioses** because they each contain three carbon atoms. The structures and names of a family of aldoses and ketoses with three, four, five, and six carbons are shown in Figure 7.2 and 7.3. *Hexoses* are the most abundant sugars in nature. Nevertheless, sugars from all these classes are important in metabolism.

Monosaccharides, either aldoses or ketoses, are often given more detailed generic names to describe both the important functional groups and the total number of carbon atoms. Thus, one can refer to *aldotetroses* and *ketotetroses, aldopentoses* and *ketopentoses, aldohexoses* and *ketohexoses,* and so on. Sometimes the ketone-containing monosaccharides are named simply by inserting the letters -ul- into the simple generic terms, such as *tetruloses, pentuloses, hexuloses, heptuloses,* and so on. The simplest monosaccharides are water-soluble, and most taste sweet.

L-isomer   **D-isomer**

Glyceraldehyde   **Dihydroxy-acetone**

FIGURE 7.1 • Structure of a simple aldose (glyceraldehyde) and a simple ketose (dihydroxyacetone).

Stereochemistry

Aldoses with at least three carbons and ketoses with at least four carbons contain **chiral centers** (Chapter 4). The nomenclature for such molecules must specify the **configuration** about each asymmetric center, and drawings of these molecules must be based on a system that clearly specifies these configurations.

ALDOTRIOSE

Carbon number

1 CHO
2 HCOH
3 CH₂OH

ᴅ-Glyceraldehyde

Carbon number

ALDOTETROSES

1 CHO
2 HCOH
3 HCOH
4 CH₂OH

ᴅ-Erythrose

1 CHO
2 HOCH
3 HCOH
4 CH₂OH

ᴅ-Threose

Carbon number

ALDOPENTOSES

1 CHO
2 HCOH
3 HCOH
4 HCOH
5 CH₂OH

ᴅ-Ribose (Rib)

1 CHO
2 HOCH
3 HCOH
4 HCOH
5 CH₂OH

ᴅ-Arabinose (Ara)

1 CHO
2 HCOH
3 HOCH
4 HCOH
5 CH₂OH

ᴅ-Xylose (Xyl)

1 CHO
2 HOCH
3 HOCH
4 HCOH
5 CH₂OH

ᴅ-Lyxose (Lyx)

Carbon number

1 CHO
2 HCOH
3 HCOH
4 HCOH
5 HCOH
6 CH₂OH

ᴅ-Allose

1 CHO
2 HOCH
3 HCOH
4 HCOH
5 HCOH
6 CH₂OH

ᴅ-Altrose

1 CHO
2 HCOH
3 HOCH
4 HCOH
5 HCOH
6 CH₂OH

ᴅ-Glucose (Glc)

1 CHO
2 HOCH
3 HOCH
4 HCOH
5 HCOH
6 CH₂OH

ᴅ-Mannose (Man)

1 CHO
2 HCOH
3 HCOH
4 HOCH
5 HCOH
6 CH₂OH

ᴅ-Gulose

1 CHO
2 HOCH
3 HCOH
4 HOCH
5 HCOH
6 CH₂OH

ᴅ-Idose

1 CHO
2 HCOH
3 HOCH
4 HOCH
5 HCOH
6 CH₂OH

ᴅ-Galactose (Gal)

1 CHO
2 HOCH
3 HOCH
4 HOCH
5 HCOH
6 CH₂OH

ᴅ-Talose

ALDOHEXOSES

FIGURE 7.2 • The structure and stereochemical relationships of ᴅ-aldoses having three to six carbons. The configuration in each case is determined by the highest numbered asymmetric carbon (shown in gray). In each row, the "new" asymmetric carbon is shown in red.

As noted in Chapter 4, the **Fischer projection** system is used almost universally for this purpose today. The structures shown in Figures 7.2 and 7.3 are Fischer projections. For monosaccharides with two or more asymmetric carbons, the prefix ᴅ or ʟ refers to the configuration of the highest numbered asymmetric carbon (the asymmetric carbon farthest from the carbonyl carbon). A monosaccharide is designated ᴅ if the hydroxyl group on the highest numbered asymmetric carbon is drawn to the right in a Fischer projection, as in ᴅ-glyceraldehyde (Figure 7.1). Note that the designation ᴅ or ʟ merely relates the
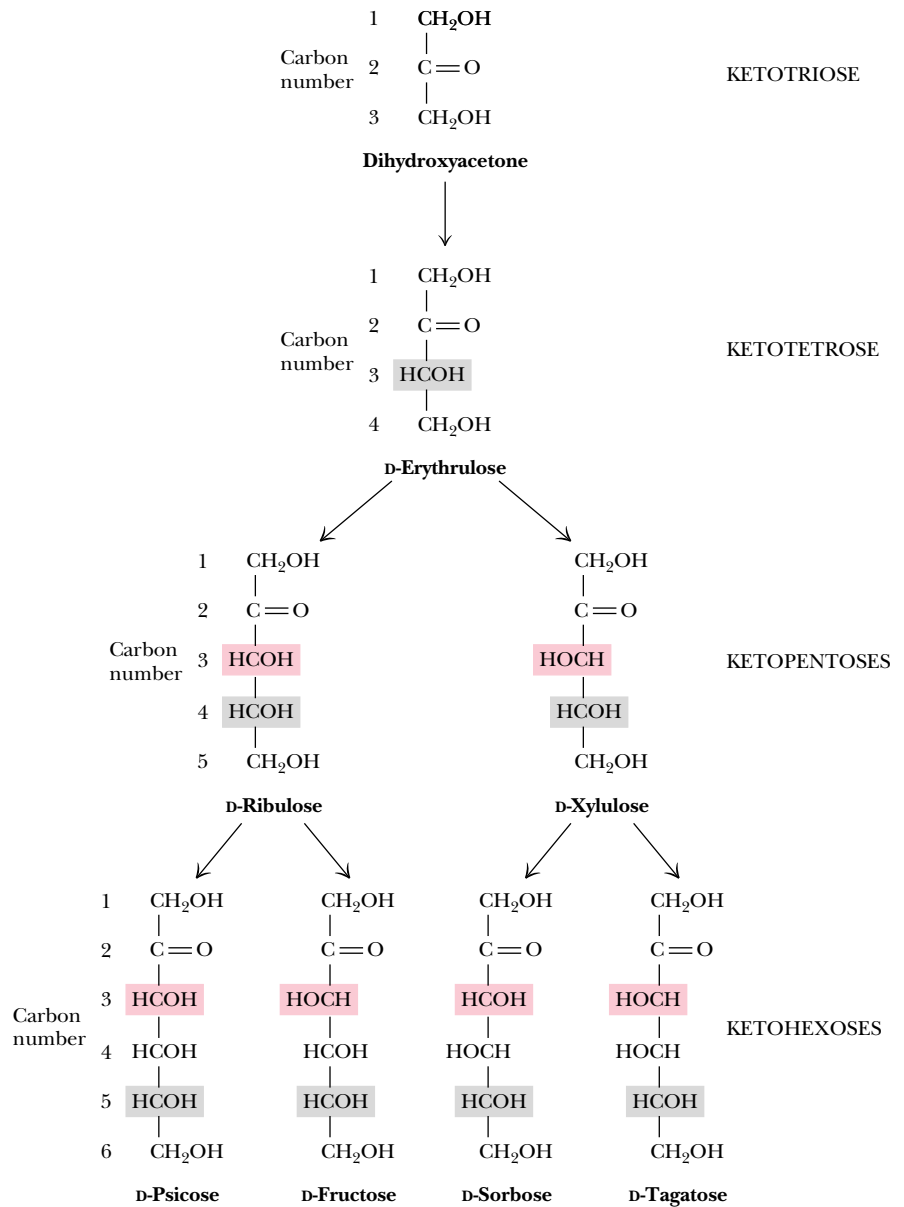
FIGURE 7.3 • The structure and stereochemical relationships of D-ketoses having three to six carbons. The configuration in each case is determined by the highest numbered asymmetric carbon (shown in gray). In each row, the "new" asymmetric carbon is shown in red.

configuration of a given molecule to that of glyceraldehyde and does *not* specify the sign of rotation of plane-polarized light. If the sign of optical rotation is to be specified in the name, the Fischer convention of D or L designations may be used along with a + (plus) or − (minus) sign. Thus, D-glucose (Figure 7.2) may also be called D(+)-glucose because it is dextrorotatory, whereas D-fructose (Figure 7.3), which is levorotatory, can also be named D(−)-fructose.

All of the structures shown in Figures 7.2 and 7.3 are D-configurations, and the D-forms of monosaccharides predominate in nature, just as L-amino acids do. These preferences, established in apparently random choices early in evolution, persist uniformly in nature because of the stereospecificity of the enzymes that synthesize and metabolize these small molecules.

L-Monosaccharides do exist in nature, serving a few relatively specialized roles. L-Galactose is a constituent of certain polysaccharides, and L-arabinose is a constituent of bacterial cell walls.

According to convention, the D- and L-forms of a monosaccharide are *mirror images* of each other, as shown in Figure 7.4 for fructose. Stereoisomers that are mirror images of each other are called **enantiomers,** or sometimes *enantiomeric pairs.* For molecules that possess two or more chiral centers, more than two stereoisomers can exist. Pairs of isomers that have opposite configurations at one or more of the chiral centers but that are not mirror images of each other are called **diastereomers** or *diastereomeric pairs.* Any two structures in a given row in Figures 7.2 and 7.3 are diastereomeric pairs. Two sugars that differ in configuration at *only one* chiral center are described as **epimers.** For example, D-mannose and D-talose are epimers and D-glucose and D-mannose are epimers, whereas D-glucose and D-talose are *not* epimers but merely diastereomers.

FIGURE 7.4 • D-Fructose and L-fructose, an enantiomeric pair. Note that changing the configuration only at C_5 would change D-fructose to L-sorbose.

Cyclic Structures and Anomeric Forms

Although Fischer projections are useful for presenting the structures of particular monosaccharides and their stereoisomers, they ignore one of the most interesting facets of sugar structure—*the ability to form cyclic structures with formation of an additional asymmetric center.* Alcohols react readily with aldehydes to form **hemiacetals** (Figure 7.5). The British carbohydrate chemist Sir Norman Haworth showed that the linear form of glucose (and other aldohexoses) could undergo a similar *intramolecular* reaction to form a *cyclic hemiacetal.* The resulting six-membered, oxygen-containing ring is similar to *pyran* and is designated a **pyranose.** The reaction is catalyzed by acid (H^+) or base (OH^-) and is readily reversible.

FIGURE 7.5

HAWORTH PROJECTION FORMULAS   FISCHER PROJECTION FORMULAS

FIGURE 7.6

In a similar manner, ketones can react with alcohols to form **hemiketals.** The analogous intramolecular reaction of a ketose sugar such as fructose yields a *cyclic hemiketal* (Figure 7.6). The five-membered ring thus formed is reminiscent of *furan* and is referred to as a **furanose.** The cyclic pyranose and furanose forms are the preferred structures for monosaccharides in aqueous solution. At equilibrium, the linear aldehyde or ketone structure is only a minor component of the mixture (generally much less than 1%).

When hemiacetals and hemiketals are formed, the carbon atom that carried the carbonyl function becomes an asymmetric carbon atom. Isomers of monosaccharides that differ only in their configuration about that carbon atom are called **anomers,** designated as α or β, as shown in Figure 7.5, and the carbonyl carbon is thus called the **anomeric carbon.** When the hydroxyl group at the anomeric carbon is on the *same side* of a Fischer projection as the oxygen atom at the highest numbered asymmetric carbon, the configuration at the anomeric carbon is α, as in α-D-glucose. When the anomeric hydroxyl is on the *opposite side* of the Fischer projection, the configuration is β, as in β-D-glucopyranose (Figure 7.5).

The addition of this asymmetric center upon hemiacetal and hemiketal formation alters the optical rotation properties of monosaccharides, and the original assignment of the α and β notations arose from studies of these properties. Early carbohydrate chemists frequently observed that the optical rotation of glucose (and other sugar) solutions could change with time, a process called **mutarotation.** This indicated that a structural change was occurring. It was eventually found that α-D-glucose has a specific optical rotation, $[\alpha]_D^{20}$, of 112.2°, and that β-D-glucose has a specific optical rotation of 18.7°. Mutarotation involves interconversion of α and β forms of the monosaccharide with intermediate formation of the linear aldehyde or ketone, as shown in Figures 7.5 and 7.6.
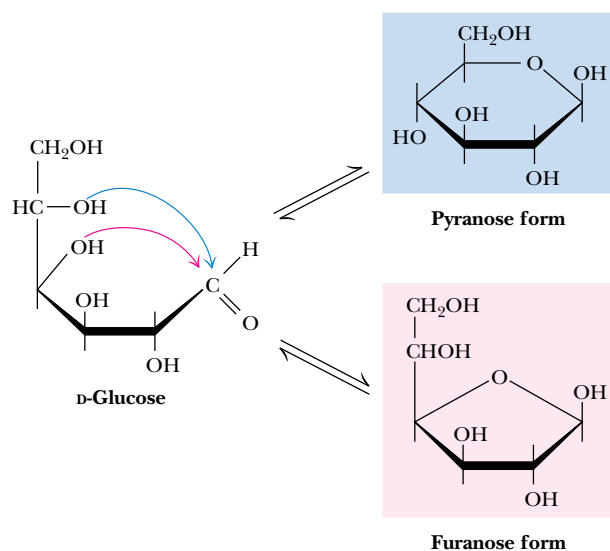
FIGURE 7.7 • D-Glucose can cyclize in two ways, forming either furanose or pyranose structures.

Haworth Projections

Another of Haworth's lasting contributions to the field of carbohydrate chemistry was his proposal to represent pyranose and furanose structures as hexagonal and pentagonal rings lying perpendicular to the plane of the paper, with thickened lines indicating the side of the ring closest to the reader. Such **Haworth projections,** which are now widely used to represent saccharide structures (Figures 7.5 and 7.6), show substituent groups extending either above or below the ring. Substituents drawn to the left in a Fischer projection are drawn above the ring in the corresponding Haworth projection. Substituents drawn to the right in a Fischer projection are below the ring in a Haworth projection. Exceptions to these rules occur in the formation of furanose forms of pentoses and the formation of furanose or pyranose forms of hexoses. In these cases, the structure must be redrawn with a rotation about the carbon whose hydroxyl group is involved in the formation of the cyclic form (Figures 7.7 and 7.8) in order to orient the appropriate hydroxyl group for ring formation. This is
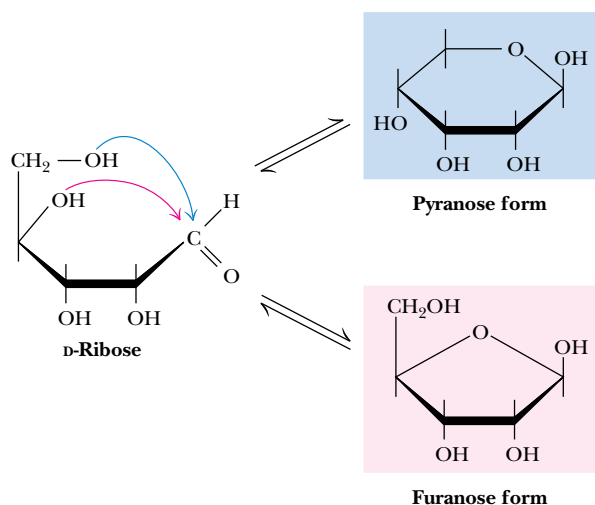
FIGURE 7.8 • D-Ribose and other five-carbon saccharides can form either furanose or pyranose structures.

merely for illustrative purposes and involves no change in configuration of the saccharide molecule.

The rules previously mentioned for assignment of α- and β-configurations can be readily applied to Haworth projection formulas. For the D-sugars, the anomeric hydroxyl group is below the ring in the α-anomer and above the ring in the β-anomer. For L-sugars, the opposite relationship holds.

As Figures 7.7 and 7.8 imply, in most monosaccharides there are two or more hydroxyl groups which can react with an aldehyde or ketone at the other end of the molecule to form a hemiacetal or hemiketal. Consider the possibilities for glucose, as shown in Figure 7.7. If the C-4 hydroxyl group reacts with the aldehyde of glucose, a five-membered ring is formed, whereas if the C-5 hydroxyl reacts, a six-membered ring is formed. The C-6 hydroxyl does not react effectively because a seven-membered ring is too strained to form a stable hemiacetal. The same is true for the C-2 and C-3 hydroxyls, and thus five- and six-membered rings are by far the most likely to be formed from six-membered monosaccharides. D-Ribose, with five carbons, readily forms either five-membered rings (α- or β-D-ribofuranose) or six-membered rings (α- or β-D-ribopyranose) (Figure 7.8). In general, aldoses and ketoses with five or more carbons can form *either* furanose or pyranose rings, and the more stable form depends on structural factors. The nature of the substituent groups on the carbonyl and hydroxyl groups and the configuration about the asymmetric carbon will determine whether a given monosaccharide prefers the pyranose or furanose structure. In general, the pyranose form is favored over the furanose ring for aldohexose sugars, although, as we shall see, furanose structures are more stable for ketohexoses.

Although Haworth projections are convenient for display of monosaccharide structures, they do not accurately portray the conformations of pyranose and furanose rings. Given C—C—C tetrahedral bond angles of 109° and C—O—C angles of 111°, neither pyranose nor furanose rings can adopt true planar structures. Instead, they take on puckered conformations, and in the case of pyranose rings, the two favored structures are the **chair conformation** and the **boat conformation,** shown in Figure 7.9. Note that the ring substituents
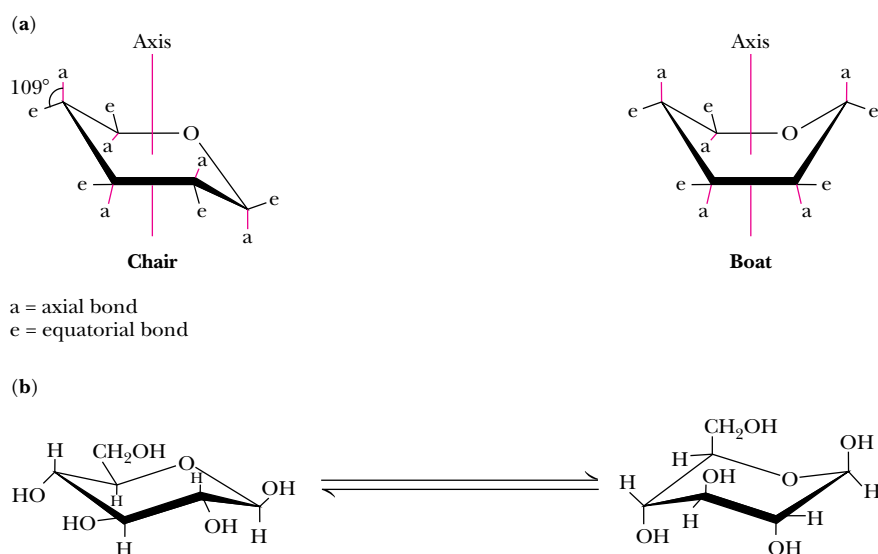
FIGURE 7.9 • (a) Chair and boat conformations of a pyranose sugar. (b) Two possible chair conformations of β-D-glucose.

in these structures can be **equatorial,** which means approximately coplanar with the ring, or **axial,** that is, parallel to an axis drawn through the ring as shown. Two general rules dictate the conformation to be adopted by a given saccharide unit. First, bulky substituent groups on such rings are more stable when they occupy equatorial positions rather than axial positions, and second, chair conformations are slightly more stable than boat conformations. For a typical pyranose, such as β-D-glucose, there are two possible chair conformations (Figure 7.9). Of all the D-aldohexoses, β-D-glucose is the only one that can adopt a conformation with all its bulky groups in an equatorial position. With this advantage of stability, it may come as no surprise that β-D-glucose is the most widely occurring organic group in nature and the central hexose in carbohydrate metabolism.

Derivatives of Monosaccharides

A variety of chemical and enzymatic reactions produce **derivatives** of the simple sugars. These modifications produce a diverse array of saccharide derivatives. Some of the most common derivations are discussed here.

Sugar Acids

Sugars with free anomeric carbon atoms are reasonably good reducing agents and will reduce hydrogen peroxide, ferricyanide, certain metals (Cu^{2+} and Ag^+), and other oxidizing agents. Such reactions convert the sugar to a **sugar acid.** For example, addition of alkaline $CuSO_4$ (called *Fehling's solution*) to an aldose sugar produces a red cuprous oxide (Cu_2O) precipitate:

$$\underset{\textbf{Aldehyde}}{\overset{\displaystyle \overset{O}{\underset{\|}{}}}{RC-H}} + 2\ Cu^{2+} + 5\ OH^- \longrightarrow \underset{\textbf{Carboxylate}}{\overset{\displaystyle \overset{O}{\underset{\|}{}}}{RC-O^-}} + Cu_2O\!\downarrow + 3\ H_2O$$
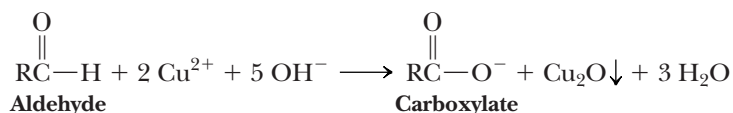
and converts the aldose to an **aldonic acid,** such as **gluconic acid** (Figure 7.10). Formation of a precipitate of red Cu_2O constitutes a positive test for an aldehyde. Carbohydrates that can reduce oxidizing agents in this way are referred to as **reducing sugars.** By quantifying the amount of oxidizing agent reduced by a sugar solution, one can accurately determine the concentration of the sugar. *Diabetes mellitus* is a condition that causes high levels of glucose in urine and blood, and frequent analysis of reducing sugars in diabetic patients is an important part of the diagnosis and treatment of this disease. Over-the-counter kits for the easy and rapid determination of reducing sugars have made this procedure a simple one for diabetics.

Monosaccharides can be oxidized enzymatically at C-6, yielding **uronic acids,** such as **D-glucuronic** and **L-iduronic** acids (Figure 7.10). L-Iduronic acid is similar to D-glucuronic acid, except for having an opposite configuration at C-5. Oxidation at both C-1 and C-6 produces **aldaric acids,** such as **D-glucaric acid.**

Sugar Alcohols

Sugar alcohols, another class of sugar derivative, can be prepared by the mild reduction (with $NaBH_4$ or similar agents) of the carbonyl groups of aldoses and ketoses. Sugar alcohols, or **alditols,** are designated by the addition of *-itol* to the name of the parent sugar (Figure 7.11). The alditols are linear molecules that cannot cyclize in the manner of aldoses. Nonetheless, alditols are characteristically sweet tasting, and **sorbitol, mannitol,** and **xylitol** are widely used to sweeten sugarless gum and mints. Sorbitol buildup in the eyes of dia-

FIGURE 7.10

D-Gluconic acid

D-Gluconic acid

D-δ-Gluconolactone

Note: D-Gluconic acid and other aldonic acids exist in equilibrium with lactone structures.

Oxidation at C–1

D-Glucose

Oxidation at C–6

D-Glucuronic acid (GlcUA)

L-Iduronic acid (IdUA)

Oxidation at C–1 and C–6

D-Glucaric acid
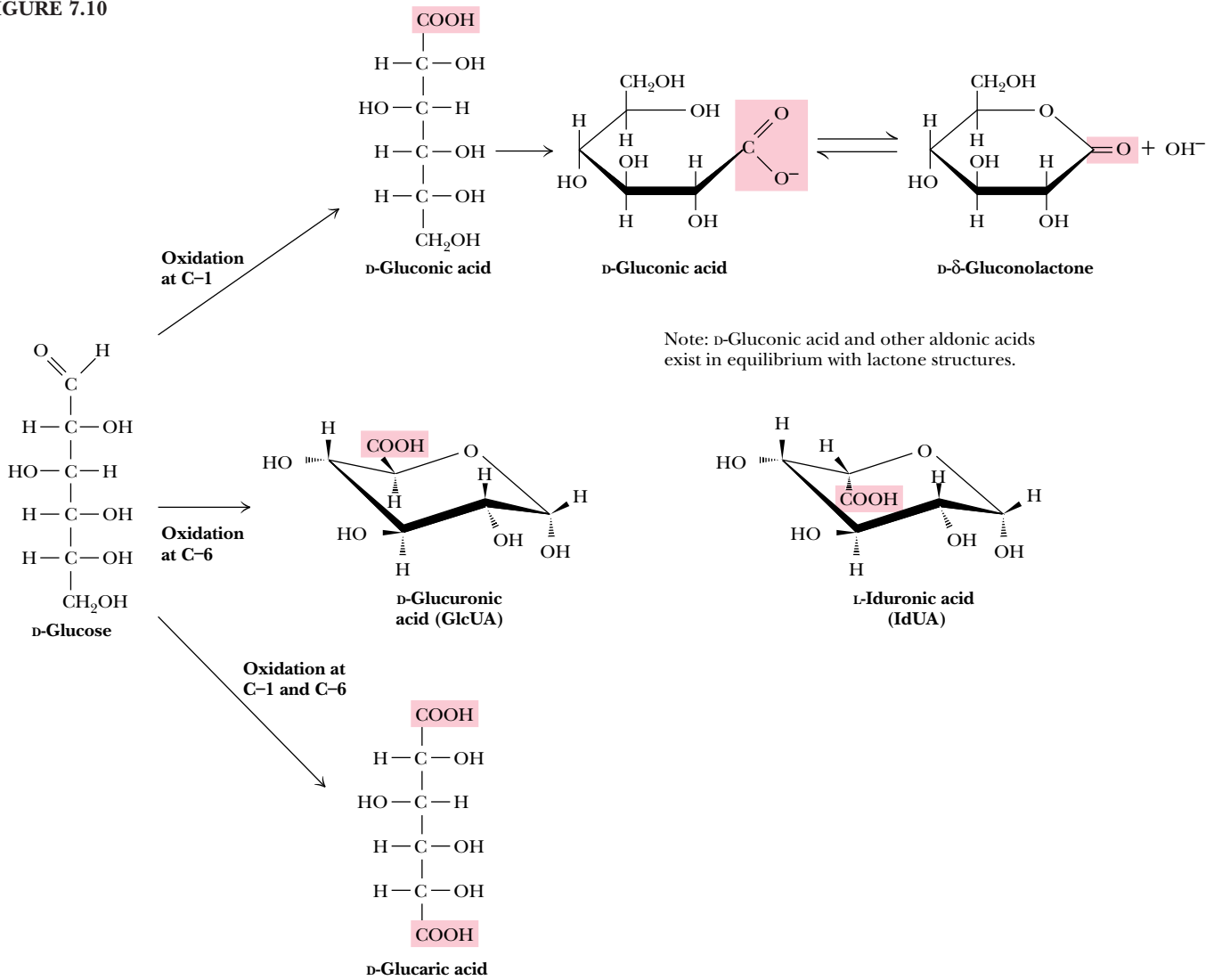
FIGURE 7.11 • Structures of some sugar alcohols.

D-Glucitol (sorbitol)

D-Mannitol

D-Xylitol

D-Glycerol

myo-**Inositol**

D-Ribitol
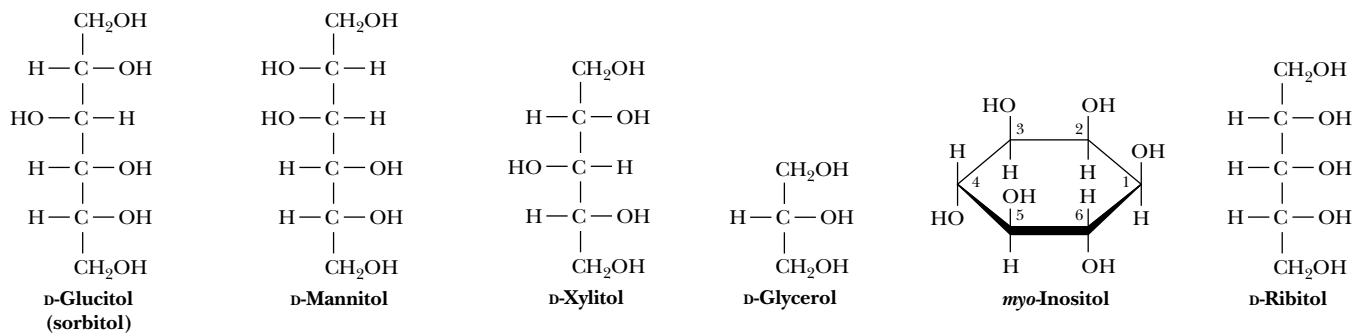
betics is implicated in cataract formation. **Glycerol** and ***myo*-inositol,** a cyclic alcohol, are components of lipids (see Chapter 8). There are nine different stereoisomers of inositol; the one shown in Figure 7.11 was first isolated from heart muscle and thus has the prefix *myo*- for muscle. **Ribitol** is a constituent of flavin coenzymes (see Chapter 20).
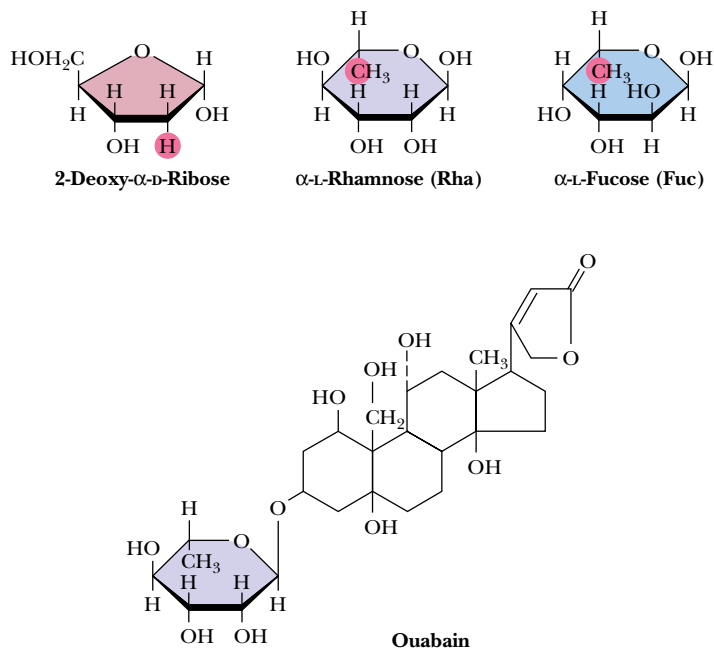
FIGURE 7.12 • Several deoxy sugars and ouabain, which contains α-ʟ-rhamnose (Rha). Hydrogen atoms highlighted in red are "deoxy" positions.

Deoxy Sugars

The **deoxy sugars** are monosaccharides with one or more hydroxyl groups replaced by hydrogens. 2-Deoxy-ᴅ-ribose (Figure 7.12), whose systematic name is 2-deoxy-ᴅ-erythropentose, is a constituent of DNA in all living things (see Chapter 11). Deoxy sugars also occur frequently in glycoproteins and polysaccharides. ʟ-Fucose and ʟ-rhamnose, both 6-deoxy sugars, are components of some cell walls, and rhamnose is a component of **ouabain,** a highly toxic *cardiac glycoside* found in the bark and root of the ouabaio tree. Ouabain is used by the East African Somalis as an arrow poison. The sugar moiety is not the toxic part of the molecule (see Chapter 10).

Sugar Esters

Phosphate esters of glucose, fructose, and other monosaccharides are important metabolic intermediates, and the ribose moiety of nucleotides such as ATP and GTP is phosphorylated at the 5′-position (Figure 7.13).
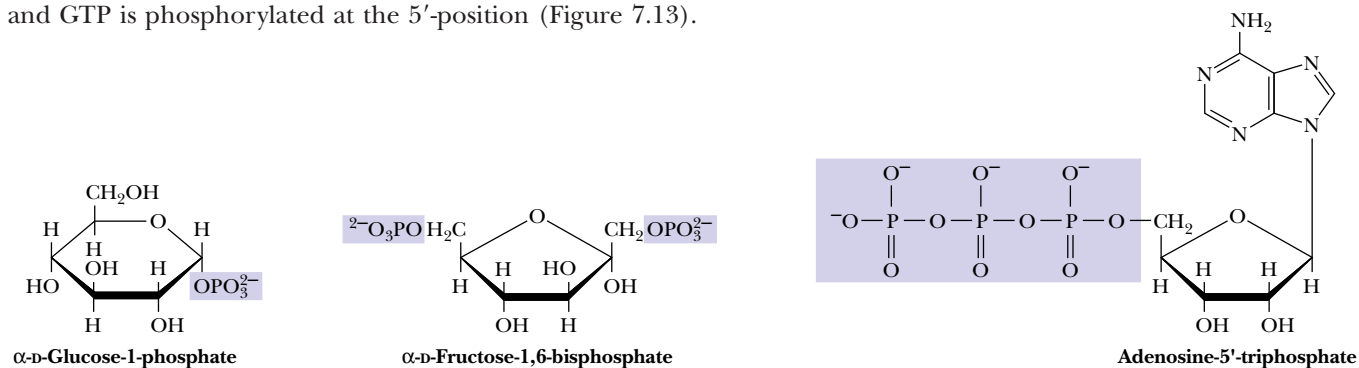
FIGURE 7.13 • Several sugar esters important in metabolism.
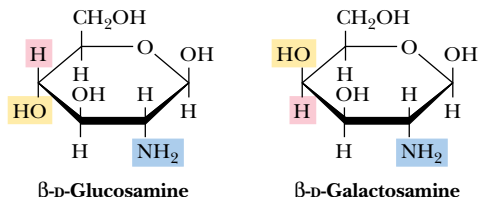
FIGURE 7.14 • Structures of D-glucosamine and D-galactosamine.

Amino Sugars

Amino sugars, including **D-glucosamine** and **D-galactosamine** (Figure 7.14), contain an amino group (instead of a hydroxyl group) at the C-2 position. They are found in many oligo- and polysaccharides, including *chitin,* a polysaccharide in the exoskeletons of crustaceans and insects.

Muramic acid and **neuraminic acid,** which are components of the polysaccharides of cell membranes of higher organisms and also bacterial cell walls, are glucosamines linked to three-carbon acids at the C-1 or C-3 positions. In muramic acid (thus named as an *ami*ne isolated from bacterial cell wall polysaccharides; *murus* is Latin for "wall"), the hydroxyl group of a lactic acid moiety makes an ether linkage to the C-3 of glucosamine. Neuraminic acid (an *ami*ne isolated from *neu*ral tissue) forms a C—C bond between the C-1 of *N*-acetylmannosamine and the C-3 of pyruvic acid (Figure 7.15). The *N*-acetyl and *N*-glycolyl derivatives of neuraminic acid are collectively known as **sialic acids** and are distributed widely in bacteria and animal systems.

Muramic acid

N-Acetyl-D-neuraminic acid (NeuNAc)

Pyruvic acid

N-Acetylmannosamine

Fischer projection

Haworth projection

Chair conformation

N-Acetyl-D-neuraminic acid (NeuNAc), a sialic acid
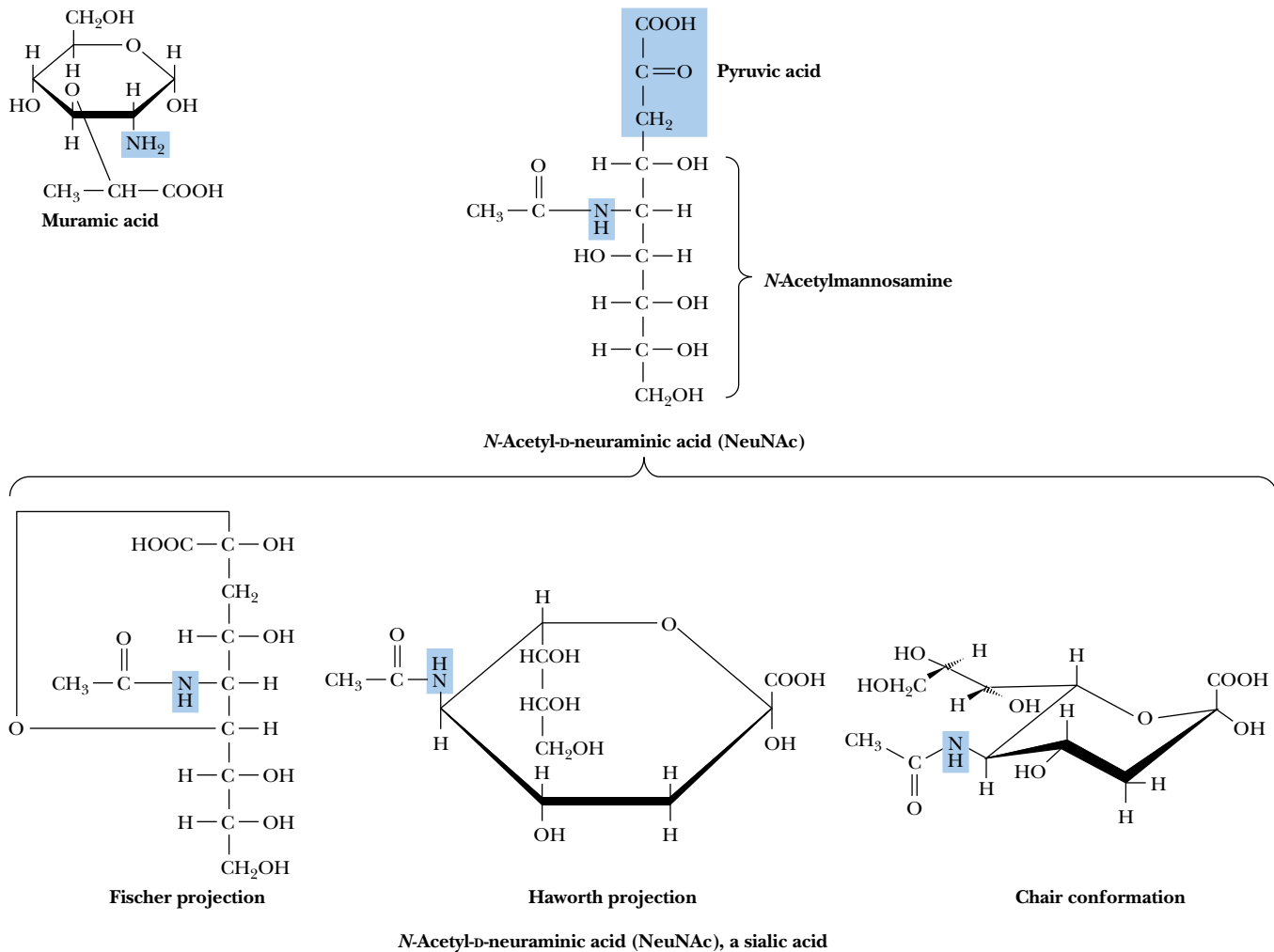
FIGURE 7.15 • Structures of muramic acid and neuraminic acid and several depictions of sialic acid.
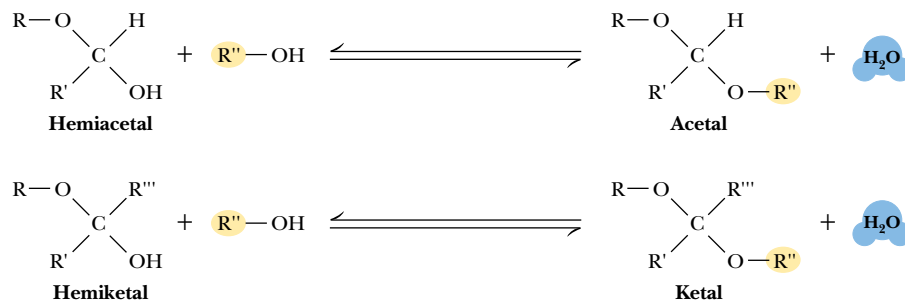
FIGURE 7.16 • Acetals and ketals can be formed from hemiacetals and hemiketals, respectively.

Acetals, Ketals, and Glycosides

Hemiacetals and hemiketals can react with alcohols in the presence of acid to form **acetals** and **ketals,** as shown in Figure 7.16. This reaction is another example of a *dehydration synthesis* and is similar in this respect to the reactions undergone by amino acids to form peptides and nucleotides to form nucleic acids. The pyranose and furanose forms of monosaccharides react with alcohols in this way to form **glycosides** with retention of the α- or β-configuration at the C-1 carbon. The new bond between the anomeric carbon atom and the oxygen atom of the alcohol is called a **glycosidic bond.** Glycosides are named according to the parent monosaccharide. For example, *methyl-β-D-glucoside* (Figure 7.17) can be considered a derivative of β-D-glucose.

7.3 • Oligosaccharides

Given the relative complexity of oligosaccharides and polysaccharides in higher organisms, it is perhaps surprising that these molecules are formed from relatively few different monosaccharide units. (In this respect, the oligo- and polysaccharides are similar to proteins; both form complicated structures based on a small number of different building blocks.) Monosaccharide units include the hexoses glucose, fructose, mannose, and galactose and the pentoses ribose and xylose.

Disaccharides

The simplest oligosaccharides are the **disaccharides,** which consist of two monosaccharide units linked by a glycosidic bond. As in proteins and nucleic acids, each individual unit in an oligosaccharide is termed a *residue.* The disaccharides shown in Figure 7.18 are all commonly found in nature, with sucrose, maltose, and lactose being the most common. Each is a mixed acetal, with one hydroxyl group provided intramolecularly and one hydroxyl from the other monosaccharide. Except for sucrose, each of these structures possesses one free unsubstituted anomeric carbon atom, and thus each of these disaccharides is a reducing sugar. The end of the molecule containing the free anomeric carbon is called the **reducing end,** and the other end is called the **nonreducing end.** In the case of sucrose, both of the anomeric carbon atoms are substituted, that is, neither has a free —OH group. The substituted anomeric carbons cannot be converted to the aldehyde configuration and thus cannot participate in

Methyl-α-D-glucoside

Methyl-β-D-glucoside
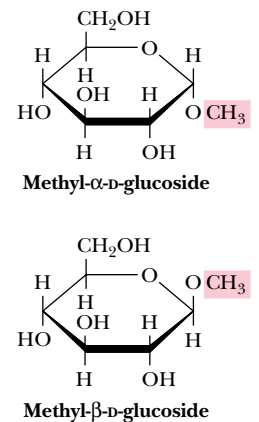
FIGURE 7.17 • The anomeric forms of methyl-D-glucoside.

Free anomeric carbon
(reducing end)

Lactose (galactose-β-1,4-glucose)

Maltose (glucose-α-1,4-glucose)

Sucrose (glucose-α-1,2-fructose)

Cellobiose (glucose-β-1,4-glucose)

Isomaltose (glucose-α-1,6-glucose)

Simple sugars

Glucose

Galactose
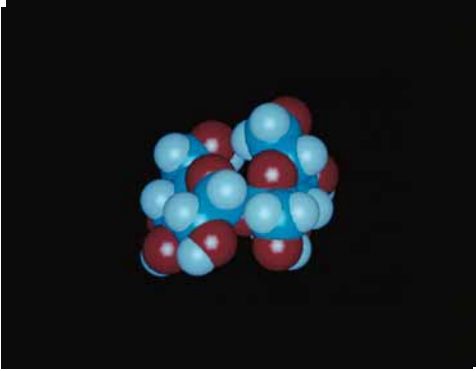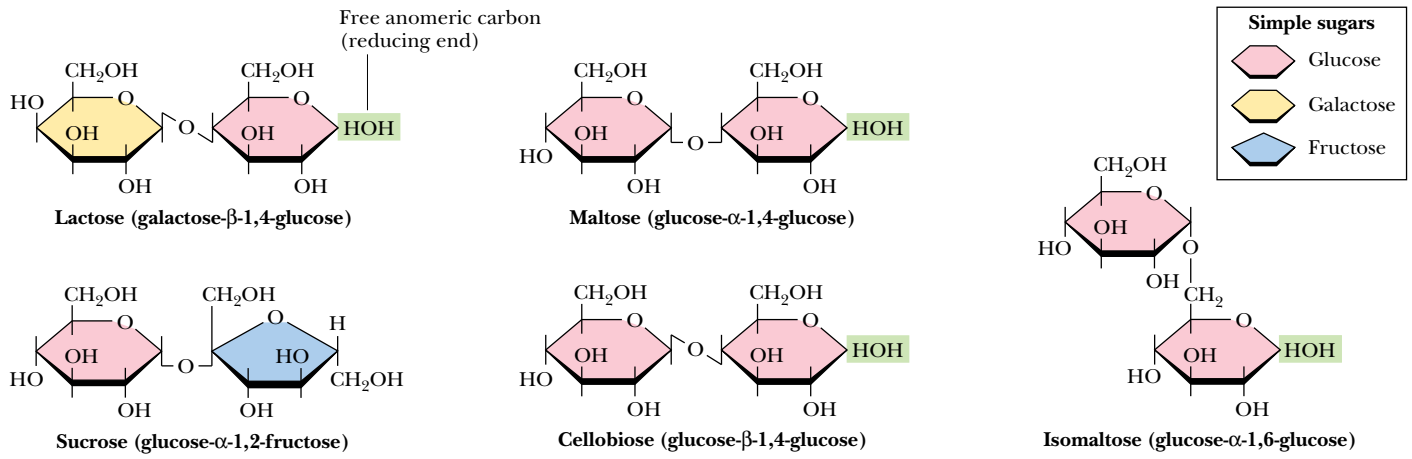
Fructose

FIGURE 7.18 • The structures of several important disaccharides. Note that the notation —HOH means that the configuration can be either α or β. If the —OH group is above the ring, the configuration is termed β. The configuration is α if the —OH group is below the ring as shown. Also note that sucrose has no free anomeric carbon atoms.

Sucrose

the oxidation–reduction reactions characteristic of reducing sugars. Thus, sucrose is *not* a reducing sugar.

Maltose, isomaltose, and cellobiose are all **homodisaccharides** because they each contain only one kind of monosaccharide, namely, glucose. **Maltose** is produced from starch (a polymer of α-D-glucose produced by plants) by the action of amylase enzymes and is a component of malt, a substance obtained by allowing grain (particularly barley) to soften in water and germinate. The enzyme **diastase,** produced during the germination process, catalyzes the hydrolysis of starch to maltose. Maltose is used in beverages (malted milk, for example), and because it is fermented readily by yeast, it is important in the brewing of beer. In both maltose and cellobiose, the glucose units are **1→4 linked,** meaning that the C-1 of one glucose is linked by a glycosidic bond to the C-4 oxygen of the other glucose. The only difference between them is in the configuration at the glycosidic bond. Maltose exists in the α-configuration, whereas cellobiose is β. **Isomaltose** is obtained in the hydrolysis of some polysaccharides (such as dextran), and **cellobiose** is obtained from the acid hydrolysis of cellulose. Isomaltose also consists of two glucose units in a glycosidic bond, but in this case, C-1 of one glucose is linked to C-6 of the other, and the configuration is α.

The complete structures of these disaccharides can be specified in shorthand notation by using abbreviations for each monosaccharide, α or β, to denote configuration, and appropriate numbers to indicate the nature of the linkage. Thus, cellobiose is Glcβ1–4Glc, whereas isomaltose is Glcα1–6Glc. Often the glycosidic linkage is written with an arrow so that cellobiose and isomaltose would be Glcβ1→4Glc and Glcα1→6Glc, respectively. Because the linkage carbon on the first sugar is always C-1, a newer trend is to drop the 1- or

A DEEPER LOOK

Trehalose—A Natural Protectant for Bugs

Insects use an open circulatory system to circulate **hemolymph** (insect blood). The "blood sugar" is not glucose but rather **trehalose,** an unusual, nonreducing disaccharide (see Figure). Trehalose is found typically in organisms that are naturally subject to temperature variations and other environmental stresses—bacterial spores, fungi, yeast, and many insects. (Interestingly, honeybees do not have trehalose in their hemolymph, perhaps because they practice a colonial, rather than solitary, lifestyle. Bee colonies maintain a rather constant temperature of 18°C, protecting the residents from large temperature changes.)

What might explain this correlation between trehalose utilization and environmentally stressful lifestyles? Konrad Bloch* suggests that trehalose may act as a natural cryoprotectant. Freezing and thawing of biological tissues frequently causes irreversible structural changes, destroying biological activity. High concentrations of polyhydroxy compounds, such as sucrose and glycerol, can protect biological materials from such damage.

Trehalose is particularly well-suited for this purpose and has been shown to be superior to other polyhydroxy compounds, especially at low concentrations. Support for this novel idea comes from studies by P. A. Attfield,[†] which show that trehalose levels in the yeast *Saccharomyces cerevisiae* increase significantly during exposure to high salt and high growth temperatures—the same conditions that elicit the production of heat-shock proteins!
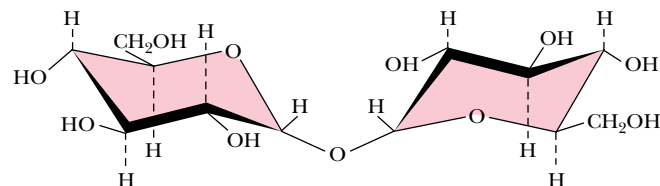
*Bloch, K., 1994. *Blondes in Venetian Paintings, the Nine-Banded Armadillo, and Other Essays in Biochemistry.* New Haven: Yale University Press.
[†]Attfield, P. A., 1987. Trehalose accumulates in *Saccharomyces cerevisiae* during exposure to agents that induce heat shock responses. *FEBS Letters* **225:**259.

1→ and describe these simply as Glcβ4Glc and Glcα6Glc, respectively. More complete names can also be used, however, so that maltose would be O-α-D-glucopyranosyl-(1→4)-D-glucopyranose. Cellobiose, because of its β-glycosidic linkage, is formally O-β-D-glucopyranosyl-(1→4)-D-glucopyranose.

β-D-lactose (O-β-D-Galactopyranosyl-(1→4)-D-glucopyranose) (Figure 7.18) is the principal carbohydrate in milk and is of critical nutritional importance to mammals in the early stages of their lives. It is formed from D-galactose and D-glucose via a β(1→4) link, and because it has a free anomeric carbon, it is capable of mutarotation and is a reducing sugar. It is an interesting quirk of nature that lactose cannot be absorbed directly into the bloodstream. It must first be broken down into galactose and glucose by **lactase,** an intestinal enzyme that exists in young, nursing mammals but is not produced in significant quantities in the mature mammal. Most humans, with the exception of certain groups in Africa and northern Europe, produce only low levels of lactase. For most individuals, this is not a problem, but some cannot tolerate lactose and experience intestinal pain and diarrhea upon consumption of milk.

Sucrose, in contrast, is a disaccharide of almost universal appeal and tolerance. Produced by many higher plants and commonly known as *table sugar,* it is one of the products of photosynthesis and is composed of fructose and glucose. Sucrose has a specific optical rotation, $[\alpha]_D^{20}$, of +66.5°, but an equimolar mixture of its component monosaccharides has a net negative rotation ($[\alpha]_D^{20}$ of glucose is +52.5° and of fructose is −92°). Sucrose is hydrolyzed by the enzyme **invertase,** so named for the inversion of optical rotation accompanying this reaction. Sucrose is also easily hydrolyzed by dilute acid, apparently because the fructose in sucrose is in the relatively unstable furanose form. Although sucrose and maltose are important to the human diet, they are not taken up directly in the body. In a manner similar to lactose, they are first hydrolyzed by **sucrase** and **maltase,** respectively, in the human intestine.

𝒜 D E E P E R   L O O K

Honey—An Ancestral Carbohydrate Treat

Honey, the first sweet known to humankind, is the only sweetening agent that can be stored and used exactly as produced in nature. Bees process the nectar of flowers so that their final product is able to survive long-term storage at ambient temperature. Used as a ceremonial material and medicinal agent in earliest times, honey was not regarded as a food until the Greeks and Romans. Only in modern times have cane and beet sugar surpassed honey as the most frequently used sweetener. What is the chemical nature of this magical, viscous substance?

The bees' processing of honey consists of (1) reducing the water content of the nectar (30 to 60%) to the self-preserving range of 15 to 19%, (2) hydrolyzing the significant amount of sucrose in nectar to glucose and fructose by the action of the enzyme invertase, and (3) producing small amounts of gluconic acid from glucose by the action of the enzyme **glucose oxidase.** Most of the sugar in the final product is glucose and fructose, and the final product is supersaturated with respect to these monosaccharides. Honey actually consists of an emulsion of microscopic glucose hydrate and fructose hydrate crystals in a thick syrup. Sucrose accounts for only about 1% of the sugar in the final product, with fructose at about 38% and glucose at 31% by weight.

The figure shows a ^{13}C nuclear magnetic resonance spectrum of honey from a mixture of wildflowers in southeastern Pennsylvania. Interestingly, five major hexose species contribute to this spectrum. Although most textbooks show fructose exclusively in its furanose form, the predominant form of fructose (67% of total fructose) is β-D-fructopyranose, with the β- and α-fructofuranose forms accounting for 27% and 6% of the fructose, respectively. In polysaccharides, fructose invariably prefers the furanose form, but free fructose (and crystalline fructose) is predominantly β-fructopyranose.

α-D-Fructopyranose

β-D-Fructopyranose

α-D-Fructofuranose

β-D-Fructofuranose

Honey

α-D-Glucopyranose
β-D-Glucopyranose
α-D-Fructofuranose
β-D-Fructofuranose
β-D-Fructopyranose
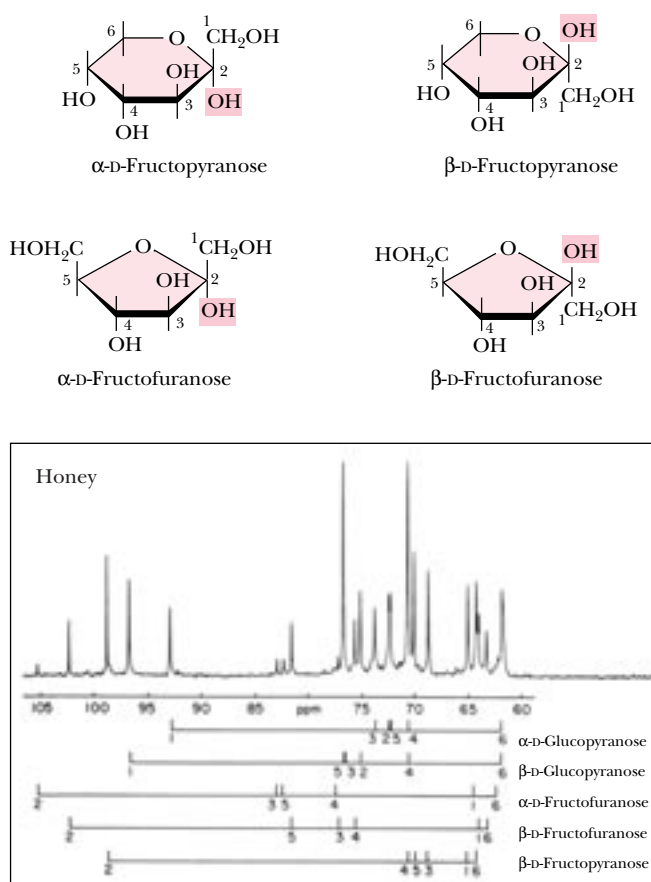
White, J. W., 1978. Honey. *Advances in Food Research* **24:**287–374.

Prince, R. C., Gunson, D. E., Leigh, J. S., and McDonald, G. G., 1982. The predominant form of fructose is a pyranose, not a furanose ring. *Trends in Biochemical Sciences* **7:**239–240.

Melezitose (a constituent of honey)
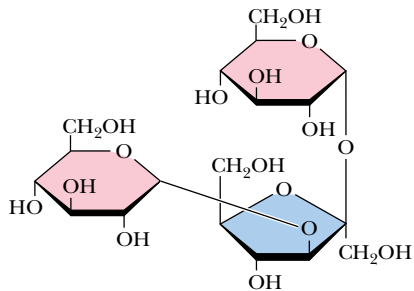
Amygdalin (occurs in seeds of *Rosaceae*; glycoside of bitter almonds, in kernels of cherries, peaches, apricots)
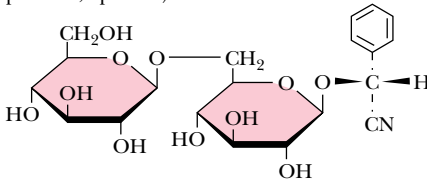
Laetrile (claimed to be an anticancer agent, but there is no rigorous scientific evidence for this)

Cycloheptaamylose (a breakdown product of starch; useful in chromatographic separations)

Stachyose (a constituent of many plants: white jasmine, yellow lupine, soybeans, lentils, etc.; causes flatulence since humans cannot digest it)
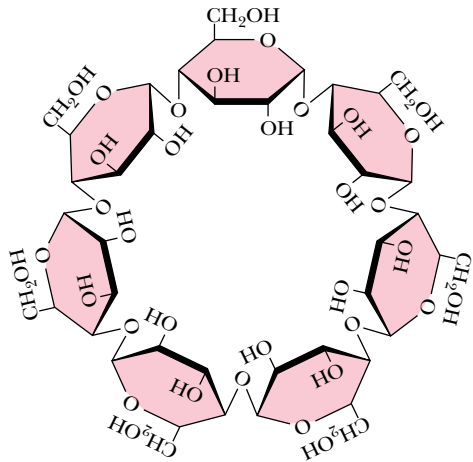
Dextrantriose (a constituent of saké and honeydew)
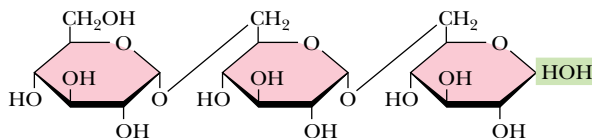
FIGURE 7.19 • The structures of some interesting oligosaccharides.

Higher Oligosaccharides

In addition to the simple disaccharides, many other oligosaccharides are found in both prokaryotic and eukaryotic organisms, either as naturally occurring substances or as hydrolysis products of natural materials. Figure 7.19 lists a number of simple oligosaccharides, along with descriptions of their origins and interesting features. Several are constituents of the sweet nectars or saps exuded or extracted from plants and trees. One particularly interesting and useful group of oligosaccharides is the **cycloamyloses.** These oligosaccharides are cyclic structures, and in solution they form molecular "pockets" of various diameters. These pockets are surrounded by the chiral carbons of the saccharides themselves and are able to form stereospecific inclusion complexes with chiral molecules that can fit into the pockets. Thus, mixtures of stereoisomers of small organic molecules can be separated into pure isomers on columns of **cycloheptaamylose,** for example.

Stachyose is typical of the oligosaccharide components found in substantial quantities in beans, peas, bran, and whole grains. These oligosaccharides are not digested by stomach enzymes, but *are* metabolized readily by bacteria in the intestines. This is the source of the flatulence that often accompanies the consumption of such foods. Commercial products are now available that assist in the digestion of the gas-producing components of these foods. These products contain an enzyme that hydrolyzes the culprit oligosaccharides in the stomach before they become available to intestinal microorganisms.
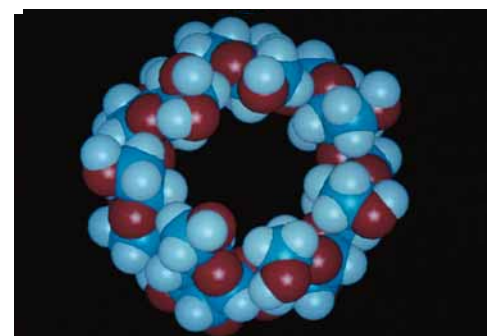
Cycloheptaamylose
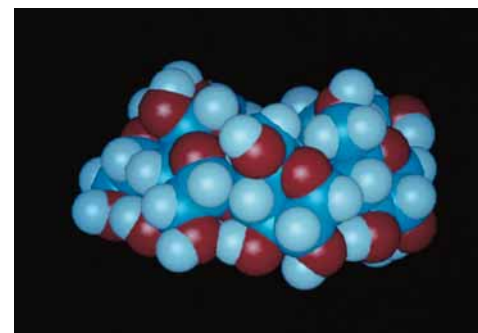
Cycloheptaamylose (side view)

225

Another notable glycoside is **amygdalin,** which occurs in bitter almonds and in the kernels or pits of cherries, peaches, and apricots. Hydrolysis of this substance and subsequent oxidation yields **laetrile,** which has been claimed by some to have anticancer properties. There is no scientific evidence for these claims, and the U.S. Food and Drug Administration has never approved laetrile for use in the United States.

Oligosaccharides also occur widely as components (via glycosidic bonds) of *antibiotics* derived from various sources. Figure 7.20 shows the structures of a few representative carbohydrate-containing antibiotics. Some of these antibiotics also show antitumor activity. One of the most important of this type is **bleomycin A$_2$,** which is used clinically against certain tumors.

Bleomycin A$_2$ (an antitumor agent used clinically against specific tumors)

Aburamycin C (an antibiotic and antitumor agent)

Sulfurmycin B (active against Gram-positive bacteria, mycobacteria, and tumors)

Streptomycin (a broad spectrum antibiotic)
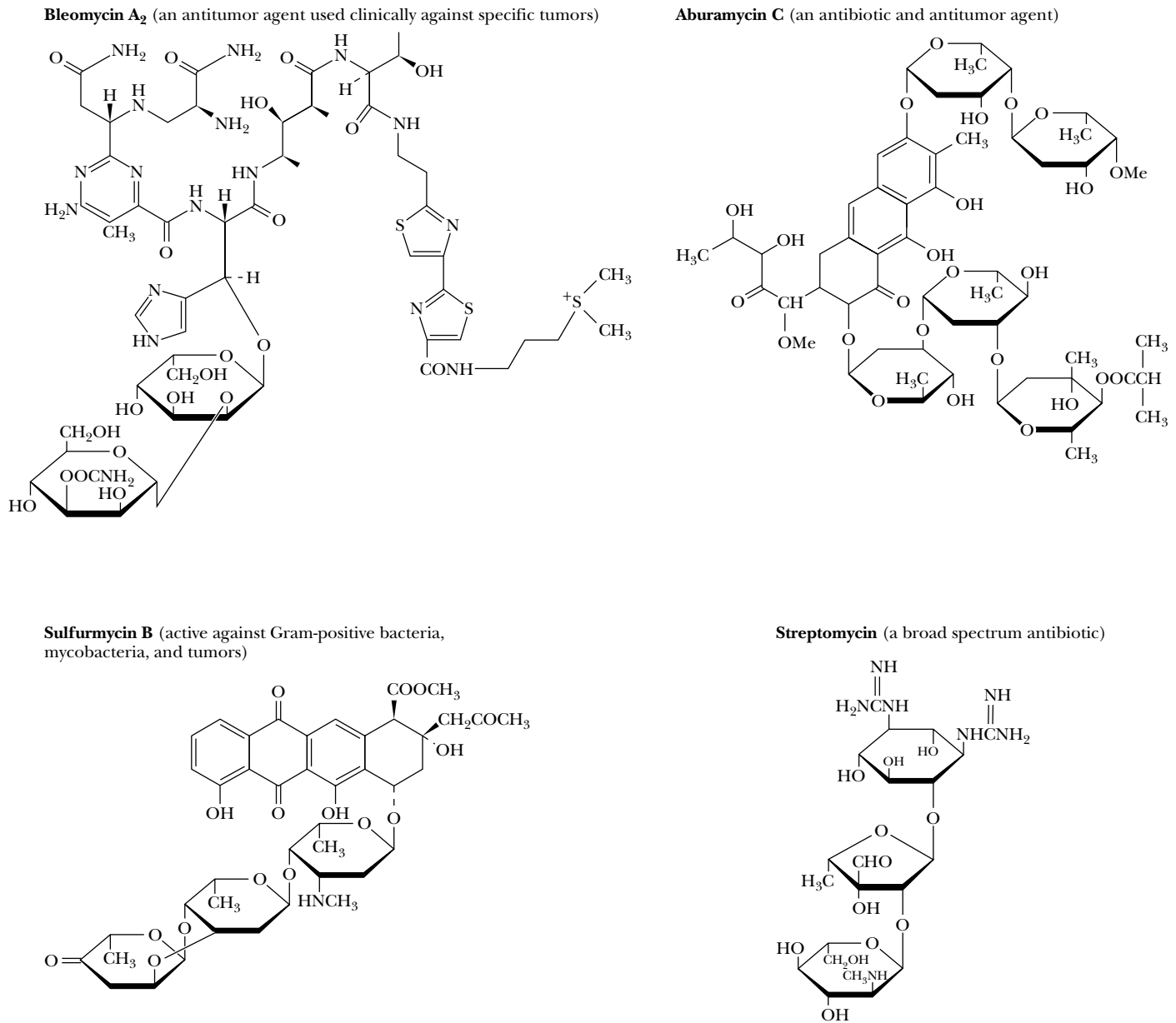
FIGURE 7.20 • Some antibiotics are oligosaccharides or contain oligosaccharide groups.

7.4 • Polysaccharides

Structure and Nomenclature

By far the majority of carbohydrate material in nature occurs in the form of polysaccharides. By our definition, polysaccharides include not only those substances composed only of glycosidically linked sugar residues but also molecules that contain polymeric saccharide structures linked via covalent bonds to amino acids, peptides, proteins, lipids, and other structures.

Polysaccharides, also called **glycans,** consist of monosaccharides and their derivatives. If a polysaccharide contains only one kind of monosaccharide molecule, it is a **homopolysaccharide,** or **homoglycan,** whereas those containing more than one kind of monosaccharide are **heteropolysaccharides.** The most common constituent of polysaccharides is D-glucose, but D-fructose, D-galactose, L-galactose, D-mannose, L-arabinose, and D-xylose are also common. Common monosaccharide derivatives in polysaccharides include the amino sugars (D-glucosamine and D-galactosamine), their derivatives (*N*-acetylneuraminic acid and *N*-acetylmuramic acid), and simple sugar acids (glucuronic and iduronic acids). Homopolysaccharides are often named for the sugar unit they contain, so that glucose homopolysaccharides are called **glucans,** while mannose homopolysaccharides are **mannans.** Other homopolysaccharide names are just as obvious: *galacturonans, arabinans,* and so on. Homopolysaccharides of uniform linkage type are often named by including notation to denote ring size and linkage type. Thus, cellulose is a *(1→4)-β-D-glucopyranan.* Polysaccharides differ not only in the nature of their component monosaccharides but also in the length of their chains and in the amount of chain branching that occurs. Although a given sugar residue has only one anomeric carbon and thus can form only one glycosidic linkage with hydroxyl groups on other molecules, each sugar residue carries several hydroxyls, one or more of which may be an acceptor of glycosyl substituents (Figure 7.21). This ability to form branched structures distinguishes polysaccharides from proteins and nucleic acids, which occur only as linear polymers.
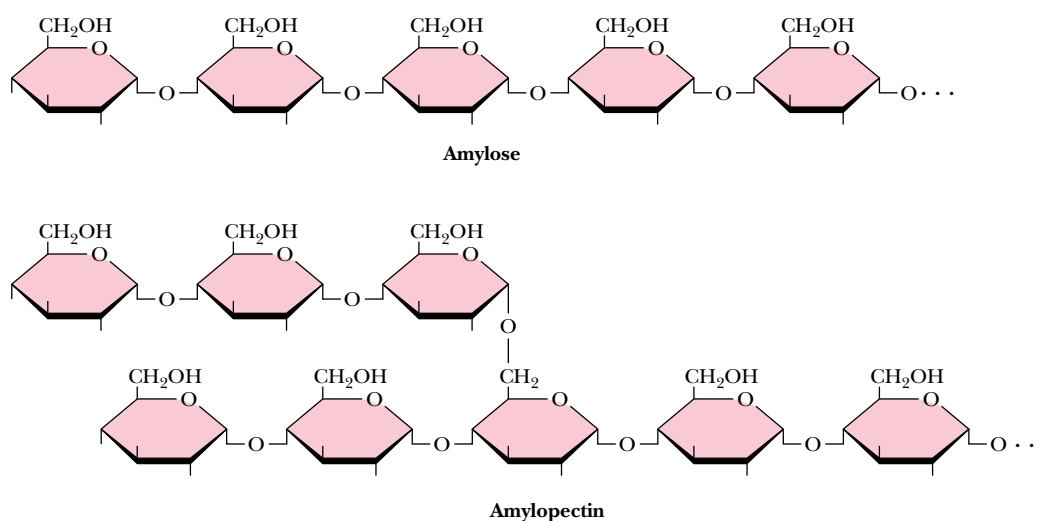
FIGURE 7.21 • Amylose and amylopectin are the two forms of starch. Note that the linear linkages are $\alpha(1\rightarrow4)$, but the branches in amylopectin are $\alpha(1\rightarrow6)$. Branches in polysaccharides can involve any of the hydroxyl groups on the monosaccharide components. Amylopectin is a highly branched structure, with branches occurring every 12 to 30 residues.

Polysaccharide Functions

The functions of many individual polysaccharides cannot be assigned uniquely, and some of their functions may not yet be appreciated. Traditionally, biochemistry textbooks have listed the functions of polysaccharides as storage materials, structural components, or protective substances. Thus, *starch, glycogen,* and other storage polysaccharides, as readily metabolizable food, provide energy reserves for cells. *Chitin* and *cellulose* provide strong support for the skeletons of arthropods and green plants, respectively. Mucopolysaccharides, such as the *hyaluronic acids,* form protective coats on animal cells. In each of these cases, the relevant polysaccharide is either a homopolymer or a polymer of small repeating units. Recent research indicates, however, that oligosaccharides and polysaccharides with varied structures may also be involved in much more sophisticated tasks in cells, including a variety of cellular recognition and intercellular communication events, as discussed later.

Storage Polysaccharides

Storage polysaccharides are an important carbohydrate form in plants and animals. It seems likely that organisms store carbohydrates in the form of polysaccharides rather than as monosaccharides to lower the osmotic pressure of the sugar reserves. Because osmotic pressures depend only on *numbers of molecules,* the osmotic pressure is greatly reduced by formation of a few polysaccharide molecules out of thousands (or even millions) of monosaccharide units.

Starch

By far the most common storage polysaccharide in plants is **starch,** which exists in two forms: **α-amylose** and **amylopectin,** the structures of which are shown in Figure 7.21. Most forms of starch in nature are 10 to 30% α-amylose and 70 to 90% amylopectin. Typical cornstarch produced in the United States is about 25% α-amylose and 75% amylopectin. α-Amylose is composed of linear chains of D-glucose in $\alpha(1\rightarrow4)$ linkages. The chains are of varying length, having molecular weights from several thousand to half a million. As can be seen from the structure in Figure 7.21, the chain has a reducing end and a nonreducing end. Although poorly soluble in water, α-amylose forms micelles in which the polysaccharide chain adopts a helical conformation (Figure 7.22). Iodine reacts with α-amylose to give a characteristic blue color, which arises from the insertion of iodine into the middle of the hydrophobic amylose helix.

In contrast to α-amylose, amylopectin, the other component of typical starches, is a highly branched chain of glucose units (Figure 7.21). Branches occur in these chains every 12 to 30 residues. The average branch length is between 24 and 30 residues, and molecular weights of amylopectin molecules can range up to 100 million. The linear linkages in amylopectin are $\alpha(1\rightarrow4)$, whereas the branch linkages are $\alpha(1\rightarrow6)$. As is the case for α-amylose, amylopectin forms micellar suspensions in water; iodine reacts with such suspensions to produce a red-violet color.

Starch is stored in plant cells in the form of granules in the stroma of plastids (plant cell organelles) of two types: **chloroplasts,** in which photosynthesis takes place, and **amyloplasts,** plastids that are specialized starch accumulation bodies. When starch is to be mobilized and used by the plant that stored it, it must be broken down into its component monosaccharides. Starch is split into its monosaccharide elements by stepwise phosphorolytic cleavage of glucose units, a reaction catalyzed by **starch phosphorylase** (Figure 7.23). This is formally an $\alpha(1\rightarrow4)$-glucan phosphorylase reaction, and at each step, the prod-
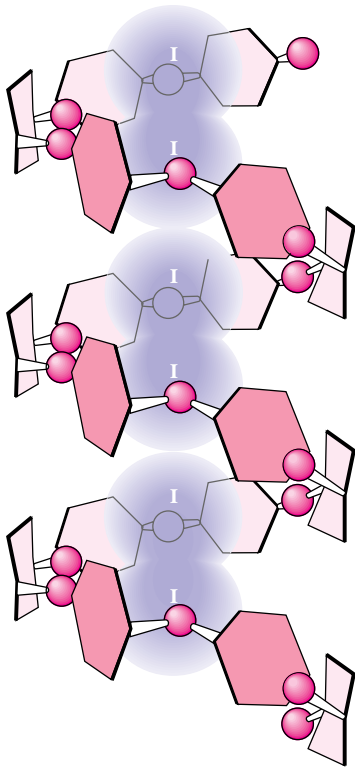
FIGURE 7.22 • Suspensions of amylose in water adopt a helical conformation. Iodine (I_2) can insert into the middle of the amylose helix to give a blue color that is characteristic and diagnostic for starch.
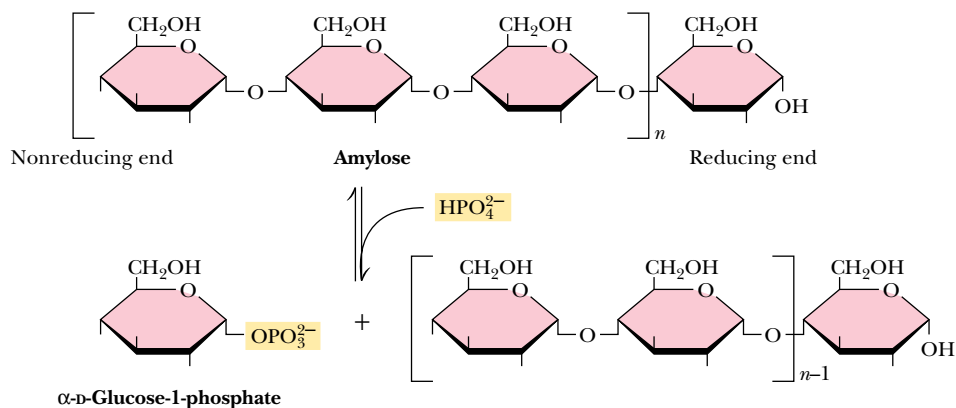
FIGURE 7.23 • The starch phosphorylase reaction cleaves glucose residues from amylose, producing α-ᴅ-glucose-1-phosphate.

ucts are one molecule of glucose-1-phosphate and a starch molecule with one less glucose unit. In α-amylose, this process continues all along the chain until the end is reached. However, the $\alpha(1\rightarrow6)$ branch points of amylopectin are not susceptible to cleavage by phosphorylase, and thorough digestion of amylopectin by phosphorylase leaves a *limit dextrin,* which must be attacked by an $\alpha(1\rightarrow6)$-glucosidase to cleave the $1\rightarrow6$ branch points and allow complete hydrolysis of the remaining $1\rightarrow4$ linkages. Glucose-1-phosphate units are thus delivered to the plant cell, suitable for further processing in glycolytic pathways (see Chapter 19).

In animals, digestion and use of plant starches begins in the mouth with **salivary α-amylase** ($\alpha(1\rightarrow4)$-glucan 4-glucanohydrolase), the major enzyme secreted by the salivary glands. Although the capability of making and secreting salivary α-amylases is widespread in the animal world, some animals (such as cats, dogs, birds, and horses) do not secrete them. Salivary α-amylase is an **endoamylase** that splits $\alpha(1\rightarrow4)$ glycosidic linkages only within the chain. Raw starch is not very susceptible to salivary endoamylase. However, when suspensions of starch granules are heated, the granules swell, taking up water and causing the polymers to become more accessible to enzymes. Thus, cooked starch is more digestible. In the stomach, salivary α-amylase is inactivated by the lower pH, but pancreatic secretions also contain α-amylase. **β-Amylase,** an enzyme absent in animals but prevalent in plants and microorganisms, cleaves disaccharide (maltose) units from the termini of starch chains and is an **exoamylase.** Neither α-amylase nor β-amylase, however, can cleave the $\alpha(1\rightarrow6)$ branch points of amylopectin, and once again, $\alpha(1\rightarrow6)$-glucosidase is required to cleave at the branch points and allow complete hydrolysis of starch amylopectin.

Glycogen

The major form of storage polysaccharide in animals is **glycogen.** Glycogen is found mainly in the liver (where it may amount to as much as 10% of liver mass) and skeletal muscle (where it accounts for 1 to 2% of muscle mass). Liver glycogen consists of granules containing highly branched molecules, with $\alpha(1\rightarrow6)$ branches occurring every 8 to 12 glucose units. Like amylopectin, glycogen yields a red-violet color with iodine. Glycogen can be hydrolyzed by both α- and β-amylases, yielding glucose and maltose, respectively, as products and can also be hydrolyzed by **glycogen phosphorylase,** an enzyme present in liver and muscle tissue, to release glucose-1-phosphate.
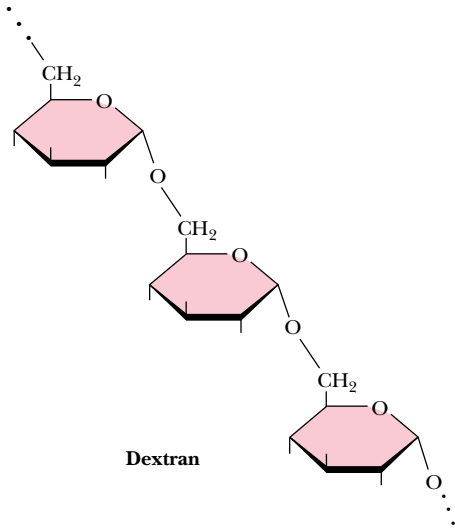
FIGURE 7.24 • Dextran is a branched polymer of D-glucose units. The main chain linkage is $\alpha(1\rightarrow6)$, but $1\rightarrow2$, $1\rightarrow3$, or $1\rightarrow4$ branches can occur.

Dextran

Another important family of storage polysaccharides are the **dextrans,** which are $\alpha(1\rightarrow6)$-linked polysaccharides of D-glucose with branched chains found in yeast and bacteria (Figure 7.24). Because the main polymer chain is $\alpha(1\rightarrow6)$ linked, the repeating unit is *isomaltose,* Glc$\alpha(1\rightarrow6)$-Glc. The branch points may be $1\rightarrow2$, $1\rightarrow3$, or $1\rightarrow4$ in various species. The degree of branching and the average chain length between branches depend on the species and strain of the organism. Bacteria growing on the surfaces of teeth produce extracellular accumulations of dextrans, an important component of *dental plaque.* Bacterial dextrans are frequently used in research laboratories as the support medium for column chromatography of macromolecules. Dextran chains cross-linked with epichlorohydrin yield the structure shown in Figure 7.25. These preparations (known by various trade names such as Sephadex and Bio-gel) are extremely hydrophilic and swell to form highly hydrated gels in water. Depending on the degree of cross-linking and the size of the gel particle, these materials form gels containing from 50 to 98% water. Dextran can also be cross-linked with other agents, forming gels with slightly different properties.

Structural Polysaccharides

Cellulose

The **structural polysaccharides** have properties that are dramatically different from those of the storage polysaccharides, even though the compositions of these two classes are similar. The structural polysaccharide **cellulose** is the most
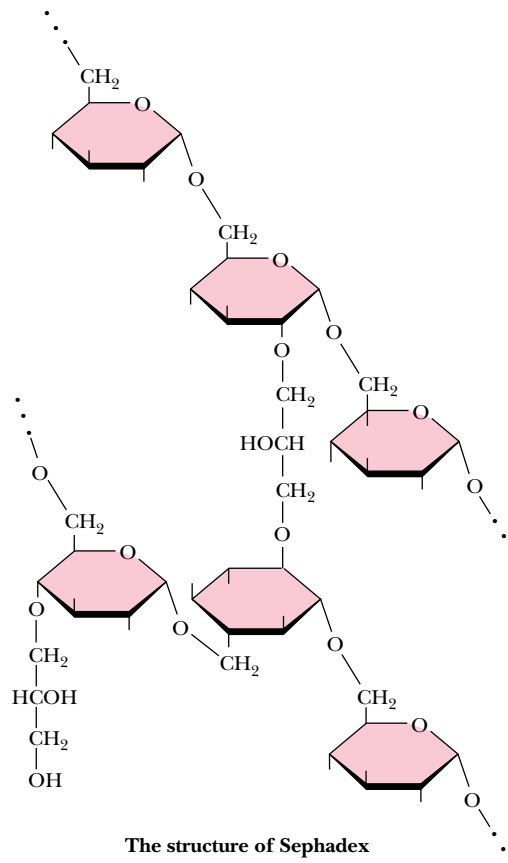
FIGURE 7.25 • Sephadex gels are formed from dextran chains cross-linked with epichlorohydrin. The degree of cross-linking determines the chromatographic properties of Sephadex gels. Sephacryl gels are formed by cross-linking of dextran polymers with *N,N′*-methylene bisacrylamide.

The structure of Sephadex

α-1,4-Linked D-glucose units

(a)

β-1,4-Linked D-glucose units

(b)
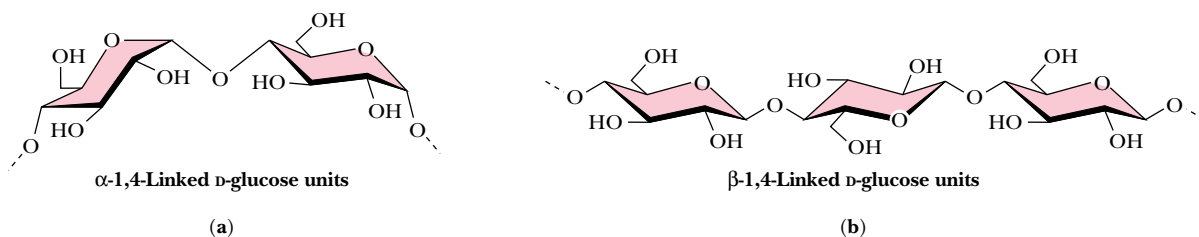
FIGURE 7.26 • (a) Amylose, composed exclusively of the relatively bent $\alpha(1\rightarrow4)$ linkages, prefers to adopt a helical conformation, whereas (b) cellulose, with $\beta(1\rightarrow4)$-glycosidic linkages, can adopt a fully extended conformation with alternating 180° flips of the glucose units. The hydrogen bonding inherent in such extended structures is responsible for the great strength of tree trunks and other cellulose-based materials.

abundant natural polymer found in the world. Found in the cell walls of nearly all plants, cellulose is one of the principal components providing physical structure and strength. The wood and bark of trees are insoluble, highly organized structures formed from cellulose and also from *lignin* (see Figure 27.35). It is awe-inspiring to look at a large tree and realize the amount of weight supported by polymeric structures derived from sugars and organic alcohols. Cellulose also has its delicate side, however. *Cotton,* whose woven fibers make some of our most comfortable clothing fabrics, is almost pure cellulose. Derivatives of cellulose have found wide use in our society. **Cellulose acetates** are produced by the action of acetic anhydride on cellulose in the presence of sulfuric acid and can be spun into a variety of fabrics with particular properties. Referred to simply as *acetates,* they have a silky appearance, a luxuriously soft feel, and a deep luster and are used in dresses, lingerie, linings, and blouses.

Cellulose is a linear homopolymer of D-glucose units, just as in α-amylose. The structural difference, which completely alters the properties of the polymer, is that in cellulose the glucose units are linked by $\beta(1\rightarrow4)$-glycosidic bonds, whereas in α-amylose the linkage is $\alpha(1\rightarrow4)$. The conformational difference between these two structures is shown in Figure 7.26. The $\alpha(1\rightarrow4)$-linkage sites of amylose are naturally bent, conferring a gradual turn to the polymer chain, which results in the helical conformation already described (see Figure 7.22). The most stable conformation about the $\beta(1\rightarrow4)$ linkage involves alternating 180° flips of the glucose units along the chain so that the chain adopts a fully extended conformation, referred to as an **extended ribbon.** Juxtaposition of several such chains permits efficient interchain hydrogen bonding, the basis of much of the strength of cellulose.

The structure of one form of cellulose, determined by X-ray and electron diffraction data, is shown in Figure 7.27. The flattened sheets of the chains lie side by side and are joined by hydrogen bonds. These sheets are laid on top of one another in a way that staggers the chains, just as bricks are staggered to give strength and stability to a wall. Cellulose is extremely resistant to hydrolysis, whether by acid or by the digestive tract amylases described earlier. As a result, most animals (including humans) cannot digest cellulose to any significant degree. Ruminant animals, such as cattle, deer, giraffes, and camels, are an exception because bacteria that live in the rumen (Figure 7.28) secrete the enzyme **cellulase,** a β-glucosidase effective in the hydrolysis of cellulose. The resulting glucose is then metabolized in a fermentation process to the benefit of the host animal. Termites and shipworms (*Teredo navalis*) similarly digest cellulose because their digestive tracts also contain bacteria that secrete cellulase.

FIGURE 7.27 • The structure of cellulose, showing the hydrogen bonds (blue) between the sheets, which strengthen the structure. Intrachain hydrogen bonds are in red and interchain hydrogen bonds are in green.

Intrachain hydrogen bond

Interchain hydrogen bond

Intersheet hydrogen bond

Esophagus

Omasum

Small intestine

Reticulum

Abomasum
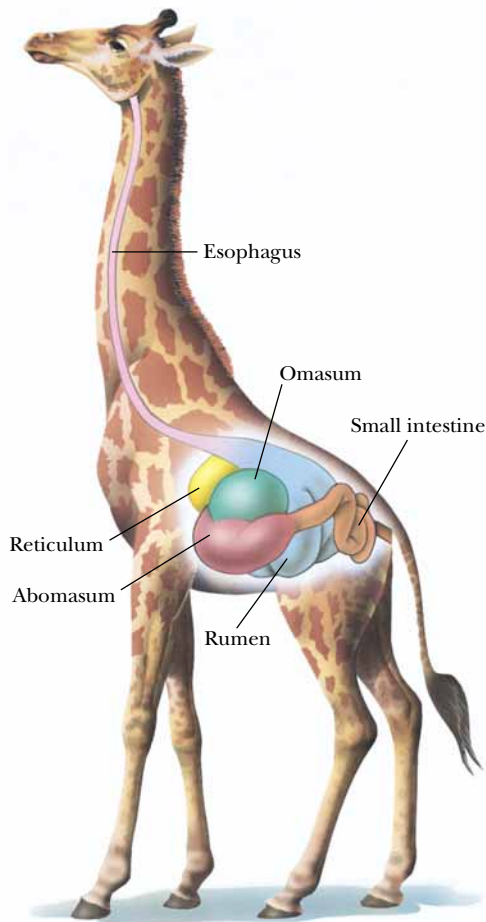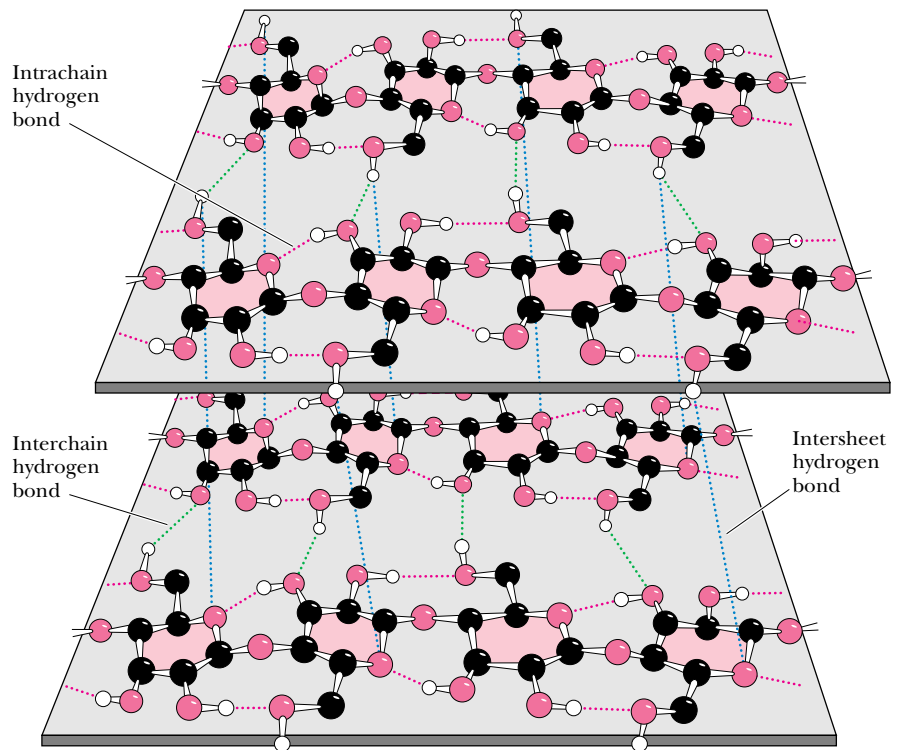
Rumen

FIGURE 7.28 • Giraffes, cattle, deer, and camels are ruminant animals that are able to metabolize cellulose, thanks to bacterial cellulase in the rumen, a large first compartment in the stomach of a ruminant.

Chitin

A polysaccharide that is similar to cellulose, both in its biological function and its primary, secondary, and tertiary structure, is **chitin.** Chitin is present in the cell walls of fungi and is the fundamental material in the exoskeletons of crustaceans, insects, and spiders. The structure of chitin, an extended ribbon, is identical to cellulose, except that the —OH group on each C-2 is replaced by —NHCOCH$_3$, so that the repeating units are *N-acetyl-D-glucosamines* in $\beta(1\rightarrow4)$ linkage. Like cellulose (Figure 7.27), the chains of chitin form extended ribbons (Figure 7.29) and pack side by side in a crystalline, strongly hydrogen-bonded form. One significant difference between cellulose and chitin is whether the chains are arranged in **parallel** (all the reducing ends together at one end of a packed bundle and all the nonreducing ends together at the other end) or **antiparallel** (each sheet of chains having the chains arranged oppositely from the sheets above and below). Natural cellulose seems to occur only in parallel arrangements. Chitin, however, can occur in three forms, sometimes all in the same organism. α-*Chitin* is an all-parallel arrangement of the chains, whereas β-*chitin* is an antiparallel arrangement. In δ-*chitin*, the structure is thought to involve pairs of parallel sheets separated by single antiparallel sheets.

Chitin is the earth's second most abundant carbohydrate polymer (after cellulose), and its ready availability and abundance offer opportunities for industrial and commercial applications. Chitin-based coatings can extend the shelf life of fruits, and a chitin derivative that binds to iron atoms in meat has been found to slow the reactions that cause rancidity and flavor loss. Without such a coating, the iron in meats activates oxygen from the air, forming reactive free radicals that attack and oxidize polyunsaturated lipids, causing most of the flavor loss associated with rancidity. Chitin-based coatings coordinate the iron atoms, preventing their interaction with oxygen.

Cellulose

Chitin

N–Acetylglucosamine units

Mannan

Mannose units

Poly (D-Mannuronate)

Poly (L-Guluronate)
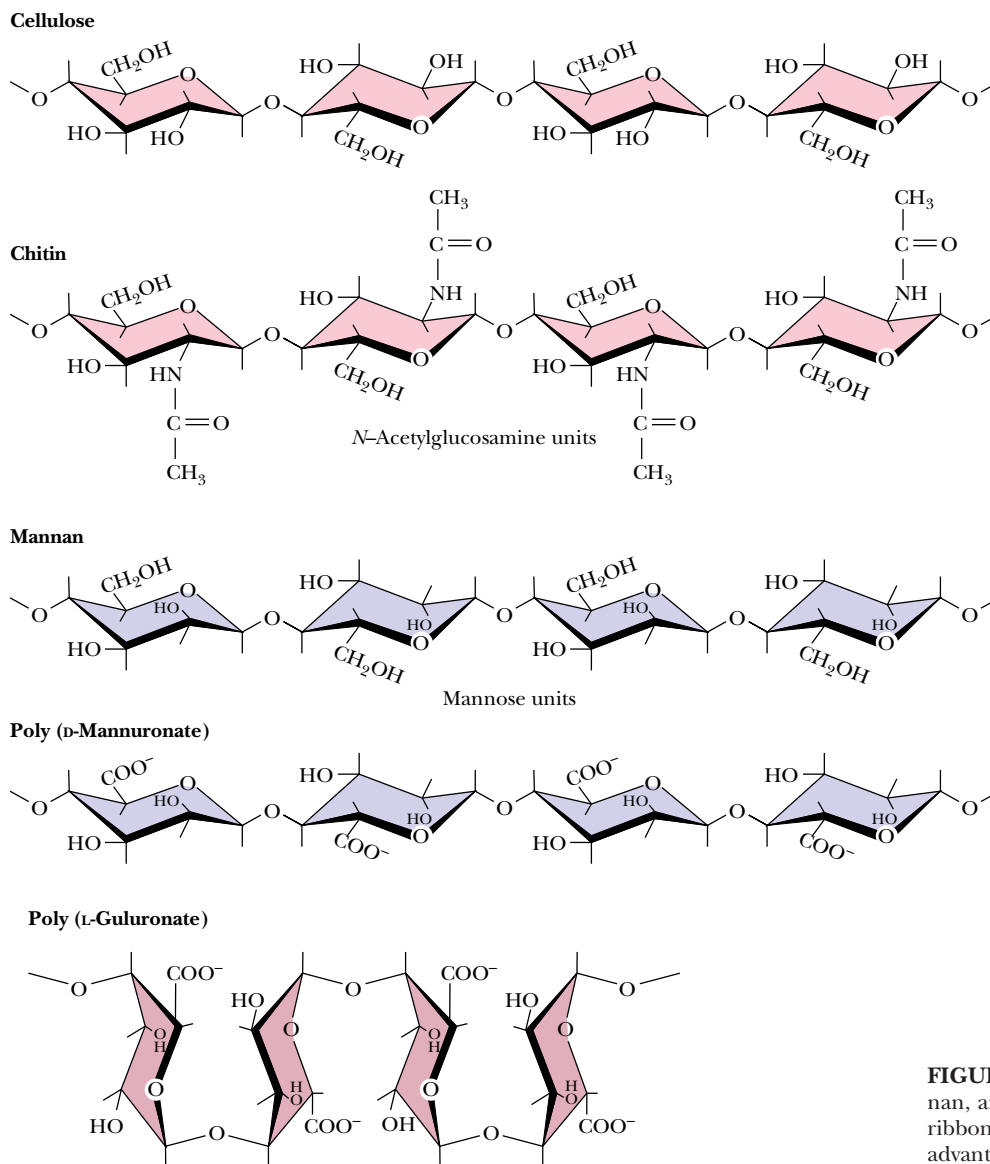
FIGURE 7.29 • Like cellulose, chitin, mannan, and poly(D-mannuronate) form extended ribbons and pack together efficiently, taking advantage of multiple hydrogen bonds.

Alginates

A family of novel extended ribbon structures that bind metal ions, particularly calcium, in their structure are the **alginate** polysaccharides of marine brown algae *(Phaeophyceae)*. These include **poly(β-D-mannuronate)** and **poly(α-L-guluronate),** which are (1→4) linked chains formed from *β-mannuronic acid* and α-*L-guluronic acid,* respectively. Both of these homopolymers are found together in most marine alginates, although to widely differing extents, and mixed chains containing both monomer units are also found. As shown in Figure 7.29, the conformation of poly(β-D-mannuronate) is similar to that of cellulose. In the solid state, the free form of the polymer exists in cellulose-like form. However, complexes of the polymer with cations (such as lithium, sodium, potassium, and calcium) adopt a threefold helix structure, presumably to accommodate the bound cations. For poly(α-L-guluronate) (Figure 7.29), the axial–axial configuration of the glycosidic linkage leads to a distinctly buckled ribbon with limited flexibility. Cooperative interactions between such buckled ribbons can only

$\mathcal{A}$ **D E E P E R   L O O K**

Billiard Balls, Exploding Teeth, and Dynamite—
The Colorful History of Cellulose

Although humans cannot digest it and most people's acquaintance with cellulose is limited to comfortable cotton clothing, cellulose has enjoyed a colorful and varied history of utilization. In 1838, Théophile Pelouze in France found that paper or cotton could be made explosive if dipped in concentrated nitric acid. Christian Schönbein, a professor of chemistry at the University of Basel, prepared "nitrocotton" in 1845 by dipping cotton in a mixture of nitric and sulfuric acids and then washing the material to remove excess acid. In 1860, Major E. Schultze of the Prussian army used the same material, now called **guncotton,** as a propellant replacement for gunpowder, and its preparation in brass cartridges soon made it popular for this purpose. The only problem was that it was too explosive and could detonate unpredictably in factories where it was produced. The entire town of Faversham, England, was destroyed in such an accident. In 1868, Alfred Nobel mixed guncotton with ether and alcohol, thus preparing **nitrocellulose,** and in turn mixed this with nitroglycerine and sawdust to produce **dynamite.** Nobel's income from dynamite and also

from his profitable development of the Russian oil fields in Baku eventually formed the endowment for the Nobel Prizes.

In 1869, concerned over the precipitous decline (from hunting) of the elephant population in Africa, the billiard ball manufacturers Phelan and Collander offered a prize of $10,000 for production of a substitute for ivory. Brothers Isaiah and John Hyatt in Albany, New York, produced a substitute for ivory by mixing guncotton with camphor, then heating and squeezing it to produce **celluloid.** This product found immediate uses well beyond billiard balls. It was easy to shape, strong, and resilient, and it exhibited a high tensile strength. Celluloid was used eventually to make dolls, combs, musical instruments, fountain pens, piano keys, and a variety of other products. The Hyatt brothers eventually formed the Albany Dental Company to make false teeth from celluloid. Because camphor was used in their production, the company advertised that their teeth smelled "clean," but, as reported in the *New York Times* in 1875, the teeth also occasionally exploded!

Portions adapted from Burke, J., 1996. *The Pinball Effect: How Renaissance Water Gardens Made the Carburetor Possible and Other Journeys Through Knowledge.* New York: Little, Brown, & Company.

be strong if the interstices are filled effectively with water molecules or metal ions. Figure 7.30 shows a molecular model of a Ca^{2+}-induced dimer of poly(α-L-guluronate).

Agarose

An important polysaccharide mixture isolated from marine red algae (*Rhodophyceae*) is **agar,** which consists of two components, **agarose** and **agaropectin.** Agarose (Figure 7.31) is a chain of alternating D-galactose and 3,6-anhydro-L-galactose, with side chains of 6-methyl-D-galactose. Agaropectin is similar, but contains in addition sulfate ester side chains and D-glucuronic acid. The three-dimensional structure of agarose is a double helix with a threefold screw axis, as shown in Figure 7.31. The central cavity is large enough to accommodate water molecules. Agarose and agaropectin readily form gels containing large amounts (up to 99.5%) of water. Agarose can be processed to remove most of the charged groups, yielding a material (trade name Sepharose) useful for purification of macromolecules in gel exclusion chromatography. Pairs of chains form double helices that subsequently aggregate in bundles to form a stable gel, as shown in Figure 7.32.

Glycosaminoglycans

A class of polysaccharides known as **glycosaminoglycans** is involved in a variety of extracellular (and sometimes intracellular) functions. Glycosaminoglycans consist of linear chains of repeating disaccharides in which one of the monosaccharide units is an amino sugar and one (or both) of the monosaccharide units contains at least one negatively charged sulfate or carboxylate group. The repeating disaccharide structures found commonly in glycosaminoglycans are
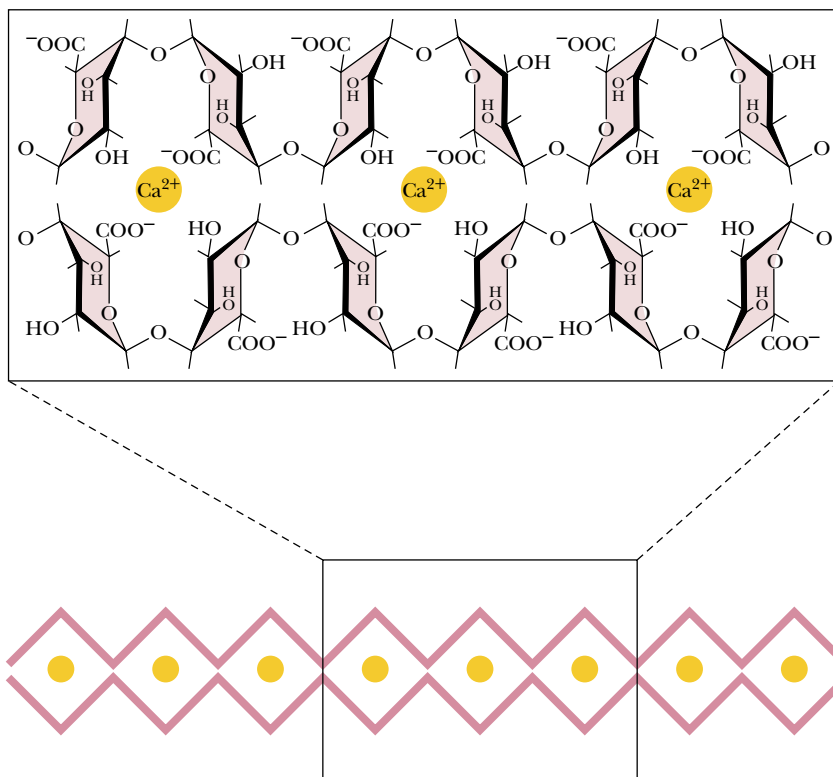
FIGURE 7.30 • Poly(α-L-guluronate) strands dimerize in the presence of Ca^{2+}, forming a structure known as an "egg carton."

Agarose

3,6-anhydro bridge

Agarose double helix

FIGURE 7.31 • The favored conformation of agarose in water is a double helix with a three-fold screw axis.

shown in Figure 7.33. **Heparin,** with the highest net negative charge of the disaccharides shown, is a natural anticoagulant substance. It binds strongly to *antithrombin III* (a protein involved in terminating the clotting process) and inhibits blood clotting. **Hyaluronate** molecules may consist of as many as 25,000 disaccharide units, with molecular weights of up to 10^7. Hyaluronates are impor-

Soluble agarose   Initial gel   Final gel structure

$t \approx 45°C$

$t = 100°C$

FIGURE 7.32 • The ability of agarose to assemble in complex bundles to form gels in aqueous solution makes it useful in numerous chromatographic procedures, including gel exclusion chromatography and electrophoresis. Cells grown in culture can be embedded in stable agarose gel "threads" so that their metabolic and physiological properties can be studied.

FIGURE 7.33 • Glycosaminoglycans are formed from repeating disaccharide arrays. Glycosaminoglycans are components of the proteoglycans.

tant components of the vitreous humor in the eye and of *synovial fluid,* the lubricant fluid of joints in the body. The **chondroitins** and **keratan sulfate** are found in tendons, cartilage, and other connective tissue, whereas **dermatan sulfate,** as its name implies, is a component of the extracellular matrix of skin. Glycosaminoglycans are fundamental constituents of *proteoglycans* (discussed later).

PROBLEMS

1. Draw Haworth structures for the two possible isomers of D-altrose (Figure 7.2) and D-psicose (Figure 7.3).

2. Give the systematic name for stachyose (Figure 7.19).

3. Trehalose, a disaccharide produced in fungi, has the following structure:
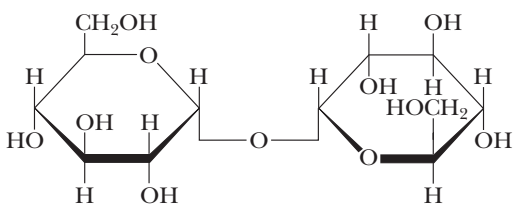
a. What is the systematic name for this disaccharide?
b. Is trehalose a reducing sugar? Explain.

4. Draw a Fischer projection structure for L-sorbose (D-sorbose is shown in Figure 7.3).

5. α-D-Glucose has a specific rotation, $[\alpha]_D^{20}$, of +112.2°, whereas β-D-glucose has a specific rotation of +18.7°. What is the composition of a mixture of α-D- and β-D-glucose, which has a specific rotation of 83.0°?

6. A 0.2-g sample of amylopectin was analyzed to determine the fraction of the total glucose residues that are branch points in the structure. The sample was exhaustively methylated and then digested, yielding 50 μmol of 2,3-dimethylglucose and 0.4 μmol of 1, 2, 3, 6-tetramethylglucose.

a. What fraction of the total residues are branch points?
b. How many reducing ends does this amylopectin have?

FURTHER READING

Aspinall, G. O., 1982. *The Polysaccharides,* Vols. 1 and 2. New York: Academic Press.

Collins, P. M., 1987. *Carbohydrates.* London: Chapman and Hall.

Davison, E. A., 1967. *Carbohydrate Chemistry.* New York: Holt, Rinehart and Winston.

Feeney, R. E., Burcham, T. S., and Yeh, Y., 1986. Antifreeze glycoproteins from polar fish blood. *Annual Review of Biophysical Chemistry* **15:**59–78.

Jentoft, N., 1990. Why are proteins O-glycosylated? *Trends in Biochemical Sciences* **155:**291–294.

Kjellen, L., and Lindahl, U., 1991. Proteoglycans: Structures and interactions. *Annual Review of Biochemistry* **60:**443–475.

Lennarz, W. J., 1980. *The Biochemistry of Glycoproteins and Proteoglycans.* New York: Plenum Press.

Lodish, H. F., 1991. Recognition of complex oligosaccharides by the multisubunit asialoglycoprotein receptor. *Trends in Biochemical Sciences* **16:**374–377.

McNeil, M., Darvill, A. G., Fry, S. C., and Albersheim, P., 1984. Structure and function of the primary cell walls of plants. *Annual Review of Biochemistry* **53:**625–664.

Pigman, W., and Horton, D., 1972. *The Carbohydrates.* New York: Academic Press.

Rademacher, T. W., Parekh, R. B., and Dwek, R. A., 1988. Glycobiology. *Annual Review of Biochemistry* **57:**785–838.

Ruoslahti, E., 1989. Proteoglycans in cell regulation. *Journal of Biological Chemistry* **264:**13369–13372.

Sharon, N., 1980. Carbohydrates. *Scientific American* **243:**90–102.

Sharon, N., 1984. Glycoproteins. *Trends in Biochemical Sciences* **9:**198–202.

Chapter 8

Lipids

*"The mighty whales which swim in a sea of water, and have a sea of oil swimming in them." Herman Melville, "Extracts." Moby Dick. New York: Penguin Books, 1972. (Humpback whale (*Megaptera novaeangliae*) breaching, Cape Cod, MA; photo © Steven Morello/Peter Arnold, Inc.)*

Lipids are a class of biological molecules defined by low solubility in water and high solubility in nonpolar solvents. As molecules that are largely hydrocarbon in nature, lipids represent highly reduced forms of carbon and, upon oxidation in metabolism, yield large amounts of energy. Lipids are thus the molecules of choice for metabolic energy storage.

The lipids found in biological systems are either **hydrophobic** (containing only nonpolar groups) or **amphipathic,** which means they possess both polar and nonpolar groups. The hydrophobic nature of lipid molecules allows membranes to act as effective barriers to more polar molecules. In this chapter, we discuss the chemical and physical properties of the various classes of lipid molecules. The following chapter considers membranes, whose properties depend intimately on their lipid constituents.

8.1 • Fatty Acids

A **fatty acid** is composed of a long hydrocarbon chain ("tail") and a terminal carboxyl group (or "head"). The carboxyl group is normally ionized under physiological conditions. Fatty acids occur in large amounts in biological systems, but rarely in the free, uncomplexed state. They typically are esterified to glycerol or other backbone structures. Most of the fatty acids found in nature have an even number of carbon atoms (usually 14 to 24). Certain marine organisms, however, contain substantial amounts of fatty acids with odd numbers of carbon atoms. Fatty acids are either **saturated** (all carbon–carbon bonds are single bonds) or **unsaturated** (with one or more double bonds in the hydrocarbon chain). If a fatty acid has a single double bond, it is said to be **monounsaturated,** and if it has more than one, **polyunsaturated.** Fatty acids can be named or described in at least three ways, as listed in Table 8.1. For example, a fatty acid composed of an 18-carbon chain with no double bonds can be called by its systematic name (**octadecanoic acid**), its common name (stearic acid), or its shorthand notation, in which the number of carbons is followed by a colon and the number of double bonds in the molecule (18:0 for stearic acid). The structures of several fatty acids are given in Figure 8.1. **Stearic acid** (18:0) and **palmitic acid** (16:0) are the most common saturated fatty acids in nature.

Free rotation around each of the carbon–carbon bonds makes saturated fatty acids extremely flexible molecules. Owing to steric constraints, however, the fully extended conformation (Figure 8.1) is the most stable for saturated fatty acids. Nonetheless, the degree of stabilization is slight, and (as will be seen) saturated fatty acid chains adopt a variety of conformations.

Unsaturated fatty acids are slightly more abundant in nature than saturated fatty acids, especially in higher plants. The most common unsaturated fatty acid

Table 8.1

Common Biological Fatty Acids				
Number of Carbons	**Common Name**	**Systematic Name**	**Symbol**	**Structure**
Saturated fatty acids				
12	Lauric acid	Dodecanoic acid	12:0	$CH_3(CH_2)_{10}COOH$
14	Myristic acid	Tetradecanoic acid	14:0	$CH_3(CH_2)_{12}COOH$
16	Palmitic acid	Hexadecanoic acid	16:0	$CH_3(CH_2)_{14}COOH$
18	Stearic acid	Octadecanoic acid	18:0	$CH_3(CH_2)_{16}COOH$
20	Arachidic acid	Eicosanoic acid	20:0	$CH_3(CH_2)_{18}COOH$
22	Behenic acid	Docosanoic acid	22:0	$CH_3(CH_2)_{20}COOH$
24	Lignoceric acid	Tetracosanoic acid	24:0	$CH_3(CH_2)_{22}COOH$
Unsaturated fatty acids (all double bonds are *cis*)				
16	Palmitoleic acid	9-Hexadecenoic acid	16:1	$CH_3(CH_2)_5CH{=}CH(CH_2)_7COOH$
18	Oleic acid	9-Octadecenoic acid	18:1	$CH_3(CH_2)_7CH{=}CH(CH_2)_7COOH$
18	Linoleic acid	9,12-Octadecadienoic acid	18:2	$CH_3(CH_2)_4(CH{=}CHCH_2)_2(CH_2)_6COOH$
18	α-Linolenic acid	9,12,15-Octadecatrienoic acid	18:3	$CH_3CH_2(CH{=}CHCH_2)_3(CH_2)_6COOH$
18	γ-Linolenic acid	6,9,12-Octadecatrienoic acid	18:3	$CH_3(CH_2)_4(CH{=}CHCH_2)_3(CH_2)_3COOH$
20	Arachidonic acid	5,8,11,14-Eicosatetraenoic acid	20:4	$CH_3(CH_2)_4(CH{=}CHCH_2)_4(CH_2)_2COOH$
24	Nervonic acid	15-Tetracosenoic acid	24:1	$CH_3(CH_2)_7CH{=}CH(CH_2)_{13}COOH$

Palmitic acid

Stearic acid
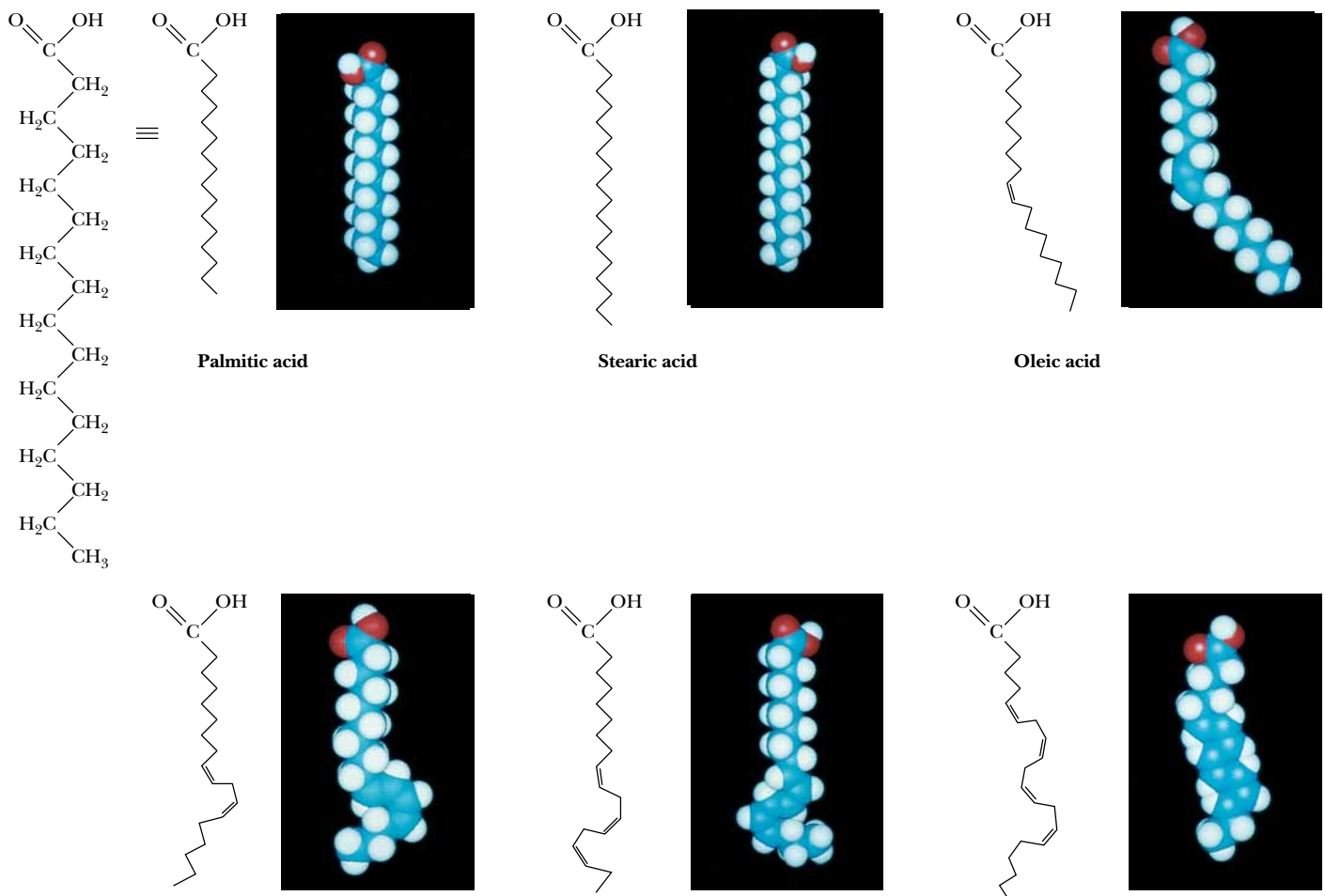
Oleic acid

FIGURE 8.1 • The structures of some typical fatty acids. Note that most natural fatty acids contain an even number of carbon atoms and that the double bonds are nearly always *cis* and rarely conjugated.

is **oleic acid,** or 18:1(9), with the number in parentheses indicating that the double bond is between carbons 9 and 10. The number of double bonds in an unsaturated fatty acid varies typically from one to four, but, in the fatty acids found in most bacteria, this number rarely exceeds one.

The double bonds found in fatty acids are nearly always in the *cis* configuration. As shown in Figure 8.1, this causes a bend or "kink" in the fatty acid chain. This bend has very important consequences for the structure of biological membranes. Saturated fatty acid chains can pack closely together to form ordered, rigid arrays under certain conditions, but unsaturated fatty acids prevent such close packing and produce flexible, fluid aggregates.

Some fatty acids are not synthesized by mammals and yet are necessary for normal growth and life. These *essential fatty acids* include **linoleic** and **γ-linolenic acids.** These must be obtained by mammals in their diet (specifically from plant sources). **Arachidonic acid,** which is not found in plants, can only be synthesized by mammals from linoleic acid. At least one function of the essential fatty acids is to serve as a precursor for the synthesis of **eicosanoids,** such as

Fatty Acids in Food: Saturated Versus Unsaturated

Fats consumed in the modern human diet vary widely in their fatty acid compositions. The table below provides a brief summary. The incidence of cardiovascular disease is correlated with diets high in saturated fatty acids. By contrast, a diet that is relatively higher in unsaturated fatty acids (especially polyunsaturated fatty acids) may reduce the risk of heart attacks and strokes. Corn oil, abundant in the United States and high in (polyunsaturated) linoleic acid, is an attractive dietary choice. *Margarine* made from corn, safflower, or sunflower oils is much lower in saturated fatty acids than is butter, which is made from milk fat. However, margarine may present its own health risks. Its fatty acids contain *trans*-double bonds (introduced by the hydrogenation process), which may also contribute to cardiovascular disease. (Margarine was invented by a French chemist, H. Mège Mouriès, who won a prize from Napoleon III in 1869 for developing a substitute for butter.)

Although vegetable oils usually contain a higher proportion of unsaturated fatty acids than do animal oils and fats, several plant oils are actually high in saturated fats. Palm oil is low in polyunsaturated fatty acids and particularly high in (saturated) palmitic acid (whence the name *palmitic*). Coconut oil is particularly high in lauric and myristic acids (both saturated) and contains very few unsaturated fatty acids.

Some of the fatty acids found in the diets of developed nations (often 1 to 10 g of daily fatty acid intake) are *trans* fatty acids—fatty acids with one or more double bonds in the *trans* configuration. Some of these derive from dairy fat and ruminant meats, but the bulk are provided by partially hydrogenated vegetable or fish oils. Substantial evidence now exists to indicate that *trans* fatty acids may have deleterious health consequences. Numerous studies have shown that *trans* fatty acids raise plasma LDL cholesterol levels when exchanged for *cis*-unsaturated fatty acids in the diet and may also lower HDL cholesterol levels and raise triglyceride levels. The effects of *trans* fatty acids on LDL, HDL, and cholesterol levels are similar to those of saturated fatty acids, and diets aimed at reducing the risk of coronary heart disease should be low in both *trans* and saturated fatty acids.

Oleic acid
cis double bond

Elaidic acid
trans double bond
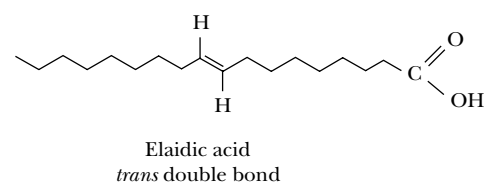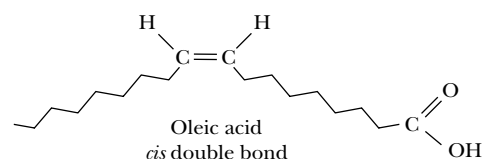
Structure of *cis* and *trans* monounsaturated C_{18} fatty acids.

Fatty Acid Compositions of Some Dietary Lipids*					
Source	Lauric and Myristic	Palmitic	Stearic	Oleic	Linoleic
Beef	5	24–32	20–25	37–43	2–3
Milk		25	12	33	3
Coconut	74	10	2	7	—
Corn		8–12	3–4	19–49	34–62
Olive		9	2	84	4
Palm		39	4	40	8
Safflower		6	3	13	78
Soybean		9	6	20	52
Sunflower		6	1	21	66

Data from *Merck Index*, 10th ed. Rahway, NJ: Merck and Co.; and Wilson, et al., 1967, *Principles of Nutrition*, 2nd ed. New York: Wiley.

*Values are percentages of total fatty acids.

Lactobacillic acid

$CH_3(CH_2)_5HC \underline{\hspace{1cm}} CH(CH_2)_9COOH$

CH_2

Tuberculostearic acid

$CH_3(CH_2)_7CH(CH_2)_8COOH$

CH_3
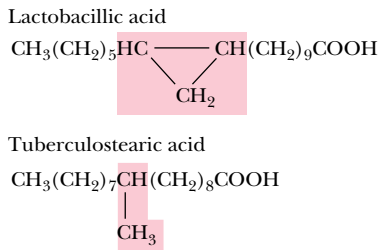
FIGURE 8.2 • Structures of two unusual fatty acids: lactobacillic acid, a fatty acid containing a cyclopropane ring, and tuberculostearic acid, a branched-chain fatty acid.

prostaglandins, a class of compounds that exert hormone-like effects in many physiological processes (discussed in Chapter 25).

In addition to unsaturated fatty acids, several other modified fatty acids are found in nature. Microorganisms, for example, often contain branched-chain fatty acids, such as **tuberculostearic acid** (Figure 8.2). When these fatty acids are incorporated in membranes, the methyl group constitutes a local structural perturbation in a manner similar to the double bonds in unsaturated fatty acids (see Chapter 9). Some bacteria also synthesize fatty acids containing cyclic structures such as cyclopropane, cyclopropene, and even cyclopentane rings.

8.2 • Triacylglycerols

A significant number of the fatty acids in plants and animals exist in the form of **triacylglycerols** (also called **triglycerides**). Triacylglycerols are a major energy reserve and the principal neutral derivatives of glycerol found in animals. These molecules consist of a glycerol esterified with three fatty acids (Figure 8.3). If all three fatty acid groups are the same, the molecule is called a simple triacylglycerol. Examples include **tristearoylglycerol** (common name *tristearin*) and **trioleoylglycerol** (*triolein*). Mixed triacylglycerols contain two or three different fatty acids. Triacylglycerols in animals are found primarily in the adipose tissue (body fat), which serves as a depot or storage site for lipids. Monoacylglycerols and diacylglycerols also exist, but are far less common than the triacylglycerols. Most natural plant and animal fat is composed of mixtures of simple and mixed triacylglycerols.

Acylglycerols can be hydrolyzed by heating with acid or base or by treatment with lipases. Hydrolysis with alkali is called **saponification** and yields salts of free fatty acids and glycerol. This is how **soap** (a metal salt of an acid derived from fat) was made by our ancestors. One method used potassium hydroxide (*potash*) leached from wood ashes to hydrolyze animal fat (mostly triacylglycerols). (The tendency of such soaps to be precipitated by Mg^{2+} and Ca^{2+} ions in hard water makes them less useful than modern detergents.) When the fatty acids esterified at the first and third carbons of glycerol are different, the sec-

$H_2C \underline{\hspace{0.5cm}} CH \underline{\hspace{0.5cm}} CH_2$

HO   OH   OH

Glycerol

$H_2C \underline{\hspace{0.5cm}} CH \underline{\hspace{0.5cm}} CH_2$

O   O   O

$O=C$ $C=O$ $C=O$

**Tristearin
(a simple triacylglycerol)**

$H_2C \underline{\hspace{0.5cm}} CH \underline{\hspace{0.5cm}} CH_2$

O   O   O

$O=C$ $C=O$ $C=O$

Myristic   Palmitoleic

Stearic

A mixed triacylglycerol
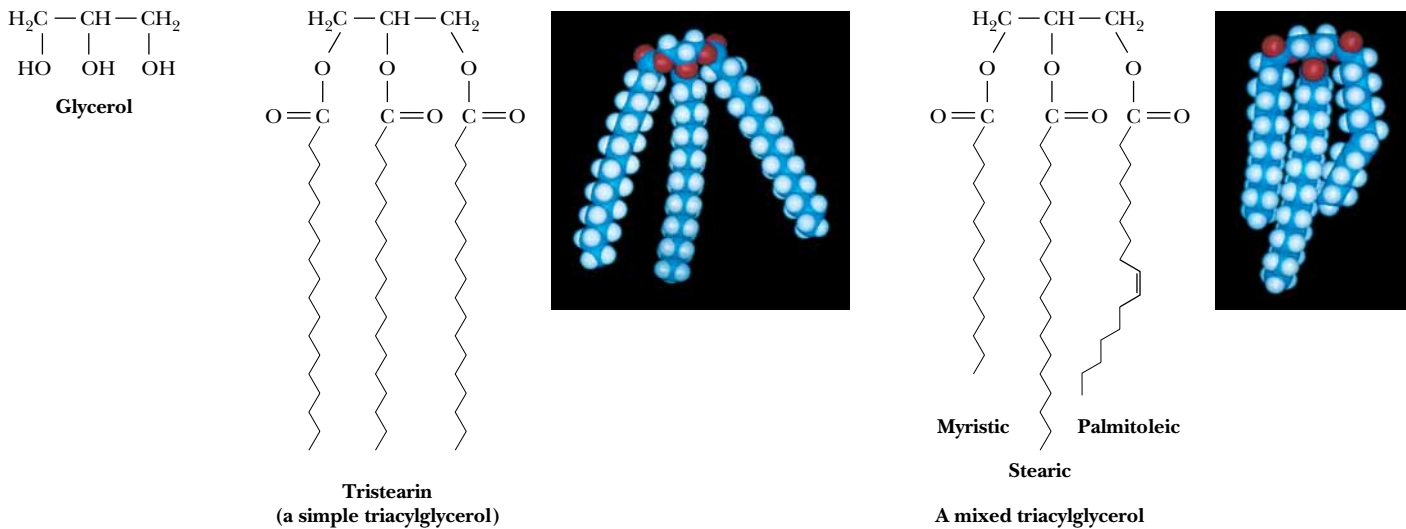
FIGURE 8.3 • Triacylglycerols are formed from glycerol and fatty acids.

Polar Bears Use Triacylglycerols to Survive Long Periods of Fasting

The polar bear is magnificently adapted to thrive in its harsh Arctic environment. Research by Malcolm Ramsey (at the University of Saskatchewan in Canada) and others has shown that polar bears eat only during a few weeks out of the year and then fast for periods of 8 months or more, consuming no food or water during that time. Eating mainly in the winter, the adult polar bear feeds almost exclusively on seal blubber (largely composed of triacylglycerols), thus building up its own triacylglycerol reserves. Through the Arctic summer, the polar bear maintains normal physical activity, roaming over long distances, but relies entirely on its body fat for sustenance, burning as much as 1 to 1.5 kg of fat per day. It neither urinates nor defecates for extended periods. All the water needed to sustain life is provided from the metabolism of triacylglycerides (because oxidation of fatty acids yields carbon dioxide and water).

Ironically, the word *Arctic* comes from the ancient Greeks, who understood that the northernmost part of the earth lay under the stars of the constellation Ursa Major, the Great Bear. Although unaware of the polar bear, they called this region *Arktikós,* which means "the country of the great bear."

(*Thomas D. Mangelsen/Images of Nature*)

ond carbon is asymmetric. The various acylglycerols are normally soluble in benzene, chloroform, ether, and hot ethanol. Although triacylglycerols are insoluble in water, mono- and diacylglycerols readily form organized structures in water (discussed later), owing to the polarity of their free hydroxyl groups.

Triacylglycerols are rich in highly reduced carbons and thus yield large amounts of energy in the oxidative reactions of metabolism. Complete oxidation of 1 g of triacylglycerols yields about 38 kJ of energy, whereas proteins and carbohydrates yield only about 17 kJ/g. Also, their hydrophobic nature allows them to aggregate in highly anhydrous forms, whereas polysaccharides and proteins are highly hydrated. For these reasons, triacylglycerols are the molecules of choice for energy storage in animals. Body fat (mainly triacylglycerols) also provides good insulation. Whales and Arctic mammals rely on body fat for both insulation and energy reserves.

8.3 • Glycerophospholipids

A 1,2-diacylglycerol that has a phosphate group esterified at carbon atom 3 of the glycerol backbone is a **glycerophospholipid,** also known as a *phosphoglyceride* or a *glycerol phosphatide* (Figure 8.4). These lipids form one of the largest classes of natural lipids and one of the most important. They are essential components of cell membranes and are found in small concentrations in other parts of the cell. It should be noted that all glycerophospholipids are members of the broader class of lipids known as **phospholipids.**

The numbering and nomenclature of glycerophospholipids present a dilemma in that the number 2 carbon of the glycerol backbone of a phos-
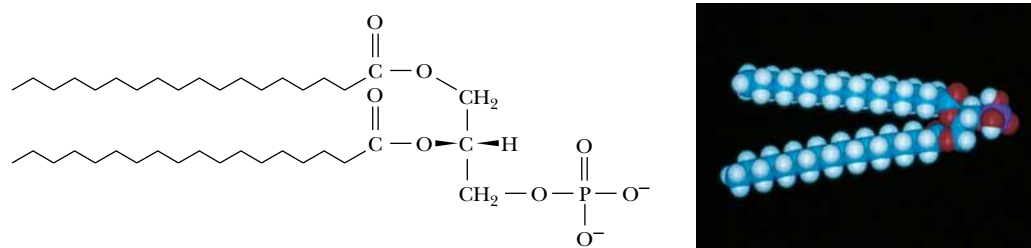
FIGURE 8.4 • Phosphatidic acid, the parent compound for glycerophospholipids.

pholipid is asymmetric. It is possible to name these molecules either as D- or L-isomers. Thus, glycerol phosphate itself can be referred to either as D-glycerol-1-phosphate or as L-glycerol-3-phosphate (Figure 8.5). Instead of naming the glycerol phosphatides in this way, biochemists have adopted the *stereospecific numbering* or *sn-* system. In this system, the *pro-S* position of a prochiral atom is denoted as the *1-position,* the prochiral atom as the *2-position,* and so on. When this scheme is used, the prefix *sn-* precedes the molecule name (glycerol phosphate in this case) and distinguishes this nomenclature from other approaches. In this way, the glycerol phosphate in natural phosphoglycerides is named *sn*-glycerol-3-phosphate.

The Most Common Phospholipids

Phosphatidic acid, the parent compound for the glycerol-based phospholipids (Figure 8.4), consists of *sn*-glycerol-3-phosphate, with fatty acids esterified at the 1- and 2-positions. Phosphatidic acid is found in small amounts in most natural systems and is an important intermediate in the biosynthesis of the more common glycerophospholipids (Figure 8.6). In these compounds, a

---

𝒜 D E E P E R   L O O K

Prochirality

If a tetrahedral center in a molecule has two identical substituents, it is referred to as **prochiral** since, if either of the like substituents is converted to a different group, the tetrahedral center then becomes chiral. Consider glycerol: the central carbon of glycerol is prochiral since replacing either of the —CH₂OH groups would make the central carbon chiral. Nomenclature for prochiral centers is based on the (R,S) system (in Chapter 3). To name the otherwise identical substituents of a prochiral center, imagine

increasing slightly the priority of one of them (by substituting a deuterium for a hydrogen, for example) as shown: the resulting molecule has an (S)-configuration about the (now chiral) central carbon atom. The group that contains the deuterium is thus referred to as the *pro-S* group. As a useful exercise, you should confirm that labeling the other CH₂OH group with a deuterium produces the (R)-configuration at the central carbon, so that this latter CH₂OH group is the *pro-R* substituent.

Glycerol

1-d, 2(S)-Glycerol
(S-configuration at C-2)

pro-*S* position ────────▶ CH_2OH $CH_2OPO_3^{2-}$

$HO-\overset{|}{\underset{|}{C}}-H$ ≡ $H-\overset{|}{\underset{|}{C}}-OH$

pro-*R* position ────────▶ $CH_2OPO_3^{2-}$ CH_2OH

L-Glycerol-3-phosphate   **D-Glycerol-1-phosphate**

sn-**Glycerol-3-phosphate**
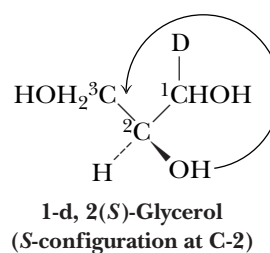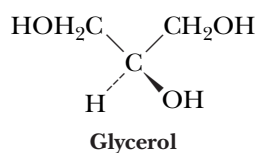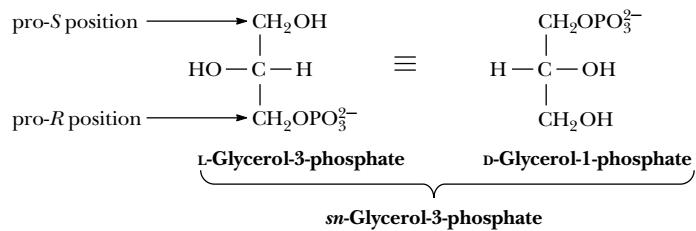
FIGURE 8.5 • The absolute configuration of *sn*-glycerol-3-phosphate. The pro-(*R*) and pro-(*S*) positions of the parent glycerol are also indicated.

Phosphatidylcholine
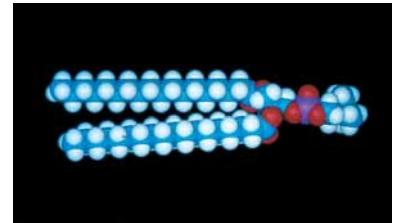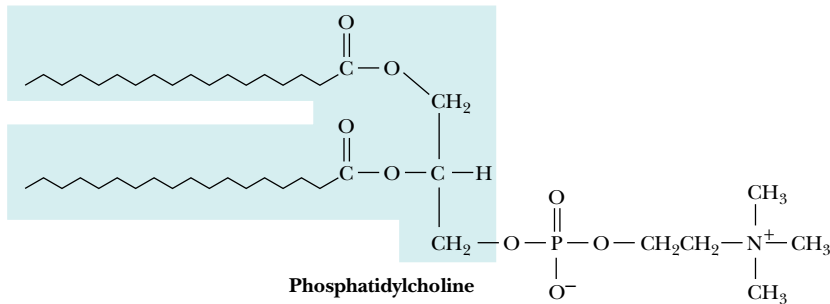
GLYCEROLIPIDS WITH OTHER HEAD GROUPS:

Phosphatidylethanolamine

Phosphatidylserine

Phosphatidylglycerol
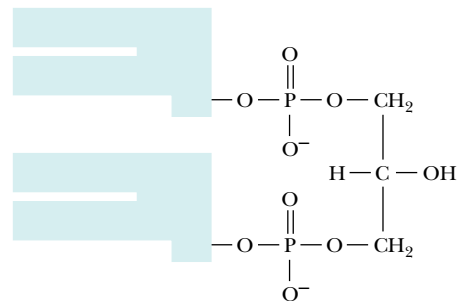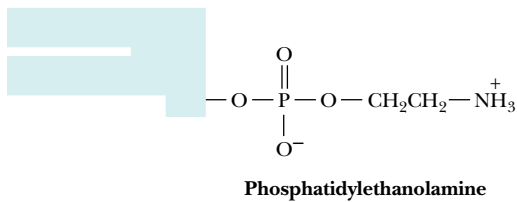
Diphosphatidylglycerol (Cardiolipin)
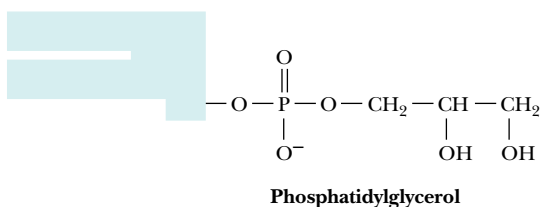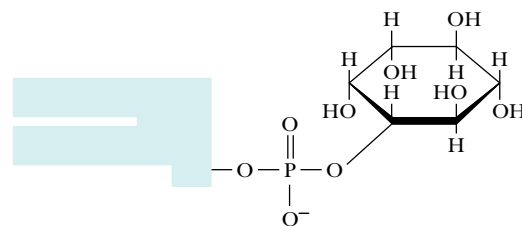
Phosphatidylinositol
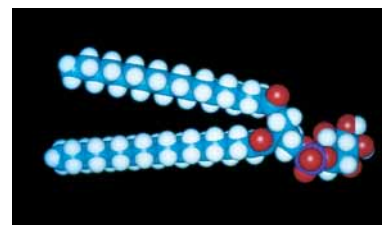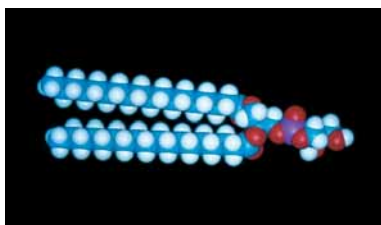
FIGURE 8.6 • Structures of several glycerophospholipids and space-filling models of phosphatidylcholine, phosphatidylglycerol, and phosphatidylinositol.

variety of polar groups are esterified to the phosphoric acid moiety of the molecule. The phosphate, together with such esterified entities, is referred to as a "head" group. Phosphatides with choline or ethanolamine are referred to as **phosphatidylcholine** (known commonly as **lecithin**) or **phosphatidylethanolamine,** respectively. These phosphatides are two of the most common constituents of biological membranes. Other common *head groups* found in phosphatides include glycerol, serine, and inositol (Figure 8.6). Another kind of glycerol phosphatide found in many tissues is **diphosphatidylglycerol.** First observed in heart tissue, it is also called **cardiolipin.** In cardiolipin, a phosphatidylglycerol is esterified through the C-1 hydroxyl group of the glycerol moiety of the head group to the phosphoryl group of another phosphatidic acid molecule.

$\mathcal{A}$ DEEPER LOOK

Glycerophospholipid Degradation: One of the Effects of Snake Venoms

The venoms of poisonous snakes contain (among other things) a class of enzymes known as **phospholipases,** enzymes that cause the breakdown of phospholipids. For example, the venoms of the eastern diamondback rattlesnake (*Crotalus adamanteus*) and the Indian cobra (*Naja naja*) both contain phospholipase A_2, which catalyzes the hydrolysis of fatty acids at the C-2 position of glycerophospholipids.

The phospholipid breakdown product of this reaction, *lysolecithin,* acts as a detergent and dissolves the membranes of red blood cells, causing them to rupture. Indian cobras kill several thousand people each year.
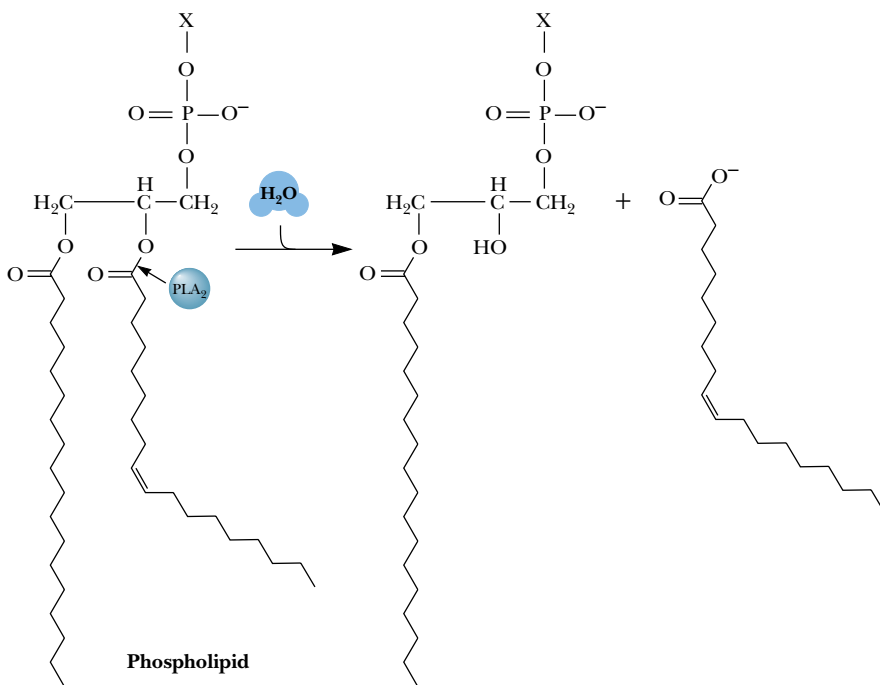
Eastern diamondback rattlesnake. *(Dr. E. R. Degginger)*

Phospholipid

Indian cobra. *(Dr. E. R. Degginger)*

FIGURE 8.7 • A space-filling model of 1-stearoyl-2-oleoyl-phosphatidylcholine.

Phosphatides exist in many different varieties, depending on the fatty acids esterified to the glycerol group. As we shall see, the nature of the fatty acids can greatly affect the chemical and physical properties of the phosphatides and the membranes that contain them. In most cases, glycerol phosphatides have a saturated fatty acid at position 1 and an unsaturated fatty acid at position 2 of the glycerol. Thus, **1-stearoyl-2-oleoyl-phosphatidylcholine** (Figure 8.7) is a common constituent in natural membranes, but **1-linoleoyl-2-palmitoylphosphatidylcholine** is not.

Both structural and functional strategies govern the natural design of the many different kinds of glycerophospholipid head groups and fatty acids. The structural roles of these different glycerophospholipid classes are described in Chapter 9. Certain phospholipids, including phosphatidylinositol and phosphatidylcholine, participate in complex cellular signaling events. These roles, appreciated only in recent years, are described in Chapter 34.

Ether Glycerophospholipids

Ether glycerophospholipids possess an ether linkage instead of an acyl group at the C-1 position of glycerol (Figure 8.8). One of the most versatile biochemical signal molecules found in mammals is **platelet activating factor,** or **PAF,** a unique ether glycerophospholipid (Figure 8.9). The alkyl group at C-1 of PAF is typically a 16-carbon chain, but the acyl group at C-2 is a 2-carbon acetate unit. By virtue of this acetate group, PAF is much more water-soluble
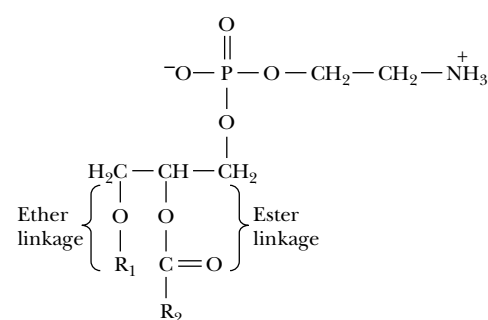
FIGURE 8.8 • A 1-alkyl 2-acyl-phosphatidylethanolamine (an ether glycerophospholipid).

Platelet Activating Factor: A Potent Glyceroether Mediator

Platelet activating factor (PAF) was first identified by its ability (at low levels) to cause platelet aggregation and dilation of blood vessels, but it is now known to be a potent mediator in inflammation, allergic responses, and shock. PAF effects are observed at tissue concentrations as low as 10^{-12} *M.* PAF causes a dramatic inflammation of air passages and induces asthma-like symptoms in laboratory animals. **Toxic-shock syndrome** occurs when fragments of destroyed bacteria act as toxins and induce the synthesis of PAF. This results in a drop in blood pressure and a reduced volume of blood pumped by the heart, which leads to shock and, in severe cases, death.

Beneficial effects have also been attributed to PAF. In reproduction, PAF secreted by the fertilized egg is instrumental in the implantation of the egg in the uterine wall. PAF is produced in significant quantities in the lungs of the fetus late in pregnancy and may stimulate the production of fetal lung surfactant, a protein–lipid complex that prevents collapse of the lungs in a newborn infant.
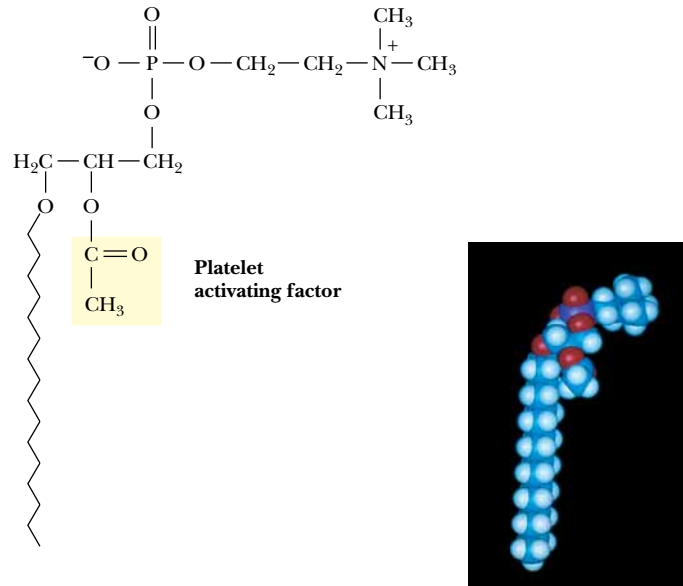
FIGURE 8.9 • The structure of 1-alkyl 2-acetyl-phosphatidylcholine, also known as platelet activating factor or PAF.

than other lipids, allowing PAF to function as a soluble messenger in signal transduction.

Plasmalogens are ether glycerophospholipids in which the alkyl moiety is *cis*-α,β-unsaturated (Figure 8.10). Common plasmalogen head groups include choline, ethanolamine, and serine. These lipids are referred to as phosphatidal choline, phosphatidal ethanolamine, and phosphatidal serine.
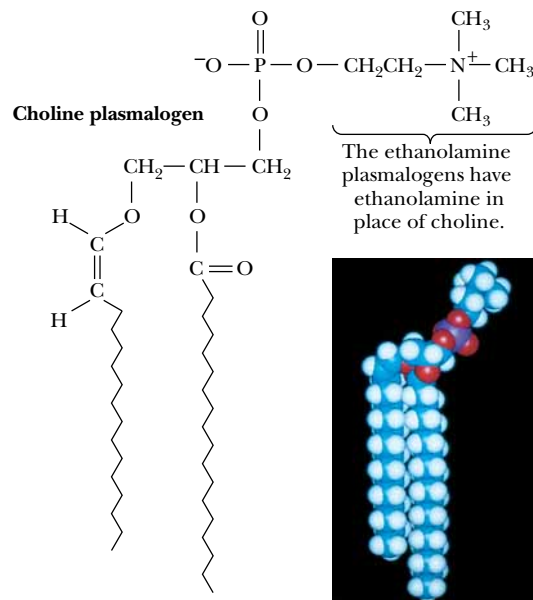
FIGURE 8.10 • The structure and a space-filling model of a choline plasmalogen.
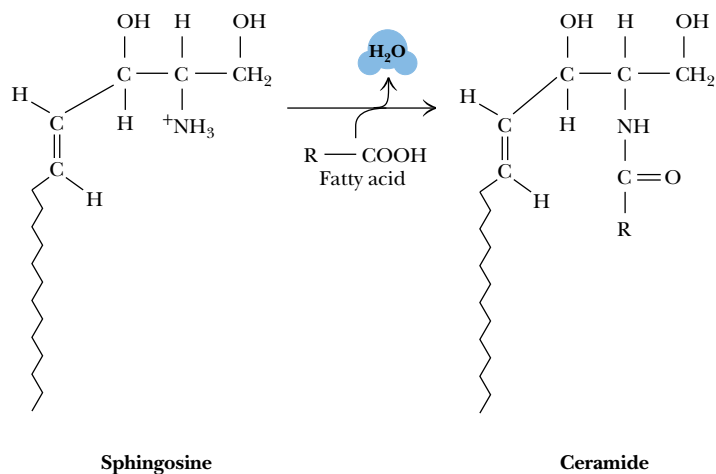
FIGURE 8.11 • Formation of an amide linkage between a fatty acid and sphingosine produces a ceramide.

8.4 • Sphingolipids

Sphingolipids represent another class of lipids found frequently in biological membranes. An 18-carbon amino alcohol, **sphingosine** (Figure 8.11), forms the backbone of these lipids rather than glycerol. Typically, a fatty acid is joined to a sphingosine via an amide linkage to form a **ceramide. Sphingomyelins** represent a phosphorus-containing subclass of sphingolipids and are especially important in the nervous tissue of higher animals. A **sphingomyelin** is formed by the esterification of a phosphorylcholine or a phosphorylethanolamine to the 1-hydroxy group of a ceramide (Figure 8.12).

**Choline sphingomyelin
with stearic acid**
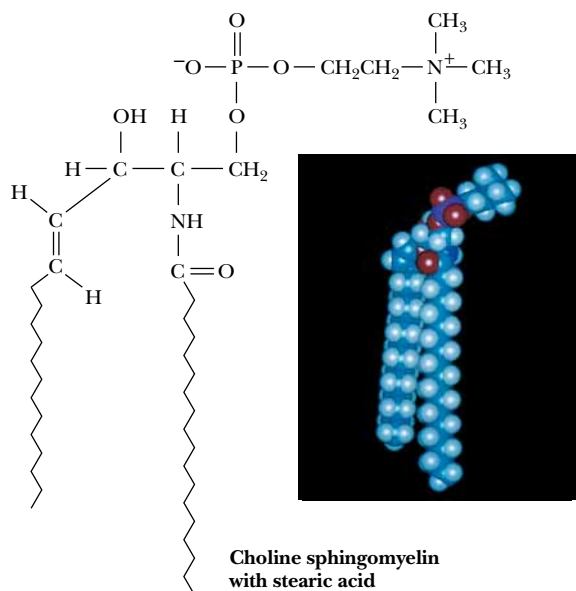
FIGURE 8.12 • A structure and a space-filling model of a choline sphingomyelin formed from stearic acid.

β-D-galactose

CH₂OH ... (structure)
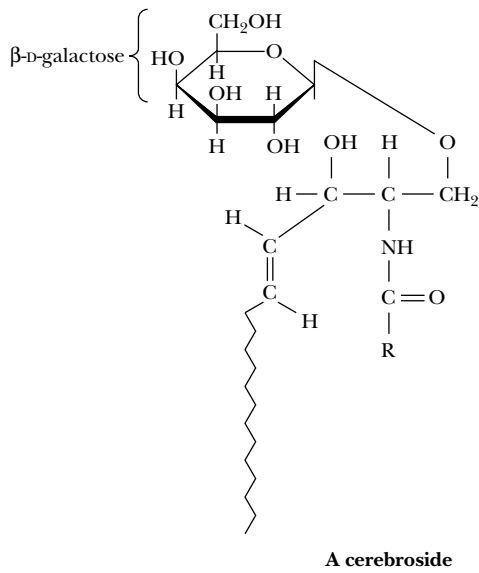
A cerebroside

FIGURE 8.13 • The structure of a cerebroside. Note the sphingosine backbone.

There is another class of ceramide-based lipids which, like the sphingomyelins, are important components of muscle and nerve membranes in animals. These are the **glycosphingolipids,** and they consist of a ceramide with one or more sugar residues in a β-glycosidic linkage at the 1-hydroxyl moiety. The neutral glycosphingolipids contain only neutral (uncharged) sugar residues. When a single glucose or galactose is bound in this manner, the molecule is a **cerebroside** (Figure 8.13). Another class of lipids is formed when a sulfate is esterified at the 3-position of the galactose to make a **sulfatide.** Gangliosides (Figure 8.14) are more complex glycosphingolipids that consist of a ceramide backbone with three or more sugars esterified, one of these being a **sialic acid** such as *N*-acetylneuraminic acid. These latter compounds are referred to as *acidic glycosphingolipids,* and they have a net negative charge at neutral pH.

The glycosphingolipids have a number of important cellular functions, despite the fact that they are present only in small amounts in most membranes. Glycosphingolipids at cell surfaces appear to determine, at least in part, certain elements of tissue and organ specificity. Cell–cell recognition and tissue immunity appear to depend upon specific glycosphingolipids. Gangliosides are present in nerve endings and appear to be important in nerve impulse transmission. A number of genetically transmitted diseases involve the accumulation of specific glycosphingolipids due to an absence of the enzymes needed for their degradation. Such is the case for ganglioside G_{M2} in the brains of *Tay-Sachs disease* victims, a rare but fatal disease characterized by a red spot on the retina, gradual blindness, and loss of weight, especially in infants and children.

G_{M1}
G_{M2}
G_{M3}

D-Galactose   *N*-Acetyl-D-galactosamine   D-Galactose   D-Glucose

N-Acetylneuraminidate
(sialic acid)

Gangliosides G_{M1}, G_{M2}, and G_{M3}
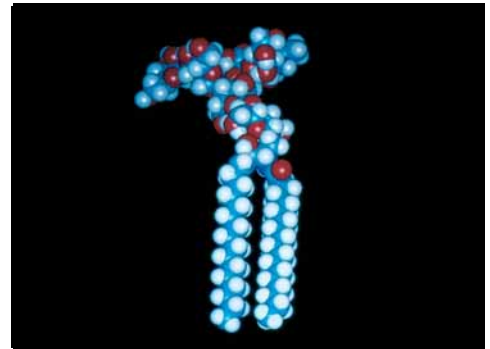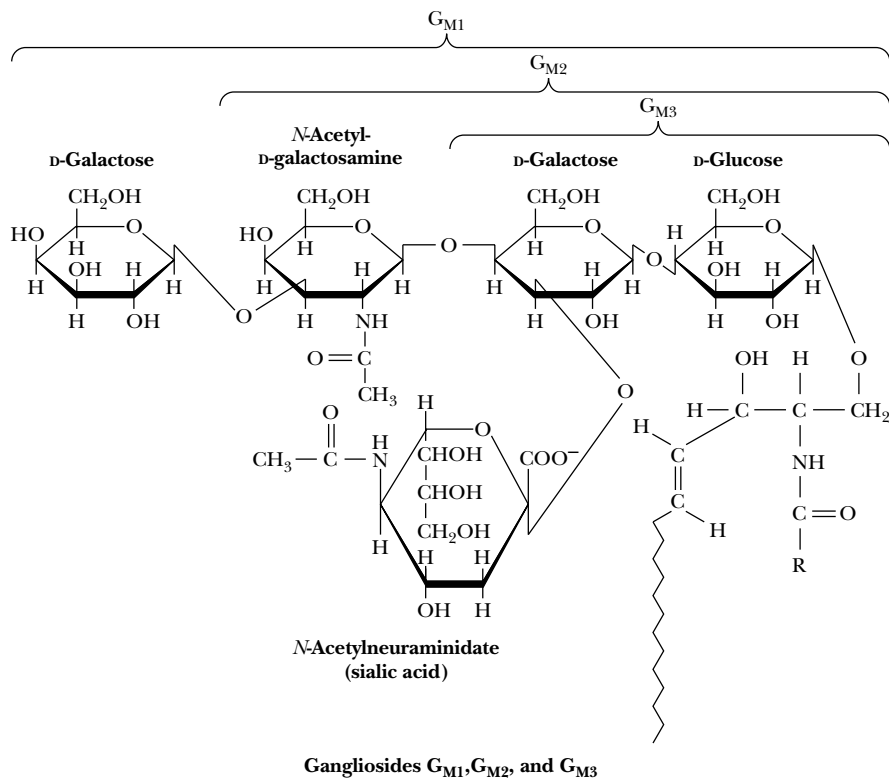
FIGURE 8.14 • The structures of several important gangliosides. Also shown is a space-filling model of ganglioside G_{M1}.

Moby Dick and Spermaceti: A Valuable Wax from Whale Oil

When oil from the head of the sperm whale is cooled, **spermaceti,** a translucent wax with a white, pearly luster, crystallizes from the mixture. Spermaceti, which makes up 11% of whale oil, is composed mainly of the wax **cetyl palmitate:**

$$CH_3(CH_2)_{14}—COO—(CH_2)_{15}CH_3$$

as well as smaller amounts of cetyl alcohol:

$$HO—(CH_2)_{15}CH_3$$

Spermaceti and cetyl palmitate have been widely used in the making of cosmetics, fragrant soaps, and candles.

In the literary classic *Moby Dick,* Herman Melville describes Ishmael's impressions of spermaceti, when he muses that the waxes "discharged all their opulence, like fully ripe grapes their wine; as I snuffed that uncontaminated aroma—literally and truly, like the smell of spring violets."*

*Melville, H., *Moby Dick,* Octopus Books, London, 1984, p. 205 (Adapted from *Chemistry in Moby Dick,* Waddell, T. G., and Sanderlin, R. R. (1986), *Journal of Chemical Education* **63:**1019–1020.)

8.5 • Waxes

Waxes are esters of long-chain alcohols with long-chain fatty acids. The resulting molecule can be viewed (in analogy to the glycerolipids) as having a weakly polar head group (the ester moiety itself) and a long, nonpolar tail (the hydrocarbon chains) (Figure 8.15). Fatty acids found in waxes are usually saturated. The alcohols found in waxes may be saturated or unsaturated and may include sterols, such as cholesterol (see later section). Waxes are water-insoluble due to the weakly polar nature of the ester group. As a result, this class of molecules confers water-repellant character to animal skin, to the leaves of certain plants, and to bird feathers. The glossy surface of a polished apple results from a wax coating. **Carnauba wax,** obtained from the fronds of a species of palm tree in Brazil, is a particularly hard wax used for high gloss finishes, such as in automobile wax, boat wax, floor wax, and shoe polish. **Lanolin,** a component of wool wax, is used as a base for pharmaceutical and cosmetic products because it is rapidly assimilated by human skin.
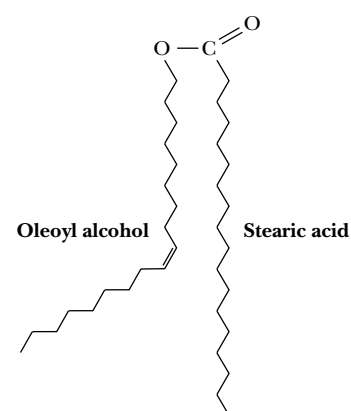
FIGURE 8.15 • An example of a wax. Oleoyl alcohol is esterified to stearic acid in this case.

8.6 • Terpenes

The **terpenes** are a class of lipids formed from combinations of two or more molecules of 2-methyl-1,3-butadiene, better known as **isoprene** (a five-carbon unit that is abbreviated C_5). A **monoterpene** (C_{10}) consists of two isoprene units, a **sesquiterpene** (C_{15}) consists of three isoprene units, a **diterpene** (C_{20}) has four isoprene units, and so on. Isoprene units can be linked in terpenes to form straight chain or cyclic molecules, and the usual method of linking isoprene units is head to tail (Figure 8.16). Monoterpenes occur in all higher plants, while sesquiterpenes and diterpenes are less widely known. Several examples of these classes of terpenes are shown in Figure 8.17. The **triterpenes** are C_{30} terpenes and include **squalene** and **lanosterol,** two of the precursors of cholesterol and other steroids (discussed later). **Tetraterpenes** (C_{40}) are less common but include the carotenoids, a class of colorful photosynthetic pigments. β-Carotene is the precursor of vitamin A, while lycopene, similar to β-carotene but lacking the cyclopentene rings, is a pigment found in tomatoes.
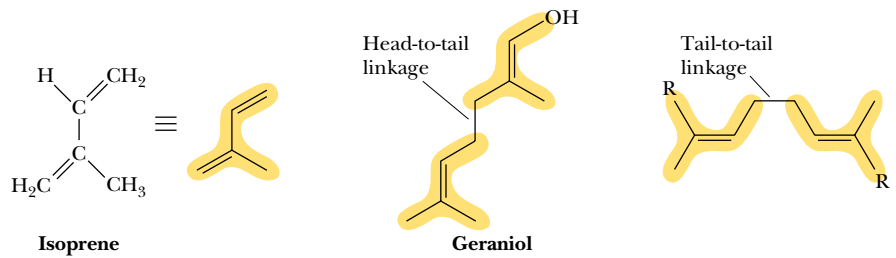
FIGURE 8.16 • The structure of isoprene (2-methyl-1,3-butadiene) and the structure of head-to-tail and tail-to-tail linkages. Isoprene itself can be formed by distillation of natural rubber, a linear head-to-tail polymer of isoprene units.

Long-chain polyisoprenoid molecules with a terminal alcohol moiety are called **polyprenols.** The **dolichols,** one class of polyprenols (Figure 8.18), consist of 16 to 22 isoprene units and, in the form of dolichyl phosphates, function to carry carbohydrate units in the biosynthesis of glycoproteins in animals. Polyprenyl groups serve to *anchor* certain proteins to biological membranes (discussed in Chapter 9).
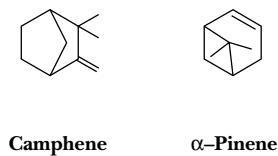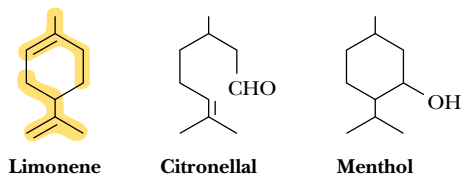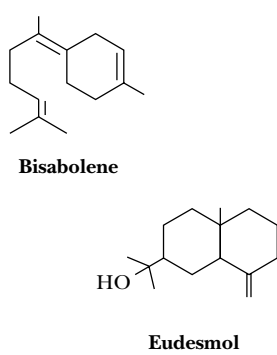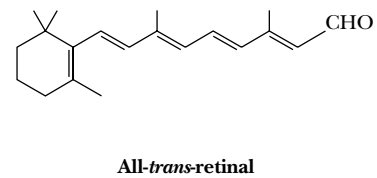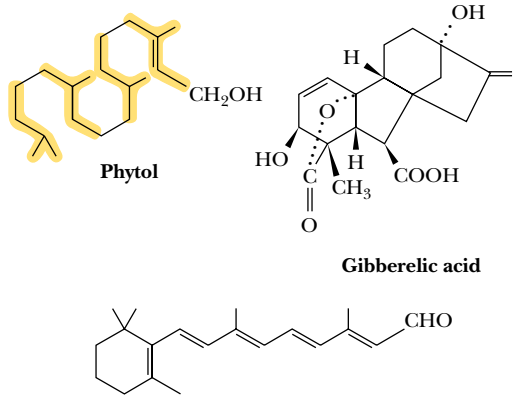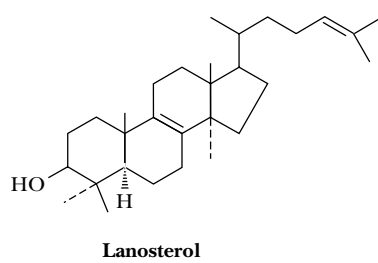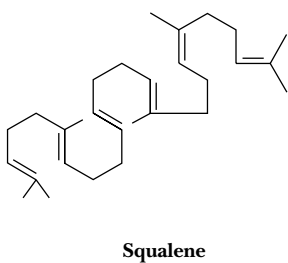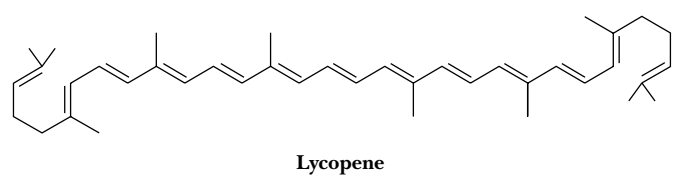
FIGURE 8.17 • Many monoterpenes are readily recognized by their characteristic flavors or odors (limonene in lemons; citronellal in roses, geraniums, and some perfumes; pinene in turpentine; and menthol from peppermint, used in cough drops and nasal inhalers). The diterpenes, which are C_{20} terpenes, include retinal (the essential light-absorbing pigment in rhodopsin, the photoreceptor protein of the eye), phytol (a constituent of chlorophyll), and the gibberellins (potent plant hormones). The triterpene lanosterol is a constituent of wool fat. Lycopene is a carotenoid found in ripe fruit, especially tomatoes.

Dolichol phosphate

Coenzyme Q (Ubiquinone, UQ)

Vitamin E (α-tocopherol)

Vitamin K₁
(phylloquinone)

Undecaprenyl alcohol (bactoprenol)
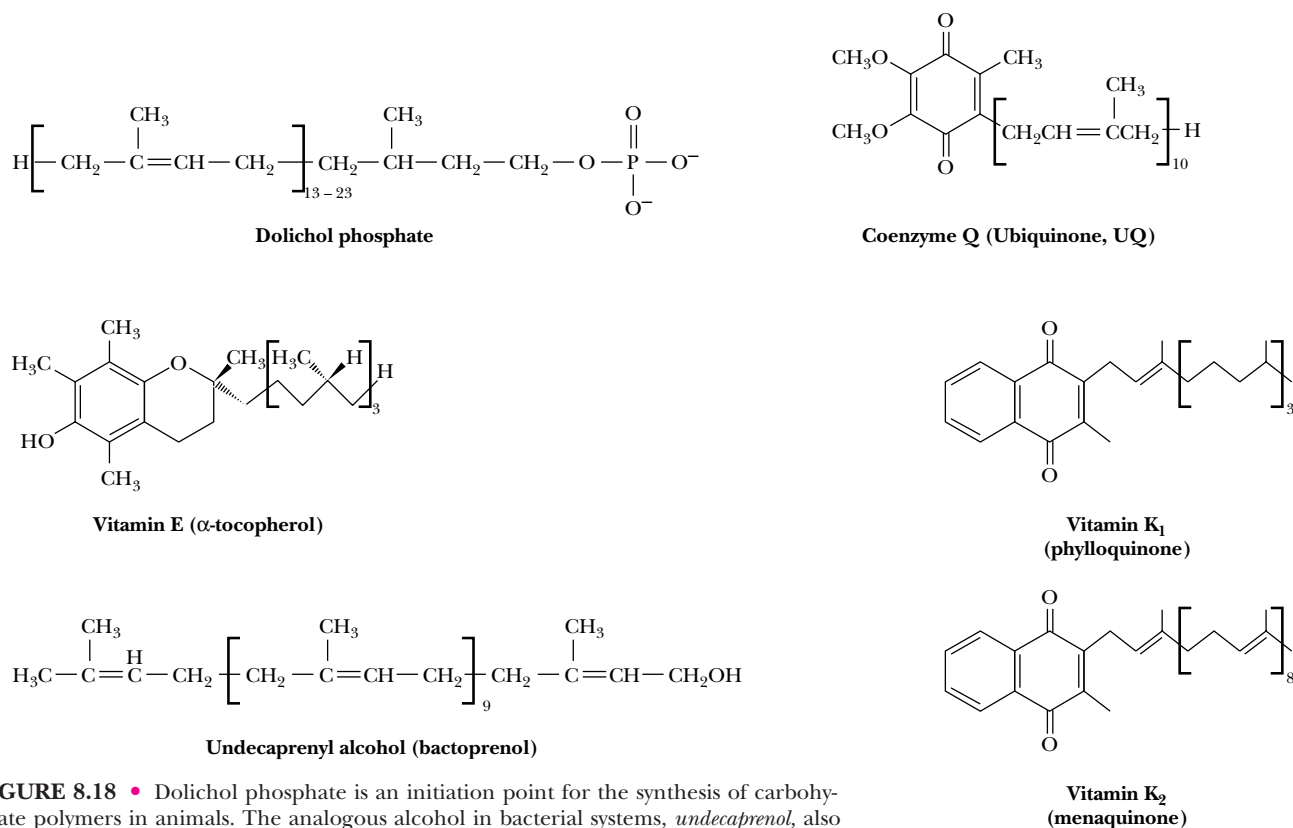
FIGURE 8.18 • Dolichol phosphate is an initiation point for the synthesis of carbohydrate polymers in animals. The analogous alcohol in bacterial systems, *undecaprenol,* also known as *bactoprenol,* consists of 11 isoprene units. Undecaprenyl phosphate delivers sugars from the cytoplasm for the synthesis of cell wall components such as peptidoglycans, lipopolysaccharides, and glycoproteins. Polyprenyl compounds also serve as the side chains of vitamin K, the ubiquinones, plastoquinones, and tocopherols (such as vitamin E).

Vitamin K₂
(menaquinone)

𝒜 D E E P E R L O O K

Why Do Plants Emit Isoprene?

he Blue Ridge Mountains of Virginia are so-named for the misty blue vapor or haze that hangs over them through much of the summer season. This haze is composed in part of isoprene that is produced and emitted by the plants and trees of the mountains. Global emission of isoprene from vegetation is estimated at 3×10^{14} g/yr. Plants frequently emit as much as 15% of the carbon fixed in photosynthesis as isoprene, and Thomas Sharkey, a botanist at the University of Wisconsin, has shown that the kudzu plant can emit as much as 67% of its fixed carbon as isoprene as the result of water stress. Why should plants and trees emit large amounts of isoprene and other hydrocarbons? Sharkey has shown that an isoprene atmosphere or "blanket" can protect leaves from irreversible damage induced by high (summer-like) temperatures. He hypothesizes that isoprene in the air around plants dissolves into leaf-cell membranes, altering the lipid bilayer and/or lipid–protein and protein–protein interactions within the membrane to increase thermal tolerance.

Blue Ridge Mountains. *(Randy Wells/Tony Stone Images)*

$\mathcal{H}$ UMAN BIOCHEMISTRY

Coumarin or Warfarin—Agent of Life or Death

The isoprene-derived molecule whose structure is shown here is known alternately as **Coumarin** and **warfarin.** By the former name, it is a widely prescribed anticoagulant. By the latter name, it is a component of rodent poisons. How can the same chemical species be used for such disparate purposes? The key to both uses lies in its ability to act as an antagonist of vitamin K in the body.

Vitamin K stimulates the carboxylation of glutamate residues on certain proteins, including some proteins in the blood-clotting cascade (including **prothrombin, Factor VII, Factor IX, and Factor X,** which undergo a Ca^{2+}-dependent conformational change in the course of their biological activity, as well as **protein C** and **protein S,** two regulatory proteins). Carboxylation of these coagulation factors is catalyzed by a carboxylase that requires the reduced form of vitamin K (vitamin KH_2), molecular oxygen, and carbon dioxide. KH_2 is oxidized to vitamin K epoxide, which is recycled to KH_2 by the enzymes **vitamin K epoxide reductase** (1) and **vitamin K reductase** (2, 3). Coumarin/warfarin exerts its anti-coagulant effect by inhibiting vitamin K epoxide reductase and possibly also vitamin K reductase. This inhibition depletes vitamin KH_2 and reduces the activity of the carboxylase.

Coumarin/warfarin, given at a typical dosage of 4 to 5 mg/day, prevents the deleterious formation in the bloodstream of small blood clots and thus reduces the risk of heart attacks and strokes for individuals whose arteries contain sclerotic plaques. Taken in much larger doses, as for example in rodent poisons, Coumarin/warfarin can cause massive hemorrhages and death.

Warfarin (Coumarin)
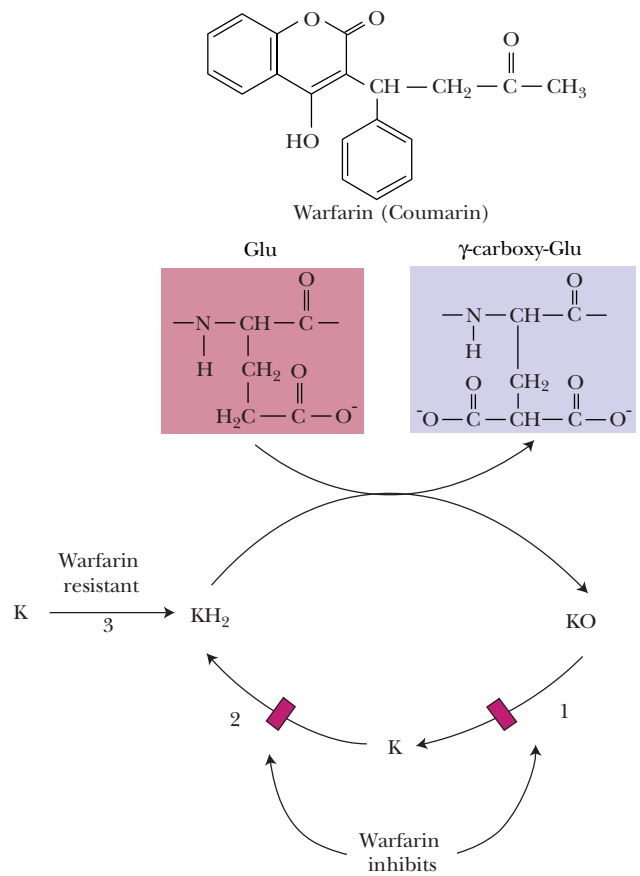
8.7 • Steroids

Cholesterol

A large and important class of terpene-based lipids is the **steroids.** This molecular family, whose members effect an amazing array of cellular functions, is based on a common structural motif of three six-membered rings and one five-membered ring all fused together. **Cholesterol** (Figure 8.19) is the most common steroid in animals and the precursor for all other animal steroids. The numbering system for cholesterol applies to all such molecules. Many steroids contain methyl groups at positions 10 and 13 and an 8- to 10-carbon alkyl side chain at position 17. The polyprenyl nature of this compound is particularly evident in the side chain. Many steroids contain an oxygen at C-3, either a hydroxyl group in sterols or a carbonyl group in other steroids. Note also that the carbons at positions 10 and 13 and the alkyl group at position 17 are nearly always oriented on the same side of the steroid nucleus, the β-orientation. Alkyl groups that extend from the other side of the steroid backbone are in an α-orientation.
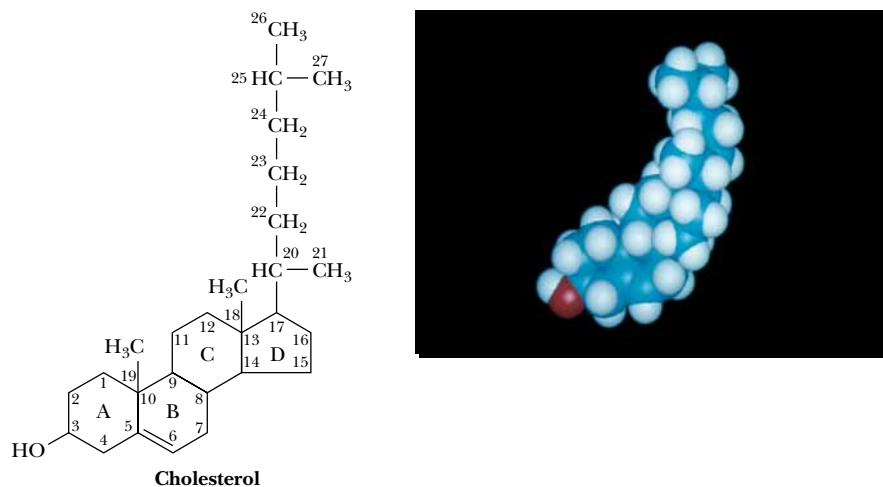
FIGURE 8.19 • The structure of cholesterol, shown with steroid ring designations and carbon numbering.

Cholesterol is a principal component of animal cell plasma membranes, and much smaller amounts of cholesterol are found in the membranes of intracellular organelles. The relatively rigid fused ring system of cholesterol and the weakly polar alcohol group at the C-3 position have important consequences for the properties of plasma membranes. Cholesterol is also a component of *lipoprotein complexes* in the blood, and it is one of the constituents of *plaques* that form on arterial walls in *atherosclerosis.*

Steroid Hormones

Steroids derived from cholesterol in animals include five families of hormones (the androgens, estrogens, progestins, glucocorticoids and mineralocorticoids) and bile acids (Figure 8.20). **Androgens** such as **testosterone** and **estrogens** such as **estradiol** mediate the development of sexual characteristics and sexual function in animals. The **progestins** such as **progesterone** participate in control of
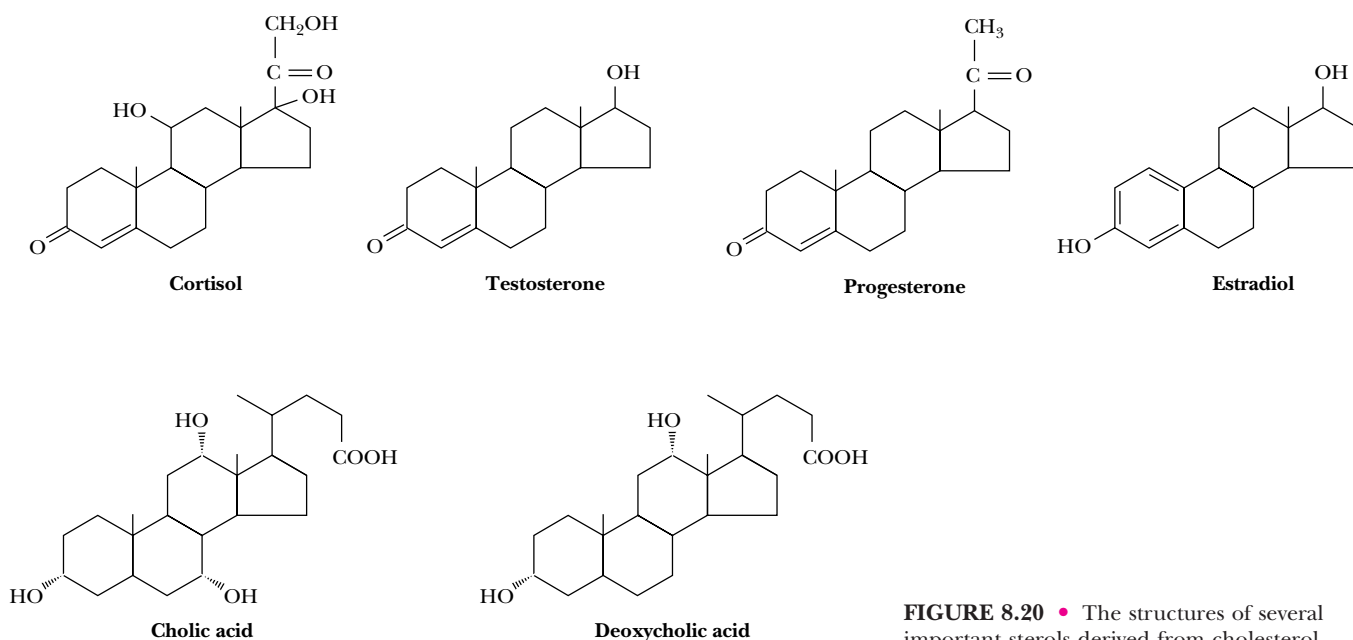
FIGURE 8.20 • The structures of several important sterols derived from cholesterol.

the menstrual cycle and pregnancy. **Glucocorticoids (cortisol,** for example) participate in the control of carbohydrate, protein, and lipid metabolism, whereas the **mineralocorticoids** regulate salt (Na^+, K^+, and Cl^-) balances in tissues. The **bile acids** (including **cholic** and **deoxycholic acid**) are detergent molecules secreted in bile from the gallbladder that assist in the absorption of dietary lipids in the intestine.

ℋUMAN BIOCHEMISTRY

Plant Sterols—Natural Cholesterol Fighters

Dietary guidelines for optimal health call for reducing the intake of cholesterol. One strategy for doing so involves the plant sterols, including sitosterol, stigmasterol, stigmastanol, and campesterol, shown in the figure. Despite their structural similarity to cholesterol, minor isomeric differences and/or the presence of methyl and ethyl groups in the side chains of these substances result in their poor absorption by intestinal mucosal cells. Interestingly, although plant sterols are not effectively absorbed by the body, they nonetheless are highly effective in blocking the absorption of cholesterol itself by intestinal cells.

The practical development of plant sterol drugs as cholesterol-lowering agents will depend both on structural features of the sterols themselves and on the form of the administered agent. For example, the unsaturated sterol sitosterol is poorly absorbed in the human intestine, whereas sitostanol, the saturated analog, is almost totally unabsorbable. In addition, there is evidence that plant sterols administered in a soluble, micellar form (see page 261 for a description of micelles) are more effective in blocking cholesterol absorption than plant sterols administered in a solid, crystalline form.

Stigmastanol

α_1- Sitosterol

Stigmasterol

β-Sitosterol

Campesterol
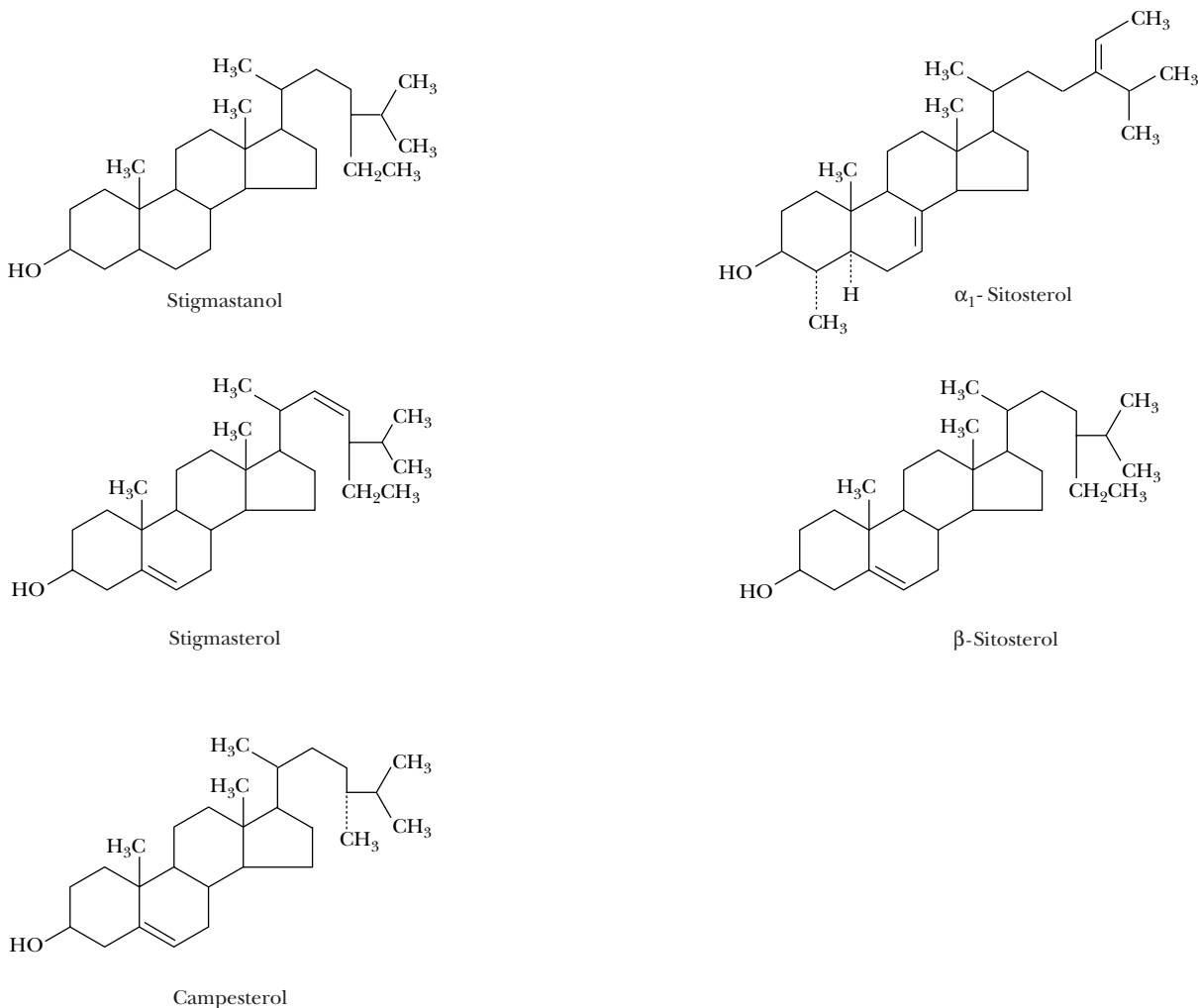
17β-Hydroxysteroid Dehydrogenase 3 Deficiency

Testosterone, the principal male sex steroid hormone, is synthesized in five steps from cholesterol, as shown below. In the last step, five isozymes catalyze the 17β-hydroxysteroid dehydrogenase reactions that interconvert 4-androstenedione and testosterone. Defects in the synthesis or action of testosterone can impair the development of the male phenotype during embryogenesis and cause the disorders of human sexuality termed male pseudohermaphroditism. Specifically, mutations in isozyme 3 of the 17β-hydroxysteroid dehydrogenase in the fetal testis impair the for-

mation of testosterone and give rise to genetic males with female external genitalia and blind-ending vaginas. Such individuals are typically raised as females but virilize at puberty, due to an increase in serum testosterone, and develop male hair growth patterns. Fourteen different mutations of 17β-hydroxysteroid dehydrogenase 3 have been identified in 17 affected families in the United States, the Middle East, Brazil, and Western Europe. These families account for about 45% of the patients with this disorder reported in scientific literature.
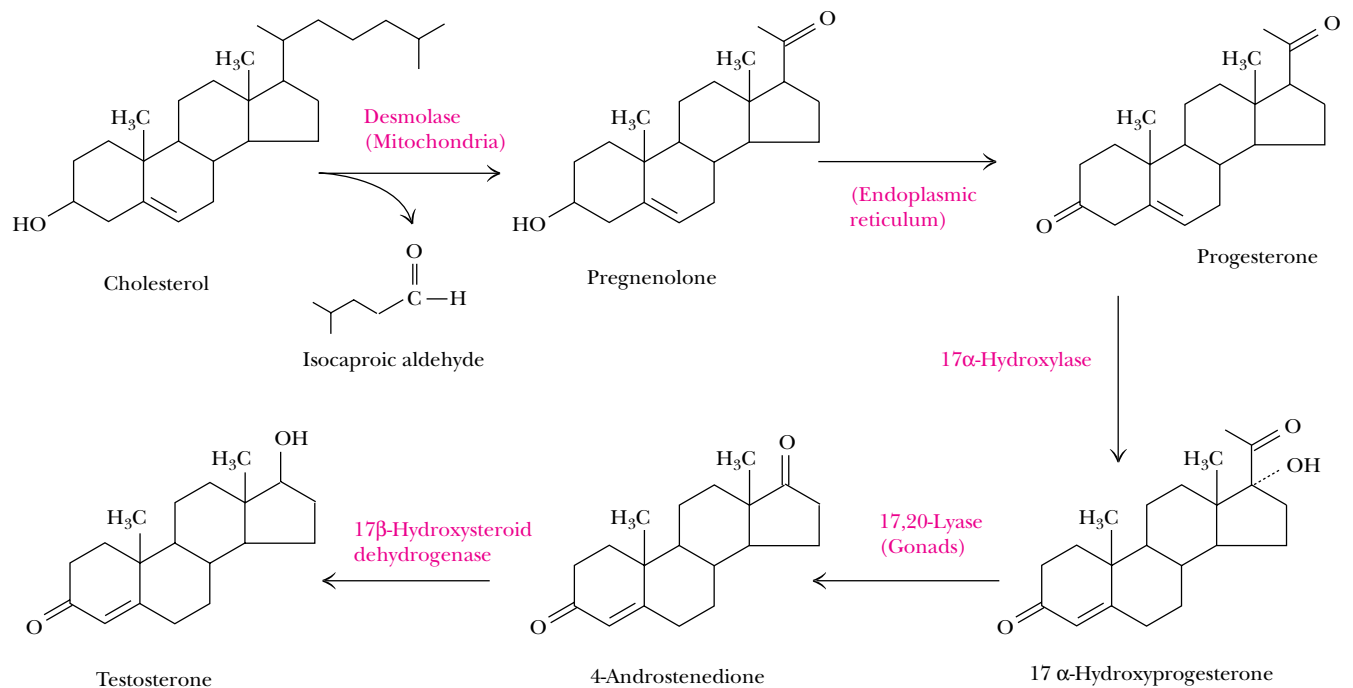
PROBLEMS

1. Draw the structures of (a) all the possible triacylglycerols that can be formed from glycerol with stearic and arachidonic acid, and (b) all the phosphatidylserine isomers that can be formed from palmitic and linolenic acids.

2. Describe in your own words the structural features of
a. a ceramide, and how it differs from a cerebroside.
b. a phosphatidylethanolamine, and how it differs from a phosphatidylcholine.
c. an ether glycerophospholipid, and how it differs from a plasmalogen.
d. a ganglioside, and how it differs from a cerebroside.
e. testosterone, and how it differs from estradiol.

3. From your memory of the structures, name
a. the glycerophospholipids that carry a net positive charge.
b. the glycerophospholipids that carry a net negative charge.
c. the glycerophospholipids that have zero net charge.

4. Compare and contrast two individuals, one of whose diet consists largely of meats containing high levels of cholesterol, and the other of whose diet is rich in plant sterols. Are their risks of cardiovascular disease likely to be similar or different? Explain your reasoning.

5. James G. Watt, Secretary of the Interior (1981–1983) in Ronald Reagan's first term, provoked substantial controversy by stating publicly that trees cause significant amounts of air pollution. Based on your reading of this chapter, evaluate Watt's remarks.

6. In a departure from his usual and highly popular westerns, author Louis L'Amour wrote a novel in 1987, *Best of the Breed* (Bantam Press), in which a military pilot of native American ancestry is shot down over the former Soviet Union and is forced to use the survival skills of his ancestral culture to escape his enemies. On the rare occasions when he is able to trap and kill an animal for food, he selectively eats the fat, not the meat. Based on your reading of this chapter, what is his reasoning for doing so?

257

FURTHER READING

Anderson, S., Russell, D. W., and Wilson, J. D., 1996. 17β-Hydroxysteroid dehydrogenase 3 deficiency. *Trends in Endocrinology and Metabolism* **7:**121–126.

Chakrin, L. W., and Bailey, D. M., 1984. *The Leukotrienes—Chemistry and Biology.* Orlando: Academic Press.

DeLuca, H. F., and Schneos, H. K., 1983. Vitamin D: recent advances. *Annual Review of Biochemistry* **52:**411–439.

Denke, M. A., 1995. Lack of efficacy of low-dose sitostanol therapy as an adjunct to a cholesterol-lowering diet in men with moderate hypercholesterolemia. *American Journal of Clinical Nutrition* **61:**392–396.

Dowd, P., Ham, S.-W., Naganathan, S., and Hershline, R., 1995. The mechanism of action of vitamin K. *Annual Review of Nutrition* **15:**419–440.

Hakamori, S., 1986. Glycosphingolipids. *Scientific American* **254:**44–53.

Hirsh, J., Dalen, J. E., Deykin, D., Poller, L., and Bussey, H., 1995. Oral anticoagulants: Mechanism of action, clinical effectiveness, and optimal therapeutic range. *Chest* **108:**231S–246S.

Katan, M. B., Zock, P. L., and Mensink, R. P., 1995. *Trans* fatty acids and their effects on lipoproteins in humans. *Annual Review of Biochemistry* **15:**473–493.

Keuhl, F. A., and Egan, R. W., 1980. Prostaglandins, arachidonic acid and inflammation. *Science* **210:**978–984.

Robertson, R. N., 1983. *The Lively Membranes.* Cambridge: Cambridge University Press.

Seachrist, L., 1996. A fragrance for cancer treatment and prevention. *The Journal of NIH Research* **8:**43.

Sharkey, T. D., 1995. Why plants emit isoprene. *Nature* **374:**769.

Sharkey, T. D., 1996. Emission of low molecular-mass hydrocarbons from plants. *Trends in Plant Science* **1:**78–82.

Vance, D. E., and Vance, J. E. (eds.), 1985. *Biochemistry of Lipids and Membranes.* Menlo Park, CA.: Benjamin-Cummings.

Vanhanen, H. T., Blomqvist, S., Ehnholm, C., et al., 1993. Serum cholesterol, cholesterol precursors, and plant sterols in hypercholesterolemic subjects with different apoE phenotypes during dietary sitostanol ester treatment. *Journal of Lipid Research* **34:**1535–1544.

$\mathcal{C}$hapter 9

Membranes and Cell Surfaces
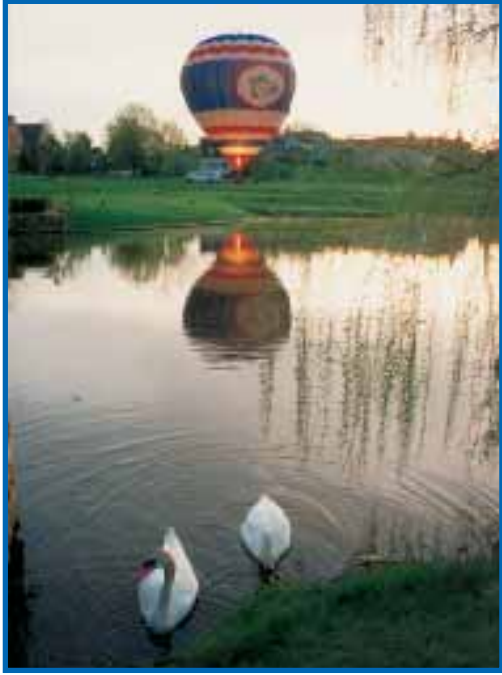
Membranes are thin envelopes that define the volume of cells, like this hot-air balloon is defined in space by its colorful envelope. (Boar's Head Inn Balloon, Charlottesville, VA, by Larry Swank)

Membranes serve a number of essential cellular functions. They constitute the boundaries of cells and intracellular organelles, and they provide a surface where many important biological reactions and processes occur. Membranes have proteins that mediate and regulate the transport of metabolites, macromolecules, and ions. Hormones and many other biological signal molecules and regulatory agents exert their effects via interactions with membranes. Photosynthesis, electron transport, oxidative phosphorylation, muscle contraction, and electrical activity all depend on membranes and membrane proteins. Thirty percent of the genes of at least one organism, *Mycoplasma genitalium* (whose entire genome has been sequenced), are thought to encode membrane proteins.

259

Biological membranes are uniquely organized arrays of lipids and proteins (either of which may be decorated with carbohydrate groups). The lipids found in biological systems are often **amphipathic,** signifying that they possess both polar and nonpolar groups. The hydrophobic nature of lipid molecules allows membranes to act as effective barriers to polar molecules. The polar moieties of amphipathic lipids typically lie at the surface of membranes, where they interact with water. Proteins interact with the lipids of membranes in a variety of ways. Some proteins associate with membranes via electrostatic interactions with polar groups on the membrane surface, whereas other proteins are embedded to various extents in the hydrophobic core of the membrane. Other proteins are *anchored* to membranes via covalently bound lipid molecules that associate strongly with the hydrophobic membrane core.

This chapter discusses the composition, structure, and dynamic processes of biological membranes.

9.1 • Membranes

Cells make use of many different types of membranes. All cells have a cytoplasmic membrane, or *plasma membrane,* that functions (in part) to separate the cytoplasm from the surroundings. In the early days of biochemistry, the plasma membrane was not accorded many functions other than this one of partition. We now know that the plasma membrane is also responsible for (1) the exclusion of certain toxic ions and molecules from the cell, (2) the accumulation of cell nutrients, and (3) energy transduction. It functions in (4) cell locomotion, (5) reproduction, (6) signal transduction processes, and (7) interactions with molecules or other cells in the vicinity.

Even the plasma membranes of prokaryotic cells (bacteria) are complex (Figure 9.1). With no intracellular organelles to divide and organize the work, bacteria carry out processes either at the plasma membrane or in the cyto-

(a)

(b)

(c)

(d)
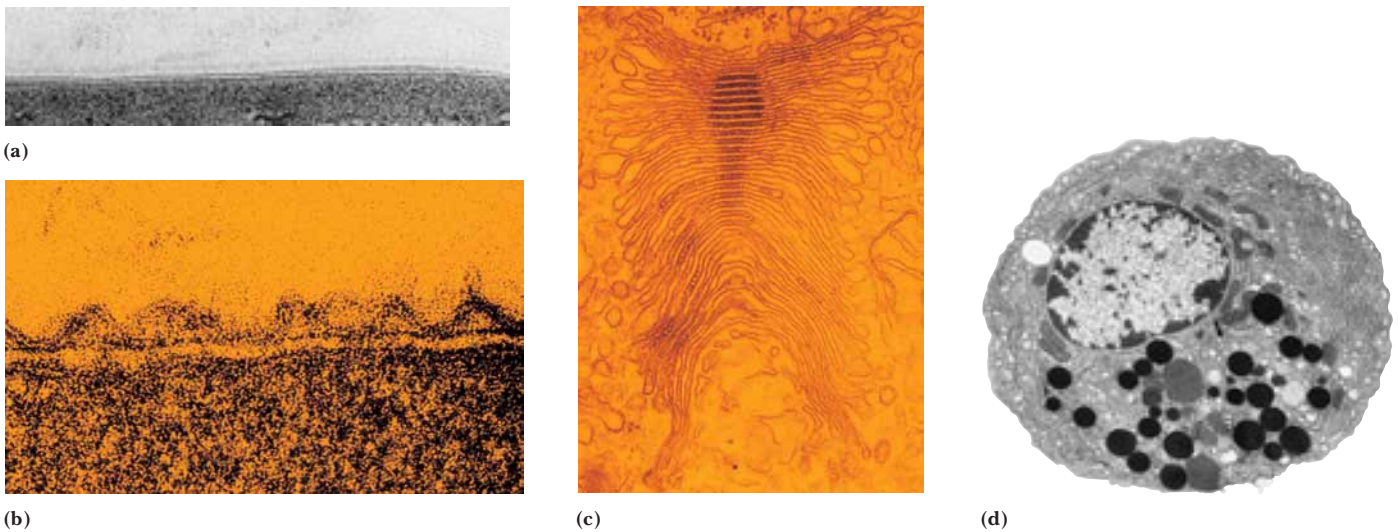
FIGURE 9.1 • Electron micrographs of several different membrane structures: (a) *Menoidium,* a protozoan; (b) Gram-negative envelope of *Aquaspirillum serpens;* (c) Golgi apparatus; (d) pancreatic acinar cell. *(a, T. T. Beveridge/Visuals Unlimited; b, © Cabisco/Visuals Unlimited; c, d, © D. W. Fawcett/Photo Researchers, Inc.)*

plasm itself. Eukaryotic cells, however, contain numerous intracellular organelles that perform specialized tasks. Nucleic acid biosynthesis is handled in the nucleus; mitochondria are the site of electron transport, oxidative phosphorylation, fatty acid oxidation, and the tricarboxylic acid cycle; and secretion of proteins and other substances is handled by the endoplasmic reticulum and the Golgi apparatus. This partitioning of labor is not the only contribution of the membranes in these cells. Many of the processes occurring in these organelles (or in the prokaryotic cell) actively involve membranes. Thus, some of the enzymes involved in nucleic acid metabolism are membrane-associated. The electron transfer chain and its associated system for ATP synthesis are embedded in the mitochondrial membrane. Many enzymes responsible for aspects of lipid biosynthesis are located in the endoplasmic reticulum membrane.

Spontaneously Formed Lipid Structures

Monolayers and Micelles

Amphipathic lipids spontaneously form a variety of structures when added to aqueous solution. All these structures form in ways that minimize contact between the hydrophobic lipid chains and the aqueous milieu. For example, when small amounts of a fatty acid are added to an aqueous solution, a monolayer is formed at the air–water interface, with the polar head groups in contact with the water surface and the hydrophobic tails in contact with the air (Figure 9.2). Few lipid molecules are found as monomers in solution.

Further addition of fatty acid eventually results in the formation of micelles. **Micelles** formed from an amphipathic lipid in water position the hydrophobic tails in the center of the lipid aggregation with the polar head groups facing outward. Amphipathic molecules that form micelles are characterized by a unique **critical micelle concentration,** or **CMC.** Below the CMC, individual lipid molecules predominate. Nearly all the lipid added above the CMC, however, spontaneously forms micelles. Micelles are the preferred form of aggregation in water for detergents and soaps. Some typical CMC values are listed in Figure 9.3.
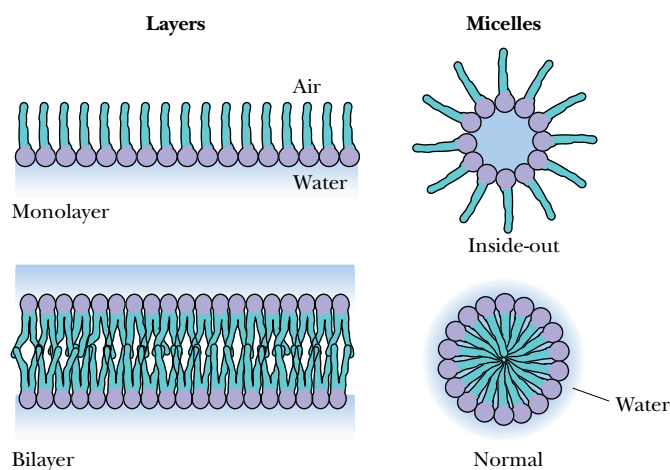
FIGURE 9.2 • Several spontaneously formed lipid structures.

Structure	M_r	CMC	Micelle M_r
Triton X-100 $CH_3-C(CH_3)_2-CH_2-C(CH_3)_2-C_6H_4-(OCH_2CH_2)_{10}-OH$	625	0.24 mM	90–95,000
Octyl glucoside	292	25 mM	
$C_{12}E_8$ (Dodecyl octaoxyethylene ether) $C_{12}H_{25}-(OCH_2CH_2)_8-OH$	538	0.071 mM	

FIGURE 9.3 • The structures of some common detergents and their physical properties. Micelles formed by detergents can be quite large. Triton X-100, for example, typically forms micelles with a total molecular mass of 90 to 95 kD. This corresponds to approximately 150 molecules of Triton X-100 per micelle.

Bilayer

(a)

Unilamellar vesicle
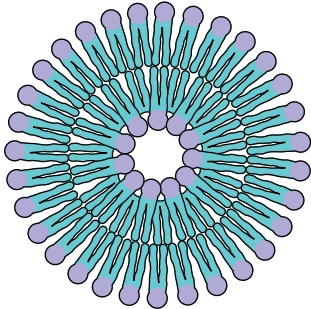
(b)

Multilamellar vesicle
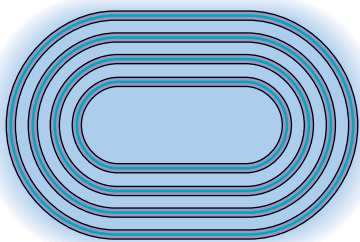
(c)

(d)

FIGURE 9.4 • Drawings of (a) a bilayer, (b) a unilamellar vesicle, (c) a multilamellar vesicle, and (d) an electron micrograph of a multilamellar Golgi structure (× 94,000).
(d, David Phillips/Visuals Unlimited)

Lipid Bilayers

Lipid bilayers consist of back-to-back arrangements of monolayers (Figure 9.2). Phospholipids prefer to form bilayer structures in aqueous solution because their pairs of fatty acyl chains do not pack well in the interior of a micelle. Phospholipid bilayers form rapidly and spontaneously when phospholipids are added to water, and they are stable structures in aqueous solution. As opposed to micelles, which are small, self-limiting structures of a few hundred molecules, bilayers may form spontaneously over large areas (10^8 nm^2 or more). Because exposure of the edges of the bilayer to solvent is highly unfavorable, extensive bilayers normally wrap around themselves and form closed vesicles (Figure 9.4). The nature and integrity of these vesicle structures are very much dependent on the lipid composition. Phospholipids can form either *unilamellar vesicles* (with a single lipid bilayer) known as *liposomes,* or *multilamellar vesicles*. These latter structures are reminiscent of the layered structure of onions. Multilamellar vesicles were discovered by Sir Alex Bangham and are sometimes referred to as "Bangosomes" in his honor.

Liposomes are highly stable structures that can be subjected to manipulations such as gel filtration chromatography and dialysis. With such methods, it is possible to prepare liposomes having different inside and outside solution compositions. Liposomes can be used as drug and enzyme delivery systems in therapeutic applications. For example, liposomes can be used to introduce contrast agents into the body for diagnostic imaging procedures, including *computerized tomography (CT)* and *magnetic resonance imaging (MRI)* (Figure 9.5). Liposomes can fuse with cells, mixing their contents with the intracellular medium. If methods can be developed to target liposomes to selected cell populations, it may be possible to deliver drugs, therapeutic enzymes, and contrast agents to particular kinds of cells (such as cancer cells).

That vesicles and liposomes form at all is a consequence of the amphipathic nature of the phospholipid molecule. Ionic interactions between the
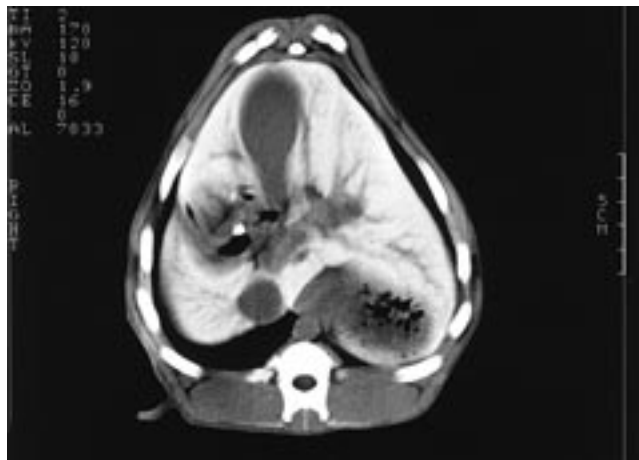
FIGURE 9.5 • A computerized tomography (CT) image of the upper abdomen of a dog, following administration of liposome-encapsulated iodine, a contrast agent that improves the light/dark contrast of objects in the image. The spine is the bright white object at the bottom and the other bright objects on the periphery are ribs. The liver (white) occupies most of the abdominal space. The gallbladder (bulbous object at the center top) and blood vessels appear dark in the image. The liposomal iodine contrast agent has been taken up by Kuppfer cells, which are distributed throughout the liver, except in tumors. The dark object in the lower right is a large tumor. None of these anatomical features would be visible in a CT image in the absence of the liposomal iodine contrast agent. *(Courtesy of Walter Perkins, The Liposome Co., Inc., Princeton, NJ, and Brigham and Women's Hospital, Boston, MA)*

polar head groups and water are maximized, whereas hydrophobic interactions (see Chapter 2) facilitate the association of hydrocarbon chains in the interior of the bilayer. The formation of vesicles results in a favorable increase in the entropy of the solution, because the water molecules are not required to order themselves around the lipid chains. It is important to consider for a moment the physical properties of the bilayer membrane, which is the basis of vesicles and also of natural membranes. Bilayers have a polar surface and a nonpolar core. This hydrophobic core provides a substantial barrier to ions and other polar entities. The rates of movement of such species across membranes are thus quite slow. However, this same core also provides a favorable environment for nonpolar molecules and hydrophobic proteins. We will encounter numerous cases of hydrophobic molecules that interact with membranes and regulate biological functions in some way by binding to or embedding themselves in membranes.

Fluid Mosaic Model

In 1972, S. J. Singer and G. L. Nicolson proposed the **fluid mosaic model** for membrane structure, which suggested that membranes are dynamic structures composed of proteins and phospholipids. In this model, the phospholipid bilayer is a *fluid* matrix, in essence, a two-dimensional solvent for proteins. Both lipids and proteins are capable of rotational and lateral movement.

Singer and Nicolson also pointed out that proteins can be associated with the surface of this bilayer or embedded in the bilayer to varying degrees (Figure 9.6).They defined two classes of membrane proteins. The first, called **peripheral proteins** (or **extrinsic proteins**), includes those that do not penetrate the bilayer to any significant degree and are associated with the membrane by virtue
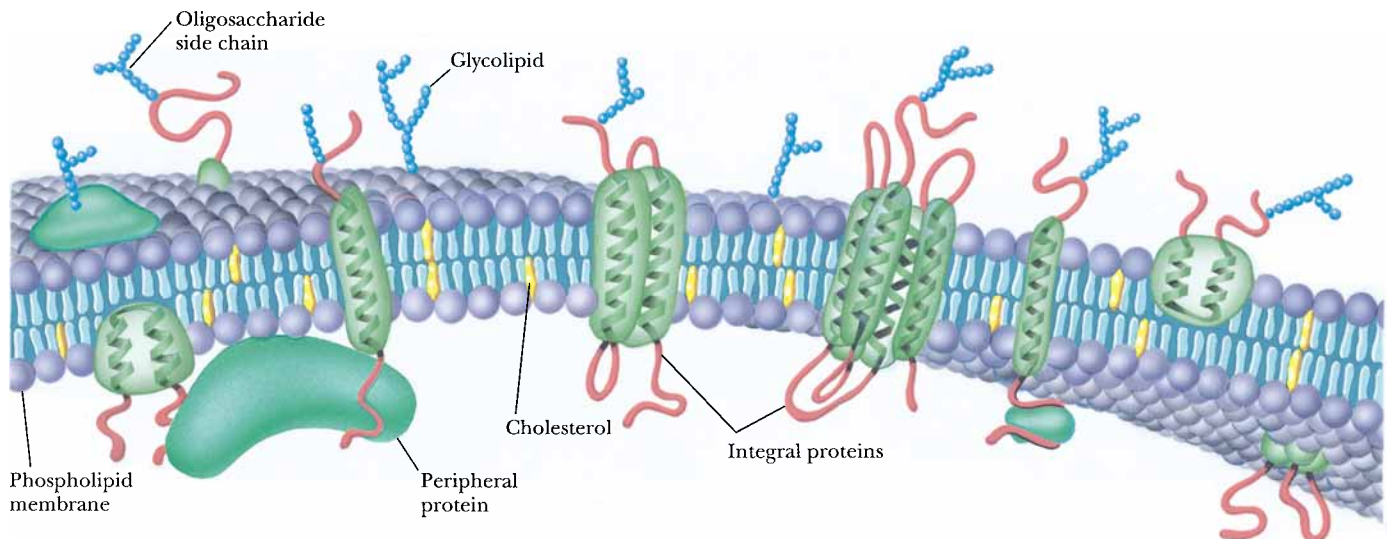
FIGURE 9.6 • The fluid mosaic model of membrane structure proposed by S. J. Singer and G. L. Nicolson. In this model, the lipids and proteins are assumed to be mobile, so that they can move rapidly and laterally in the plane of the membrane. Transverse motion may also occur, but it is much slower.

of ionic interactions and hydrogen bonds between the membrane surface and the surface of the protein. Peripheral proteins can be dissociated from the membrane by treatment with salt solutions or by changes in pH (treatments that disrupt hydrogen bonds and ionic interactions). **Integral proteins** (or **intrinsic proteins**), in contrast, possess hydrophobic surfaces that can readily penetrate the lipid bilayer itself, as well as surfaces that prefer contact with the aqueous medium. These proteins can either insert into the membrane or extend all the way across the membrane and expose themselves to the aqueous solvent on both sides. Singer and Nicolson also suggested that a portion of the bilayer lipid interacts in specific ways with integral membrane proteins and that these interactions might be important for the function of certain membrane proteins. Because of these intimate associations with membrane lipid, integral proteins can only be removed from the membrane by agents capable of breaking up the hydrophobic interactions within the lipid bilayer itself (such as detergents and organic solvents). The fluid mosaic model has become the paradigm for modern studies of membrane structure and function.

Membrane Bilayer Thickness

The Singer–Nicolson model suggested a value of approximately 5 nm for membrane thickness, the same thickness as a lipid bilayer itself. Low angle X-ray diffraction studies in the early 1970s showed that many natural membranes were approximately 5 nm in thickness and that the interiors of these membranes were low in electron density. This is consistent with the arrangement of bilayers having the hydrocarbon tails (low in electron density) in the interior of the membrane. The outside edges of these same membranes were shown to be of high electron density, which is consistent with the arrangement of the polar lipid head groups on the outside surfaces of the membrane.

Hydrocarbon Chain Orientation in the Bilayer

An important aspect of membrane structure is the orientation or ordering of lipid molecules in the bilayer. In the bilayers sketched in Figures 9.2 and 9.4, the long axes of the lipid molecules are portrayed as being perpendicular (or

normal) to the plane of the bilayer. In fact, the hydrocarbon tails of phospholipids may tilt and bend and adopt a variety of orientations. Typically, the portions of a lipid chain near the membrane surface lie most nearly perpendicular to the membrane plane, and lipid chain ordering decreases toward the end of the chain (toward the middle of the bilayer).

Membrane Bilayer Mobility

The idea that lipids and proteins could move rapidly in biological membranes was a relatively new one when the fluid mosaic model was proposed. Many of the experiments designed to test this hypothesis involved the use of specially designed probe molecules. The first experiment demonstrating protein lateral movement in the membrane was described by L. Frye and M. Edidin in 1970. In this experiment, human cells and mouse cells were allowed to fuse together. Frye and Edidin used fluorescent antibodies to determine whether integral membrane proteins from the two cell types could move and intermingle in the newly formed, fused cells. The antibodies specific for human cell proteins were labeled with rhodamine, a red fluorescent marker, and the antibodies specific for mouse cell proteins were labeled with fluorescein, a green fluorescent marker. When both types of antibodies were added to newly fused cells, the binding pattern indicated that integral membrane proteins from the two cell types had moved laterally and were dispersed throughout the surface of the fused cell (Figure 9.7). This clearly demonstrated that integral membrane proteins possess significant lateral mobility.

Just how fast can proteins move in a biological membrane? Many membrane proteins can move laterally across a membrane at a rate of a few microns per minute. On the other hand, some integral membrane proteins are much more restricted in their lateral movement, with diffusion rates of about 10 nm/sec or even slower. These latter proteins are often found to be anchored to the *cytoskeleton* (Chapter 17), a complex latticelike structure that maintains the cell's shape and assists in the controlled movement of various substances through the cell.

Lipids also undergo rapid lateral motion in membranes. A typical phospholipid can diffuse laterally in a membrane at a linear rate of several microns per second. At that rate, a phospholipid could travel from one end of a bacterial cell to the other in less than a second or traverse a typical animal cell in a few minutes. On the other hand, *transverse* movement of lipids (or proteins) from one face of the bilayer to the other is much slower (and much less likely). For example, it can take as long as several days for half the phospholipids in a bilayer vesicle to "flip" from one side of the bilayer to the other.

Membranes Are Asymmetric Structures

Biological membranes are **asymmetric** structures. There are several kinds of asymmetry to consider. Both the lipids and the proteins of membranes exhibit lateral and transverse asymmetries. **Lateral asymmetry** arises when lipids or proteins of particular types cluster in the plane of the membrane.

Lipids Exhibit Lateral Membrane Asymmetry

Lipids in model systems are often found in asymmetric clusters (see Figure 9.8). Such behavior is referred to as a **phase separation,** which arises either spontaneously or as the result of some extraneous influence. Phase separations can be induced in model membranes by divalent cations, which interact with negatively charged moieties on the surface of the bilayer. For example, Ca^{2+} induces phase separations in membranes formed from phosphatidylserine (PS)

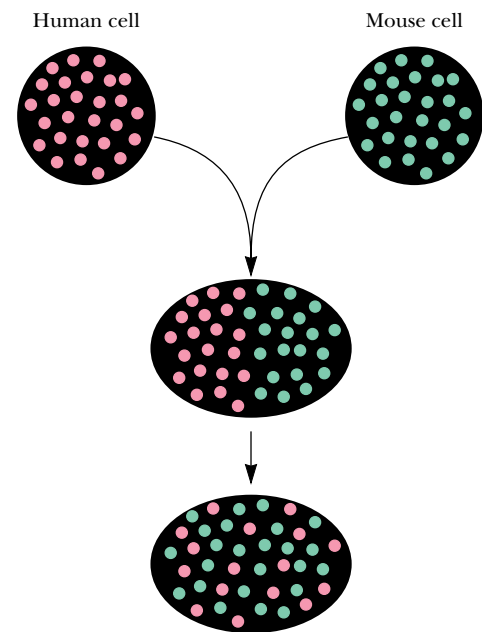Human cell   Mouse cell

FIGURE 9.7 • The Frye–Edidin experiment. Human cells with membrane antigens for red fluorescent antibodies were mixed and fused with mouse cells having membrane antigens for green fluorescent antibodies. Treatment of the resulting composite cells with red- and green-fluorescent–labeled antibodies revealed a rapid mixing of the membrane antigens in the composite membrane. This experiment demonstrated the lateral mobility of membrane proteins.
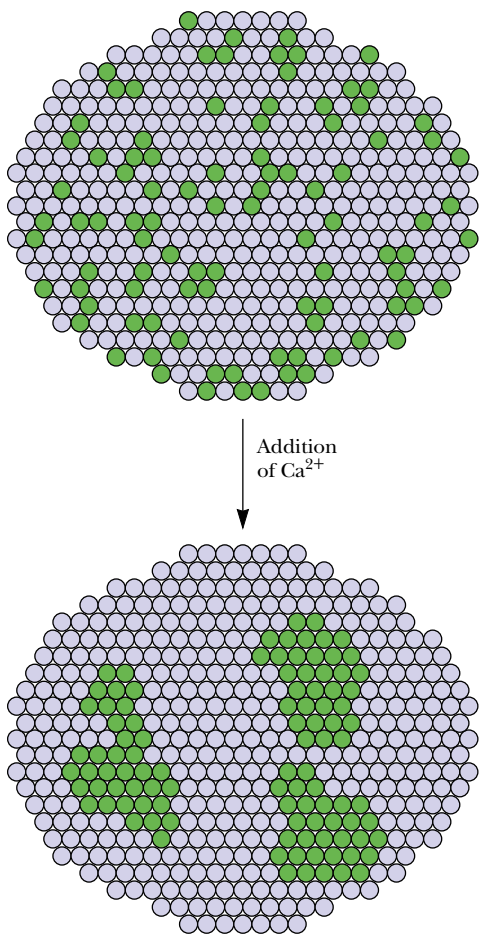
FIGURE 9.8 • An illustration of the concept of lateral phase separations in a membrane. Phase separations of phosphatidylserine (green circles) can be induced by divalent cations such as Ca^{2+}.

and phosphatidylethanolamine (PE) or from PS, PE, and phosphatidylcholine. Ca^{2+} added to these membranes forms complexes with the negatively charged serine carboxyls, causing the PS to cluster and separate from the other lipids. Such metal-induced lipid phase separations have been shown to regulate the activity of membrane-bound enzymes.

There are other ways in which the lateral organization (and asymmetry) of lipids in biological membranes can be altered. For example, cholesterol can intercalate between the phospholipid fatty acid chains, its polar hydroxyl group associated with the polar head groups. In this manner, patches of cholesterol and phospholipids can form in an otherwise homogeneous sea of pure phospholipid. This lateral asymmetry can in turn affect the function of membrane proteins and enzymes. The lateral distribution of lipids in a membrane can also be affected by proteins in the membrane. Certain integral membrane proteins prefer associations with specific lipids. Proteins may select unsaturated lipid chains over saturated chains or may prefer a specific head group over others.

Proteins Exhibit Lateral Membrane Asymmetry

Membrane proteins in many cases are randomly distributed through the plane of the membrane. This was one of the corollaries of the fluid mosaic model of Singer and Nicholson and has been experimentally verified using electron microscopy. Electron micrographs show that integral membrane proteins are often randomly distributed in the membrane, with no apparent long-range order.

However, membrane proteins can also be distributed in nonrandom ways across the surface of a membrane. This can occur for several reasons. Some proteins must interact intimately with certain other proteins, forming multi-subunit complexes that perform specific functions in the membrane. A few integral membrane proteins are known to *self-associate* in the membrane, forming large multimeric clusters. **Bacteriorhodopsin,** a light-driven proton pump protein, forms such clusters, known as "purple patches," in the membranes of *Halobacterium halobium* (Figure 9.9). The bacteriorhodopsin protein in these purple patches forms highly ordered, two-dimensional crystals.

Transverse Membrane Asymmetry

Membrane asymmetries in the **transverse** direction (from one side of the membrane to the other) can be anticipated when one considers that many properties of a membrane depend upon its two-sided nature. Properties that are a consequence of membrane "sidedness" include membrane transport, which is driven in one direction only, the effects of hormones at the outsides of cells, and the immunological reactions that occur between cells (necessarily involving only the outside surfaces of the cells). One would surmise that the proteins involved in these and other interactions must be arranged asymmetrically in the membrane.

Protein Transverse Asymmetry

Protein transverse asymmetries have been characterized using chemical, enzymatic, and immunological labeling methods. Working with **glycophorin,** the major glycoprotein in the erythrocyte membrane (discussed in Section 9.2), Mark Bretscher was the first to demonstrate the asymmetric arrangement of an integral membrane protein. Treatment of whole erythrocytes with trypsin released the carbohydrate groups of glycophorin (in the form of several small glycopeptides). Because trypsin is much too large to penetrate the erythrocyte membrane, the N-terminus of glycophorin, which contains the carbohydrate
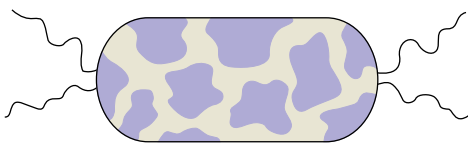

FIGURE 9.9 • The purple patches of *Halobacterium halobium.*

moieties, must be exposed to the outside surface of the membrane. Bretscher showed that [^{35}S]-formylmethionylsulfone methyl phosphate could label the C-terminus of glycophorin with ^{35}S in erythrocyte membrane fragments but not in intact erythrocytes. This clearly demonstrated that the C-terminus of glycophorin is uniformly exposed to the interior surface of the erythrocyte membrane. Since that time, many integral membrane proteins have been shown to be oriented uniformly in their respective membranes.

Lipid Transverse Asymmetry

Phospholipids are also distributed asymmetrically across many membranes. In the erythrocyte, phosphatidylcholine (PC) comprises about 30% of the total phospholipid in the membrane. Of this amount, 76% is found in the outer monolayer and 24% is found in the inner monolayer. Since this early observation, the lipids of many membranes have been found to be asymmetrically distributed between the inner and outer monolayers. Figure 9.10 shows the asymmetric distribution of phospholipids observed in the human erythrocyte membrane. Asymmetric lipid distributions are important to cells in several ways. The carbohydrate groups of glycolipids (and of glycoproteins) always face the outside surface of plasma membranes where they participate in cell recognition phenomena. Asymmetric lipid distributions may also be important to various integral membrane proteins, which may prefer particular lipid classes in the inner and outer monolayers. The total charge on the inner and outer surfaces of a membrane depends on the distribution of lipids. The resulting charge differences affect the membrane potential, which in turn is known to modulate the activity of certain ion channels and other membrane proteins.

How are transverse lipid asymmetries created and maintained in cell membranes? From a thermodynamic perspective, these asymmetries could only occur by virtue of asymmetric syntheses of the bilayer itself or by energy-dependent asymmetric transport mechanisms. Without at least one of these, lipids of all kinds would eventually distribute equally between the two monolayers of a membrane. In eukaryotic cells, phospholipids, glycolipids, and cholesterol are synthesized by enzymes located in (or on the surface of) the endoplasmic reticulum (ER) and the Golgi system (discussed in Chapter 25). Most if not all of these biosynthetic processes are asymmetrically arranged across the membranes of the ER and Golgi. There is also a separate and continuous flow of phospholipids, glycolipids, and cholesterol from the ER and Golgi to other membranes in the cell, including the plasma membrane. This flow is mediated by specific **lipid transfer proteins.** Most cells appear to contain such proteins.
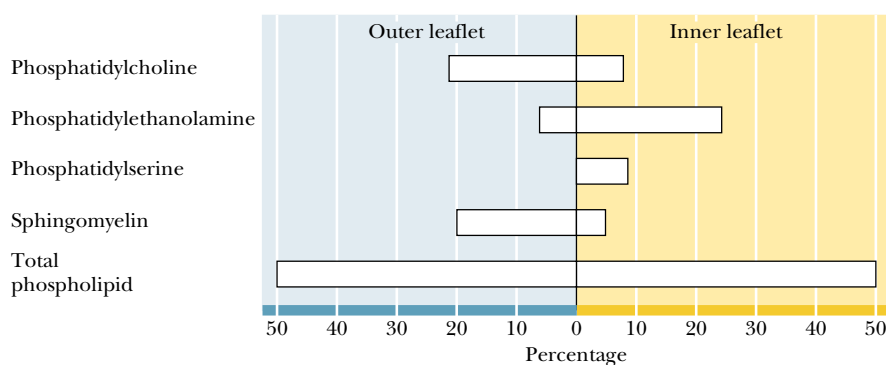
FIGURE 9.10 • Phospholipids are arranged asymmetrically in most membranes, including the human erythrocyte membrane, as shown here. Values are mole percentages. *(After Rothman and Lenard, 1977.* Science ***194:****1744.)*

Flippase protein

1 Lipid molecule diffuses
   to flippase protein

2 Flippase flips lipid to
   opposite side of bilayer

3 Lipid diffuses away from
   flippase
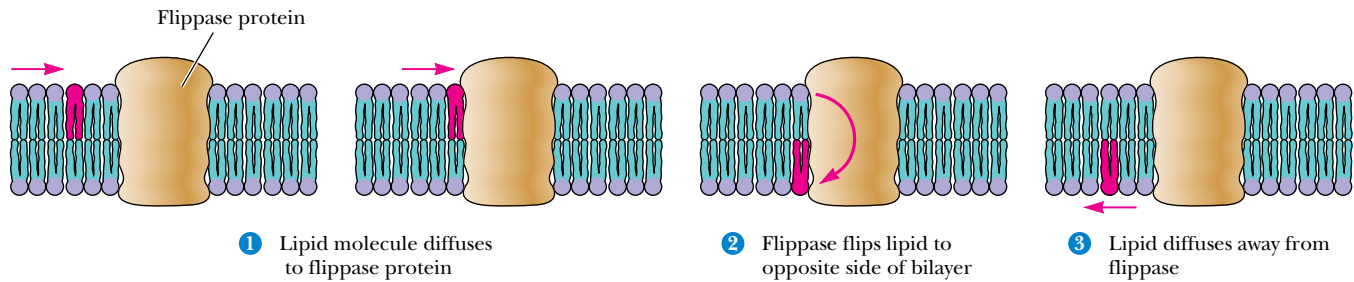
FIGURE 9.11 • Phospholipids can be "flipped" across a bilayer membrane by the action of flippase proteins. When, by normal diffusion through the bilayer, the lipid encounters a flippase, it can be moved quickly to the other face of the bilayer.

Flippases: Proteins That Flip Lipids Across the Membrane

Proteins that can "flip" phospholipids from one side of a bilayer to the other have also been identified in several tissues (Figure 9.11). Called **flippases,** these proteins reduce the half-time for phospholipid movement across a membrane from 10 days or more to a few minutes or less. Some of these systems may operate passively, with no required input of energy, but passive transport alone cannot establish or maintain asymmetric transverse lipid distributions. However, rapid phospholipid movement from one monolayer to the other occurs in an *ATP-dependent* manner in erythrocytes. Energy-dependent lipid flippase activity may be responsible for the creation and maintenance of transverse lipid asymmetries.

Membrane Phase Transitions

Lipids in bilayers undergo radical changes in physical state over characteristic narrow temperature ranges. These changes are in fact true **phase transitions,** and the temperatures at which these changes take place are referred to as **transition temperatures** or **melting temperatures** (T_m). These phase transitions involve substantial changes in the organization and motion of the fatty acyl chains within the bilayer. The bilayer below the phase transition exists in a closely packed gel state, with the fatty acyl chains relatively immobilized in a tightly packed array (Figure 9.12). In this state, the anti conformation is adopted by all the carbon–carbon bonds in the lipid chains. This leaves the lipid chains in their fully extended conformation. As a result, the surface area per lipid is minimal and the bilayer thickness is maximal. Above the transition temperature, a liquid crystalline state exists in which the mobility of fatty acyl chains is intermediate between solid and liquid alkane. In this more fluid, liquid crystalline state, the carbon–carbon bonds of the lipid chains more readily adopt gauche conformations (Figure 9.13). As a result, the surface area per lipid increases and the bilayer thickness decreases by 10 to 15%.

Gel   Heat   Liquid crystal
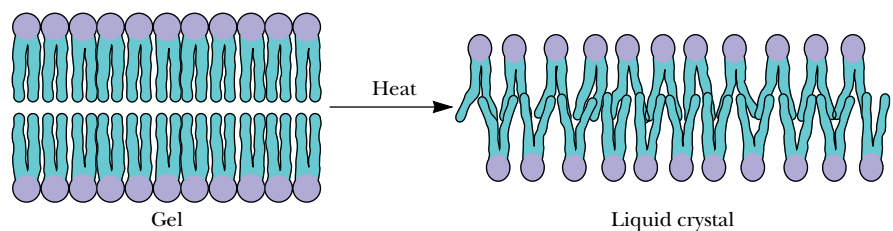
FIGURE 9.12 • An illustration of the gel-to-liquid crystalline phase transition, which occurs when a membrane is warmed through the transition temperature, T_m. Notice that the surface area must increase and the thickness must decrease as the membrane goes through a phase transition. The mobility of the lipid chains increases dramatically.
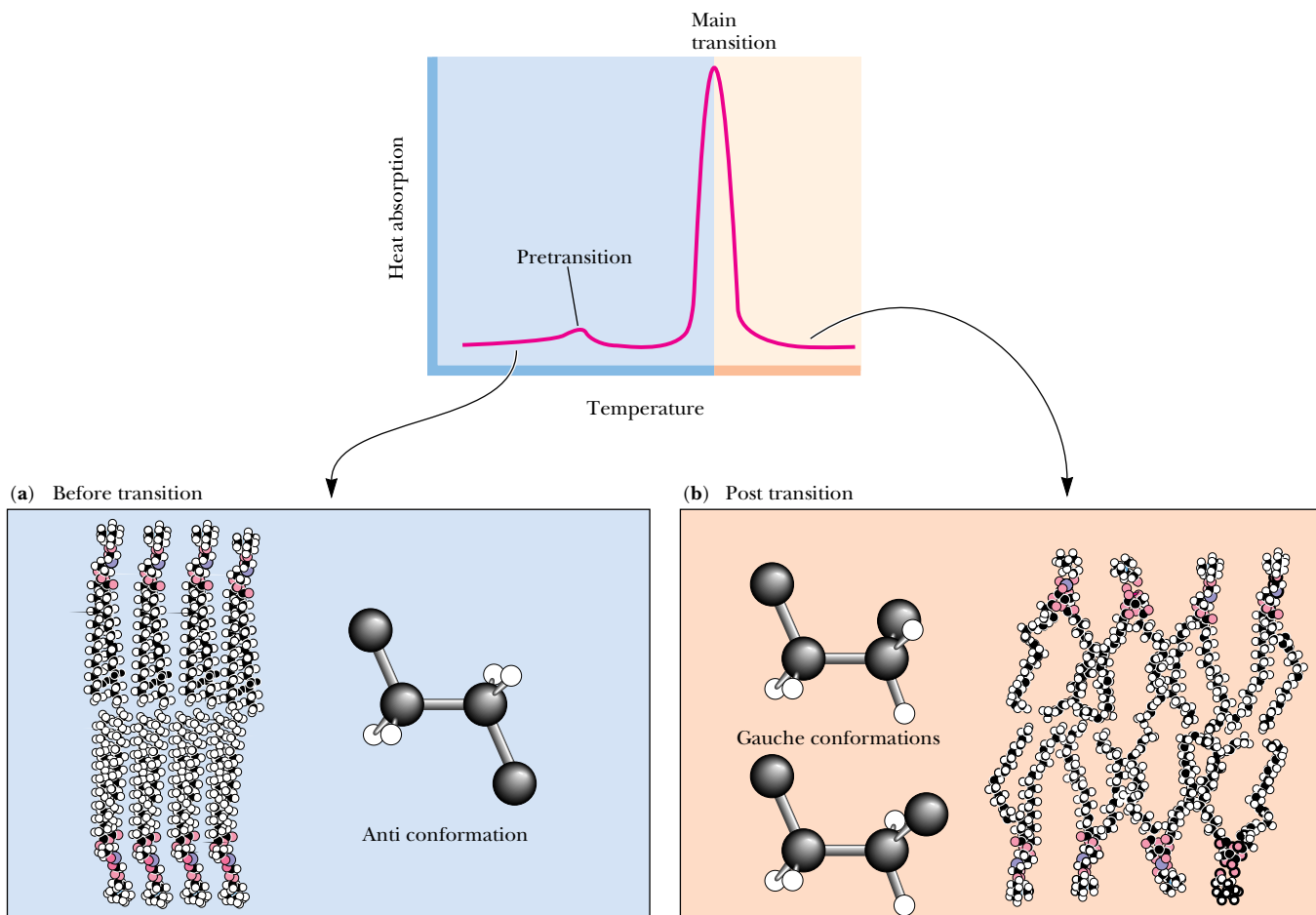
FIGURE 9.13 • Membrane lipid phase transitions can be detected and characterized by measuring the rate of absorption of heat by a membrane sample in a calorimeter (see Chapter 3 for a detailed discussion of calorimetry). Pure, homogeneous bilayers (containing only a single lipid component) give sharp calorimetric peaks. Egg PC contains a variety of fatty acid chains and thus yields a broad calorimetric peak. Below the phase transition, lipid chains primarily adopt the anti conformation. Above the phase transition, lipid chains have absorbed a substantial amount of heat. This is reflected in the adoption of higher-energy conformations, including the gauche conformations shown.

The sharpness of the transition in pure lipid preparations shows that the phase change is a cooperative behavior. This is to say that the behavior of one or a few molecules affects the behavior of many other molecules in the vicinity. The sharpness of the transition then reflects the number of molecules that are acting in concert. Sharp transitions involve large numbers of molecules all "melting" together.

Phase transitions have been characterized in a number of different pure and mixed lipid systems. Table 9.1 shows a comparison of the transition temperatures observed for several different phosphatidylcholines with different fatty acyl chain compositions. General characteristics of bilayer phase transitions include the following:

1. The transitions are always endothermic; heat is absorbed as the temperature increases through the transition (Figure 9.13).
2. Particular phospholipids display characteristic transition temperatures (T_m). As shown in Table 9.1, T_m increases with chain length, decreases with unsaturation, and depends on the nature of the polar head group.
3. For pure phospholipid bilayers, the transition occurs over a narrow temperature range. The phase transition for dimyristoyl lecithin has a peak width of about 0.2°C.
4. Native biological membranes also display characteristic phase transitions, but these are broad and strongly dependent on the lipid and protein composition of the membrane.

Table 9.1

Phase Transition Temperatures for Phospholipids in Water

Phospholipid	Transition Temperature (T_m), °C
Dipalmitoyl phosphatidic acid (Di 16:0 PA)	67
Dipalmitoyl phosphatidylethanolamine (Di 16:0 PE)	63.8
Dipalmitoyl phosphatidylcholine (Di 16:0 PC)	41.4
Dipalmitoyl phosphatidylglycerol (Di 16:0 PG)	41.0
Dilauroyl phosphatidylcholine (Di 14:0 PC)	23.6
Distearoyl phosphatidylcholine (Di 18:0 PC)	58
Dioleoyl phosphatidylcholine (Di 18:1 PC)	-22
1-Stearoyl-2-oleoyl-phosphatidylcholine (1-18:0, 2-18:1 PC)	3
Egg phosphatidylcholine (Egg PC)	-15

Adapted from Jain, M., and Wagner, R. C., 1980. *Introduction to Biological Membranes.* New York: John Wiley and Sons; Martonosi, A., ed., 1982. *Membranes and Transport,* Vol. 1. New York: Plenum Press.

5. With certain lipid bilayers, a change of physical state referred to as a *pretransition* occurs 5° to 15°C below the phase transition itself. These pretransitions involve a tilting of the hydrocarbon chains.
6. A volume change is usually associated with phase transitions in lipid bilayers.
7. Bilayer phase transitions are sensitive to the presence of solutes that interact with lipids, including multivalent cations, lipid-soluble agents, peptides, and proteins.

Cells adjust the lipid composition of their membranes to maintain proper fluidity as environmental conditions change.

9.2 • Structure of Membrane Proteins

The lipid bilayer constitutes the fundamental structural unit of all biological membranes. Proteins, in contrast, carry out essentially all of the active functions of membranes, including transport activities, receptor functions, and other related processes. As suggested by Singer and Nicolson, most membrane proteins can be classified as peripheral or integral. The **peripheral proteins** are globular proteins that interact with the membrane mainly through electrostatic and hydrogen-bonding interactions with integral proteins. Although peripheral proteins are not discussed further here, many proteins of this class are described in the context of other discussions throughout this textbook. **Integral proteins** are those that are strongly associated with the lipid bilayer, with a portion of the protein embedded in, or extending all the way across, the lipid bilayer. Another class of proteins not anticipated by Singer and Nicolson, the **lipid-anchored proteins,** are important in a variety of functions in different cells and tissues. These proteins associate with membranes by means of a variety of covalently linked lipid anchors.

Integral Membrane Proteins

Despite the diversity of integral membrane proteins, most fall into two general classes. One of these includes proteins attached or anchored to the membrane by only a small hydrophobic segment, such that most of the protein extends out into the water solvent on one or both sides of the membrane. The other class includes those proteins that are more or less globular in shape and more totally embedded in the membrane, exposing only a small surface to the water solvent outside the membrane. In general, those structures of integral membrane protein within the nonpolar core of the lipid bilayer are dominated by α-helices or β-sheets because these secondary structures neutralize the highly polar N—H and C=O functions of the peptide backbone through H-bond formation.

A Protein with a Single Transmembrane Segment

In the case of the proteins that are anchored by a small hydrophobic polypeptide segment, that segment often takes the form of a single α-helix. One of the best examples of a membrane protein with such an α-helical structure is **glycophorin.** Most of glycophorin's mass is oriented on the outside surface of the cell, exposed to the aqueous milieu (Figure 9.14). A variety of hydrophilic oligosaccharide units are attached to this extracellular domain. These oligosaccharide groups constitute the ABO and MN blood group antigenic specifici-

FIGURE 9.14 • Glycophorin A spans the membrane of the human erythrocyte via a single α-helical transmembrane segment. The C-terminus of the peptide, whose sequence is shown here, faces the cytosol of the erythrocyte; the N-terminal domain is extracellular. Points of attachment of carbohydrate groups are indicated.

ties of the red cell. This extracellular portion of the protein also serves as the receptor for the influenza virus. Glycophorin has a total molecular weight of about 31,000 and is approximately 40% protein and 60% carbohydrate. The glycophorin primary structure consists of a segment of 19 hydrophobic amino acid residues with a short hydrophilic sequence on one end and a longer hydrophilic sequence on the other end. The 19-residue sequence is just the right length to span the cell membrane if it is coiled in the shape of an α-helix. The large hydrophilic sequence includes the amino terminal residue of the polypeptide chain.

Numerous other membrane proteins are also attached to the membrane by means of a single hydrophobic α-helix, with hydrophilic segments extending into either the cytoplasm or the extracellular space. These proteins often function as receptors for extracellular molecules or as recognition sites that allow the immune system to recognize and distinguish the cells of the host organism from invading foreign cells or viruses. The proteins that represent the *major transplantation antigens H2* in mice and *human leukocyte associated (HLA) proteins* in humans are members of this class. Other such proteins include the *surface immunoglobulin receptors* on B lymphocytes and the *spike proteins* of many membrane viruses. The function of many of these proteins depends primarily on their extracellular domain, and thus the segment facing the intracellular surface is often a shorter one.

Bacteriorhodopsin: A 7-Transmembrane Segment Protein

Membrane proteins that take on a more globular shape, instead of the rodlike structure previously described, are often involved with transport activities and other functions requiring a substantial portion of the peptide to be embedded in the membrane. These proteins may consist of numerous hydrophobic α-helical segments joined by hinge regions so that the protein winds in a zig-zag pattern back and forth across the membrane. A well-characterized example of such a protein is **bacteriorhodopsin,** which clusters in purple patches in the membrane of the bacterium *Halobacterium halobium.* The name *Halobacterium* refers to the fact that this bacterium thrives in solutions having high concentrations of sodium chloride, such as the salt beds of San Francisco Bay. *Halobacterium* carries out a light-driven proton transport by means of bacteriorhodopsin, named in reference to its spectral similarities to rhodopsin in the rod outer segments of the mammalian retina. When this organism is deprived of oxygen for oxidative metabolism, it switches to the capture of energy from sunlight, using this energy to pump protons out of the cell. The proton gradient generated by such light-driven proton pumping represents potential energy, which is exploited elsewhere in the membrane to synthesize ATP.

Bacteriorhodopsin clusters in hexagonal arrays (Figure 9.15) in the purple membrane patches of *Halobacterium,* and it was this orderly, repeating arrangement of proteins in the membrane that enabled Nigel Unwin and Richard Henderson in 1975 to determine the bacteriorhodopsin structure. The polypeptide chain crosses the membrane seven times, in seven α-helical segments, with very little of the protein exposed to the aqueous milieu. The bacteriorhodopsin structure has become a model of globular membrane protein structure. Many other integral membrane proteins contain numerous hydrophobic sequences that, like those of bacteriorhodopsin, could form α-helical transmembrane segments. For example, the amino acid sequence of the sodium–potassium transport ATPase contains ten hydrophobic segments of length sufficient to span the plasma membrane. By analogy with bacteriorhodopsin, one would expect that these segments form a globular hydrophobic core that anchors the ATPase in the membrane. The helical segments may also account for the transport properties of the enzyme itself.

Treating Allergies at the Cell Membrane

Allergies represent overreactions of the immune system caused by exposure to foreign substances referred to as allergens. The inhalation of allergens, such as pollen, pet dander, and dust, can cause a variety of allergic responses, including itchy eyes, a runny nose, shortness of breath, and wheezing. Allergies can also be caused by food, drugs, dyes, and other chemicals.

The visible symptoms of such an allergic response are caused by the release of **histamine** (see figure) by mast cells, a type of cell found in loose connective tissue. Histamine dilates blood vessels, increases the permeability of capillaries (allowing antibodies to pass from the capillaries to surrounding tissue), and constricts bronchial air passages. Histamine acts by binding to specialized membrane proteins called **histamine H1 receptors.** These integral membrane proteins possess seven transmembrane α-helical segments, with an extracellular amino terminus and a cytoplasmic carboxy terminus. When histamine binds to the extracellular domain of an H1 receptor, the intracellular domain undergoes a conformation change that stimulates a GTP-binding protein, which in turn activates the allergic response in the affected cell.

A variety of highly effective **antihistamine** drugs are available for the treatment of allergy symptoms. These drugs share the property of binding tightly to histamine H1 receptors, without eliciting the same effects as histamine itself. They are referred to as **histamine H1 receptor antagonists** because they prevent the binding of histamine to the receptors. The structures of Allegra (made by Hoechst Marion Roussel, Inc.), Claritin (by Schering-Plough Corp.), and Zyrtec (by Pfizer) are all shown at right.
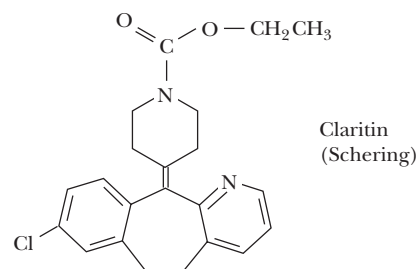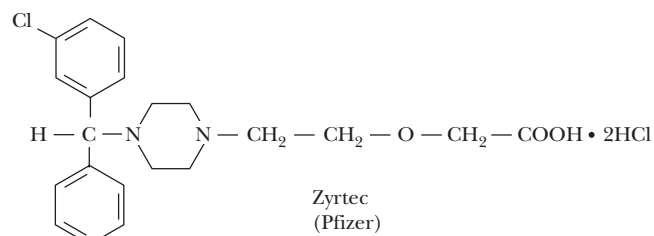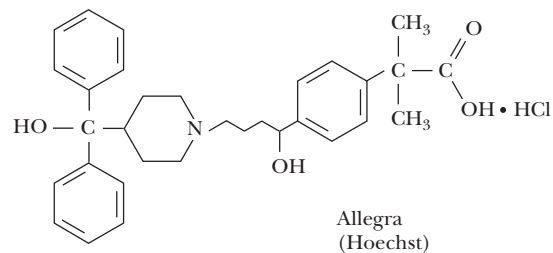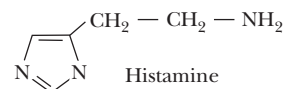
The structures of histamine and three antihistamine drugs. ▶
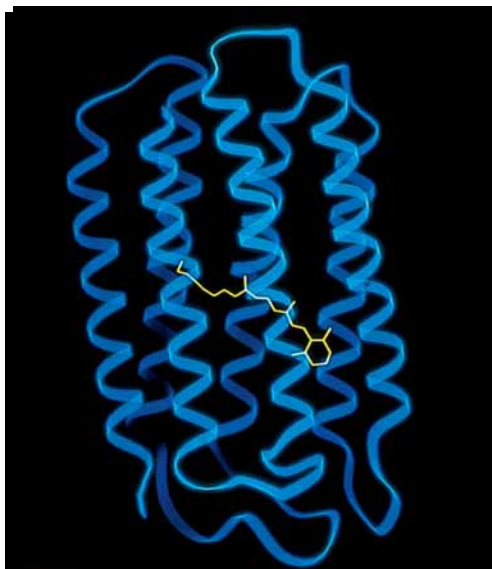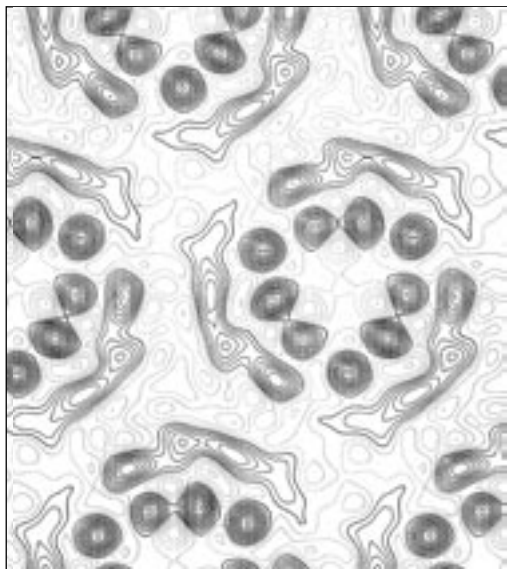
FIGURE 9.15 • An electron density profile illustrating the three centers of threefold symmetry in arrays of bacterio-rhodopsin in the purple membrane of *Halobacterium halobium,* together with a computer-generated model showing the seven α-helical transmembrane segments in bacteriorhodopsin. *(Electron density map from Stoecknius, W., 1980. Purple membrane of halobacteria: A new light-energy converter.* Accounts of Chemical Research *13:337–344. Model on right from Henderson, R., 1990. Model for the structure of bacteriorhodopsin based on high-resolution electron cryo-microscopy.* Journal of Molecular Biology *213:899–929.)*
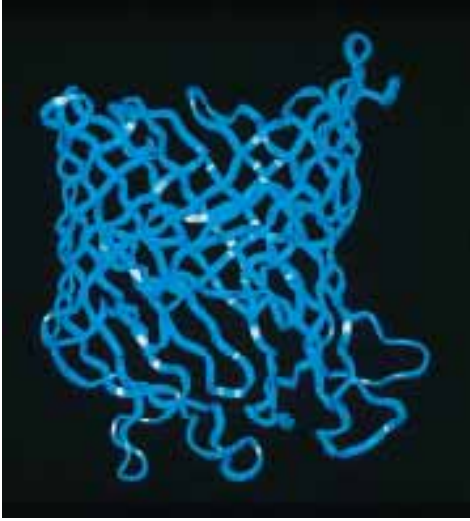
FIGURE 9.16 • The three-dimensional structure of maltoporin from *E. coli.*

Porins—A β-Sheet Motif for Membrane Proteins

The β-sheet is another structural motif that provides extensive hydrogen bonding for transmembrane peptide segments. **Porin** proteins found in the outer membranes (OM) of Gram-negative bacteria such as *Escherichia coli,* and also in the outer mitochondrial membranes of eukaryotic cells, span their respective membranes with large β-sheets. A good example is **maltoporin,** also known as **LamB protein** or **lambda receptor,** which participates in the entry of maltose and maltodextrins into *E. coli.* Maltoporin is active as a trimer. The 421-residue monomer is an aesthetically pleasing 18-strand β-barrel (Figure 9.16). The β-strands are connected to their nearest neighbors either by long loops or by β-turns (Figure 9.17). The long loops are found at the end of the barrel that is exposed to the cell exterior, whereas the turns are located on the intracellular face of the barrel. Three of the loops fold into the center of the barrel.

The amino acid compositions and sequences of the β-strands in porin proteins are novel. Polar and nonpolar residues alternate along the β-strands, with polar residues facing the central pore or cavity of the barrel and nonpolar residues facing out from the barrel where they can interact with the hydrophobic lipid milieu of the membrane. The smallest diameter of the porin channel is about 5 Å. Thus, a maltodextrin polymer (composed of two or more glucose units) must pass through the porin in an extended conformation (like a spaghetti strand).

Lipid-Anchored Membrane Proteins

Certain proteins are found to be covalently linked to lipid molecules. For many of these proteins, covalent attachment of lipid is required for association with a membrane. The lipid moieties can insert into the membrane bilayer, effectively **anchoring** their linked proteins to the membrane. Some proteins with covalently linked lipid normally behave as soluble proteins; others are integral
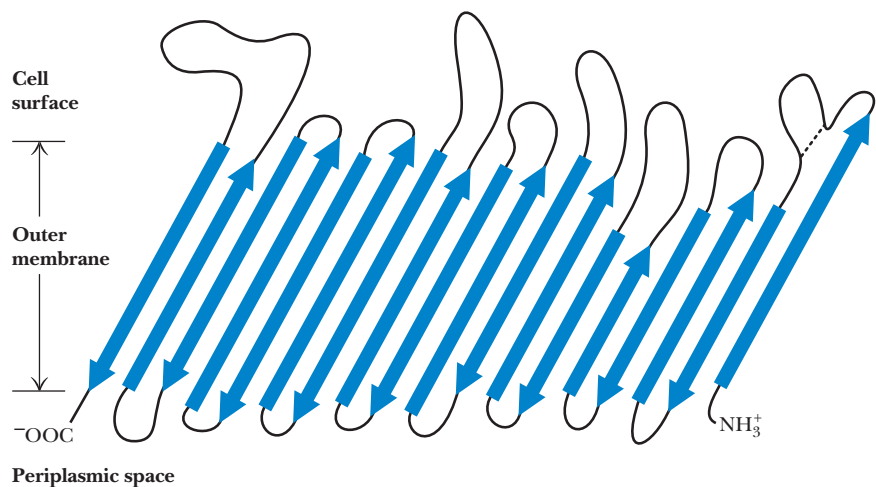
FIGURE 9.17 • The arrangement of the peptide chain in maltoporin from *E. coli.*

$\mathcal{A}$ D E E P E R L O O K

Exterminator Proteins—Biological Pest Control at the Membrane

Control of biological pests, including mosquitoes, houseflies, gnats, and tree-consuming predators like the eastern tent caterpillar, is frequently achieved through the use of microbial membrane proteins. For example, several varieties of *Bacillus thurigiensis* produce proteins that bind to cell membranes in the digestive systems of insects that consume them, creating transmembrane ion channels. Leakage of Na^+, K^+, and H^+ ions through these membranes in the insect gut destroys crucial ion gradients and interferes with digestion of food. Insects that ingest these toxins eventually die of starvation. *B. thurigiensis* toxins account for more than 90% of sales of biological pest control agents.

B. thurigiensis is a common Gram-positive, spore-forming soil bacterium that produces **inclusion bodies,** microcrystalline clusters of many different proteins. These crystalline proteins, called **δ-endotoxins,** are the ion channel toxins that are sold commercially for pest control. Most such endotoxins are **protoxins,** which are inactive until cleaved to smaller, active proteins by proteases in the gut of a susceptible insect. One such crystalline protoxin,

lethal to mosquitoes, is a 27 kD protein, which is cleaved to form the active 25 kD toxin in the mosquito. This toxin has no effect on membranes at neutral pH, but at pH 9.5 (the pH of the mosquito gut) the toxin forms cation channels in the gut membranes.

This 25 kD protein is not toxic to tent caterpillars, but a larger, 130 kD protein in the *B. thurigiensis* inclusion bodies is cleaved by a caterpillar gut protease to produce a 55 kD toxin that is active in the caterpillar. Remarkably, the strain of *B. thurigiensis* known as *azawai* produces a protoxin with dual specificity: in the caterpillar gut, this 130 kD protein is cleaved to form a 55 kD toxin active in the caterpillar. However, when the same 130 kD protoxin is consumed by mosquitoes or houseflies, it is cleaved to form a 53 kD protein (15 amino acid residues shorter than the caterpillar toxin) that is toxic to these latter organisms. Understanding the molecular basis of the toxicity and specificity of these proteins and the means by which they interact with membranes to form lethal ion channels is a fascinating biochemical challenge with far-reaching commercial implications.

membrane proteins and remain membrane-associated even when the lipid is removed. Covalently bound lipid in these latter proteins can play a role distinct from membrane anchoring. In many cases, attachment to the membrane via the lipid anchor serves to modulate the activity of the protein.

Another interesting facet of lipid anchors is that they are transient. Lipid anchors can be reversibly attached to and detached from proteins. This provides a "switching device" for altering the affinity of a protein for the membrane. Reversible lipid anchoring is one factor in the control of **signal transduction pathways** in eukaryotic cells (Chapter 34).

Four different types of lipid-anchoring motifs have been found to date. These are **amide-linked myristoyl** anchors, **thioester-linked fatty acyl** anchors, **thioether-linked prenyl** anchors, and **amide-linked glycosyl phosphatidylinositol** anchors. Each of these anchoring motifs is used by a variety of membrane proteins, but each nonetheless exhibits a characteristic pattern of structural requirements.

Amide-Linked Myristoyl Anchors

Myristic acid may be linked via an amide bond to the α-amino group of the N-terminal glycine residue of selected proteins (Figure 9.18). The reaction is referred to as ***N*-myristoylation** and is catalyzed by *myristoyl–CoA:protein* N-*myristoyltransferase,* known simply as **NMT.** *N*-Myristoyl-anchored proteins include the catalytic subunit of *cAMP-dependent protein kinase,* the *pp60^{src} tyrosine kinase,* the phosphatase known as *calcineurin B,* the α-subunit of *G proteins* (involved in GTP-dependent transmembrane signaling events), and the *gag proteins* of certain retroviruses, including the HIV-1 virus that causes AIDS.

FIGURE 9.18 • Certain proteins are anchored to biological membranes by lipid anchors. Particularly common are the *N*-myristoyl– and *S*-palmitoyl–anchoring motifs shown here. *N*-Myristoylation always occurs at an N-terminal glycine residue, whereas thioester linkages occur at cysteine residues within the polypeptide chain. G-protein–coupled receptors, with seven transmembrane segments, may contain one (and sometimes two) palmitoyl anchors in thioester linkage to cysteine residues in the C-terminal segment of the protein.
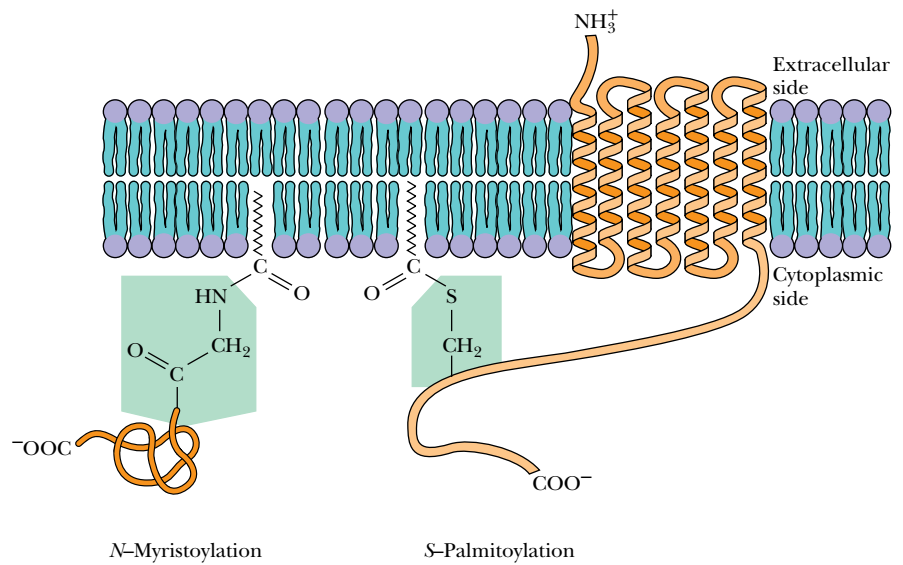
Thioester-Linked Fatty Acyl Anchors

A variety of cellular and viral proteins contain fatty acids covalently bound via ester linkages to the side chains of cysteine and sometimes to serine or threonine residues within a polypeptide chain (Figure 9.18). This type of fatty acyl chain linkage has a broader fatty acid specificity than *N*-myristoylation. Myristate, palmitate, stearate, and oleate can all be esterified in this way, with the C_{16} and C_{18} chain lengths being most commonly found. Proteins anchored to membranes via fatty acyl thioesters include *G-protein-coupled receptors,* the *surface glycoproteins* of several viruses, and the *transferrin receptor* protein.

Thioether-Linked Prenyl Anchors

As noted in Chapter 7, polyprenyl (or simply prenyl) groups are long-chain polyisoprenoid groups derived from isoprene units. Prenylation of proteins destined for membrane anchoring can involve either **farnesyl** or **geranylgeranyl** groups (Figure 9.19). The addition of a prenyl group typically occurs at the cysteine residue of a carboxy-terminal CAAX sequence of the target protein, where C is cysteine, A is any aliphatic residue, and X can be any amino acid. As shown in Figure 9.19, the result is a thioether-linked farnesyl or geranylgeranyl group. Once the prenylation reaction has occurred, a specific protease cleaves the three carboxy-terminal residues, and the carboxyl group of the now terminal Cys is methylated to produce an ester. All of these modifications appear to be important for subsequent activity of the prenyl-anchored protein. Proteins anchored to membranes via prenyl groups include *yeast mating factors,* the *p21^{ras} protein* (the protein product of the *ras* oncogene; see Chapter 34), and the *nuclear lamins,* structural components of the lamina of the inner nuclear membrane.

Glycosyl Phosphatidylinositol Anchors

Glycosyl phosphatidylinositol, or **GPI,** groups are structurally more elaborate membrane anchors than fatty acyl or prenyl groups. GPI groups modify the carboxy-terminal amino acid of a target protein via an ethanolamine residue linked to an oligosaccharide, which is linked in turn to the inositol moiety of a phosphatidylinositol (Figure 9.20). The oligosaccharide typically consists of
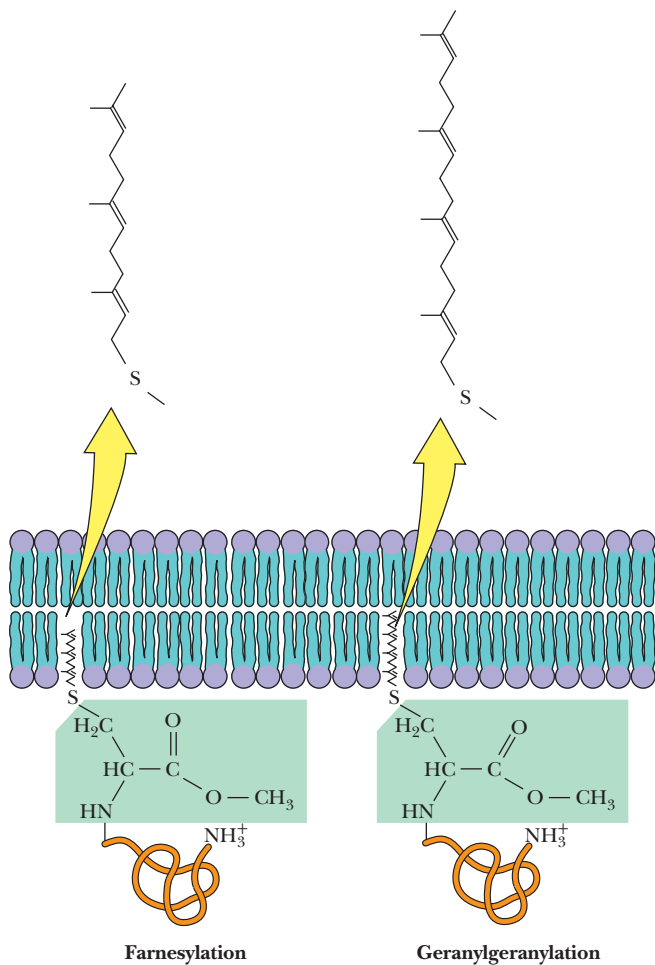
FIGURE 9.19 • Proteins containing the C-terminal sequence CAAX can undergo prenylation reactions that place thioether-linked farnesyl or geranylgeranyl groups at the cysteine side chain. Prenylation is accompanied by removal of the AAX peptide and methylation of the carboxyl group of the cysteine residue, which has become the C-terminal residue.

Farnesylation

Geranylgeranylation

Key:

E = Ethanolamine
Gal = Galactose
M = Mannose
GN = Glucosamine
I = Inositol

Vesicular stomatitis glycoprotein

Acetylcholinesterase

Thyroglobulin 1
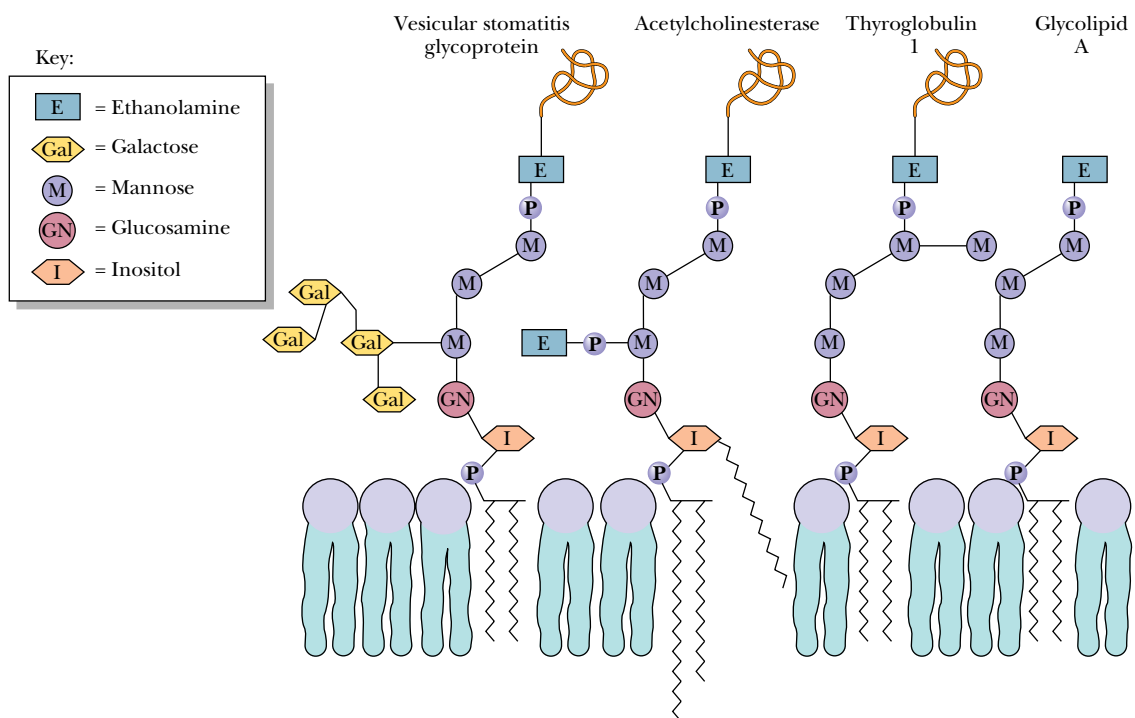
Glycolipid A

FIGURE 9.20 • The glycosyl phosphatidylinositol (GPI) moiety is an elaborate lipid-anchoring group. Note the core of three mannose residues and a glucosamine. Additional modifications may include fatty acids at the inositol and glycerol —OH groups.

A Prenyl Protein Protease Is a New Chemotherapy Target

The protein called p21^{ras} or simply Ras is a small GTP-binding protein involved in cell signaling pathways that regulate growth and cell division. Mutant forms of Ras cause uncontrolled cell growth, and Ras mutations are involved in one third of all human cancers. Because the signaling activity of Ras is dependent on prenylation, the prenylation reaction itself, as well as the proteolysis of the -AAX motif and the methylation of the prenylated Cys residue, have been considered targets for development of new chemotherapy strategies.

Farnesyl transferase from rat cells is a heterodimer consisting of a 48 kD α-subunit and a 46 kD β-subunit. In the structure shown here, helices 2 to 15 of the α-subunit are folded into seven short coiled coils that together form a crescent-shaped envelope partially surrounding the β-subunit. Twelve helices of the β-subunit form a novel barrel motif that creates the active site of the enzyme. Farnesyl transferase inhibitors, one of which is shown here, are potent suppressors of tumor growth in mice, but their value in humans has not been established.

Mutations that inhibit prenyl transferases cause defective growth or death of cells, raising questions about the usefulness of prenyl transferase inhibitors in chemotherapy. However, Victor Boyartchuk and his colleagues at the University of California, Berkeley, and Acacia Biosciences have shown that the protease that cleaves the -AAX motif from Ras following the prenylation reaction may be a better chemotherapeutic target. They have identified two genes for the prenyl protein protease in the yeast *Saccharomyces cerevisiae* and have shown that deletion of these genes results in loss of proteolytic processing of prenylated proteins, including Ras. Interestingly, normal yeast cells are unaffected by this gene deletion. However, in yeast cells that carry mutant forms of Ras and that display aberrant growth behaviors, deletion of the protease gene restores normal growth patterns. If these remarkable results translate from yeast to human tumor cells, inhibitors of CAAX proteases may be more valuable chemotherapeutic agents than prenyl transferase inhibitors.

The structure of the farnesyl transferase heterodimer. A novel barrel structure is formed from 12 helical segments in the β-subunit (purple). The α-subunit (yellow) consists largely of seven successive pairs of α-helices that form a series of right-handed antiparallel coiled coils running along the bottom of the structure. These "helical hairpins" are arranged in a double-layered, right-handed superhelix resulting in a cresent-shaped subunit that envelopes part of the subunit.

The farnesylation and subsequent processing of the Ras protein. Following farnesylation by the FTase, the carboxy-terminal VLS peptide is removed by a prenyl protein-specific endoprotease (PPSEP) in the ER, and then a prenylprotein-specific methyltransferase (PPSMT) donates a methyl group from S-adenosylmethionine (SAM) to the carboxy-terminal S-farnesylated cysteine. Finally, palmitates are added to cysteine residues near the C-terminus of the protein.

2(S)-{(S)-[2(R)-amino-3-mercapto]propylamino-3(S)-methyl}pentyloxy-3-phenylpropionyl-methioninesulfone methyl ester

The structure of I-739,749, a farnesyl transferase inhibitor that is a potent tumor growth suppressor.

a conserved tetrasaccharide core of three mannose residues and a glucosamine, which can be altered by modifications of the mannose residues or addition of galactosyl side chains of various sizes, extra phosphoethanolamines, or additional *N*-acetylgalactose or mannosyl residues (Figure 9.20). The inositol moiety can also be modified by an additional fatty acid, and a variety of fatty acyl groups are found linked to the glycerol group. GPI groups anchor a wide variety of *surface antigens, adhesion molecules,* and *cell surface hydrolases* to plasma membranes in various eukaryotic organisms. GPI anchors have not yet been observed in prokaryotic organisms or plants.

9.3 • Membranes and Cell-Surface Polysaccharides

Bacterial Cell Walls

Some of nature's most interesting polysaccharide structures are found in *bacterial cell walls*. Given the strength and rigidity provided by polysaccharide structures, it is not surprising that bacteria use such structures to provide protection for their cellular contents. Bacteria normally exhibit high internal osmotic pressures and frequently encounter variable, often hypotonic exterior conditions. The rigid cell walls synthesized by bacteria maintain cell shape and size and prevent swelling or shrinkage that would inevitably accompany variations in solution osmotic strength.

Peptidoglycan

Bacteria are conveniently classified as either **Gram-positive** or **Gram-negative** depending on their response to the so-called *Gram stain*. Despite substantial differences in the various structures surrounding these two types of cells, nearly all bacterial cell walls have a strong, protective peptide–polysaccharide layer called **peptidoglycan.** Gram-positive bacteria have a thick (approximately 25 nm) cell wall consisting of multiple layers of peptidoglycan. This thick cell wall surrounds the bacterial plasma membrane. Gram-negative bacteria, in contrast, have a much thinner (2 to 3 nm) cell wall consisting of a single layer of peptidoglycan sandwiched between the inner and outer lipid bilayer membranes. In either case, peptidoglycan, sometimes called **murein** (from the Latin *murus* for "wall"), is a continuous cross-linked structure—in essence, a single molecule—built around the cell. The structure is shown in Figure 9.21. The backbone is a $\beta(1\rightarrow4)$ linked polymer of alternating *N*-acetylglucosamine and *N*-acetylmuramic acid units. This part of the structure is similar to chitin, but it is joined to a tetrapeptide, usually L-Ala·D-Glu·L-Lys·D-Ala, in which the L-lysine is linked to the γ-COOH of D-glutamate. The peptide is linked to the *N*-acetylmuramic acid units via its D-lactate moiety. The ϵ-amino group of lysine in this peptide is linked to the —COOH of D-alanine of an adjacent tetrapeptide. In Gram-negative cell walls, the lysine ϵ-amino group forms a *direct amide bond* with this D-alanine carboxyl (Figure 9.22). In Gram-positive cell walls, a **pentaglycine chain** bridges the lysine ϵ-amino group and the D-Ala carboxyl group.

Cell Walls of Gram-Negative Bacteria

In Gram-negative bacteria, the peptidoglycan wall is the rigid framework around which is built an elaborate membrane structure (Figure 9.23). The peptidoglycan layer encloses the *periplasmic space* and is attached to the outer membrane via a group of **hydrophobic proteins.** These proteins, each having 57 amino acid residues, are attached through amide linkages from the side chains of C-terminal lysines of the proteins to diaminopimelic acid groups on the
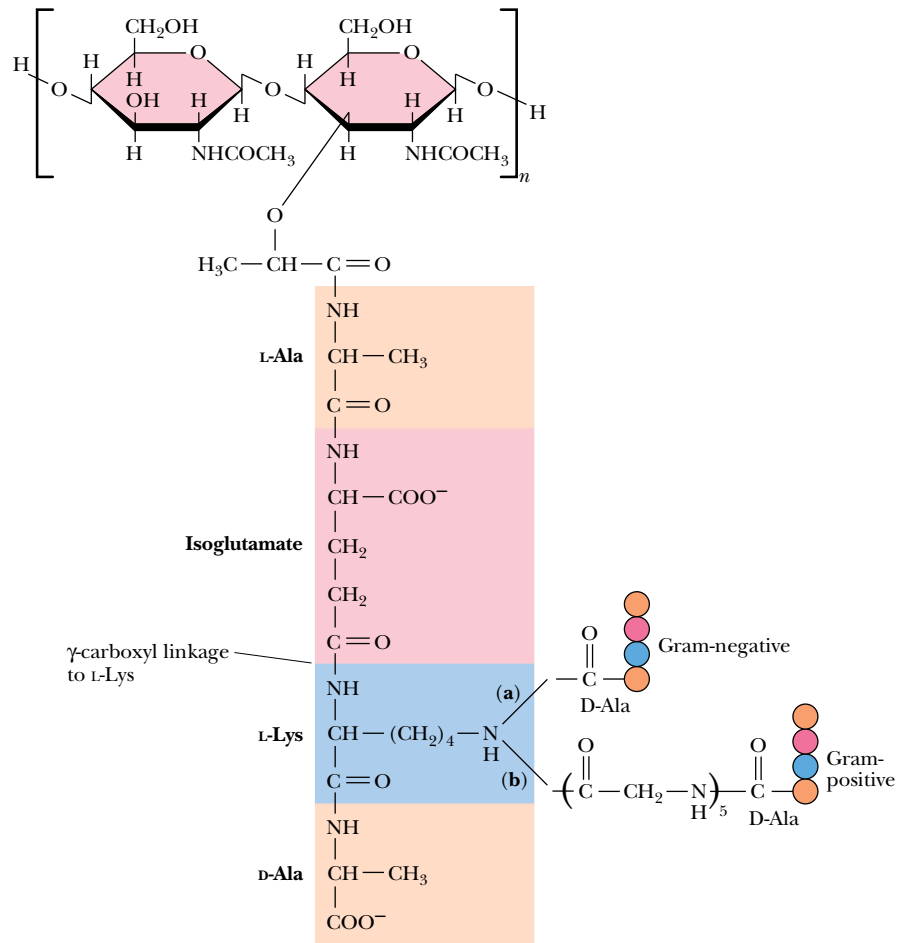
FIGURE 9.21 • The structure of peptidoglycan. The tetrapeptides linking adjacent backbone chains contain an unusual γ-carboxyl linkage.
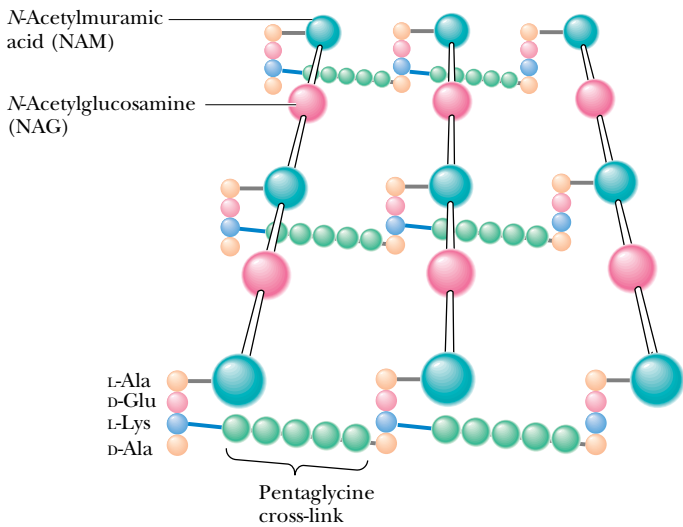
FIGURE 9.22 • (a) The cross-link in Gram-positive cell walls is a pentaglycine bridge. (b) In Gram-negative cell walls, the linkage between the tetrapeptides of adjacent carbohydrate chains in peptidoglycan involves a direct amide bond between the lysine side chain of one tetrapeptide and D-alanine of the other.
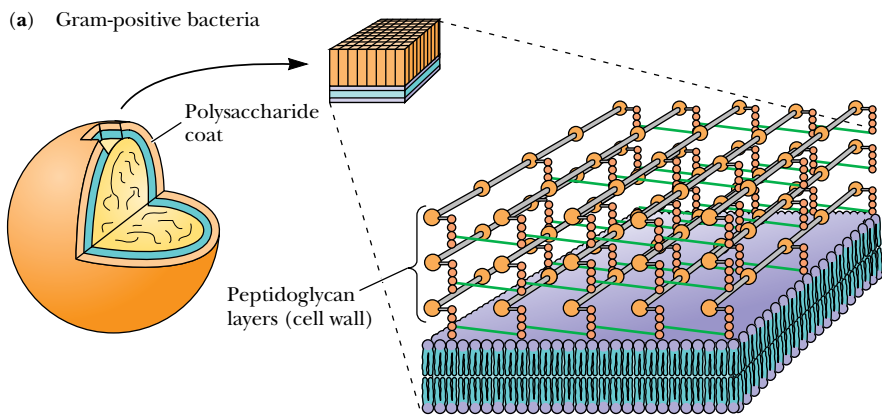
(a) Gram-positive bacteria

Polysaccharide coat

Peptidoglycan layers (cell wall)

(b) Gram-negative bacteria

Lipopoly-saccharide

Outer lipid bilayer membrane

Cell wall — Peptidoglycan

Inner lipid bilayer membrane

Lipoprotein
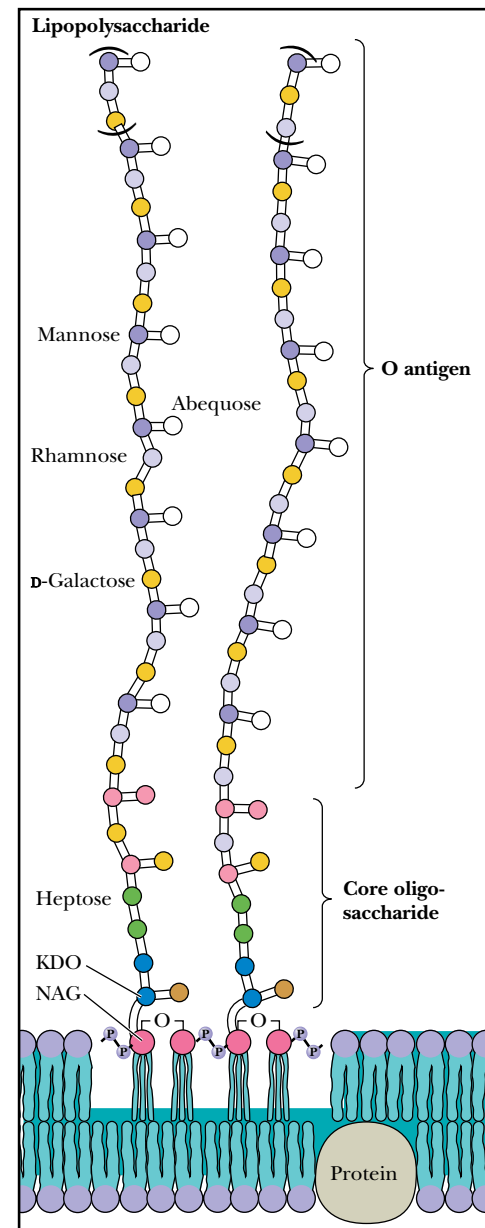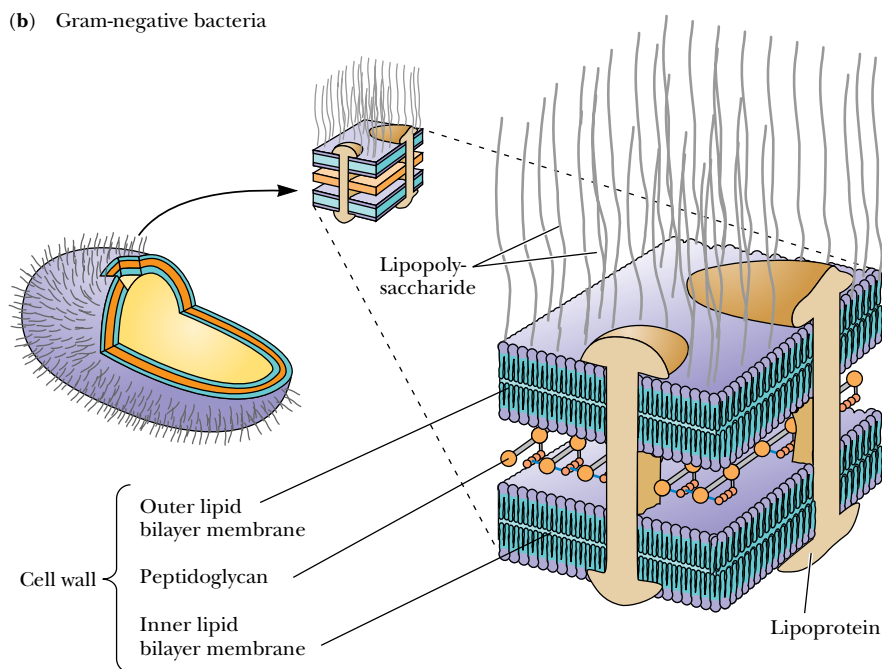
FIGURE 9.23 • The structures of the cell wall and membrane(s) in Gram-positive and Gram-negative bacteria. The Gram-positive cell wall is thicker than that in Gram-negative bacteria, compensating for the absence of a second (outer) bilayer membrane.

Lipopolysaccharide

Mannose

Abequose

O antigen

Rhamnose

D-Galactose

Heptose

Core oligo-saccharide

KDO

NAG

Protein

peptidoglycan. Diaminopimelic acid replaces one of the D-alanine residues in about 10% of the peptides of the peptidoglycan. On the other end of the hydrophobic protein, the N-terminal residue, a serine, makes a covalent bond to a lipid that is part of the outer membrane.

As shown in Figure 9.24, the outer membrane of Gram-negative bacteria is coated with a highly complex **lipopolysaccharide,** which consists of a lipid group (anchored in the outer membrane) joined to a polysaccharide made up of long chains with many different and characteristic repeating structures

Lipopolysaccharides

Outer cell wall

Peptidoglycan

Plasma membrane
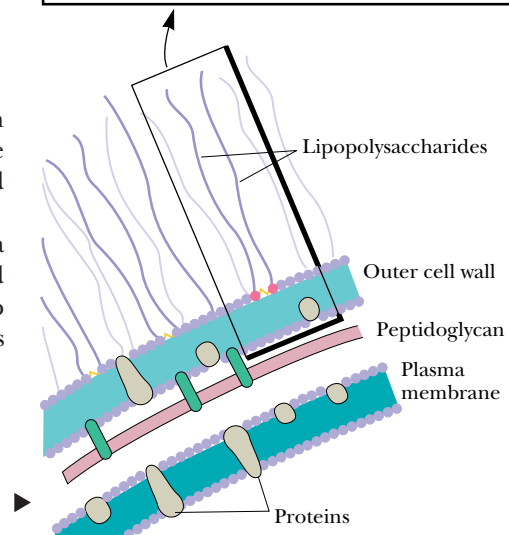
FIGURE 9.24 • Lipopolysaccharide (LPS) coats the outer membrane of Gram-negative bacteria. The lipid portion of the LPS is embedded in the outer membrane and is linked to a complex polysaccharide.

Proteins

281

(Figure 9.24). These many different unique units determine the antigenicity of the bacteria; that is, animal immune systems recognize them as foreign substances and raise antibodies against them. As a group, these **antigenic determinants** are called the **O antigens,** and there are thousands of different ones. The *Salmonella* bacteria alone have well over a thousand known O antigens that have been organized into 17 different groups. The great variation in these O antigen structures apparently plays a role in the recognition of one type of cell by another and in evasion of the host immune system.

Cell Walls of Gram-Positive Bacteria

In Gram-positive bacteria, the cell exterior is less complex than for Gram-negative cells. Having no outer membrane, Gram-positive cells compensate with a thicker wall. Covalently attached to the peptidoglycan layer are **teichoic acids,** which often account for 50% of the dry weight of the cell wall (Figure 9.25). The teichoic acids are polymers of *ribitol phosphate* or *glycerol phosphate* linked by phosphodiester bonds. In these heteropolysaccharides, the free hydroxyl groups of the ribitol or glycerol are often substituted by glycosidically linked monosaccharides (often glucose or *N*-acetylglucosamine) or disaccharides. D-Alanine is sometimes found in ester linkage to the saccharides. Teichoic acids are not confined to the cell wall itself, and they may be present in the inner membranes of these bacteria. Many teichoic acids are antigenic, and they also serve as the receptors for bacteriophages in some cases.

Cell Surface Polysaccharides

Compared to bacterial cells, which are identical within a given cell type (except for O antigen variations), animal cells display a wondrous diversity of structure, constitution, and function. Although each animal cell contains, in its genetic material, the instructions to replicate the entire organism, each differentiated

FIGURE 9.25 • Teichoic acids are covalently linked to the peptidoglycan of Gram-positive bacteria. These polymers of (a, b) glycerol phosphate or (c) ribitol phosphate are linked by phosphodiester bonds.
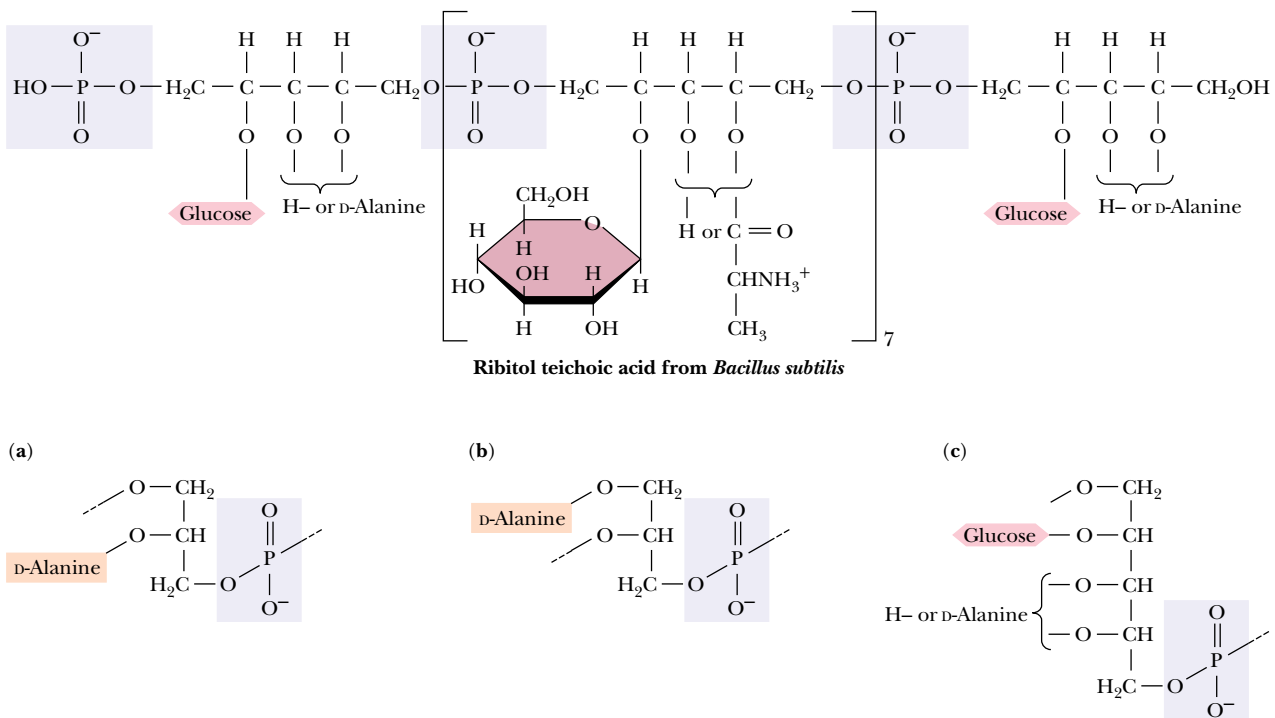
animal cell carefully controls its composition and behavior within the organism. A great part of each cell's uniqueness begins at the cell surface. This surface uniqueness is critical to each animal cell because cells spend their entire life span in intimate contact with other cells and must therefore communicate with one another. That cells are able to pass information among themselves is evidenced by numerous experiments. For example, heart *myocytes,* when grown in culture (in glass dishes) establish *synchrony* when they make contact, so that they "beat" or contract in unison. If they are removed from the culture and separated, they lose their synchronous behavior, but if allowed to reestablish cell-to-cell contact, they spontaneously restore their synchronous contractions.

𝓗 U M A N B I O C H E M I S T R Y

Selectins, Rolling Leukocytes, and the Inflammatory Response

Human bodies are constantly exposed to a plethora of bacteria, viruses, and other inflammatory substances. To combat these infectious and toxic agents, the body has developed a carefully regulated inflammatory response system. Part of that response is the orderly migration of leukocytes to sites of inflammation. Leukocytes literally roll along the vascular wall and into the tissue site of inflammation. This rolling movement is mediated by reversible adhesive interactions between the leukocytes and the vascular surface.

 These interactions involve adhesion proteins called **selectins,** which are found both on the rolling leukocytes and on the endothelial cells of the vascular walls. Selectins have a characteristic domain structure, consisting of an N-terminal extracellular lectin domain, a single epidermal growth factor (EGR) domain, a series of two to nine short consensus repeat (SCR) domains, a single transmembrane segment, and a short cytoplasmic domain. Lectin domains, first characterized in plants, bind carbohydrates with high affinity and specificity. Selectins of three types are known—**E-selectins, L-selectins,** and **P-selectins.** L-selectin is found on the surfaces of leukocytes, including neutrophils and lymphocytes, and binds to carbohydrate ligands on endothelial cells. The presence of L-selectin is a necessary component of leukocyte rolling. P-selectin and E-selectin are located on the vascular endothelium and bind with carbohydrate ligands on leukocytes. Typical neutrophil cells possess 10,000 to 20,000 P-selectin binding sites. Selectins are expressed on the surfaces of their respective cells by exposure to inflammatory signal molecules, such as histamine, hydrogen peroxide, and bacterial endotoxins. P-selectins, for example, are stored in intracellular granules and are transported to the cell membrane within seconds to minutes of exposure to a triggering agent.

 Substantial evidence supports the hypothesis that selectin–carbohydrate ligand interactions modulate the rolling of leukocytes along the vascular wall. Studies with L-selectin–deficient and P-selectin–deficient leukocytes show that L-selectins mediate weaker adherence of the leukocyte to the vascular wall and promote faster rolling along the wall. P-selectins conversely promote stronger adherence and slower rolling. Thus, leukocyte rolling velocity in the inflammatory response could be modulated by variable exposure of P-selectins and L-selectins at the surfaces of endothelial cells and leukocytes, respectively.
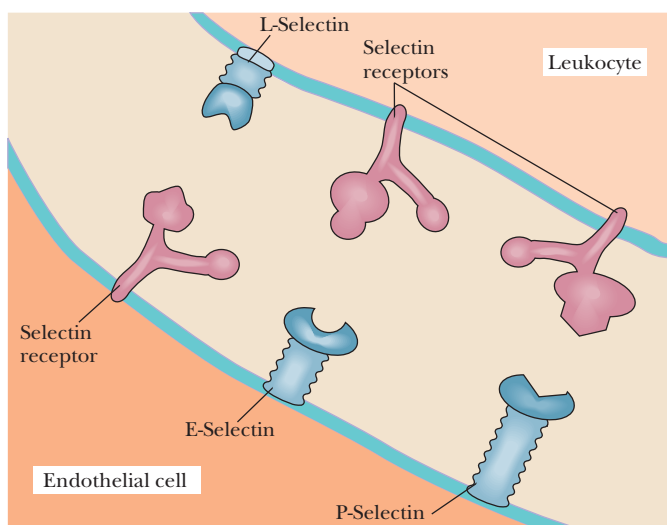
A diagram showing the interactions of selectins with their receptors.
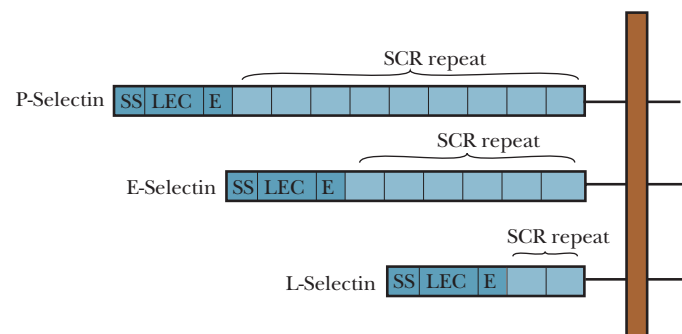
The selectin family of adhesion proteins.

Kidney cells grown in culture with liver cells seek out and make contact with other kidney cells and avoid contact with liver cells. Cells grown in culture grow freely until they make contact with one another, at which point growth stops, a phenomenon well known as **contact inhibition.** One important characteristic of cancerous cells is the loss of contact inhibition.

As these and many other related phenomena show, it is clear that molecular structures on one cell are recognizing and responding to molecules on the adjacent cell or to molecules in the **extracellular matrix,** the complex "soup" of connective proteins and other molecules that exists outside of and among cells. Many of these interactions involve *glycoproteins* on the cell surface and *proteoglycans* in the extracellular matrix. The "information" held in these special carbohydrate-containing molecules is not encoded directly in the genes (as with proteins), but is determined instead by expression of the appropriate enzymes that assemble carbohydrate units in a characteristic way on these molecules. Also, by virtue of the several hydroxyl linkages that can be formed with each carbohydrate monomer, these structures can be more information-rich than proteins and nucleic acids, which can form only linear polymers. A few of these glycoproteins and their unique properties are described in the following sections.

9.4 • Glycoproteins

Many proteins found in nature are **glycoproteins** because they contain covalently linked oligo- and polysaccharide groups. The list of known glycoproteins includes structural proteins, enzymes, membrane receptors, transport proteins, and immunoglobulins, among others. In most cases, the precise function of the bound carbohydrate moiety is not understood.

Carbohydrate groups may be linked to polypeptide chains via the hydroxyl groups of serine, threonine, or hydroxylysine residues (in **O-linked saccharides**) (Figure 9.26a) or via the amide nitrogen of an asparagine residue (in **N-linked saccharides**) (Figure 9.26b). The carbohydrate residue linked to the protein in O-linked saccharides is usually an *N*-acetylgalactosamine, but mannose, galactose, and xylose residues linked to protein hydroxyls are also found (Figure 9.26a). Oligosaccharides O-linked to glycophorin (see Figure 9.14) involve *N*-acetylgalactosamine linkages and are rich in sialic acid residues (Figure 9.14). N-linked saccharides always have a unique core structure composed of two *N*-acetylglucosamine residues linked to a branched mannose triad (Figure 9.26b, c). Many other sugar units may be linked to each of the mannose residues of this branched core.

O-Linked saccharides are often found in cell surface glycoproteins and in **mucins,** the large glycoproteins that coat and protect mucous membranes in the respiratory and gastrointestinal tracts in the body. Certain viral glycoproteins also contain O-linked sugars. O-Linked saccharides in glycoproteins are often found clustered in richly glycosylated domains of the polypeptide chain. Physical studies on mucins show that they adopt rigid, extended structures so that an individual mucin molecule ($M_r = 10^7$) may extend over a distance of 150 to 200 nm in solution. Inherent steric interactions between the sugar residues and the protein residues in these cluster regions cause the peptide core to fold into an extended and relatively rigid conformation. This interesting effect may be related to the function of O-linked saccharides in glycoproteins. It allows aggregates of mucin molecules to form extensive, intertwined networks, even at low concentrations. These viscous networks protect the mucosal surface of the respiratory and gastrointestinal tracts from harmful environmental agents.

(**a**) O-linked saccharides

β-Galactosyl–1,3–α-*N*-acetylgalactosyl-serine

α-Xylosyl-threonine

α-Mannosyl-serine
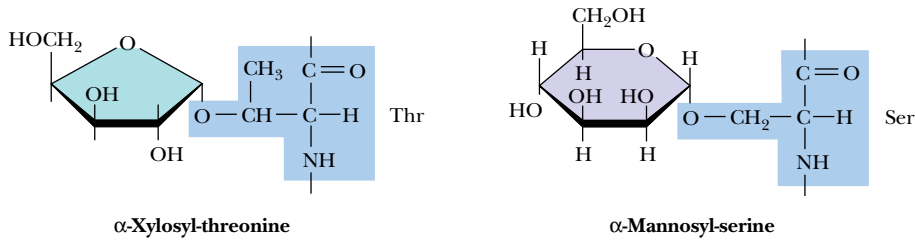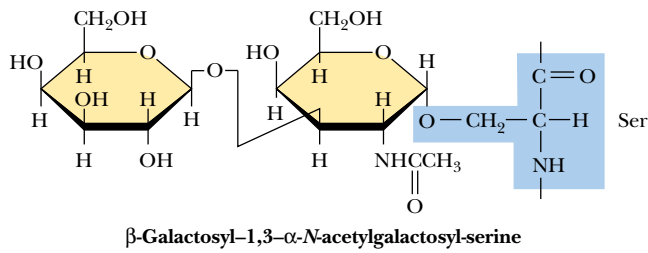
(**b**) Core oligosaccharides in N-linked glycoproteins
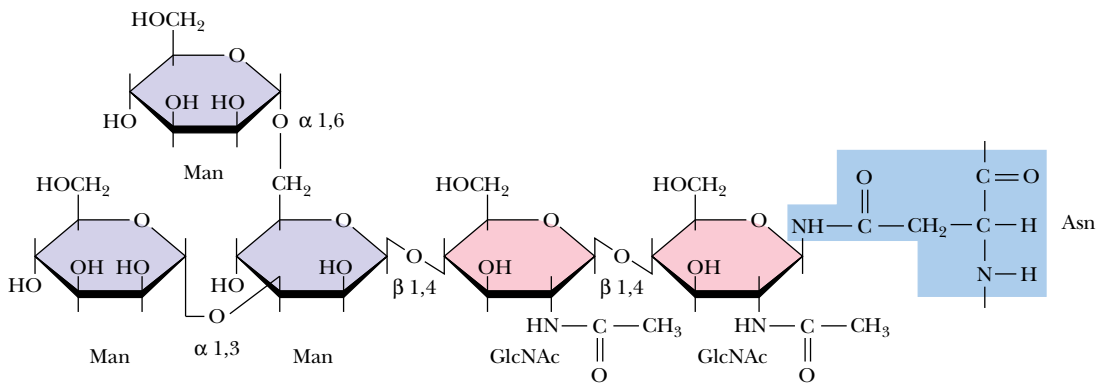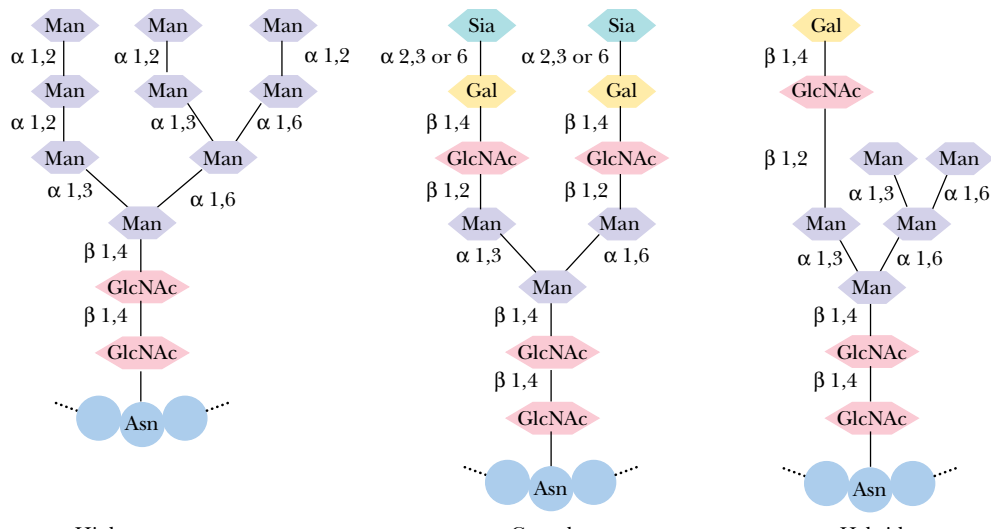
(**c**) N-linked glycoproteins

FIGURE 9.26 • The carbohydrate moieties of glycoproteins may be linked to the protein via (a) serine or threonine residues (in the O-linked saccharides) or (b) asparagine residues (in the N-linked saccharides). (c) N-Linked glycoproteins are of three types: high mannose, complex, and hybrid, the latter of which combines structures found in the high mannose and complex saccharides.
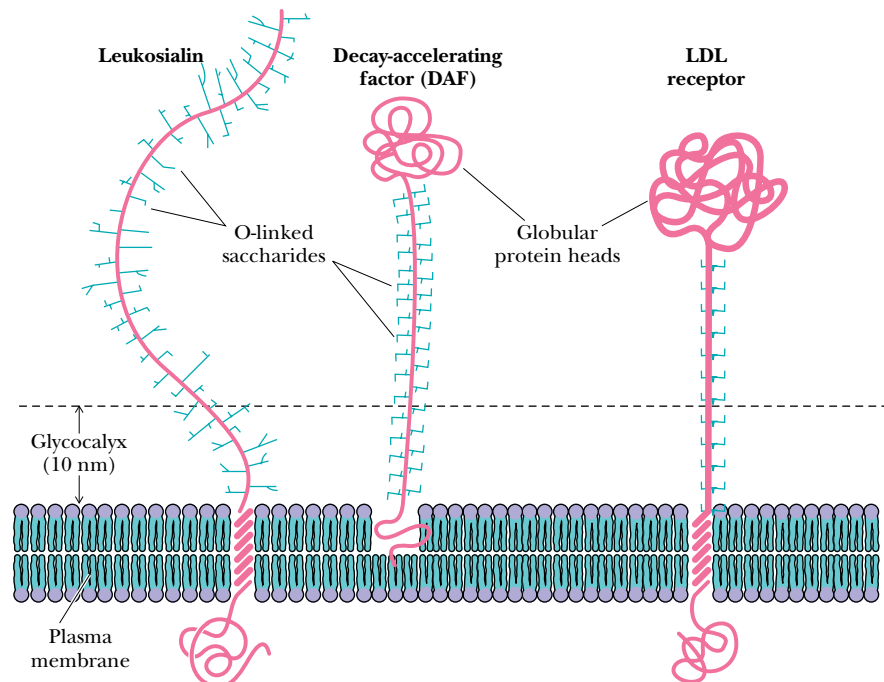
FIGURE 9.27 • The O-linked saccharides of glycoproteins appear in many cases to adopt extended conformations that serve to extend the functional domains of these proteins above the membrane surface. *(Adapted from Jentoft, N., 1990,* Trends in Biochemical Sciences *15:291–294.)*

There appear to be two structural motifs for membrane glycoproteins containing O-linked saccharides. Certain glycoproteins, such as **leukosialin,** are O-glycosylated throughout much or most of their extracellular domain (Figure 9.27). Leukosialin, like mucin, adopts a highly extended conformation, allowing it to project great distances above the membrane surface, perhaps protecting the cell from unwanted interactions with macromolecules or other cells. The second structural motif is exemplified by the **low density lipoprotein (LDL) receptor** and by **decay accelerating factor (DAF).** These proteins contain a highly O-glycosylated stem region that separates the transmembrane domain from the globular, functional extracellular domain. The O-glycosylated stem serves to raise the functional domain of the protein far enough above the membrane surface to make it accessible to the extracellular macromolecules with which it interacts.

Antifreeze Glycoproteins

A unique family of O-linked glycoproteins permits fish to live in the icy seawater of the Arctic and Antarctic regions where water temperature may reach as low as $-1.9°C$. **Antifreeze glycoproteins (AFGPs)** are found in the blood of nearly all Antarctic fish and at least five Arctic fish. These glycoproteins have the peptide structure

$$[\text{Ala-Ala-Thr}]_n\text{-Ala-Ala}$$

where n can be 4, 5, 6, 12, 17, 28, 35, 45, or 50. Each of the threonine residues is glycosylated with the disaccharide β-galactosyl-$(1\rightarrow3)$-α-N-acetylgalactos-

β-Galactosyl–1,3–α-N-acetylgalactosamine

Repeating unit of antifreeze glycoproteins
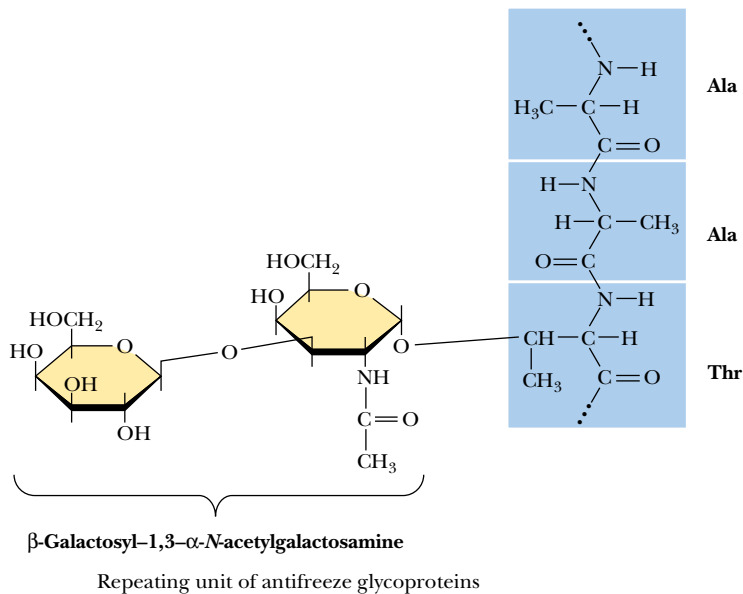
FIGURE 9.28 • The structure of the repeating unit of antifreeze glycoproteins, a disaccharide consisting of β-galactosyl-(1→3)-α-N-acetylgalactosamine in glycosidic linkage to a threonine residue.

amine (Figure 9.28). This glycoprotein adopts a **flexible rod** conformation with regions of threefold left-handed helix. The evidence suggests that antifreeze glycoproteins may inhibit the formation of ice in the fish by binding specifically to the growth sites of ice crystals, inhibiting further growth of the crystals.

N-Linked Oligosaccharides

N-Linked oligosaccharides are found in many different proteins, including immunoglobulins G and M, ribonuclease B, ovalbumin, and peptide hormones (Figure 9.29). Many different functions are known or suspected for N-glycosylation of proteins. Glycosylation can affect the physical and chemical properties of proteins, altering solubility, mass, and electrical charge. Carbohydrate moieties have been shown to stabilize protein conformations and protect proteins against proteolysis. Eukaryotic organisms use posttranslational additions of N-linked oligosaccharides to direct selected proteins to various intracellular organelles.

Oligosaccharide Cleavage as a Timing Device for Protein Degradation

The slow cleavage of monosaccharide residues from N-linked glycoproteins circulating in the blood targets these proteins for degradation by the organism. The liver contains specific receptor proteins that recognize and bind glycoproteins that are ready to be degraded and recycled. Newly synthesized serum glycoproteins contain N-linked **triantennary** (three-chain) oligosaccharides having structures similar to those in Figure 9.30, in which sialic acid residues cap galactose residues. As these glycoproteins circulate, enzymes on the blood vessel walls cleave off the sialic acid groups, exposing the galactose residues. In
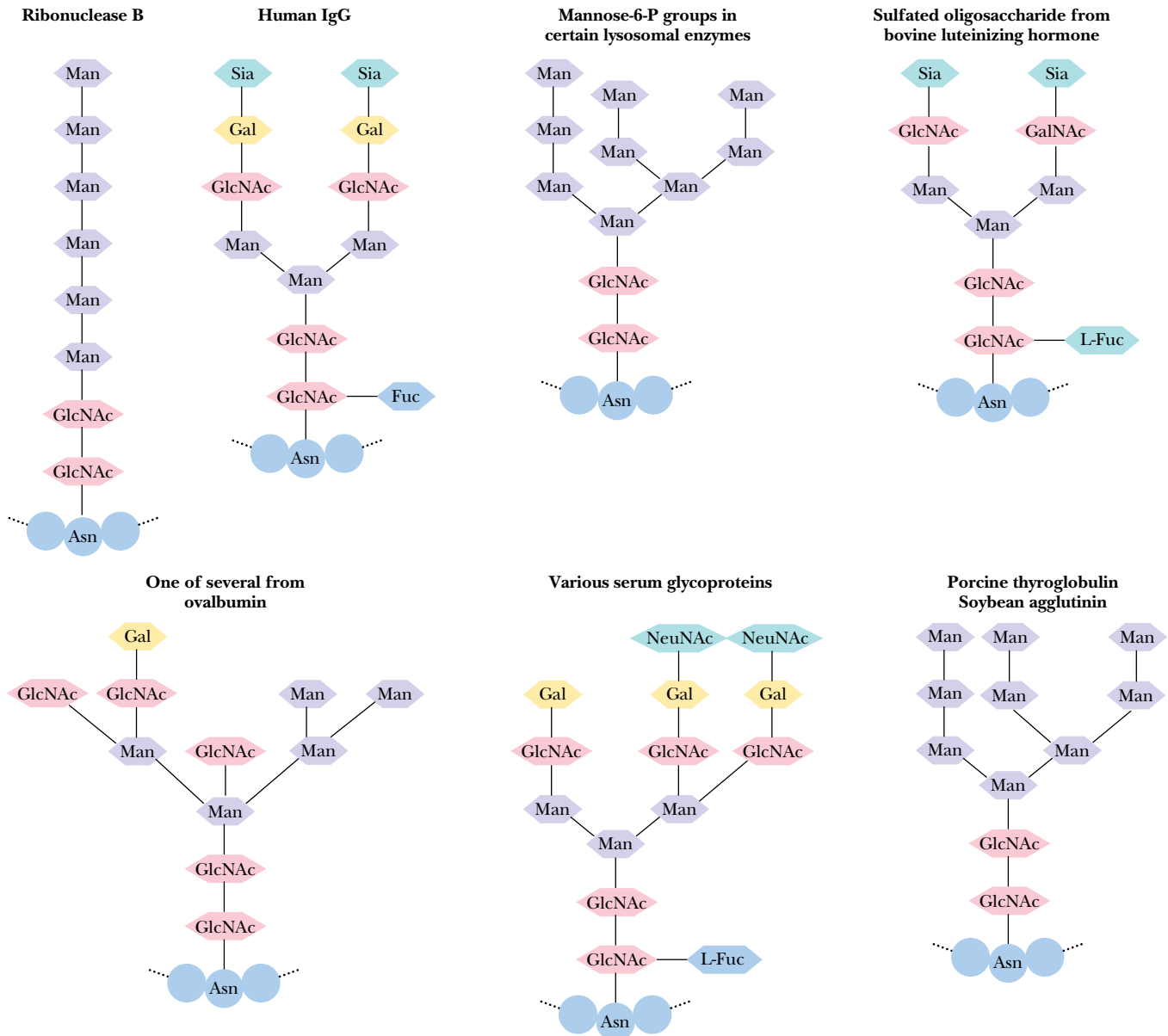
FIGURE 9.29 • Some of the oligosaccharides found in N-linked glycoproteins.

the liver, the **asialoglycoprotein receptor** binds the exposed galactose residues of these glycoproteins with very high affinity ($K_D = 10^{-9}$ to 10^{-8} M). The complex of receptor and glycoprotein is then taken into the cell by **endocytosis,** and the glycoprotein is degraded in cellular lysosomes. Highest affinity binding of glycoprotein to the asialoglycoprotein receptor requires three free galactose residues. Oligosaccharides with only one or two exposed galactose residues bind less tightly. This is an elegant way for the body to keep track of how long glycoproteins have been in circulation. Over a period of time, anywhere from a few hours to weeks, the sialic acid groups are cleaved one by one. The longer the glycoprotein circulates and the more sialic acid residues are removed, the more galactose residues become exposed so that the glycoprotein is eventually bound to the liver receptor.
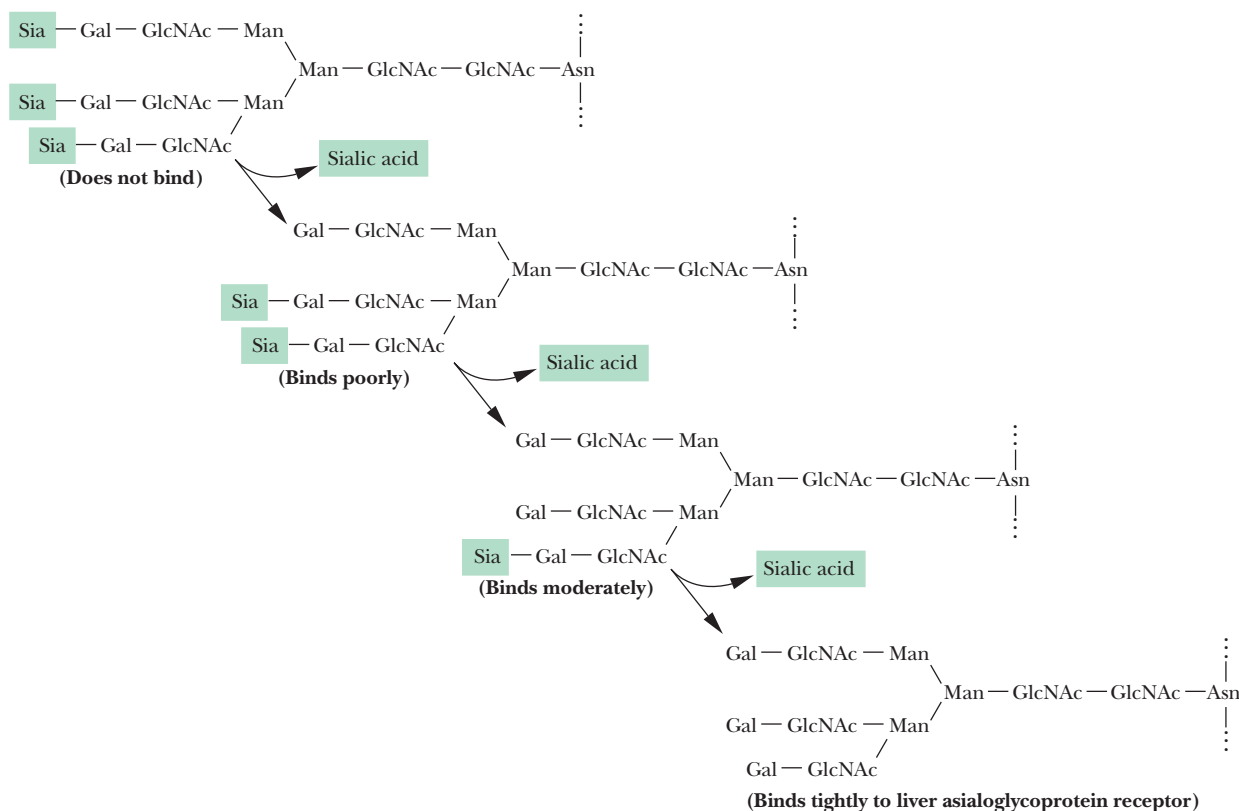
FIGURE 9.30 • Progressive cleavage of sialic acid residues exposes galactose residues. Binding to the asialoglycoprotein receptor in the liver becomes progressively more likely as more Gal residues are exposed.

9.5 • Proteoglycans

Proteoglycans are a family of glycoproteins whose carbohydrate moieties are predominantly **glycosaminoglycans.** The structures of only a few proteoglycans are known, and even these few display considerable diversity (Figure 9.31). They range in size from **serglycin,** having 104 amino acid residues (10.2 kD) to **versican,** having 2409 residues (265 kD). Each of these proteoglycans contains one or two types of covalently linked glycosaminoglycans (Table 9.2). In the known proteoglycans, the glycosaminoglycan units are O-linked to serine residues of Ser-Gly dipeptide sequences. Serglycin is named for a unique central domain of 49 amino acids composed of alternating serine and glycine residues. The **cartilage matrix proteoglycan** contains 117 Ser-Gly pairs to which chondroitin sulfates attach. **Decorin,** a small proteoglycan secreted by fibroblasts and found in the extracellular matrix of connective tissues, contains only three Ser-Gly pairs, only one of which is normally glycosylated. In addition to glycosaminoglycan units, proteoglycans may also contain other N-linked and O-linked oligosaccharide groups.

Functions of Proteoglycans

Proteoglycans may be *soluble* and located in the extracellular matrix, as is the case for serglycin, versican, and the cartilage matrix proteoglycan, or they may be *integral transmembrane proteins,* such as **syndecan.** Both types of proteoglycan

(a) Versican

NH$_3^+$

Hyaluronic acid binding domain (link-protein like)

Chondroitin sulfate

Protein core

Epidermal growth factor-like domains

COO$^-$

(b) Serglycin

NH$_3^+$

Ser/Gly protein core

COO$^-$

Chondroitin sulfate

(c) Decorin

NH$_3^+$

Chondroitin/dermatan sulfate chain

COO$^-$

(d) Syndecan

Heparan sulfate

NH$_3^+$

Extracellular domain

Chondroitin sulfate

Cytoplasmic domain

COO$^-$

Transmembrane domain

(e) Rat cartilage proteoglycan

Chondroitin sulfate

O–linked oligosaccharides

Keratan sulfate

N–linked oligosaccharides

FIGURE 9.31 • The known proteoglycans include a variety of structures. The carbohydrate groups of proteoglycans are predominantly glycosaminoglycans O-linked to serine residues. Proteoglycans include both soluble proteins and integral transmembrane proteins.

appear to function by interacting with a variety of other molecules through their glycosaminoglycan components and through specific receptor domains in the polypeptide itself. For example, syndecan (from the Greek *syndein* meaning "to bind together") is a transmembrane proteoglycan that associates intracellularly with the actin cytoskeleton (Chapter 17). Outside the cell, it interacts with **fibronectin,** an extracellular protein that binds to several cell surface proteins and to components of the extracellular matrix. The ability of syndecan to participate in multiple interactions with these target molecules allows them to act as a sort of "glue" in the extracellular space, linking components of the extracellular matrix, facilitating the binding of cells to the matrix, and mediating the binding of growth factors and other soluble molecules to the matrix and to cell surfaces (Figure 9.32).

Table 9.2

Some Proteoglycans of Known Sequence

Proteoglycan	Glycosaminoglycan	Protein M_r	Number of Amino Acid Residues
Secreted or extracellular matrix proteoglycans			
Large aggregating cartilage proteoglycans	CS/KS[*]	220,952	2124
Versican	CS/DS	265,048	2409
Decorin	CS/DS	38,000	329
Intracellular granule proteoglycan			
Serglycin (PG19)	CS/DS	10,190	104
Membrane-intercalated proteoglycans			
Syndecan	HS/CS	38,868	311

[*]CS, chondroitin sulfate; DS, dermatan sulfate; HS, heparan sulfate (an analog of heparin); KS, keratan sulfate. These glycosaminoglycans are polymers consisting of the repeating disaccharides: glucuronic acid *N*-acetylgalactosamine (CS), iduronic acid *N*-acetylgalactosamine (DS), iduronic acid *N*-acetylglucosamine (HS and heparin), and galactose *N*-acetylglucosamine (KS). DS, HS, and heparin also contain some disaccharide units in which the uronic acid is glucuronic acid instead of iduronic acid. These glycosaminoglycans and CS are generally bound to the hydroxyl group of a serine residue to give the sequence (disaccharide) *n*GlcUA-Gal-Gal-Xyl-*O* Ser. Keratan sulfate has a different linkage region and can be either O- or N-linked. The sugars in the repeating disaccharide unit are sulfated to various degrees. By comparison, hyaluronic acid is a polymer of glucuronic acid and glucosamine that is not sulfated and does not attach covalently to a protein core.

Adapted from Ruoslahti, E., 1989. *Journal of Biological Chemistry* **264:**13369–13372.
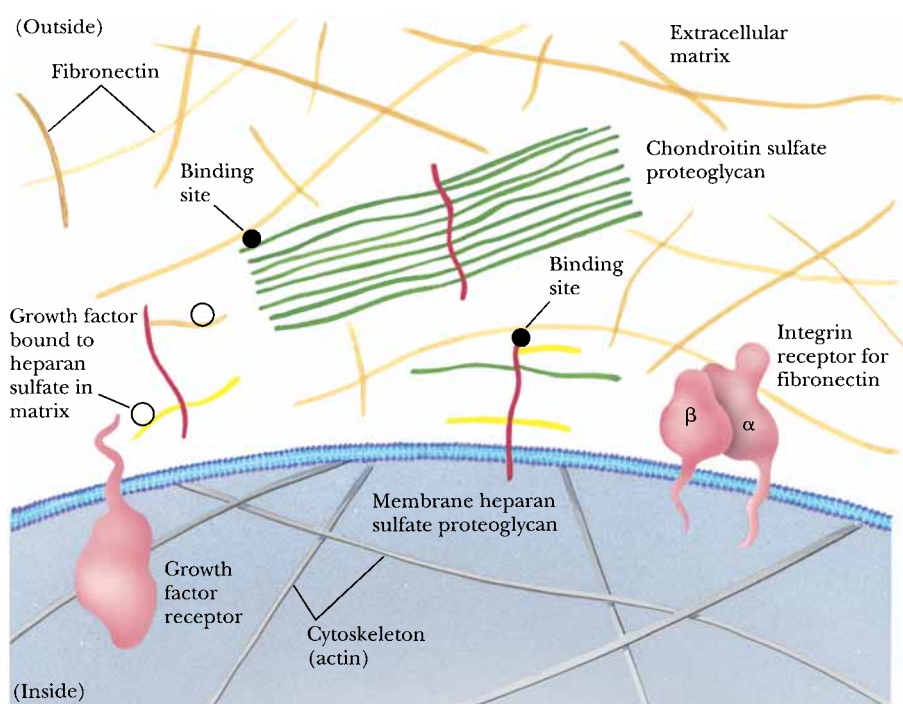
FIGURE 9.32 • Proteoglycans serve a variety of functions on the cytoplasmic and extracellular surfaces of the plasma membrane. Many of these functions appear to involve the binding of specific proteins to the glycosaminoglycan groups.

FIGURE 9.33 • A portion of the structure of heparin, a carbohydrate having anticoagulant properties. It is used by blood banks to prevent the clotting of blood during donation and storage and also by physicians to prevent the formation of life-threatening blood clots in patients recovering from serious injury or surgery. This sulfated pentasaccharide sequence in heparin binds with high affinity to antithrombin III, accounting for this anticoagulant activity. The 3-O-sulfate marked by an asterisk is essential for high-affinity binding of heparin to antithrombin III.
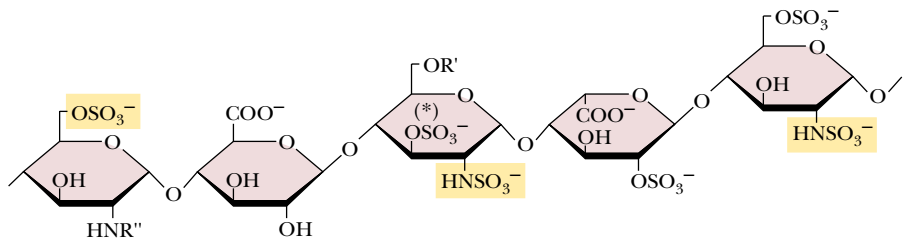
Many of the functions of proteoglycans involve the binding of specific proteins to the glycosaminoglycan groups of the proteoglycan. The glycosaminoglycan binding sites on these specific proteins contain multiple basic amino acid residues. The amino acid sequences BBXB and BBBXXB (where B is a basic amino acid and X is any amino acid) recur repeatedly in these binding domains. Basic amino acids such as lysine and arginine provide charge neutralization for the negative charges of glycosaminoglycan residues, and in many cases, the binding of extracellular matrix proteins to glycosaminoglycans is primarily charge-dependent. For example, more highly sulfated glycosaminoglycans bind more tightly to fibronectin. Certain protein–glycosaminoglycan interactions, however, require a specific carbohydrate sequence. A particular pentasaccharide sequence in heparin, for example, binds tightly to antithrombin III (Figure 9.33), accounting for the anticoagulant properties of heparin. Other glycosaminoglycans interact much more weakly.

Proteoglycans May Modulate Cell Growth Processes

Several lines of evidence raise the possibility of modulation or regulation of cell growth processes by proteoglycans. First, heparin and heparan sulfate are known to inhibit cell proliferation in a process involving internalization of the glycosaminoglycan moiety and its migration to the cell nucleus. Second, **fibroblast growth factor** binds tightly to heparin and other glycosaminoglycans, and the heparin–growth factor complex protects the growth factor from degradative enzymes, thus enhancing its activity. There is evidence that binding of fibroblast growth factors by proteoglycans and glycosaminoglycans in the extracellular matrix creates a reservoir of growth factors for cells to use. Third, **transforming growth factor β** has been shown to stimulate the synthesis and secretion of proteoglycans in certain cells. Fourth, several proteoglycan core proteins, including versican and **lymphocyte homing receptor,** have domains similar in sequence to **epidermal growth factor** and **complement regulatory factor.** These growth factor domains may interact specifically with growth factor receptors in the cell membrane in processes that are not yet understood.

Proteoglycans Make Cartilage Flexible and Resilient

Cartilage matrix proteoglycan is responsible for the flexibility and resilience of cartilage tissue in the body. In cartilage, long filaments of hyaluronic acid are studded or coated with proteoglycan molecules, as shown in Figure 9.34. The hyaluronate chains can be as long as 4 μm and can coordinate 100 or more proteoglycan units. Cartilage proteoglycan possesses a **hyaluronic acid binding domain** on the NH$_2$-terminal portion of the polypeptide, which binds to hyaluronate with the assistance of a **link protein.** The proteoglycan–hyaluronate aggregates can have molecular weights of 2 million or more.

The proteoglycan–hyaluronate aggregates are highly hydrated by virtue of strong interactions between water molecules and the polyanionic complex.

When cartilage is compressed (such as when joints absorb the impact of walking or running), water is briefly squeezed out of the cartilage tissue and then reabsorbed when the stress is diminished. This reversible hydration gives cartilage its flexible, shock-absorbing qualities and cushions the joints during physical activities that might otherwise injure the involved tissues.
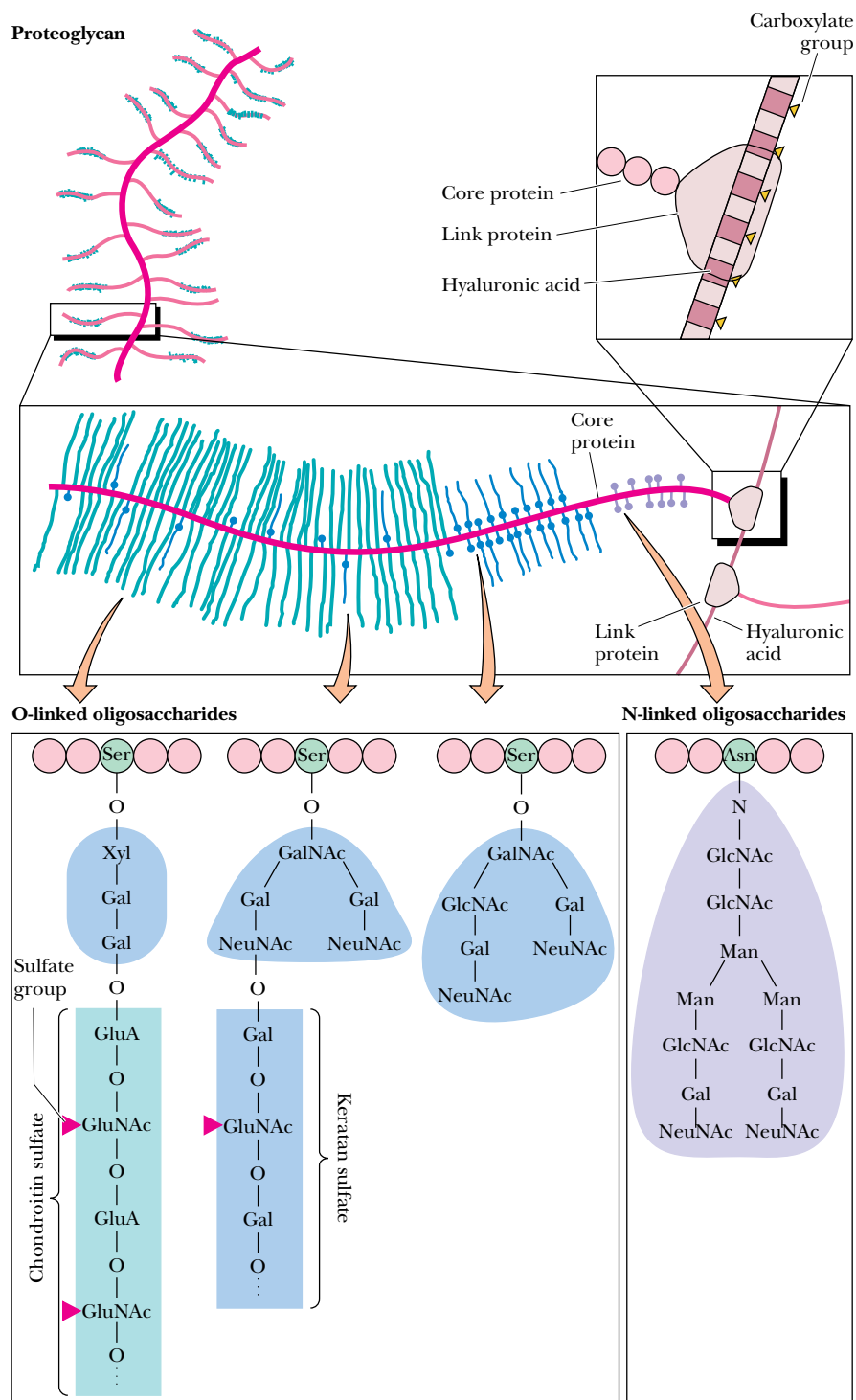
FIGURE 9.34 • Hyaluronate (see Figure 7.33) forms the backbone of proteoglycan structures, such as those found in cartilage. The proteoglycan subunits consist of a core protein containing numerous O-linked and N-linked glycosaminoglycans. In cartilage, these highly hydrated proteoglycan structures are enmeshed in a network of collagen fibers. Release (and subsequent reabsorption) of water by these structures during compression accounts for the shock-absorbing qualities of cartilaginous tissue.

PROBLEMS

1. In Problem 1(b) in chapter 8 (page 257) you were asked to draw all the phosphatidylserine isomers that can be formed from palmitic and linolenic acids. Which of the PS isomers are not likely to be found in biological membranes?

2. The purple patches of the *Halobacterium halobium* membrane, which contain the protein bacteriorhodopsin, are approximately 75% protein and 25% lipid. If the protein molecular weight is 26,000 and an average phospholipid has a molecular weight of 800, calculate the phospholipid to protein mole ratio.

3. Sucrose gradients for separation of membrane proteins must be able to separate proteins and protein–lipid complexes having a wide range of densities, typically 1.00 to 1.35 g/mL.

a. Consult reference books (such as the *CRC Handbook of Biochemistry*) and plot the density of sucrose solutions versus percent sucrose by weight (g sucrose per 100 g solution), and versus percent by volume (g sucrose per 100 mL solution). Why is one plot linear and the other plot curved?

b. What would be a suitable range of sucrose concentrations for separation of three membrane-derived protein–lipid complexes with densities of 1.03, 1.07, and 1.08 g/mL?

4. Phospholipid lateral motion in membranes is characterized by a diffusion coefficient of about 1×10^{-8} cm^2/sec. The distance traveled in two dimensions (across the membrane) in a given time is $r = (4Dt)^{1/2}$, where r is the distance traveled in centimeters, D is the diffusion coefficient, and t is the time during which diffusion occurs. Calculate the distance traveled by a phospholipid across a bilayer in 10 msec (milliseconds).

5. Protein lateral motion is much slower than that of lipids because proteins are larger than lipids. Also, some membrane proteins can diffuse freely through the membrane, whereas others are bound or anchored to other protein structures in the membrane. The diffusion constant for the membrane protein fibronectin is approximately 0.7×10^{-12} cm^2/sec, whereas that for rhodopsin is about 3×10^{-9} cm^2/sec.

a. Calculate the distance traversed by each of these proteins in 10 msec.

b. What could you surmise about the interactions of these proteins with other membrane components?

6. Discuss the effects on the lipid phase transition of pure dimyristoyl phosphatidylcholine vesicles of added (a) divalent cations, (b) cholesterol, (c) distearoyl phosphatidylserine, (d) dioleoyl phosphatidylcholine, and (e) integral membrane proteins.

FURTHER READING

Aspinall, G. O., 1982. *The Polysaccharides,* Vols. 1 and 2. New York: Academic Press.

Bennett, V., 1985. The membrane skeleton of human erythrocytes and its implications for more complex cells. *Annual Review of Biochemistry* **54:**273–304.

Bretscher, M., 1985. The molecules of the cell membrane. *Scientific American* **253:**100–108.

Collins, P. M., 1987. *Carbohydrates.* London: Chapman and Hall.

Davison, E. A., 1967. *Carbohydrate Chemistry.* New York: Holt, Rinehart and Winston.

Dawidowicz, E. A., 1987. Dynamics of membrane lipid metabolism and turnover. *Annual Review of Biochemistry* **56:**43–61.

Doering, T. L., Masterson, W. J., Hart, G. W., and Englund, P. T., 1990. Biosynthesis of glycosyl phosphatidylinositol membrane anchors. *Journal of Biological Chemistry* **265:**611–614.

Fasman, G. D., and Gilbert, W. A., 1990. The prediction of transmembrane protein sequences and their conformation: An evaluation. *Trends in Biochemical Sciences* **15:**89–92.

Feeney, R. E., Burcham, T. S., and Yeh, Y., 1986. Antifreeze glycoproteins from polar fish blood. *Annual Review of Biophysical Chemistry* **15:**59–78.

Frye, C. D., and Edidin, M., 1970. The rapid intermixing of cell surface antigens after formation of mouse–human heterokaryons. *Journal of Cell Science* **7:**319–335.

Gelb, M. H., 1997. Protein prenylation, et cetera: Signal transduction in two dimensions. *Science* **275:**1750–1751.

Glomset, J. A., Gelb, M. H., and Farnsworth, C. C., 1990. Prenyl proteins in eukaryotic cells: A new type of membrane anchor. *Trends in Biochemical Sciences* **15:**139–142.

Gordon, J. I., Duronio, R. J., Rudnick, D. A., Adams, S. P., and Gokel, G. W., 1991. Protein *N*-myristoylation. *Journal of Biological Chemistry* **266:** 8647–8650.

Jain, M. K., 1988. *Introduction to Biological Membranes,* 2nd ed. New York: John Wiley & Sons.

Jennings, M. L., 1989. Topography of membrane proteins. *Annual Review of Biochemistry* **58:**999–1027.

Jentoft, N., 1990. Why are proteins O-glycosylated? *Trends in Biochemical Sciences* **15:**291–294.

Kjellen, L., and Lindahl, U., 1991. Proteoglycans: Structures and interactions. *Annual Review of Biochemistry* **60:**443–475.

Knowles, B. H., Blatt, M. R., Tester, M., et al., 1989. A cytosolic δ-endotoxin from *Bacillus thurigiensis var. israelensis* forms cation-selective channels in planar lipid bilayers. *FEBS Letters* **244:**259–262.

Koblan, K. S., Kohl, N. E., Omer, C. A., et al., 1996. Farnesyltransferase inhibitors: A new class of cancer chemotherapeutics. *Biochemical Society Transactions* **24:**688–692.

Lasky, L. A., 1995. Selectin–carbohydrate interactions and the initiation of the inflammatory response. *Annual Review of Biochemistry* **64:**113–139.

Lennarz, W. J., 1980. *The Biochemistry of Glycoproteins and Proteoglycans.* New York: Plenum Press.

Lodish, H. F., 1991. Recognition of complex oligosaccharides by the multisubunit asialoglycoprotein receptor. *Trends in Biochemical Sciences* **16:**374 –377.

Marchesi, V. T., 1984. Structure and function of the erythrocyte membrane skeleton. *Progress in Clinical Biology Research* **159:**1–12.

Marchesi, V. T., 1985. Stabilizing infrastructure of cell membranes. *Annual Review of Cell Biology* **1:**531–561.

McNeil, M., Darvill, A. G., Fry, S. C., and Albersheim, P., 1984. Structure and function of the primary cell walls of plants. *Annual Review of Biochemistry* **53:**625–664.

Op den Kamp, J. A. F., 1979. Lipid asymmetry in membranes. *Annual Review of Biochemistry* **48:**47–71.

Park, H-W., Boduluri, S. R., Moomaw, J. F., et al., 1997. Crystal structure of protein farnesyltransferase at 2.25 Angstrom resolution. *Science* **275:** 1800–1804.

Pigman, W., and Horton, D., 1972. *The Carbohydrates.* New York: Academic Press.

Rademacher, T. W., Parekh, R. B., and Dwek, R. A., 1988. Glycobiology. *Annual Review of Biochemistry* **57:**785–838.

Robertson, R. N., 1983. *The Lively Membranes.* Cambridge: Cambridge University Press.

Ruoslahti, E., 1989. Proteoglycans in cell regulation. *Journal of Biological Chemistry* **264:**13369–13372.

Seelig, J., and Seelig, A., 1981. Lipid conformation in model membranes and biological membranes. *Quarterly Review of Biophysics* **13:**19–61.

Sefton, B., and Buss, J. E., 1987. The covalent modification of eukaryotic proteins with lipid. *Journal of Cell Biology* **104:**1449–1453.

Sharon, N., 1980. Carbohydrates. *Scientific American* **243:**90–102.

Sharon, N., 1984. Glycoproteins. *Trends in Biochemical Sciences* **9:**198–202.

Singer, S. J., and Nicolson, G. L., 1972. The fluid mosaic model of the structure of cell membranes. *Science* **175:**720–731.

Singer, S. J., and Yaffe, M. P., 1990. Embedded or not? Hydrophobic sequences and membranes. *Trends in Biochemical Sciences* **15:**369–373.

Tanford, C., 1980. *The Hydrophobic Effect: Formation of Micelles and Biological Membranes,* 2nd ed. New York: Wiley-Interscience.

Towler, D. A., Gordon, J. I., Adams, S. P., and Glaser, L., 1988. The biology and enzymology of eukaryotic protein acylation. *Annual Review of Biochemistry* **57:**69–99.

Unwin, N., and Henderson, R., 1984. The structure of proteins in biological membranes. *Scientific American* **250:**78–94.

Wirtz, K. W. A., 1991. Phospholipid transfer proteins. *Annual Review of Biochemistry* **60:**73–99.

It takes a membrane to make sense out of disorder in biology. You have to be able to catch energy and hold it, storing precisely the needed amount and releasing it in measured shares. A cell does this, and so do the organelles inside. . . . To stay alive, you have to be able to hold out against equilibrium, maintain imbalance, bank against entropy, and you can only transact this business with membranes in our kind of world.

LEWIS THOMAS, "The World's Biggest Membrane," *The Lives of a Cell* (1974)

*C*hapter 10

Membrane Transport

"Drawbridge at Arles with a Group of Washerwomen" (1888) by Vincent van Gogh (Rijksmuseum Kroller-Muller; photo by Erich Lessing/Art Resource)

Transport processes are vitally important to all life forms because all cells must exchange materials with their environment. Cells must obviously have ways to bring nutrient molecules into the cell and ways to send waste products and toxic substances out. Also, inorganic electrolytes must be able to pass in and out of cells and across organelle membranes. All cells maintain **concentration gradients** of various metabolites across their plasma membranes and also across the membranes of intracellular organelles. By their very nature, cells maintain a very large amount of potential energy in the form of such concentration gradients. Sodium and potassium ion gradients across the plasma membrane mediate the transmission of nerve impulses and the normal functions of the brain, heart, kidneys, and liver, among other organs. Storage and release of calcium from cellular compartments controls muscle contraction, and also the response of many cells to hormonal signals. High acid concentrations in the stomach are required for the digestion of food. Extremely high hydrogen ion gradients

are maintained across the plasma membranes of the mucosal cells lining the stomach in order to maintain high acid levels in the stomach yet protect the cells that constitute the stomach walls from the deleterious effects of such acid.

In this chapter, we shall consider the molecules and mechanisms that mediate these transport activities. In nearly every case, the molecule or ion transported is water-soluble, yet moves across the hydrophobic, impermeable lipid membrane at a rate high enough to serve the metabolic and physiologic needs of the cell. This perplexing problem is solved in each case by a specific transport protein. The transported species either diffuses through a channel-forming protein or is carried by a carrier protein. Transport proteins are all classed as **integral membrane proteins** (Chapter 9), ranging in size from small peptides to large, multisubunit protein complexes.

Some transport proteins merely provide a path for the transported species, whereas others couple an enzymatic reaction with the transport event. In all cases, transport behavior depends on the interactions of the transport protein not only with solvent water but with the lipid milieu of the membrane as well. The dynamic and asymmetric nature of the membrane and its components (Chapter 9) plays an important part in the function of these transport systems.

From a thermodynamic and kinetic perspective, there are only three types of membrane transport processes: *passive diffusion, facilitated diffusion,* and *active transport.* To be thoroughly appreciated, membrane transport phenomena must be considered in terms of thermodynamics. Some of the important kinetic considerations also will be discussed.

10.1 • Passive Diffusion

Passive diffusion is the simplest transport process. In passive diffusion, the transported species moves across the membrane in the thermodynamically favored direction without the help of any specific transport system/molecule. For an uncharged molecule, passive diffusion is an entropic process, in which movement of molecules across the membrane proceeds until the concentration of the substance on both sides of the membrane is the same. For an uncharged molecule, the free energy difference between side 1 and side 2 of a membrane (Figure 10.1) is given by

$$\Delta G = G_2 - G_1 = RT \ln \frac{[C_2]}{[C_1]} \tag{10.1}$$

The difference in concentrations, $[C_2] - [C_1]$, is termed the **concentration gradient,** and ΔG here is the **chemical potential difference.**

Passive Diffusion of a Charged Species

For a charged species, the situation is slightly more complicated. In this case, the movement of a molecule across a membrane depends on its **electrochemical potential.** This is given by

$$\Delta G = G_2 - G_1 = RT \ln \frac{[C_2]}{[C_1]} + Z\mathscr{F}\Delta\psi \tag{10.2}$$

where Z is the **charge** on the transported species, $\mathscr{F}$ is **Faraday's constant** (the charge on 1 mole of electrons = 96,485 coulombs/mol = 96,485 joules/volt • mol, because 1 volt = 1 joule/coulomb), and $\Delta\psi$ is the electric potential difference (that is, voltage difference) across the membrane. The second term in the expression thus accounts for the movement of a charge across a potential

Membrane

Side 1 | Side 2

Concentration C_1 Concentration C_2

$$\Delta G = RT \ln \frac{[C_2]}{[C_1]}$$
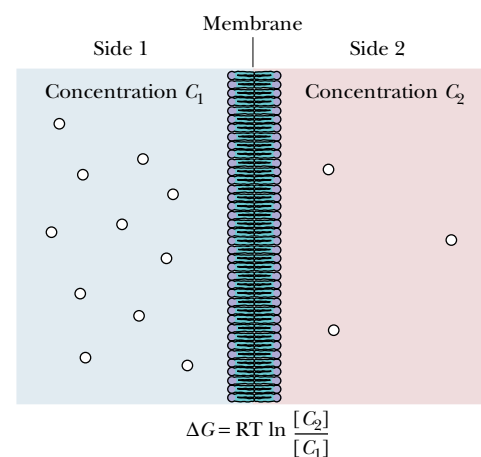
FIGURE 10.1 • Passive diffusion of an uncharged species across a membrane depends only on the concentrations (C_1 and C_2) on the two sides of the membrane.

$$\Psi_2-\Psi_1 = \Delta\Psi > 0$$
$$Z = -1$$
$$Z\mathcal{F}\Delta\Psi < 0$$
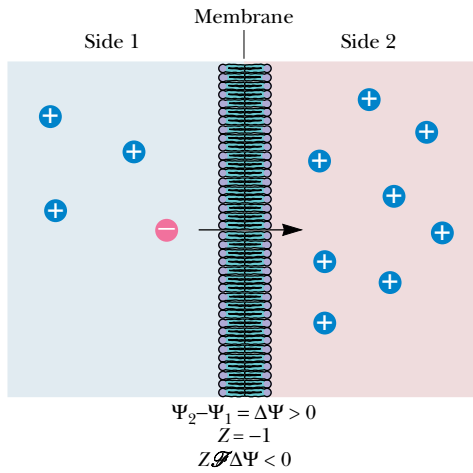
FIGURE 10.2 • The passive diffusion of a charged species across a membrane depends upon the concentration and also on the charge of the particle, *Z,* and the electrical potential difference across the membrane, $\Delta\psi$.
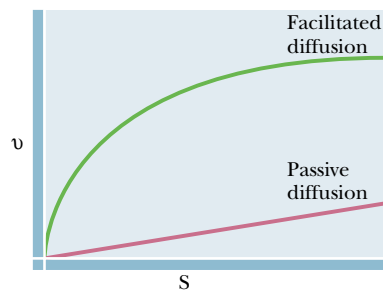
FIGURE 10.3 • Passive diffusion and facilitated diffusion may be distinguished graphically. The plots for facilitated diffusion are similar to plots of enzyme-catalyzed processes (Chapter 14) and they display saturation behavior.

difference. Note that the effect of this second term on ΔG depends on the magnitude and the sign of both Z and $\Delta\psi$. For example, as shown in Figure 10.2, if side 2 has a higher potential than side 1 (so that $\Delta\psi$ is positive), for a negatively charged ion the term $Z\mathcal{F}\Delta\psi$ makes a negative contribution to ΔG.

In other words, the negative charge is spontaneously attracted to the more positive potential—and ΔG is negative. In any case, if the sum of the two terms on the right side of Equation 10.2 is a negative number, transport of the ion in question from side 1 to side 2 would occur spontaneously. The driving force for passive transport is the ΔG term for the transported species itself.

10.2 • Facilitated Diffusion

The transport of many substances across simple lipid bilayer membranes via passive diffusion is far too slow to sustain life processes. On the other hand, the transport rates for many ions and small molecules across actual biological membranes is much higher than anticipated from passive diffusion alone. This difference is due to specific proteins in the membrane that **facilitate** transport of these species across the membrane. Similar proteins capable of effecting **facilitated diffusion** of a variety of solutes are present in essentially all natural membranes. Such proteins have two features in common: (a) they facilitate net movement of solutes only in the thermodynamically favored direction (that is, $\Delta G < 0$), and (b) they display a measurable affinity and specificity for the transported solute. Consequently, facilitated diffusion rates display **saturation behavior** similar to that observed with substrate binding by enzymes (Chapter 14). Such behavior provides a simple means for distinguishing between passive diffusion and facilitated diffusion experimentally. The dependence of transport rate on solute concentration takes the form of a rectangular hyperbola (Figure 10.3), so that the transport rate approaches a limiting value, V_{max}, at very high solute concentration. Figure 10.3 also shows the graphical behavior exhibited by simple passive diffusion. Because passive diffusion does not involve formation of a specific solute:protein complex, the plot of rate versus concentration is linear, not hyperbolic.

Glucose Transport in Erythrocytes Occurs by Facilitated Diffusion

Many transport processes in a variety of cells occur by facilitated diffusion. Table 10.1 lists just a few of these. The **glucose transporter** of erythrocytes illustrates many of the important features of facilitated transport systems. Although glucose transport operates variously by passive diffusion, facilitated diffusion, or active transport mechanisms, depending on the particular cell, the **glucose transport system** of erythrocytes (red blood cells) operates exclusively by facilitated diffusion. The erythrocyte glucose transporter has a molecular mass of approximately 55 kD and is found on SDS polyacrylamide electrophoresis gels (Figure 10.4) as **band 4.5.** Typical erythrocytes contain around 500,000 copies of this protein. The active form of this transport protein in the erythrocyte membrane is a trimer. Hydropathy analysis of the amino acid sequence of the erythrocyte glucose transporter has provided a model for the structure of the protein (Figure 10.5). In this model, the protein spans the membrane 12 times, with both the N- and C-termini located on the cytoplasmic side. Transmembrane segments M7, M8, and M11 comprise a hydrophilic transmembrane channel, with segments M9 and M10 forming a relatively hydrophobic pocket adjacent to the glucose-binding site. Cytochalasin B, a fungal metabolite (Figure 10.6), is a competitive inhibitor of glucose transport. The mechanism of glucose transport is not well understood. An **alternating conformation model,** in

Table 10.1

Facilitated Transport Systems			
Permeant	**Cell Type**	K_m **(mM)**	V_{max} **(mM/min)**
D-Glucose	Erythrocyte	4–10	100–500
Chloride	Erythrocyte	25–30	
cAMP	Erythrocyte	0.0047	0.028
Phosphate	Erythrocyte	80	2.8
D-Glucose	Adipocytes	20	
D-Glucose	Yeast	5	
Sugars and amino acids	Tumor cells	0.5–4	2–6
D-Glucose	Rat liver	30	
D-Glucose	*Neurospora crassa*	8.3	46
Choline	Synaptosomes	0.083	
L-Valine	*Arthrobotrys conoides*	0.15–0.75	

Source: Adapted from Jain, M., and Wagner, R., 1980. *Introduction to Biological Membranes.* New York: Wiley.

which the glucose-binding site is alternately exposed to the cytoplasmic and extracellular surfaces of the membrane, has been proposed but remains controversial. Many other glucose transport proteins with sequences that are homologous to the erythrocyte glucose transporter have been identified in muscle, liver, and most other animal tissues. The reduced ability of insulin to stimulate glucose transport in diabetic patients is due to reduced expression of some, but not all, of these glucose transport proteins.
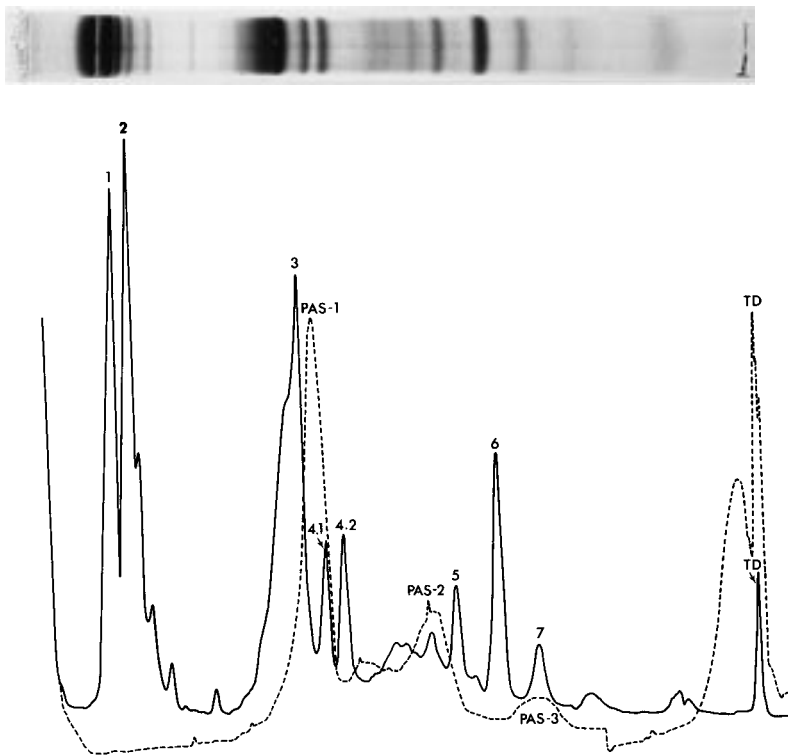
FIGURE 10.4 • SDS-gel electrophoresis of erythrocyte membrane proteins (*top*) and a densitometer tracing of the same gel (*bottom*). The region of the gel between band 4.2 and band 5 is referred to as zone 4.5 or "band 4.5." The bands are numbered from the top of the gel (high molecular weights) to the bottom (low molecular weights). Band 3 is the anion-transporting protein and band 4.5 is the glucose transporter. The dashed line shows the staining of the gel by periodic acid–Schiff's reagent (PAS), which stains carbohydrates. Three "PAS bands" (PAS-1, PAS-2, PAS-3) indicate the positions of glycoproteins in the gel. *(Photo courtesy of Theodore Steck, University of Chicago)*
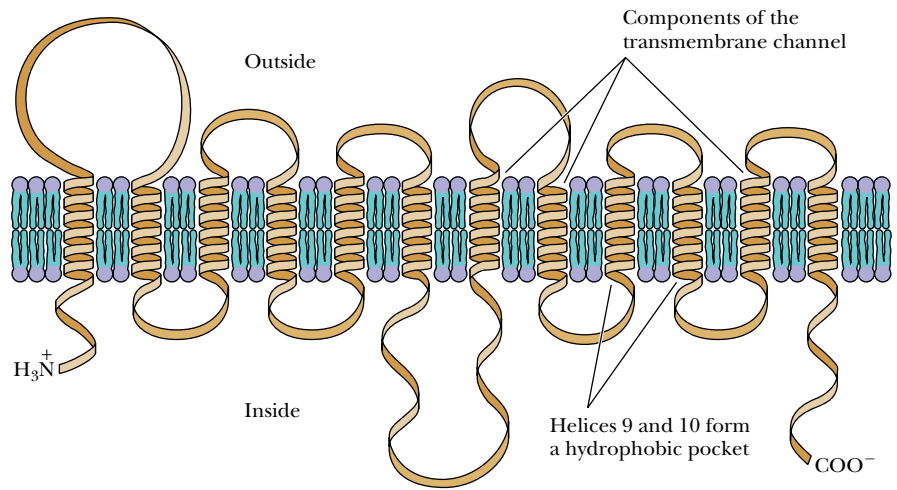
FIGURE 10.5 • A model for the arrangement of the glucose transport protein in the erythrocyte membrane. Hydropathy analysis is consistent with 12 transmembrane helical segments.
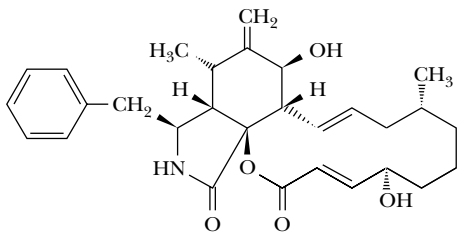
FIGURE 10.6 • The structure of cytochalasin B.

The Anion Transporter of Erythrocytes Also Operates by Facilitated Diffusion

The **anion transport system** is another facilitated diffusion system of the erythrocyte membrane. Chloride and bicarbonate (HCO_3^-) ions are exchanged across the red cell membrane by a 95-kD transmembrane protein. This protein is abundant in the red cell membrane and is represented by **band 3** on SDS electrophoresis gels (Figure 10.4). The gene for the human erythrocyte anion transporter has been sequenced and hydropathy analysis has yielded a model for the arrangement of the protein in the red cell membrane (Figure 10.7). The model has 14 transmembrane segments, and the sequence includes 3 regions: a hydrophilic, cytoplasmic domain (residues 1 through 403) that interacts with numerous cytoplasmic and membrane proteins; a hydrophobic domain (residues 404 through 882) that comprises the anion transporting channel; and an acidic, C-terminal domain (residues 883 through 911). This transport system facilitates a one-for-one exchange of chloride and bicarbonate, so that the net transport process is electrically neutral. The net direction of anion flow through this protein depends on the sum of the chloride and bicarbonate concentration gradients. Typically, carbon dioxide is collected by red cells in respiring tissues (by means of $Cl^- \rightleftharpoons HCO_3^-$ exchange) and is then carried in the blood to the lungs, where bicarbonate diffuses out of the erythrocytes in exchange for Cl^- ions.

FIGURE 10.7 • A model for the arrangement of the anion transport protein in the membrane, based on hydropathy analysis.
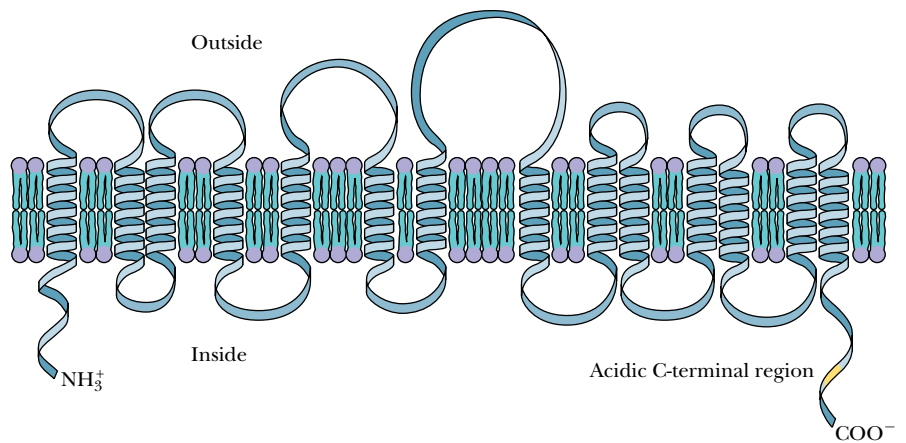
10.3 • Active Transport Systems

Passive and facilitated diffusion systems are relatively simple, in the sense that the transported species flow downhill energetically, that is, from high concentration to low concentration. However, other transport processes in biological systems must be *driven* in an energetic sense. In these cases, the transported species moves from low concentration to high concentration, and thus the transport requires *energy input.* As such, it is considered an **active transport system.** The most common energy input is **ATP hydrolysis** (see Chapter 3), with hydrolysis being *tightly coupled* to the transport event. Other energy sources also drive active transport processes, including *light energy* and the *energy stored in ion gradients* (concentration differences of an ion (or solute) across a membrane represent an energized state (see Chapter 21)). The original ion gradient is said to arise from a **primary active transport** process, and the transport that depends on the ion gradient for its energy input is referred to as a **secondary active transport** process (see discussion of amino acid and sugar transport, Section 10.6). When transport results in a net movement of electric charge across the membrane, it is referred to as an **electrogenic transport** process. If no net movement of charge occurs during transport, the process is electrically neutral.

All Active Transport Systems Are Energy-Coupling Devices

Hydrolysis of ATP is essentially a chemical process, whereas movement of species across a membrane is a mechanical process (that is, movement). An active transport process that depends on ATP hydrolysis thus couples chemical free energy to mechanical (translational) free energy. The bacteriorhodopsin protein in *Halobacterium halobium* couples light energy and mechanical energy. Oxidative phosphorylation (Chapter 21) involves coupling between electron transport, proton translocation, and the capture of chemical energy in the form of ATP synthesis. Similarly, the overall process of photosynthesis (Chapter 22) amounts to a coupling between captured light energy, proton translocation, and chemical energy stored in ATP.

10.4 • Transport Processes Driven by ATP

Monovalent Cation Transport: Na^+,K^+-ATPase

All animal cells actively extrude Na^+ ions and accumulate K^+ ions. These two transport processes are driven by **Na^+,K^+-ATPase,** also known as the **sodium pump,** an integral protein of the plasma membrane. Most animal cells maintain cytosolic concentrations of Na^+ and K^+ of 10 mM and 100 mM, respectively. The extracellular milieu typically contains about 100 to 140 mM Na^+ and 5 to 10 mM K^+. Potassium is required within the cell to activate a variety of processes, whereas high intracellular sodium concentrations are inhibitory. The transmembrane gradients of Na^+ and K^+ and the attendant gradients of Cl^- and other ions provide the means by which neurons communicate (see Chapter 34). They also serve to regulate cellular volume and shape. Animal cells also depend upon these Na^+ and K^+ gradients to drive transport processes involving amino acids, sugars, nucleotides, and other substances. In fact, maintenance of these Na^+ and K^+ gradients consumes large amounts of energy in animal cells—20 to 40% of total metabolic energy in many cases and up to 70% in neural tissue.

The Na^+- and K^+-dependent ATPase comprises two subunits, an α-subunit of 1016 residues (120 kD) and a 35-kD β-subunit. The sodium pump actively
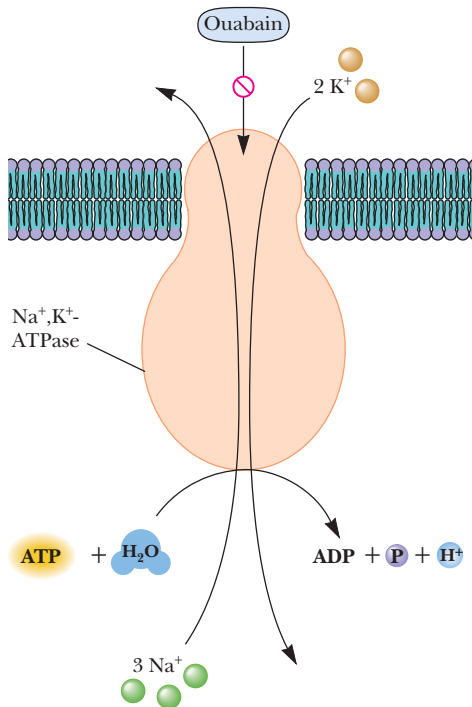
FIGURE 10.8 • A schematic diagram of the Na⁺,K⁺-ATPase in mammalian plasma membrane. ATP hydrolysis occurs on the cytoplasmic side of the membrane, Na⁺ ions are transported out of the cell, and K⁺ ions are transported in. The transport stoichiometry is 3 Na⁺ out and 2 K⁺ in per ATP hydrolyzed. The specific inhibitor ouabain (Figure 7.12) and other cardiac glycosides inhibit Na⁺,K⁺-ATPase by binding on the extracellular surface of the pump protein.

pumps three Na⁺ ions out of the cell and two K⁺ ions into the cell per ATP hydrolyzed:

$$ATP^{4-} + H_2O + 3Na^+(\text{inside}) + 2K^+(\text{outside}) \rightarrow ADP^{3-} +$$
$$H_2PO_4^- + 3Na^+(\text{outside}) + 2K^+(\text{inside}) \quad (10.3)$$
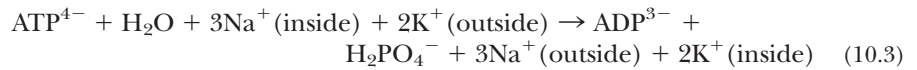
ATP hydrolysis occurs on the cytoplasmic side of the membrane (Figure 10.8), and the net movement of one positive charge outward per cycle makes the sodium pump electrogenic in nature.

Hydropathy analysis of the amino acid sequences of the α- and β-subunits and chemical modification studies have led to a model for the arrangement of the ATPase in the plasma membrane (Figure 10.9). The model describes 10 transmembrane α-helices in the α-subunit, with two large cytoplasmic domains. The larger of these, between transmembrane segments 4 and 5, has been implicated as the ATP-binding domain. The enzyme is covalently phosphorylated at an aspartate residue on the α-subunit in the course of ATP hydrolysis. The covalent E-P intermediate was trapped and identified using tritiated sodium borohydride (Figure 10.10).

A minimal mechanism for Na⁺,K⁺-ATPase postulates that the enzyme cycles between two principal conformations, denoted E_1 and E_2 (Figure 10.11). E_1 has a high affinity for Na⁺ and ATP and is rapidly phosphorylated in the presence of Mg^{2+} to form E_1-P, a state which contains *three occluded Na⁺ ions* (occluded in the sense that they are tightly bound and not easily dissociated from the enzyme in this conformation). A conformation change yields E_2-P, a form of the enzyme with relatively low affinity for Na⁺, but a high affinity for K⁺. This state presumably releases 3 Na⁺ ions and binds 2 K⁺ ions on the outside of the cell. Dephosphorylation leaves E_2K_2, a form of the enzyme with *two*

FIGURE 10.9 • A model for the arrangement of Na⁺,K⁺-ATPase in the plasma membrane. The large cytoplasmic domain between transmembrane segments 4 and 5 contains the ATP-binding site and the aspartate residue that is phosphorylated during the catalytic cycle. The β-subunit contains one transmembrane segment and a large extracellular carboxy-terminal segment.
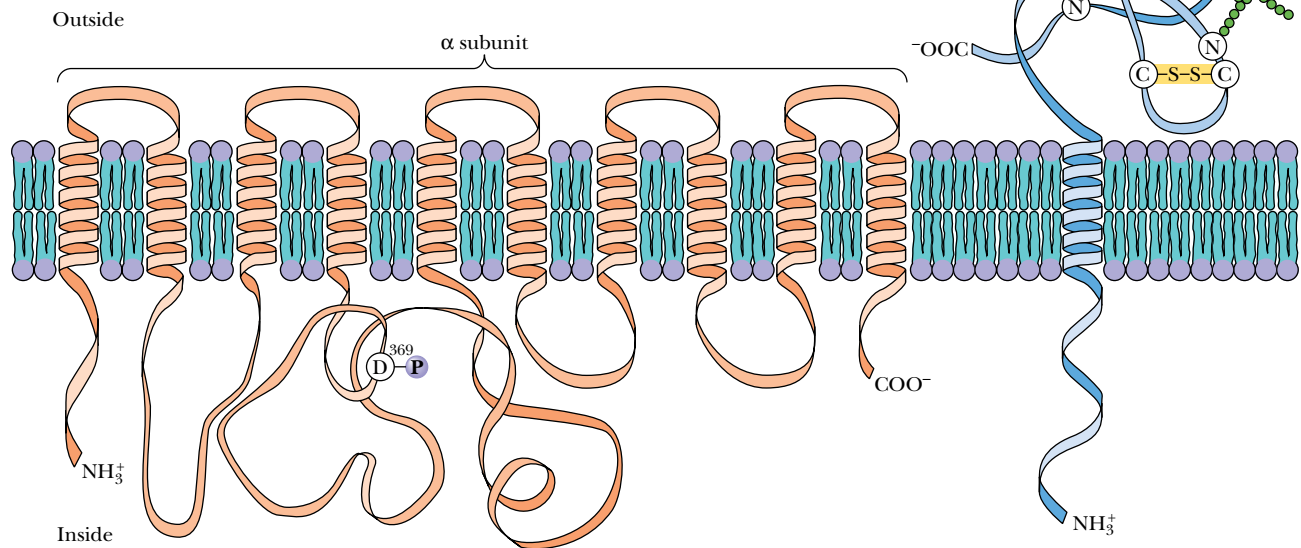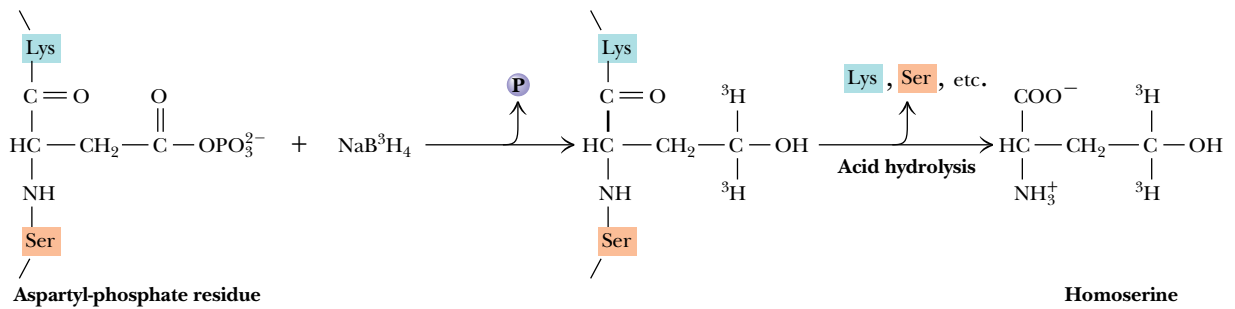
FIGURE 10.10 • The reaction of tritiated sodium borohydride with the aspartyl phosphate at the active site of Na^+,K^+-ATPase. Acid hydrolysis of the enzyme following phosphorylation and sodium borohydride treatment yields a tripeptide containing serine, homoserine (derived from the aspartyl-phosphate), and lysine as shown. The site of phosphorylation is Asp^{369} in the large cytoplasmic domain of the ATPase.
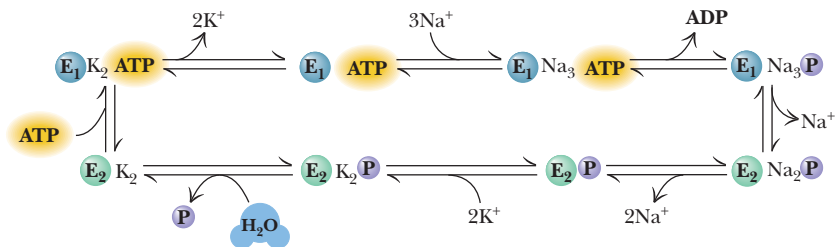
FIGURE 10.11 • A mechanism for Na^+,K^+-ATPase. The model assumes two principal conformations, E_1 and E_2. Binding of Na^+ ions to E_1 is followed by phosphorylation and release of ADP. Na^+ ions are transported and released and K^+ ions are bound before dephosphorylation of the enzyme. Transport and release of K^+ ions complete the cycle.

occluded K^+ ions. A conformation change, which appears to be accelerated by the binding of ATP (with a relatively low affinity), releases the bound K^+ inside the cell and returns the enzyme to the E_1: ATP state. Enzyme forms with occluded cations represent states of the enzyme with cations bound in the transport channel. The alternation between high and low affinities for Na^+, K^+, and ATP serves to tightly couple the hydrolysis of ATP and ion binding and transport.

Na^+,K^+-ATPase Is Inhibited by Cardiac Glycosides

Plant and animal steroids such as *ouabain* (Figure 10.12) specifically inhibit Na^+,K^+-ATPase and ion transport. These substances are traditionally referred to as **cardiac glycosides** or **cardiotonic steroids,** both names derived from the potent effects of these molecules on the heart. These molecules all possess a *cis*-configuration of the C-D ring junction, an unsaturated lactone ring (5- or 6-membered) in the β-configuration at C-17, and a β-OH at C-14. There may be one or more sugar residues at C-3. The sugar(s) are not required for inhibition, but do contribute to water solubility of the molecule. Cardiac glycosides bind exclusively to the extracellular surface of Na^+,K^+-ATPase when it is in the E_2-P state, forming a very stable E_2-P (cardiac glycoside) complex.

Medical researchers studying high blood pressure have consistently found that people with hypertension have high blood levels of some sort of Na^+,K^+-
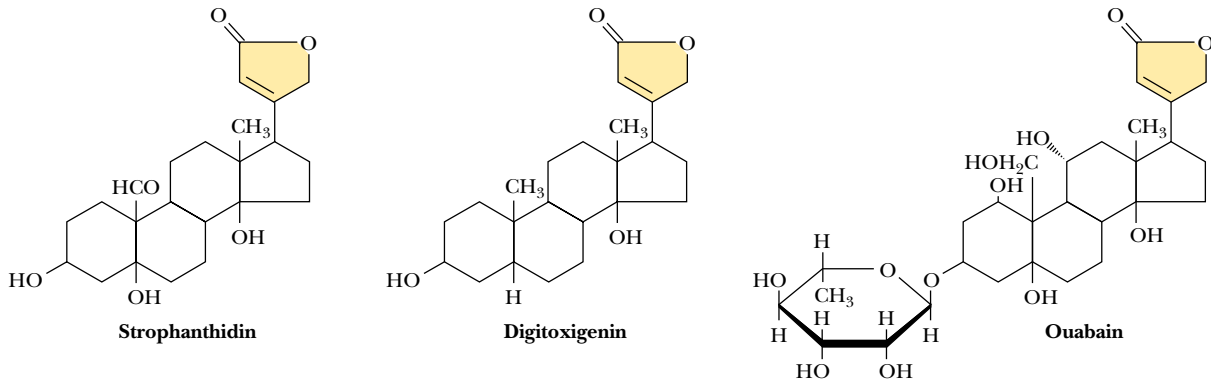
FIGURE 10.12 • The structures of several cardiac glycosides. The lactose rings are yellow.

ATPase inhibitor. In such patients, inhibition of the sodium pump in the cells lining the blood vessel wall results in accumulation of sodium and calcium in these cells and the narrowing of the vessels to create hypertension. An 8-year study aimed at the isolation and identification of the agent responsible for these effects by researchers at the University of Maryland Medical School and the Upjohn Laboratories in Michigan recently yielded a surprising result. Mass spectrometric analysis of compounds isolated from many hundreds of gallons of blood plasma has revealed that the hypertensive agent is ouabain itself or a closely related molecule!

Calcium Transport: Ca^{2+}-ATPase

Calcium, an ion acting as a cellular signal in virtually all cells (see Chapter 34), plays a special role in muscles. It is the signal that stimulates muscles to contract (Chapter 17). In the resting state, the levels of Ca^{2+} near the muscle fibers are very low (approximately 0.1 μM), and nearly all of the calcium ion in muscles is sequestered inside a complex network of vesicles called the **sarcoplasmic reticulum,** or **SR** (see Figure 17.2). Nerve impulses induce the sarcoplasmic reticulum membrane to quickly release large amounts of Ca^{2+}, with cytosolic levels rising to approximately 10 μM. At these levels, Ca^{2+} stimulates contraction. Relaxation of the muscle requires that cytosolic Ca^{2+} levels be reduced to their resting levels. This is accomplished by an ATP-driven Ca^{2+} transport protein known as the **Ca^{2+}-ATPase.** This enzyme is the most abundant protein in the SR membrane, accounting for 70 to 80% of the SR protein. Ca^{2+}-ATPase bears many similarities to the Na$^+$,K$^+$-ATPase. It has an α-subunit of the same approximate size, it forms a covalent E-P intermediate during ATP hydrolysis, and its mechanism of ATP hydrolysis and ion transport is similar in many ways to that of the sodium pump.

The amino acid sequence of the α-subunit is homologous with the sodium pump α-subunit, particularly around the phosphorylation site and the ATP-binding site (Figure 10.13). Ten transmembrane helical segments are predicted from hydropathy analysis, as well as a "stalk" consisting of five helical segments (Figure 10.14). This stalk lies between the membrane surface and the globular cytoplasmic domain containing the nucleotide-binding domain and the site of phosphorylation. The E-P formed by SR Ca^{2+}-ATPase is an aspartyl phosphate like that of Na$^+$,K$^+$-ATPase, in this case Asp residue 351.

(a) Phosphorylation domain

	Res. no.																	
Na+, K+-ATPase, α	363	T	S	T	I	C	S	D	K	T	G	T	L	T	Q	N	R	M
H+, K+-ATPase	379	T	S	V	I	C	S	D	K	T	G	T	L	T	Q	N	R	M
Ca2+-ATPase, SR	345	T	S	V	I	C	S	D	K	T	G	T	L	T	T	N	Q	M
H+-ATPase, yeast	372	V	E	I	L	C	S	D	K	T	G	T	L	T	K	N	K	L
K+-ATPase, Streptococcus faecalis	273	L	D	V	I	M	L	D	K	T	G	T	L	T	Q	G	K	F
F1 ATPase, E. coli	280	Q	E	R	I	T	S	T	K	T	G	S	I	T	S	V	Q	A
F1 ATPase, bovine	293	Q	E	R	I	T	T	T	K	K	G	S	I	T	S	V	Q	A

(b) Segment-binding FITC, an ATP-site probe for ATPases

Na+, K+-ATPase, α	496	P	Q	H	L	L	V	M	K	G	A	P	E	R	I	L	D	R	C	S	S
H+, K+-ATPase	510	P	R	H	L	L	V	M	K	G	A	P	E	R	V	L	E	R	C	S	S
Ca2+-ATPase, SR	508	V	G	N	K	M	F	V	K	G	A	P	E	G	V	I	D	R	C	N	Y
Ca2+-ATPase, plasma membrane						M	Y	S	K	G	A	S	E	I	I	L	R				
H+-ATPase, yeast	467	G	E	R	I	V	C	V	K	G	A	P	L	S	A	L	K	T	V	E	E
H+-ATPase, Neurospora	467	G	E	R	I	T	C	V	K	G	A	P	L	F	V	L	K	T	V	E	E

(c) ATP-binding region

Na+, K+-ATPase, α	543	L	G	E	R	V	—	L	G	F	C	H	L	F	L	P	D	E	Q	F	P
H+, K+-ATPase	613	L	K	C	R	T	—	A	G	I	R	V	I	M	V	T	G	D	H	P	I
Ca2+-ATPase, SR	611	Q	L	C	R	D	—	A	G	I	R	V	I	M	I	T	G	D	N	K	G
H+-ATPase, Neurospora	544	C	E	A	K	T	—	L	G	L	S	I	K	M	L	T	G	D	A	V	G
H+-ATPase, yeast	545	S	E	A	R	H	—	L	G	L	R	V	K	M	L	T	G	D	A	V	G
F1 ATPase, bovine	243	E	Y	F	R	D	Q	E	G	Q	D	V	L	L	F	I	D	N	I	F	R
F1ATPase, E.coli	267	E	Y	F	R	D	—	R	G	E	D	A	L	I	I	Y	D	D	L	S	K
ATP-ADP exchange protein	277	V	L	—	R	G	N	G	G	A	F	V	L	V	L	Y	D	E	I	K	K
Adenylate kinase	104	E	F	E	R	K	—	I	G	Q	P	T	L	L	L	Y	V	D	A	G	P
Phosphofructokinase	87	E	Q	L	K	K	—	H	G	I	Q	G	L	V	V	I	G	G	D	G	S

(d) Segment-binding active-site probes in Na+, K+-ATPase

Na+, K+ATPase, α	701	Q	G	A	I	V	A	V	T	G	D	G	V	N	D	S	P	A	L	K	K
H+, K+-ATPase	717	L	G	A	I	V	A	V	T	G	D	G	V	N	D	S	P	A	L	K	K
Ca2+-ATPase, SR	694	Y	D	E	I	T	A	M	T	G	D	G	V	N	D	A	P	A	L	K	K
H+-ATPase, Neurospora	625	R	G	Y	L	V	A	M	T	G	D	G	V	N	D	A	P	S	L	K	K
H+-ATPase, yeast	625	R	G	Y	L	V	A	M	T	G	D	G	V	N	D	A	P	S	L	K	K
K+-ATPase, Streptococcus faecalis	467	Q	G	K	K	V	I	M	V	G	D	G	I	N	D	A	P	S	L	A	R
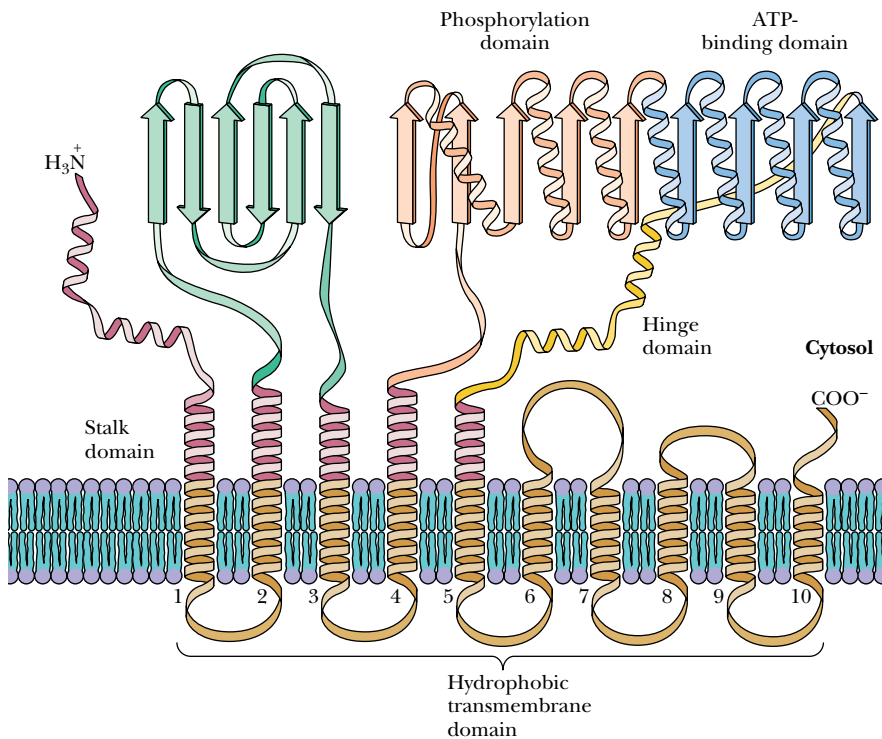
▲ **FIGURE 10.13** • Some of the sequence homologies in the nucleotide binding and phosphorylation domains of Na+,K+-ATPase, Ca2+-ATPase, and gastric H+,K+-ATPase. *(Adapted from Jørgensen, P. L., and Andersen, J. P., 1988. Structural basis for E_1 - E_2 conformational transitions in Na+,K+-pump and Ca2+-pump proteins. Journal of Membrane Biology 103:95–120)*

◀ **FIGURE 10.14** • The arrangement of Ca2+-ATPase in the sarcoplasmic reticulum membrane. Ten transmembrane segments are postulated on the basis of hydropathy analysis.
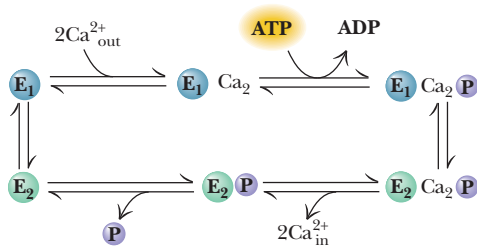
FIGURE 10.15 • A mechanism for Ca^{2+}-ATPase from sarcoplasmic reticulum. Note the similarity to the mechanism of Na^+,K^+-ATPase (see also Figure 10.11). ("Out" here represents the cytosol; "in" represents the lumen of the SR.)

Two Ca^{2+} ions are transported into the SR per ATP hydrolyzed by this enzyme, and the mechanism (Figure 10.15) appears to involve two major conformations, E_1 and E_2, just as the Na^+,K^+-ATPase mechanism does. Calcium ions are strongly occluded in the E_1-Ca_2-P state, and these occluded ions do not dissociate from the enzyme until the enzyme converts to the E_2-Ca_2-P state, which has a very low affinity for Ca^{2+}. In the E_1-Ca_2-P state, the transported Ca^{2+} ions are bound in the transport channel.

$\mathcal{H}$UMAN BIOCHEMISTRY

Cardiac Glycosides: Potent Drugs from Ancient Times

The cardiac glycosides have a long and colorful history. Many species of plants producing these agents grow in tropical regions and have been used by natives in South America and Africa to prepare poisoned arrows used in fighting and hunting. Zulus in South Africa, for example, have used spears tipped with cardiac glycoside poisons. The sea onion, found commonly in southern Europe and northern Africa, was used by the Romans and the Egyptians as a cardiac stimulant, diuretic, and expectorant. The Chinese have long used a medicine made from the skins of certain toads for similar purposes. Cardiac glycosides are also found in several species of domestic plants, including the foxglove, lily of the valley, oleander (figure), and milkweed plant. Monarch butterflies acquire these compounds by feeding on milkweed and then storing the cardiac glycosides in their exoskeletons. Cardiac glycosides deter predation of monarch butterflies by birds, which learn by experience not to feed on monarchs. Viceroy butterflies mimic monarchs in overall appearance. Although viceroys contain no cardiac glycosides and are edible, they are avoided by birds that mistake them for monarchs.

In 1785, the physician and botanist William Withering described the medicinal uses for agents derived from the foxglove plant. In modern times, **digitalis** (a preparation from dried leaves of the foxglove, *Digitalis purpurea*) and other purified cardiotonic steroids have been used to increase the contractile force of heart muscle, to slow the rate of beating, and to restore normal function in hearts undergoing fibrillation (a condition in which heart valves do not open and close rhythmically, but rather remain partially open, fluttering in an irregular and ineffective way). Inhibition of the cardiac sodium pump increases the intracellular Na^+ concentration, leading to stimulation of the Na^+-Ca^{2+} exchanger, which extrudes sodium in exchange for inward movement of calcium. Increased intracellular Ca^{2+} stimulates muscle contraction. Careful use of digitalis drugs has substantial therapeutic benefit for heart patients.

(b) Monarch butterfly

(c) Viceroy

(a) Cardiac glycoside inhibitors of Na^+,K^+-ATPase are produced by many plants, including foxglove, lily of the valley, milkweed, and oleander (shown here). (b) The monarch butterfly, which concentrates cardiac glycosides in its exoskeleton, is shunned by predatory birds. (c) Predators also avoid the viceroy, even though it contains no cardiac glycosides, because it is similar in appearance to the monarch.

(a) Oleander

The Gastric H$^+$,K$^+$-ATPase

Production of protons is a fundamental activity of cellular metabolism, and proton production plays a special role in the stomach. The highly acidic environment of the stomach is essential for the digestion of food in all animals. The pH of the stomach fluid is normally 0.8 to 1. The pH of the parietal cells of the gastric mucosa in mammals is approximately 7.4. This represents a **pH gradient** across the mucosal cell membrane of 6.6, the largest known transmembrane gradient in eukaryotic cells. This enormous gradient must be maintained constantly so that food can be digested in the stomach without damage to the cells and organs adjacent to the stomach. The gradient of H$^+$ is maintained by an **H$^+$,K$^+$-ATPase,** which uses the energy of hydrolysis of ATP to pump H$^+$ out of the mucosal cells and into the stomach interior in exchange for K$^+$ ions. This transport is electrically neutral, and the K$^+$ that is transported into the mucosal cell is subsequently pumped back out of the cell together with Cl$^-$ in a second electroneutral process (Figure 10.16). Thus, the net transport effected by these two systems is the movement of HCl into the interior of the stomach. (Only a small amount of K$^+$ is needed because it is recycled.) The H$^+$,K$^+$-ATPase bears many similarities to the plasma membrane Na$^+$,K$^+$-ATPase and the SR Ca^{2+}-ATPase described above. It has a similar molecular weight, forms an E-P intermediate, and many parts of its peptide sequence are homologous with the Na$^+$,K$^+$-ATPase and Ca^{2+}-ATPase (Figure 10.13).
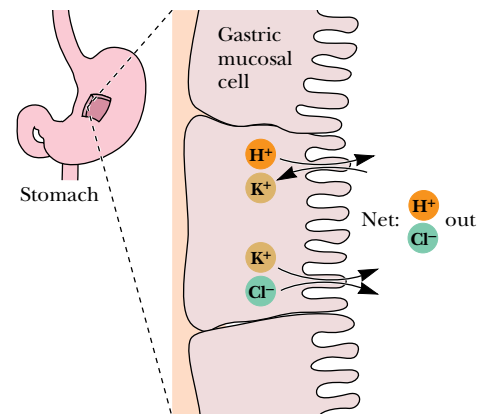
FIGURE 10.16 • The H$^+$,K$^+$-ATPase of gastric mucosal cells mediates proton transport into the stomach. Potassium ions are recycled by means of an associated K$^+$/Cl$^-$ cotransport system. The action of these two pumps results in net transport of H$^+$ and Cl$^-$ into the stomach.

Bone Remodeling by Osteoclast Proton Pumps

Other proton-translocating ATPases exist in eukaryotic and prokaryotic systems. **Vacuolar ATPases** are found in vacuoles, lysosomes, endosomes, Golgi, chromaffin granules, and coated vesicles. Various H$^+$-transporting ATPases occur in yeast and bacteria as well. H$^+$-transporting ATPases found in **osteoclasts** (multinucleate cells that break down bone during normal bone remodeling) provide a source of circulating calcium for soft tissues such as nerves and muscles. About 5% of bone mass in the human body undergoes remodeling at any given time. Once growth is complete, the body balances formation of new bone tissue by cells called **osteoblasts** with resorption of existing bone matrix by osteoclasts. Osteoclasts possess proton pumps—similar to vacuolar ATPases—on the portion of the plasma membrane that attaches to the bone. This region of the osteoclast membrane is called the ruffled border. The osteoclast attaches to the bone in the manner of a cup turned upside down on a saucer (Figure 10.17), leaving an extracellular space between the bone surface and the cell. The H$^+$-ATPases in the ruffled border pump protons into this space, creating an acidic solution that dissolves the bone mineral matrix. Bone mineral is primarily an inorganic mixture of calcium carbonate and hydroxyapatite (calcium phosphate). In this case, transport of protons out of the osteoclasts lowers the pH of the extracellular space near the bone to about 4, solubilizing the hydroxyapatite.
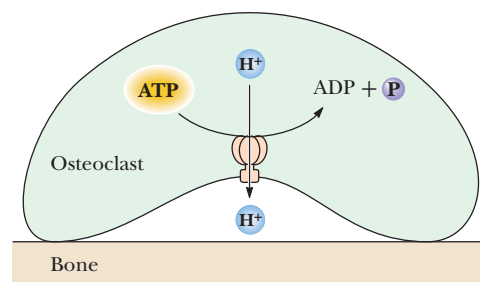
FIGURE 10.17 • Proton pumps cluster on the ruffled border of osteoclast cells and function to pump protons into the space between the cell membrane and the bone surface. High proton concentration in this space dissolves the mineral matrix of the bone.

ATPases That Transport Peptides and Drugs

Species other than protons and inorganic ions are also transported across certain membranes by specialized ATPases. Yeast (*Saccharomyces cerevisiae*) has one such system. Yeasts exist in two haploid mating types, designated **a** and **α.** Each mating type produces a mating factor (**a-factor** or **α-factor,** respectively) and responds to the mating factor of the opposite type. The α-factor is a peptide that is inserted into the ER during translation on the ribosome. α-Factor is glycosylated in the ER and then secreted from the cell. On the other hand, the

Outside
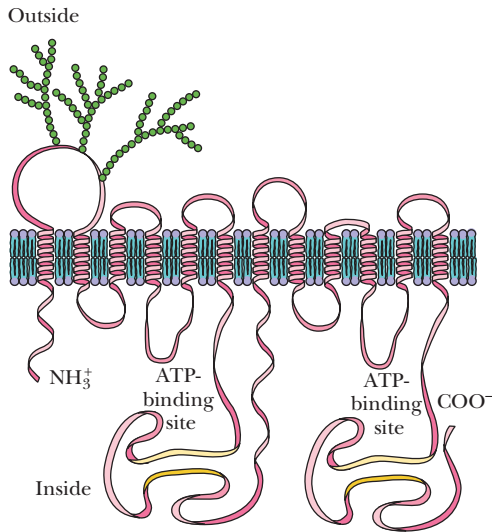
FIGURE 10.18 • A model for the structure of the a-factor transport protein in the yeast plasma membrane. Gene duplication has yielded a protein with two identical halves, each half containing six transmembrane helical segments and an ATP-binding site. Like the yeast a-factor transporter, the multidrug transporter is postulated to have 12 transmembrane helices and 2 ATP-binding sites.

a-factor is a 12-amino acid peptide made from a short precursor. Export of this peptide from the cell is carried out by a 1290-residue protein, which consists of two identical halves joined together—a tandem duplication. Each half contains six putative transmembrane segments arranged in pairs, and a conserved hydrophilic cytoplasmic domain containing a consensus sequence for an ATP-binding site (Figure 10.18). This protein uses the energy of ATP hydrolysis to export the 12-residue a-factor from the cell. In yeast cells that produce mutant forms of the a-factor ATPase, a-factor is not excreted and accumulates to high levels inside the cell.

Proteins very similar to the yeast a-factor transporter have been identified in a variety of prokaryotic and eukaryotic cells, and one of these appears to be responsible for the acquisition of **drug resistance** in many human malignancies. Clinical treatment of human cancer often involves chemotherapy, the treatment with one or more drugs that selectively inhibit the growth and proliferation of tumorous tissue. However, the efficacy of a given chemotherapeutic drug often decreases with time, owing to an acquired resistance. Even worse, the acquired resistance to a single drug usually results in a simultaneous resistance to a wide spectrum of drugs with little structural or even functional similarity to the original drug, a phenomenon referred to as **multidrug resistance,** or **MDR.** This perplexing problem has been traced to the induced expression of a 170-kD plasma membrane glycoprotein known as the **P-glycoprotein** or the **MDR ATPase.** Like the yeast a-factor transporter, MDR ATPase is a tandem repeat, each half consisting of a hydrophobic sequence with six transmembrane segments followed by a hydrophilic, cytoplasmic sequence containing a consensus ATP-binding site (Figure 10.18). The protein uses the energy of ATP hydrolysis to actively transport a wide variety of drugs (Figure 10.19) out of the cell. Ironically, it is probably part of a sophisticated protection system for the cell and the organism. Organic molecules of various types and structures that might diffuse across the plasma membrane are apparently recognized by this

FIGURE 10.19 • Some of the cytotoxic drugs that are transported by the MDR ATPase.
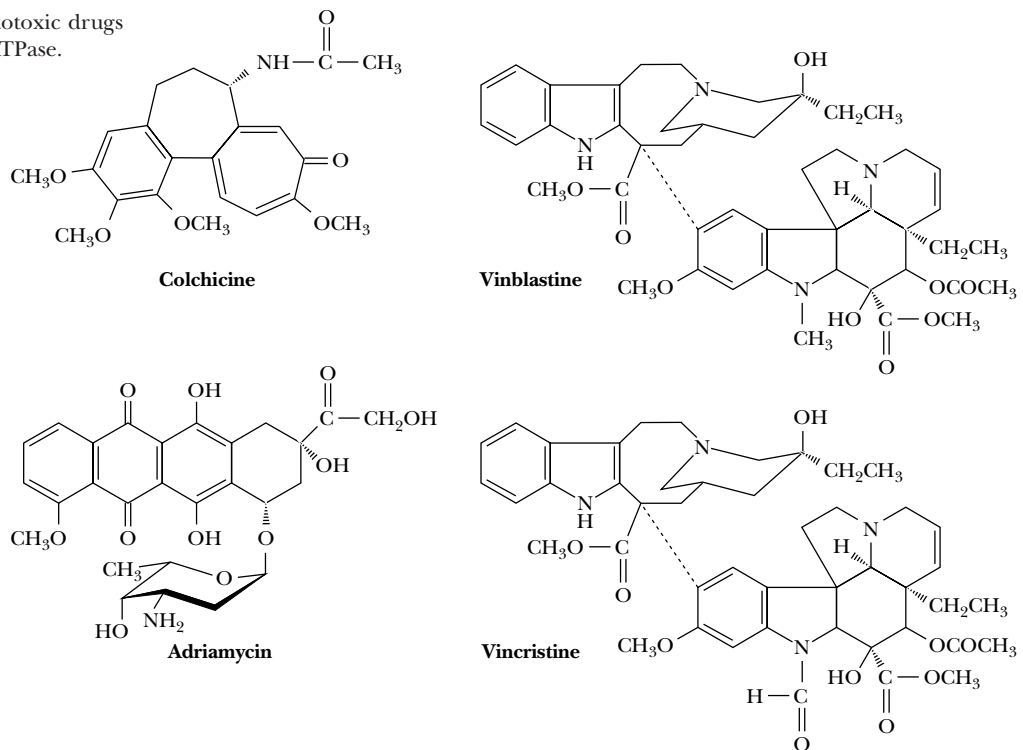
protein and actively extruded from the cell. Despite the cancer-fighting nature of chemotherapeutic agents, the MDR ATPase recognizes these agents as cellular intruders and rapidly removes them. It is not yet understood how this large protein can recognize, bind, and transport such a broad group of diverse molecules, but it is known that the yeast a-factor ATPase and the MDR ATPase are just two members of a **superfamily** of transport proteins, many of whose functions are not yet understood.

10.5 • Transport Processes Driven by Light

As noted previously, certain biological transport processes are driven by light energy rather than by ATP. Two well-characterized systems are **bacteriorhodopsin,** the light-driven H^+-pump, and **halorhodopsin,** the light-driven Cl^--pump, of *Halobacterium halobium,* an archaebacterium that thrives in high-salt media. *H. halobium* grows optimally at an NaCl concentration of 4.3 *M.* It was extensively characterized by Walther Stoeckenius, who found it growing prolifically in the salt pools near San Francisco Bay, where salt is commercially extracted from seawater. *H. halobium* carries out normal respiration if oxygen and metabolic energy sources are plentiful. However, when these substrates are lacking, *H. halobium* survives by using bacteriorhodopsin and halorhodopsin to capture light energy. In oxygen- and nutrient-deficient conditions, **purple patches** appear on the surface of *H. halobium* (Figure 10.20). These purple patches of membrane are 75% protein, the only protein being **bacteriorhodopsin (bR).** The purple color arises from a retinal molecule that is covalently bound in a Schiff base linkage with an ϵ-NH_2 group of Lys^{216} on each bacteriorhodopsin protein (Figure 10.21). Bacteriorhodopsin is a 26-kD transmembrane protein that packs so densely in the membrane that it naturally forms a two-dimensional crystal in the plane of the membrane. The structure of bR has been elucidated by image enhancement analysis of electron microscopic data, which reveals seven transmembrane helical protein segments. The retinal moiety lies parallel to the membrane plane, about 1 nm below the membrane's outer surface (Figure 9.15).

A Model for Light-Driven Proton Transport

The mechanism of the light-driven transport of protons by bacteriorhodopsin is complex, but a partial model has emerged (Figure 10.22). A series of intermediate states, named for the wavelengths (in nm) of their absorption spectra, has been identified. Absorption of a photon of light by the bR_{568} form (in which the Schiff base at Lys^{216} is protonated) converts the retinal from the all-*trans* configuration to the 13-*cis* isomer. Passage through several different intermediate states results in outward transport of 2 H^+ ions per photon absorbed, and the return of the bound retinal to the all-*trans* configuration. It appears that the transported protons are in fact protons from the protonated Schiff base. The proton gradient thus established represents chemical energy that can be used by *H. halobium* to drive ATP synthesis and the movement of molecules across the cell membrane (see Chapter 21).

FIGURE 10.20 • A schematic drawing of *Halobacterium halobium.* The purple patches contain bacteriorhodopsin (bR).
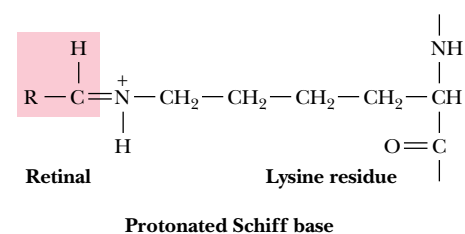
FIGURE 10.21 • The Schiff base linkage between the retinal chromophore and Lys^{216}.

FIGURE 10.22 • The reaction cycle of bacteriorhodopsin. The intermediate states are indicated by letters, with subscripts to indicate the absorption maxima of the states. Also indicated for each state is the configuration of the retinal chromophore (all-*trans* or 13-*cis*) and the protonation state of the Schiff base (C=N: or C=N⁺H).
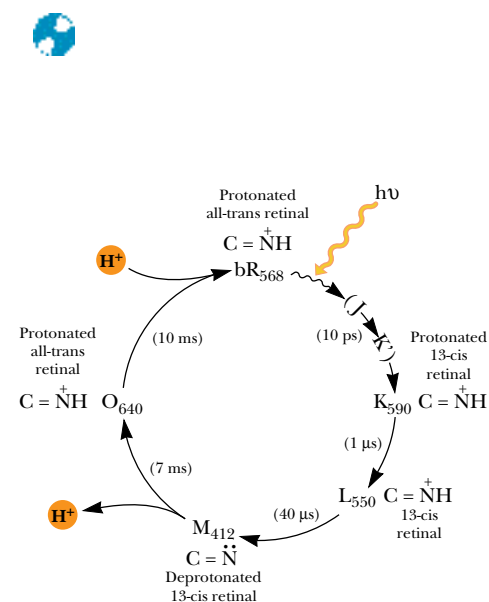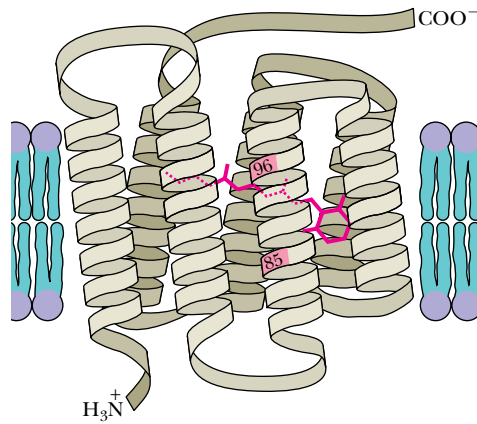
FIGURE 10.23 • The folding of halorhodopsin with the transmembrane segments indicated. The only lysine residue in the protein is Lys^{242}, to which the retinal chromophore is covalently linked.

Light-Driven Chloride Transport in *H. halobium*

Anion transport, on the other hand, is handled by a second light-driven ion pump in the *H. halobium* membrane. The inward transport of Cl$^-$ ion is mediated by *halorhodopsin,* a 27-kD protein whose primary structure and arrangement in the membrane (Figure 10.23) is very similar to that of bacteriorhodopsin. Although halorhodopsin does not exist naturally as a tightly packed two-dimensional crystal in the membrane, it does have a retinal chromophore, bound covalently at Lys^{242}, the only lysine in the protein. The transmembrane portion of halorhodopsin is 36% homologous with bacteriorhodopsin. The conserved residues are concentrated in the central core formed in both proteins by the seven transmembrane helices (Figure 10.24). Like bacteriorhodopsin, halorhodopsin undergoes a cycle of light-driven con-
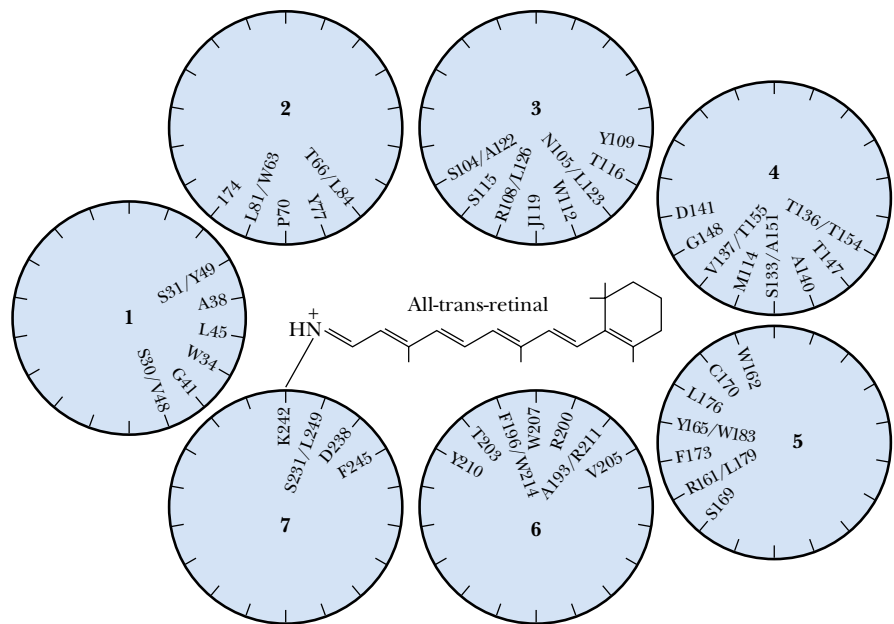
FIGURE 10.24 • A helical wheel model of halorhodopsin. The amino acids facing the polar, hydrophilic core of the protein are shown. Of these 60 residues, 36 are conserved between halorhodopsin and bacteriorhodopsin. *(Adapted from Oesterhelt, D., and Tittor, J., 1989.* Trends in Biochemical Sciences *14:57–61.)*

formational changes (Figure 10.25), but no deprotonation of the Schiff base occurs during the halorhodopsin photocycle. Given the striking similarity of structures for these two proteins, it is intriguing to ask why bacteriorhodopsin pumps H^+ but not Cl^- and why halorhodopsin pumps Cl^- but not H^+. The first question may be answered by the work of H. G. Khorana and his coworkers, who replaced Asp^{85} and Asp^{96} in bacteriorhodopsin with asparagine and found that either substitution caused a drastic reduction in H^+ transport. Dieter Oesterhelt and coworkers have shown that Asp^{85} and Asp^{96} are important in the deprotonation and reprotonation, respectively, of the Schiff base in bacteriorhodopsin. The absence of these two crucial residues in halorhodopsin may explain why the latter protein can't reversibly deprotonate the Schiff base and why halorhodopsin doesn't pump protons.

FIGURE 10.25 • The photocycle of light-adapted halorhodopsin (hR), shown in the presence and absence of chloride. The superscripts indicate the maxima of the difference spectra between hR and the intermediates.

10.6 • Transport Processes Driven by Ion Gradients

Amino Acid and Sugar Transport

The gradients of H^+, Na^+, and other cations and anions established by ATPases and other energy sources can be used for **secondary active transport** of various substrates. The best-understood systems use Na^+ or H^+ gradients to transport amino acids and sugars in certain cells. Many of these systems operate as **symports,** with the ion and the transported amino acid or sugar moving in the same direction (that is, into the cell). In **antiport** processes, the ion and the other transported species move in opposite directions. (For example, the anion transporter of erythrocytes is an antiport.) **Proton symport** proteins are used by *E. coli* and other bacteria to accumulate lactose, arabinose, ribose, and a variety of amino acids. *E. coli* also possesses Na^+-symport systems for melibiose as well as for glutamate and other amino acids.

Table 10.2 lists several systems that transport amino acids into mammalian cells. The accumulation of neutral amino acids in the liver by System A rep-

Table 10.2

Some Mammalian Amino Acid Transport Systems			
System Designation	Ion Dependence	Amino Acids Transported	Cellular Source
A	Na^+	Neutral amino acids	
ASC	Na^+	Neutral amino acids	
L	Na^+-independent	Branched-chain and aromatic amino acids	Ehrlich ascites cells Chinese hamster ovary cells Hepatocytes
N	Na^+	Nitrogen-containing side chains (Gln, Asn, His, etc.)	
y^+	Na^+-independent	Cationic amino acids	
x_{AG}^-	Na^+	Aspartate and glutamate	Hepatocytes
P	Na^+	Proline	Chinese hamster ovary cells

Adapted from: Collarini, E. J., and Oxender, D. L., 1987. Mechanisms of transport of amino acids across membranes. *Annual Review of Nutrition* **7:**75–90.
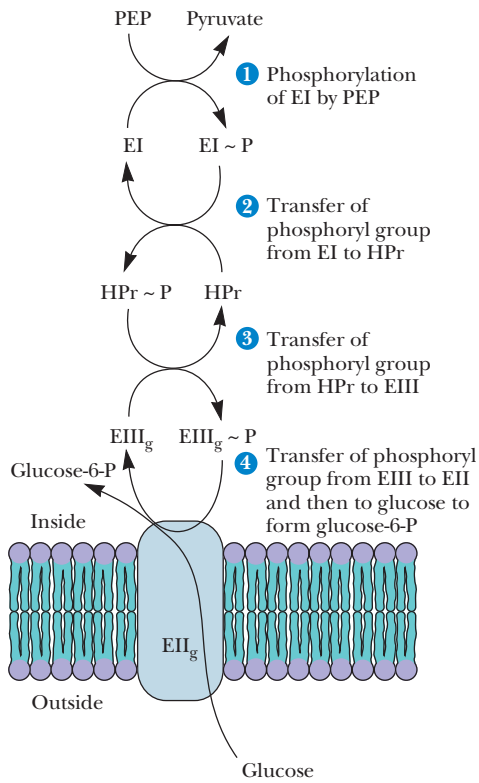
FIGURE 10.26 • Glucose transport in *E. coli* is mediated by the PEP-dependent phospho-transferase system. Enzyme I is phosphorylated in the first step by PEP. Successive phosphoryl transfers to HPr and Enzyme III in Steps 2 and 3 are followed by transport and phosphorylation of glucose. Enzyme II is the sugar transport channel.

resents an important metabolic process. Thus, plasma membrane transport of alanine is the rate-limiting step in hepatic alanine metabolism. This system is normally expressed at low levels in the liver, but substrate deprivation and hormonal activation both stimulate System A expression.

10.7 • Group Translocation

Certain bacteria possess a novel and versatile system for the inward transport of certain sugars. In this process, the sugar becomes phosphorylated during its transport across the membrane; that is, transport and phosphorylation are tightly coupled. This type of process, in which a chemical modification accompanies transport, has been denoted **group translocation.** Several such systems are known, but the best understood is the **phosphoenolpyruvate:glucose phosphotransferase system,** or simply the **phosphotransferase system** (or **PTS**), discovered by Saul Roseman of Johns Hopkins University in 1964. The advantage of this system lies in the fact that the sugars, once phosphorylated, are trapped in the cell. Membranes are permeable to simple sugars but impermeable to sugar phosphates, which are negatively charged. The overall reaction for the phosphotransferase is:

$$\text{Sugar}_\text{outside} + \text{PEP}_\text{inside} \longrightarrow \text{sugar-P}_\text{inside} + \text{pyruvate}_\text{inside}$$
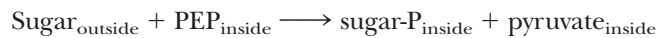
The subscripts illustrate an important point: the phosphoryl transfer occurs entirely on the inside surface of the bacterial membrane.

Several unique features distinguish the phosphotransferase. First, phosphoenolpyruvate is both the phosphoryl donor and the energy source for sugar transport. Second, four different proteins are required for this transport. Two of these proteins (**Enzyme I** and **HPr**) are general and are required for the phosphorylation of all PTS-transported sugars. The other two proteins (**Enzyme II** and **Enzyme III**) are specific for the particular sugar to be transported.

The first step in the phosphotransferase reaction (Figure 10.26) is the phosphorylation of Enzyme I by PEP to form a reactive phosphohistidine intermediate (Figure 10.27). This is followed by phosphoryl transfer to a histidyl residue of HPr, followed by phosphorylation of Enzyme III. At the same time, the sugar to be transported is bound on the outside surface of the cell by Enzyme II, which constitutes the sugar transport channel. As the sugar is moved to the inside surface of the membrane, the phosphoryl group is transferred from Enzyme III to the sugar, forming the desired sugar phosphate, which is
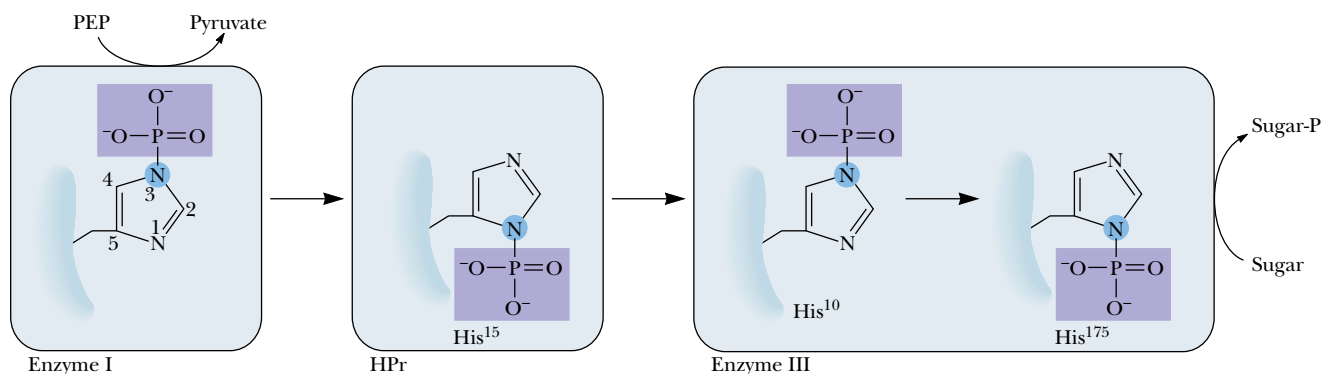
FIGURE 10.27 • The path of the phosphoryl group through the PTS mechanism. Reactive phosphohistidine intermediates of Enzyme I, HPr, and Enzyme III transfer phosphoryl groups from PEP to the transported sugar.

released into the cytoplasm. (In some cases, for example the *E. coli* mannitol system, no Enzyme III has been identified. In these cases, the C-terminal end of the relevant Enzyme II, which resembles an Enzyme III-type sequence, substitutes for Enzyme III.)

10.8 • Specialized Membrane Pores

Porins in Gram-Negative Bacterial Membranes

The membrane transport systems described previously (and many others like them) are relatively specific and function to transport either a single substrate or a very limited range of substrates under normal conditions. At the same time, several rather nonspecific systems also carry out transport processes. One such class of nonspecific transport proteins is found in the outer membranes of Gram-negative bacteria and mitochondria. Low-molecular-weight nutrients and certain other molecules, such as some antibiotics, cross this outer membrane, but larger molecules such as proteins cannot. The ability of the outer membrane to act as a molecular sieve is due to proteins called **porins** (Chapter 9). Alternatively, these molecules have been referred to as **peptidoglycan-associated proteins** or simply **matrix proteins. General porins** form nonspecific pores across the outer membrane and sort molecules according to molecular size, whereas **specific porins** contain binding sites for particular substrates. Porins from several organisms have been isolated and characterized (Table 10.3). Molecular masses of the porins generally range from 30 kD to 50 kD. Most (but not all) porins are arranged in the outer membrane as trimers of identical subunits. The molecular exclusion limits clearly depend on the size of the pore formed by the porin molecule. The pores formed by *E. coli* and *S. typhimurium* porins are relatively small, but porin F from *Pseudomonas aeruginosa* creates a much larger pore, with an exclusion limit of approximately 6 kD. Specific porins *LamB* and *Tsx* of *E. coli* and porins *P* and *DI* of *P. aeruginosa* possess specific binding sites for maltose and related oligosaccharides (Table 10.4), nucleosides, anions, and glucose, respectively.

Table 10.3

Properties of Some General Porins		
Porin and Bacterial Source	**Pore Diameter (nm)**	**M_r Exclusion Limit**
E. coli		
OmpF	1.2	
OmpC	1.1	600
PhoE	1.2	
S. typhimurium		
M_r 38,000	1.4	
M_r 39,000	1.4	700
M_r 40,000	1.4	
P. aeruginosa		
F	2.2	6000

Source: Adapted from Benz, R., 1984. Structure and selectivity of porin channels. *Current Topics in Membrane Transport* **21:**199–219; and Benz, R., 1988. Structure and function of porins from Gram-negative bacteria. *Annual Review of Microbiology* **42:**359–393.

Table 10.4

Binding and Permeation Properties of the LamB Channel for Different Sugars

Sugar	K_s (mM)*	P (s^{-1})†
Maltose	10	100
Maltotriose	0.40	66
Maltoheptaose	0.067	2.5
Lactose	56	9
Sucrose	15	2.5
D-Glucose	110	290
L-Glucose	46	—
D-Galactose	42	225
D-Fructose	600	135
D-Mannose	160	160
Stachyose	50	<1

*Half-saturation constant (concentration for 50% saturation of the transport protein).
†Rate of permeation relative to that of maltose. Data adjusted to 100 s^{-1} for maltose. The LamB-containing liposomes were added to buffer solutions containing 40 mM of the corresponding test sugars.

Source: Adapted from Benz, R. 1988. Structure and function of porins from Gram-negative bacteria. *Annual Review of Microbiology* **42:**359–393.

Porins show high degrees of sequence homology and similarity. The most intriguing feature of porin secondary and tertiary structure is this: In contrast to nearly all other membrane proteins that adopt α-helical structures in the transmembrane segments, porins show little or no evidence of α-helical domains and segments. Instead, the porins and other outer membrane proteins adopt β-sheet structures for their membrane-spanning segments. Models of membrane insertion, which involve β-strands arranged perpendicular to the membrane plane, have been proposed for several porins (Figure 10.28). The crystal structure of the porin from *Rhodobacter capsulatus* shows a trimer in which each monomer forms a pore (Figure 10.29). The monomer pore consists of a 16-stranded β-barrel that traverses the membrane as a tube. The tube is nar-
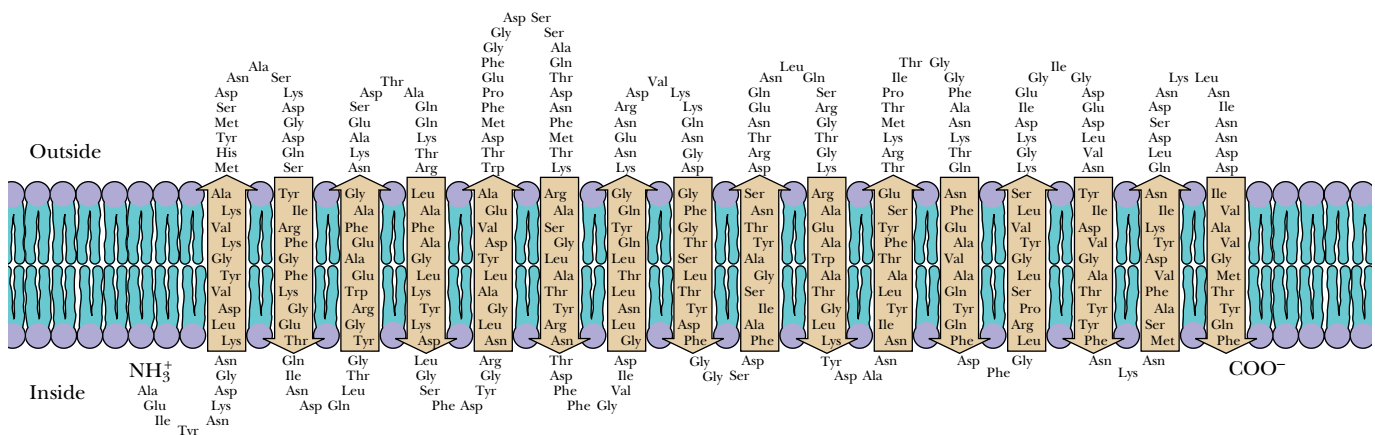
FIGURE 10.28 • A model for the arrangement of the porin PhoE in the outer membrane of *E. coli*. The transmembrane segments are strands of β-sheet.

(a)   (b)   (c)
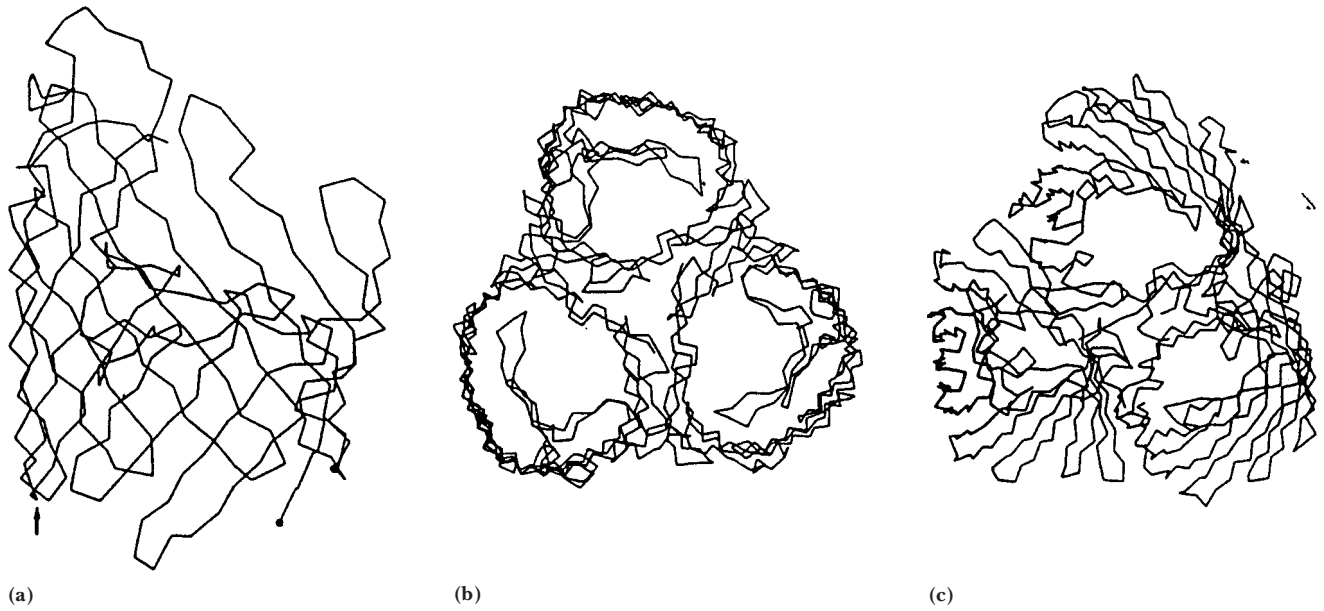
FIGURE 10.29 • Three-dimensional reconstruction of porin from *Rhodobacter capsulatus.* Drawings of (a) side view of porin monomer showing β-sheet structure. (b) Top view and (c) nearly top view of porin trimer.

rowed near the center by peptide chain segments protruding from the inner wall of the barrel. These chain segments form an "eyelet" about 1 nm long and 0.6 to 1 nm across. The eyelet is postulated to determine the exclusion limit for particles diffusing through the pore.

Porins and the other outer membrane proteins of Gram-negative bacteria appear to be the only known membrane proteins that have chosen the β-strand over the α-helix. Why might this be? Among other reasons, there is an advantage of genetic economy in the use of β-strands to traverse the membrane instead of α-helices. An α-helix requires 21 to 25 amino acid residues to span a typical biological membrane; a β-strand can cross the same membrane with 9 to 11 residues. Therefore, a given amount of genetic information could encode a larger number of membrane-spanning segments using a β-strand motif instead of α-helical arrays. Further, β-strands can present alternating hydrophobic and hydrophilic R groups along their length, with hydrophobic R groups facing the lipid bilayer and hydrophilic R groups facing the water-filled channel (Chapter 9).

The Pore-Forming Toxins

Many organisms produce lethal molecules known as **pore-forming toxins,** which insert themselves in a host cell's plasma membrane to form a channel or pore. Pores formed by such toxins can kill the host cell by collapsing ion gradients or by facilitating the entry of toxic agents into the cell. Produced by a variety of organisms and directed toward a similarly diverse range of target cells, these toxins nonetheless share certain features in common. The structures of these remarkable toxins have provided valuable insights into the mechanisms of their membrane insertion and also into the architecture of membrane proteins.

Colicins are pore-forming proteins, produced by certain strains of *E. coli,* that kill or inhibit the growth of other, competing bacteria and even other strains of *E. coli* (a process known as *allelopathy*). Channel-forming colicins are released as soluble monomers. Upon encountering a host cell, the colicin molecule traverses the bacterial outer membrane and periplasm, then inserts itself

FIGURE 10.30 • The structure of colicin Ia. Colicin Ia, with a total length of 210 Å, spans the periplasmic space of a Gram-negative bacterium host, with the R (receptor-binding) domain (blue) anchored to proteins in the outer membrane and the C domain (violet) forming a channel in the inner membrane. The T (translocation) domain is shown in red. The image on the right shows details of the C domain, including helices 8 and 9 (green), which are highly hydrophobic.

FIGURE 10.31 • The umbrella model of membrane channel protein insertion. Hydrophobic helices insert directly into the core of the membrane, with amphipathic helices arrayed on the surface like an open umbrella. A trigger signal (low pH or a voltage gradient) draws some of the amphipathic helices into and across the membrane, causing the pore to open.

into the inner (plasma) membrane. The channel thus formed is monomeric and a single colicin molecule can kill a host cell. The structure of colicin Ia, a 626-residue protein, is shown in Figure 10.30. It consists of three domains, termed the **T (translocation) domain,** the **R (receptor-binding) domain,** and the **C (channel-forming) domain.** The T domain mediates translocation across the outer membrane, the R domain binds to an outer-membrane receptor, and the C-domain creates a voltage-gated channel across the inner membrane. The T, R, and C domains are separated by long (160 Å) α-helical segments. The peptide is folded at the R domain, so that the C and T domains are juxtaposed and the two long helices form an underwound antiparallel coiled coil. The protein is unusually elongated—210 Å from end to end—with the T and C domains at one end and R at the other. This unusual design permits colicin Ia to span the periplasmic space (which has an average width of 150 Å) and insert in the inner membrane.

The nature of the channel-forming domain provides clues to the process of channel formation in the inner membrane. The C domain consists of a 10-helix bundle, with helices 8 and 9 forming an unusually hydrophobic hairpin structure. The other eight helices are amphipathic and serve to stabilize hydrophobic helices 8 and 9 in solution. When this domain inserts in the inner membrane, helices 8 and 9 inject themselves into the hydrophobic membrane core, leaving the other helices behind on the membrane surface (Figure 10.31). Application of a transmembrane potential (voltage) then triggers the amphipathic helices to insert into the membrane, with their hydrophobic faces facing the hydrophobic bilayer and their polar faces forming the channel surface. This model is hypothetical, but it is supported by studies showing that channel opening involves dramatic structural changes and that helices 2 to 5 move across the membrane during channel opening.

Interestingly, certain other pore-forming toxins possess helix-bundle motifs that may participate in channel formation, in a manner similar to that proposed for colicin Ia. For example, the **δ-endotoxin** produced by *Bacillus thuringiensis* is toxic to Coleoptera insects (beetles) and is composed of three domains, including a seven-helix bundle, a three-sheet domain, and a β-sandwich. In the seven-helix bundle, helix 5 is highly hydrophobic, and the other six helices are amphipathic. In solution (Figure 10.32), the six amphipathic
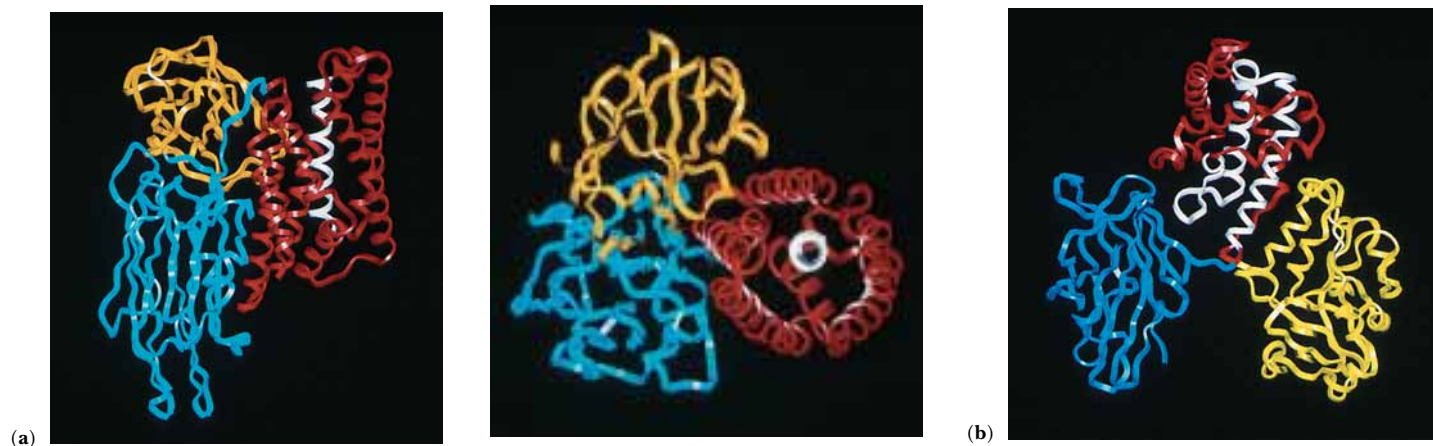
FIGURE 10.32 • The structures of (a) δ-endotoxin (two views) from *Bacillus thuringiensis* and (b) diphtheria toxin from *Corynebacterium diphtheriae*. Each of these toxins possesses a bundle of α-helices which is presumed to form the transmembrane channel when the toxin is inserted across the host membrane. In δ-endotoxin, helix 5 (white) is surrounded by 6 helices (red) in a 7-helix bundle. In diphtheria toxin, three hydrophobic helices (white) lie at the center of the transmembrane domain (red).

helices surround helix 5, with their nonpolar faces apposed to helix 5 and their polar faces directed to the solvent. Membrane insertion and channel formation may involve initial insertion of helix 5, as in Figure 10.31, followed by insertion of the amphipathic helices, so that their nonpolar faces contact the bilayer lipids and their polar faces line the channel.

There are a number of other toxins for which the helical channel model is inappropriate. These include **α-hemolysin** from *Staphylococcus aureus,* **aerolysin** from *Aeromonas hydrophila,* and the **anthrax toxin protective antigen** from *Bacillus anthracis.* The membrane-spanning domains of these proteins do not possess long stretches of hydrophobic residues that could form α-helical transmembrane segments. They do, however, contain substantial peptide segments of alternating hydrophobic and polar residues. Like the porins, such segments can adopt β-strand structures, such that one side of the β-strand is hydrophobic and the other side is polar. Oligomeric association of several such segments can produce a β-barrel motif, with the inside of the barrel lined with polar residues and the outside of the barrel coated with hydrophobic residues —a motif that can be accommodated readily in a bilayer membrane, creating a polar transmembrane channel.

α-Hemolysin, a 33.2-kD monomer protein, forms a mushroom-shaped heptameric pore, 100 Å in length, with a diameter that ranges from 14 Å to 46 Å (Figure 10.33). In this structure, each monomer contributes two β-strands 65 Å long, which are connected by a hairpin turn. The interior of the 14-stranded β-barrel structure is hydrophilic and the hydrophobic outer surface of the barrel is 28 Å wide. Pores formed by α-hemolysin in human erythrocytes, platelets, and lymphocytes allow rapid Ca^{2+} influx into these cells with toxic consequences.

Aeromonas hydrophila is a bacterium that causes diarrheal diseases and deep wound infections. These complications arise due to pore formation in sensitive cells by the protein toxin aerolysin. Proteolytic processing of the 52-kD precursor **proaerolysin** (Figure 10.34) produces the toxic form of the protein, aerolysin. Like α-hemolysin, aerolysin monomers associate to form a heptameric transmembrane pore. Michael Parker and coworkers have proposed
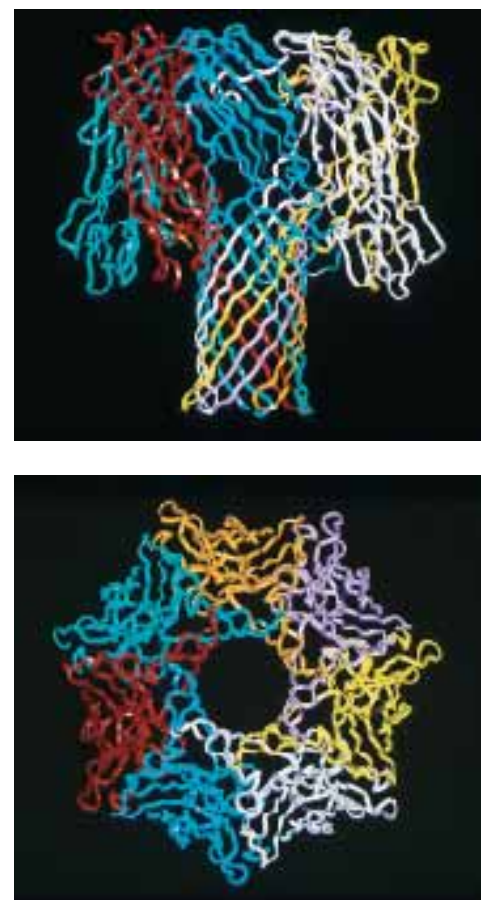
FIGURE 10.33 • The structure of the heptameric channel formed by α-hemolysin. Each of the seven subunits contributes a β-sheet hairpin to the transmembrane channel.
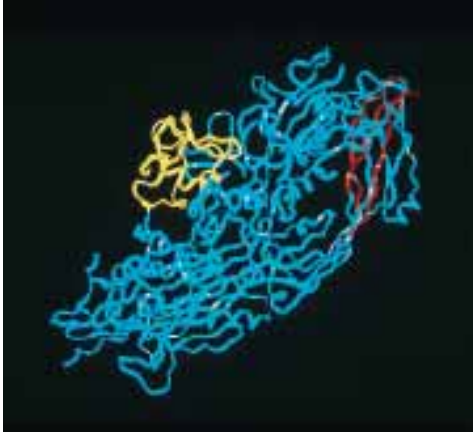
FIGURE 10.34 • The structure of proaerolysin, produced by *Aeromonas hydrophila*. Proteolysis of this precursor yields the active form, aerolysin, which is responsible for the pathogenic effects of the bacterium in deep wound infections and diarrheal diseases. Like hemolysin, aerolysin monomers associate to form heptameric membrane pores. The three β-strands that contribute to the formation of the heptameric pore are shown in red. The N-terminal domain (residues 1–80, yellow) is a small lobe that protrudes from the rest of the protein.

that each monomer in this aggregate contributes three β-strands to the β-barrel pore. Each of these β-strands (residues 277 to 287, 290 to 302, and 410 to 422) consists of alternating hydrophobic and polar residues, so that the pore once again places polar residues toward the water-filled channel and nonpolar residues facing the lipid bilayer.

Whether crossing the membrane with aggregates of amphipathic α-helices or β-barrels, these pore-forming toxins represent Nature's accommodation to a structural challenge facing all protein-based transmembrane channels: the need to provide hydrogen-bonding partners for the polypeptide backbone N—H and C=O groups in an environment (the bilayer interior) that lacks hydrogen-bond donors or acceptors. The solution to this problem is found, of course, in the extensive hydrogen-bonding possibilities of α-helices and β-sheets.

Amphipathic Helices Form Transmembrane Ion Channels

Recently, a variety of natural peptides that form transmembrane channels have been identified and characterized. Melittin (Figure 10.35) is a bee venom toxin peptide of 26 residues. The cecropins are peptides induced in *Hyalophora cecropia* (Figure 10.36) and other related silkworms when challenged by bacterial infections. These peptides are thought to form α-helical aggregates in mem-

Alamethicin I[1]:

Ac-Aib-Pro-Aib-Ala-Aib-Ala-Gln-Aib-Val-Aib-Gly-Leu-Aib-Pro-Val-Aib-Aib-Glu-Gln-Phol*

Cecropin A:

Lys-Trp-Lys-Leu-Phe-Lys-Lys-Ile-Glu-Lys-Val-Gly-Gln-Asn-Ile-Arg-Asp-Gly-Ile-Ile-Lys-Ala-Gly-Pro-Ala-Val-Ala-Val-Val-Gly-Gln-Ala-Thr-Gln-Ile-Ala-Lys-NH$_2$

Melittin:

Gly-Ile-Gly-Ala-Val-Leu-Lys-Val-Leu-Thr-Thr-Gly-Leu-Pro-Ala-Leu-Ile-Ser-Trp-Ile-Lys-Arg-Lys-Arg-Gln-Gln-NH$_2$

Magainin 2 amide:

Gly-Ile-Gly-Lys-Phe-Leu-His-Ser-Ala-Lys-Lys-Phe-Gly-Lys-Ala-Phe-Val-Gly-Glu-Ile-Met-Asn-Ser-NH$_2$

FIGURE 10.35 • The amino acid sequences of several amphipathic peptide antibiotics. α-Helices formed from these peptides cluster polar residues on one face of the helix, with nonpolar residues at other positions.

FIGURE 10.36 • Adult (*left*) and caterpillar (*right*) stages of the cecropia moth, *Hyalophora cecropia*. *(left, Greg Neise/Visuals Unlimited; right, Patti Murray/Animals, Animals)*

branes, creating an ion channel in the center of the aggregate. The unifying feature of these helices is their **amphipathic** character, with polar residues clustered on one face of the helix and nonpolar residues elsewhere. In the membrane, the polar residues face the ion channel, leaving the nonpolar residues elsewhere on the helix to interact with the hydrophobic interior of the lipid bilayer.

𝒜 D E E P E R L O O K

Melittin—How to Sting Like a Bee

The stings of many stinging insects, like wasps, hornets, and bumblebees, cause a pain that, although mild at first, increases in intensity over 2 to 30 minutes, with a following period of swelling that may last for several days. The sting of the honey bee (*Apis mellifera*), on the other hand, elicits a sharp, stabbing pain within 10 seconds. This pain may last for several minutes and is followed by several hours of swelling and itching. The immediate, intense pain is caused by **melittin,** a 26-residue peptide that constitutes about half of the 50 μg (dry weight) of material injected during the "sting" (in a total volume of only 0.5 μL). How does this simple peptide cause the intense pain that accompanies a bee sting?

The pain appears to arise from the formation of melittin pores in the membranes of **nociceptors,** free nerve endings that detect harmful ("noxious"—thus the name) stimuli of violent mechanical stress, high temperatures, and irritant chemicals. The creation of pores by melittin depends on the nociceptor membrane potential. Melittin in water solution is tetrameric. However, melittin interacting with membranes in the absence of a membrane potential is monomeric and shows no evidence of oligomer

formation. When an electrical potential (voltage) is applied across the membrane, melittin tetramers form and the membrane becomes permeable to anions such as chloride. Nociceptor membranes maintain a resting potential of 70 mV (negative inside). When melittin binds to the nociceptor membrane, the flow of chloride ions out of the cell diminishes the transmembrane potential, stimulating the nerve and triggering a pain response and also inducing melittin tetramers to dissociate. When the membrane potential is re-established, melittin tetramers reform and the cycle is repeated over and over, causing a prolonged and painful stimulation of the nociceptors. The pain of the sting eventually lessens, perhaps due to the molecules of melittin diffusing apart, so that tetramers can no longer form.

Although the honey bee's sting is unpleasant, this tiny creature is crucial to the world's agricultural economy. Honey bees produce more than $100 million worth of honey each year, and, more importantly, the pollination of numerous plants by honey bees is responsible for the production of $20 billion worth of crops in the United States alone.

Gap Junctions in Mammalian Cell Membranes

When cells lie adjacent to each other in animal tissues, they are often connected by **gap junction** structures, which permit the passive flow of small molecules from one cell to the other. Such junctions essentially connect the cells metabolically, providing a means of chemical transfer and communication. In certain tissues, such as heart muscle that is not innervated, gap junctions permit very large numbers of cells to act synchronously. Gap junctions also provide a means for transport of nutrients to cells disconnected from the circulatory system, such as the lens cells of the eye.

Gap junctions are formed from hexameric arrays of a single 32-kD protein. Each subunit of the array is cylindrical, with a length of 7.5 nm and a diameter of 2.5 nm. The subunits of the hexameric array are normally tilted with respect to the sixfold axis running down the center of the hexamer (Figure 10.37). In this conformation, a central pore having a diameter of about 1.8 to 2.0 nm is created, and small molecules (up to masses of 1 kD to 1.2 kD) can pass through unimpeded. Proteins, nucleic acids, and other large structures cannot. A complete gap junction is formed from two such hexameric arrays, one from each cell. A twisting, sliding movement of the subunits narrows the channel and closes the gap junction. This closure is a cooperative process, and a localized conformation change at the cytoplasmic end assists in the closing of the channels. Because the closing of the gap junction does not appear to involve massive conformational changes in the individual subunits, the free energy change for closure is small.

Although gap junctions allow cells to communicate metabolically under normal conditions, the ability to close gap junctions provides the tissue with an important intercellular regulation mechanism. In addition, gap junctions provide a means to protect adjacent cells if one or more cells are damaged or
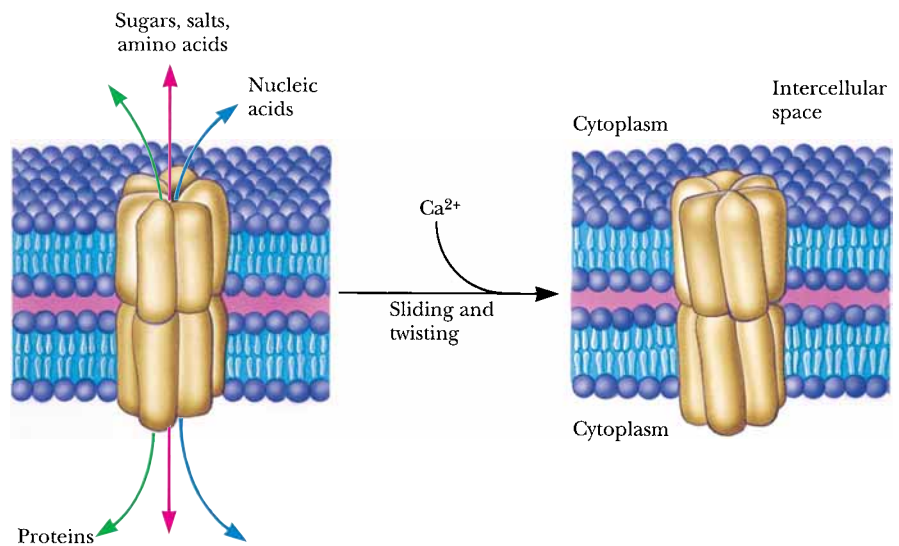
FIGURE 10.37 • Gap junctions consist of hexameric arrays of cylindrical protein subunits in the plasma membrane. The subunit cylinders are tilted with respect to the axis running through the center of the gap junction. A gap junction between cells is formed when two hexameric arrays of subunits in separate cells contact each other and form a pore through which cellular contents may pass. Gap junctions close by means of a twisting, sliding motion in which the subunits decrease their tilt with respect to the central axis. Closure of the gap junction is Ca^{2+}-dependent.

stressed. To these ends, gap junctions are sensitive to membrane potentials, hormonal signals, pH changes, and intracellular calcium levels. Dramatic changes in pH or Ca^{2+} concentration in a cell may be a sign of cellular damage or death. In order to protect neighboring cells from the propagation of such effects, gap junctions close in response to decreased pH or prolonged increases in intracellular Ca^{2+}. Under normal conditions of intracellular Ca^{2+} levels ($<10^{-7}$ M), gap junctions are open and intercellular communication is maintained. When calcium levels rise to 10^{-5} M or higher, the junctions, sensing danger, rapidly close.

10.9 • Ionophore Antibiotics

All of the transport systems examined thus far are relatively large proteins. Several small molecule toxins produced by microorganisms facilitate ion transport across membranes. Due to their relative simplicity, these molecules, the **ionophore antibiotics,** represent paradigms of the **mobile carrier** and **pore** or **channel** models for membrane transport. Mobile carriers are molecules that form complexes with particular ions and diffuse freely across a lipid membrane (Figure 10.38). Pores or channels, on the other hand, adopt a fixed orientation in a membrane, creating a hole that permits the transmembrane movement of ions. These pores or channels may be formed from monomeric or (more often) multimeric structures in the membrane.

Carriers and channels may be distinguished on the basis of their temperature dependence. Channels are comparatively insensitive to membrane phase transitions and show only a slight dependence of transport rate on temperature. Mobile carriers, on the other hand, function efficiently above a membrane phase transition, but only poorly below it. Consequently, mobile carrier systems often show dramatic increases in transport rate as the system is heated through its phase transition. Figure 10.39 displays the structures of several of these interesting molecules. As might be anticipated from the variety of structures represented here, these molecules associate with membranes and facilitate transport by different means.
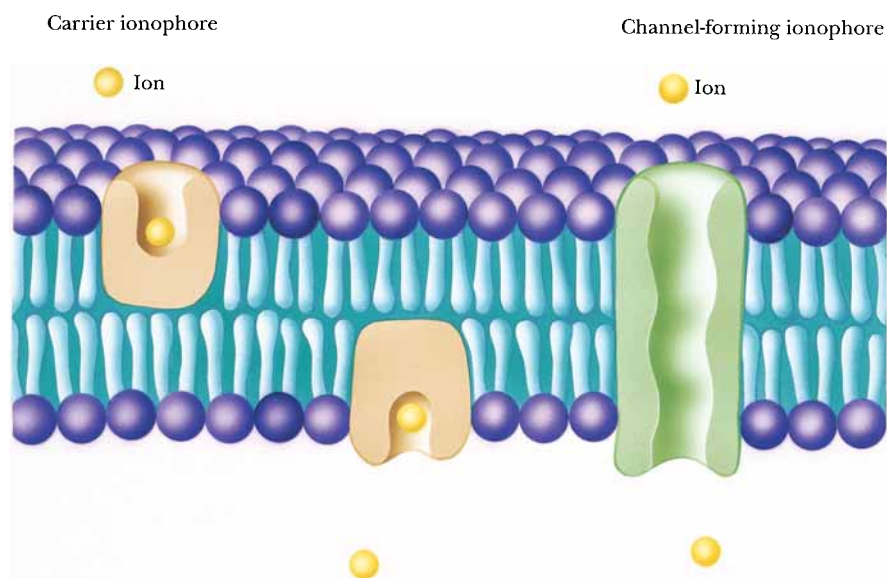
FIGURE 10.38 • Schematic drawings of mobile carrier and channel ionophores. Carrier ionophores must move from one side of the membrane to the other, acquiring the transported species on one side and releasing it on the other side. Channel ionophores span the entire membrane.
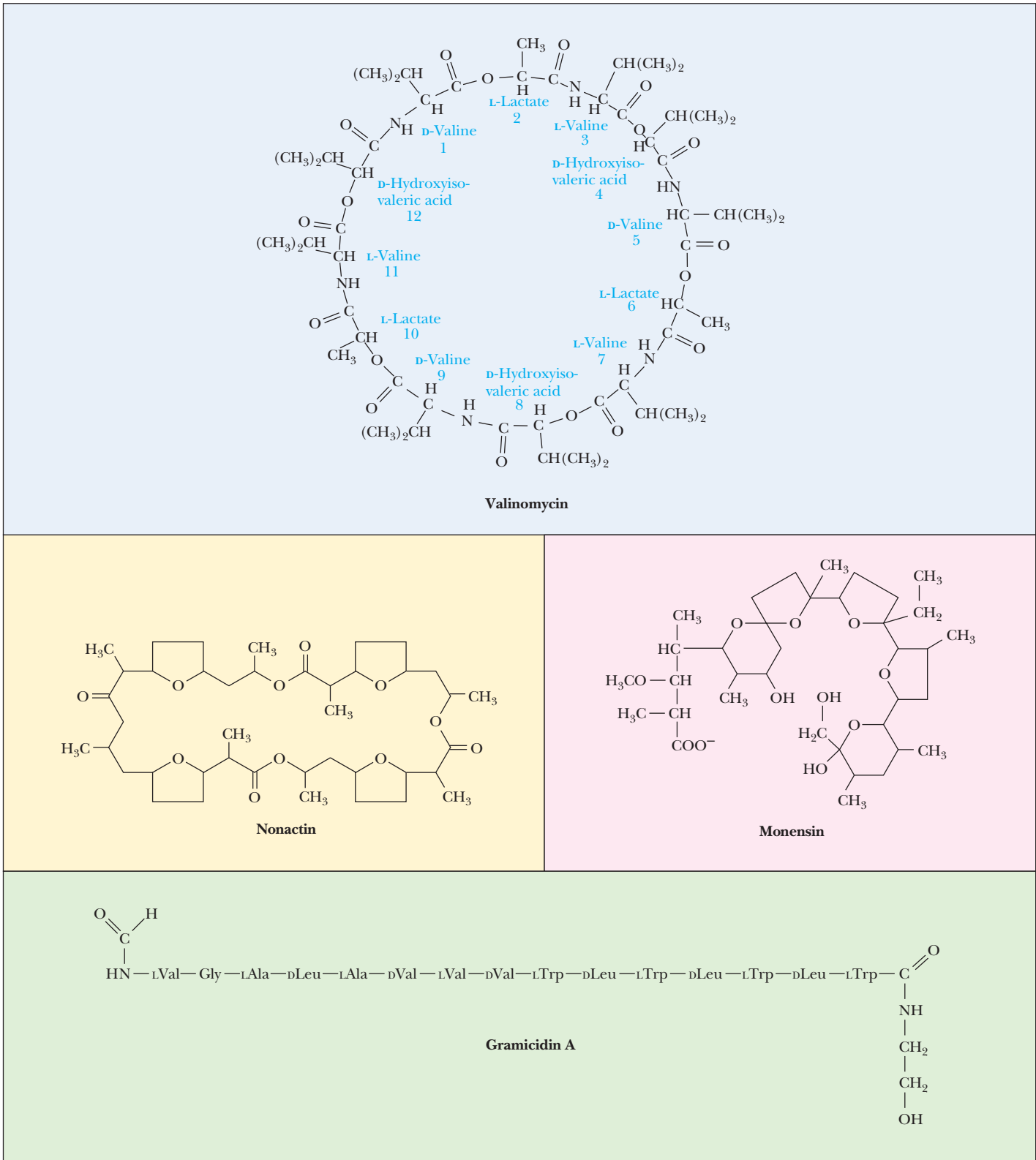
FIGURE 10.39 • Structures of several ionophore antibiotics. Valinomycin consists of three repeats of a four-unit sequence. Because it contains both peptide and ester bonds, it is referred to as a depsipeptide.
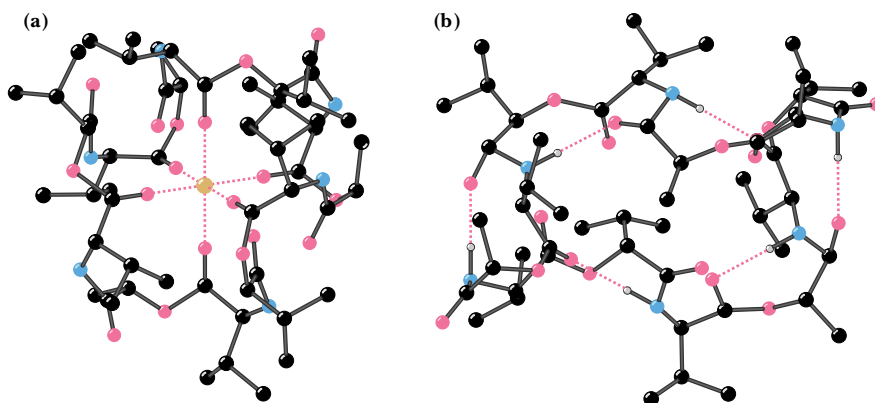
FIGURE 10.40 • The structures of (a) the valinomycin-K^+ complex and (b) uncomplexed valinomycin.

Valinomycin Is a Mobile Carrier Ionophore

Valinomycin (isolated from *Streptomyces fulvissimus*) is a cyclic structure containing 12 units made from four different residues. Two are amino acids (L-valine and D-valine); the other two residues, L-lactate and D-hydroxyisovalerate, contribute ester linkages. Valinomycin is a **depsipeptide,** that is, a molecule with both peptide and ester bonds. (Considering the 12 units in the structure, valinomycin is called a **dodecadepsipeptide.**) Valinomycin consists of the 4-unit sequence (D-valine, L-lactate, L-valine, D-hydroxyisovalerate), repeated three times to form the cyclic structure in Figure 10.39. The structures of uncomplexed valinomycin and the K^+-valinomycin complex have been studied by X-ray crystallography (Figure 10.40). The structure places K^+ at the center of the valinomycin ring, coordinated with the carbonyl oxygens of the 6 valines. The polar groups of the valinomycin structure are positioned toward the center of the ring, whereas the nonpolar groups (the methyl and isopropyl side chains) are directed outward from the ring. The hydrophobic exterior of valinomycin interacts favorably with low dielectric solvents and with the hydrophobic interiors of lipid bilayers. Moreover, the central carbonyl groups completely surround the K^+ ion, shielding it from contact with nonpolar solvents or the hydrophobic membrane interior. As a result, the K^+-valinomycin complex freely diffuses across biological membranes and effects rapid, passive K^+ transport (up to 10,000 K^+/sec) in the presence of K^+ gradients.

Valinomycin displays a striking selectivity with respect to monovalent cation binding. It binds K^+ and Rb^+ tightly, but shows about a thousandfold lower affinity for Na^+ and Li^+. The smaller ionic radii of Na^+ and Li^+ (compared to K^+ and Rb^+) may be responsible in part for the observed differences. However, another important difference between Na^+ and K^+ is shown in Table 10.5. The **free energy of hydration** for an ion is the stabilization achieved by hydrating that ion. The process of dehydration, a prerequisite to forming the ion-valinomycin complex, requires energy input. As shown in Table 10.5, considerably more energy is required to desolvate an Na^+ ion than to desolvate a K^+ ion. It is thus easier to form the K^+-valinomycin complex than to form the corresponding Na^+ complex.

Other mobile carrier ionophores include *monensin* and *nonactin* (Figure 10.39). The unifying feature in all these structures is an inward orientation of polar groups (to coordinate the central ion) and outward orientation of non-

Table 10.5

Properties of Alkali Cations

Ion	Atomic Number	Ionic Radius (nm)	Hydration Free Energy, ΔG (kJ/mol)
Li^+	3	0.06	-410
Na^+	11	0.095	-300
K^+	19	0.133	-230
Rb^+	37	0.148	-210
Cs^+	55	0.169	-200

(a)

(b)
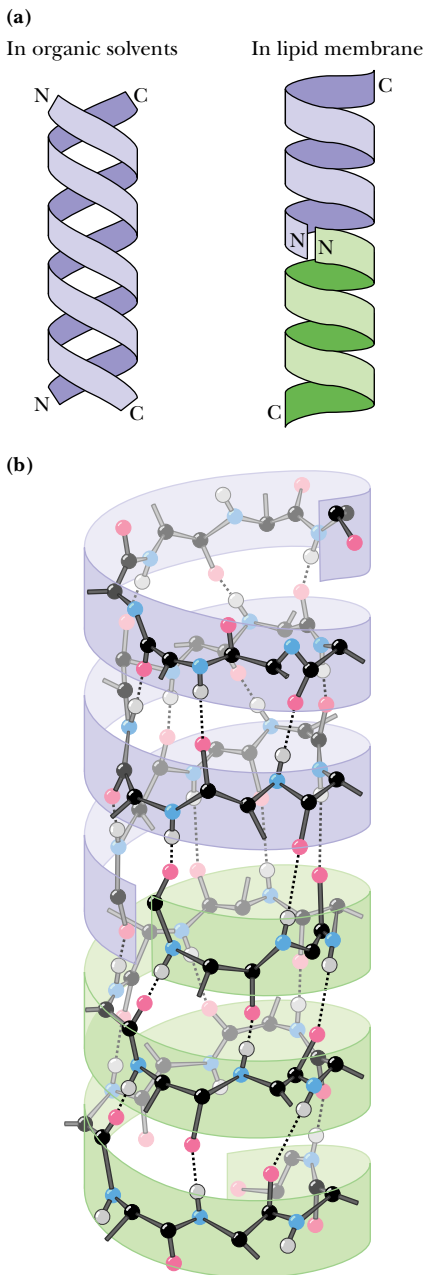
polar residues (making these complexes freely soluble in the hydrophobic membrane interior).

Gramicidin Is a Channel-Forming Ionophore

In contrast to valinomycin, all protein-derived membrane transport systems appear to function as channels, not mobile carriers. All of the proteins discussed in this chapter use multiple transmembrane segments to create channels in the membrane, through which species are transported. For this reason, it may be more relevant to consider the **pore** or **channel** ionophores. **Gramicidin** from *Bacillus brevis* (Figure 10.41) is a linear peptide of 15 residues and is a prototypical channel ionophore. Gramicidin contains alternating L- and D-residues, a formyl group at the N-terminus, and an ethanolamine at the C-terminus. The predominance of hydrophobic residues in the gramicidin structure facilitates its incorporation into lipid bilayers and membranes. Once incorporated in lipid bilayers, it permits the rapid diffusion of many different cations. Gramicidin possesses considerably less ionic specificity than does valinomycin, but permits higher transport rates. A single gramicidin channel can transport as many as 10 million K^+ ions per second. Protons and all alkali cations can diffuse through gramicidin channels, but divalent cations such as Ca^{2+} block the channel.

Gramicidin forms two different helical structures. A double helical structure predominates in organic solvents (Figure 10.41), whereas a helical dimer is formed in lipid membranes. (An α-helix cannot be formed by gramicidin, because it has both D- and L-amino acid residues.) The helical dimer is a head-to-head or amino terminus–to–amino terminus (N-to-N) dimer oriented perpendicular to the membrane surface, with the formyl groups at the bilayer center and the ethanolamine moieties at the membrane surface. The helix is unusual, with 6.3 residues per turn and a central hole approximately 0.4 nm in diameter. The hydrogen-bonding pattern in this structure, in which N—H groups alternately point up and down the axis of the helix to hydrogen-bond with carbonyl groups, is reminiscent of a β-sheet. For this reason this structure has often been referred to as a β-helix.

FIGURE 10.41 • (a) Gramicidin forms a double helix in organic solvents; a helical dimer is the preferred structure in lipid bilayers. The structure is a head-to-head, left-handed helix, with the carboxy-termini of the two monomers at the ends of the structure. (b) The hydrogen-bonding pattern resembles that of a parallel β-sheet.

PROBLEMS

1. Calculate the free energy difference at 25°C due to a galactose gradient across a membrane, if the concentration on side 1 is 2 mM and the concentration on side 2 is 10 mM.

2. Consider a phospholipid vesicle containing 10 mM Na$^+$ ions. The vesicle is bathed in a solution that contains 52 mM Na$^+$ ions, and the electrical potential difference across the vesicle membrane $\Delta\psi = \psi_{outside} - \psi_{inside} = -30$ mV. What is the electrochemical potential at 25°C for Na$^+$ ions?

3. Transport of histidine across a cell membrane was measured at several histidine concentrations:

[Histidine], μM	Transport, μmol/min
2.5	42.5
7	119
16	272
31	527
72	1220

Does this transport operate by passive diffusion or by facilitated diffusion?

4. Fructose is present outside a cell at 1 μM concentration. An active transport system in the plasma membrane transports fructose into this cell, using the free energy of ATP hydrolysis to drive fructose uptake. Assume that one fructose is transported per ATP hydrolyzed, that ATP is hydrolyzed on the intracellular surface of the membrane, and that the concentrations of ATP, ADP, and P$_i$ are 3 mM, 1 mM, and 0.5 mM, respectively. T = 298 K. What is the highest intracellular concentration of fructose that this transport system can generate? (*Hint:* Refer to Chapter 3 to recall the effects of concentration on free energy of ATP hydrolysis.)

5. The rate of K$^+$ transport across bilayer membranes reconstituted from dipalmitoylphosphatidylcholine (DPPC) and nigericin is approximately the same as that observed across membranes reconstituted from DPPC and *cecropin a* at 35°C. Would you expect the transport rates across these two membranes also to be similar at 50°C? Explain.

6. In this chapter, we have examined coupled transport systems that rely on ATP hydrolysis, on primary gradients of Na$^+$ or H$^+$, and on phosphotransferase systems. Suppose you have just discovered an unusual strain of bacteria that transports rhamnose across its plasma membrane. Suggest experiments that would test whether it was linked to any of these other transport systems.

FURTHER READING

Benz, R., 1980. Structure and function of porins from Gram-negative bacteria. *Annual Review of Microbiology* **42:**359–393.

Blair, H. C., et al., 1989. Osteoclastic bone resorption by a polarized vacuolar proton pump. *Science* **245:**855–857.

Christensen, B., et al., 1988. Channel-forming properties of cecropins and related model compounds incorporated into planar lipid membranes. *Proceedings of the National Academy of Sciences U.S.A.* **85:**5072–5076.

Choe, S., Bennett, M., Fujii, G., et al., 1992. The crystal structure of diphtheria toxin. *Nature* **357:**216–222.

Collarini, E. J., and Oxender, D., 1987. Mechanisms of transport of amino acids across membrane. *Annual Review of Nutrition* **7:**75–90.

Featherstone, C., 1990. An ATP-driven pump for secretion of yeast mating factor. *Trends in Biochemical Sciences* **15:**169–170.

Garavito, R. M., et al., 1983. X-ray diffraction analysis of matrix porin, an integral membrane protein from *Escherichia coli* outer membrane. *Journal of Molecular Biology* **164:**313–327.

Glynn, I., and Karlish, S., 1990. Occluded ions in active transport. *Annual Review of Biochemistry* **59:**171–205.

Gould, G. W., and Bell, G. I., 1990. Facilitative glucose transporters: An expanding family. *Trends in Biochemical Sciences* **15:**18–23.

Hughson, F., 1997. Penetrating insights into pore formation. *Nature Structural Biology* **4:**89–92.

Inesi, G., Sumbilla, C., and Kirtley, M., 1990. Relationships of molecular structure and function in Ca^{2+}-transport ATPase. *Physiological Reviews* **70:**749–759.

Jap, B., and Walian, P. J., 1990. Biophysics of the structure and function of porins. *Quarterly Reviews of Biophysics* **23:**367–403.

Jay, D., and Cantley, L., 1986. Structural aspects of the red cell anion exchange protein. *Annual Review of Biochemistry* **55:**511–538.

Jennings, M. L., 1989. Structure and function of the red blood cell anion transport protein. *Annual Review of Biophysics and Biophysical Chemistry* **18:**397–430.

Jørgensen, P. L., 1986. Structure, function and regulation of Na$^+$,K$^+$-ATPase in the kidney. *Kidney International* **29:**10–20.

Jørgensen, P. L., and Andersen, J. P., 1988. Structural basis for E$_1$-E$_2$ conformational transitions in Na$^+$,K$^+$-pump and Ca^{2+}-pump proteins. *Journal of Membrane Biology* **103:**95–120.

Juranka, P. F., Zastawny, R. L., and Ling, V., 1989. P-Glycoprotein: Multidrug-resistance and a superfamily of membrane-associated transport proteins. *The FASEB Journal* **3:**2583–2592.

Kaback, H. R., Bibi, E., and Roepe, P. D., 1990. β-Galactoside transport in *E. coli:* A functional dissection of lac permease. *Trends in Biochemical Sciences* **15:**309–314.

Kartner, N., and Ling, V., 1989. Multidrug resistance in cancer. *Scientific American* **260:**44–51.

Li, H., Lee, S., and Jap, B., 1997. Molecular design of aquaporin-1 water channel as revealed by electron crystallography. *Nature Structural Biology* **4:**263–265.

Li, J., Carroll, J., and Ellar, D., 1991. Crystal structure of insecticidal δ-endotoxin from *Bacillus thuringiensis* at 2.5 Å resolution. *Nature* **353:**815–821.

Matthew, M. K., and Balaram, A., 1983. A helix dipole model for alamethicin and related transmembrane channels. *FEBS Letters* **157:**1–5.

Meadow, N. D., Fox, D. K., and Roseman, S., 1990. The bacterial phosphoenolpyruvate:glycose phosphotransferase system. *Annual Review of Biochemistry* **59:**497–542.

Miller, C., 1996. A chloride channel model? *Science* **274:**738.

Oesterhelt, D., and Tittor, J., 1989. Two pumps, one principle: Light-driven ion transport in *Halobacteria. Trends in Biochemical Sciences* **14:**57–61.

Parker, M., 1997. More than one way to make a hole. *Nature Structural Biology* **4:**250–253.

Parker, M., Buckley, J., Postma, J., et al., 1994. Structure of the *Aeromonas* toxin proaerolysin in its water-soluble and membrane-channel states. *Nature* **367:**292–295.

Parker, M., Tucker, A., Tsernoglou, D., and Pattus, F., 1990. Insights into membrane insertion based on studies of colicins. *Trends in Biochemical Sciences* **15:**126–129.

Pedersen, P. L., and Carafoli, E., 1987. Ion motive ATPases. *Trends in Biochemical Sciences* **12:**146–150, 186–189.

Petosa, C., Collier, R., Klimpel, K., et al., 1997. Crystal structure of the anthrax toxin protective antigen. *Nature* **385:**833–838.

Pressman, B., 1976. Biological applications of ionophores. *Annual Review of Biochemistry* **45:**501–530.

Prince, R. C., 1990. At least one *Bacillus thuringiensis* toxin forms ion-selective pores in membranes. *Trends in Biochemical Sciences* **15:**2–3.

Prince, R., Gunson, D., and Scarpa, A., 1985. Sting like a bee! The ionophoric properties of melittin. *Trends in Biochemical Sciences* **10:**99.

Schirmer, T., Keller, T. A., Wang, Y.-F., and Rosenbusch, J. P., 1995. Structural basis for sugar translocation through maltoporin channels at 3.1 Å resolution. *Science* **267:**512–514.

Song, L., Hobaugh, M., Shustak, C., et al., 1996. Structure of staphylococcal α-hemolysin, a heptameric transmembrane pore. *Science* **274:**1859–1866.

Spudich, J. L., and Bogomolni, R. A., 1988. Sensory rhodopsins of *Halobacteria. Annual Review of Biophysics and Biophysical Chemistry* **17:**193–215.

Wade, D., et al., 1990. All-D amino acid-containing channel-forming antibiotic peptides. *Proceedings of the National Academy of Sciences U.S.A.* **87:**4761–4765.

Wallace, B. A., 1990. Gramicidin channels and pores. *Annual Review of Biophysics and Biophysical Chemistry* **19:**127–157.

Walmsley, A. R., 1988. The dynamics of the glucose transporter. *Trends in Biochemical Sciences* **13:**226–231.

Weiner, M., Freymann, D., Ghosh, P., and Stroud, R., 1997. Crystal structure of colicin Ia. *Nature* **385:**461–464.

Wheeler, T. J., and Hinkle, P., 1985. The glucose transporter of mammalian cells. *Annual Review of Physiology* **47:**503–517.

$\mathcal{C}$hapter 11

Nucleotides and cleic Acids
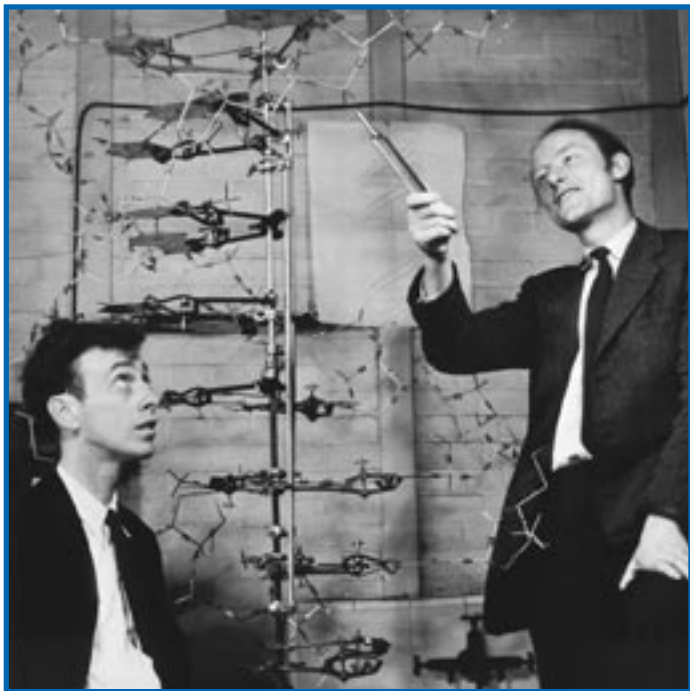
Francis Crick and James Watson point out features of their model for the structure of DNA. (© A. Barrington Brown/Science Source/Photo Researchers, Inc.)

Nucleotides and **nucleic acids** are biological molecules that possess heterocyclic nitrogenous bases as principal components of their structure. The biochemical roles of nucleotides are numerous; they participate as essential intermediates in virtually all aspects of cellular metabolism. Serving an even more central biological purpose are the nucleic acids, the elements of heredity and the agents of genetic information transfer. Just as proteins are linear polymers of amino acids, nucleic acids are linear polymers of nucleotides. Like the letters in this sentence, the orderly sequence of nucleotide residues in a nucleic acid can encode information. The two basic kinds of nucleic acids are **deoxyribonucleic acid (DNA)** and **ribonucleic acid (RNA).** Complete hydrolysis of nucleic acids liberates nitrogenous bases, a five-carbon sugar, and phosphoric acid in equal amounts. The five-carbon sugar in DNA is 2-deoxyribose; in RNA,

327
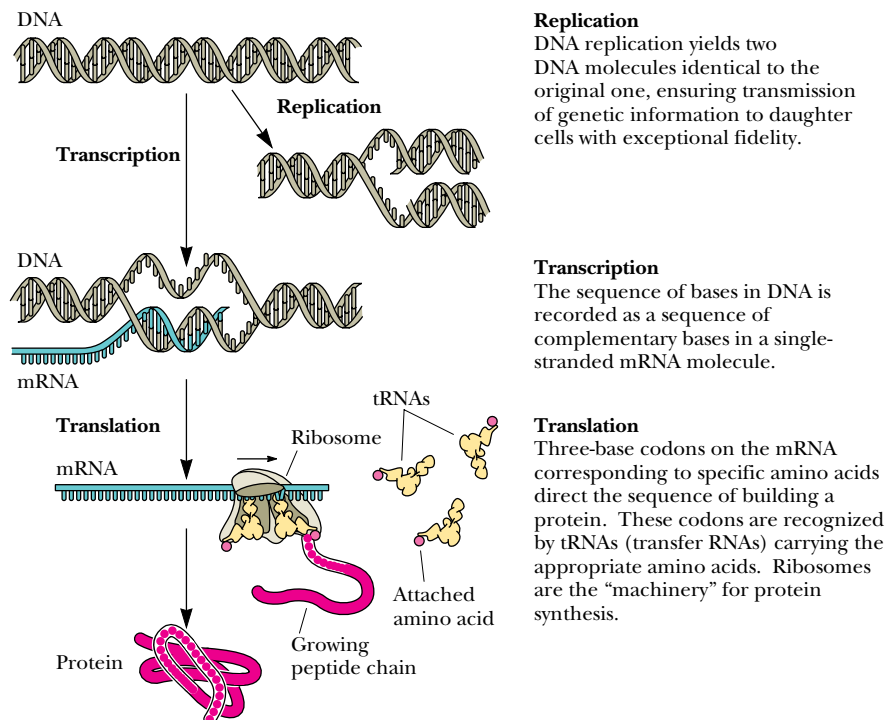
FIGURE 11.1 • The fundamental process of information transfer in cells. Information encoded in the nucleotide sequence of DNA is transcribed through synthesis of an RNA molecule whose sequence is dictated by the DNA sequence. As the sequence of this RNA is read (as groups of three consecutive nucleotides) by the protein synthesis machinery, it is translated into the sequence of amino acids in a protein. This information transfer system is encapsulated in the dogma: DNA → RNA → protein.

it is ribose. (See Chapter 7 for a detailed discussion of sugars and other carbohydrates.) DNA is the repository of genetic information in cells, while RNA serves in the transcription and translation of this information (Figure 11.1). An interesting exception to this rule is that some viruses have their genetic information stored as RNA.

This chapter describes the chemistry of nucleotides and the major classes of nucleic acids. Chapter 12 presents methods for determination of nucleic acid primary structure (nucleic acid sequencing) and describes the higher orders of nucleic acid structure. Chapter 13 introduces the *molecular biology of recombinant DNA:* the construction and uses of novel DNA molecules assembled by combining segments from other DNA molecules.

11.1 • Nitrogenous Bases

The bases of nucleotides and nucleic acids are derivatives of either **pyrimidine** or **purine.** Pyrimidines are six-membered heterocyclic aromatic rings containing two nitrogen atoms (Figure 11.2a). The atoms are numbered in a clockwise fashion, as shown in the figure. The purine ring structure is represented by the combination of a pyrimidine ring with a five-membered imidazole ring to yield a fused ring system (Figure 11.2b). The nine atoms in this system are numbered according to the convention shown.

FIGURE 11.2 • (a) The pyrimidine ring system; by convention, atoms are numbered as indicated. (b) The purine ring system, atoms numbered as shown.

Cytosine
(2-oxy-4-amino pyrimidine)

Uracil
(2-oxy-4-oxy pyrimidine)

Thymine
(2-oxy-4-oxy 5-methyl pyrimidine)

FIGURE 11.3 • The common pyrimidine bases—cytosine, uracil, and thymine—in the tautomeric forms predominant at pH 7.

The pyrimidine ring system is planar, while the purine system deviates somewhat from planarity in having a slight pucker between its imidazole and pyrimidine portions. Both are relatively insoluble in water, as might be expected from their pronounced aromatic character.

Common Pyrimidines and Purines

The common naturally occurring pyrimidines are **cytosine, uracil,** and **thymine** (5-methyluracil) (Figure 11.3). Cytosine and thymine are the pyrimidines typically found in DNA, whereas cytosine and uracil are common in RNA. To view this generality another way, the uracil component of DNA occurs as the 5-methyl variety, thymine. Various pyrimidine derivatives, such as dihydrouracil, are present as minor constituents in certain RNA molecules.

Adenine (6-amino purine) and **guanine** (2-amino-6-oxy purine), the two common purines, are found in both DNA and RNA (Figure 11.4). Other naturally occurring purine derivatives include **hypoxanthine, xanthine,** and **uric acid** (Figure 11.5). Hypoxanthine and xanthine are found only rarely as constituents of nucleic acids. Uric acid, the most oxidized state for a purine derivative, is never found in nucleic acids.

Hypoxanthine

Xanthine

Adenine
(6-amino purine)

Guanine
(2-amino-6-oxy purine)

FIGURE 11.4 • The common purine bases—adenine and guanine—in the tautomeric forms predominant at pH 7.

Uric acid

FIGURE 11.5 • Other naturally occurring purine derivatives—hypoxanthine, xanthine, and uric acid.

Properties of Pyrimidines and Purines

The aromaticity of the pyrimidine and purine ring systems and the electron-rich nature of their —OH and —NH$_2$ substituents endow them with the capacity to undergo **keto–enol tautomeric shifts.** That is, pyrimidines and purines exist as tautomeric pairs, as shown in Figure 11.6 for uracil. The keto tautomer is called a **lactam,** whereas the enol form is a **lactim.** The lactam form vastly predominates at neutral pH. In other words, pK_a values for ring nitrogen atoms 1 and 3 in uracil are greater than 8 (the pK_a value for N-3 is 9.5) (Table 11.1).

Table 11.1

Proton Dissociation Constants (pK_a Values) for Nucleotides			
Nucleotide	pK_a Base-N	pK_1 Phosphate	pK_2 Phosphate
5′-AMP	3.8 (N-1)	0.9	6.1
5′-GMP	9.4 (N-1)	0.7	6.1
	2.4 (N-7)		
5′-CMP	4.5 (N-3)	0.8	6.3
5′-UMP	9.5 (N-3)	1.0	6.4

Lactam   **Lactim**
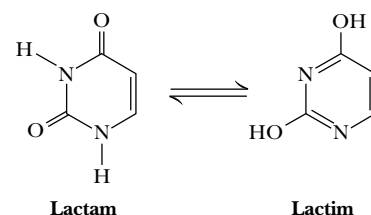
FIGURE 11.6 • The keto/enol tautomerism of uracil.
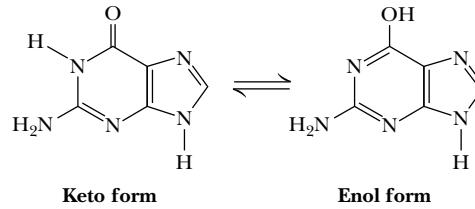
FIGURE 11.7 • The tautomerism of the purine, guanine.

Keto form   Enol form

In contrast, as might be expected from the form of cytosine that predominates at pH 7, the pK_a value for N-3 in this pyrimidine is 4.5. Similarly, tautomeric forms can be represented for purines, as given for guanine in Figure 11.7. Here, the pK_a value is 9.4 for N-1 and less than 5 for N-3. These pK_a values specify whether hydrogen atoms are associated with the various ring nitrogens at neutral pH. As such, they are important in determining whether these nitrogens serve as H-bond donors or acceptors. Hydrogen bonding between purine and pyrimidine bases is fundamental to the biological functions of nucleic acids, as in the formation of the double helix structure of DNA (see Section 11.6). The important functional groups participating in H-bond formation are the amino groups of cytosine, adenine, and guanine; the ring nitrogens at position 3 of pyrimidines and position 1 of purines; and the strongly electronegative oxygen atoms attached at position 4 of uracil and thymine, position 2 of cytosine, and position 6 of guanine (see Figure 11.21).

Another property of pyrimidines and purines is their strong absorbance of ultraviolet (UV) light, which is also a consequence of the aromaticity of their heterocyclic ring structures. Figure 11.8 shows characteristic absorption spectra of several of the common bases of nucleic acids—adenine, uracil, cytosine, and guanine—in their nucleotide forms: AMP, UMP, CMP, and GMP (see Section 11.4). This property is particularly useful in quantitative and qualitative analysis of nucleotides and nucleic acids.

11.2 • The Pentoses of Nucleotides and Nucleic Acids

Five-carbon sugars are called **pentoses** (see Chapter 7). RNA contains the pentose D-ribose, while 2-deoxy-D-ribose is found in DNA. In both instances, the pentose is in the five-membered ring form known as *furanose:* D-ribofuranose for RNA and 2-deoxy-D-ribofuranose for DNA (Figure 11.9). When these ribofuranoses are found in nucleotides, their atoms are numbered as 1′, 2′, 3′, and so on to distinguish them from the ring atoms of the nitrogenous bases. As we shall see, the seemingly minor difference of a hydroxyl group at the 2′-position has far-reaching effects on the secondary structures available to RNA and DNA, as well as their relative susceptibilities to chemical and enzymatic hydrolysis.
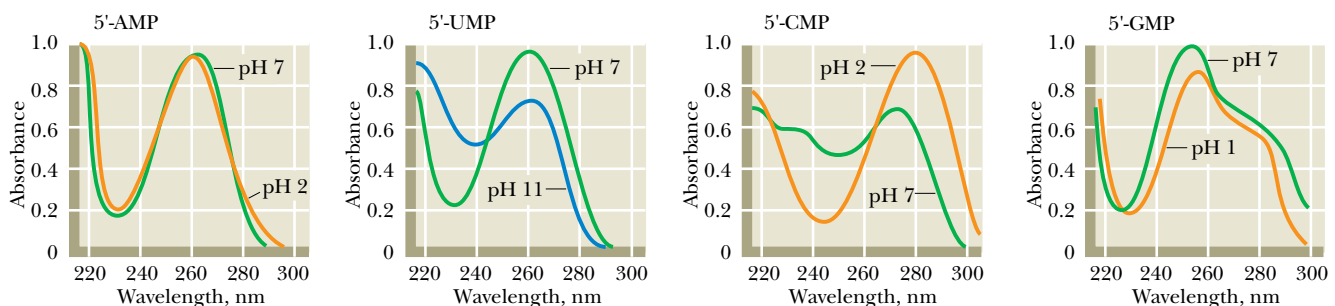
FIGURE 11.8 • The UV absorption spectra of the common ribonucleotides.
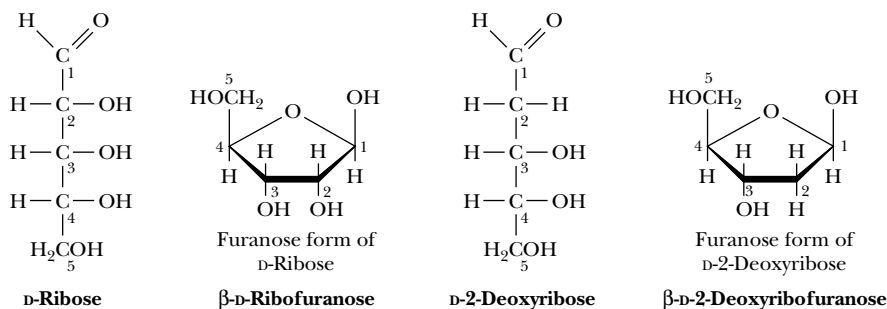
FIGURE 11.9 • Furanose structures—ribose and deoxyribose.

β-N_1-glycosidic bond in pyrimidine ribonucleosides

11.3 • Nucleosides Are Formed by Joining a Nitrogenous Base to a Sugar

Nucleosides are compounds formed when a base is linked to a sugar via a **glycosidic bond** (Figure 11.10). Glycosidic bonds by definition involve the carbonyl carbon atom of the sugar, which in cyclic structures is joined to the ring O atom (see Chapter 7). Such carbon atoms are called **anomeric.** In nucleosides, the bond is an *N*-glycoside because it connects the anomeric C-1′ to N-1 of a pyrimidine or to N-9 of a purine. Glycosidic bonds can be either α or β, depending on their orientation relative to the anomeric C atom. Glycosidic bonds in nucleosides and nucleotides are always of the β-configuration, as represented in Figure 11.10. Nucleosides are named by adding the ending *-idine* to the root name of a pyrimidine or *-osine* to the root name of a purine. The common nucleosides are thus **cytidine, uridine, thymidine, adenosine,** and **guanosine.** The structures shown in Figure 11.11 are *ribonucleosides. Deoxyribonucleosides,* in contrast, lack a 2′-OH group on the pentose. The nucleoside formed by hypoxanthine and ribose is **inosine.**

β-N_9-glycosidic bond in purine ribonucleosides

FIGURE 11.10 • β-Glycosidic bonds link nitrogenous bases and sugars to form nucleosides.

Cytidine

Uridine

Adenosine

Guanosine

Inosine, an uncommon nucleoside
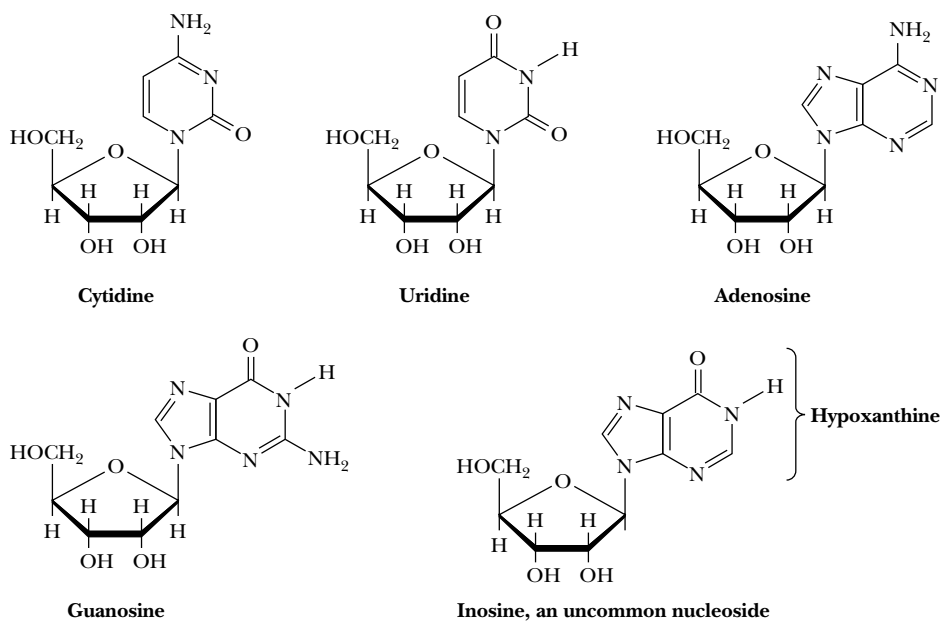
FIGURE 11.11 • The common ribonucleosides—cytidine, uridine, adenosine, and guanosine. Also, inosine drawn in anti conformation.

syn **Guanosine**   *anti* **Guanosine**   *anti* **Uridine**
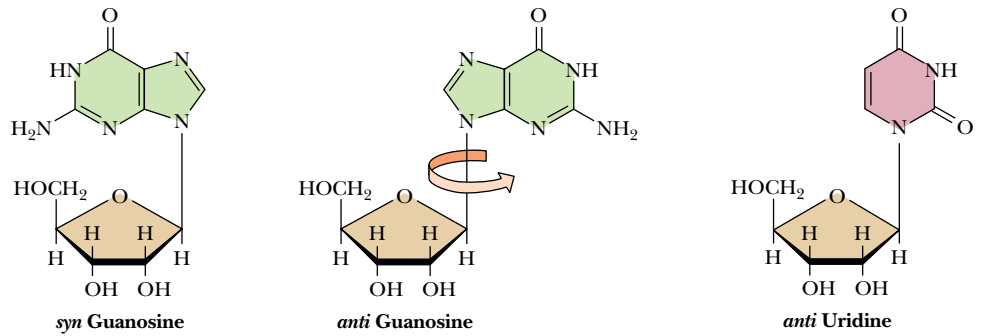
FIGURE 11.12 • Rotation around the glycosidic bond is sterically hindered; syn versus anti conformations in nucleosides are shown.

Nucleoside Conformation

In nucleosides, rotation of the base about the glycosidic bond is sterically hindered, principally by the hydrogen atom on the C-2′ carbon of the furanose. (This hindrance is most easily seen and appreciated by manipulating accurate molecular models of these structures.) Consequently, nucleosides and nucleotides (see next section) exist in either of two conformations, designated *syn* and *anti* (Figure 11.12). For pyrimidines in the syn conformation, the oxygen substituent at position C-2 lies immediately above the furanose ring; in the anti conformation, this steric interference is avoided. Consequently, pyrimidine nucleosides favor the anti conformation. Purine nucleosides can adopt either the syn or anti conformation. In either conformation, the roughly planar furanose and base rings are not coplanar but lie at approximately right angles to one another.

$\mathcal{H}$ UMAN BIOCHEMISTRY

Adenosine: A Nucleoside with Physiological Activity

For the most part, nucleosides have no biological role other than to serve as component parts of nucleotides. Adenosine is an exception. In mammals, adenosine functions as an **autocoid,** or "local hormone." This nucleoside circulates in the bloodstream, acting locally on specific cells to influence such diverse physiological phenomena as blood vessel dilation, smooth muscle contraction, neuronal discharge, neurotransmitter release, and metabolism of fat. For example, when muscles work hard, they release adenosine, causing the surrounding blood vessels to dilate, which in turn increases the flow of blood and its delivery of O_2 and nutrients to the muscles. In a different autocoid role, adenosine acts in regulating heartbeat. The natural rhythm of the heart is controlled by a pacemaker, the sinoatrial node, that cyclically sends a wave of electrical excitation to the heart muscles. By blocking the flow of electrical current, adenosine slows the heart rate. *Supraventricular tachycardia* is a heart condition characterized by a rapid heartbeat. Intravenous injection of adenosine causes a momentary interruption of the rapid cycle of contraction and restores a normal heart rate. Adenosine is licensed and marketed as *Adenocard*™ to treat supraventricular tachycardia.

In addition, adenosine is implicated in sleep regulation. During periods of extended wakefulness, extracellular adenosine levels rise as a result of metabolic activity in the brain, and this increase promotes sleepiness. During sleep, adenosine levels fall. Caffeine promotes wakefulness by blocking the interaction of extracellular adenosine with its neuronal receptors.*

Caffeine
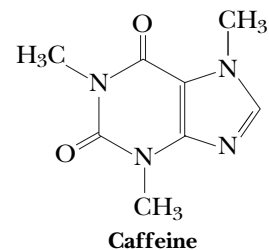
*Porrka-Heiskanen, T., et al., 1997. Adenosine: A mediator of the sleep-inducing effects of prolonged wakefulness. *Science* **276:**1265–1268.

Nucleosides Are More Water-Soluble Than Free Bases

Nucleosides are much more water-soluble than the free bases because of the hydrophilicity of the sugar moiety. Like glycosides (see Chapter 7), nucleosides are relatively stable in alkali. Pyrimidine nucleosides are also resistant to acid hydrolysis, but purine nucleosides are easily hydrolyzed in acid to yield the free base and pentose.

11.4 • Nucleotides Are Nucleoside Phosphates

A **nucleotide** results when phosphoric acid is esterified to a sugar —OH group of a nucleoside. The nucleoside ribose ring has three —OH groups available for esterification, at C-2′, C-3′, and C-5′ (although 2′-deoxyribose has only two). The vast majority of monomeric nucleotides in the cell are **ribonucleotides** having 5′-phosphate groups. Figure 11.13 shows the structures of the common four *ribonucleotides,* whose formal names are **adenosine 5′-monophosphate, guanosine 5′-monophosphate, cytidine 5′-monophosphate,** and **uridine 5′-monophosphate.** These compounds are more often referred to by their abbreviations: **5′-AMP, 5′-GMP, 5′-CMP,** and **5′-UMP,** or even more simply as **AMP, GMP, CMP,** and **UMP.** Nucleoside 3′-phosphates and nucleoside 2′-phosphates (3′-NMP and 2′-NMP, where N is a generic designation for "nucleoside") do not occur naturally, but are biochemically important as products of polynucleotide or nucleic acid hydrolysis. Because the pK_a value for the first dissociation of a proton from the phosphoric acid moiety is 1.0 or less (Table 11.1), the nucleotides have acidic properties. This acidity is implicit in the other names by which these substances are known—**adenylic acid, guanylic acid,**
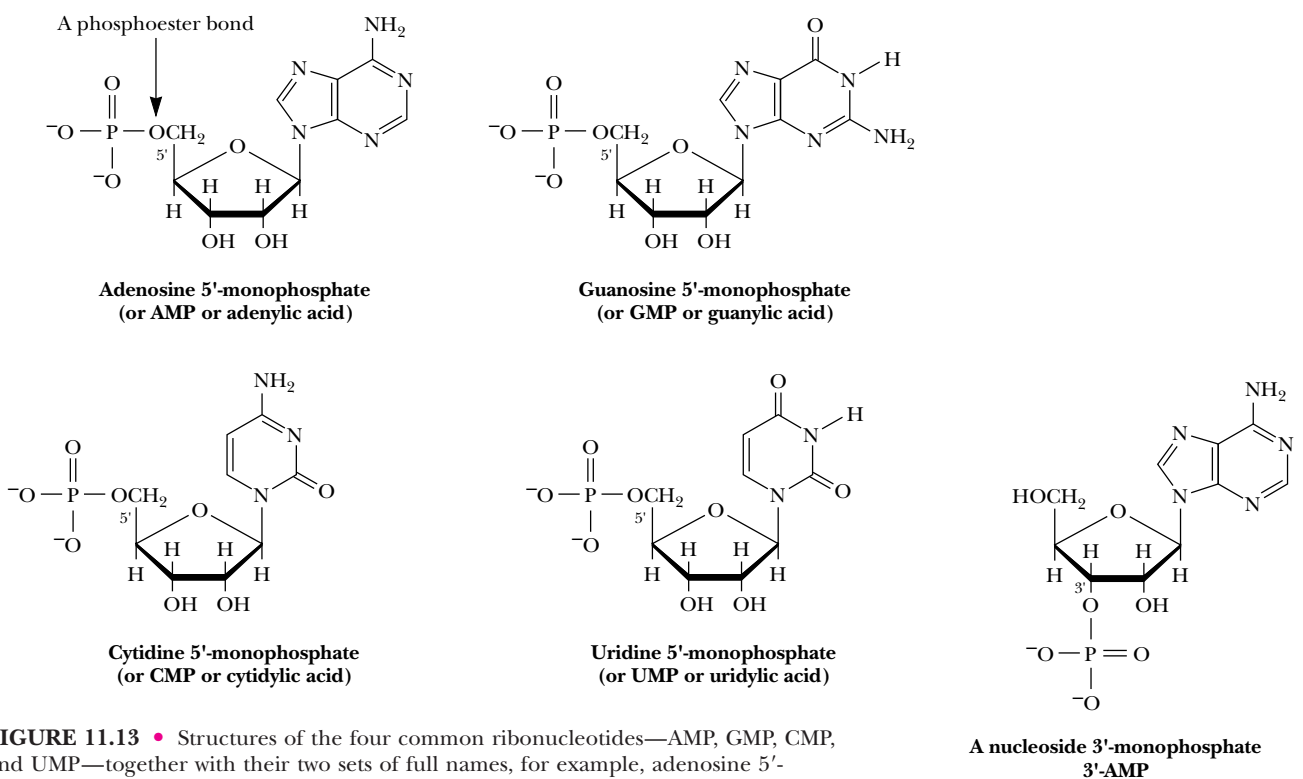
FIGURE 11.13 • Structures of the four common ribonucleotides—AMP, GMP, CMP, and UMP—together with their two sets of full names, for example, adenosine 5′-monophosphate and adenylic acid. Also shown is the nucleoside 3′-AMP.

3',5'-Cyclic AMP

3',5'-Cyclic GMP
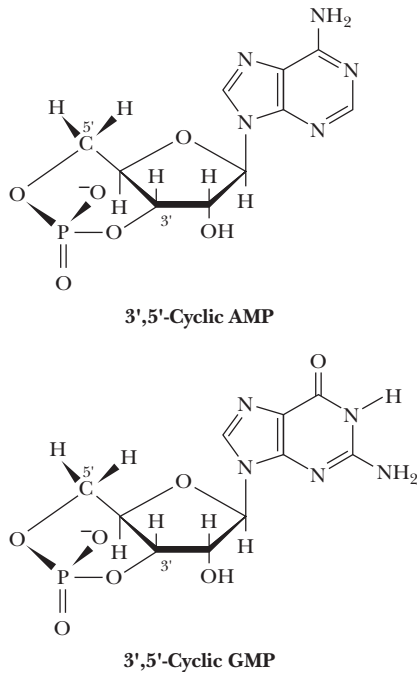
FIGURE 11.14 • Structures of the cyclic nucleotides cAMP and cGMP.

cytidylic acid, and **uridylic acid.** The pK_a value for the second dissociation, pK_2, is about 6.0, so at neutral pH or above, the net charge on a nucleoside monophosphate is -2. Nucleic acids, which are polymers of nucleoside monophosphates, derive their name from the acidity of these phosphate groups.

Cyclic Nucleotides

Nucleoside monophosphates in which the phosphoric acid is esterified to *two* of the available ribose hydroxyl groups (Figure 11.14) are found in all cells. Forming two such ester linkages with one phosphate results in a cyclic structure. **3′,5′-cyclic AMP,** often abbreviated **cAMP,** and its guanine analog **3′,5′-cyclic GMP,** or **cGMP,** are important regulators of cellular metabolism (see Part III: Metabolism and Its Regulation).

Nucleoside Diphosphates and Triphosphates

Additional phosphate groups can be linked to the phosphoryl group of a nucleotide through the formation of phosphoric anhydride linkages, as shown in Figure 11.15. Addition of a second phosphate to AMP creates **adenosine 5′-diphosphate,** or **ADP,** and adding a third yields **adenosine 5′-triphosphate,** or **ATP.** The respective phosphate groups are designated by the Greek letters α, β, and γ, starting with the α-phosphate as the one linked directly to the pentose. The abbreviations **GTP, CTP,** and **UTP** represent the other corresponding nucleoside 5′-triphosphates. Like the nucleoside 5′-monophosphates, the nucleoside 5′-diphosphates and 5′-triphosphates all occur in the free state in the cell, as do their deoxyribonucleoside phosphate counterparts, represented as dAMP, dADP, and dATP; dGMP, dGDP, and dGTP; dCMP, dCDP, and dCTP; dUMP, dUDP, and dUTP; and dTMP, dTDP, and dTTP.

Phosphate (P_i)   +   AMP (adenosine 5'-monophosphate)   Water   +   ADP (adenosine 5'-diphosphate)

Phosphate   +   ADP   ATP (adenosine 5'-triphosphate)
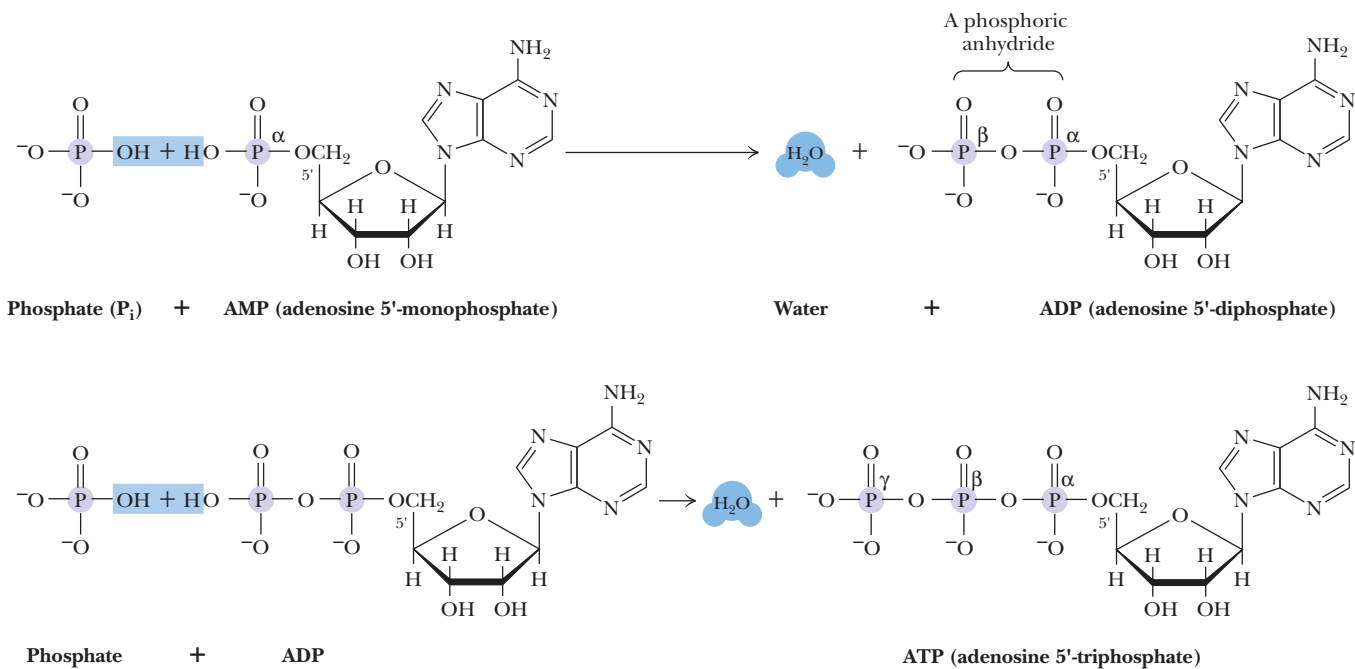
FIGURE 11.15 • Formation of ADP and ATP by the successive addition of phosphate groups via phosphoric anhydride linkages. Note the removal of equivalents of H_2O in these dehydration synthesis reactions.

NDPs and NTPs Are Polyprotic Acids

Nucleoside 5′-diphosphates (NDPs) and **nucleoside 5′-triphosphates (NTPs)** are relatively strong *polyprotic acids,* in that they dissociate three and four protons, respectively, from their phosphoric acid groups. The resulting phosphate anions on NDPs and NTPs form stable complexes with divalent cations such as Mg^{2+} and Ca^{2+}. Because Mg^{2+} is present at high concentrations (5 to 10 mM) intracellularly, NDPs and NTPs occur primarily as Mg^{2+} complexes in the cell. The phosphoric anhydride linkages in NDPs and NTPs are readily hydrolyzed by acid, liberating inorganic phosphate (often symbolized as P_i) and the corresponding NMP. A diagnostic test for NDPs and NTPs is quantitative liberation of P_i upon treatment with 1 N HCl at 100°C for 7 min.

Nucleoside 5′-Triphosphates Are Carriers of Chemical Energy

Nucleoside 5′-triphosphates are indispensable agents in metabolism because the phosphoric anhydride bonds they possess are a prime source of chemical energy to do biological work. ATP has been termed the energy currency of the cell (Chapter 3). GTP is the major energy source for protein synthesis (see Chapter 33), CTP is an essential metabolite in phospholipid synthesis (see Chapter 25), and UTP forms activated intermediates with sugars that go on to serve as substrates in the biosynthesis of complex carbohydrates and polysaccharides (see Chapter 23). The evolution of metabolism has led to the dedication of one of these four NTPs to each of the major branches of metabolism. To complete the picture, the four NTPs and their dNTP counterparts are the substrates for the synthesis of the remaining great class of biomolecules—the nucleic acids.

The Bases of Nucleotides Serve as "Information Symbols"

Virtually all of the biochemical reactions of nucleotides involve either *phosphate* or *pyrophosphate group transfer:* the release of a phosphoryl group from an NTP to give an NDP, the release of a pyrophosphoryl group to give an NMP unit, or the acceptance of a phosphoryl group by an NMP or an NDP to give an NDP or an NTP (Figure 11.16). Interestingly, the pentose and the base are *not*

FIGURE 11.16 • Phosphoryl and pyrophosphoryl group transfer, the major biochemical reactions of nucleotides.
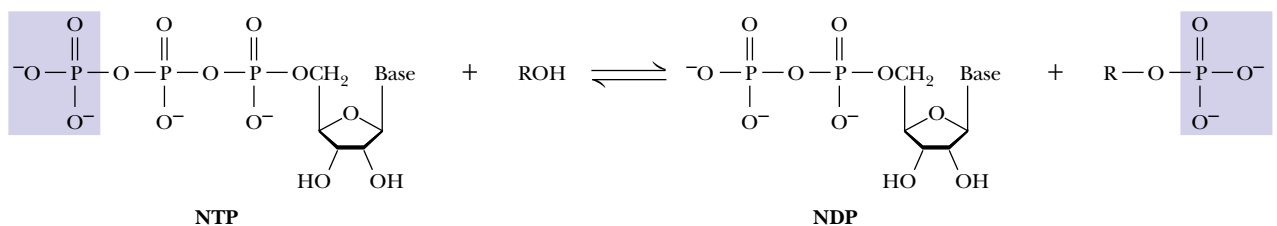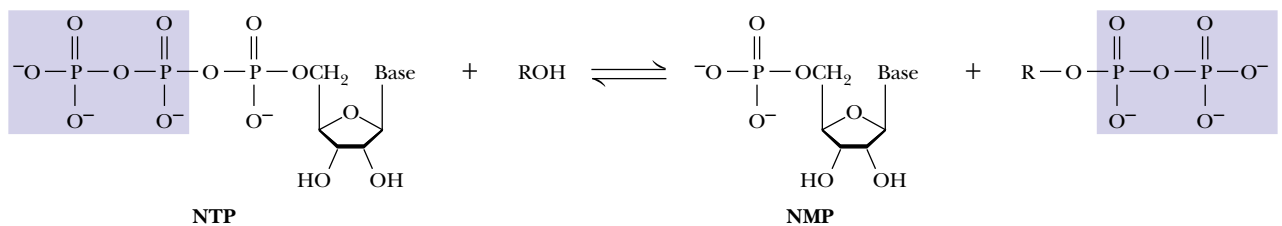
directly involved in this chemistry. However, a "division of labor" directs ATP to serve as the primary nucleotide in central pathways of energy metabolism, while GTP, for example, is used to drive protein synthesis. Thus, the various nucleotides are channeled in appropriate metabolic directions through specific recognition of the base of the nucleotide. That is, the bases of nucleotides serve solely as *information symbols* aloof from the covalent bond chemistry that goes on. This role as information symbols extends to nucleotide polymers, the nucleic acids, where the bases serve as the information symbols for the code of genetic information.

11.5 • Nucleic Acids Are Polynucleotides

Nucleic acids are linear polymers of nucleotides linked 3′ to 5′ by **phosphodiester bridges** (Figure 11.17). They are formed as 5′-nucleoside monophosphates are successively added to the 3′-OH group of the preceding nucleotide, a process that gives the polymer a directional sense. Polymers of ribonucleotides are named **ribonucleic acid,** or **RNA.** Deoxyribonucleotide polymers are called **deoxyribonucleic acid,** or **DNA.** Because C-1′ and C-4′ in deoxyribonucleotides are involved in furanose ring formation and because there is no 2′-OH, only
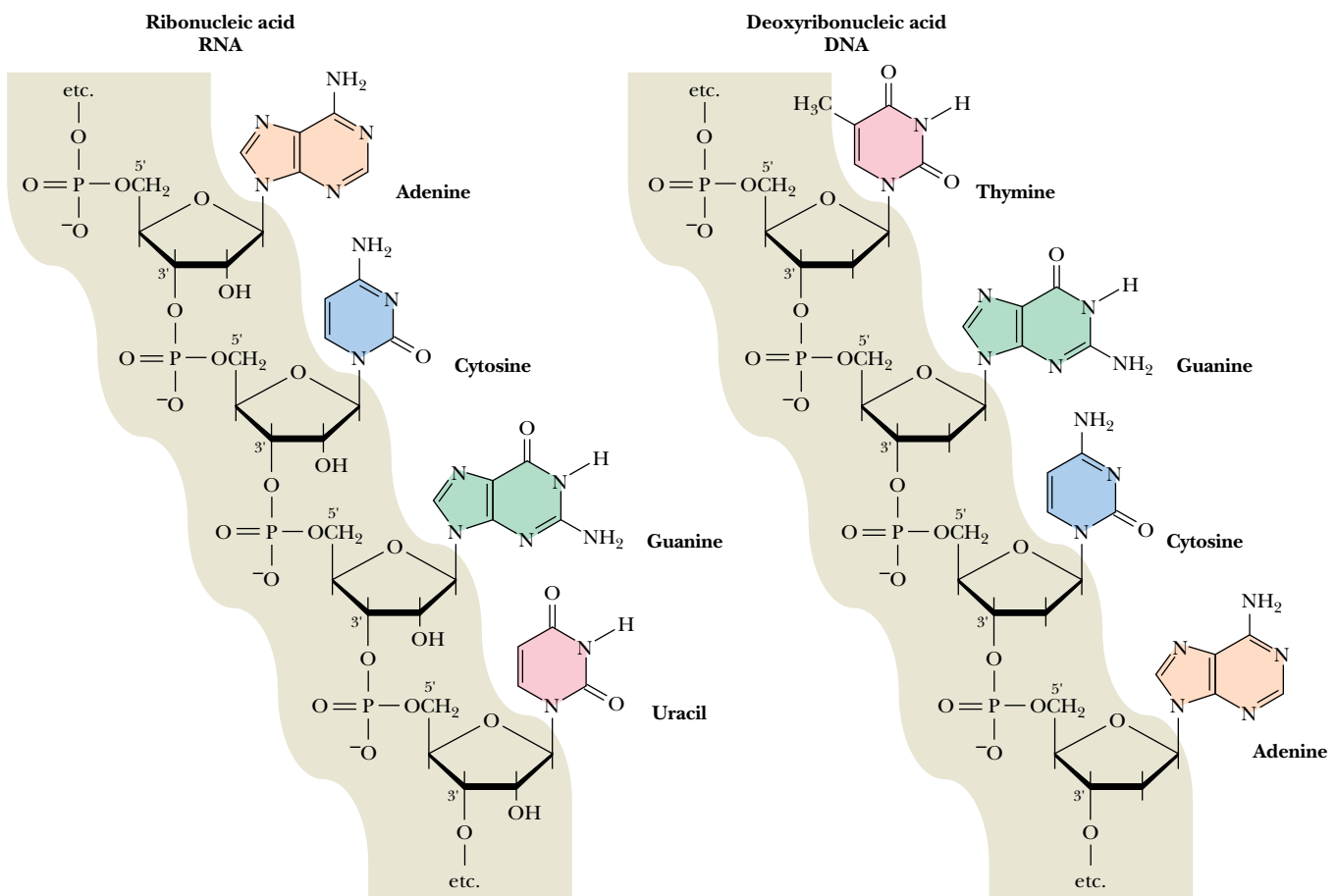
FIGURE 11.17 • 3′-5′ phosphodiester bridges link nucleotides together to form polynucleotide chains.

the 3'- and 5'-hydroxyl groups are available for internucleotide phosphodiester bonds. In the case of DNA, a polynucleotide chain may contain hundreds of millions of nucleotide units. Any structural representation of such molecules would be cumbersome at best, even for a short oligonucleotide stretch.

Shorthand Notations for Polynucleotide Structures

Several conventions have been adopted to convey the sense of polynucleotide structures. A repetitious uniformity exists in the covalent backbone of polynucleotides, in which the chain can be visualized as running from 5' to 3' along the atoms of one furanose and thence across the phosphodiester bridge to the furanose of the next nucleotide in line. Thus, this backbone can be portrayed by the symbol of a vertical line representing the furanose and a slash representing the phosphodiester link, as shown in Figure 11.18. The diagonal slash runs from the middle of a furanose line to the bottom of an adjacent one to indicate the 3'- (middle) to 5'- (bottom) carbons of neighboring furanoses joined by the phosphodiester bridge. The base attached to each furanose is indicated above it by a one-letter designation: A, C, G, or U (or T). *The convention in all notations of nucleic acid structure is to read the polynucleotide chain from the 5'-end of the polymer to the 3'-end.* Note that this reading direction actually passes through each phosphodiester from 3' to 5'.

Base Sequence

The only significant variation that commonly occurs in the chemical structure of nucleic acids is the nature of the base at each nucleotide position. These bases are not part of the sugar–phosphate backbone but instead serve as distinctive side chains, much like the R groups of amino acids along a polypeptide backbone. They give the polymer its unique identity. A simple notation of these structures is merely to list the order of bases in the polynucleotide using single capital letters—A, G, C, and U (or T). Occasionally, a lowercase "p" is written between each successive base to indicate the phosphodiester bridge, as in GpApCpGpUpA. A "p" preceding the sequence indicates that the nucleic acid carries a PO_4 on its 5'-end, as in pGpApCpGpUpA; a "p" terminating the sequence connotes the presence of a phosphate on the 3'-OH end, as in GpApCpGpUpAp.

   A more common method of representing nucleotide sequences is to omit the "p" and write only the order of bases, such as GACGUA. This notation assumes the presence of the phosphodiesters joining adjacent nucleotides. The presence of 3'- or 5'-phosphate termini, however, must still be specified, as in GACGUAp for a 3'-PO_4 terminus. To distinguish between RNA and DNA sequences, DNA sequences are typically preceded by a lowercase "d" to denote deoxy, as in d-GACGTA. From a simple string of letters such as this, any biochemistry student should be able to draw the unique chemical structure for a pentanucleotide, even though it may contain over 200 atoms.
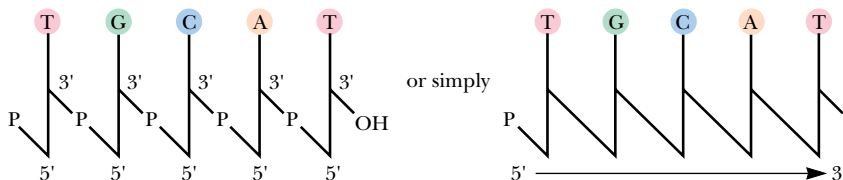
FIGURE 11.18 • Furanoses are represented by lines; phosphodiesters are represented by diagonal slashes in this shorthand notation for nucleic acid structures.

11.6 • Classes of Nucleic Acids

The two major classes of nucleic acids are DNA and RNA. DNA has only one biological role, but it is the more central one. The information to make all the functional macromolecules of the cell (even DNA itself) is preserved in DNA and accessed through transcription of the information into RNA copies. Coincident with its singular purpose, there is only a single DNA molecule (or "chromosome") in simple life forms such as viruses or bacteria. Such DNA molecules must be quite large in order to embrace enough information for making the macromolecules necessary to maintain a living cell. The *Escherichia coli* chromosome has a molecular mass of 2.9×10^9 D and contains over 9 million nucleotides. Eukaryotic cells have many chromosomes, and DNA is found principally in two copies in the diploid chromosomes of the nucleus, but it also occurs in mitochondria and in chloroplasts, where it encodes some of the proteins and RNAs unique to these organelles.

In contrast, RNA occurs in multiple copies and various forms (Table 11.2). Cells contain up to eight times as much RNA as DNA. RNA has a number of important biological functions, and on this basis, RNA molecules are categorized into several major types: **messenger RNA, ribosomal RNA,** and **transfer RNA.** Eukaryotic cells contain an additional type, **small nuclear RNA (snRNA).** With these basic definitions in mind, let's now briefly consider the chemical and structural nature of DNA and the various RNAs. Chapter 12 elaborates on methods to determine the primary structure of nucleic acids by sequencing methods and discusses the secondary and tertiary structures of DNA and RNA. Part IV, Information Transfer, includes a detailed treatment of the dynamic role of nucleic acids in the molecular biology of the cell.

DNA

The DNA isolated from different cells and viruses characteristically consists of two polynucleotide strands wound together to form a long, slender, helical molecule, the **DNA double helix.** The strands run in opposite directions; that is, they are *antiparallel* and are held together in the double helical structure through *interchain hydrogen bonds* (Figure 11.19). These H bonds pair the bases of nucleotides in one chain to complementary bases in the other, a phenomenon called **base pairing.**

Table 11.2

Various Kinds of RNA Found in an *E. coli* Cell				
Type	Sedimentation Coefficient	Molecular Weight	Number of Nucleotide Residues	Percentage of Total Cell RNA
mRNA	6–25	25,000–1,000,000	75–3,000	~2
tRNA	~4	23,000–30,000	73–94	16
rRNA	5	35,000	120 ⎫	
	16	550,000	1542 ⎬	82
	23	1,100,000	2904 ⎭	

Segment of unwound double helix
illustrating the antiparallel orientation
of the complementary strands
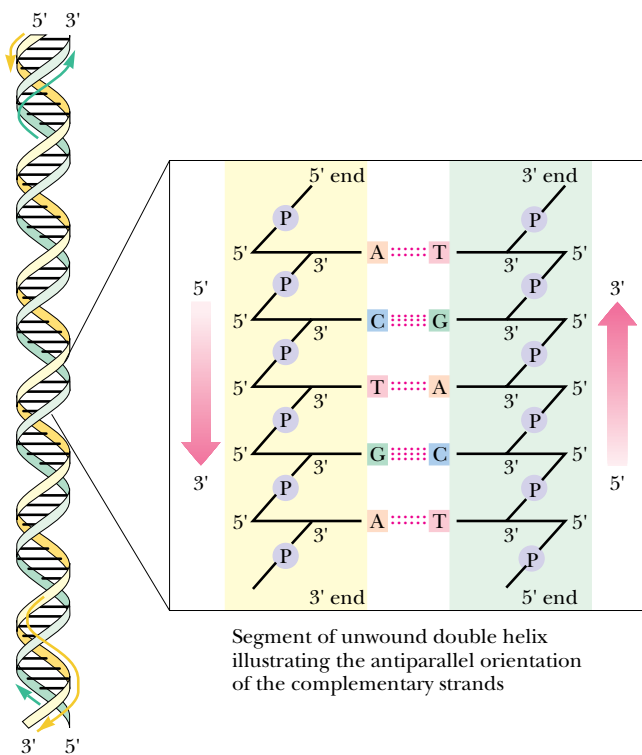
FIGURE 11.19 • The antiparallel nature of the DNA double helix.

Chargaff's Rules

A clue to the chemical basis of base pairing in DNA came from the analysis of the base composition of various DNAs by Erwin Chargaff in the late 1940s. His data showed that the four bases commonly found in DNA (A, C, G, and T) do not occur in equimolar amounts and that the relative amounts of each vary from species to species (Table 11.3). Nevertheless, Chargaff noted that certain pairs of bases, namely, adenine and thymine, and guanine and cytosine, are

Table 11.3

Molar Ratios Leading to the Formulation of Chargaff's Rules					
Source	Adenine to Guanine	Thymine to Cytosine	Adenine to Thymine	Guanine to Cytosine	Purines to Pyrimidines
Ox	1.29	1.43	1.04	1.00	1.1
Human	1.56	1.75	1.00	1.00	1.0
Hen	1.45	1.29	1.06	0.91	0.99
Salmon	1.43	1.43	1.02	1.02	1.02
Wheat	1.22	1.18	1.00	0.97	0.99
Yeast	1.67	1.92	1.03	1.20	1.0
Hemophilus influenzae	1.74	1.54	1.07	0.91	1.0
E. coli K-12	1.05	0.95	1.09	0.99	1.0
Avian tubercle bacillus	0.4	0.4	1.09	1.08	1.1
Serratia marcescens	0.7	0.7	0.95	0.86	0.9
Bacillus schatz	0.7	0.6	1.12	0.89	1.0

Source: After Chargaff, E., 1951. *Federation Proceedings* **10:**654–659.
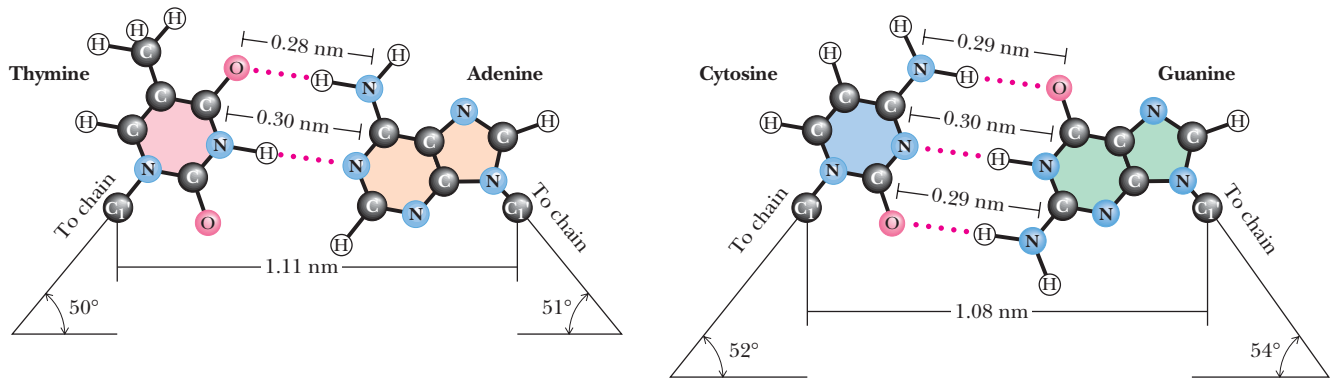
FIGURE 11.20 • The Watson–Crick base pairs A : T and G : C.
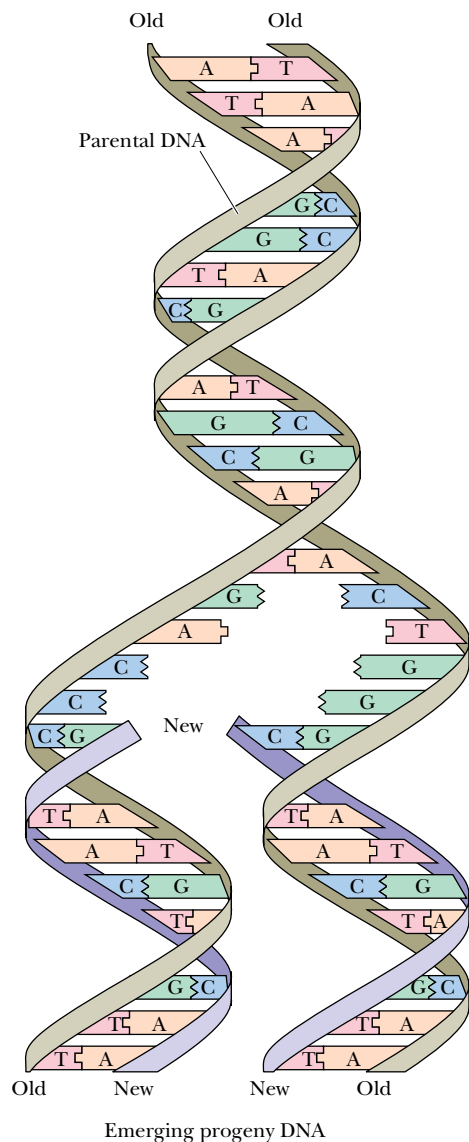
FIGURE 11.21 • Replication of DNA gives identical progeny molecules because base pairing is the mechanism determining the nucleotide sequence synthesized within each of the new strands during replication.

always found in a 1:1 ratio and that the number of pyrimidine residues always equals the number of purine residues. These findings are known as *Chargaff's rules:* **[A] = [T]; [C] = [G]; [pyrimidines] = [purines].**

Watson and Crick's Double Helix

James Watson and Francis Crick, working in the Cavendish Laboratory at Cambridge University in 1953, took advantage of Chargaff's results and the data obtained by Rosalind Franklin and Maurice Wilkins in X-ray diffraction studies on the structure of DNA to conclude that DNA was a *complementary double helix.* Two strands of deoxyribonucleic acid (sometimes referred to as the *Watson strand* and the *Crick strand*) are held together by hydrogen bonds formed between unique base pairs, always consisting of a purine in one strand and a pyrimidine in the other. Base pairing is very specific: if the purine is adenine, the pyrimidine must be thymine. Similarly, guanine pairs only with cytosine (Figure 11.20). Thus, if an A occurs in one strand of the helix, T must occupy the complementary position in the opposing strand. Likewise, a G in one dictates a C in the other. Because exceptions to this exclusive pairing of A only with T and G only with C are rare, these pairs are taken as the standard or accepted law, and the A:T and G:C base pairs are often referred to as canonical. As Watson recognized from testing various combinations of bases using structurally accurate models, the A:T pair and the G:C pair form spatially equivalent units (Figure 11.20). The backbone-to-backbone distance of an A:T pair is 1.11 nm, virtually identical to the 1.08 nm chain separation in G:C base pairs.

The DNA molecule not only conforms to Chargaff's rules but also has a profound property relating to heredity: *The sequence of bases in one strand has a complementary relationship to the sequence of bases in the other strand.* That is, the information contained in the sequence of one strand is conserved in the sequence of the other. Therefore, separation of the two strands and faithful replication of each, through a process in which base pairing specifies the nucleotide sequence in the newly synthesized strand, leads to two progeny molecules identical in every respect to the parental double helix (Figure 11.21). Elucidation of the double helical structure of DNA represented one of the most significant events in the history of science. This discovery more than any other marked the beginning of molecular biology. Indeed, upon solving the structure of DNA, Crick proclaimed in The Eagle, a pub just across from the Cavendish lab, "We have discovered the secret of life!"
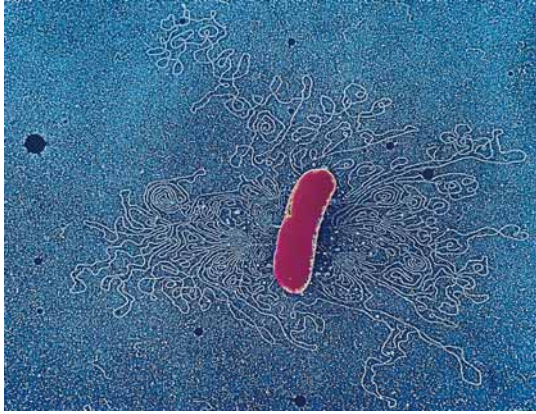
FIGURE 11.22 • If the cell walls of bacteria such as *Escherichia coli* are partially digested and the cells are then osmotically shocked by dilution with water, the contents of the cells are extruded to the exterior. In electron micrographs, the most obvious extruded component is the bacterial chromosome, shown here surrounding the cell. *(Dr. Gopal Murti/CNRI/Phototake NYC)*

Size of DNA Molecules

Because of the double helical nature of DNA molecules, their size can be represented in terms of the numbers of nucleotide base pairs they contain. For example, the *E. coli* chromosome consists of 4.64×10^6 base pairs (abbreviated bp) or 4.64×10^3 kilobase pairs (kbp). DNA is a threadlike molecule. The diameter of the DNA double helix is only 2 nm, but the length of the DNA molecule forming the *E. coli* chromosome is over 1.6×10^6 nm (1.6 mm). Because the long dimension of an *E. coli* cell is only 2000 nm (0.002 mm), its chromosome must be highly folded. Because of their long, threadlike nature, DNA molecules are easily sheared into shorter fragments during isolation procedures, and it is difficult to obtain intact chromosomes even from the simple cells of prokaryotes.

DNA in the Form of Chromosomes

DNA occurs in various forms in different cells. The single chromosome of prokaryotic cells (Figure 11.22) is typically a circular DNA molecule. Relatively little protein is associated with prokaryotic chromosomes. In contrast, the DNA molecules of eukaryotic cells, each of which defines a chromosome, are linear and richly adorned with proteins. A class of arginine- and lysine-rich basic proteins called **histones** interact ionically with the anionic phosphate groups in the DNA backbone to form **nucleosomes,** structures in which the DNA double helix is wound around a protein "core" composed of pairs of four different histone polypeptides (Figure 11.23; see also Section 12.5 in Chapter 12). Chromosomes also contain a varying mixture of other proteins, so-called **nonhistone chromosomal proteins,** many of which are involved in regulating which genes in DNA are transcribed at any given moment. The amount of DNA in a diploid mammalian cell is typically more than 1000 times that found in an *E. coli* cell. Some higher plant cells contain more than 50,000 times as much.

RNA

Messenger RNA

Messenger RNA **(mRNA)** serves to carry the information or "message" that is encoded in genes to the sites of protein synthesis in the cell, where this information is translated into a polypeptide sequence. Because mRNA molecules are transcribed copies of the protein-coding genetic units that comprise most of DNA, mRNA is said to be "the DNA-like RNA."

Histone "core" octamer
(here shown in cross section)
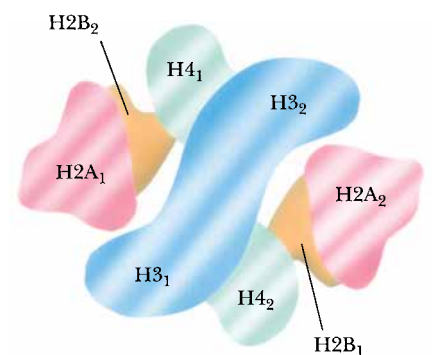
Nucleosome
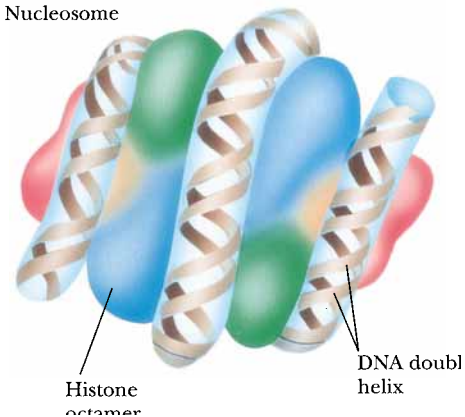
FIGURE 11.23 • A diagram of the histone octamer. Nucleosomes consist of two turns of DNA supercoiled about a histone "core" octamer.

Messenger RNA is synthesized during **transcription,** an enzymatic process in which an RNA copy is made of the sequence of bases along one strand of DNA. This mRNA then directs the synthesis of a polypeptide chain as the information that is contained within its nucleotide sequence is translated into an amino acid sequence by the protein-synthesizing machinery of the ribosomes. Ribosomal RNA and tRNA molecules are also synthesized by transcription of DNA sequences, but unlike mRNA molecules, these RNAs are not subsequently translated to form proteins. Only the genetic units of DNA sequence that encode proteins are transcribed into mRNA molecules. In prokaryotes, a single mRNA may contain the information for the synthesis of several polypeptide chains within its nucleotide sequence (Figure 11.24). In contrast, eukaryotic mRNAs encode only one polypeptide, but are more complex in that they are synthesized in the nucleus in the form of much larger precursor molecules called **heterogeneous nuclear RNA,** or **hnRNA.** hnRNA molecules contain stretches of nucleotide sequence that have no protein-coding capacity. These
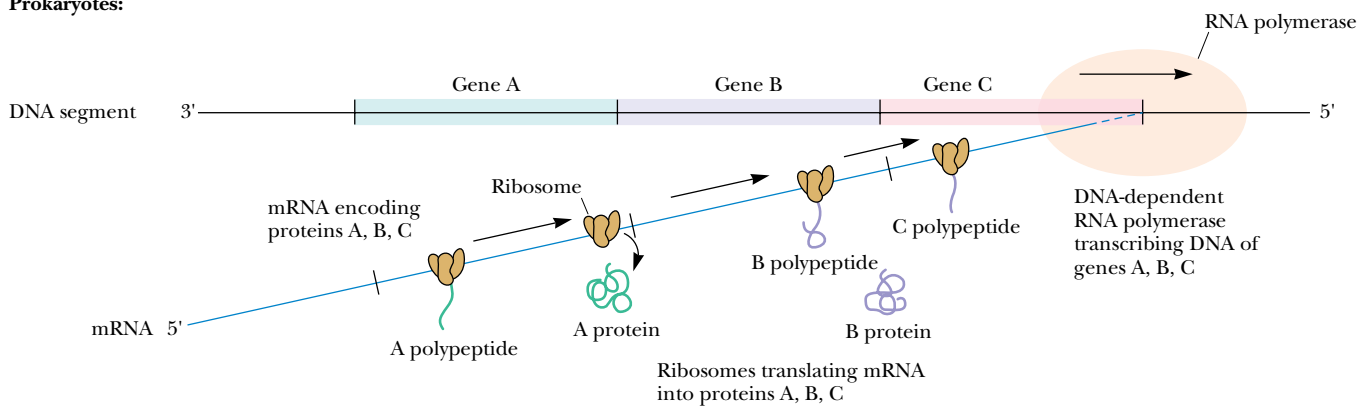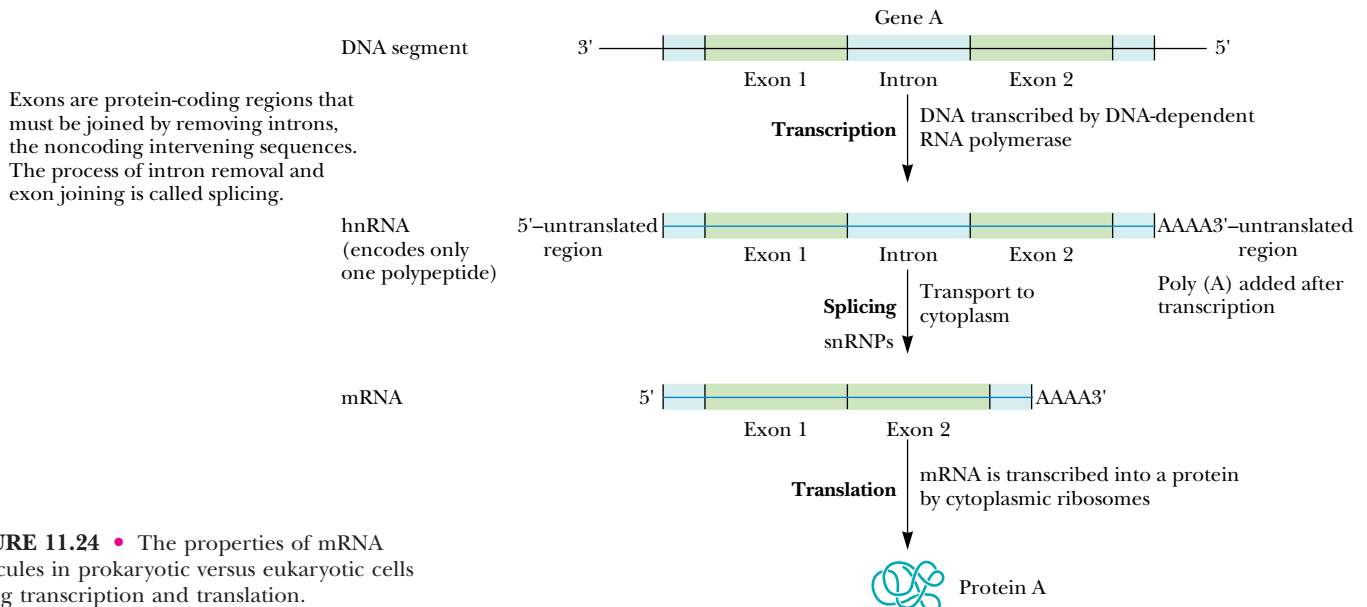
FIGURE 11.24 • The properties of mRNA molecules in prokaryotic versus eukaryotic cells during transcription and translation.

noncoding regions are called **intervening sequences** or **introns** because they intervene between coding regions, which are called **exons.** Introns interrupt the continuity of the information specifying the amino acid sequence of a protein and must be spliced out before the message can be translated. In addition, eukaryotic hnRNA and mRNA molecules have a run of 100 to 200 adenylic acid residues attached at their 3′-ends, so-called **poly(A) tails.** This polyadenylylation occurs after transcription has been completed and is believed to contribute to mRNA stability. The properties of messenger RNA molecules as they move through transcription and translation in prokaryotic versus eukaryotic cells are summarized in Figure 11.24.

Ribosomal RNA
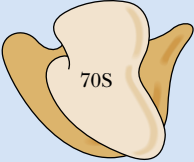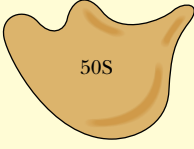
Ribosomes, the supramolecular assemblies where protein synthesis occurs, are about 65% RNA of the ribosomal RNA type. Ribosomal RNA **(rRNA)** molecules fold into characteristic secondary structures as a consequence of intramolecular hydrogen bond interactions (marginal figure). The different species of rRNA are generally referred to according to their **sedimentation coefficients**[1] (see the Appendix to Chapter 5), which are a rough measure of their relative size (Table 11.2 and Figure 11.25).

Ribosomes are composed of two subunits of different sizes that dissociate from each other if the Mg^{2+} concentration is below 10^{-3} *M*. Each subunit is
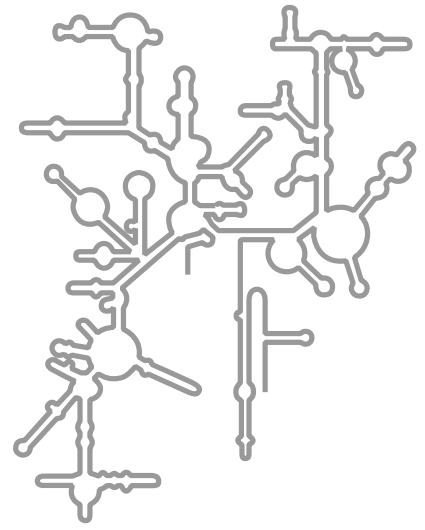
Ribosomal RNA has a complex secondary structure due to many intrastrand hydrogen bonds.

PROKARYOTIC RIBOSOMES (*E.coli*)			EUKARYOTIC RIBOSOMES (Rat)		
Ribosome			**Ribosome**		
$(2.52 \times 10^6 \text{ D})$	70S		$(4.22 \times 10^6 \text{ D})$	80S	
Subunits			**Subunits**		
	30S	50S		40S	60S
	$(0.93 \times 10^6 \text{ D})$	$(1.59 \times 10^6 \text{ D})$		$(1.4 \times 10^6 \text{ D})$	$(2.82 \times 10^6 \text{ D})$
RNA	16S RNA (1542 nucleotides)	23S RNA (2904 nucleotides)	**RNA**	18S RNA (1874 nucleotides)	28S + 5.85 RNA (4718 + 160 nucleotides)
		5S RNA (120 nucleotides)			5S RNA (120 nucleotides)
Protein			**Protein**		
	21 proteins	31 proteins		33 proteins	49 proteins

FIGURE 11.25 • The organization and composition of prokaryotic and eukaryotic ribosomes.

[1]Sedimentation coefficients are a measure of the velocity with which a particle sediments in a centrifugal force field. Sedimentation coefficients are typically expressed in **Svedbergs** (symbolized S), named to honor The Svedberg, developer of the ultracentrifuge. One S equals 10^{-13} sec.

4-Thiouridine (S⁴U) **4-Thiouridine (S^4U)**   **Inosine**   **1-Methylguanosine (m^1G)**   **N^6-Isopentenyladenosine (i^6A)**

Ribothymidine (T)   **Pseudouridine (ψ)**   **Dihydrouridine (D)**
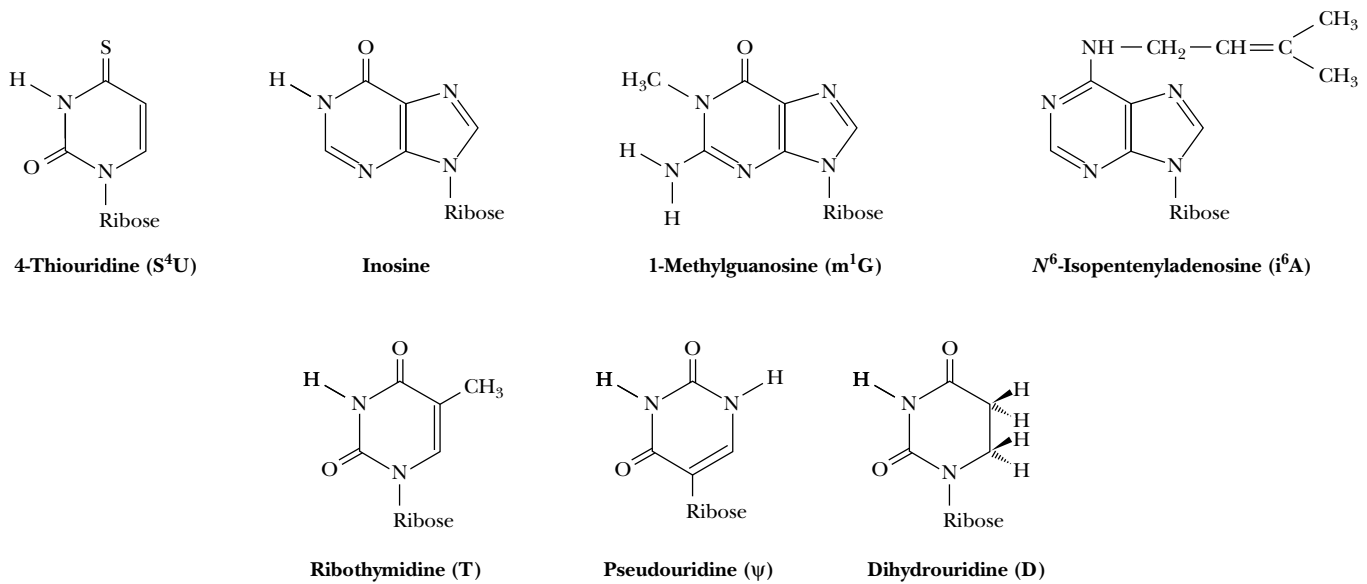
FIGURE 11.26 • Unusual bases of RNA—pseudouridine, ribothymidylic acid, and various methylated bases.

a supramolecular assembly of proteins and RNA and has a total mass of 10^6 daltons or more. *E. coli* ribosomal subunits have sedimentation coefficients of 30S (the small subunit) and 50S (the large subunit). Eukaryotic ribosomes are somewhat larger than prokaryotic ribosomes, consisting of 40S and 60S subunits. The properties of ribosomes and their rRNAs are summarized in Figure 11.25. The 30S subunit of *E. coli* contains a single RNA chain of 1542 nucleotides. This small subunit rRNA itself has a sedimentation coefficient of 16S. The large *E. coli* subunit has two rRNA molecules, a 23S (2904 nucleotides) and a 5S (120 nucleotides). The ribosomes of a typical eukaryote, the rat, have rRNA molecules of 18S (1874 nucleotides) and 28S (4718 bases), 5.8S (160 bases), and 5S (120 bases). The 18S rRNA is in the 40S subunit and the latter three are all part of the 60S subunit.

Ribosomal RNAs characteristically contain a number of specially modified nucleotides, including **pseudouridine** residues, **ribothymidylic acid,** and **methylated bases** (Figure 11.26). The central role of ribosomes in the biosynthesis of proteins is treated in detail in Chapter 33. Here we briefly note the significant point that genetic information in the nucleotide sequence of an mRNA is translated into the amino acid sequence of a polypeptide chain by ribosomes.

Transfer RNA

Transfer RNA **(tRNA)** serves as a carrier of amino acid residues for protein synthesis. Transfer RNA molecules also fold into a characteristic secondary structure (marginal figure). The amino acid is attached as an aminoacyl ester to the 3′-terminus of the tRNA. Aminoacyl-tRNAs are the substrates for protein biosynthesis. The tRNAs are the smallest RNAs (size range—23 to 30 kD) and contain 73 to 94 residues, a substantial number of which are methylated or otherwise unusually modified. Transfer RNA derives its name from its role as the carrier of amino acids during the process of protein synthesis (see Chapters 32 and 33). Each of the 20 amino acids of proteins has at least one unique tRNA species dedicated to chauffeuring its delivery to ribosomes for insertion into growing polypeptide chains, and some amino acids are served by several tRNAs. For example, five different tRNAs act in the transfer of leucine into
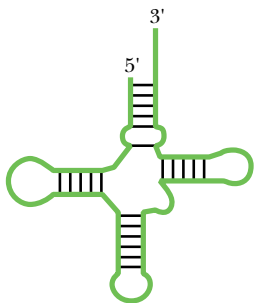
Transfer RNA also has a complex secondary structure due to many intrastrand hydrogen bonds.

proteins. In eukaryotes, there are even discrete sets of tRNA molecules for each site of protein synthesis—the cytoplasm, the mitochondrion, and, in plant cells, the chloroplast. All tRNA molecules possess a 3′-terminal nucleotide sequence that reads **-CCA,** and the amino acid is carried to the ribosome attached as an acyl ester to the free 3′-OH of the terminal A residue. These **aminoacyl-tRNAs** are the substrates of protein synthesis, the amino acid being transferred to the carboxyl end of a growing polypeptide. The peptide bond-forming reaction is a catalytic process intrinsic to ribosomes.

Small Nuclear RNAs

Small nuclear RNAs, or **snRNAs,** are a class of RNA molecules found in eukaryotic cells, principally in the nucleus. They are neither tRNA nor small rRNA molecules, although they are similar in size to these species. They contain from 100 to about 200 nucleotides, some of which, like tRNA and rRNA, are methylated or otherwise modified. No snRNA exists as naked RNA. Instead, snRNA is found in stable complexes with specific proteins forming **small nuclear ribonucleoprotein particles,** or **snRNPs,** which are about 10S in size. Their occurrence in eukaryotes, their location in the nucleus, and their relative abundance (1 to 10% of the number of ribosomes) are significant clues to their biological purpose: snRNPs are important in the processing of eukaryotic gene transcripts (hnRNA) into mature messenger RNA for export from the nucleus to the cytoplasm (Figure 11.24).

Significance of Chemical Differences Between DNA and RNA

Two fundamental chemical differences distinguish DNA from RNA:

1. DNA contains 2-deoxyribose instead of ribose.
2. DNA contains thymine instead of uracil.

What are the consequences of these differences and do they hold any significance in common? An argument can be made that, because of these differences, DNA is a more stable polymeric form than RNA. The greater stability of DNA over RNA is consistent with the respective roles these macromolecules have assumed in heredity and information transfer.

   Consider first why DNA contains thymine instead of uracil. The key observation is that *cytosine deaminates to form uracil* at a finite rate *in vivo* (Figure 11.27). Because C in one DNA strand pairs with G in the other strand, whereas U would pair with A, conversion of a C to a U could potentially result in a heritable change of a CG pair to a UA pair. Such a change in nucleotide sequence would constitute a *mutation* in the DNA. To prevent this reaction from leading to changes in nucleotide sequence, a cellular repair mechanism "proofreads" DNA, and when a U arising from C deamination is encountered, it is treated as inappropriate and is replaced by a C. If DNA normally contained U rather than T, this repair system could not readily distinguish U formed by C deamination from U correctly paired with A. However, the U in DNA is "5-methyl-U" or, as it is conventionally known, thymine (Figure 11.28). That is, the 5-methyl group on T labels it as if to say "this U belongs; do not replace it."

   The ribose 2′-OH group of RNA is absent in DNA. Consequently, the ubiquitous 3′-O of polynucleotide backbones lacks a vicinal hydroxyl neighbor in DNA. This difference leads to a greater resistance of DNA to alkaline hydrolysis, examined in detail in the following section. To view it another way, RNA is less stable than DNA because its vicinal 2′-OH group makes the 3′-phosphodiester bond susceptible to nucleophilic cleavage (Figure 11.29). For just this reason, it is selectively advantageous for the heritable form of genetic information to be DNA rather than RNA.
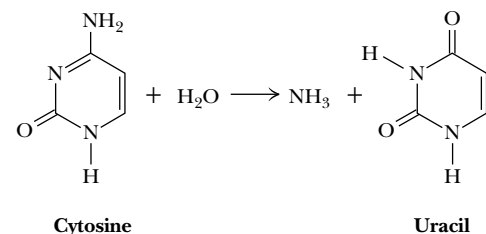

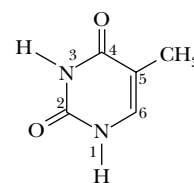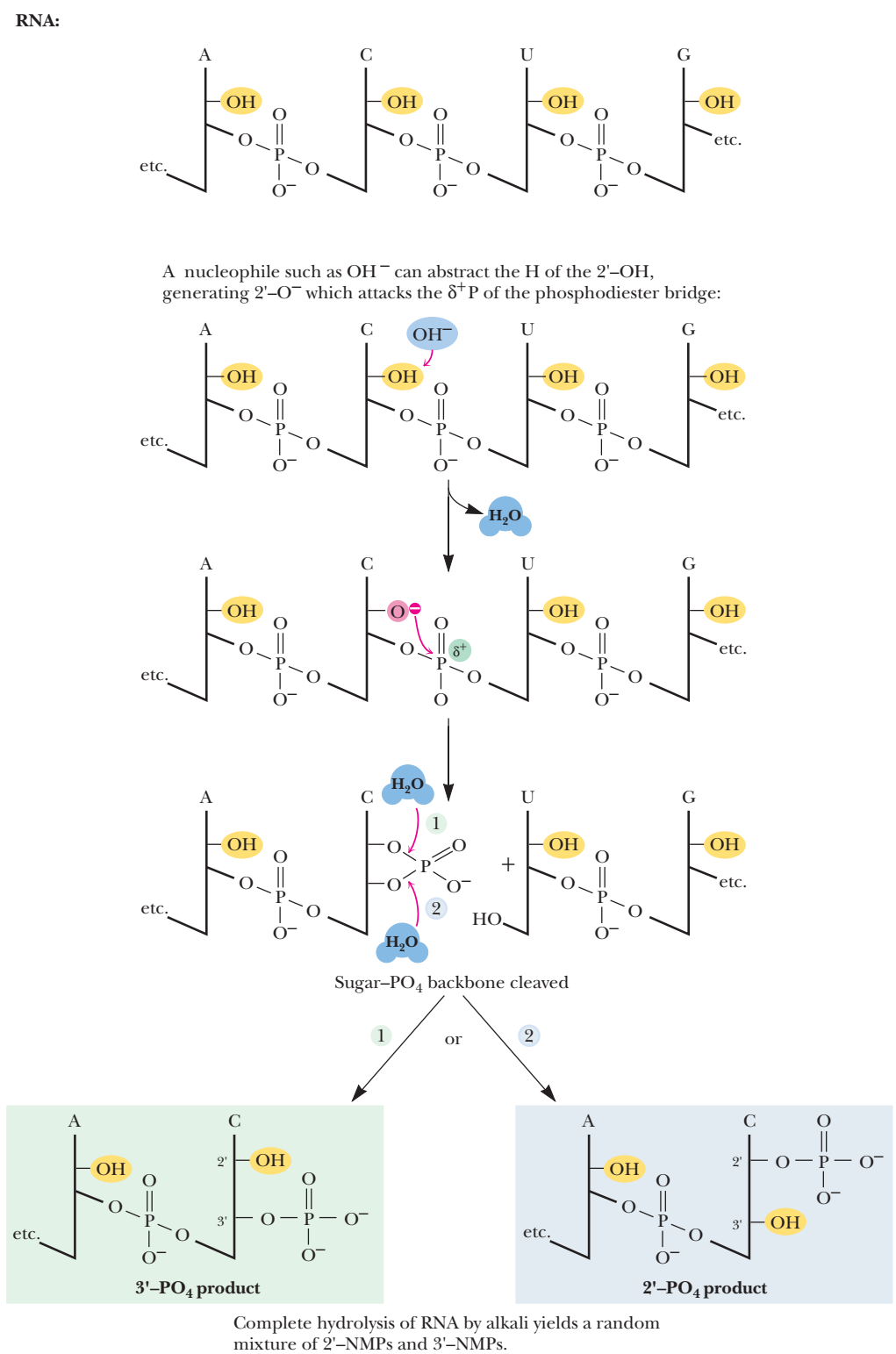**FIGURE 11.27 •** Deamination of cytosine forms uracil.
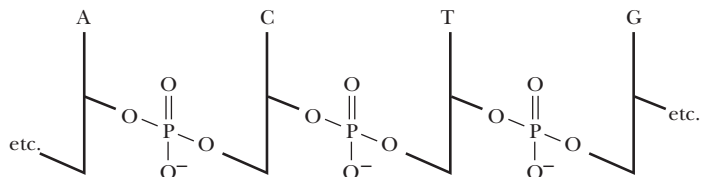

FIGURE 11.28 • The 5-methyl group on thymine labels it as a special kind of uracil.

FIGURE 11.29 • The vicinal —OH groups of RNA are susceptible to nucleophilic attack leading to hydrolysis of the phosphodiester bond and fracture of the polynucleotide chain; DNA lacks a 2'-OH vicinal to its 3'-O-phosphodiester backbone. Alkaline hydrolysis of RNA results in the formation of a mixture of 2'- and 3'-nucleoside monophosphates.

RNA:

A nucleophile such as OH^- can abstract the H of the 2'–OH, generating 2'–O^- which attacks the δ^+P of the phosphodiester bridge:

Sugar–PO_4 backbone cleaved

1 or **2**

3'–PO₄ product

2'–PO₄ product

Complete hydrolysis of RNA by alkali yields a random mixture of 2'–NMPs and 3'–NMPs.

DNA: no 2'– OH; resistant to OH^-:

346

𝒜 D E E P E R L O O K

Peptide Nucleic Acids (PNAs) Are Synthetic Mimics of DNA and RNA

Synthetic chemists have invented analogs of DNA (and RNA) in which the sugar–phosphate backbone is replaced by a peptide backbone, creating a polymer appropriately termed a *peptide nucleic acid,* or *PNA*. The PNA peptide backbone was designed so that the space between successive bases was the same as in natural DNA (see figure). PNA consists of repeating units of *N*-(2-aminoethyl)-glycine residues linked by peptide bonds; the bases are attached to this backbone through methylene carbonyl linkages. This chemistry provides six bonds along the backbone between bases and three bonds between the backbone and each base, just like natural DNA. PNA oligomers interact with DNA (and RNA) through specific base-pairing interactions, just as would be expected for a pair of complementary oligonucleotides. PNAs are resistant to nucleases and also are poor substrates for proteases. PNAs thus show great promise as specific diagnostic probes for unique DNA or RNA nucleotide sequences. PNAs also have potential application as antisense drugs (see problem 5 in the end-of-chapter problems).
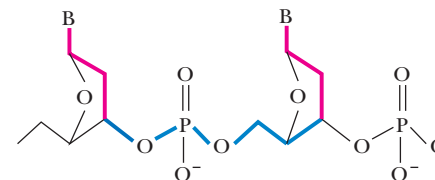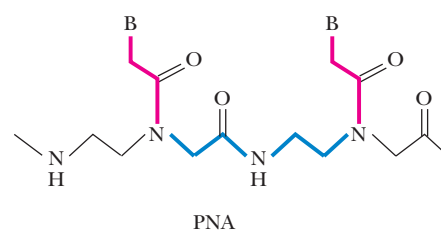
Note the repeating six bonds (in bold) between base attachments and the three-bond linker between base (B) and backbone.

Buchardt, O., et al., 1993. Peptide nucleic acids and their potential applications in biotechnology. *Trends in Biotechnology* **11:***384–386.*

11.7 • Hydrolysis of Nucleic Acids

Most reactions of nucleic acid hydrolysis break bonds in the polynucleotide backbone. Such reactions are important because they can be used to manipulate these polymeric molecules. For example, hydrolysis of polynucleotides generates smaller fragments whose nucleotide sequence can be more easily determined.

Hydrolysis by Acid or Base

RNA is relatively resistant to the effects of dilute acid, but gentle treatment of DNA with 1 mM HCl leads to hydrolysis of purine glycosidic bonds and the loss of purine bases from the DNA. The glycosidic bonds between pyrimidine bases and 2′-deoxyribose are not affected, and, in this case, the polynucleotide's sugar–phosphate backbone remains intact. The purine-free polynucleotide product is called **apurinic acid.**

DNA is not susceptible to alkaline hydrolysis. On the other hand, RNA is alkali labile and is readily hydrolyzed by dilute sodium hydroxide. Cleavage is random in RNA, and the ultimate products are a mixture of nucleoside 2′- and 3′-monophosphates. These products provide a clue to the reaction mechanism (Figure 11.29). Abstraction of the 2′-OH hydrogen by hydroxyl anion leaves a 2′-O$^-$ that carries out a nucleophilic attack on the δ^+ phosphorus atom of the phosphate moiety, resulting in cleavage of the 5′-phosphodiester bond and formation of a cyclic 2′,3′-phosphate. This cyclic 2′,3′-phosphodiester is unstable and decomposes randomly to either a 2′- or 3′-phosphate ester. DNA has no 2′-OH; therefore DNA is alkali stable.

Enzymatic Hydrolysis

Enzymes that hydrolyze nucleic acids are called **nucleases.** Virtually all cells contain various nucleases that serve important housekeeping roles in the normal course of nucleic acid metabolism. Organs that provide digestive fluids, such as the pancreas, are rich in nucleases and secrete substantial amounts to hydrolyze ingested nucleic acids. Fungi and snake venom are often good sources of nucleases. As a class, nucleases are **phosphodiesterases** because the reaction that they catalyze is the cleavage of phosphodiester bonds by H_2O. Because each internal phosphate in a polynucleotide backbone is involved in two phosphoester linkages, cleavage can potentially occur on either side of the phosphorus (Figure 11.30). Convention labels the 3′-side as *a* and the 5′-side as *b*. Cleavage on the *a* side leaves the phosphate attached to the 5′-position of the adjacent nucleotide, while *b*-side hydrolysis yields 3′-phosphate products. Enzymes or reactions that hydrolyze nucleic acids are characterized as acting at either *a* or *b*. A second convention denotes whether the nucleic acid chain was cleaved at some internal location, *endo,* or whether a terminal nucleotide residue was hydrolytically removed, *exo.* Note that exo *a* cleavage characteristically occurs at the 3′-end of the polymer, whereas exo *b* cleavage involves attack at the 5′-terminus (Figure 11.31).

Nuclease Specificity

Like most enzymes (see Chapter 14), nucleases exhibit selectivity or *specificity* for the nature of the substance on which they act. That is, some nucleases act only on DNA **(DNases),** while others are specific for RNA (the **RNases**). Still

Convention: The 3'-side of each phosphodiester is termed *a*; the 5'-side is termed *b*.

Hydrolysis of the *a* bond yields 5′–PO_4 products:

Mixture of 5' –nucleoside monophosphates (NMPs)

Hydrolysis of the *b* bond yields 3′–PO_4 products:

A 3′, 5′ –diPO_4 nucleotide from the 5′– end

A mixture of 3′– NMPs

A nucleoside from the 3′– OH end
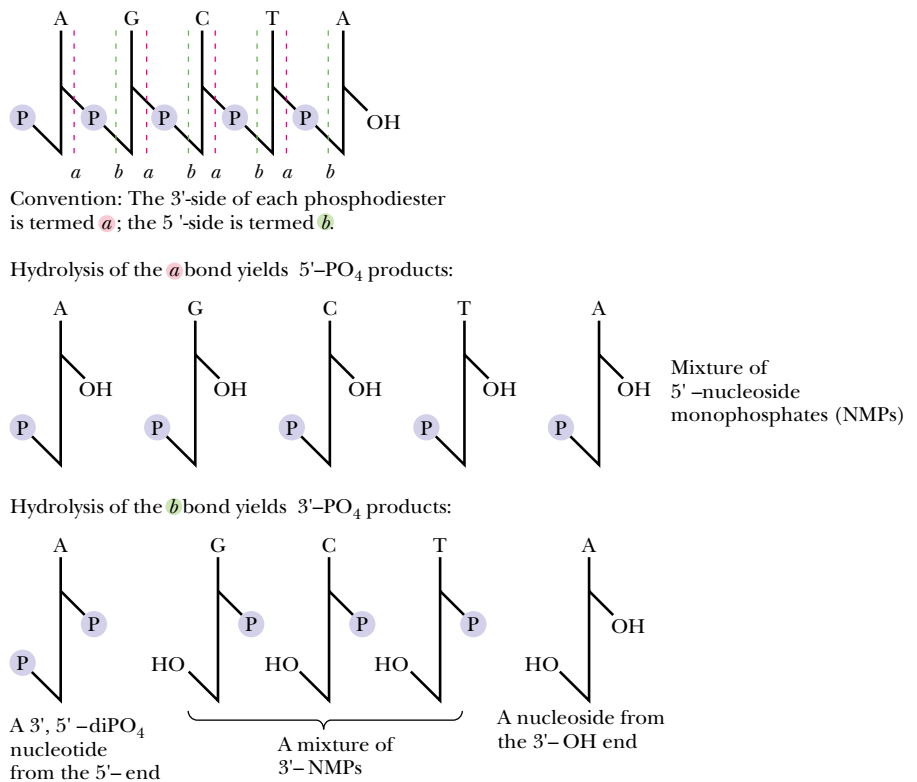
FIGURE 11.30 • Cleavage in polynucleotide chains: *a* cleavage yields 5′-phosphate products, whereas *b* cleavage gives 3′-phosphate products.

Snake venom phosphodiesterase: an "*a*" specific exonuclease:

Sequential removal of
5'–NMP from 3'–end

Snake venom
phosphodiesterase
attacks here next

5'–AMP
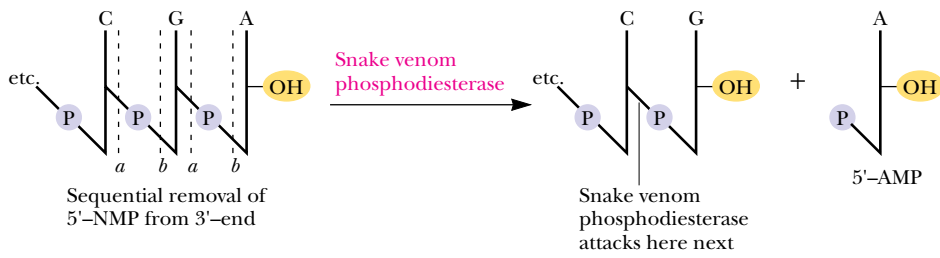
Spleen phosphodiesterase: a "*b*" specific exonuclease:

Sequential removal of
3'–NMP from 5'–end

3'–CMP

Spleen
phosphodiesterase
attacks here next
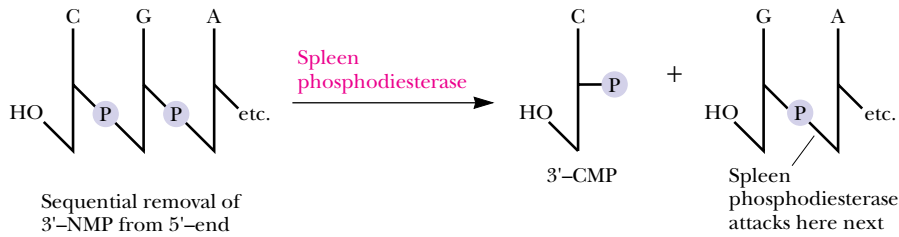
FIGURE 11.31 • Snake venom phosphodiesterase and spleen phosphodiesterase are
exonucleases that degrade polynucleotides from opposite ends.

others are nonspecific and are referred to simply as **nucleases,** as in *nuclease
S1* (see Table 11.4). Nucleases may also show specificity for only single-stranded
nucleic acids or may only act on double helices. Single-stranded nucleic acids
are abbreviated by an *ss* prefix, as in ssRNA; the prefix *ds* denotes double-
stranded. Nucleases may also display a decided preference for acting only at

Table 11.4

Specificity of Various Nucleases			
Enzyme	**DNA, RNA, or Both**	***a* or *b***	**Specificity**
Exonucleases			
Snake venom phosphodiesterase	Both	*a*	Starts at 3'-end, 5'-NMP products
Spleen phosphodiesterase	Both	*b*	Starts at 5'-end, 3'-NMP products
Endonucleases			
RNase A (pancreas)	RNA	*b*	Where 3'-PO_4 is to pyrimidine; oligos with pyrimidine 3'-PO_4 ends
Bacillus subtilis RNase	RNA	*b*	Where 3'-PO_4 is to purine; oligos with purine 3'-PO_4 ends
RNase T_1	RNA	*b*	Where 3'-PO_4 is to guanine
RNase T_2	RNA	*b*	Where 3'-PO_4 is to adenine
DNase I (pancreas)	DNA	*a*	Preferably between Py and Pu; nicks dsDNA, creating 3'-OH ends
DNase II (spleen, thymus, *Staphylococcus aureus*)	DNA	*b*	Oligo products
Nuclease S1	Both	*a*	Cleaves single-stranded but not double-stranded nucleic acids

Pancreatic RNase is an enzyme specific for *b* cleavage where a pyrimidine base lies
to the 3'–side of the phosphodiester; it acts endo. The products are oligonucleotides
with pyrimidine–3'–PO_4 ends:
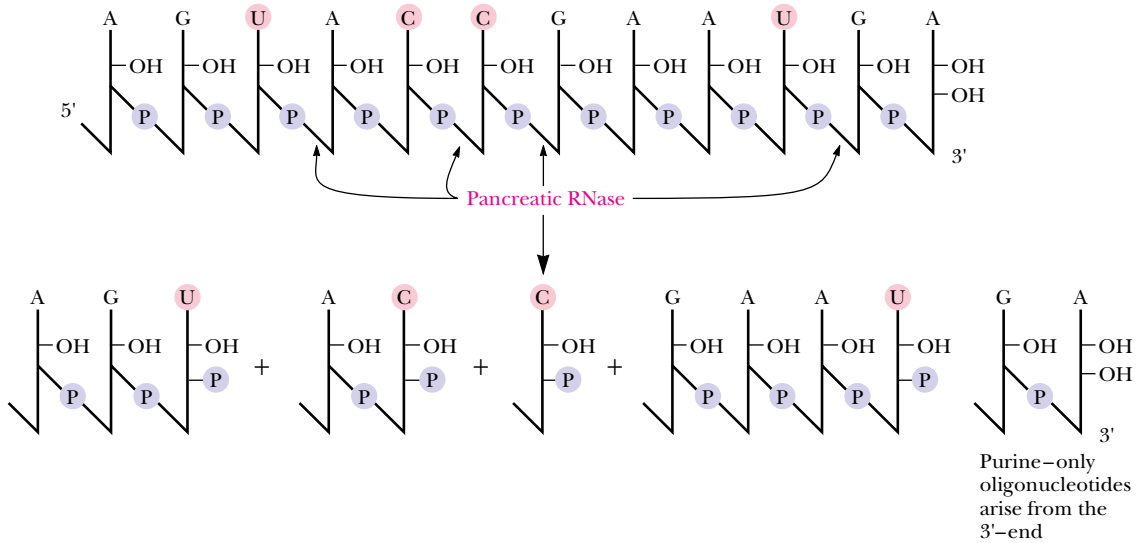
FIGURE 11.32 • An example of nuclease specificity: The specificity of RNA hydrolysis by bovine pancreatic RNase. This RNase cleaves *b* at 3'-pyrimidines, yielding oligonucleotides with pyrimidine 3'-PO_4 ends.

certain bases in a polynucleotide (Figure 11.32), or, as we shall see for *restriction endonucleases,* some nucleases will act only at a particular nucleotide sequence four to eight nucleotides in length. Table 11.4 lists the various permutations in specificity displayed by these nucleases and gives prominent examples of each. To the molecular biologist, nucleases are the surgical tools for the dissection and manipulation of nucleic acids in the laboratory.

Exonucleases degrade nucleic acids by sequentially removing nucleotides from their ends. Two in common use are *snake venom phosphodiesterase* and *bovine spleen phosphodiesterase* (Figure 11.31). Because they act on either DNA or RNA, they are referred to by the generic name *phosphodiesterase*. These two enzymes have complementary specificities. Snake venom phosphodiesterase acts by *a* cleavage and starts at the free 3'-OH end of a polynucleotide chain, liberating nucleoside 5'-monophosphates. In contrast, the bovine spleen enzyme starts at the 5'-end of a nucleic acid, cleaving *b* and releasing 3'-NMPs.

Restriction Enzymes

Restriction endonucleases are enzymes, isolated chiefly from bacteria, that have the ability to cleave double-stranded DNA. The term *restriction* comes from the capacity of prokaryotes to defend against or "restrict" the possibility of takeover by foreign DNA that might gain entry into their cells. Prokaryotes degrade foreign DNA by using their unique restriction enzymes to chop it into relatively large but noninfective fragments. Restriction enzymes are classified into three types, I, II, or III. Types I and III require ATP to hydrolyze DNA and can also catalyze chemical modification of DNA through addition of methyl groups to specific bases. Type I restriction endonucleases cleave DNA randomly, while type III recognize specific nucleotide sequences within dsDNA and cut the DNA at or near these sites.

Type II Restriction Endonucleases

Type II restriction enzymes have received widespread application in the cloning and sequencing of DNA molecules. Their hydrolytic activity is not ATP-dependent, and they do not modify DNA by methylation or other means. Most importantly, they cut DNA within or near particular nucleotide sequences that they specifically recognize. These recognition sequences are typically four or six nucleotides in length and have a twofold axis of symmetry. For example, *E. coli* has a restriction enzyme, *Eco*RI, that recognizes the hexanucleotide sequence GAATTC:

$$5'\text{——N—N—N—N—}\mathbf{G\text{—}A\text{—}A\text{—}T\text{—}T\text{—}C}\text{—N—N—N—N——}3'$$
$$3'\text{——N—N—N—N—}\mathbf{C\text{—}T\text{—}T\text{—}A\text{—}A\text{—}G}\text{—N—N—N—N——}5'$$

Note the twofold symmetry: the sequence read $5' \rightarrow 3'$ is the same in both strands.

When *Eco*RI encounters this sequence in dsDNA, it causes a staggered, double-stranded break by hydrolyzing each chain between the G and A residues:

$$5'\text{——N—N—N—N—}\mathbf{G}\quad\mathbf{A\text{—}A\text{—}T\text{—}T\text{—}C}\text{—N—N—N—N——}3'$$
$$3'\text{——N—N—N—N—}\mathbf{C\text{—}T\text{—}T\text{—}A\text{—}A}\quad\mathbf{G}\text{—N—N—N—N——}5'$$

Staggered cleavage results in fragments with protruding single-stranded 5′-ends:

$$5'\text{——N—N—N—N—}\mathbf{G}\qquad\qquad 5'\,\mathbf{A\text{—}A\text{—}T\text{—}T\text{—}C}\text{—N—N—N—N——}3'$$
$$3'\text{——N—N—N—N—}\mathbf{C\text{—}T\text{—}T\text{—}A\text{—}A}\,5'\qquad\qquad \mathbf{G}\text{—N—N—N—N——}5'$$

Because the protruding termini of *Eco*RI fragments have complementary base sequences, they can form base pairs with one another.

$$\text{——N—N—N—N—}\mathbf{G}\quad\mathbf{A\text{—}A\text{—}T\text{—}T\text{—}C}\text{—N—N—N—N——}$$
$$\text{——N—N—N—N—}\mathbf{C\text{—}T\text{—}T\text{—}A\text{—}A}\quad\mathbf{G}\text{—N—N—N—N——}$$

Therefore, DNA restriction fragments having such "sticky" ends can be joined together to create new combinations of DNA sequence. If the fragments are derived from DNA molecules of different origin, novel recombinant forms of DNA are created.

*Eco*RI leaves staggered 5′-termini. Other restriction enzymes, such as *Pst*I, which recognizes the sequence 5′-CTGCAG-3′ and cleaves between A and G, produce cohesive staggered 3′-ends. Still others, such as *Bal*I, act at the center of the twofold symmetry axis of their recognition site and generate blunt ends that are noncohesive. *Bal*I recognizes 5′-TGGCCA-3′ and cuts between G and C.

Table 11.5

Restriction Endonucleases

About 1000 restriction enzymes have been characterized. They are named by italicized three-letter codes, the first a capital letter denoting the genus of the organism of origin, while the next two letters are an abbreviation of the particular species. Because prokaryotes often contain more than one restriction enzyme, the various representatives are assigned letter and number codes as they are identified. Thus, *Eco*RI is the initial restriction endonuclease isolated from *Escherichia coli,* strain R. With one exception (*Nci*I), all known type II restriction endonucleases generate fragments with 5′-PO$_4$ and 3′-OH ends.

Enzyme	Common Isoschizomers	Recognition Sequence	Compatible Cohesive Ends
*Alu*I		AG↓CT	Blunt
*Apy*I	*Atu*I, *Eco*RII	CC↓$\left(\substack{A\\T}\right)$GG	
*Asu*II		TT↓CGAA	*Cla*I, *Hpa*II, *Taq*I
*Ava*I		G↓PyCGPuG	*Sal*I, *Xho*I, *Xma*I
*Avr*II		C↓CTAGG	
*Bal*I		TGG↓CCA	Blunt
*Bam*HI		G↓GATCC	*Bcl*I, *Bgl*II, *Mbo*I, *Sau*3A, *Xho*II
*Bcl*I		T↓GATCA	*Bam*HI, *Bgl*II, *Mbo*I, *Sau*3A, *Xho*II
*Bgl*II		A↓GATCT	*Bam*HI, *Bcl*I, *Mbo*I, *Sau*3A, *Xho*II
*Bst*EII		G↓GTNACC	
*Bst*XI		CCANNNNN↓NTGG	
*Cla*I		AT↓CGAT	*Acc*I, *Acy*I, *Asy*II, *Hpa*II, *Taq*I
*Dde*I		C↓TNAG	
*Eco*RI		G↓AATTC	
*Eco*RII	*Atu*I, *Apy*I	↓CC ($\substack{A\\T}$)GG	
*Fnu*DII	*Tha*I	CG↓CG	Blunt
*Hae*I		($\substack{A\\T}$)GG↓CC($\substack{T\\A}$)	Blunt
*Hae*II		PuGCGC↓Py	
*Hae*III		GG↓CC	Blunt
*Hinc*II		GTPy↓PuAC	Blunt
*Hin*dIII		A↓AGCTT	
*Hpa*I		GTT↓AAC	Blunt
*Hpa*II		C↓CGG	*Acc*I, *Acy*I, *Asu*II, *Cla*I, *Taq*I
*Kpn*I		GGTAC↓C	*Bam*HI, *Bcl*I, *Bgl*II, *Xho*II
*Mbo*I	*Sau*3A	↓GATC	
*Msp*I		C↓CGG	
*Mst*I		TGC↓GCA	Blunt
*Not*I		GC↓GGCCGC	
*Pst*I		CTGCA↓G	
*Sac*I	*Sst*I	GAGCT↓C	
*Sal*I		G↓TCGAC	*Ava*I, *Xho*I
*Sau*3A		↓GATC	*Bam*HI, *Bcl*I, *Bgl*II, *Mbo*I, *Xho*II
*Sfi*I		GGCCNNNN↓NGGCC	
*Sma*I	*Xma*I	CCC↓GGG	Blunt
*Sph*I		GCATG↓C	
*Sst*I	*Sac*I	GAGCT↓C	
*Taq*I		T↓CGA	*Acc*I, *Acy*I, *Asu*II, *Cla*I, *Hpa*II
*Xba*I		T↓CTAGA	
*Xho*I		C↓TCGAG	*Ava*I, *Sal*I
*Xho*II		($\substack{A\\G}$)↓GATC($\substack{T\\C}$)	*Bam*HI, *Bcl*I, *Bgl*II, *Mbo*I, *Sau*3A
*Xma*I	*Sma*I	C↓CCGGG	*Ava*I

Table 11.5 lists many of the commonly used restriction endonucleases and their recognition sites. Because these sites all have twofold symmetry, only the sequence on one strand needs to be designated.

ISOSCHIZOMERS. Different restriction enzymes sometimes recognize and cleave within identical target sequences. For example, *Mbo*I and *Sau*3A recognize the same tetranucleotide run: 5′-GATC-3′. Both cleave the DNA strands at the same position, namely, on the 5′-side of the G. Such enzymes are called **isoschizomers,** meaning that they cut at the same site. The enzyme *Bam*HI is an isoschizomer of *Mbo*I and *Sau*3A except that it has greater specificity because it acts only at hexanucleotide sequences reading GGATCC. *Bam*HI cuts between the two G's, leaving cohesive 5′-ends that can match up with *Mbo*I or *Sau*3A fragments.

schizo • from the Greek *schizein,* to split

RESTRICTION FRAGMENT SIZE. Assuming random distribution and equimolar proportions for the four nucleotides in DNA, a particular tetranucleotide sequence should occur every 4^4 nucleotides, or every 256 bases. Therefore, the fragments generated by a restriction enzyme that acts at a four-nucleotide sequence should average about 250 bp in length. "Six-cutters," enzymes such as *Eco*RI or *Bam*HI, will find their unique hexanucleotide sequences on the average once in every 4096 (4^6) bp of length. Because the genetic code is a triplet code with three bases of DNA specifying one amino acid in a polypeptide sequence, and because polypeptides typically contain at most 1000 amino acid residues, the fragments generated by six-cutters are approximately the size of prokaryotic genes. This property makes these enzymes useful in the construction and cloning of genetically useful recombinant DNA molecules. For the isolation of even larger nucleotide sequences, such as those of genes encoding large polypeptides (or those of eukaryotic genes that are disrupted by large introns), partial or limited digestion of DNA by restriction enzymes can be employed. However, restriction endonucleases that cut only at specific nucleotide sequences 8 or even 13 nucleotides in length are also available, such as *Not*I and *Sfi*I.

Restriction Mapping

The application of these sequence-specific nucleases to problems in molecular biology is considered in detail in Chapter 13, but one prominent application is described here. Because restriction endonucleases cut dsDNA at unique sites to generate large fragments, they provide a means for mapping DNA molecules that are many kilobase pairs in length. Restriction digestion of a DNA molecule is in many ways analogous to proteolytic digestion of a protein by an enzyme such as trypsin (see Chapter 5): the restriction endonuclease acts only at its specific sites so that a discrete set of nucleic acid fragments is generated. This action is analogous to trypsin cleavage only at Arg and Lys residues to yield a particular set of tryptic peptides from a given protein. The restriction fragments represent a unique collection of different-sized DNA pieces. Fortunately, this complex mixture can be resolved by *electrophoresis* (see the Appendix to Chapter 5). Electrophoresis of DNA molecules on gels of restricted pore size (as formed in agarose or polyacrylamide media) separates them according to size, the largest being retarded in their migration through the gel pores while the smallest move relatively unhindered. Figure 11.33 shows a hypothetical electrophoretogram obtained for a DNA molecule treated with two different restriction nucleases, alone and in combination. Just as cleavage of a protein with different proteases to generate overlapping fragments allows an ordering of the peptides, restriction fragments can be ordered or "mapped" according to their sizes, as deduced from the patterns depicted in Figure 11.33.

Treatment of a linear 10kb DNA molecule with endonucleases gave the following results:

Longer DNA fragments

Shorter DNA fragments

The observed electrophoretic pattern

Restriction mapping: consider the possible arrangements:

Which arrangements are correct?

Possible maps of the 10kb fragment:

Treatment with restriction endonuclease **A** gave 2 fragments, one 7 kb in size and one 3 kb in size, as judged by gel electrophoresis.

Treatment of another sample of the 10 kb DNA with restriction endonuclease **B** gave three fragments, 8.5 kb, 1.0 kb, and 0.5 kb.

Treatment of a third sample with both restriction endonucleases **A** and **B** yielded fragments 6.5, 2, 1, and 0.5 kb.

The only combinations giving the observed **A + B** digests are **1** + **5** and **2** + **7**.

To decide between these alternatives, a fixed point of reference, such as one of the ends of the fragment, must be identified or labeled. The task increases in complexity as DNA size, number of restriction sites, and/or number of restriction enzymes used increases.

FIGURE 11.33 • Restriction mapping of a DNA molecule as determined by an analysis of the electrophoretic pattern obtained for different restriction endonuclease digests. (Keep in mind that a dsDNA molecule has a unique nucleotide sequence and therefore a definite polarity; thus, fragments from one end are distinctly different from fragments derived from the other end.)

PROBLEMS

1. Draw the chemical structure of pACG.

2. Chargaff's results (Table 11.3) yielded a molar ratio of 1.56 for A to G in human DNA, 1.75 for T to C, 1.00 for A to T, and 1.00 for G to C. Given these values, what are the mole fractions of A, C, G, and T in human DNA?

3. Adhering to the convention of writing nucleotide sequences in the $5' \rightarrow 3'$ direction, what is the nucleotide sequence of the DNA strand that is complementary to d-ATCGCAACTGTCACTA?

4. Messenger RNAs are synthesized by RNA polymerases that read along a DNA template strand in the $3' \rightarrow 5'$ direction, polymerizing ribonucleotides in the $5' \rightarrow 3'$ direction (see Figure 11.24). Give the nucleotide sequence $(5' \rightarrow 3')$ of the DNA template strand from which the following mRNA segment was transcribed: 5'-UAGUGACAGUUGCGAU-3'.

5. The DNA strand that is complementary to the template strand copied by RNA polymerase during transcription has a nucleotide

sequence identical to that of the RNA being synthesized (except T residues are found in the DNA strand at sites where U residues occur in the RNA). An RNA transcribed from this nontemplate DNA strand would be complementary to the mRNA synthesized by RNA polymerase. Such an RNA is called antisense RNA. A promising strategy to thwart the deleterious effects of genes activated in disease states (such as cancer) is to generate antisense RNAs in affected cells. These antisense RNAs would form double-stranded hybrids with mRNAs transcribed from the activated genes and prevent their translation into protein. Suppose transcription of a cancer-activated gene yielded an mRNA whose sequence included the segment 5′-

UACGGUCUAAGCUGA. What is the corresponding nucleotide sequence $(5′ \rightarrow 3′)$ of the template strand in a DNA duplex that might be introduced into these cells so that an antisense RNA could be transcribed from it?

6. A 10-kb DNA fragment digested with restriction endonuclease *Eco*RI yielded fragments 4 kb and 6 kb in size. When digested with *Bam*HI, fragments 1, 3.5, and 5.5 kb were generated. Concomitant digestion with both *Eco*RI and *Bam*HI yielded fragments 0.5, 1, 3, and 5.5 kb in size. Give a possible restriction map for the original fragment.

FURTHER READING

Adams, R. L. P., Knowler, J. T., and Leader, D. P., 1992. *The Biochemistry of the Nucleic Acids,* 11th ed. New York: Chapman and Hall (Methuen and Co., distrib.).

Gray, M. W., and Cedergren, R., eds., 1993. The New Age of RNA. *The FASEB Journal* **7:**4–239. A collection of articles emphasizing the new appreciation for RNA in protein synthesis, in evolution, and as a catalyst.

Judson, H. F., 1979. *The Eighth Day of Creation.* New York: Simon and Schuster.

Maniatis, T., Frisch, E. F., and Sambrook, J., 1989. *Molecular Cloning: A Laboratory Manual,* 2nd ed. Cold Spring Harbor, NY: Cold Spring Harbor Laboratory.

Watson, J. D., Hopkins, N. H., Roberts, J. W., Steitz, J. A., and Weiner, A. M., 1987. *The Molecular Biology of the Gene,* Vol. I, *General Principles,* 4th ed. Menlo Park, CA: Benjamin/Cummings.

Chapter 12

Structure of Nucleic Acids

The Structure of DNA: "A melody for the eye of the intellect, with not a note wasted."

Horace Freeland Judson, *The Eighth Day of Creation*

"Scherzo in D&A" (detail) by David E. Rodale (1955–1985)

Chapter 11 presented the structure and chemistry of nucleotides and how these units are joined via phosphodiester bonds to form nucleic acids, the biological polymers for information storage and transmission. In this chapter, we investigate biochemical methods that reveal this information by determining the sequential order of nucleotides in a polynucleotide, the so-called **primary structure** of nucleic acids. Then, we consider the higher orders of structure in the nucleic acids, the secondary and tertiary levels. Although the focus here is primarily on the structural and chemical properties of these macromolecules, it is fruitful to keep in mind the biological roles of these remarkable substances. The sequence of nucleotides in nucleic acids is the embodiment of genetic information (see Part IV). We can anticipate that the cellular mechanisms for accessing this information, as well as reproducing it with high fidelity, will be illuminated by knowledge of the chemical and structural qualities of these polymers.

12.1 • The Primary Structure of Nucleic Acids

As recently as 1975, determining the primary structure of nucleic acids (the nucleotide sequence) was a more formidable problem than amino acid sequencing of proteins, simply because nucleic acids contain only four unique monomeric units whereas proteins have twenty. With only four, there are *apparently* fewer specific sites for selective cleavage, distinctive sequences are more difficult to recognize, and the likelihood of ambiguity is greater. The much greater number of monomeric units in most polynucleotides as compared to polypeptides is a further difficulty. Two important breakthroughs reversed this situation so that now sequencing nucleic acids is substantially easier than sequencing polypeptides. One was the discovery of *restriction endonucleases* that cleave DNA at specific oligonucleotide sites, generating unique fragments of manageable size (see Chapter 11). The second is the power of *polyacrylamide gel electrophoresis* separation methods to resolve nucleic acid fragments that differ from one another in length by just one nucleotide.

Sequencing Nucleic Acids

Two basic protocols for nucleic acid sequencing are in widespread use: the **chain termination** or **dideoxy method** of F. Sanger and the **base-specific chemical cleavage method** developed by A. M. Maxam and W. Gilbert. Because both methods are carried out on nanogram amounts of DNA, very sensitive analytical techniques are used to detect the DNA chains following electrophoretic separation on polyacrylamide gels. Typically, the DNA molecules are labeled with radioactive ^{32}P,[1] and following electrophoresis, the pattern of their separation is visualized by **autoradiography.** A piece of X-ray film is placed over the gel and the radioactive disintegrations emanating from ^{32}P decay create a pattern on the film that is an accurate image of the resolved oligonucleotides. Recently, sensitive biochemical and chemiluminescent methods have begun to supersede the use of radioisotopes as tracers in these experiments.

Chain Termination or Dideoxy Method

To appreciate the rationale of the chain termination or dideoxy method, we first must briefly examine the biochemistry of DNA replication. DNA is a double-helical molecule. In the course of its replication, the sequence of nucleotides in one strand is copied in a complementary fashion to form a new second strand by the enzyme **DNA polymerase.** Each original strand of the double helix serves as **template** for the biosynthesis that yields two daughter DNA duplexes from the parental double helix (Figure 12.1). DNA polymerase carries out this reaction *in vitro* in the presence of the four deoxynucleotide monomers and copies single-stranded DNA, provided a double-stranded region of DNA is artificially generated by adding a **primer.** This primer is merely an oligonucleotide capable of forming a short stretch of dsDNA by base pairing with the ssDNA (Figure 12.2). The primer must have a free 3′-OH end from which the new polynucleotide chain can grow as the first residue is added in the initial step of the polymerization process. DNA polymerases synthesize new strands by adding successive nucleotides in the 5′ → 3′ direction.

FIGURE 12.1 • DNA replication yields two daughter DNA duplexes identical to the parental DNA molecule. Each original strand of the double helix serves as a template, and the sequence of nucleotides in each of these strands is copied to form a new complementary strand by the enzyme DNA polymerase. By this process, biosynthesis yields two daughter DNA duplexes from the parental double helix.

---

[1]Because its longer half-life and lower energy make it more convenient to handle, ^{35}S is replacing ^{32}P as the radioactive tracer of choice in sequencing by the Sanger method. ^{35}S-α-labeled deoxynucleotide analogs provide the source for incorporating radioactivity into DNA.

FIGURE 12.2 • DNA polymerase copies ssDNA *in vitro* in the presence of the four deoxynucleotide monomers, provided a double-stranded region of DNA is artificially generated by adding a primer, an oligonucleotide capable of forming a short stretch of dsDNA by base pairing with the ssDNA. The primer must have a free 3′-OH end from which the new polynucleotide chain can grow as the first residue is added in the initial step of the polymerization process.
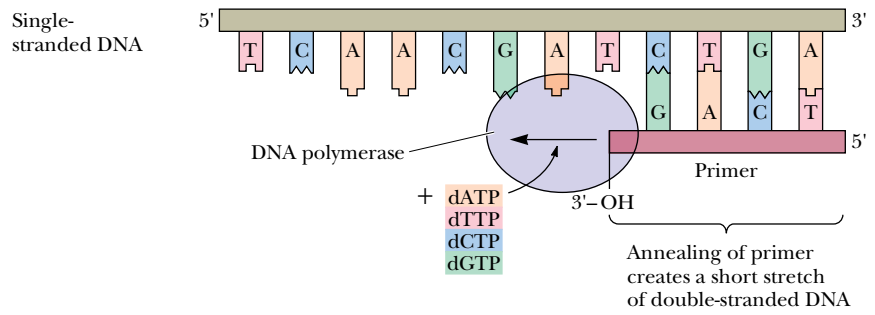
Chain Termination Protocol

In the chain termination method of DNA sequencing, a DNA fragment of unknown sequence serves as template in a polymerization reaction using some type of DNA polymerase, usually *Sequenase 2*®, a genetically engineered version of bacteriophage T7 DNA polymerase that lacks all traces of exonuclease activity that might otherwise degrade the DNA. The primer requirement is met by an appropriate oligonucleotide (this method is also known as the **primed synthesis method** for this reason). Four parallel reactions are run; all four contain the four deoxynucleoside triphosphates dATP, dGTP, dCTP, and dTTP, which are the substrates for DNA polymerase (Figure 12.3 on the facing page). In each of the four reactions, a different 2′,3′-**di**deoxynucleotide is included, and it is these dideoxynucleotides that give the method its name.

Because dideoxynucleotides lack 3′-OH groups, these nucleotides cannot serve as acceptors for 5′-nucleotide addition in the polymerization reaction, and thus the chain is terminated where they become incorporated. The concentrations of the four deoxynucleotides and the single dideoxynucleotide in each reaction mixture are adjusted so that the dideoxynucleotide is incorporated infrequently. Therefore, base-specific premature chain termination is only a random, occasional event, and a population of new strands of varying length is synthesized. Four reactions are run, one for each dideoxynucleotide, so that termination, although random, can occur everywhere in the sequence. In each mixture, each newly synthesized strand has a dideoxynucleotide at its 3′-end, and its presence at that position demonstrates that a base of that particular kind was specified by the template. A radioactively labeled dNTP is included in each reaction mixture to provide a tracer for the products of the polymerization process.

Reading Dideoxy Sequencing Gels

The sequencing products are visualized by autoradiography (or similar means) following their separation according to size by polyacrylamide gel electrophoresis (Figure 12.3). Because the smallest fragments migrate fastest upon electrophoresis and because fragments differing by only single nucleotides in length are readily resolved, the autoradiogram of the gel can be read from bottom to top, noting which lane has the next largest band at each step. Thus, the gel in Figure 12.3 is read AGCGTAGC (5′ → 3′). Because of the way DNA polymerase acts, this observed sequence is complementary to the corresponding unknown template sequence. Knowing this, the template sequence now can be written GCTACGCT (5′ → 3′).
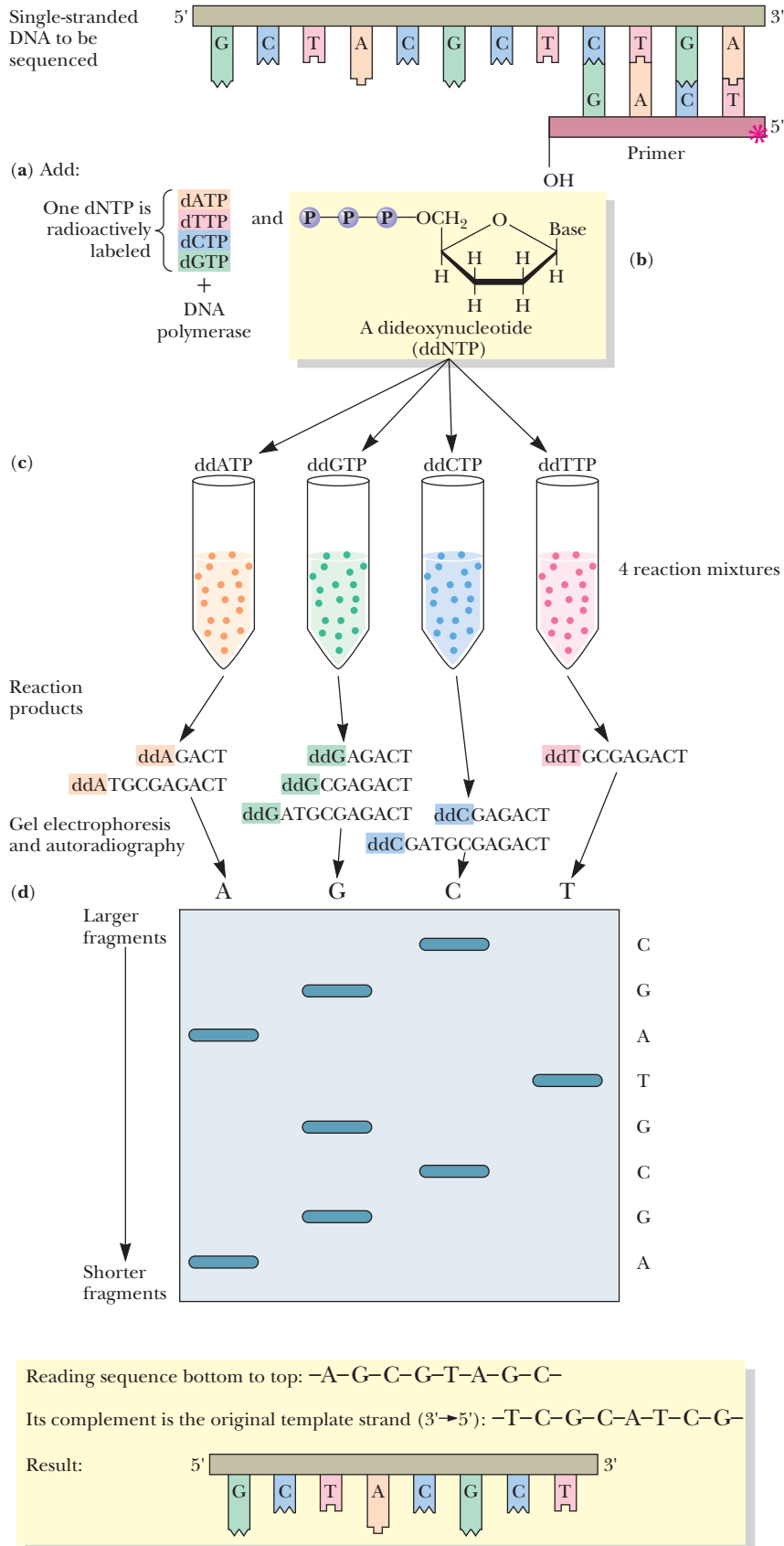
FIGURE 12.3 • The chain termination or dideoxy method of DNA sequencing. (a) DNA polymerase reaction. (b) Structure of dideoxynucleotide. (c) Four reaction mixtures with nucleoside triphosphates plus one dideoxynucleoside triphosphate. (d) Electrophoretogram. Note that the nucleotide sequence as read from the bottom to the top of the gel is the order of nucleotide addition carried out by DNA polymerase.

Base-Specific Chemical Cleavage Method

The base-specific chemical cleavage (or Maxam–Gilbert) method starts with a single-stranded DNA that is labeled at one end with radioactive ^{32}P. (Double-stranded DNA can be used if only one strand is labeled at only one of its ends.) The DNA strand is then randomly cleaved by reactions that specifically fragment its sugar–phosphate backbone only where certain bases have been chemically removed. There is no unique reaction for each of the four bases. However,
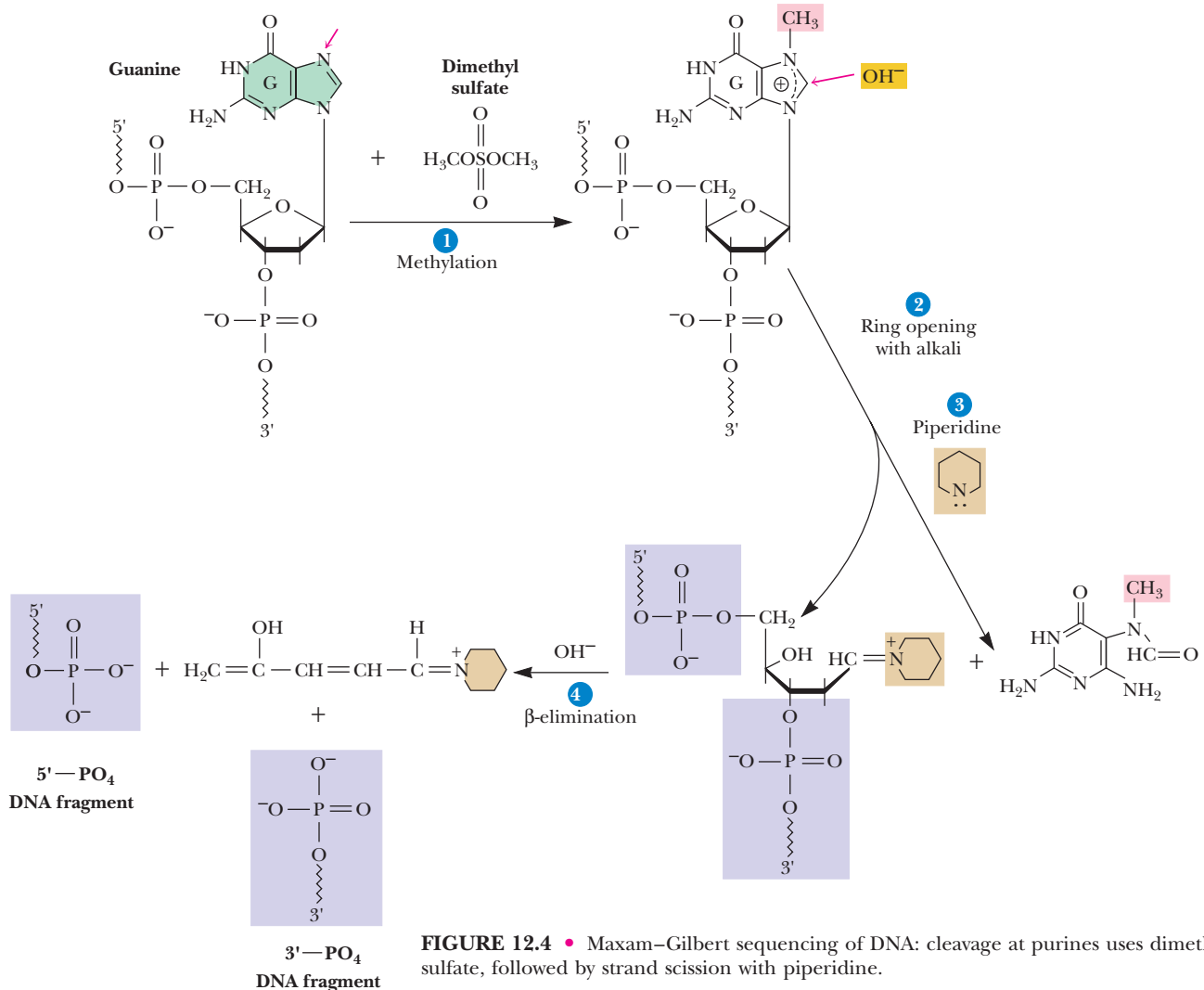
FIGURE 12.4 • Maxam–Gilbert sequencing of DNA: cleavage at purines uses dimethyl sulfate, followed by strand scission with piperidine.

Cleavage at G using dimethyl sulfate, followed by strand scission with piperidine: Under alkaline conditions, **dimethyl sulfate** reacts with guanine to methylate it at the 7-position **(1).** This substitution leads to instability of the N-9 glycosidic bond, so that in the presence of OH⁻ and the secondary amine **piperidine (2),** the purine ring is degraded and released. A β-elimination reaction facilitated by piperidine **(3)** then causes the excision of the naked deoxyribose moiety from the sugar–phosphate backbone, with consequent scission of the DNA strand to yield 5′- and 3′-fragments.

Cleavage at A or G: If the DNA is first treated with acid, dimethyl sulfate methylates adenine at the 3-position as well as guanine at the 7-position (not shown). Subsequent reaction with OH⁻ and piperidine triggers degradation and displacement of the methylated A or G purine base and strand scission, essentially as indicated here for reaction of dimethyl sulfate with guanine.
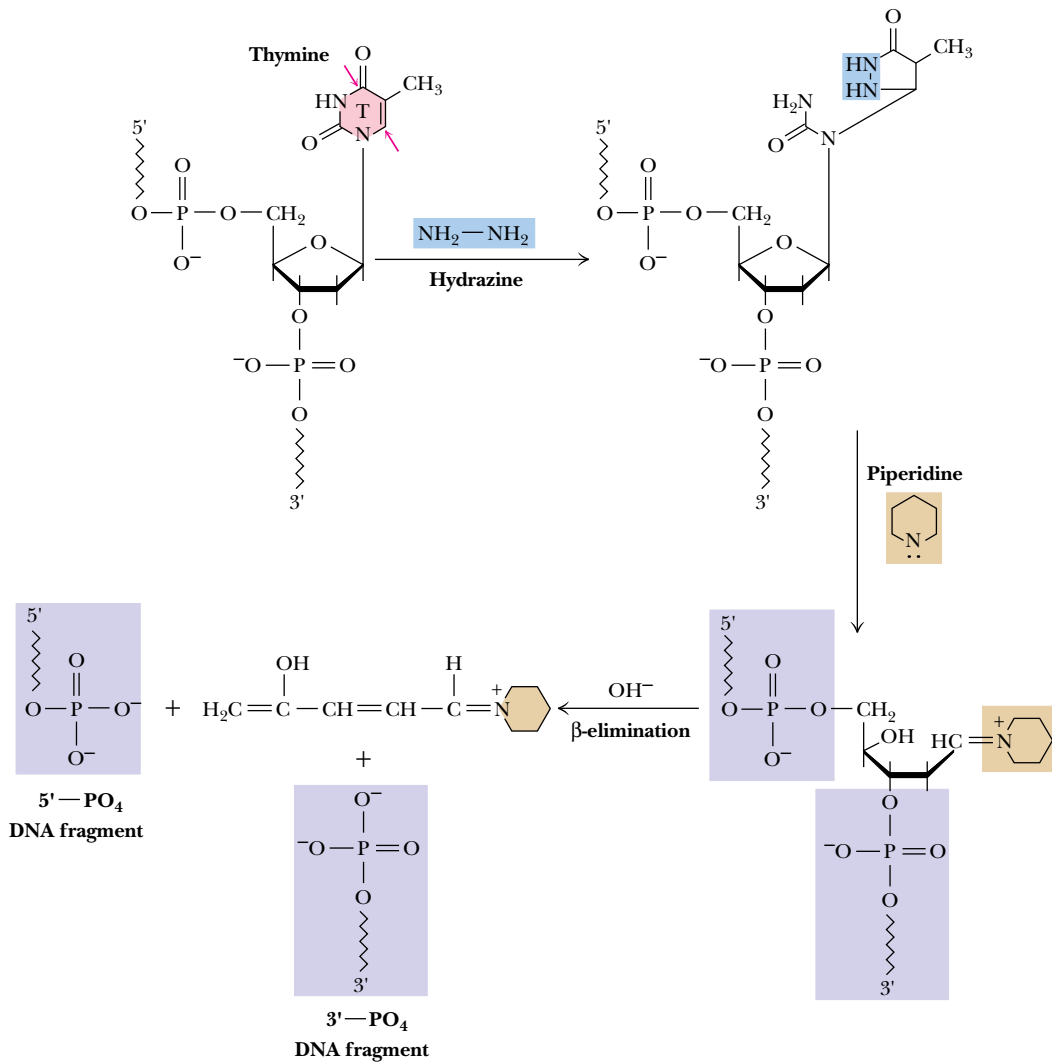
FIGURE 12.5 • Maxam–Gilbert sequencing of DNA: hydrolysis of pyrimidine rings by hydrazine. Hydrazine (H_2N-NH_2) attacks across the C-4 and C-6 atoms of pyrimidines to open the ring. This degradation subsequently leads to modification of the deoxyribose, rendering it susceptible to β-elimination by piperidine in the presence of hydroxide ion. Shown here is the excision of a T residue. As in Figure 12.4, 5′- and 3′-fragments are produced. The presence of high salt concentrations protects T (but not C) from reaction with hydrazine. In the presence of 2 *M* NaCl, the reaction shown here occurs only at C residues.

there is a reaction specific to G only and a purine-specific reaction that removes A or G (Figure 12.4). Thus, the difference in these two reactions is a specific indication of where A occurs. Similarly, there is a cleavage reaction specific for the pyrimidines (C+T) (Figure 12.5), which, if run in the presence of 1 or 2 *M* NaCl, works only with C. Differences in these two are thus attributable to the presence of T in the nucleotide sequence.

Note that the key to Maxam–Gilbert sequencing is to modify a base chemically so that it is removed from its sugar. Then piperidine excises the sugar from its 5′- and 3′-links in a β-elimination reaction. The conditions of chemical cleavage described in Figures 12.4 and 12.5 are generally adjusted so that,

G   A+G   C+T   C

A
T
C
T
G
A
C
C
C
T
A
G
T
C
C
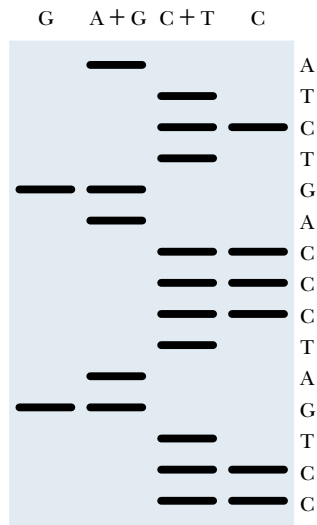
5' *³²P–TCCTGATCCCAGTCTA 3'
5' ATCTGACCCTAGTCCT–³²P* 3'

A T G C

◄ **FIGURE 12.6 •** Autoradiogram of a hypothetical electrophoretic pattern obtained for four reaction mixtures, performed as described in Figures 12.4 and 12.5 and run in the four lanes G, A+G, C+T, and C, respectively. Reading this pattern from the bottom up yields the sequence CCTGATCCCAGTCTA. The correct $5' \rightarrow 3'$ order is determined by knowing which end of the ssDNA was ³²P-labeled. If the 5'-end was ³²P-labeled, only the 5'-fragments will be evident on the autoradiogram; the 3'-ends will be invisible. Similarly, if the 3'-end was originally labeled, only the 3'-fragments light up the autoradiogram. Assuming that the 5'-end was labeled, the sequence would be CCTGATCCCAGTCTA. If it were the 3'-end, the sequence read in the $5' \rightarrow 3'$ convention would be ATCTGACCC-TAGTCC. An interesting feature of the Maxam–Gilbert sequencing procedure is that the base that is "read" in the ladder is actually not present in the oligonucleotide that identi-fies it. Thus, an unidentified base bears the label at the end of the smallest fragment; this unidentified base is the one that preceded the first identified base. For example, an oligonucleotide of either

³²P-5'-**(A,C,G,T)CCTGATCCCAGTCTA**-3'

or

5'-**ATCTGACCCTAGTCC(A,C,G,T)**-3'-³²P

would yield the same pattern in the autoradiogram. (Indication here of T as the end-labeled nucleotide is arbitrary.)

on average, only a single scission occurs per DNA molecule. However, because a very large number of DNA molecules exist in each reaction mixture, the products are a random collection of different-sized fragments wherein the occurrence of any base is represented by its unique pair of 5'- and 3'-cleavage products. These products form a complete set, the members of which differ in length by only one nucleotide, and they can be resolved by gel electrophore-sis into a "ladder," which can be visualized by autoradiography of the gel if the DNA fragments are radioactively labeled (Figure 12.6).

In principle, the Maxam–Gilbert method can provide the total sequence of a dsDNA molecule just by determining the purine positions on one strand and then the purines on the complementary strand. Complementary base-pair-ing rules then reveal the pyrimidines along each strand, T complementary to where A is, C complementary to where G occurs. (The analogous approach of locating the pyrimidines on each strand would also provide sufficient infor-mation to write the total sequence.)

With current technology, it is possible to read the order of as many as 400 bases from the autoradiogram of a sequencing gel (Figure 12.7). The actual chemical or enzymatic reactions, electrophoresis, and autoradiography are now routine, and a skilled technician can sequence about 1 kbp per week using these manual techniques. The major effort in DNA sequencing is in the isola-tion and preparation of fragments of interest, such as cloned genes.

Automated DNA Sequencing

In recent years, automated DNA sequencing machines capable of identifying about 10^4 bases per day have become commercially available. One clever inno-vation has been the use of fluorescent dyes of different colors to uniquely label the primer DNA introduced into the four sequencing reactions; for example, red for the A reaction, blue for T, green for G, and yellow for C. Then, all four reaction mixtures can be combined and run together on one electrophoretic
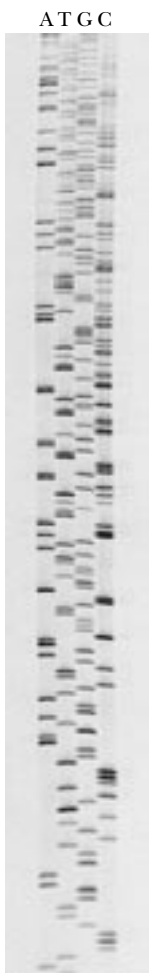
◄ **FIGURE 12.7 •** A photograph of the autoradiogram from an actual sequencing gel. A portion of the DNA sequence of *nit-6,* the *Neurospora* gene encoding the enzyme nitrite reductase. *(James D. Colandene, University of Virginia)*
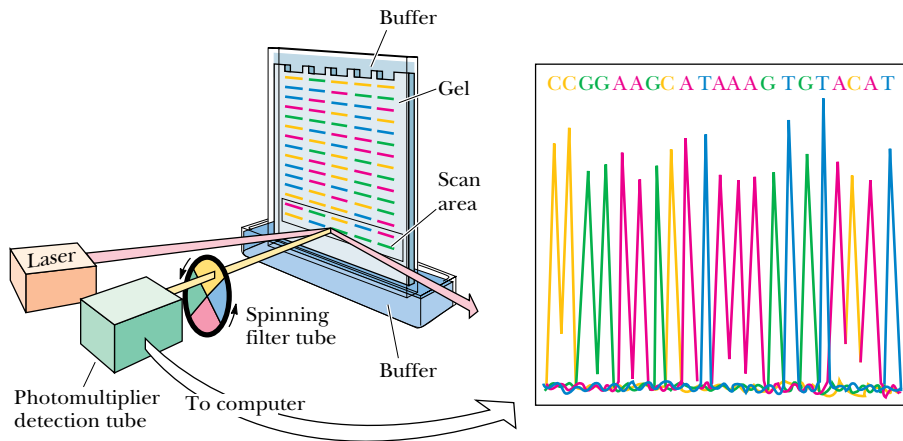
FIGURE 12.8 • Schematic diagram of the methodology used in fluorescent labeling and automated sequencing of DNA. Four reactions are set up, one for each base, and the primer in each is end-labeled with one of four different fluorescent dyes; the dyes serve to color-code the base-specific sequencing protocol (a unique dye is used in each dideoxynucleotide reaction). The four reaction mixtures are then combined and run in one lane. Thus, each lane in the gel represents a different sequencing experiment. As the differently sized fragments pass down the gel, a laser beam excites the dye in the scan area. The emitted energy passes through a rotating color filter and is detected by a fluorometer. The color of the emitted light identifies the final base in the fragment. *(Applied Biosystems, Inc., Foster City, CA)*

gel slab. As the oligonucleotides are separated and pass to the bottom of the gel, each is illuminated by a low-power argon laser beam that causes the dye attached to the primer to fluoresce. The color of the fluorescence is detected automatically, revealing the identity of the primer, and hence the base, immediately (Figure 12.8). The development of such automation has opened the possibility for sequencing the entire human genome, some 2.9 billion bp. Even so, if 100 automated machines operating at peak efficiency were dedicated to the task, it would still take at least 8 years to complete!

12.2 • The ABZs of DNA Secondary Structure

Double-stranded DNA molecules assume one of three secondary structures, termed A, B, and Z. Fundamentally, double-stranded DNA is a regular two-chain structure with hydrogen bonds formed between opposing bases on the two chains (see Chapter 11). Such H-bonding is possible only when the two chains are antiparallel. The polar sugar–phosphate backbones of the two chains are on the outside. The bases are stacked on the inside of the structure; these heterocyclic bases, as a consequence of their π-electron clouds, are hydrophobic on their flat sides. One purely hypothetical conformational possibility for a two-stranded arrangement would be a ladderlike structure (Figure 12.9) in which the base pairs are fixed at 0.6 nm apart because this is the distance between adjacent sugars in the DNA backbone. Because H_2O molecules would be accessible to the spaces between the hydrophobic surfaces of the bases, this conformation is energetically unfavorable. This ladderlike structure converts to a helix when given a simple right-handed twist. Helical twisting brings the base-pair rungs of the ladder closer together, stacking them 0.34 nm apart, without affecting the sugar–sugar distance of 0.6 nm. Because this helix repeats itself approximately every 10 bp, its **pitch** is 3.4 nm. This is the major conformation of DNA in solution and it is called **B-DNA.**
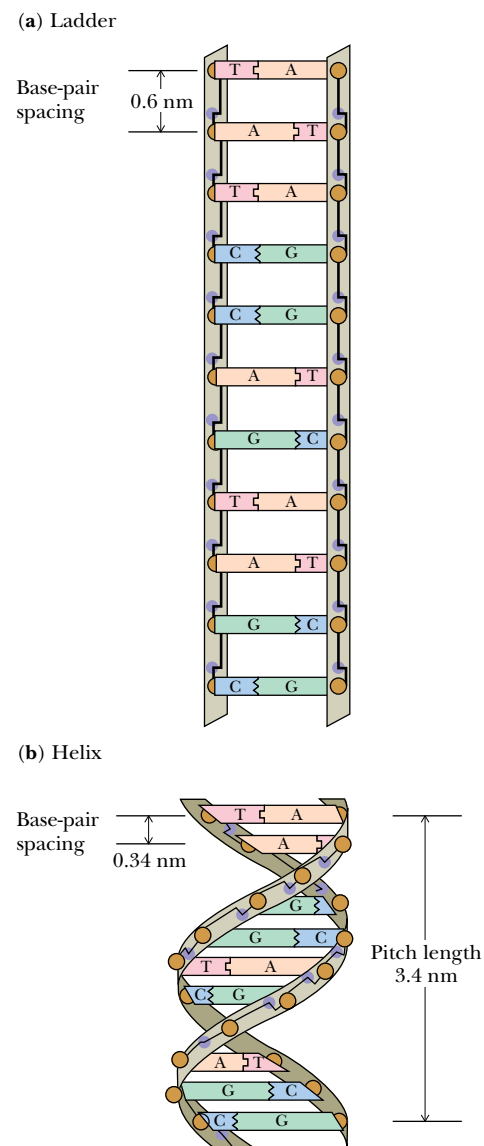
FIGURE 12.9 • (a) Double-stranded DNA as an imaginary ladderlike structure. (b) A simple right-handed twist converts the ladder to a helix.

Structural Equivalence of Watson–Crick Base Pairs

As indicated in Chapter 11, the base pairing in DNA is very specific: the purine adenine pairs with the pyrimidine thymine; the purine guanine pairs with the pyrimidine cytosine. Further, the A:T pair and G:C pair have virtually identical dimensions (Figure 12.10). Watson and Crick realized that units of such similarity could serve as spatially invariant substructures to build a polymer whose exterior dimensions would be uniform along its length, regardless of the sequence of bases.

The DNA Double Helix Is a Stable Structure

Several factors account for the stability of the double-helical structure of DNA. First, both internal and external hydrogen bonds stabilize the double helix. The two strands of DNA are held together by H-bonds that form between the complementary purines and pyrimidines, two in an A:T pair and three in a G:C pair (Figure 12.10), while polar atoms in the sugar–phosphate backbone form external H bonds with surrounding water molecules. Second, the negatively charged phosphate groups are all situated on the exterior surface of the helix in such a way that they have minimal effect on one another and are free to interact electrostatically with cations in solution such as Mg^{2+}. Third, the core of the helix consists of the base pairs, which, in addition to being H-bonded, stack together through hydrophobic interactions and van der Waals forces that contribute significantly to the overall stabilizing energy.

A stereochemical consequence of the way A:T and G:C base pairs form is that the sugars of the respective nucleotides have opposite orientations, and thus the sugar–phosphate backbones of the two chains run in opposite or
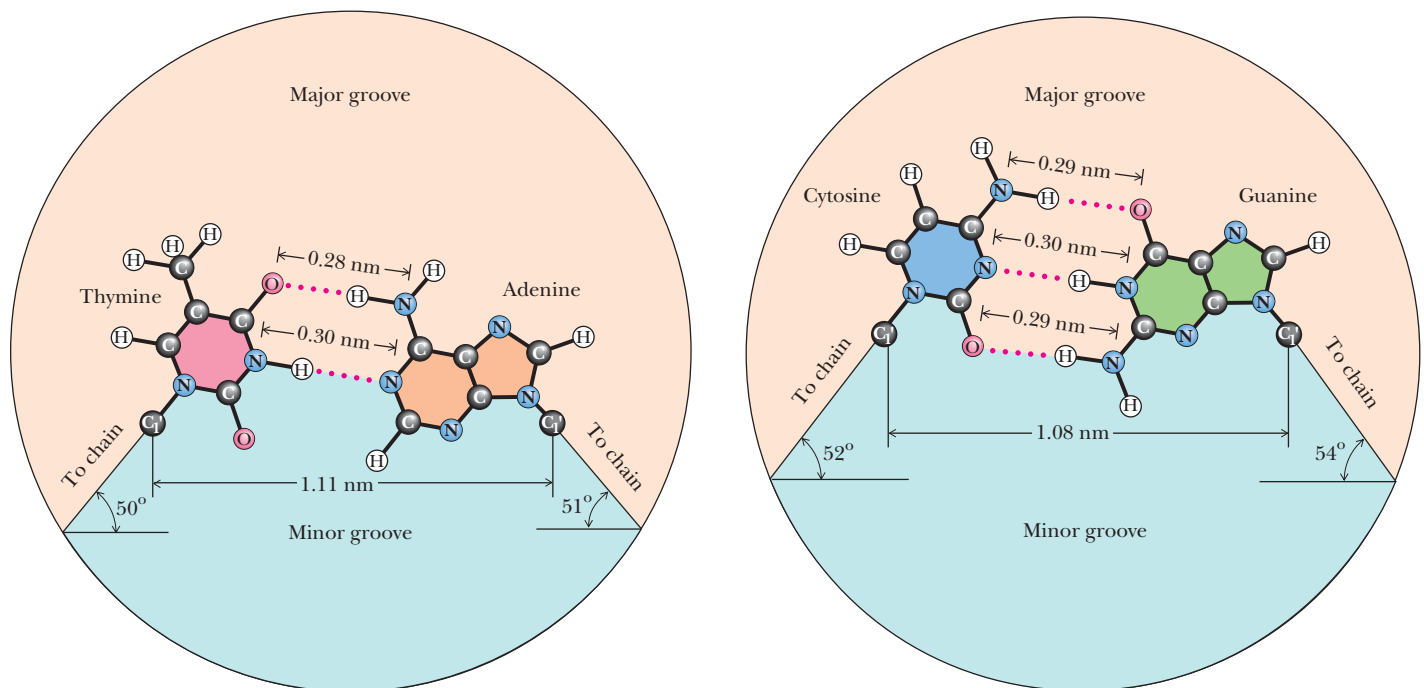
FIGURE 12.10 • Watson–Crick A:T and G:C base pairs. All H bonds in both base pairs are straight, with each H atom pointing directly at its acceptor N or O atom. Linear H bonds are the strongest. The mandatory binding of larger purines with smaller pyrimidines leads to base pairs that have virtually identical dimensions, allowing the two sugar–phosphate backbones to adopt identical helical conformations.
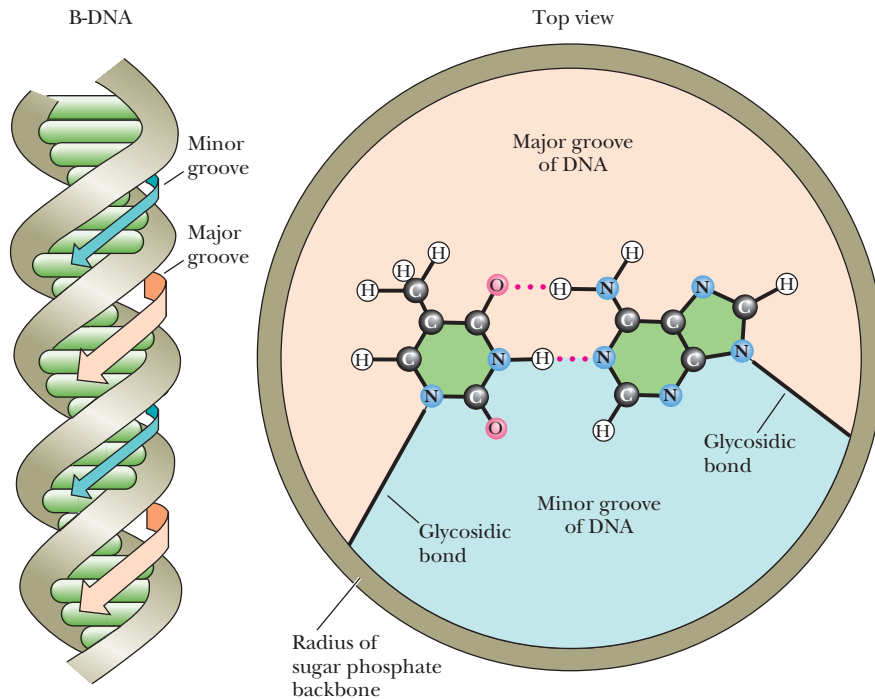
FIGURE 12.11 • The bases in a base pair are not directly across the helix axis from one another along some diameter but rather are slightly displaced. This displacement, and the relative orientation of the glycosidic bonds linking the bases to the sugar–phosphate backbone, leads to differently sized grooves in the cylindrical column created by the double helix, the major groove and the minor groove, each coursing along its length.

Two base pairs with 32° of right-handed helical twist: the *minor-groove edges are drawn with heavy shading.*

Propeller twist, as in (2), allows greater overlap of bases within the same strand and reduces the area of contact between the bases and water.

Propeller-twisted base pairs. Note how the hydrogen bonds between bases are distorted by this motion, yet remain intact. The minor-groove edges of the bases are shaded.

"antiparallel" directions. Furthermore, the two glycosidic bonds holding the bases in each base pair are not directly across the helix from each other, defining a common diameter (Figure 12.11). Consequently, the sugar–phosphate backbones of the helix are not equally spaced along the helix axis, and the grooves between them are not the same size. Instead, the intertwined chains create a **major groove** and a **minor groove** (Figure 12.11). The edges of the base pairs have a specific relationship to these grooves. The "top" edges of the base pairs ("top" as defined by placing the glycosidic bond at the bottom, as in Figure 12.10) are exposed along the interior surface or "floor" of the major groove; the base-pair edges nearest to the glycosidic bond form the interior surface of the minor groove. Some proteins that bind to DNA can actually recognize specific nucleotide sequences by "reading" the pattern of H-bonding possibilities presented by the edges of the bases in these grooves. Such DNA–protein interactions provide one step toward understanding how cells regulate the expression of genetic information encoded in DNA (see Chapter 32).

Conformational Variation in Double-Helical Structures

In solution, DNA ordinarily assumes the structure we have been discussing: B-DNA. However, nucleic acids also occur naturally in other double-helical forms. The base-pairing arrangement remains the same, but the sugar–phosphate groupings that constitute the backbone are inherently flexible and can adopt different conformations. One conformational variation is **propeller twist** (Figure 12.12). Propeller twist allows greater overlap between successive bases along a strand of DNA and diminishes the area of contact between bases and solvent water.
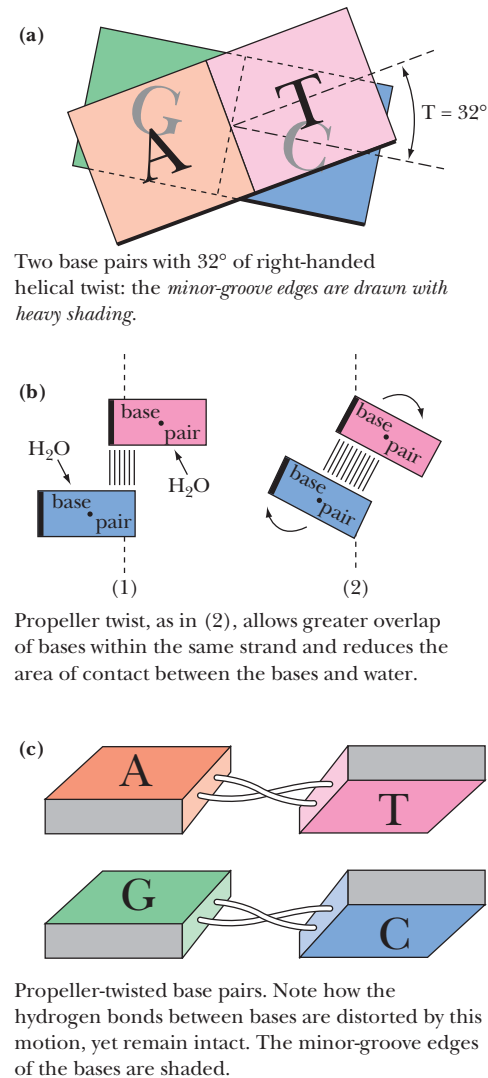
FIGURE 12.12 • Helical twist and propeller twist in DNA. (a) Successive base pairs in B-DNA show a rotation with respect to each other (so-called helical twist) of 36° or so, as viewed down the cylindrical axis of the DNA. (b) Rotation in a different dimension— **propellor twist**—allows the hydrophobic surfaces of bases to overlap better. The view here is edge-on to two successive bases in one DNA strand (as if the two bases on the right-hand strand of DNA in (a) were viewed from the right-hand margin of the page; dots represent end-on views down the glycosidic bonds). Clockwise rotation (as shown here) has a positive sign. (c) The two bases on the left-hand strand of DNA in (a) also show positive propellor twist (a clockwise rotation of the two bases in (a) as viewed from the left-hand margin of the paper). *(Adapted from Figure 3.4 in Callandine, C. R., and Drew, H. R., 1992.* Understanding DNA: The Molecule and How It Works. *London: Academic Press.)*
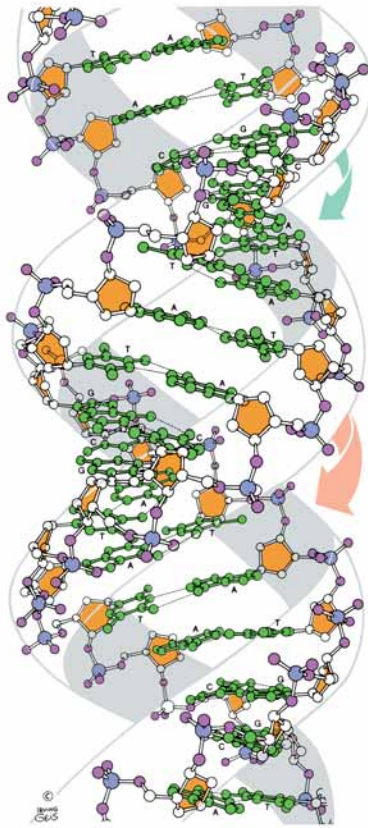
A
DNA
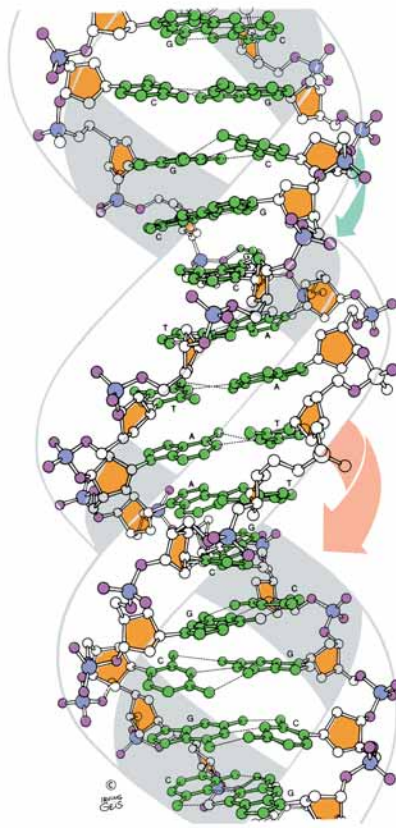
B
DNA
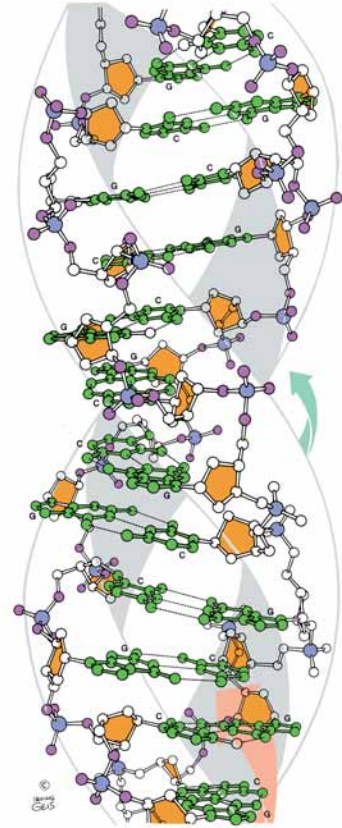
Z
DNA
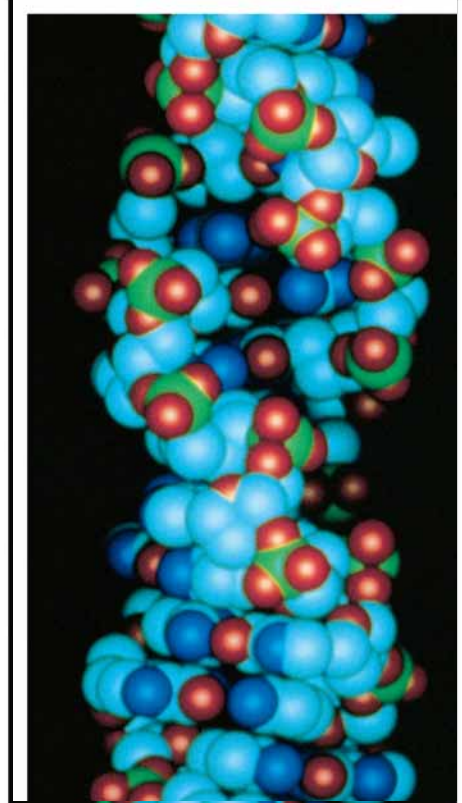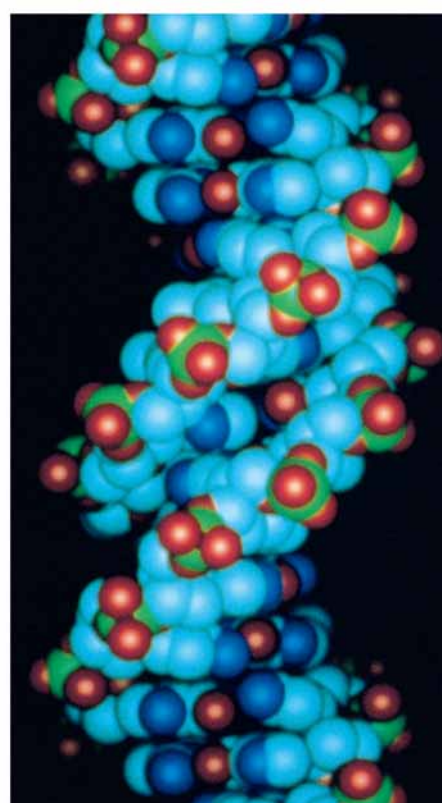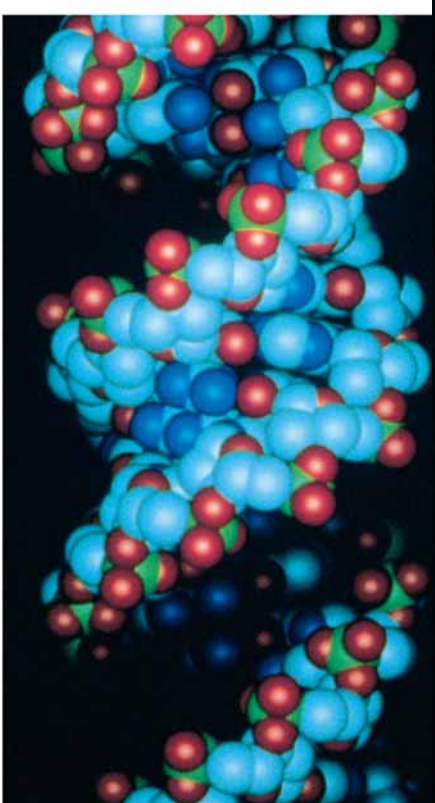
Alternative Form of Right-Handed DNA

An alternative form of the right-handed double helix is **A-DNA.** A-DNA molecules differ in a number of ways from B-DNA. The pitch, or distance required to complete one helical turn, is different. In B-DNA, it is 3.4 nm, whereas in A-DNA it is 2.46 nm. One turn in A-DNA requires 11 bp to complete. Depending on local sequence, 10 to 10.6 bp define one helical turn in B-form DNA. In A-DNA, the base pairs are no longer nearly perpendicular to the helix axis but instead are tilted 19° with respect to this axis. Successive base pairs occur every 0.23 nm along the axis, as opposed to 0.332 nm in B-DNA. The B-form of DNA is thus longer and thinner than the short, squat A-form, which has its base pairs displaced around, rather than centered on, the helix axis. Figure 12.13 shows the relevant structural characteristics of the A- and B-forms of DNA. (Z-DNA, another form of DNA to be discussed shortly, is also depicted in Figure 12.13.) A comparison of the structural properties of A-, B-, and Z-DNA is summarized in Table 12.1.

   Although relatively dehydrated DNA fibers can be shown to adopt the A-conformation under physiological conditions, it is unclear whether DNA ever assumes this form *in vivo*. However, double-helical DNA:RNA hybrids probably have an A-like conformation. The 2′-OH in RNA sterically prevents dou-

A
DNA

B
DNA

Z
DNA
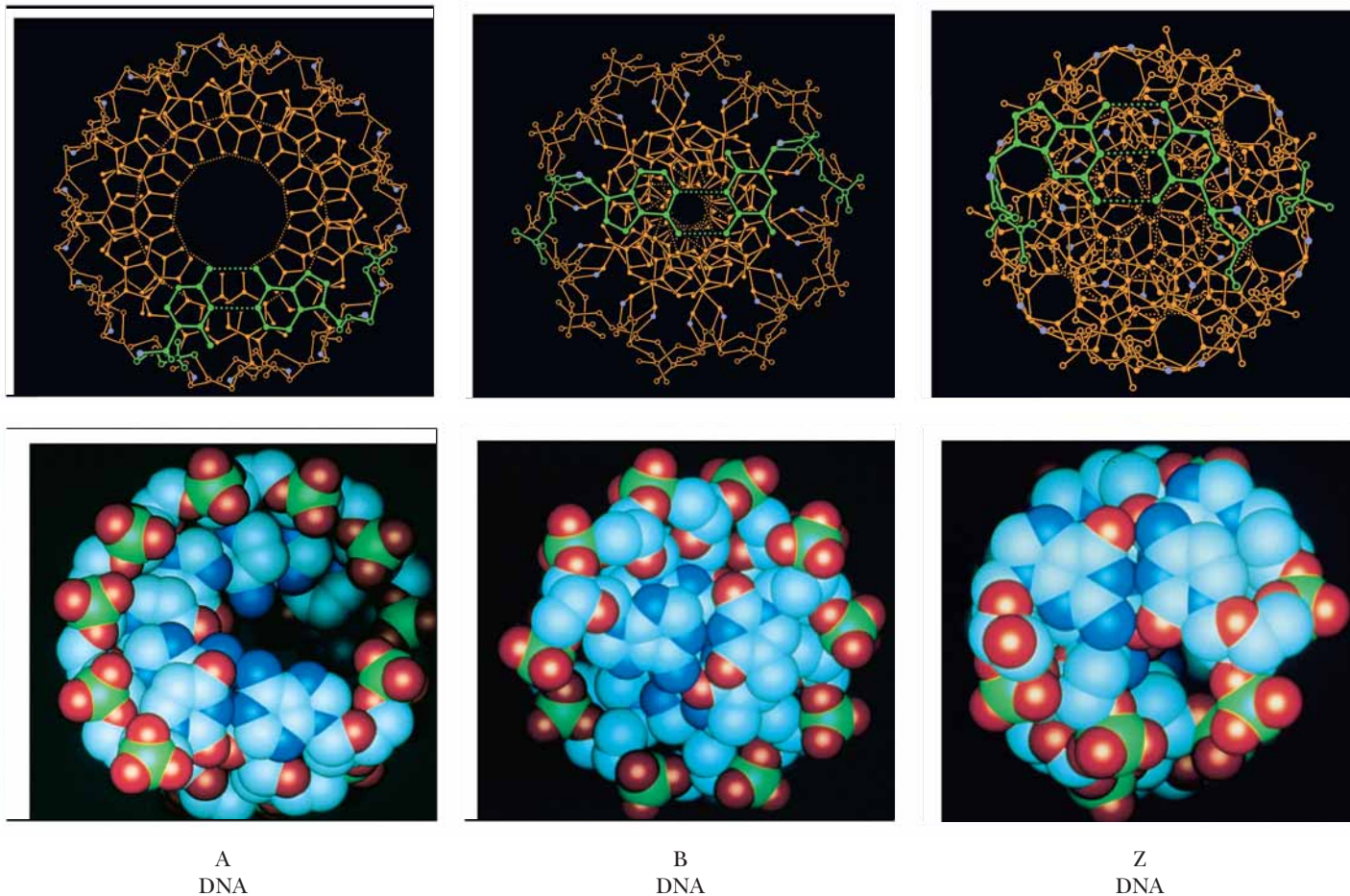
FIGURE 12.13 • *(here and on the facing page)* Comparison of the A-, B-, and Z-forms of the DNA double helix. The distance required to complete one helical turn is shorter in A-DNA than it is in B-DNA. The alternating pyrimidine–purine sequence of Z-DNA is the key to the "left-handedness" of this helix. *(Robert Stodola, Fox Chase Cancer Research Center, and Irving Geis)*

Table 12.1

Comparison of the Structural Properties of A-, B-, and Z-DNA

	Double Helix Type		
	A	B	Z
Overall proportions	Short and broad	Longer and thinner	Elongated and slim
Rise per base pair	2.3 Å	3.32 Å ± 0.19 Å	3.8 Å
Helix packing diameter	25.5 Å	23.7 Å	18.4 Å
Helix rotation sense	Right-handed	Right-handed	Left-handed
Base pairs per helix repeat	1	1	2
Base pairs per turn of helix	~11	~10	12
Mean rotation per base pair	33.6°	35.9° ± 4.2°	−60°/2
Pitch per turn of helix	24.6 Å	33.2 Å	45.6 Å
Base-pair tilt from the perpendicular	+19°	−1.2° ± 4.1°	−9°
Base-pair mean propeller twist	+18°	+16° ± 7°	~0°
Helix axis location	Major groove	Through base pairs	Minor groove
Major groove proportions	Extremely narrow but very deep	Wide and with intermediate depth	Flattened out on helix surface
Minor groove proportions	Very broad but shallow	Narrow and with intermediate depth	Extremely narrow but very deep
Glycosyl bond conformation	anti	anti	anti at C, syn at G

Adapted from Dickerson, R. L., et al., 1982. *Cold Spring Harbor Symposium on Quantitative Biology* **47**:14.

ble-helical regions of RNA chains from adopting the B-form helical arrangement. Importantly, double-stranded regions in RNA chains assume an A-like conformation, with their bases strongly tilted with respect to the helix axis.

Z-DNA: A Left-Handed Double Helix

Z-DNA was first recognized by Alexander Rich and his colleagues at MIT in X-ray analysis of the synthetic deoxynucleotide dCpGpCpGpCpG, which crystallized into an antiparallel double helix of unexpected conformation. The alternating pyrimidine–purine (Py–Pu) sequence of this oligonucleotide is the key to its unusual properties. The *N*-glycosyl bonds of G residues in this alternating copolymer are rotated 180° with respect to their conformation in B-DNA, so that now the purine ring is in the syn rather than the anti conformation (Figure 12.14). The C residues remain in the anti form. Because the G ring is "flipped," the C ring must also flip to maintain normal Watson–Crick base pairing. However, pyrimidine nucleosides do not readily adopt the syn conformation because it creates steric interference between the pyrimidine C-2 oxy substituent and atoms of the pentose. Because the cytosine ring does not rotate relative to the pentose, the whole C nucleoside (base and sugar) must flip 180° (Figure 12.15). It is topologically possible for the G to go syn and the C nucleoside to undergo rotation by 180° without breaking and re-forming the G:C hydrogen bonds. In other words, the B to Z structural transition can take place without disruption of the bonding relationships among the atoms involved.

Because alternate nucleotides assume different conformations, the repeating unit on a given strand in the Z-helix is the dinucleotide. That is, for any number of bases, *n*, along one strand, *n* − 1 dinucleotides must be considered. For example, a GpCpGpC subset of sequence along one strand is comprised

Deoxyguanosine in B-DNA (anti position) Deoxyguanosine in Z-DNA (syn position)
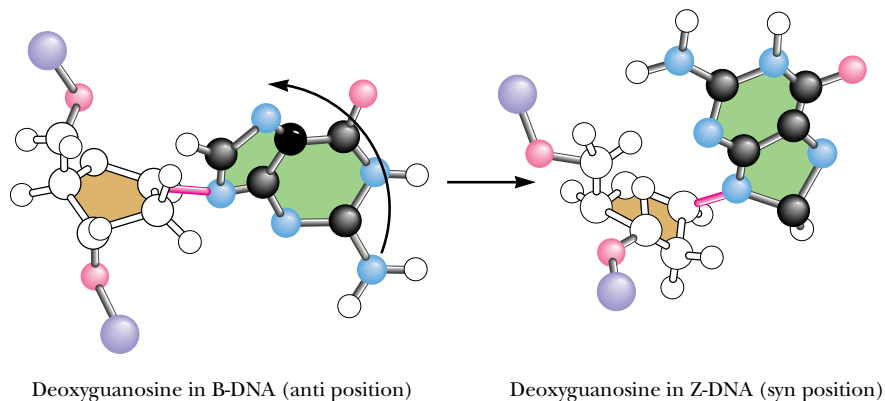
FIGURE 12.14 • Comparison of the deoxy-guanosine conformation in B- and Z-DNA. In B-DNA, the Cl′−N-9 glycosyl bond is always in the anti position *(left)*. In contrast, in the left-handed Z-DNA structure, this bond rotates (as shown) to adopt the syn conformation.

of *three* successive dinucleotide units: GpC, CpG, and GpC. (In B-DNA, the nucleotide conformations are essentially uniform and the repeating unit is the mononucleotide.) It follows that the CpG sequence is distinct conformation-ally from the GpC sequence along the alternating copolymer chains in the Z-double helix. The conformational alterations going from B to Z realign the sugar–phosphate backbone along a zigzag course that has a left-handed ori-entation (Figure 12.13), thus the designation *Z-DNA*. Note that in any GpCpGp subset, the sugar–phosphates of GpC form the horizontal "zig" while the CpG backbone segment forms the vertical "zag." The mean rotation angle circum-scribed around the helix axis is −15° for a CpG step and −45° for a GpC step (giving −60° for the dinucleotide repeat). The minus sign denotes a left-handed or counterclockwise rotation about the helix axis. Z-DNA is more elon-gated and slimmer than B-DNA.
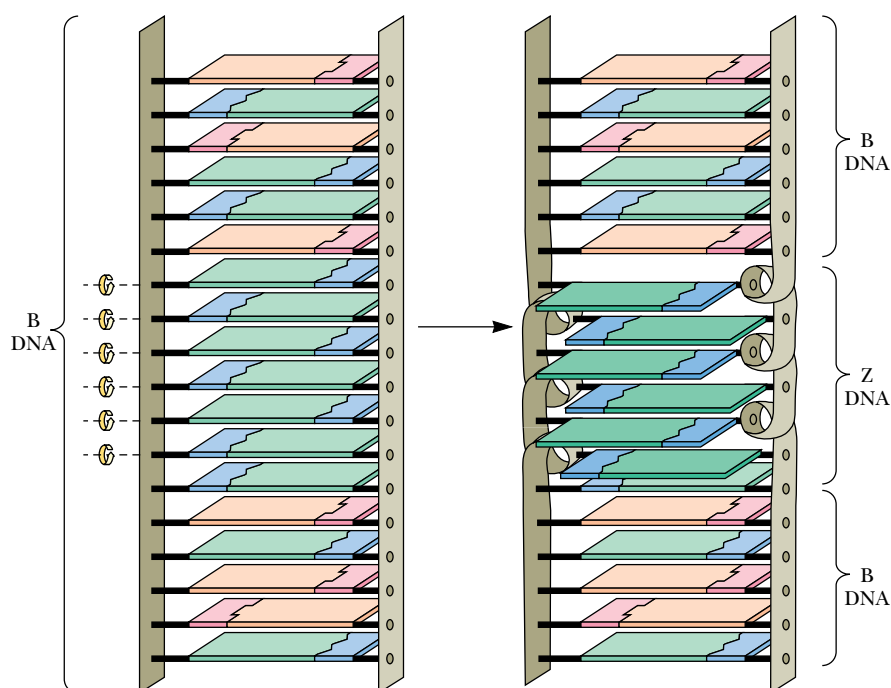
FIGURE 12.15 • The change in topological relationships of base pairs from B- to Z-DNA. A six-base-pair segment of B-DNA is converted to Z-DNA through rotation of the base pairs, as indicated by the curved arrows. The purine rings (green) of the deoxyguano-sine nucleosides rotate via an anti to syn change in the conformation of the guanine–deoxyribose glycosidic bond; the pyrimidine rings (blue) are rotated by flipping the entire deoxycytidine nucleoside (base *and* deoxyri-bose). As a consequence of these conforma-tional changes, the base pairs in the Z-DNA region no longer share π,π stacking interac-tions with adjacent B-DNA regions.

Cytosine Methylation and Z-DNA

The Z-form can arise in sequences that are not strictly alternating Py–Pu. For example, the hexanucleotide ^{m5}CGAT^{m5}CG, a Py-Pu-Pu-Py-Py-Pu sequence containing two 5-methylcytosines (^{m5}C), crystallizes as Z-DNA. Indeed, the *in vivo* methylation of C at the 5-position is believed to favor a B to Z switch because, in B-DNA, these hydrophobic methyl groups would protrude into the aqueous environment of the major groove and destabilize its structure. In Z-DNA, the same methyl groups can form a stabilizing hydrophobic patch. It is likely that the Z-conformation naturally occurs in specific regions of cellular DNA, which otherwise is predominantly in the B-form. Furthermore, because methylation is implicated in gene regulation, the occurrence of Z-DNA may affect the expression of genetic information (see Part IV, Information Transfer).

The Double Helix in Solution

The long-range structure of B-DNA in solution is not a rigid, linear rod. Instead, DNA behaves as a dynamic, flexible molecule. Localized thermal fluctuations temporarily distort and deform DNA structure over short regions. Base and backbone ensembles of atoms undergo elastic motions on a time scale of nanoseconds. To some extent, these effects represent changes in rotational angles of the bonds comprising the polynucleotide backbone. These changes are also influenced by sequence-dependent variations in base-pair stacking. The consequence is that the helix bends gently. When these variations are summed over the great length of a DNA molecule, the net result of these bending motions is that, at any given time, the double helix assumes a roughly spherical shape, as might be expected for a long, semi-rigid rod undergoing apparently random coiling. It is also worth noting that, on close scrutiny, the surface of the double helix is *not* that of a totally featureless, smooth, regular "barber pole" structure. Different base sequences impart their own special signatures to the molecule by subtle influences on such factors as the groove width, the angle between the helix axis and base planes, and the mechanical rigidity. Certain regulatory proteins bind to specific DNA sequences and participate in activating or suppressing expression of the information encoded therein. These proteins bind at unique sites by virtue of their ability to recognize novel structural characteristics imposed on the DNA by the local nucleotide sequence.

Intercalating Agents Distort the Double Helix

intercalate • to insert between others

Aromatic macrocycles, flat hydrophobic molecules composed of fused, heterocyclic rings, such as **ethidium bromide, acridine orange,** and **actinomycin D** (Figure 12.16), can insert between the stacked base pairs of DNA. The bases are forced apart to accommodate these so-called **intercalating agents,** causing an unwinding of the helix to a more ladderlike structure. The deoxyribose–phosphate backbone is almost fully extended as successive base pairs are displaced 0.7 nm from one another, and the rotational angle about the helix axis between adjacent base pairs is reduced from 36° to 10°.

Dynamic Nature of the DNA Double Helix in Solution

Intercalating substances insert with ease into the double helix, indicating that the van der Waals bonds they form with the bases sandwiching them are more favorable than similar bonds between the bases themselves. Furthermore, the fact that these agents slip in suggests that the double helix must temporarily unwind and present gaps for these agents to occupy. That is, the DNA double helix in solution must be represented by a set of metastable alternatives to the standard B-conformation. These alternatives constitute a flickering repertoire of dynamic structures.

Sar = Sarcosine = H_3C — N — CH_2 — COOH (N-Methylglycine)
                          |
                          H

Meval = Mevalonic acid = $HOCH_2$ — CH_2 — C — CH_2 — COOH
                                              |
                                    CH_3 above C, OH below C
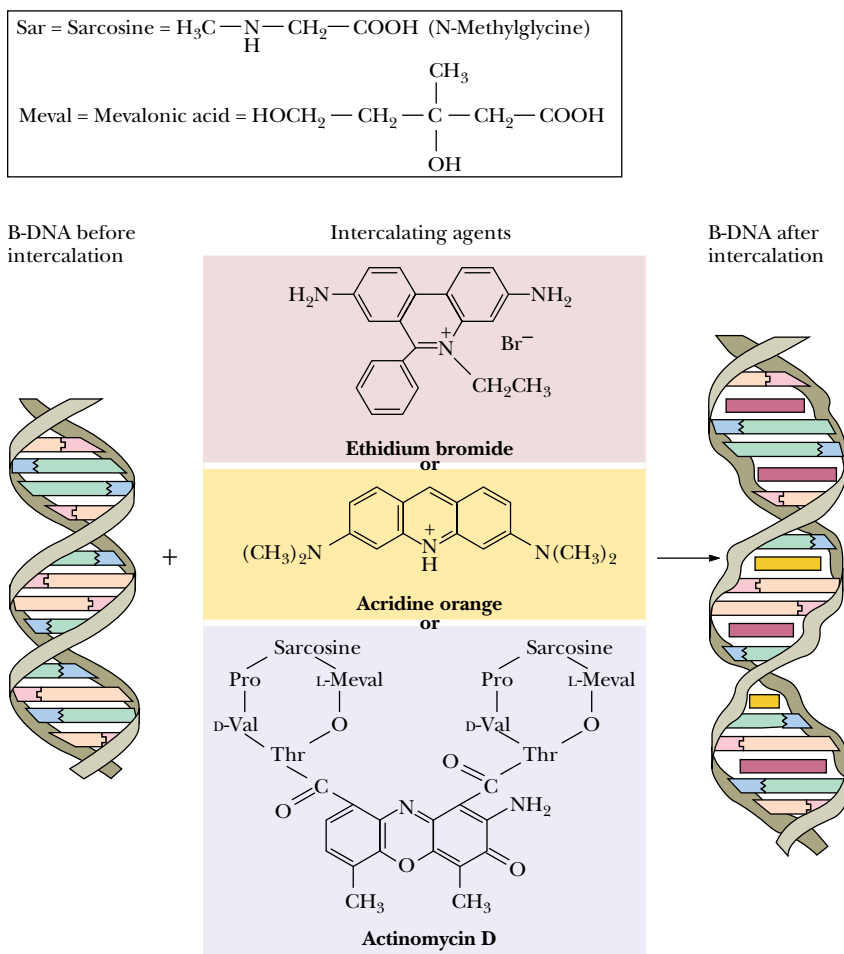
FIGURE 12.16 • The structures of ethidium bromide, acridine orange, and actinomycin D, three intercalating agents, and their effects on DNA structure.

12.3 • Denaturation and Renaturation of DNA

Thermal Denaturation and Hyperchromic Shift

When duplex DNA molecules are subjected to conditions of pH, temperature, or ionic strength that disrupt hydrogen bonds, the strands are no longer held together. That is, the double helix is **denatured** and the strands separate as individual random coils. If temperature is the denaturing agent, the double helix is said to *melt*. The course of this dissociation can be followed spectrophotometrically because the relative absorbance of the DNA solution at 260 nm increases as much as 40% as the bases unstack. This absorbance increase, or **hyperchromic shift,** is due to the fact that the aromatic bases in DNA interact via their π electron clouds when stacked together in the double helix. Because the UV absorbance of the bases is a consequence of π electron transitions, and because the potential for these transitions is diminished when the bases stack, the bases in duplex DNA absorb less 260-nm radiation than expected for their numbers. Unstacking alleviates this suppression of UV absorbance. The rise in absorbance coincides with strand separation, and the midpoint of the absorbance increase is termed the **melting temperature,** T_m

FIGURE 12.17 • Heat denaturation of DNA from various sources, so-called melting curves. The midpoint of the melting curve is defined as the melting temperature, T_m. *(From Marmur, J., 1959. Nature **183**:1427–1429.)*
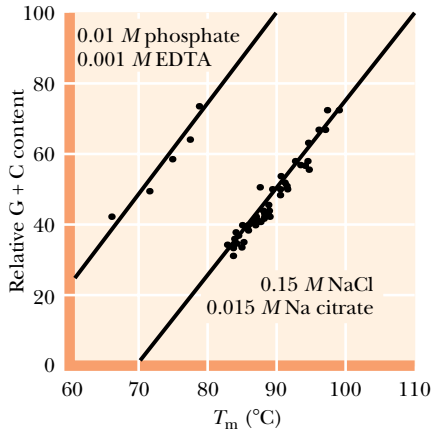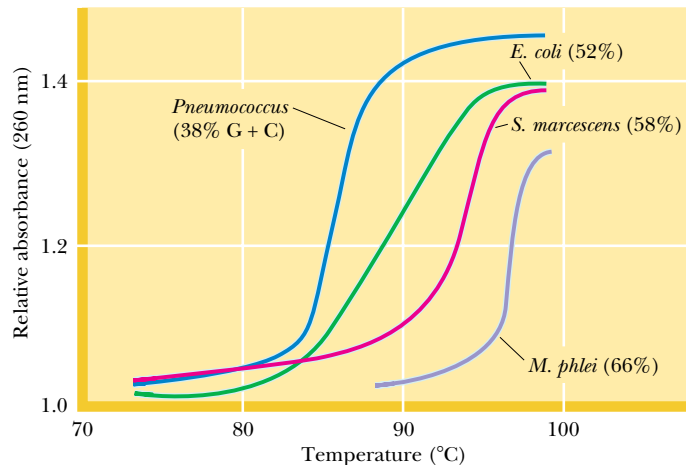
FIGURE 12.18 • The dependence of melting temperature on relative (G + C) content in DNA. Note that T_m increases if ionic strength is raised at constant pH (pH 7); 0.01 *M* phosphate+0.001 *M* EDTA versus 0.15 *M* NaCl/0.015 *M* Na citrate. In 0.15 *M* NaCl/0.015 *M* Na citrate, duplex DNA consisting of 100% A:T pairs melts at less than 70°C, whereas DNA of 100% G:C has a T_m greater than 110°C. *(From Marmur, J., and Doty, P., 1962. Journal of Molecular Biology **5**:120.)*

(Figure 12.17). DNAs differ in their T_m values because they differ in relative G + C content. The higher the G + C content of a DNA, the higher its melting temperature because G:C pairs are held by three H bonds whereas A:T pairs have only two. The dependence of T_m on the G + C content is depicted in Figure 12.18. Also note that T_m is dependent on the ionic strength of the solution; the lower the ionic strength, the lower the melting temperature. At 0.2 *M* Na^+, $T_m = 69.3 + 0.41(\% \text{ G} + \text{C})$. Ions suppress the electrostatic repulsion between the negatively charged phosphate groups in the complementary strands of the helix, thereby stabilizing it. (DNA in pure water melts even at room temperature.) At high concentrations of ions, T_m is raised and the transition between helix and coil is sharp.

pH Extremes or Strong H-Bonding Solutes Also Denature DNA Duplexes

At pH values greater than 10, extensive deprotonation of the bases occurs, destroying their hydrogen bonding potential and denaturing the DNA duplex. Similarly, extensive protonation of the bases below pH 2.3 disrupts base pairing. Alkali is the preferred denaturant because, unlike acid, it does not hydrolyze the glycosidic linkages in the sugar–phosphate backbone. Small solutes that readily form H bonds are also DNA denaturants at temperatures below T_m if present in sufficiently high concentrations to compete effectively with the H-bonding between the base pairs. Examples include formamide and urea.

DNA Renaturation

Denatured DNA will **renature** to re-form the duplex structure if the denaturing conditions are removed (that is, if the solution is cooled, the pH is returned to neutrality, or the denaturants are diluted out). Renaturation requires reassociation of the DNA strands into a double helix, a process termed **reannealing.** For this to occur, the strands must realign themselves so that their complementary bases are once again in register and the helix can be zippered up (Figure 12.19). Renaturation is dependent both on DNA concentration and time. Many of the realignments are imperfect, and thus the strands must dissociate again to allow for proper pairings to be formed. The process occurs more quickly if the temperature is warm enough to promote diffusion of the large DNA molecules but not so warm as to cause melting.
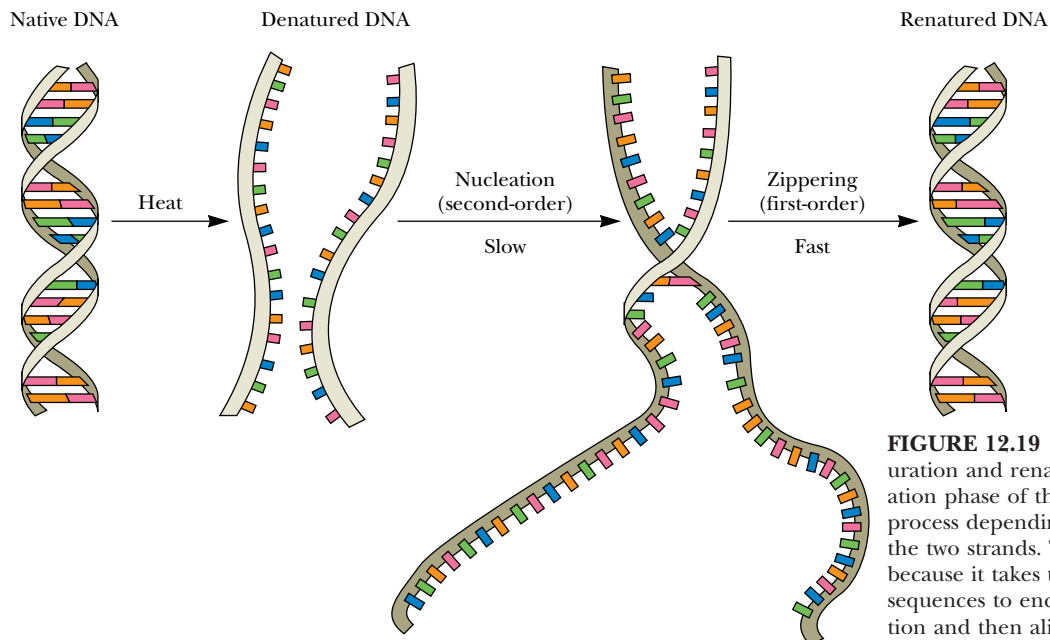
FIGURE 12.19 • Steps in the thermal denaturation and renaturation of DNA. The nucleation phase of the reaction is a second-order process depending on sequence alignment of the two strands. This process takes place slowly because it takes time for complementary sequences to encounter one another in solution and then align themselves in register. Once the sequences are aligned, the strands zipper up quickly.

Renaturation Rate and DNA Sequence Complexity—c_0t Curves

The renaturation rate of DNA is an excellent indicator of the sequence complexity of DNA. For example, bacteriophage T_4 DNA contains about 2×10^5 nucleotide pairs, whereas *Escherichia coli* DNA possesses 4.64×10^6. *E. coli* DNA is considerably more complex in that it encodes more information. Expressed another way, for any given amount of DNA (in grams), the sequences represented in an *E. coli* sample are more heterogeneous, that is, more dissimilar from one another, than those in an equal weight of phage T_4 DNA. Therefore, it will take the *E. coli* DNA strands longer to find their complementary partners and reanneal. This situation can be analyzed quantitatively.

If c is the concentration of single-stranded DNA at time t, then the second-order rate equation for two complementary strands coming together is given by the rate of decrease in c:

$$-dc/dt = k_2 c^2$$

where k_2 is the second-order rate constant. Starting with a concentration, c_0, of completely denatured DNA at $t = 0$, the amount of single-stranded DNA remaining at some time t is

$$c/c_0 = 1/(1 + k_2 c_0 t)$$

where the units of c are mol of nucleotide per L and t is in seconds. The time for half of the DNA to renature (when $c/c_0 = 0.5$) is defined as $t = t_{1/2}$. Then,

$$0.5 = 1/(1 + k_2 c_0 t_{1/2}) \quad \text{and thus} \quad 1 + k_2 c_0 t_{1/2} = 2$$

yielding

$$c_0 t_{1/2} = 1/k_2$$

A graph of the fraction of single-stranded DNA reannealed (c/c_0) as a function of $c_0 t$ on a semilogarithmic plot is referred to as a **c_0t** (pronounced "cot") **curve** (Figure 12.20). The rate of reassociation can be followed spectrophotometrically by the UV absorbance decrease as duplex DNA is formed. Note that

FIGURE 12.20 • These c_0t curves show the rates of reassociation of denatured DNA from various sources and illustrate how the rate of reassociation is inversely proportional to genome complexity. The DNA sources are as follows: poly A+poly U, a synthetic DNA duplex of poly A and poly U polynucleotide chains; mouse satellite DNA, a fraction of mouse DNA in which the same sequence is repeated many thousands of times; MS-2 dsRNA, the double-stranded form of RNA found during replication of MS-2, a simple bacteriophage; T4 DNA, the DNA of a more complex bacteriophage; *E. coli* DNA, bacterial DNA; calf DNA (nonrepetitive fraction), mammalian DNA (calf) from which the highly repetitive DNA fraction (satellite DNA) has been removed. Arrows indicate the genome size (in bp) of the various DNAs. *(From Britten, R. J., and Kohne, D. E., 1968.* Science **161:***529–540.)*
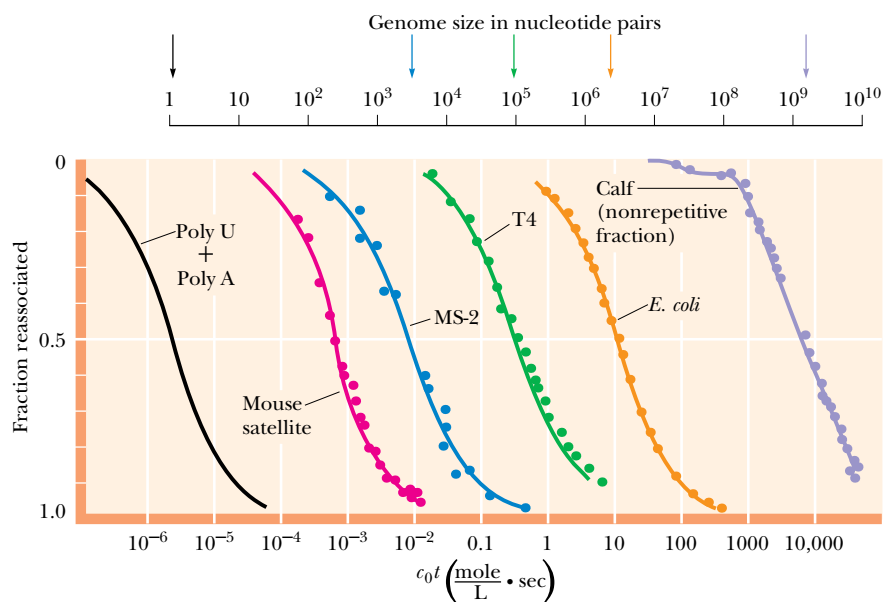
relatively more complex DNAs take longer to renature, as reflected by their greater $c_0t_{1/2}$ values. Poly A and poly U (Figure 12.20) are minimally complex in sequence and anneal rapidly to form a double-stranded A:U polynucleotide. *Mouse satellite DNA* is a highly repetitive subfraction of mouse DNA. Its lack of sequence heterogeneity is seen in its low $c_0t_{1/2}$ value. MS-2 is a small bacteriophage whose genetic material is RNA. Calf thymus DNA is the mammalian representative in Figure 12.20.

Nucleic Acid Hybridization

If DNA from two different species are mixed, denatured, and allowed to cool slowly so that reannealing can occur, artificial **hybrid duplexes** may form, provided the DNA from one species is similar in nucleotide sequence to the DNA of the other. The degree of hybridization is a measure of the sequence similarity or *relatedness* between the two species. Depending on the conditions of the experiment, about 25% of the DNA from a human forms hybrids with mouse DNA, implying that some of the nucleotide sequences (genes) in humans are very similar to those in mice. Mixed RNA:DNA hybrids can be created *in vitro* if single-stranded DNA is allowed to anneal with RNA copies of itself, such as those formed when genes are transcribed into mRNA molecules.

Nucleic acid hybridization is a commonly employed procedure in molecular biology. First, it can reveal evolutionary relationships. Second, it gives researchers the power to identify specific genes selectively against a vast background of irrelevant genetic material. An appropriately labeled oligo- or polynucleotide, referred to as a **probe,** is constructed so that its sequence is complementary to a target gene. The probe specifically base pairs with the target gene, allowing identification and subsequent isolation of the gene. Also, the quantitative expression of genes (in terms of the amount of mRNA synthesized) can be assayed by hybridization experiments.

Buoyant Density of DNA

Not only the melting temperature of DNA but also its density in solution is dependent on relative G:C content. G:C-rich DNA has a significantly higher density than A:T-rich DNA. Furthermore, a linear relationship exists between the buoyant densities of DNA from different sources and their G:C content
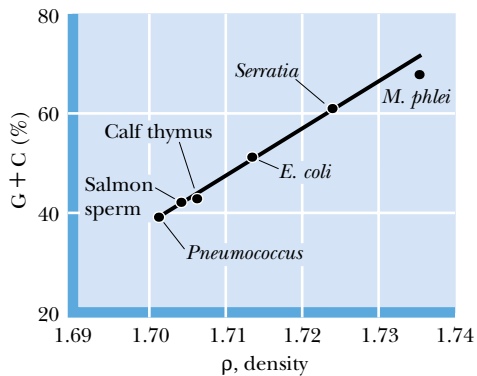
FIGURE 12.21 • The relationship of the densities (in g/mL) of DNAs from various sources and their G:C content. *(From Doty, P., 1961.* Harvey Lectures **55:***103.)*

(Figure 12.21). The density of DNA, ρ (in g/mL), as a function of its G:C content is given by the equation $\rho = 1.660 + 0.098(GC)$, where (GC) is the mole fraction of (G + C) in the DNA. Because of its relatively high density, DNA can be purified from cellular material by a form of density gradient centrifugation known as *isopycnic centrifugation* (see Appendix to this chapter).

12.4 • Supercoils and Cruciforms: Tertiary Structure in DNA

The conformations of DNA discussed thus far are variations sharing a common secondary structural theme, the double helix, in which the DNA is assumed to be in a regular, linear form. DNA can also adopt regular structures of higher complexity in several ways. For example, many DNA molecules are circular. Most, if not all, bacterial chromosomes are covalently closed, circular DNA duplexes, as are almost all plasmid DNAs. **Plasmids** are naturally occurring, self-replicating, circular, extrachromosomal DNA molecules found in bacteria; plasmids carry genes specifying novel metabolic capacities advantageous to the host bacterium. Various animal virus DNAs are circular as well.

Supercoils

In duplex DNA, the two strands are wound about each other once every 10 bp, that is, once every turn of the helix. Double-stranded circular DNA (or linear DNA duplexes whose ends are not free to rotate), form **supercoils** if the strands are underwound (*negatively supercoiled*) or overwound (*positively supercoiled*) (Figure 12.22). Underwound duplex DNA has fewer than the natural number of turns, whereas overwound DNA has more. DNA supercoiling is analogous to twisting or untwisting a two-stranded rope so that it is torsionally stressed. Negative supercoiling introduces a torsional stress that favors unwinding of the right-handed B-DNA double helix, while positive supercoiling overwinds such a helix. Both forms of supercoiling compact the DNA so that it sediments faster upon ultracentrifugation or migrates more rapidly in an electrophoretic gel in comparison to **relaxed DNA** (DNA that is not supercoiled).

Linking Number

The basic parameter characterizing supercoiled DNA is the **linking number** (L). This is the number of times the two strands are intertwined, and, provided both strands remain covalently intact, L cannot change. In a relaxed circular

(a)

(b)

(c)

Toroidal spirals within supercoil

Interwound supercoil

Base of loop
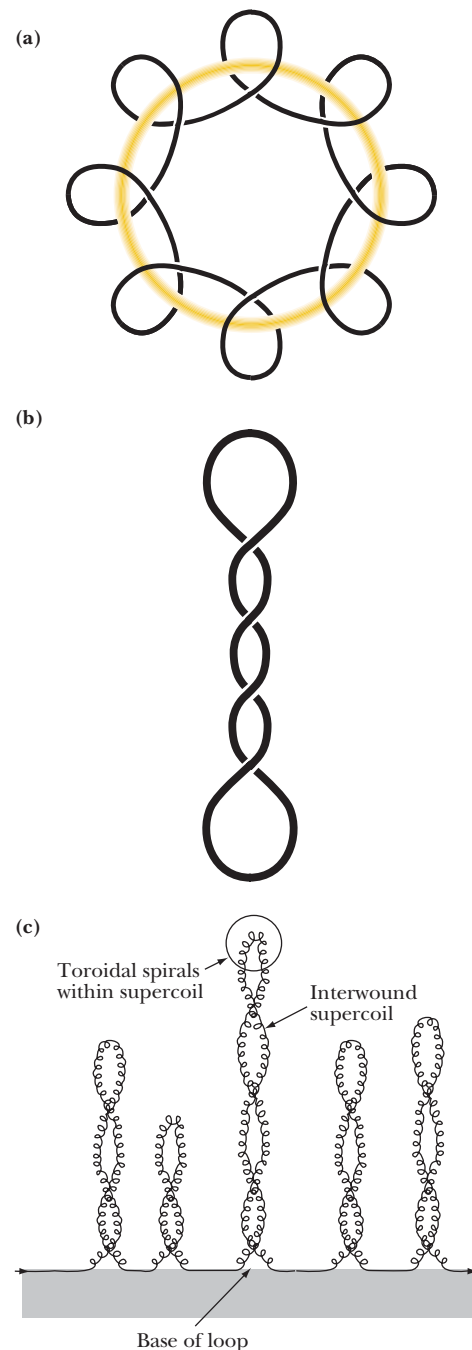
FIGURE 12.22 • Toroidal and interwound varieties of DNA supercoiling. (a) The DNA is coiled in a spiral fashion about an imaginary toroid. (b) The DNA interwinds and wraps about itself. (c) Supercoils in long, linear DNA arranged into loops whose ends are restrained —a model for chromosomal DNA. *(Adapted from Figures 6.1 and 6.2 in Callandine, C. R., and Drew, H. R., 1992.* Understanding DNA: The Molecule and How It Works. *London: Academic Press.)*
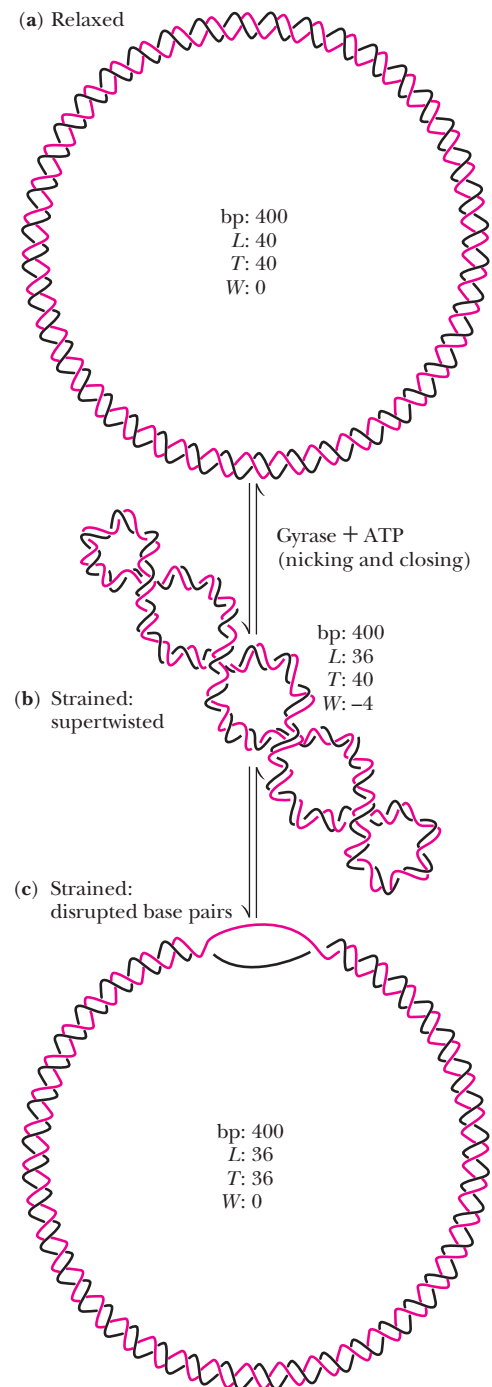
DNA loop

(+) node   (−) node

ATP

(+) node   (−) node

DNA is cut and a conformational change allows the DNA to pass through. Gyrase religates the DNA and then releases it.

ADP + P
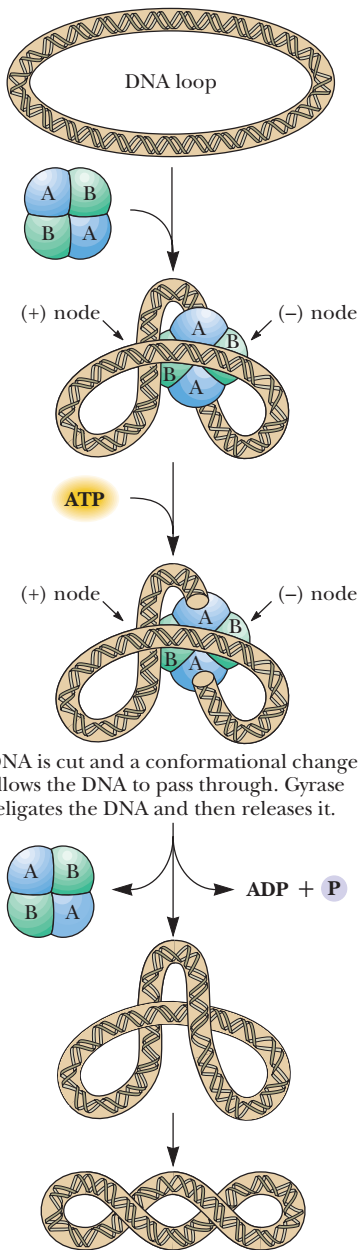
FIGURE 12.24 • A simple model for the action of bacterial DNA gyrase (topoisomerase II). The A-subunits cut the DNA duplex and then hold onto the cut ends. Conformational changes occur in the enzyme that allow a continuous region of the DNA duplex to pass between the cut ends and into an internal cavity of the protein. The cut ends are then re-ligated, and the intact DNA duplex is released from the enzyme. The released intact circular DNA now contains two negative supercoils as a consequence of DNA gyrase action.

(a) Positive supercoiling

| $T = 0$ $W = 0$ | $T = +3$ $W = 0$ | $T = +2$ $W = +1$ | $T = +1$ $W = +2$ | $T = 0$ $W = +3$ |

$L = 0$ $\qquad\qquad L = +3$

(1)   (2)   (3)   (4)   (5)

(b) Negative supercoiling

| $T = 0$ $W = 0$ | $T = -3$ $W = 0$ | $T = -2$ $W = -1$ | $T = -1$ $W = -2$ | $T = 0$ $W = -3$ |

$L = 0$ $\qquad\qquad L = -3$

(1)   (2)   (3)   (4)   (5)
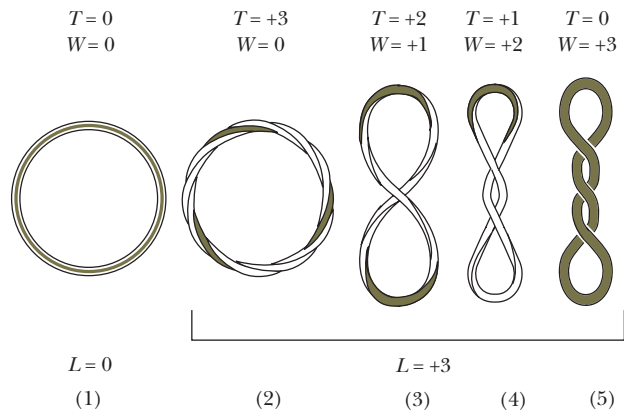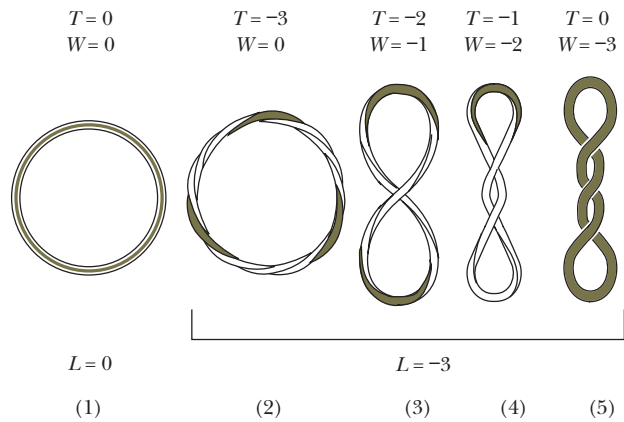
FIGURE 12.23 • Supercoiled DNA topology. *(Adapted from Figures 6.5 and 6.6 in Callandine, C. R., and Drew, H. R., 1992.* Understanding DNA: The Molecule and How It Works. *London: Academic Press.)*

DNA duplex of 400 bp, L is 40 (assuming 10 bp per turn in B-DNA). The linking number for relaxed DNA is usually taken as the reference parameter and is written as L_0. L can be equated to the **twist** (T) and **writhe** (W) of the duplex, where twist is the number of helical turns and writhe is the number of supercoils:

$$L = T + W$$

Figure 12.23a shows the values of T and W for various positively and negatively supercoiled circular DNAs. In any closed, circular DNA duplex that is relaxed, $W = 0$. A relaxed circular DNA of 400 bp has 40 helical turns, $T = L = 40$. This linking number can only be changed by breaking one or both strands of the DNA, winding them tighter or looser, and rejoining the ends. Enzymes capable of carrying out such reactions are called **topoisomerases** because they change the topological state of DNA. Topoisomerase falls into two basic classes, I and II. Topoisomerases of the I type cut one strand of a DNA double helix, pass the other strand through, and then rejoin the cut ends. Topoisomerase II enzymes cut both strands of a dsDNA, pass a region of the DNA duplex between the cut ends, and then rejoin the ends (Figure 12.24). Topoisomerases are important players in DNA replication (see Chapter 30).

DNA Gyrase

The bacterial enzyme **DNA gyrase** is a topoisomerase that introduces negative supercoils into DNA in the manner shown in Figure 12.24. Suppose DNA gyrase puts four negative supercoils into the 400-bp circular duplex, then $W = -4$, T remains the same, and $L = 36$ (Figure 12.25). In actuality, the negative supercoils cause a torsional stress on the molecule so that T tends to decrease; that is, the helix becomes a bit unwound so that base pairs are separated. The extreme would be that T would decrease by 4 and the supercoiling would be removed ($T = 36$, $L = 36$, and $W = 0$). Usually the real situation is a compromise in which the negative value of W is reduced, T decreases slightly, and these changes are distributed over the length of the circular duplex so that no localized unwinding of the helix ensues. Although the parameters T and W are conceptually useful, neither can be measured experimentally at the present time.

Superhelix Density

The difference between the linking number of a DNA and the linking number of its relaxed form is ΔL: $\Delta L = (L - L_0)$. In our example with four negative supercoils, $\Delta L = -4$. The **superhelix density** or **specific linking difference** is defined as $\Delta L/L_0$ and is sometimes termed *sigma, σ*. For our example, $\sigma = -4/40$, or -0.1. As a ratio, σ is a measure of supercoiling that is independent of length. Its sign reflects whether the supercoiling tends to unwind (*negative σ*) or overwind (*positive σ*) the helix. In other words, the superhelix density states the number of supercoils per 10 bp, which also is the same as the number of supercoils per B-DNA repeat. Circular DNA isolated from natural sources is always found in the underwound, negatively supercoiled state.

Toroidal Supercoiled DNA

Negatively supercoiled DNA can arrange into a toroidal state (Figure 12.26). The toroidal state of negatively supercoiled DNA is stabilized by wrapping around proteins which serve as spools for the DNA "ribbon." This toroidal con-

(a) Relaxed

bp: 400
L: 40
T: 40
W: 0

Gyrase + ATP
(nicking and closing)

bp: 400
L: 36
T: 40
W: –4

(b) Strained: supertwisted

(c) Strained: disrupted base pairs

bp: 400
L: 36
T: 36
W: 0

FIGURE 12.25 • A 400-bp circular DNA molecule in different topological states: (a) relaxed, (b) negative supercoils distributed over the entire length, and (c) negative supercoils creating a localized single-stranded region. Negative supercoiling has the potential to cause localized unwinding of the DNA double helix so that single-stranded regions (or bubbles) are created.

(a) $T = -2$, $W = 0$

Protein spool

(b) $T = 0$, $W = -2$

(c) $T = 0$, $W = -2$

FIGURE 12.26 • Supercoiled DNA in a toroidal form wraps readily around protein "spools." A twisted segment of linear DNA with two negative supercoils (a) can collapse into a toroidal conformation if its ends are brought closer together (b). Wrapping the DNA toroid around a protein "spool" stabilizes this conformation of supercoiled DNA (c). *(Adapted from Figure 6.6 in Callandine, C. R., and Drew, H. R., 1992.* Understanding DNA: The Molecule and How It Works. *London: Academic Press.)*

FIGURE 12.27 • The formation of a cruciform structure from a palindromic sequence within DNA. The self-complementary inverted repeats can rearrange to form hydrogen-bonded cruciform loops.

formation of DNA is found in protein : DNA interactions that are the basis of phenomena as diverse as chromosome structure (see Figure 12.31) and gene expression.

Cruciforms

Palindromes are words, phrases, or sentences that are the same when read backward or forward, such as "radar," "sex at noon taxes," "Madam, I'm Adam," and "a man, a plan, a canal, Panama." DNA sequences that are **inverted repeats,** or palindromes, have the potential to form a tertiary structure known as a **cruciform** (literally meaning "cross-shaped") if the normal interstrand base pairing is replaced by intrastrand pairing (Figure 12.27). In effect, each DNA strand folds back on itself in a hairpin structure to align the palindrome in base-pairing register. Such cruciforms are never as stable as normal DNA duplexes because an unpaired segment must exist in the loop region. However, negative supercoiling causes a localized disruption of hydrogen bonding between base pairs in DNA and may promote formation of cruciform loops. Cruciform structures have a twofold rotational symmetry about their centers and potentially create distinctive recognition sites for specific DNA-binding proteins.

12.5 • Chromosome Structure

A typical human cell is 20 μm in diameter. Its genetic material consists of 23 pairs of dsDNA molecules in the form of **chromosomes,** the average length of which is 3×10^9 bp/23 or 1.3×10^8 nucleotide pairs. At 0.34 nm/bp in B-DNA, this represents a DNA molecule 5 cm long. Together, these 46 dsDNA molecules amount to more than 2 m of DNA that must be packaged into a nucleus perhaps 5μm in diameter! Clearly, the DNA must be condensed by a factor of more than 10^5. This remarkable task is accomplished by neatly wrapping the DNA around protein spools called **nucleosomes** and then packing the nucleosomes to form a helical filament that is arranged in loops associated with the **nuclear matrix,** a skeleton or scaffold of proteins providing a structural framework within the nucleus.

Table 12.2

Properties of Histones

Histone	Ratio of Lysine to Arginine	M_r	Copies per Nucleosome
H1	59/3	21,200	1 (not in bead)
H2A	13/13	14,100	2 (in bead)
H2B	20/8	13,900	2 (in bead)
H3	13/17	15,100	2 (in bead)
H4	11/14	11,400	2 (in bead)

Nucleosomes

The DNA in a eukaryotic cell nucleus during the interphase between cell divisions exists as a nucleoprotein complex called **chromatin.** The proteins of chromatin fall into two classes: **histones** and **nonhistone chromosomal proteins.** Histones are abundant structural proteins, whereas the nonhistone class is represented only by a few copies each of many diverse proteins involved in genetic regulation. The histones are relatively small, positively charged arginine- or lysine-rich proteins that interact via ionic bonds with the negatively charged phosphate groups on the polynucleotide backbone. Five distinct histones are known: **H1, H2A, H2B, H3,** and **H4** (Table 12.2). Pairs of histones H2A, H2B, H3, and H4 aggregate to form an octameric core structure, which is the core of the **nucleosome,** around which the DNA helix is wound (see Figure 11.23).

If chromatin is swelled suddenly in water and prepared for viewing in the electron microscope, the nucleosomes are evident as "beads on a string," dsDNA being the string (Figure 12.28). The structure of the histone octamer core has been determined by X-ray crystallography without DNA by E. N. Moudrianakis's laboratory (Figure 12.29) and wrapped with DNA by T. J.
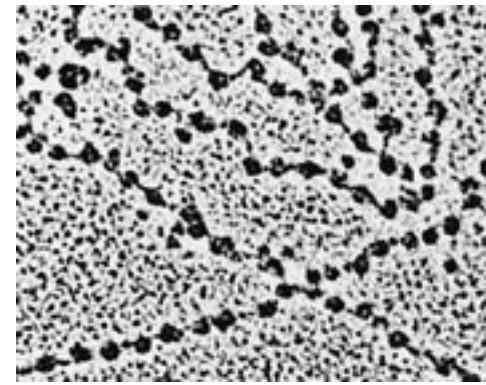
FIGURE 12.28 • Electron micrograph of *Drosophila melanogaster* chromatin after swelling reveals the presence of nucleosomes as "beads on a string." *(Electron micrograph courtesy of Oscar L. Miller, Jr., of the University of Virginia)*

(a)   (b)   (c)   (d)
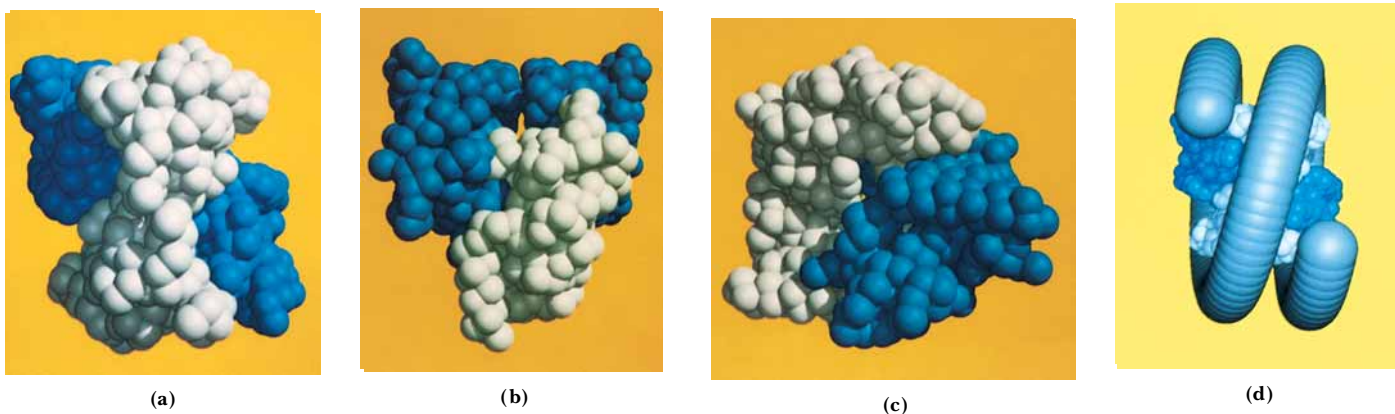
FIGURE 12.29 • Four orthogonal views of the histone octamer as determined by X-ray crystallography: (a) front view; (b) top view; and (c) disk view, that is, as viewed down the long axis of the chromatin fiber. In the (c) perspective, the DNA duplex would wrap around the octamer, with the axis of the DNA supercoil perpendicular to the plane of the picture. (d) Suggested appearance of the nucleosome when wrapped with DNA. *(Photographs courtesy of Evangelos N. Moudrianakis of Johns Hopkins University)*

FIGURE 12.30 • (a) Deduced structure of the nucleosome core particle wrapped with 1.65 turns of DNA (146 bp). The DNA is shown as a ribbon. (*left*) View down the axis of the nucleosome; (*right*) view perpendicular to the axis. (b) One-half of the nucleosome core particle with 73 bp of DNA, as viewed down the nucleosome axis. Note that the DNA does not wrap in a uniform circle about the histone core, but instead follows a course consisting of a series of somewhat straight segments separated by bends. (*Adapted from Luger, C., et al., 1997. Crystal structure of the nucleosome core particle at 2.8 Å resolution. Nature **389**:251–260. Photos courtesy of T. J. Richmond, ETH-Hönggerberg, Zurich, Switzerland.*)

Richmond and collaborators (Figure 12.30). The octamer (Figure 12.29) has surface landmarks that guide the course of the DNA around the octamer; 146 bp of B-DNA in a flat, left-handed superhelical conformation make 1.65 turns around the histone core (Figure 12.30), which itself is a protein superhelix consisting of a spiral array of the four histone dimers. Histone 1, a three-domain protein, serves to seal the ends of the DNA turns to the nucleosome core and to organize the additional 40 to 60 bp of DNA that link consecutive nucleosomes.

Organization of Chromatin and Chromosomes

solenoid • a coil wound in the form of a helix

A higher order of chromatin structure is created when the nucleosomes, in their characteristic beads-on-a-string motif, are wound in the fashion of a *solenoid* having six nucleosomes per turn (Figure 12.31). The resulting 30-nm filament contains about 1200 bp in each of its solenoid turns. Interactions between the respective H1 components of successive nucleosomes stabilize the 30-nm filament. This 30-nm filament then forms long DNA loops of variable length, each containing on average between 60,000 and 150,000 bp. Electron microscopic analysis of human chromosome 4 suggests that 18 such loops are then arranged radially about the circumference of a single turn to form a **miniband unit** of the chromosome. According to this model, approximately 10^6 of these minibands are arranged along a central axis in each of the chromatids of human chromosome 4 that form at mitosis (Figure 12.31). Despite intensive study, much of the higher-order structure of chromosomes remains a mystery.

		Base pairs per turn	Packing ratio
DNA double helix	2 nm	10	1
"Beads on a string" chromatin form	11 nm	80	6–7
Solenoid (six nucleosomes per turn)	30 nm	1200	~40
Loops (50 turns per loop)	~ 0.25 µm	60,000	680
Miniband (18 loops)	0.84 µm	~1.1×10^6	1.2×10^4
Chromosome (stacked minibands)	0.84 µm	18 loops/ miniband	1.2×10^4

Matrix

FIGURE 12.31 • A model for chromosome structure, human chromosome 4. The 2-nm DNA helix is wound twice around histone octamers to form 10-nm nucleosomes, each of which contains 160 bp (80 per turn). These nucleosomes are then wound in solenoid fashion with six nucleosomes per turn to form a 30-nm filament. In this model, the 30-nm filament forms long DNA loops, each containing about 60,000 bp, which are attached at their base to the nuclear matrix. Eighteen of these loops are then wound radially around the circumference of a single turn to form a miniband unit of a chromosome. Approximately 10^6 of these minibands occur in each chromatid of human chromosome 4 at mitosis.

$\mathscr{H}$ UMAN BIOCHEMISTRY

Telomeres and Tumors

Eukaryotic chromosomes are linear. The ends of chromosomes have specialized structures known as **telomeres.** The telomeres of virtually all eukaryotic chromosomes consist of short, tandemly repeated nucleotide sequences at the ends of the chromosomal DNA. For example, the telomeres of human germline (sperm and egg) cells contain between 1000 and 1700 copies of the hexameric repeat TTAGGG (see figure). Telomeres are believed to be responsible for maintaining chromosomal integrity by protecting against DNA degradation or rearrangement. Telomeres are added to the ends of chromosomal DNA by an RNA-containing enzyme known as **telomerase** (Chapter 30); telomerase is an unusual DNA polymerase that was discovered in 1985 by Elizabeth Blackburn and Carol Greider of the University of California, San Francisco.

However, most normal somatic cells lack telomerase. Consequently, upon every cycle of cell division when the cell replicates its DNA, about 50-nucleotide portions are lost from the end of each telomere. Thus, over time, the telomeres of somatic cells in animals become shorter and shorter, eventually leading to chromosome instability and cell death. This phenomenon has led some scientists to espouse a "telomere theory of aging" that implicates telomere shortening as the principal factor in cell, tissue, and even organism aging. Interestingly, cancer cells appear "immortal" because they continue to reproduce indefinitely. A survey of 20 different tumor types by Geron Corporation of Menlo Park, California, revealed that all contained telomerase activity.

(a)

(b)
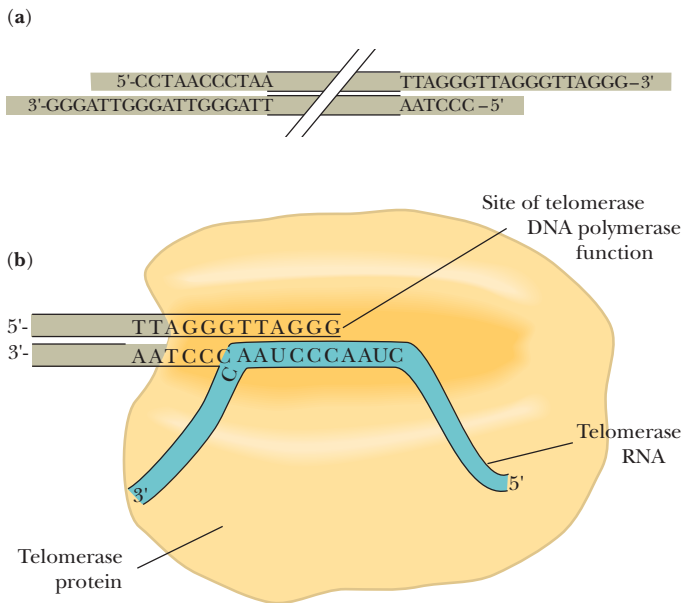
(a) Telomeres on human chromosomes consist of the hexanucleotide sequence TTAGGG repeated between 1000 and 1700 times. These TTAGGG tandem repeats are attached to the 3′-ends of the DNA strands and are paired with the complementary sequence 3′-AATCCC-5′ on the other DNA strand. Thus, a G-rich region is created at the 3′-end of each DNA strand and a C-rich region is created at the 5′-end of each DNA strand. Typically, at each end of the chromosome, the G-rich strand protrudes 12 to 16 nucleotides beyond its complementary C-rich strand. (b) Like other telomerases, human telomerase is a ribonucleoprotein. The ribonucleic acid of human telomerase is an RNA molecule 962 nucleotides long. This RNA serves as the template for the DNA polymerase activity of telomerase. Nucleotides 46 to 56 of this RNA are CUAA**CCCUAA**C and provide the template function for the telomerase-catalyzed addition of TTAGGG units to the 3′-end of a DNA strand.

12.6 • Chemical Synthesis of Nucleic Acids

Laboratory synthesis of oligonucleotide chains of defined sequence presents some of the same problems encountered in chemical synthesis of polypeptides (see Chapter 5). First, functional groups on the monomeric units (in this case, bases) are reactive under conditions of polymerization and therefore must be protected by blocking agents. Second, to generate the desired sequence, a phosphodiester bridge must be formed between the 3′-O of one nucleotide (B) and the 5′-O of the preceding one (A) in a way that precludes the unwanted bridging of the 3′-O of A with the 5′-O of B. Finally, recoveries at each step must be high so that overall yields in the multistep process are acceptable. As in peptide synthesis (see Chapter 5), *solid phase methods* are used to overcome some

of these problems. Commercially available automated instruments, called **DNA synthesizers** or "gene machines," are capable of carrying out the synthesis of oligonucleotides of 150 bases or more.

Phosphoramidite Chemistry

Phosphoramidite chemistry is currently the accepted method of oligonucleotide synthesis. The general strategy involves the sequential addition of nucleotide units as *nucleoside phosphoramidite* derivatives to a nucleoside covalently attached to the insoluble resin. Excess reagents, starting materials, and side products are removed after each step by filtration. After the desired oligonucleotide has been formed, it is freed of all blocking groups, hydrolyzed from the resin, and purified by gel electrophoresis. The four-step cycle is shown in Figure 12.32. Chemical synthesis takes place in the $3' \rightarrow 5'$ direction (the reverse of the biological polymerization direction).
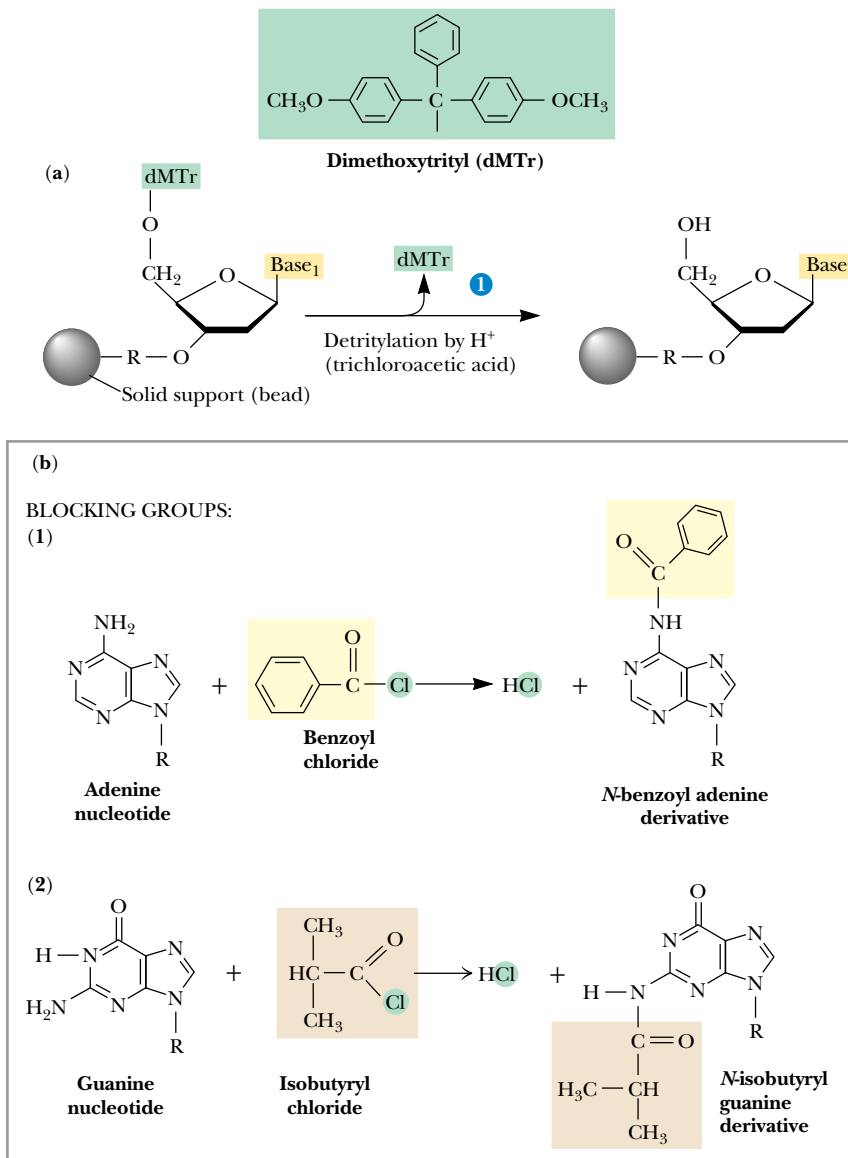
FIGURE 12.32 • Solid phase oligonucleotide synthesis. The four-step cycle starts with the first base in nucleoside form (N-1) attached by its 3′-OH group to an insoluble, inert resin or matrix, typically either controlled pore glass (CPG) or silica beads. Its 5′-OH is blocked with a dimethoxytrityl (DMTr) group (a). If the base has reactive —NH$_2$ functions, as in A, G, or C, then *N*-benzoyl or *N*-isobutyryl derivatives are used to prevent their reaction (b). In step 1, the DMTr protecting group is removed by trichloroacetic acid treatment. Step 2 is the coupling step: the second base (N-2) is added in the form of a nucleoside phosphoramidite derivative whose 5′-OH bears a DMTr blocking group so it cannot polymerize with itself (c). *(Figure continued on following page.)*

(**c**)

FIGURE 12.32 (continued) • The presence of a weak acid, such as tetrazole, activates the phosphoramidite, and it rapidly reacts with the free 5′-OH of N-1, forming a dinucleotide linked by a phosphite group. Chemical synthesis thus takes place in the 3′ → 5′ direction. Unreacted free 5′-OHs of N-1 (usually only 2–6% of the total) are blocked from further participation in the polymerization process by acetylation with acetic anhydride in step 3, referred to as *capping*. The phosphite linkage between N-1 and N-2 is highly reactive and, in step 4, it is oxidized by aqueous iodine (I$_2$) to form the desired more stable phosphate group. This completes the cycle. Subsequent cycles add successive residues to the resin-immobilized chain. When the chain is complete, it is cleaved from the support with NH$_4$OH, which also removes the *N*-benzoyl and *N*-isobutyryl protecting groups from the amino functions on the A, G, and C residues.

Chemically Synthesized Genes

Table 12.3 lists some of the genes that have been chemically synthesized. Because protein-coding genes are characteristically much larger than the 150-bp practical limit on oligonucleotide synthesis, their synthesis involves joining a series of oligonucleotides to assemble the overall sequence. A prime example of such synthesis is the gene for rhodopsin.

Figure 12.33 illustrates the strategy used in the total synthesis of the gene for bovine rhodopsin. This gene, which is 1057 base pairs long, encodes the 348 amino-acid photoreceptor protein of the vertebrate retina. Theoretically, no gene is beyond the scope of these methods, a fact that opens the door to an incredibly exciting range of possibilities for investigating structure–function relationships in the organization and expression of hereditary material.

Table 12.3

Some Chemically Synthesized Genes

Gene	Size (bp)
tRNA	126
α-Interferon	542
Secretin	81
γ-Interferon	453
Rhodopsin	1057
Proenkephalin	77
Connective tissue activating peptide III	280
Lysozyme	385
Tissue plasminogen activator	1610
c-Ha-ras	576
RNase T1	324
Cytochrome b_5	330
Bovine intestinal Ca-binding protein	298
Hirudin	226
RNase A	375
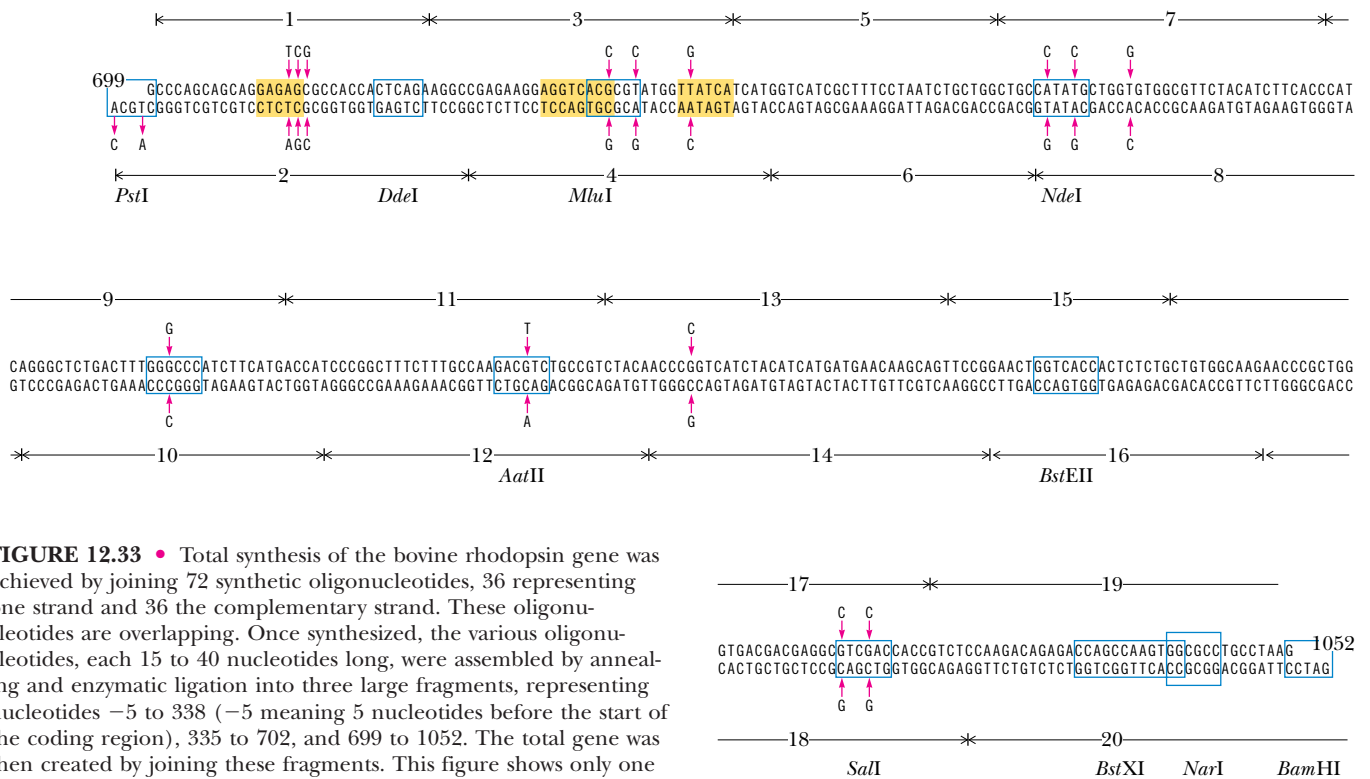
FIGURE 12.33 • Total synthesis of the bovine rhodopsin gene was achieved by joining 72 synthetic oligonucleotides, 36 representing one strand and 36 the complementary strand. These oligonucleotides are overlapping. Once synthesized, the various oligonucleotides, each 15 to 40 nucleotides long, were assembled by annealing and enzymatic ligation into three large fragments, representing nucleotides −5 to 338 (−5 meaning 5 nucleotides before the start of the coding region), 335 to 702, and 699 to 1052. The total gene was then created by joining these fragments. This figure shows only one fragment (fragment PB, comprising nucleotides 699 through 1052), assembled from 20 complementary oligonucleotides whose ends overlap. Odd-numbered oligonucleotides (1, 3, 5, . . .) compose the 5′ → 3′ strand; even-numbered ones (2, 4, 6, . . .) represent the 3′ → 5′ strand. (Vertical arrows indicate nucleotides that were changed from the native gene sequence. Restriction sites are shown boxed in blue lines; those removed from the gene through nucleotide substitutions are shown as yellow shaded boxes.) Note the single-stranded overhangs at either end of the 3′ → 5′ strand. The sequences at these overhangs correspond to restriction endonuclease sites (*Pst*I and *Bam*H1), which facilitate subsequent manipulation of the fragment in gene assembly and cloning.

12.7 • Secondary and Tertiary Structure of RNA

RNA molecules (see Chapter 11) are typically single-stranded. Nevertheless, they are often rich in double-stranded regions that form when complementary sequences within the chain come together and join via **intrastrand hydrogen bonding.** RNA strands cannot fold to form B-DNA type double helices because their 2′-OH groups are a steric hindrance to this conformation. Instead, RNA double helices adopt a conformation similar to the A-form of DNA, having about 11 bp per turn, and the bases strongly tilted from the plane perpendicular to the helix axis (see Figure 12.13). Both tRNA and rRNA have characteristic secondary structures formed in this manner. Secondary structures are presumed to exist in mRNA species as well, although their nature is as yet little understood. (The functions of tRNA, rRNA, and mRNA are discussed in detail in Part IV: Information Transfer.)

Transfer RNA

In tRNA molecules, which contain from 73 to 94 nucleotides in a single chain, a majority of the bases are hydrogen-bonded to one another. Figure 12.34 shows the structure that typifies tRNAs. *Hairpin turns* bring complementary stretches of bases in the chain into contact so that double-helical regions form. Because of the arrangement of the complementary stretches along the chain, the overall pattern of H-bonding can be represented as a *cloverleaf.* Each cloverleaf consists of four H-bonded segments—three loops and the stem where the 3′- and 5′-ends of the molecule meet. These four segments are designated the ***acceptor stem,*** the ***D loop,*** the ***anticodon loop,*** and the ***TψC loop.***
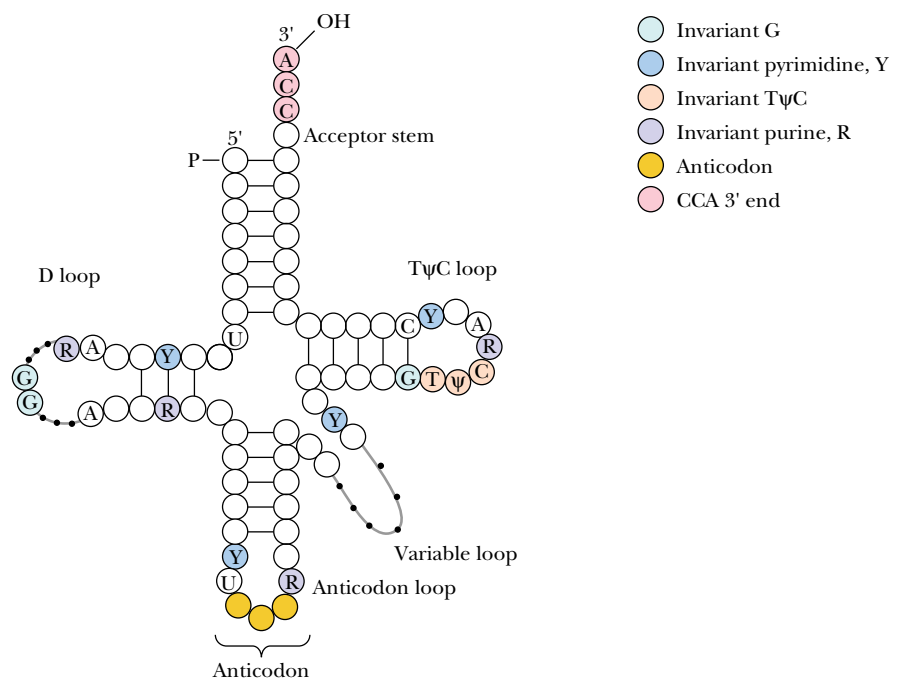
FIGURE 12.34 • A general diagram for the structure of tRNA. The positions of invariant bases as well as bases that seldom vary are shown in color. The numbering system is based on yeast tRNA^{Phe}. R = purine; Y = pyrimidine. Dotted lines denote sites in the D loop and variable loop regions where varying numbers of nucleotides are found in different tRNAs.

tRNA Secondary Structure

The *acceptor stem* is where the amino acid is linked to form the aminoacyl-tRNA derivative, which serves as the amino acid–donating species in protein synthesis; this is the physiological role of tRNA. The amino acid adds to the 3′-OH of the 3′-terminal A nucleotide (Figure 12.35). The 3′-end of tRNA is invariantly CCA-3′-OH. This CCA sequence plus a fourth nucleotide extends beyond the double-helical portion of the acceptor stem. The *D loop* is so named because this tRNA loop often contains dihydrouridine, or D, residues. In addition to dihydrouridine, tRNAs characteristically contain a number of unusual bases, including inosine, thiouridine, pseudouridine, and hypermethylated purines (see Figure 11.26). The *anticodon loop* consists of a double-helical segment and seven unpaired bases, three of which are the **anticodon.** (The anticodon is the three-nucleotide unit that recognizes and base pairs with a particular mRNA **codon,** a complementary three-base unit in mRNA which is the genetic information that specifies an amino acid.) Reading 3′ → 5′, the anticodon is invariably preceded by a purine (often an alkylated one) and followed by a U. Anticodon base pairing to the codon on mRNA allows a particular tRNA species to deliver its amino acid to the protein-synthesizing apparatus. It represents the key event in translating the information in the nucleic acid sequence so that the appropriate amino acid is inserted at the right place in the amino acid sequence of the protein being synthesized. Next along the tRNA sequence in the 5′ → 3′ direction comes a loop that varies from tRNA to tRNA in the number of residues that it has, the so-called **extra** or **variable loop.** The last loop in the tRNA, reading 5′ → 3′, is the **TψC loop,** which contains seven unpaired bases including the sequence TψC, where ψ is the symbol for **pseudouridine.** Ribosomes bind tRNAs through recognition of this TψC loop. Almost all of the invariant residues common to tRNAs lie within the non–hydrogen-bonded regions of the cloverleaf structure (Figure 12.34). Figure 12.36 depicts the complete nucleotide sequence and cloverleaf structure of yeast alanine tRNA.
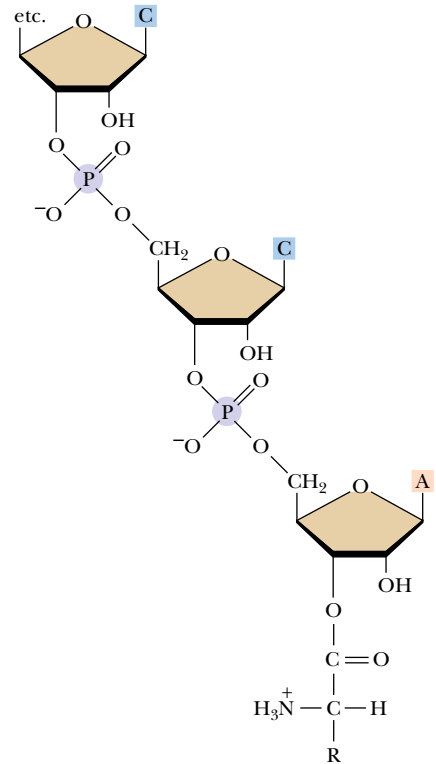
FIGURE 12.35 • Amino acids are linked to the 3′-OH end of tRNA molecules by an ester bond formed between the carboxyl group of the amino acid and the 3′-OH of the terminal ribose of the tRNA.
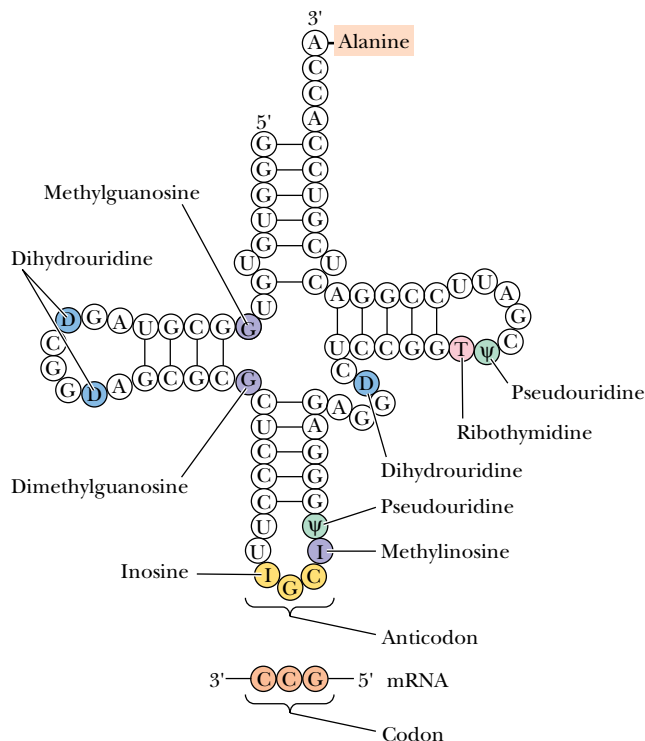
FIGURE 12.36 • The complete nucleotide sequence and cloverleaf structure of yeast alanine tRNA.

tRNA Tertiary Structure

Tertiary structure in tRNA arises from hydrogen-bonding interactions between bases in the D loop with bases in the variable and TψC loops, as shown for yeast phenylalanine tRNA in Figure 12.37. Note that these H bonds involve the invariant nucleotides of tRNAs, thus emphasizing the importance of the tertiary structure they create to the function of tRNAs in general. These H bonds fold the D and TψC arms together and bend the cloverleaf into the stable L-shaped tertiary form (Figure 12.38). Many of these H bonds involve base pairs that are not canonical A:T or G:C pairings (Figure 12.38). The amino acid acceptor stem is at one end of the L, separated by 7 nm or so from the anticodon at the opposite end of the L. The D and TψC loops form the corner of the L. In the L-conformation, the bases are oriented to maximize hydrophobic stacking interactions between their flat faces. Such stacking is a second major factor contributing to L-form stabilization.

Ribosomal RNA

rRNA Secondary Structure

Ribosomes, the protein-synthesizing machinery of cells, are composed of two **subunits,** called **small** and **large,** and ribosomal RNAs are integral components of these subunits (see Table 11.2). A large degree of *intrastrand sequence com-*

FIGURE 12.37 • Tertiary interactions in yeast phenylalanine tRNA. The molecule is presented in the conventional cloverleaf secondary structure generated by intrastrand hydrogen bonding. Solid lines connect bases that are hydrogen-bonded when this cloverleaf pattern is folded into the characteristic tRNA tertiary structure (see also Figure 12.36).

(a)

(b)
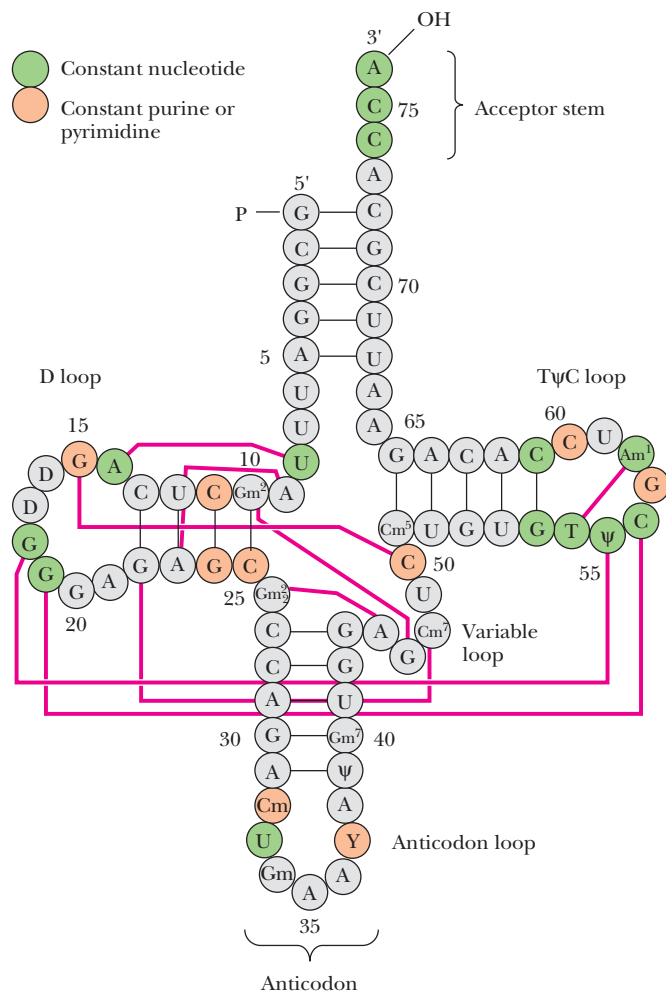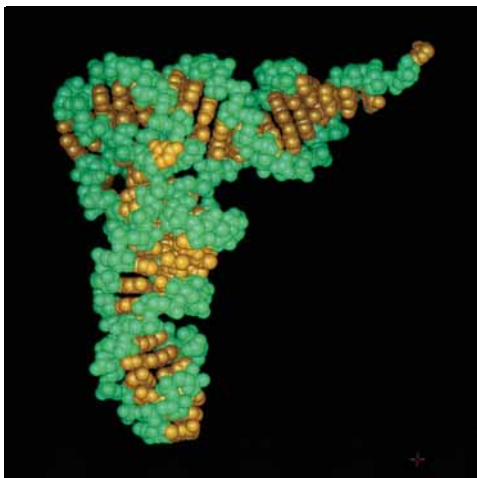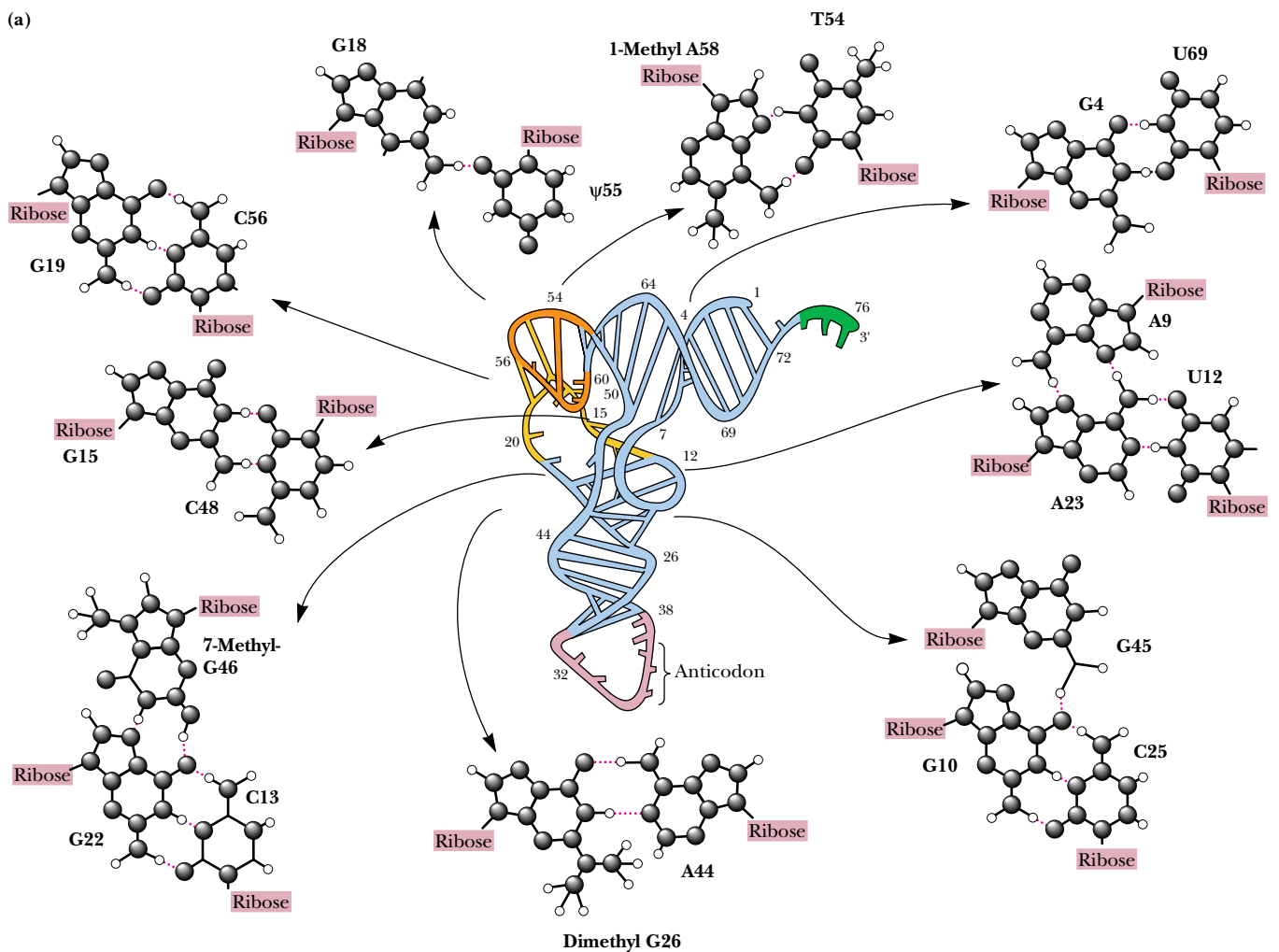
FIGURE 12.38 ● (a) The three-dimensional structure of yeast phenylalanine tRNA as deduced from X-ray diffraction studies of its crystals. The tertiary folding is illustrated in the center of the diagram with the ribose–phosphate backbone presented as a continuous ribbon; H bonds are indicated by crossbars. Unpaired bases are shown as short, unconnected rods. The anticodon loop is at the bottom and the -CCA 3′-OH acceptor end is at the top right. The various types of noncanonical hydrogen-bonding interactions observed between bases surround the central molecule. Three of these structures show examples of unusual H-bonded interactions involving three bases; these interactions aid in establishing tRNA tertiary structure. (b) A space-filling model of the molecule. *(After Kim, S. H., in Schimmel, P., Söll, D., and Abelson, J. N., eds., 1979.* Transfer RNA: Structure, Properties, and Recognition. *New York: Cold Spring Harbor Laboratory.)*

plementarity is found in all rRNA strands, and all assume a highly folded pattern that allows base pairing between these complementary segments. Figure 12.39 shows the secondary structure assigned to the *E. coli* 16S rRNA. This structure is based on alignment of the nucleotide sequence into H-bonding segments. The reliability of these alignments is then tested through a comparative analysis of whether identical secondary structures can be predicted from
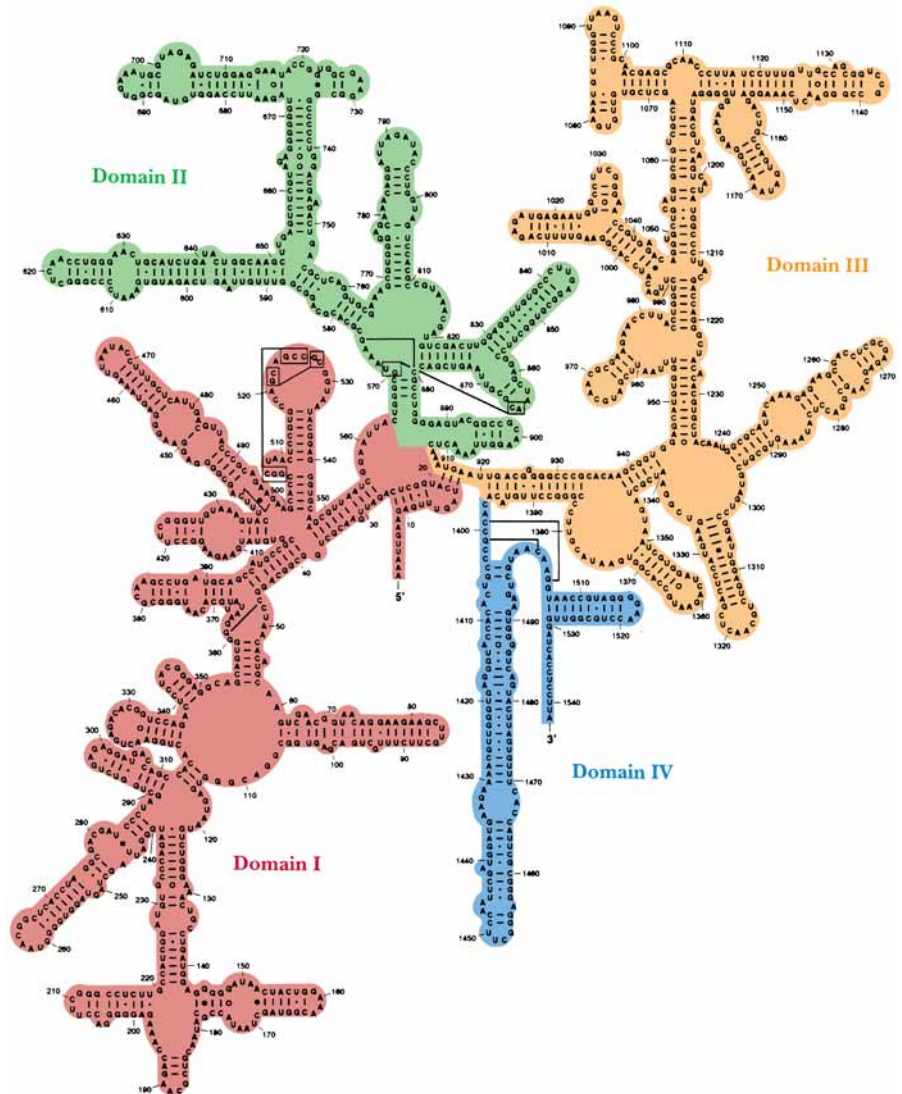
FIGURE 12.39 • The proposed secondary structure for *E. coli* 16S rRNA, based on comparative sequence analysis in which the folding pattern is assumed to be conserved across different species. The molecule can be subdivided into four domains—**I, II, III,** and **IV**—on the basis of contiguous stretches of the chain that are closed by long-range base-pairing interactions. **I,** the 5′-domain, includes nucleotides 27 through 556. **II,** the central domain, runs from nucleotide 564 to 912. Two domains comprise the 3′-end of the molecule. **III,** the major one, comprises nucleotides 923 to 1391. **IV,** the 3′-terminal domain, covers residues 1392 to 1541.

nucleotide sequences of 16S-like rRNAs from other species. If so, then such structures are apparently conserved. The approach is based on the thesis that, because ribosomal RNA species (regardless of source) serve common roles in protein synthesis, it may be anticipated that they share structural features. The structure is marvelously rich in short, helical segments separated and punctuated by single-stranded loops.

Comparison of rRNAs from Various Species

If a phylogenetic comparison is made of the 16S-like rRNAs from an archaebacterium (*Halobacterium volcanii*), a eubacterium (*E. coli*), and a eukaryote (the yeast *Saccharomyces cerevisiae*), a striking similarity in secondary structure emerges (Figure 12.40). Remarkably, these secondary structures are similar despite the fact that the nucleotide sequences of these rRNAs themselves exhibit a low degree of similarity. Apparently, evolution is acting at the level of rRNA secondary structure, not rRNA nucleotide sequence. Similar conserved folding patterns are seen for the 23S-like and 5S-like rRNAs that reside in the

(a)
E. coli (a eubacterium)

(b)
H. volcanii (an archaebacterium)

(c)
S. cerevisiae (yeast, a lower eukaryote)
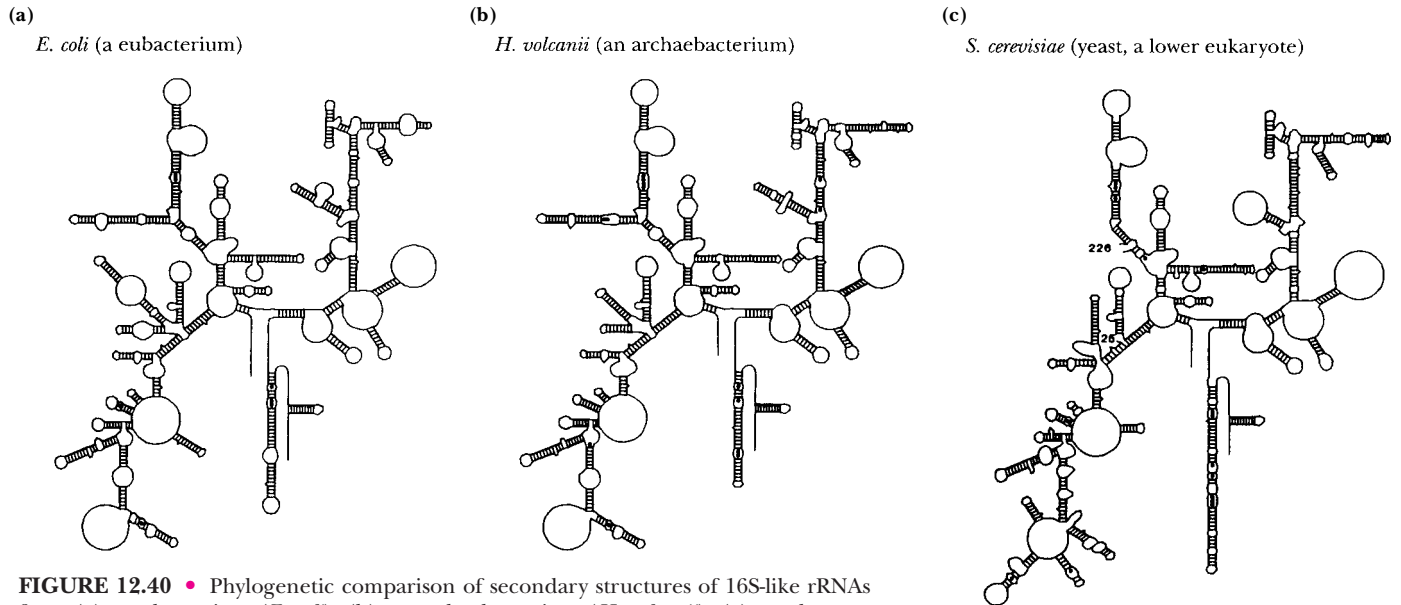
FIGURE 12.40 • Phylogenetic comparison of secondary structures of 16S-like rRNAs from (a) a eubacterium (*E. coli*), (b) an archaebacterium (*H. volcanii*), (c) a eukaryote (*S. cerevisiae,* a yeast).

large ribosomal subunits of various species. An insightful conclusion may be drawn regarding the persistence of such strong secondary structure conservation despite the millennia that have passed since these organisms diverged: *all ribosomes are constructed to a common design and all function in a similar manner.*

rRNA Tertiary Structure

Despite the unity in secondary structural patterns, little is known about the three-dimensional, or tertiary, structure of rRNAs. Even less is known about the quaternary interactions that occur when ribosomal proteins combine with rRNAs and when the ensuing ribonucleoprotein complexes, the small and large subunits, come together to form the complete ribosome. Furthermore, assignments of functional roles to rRNA molecules are still tentative and approximate. (We return to these topics in Chapter 33.)

PROBLEMS

1. The oligonucleotide d-ATGCCTGACT was subjected to sequencing by (a) Sanger's dideoxy method and (b) Maxam and Gilbert's chemical cleavage method, and the products were analyzed by electrophoresis on a polyacrylamide gel. Draw diagrams of the gel-banding patterns obtained for (a) and (b).

2. The result of sequence determination of an oligonucleotide as performed by the Sanger dideoxy chain termination method is displayed at right.

What is the sequence of the original oligonucleotide? A second sample of the oligonucleotide was 3′-end labeled with ^{32}P and then subjected to the Maxam–Gilbert chemical cleavage sequencing protocol. Draw a diagram depicting the pattern seen on the autoradiogram of the Maxam–Gilbert sequencing gel.

A	C	G	T

---------			

3. X-ray diffraction studies indicate the existence of a novel double-stranded DNA helical conformation in which ΔZ (the rise per base pair) $= 0.32$ nm and P (the pitch) $= 3.36$ nm. What are the other parameters of this novel helix: (a) the number of base pairs per turn, (b) $\Delta\phi$ (the mean rotation per base pair), and (c) c (the true repeat)?

4. A 41.5-nm-long duplex DNA molecule in the B-conformation adopts the A-conformation upon dehydration. How long is it now? What is its approximate number of base pairs?

5. If 80% of the base pairs in a duplex DNA molecule (12.5 kbp) are in the B-conformation and 20% are in the Z-conformation, what is the length of the molecule?

6. A "relaxed," circular, double-stranded DNA molecule (1600 bp) is in a solution where conditions favor 10 bp per turn. What is the value of L_0 for this DNA molecule? Suppose DNA gyrase introduces 12 negative supercoils into this molecule. What are the values of L, W, and T now? What is the superhelical density, σ?

7. Suppose one double-helical turn of a superhelical DNA molecule changes conformation from B-form to Z-form. What are the changes in L, W, and T? Why do you suppose the transition of DNA from B-form to Z-form is favored by negative supercoiling?

8. There is one nucleosome for every 200 bp of eukaryotic DNA. How many nucleosomes are in a diploid human cell? Nucleosomes can be approximated as disks 11 nm in diameter and 6 nm long. If all the DNA molecules in a diploid human cell are in the B-conformation, what is the sum of their lengths? If this DNA is now arrayed on nucleosomes in the "beads-on-a-string" motif, what is its approximate total length?

9. The characteristic secondary structures of tRNA and rRNA molecules are achieved through intrastrand hydrogen bonding. Even for the small tRNAs, remote regions of the nucleotide sequence interact via H-bonding when the molecule adopts the cloverleaf pattern. Using Figure 12.34 as a guide, draw the primary structure of a tRNA and label the positions of its various self-complementary regions.

10. Using the data in Table 11.3, arrange the DNAs from the following sources in order of increasing T_m: human, salmon, wheat, yeast, *E. coli.*

11. The DNAs from mice and rats have (G+C) contents of 44% and 40%, respectively. Calculate the T_ms for these DNAs in 0.2 M NaCl. If samples of these DNAs were inadvertently mixed, how might they be separated from one another? Describe the procedure and the results (hint: see the Appendix to this chapter).

12. Calculate the density (ρ) of avian tubercle bacillus DNA from the data presented in Table 11.3 and the equation $\rho = 1.660 + 0.098(GC)$, where (GC) is the mole fraction of (G+C) in DNA.

FURTHER READING

Adams, R. L. P., Knowler, J. T., and Leader, D. P., 1992. *The Biochemistry of the Nucleic Acids,* 11th ed. London: Chapman and Hall.

Arents, G., et al*.,* 1991. The nucleosome core histone octamer at 3.1 Å resolution: A tripartite protein assembly and a left-hand superhelix. *Proceedings of the National Academy of Sciences U.S.A.* **88:**10148–10152.

Axelrod, N., 1996. Of telomeres and tumors. *Nature Medicine* **2:**158–159.

Callandine, C. R., and Drew, H. R., 1992. *Understanding DNA: The Molecule and How It Works.* London: Academic Press.

Ferretti, L., Karnik, S. S., Khorana, H. G., Nassal, M., and Oprian, D. D., 1986. Total synthesis of a gene for bovine rhodopsin. *Proceedings of the National Academy of Sciences U.S.A.* **83:**599–603.

Kornberg, A., and Baker, T. A., 1991. *DNA Replication,* 2nd ed. New York: W.H. Freeman and Co.

Luger, C., et al., 1997. Crystal structure of the nucleosome core particle at 2.8 Å resolution. *Nature* **389:**251–260.

Noller, H. F., 1984. Structure of ribosomal RNA. *Annual Review of Biochemistry* **53:**119–162.

Pienta, K. J., and Coffey, D. S., 1984. A structural analysis of the role of the nuclear matrix and DNA loops in the organization of the nucleus and chromosomes. In Cook, P. R., and Laskey, R. A., eds., Higher Order Structure in the Nucleus. *Journal of Cell Science* Supplement **1:**123–135.

Rhodes, D., 1997. The nucleosome core all wrapped up. *Nature* **389:**231–233.

Rich, A., Nordheim, A., and Wang, A. H.-J., 1984. The chemistry and biology of left-handed Z-DNA. *Annual Review of Biochemistry* **53:**791–846.

Wand, B.-C., et al., 1994. The octameric histone core of the nucleosome. *Journal of Molecular Biology* **236:**179–188.

Watson, J. D., Hopkins, N. H., Roberts, J. W., Steitz, J. A., and Weiner, A. M., 1987. *The Molecular Biology of the Gene,* Vol. I, *General Principles,* 4th ed. Menlo Park, CA: Benjamin/Cummings.

Watson, J. D., ed., 1983. Structures of DNA. *Cold Spring Harbor Symposia on Quantitative Biology,* Volume XLVII. New York: Cold Spring Harbor Laboratory.

Wu, R., 1993. Development of enzyme-based methods for DNA sequence analysis and their application in genome projects. *Methods in Enzymology* **67:**431–468.

$\mathcal{A}$ppendix to Chapter 12

Isopycnic Centrifugation and Buoyant Density of DNA

Density gradient ultracentrifugation is a variant of the basic technique of ultracentrifugation (discussed in the Appendix to Chapter 5). Density gradient centrifugation can be used to isolate DNA. The densities of DNAs are about the same as concentrated solutions of cesium chloride, CsCl (1.6 to 1.8 g/mL). Centrifugation of CsCl solutions at very high rotational speeds, where the centrifugal force becomes 10^5 times stronger than the force of gravity, causes the formation of a density gradient within the solution. This gradient is the result of a balance that is established between the sedimentation of the salt ions toward the bottom of the tube and their diffusion upward toward regions of lower concentration. If DNA is present in the centrifuged CsCl solution, it moves to a position of equilibrium in the gradient equivalent to its buoyant density (Figure A12.1). For this reason, this technique is also called **isopycnic centrifugation.**

Cesium chloride centrifugation is an excellent means of removing RNA and proteins in the purification of DNA. The density of DNA is typically slightly greater than 1.7 g/cm^3, while the density of RNA is more than 1.8 g/cm^3. Proteins have densities less than 1.3 g/cm^3. In CsCl solutions of appropriate density, the DNA bands near the center of the tube, RNA pellets to the bottom, and the proteins float near the top. Single-stranded DNA is denser than double-helical DNA. The irregular structure of randomly coiled ssDNA allows the atoms to pack together through van der Waals interactions. These interactions compact the molecule into a smaller volume than that occupied by a hydrogen-bonded double helix.

The net movement of solute particles in an ultracentrifuge is the result of two processes: diffusion (from regions of higher concentration to regions of lower concentration) and sedimentation due to centrifugal force (in the direction away from the axis of rotation). In general, diffusion rates for molecules are inversely proportional to their molecular weight—larger molecules diffuse more slowly than smaller ones. On the other hand, sedimentation rates increase with increasing molecular weight. A macromolecular species that has reached its position of equilibrium in isopycnic centrifugation has formed a concentrated band of material.

Essentially three effects are influencing the movement of the molecules in creating this concentration zone: (1) diffusion away to regions of lower concentration; (2) sedimentation of molecules situated at positions of slightly lower solution density in the density gradient; and (3) flotation (buoyancy or "reverse sedimentation") of molecules that have reached positions of slightly greater solution density in the gradient. The consequence of the physics of these effects is that, at equilibrium, *the width of the concentration band established by the macro-*

molecular species is inversely proportional to the square root of its molecular weight. That is, a population of large molecules will form a concentration band that is narrower than the band formed by a population of small molecules. For example, the band width formed by dsDNA will be less than the band width formed by the same DNA when dissociated into ssDNA.
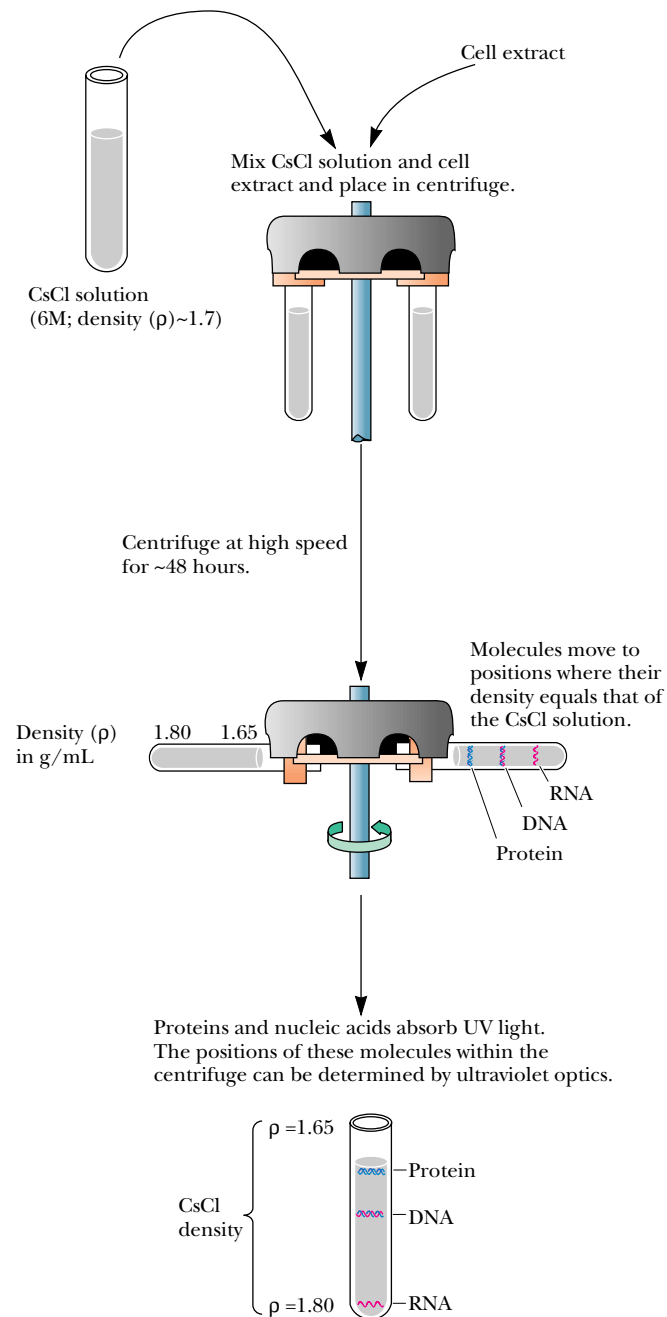
FIGURE A12.1 • Density gradient centrifugation is a common method of separating macromolecules, particularly nucleic acids, in solution. A cell extract is mixed with a solution of CsCl to a final density of about 1.7 g/cm^3 and centrifuged at high speed (40,000 rpm, giving relative centrifugal forces of about 200,000 *g*). The biological macromolecules in the extract will move to equilibrium positions in the CsCl gradient that reflect their buoyant densities.

*C*hapter 13

Recombinant DNA: Cloning and Creation of Chimeric Genes

The Chimera of Arezzo, of Etruscan origin and probably from the 5th century B.C., was found near Arezzo, Italy, in 1553. Chimeric animals existed only in the imagination of the ancients. But the ability to create chimeric DNA molecules is a very real technology that has opened up a whole new field of scientific investigation. (Scala/Art Resource, Chimera, Museo Archeologico, Florence, Italy)

In the early 1970s, technologies for the laboratory manipulation of nucleic acids emerged. In turn, these technologies led to the construction of DNA molecules composed of nucleotide sequences taken from different sources. The products of these innovations, **recombinant DNA molecules,**[1] opened exciting new avenues of investigation in molecular biology and genetics, and a new field

[1]The advent of molecular biology, like that of most scientific disciplines, has generated a jargon all its own. Learning new fields often requires gaining familiarity with a new vocabulary. We will soon see that many words—*vector, amplification,* and *insert* are but a few examples—have been bent into new meanings to describe the marvels of this new biology.

amplification • the production of multiple copies

was born—**recombinant DNA technology. Genetic engineering** is the application of this technology to the manipulation of genes. These advances were made possible by methods for **amplification** of any particular DNA segment, regardless of source, within bacterial host cells. Or, in the language of recombinant DNA technology, the **cloning** of virtually any DNA sequence became feasible.

13.1 • Cloning

In classical biology, a *clone* is a population of identical organisms derived from a single parental organism. For example, the members of a colony of bacterial cells that arise from a single cell on a petri plate are clones. Molecular biology has borrowed the term to mean a collection of molecules or cells all identical to an original molecule or cell. So, if the original cell on the petri plate harbored a recombinant DNA molecule in the form of a plasmid, the plasmids within the millions of cells in a bacterial colony represent a clone of the original DNA molecule, and these molecules can be isolated and studied. Furthermore, if the cloned DNA molecule is a gene (or part of a gene), that is, it encodes a functional product, a new avenue to isolating and studying this product has opened. Recombinant DNA methodology offers exciting new vistas in biochemistry.

Plasmids

Plasmids are naturally occurring, circular, extrachromosomal DNA molecules (see Chapter 12). Natural strains of the common colon bacterium *Escherichia coli* isolated from various sources harbor diverse plasmids. Often these plasmids carry genes specifying novel metabolic activities that are advantageous to the host bacterium. These activities range from catabolism of unusual organic substances to metabolic functions that endow the host cells with resistance to antibiotics, heavy metals, or bacteriophages. Plasmids that are able to perpetuate themselves in *E. coli,* the bacterium favored by bacterial geneticists and molecular biologists, have become the darlings of recombinant DNA technology. Because restriction endonuclease digestion of plasmids can generate fragments with overlapping or "sticky" ends, artificial plasmids can be constructed by ligating different fragments together. Such artificial plasmids were among the earliest recombinant DNA molecules. These recombinant molecules can be autonomously replicated, and hence propagated, in suitable bacterial host cells, provided they still possess a site signaling where DNA replication can begin (a so-called **origin of replication** or *ori* sequence).

ligation • the act of joining

Plasmids as Cloning Vectors

The idea arose that "foreign" DNA sequences could be inserted into artificial plasmids and that these foreign sequences would be carried into *E. coli* and propagated as part of the plasmid. That is, these plasmids could serve as **cloning vectors** to carry genes. (The word *vector* is used here in the sense of "a vehicle or carrier.") Plasmids useful as cloning vectors possess three common features: **a replicator, a selectable marker,** and **a cloning site** (Figure 13.1). A *replicator* is an origin of replication, or *ori.* The *selectable marker* is typically a gene conferring resistance to an antibiotic. Only those cells containing the cloning vector will grow in the presence of the antibiotic. Therefore, growth on antibiotic-containing media "selects for" plasmid-containing cells. Typically, the *cloning*

site is a sequence of nucleotides representing one or more restriction endonuclease cleavage sites. Cloning sites are located where the insertion of foreign DNA neither disrupts the plasmid's ability to replicate nor inactivates essential markers.

Virtually Any DNA Sequence Can Be Cloned

Nuclease cleavage at a restriction site opens, or *linearizes,* the circular plasmid so that a foreign DNA fragment can be inserted. The ends of this linearized plasmid are joined to the ends of the fragment so that the circle is closed again, creating a recombinant plasmid (Figure 13.2). **Recombinant plasmids** are hybrid DNA molecules consisting of plasmid DNA sequences plus inserted DNA elements (called *inserts*). Such hybrid molecules are also called **chimeric constructs** or **chimeric plasmids.** (The term *chimera* is borrowed from mythology and refers to a beast composed of the body and head of a lion, the heads of a goat and a snake, and the wings of a bat.) The presence of foreign DNA sequences does not adversely affect replication of the plasmid, so chimeric plasmids can be propagated in bacteria just like the original plasmid. Bacteria often harbor several hundred copies of common cloning vectors per cell. Hence, large amounts of a cloned DNA sequence can be recovered from bacterial cultures. The enormous power of recombinant DNA technology stems in part from the fact that *virtually any DNA sequence can be selectively cloned and amplified in this manner.* DNA sequences that are difficult to clone include inverted repeats, origins of replication, centromeres, and telomeres. The only practical limitation is the size of the foreign DNA segment: most plasmids with inserts larger than about 10 kbp are not replicated efficiently.

Bacterial cells may harbor one or many copies of a particular plasmid, depending on the nature of the plasmid replicator. That is, plasmids are classified as *high copy number* or *low copy number*. The copy number of most genetically engineered plasmids is high (200 or so), but some are lower.

FIGURE 13.2 • Foreign DNA sequences can be inserted into plasmid vectors by opening the circular plasmid with a restriction endonuclease. The ends of the linearized plasmid DNA are then joined with the ends of a foreign sequence, reclosing the circle to create a chimeric plasmid.

FIGURE 13.3 • Restriction endonuclease *Eco*RI cleaves double-stranded DNA. The recognition site for *Eco*RI is the hexameric sequence GAATTC:

<div align="center">

5′ . . . NpNpNpNp**GpApApTpTpC**pNpNpNpNp . . . 3′

3′ . . . NpNpNpNp**CpTpTpApApG**pNpNpNpNp . . . 5′

</div>

Cleavage occurs at the G residue on each strand so that the DNA is cut in a staggered fashion, leaving 5′-overhanging single-stranded ends (sticky ends):

<div align="center">

5′ . . . NpNpNpNp**G**   **pApApTpTpC**pNpNpNpNp . . . 3′

3′ . . . NpNpNpNp**CpTpTpApAp**   **G**pNpNpNpNp . . . 5′

</div>

An *Eco*RI restriction fragment of foreign DNA can be inserted into a plasmid having an *Eco*RI cloning site by (a) cutting the plasmid at this site with *Eco*RI, annealing the linearized plasmid with the *Eco*RI foreign DNA fragment, and (b) sealing the nicks with DNA ligase.

Construction of Chimeric Plasmids

Creation of chimeric plasmids requires joining the ends of the foreign DNA insert to the ends of a linearized plasmid (Figure 13.2). This ligation is facilitated if the ends of the plasmid and the insert have complementary, single-stranded overhangs. Then these ends can base-pair with one another, annealing the two molecules together. One way to generate such ends is to cleave the DNA with restriction enzymes that make staggered cuts; many such restriction endonucleases are available (see Table 11.5). For example, if the sequence to be inserted is an *Eco*RI fragment and the plasmid is cut with *Eco*RI, the single-stranded sticky ends of the two DNAs can anneal (Figure 13.3). The interruptions in the sugar–phosphate backbone of DNA can then be sealed with DNA ligase to yield a covalently closed, circular chimeric plasmid. DNA ligase is an enzyme that covalently links adjacent 3′-OH and 5′-PO₄ groups. An inconvenience of this strategy is that *any* pair of *Eco*RI sticky ends can anneal with each other. So, plasmid molecules can reanneal with themselves, as can the foreign DNA restriction fragments. These DNAs can be eliminated by selection schemes designed to identify only those bacteria containing chimeric plasmids.

Blunt-end ligation is an alternative method for joining different DNAs. This method depends on the ability of **phage T4 DNA ligase** to covalently join the ends of any two DNA molecules (even those lacking 3′- or 5′-overhangs) (Figure 13.4). Some restriction endonucleases cut DNA so that blunt ends are formed (see Table 11.5). Because there is no control over which pair of DNAs are blunt-end ligated by T4 DNA ligase, strategies to identify the desired products must be applied.
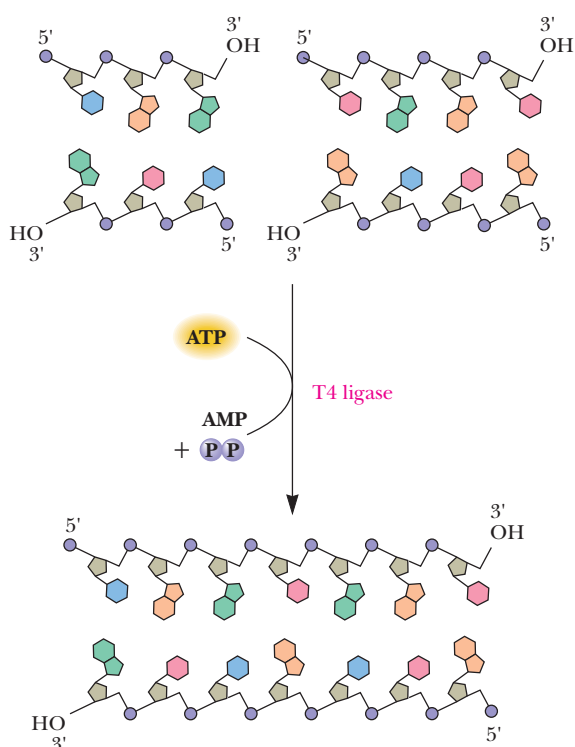
FIGURE 13.4 • Blunt-end ligation using phage T4 DNA ligase, which catalyzes the ATP-dependent ligation of DNA molecules. AMP and PP$_i$ are by-products.

A great number of variations on these basic themes have emerged. For example, short synthetic DNA duplexes whose nucleotide sequence consists of little more than a restriction site can be blunt-end ligated onto any DNA. These short DNAs are known as **linkers.** Cleavage of the ligated DNA with the restriction enzyme then leaves tailor-made sticky ends useful in cloning reactions (Figure 13.5). Similarly, many vectors contain a **polylinker** cloning site, a short region of DNA sequence bearing numerous restriction sites.

Promoters and Directional Cloning

Note that the strategies discussed thus far create hybrids in which the orientation of the DNA insert within the chimera is random. Sometimes it is desirable to insert the DNA in a particular orientation. For example, an experimenter might wish to insert a particular DNA (a gene) in a vector so that its gene product is synthesized. To do this, the DNA must be placed downstream from a **promoter.** A promoter is a nucleotide sequence lying upstream of a

FIGURE 13.5 • (a) The use of linkers to create tailor-made ends on cloning fragments. Synthetic oligonucleotide duplexes whose sequences represent *Eco*RI restriction sites are blunt-end ligated to a DNA molecule using T4 DNA ligase. Note that the ligation reaction can add multiple linkers on each end of the blunt-ended DNA. *Eco*RI digestion removes all but the terminal one, leaving the desired 5′-overhangs. (b) Cloning vectors often have polylinkers consisting of a multiple array of restriction sites at their cloning sites, so restriction fragments generated by a variety of endonucleases can be incorporated into the vector. Note that the polylinker is engineered not only to have multiple restriction sites but also to have an uninterrupted sequence of codons, so this region of the vector has the potential for translation into protein. The sequence shown is the cloning site for the vectors M13mp7 and pUC7; the colored amino acid residues are contiguous with the coding sequence of the *lacZ* gene carried by this vector (see Figure 13.18). *(a, Adapted from Figure 3.16.3; b, adapted from Figure 1.14.2, in Ausubel, F. M., et al., 1987,* Current Protocols in Molecular Biology. *New York: John Wiley & Sons.)*

gene that controls expression of the gene. RNA polymerase molecules bind specifically at promoters and initiate transcription of adjacent genes, copying template DNA into RNA products. One way to insert DNA so that it will be properly oriented with respect to the promoter is to create DNA molecules whose ends have different overhangs. Ligation of such molecules into the plasmid vector can only take place in one orientation, to give **directional cloning** (Figure 13.6).
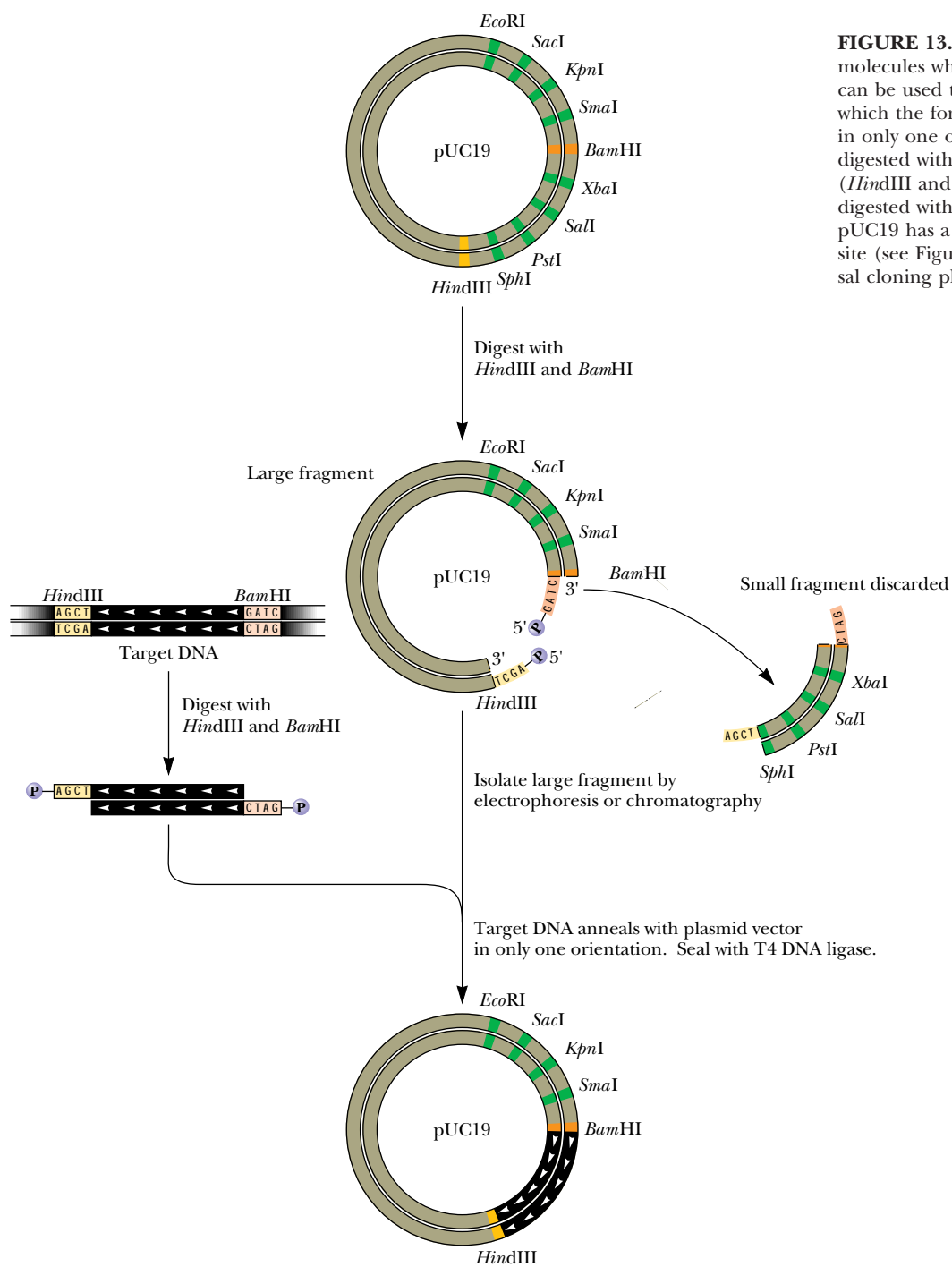
FIGURE 13.6 • Directional cloning. DNA molecules whose ends have different overhangs can be used to form chimeric constructs in which the foreign DNA can enter the plasmid in only one orientation. The foreign DNA is digested with two different restriction enzymes (*Hin*dIII and *Bam*HI), and the plasmid is digested with the same two enzymes. Note that pUC19 has a polylinker or universal cloning site (see Figure 13.5b); pUC stands for universal cloning plasmid.

Biologically Functional Chimeric Plasmids

The first biologically functional chimeric DNA molecules constructed *in vitro* were assembled from parts of different plasmids in 1973 by Stanley Cohen, Annie Chang, Herbert Boyer, and Robert Helling. These plasmids were used to **transform** recipient *E. coli* cells (*transformation* means the uptake and repli-

3 *tet*^{r} gene is split by the insertion of DNA fragment. *amp*^{r} gene remains intact.

amp^r gene remains intact

Chimeric plasmid

2 *Bam*HI restriction fragment of DNA to be cloned is inserted into the *Bam*HI site of *tet*^{r}.

pBR322
(4363 bases)

1 A plasmid with genes for ampicillin resistance (*amp*^{r}) and tetracycline resistance (*tet*^{r}). A *Bam*HI restriction site is located within the *tet*^{r} gene.

4 Suspend 20 ng plasmid DNA + 10^7 *E.coli* cells in $CaCl_2$ solution.

42°C, 2 min.

5 Plate bacteria on ampicillin media.

37°C, overnight

Tetracycline-containing medium

37°C, overnight

Ampicillin-containing medium

8 Only *tet*^{r} colonies appear; *tet*^{s} colonies can be recovered from *amp*^{r} plate by comparing two plates.

7 Using velvet-covered disk, bacterial colonies are lifted from surface of agar *amp*$^+$ plate and pressed briefly to surface of plate containing tetracycline media.

6 Only ampicillin-resistant (*amp*^{r}) bacterial colonies grow.

FIGURE 13.7 • A typical bacterial transformation experiment. Here the plasmid pBR322 is the cloning vector. (1) Cleavage of pBR322 with restriction enzyme *Bam*H1, followed by (2) annealing and ligation of inserts generated by *Bam*H1 cleavage of some foreign DNA, (3) creates a chimeric plasmid. (4) The chimeric plasmid is then used to transform Ca^{2+}-treated heat-shocked *E. coli* cells, and the bacterial sample is plated on a petri plate. (5) Following incubation of the petri plate overnight at 37°C, (6) colonies of *amp*^{r} bacteria are evident. (7) Replica plating of these bacteria on plates of tetracycline-containing media (8) reveals which colonies are *tet*^{r} and which are tetracycline sensitive (*tet*^{s}). Only the *tet*^{s} colonies possess plasmids with foreign DNA inserts.

cation of exogenous DNA by a recipient cell; see Chapter 29). The bacterial cells were rendered somewhat permeable to DNA by Ca^{2+} treatment and a brief 42°C heat shock. Although less than 0.1% of the Ca^{2+}-treated bacteria became competent for transformation following such treatment, transformed bacteria could be selected by their resistance to certain antibiotics (Figure 13.7). Consequently, the chimeric plasmids must have been biologically functional in at least two aspects: they replicated stably within their hosts and they expressed the drug resistance markers they carried.

In general, plasmids used as cloning vectors are engineered to be small, 2.5 kbp to about 10 kbp in size, so that the size of the insert DNA can be maximized. These plasmids have only a single origin of replication, so the time necessary for complete replication depends on the size of the plasmid. Under selective pressure in a growing culture of bacteria, overly large plasmids are prone to delete any nonessential "genes," such as any foreign inserts. Such deletion would thwart the purpose of most cloning experiments. The useful upper limit on cloned inserts in plasmids is about 10 kbp. Many eukaryotic genes exceed this size.

Bacteriophage λ as a Cloning Vector

The genome of bacteriophage λ (lambda) (Figure 13.8) is a 48.5-kbp linear DNA molecule that is packaged into the head of the bacteriophage. The middle one-third of this genome is not essential to phage infection, so λ phage DNA has been engineered so that foreign DNA molecules up to 16 kbp can be inserted into this region for cloning purposes. *In vitro* packaging systems are then used to package the chimeric DNA into phage heads which, when assembled with phage tails, form infective phage particles. Bacteria infected with these recombinant phage produce large numbers of phage progeny before they lyse, and large amounts of recombinant DNA can be easily purified from the lysate.

Cosmids

The DNA incorporated into phage heads by bacteriophage λ packaging systems must satisfy only a few criteria. It must possess a 14-bp sequence known as *cos* (which stands for *co*hesive end *s*ite) at each of its ends, and these *cos* sequences must be separated by no fewer than 36 kbp and no more than 51 kbp of DNA. Essentially any DNA satisfying these minimal requirements will be packaged and assembled into an infective phage particle. Other cloning features such as an *ori*, selectable markers, and a polylinker are joined to the *cos* sequence so that the cloned DNA can be propagated and selected in host cells. These features have been achieved by placing *cos* sequences on either side of cloning sites in plasmids to create **cosmid vectors** that are capable of carrying DNA inserts about 40 kbp in size (Figure 13.9). Because cosmids lack essential phage genes, they reproduce in host bacteria as plasmids.

Shuttle Vectors

Shuttle vectors are plasmids capable of propagating and transferring ("shuttling") genes between two different organisms, one of which is typically a prokaryote (*E. coli*) and the other a eukaryote (for example, yeast). Shuttle vectors must have unique origins of replication for each cell type as well as different markers for selection of transformed host cells harboring the vector (Figure 13.10). Shuttle vectors have the advantage that eukaryotic genes can be cloned in bacterial hosts, yet the expression of these genes can be analyzed in appropriate eukaryotic backgrounds.

FIGURE 13.8 • Electron micrograph of bacteriophage λ. *(Robley C. Williams, University of California/BPS)*
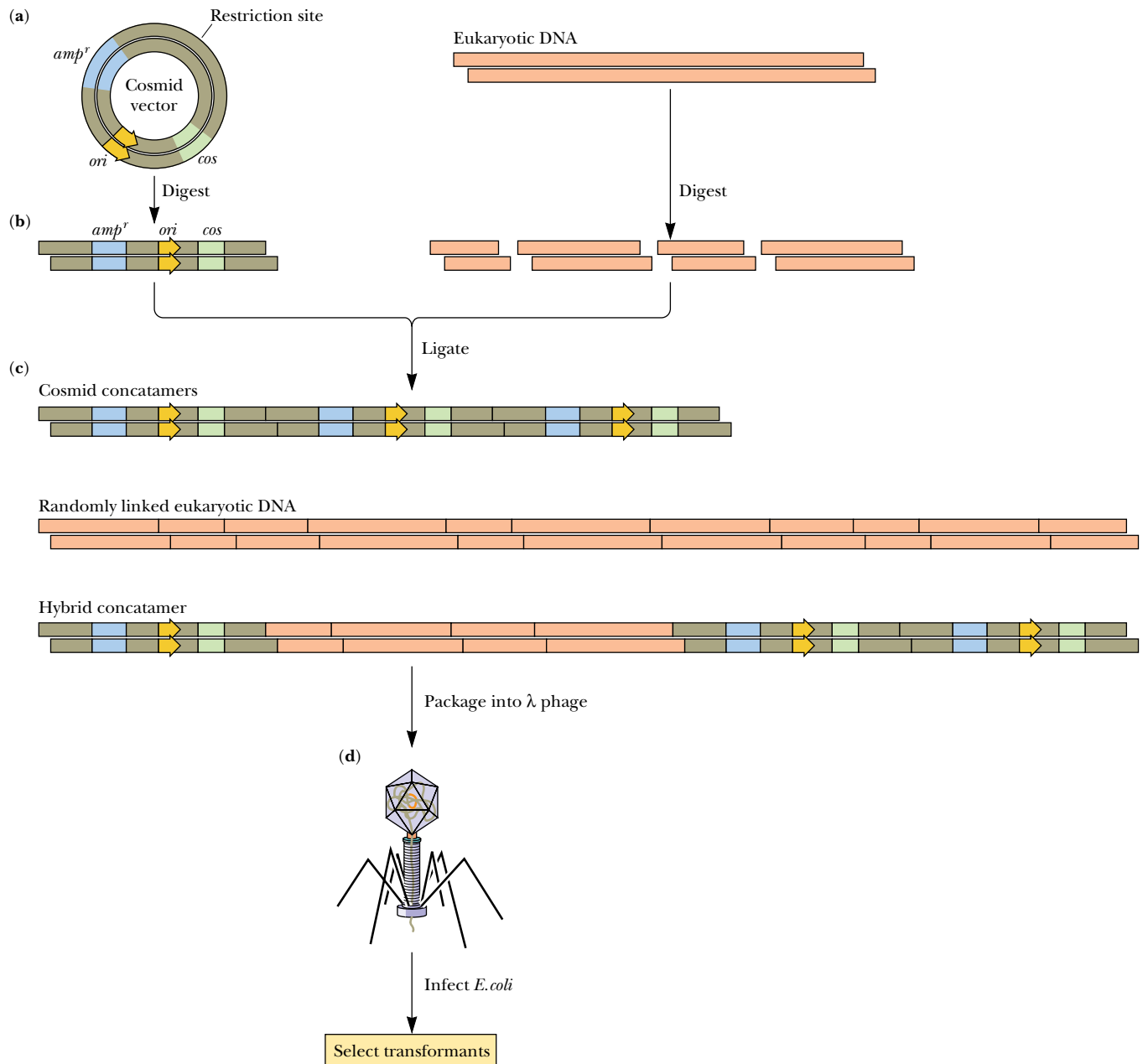
FIGURE 13.9 • Cosmid vectors for cloning large DNA fragments. (a) Cosmid vectors are plasmids that carry a selectable marker such as *amp^r*, an origin of replication (*ori*), a polylinker suitable for insertion of foreign DNA, and (b) a *cos* sequence. Both the plasmid and the foreign DNA to be cloned are cut with a restriction enzyme, and the two DNAs are then ligated together. (c) The ligation reaction leads to the formation of hybrid concatamers, molecules in which plasmid sequences and foreign DNAs are linked in series in no particular order. The bacteriophage λ packaging extract contains the restriction enzyme that recognizes *cos* sequences and cleaves at these sites. (d) DNA molecules of the proper size (36 to 51 kbp) are packaged into phage heads, forming infective phage particles. (e) The *cos* sequence is

$$\downarrow$$

5′-TACG**GGGCGGCGACCT**CGCG-3′

3′-ATGC**CCCGCCGCTGGA**GCGC-5′

$$\uparrow$$
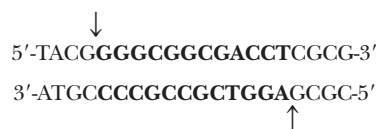
Endonuclease cleavage at the sites indicated by arrows leaves 12-bp cohesive ends. *(a–d, Adapted from Figure 1.10.7 in Ausubel, F. M., et al., eds., 1987. Current Protocols in Molecular Biology. New York: John Wiley & Sons; e, from Figure 4 in Murialdo, H., 1991. Annual Review of Biochemistry **60**:136.)*
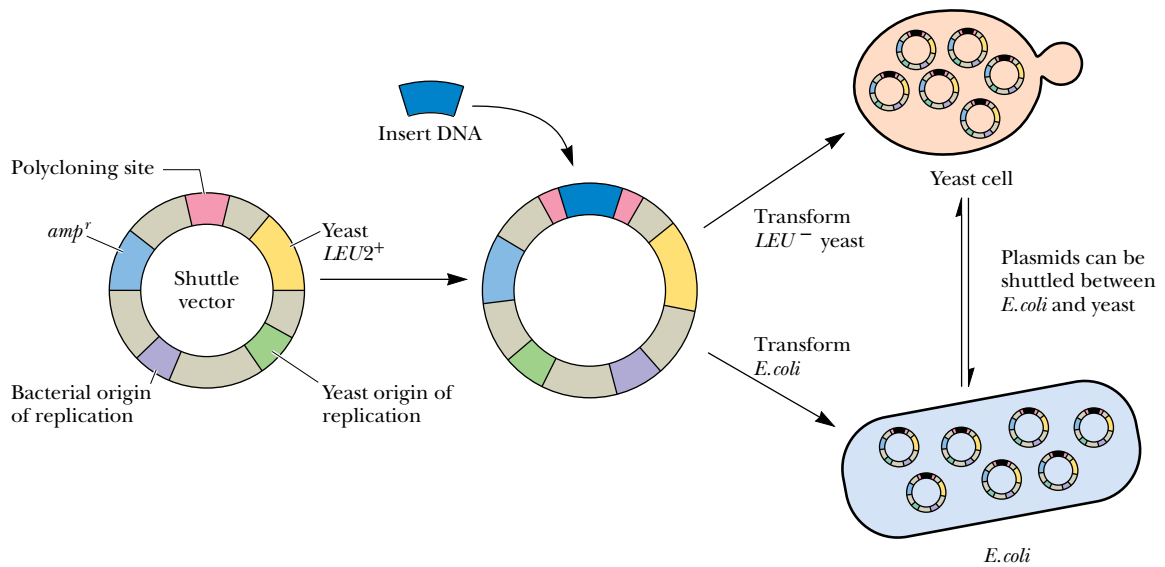
FIGURE 13.10 • A typical shuttle vector. This vector has both yeast and bacterial origins of replication, *amp*^{r} (ampicillin resistance gene for selection in *E. coli*) and *LEU2*$^+$, a gene in the yeast pathway for leucine biosynthesis. The recipient yeast cells are *LEU2*$^-$ (defective in this gene) and thus require leucine for growth. *LEU2*$^-$ yeast cells transformed with this shuttle vector can be selected on medium lacking any leucine supplement. *(Adapted from Figure 19-5 in Watson J. D., et al., 1987. The Molecular Biology of the Gene. Menlo Park, CA: Benjamin-Cummings.)*

Artificial Chromosomes

DNA molecules 2 megabase pairs in length have been successfully propagated in yeast by creating **yeast artificial chromosomes** or **YACs.** Further, such YACs have been transferred into transgenic mice for the analysis of large genes or multigenic DNA sequences *in vivo,* that is, within the living animal. For these large DNAs to be replicated in the yeast cell, YAC constructs must include not only an origin of replication (known in yeast terminology as an *autonomously replicating sequence* or *ARS*) but also a centromere and telomeres. Recall that centromeres provide the site for attachment of the chromosome to the spindle during mitosis and meiosis, and telomeres are nucleotide sequences defining the ends of chromosomes. Telomeres are essential for proper replication of the chromosome.

13.2 • DNA Libraries

A DNA library is a set of cloned fragments that collectively represent the genes of a particular organism. Particular genes can be isolated from DNA libraries, much as books can be obtained from conventional libraries. The secret is knowing where and how to look.

Genomic Libraries

Any particular gene constitutes only a small part of an organism's genome. For example, if the organism is a mammal whose entire genome encompasses some 10^6 kbp and the gene is 10 kbp, then the gene represents only 0.001% of the total nuclear DNA. It is impractical to attempt to recover such rare sequences directly from isolated nuclear DNA because of the overwhelming amount of

extraneous DNA sequences. Instead, a **genomic library** is prepared by isolating total DNA from the organism, digesting it into fragments of suitable size, and cloning the fragments into an appropriate vector. This approach is called *shotgun cloning* because the strategy has no way of targeting a particular gene but instead seeks to clone all the genes of the organism at one time. The intent is that at least one recombinant clone will contain at least part of the gene of interest. Usually, the isolated DNA is only partially digested by the chosen restriction endonuclease so that not every restriction site is cleaved in every DNA molecule. Then, even if the gene of interest contains a susceptible restriction site, some intact genes might still be found in the digest. Genomic libraries have been prepared from hundreds of different species.

Many clones must be created to be confident that the genomic library contains the gene of interest. The probability, *P*, that some number of clones, *N*, contains a particular fragment representing a fraction, *f*, of the genome is

$$P = 1 - (1 - f)^N$$

Thus,

$$N = \ln (1 - P)/\ln (1 - f)$$

For example, if the library consists of 10-kbp fragments of the *E. coli* genome (4640 kbp total), over 2000 individual clones must be screened to have a 99% probability ($P = 0.99$) of finding a particular fragment. Since $f = 10/4640 = 0.0022$ and $P = 0.99$, $N = 2093$. For a 99% probability of finding a particular

---

$\mathcal{C}$RITICAL DEVELOPMENTS IN BIOCHEMISTRY

Combinatorial Libraries

Specific recognition and binding of other molecules is a defining characteristic of any protein or nucleic acid. Often, target ligands of a particular protein are unknown, or, in other instances, a unique ligand for a known protein may be sought in the hope of blocking the activity of the protein or otherwise perturbing its function. **Combinatorial libraries** are the products of emerging strategies to facilitate the identification and characterization of possible ligands for a protein. These strategies are also applicable to the study of nucleic acids. Unlike genomic libraries, combinatorial libraries consist of synthetic oligomers. Arrays of synthetic oligonucleotides printed as tiny dots on miniature solid supports are known as **DNA chips.** Specifically, combinatorial libraries contain very large numbers of chemically synthesized molecules (such as peptides or oligonucleotides) with randomized sequences or structures. Such libraries are designed and constructed with the hope that one molecule among a vast number will be recognized as a ligand by the protein (or nucleic acid) of interest. If so, perhaps that molecule will be useful in a pharmaceutical application, for instance as a drug to treat a disease involving the protein to which it binds.

An example of this strategy is the preparation of a **synthetic combinatorial library** of hexapeptides. The maximum number of sequence combinations for hexapeptides is 20^6 or 64,000,000. One approach to simplify preparation and screening possibilities for such a library is to specify the first two amino acids in the hexa-

peptide while the next four are randomly chosen. In this approach, 400 libraries (20^2) are synthesized, each of which is unique in terms of the amino acids at positions 1 and 2 but random at the other four positions (as in *AAXXXX, ACXXXX, ADXXXX,* etc.) so that each of the 400 libraries contains 20^4 or 160,000 different sequence combinations. Screening these libraries with the protein of interest reveals which of the 400 libraries contains a ligand with high affinity. This library is then systematically expanded by specifying the first 3 amino acids (knowing from the chosen 1-of-400 libraries which amino acids are best as the first 2); only 20 synthetic libraries (each containing 20^3 or 8000 hexapeptides) are made here (one for each third-position possibility, the remaining three positions being randomized). Selection for ligand binding, again with the protein of interest, reveals the best of these 20, and this particular library is then varied systematically at the fourth position, creating 20 more libraries (each containing 20^2 or 400 hexapeptides). This cycle of synthesis, screening, and selection is repeated until all six positions in the hexapeptide are optimized to create the best ligand for the protein. A variation on this basic strategy using synthetic oligonucleotides rather than peptides identified a unique 15-mer (sequence GGTTGGTGTGGTTGG) with high affinity ($K_D = 2.7$ nM) toward thrombin, a serine protease in the blood coagulation pathway. Thrombin is a major target for the pharmacological prevention of clot formation in coronary thrombosis.

(From Cortese, R., 1996. Combinatorial Libraries: Synthesis, Screening and Application Potential. *Berlin: Walter de Gruyter.)*

FIGURE 13.11 • Screening a genomic library by colony hybridization (or plaque hybridization). Host bacteria transformed with a plasmid-based genomic library or infected with a bacteriophage-based genomic library are plated on a petri plate and incubated overnight to allow bacterial colonies (or phage plaques) to form. A replica of the bacterial colonies (or plaques) is then obtained by overlaying the plate with a nitrocellulose disc (1). Nitrocellulose strongly binds nucleic acids; single-stranded nucleic acids are bound more tightly than double-stranded nucleic acids. (Nylon membranes with similar nucleic acid– and protein-binding properties are also used.) Once the nitrocellulose disc has taken up an impression of the bacterial colonies (or plaques), it is removed and the petri plate is set aside and saved. The disc is treated with 2 *M* NaOH, neutralized, and dried (2). NaOH both lyses any bacteria (or phage particles) and dissociates the DNA strands. When the disc is dried, the DNA strands become immobilized on the filter. The dried disc is placed in a sealable plastic bag, and a solution containing heat-denatured (single-stranded), labeled probe is added (3). The bag is incubated to allow annealing of the probe DNA to any target DNA sequences that might be present on the nitrocellulose. The filter is then washed, dried, and placed on a piece of X-ray film to obtain an autoradiogram (4). The position of any spots on the X-ray film reveals where the labeled probe has hybridized with target DNA (5). The location of these spots can be used to recover the genomic clone from the bacteria (or plaques) on the original petri plate.

Master plate of bacteria colonies (or phage plaques)

1 Replicate onto nitrocellulose disc

2 Treat with NaOH; neutralize, dry

Denatured DNA bound to nitrocellulose

3 Place nitrocellulose filter in sealable plastic bag with solution of labeled DNA probe

4 Wash filter, prepare autoradiograph and compare with master plate

Radioactive probe will hybridize with its complementary DNA

5 Darkening identifies colonies (plaques) containing the DNA desired

Autoradiograph film

sequence within the 3×10^6 kbp human genome, *N* would equal almost 1.4 million if the cloned fragments averaged 10 kbp in size. The need for cloning vectors capable of carrying very large DNA inserts becomes obvious from these numbers.

Screening Libraries

A common method of screening plasmid-based genomic libraries is to carry out a **colony hybridization experiment.** The protocol is similar for phage-based libraries except that bacteriophage plaques, not bacterial colonies, are screened. In a typical experiment, host bacteria containing either a plasmid-based or bacteriophage-based library are plated out on a petri dish and allowed to grow overnight to form colonies (or in the case of phage libraries, plaques) (Figure 13.11). A replica of the bacterial colonies (or plaques) is then obtained by overlaying the plate with a nitrocellulose disc. The disc is removed, treated with alkali to dissociate bound DNA duplexes into single-stranded DNA, dried, and placed in a sealed bag with labeled probe (see the box on Southern blotting). If the probe DNA is duplex DNA, it must be denatured by heating at 70°C. The probe and target DNA complementary sequences must be in a single-stranded form if they are to hybridize with one another. Any DNA sequences complementary to probe DNA will be revealed by autoradiography of the nitrocellulose disc. Bacterial colonies (phage plaques) containing clones bearing target DNA are identified on the film and can be recovered from the master plate.

Probes for Southern Hybridization

Clearly, specific probes are essential reagents if the goal is to identify a particular gene against a background of innumerable DNA sequences. Usually, the probes that are used to screen libraries are nucleotide sequences that are complementary to some part of the target gene. To make useful probes requires some information about the gene's nucleotide sequence. Sometimes such information is available. Alternatively, if the amino acid sequence of the protein encoded by the gene is known, it is possible to work backward through the genetic code to the DNA sequence (Figure 13.12). Because the genetic code is *degenerate* (that is, several codons may specify the same amino acid; see
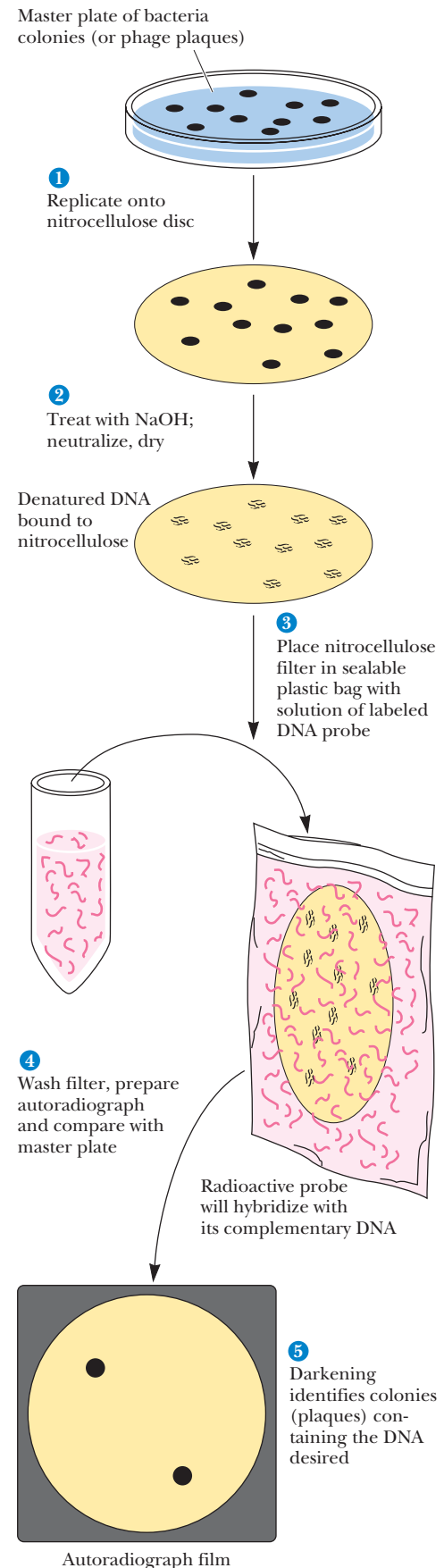
Known amino acid sequence:

Phe	Met	Glu	Trp	His	Lys	Asn

Possible mRNA sequence:

UUU	AUG	GAA	UGG	CAU	AGG	AAU
UUC		GAG		CAC	AAA	AAC

❶

Nitrocellulose filter replica of bacterial colonies carrying different DNA fragments

❷

Synthesize 32 possible DNA oligonucleotides and end label with radioactive ^{32}P

❸

Incubate nitrocellulose filter with probe solution in plastic bag

❹

Hybridization of the correct oligonucleotide to the DNA

❺

Detection by autoradiography

Autoradiograph film
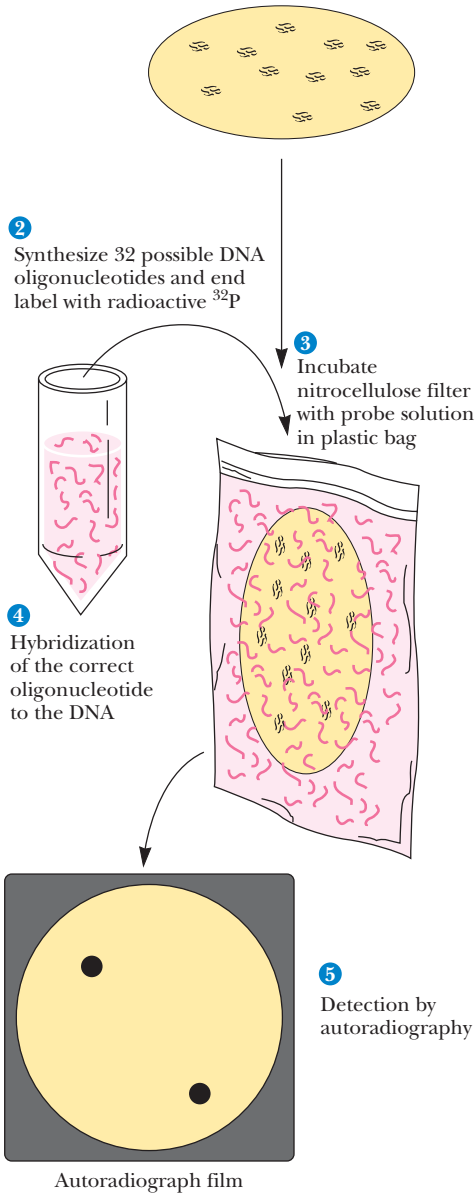
FIGURE 13.12 • Cloning genes using oligonucleotide probes designed from a known amino acid sequence. A radioactively labeled set of DNA (degenerate) oligonucleotides representing all possible mRNA coding sequences is synthesized. (In this case, there are 2^5, or 32.) The complete mixture is used to probe the genomic library by colony hybridization (see Figure 13.11). *(Adapted from Figure 19-18 in Watson, J. D., et al., 1987.* Molecular Biology of the Gene. *Menlo Park, CA: Benjamin-Cummings.)*

Chapter 32), probes designed by this approach are usually **degenerate oligonucleotides** about 17 to 50 residues long (such oligonucleotides are so-called 17- to 50-mers). The oligonucleotides are synthesized so that different bases are incorporated at sites where degeneracies occur in the codons. The final preparation thus consists of a mixture of equal-length oligonucleotides whose sequences vary to accommodate the degeneracies. Presumably, one oligonucleotide sequence in the mixture will hybridize with the target gene. These oligonucleotide probes are at least 17-mers because shorter degenerate oligonucleotides might hybridize with sequences unrelated to the target sequence.

A piece of DNA from the corresponding gene in a related organism can also be used as a probe in screening a library for a particular gene. Such probes are termed **heterologous probes** because they are not derived from the homologous (same) organism.

Problems arise if a complete eukaryotic gene is the cloning target; eukaryotic genes can be tens or even hundreds of kilobase pairs in size. Genes this size are fragmented in most cloning procedures. Thus, the DNA identified by the probe may represent a clone that carries only part of the desired gene. However, most cloning strategies are based on a partial digestion of the genomic DNA, a technique that generates an overlapping set of genomic fragments. This being so, DNA segments from the ends of the identified clone can now be used to probe the library for clones carrying DNA sequences that flanked the original isolate in the genome. Repeating this process ultimately yields the complete gene among a subset of overlapping clones.

cDNA Libraries

cDNAs are DNA molecules copied from mRNA templates. cDNA libraries are constructed by synthesizing cDNA from purified cellular mRNA. These libraries present an alternative strategy for gene isolation, especially eukaryotic genes. Because most eukaryotic mRNAs carry 3′-poly(A) tails, mRNA can be selectively isolated from preparations of total cellular RNA by oligo(dT)-cellulose chromatography (Figure 13.13). DNA copies of the purified mRNAs are synthesized by first annealing short oligo(dT) chains to the poly(A) tails. These oligo(dT) chains serve as primers for reverse transcriptase–driven synthesis of DNA (Figure 13.14). (Random oligonucleotides can also be used as primers, with the advantages being less dependency on poly(A) tracts and increased likelihood of creating clones representing the 5′-ends of mRNAs.) **Reverse transcriptase** is an enzyme that synthesizes a DNA strand, copying RNA as the template. DNA polymerase is then used to copy the DNA strand and form a double-stranded (duplex DNA) molecule. Linkers are then added to the DNA duplexes rendered from the mRNA templates, and the cDNA is cloned into a suitable vector. Once a cDNA derived from a particular gene has been identified, the cDNA becomes an effective probe for screening genomic libraries for isolation of the gene itself.

Because different cell types in eukaryotic organisms express selected subsets of genes, RNA preparations from cells or tissues in which genes of interest are selectively transcribed are enriched for the desired mRNAs. cDNA
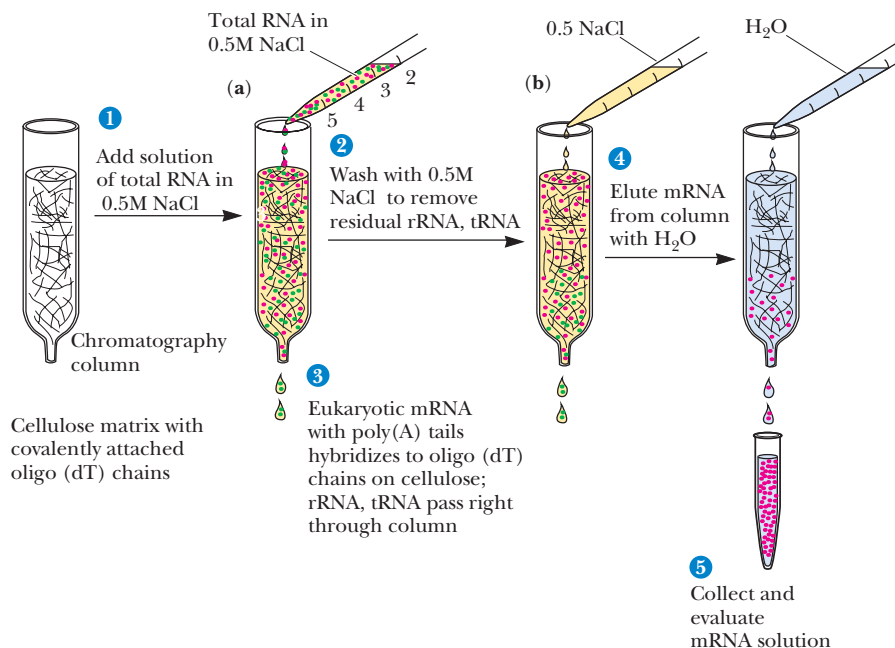
FIGURE 13.13 • Isolation of eukaryotic mRNA via oligo(dT)-cellulose chromatography. (a) In the presence of 0.5 *M* NaCl, the poly(A) tails of eukaryotic mRNA anneal with short oligo(dT) chains covalently attached to an insoluble chromatographic matrix such as cellulose. Other RNAs, such as rRNA (green), pass right through the chromatography column. (b) The column is washed with more 0.5 *M* NaCl to remove residual contaminants. (c) Then the poly(A) mRNA is recovered by washing the column with water because the base pairs formed between the poly(A) tails of the mRNA and the oligo(dT) chains are unstable in solutions of low ionic strength.
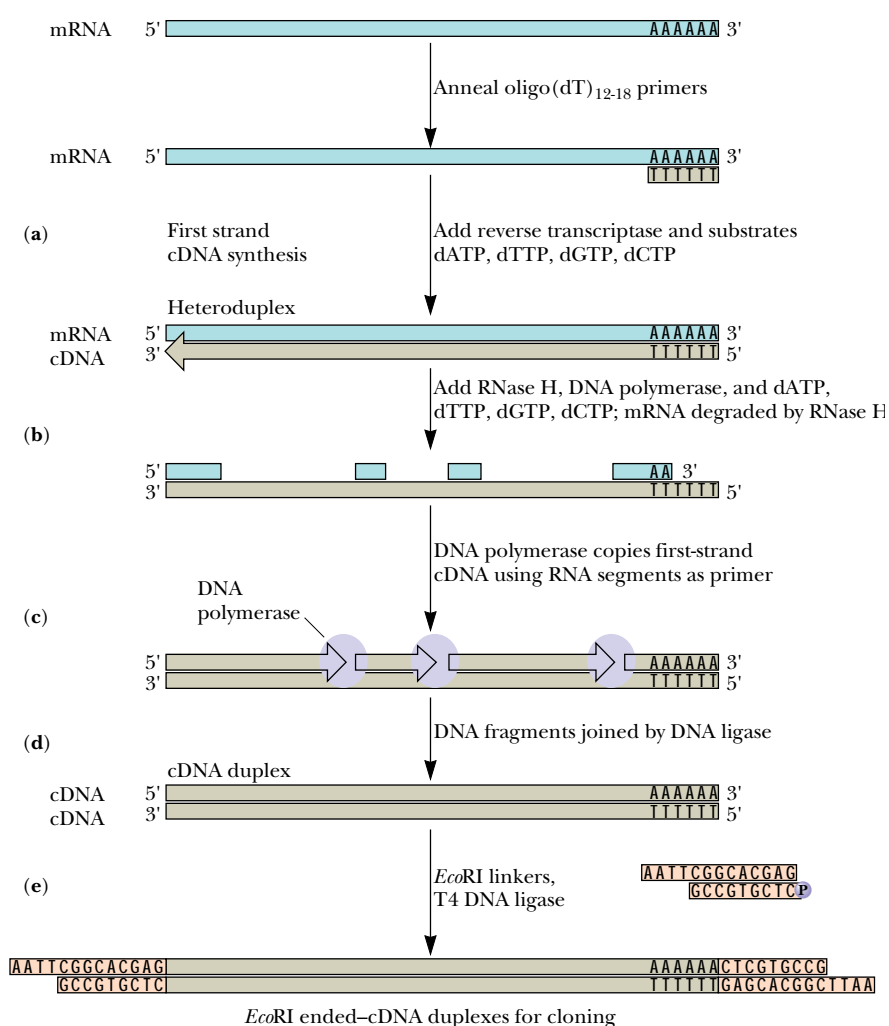
FIGURE 13.14 • Reverse transcriptase–driven synthesis of cDNA from oligo(dT) primers annealed to the poly(A) tails of purified eukaryotic mRNA. (a) Oligo(dT) chains serve as primers for synthesis of a DNA copy of the mRNA by reverse transcriptase. Following completion of first-strand cDNA synthesis by reverse transcriptase, RNase H and DNA polymerase are added (b). RNase H specifically digests RNA strands in DNA:RNA hybrid duplexes. DNA polymerase copies the first-strand cDNA, using as primers the residual RNA segments after RNase H has created nicks and gaps (c). DNA polymerase has a $5' \rightarrow 3'$ exonuclease activity that removes the residual RNA as it fills in with DNA. The nicks remaining in the second-strand DNA are sealed by DNA ligase (d), yielding duplex cDNA. *Eco*RI adapters with 5′-overhangs are then ligated onto the cDNA duplexes (e) using phage T4 DNA ligase to create *Eco*RI-ended cDNA for insertion into a cloning vector.

$\mathcal{C}$ RITICAL DEVELOPMENTS IN BIOCHEMISTRY

Identifying Specific DNA Sequences by Southern Blotting (Southern Hybridization)

Any given DNA fragment is unique solely by virtue of its specific nucleotide sequence. The only practical way to find one particular DNA segment among a vast population of different DNA fragments (such as you might find in genomic DNA preparations) is to exploit its sequence specificity to identify it. In 1975, E. M. Southern invented a technique capable of doing just that.

Electrophoresis

Southern first fractionated a population of DNA fragments according to size by gel electrophoresis (see step 2 in figure). The electrophoretic mobility of a nucleic acid is inversely proportional to its molecular mass. Polyacrylamide gels are suitable for separation of nucleic acids of 25 to 2000 bp. Agarose gels are better if the DNA fragments range up to 10 times this size. Most preparations of genomic DNA show a broad spectrum of sizes, from less than 1 kbp to more than 20 kbp. Typically, no discrete-size fragments are evident following electrophoresis, just a "smear" of DNA throughout the gel.

Blotting

Once the fragments have been separated by electrophoresis (step 3), the gel is soaked in a solution of NaOH. Alkali denatures duplex DNA, converting it to single-stranded DNA. After the pH of the gel is adjusted to neutrality with buffer, a sheet of nitrocellulose soaked in a concentrated salt solution is then placed over the gel (c), and salt solution is drawn through the gel in a direction perpendicular to the direction of electrophoresis (step 4). The salt solution is pulled through the gel in one of three ways: capillary action (*blotting*), suction (*vacuum blotting*), or electrophoresis (*electroblotting*). The movement of salt solution through the gel carries the DNA to the nitrocellulose sheet. Nitrocellulose binds single-stranded DNA molecules very tightly, effectively immobilizing them in place on the sheet.* Note that the distribution pattern of the electrophoretically separated DNA is maintained when the single-stranded DNA molecules bind to the nitrocellulose sheet (step 5 in figure). Next, the nitrocellulose is dried by baking in a vacuum oven;[†] baking tightly fixes the single-stranded DNAs to the nitrocellulose. Next, in the *prehybridization step,* the nitrocellulose sheet is incubated with a solution containing protein (serum albumin, for example) and/or a detergent such as sodium dodecyl sulfate. The protein and detergent molecules saturate any remaining binding sites for DNA on the nitrocellulose. Thus, no more DNA can bind nonspecifically to the nitrocellulose sheet.

Hybridization

To detect a particular DNA within the electrophoretic smear of countless DNA fragments, the prehybridized nitrocellulose sheet is incubated in a sealed plastic bag with a solution of specific probe molecules (step 6 in figure). A **probe** is usually a single-stranded DNA of defined sequence that is distinctively labeled, either with a radioactive isotope (such as ^{32}P) or some other easily detectable tag. The nucleotide sequence of the probe is designed to be complementary to the sought-for or *target* DNA fragment. The single-stranded probe DNA **anneals** with the single-stranded target DNA bound to the nitrocellulose through specific base pairing to form a DNA duplex. This annealing, or **hybridization** as it is usually called, labels the target DNA, revealing its position on the nitrocellulose. For example, if the probe is ^{32}P-labeled, its location can be detected by autoradiographic exposure of a piece of X-ray film laid over the nitrocellulose sheet (step 7 in figure).

Southern's procedure has been extended to the identification of specific RNA and protein molecules. In a play on Southern's name, the identification of particular RNAs following separation by gel electrophoresis, blotting, and probe hybridization is called **Northern blotting.** The analogous technique for identifying protein molecules is termed **Western blotting.** In Western blotting, the probe of choice is usually an antibody specific for the target protein.

The Southern blotting technique involves the transfer of electrophoretically separated DNA fragments to a nitrocellulose sheet and subsequent detection of specific DNA sequences. A preparation of DNA fragments [typically a restriction digest, (1)] is separated according to size by gel electrophoresis (2). The separation pattern can be visualized by soaking the gel in ethidium bromide to stain the DNA and then illuminating the gel with UV light (3). Ethidium bromide molecules intercalated between the hydrophobic bases of DNA are fluorescent under UV light. The gel is soaked in strong alkali to denature the DNA and then neutralized in buffer. Next, the gel is placed on a sheet of nitrocellulose (or DNA-binding nylon membrane), and concentrated salt solution is passed through the gel (4) to carry the DNA fragments out of the gel where they are bound tightly to the nitrocellulose (5). Incubation of the nitrocellulose sheet with a solution of labeled, single-stranded probe DNA (6) allows the probe to hybridize with target DNA sequences complementary to it. The location of these target sequences is then revealed by an appropriate means of detection, such as autoradiography (7). ▶

---

*The underlying cause of DNA binding to nitrocellulose is not clear, but probably involves a combination of hydrogen bonding, hydrophobic interactions, and salt bridges.
[†]Vacuum drying is essential because nitrocellulose reacts violently with O_2 if heated. For this reason, nylon-based membranes are preferable to nitrocellulose membranes.

1 Digest DNA with restriction endonucleases

DNA

DNA restriction fragments

2 Perform agarose gel electrophoresis on the DNA fragments from different digests

Buffer solution

Agarose gel

3 DNA fragments fractionated by size (visible under UV light if gel is soaked in ethidium bromide)

Longer DNA fragments

Shorter DNA fragments

Soak gel in NaOH, neutralize

4 Transfer (blot) gel to nitrocellulose filter using Southern blot technique

Weight

Garrett & Grisham
Biochemistry

Absorbent paper

Nitrocellulose filter

Gel

Wick

Buffer

5 DNA fragments are bound to the filter in positions identical to those on the gel

6 Hybridize filter with radioactively labeled probe.

Radioactive probe solution

7 Expose filter to X-ray film. Resulting autoradiograph shows hybridized DNA fragments

$\mathcal{H}$UMAN BIOCHEMISTRY

The Human Genome Project

The Human Genome Project is a collaborative international, government- and private-sponsored effort to map and sequence the entire human genome, some 3 billion base pairs distributed among the two sex chromosomes (**X** and **Y**) and 22 **autosomes** (chromosomes that are not sex chromosomes). Initial work identified and mapped at least 3000 genetic **markers** (genes or other recognizable loci on the DNA), evenly distributed throughout the chromosomes at roughly 100-kb intervals. At the same time, determination of the entire nucleotide sequence of the human genome began. The target date for completion is 2005. An ancillary part of the project is sequencing the genomes of other species (such as yeast, *Drosophila melanogaster* [the fruit fly], mice, and *Arabidopsis thaliana* [a plant]) to reveal comparative aspects of genetic and sequence organization (Table 13.1). Information about whole genome sequences of organisms has created a new branch of science called **functional genomics.** Functional genomics addresses global issues of gene expression, such as looking at *all* the genes that are activated during major metabolic shifts (as from growth under aerobic to growth under anaerobic conditions) or during embryogenesis and development of organisms. Functional genomics also provides new insights into evolutionary relationships between organisms.

The Human Genome Project is also vital to medicine. A number of human diseases have been traced to genetic defects, whose positions within the human genome have been identified. Among these are

> *cystic fibrosis* gene
>
> *Duchenne muscular dystrophy* gene* (at 2.4 megabases, the largest known gene in any organism)
>
> *Huntington's disease* gene
>
> *neurofibromatosis* gene
>
> *neuroblastoma* gene (a form of brain cancer)
>
> *amyotrophic lateral sclerosis* gene (Lou Gehrig's disease)
>
> *fragile X-linked mental retardation* gene*

as well as genes associated with the development of diabetes, breast cancer, colon cancer, and affective disorders such as *schizophrenia* and *bipolar affective disorder* (manic depression).

Table 13.1

Completed Genome Nucleotide Sequences	
Genome	**Genome Size[1] (Year Completed)**
Bacteriophage ϕX174	0.0054 (1977)
Bacteriophage λ	0.048 (1982)
Marchantia[2] chloroplast genome	0.187 (1986)
Vaccinia virus	0.192 (1990)
Cytomegalovirus (CMV)	0.229 (1991)
Marchantia[2] mitochondrial genome	0.187 (1992)
Variola (smallpox) virus	0.186 (1993)
Hemophilus influenzae[3] (Gram-negative bacterium)	1.830 (1995)
Mycobacterium genatalium (mycobacterium)	0.58 (1995)
Methanococcus jannaschii (archaebacterium)	1.67 (1996)
Escherichia coli (Gram-negative bacterium)	4.64 (1996)
Saccharomyces cerevisiae (yeast)	12.067 (1996)
Bacillus subtilis (Gram-positive bacterium)	4.21 (1997)
Arabidopsis thaliana (green plant)	100 (?)
Caenorhabditis elegans (simple animal: nematode worm)	100 (1998?)
Drosophila melanogaster (fruit fly)	165 (?)
Homo sapiens (human)	2900 (2005?)

[1]Genome size is given as millions of base pairs (mb).
[2]*Marchantia* is a bryophyte (a nonvascular green plant).
[3]The first complete sequence for the genome of a free-living organism.

*X-chromosome linked gene. As of 1992, more than 100 disease-related genes had been mapped to this chromosome.

libraries prepared from such mRNA are representative of the pattern and extent of gene expression that uniquely define particular kinds of differentiated cells. cDNA libraries of many normal and diseased human cell types are commercially available, including cDNA libraries of many tumor cells. Comparison of normal and abnormal cDNA libraries, in conjunction with two-dimensional gel electrophoretic analysis (see Appendix to Chapter 5) of the proteins produced in normal and abnormal cells, is a promising new strategy in clinical medicine to understand disease mechanisms.

Expression Vectors

Expression vectors are engineered so that any cloned insert can be transcribed into RNA, and, in many instances, even translated into protein. cDNA expression libraries can be constructed in specially designed vectors derived from either plasmids or bacteriophage λ. Proteins encoded by the various cDNA clones within such expression libraries can be synthesized in the host cells, and if suitable assays are available to identify a particular protein, its corresponding cDNA clone can be identified and isolated. Expression vectors designed for RNA expression or protein expression, or both, are available.

RNA Expression

A vector for *in vitro* expression of DNA inserts as RNA transcripts can be constructed by putting a highly efficient promoter adjacent to a versatile cloning site. Figure 13.15 depicts such an expression vector. Linearized recombinant vector DNA is transcribed *in vitro* using SP6 RNA polymerase. Large amounts of RNA product can be obtained in this manner; if radioactive ribonucleotides are used as substrates, labeled RNA molecules useful as probes are made.

Protein Expression

Because cDNAs are DNA copies of mRNAs, cDNAs are uninterrupted copies of the exons of expressed genes. Because cDNAs lack introns, it is feasible to express these cDNA versions of eukaryotic genes in prokaryotic hosts that cannot process the complex primary transcripts of eukaryotic genes. To express a eukaryotic protein in *E. coli,* the eukaryotic cDNA must be cloned in an *expression vector* that contains regulatory signals for both transcription and translation. Accordingly, a *promoter* where RNA polymerase initiates transcription as well as a *ribosome binding site* to facilitate translation are engineered into the vector just upstream from the restriction site for inserting foreign DNA. The AUG initiation codon that specifies the first amino acid in the protein (the *translation start site*) is contributed by the insert (Figure 13.16).

Strong promoters have been constructed that drive the synthesis of foreign proteins to levels equal to 30% or more of total *E. coli* cellular protein. An example is the hybrid promoter, p_{tac}, which was created by fusing part of the promoter for the *E. coli* genes encoding the enzymes of lactose metabolism (the *lac* promoter) with part of the promoter for the genes encoding the enzymes of tryptophan biosynthesis (the *trp* promoter) (Figure 13.17). In cells carrying p_{tac} expression vectors, the p_{tac} promoter is not induced to drive transcription of the foreign insert until the cells are exposed to *inducers* that lead to its activation. Analogs of lactose (a β-galactoside) such as *isopropyl-β-thiogalactoside,* or **IPTG,** are excellent inducers of p_{tac}. Thus, expression of the foreign protein is easily controlled. (See Chapter 31 for detailed discussions of inducible gene expression.) The bacterial production of valuable eukaryotic proteins represents one of the most important uses of recombinant DNA technology. For example, human insulin for the clinical treatment of diabetes is now produced in bacteria.

Analogous systems for expression of foreign genes in eukaryotic cells include vectors carrying promoter elements derived from mammalian viruses, such as *simian virus 40 (SV40),* the *Epstein–Barr virus,* and the human *cytomegalovirus (CMV).* A system for high-level expression of foreign genes uses insect cells infected with the *baculovirus* expression vector. **Baculoviruses** infect *lepidopteran* insects (butterflies and moths). In engineered baculovirus vectors, the foreign gene is cloned downstream of the promoter for **polyhedrin,** a major viral-encoded structural protein, and the recombinant vector is incorporated
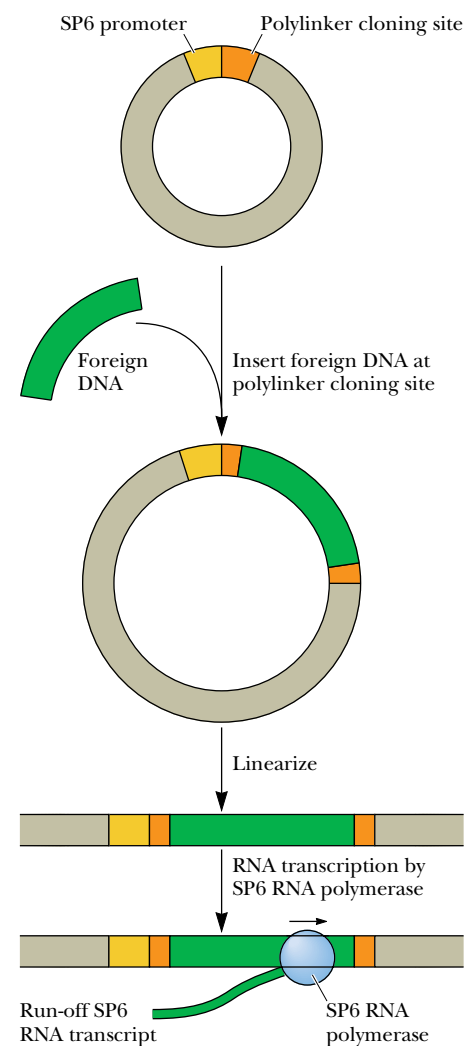
FIGURE 13.15 • Expression vectors carrying the promoter recognized by the RNA polymerase of bacteriophage SP6 are useful for making RNA transcripts *in vitro.* SP6 RNA polymerase works efficiently *in vitro* and recognizes its specific promoter with high specificity. These vectors typically have a polylinker adjacent to the SP6 promoter. Successive rounds of transcription initiated by SP6 RNA polymerase at its promoter lead to the production of multiple RNA copies of any DNA inserted at the polylinker. Before transcription is initiated, the circular expression vector is linearized by a single cleavage at or near the end of the insert so that transcription terminates at a fixed point.
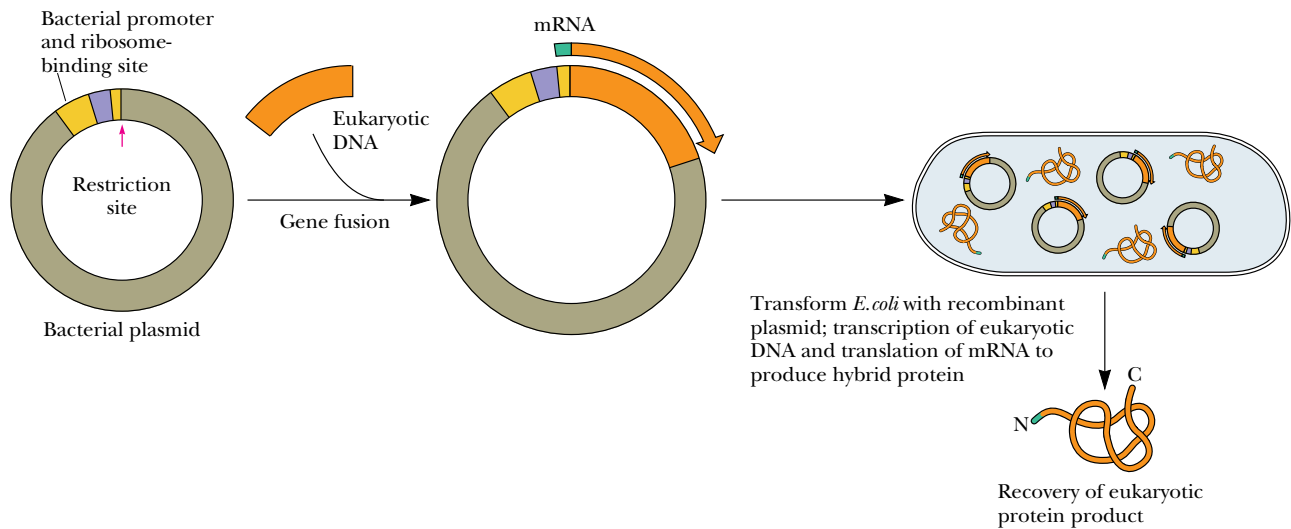
FIGURE 13.16 • A typical expression-cloning vector. Eukaryotic coding sequences are inserted at the restriction site just downstream from a promoter region where RNA polymerase binds and initiates transcription. Transcription proceeds through a region encoding a bacterial ribosome-binding site and into the cloned insert. The presence of the bacterial ribosome-binding site in the RNA transcript ensures that the RNA can be translated into protein by the ribosomes of the host bacteria. *(Adapted from Figure 19-5 from* Molecular Biology of the Gene, *4th edition. Copyright 1987 by James D. Watson. Reprinted by permission of Benjamin/Cummings Publishing Co., Inc.)*
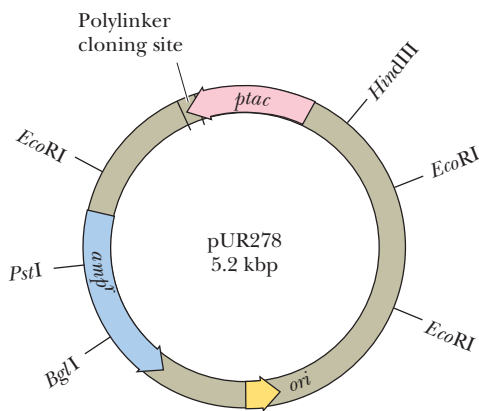
FIGURE 13.17 • A p_{tac} protein expression vector contains the hybrid promoter p_{tac} derived from fusion of the *lac* and *trp* promoters. Expression from p_{tac} is more than 10 times greater than expression from either the *lac* or *trp* promoter alone. Isopropyl-β-D-thiogalactoside, or IPTG, induces expression from p_{tac} as well as *lac*.

into insect cells grown in culture. Expression from the polyhedrin promoter can lead to accumulation of the foreign gene product to levels as high as 500 mg/L.

Screening cDNA Expression Libraries with Antibodies

Antibodies that specifically cross-react with a particular protein of interest are often available. If so, these antibodies can be used to screen a cDNA expression library to identify and isolate cDNA clones encoding the protein. The cDNA library is introduced into host bacteria, which are plated out and grown overnight, as in the colony hybridization scheme previously described. DNA-binding nylon membranes are placed on the plates to obtain a replica of the bacterial colonies. The nylon membrane is then incubated under conditions that induce protein synthesis from the cloned cDNA inserts, and the cells are treated to release the synthesized protein. The synthesized protein binds tightly to the nylon membrane, which can then be incubated with the specific antibody. Binding of the antibody to its target protein product reveals the position of any cDNA clones expressing the protein, and these clones can be recovered from the original plate. Like other libraries, expression libraries can be screened with oligonucleotide probes, too.

Fusion Protein Expression

Some expression vectors carry cDNA inserts cloned directly into the coding sequence of a vector-borne protein-coding gene (Figure 13.18). Translation of the recombinant sequence leads to synthesis of a *hybrid protein* or *fusion protein*. The N-terminal region of the fused protein represents amino acid sequences encoded in the vector, whereas the remainder of the protein is encoded by the foreign insert. Keep in mind that the triplet codon sequence within the cloned insert must be in phase with codons contributed by the vector sequences to make the right protein. The N-terminal protein sequence contributed by the vector can be chosen to suit purposes. Furthermore, adding an N-terminal sig-

Codon: Cys Gln Lys Gly Asp Pro Ser Thr Leu Glu Ser Leu Ser Met
Cloning site: TGT CAA AAA GGG GAT CCG TCG ACT CTA GAA AGC TTA TCG ATG
                        *Bam*HI   *Sal*I   *Xba*I   *Hin*dIII   *Cla*I
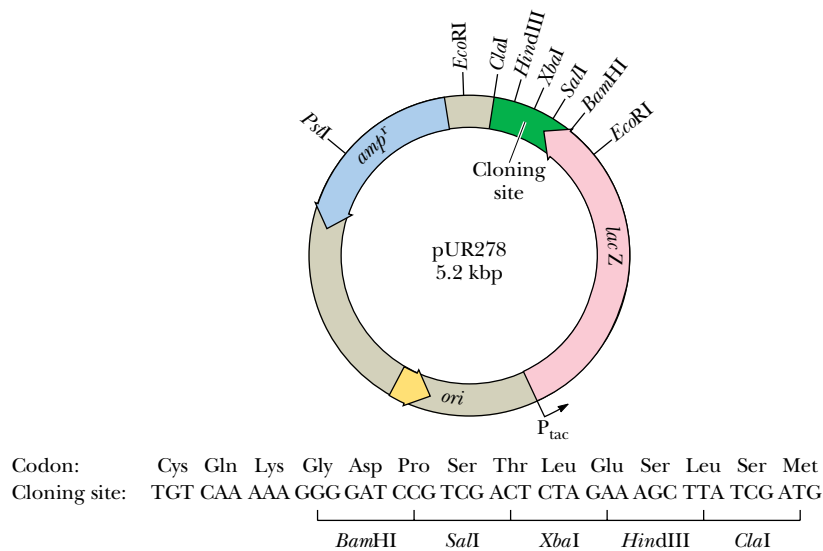
FIGURE 13.18 • A typical expression vector for the synthesis of a hybrid protein. The cloning site is located at the end of the coding region for the protein β-galactosidase. Insertion of foreign DNAs at this site fuses the foreign sequence to the β-galactosidase coding region (the *lacZ* gene). IPTG induces the transcription of the *lacZ* gene from its promoter p_{lac}, causing expression of the fusion protein. *(Adapted from Figure 1.5.4 in Ausubel, F. M., et al.,1987.* Current Protocols in Molecular Biology. *New York: John Wiley & Sons.)*

nal sequence that targets the hybrid protein for secretion from the cell simplifies recovery of the fusion protein. A variety of gene fusion systems have been developed to facilitate isolation of a specific protein encoded by a cloned insert. The isolation procedures are based on affinity chromatography purification of the fusion protein through exploitation of the unique ligand-binding properties of the vector-encoded protein (Table 13.2).

β-Galactosidase and Blue or White Selection

One version of these fusion protein expression vectors places the cloning site at the end of the coding region of the protein *β-galactosidase,* so that among other things the fusion protein is attached to β-galactosidase and can be recovered by purifying the β-galactosidase activity. Alternatively, placing the cloning site within the β-galactosidase coding region means that cloned inserts disrupt the β-galactosidase amino acid sequence, inactivating its enzymatic activity. This property has been exploited in developing a visual screening protocol that dis-

Table 13.2

Gene Fusion Systems for Isolation of Cloned Fusion Proteins

Gene Product	Origin	Molecular Mass (kD)	Secreted?[1]	Affinity Ligand
β-Galactosidase	*E. coli*	116	No	*p*-Aminophenyl-β-D-thiogalactoside (APTG)
Protein A	*S. aureus*	31	Yes	Immunoglobulin G (IgG)
Chloramphenicol acetyltransferase (CAT)	*E. coli*	24	Yes	Chloramphenicol
Streptavidin	*Streptomyces*	13	Yes	Biotin
Glutathione-S-transferase (GST)	*E. coli*	26	No	Glutathione
Maltose-binding protein (MBP)	*E. coli*	40	Yes	Starch

[1]This indicates whether combined secretion–fusion gene systems have led to secretion of the protein product from the cells, which simplifies its isolation and purification.

Adapted from Uhlen, M., and Moks, T., 1990. Gene fusions for purpose of expression: An introduction. *Methods in Enzymology* **185:**129–143.
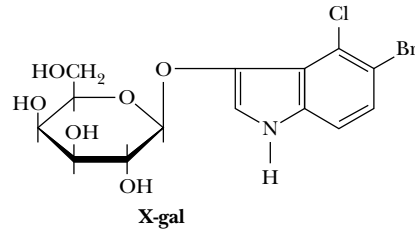
FIGURE 13.19 • The structure of 5-bromo-4-chloro-3-indolyl-β-D-galactopyranoside, or X-gal.

tinguishes those clones in the library that bear inserts from those that lack them.

Cells that have been transformed with a plasmid-based β-galactosidase expression cDNA library (or infected with a similar library constructed in a bacteriophage λ–based β-galactosidase fusion vector) are plated on media containing *5-bromo-4-chloro-3-indolyl-β-D-galactopyranoside,* or **X-gal** (Figure 13.19). X-gal is a *chromogenic substrate,* a colorless substance that upon enzymatic reaction yields a colored product. Following induction with IPTG, bacterial colonies (or plaques) harboring vectors in which the β-galactosidase gene is intact (those vectors lacking inserts) express an active β-galactosidase that cleaves X-gal, liberating 5-bromo-4-chloro-indoxyl, which dimerizes to form an indigo blue product. These blue colonies (or plaques) represent clones that lack inserts. The β-galactosidase gene is inactivated in clones with inserts, so those colonies (or plaques) that remain "white" (actually, colorless) are recombinant clones.

Reporter Gene Constructs

Potential regulatory regions of genes (such as promoters) can be investigated by placing these regulatory sequences into plasmids upstream of a gene, called a **reporter gene,** whose expression is easy to measure. Such chimeric plasmids are then introduced into cells of choice (including eukaryotic cells) to assess the potential function of the nucleotide sequence in regulation because expression of the reporter gene serves as a report on the effectiveness of the regulatory element. A number of different genes have been used as reporter genes, such as the *lacZ* gene. A reporter gene with many inherent advantages is that encoding the **green fluorescent protein** (or **GFP**), described in Chapter 4. Unlike the protein expressed by other reporter gene systems, GFP does not require any substrate to measure its activity, nor is it dependent on any cofactor or prosthetic group. Detection of GFP requires only irradiation with near UV or blue light (400-nm light is optimal), and the green fluorescence (light of 500 nm) that results is easily observed with the naked eye, although it can also be measured precisely with a fluorometer. Figure 13.20 demonstrates the use of GFP as a reporter gene.
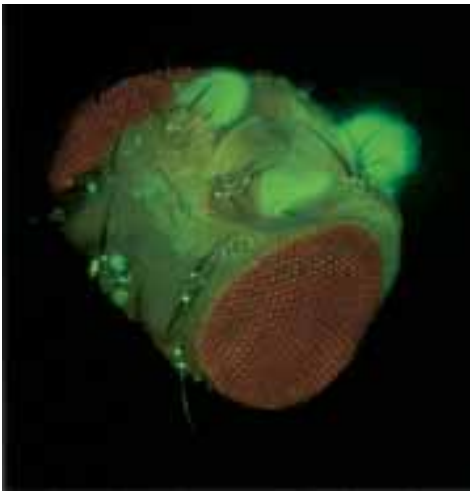
FIGURE 13.20 • Green fluorescent protein (GFP) as a reporter gene. The promoter from the *per* gene was placed upstream of the GFP gene in a plasmid and transformed into *Drosophila* (fruit flies). The *per* gene encodes a protein involved in establishing the circadian (daily) rhythmic activity of fruit flies. The fluorescence shown here in an isolated fly head follows a 24-hour rhythmic pattern and occurs to a lesser extent throughout the entire fly, indicating that *per* gene expression can occur in cells throughout the animal. Such uniformity suggests that individual cells have their own independent clocks. *(Image courtesy of Jeffrey D. Plautz and Steve A. Kay, Scripps Research Institute, La Jolla, California. See also Plautz, J. D., et al., 1997. Science **278:**1632–1635.)*

The Two-Hybrid System to Identify Proteins Involved in Specific Protein–Protein Interactions

Specific interactions between proteins (so-called protein–protein interactions) lie at the heart of many essential biological processes. Stanley Fields, Cheng-Ting Chien, and their collaborators have invented a method to identify specific protein–protein interactions *in vivo* through expression of a reporter gene whose transcription is dependent on a functional transcriptional activator, the *GAL4* protein. The *GAL4* protein consists of two domains: a DNA-binding (or **DB**) domain and a transcriptional activation (or **TA**) domain. Even if expressed as separate proteins, these two domains will still work, provided they can be brought together. The method depends on two separate plasmids encoding two hybrid proteins, one consisting of the *GAL4* DB domain fused to protein X, and the other consisting of the *GAL4* TA domain fused to protein Y (figure, part a). If proteins X and Y interact in a specific protein–protein interaction, the *GAL4* DB and TA domains are brought together so that transcription of a reporter gene driven by the *GAL4* promoter can take place (figure, part b). Protein X, fused to the *GAL4*-DNA binding domain (DB), serves as the "bait" to fish for the protein Y "target" and its fused *GAL4* TA domain. This method can be used to screen cells for protein "targets" that interact specifically with a particular "bait" protein. To do so, cDNAs encoding proteins from the cells of interest are inserted into the TA-containing plasmid to create fusions of the cDNA coding sequences with the *GAL4* TA domain coding sequences, so a fusion protein library is expressed. Identification of a target of the "bait" protein by this method also yields directly a cDNA version of the gene encoding the "target" protein.

(a)

(b)
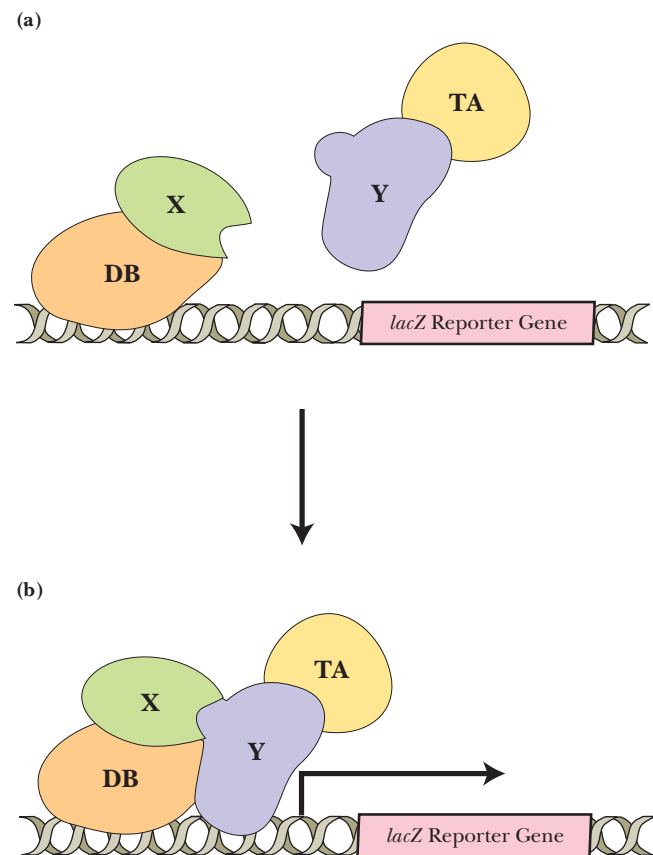
13.3 • Polymerase Chain Reaction (PCR)

Polymerase chain reaction or **PCR** is a technique for dramatically amplifying the amount of a specific DNA segment. A preparation of denatured DNA containing the segment of interest serves as template for DNA polymerase, and two specific oligonucleotides serve as primers for DNA synthesis (as in Figure 13.21). These primers, designed to be complementary to the two 3′-ends of the specific DNA segment to be amplified, are added in excess amounts of 1000 times or greater (Figure 13.21). They prime the DNA polymerase–catalyzed synthesis of the two complementary strands of the desired segment, effectively doubling its concentration in the solution. Then the DNA is heated to dissociate the DNA duplexes and then cooled so that primers bind to both the newly formed and the old strands. Another cycle of DNA synthesis ensues. The protocol has been automated through the invention of **thermal cyclers** that alternately heat the reaction mixture to 95°C to dissociate the DNA, followed by cooling, annealing of primers, and another round of DNA synthesis. The isolation of heat-stable DNA polymerases from thermophilic bacteria (such as the
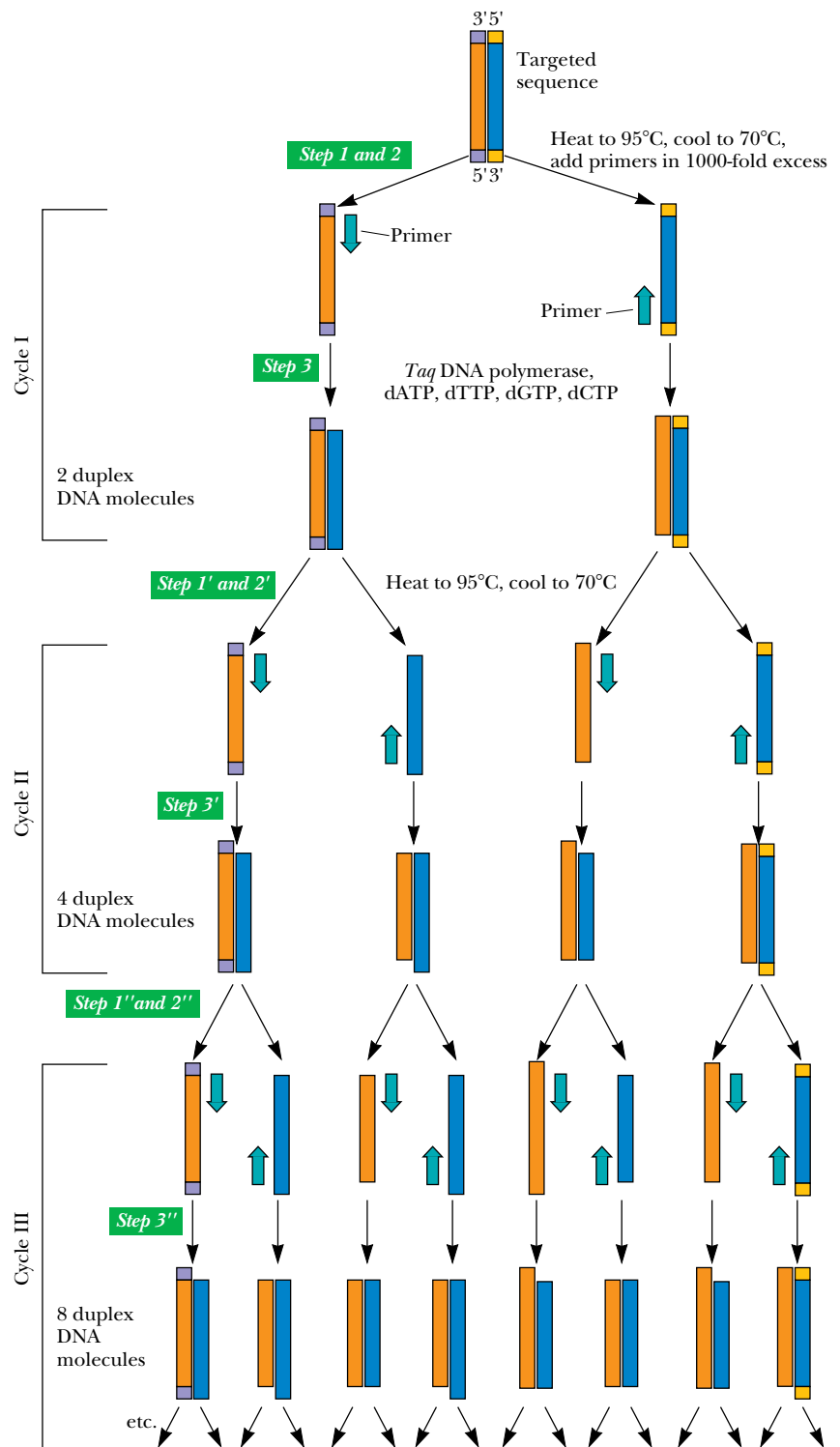
FIGURE 13.21 • Polymerase chain reaction (PCR). Oligonucleotides complementary to a given DNA sequence prime the synthesis of only that sequence. Heat-stable *Taq* DNA polymerase survives many cycles of heating. Theoretically, the amount of the specific primed sequence is doubled in each cycle.

Taq DNA polymerase from *Thermus aquaticus*) has made it unnecessary to add fresh enzyme for each round of synthesis. Because the amount of target DNA theoretically doubles each round, 25 rounds would increase its concentration about 33 million times. In practice, the increase is actually more like a million times, which is more than ample for gene isolation. Thus, starting with a tiny

amount of total genomic DNA, a particular sequence can be produced in quantity in a few hours.

PCR amplification is an effective cloning strategy if sequence information for the design of appropriate primers is available. Because DNA from a single cell can be used as a template, the technique has enormous potential for the clinical diagnosis of infectious diseases and genetic abnormalities. With PCR techniques, DNA from a single hair or sperm can be analyzed to identify particular individuals in criminal cases without ambiguity. **RT-PCR,** a variation on the basic PCR method, is useful when the nucleic acid to be amplified is an RNA (such as mRNA). Reverse transcriptase (RT) is used to synthesize a cDNA strand complementary to the RNA, and this cDNA serves as the template for further cycles of PCR.

In Vitro Mutagenesis

The advent of recombinant DNA technology has made it possible to clone genes, manipulate them *in vitro,* and express them in a variety of cell types under various conditions. The function of any protein is ultimately dependent on its amino acid sequence, which in turn can be traced to the nucleotide sequence of its gene. The introduction of purposeful changes in the nucleotide sequence of a cloned gene represents an ideal way to make specific structural changes in a protein. The effects of these changes on the protein's function can then be studied. Such changes constitute *mutations* introduced *in vitro* into the gene. *In vitro* **mutagenesis** makes it possible to alter the nucleotide sequence of a cloned gene systematically, as opposed to the chance occurrence of mutations in natural genes.

One efficient technique for *in vitro* mutagenesis is **PCR-based mutagenesis.** Mutant primers are added to a PCR reaction in which the gene (or segment of a gene) is undergoing amplification. The *mutant primers* are primers whose sequence has been specifically altered to introduce a directed change at a particular place in the nucleotide sequence of the gene being amplified (Figure 13.22). Mutant versions of the gene can then be cloned and expressed to determine any effects of the mutation on the function of the gene product.

13.4 • Recombinant DNA Technology: An Exciting Scientific Frontier

The strategies and methodologies described in this chapter are but an overview of the repertoire of experimental approaches that have been devised by molecular biologists in order to manipulate DNA and the information inherent in it. The enormous success of recombinant DNA technology means that the molecular biologist's task in searching genomes for genes is now akin to that of a lexicographer compiling a dictionary, a dictionary in which the "letters," i.e., the nucleotide sequences, spell out not words, but genes and what they mean. Molecular biologists have no index or alphabetic arrangement to serve as a guide through the vast volume of information in a genome; nevertheless, this information and its organization are rapidly being disclosed by the imaginative efforts and diligence of these scientists and their growing arsenal of analytical schemes.

Recombinant DNA technology now verges on the ability to engineer at will the genetic constitution of organisms for desired ends. The commercial production of therapeutic biomolecules in microbial cultures is already established (for example, the production of human insulin in quantity in *E. coli* cells). Agricultural crops with desired attributes, such as enhanced resistance to her-

Gene in plasmid with mutation target site X

Thermal denaturation; anneal mutagenic primers which also introduce a unique restriction site

***Taq* DNA polymerase; many cycles of PCR**

Many copies of plasmid with desired site-specific mutation

Transform *E.coli* cells. Screen single colonies for plasmids with unique restriction site (≡ mutant gene)
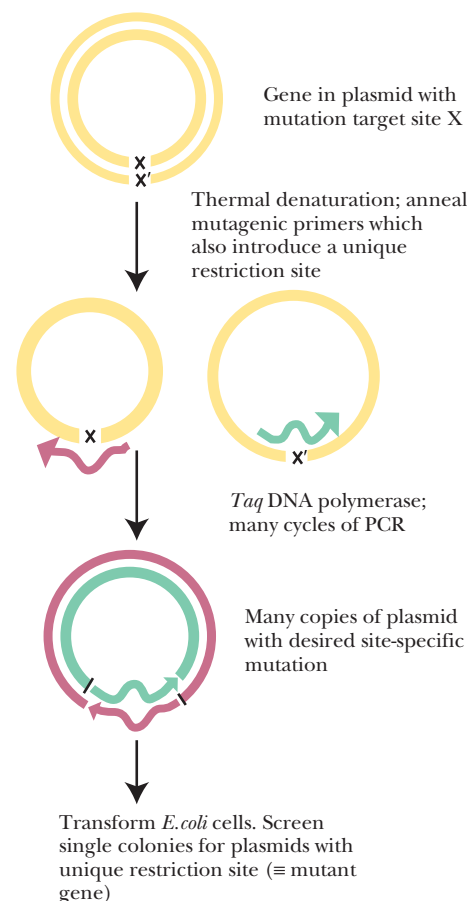
FIGURE 13.22 • One method of PCR-based site-directed mutagenesis. Template DNA strands are separated by increased temperature, and the single strands are amplified by PCR using mutagenic primers (represented as bent arrows) whose sequences introduce a single base substitution at site *X* (and its complementary base *X'*; thus the desired amino acid change in the protein encoded by the gene). Ideally, the mutagenic primers also introduce a unique restriction site into the plasmid that was not present before. Following many cycles of PCR, the DNA product can be used to transform *E. coli* cells. Single colonies of the transformed cells can be picked. The plasmid DNA within each colony can be isolated and screened for the presence of the mutation by screening for the presence of the unique restriction site by restriction endonuclease cleavage. For example, the nucleotide sequence *GGATCT* within a gene codes for amino acid residues Gly-Ser. Using mutagenic primers of nucleotide sequence *AGATCT* (and its complement *AGATCT*) changes the amino acid sequence from Gly-Ser to Arg-Ser and creates a *Bgl*II restriction site (see Table 11.5). Gene expression of the isolated mutant plasmid in *E. coli* allows recovery and analysis of the mutant protein.

*H*UMAN BIOCHEMISTRY

The Biochemical Defects in Cystic Fibrosis and ADA⁻ SCID

The gene defective in cystic fibrosis codes for CFTR (cystic fibrosis transmembrane conductance regulator), a membrane protein that pumps Cl⁻ out of cells. If this Cl⁻ pump is defective, Cl⁻ ions remain in cells, which then take up water from the surrounding mucus by osmosis. The mucus thickens and accumulates in various organs, including the lungs, where its presence favors infections such as pneumonia. Left untreated, children with cystic fibrosis seldom survive past the age of 5 years.

ADA⁻ SCID (adenosine deaminase–defective severe combined immunodeficiency) is a fatal genetic disorder caused by defects in the gene that encodes adenosine deaminase (ADA).

The consequence of ADA deficiency is accumulation of adenosine and 2′-deoxyadenosine, substances toxic to lymphocytes, important cells in the immune response. 2′-Deoxyadenosine is particularly toxic because its presence leads to accumulation of its nucleotide form, dATP, an essential substrate in DNA synthesis. Elevated levels of dATP actually block DNA replication and cell division by inhibiting synthesis of the other deoxynucleoside 5′-triphosphates (see Chapter 27). Accumulation of dATP also leads to selective depletion of cellular ATP, robbing cells of energy. Children with ADA⁻ SCID fail to develop normal immune responses and are susceptible to fatal infections, unless kept in protective isolation.

bicides, are in cultivation. The rat growth hormone gene has been cloned and transferred into mouse embryos, creating *transgenic mice* that at adulthood are twice normal size (see Chapter 29). Already, transgenic versions of domestic animals such as pigs, sheep, and even fish have been developed for human benefit. Perhaps most important, in a number of instances, clinical trials have been approved for **gene replacement therapy** (or, more simply, *gene therapy*) to correct particular human genetic disorders.

Human Gene Therapy

Human gene therapy seeks to repair the damage caused by a genetic deficiency through introduction of a functional version of the defective gene. To achieve this end, a cloned variant of the gene must be incorporated into the organism in such a manner that it is expressed only at the proper time *and* only in appropriate cell types. At this time, these conditions impose serious technical and clinical difficulties. Many gene therapies have received approval from the National Institutes of Health for trials in human patients, including the introduction of gene constructs into patients. Among these are constructs designed to cure ADA⁻ SCID (**s**evere **c**ombined **i**mmuno**d**eficiency due to adenosine deaminase [ADA] deficiency), neuroblastoma, or cystic fibrosis, or to treat cancer through expression of the E1A and p53 tumor suppressor genes.

A basic strategy in human gene therapy involves incorporation of a functional gene into target cells. The gene is typically in the form of an **expression cassette** consisting of a cDNA version of the gene downstream from a promoter that drives expression of the gene. A vector carrying such an expression cassette is introduced into target cells, either *ex vivo* via gene transfer into cultured cells in the laboratory and administration of the modified cells to the patient, or *in vivo* via direct incorporation of the gene into the cells of the patient. Because retroviruses can transfer their genetic information directly into the genome of host cells, retroviruses provide one route to permanent modification of host cells *ex vivo*. A replication-deficient version of *Maloney murine leukemia virus* can serve as a vector for expression cassettes up to 9 kb in size. Figure 13.23 describes a strategy for retrovirus vector–mediated gene delivery. In this strategy, it is hoped that the expression cassette will become stably integrated into the DNA of the patient's own cells and expressed to pro-
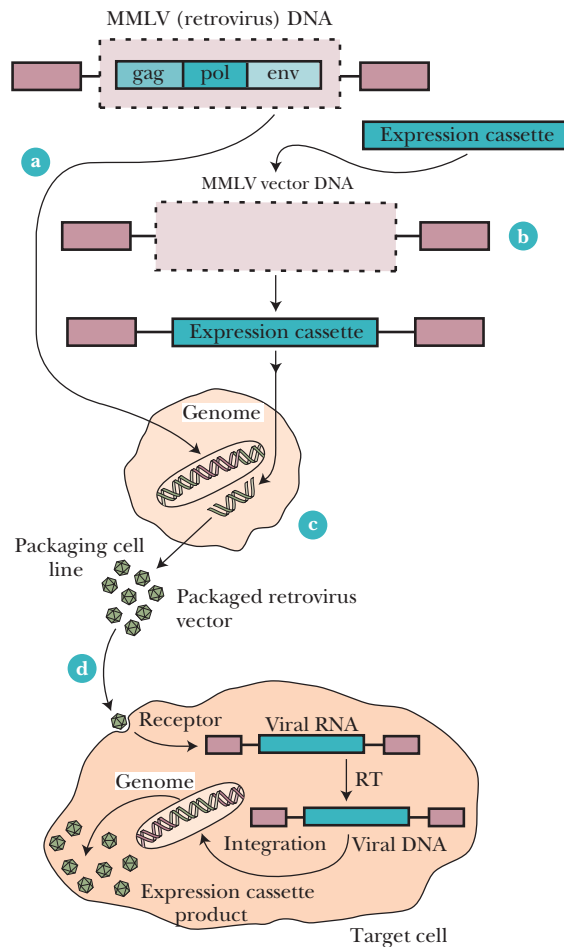
FIGURE 13.23 • Retrovirus-mediated gene delivery *ex vivo*. Retroviruses are RNA viruses that replicate their RNA genome by first making a DNA intermediate. The Maloney murine leukemia virus (MMLV) is the retrovirus used in human gene therapy. Deletion of the essential genes *gag, pol,* and *env* from MMLV makes it replication-deficient (so it can't reproduce) (a) and creates a space for insertion of an expression cassette (b). The modified MMLV acts as a vector for the expression cassette; although replication-defective, it is still infectious. Infection of a packaging cell line that carries intact *gag, pol,* and *env* genes allows the modified MMLV to reproduce (c), and the packaged retroviral viruses can be collected and used to infect a patient (d). In the cytosol of the patient's cells, a DNA copy of the viral RNA is synthesized by viral reverse transcriptase, which accompanies the viral RNA into the cells. This DNA is then randomly integrated into the host cell genome, where its expression leads to production of the expression cassette product. *(Adapted from Figure 1 in Crystal, R. G., 1995. Transfer of genes to humans: Early lessons and obstacles to success.* Science ***270**:404.)*

duce the desired gene product. Alternatively, *adenovirus* vectors that can carry expression cassettes up to 7.5 kb are a possible *in vivo* approach to human gene therapy (Figure 13.24). Recombinant, replication-deficient adenoviruses enter target cells via specific receptors on the target cell surface; the transferred genetic information is expressed directly from the adenovirus recombinant DNA and is never incorporated into the host cell genome. Although many problems remain to be solved, human gene therapy as a clinical strategy is feasible.
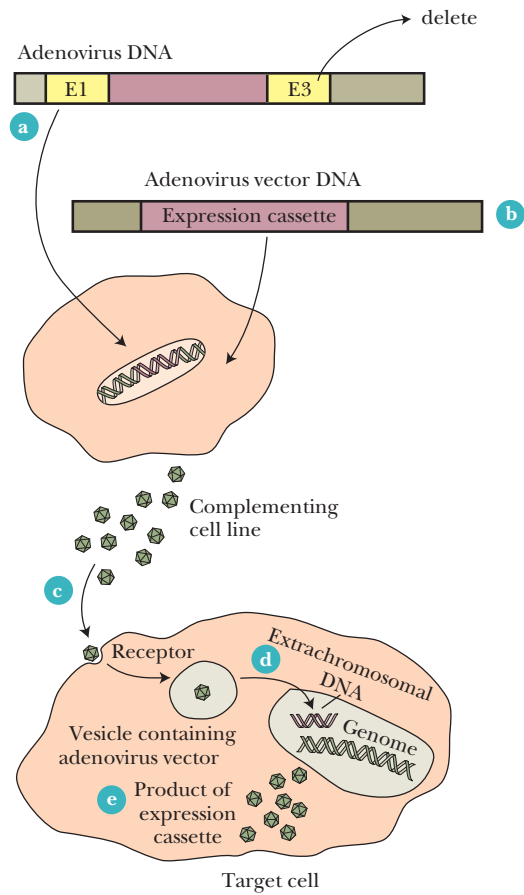
FIGURE 13.24 • Adenovirus-mediated gene delivery *in vivo*. Adenoviruses are DNA viruses. The adenovirus genome (36 kb) is divided into *early genes* (E1 through E4) and *late genes* (L1 to L5) (a). Adenovirus vectors are generated by deleting gene E1 (and sometimes E3 if more space for an expression cassette is needed) (b); deletion of E1 renders the adenovirus incapable of replication unless introduced into a complementing cell line carrying the E1 gene (c). Adenovirus progeny from the complementing cell line can be used to infect a patient. In the patient, the adenovirus vector with its expression cassette enters the cells via specific receptors (d). Its linear dsDNA ultimately gains access to the cell nucleus, where it functions extrachromosomally and expresses the product of the expression cassette (e). *(Adapted from Figure 2 in Crystal, R. G., 1995. Transfer of genes to humans: Early lessons and obstacles to success.* Science **270:**404.)

PROBLEMS

1. A DNA fragment isolated from an *Eco*RI digest of genomic DNA was combined with a plasmid vector linearized by *Eco*RI digestion so sticky ends could anneal. Phage T4 DNA ligase was then added to the mixture. List all possible products of the ligation reaction.

2. The nucleotide sequence of a polylinker in a particular plasmid vector is

—GAATTCCCGGGGATCCTCTAGAGTCGACCTGCAGGCATGC—

This polylinker contains restriction sites for *Bam*HI, *Eco*RI, *Pst*I, *Sal*I, *Sma*I, *Sph*I, and *Xba*I. Indicate the location of each restriction site in this sequence. (See Table 11.5 of restriction enzymes for their cleavage sites.)

3. A vector has a polylinker containing restriction sites in the following order: *Hin*dIII, *Sac*I, *Xho*I, *Bgl*II, *Xba*I, and *Cla*I.
a. Give a possible nucleotide sequence for the polylinker.
b. The vector is digested with *Hin*dIII and *Cla*I. A DNA segment contains a *Hin*dIII restriction site fragment 650 bases upstream from a *Cla*I site. This DNA fragment is digested with *Hin*dIII and *Cla*I, and the resulting *Hin*dIII–*Cla*I fragment is directionally cloned into the *Hin*dIII–*Cla*I–digested vector. Give the nucleotide sequence at each end of the vector and the insert and show that the insert can be cloned into the vector in only one orientation.

4. Yeast (*Saccharomyces cerevisiae*) has a genome size of 1.21×10^7 bp. If a genomic library of yeast DNA was constructed in a bacteriophage λ vector capable of carrying 16-kbp inserts, how many indi-

vidual clones would have to be screened to have a 99% probability of finding a particular fragment?

5. The South American lungfish has a genome size of 1.02×10^{11} bp. If a genomic library of lungfish DNA was constructed in a cosmid vector capable of carrying inserts averaging 45 kbp in size, how many individual clones would have to be screened to have a 99% probability of finding a particular DNA fragment?

6. Given the following short DNA duplex of sequence $(5' \rightarrow 3')$

ATGCCGTAGTCGATCATTACGATAGCATAGCACAGGGATCCA-CATGCACACACATGACATAGGACAGATAGCAT

what oligonucleotide primers (17-mers) would be required for PCR amplification of this duplex?

7. Figure 13.5b shows a polylinker that falls within the β-galac-tosidase coding region of the *lacZ* gene. This polylinker serves as a cloning site in a fusion protein expression vector where the closed insert is expressed as a β-galactosidase fusion protein. Assume the vector polylinker was cleaved with *Bam*HI and then

ligated with an insert whose sequence reads

GATCCATTTATCCACCGGAGAGCTGGTATCCCCAAAAGACG-GCC . . .

What is the amino acid sequence of the fusion protein? Where is the junction between β-galactosidase and the sequence encoded by the insert? (Consult the genetic code table on the inside front cover to decipher the amino acid sequence.)

8. The amino acid sequence across a region of interest in a protein is

Asn-Ser-Gly-Met-His-Pro-Gly-Lys-Leu-Ala-Ser-Trp-Phe-Val-Gly-Asn-Ser

The nucleotide sequence encoding this region begins and ends with an *Eco*RI site, making it easy to clone out the sequence and amplify it by the polymerase chain reaction (PCR). Give the nucleotide sequence of this region. Suppose you wished to change the middle Ser residue to a Cys to study the effects of this change on the protein's activity. What would be the sequence of the mutant oligonucleotide you would use for PCR amplification?

FURTHER READING

Ausubel, F. M., Brent, R., Kingston, R. E., et al., eds., 1987. *Current Protocols in Molecular Biology.* New York: John Wiley & Sons. A popular cloning manual.

Berger, S. L., and Kimmel, A. R., eds., 1987. *Guide to Molecular Cloning Techniques. Methods in Enzymology,* Volume 152. New York: Academic Press.

Bolivar, F., Rodriguez, R. L., Greene, P. J., et al., 1977. Construction and characterization of new cloning vehicles. II. A multipurpose cloning system. *Gene* **2:**95–113. A paper describing one of the early plasmid cloning systems.

Chalfie, M., et al., 1994. Green fluorescent protein as a marker for gene expression. *Science* **263:**802–805.

Chien, C.-T., et al., 1991. The two-hybrid system: A method to identify and clone genes for proteins that interact with a protein of interest. *Proceedings of the National Academy of Sciences U.S.A.* **88:**9578–9582.

Cohen, S. N., Chang, A. C. Y., Boyer, H. W., and Helling, R. B., 1973. Construction of biologically functional bacterial plasmids *in vitro. Proceedings of the National Academy of Sciences U.S.A.* **70:**3240–3244. The classic paper on the construction of chimeric plasmids.

Cortese, R., 1996. *Combinatorial Libraries: Synthesis, Screening and Application Potential.* Berlin: Walter de Gruyter.

Crystal, R. G., 1995. Transfer of genes to humans: Early lessons and obstacles to success. *Science* **270:**404–410.

Goeddel, D. V., ed., 1990. *Gene Expression Technology. Methods in Enzymology,* Volume 185. New York: Academic Press.

Grunstein, M., and Hogness, D. S., 1975. Colony hybridization: A specific method for the isolation of cloned DNAs that contain a specific gene. *Proceedings of the National Academy of Sciences U.S.A.* **72:**3961–3965. Article describing the colony hybridization technique for specific gene isolation.

Guyer, M., 1992. A comprehensive genetic linkage map for the human genome. *Science* **258:**67–86. M. Guyer is the corresponding author for the American/French NIH/CEPH (National Institutes of Health/Centre Etude du Polymorphisme Humain) Collaborative Mapping Group. This article is part of the October 2, 1992, issue of *Science* (Volume 258, Number 1), which presents an update of progress on the Human Genome Project. See also the 1995 genome issue of *Science,* Volume 270, Number 5235, October 20, 1995.

Jackson, D. A., Symons, R. H., and Berg, P., 1972. Biochemical method for inserting new genetic information into DNA of simian virus 40: Circular SV40 DNA molecules containing lambda phage genes and the galactose operon of *E. coli. Proceedings of the National Academy of Sciences U.S.A.* **69:**2904–2909.

Luckow, V. A., and Summers, M. D., 1988. Trends in the development of baculovirus expression vectors. *Biotechnology* **6:**47–55.

Lyon, J., and Gorner, P., 1995. *Altered Fates. Gene Therapy and the Retooling of Human Life.* New York: Norton.

Maniatis, T., Hardison, R. C., Lacy, E., et al., 1978. The isolation of structural genes from libraries of eucaryotic DNA. *Cell* **15:**687–701.

Morgan, R. A., and Anderson, W. F., 1993. Human gene therapy. *Annual Review of Biochemistry* **62:**191–217.

Murialdo, H., 1991. Bacteriophage lambda DNA maturation and packaging. *Annual Review of Biochemistry* **60:**125–153. Review of the biochemistry of packaging DNA into λ phage heads.

Palese, P., and Roizman, B., 1996. Genetic engineering of viruses and of virus vectors: A preface. *Proceedings of the National Academy of Sciences U.S.A.* **93:**11287–11425. A preface to a series of papers from a colloquium on genetic engineering and methods in gene therapy.

Peterson, K. R., et al., 1997. Production of transgenic mice with yeast artificial chromosomes. *Trends in Genetics* **13:**61–66.

Saiki, R. K., Gelfand, D. H., Stoeffel, B., et al., 1988. Primer-directed amplification of DNA with a thermostable DNA polymerase. *Science* **239:**487–491. Discussion of the polymerase chain reaction procedure.

Sambrook, J., Fritsch, E. F., and Maniatis, T., 1989. *Molecular Cloning,* 2nd ed. Long Island: Cold Spring Harbor Laboratory Press. (This cloning manual is familiarly referred to as "Maniatis.")

Scriver, C. R., Beaudet, A. L., Sly, W. S., and Valle, D., eds. 1995. *The Metabolic and Molecular Bases of Inherited Disease.* The seventh edition of this classic work contains contributions from over 300 authors. A three-volume treatise, it is the definitive source on the molecular basis of inherited diseases.

Southern, E. M., 1975. Detection of specific sequences among DNA fragments separated by gel electrophoresis. *Journal of Molecular Biology* **98:**503–517. The classic paper on the identification of specific DNA sequences through hybridization with unique probes.

Southern, E. M., 1996. DNA chips: Analysing sequence by hybridization to oligonucleotides on a large scale. *Trends in Genetics* **12:**110–115.

Timmer, W. C., and Villalobos, J. M., 1993. The polymerase chain reaction. *The Journal of Chemical Education* **70:**273–280.

Young, R. A., and Davis, R. W., 1983. Efficient isolation of genes using antibody probes. *Proceedings of the National Academy of Sciences U.S.A.* **80:**1194–1198. Using antibodies to screen protein expression libraries to isolate the structural gene for a specific protein.

$\mathcal{P}$art II

Protein Dynamics

Protein dynamics—the action of enzymes and molecular motors—provides the key to understanding the biochemistry of this cheetah and the grasses through which it runs. (Frank Lane/Parfitt/Tony Stone Images)

*C*hapter 14

Enzyme Kinetics

"Alice and the Queen of Hearts," illustrated by John Tenniel, *The Nursery Alice.* (Mary Evans Picture Library, London)

Living organisms seethe with metabolic activity. Thousands of chemical reactions are proceeding very rapidly at any given instant within all living cells. Virtually all of these transformations are mediated by **enzymes,** proteins (and occasionally RNA) specialized to catalyze metabolic reactions. The substances transformed in these reactions are often organic compounds that show little tendency for reaction outside the cell. An excellent example is glucose, a sugar that can be stored indefinitely on the shelf with no deterioration. Most cells quickly oxidize glucose, producing carbon dioxide and water and releasing lots of energy:

$$C_6H_{12}O_6 + 6\ O_2 \longrightarrow 6\ CO_2 + 6\ H_2O + 2870\ kJ\ of\ energy$$
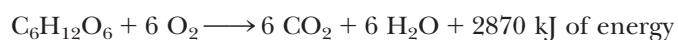
(-2870 kJ/mol is the standard free energy change [$\Delta G°'$] for the oxidation of glucose; see Chapter 3). In chemical terms, 2870 kJ is a large amount of energy, and glucose can be viewed as an energy-rich compound even though at ambi-
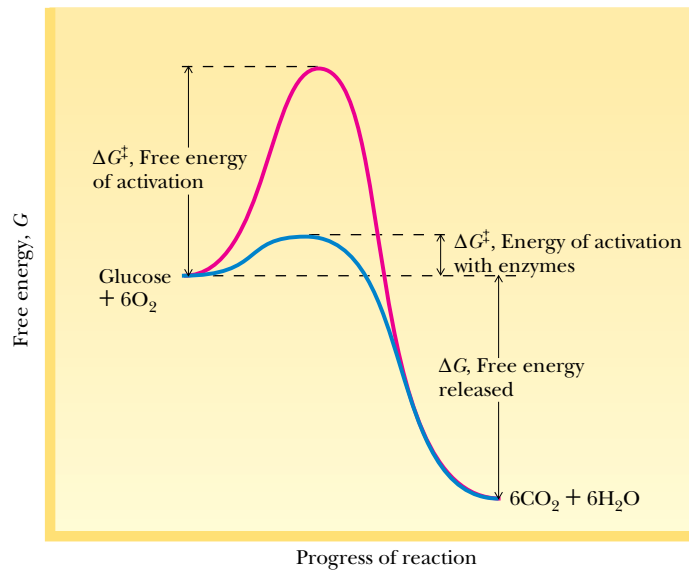
FIGURE 14.1 • Reaction profile showing large $\Delta G^{\ddagger}$ for glucose oxidation, free energy change of $-2,870$ kJ/mol; catalysts lower $\Delta G^{\ddagger}$, thereby accelerating rate.

ent temperature it is not readily reactive with oxygen outside of cells. Stated another way, glucose represents **thermodynamic potentiality:** its reaction with oxygen is strongly exergonic, but it just doesn't occur under normal conditions. On the other hand, enzymes can catalyze such thermodynamically favorable reactions so that they proceed at extraordinarily rapid rates (Figure 14.1). In glucose oxidation and countless other instances, enzymes provide cells with the ability to exert *kinetic control over thermodynamic potentiality*. That is, living systems use enzymes to accelerate and control the rates of vitally important biochemical reactions.

Enzymes Are the Agents of Metabolic Function

Acting in sequence, enzymes form metabolic pathways by which nutrient molecules are degraded, energy is released and converted into metabolically useful forms, and precursors are generated and transformed to create the literally thousands of distinctive biomolecules found in any living cell (Figure 14.2). Situated at key junctions of metabolic pathways are specialized **regulatory enzymes** capable of sensing the momentary metabolic needs of the cell and adjusting their catalytic rates accordingly. The responses of these enzymes ensure the harmonious integration of the diverse and often divergent metabolic activities of cells so that the living state is promoted and preserved.

14.1 • Enzymes—Catalytic Power, Specificity, and Regulation

Enzymes are characterized by three distinctive features: **catalytic power, specificity,** and **regulation.**

Catalytic Power

Enzymes display enormous catalytic power, accelerating reaction rates as much as 10^{16} over uncatalyzed levels, which is far greater than any synthetic catalysts can achieve, and enzymes accomplish these astounding feats in dilute aqueous
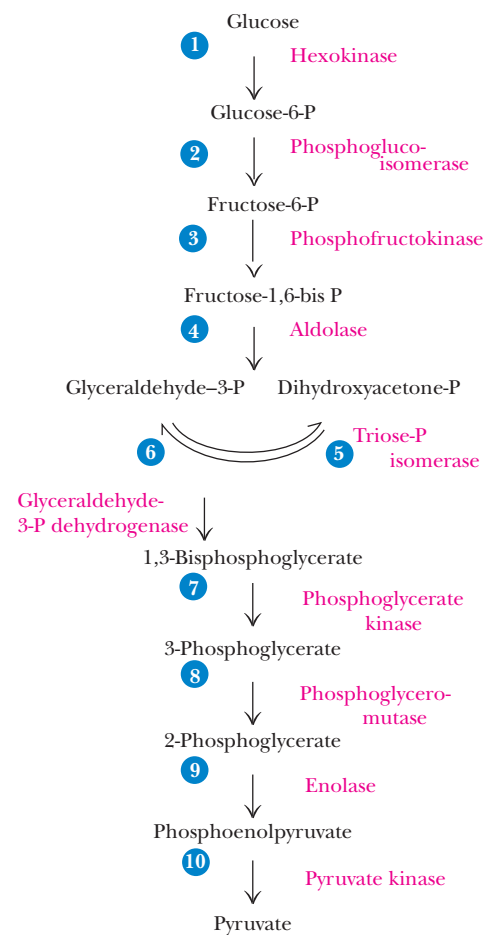
FIGURE 14.2 • The breakdown of glucose by *glycolysis* provides a prime example of a metabolic pathway. Ten enzymes mediate the reactions of glycolysis. Enzyme 4, *fructose 1,6, biphosphate aldolase,* catalyzes the C—C bond–breaking reaction in this pathway.

solutions under mild conditions of temperature and pH. For example, the enzyme jack bean *urease* catalyzes the hydrolysis of urea:

$$\underset{\displaystyle H_2N-\overset{\displaystyle \overset{O}{\|}}{C}-NH_2}{} + 2\,H_2O + H^+ \longrightarrow 2\,NH_4^+ + HCO_3^-$$
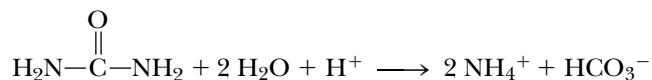
At 20°C, the rate constant for the enzyme-catalyzed reaction is 3×10^4/sec; the rate constant for the uncatalyzed hydrolysis of urea is 3×10^{-10}/sec. Thus, 10^{14} is the ratio of the catalyzed rate to the uncatalyzed rate of reaction. Such a ratio is defined as the relative **catalytic power** of an enzyme, so the catalytic power of urease is 10^{14}.

Specificity

A given enzyme is very selective, both in the substances with which it interacts and in the reaction that it catalyzes. The substances upon which an enzyme acts are traditionally called **substrates.** In an enzyme-catalyzed reaction, none of the substrate is diverted into nonproductive side-reactions, so no wasteful by-products are produced. It follows then that the products formed by a given enzyme are also very specific. This situation can be contrasted with your own experiences in the organic chemistry laboratory, where yields of 50% or even 30% are viewed as substantial accomplishments (Figure 14.3). The selective qualities of an enzyme are collectively recognized as its **specificity.** Intimate interaction between an enzyme and its substrates occurs through molecular recognition based on structural complementarity; such mutual recognition is the basis of specificity. The specific site on the enzyme where substrate binds and catalysis occurs is called the **active site.**
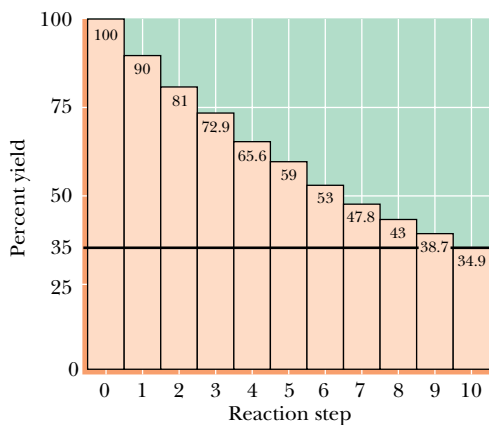
FIGURE 14.3 • A 90% yield over 10 steps, for example, in a metabolic pathway, gives an overall yield of 35%. Therefore, yields in biological reactions *must be substantially greater;* otherwise, unwanted by-products would accumulate to unacceptable levels.

Regulation

Regulation of enzyme activity is achieved in a variety of ways, ranging from controls over the amount of enzyme protein produced by the cell to more rapid, reversible interactions of the enzyme with metabolic inhibitors and activators. Chapter 15 is devoted to discussions of enzyme regulation. Because most enzymes are proteins, we can anticipate that the functional attributes of enzymes are due to the remarkable versatility found in protein structures.

Enzyme Nomenclature

Traditionally, enzymes often were named by adding the suffix *-ase* to the name of the substrate upon which they acted, as in *urease* for the urea-hydrolyzing enzyme or *phosphatase* for enzymes hydrolyzing phosphoryl groups from organic phosphate compounds. Other enzymes acquired names bearing little resemblance to their activity, such as the peroxide-decomposing enzyme *catalase* or the proteolytic enzymes (*proteases*) of the digestive tract, *trypsin* and *pepsin.* Because of the confusion that arose from these trivial designations, an International Commission on Enzymes was established in 1956 to create a systematic basis for enzyme nomenclature. Although common names for many enzymes remain in use, all enzymes now are classified and formally named according to the reaction they catalyze. Six classes of reactions are recognized (Table 14.1). Within each class are subclasses, and under each subclass are sub-subclasses within which individual enzymes are listed. Classes, subclasses, sub-subclasses, and individual entries are each numbered, so that a series of four numbers serves to specify a particular enzyme. A systematic name, descriptive

Table 14.1

Systematic Classification of Enzymes According to the Enzyme Commission

E.C. Number	Systematic Name and Subclasses
1	*Oxidoreductases* (oxidation–reduction reactions)
1.1	Acting on CH—OH group of donors
1.1.1	With NAD or NADP as acceptor
1.1.3	With O_2 as acceptor
1.2	Acting on the ⟩C=O group of donors
1.2.3	With O_2 as acceptor
1.3	Acting on the CH—CH group of donors
1.3.1	With NAD or NADP as acceptor
2	*Transferases* (transfer of functional groups)
2.1	Transferring C-1 groups
2.1.1	Methyltransferases
2.1.2	Hydroxymethyltransferases and formyltransferases
2.1.3	Carboxyltransferases and carbamoyltransferases
2.2	Transferring aldehydic or ketonic residues
2.3	Acyltransferases
2.4	Glycosyltransferases
2.6	Transferring N-containing groups
2.6.1	Aminotransferases
2.7	Transferring P-containing groups
2.7.1	With an alcohol group as acceptor
3	*Hydrolases* (hydrolysis reactions)
3.1	Cleaving ester linkage
3.1.1	Carboxylic ester hydrolases
3.1.3	Phosphoric monoester hydrolases
3.1.4	Phosphoric diester hydrolases
4	*Lyases* (addition to double bonds)
4.1	C=C lyases
4.1.1	Carboxy lyases
4.1.2	Aldehyde lyases
4.2	C=O lyases
4.2.1	Hydrolases
4.3	C=N lyases
4.3.1	Ammonia-lyases
5	*Isomerases* (isomerization reactions)
5.1	Racemases and epimerases
5.1.3	Acting on carbohydrates
5.2	Cis-trans isomerases
6	*Ligases* (formation of bonds with ATP cleavage)
6.1	Forming C—O bonds
6.1.1	Amino acid–RNA ligases
6.2	Forming C—S bonds
6.3	Forming C—N bonds
6.4	Forming C—C bonds
6.4.1	Carboxylases

of the reaction, is also assigned to each entry. To illustrate, consider the enzyme that catalyzes this reaction:

$$\text{ATP} + \text{D-glucose} \longrightarrow \text{ADP} + \text{D-glucose-6-phosphate}$$

A phosphate group is transferred from ATP to the C-6-OH group of glucose, so the enzyme is a *transferase* (Class 2, Table 14.1). Subclass 7 of transferases is

enzymes transferring phosphorus-containing groups, and sub-subclass 1 covers those *phosphotransferases with an alcohol group as an acceptor.* Entry 2 in this sub-subclass is **ATP: D-glucose-6-phosphotransferase,** and its classification number is **2.7.1.2.** In use, this number is written preceded by the letters **E.C.,** denoting the Enzyme Commission. For example, entry 1 in the same sub-subclass is E.C.2.7.1.1, ATP: D-hexose-6-phosphotransferase, an ATP-dependent enzyme that transfers a phosphate to the 6-OH of hexoses (that is, it is nonspecific regarding its hexose acceptor). These designations can be cumbersome, so in everyday usage, trivial names are employed frequently. The glucose-specific enzyme, E.C.2.7.1.2, is called *glucokinase* and the nonspecific E.C.2.7.1.1 is known as *hexokinase. Kinase* is a trivial term for enzymes that are ATP-dependent phosphotransferases.

Coenzymes

Many enzymes carry out their catalytic function relying solely on their protein structure. Many others require nonprotein components, called **cofactors** (Table 14.2). Cofactors may be metal ions or organic molecules referred to as **coenzymes.** Cofactors, because they are structurally less complex than proteins, tend to be stable to heat (incubation in a boiling water bath). Typically, proteins are denatured under such conditions. Many coenzymes are vitamins or contain vitamins as part of their structure. Usually coenzymes are actively involved in the catalytic reaction of the enzyme, often serving as intermediate carriers of functional groups in the conversion of substrates to products. In most cases, a coenzyme is firmly associated with its enzyme, perhaps even by covalent bonds, and it is difficult to

Table 14.2

Enzyme Cofactors: Some Metal Ions and Coenzymes and the Enzymes with Which They Are Associated

Metal Ions and Some Enzymes That Require Them		Coenzymes Serving as Transient Carriers of Specific Atoms or Functional Groups		Representative Enzymes Using Coenzymes
Metal Ion	Enzyme	Coenzyme	Entity Transferred	
Fe^{2+} or Fe^{3+}	Cytochrome oxidase	Thiamine pyrophosphate (TPP)	Aldehydes	Pyruvate dehydrogenase
	Catalase	Flavin adenine dinucleotide (FAD)	Hydrogen atoms	Succinate dehydrogenase
	Peroxidase	Nicotinamide adenine dinucleotide (NAD)	Hydride ion (H^-)	Alcohol dehydrogenase
Cu^{2+}	Cytochrome oxidase			
Zn^{2+}	DNA polymerase	Coenzyme A (CoA)	Acyl groups	Acetyl-CoA carboxylase
	Carbonic anhydrase	Pyridoxal phosphate (PLP)	Amino groups	Aspartate aminotransferase
	Alcohol dehydrogenase	5′-Deoxyadenosylcobalamin (vitamin B_{12})	H atoms and alkyl groups	Methylmalonyl-CoA mutase
Mg^{2+}	Hexokinase			
	Glucose-6-phosphatase	Biotin (biocytin)	CO_2	Propionyl-CoA carboxylase
Mn^{2+}	Arginase	Tetrahydrofolate (THF)	Other one-carbon groups	Thymidylate synthase
K^+	Pyruvate kinase (also requires Mg^{2+})			
Ni^{2+}	Urease			
Mo	Nitrate reductase			
Se	Glutathione peroxidase			

separate the two. Such tightly bound coenzymes are referred to as **prosthetic groups** of the enzyme. The catalytically active complex of protein and prosthetic group is called the **holoenzyme.** The protein without the prosthetic group is called the **apoenzyme;** it is catalytically inactive.

14.2 • Introduction to Enzyme Kinetics

Kinetics is the branch of science concerned with the rates of chemical reactions. The study of **enzyme kinetics** addresses the biological roles of enzymatic catalysts and how they accomplish their remarkable feats. In enzyme kinetics, we seek to determine the maximum reaction velocity that the enzyme can attain and its binding affinities for substrates and inhibitors. Coupled with studies on the structure and chemistry of the enzyme, analysis of the enzymatic rate under different reaction conditions yields insights regarding the enzyme's mechanism of catalytic action. Such information is essential to an overall understanding of metabolism.

Significantly, this information can be exploited to control and manipulate the course of metabolic events. The science of pharmacology relies on such a strategy. **Pharmaceuticals,** or **drugs,** are often special inhibitors specifically targeted at a particular enzyme in order to overcome infection or to alleviate illness. A detailed knowledge of the enzyme's kinetics is indispensable to rational drug design and successful pharmacological intervention.

Review of Chemical Kinetics

Before beginning a quantitative treatment of enzyme kinetics, it will be fruitful to review briefly some basic principles of chemical kinetics. **Chemical kinetics** is the study of the rates of chemical reactions. Consider a reaction of overall stoichiometry

$$A \longrightarrow P$$

Although we treat this reaction as a simple, one-step conversion of A to P, it more likely occurs through a sequence of elementary reactions, each of which is a simple molecular process, as in

$$A \longrightarrow I \longrightarrow J \longrightarrow P$$

where I and J represent intermediates in the reaction. Precise description of all of the elementary reactions in a process is necessary to define the overall reaction mechanism for $A \rightarrow P$.

Let us assume that $A \rightarrow P$ *is* an elementary reaction and that it is spontaneous and essentially irreversible. Irreversibility is easily assumed if the rate of P conversion to A is very slow *or* the concentration of P (expressed as [P]) is negligible under the conditions chosen. The **velocity,** v, or **rate,** of the reaction $A \rightarrow P$ is the amount of P formed or the amount of A consumed per unit time, t. That is,

$$v = \frac{d[P]}{dt} \quad \text{or} \quad v = \frac{-d[A]}{dt} \qquad (14.1)$$

The mathematical relationship between reaction rate and concentration of reactant(s) is the **rate law.** For this simple case, the rate law is

$$v = \frac{-d[A]}{dt} = k[A] \qquad (14.2)$$

From this expression, it is obvious that the rate is proportional to the concentration of A, and k is the proportionality constant, or **rate constant.** k has the units of $(time)^{-1}$, usually sec^{-1}. v is a function of [A] to the first power, or, in the terminology of kinetics, v is first-order with respect to A. For an elementary reaction, the **order** for any reactant is given by its exponent in the rate equation. The number of molecules that must simultaneously interact is defined as the **molecularity** of the reaction. Thus, the simple elementary reaction of A→P is a **first-order reaction.** Figure 14.4 portrays the course of a first-order reaction as a function of time. The rate of decay of a radioactive isotope, like ^{14}C or ^{32}P, is a first-order reaction, as is an intramolecular rearrangement, such as A→P. Both are **unimolecular reactions** (the molecularity equals 1).

Biomolecular Reactions

Consider the more complex reaction, where two molecules must react to yield products:

$$A + B \longrightarrow P + Q$$

Assuming this reaction is an elementary reaction, its molecularity is 2; that is, it is a **bimolecular reaction.** The velocity of this reaction can be determined from the rate of disappearance of either A or B, or the rate of appearance of P or Q:

$$v = \frac{-d[A]}{dt} = \frac{-d[B]}{dt} = \frac{d[P]}{dt} = \frac{d[Q]}{dt} \tag{14.3}$$

The rate law is

$$v = k[A][B] \tag{14.4}$$

The rate is proportional to the concentrations of both A and B. Because it is proportional to the product of two concentration terms, the reaction is **second-order** overall, first-order with respect to A and first-order with respect to B. (Were the elementary reaction 2A→P + Q, the rate law would be $v = k[A]^2$, second-order overall and second-order with respect to A.) Second-order rate constants have the units of $(concentration)^{-1}(time)^{-1}$, as in $M^{-1}sec^{-1}$.

Molecularities greater than two are rarely found (and greater than three, never). When the overall stoichiometry of a reaction is greater than two (for example, as in A + B + C→ or 2A + B→), the reaction almost always proceeds via uni- or bimolecular elementary steps, and the overall rate obeys a simple first- or second-order rate law.

FIGURE 14.4 • Plot of the course of a first-order reaction. The half-time, $t_{1/2}$, is the time for one-half of the starting amount of A to disappear.
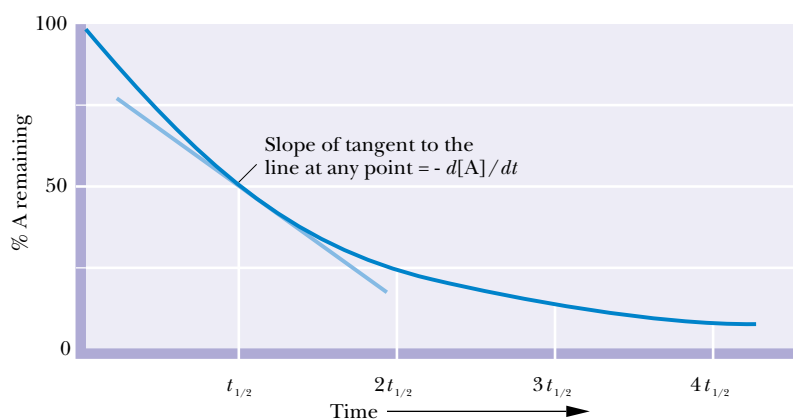
At this point, it may be useful to remind ourselves of an important caveat that is the first principle of kinetics: *Kinetics cannot prove a hypothetical mechanism.* Kinetic experiments can only rule out various alternative hypotheses because they don't fit the data. However, through thoughtful kinetic studies, a process of elimination of alternative hypotheses leads ever closer to the reality.

Free Energy of Activation and the Action of Catalysts

In a first-order chemical reaction, the conversion of A to P occurs because, at any given instant, a fraction of the A molecules has the energy necessary to achieve a reactive condition known as the **transition state.** In this state, the probability is very high that the particular rearrangement accompanying the A→P transition will occur. This transition state sits at the apex of the energy profile in the energy diagram describing the energetic relationship between A and P (Figure 14.5). The average free energy of A molecules defines the initial state and the average free energy of P molecules is the final state along the reaction coordinate. The rate of any chemical reaction is proportional to the concentration of reactant molecules (A in this case) having this transition-state energy. Obviously, the higher this energy is above the average energy, the smaller the fraction of molecules that will have this energy, and the slower the reaction will proceed. The height of this energy barrier is called the **free energy of activation, $\Delta G^{\ddagger}$.** Specifically, $\Delta G^{\ddagger}$ is the energy required to raise the average energy of one mole of reactant (at a given temperature) to the transition-state energy. The relationship between activation energy and the rate constant of the reaction, k, is given by the **Arrhenius equation:**

$$k = Ae^{-\Delta G^{\ddagger}/RT} \tag{14.5}$$
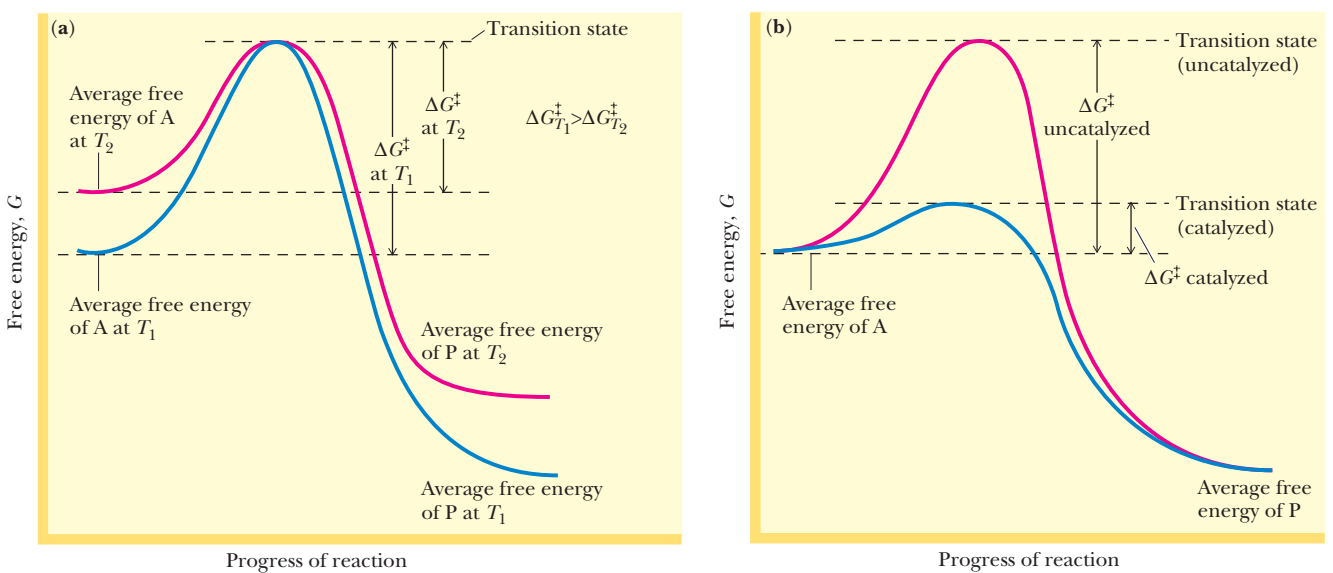
FIGURE 14.5 • Energy diagram for a chemical reaction (A→P) and the effects of (a) raising the temperature from T_1 to T_2 or (b) adding a catalyst. Raising the temperature raises the average energy of A molecules, which increases the population of A molecules having energies equal to the activation energy for the reaction, thereby increasing the reaction rate. In contrast, the average free energy of A molecules remains the same in uncatalyzed versus catalyzed reactions (conducted at the same temperature). The effect of the catalyst is to lower the free energy of activation for the reaction.

where A is a constant for a particular reaction (not to be confused with the reactant species, A, that we're discussing). Another way of writing this is $1/k = (1/A)e^{\Delta G^{\ddagger}/RT}$. That is, k is inversely proportional to $e^{\Delta G^{\ddagger}/RT}$. Therefore, if the energy of activation decreases, the reaction rate increases.

Decreasing $\Delta G^{\ddagger}$ Increases Reaction Rate

We are familiar with two general ways that rates of chemical reactions may be accelerated. First, the temperature can be raised. This will increase the average energy of reactant molecules, which in effect lowers the energy needed to reach the transition state (Figure 14.5a). The rates of many chemical reactions are doubled by a 10°C rise in temperature. Second, the rates of chemical reactions can also be accelerated by **catalysts.** Catalysts work by lowering the energy of activation rather than by raising the average energy of the reactants (Figure 14.5b). Catalysts accomplish this remarkable feat by combining transiently with the reactants in a way that promotes their entry into the reactive, transition-state condition. Two aspects of catalysts are worth noting: (a) they are regenerated after each reaction cycle (A→P), and so can be used over and over again; and (b) catalysts have *no* effect on the overall free energy change in the reaction, the free energy difference between A and P (Figure 14.5b).

14.3 • Kinetics of Enzyme-Catalyzed Reactions

Examination of the change in reaction velocity as the reactant concentration is varied is one of the primary measurements in kinetic analysis. Returning to A→P, a plot of the reaction rate as a function of the concentration of A yields a straight line whose slope is k (Figure 14.6). The more A that is available, the greater the rate of the reaction, v. Similar analyses of enzyme-catalyzed reactions involving only a single substrate yield remarkably different results (Figure 14.7). At low concentrations of the substrate S, v is proportional to [S], as expected for a first-order reaction. However, v does not increase proportionally as [S] increases, but instead begins to level off. At high [S], v becomes virtually independent of [S] and approaches a maximal limit. The value of v at this limit is written V_{max}. Because rate is no longer dependent on [S] at these high concentrations, the enzyme-catalyzed reaction is now obeying **zero-order**

FIGURE 14.6 • A plot of v versus [A] for the unimolecular chemical reaction, A→P, yields a straight line having a slope equal to k.

FIGURE 14.7 • Substrate saturation curve for an enzyme-catalyzed reaction. The amount of enzyme is constant, and the velocity of the reaction is determined at various substrate concentrations. The reaction rate, v, as a function of [S] is described by a rectangular hyperbola. At very high [S], $v = V_{max}$. That is, the velocity is limited only by conditions (temperature, pH, ionic strength) and by the amount of enzyme present; v becomes independent of [S]. Such a condition is termed *zero-order kinetics*. Under zero-order conditions, velocity is directly dependent on [enzyme]. The H_2O molecule provides a rough guide to scale. The substrate is bound at the active site of the enzyme.
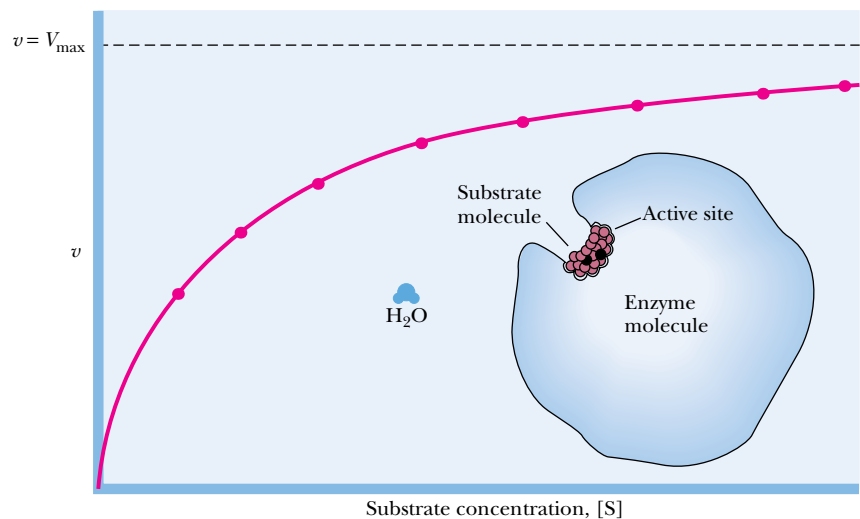
kinetics; that is, the rate is independent of the reactant (substrate) concentration. This behavior is a **saturation effect:** when v shows no increase even though [S] is increased, the system is saturated with substrate. Such plots are called **substrate saturation curves.** The physical interpretation is that every enzyme molecule in the reaction mixture has its substrate-binding site occupied by S. Indeed, such curves were the initial clue that an enzyme interacts directly with its substrate by binding it.

The Michaelis–Menten Equation

Lenore Michaelis and Maud L. Menten proposed a general theory of enzyme action in 1913 consistent with observed enzyme kinetics. Their theory was based on the assumption that the enzyme, E, and its substrate, S, associate reversibly to form an enzyme-substrate complex, ES:

$$\text{E} + \text{S} \underset{k_{-1}}{\overset{k_1}{\rightleftharpoons}} \text{ES} \qquad (14.6)$$

This association/dissociation is assumed to be a rapid equilibrium, and K_s is the *enzyme:substrate dissociation constant.* At equilibrium,

$$k_{-1}[\text{ES}] = k_1[\text{E}][\text{S}] \qquad (14.7)$$

and

$$K_S = \frac{[\text{E}][\text{S}]}{[\text{ES}]} = \frac{k_{-1}}{k_1} \qquad (14.8)$$

Product, P, is formed in a second step when ES breaks down to yield E + P.

$$\text{E} + \text{S} \underset{k_{-1}}{\overset{k_1}{\rightleftharpoons}} \text{ES} \overset{k_2}{\longrightarrow} \text{E} + \text{P} \qquad (14.9)$$

E is then free to interact with another molecule of S.

Steady-State Assumption

The interpretations of Michaelis and Menten were refined and extended in 1925 by Briggs and Haldane, by assuming the concentration of the enzyme–substrate complex ES quickly reaches a constant value in such a dynamic system. That is, ES is formed as rapidly from E + S as it disappears by its two possible fates: dissociation to regenerate E + S, and reaction to form E + P. This assumption is termed the **steady-state assumption** and is expressed as

$$\frac{d[\text{ES}]}{dt} = 0 \qquad (14.10)$$

That is, the change in concentration of ES with time, t, is 0. Figure 14.8 illustrates the time course for formation of the ES complex and establishment of the steady-state condition.

Initial Velocity Assumption

One other simplification will be advantageous. Because enzymes accelerate the rate of the reverse reaction as well as the forward reaction, it would be helpful to ignore any back reaction by which E + P might form ES. The velocity of this back reaction would be given by $v = k_{-2}[\text{E}][\text{P}]$. However, if we observe only the *initial velocity* for the reaction immediately after E and S are mixed in the absence of *P*, the rate of any back reaction is negligible because its rate will
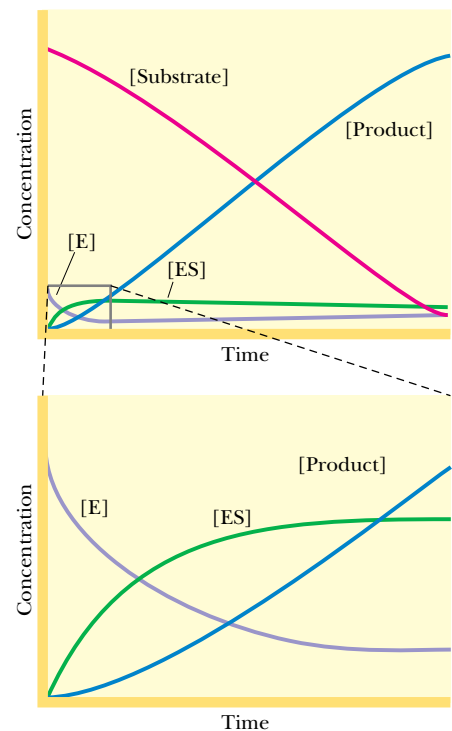
FIGURE 14.8 • Time course for the consumption of substrate, the formation of product, and the establishment of a steady-state level of the enzyme-substrate [ES] complex for a typical enzyme obeying the Michaelis–Menten, Briggs–Haldane models for enzyme kinetics. The early stage of the time course is shown in greater magnification in the bottom graph.

be proportional to [P], and [P] is essentially 0. Given such simplification, we now analyze the system described by Equation (14.9) in order to describe the initial velocity v as a function of [S] and amount of enzyme.

The total amount of enzyme is fixed and is given by the formula

$$\text{Total enzyme, } [E_T] = [E] + [ES] \tag{14.11}$$

where [E] = free enzyme and [ES] = the amount of enzyme in the enzyme–substrate complex. From Equation (14.9), the rate of [ES] formation is

$$v_f = k_1([E_T] - [ES])[S]$$

where

$$[E_T] - [ES] = [E] \tag{14.12}$$

From Equation (14.9), the rate of [ES] disappearance is

$$v_d = k_{-1}[ES] + k_2[ES] = (k_{-1} + k_2)[ES] \tag{14.13}$$

At steady state, $d[ES]/dt = 0$, and therefore, $v_f = v_d$.
So,

$$k_1([E_T] - [ES])[S] = (k_{-1} + k_2)[ES] \tag{14.14}$$

Rearranging gives

$$\frac{([E_T] - [ES])[S]}{[ES]} = \frac{(k_{-1} + k_2)}{k_1} \tag{14.15}$$

The Michaelis Constant, K_m

The ratio of constants $(k_{-1} + k_2)/k_1$ is itself a constant and is defined as the **Michaelis constant, K_m**

$$K_m = \frac{(k_{-1} + k_2)}{k_1} \tag{14.16}$$

Note from (14.15) that K_m is given by the ratio of two concentrations $(([E_T] - [ES])$ and [S]) to one ([ES]), so K_m has the units of *molarity*. From Equation (14.15), we can write

$$\frac{([E_T] - [ES])[S]}{[ES]} = K_m \tag{14.17}$$

which rearranges to

$$[ES] = \frac{[E_T][S]}{K_m + [S]} \tag{14.18}$$

Now, the most important parameter in the kinetics of any reaction is the **rate of product formation.** This rate is given by

$$v = \frac{d[P]}{dt} \tag{14.19}$$

and for this reaction

$$v = k_2[ES] \tag{14.20}$$

Substituting the expression for [ES] from Equation (14.18) into (14.20) gives

$$v = \frac{k_2[E_T][S]}{K_m + [S]} \tag{14.21}$$

The product $k_2[E_T]$ has special meaning. When [S] is high enough to saturate all of the enzyme, the velocity of the reaction, v, is maximal. At saturation, the

amount of [ES] complex is equal to the total enzyme concentration, E_T, its maximum possible value. From Equation (14.20), the initial velocity v then equals $k_2[E_T] = V_{max}$. Written symbolically, when $[S] \gg [E_T]$ (and K_m), $[E_T] = [ES]$ and $v = V_{max}$. Therefore,

$$V_{max} = k_2[E_T] \tag{14.22}$$

Substituting this relationship into the expression for v gives the **Michaelis–Menten equation**

$$v = \frac{V_{max}[S]}{K_m + [S]} \tag{14.23}$$

This equation says that the rate of an enzyme-catalyzed reaction, v, at any moment is determined by two constants, K_m and V_{max}, *and* the concentration of substrate at that moment.

When $[S] = K_m$, $v = V_{max}/2$

We can provide an operational definition for the constant K_m by rearranging Equation (14.23) to give

$$K_m = [S]\left(\frac{V_{max}}{v} - 1\right) \tag{14.24}$$

Then, at $v = V_{max}/2$, $K_m = [S]$. That is, K_m is defined by the substrate concentration that gives a velocity equal to one-half the maximal velocity. Table 14.3 gives the K_m values of some enzymes for their substrates.

Relationships Between V_{max}, K_m, and Reaction Order

The Michaelis–Menten equation (14.23) describes a curve known from analytical geometry as a *rectangular hyperbola*.[1] In such curves, as [S] is increased, v approaches the limiting value, V_{max}, in an asymptotic fashion. V_{max} can be approximated experimentally from a substrate saturation curve (Figure 14.7), and K_m can be derived from $V_{max}/2$, so the two constants of the Michaelis–Menten equation can be obtained from plots of v versus [S]. Note, however, that actual estimation of V_{max}, and consequently K_m, is only approximate from such graphs. That is, according to Equation (14.23), in order to get $v = 0.99 \ V_{max}$, [S] must equal 99 K_m, a concentration that may be difficult to achieve in practice.

From Equation (14.23), when $[S] \gg K_m$, then $v = V_{max}$. That is, v is no longer dependent on [S], so the reaction is obeying zero-order kinetics. Also, when $[S] < K_m$, then $v \approx (V_{max}/K_m)[S]$. That is, the rate, v, approximately follows a first-order rate equation, $v = k'[A]$, where $k' = V_{max}/K_m$.

K_m and V_{max}, once known explicitly, define the rate of the enzyme-catalyzed reaction, *provided:*

1. The reaction involves only one substrate, *or* if the reaction is multisubstrate, the concentration of only one substrate is varied while the concentration of all other substrates is held constant.
2. The reaction $ES \rightarrow E + P$ is irreversible, *or* the experiment is limited to observing only initial velocities where $[P] = 0$.
3. $[S]_0 > [E_T]$ and $[E_T]$ is held constant.
4. All other variables that might influence the rate of the reaction (temperature, pH, ionic strength, and so on) are constant.

---

[1] A proof that the Michaelis–Menten equation describes a rectangular hyperbola is given by Naqui, A., 1986. Where are the asymptotes of Michaelis–Menten? *Trends in Biochemical Sciences* **11:**64–65.

Table 14.3

K_m Values for Some Enzymes		
Enzyme	**Substrate**	**K_m (mM)**
Carbonic anhydrase	CO_2	12
Chymotrypsin	N-Benzoyltyrosinamide	2.5
	Acetyl-L-tryptophanamide	5
	N-Formyltyrosinamide	12
	N-Acetyltyrosinamide	32
	Glycyltyrosinamide	122
Hexokinase	Glucose	0.15
	Fructose	1.5
β-Galactosidase	Lactose	4
Glutamate dehydrogenase	NH_4^+	57
	Glutamate	0.12
	α-Ketoglutarate	2
	NAD^+	0.025
	NADH	0.018
Aspartate aminotransferase	Aspartate	0.9
	α-Ketoglutarate	0.1
	Oxaloacetate	0.04
	Glutamate	4
Threonine deaminase	Threonine	5
Arginyl-tRNA synthetase	Arginine	0.003
	tRNA^{Arg}	0.0004
	ATP	0.3
Pyruvate carboxylase	HCO_3^-	1.0
	Pyruvate	0.4
	ATP	0.06
Penicillinase	Benzylpenicillin	0.05
Lysozyme	Hexa-N-acetylglucosamine	0.006

Enzyme Units

In many situations, the actual molar amount of the enzyme is not known. However, its amount can be expressed in terms of the activity observed. The International Commission on Enzymes defines **One International Unit** of enzyme as *the amount that catalyzes the formation of one micromole of product in one minute.* (Because enzymes are very sensitive to factors such as pH, temperature, and ionic strength, the conditions of assay must be specified.) Another definition for units of enzyme activity is the **katal.** One katal is *that amount of enzyme catalyzing the conversion of one mole of substrate to product in one second.* Thus, one katal equals 6×10^7 international units.

Turnover Number

The **turnover number** of an enzyme, k_{cat}, is a measure of its maximal catalytic activity. k_{cat} is defined as the number of substrate molecules converted into product per enzyme molecule per unit time when the enzyme is saturated with substrate. The turnover number is also referred to as the **molecular activity** of the enzyme. For the simple Michaelis–Menten reaction (14.9) under conditions of initial velocity measurements, $k_2 = k_{cat}$. Provided the concentration of

enzyme, $[E_T]$, in the reaction mixture is known, k_{cat} can be determined from V_{max}. At saturating $[S]$, $v = V_{max} = k_2[E_T]$. Thus,

$$k_2 = \frac{V_{max}}{[E_T]} = k_{cat} \tag{14.25}$$

The term k_{cat} represents the kinetic efficiency of the enzyme. Table 14.4 lists turnover numbers for some representative enzymes. Catalase has the highest turnover number known; each molecule of this enzyme can degrade 40 million molecules of H_2O_2 in one second! At the other end of the scale, lysozyme requires 2 seconds to cleave a glycosidic bond in its glycan substrate.

k_{cat}/K_m

Under physiological conditions, $[S]$ is seldom saturating, and k_{cat} itself is not particularly informative. That is, the *in vivo* ratio of $[S]/K_m$ usually falls in the range of 0.01 to 1.0, so active sites often are not filled with substrate. Nevertheless, we can derive a meaningful index of the efficiency of Michaelis–Menten-type enzymes under these conditions by employing the following equations. As presented in Equation (14.23), if

$$v = \frac{V_{max}[S]}{K_m + [S]}$$

and $V_{max} = k_{cat}[E_T]$, then

$$v = \frac{k_{cat}[E_T][S]}{K_m + [S]} \tag{14.26}$$

When $[S] \ll K_m$, the concentration of free enzyme, $[E]$, is approximately equal to $[E_T]$, so that

$$v = \left(\frac{k_{cat}}{K_m}\right)[E][S] \tag{14.27}$$

That is, k_{cat}/K_m is an *apparent second-order rate constant* for the reaction of E and S to form product. Because K_m is inversely proportional to the affinity of the enzyme for its substrate and k_{cat} is directly proportional to the kinetic efficiency of the enzyme, k_{cat}/K_m provides an index of the catalytic efficiency of an enzyme operating at substrate concentrations substantially below saturation amounts.

An interesting point emerges if we restrict ourselves to the simple case where $k_{cat} = k_2$. Then

$$\frac{k_{cat}}{K_m} = \frac{k_1 k_2}{(k_{-1} + k_2)} \tag{14.28}$$

But k_1 must always be greater than or equal to $k_1 k_2/(k_{-1} + k_2)$. That is, the reaction can go no faster than the rate at which E and S come together. Thus, k_1 sets the upper limit for k_{cat}/K_m. In other words, *the catalytic efficiency of an enzyme cannot exceed the diffusion-controlled rate of combination of E and S to form ES.* In H_2O, the rate constant for such diffusion is approximately $10^9/M \cdot \sec$. Those enzymes that are most efficient in their catalysis have k_{cat}/K_m ratios approaching this value. Their catalytic velocity is limited only by the rate at which they encounter S; enzymes this efficient have achieved so-called *catalytic perfection.* All E and S encounters lead to reaction because such "catalytically perfect" enzymes can channel S to the active site, regardless of where S hits E. Table 14.5 lists the kinetic parameters of several enzymes in this category. Note that k_{cat} and K_m both show a substantial range of variation in this table, even though their ratio falls around $10^8/M \cdot \sec$.

Table 14.4

Values of k_{cat} (Turnover Number) for Some Enzymes

Enzyme	k_{cat} $(\sec^{-1})$
Catalase	40,000,000
Carbonic anhydrase	1,000,000
Acetylcholinesterase	14,000
Penicillinase	2,000
Lactate dehydrogenase	1,000
Chymotrypsin	100
DNA polymerase I	15
Lysozyme	0.5

Table 14.5

Enzymes Whose k_{cat}/K_m Approaches the Diffusion-Controlled Rate of Association with Substrate

Enzyme	Substrate	k_{cat} (sec^{-1})	K_m (M)	k_{cat}/K_m (sec^{-1} M^{-1})
Acetylcholinesterase	Acetylcholine	1.4×10^4	9×10^{-5}	1.6×10^8
Carbonic	CO_2	1×10^6	0.012	8.3×10^7
anhydrase	HCO_3^-	4×10^5	0.026	1.5×10^7
Catalase	H_2O_2	4×10^7	1.1	4×10^7
Crotonase	Crotonyl-CoA	5.7×10^3	2×10^{-5}	2.8×10^8
Fumarase	Fumarate	800	5×10^{-6}	1.6×10^8
	Malate	900	2.5×10^{-5}	3.6×10^7
Triosephosphate isomerase	Glyceraldehyde-3-phosphate*	4.3×10^3	1.8×10^{-5}	2.4×10^8
β-Lactamase	Benzylpenicillin	2×10^3	2×10^{-5}	1×10^8

*K_m for glyceraldehyde-3-phosphate is calculated on the basis that only 3.8% of the substrate in solution is unhydrated and therefore reactive with the enzyme.

Adapted from Fersht, A. 1985. *Enzyme Structure and Mechanism,* 2nd ed. New York: W.H. Freeman & Co.

Linear Plots Can Be Derived from the Michaelis–Menten Equation

Because of the hyperbolic shape of v versus [S] plots, V_{max} can only be determined from an extrapolation of the asymptotic approach of v to some limiting value as [S] increases indefinitely (Figure 14.7); and K_m is derived from that value of [S] giving $v = V_{max}/2$. However, several rearrangements of the Michaelis–Menten equation transform it into a straight-line equation. The best known of these is the **Lineweaver–Burk double-reciprocal plot:**

Taking the reciprocal of both sides of the Michaelis–Menten equation, Equation (14.23), yields the equality

$$\frac{1}{v} = \left(\frac{K_m}{V_{max}}\right)\left(\frac{1}{[S]}\right) + \frac{1}{V_{max}} \tag{14.29}$$

This conforms to $y = mx + b$ (the equation for a straight line), where $y = 1/v$; m, the slope, is K_m/V_{max}; $x = 1/[S]$; and $b = 1/V_{max}$. Plotting $1/v$ versus $1/[S]$ gives a straight line whose x-intercept is $-1/K_m$, whose y-intercept is $1/V_{max}$, and whose slope is K_m/V_{max} (Figure 14.9).

The **Hanes–Woolf plot** is another rearrangement of the Michaelis–Menten equation that yields a straight line:

Multiplying both sides of Equation (14.29) by [S] gives

$$\frac{[S]}{v} = [S]\left(\frac{K_m}{V_{max}}\right)\left(\frac{1}{[S]}\right) + \frac{[S]}{V_{max}} = \frac{K_m}{V_{max}} + \frac{[S]}{V_{max}} \tag{14.30}$$

and

$$\frac{[S]}{v} = \left(\frac{1}{V_{max}}\right)[S] + \frac{K_m}{V_{max}} \tag{14.31}$$

Graphing $[S]/v$ versus [S] yields a straight line where the slope is $1/V_{max}$, the

An Example of the Effect of Amino Acid Substitutions on K_m and k_{cat}: Wild-Type and Mutant Forms of Human Sulfite Oxidase

Mammalian sulfite oxidase is the last enzyme in the pathway for degradation of sulfur-containing amino acids. Sulfite oxidase (SO) catalyzes the oxidation of sulfite (SO_3^{2-}) to sulfate (SO_4^{2-}), using the heme-containing protein, cytochrome *c*, as electron acceptor:

$$SO_3^{2-} + 2 \text{ cytochrome } c_{oxidized} + H_2O \rightleftharpoons$$
$$SO_4^{2-} + 2 \text{ cytochrome } c_{reduced} + 2 \text{ H}^+$$
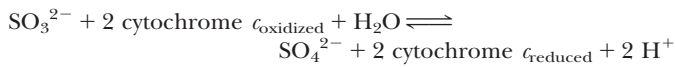
Isolated sulfite oxidase deficiency is a rare and often fatal genetic disorder in humans. The disease is characterized by severe neurological abnormalities, revealed as convulsions shortly after birth. R. M. Garrett and K. V. Rajagopalan at Duke University Medical Center have isolated the human cDNA for sulfite oxidase from the cells of normal (*wild-type*) and SO-deficient individuals. Expression of these SO cDNAs in transformed *Escherichia coli* cells allowed the isolation and kinetic analysis of wild-type and mutant forms of SO, including one (designated R160Q) in which the Arg at position 160 in the polypeptide chain is replaced by Gln. A genetically engineered version of SO (designated R160K) in which Lys replaces Arg[160] was also studied.

Kinetic Constants for Wild-Type and Mutant Sulfite Oxidase

Enzyme	$K_m^{sulfite}$ (μM)	$k_{cat}(sec^{-1})$	k_{cat}/K_m ($10^6\ M^{-1}sec^{-1}$)
Wild-type	17	18	1.1
R160Q	1900	3	0.0016
R160K	360	5.5	0.015

Replacing R[160] in sulfite oxidase by Q increases K_m, decreases k_{cat}, and markedly diminishes the catalytic efficiency (k_{cat}/K_m) of the enzyme. The R160K mutant enzyme has properties intermediate between wild-type and the R160Q mutant form. The substrate, SO_3^{2-}, is strongly anionic, and R[160] is one of several Arg residues situated within the SO substrate-binding site. Positively charged side chains in the substrate-binding site facilitate SO_3^{2-} binding and catalysis, with Arg being optimal in this role.

---

y-intercept is K_m/V_{max}, and the *x*-intercept is $-K_m$, as shown in Figure 14.10. The common advantage of these plots is that they allow both K_m and V_{max} to be accurately estimated by extrapolation of straight lines rather than asymptotes. Computer fitting of *v* versus [S] data to the Michaelis–Menten equation is more commonly done than graphical plotting.

$$\frac{1}{v} = \frac{K_m}{V_{max}}\left(\frac{1}{[S]}\right) + \frac{1}{V_{max}}$$
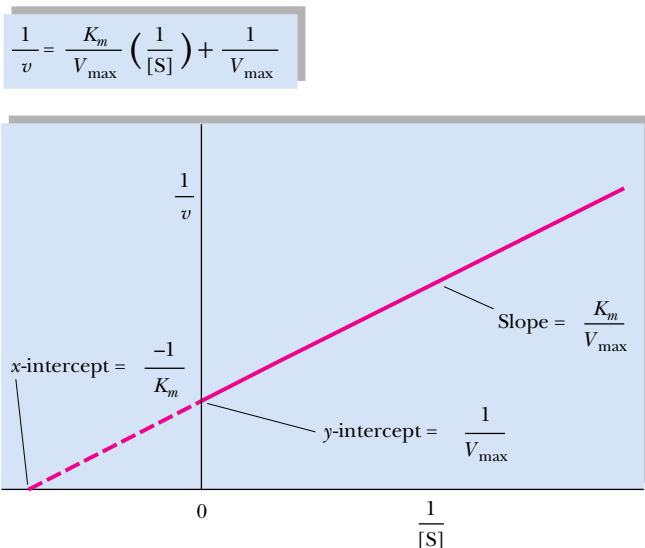
FIGURE 14.9 • The Lineweaver–Burk double-reciprocal plot, depicting extrapolations that allow the determination of the *x*- and *y*-intercepts and slope.

$$\frac{[S]}{v} = \left(\frac{1}{V_{max}}\right)[S] + \frac{K_m}{V_{max}}$$
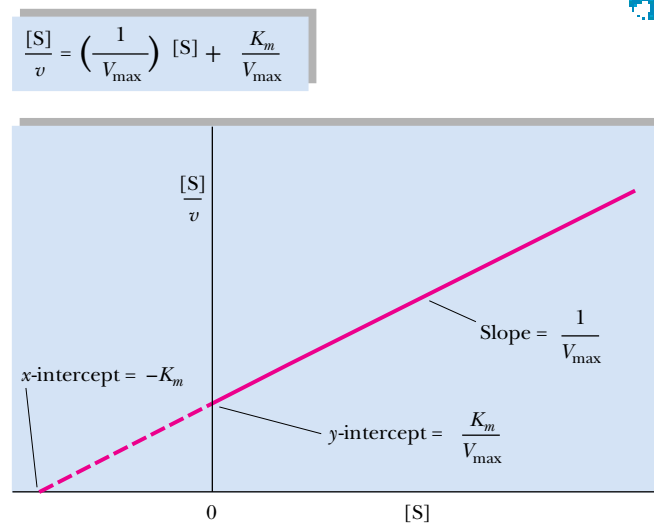
FIGURE 14.10 • A Hanes–Wolff plot of [S]/*v* versus [S], another straight-line rearrangement of the Michaelis–Menten equation.

Departures from Linearity: A Hint of Regulation?

If the kinetics of the reaction disobey the Michaelis–Menten equation, the violation is revealed by a departure from linearity in these straight-line graphs. We shall see in the next chapter that such deviations from linearity are characteristic of the kinetics of regulatory enzymes known as **allosteric enzymes.** Such regulatory enzymes are very important in the overall control of metabolic pathways.

Effect of pH on Enzymatic Activity

Enzyme-substrate recognition and the catalytic events that ensue are greatly dependent on pH. An enzyme possesses an array of ionizable side chains and prosthetic groups that not only determine its secondary and tertiary structure but may also be intimately involved in its active site. Further, the substrate itself often has ionizing groups, and one or another of the ionic forms may preferentially interact with the enzyme. Enzymes in general are active only over a limited pH range and most have a particular pH at which their catalytic activity is optimal. These effects of pH may be due to effects on K_m or V_{max} or both. Figure 14.11 illustrates the relative activity of four enzymes as a function of pH. Although the pH optimum of an enzyme often reflects the pH of its normal environment, the optimum may not be precisely the same. This difference suggests that the pH-activity response of an enzyme may be a factor in the intracellular regulation of its activity.

Effect of Temperature on Enzymatic Activity

Like most chemical reactions, the rates of enzyme-catalyzed reactions generally increase with increasing temperature. However, at temperatures above 50° to 60°C, enzymes typically show a decline in activity (Figure 14.12). Two effects are operating here: (a) the characteristic increase in reaction rate with temperature, and (b) thermal denaturation of protein structure at higher tem-
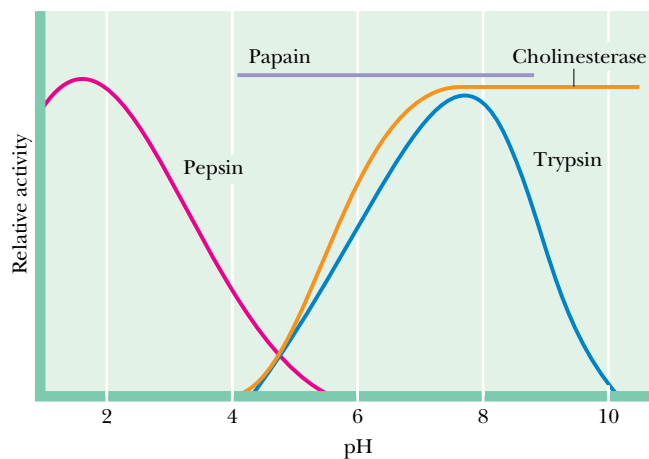
Optimum pH of Some Enzymes	
Enzyme	Optimum pH
Pepsin	1.5
Catalase	7.6
Trypsin	7.7
Fumarase	7.8
Ribonuclease	7.8
Arginase	9.7

FIGURE 14.11 • The pH activity profiles of four different enzymes. *Trypsin,* an intestinal protease, has a slightly alkaline pH optimum, whereas *pepsin,* a gastric protease, acts in the acidic confines of the stomach and has a pH optimum near 2. *Papain,* a protease found in papaya, is relatively insensitive to pHs between 4 and 8. *Cholinesterase* activity is pH-sensitive below pH 7 but not between pH 7 and 10. The cholinesterase pH activity profile suggests that an ionizable group with a pK' near 6 is essential to its activity. Might it be a histidine residue within the active site?

peratures. Most enzymatic reactions double in rate for every 10°C rise in temperature (that is, $Q_{10} = 2$, where Q_{10} is defined as *the ratio of activities at two temperatures 10° apart*) as long as the enzyme is stable and fully active. Some enzymes, those catalyzing reactions having very high activation energies, show proportionally greater Q_{10} values. The increasing rate with increasing temperature is ultimately offset by the instability of higher orders of protein structure at elevated temperatures, where the enzyme is inactivated. Not all enzymes are quite so thermally labile. For example, the enzymes of thermophilic bacteria (*thermophilic* = "heat-loving") found in geothermal springs retain full activity at temperatures in excess of 85°C.

14.4 • Enzyme Inhibition

If the velocity of an enzymatic reaction is decreased or **inhibited,** the kinetics of the reaction obviously have been perturbed. Systematic perturbations are a basic tool of experimental scientists; much can be learned about the normal workings of any system by inducing changes in it and then observing the effects of the change. The study of enzyme inhibition has contributed significantly to our understanding of enzymes.

Reversible Versus Irreversible Inhibition

Enzyme inhibitors are classified in several ways. The inhibitor may interact either reversibly or irreversibly with the enzyme. **Reversible inhibitors** interact with the enzyme through noncovalent association/dissociation reactions. In contrast, **irreversible inhibitors** usually cause stable, covalent alterations in the enzyme. That is, the consequence of irreversible inhibition is a decrease in the concentration of active enzyme. The kinetics observed are consistent with this interpretation, as we shall see later.

Reversible Inhibition

Reversible inhibitors fall into two major categories: competitive and noncompetitive (although other more unusual and rare categories are known). **Competitive inhibitors** are characterized by the fact that the substrate and inhibitor compete for the same binding site on the enzyme, the so-called **active site** or **S-binding site.** Thus, increasing the concentration of S favors the likelihood of S binding to the enzyme instead of the inhibitor, I. That is, high [S] can overcome the effects of I. The other major type, noncompetitive inhibition, cannot be overcome by increasing [S]. The two types can be distinguished by the particular patterns obtained when the kinetic data are analyzed in linear plots, such as double-reciprocal (Lineweaver–Burk) plots. A general formulation for common inhibitor interactions in our simple enzyme kinetic model would include

$$\text{E} + \text{I} \rightleftharpoons \text{EI} \quad \text{and/or} \quad \text{I} + \text{ES} \rightleftharpoons \text{IES} \qquad (14.32)$$

That is, we consider here reversible combinations of the inhibitor with E and/or ES.

Competitive Inhibition

Consider the following system

$$\text{E} + \text{S} \underset{k_{-1}}{\overset{k_1}{\rightleftharpoons}} \text{ES} \overset{k_2}{\longrightarrow} \text{E} + \text{P} \qquad \text{E} + \text{I} \underset{k_{-3}}{\overset{k_3}{\rightleftharpoons}} \text{EI} \qquad (14.33)$$
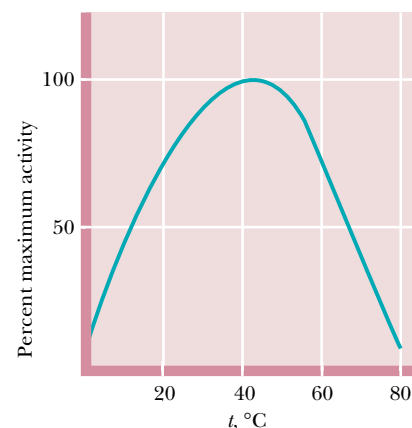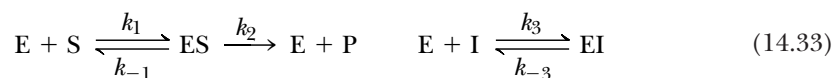
FIGURE 14.12 • The effect of temperature on enzyme activity. The relative activity of an enzymatic reaction as a function of temperature. The decrease in the activity above 50°C is due to thermal denaturation.

Table 14.6

The Effect of Various Types of Inhibitors on the Michaelis–Menten Rate Equation and on Apparent K_m and Apparent V_{max}

Inhibition Type	Rate Equation	Apparent K_m	Apparent V_{max}
None	$v = V_{max}[S]/(K_m + [S])$	K_m	V_{max}
Competitive	$v = V_{max}[S]/([S] + K_m(1 + [I]/K_I))$	$K_m(1 + [I]/K_I)$	V_{max}
Noncompetitive	$v = (V_{max}[S]/(1 + [I]/K_I))/(K_m + [S])$	K_m	$V_{max}/(1 + [I]/K_I)$
Mixed	$v = V_{max}[S]/((1 + [I]/K_I)K_m + (1 + [I]/K_I'[S]))$	$K_m(1 + [I]/K_I)/(1 + [I]/K_I')$	$V_{max}/(1 + [I]/K_I')$

K_I is defined as the enzyme:inhibitor dissociation constant $K_I = [E][I]/[EI]$; K_I' is defined as the enzyme substrate complex:inhibitor dissociation constant $K_I' = [ES][I]/[ESI]$

where an inhibitor, I, binds *reversibly* to the enzyme at the same site as S. S-binding and I-binding are mutually exclusive, *competitive* processes. Formation of the ternary complex, EIS, where both S and I are bound, is physically impossible. This condition leads us to anticipate that S and I must share a high degree of structural similarity because they bind at the same site on the enzyme. Also notice that, in our model, EI does not react to give rise to E + P. That is, I is not changed by interaction with E. The rate of the product-forming reaction is $v = k_2[ES]$.

It is revealing to compare the equation for the uninhibited case, Equation (14.23) (the Michaelis–Menten equation) with Equation (14.43) for the rate of the enzymatic reaction in the presence of a fixed concentration of the competitive inhibitor, [I]

$$v = \frac{V_{max}[S]}{[S] + K_m}$$

$$v = \frac{V_{max}[S]}{[S] + K_m\left(1 + \dfrac{[I]}{K_I}\right)}$$

(see also Table 14.6). The K_m term in the denominator in the inhibited case is increased by the factor $(1 + [I]/K_I)$; thus, v is less in the presence of the inhibitor, as expected. Clearly, in the absence of I, the two equations are identical. Figure 14.13 shows a Lineweaver–Burk plot of competitive inhibition.

FIGURE 14.13 • Lineweaver–Burk plot of competitive inhibition, showing lines for no I, [I], and 2[I]. Note that when [S] is infinitely large $(1/[S] = 0)$, V_{max} is the same, whether I is present or not. In the presence of I, the negative x-intercept $= -1/K_m(1 + [I]/K_I)$.
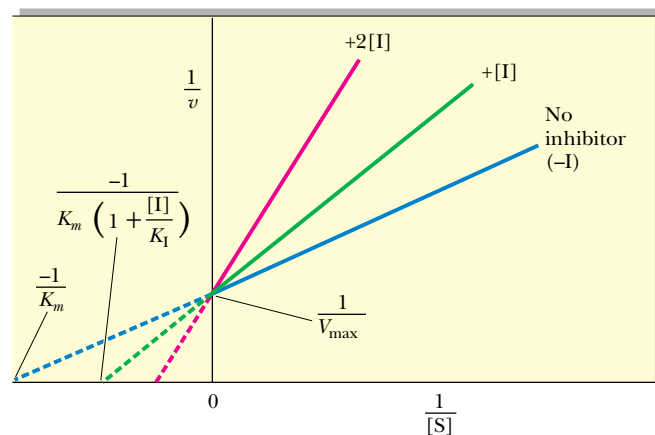
𝒜 D E E P E R L O O K

The Equations of Competitive Inhibition

Given the relationships between E, S, and I described previously and recalling the steady-state assumption that $d[ES]/dt = 0$, from Equations (14.14) and (14.16) we can write

$$[ES] = \frac{k_1[E][S]}{(k_2 + k_{-1})} = \frac{[E][S]}{K_m} \tag{14.34}$$

Assuming that $E + I \rightleftharpoons EI$ reaches rapid equilibrium, the rate of EI formation, $v_f' = k_3[E][I]$, and the rate of disappearance of EI, $v_d' = k_{-3}[EI]$, are equal. So,

$$k_3[E][I] = k_{-3}[EI] \tag{14.35}$$

Therefore,

$$[EI] = \left(\frac{k_3}{k_{-3}}\right)[E][I] \tag{14.36}$$

If we define K_I as k_{-3}/k_3, an *enzyme-inhibitor dissociation constant,* then

$$[EI] = \frac{[E][I]}{K_I} \tag{14.37}$$

knowing $[E_T] = [E] + [ES] + [EI]$. Then

$$[E_T] = [E] + \frac{[E][S]}{K_m} + \frac{[E][I]}{K_I} \tag{14.38}$$

Solving for [E] gives

$$[E] = \frac{K_I K_m [E_T]}{(K_I K_m + K_I[S] + K_m[I])} \tag{14.39}$$

Because the rate of product formation is given by $v = k_2[ES]$, from Equation (14.34) we have

$$v = \frac{k_2[E][S]}{K_m} \tag{14.40}$$

So,

$$v = \frac{(k_2 K_I[E_T][S])}{(K_I K_m + K_I[S] + K_m[I])} \tag{14.41}$$

Because $V_{max} = k_2[E_T]$,

$$v = \frac{V_{max}[S]}{K_m + [S] + \frac{K_m[I]}{K_I}} \tag{14.42}$$

or

$$v = \frac{V_{max}[S]}{[S] + K_m\left(1 + \frac{[I]}{K_I}\right)} \tag{14.43}$$

Several features of competitive inhibition are evident. First, at a given [I], v decreases ($1/v$ increases). When [S] becomes infinite, $v = V_{max}$ and is unaffected by I because all of the enzyme is in the ES form. Note that the value of the $-x$-intercept decreases as [I] increases. This $-x$-intercept is often termed the *apparent* K_m (or K_{mapp}) because it is the K_m apparent under these conditions. The diagnostic criterion for competitive inhibition is that V_{max} is unaffected by I; that is, all lines share a common y-intercept. This criterion is also the best experimental indication of binding at the same site by two substances. Competitive inhibitors resemble S structurally.

Succinate Dehydrogenase—A Classic Example of Competitive Inhibition

The enzyme *succinate dehydrogenase (SDH)* is competitively inhibited by malonate. Figure 14.14 shows the structures of succinate and malonate. The structural similarity between them is obvious and is the basis of malonate's ability to mimic succinate and bind at the active site of SDH. However, unlike succinate, which is oxidized by SDH to form fumarate, malonate cannot lose two hydrogens; consequently, it is unreactive.

Noncompetitive Inhibition

Noncompetitive inhibitors interact with both E and ES (or with S and ES, but this is a rare and specialized case). Obviously, then, the inhibitor is not binding to the same site as S, and the inhibition cannot be overcome by raising [S]. There are two types of noncompetitive inhibition: pure and mixed.

FIGURE 14.14 • Structures of succinate, the substrate of succinate dehydrogenase (SDH), and malonate, the competitive inhibitor. Fumarate (the product of SDH action on succinate) is also shown.
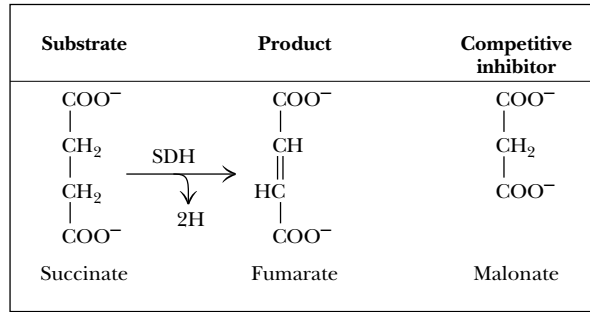
Pure Noncompetitive Inhibition

In this situation, the binding of I by E has no effect on the binding of S by E. That is, S and I bind at different sites on E, and binding of I does not affect binding of S. Consider the system

$$E + I \underset{}{\overset{K_I}{\rightleftharpoons}} EI \qquad ES + I \underset{}{\overset{K_I'}{\rightleftharpoons}} IES \qquad (14.44)$$
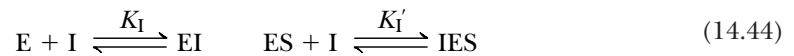
Pure noncompetitive inhibition occurs if $K_I = K_I'$. This situation is relatively uncommon; the Lineweaver–Burk plot for such an instance is given in Figure 14.15. Note that K_m is unchanged by I (the *x*-intercept remains the same, with or without I). Note also that V_{max} decreases. A similar pattern is seen if the amount of enzyme in the experiment is decreased. Thus, it is as if I lowered [E].

Mixed Noncompetitive Inhibition

In this situation, the binding of I by E influences the binding of S by E. Either the binding sites for I and S are near one another or conformational changes in E caused by I affect S binding. In this case, K_I and K_I', as defined previously, are not equal. Both K_m and V_{max} are altered by the presence of I, and K_m/V_{max} is not constant (Figure 14.16). This inhibitory pattern is commonly encountered. A reasonable explanation is that the inhibitor is binding at a site distinct from the active site, yet is influencing the binding of S at the active site.

FIGURE 14.15 • Lineweaver–Burk plot of pure noncompetitive inhibition. Note that I does not alter K_m but that it decreases V_{max}. In the presence of I, the *y*-intercept is equal to $(1/V_{max})(1 + I/K_I)$.

(a) $K_I < K_I'$

(b) $K_I' < K_I$
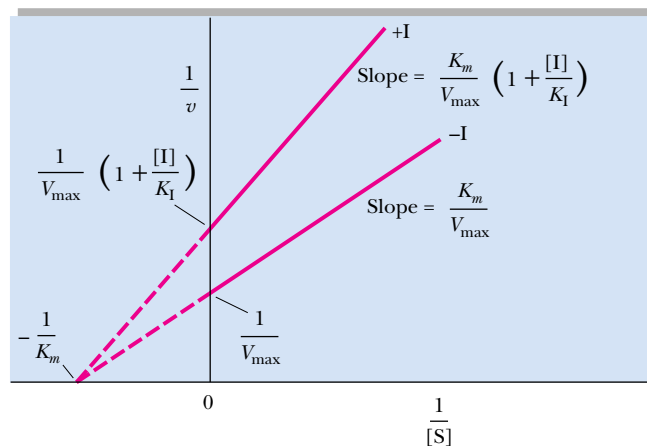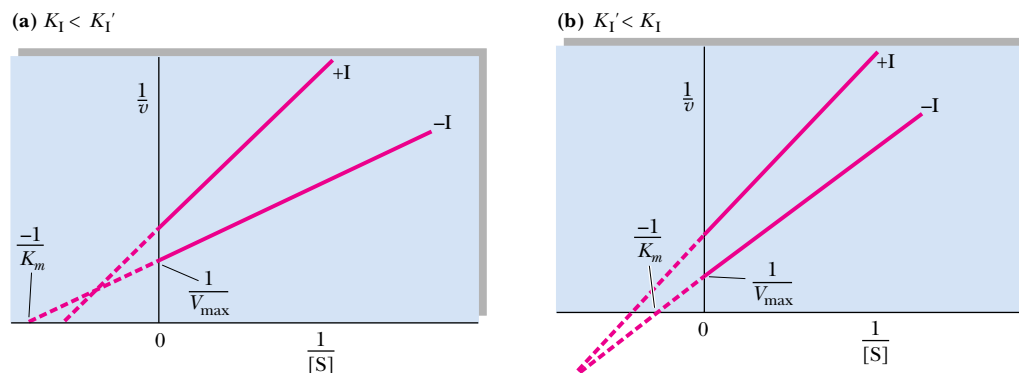
FIGURE 14.16 • Lineweaver–Burk plot of mixed noncompetitive inhibition. Note that both intercepts and the slope change in the presence of I. (a) When K_I is less than K_I'; (b) when K_I is greater than K_I'.

Presumably, these effects are transmitted via alterations in the protein's conformation. Table 14.6 includes the rate equations and apparent K_m and V_{max} values for both types of noncompetitive inhibition.

Irreversible Inhibition

If the inhibitor combines irreversibly with the enzyme—for example, by covalent attachment—the kinetic pattern seen is like that of noncompetitive inhibition, because the net effect is a loss of active enzyme. Usually, this type of inhibition can be distinguished from the noncompetitive, reversible inhibition case since the reaction of I with E (and/or ES) is not instantaneous. Instead, there is a *time-dependent decrease in enzymatic activity* as $E + I \rightarrow EI$ proceeds, and the rate of this inactivation can be followed. Also, unlike reversible inhibitions, dilution or dialysis of the enzyme:inhibitor solution does not dissociate the EI complex and restore enzyme activity.

Suicide Substrates—Mechanism-Based Enzyme Inactivators

Suicide substrates are inhibitory substrate analogs designed so that, via normal catalytic action of the enzyme, a very reactive group is generated. This reactive group then forms a covalent bond with a nearby functional group within the active site of the enzyme, thereby causing irreversible inhibition. Suicide substrates, also called *Trojan horse substrates,* are a type of **affinity label.** As substrate analogs, they bind with specificity and high affinity to the enzyme active site; in their reactive form, they become covalently bound to the enzyme. This covalent link effectively labels a particular functional group within the active site, identifying the group as a key player in the enzyme's catalytic cycle.

Penicillin—A Suicide Substrate

Several drugs in current medical use are mechanism-based enzyme inactivators. For example, the antibiotic **penicillin** exerts its effects by covalently reacting with an essential serine residue in the active site of *glycoprotein peptidase,* an enzyme that acts to cross-link the peptidoglycan chains during synthesis of bacterial cell walls (Figure 14.17). Once cell wall synthesis is blocked, the bacterial cells are very susceptible to rupture by osmotic lysis, and bacterial growth is halted.
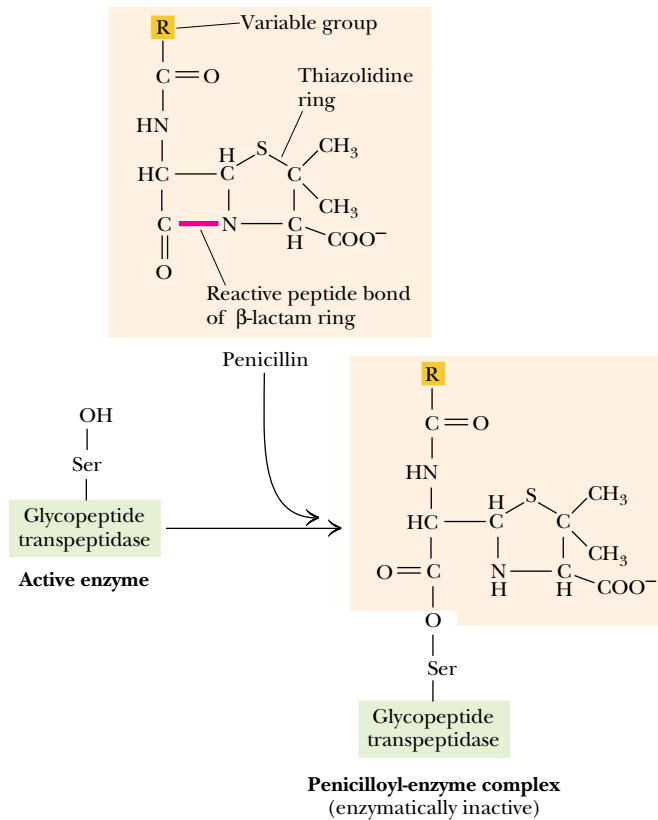
FIGURE 14.17 • Penicillin is an irreversible inhibitor of the enzyme *glycoprotein peptidase,* which catalyzes an essential step in bacterial cell wall synthesis. Penicillin consists of a thiazolidine ring fused to a β-lactam ring to which a variable group R is attached. A reactive peptide bond in the β-lactam ring covalently attaches to a serine residue in the active site of the glycopeptide transpeptidase. (The conformation of penicillin around its reactive peptide bond resembles the transition state of the normal glycoprotein peptidase substrate.) The penicilloyl–enzyme complex is catalytically inactive. The bond between the enzyme and penicillin is indefinitely stable; that is, penicillin binding is irreversible.

14.5 • Kinetics of Enzyme-Catalyzed Reactions Involving Two or More Substrates

Thus far, we have considered only the simple case of enzymes that act upon a single substrate, S. This situation is not common. Usually, enzymes catalyze reactions in which two (or even more) substrates take part.

Consider the case of an enzyme catalyzing a reaction involving two substrates, A and B, and yielding the products P and Q:

$$A + B \xrightarrow{\text{enzyme}} P + Q \qquad (14.45)$$

Such a reaction is termed a **bisubstrate reaction.** In general, bisubstrate reactions proceed by one of two possible routes:

1. Both A and B are bound to the enzyme and then reaction occurs to give P + Q:

$$E + A + B \longrightarrow AEB \longrightarrow PEQ \longrightarrow E + P + Q \qquad (14.46)$$
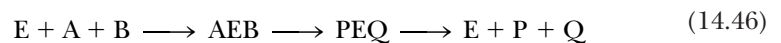
Reactions of this type are defined as **sequential** or **single-displacement reactions.** They can be either of two distinct classes:

a. **random,** where either A or B may bind to the enzyme first, followed by the other substrate, or

b. **ordered,** where A, designated the *leading substrate,* must bind to E first before B can be bound.

Both classes of single-displacement reactions are characterized by lines that intersect to the left of the $1/v$ axis in Lineweaver–Burk double-reciprocal plots (Figure 14.18).

2. The other general possibility is that one substrate, A, binds to the enzyme and reacts with it to yield a chemically modified form of the enzyme (E′) plus the product, P. The second substrate, B, then reacts with E′, regenerating E and forming the other product, Q.

$$E + A \longrightarrow EA \longrightarrow E'P \longrightarrow E' \longrightarrow E'B \longrightarrow EQ \longrightarrow E + Q$$
$$\searrow \qquad \nearrow$$
$$P \qquad B$$

$$(14.47)$$
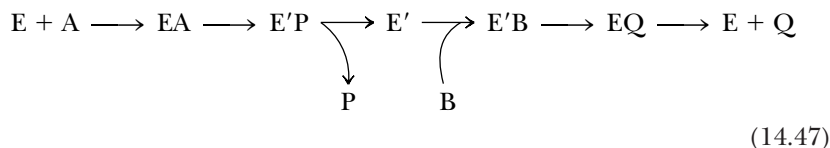
Reactions that fit this model are called **ping-pong** or **double-displacement reactions.** Two distinctive features of this mechanism are the obligatory formation of a modified enzyme intermediate, E′, and the pattern of parallel lines obtained in double-reciprocal plots (Figure 14.19).

Random, Single-Displacement Reactions

In this type of sequential reaction, all possible binary enzyme : substrate complexes (AE, EB, QE, EP) are formed rapidly and reversibly when the enzyme is added to a reaction mixture containing A, B, P, and Q:

$$A + E \rightleftharpoons AE \qquad\qquad QE \rightleftharpoons Q + E$$
$$\searrow \qquad\qquad \nearrow$$
$$AEB \rightleftharpoons QEP \qquad (14.48)$$
$$\nearrow \qquad\qquad \searrow$$
$$E + B \rightleftharpoons EB \qquad\qquad EP \rightleftharpoons E + P$$
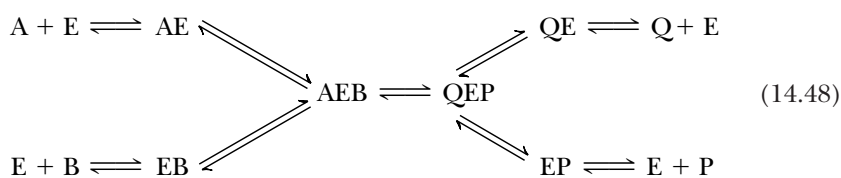
The rate-limiting step is the reaction AEB→QEP. It doesn't matter whether A or B binds first to E, or whether Q or P is released first from QEP. Sometimes,

Double-reciprocal form of the rate equation:
$$\frac{1}{v} = \frac{1}{V_{max}}\left(K_m^A + \frac{K_S^A\,K_m^B}{[B]}\right)\left(\frac{1}{[A]} + \frac{1}{V_{max}}\left(1 + \frac{K_m^B}{[B]}\right)\right)$$

Slopes are given by
$$\frac{1}{V_{max}}\left(K_m^A + \frac{K_S^A\,K_m^B}{[B]}\right)$$

$$\frac{1}{V_{max}}\left(1 - \frac{K_m^A}{K_S^A}\right)$$

$$-\frac{1}{K_S^A} \qquad 0 \qquad \frac{1}{[A]}$$
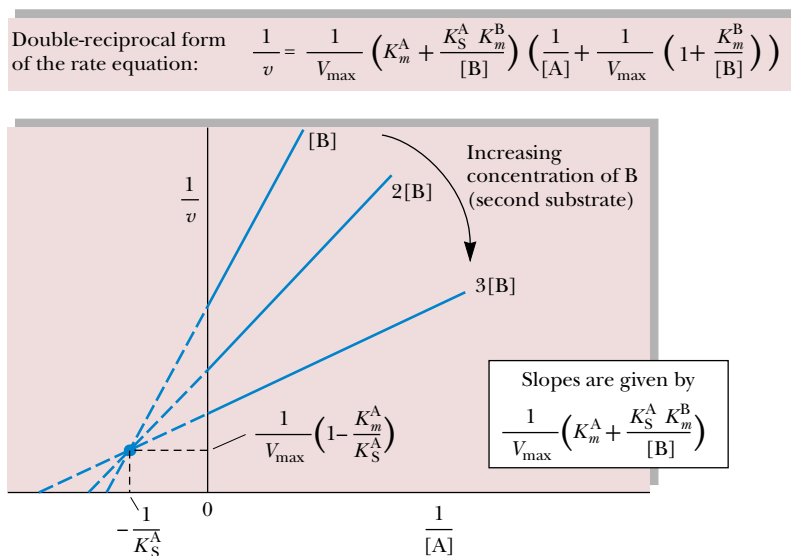
FIGURE 14.18 • Single-displacement bisubstrate mechanism. Double-reciprocal plots of the rates observed with different fixed concentrations of one substrate (B here) are graphed versus a series of concentrations of A. Note that, in these Lineweaver–Burk plots for single-displacement bisubstrate mechanisms, the lines intersect to the left of the $1/v$ axis.

Double-reciprocal form of the rate equation:

$$\frac{1}{v} = \frac{K_m^A}{V_{max}} \left(\frac{1}{[A]}\right) + \left(1 + \frac{K_m^B}{[B]}\right) \left(\frac{1}{V_{max}}\right)$$
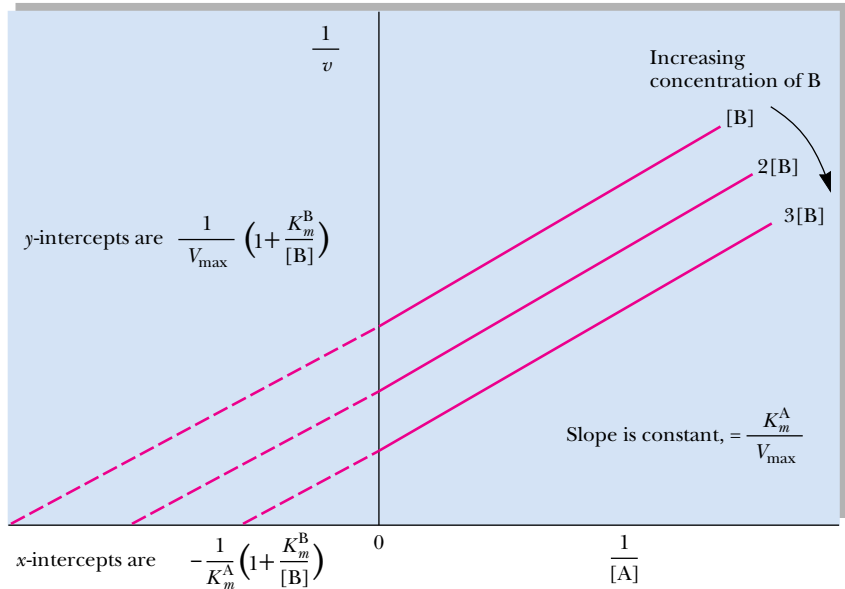
FIGURE 14.19 • Double-displacement (ping-pong) bisubstrate mechanisms are characterized by Lineweaver–Burk plots of parallel lines when double-reciprocal plots of the rates observed with different fixed concentrations of the second substrate, B, are graphed versus a series of concentrations of A.

reactions that follow this random order of addition of substrates to E can be distinguished mechanistically from reactions obeying an ordered, single-displacement mechanism, *if* A has *no* influence on the binding constant for B (and vice versa); that is, the mechanism is purely random. Then, the lines in a Lineweaver–Burk plot intersect at the $1/[A]$ axis (Figure 14.20).

Creatine Kinase Acts by a Random, Single-Displacement Mechanism

An example of a random, single-displacement mechanism is seen in the enzyme *creatine kinase,* a phosphoryl-transfer enzyme that uses ATP as a phosphoryl
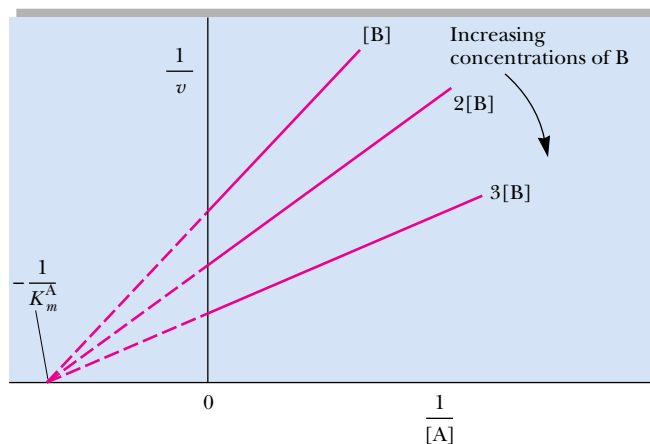
FIGURE 14.20 • Random, single-displacement bisubstrate mechanism where A does not affect B binding, and vice versa. Note that the lines intersect at the $1/[A]$ axis. (If [B] were varied in an experiment with several fixed concentrations of A, the lines would intersect at the $1/[B]$ axis in a $1/v$ versus $1/[B]$ plot.)

donor to form creatine phosphate (CrP) from creatine (Cr). Creatine-P is an important reservoir of phosphate-bond energy in muscle cells (Figure 14.21).

$$\text{ATP} + \text{E} \rightleftharpoons \text{ATP:E} \qquad\qquad \text{ADP:E} \rightleftharpoons \text{ADP} + \text{E}$$

$$\text{ATP:E:Cr} \rightleftharpoons \text{ADP:E:CrP}$$

$$\text{E} + \text{Cr} \rightleftharpoons \text{E:Cr} \qquad\qquad \text{E:CrP} \rightleftharpoons \text{E} + \text{CrP}$$
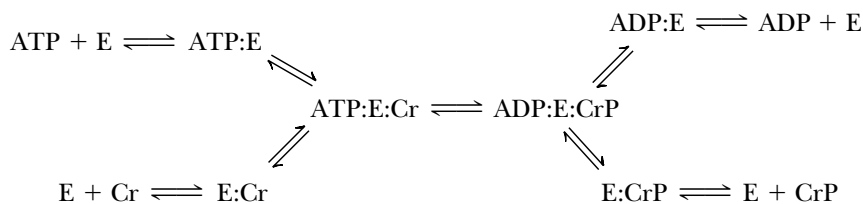
The overall direction of the reaction will be determined by the relative concentrations of ATP, ADP, Cr, and CrP and the equilibrium constant for the reaction. The enzyme can be considered to have two sites for substrate (or product) binding: an adenine nucleotide site, where ATP or ADP binds, and a creatine site, where Cr or CrP is bound. In such a mechanism, ATP and ADP compete for binding at their unique site, while Cr and CrP compete at the specific Cr-, CrP-binding site. Note that no modified enzyme form (E′), such as an E-PO₄ intermediate, appears here. The reaction is characterized by rapid and reversible binary ES complex formation, followed by addition of the remaining substrate, and the rate-determining reaction taking place within the ternary complex.

Ordered, Single-Displacement Reactions

In this case, the **leading substrate,** A (also called the **obligatory** or **compulsory substrate**), must bind first. Then the second substrate, B, binds. Strictly speaking, B cannot bind to free enzyme in the absence of A. Reaction between A and B occurs in the ternary complex, and is usually followed by an ordered release of the products of the reaction, P and Q. In the schemes below, Q is the product of A and is released last. One representation, suggested by W. W. Cleland, follows:

$$
\begin{array}{ccccccc}
\text{A} & & \text{B} & & \text{P} & & \text{Q} \\
\downarrow & & \downarrow & & \uparrow & & \uparrow \\
\text{E} \rule{1em}{0.4pt} \text{AE} & \rule{1em}{0.4pt} & \text{AEB} & \rightleftharpoons & \text{QEP} \rule{1em}{0.4pt} \text{QE} & \rule{1em}{0.4pt} & \text{E}
\end{array}
\qquad (14.49)
$$
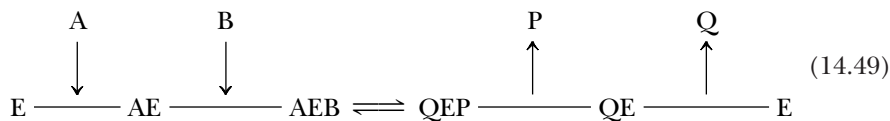
Another way of portraying this mechanism is as follows:
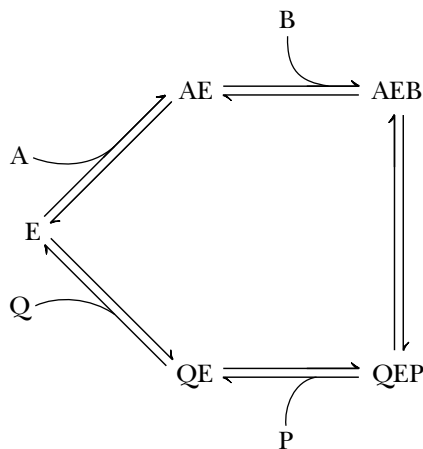
Note that A and Q are competitive for binding to the free enzyme, E, but not A and B (or Q and B).
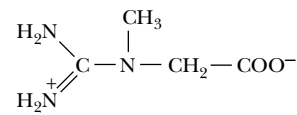
Creatine
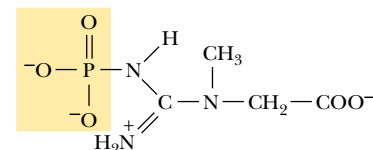
Creatine–P

FIGURE 14.21 • The structures of creatine and creatine phosphate, guanidinium compounds that are important in muscle energy metabolism.

NAD^+-Dependent Dehydrogenases Show Ordered Single-Displacement Mechanisms

Nicotinamide adenine dinucleotide (NAD^+)-dependent dehydrogenases are enzymes that typically behave according to the kinetic pattern just described. A general reaction of these dehydrogenases is

$$NAD^+ + BH_2 \rightleftharpoons NADH + H^+ + B$$
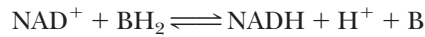
The leading substrate (A) is nicotinamide adenine dinucleotide (NAD^+), and NAD^+ and NADH (product Q) compete for a common site on E. A specific example is offered by *alcohol dehydrogenase (ADH):*

$$\underset{\text{(A)}}{NAD^+} + \underset{\substack{\text{ethanol} \\ \text{(B)}}}{CH_3CH_2OH} \rightleftharpoons \underset{\text{(Q)}}{NADH} + H^+ + \underset{\substack{\text{acetaldehyde} \\ \text{(P)}}}{CH_3CHO}$$
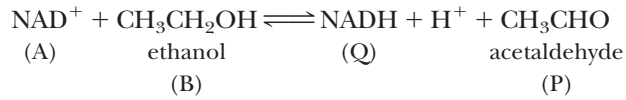
We can verify that this ordered mechanism is not random by demonstrating that no B (ethanol) is bound to E in the absence of A (NAD^+).

Double-Displacement (Ping-Pong) Reactions

Reactions conforming to this kinetic pattern are characterized by the fact that the product of the enzyme's reaction with A (called P in the following schemes) is released *prior* to reaction of the enzyme with the second substrate, B. As a result of this process, the enzyme, E, is converted to a modified form, E′, which then reacts with B to give the second product, Q, and regenerate the unmodified enzyme form, E:
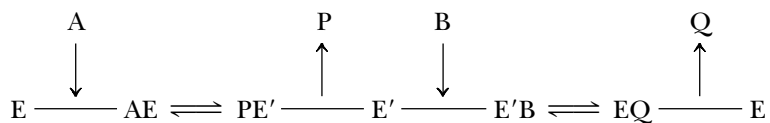
or
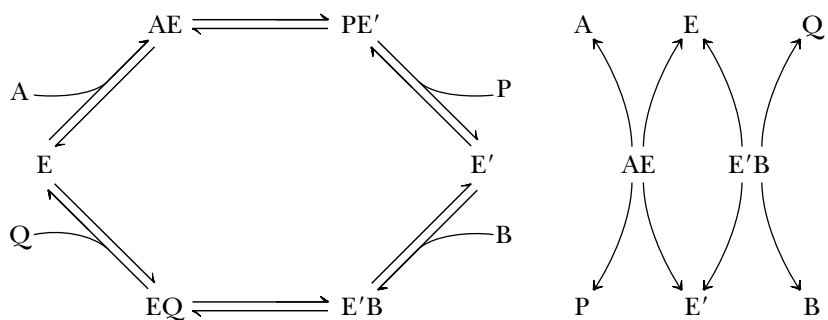
Note that these schemes predict that A and Q compete for the free enzyme form, E, while B and P compete for the modified enzyme form, E′. A and Q do not bind to E′, nor do B and P combine with E.

Aminotransferases Show Double-Displacement Catalytic Mechanisms

One class of enzymes that follow a ping-pong-type mechanism are *aminotransferases* (previously known as transaminases). These enzymes catalyze the transfer of an amino group from an amino acid to an α–keto acid. The products are a new amino acid and the keto acid corresponding to the carbon skeleton of the amino donor:

$$\text{amino acid}_1 + \text{keto acid}_2 \longrightarrow \text{keto acid}_1 + \text{amino acid}_2$$
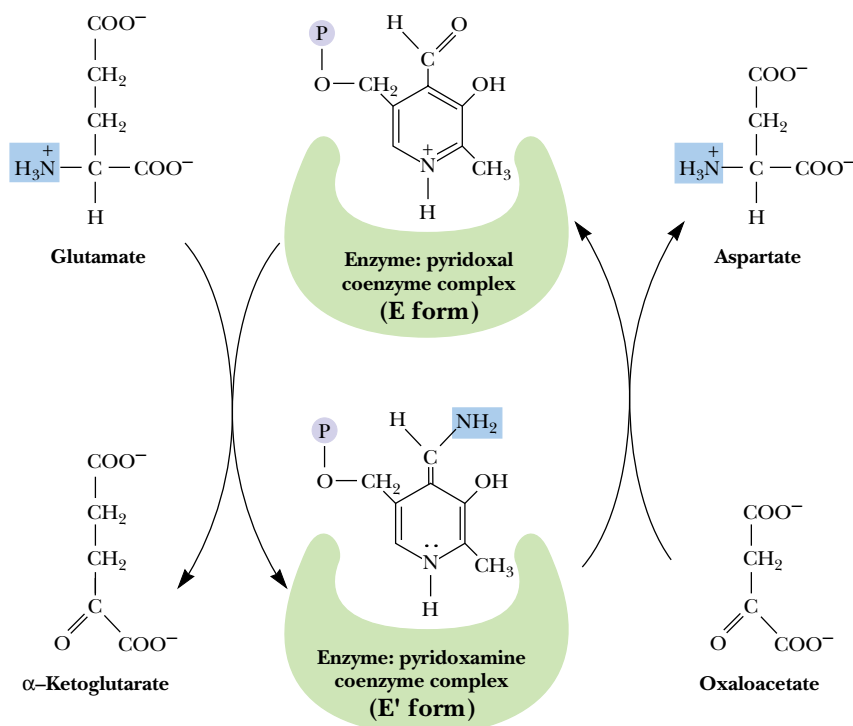
FIGURE 14.22 • *Glutamate : aspartate aminotransferase,* an enzyme conforming to a double-displacement bisubstrate mechanism. Glutamate : aspartate aminotransferase is a pyridoxal phosphate–dependent enzyme. The pyridoxal serves as the —NH$_2$ acceptor from glutamate to form pyridoxamine. Pyridoxamine is then the amino donor to oxaloacetate to form asparate and regenerate the pyridoxal coenzyme form. (The pyridoxamine : enzyme is the E′ form.)

A specific example would be *glutamate : aspartate aminotransferase.* Figure 14.22 depicts the scheme for this mechanism. Note that glutamate and aspartate are competitive for E, and that oxaloacetate and α-ketoglutarate compete for E′. In glutamate : aspartate aminotransferase, an enzyme-bound coenzyme, *pyridoxal phosphate* (a vitamin B$_6$ derivative), serves as the amino group acceptor/donor in the enzymatic reaction. The unmodified enzyme form, E, has the coenzyme in the aldehydic pyridoxal form, whereas the modified enzyme form, E′, is actually pyridoxamine phosphate (Figure 14.22). Not all enzymes displaying ping-pong–type mechanisms require coenzymes as carriers for the chemical substituent transferred in the reaction.

Diagnosis of Bisubstrate Mechanisms

Kineticists rely on a number of diagnostic tests for the assignment of a reaction mechanism to a specific enzyme. One is the graphic analysis of the kinetic patterns observed. It is usually easy to distinguish between single- and double-displacement reactions in this manner, and examining competitive effects between substrates aids in assigning reactions to random versus ordered patterns of S-binding. A second diagnostic test is to determine whether the enzyme catalyzes an exchange reaction. Consider as an example the two enzymes *sucrose phosphorylase* and *maltose phosphorylase.* Both catalyze the phosphorolysis of a disaccharide and both yield glucose-1-phosphate and a free hexose:

$$\text{sucrose} + \text{P}_i \rightleftharpoons \text{glucose-1-phosphate} + \text{fructose}$$

$$\text{maltose} + \text{P}_i \rightleftharpoons \text{glucose-1-phosphate} + \text{glucose}$$
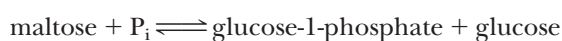
Interestingly, in the absence of sucrose and fructose, sucrose phosphorylase will catalyze the exchange of inorganic phosphate, P_i, into glucose-1-phosphate. This reaction can be followed by using $^{32}P_i$ as a radioactive tracer and observing the appearance of ^{32}P into glucose-1-phosphate:

$$^{32}P_i + \text{G-1-P} \rightleftharpoons P_i + \text{G-1-}^{32}P$$
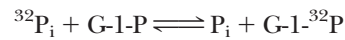
Maltose phosphorylase cannot carry out a similar reaction. The ^{32}P exchange reaction of sucrose phosphorylase is accounted for by a double-displacement mechanism where $E' = $ E-glucose:

$$\text{sucrose} + E \rightleftharpoons \text{E-glucose} + \text{fructose}$$

$$\text{E-glucose} + P_i \rightleftharpoons E + \text{glucose-1-phosphate}$$
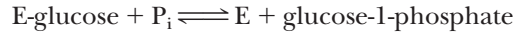
Thus, in the presence of just $^{32}P_i$ and glucose-1-phosphate, sucrose phosphorylase still catalyzes the second reaction and radioactive P_i is incorporated into glucose-1-phosphate over time.

Maltose phosphorylase proceeds via a single-displacement reaction that necessarily requires the formation of a ternary maltose : E : P_i (or glucose : E : glucose-1-phosphate) complex for any reaction to occur. Exchange reactions are a characteristic of enzymes that obey double-displacement mechanisms at some point in their catalysis.

Multisubstrate Reactions

Thus far, we have considered enzyme-catalyzed reactions involving one or two substrates. How are the kinetics described in those cases in which more than two substrates participate in the reaction? An example might be the glycolytic enzyme *glyceraldehyde-3-phosphate dehydrogenase* (Chapter 19):

$$\text{NAD}^+ + \text{glyceraldehyde-3-P} + P_i \longrightarrow \text{NADH} + H^+ + \text{1,3-bisphosphoglycerate}$$

Many other multisubstrate examples abound in metabolism. In effect, these situations are managed by realizing that the interaction of the enzyme with its many substrates can be treated as a series of uni- or bisubstrate steps in a multistep reaction pathway. Thus, the complex mechanism of a multisubstrate reaction is resolved into a sequence of steps, each of which obeys the single- and double-displacement patterns just discussed.

14.6 • RNA and Antibody Molecules as Enzymes: Ribozymes and Abzymes

Catalytic RNA Molecules: Ribozymes

It was long assumed that all enzymes are proteins. However, in recent years, more and more instances of biological catalysis by RNA molecules have been discovered. These catalytic RNAs, or **ribozymes,** satisfy several enzymatic criteria: They are substrate-specific, they enhance the reaction rate, and they emerge from the reaction unchanged. For example, RNase P, an enzyme responsible for the formation of mature tRNA molecules from tRNA precursors, requires an RNA component as well as a protein subunit for its activity in the cell. *In vitro,* the protein alone is incapable of catalyzing the maturation reaction, but the RNA component by itself can carry out the reaction under appropriate conditions. In another case, in the ciliated protozoan *Tetrahymena,* formation of mature ribosomal RNA from a pre-rRNA precursor involves the removal of an internal RNA segment and the joining of the two ends in a process known as **splicing out.** The excision of this intervening internal sequence of RNA and
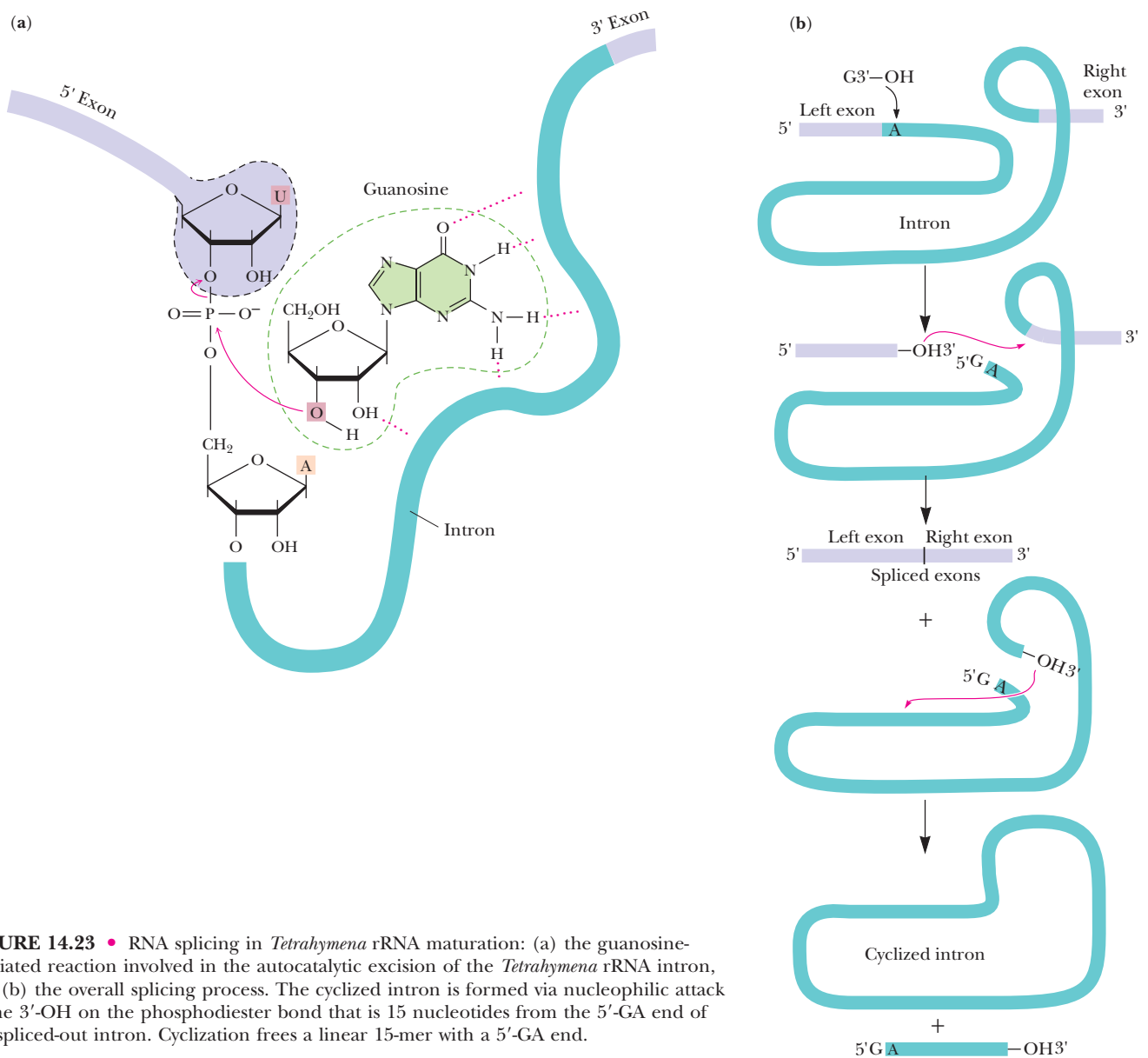
FIGURE 14.23 • RNA splicing in *Tetrahymena* rRNA maturation: (a) the guanosine-mediated reaction involved in the autocatalytic excision of the *Tetrahymena* rRNA intron, and (b) the overall splicing process. The cyclized intron is formed via nucleophilic attack of the 3′-OH on the phosphodiester bond that is 15 nucleotides from the 5′-GA end of the spliced-out intron. Cyclization frees a linear 15-mer with a 5′-GA end.

ligation of the ends is, remarkably, catalyzed by the intervening sequence of RNA itself, in the presence of Mg^{2+} and a free molecule of guanosine nucleoside or nucleotide (Figure 14.23). *In vivo,* the intervening sequence RNA probably acts only in splicing itself out; *in vitro,* however, it can act many times, turning over like a true enzyme.

Protein-Free 50S Ribosomal Subunits Catalyze Peptide Bond Formation In Vitro

Perhaps the most significant case of catalysis by RNA occurs in protein synthesis. Harry F. Noller and his colleagues have found that the **peptidyl transferase reaction,** which is the reaction of peptide bond formation during protein synthesis (Figure 14.24), can be catalyzed by 50S ribosomal subunits (see Chapter 12) from which virtually all of the protein has been removed. These
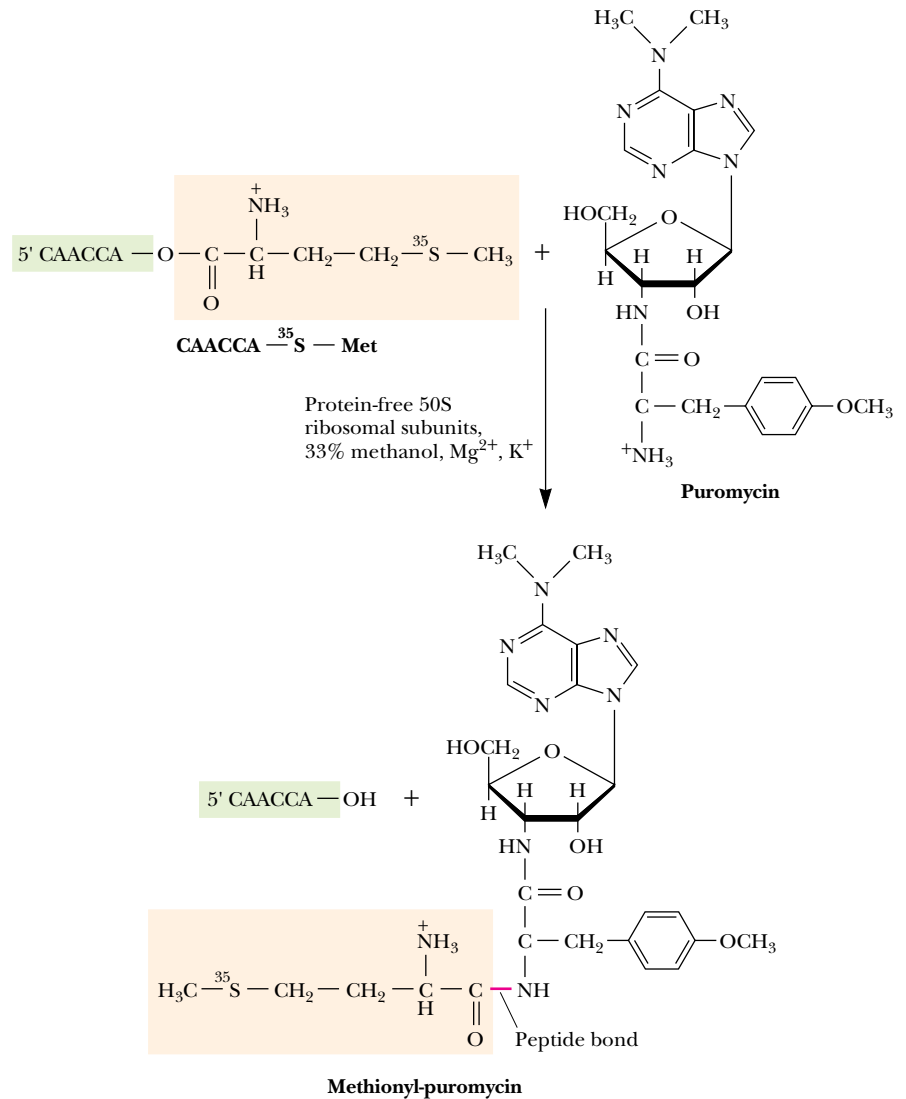
FIGURE 14.24 • Protein-free 50S ribosomal subunits have peptidyl transferase activity. Peptidyl transferase is the name of the enzymatic function that catalyzes peptide bond formation. The presence of this activity in protein-free 50S ribosomal subunits was demonstrated using a model assay for peptide bond formation in which an aminoacyl-tRNA analog (a short RNA oligonucleotide of sequence CAACCA carrying ^{35} S-labeled methionine attached at its 3′-OH end) served as the peptidyl donor and puromycin (another aminoacyl-tRNA analog) served as the peptidyl acceptor. Activity was measured by monitoring the formation of ^{35} S-labeled methioninyl-puromycin.

experiments imply that just the 23S rRNA by itself is capable of catalyzing peptide bond formation. Also, the laboratory of Thomas Cech has created a synthetic 196-nucleotide-long ribozyme capable of performing the peptidyl transferase reaction.

Several features of these "RNA enzymes," or **ribozymes,** lead to the realization that their biological efficiency does not challenge that achieved by proteins. First, RNA enzymes often do not fulfill the criterion of catalysis *in vivo* because they act only once in intramolecular events such as self-splicing. Second, the catalytic rates achieved by RNA enzymes *in vivo* and *in vitro* are

(a)

Hydroxy ester

Cyclic transition state

δ-Lactone

(b)

Cyclic phosphonate ester
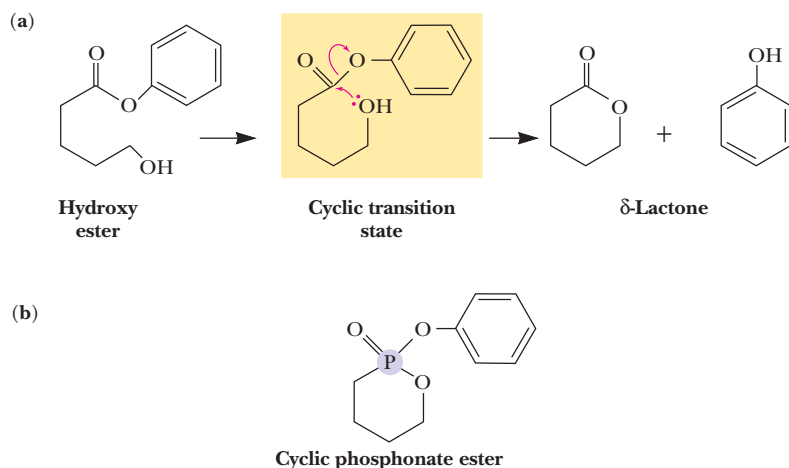
FIGURE 14.25 • Catalytic antibodies are designed to specifically bind the transition-state intermediate in a chemical reaction. (a) The intramolecular hydrolysis of a hydroxy ester to yield as products a δ-lactone and the alcohol phenol. Note the cyclic transition state. (b) The cyclic phosphonate ester analog of the cyclic transition state. Antibodies raised against this phosphonate ester act as *enzymes:* they are catalysts that markedly accelerate the rate of ester hydrolysis.

significantly enhanced by the participation of protein subunits. Nevertheless, the fact that RNA can catalyze certain reactions is experimental support for the idea that a primordial world dominated by RNA molecules existed before the evolution of DNA and proteins.

Catalytic Antibodies: Abzymes

Antibodies are *immunoglobulins,* which, of course, are proteins. Like other antibodies, **catalytic antibodies,** so-called **abzymes,** are elicited in an organism in response to immunological challenge by a foreign molecule called an **antigen** (see Chapter 29 for discussions on the molecular basis of immunology). In this case, however, the antigen is purposefully engineered to be *an analog of the transition-state intermediate in a reaction.* The rationale is that a protein specific for binding the transition-state intermediate of a reaction will promote entry of the normal reactant into the reactive, transition-state conformation. Thus, a catalytic antibody facilitates, or catalyzes, a reaction by forcing the conformation of its substrate in the direction of its transition state. (A prominent explanation for the remarkable catalytic power of conventional enzymes is their great affinity for the transition-state intermediates in the reactions they catalyze; see Chapter 16.)

One strategy has been to prepare ester analogs by substituting a phosphorus atom for the carbon in the ester group (Figure 14.25). The phosphocompound mimics the natural transition state of ester hydrolysis, and antibodies elicited against these analogs act like enzymes in accelerating the rate of ester hydrolysis as much as 1000-fold. Abzymes have been developed for a number of other classes of reactions, including C—C bond formation via aldol condensation (the reverse of the aldolase reaction [see Figure 14.2, reaction 4 and Chapter 19]) and the pyridoxal 5′-P-dependent aminotransferase reaction shown in Figure 14.22. In this latter instance, N^α-(5′-phosphopyridoxyl)-lysine (Figure 14.26a) coupled to a carrier protein served as the antigen. An antibody raised against this antigen catalyzed the conversion of D-alanine and pyridoxal 5′-P to pyruvate and pyridoxamine 5′-P (Figure 14.26b). This biotechnology offers the real possibility of creating **"designer enzymes,"** specially tailored enzymes designed to carry out specific catalytic processes.

(a)

(b)
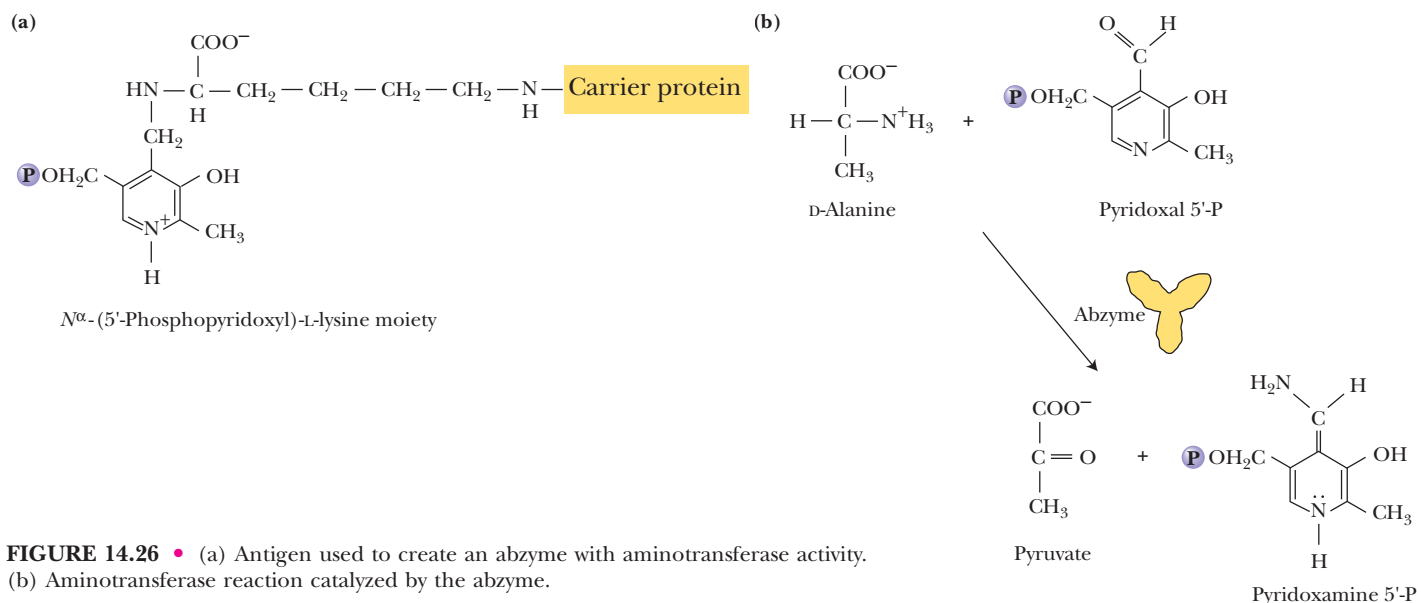
FIGURE 14.26 • (a) Antigen used to create an abzyme with aminotransferase activity. (b) Aminotransferase reaction catalyzed by the abzyme.

PROBLEMS

1. According to the Michaelis–Menten equation, what is the v/V_{max} ratio when $[S] = 4\ K_m$?

2. If $V_{max} = 100\ \mu mol/mL\ sec$ and $K_m = 2\ mM$, what is the velocity of the reaction when $[S] = 20\ mM$?

3. For a Michaelis–Menten reaction, $k_1 = 7 \times 10^7/M \cdot sec$, $k_{-1} = 1 \times 10^3/sec$, and $k_2 = 2 \times 10^4/sec$. What are the values of K_S and K_m? Does substrate binding approach equilibrium or does it behave more like a steady-state system?

4. The following kinetic data were obtained for an enzyme in the absence of any inhibitor (1), and in the presence of two different inhibitors (2) and (3) at 5 mM concentration. Assume $[E_T]$ is the same in each experiment.

[S] (mM)	(1) $v(\mu mol/mL\ sec)$	(2) $v(\mu mol/mL\ sec)$	(3) $v(\mu mol/mL\ sec)$
1	12	4.3	5.5
2	20	8	9
4	29	14	13
8	35	21	16
12	40	26	18

a. Determine V_{max} and K_m for the enzyme.

b. Determine the type of inhibition and the K_I for each inhibitor.

5. The general rate equation for an ordered, single-displacement reaction where A is the leading substrate is

$$v = \frac{V_{max}[A][B]}{(K_S^A K_m^B + K_m^A[B] + K_m^B[A] + [A][B])}$$

Write the Lineweaver–Burk (double-reciprocal) equivalent of this equation, and from it calculate algebraic expressions for (a) the slope; (b) the *y*-intercepts; and (c) the horizontal and vertical coordinates of the point of intersection when $1/v$ is plotted versus $1/[B]$ at various *fixed* concentrations of A.

6. The following graphical patterns obtained from kinetic experiments have several possible interpretations depending on the nature of the experiment and the variables being plotted. Give at least two possibilities for each.
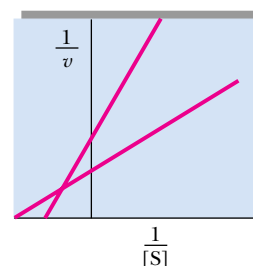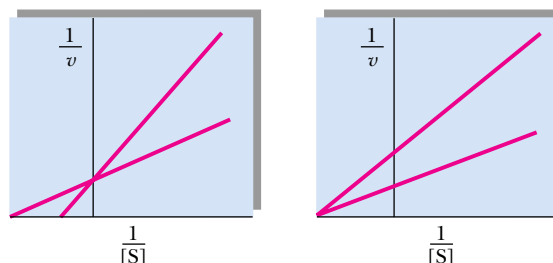
7. Liver alcohol dehydrogenase (ADH) is relatively nonspecific and will oxidize ethanol or other alcohols, including methanol. Methanol oxidation yields formaldehyde, which is quite toxic, causing, among other things, blindness. Mistaking it for the cheap

wine he usually prefers, my dog Clancy ingested about 50 mL of windshield washer fluid (a solution 50% in methanol.) Knowing that methanol would be excreted eventually by Clancy's kidneys if its oxidation could be blocked, and realizing that, in terms of methanol oxidation by ADH, ethanol would act as a competitive inhibitor, I decided to offer Clancy some wine. How much of Clancy's favorite vintage (12% ethanol) must he consume in order to lower the activity of his ADH on methanol to 5% of its normal value if the K_m values of canine ADH for ethanol and methanol are 1 millimolar and 10 millimolar, respectively? (The K_I for ethanol in its role as competitive inhibitor of methanol oxidation by ADH is the same as its K_m.) Both the methanol and ethanol will quickly distribute throughout Clancy's body fluids, which amount to about 15 L. Assume the densities of 50% methanol and the wine are both 0.9 g/mL.

FURTHER READING

Bell, J. E., and Bell, E. T., 1988. *Proteins and Enzymes.* Englewood Cliffs, NJ: Prentice-Hall. This text describes the structural and functional characteristics of proteins and enzymes.

Boyer, P. D., 1970. *The Enzymes,* Vols. I and II. New York: Academic Press. An edition for students seeking advanced knowledge on enzymes.

Cate, J. H., et al., 1996. Crystal structure of a group I ribozyme domain: Principles of RNA packing. *Science* **273:**1678.

Cech, T. R., and Bass, B. L., 1986. Biological catalysis by RNA. *Annual Review of Biochemistry* **55:**599–629. A review of the early evidence that RNA can act like an enzyme.

Cech, T. R., et al., 1992. RNA catalysis by a group I ribozyme: Developing a model for transition-state stabilization. *Journal of Biological Chemistry* **267:**17479–17482.

Dixon, M., et al., 1979. *Enzymes,* 3rd ed. New York: Academic Press. A classic work on enzyme kinetics and the properties of enzymes.

Fersht, A., 1985. *Enzyme Structure and Mechanism,* 2nd ed. Reading, PA: Freeman & Co. A monograph on the structure and action of enzymes.

Garrett, R. M., et al., 1998. Human sulfite oxidase R160Q: Identification of the mutation in a sulfite oxidase-deficient patient and expression and characterization of the mutant enzyme. *Proceedings of the National Academy of Sciences USA* **95:** 6394–6398.

Garrett, R. M., and Rajagopalan, K. V., 1996. Site-directed mutagenesis of recombinant sulfite oxidase. *Journal of Biological Chemistry* **271:**7387–7391.

Gray, C. J., 1971. *Enzyme-Catalyzed Reactions.* New York: Van Nostrand Reinhold. A monograph on quantitative aspects of enzyme kinetics.

Hsieh, L. C., Yonkovich, S., Kochersperger, L., and Schultz, P. G., 1993. Controlling chemical reactivity with antibodies. *Science* **260:**337–339.

International Union of Biochemistry and Molecular Biology Nomenclature Committee, 1992. *Enzyme Nomenclature.* New York: Academic Press. A reference volume and glossary on the official classification and nomenclature of enzymes.

Janda, K. D., 1997. Chemical selection for catalysis in combinatorial antibody libraries. *Science* **275:**945.

Janda, K. D., Shevlin, C. G., and Lerner, R. A., 1993. Antibody catalysis of a disfavored chemical transformation. *Science* **259:**490–493.

Kisker, C., et al., 1997. Molecular basis of sulfite oxidase deficiency from the structure of sulfite oxidase. *Cell* **91:**973–983.

Landry, D. W., Zhao, K., Yang, G. X., et al., 1993. Antibody-catalyzed degradation of cocaine. *Science* **259:**1899–1901.

Napper, A. D., Benkovic, S. J., Tramantano, A., and Lerner, R. A., 1987. A stereospecific cyclization catalyzed by an antibody. *Science* **237:**1041–1043.

Noller, H. F., Hoffarth, V., and Zimniak, L., 1992. Unusual resistance of peptidyl transferase to protein extraction procedures. *Science* **256:**1416–1419.

Piccirilli, J. A., McConnell, T. S., Zaug, A. J., et al., 1992. Aminoacyl esterase activity of *Tetrahymena* ribozyme. *Science* **256:**1420–1424.

Scott, W. G., and Klug, A., 1996. Ribozymes: Structure and mechanism in RNA catalysis. *Trends in Biochemical Sciences* **21:**220–224.

Scott, W. G., et al., 1996. Capturing the structure of a catalytic RNA intermediate: The hammerhead ribozyme. *Science* **274:**2065.

Segel, I. H., 1976. *Biochemical Calculations,* 2nd ed. New York: John Wiley & Sons. An excellent guide to solving problems in enzyme kinetics.

Silverman, R. B., 1988. *Mechanism-Based Enzyme Inactivation: Chemistry and Enzymology,* Vols. I and II. Boca Raton, FL: CRC Press.

Smith, W. G., 1992. *In vivo* kinetics and the reversible Michaelis–Menten model. *Journal of Chemical Education* **12:**981–984.

Steitz, T. A., and Steitz, J. A., 1993. A general two-metal-ion mechanism for catalytic RNA. *Proceedings of the National Academy of Sciences USA* **90:**6498–6502.

Wagner, J., Lerner, R. A., and Barbas, C. F., III, 1995. Efficient adolase catalytic antibodies that use the enamine mechanism of natural enzymes. *Science* **270:**1797–1800. See also the discussion entitled "Aldolase antibody" in *Science* **270:**1737.

Watson, J. D., ed., 1987. Evolution of catalytic function. *Cold Spring Harbor Symposium on Quantitative Biology* **52:**1–955. Publications from a symposium on the nature and evolution of catalytic biomolecules (proteins and RNA) prompted by the discovery that RNA could act catalytically.

Wirsching, P., et al., 1995. Reactive immunization. *Science* **270:**1775–1783. Description of *reactive immunization,* in which a highly reactive compound is used as antigen. Antibodies raised against such an antigen show catalytic activity for the chemical reaction that the antigen undergoes.

Zaug, A. J., and Cech, T. R., 1986. The intervening sequence RNA of *Tetrahymena* is an enzyme. *Science* **231:**470–475.

Zhang, B., and Cech, T. R., 1997. Peptide bond formation by *in vitro* selected ribozymes. *Nature* **390:**96–100.

Allostery is the key chemical process that makes possible intracellular and intercellular regulation: "... the molecular interactions which ensure the transmission and interpretation of (regulatory) signals rest upon (allosteric) proteins endowed with discriminatory stereospecific recognition properties."

JACQUES MONOD in *Chance and Necessity*

*C*hapter 15

Enzyme Specificity and Regulation

*Metabolic regulation is achieved through an exquisitely balanced interplay among enzymes and small molecules, a process symbolized by the delicate balance of forces in this mobile. (*Sea Scape *by Alexander Calder/Whitney Museum of American Art, NY)*

The extraordinary ability of an enzyme to catalyze only one particular reaction is a quality known as **specificity** (Chapter 14). Specificity means an enzyme acts only on a specific substance, its substrate, invariably transforming it into a specific product. That is, an enzyme binds only certain compounds, and then, only a specific reaction ensues. Some enzymes show absolute specificity, catalyzing the transformation of only one specific substrate to yield a unique product. Other enzymes carry out a particular reaction but act on a class of compounds. For example, *hexokinase* (ATP : hexose-6-phosphotransferase) will carry out the ATP-dependent phosphorylation of a number of hexoses at the 6-position, including glucose.

15.1 • Specificity Is the Result of Molecular Recognition

An enzyme molecule is typically orders of magnitude larger than its substrate. Its active site comprises only a small portion of the overall enzyme structure. The active site is part of the conformation of the enzyme molecule arranged to create a special pocket or cleft whose three-dimensional structure is complementary to the structure of the substrate. The enzyme and the substrate molecules "recognize" each other through this structural complementarity. The substrate binds to the enzyme through relatively weak forces—H bonds, ionic bonds (salt bridges), and van der Waals interactions between sterically complementary clusters of atoms. Specificity studies on enzymes entail an examination of the rates of the enzymatic reaction obtained with various **structural analogs** of the substrate. By determining which functional and structural groups within the substrate affect binding or catalysis, enzymologists can map the properties of the active site, analyzing questions such as: Can it accommodate sterically bulky groups? Are ionic interactions between E and S important? Are H bonds formed?

The "Lock and Key" Hypothesis

Pioneering enzyme specificity studies at the turn of the century by the great organic chemist Emil Fischer led to the notion of an enzyme resembling a **"lock"** and its particular substrate the **"key."** This analogy captures the essence of the specificity that exists between an enzyme and its substrate, but enzymes are not rigid templates like locks.

The "Induced Fit" Hypothesis

Enzymes are highly flexible, conformationally dynamic molecules, and many of their remarkable properties, including substrate binding and catalysis, are due to their structural pliancy. Realization of the conformational flexibility of proteins led Daniel Koshland to hypothesize that the binding of a substrate (S) by an enzyme is an interactive process. That is, the shape of the enzyme's active site is actually modified upon binding S, in a process of dynamic recognition between enzyme and substrate aptly called **induced fit.** In essence, substrate binding alters the conformation of the protein, so that the protein and the substrate "fit" each other more precisely. The process is truly interactive in that the conformation of the substrate also changes as it adapts to the conformation of the enzyme.

This idea also helps to explain some of the mystery surrounding the enormous catalytic power of enzymes: In enzyme catalysis, precise orientation of catalytic residues comprising the active site is necessary for the reaction to occur; substrate binding induces this precise orientation by the changes it causes in the protein's conformation.

"Induced Fit" and the Transition-State Intermediate

The catalytically active enzyme:substrate complex is an interactive structure in which the enzyme causes the substrate to adopt a form that mimics the transition-state intermediate of the reaction. Thus, a poor substrate would be one that was less effective in directing the formation of an optimally active enzyme:transition-state intermediate conformation. This active conformation of the enzyme molecule is thought to be relatively unstable in the absence of substrate, and free enzyme thus reverts to a conformationally different state.

(a) **(b)**

Glucose

Glycerol

Water

Active site
cleft

Glucose

Solvent-
inaccessible
active site lining

Hexokinase molecule
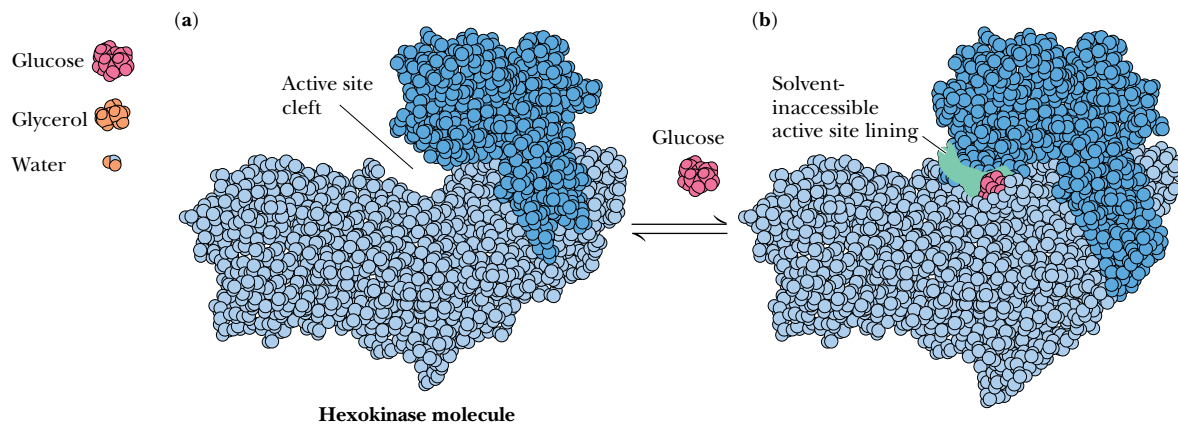
FIGURE 15.1 • A drawing, roughly to scale, of H_2O, glycerol, glucose, and an idealized hexokinase molecule. Note the two domains of structure in hexokinase, (a), between which the active site is located. Binding of glucose induces a conformational change in hexokinase. The two domains close together, creating the catalytic site (b). The shaded area in (b) represents solvent-inaccessible surface area in the active site cleft that results when the enzyme binds substrate.

Specificity and Reactivity

Consider, for example, why hexokinase catalyzes the ATP-dependent phosphorylation of hexoses but not smaller phosphoryl-group acceptors such as glycerol, ethanol, or even water. Surely these smaller compounds are not sterically forbidden from approaching the active site of hexokinase (Figure 15.1). Indeed, water should penetrate the active site easily and serve as a highly effective phosphoryl-group acceptor. Accordingly, hexokinase should display high ATPase activity. It does not. Only the binding of hexoses induces hexokinase to assume its fully active conformation.

In Chapter 16, we explore in greater detail the factors that contribute to the remarkable catalytic power of enzymes and examine specific examples of enzyme reaction mechanisms. Here we focus on another essential feature of enzymes: *the regulation of their activity.*

15.2 • Controls Over Enzymatic Activity— General Considerations

The activity displayed by enzymes is affected by a variety of factors, some of which are essential to the harmony of metabolism.

1. The enzymatic rate, $v = d[P]/dt$, "slows down" as product accumulates and equilibrium is approached. The apparent decrease in rate is due to the conversion of P to S by the reverse reaction as [P] rises. Once $[P]/[S] = K_{eq}$, no further reaction is apparent. K_{eq} defines thermodynamic equilibrium. Enzymes have no influence on the thermodynamics of a reaction. Also, product inhibition can be a kinetically valid phenomenon: Some enzymes are actually inhibited by the products of their action.
2. The availability of substrates and cofactors will determine the enzymatic reaction rate. In general, enzymes have evolved such that their K_m values approximate the prevailing *in vivo* concentration of their substrates. (It is also true that the concentration of some enzymes in cells is within an order of magnitude or so of the concentrations of their substrates.)

3. There are genetic controls over the amounts of enzyme synthesized (or degraded) by cells. If the gene encoding a particular enzyme protein is turned on or off, changes in the amount of enzyme activity soon follow. **Induction,** which is the activation of enzyme synthesis, and **repression,** which is the shutdown of enzyme synthesis, are important mechanisms for the regulation of metabolism. By controlling the amount of an enzyme that is present at any moment, cells can either activate or terminate various metabolic routes. Genetic controls over enzyme levels have a response time ranging from minutes in rapidly dividing bacteria to hours (or longer) in higher eukaryotes.

4. Enzymes can be regulated by **covalent modification,** the reversible covalent attachment of a chemical group. For example, a fully active enzyme can be converted into an inactive form simply by the covalent attachment of a functional group, such as a phosphoryl moiety (Figure 15.2). Alternatively, some enzymes exist in an inactive state unless specifically converted into the active form through covalent addition of a functional group. Covalent modification reactions are catalyzed by special **converter enzymes,** which are themselves subject to metabolic regulation. Although covalent modification represents a stable alteration of the enzyme, a different converter enzyme operates to remove the modification, so that when the conditions that favored modification of the enzyme are no longer present, the process can be reversed, restoring the enzyme to its unmodified state. Many examples of covalent modification at important metabolic junctions will be encountered in our discussions of metabolic pathways. Because covalent modification events are enzyme-catalyzed, they occur very quickly, with response times of seconds or even less for significant changes in metabolic activity. The 1992 Nobel Prize in physiology or medicine was awarded to Edmond Fischer and Edwin Krebs for their pioneering studies of reversible protein phosphorylation as an important means of cellular regulation.

5. Enzymatic activity can also be activated or inhibited through noncovalent interaction of the enzyme with small molecules (metabolites) other than the substrate. This form of control is termed **allosteric regulation,** because the activator or inhibitor binds to the enzyme at a site *other* than (*allo* means "other") the active site. Further, such allosteric regulators, or **effector molecules,** are often quite different sterically from the substrate. Because this form of regulation results simply from reversible binding of regulatory ligands to the enzyme, the cellular response time can be virtually instantaneous.
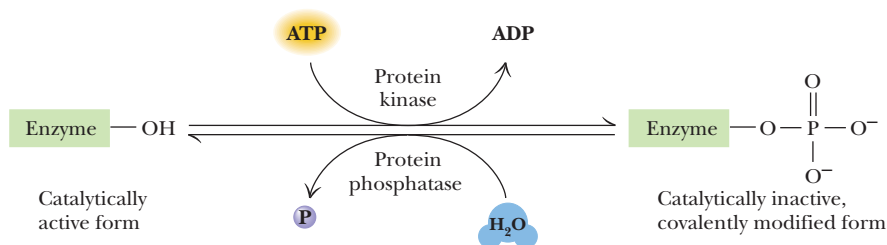
FIGURE 15.2 • Enzymes regulated by covalent modification are called **interconvertible enzymes.** The enzymes (*protein kinase* and *protein phosphatase,* in the example shown here) catalyzing the conversion of the interconvertible enzyme between its two forms are called **converter enzymes.** In this example, the free enzyme form is catalytically active, whereas the phosphoryl-enzyme form represents an inactive state. The —OH on the interconvertible enzyme represents an —OH group on a specific amino acid side chain in the protein (for example, a particular Ser residue) capable of accepting the phosphoryl group.

6. Specialized controls: Enzyme regulation is an important matter to cells, and evolution has provided a variety of additional options, including zymogens, isozymes, and modulator proteins.

Zymogens

Most proteins become fully active as their synthesis is completed and they spontaneously fold into their native, three-dimensional conformations. Some proteins, however, are synthesized as inactive precursors, called **zymogens** or **proenzymes,** that only acquire full activity upon specific proteolytic cleavage of one or several of their peptide bonds. Unlike allosteric regulation or covalent modification, zymogen activation by specific proteolysis is an irreversible process. Activation of enzymes and other physiologically important proteins by specific proteolysis is a strategy frequently exploited by biological systems to switch on processes at the appropriate time and place, as the following examples illustrate.

INSULIN.   Some protein hormones are synthesized in the form of inactive precursor molecules, from which the active hormone is derived by proteolysis. For instance, **insulin,** an important metabolic regulator, is generated by proteolytic excision of a specific peptide from **proinsulin** (Figure 15.3).

PROTEOLYTIC ENZYMES OF THE DIGESTIVE TRACT.   Enzymes of the digestive tract that serve to hydrolyze dietary proteins are synthesized in the stomach and pancreas as zymogens (Table 15.1). Only upon proteolytic activation are these enzymes able to form a catalytically active substrate-binding site. The activation of chymotrypsinogen is an interesting example (Figure 15.4). **Chymotrypsinogen** is a 245-residue polypeptide chain cross-linked by five disulfide bonds. Chymotrypsinogen is converted to an enzymatically active form called π-chymotrypsin when trypsin cleaves the peptide bond joining Arg^{15} and Ile^{16}. The enzymatically active π-chymotrypsin acts upon other π-chymotrypsin molecules, excising two dipeptides, Ser^{14}-Arg^{15} and Thr^{147}-Asn^{148}. The end product of this processing pathway is the mature protease **α-chymotrypsin,** in which the three peptide chains, A (residues 1 through 13), B (residues 16 through 146), and C (residues 149 through 245), remain together because they are linked by two disulfide bonds, one from A to B, and one from B to C. It is interesting to note that the transformation of inactive chymotrypsinogen to active π-chymotrypsin requires the cleavage of just one particular peptide bond.

BLOOD CLOTTING.   The formation of blood clots is the result of a series of zymogen activations (Figure 15.5). The amplification achieved by this cascade of enzymatic activations allows blood clotting to occur rapidly in response to injury. Seven of the clotting factors in their active form are serine proteases:
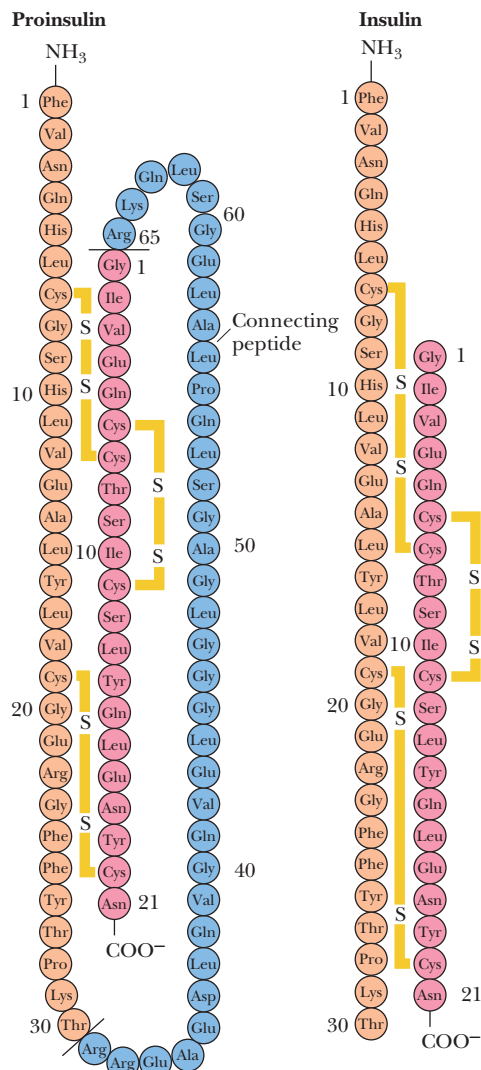
FIGURE 15.3 • Proinsulin is an 86-residue precursor to insulin (the sequence shown here is human proinsulin). Proteolytic removal of residues 31 to 65 yields insulin. Residues 1 through 30 (the B chain) remain linked to residues 66 through 87 (the A chain) by a pair of interchain disulfide bridges.

Table 15.1

Pancreatic and Gastric Zymogens		
Origin	**Zymogen**	**Active Protease**
Pancreas	Trypsinogen	Trypsin
Pancreas	Chymotrypsinogen	Chymotrypsin
Pancreas	Procarboxypeptidase	Carboxypeptidase
Pancreas	Proelastase	Elastase
Stomach	Pepsinogen	Pepsin

Chymotrypsinogen (inactive zymogen)

Cleavage at Arg^{15}
by trypsin

π-Chymotrypsin (active enzyme)

Self digestion at Leu^{13},
Tyr^{146}, and Asn^{148} by
π-chymotrypsin

α-Chymotrypsin (active enzyme)
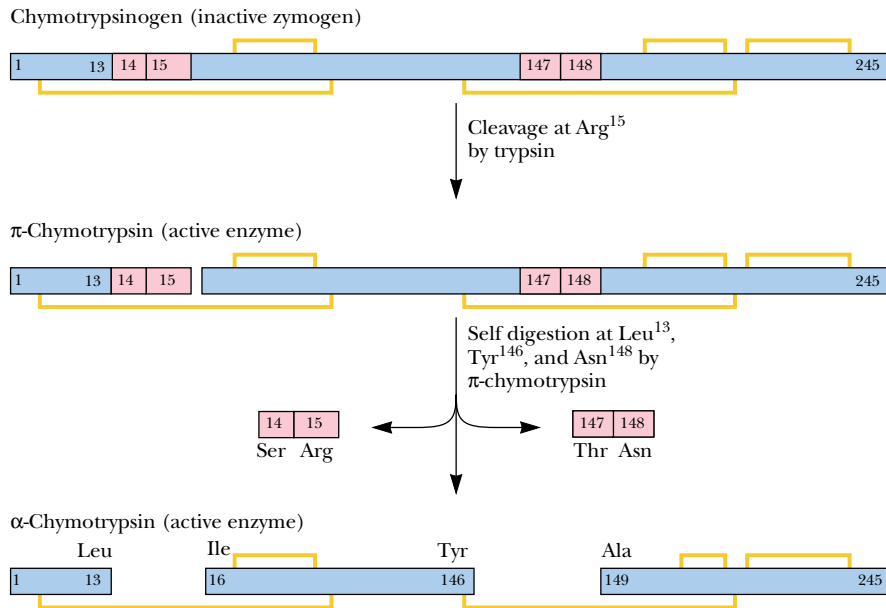
FIGURE 15.4 • The proteolytic activation of chymotrypsinogen.

kallikrein, XII$_a$, XI$_a$, IX$_a$, VII$_a$, X$_a$, and **thrombin.** Two routes to blood clot formation exist. The **intrinsic pathway** is instigated when the blood comes into physical contact with abnormal surfaces caused by injury; the **extrinsic pathway** is initiated by factors released from injured tissues. The pathways merge at Factor X and culminate in clot formation. Thrombin excises peptides rich
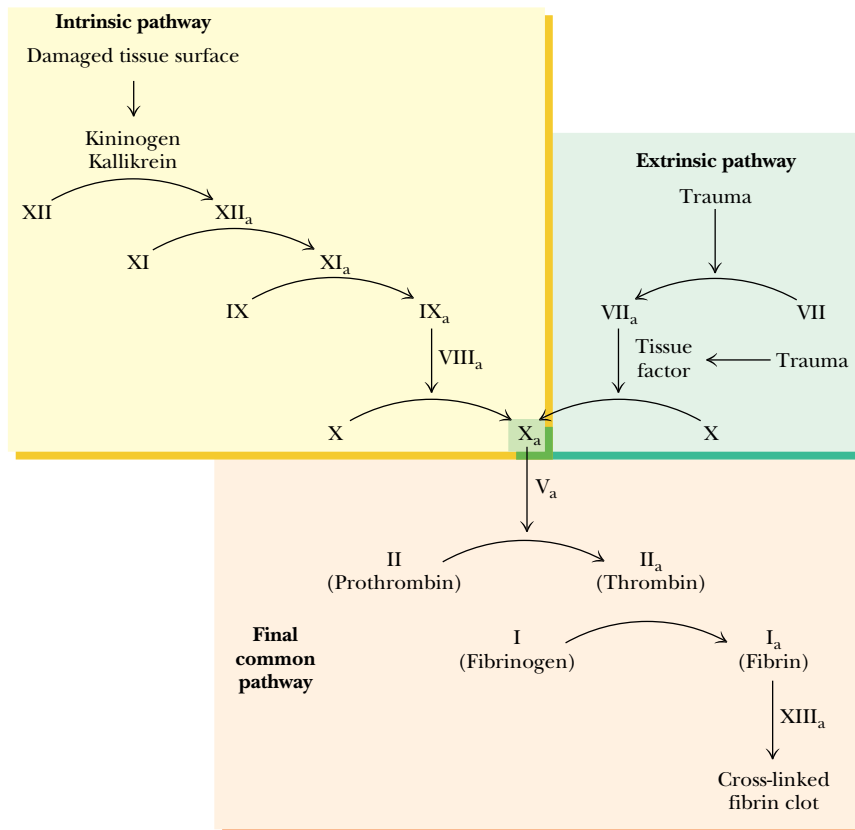
FIGURE 15.5 • The cascade of activation steps leading to blood clotting. The intrinsic and extrinsic pathways converge at Factor X, and the final common pathway involves the activation of thrombin and its conversion of fibrinogen into fibrin, which aggregates into ordered filamentous arrays that become cross-linked to form the clot.

𝒜 D E E P E R   L O O K

Protein Kinases: Target Recognition and Intrasteric Control

Protein kinases are converter enzymes that catalyze the ATP-dependent phosphorylation of serine, threonine, and/or tyrosine hydroxyl groups in target proteins (table). Phosphorylation introduces a bulky group bearing two negative charges, causing conformational changes that alter the target protein's function. (Unlike a phosphoryl group, no amino acid side chain can provide *two* negative charges.) Protein kinases represent a protein superfamily whose members are widely diverse in terms of size, subunit structure, and subcellular localization. Nevertheless, all share a common catalytic mechanism based on a conserved catalytic core/kinase domain of approximately 260 amino acid residues (see figure). Protein kinases are classified as Ser/Thr- and/or Tyr-specific and are subclassified in terms of the allosteric activators they require *and* the consensus amino acid sequence within the target protein that is recognized by the kinase. For example, cAMP-dependent protein kinase **(PKA)** phosphorylates proteins having Ser or Thr residues within an $R(R/K)X(S^*/T^*)$ target consensus sequence (* denotes the residue that becomes phosphorylated). That is, PKA phosphorylates Ser or Thr residues that occur in an Arg-(Arg or Lys)-(any amino acid)-(Ser or Thr) sequence segment (table).

Targeting of protein kinases to particular consensus sequence elements within proteins creates a means to regulate these kinases by **intrasteric control.** Intrasteric control occurs when a regulatory subunit (or protein domain) has a **pseudosubstrate sequence** that mimics the target sequence but lacks a OH-bearing side chain at the right place. For example, the cAMP-binding regulatory subunits of PKA (R subunits in Figure 15.7) possess the pseudosubstrate sequence RRGA*I and this sequence binds to the active site of PKA catalytic subunits, blocking their activity. This pseudosubstrate sequence has an alanine residue where serine occurs in the PKA target sequence; Ala is sterically similar to serine but lacks a phosphorylatable OH-group. When

these PKA regulatory subunits bind cAMP, they undergo a conformational change and dissociate from the catalytic (C) subunits, and the active site of PKA is free to bind and phosphorylate its targets.

The abundance of many protein kinases in cells is an indication of the great importance of protein phosphorylation in cellular regulation. Exactly 113 protein kinase genes have been recognized in yeast, and it is estimated that the human genome encodes more than 1000 different protein kinases. **Tyrosine kinases** (protein kinases that phosphorylate Tyr residues) occur only in multicellular organisms (yeast has no tyrosine kinases). Tyrosine kinases are components of signaling pathways involved in cell–cell communication (see Chapter 34).
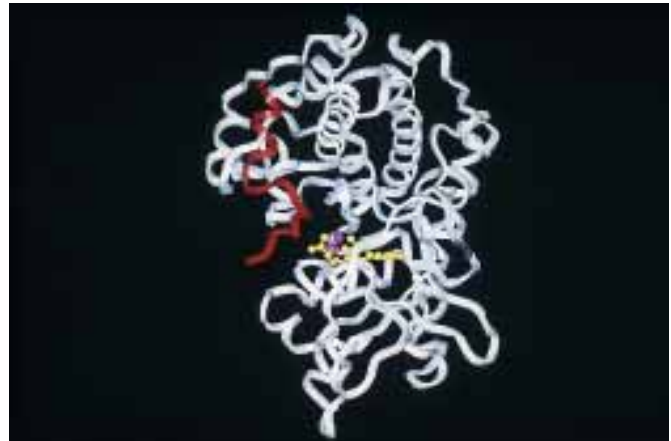
Cyclic AMP-dependent protein kinase is shown complexed with a pseudosubstrate peptide (red). This complex also includes ATP (yellow) and two Mn^{2+} ions (violet) bound at the active site.

in negative charge from **fibrinogen,** converting it to **fibrin,** a molecule with a different surface charge distribution. Fibrin readily aggregates into ordered fibrous arrays that are subsequently stabilized by covalent cross-links. Thrombin specifically cleaves Arg-Gly peptide bonds and is homologous to trypsin, which is also a serine protease (recall that trypsin acts only at Arg and Lys residues).

Isozymes

A number of enzymes exist in more than one quaternary form, differing in their relative proportions of structurally equivalent but catalytically distinct polypeptide subunits. A classic example is mammalian **lactate dehydrogenase (LDH),** which exists as five different isozymes, depending on the tetrameric association of two different subunits, A and B: A_4, A_3B, A_2B_2, AB_3, and B_4 (Figure 15.6). The kinetic properties of the various LDH isozymes differ in terms of their relative affinities for the various substrates and their sensitivity to inhibition by product. Different tissues express different isozyme forms, as appropriate to their particular metabolic needs. By regulating the relative

Classification of Protein Kinases

Protein Kinase Class	Target Sequence*	Activators
I. Ser/Thr protein kinases		
A. Cyclic nucleotide–dependent		
cAMP-dependent (PKA)	—R(R/K)X(S*/T*)—	cAMP
cGMP-dependent	—(R/K)KKX(S*/T*)—	cGMP
B. Ca^{2+}-calmodulin (CaM)–dependent		
Phosphorylase kinase (PhK)	—KRKQIS*VRGL—	phosphorylation by PKA
Myosin light-chain kinase (MLCK)	—KKRPQRATS*NV—	Ca^{2+}CaM
C. Protein kinase C (PKC)		Ca^{2+}, diacylglycerol
D. Mitogen-activated protein kinases	—PXX(S*/T*)P—	phosphorylation
(MAP kinases)		by MAPK kinase
E. G protein–coupled receptors		
β-Adrenergic receptor kinase (BARK)		
Rhodopsin kinase		
II. Ser/Thr/Tyr protein kinases		
MAP kinase kinase (MAPK kinase)	—TEY—	phosphorylation by *Raf* (a protein kinase)
III. Tyr protein kinases		
A. Cytosolic tyrosine kinases (*src, fgr, abl,* etc.)		
B. Receptor tyrosine kinases (RTKs)		
Plasma membrane receptors for hormones such as *epidermal growth factor* (EGF) or *platelet-derived growth factor* (PDGF)		

*X denotes any amino acid.
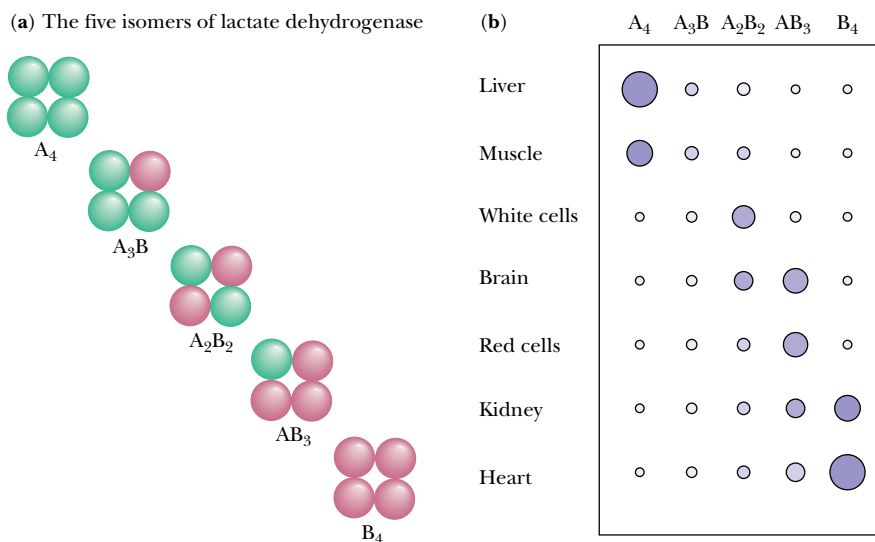
FIGURE 15.6 • The isozymes of lactate dehydrogenase (LDH). Active muscle tissue becomes anaerobic and produces pyruvate from glucose via glycolysis (Chapter 19). It needs LDH to regenerate NAD^+ from NADH so glycolysis can continue. The lactate produced is released into the blood. The muscle LDH isozyme (A_4) works best in the NAD^+-regenerating direction. Heart tissue is aerobic and uses lactate as a fuel, converting it to pyruvate via LDH and using the pyruvate to fuel the citric acid cycle to obtain energy. The heart LDH isozyme (B_4) is inhibited by excess pyruvate so the fuel won't be wasted.

amounts of A and B subunits they synthesize, the cells of various tissues control which isozymic forms are likely to assemble, and, thus, which kinetic parameters prevail.

Modulator Proteins

Modulator proteins are yet another way that cells mediate metabolic activity. **Modulator proteins** are proteins that bind to enzymes, and by binding, influence the activity of the enzyme. For example, some enzymes, such as *cAMP-dependent protein kinase* (Chapter 23), exist as dimers of catalytic subunits and regulatory subunits. These regulatory subunits are *modulator proteins* that suppress the activity of the catalytic subunits. Dissociation of the regulatory subunits (modulator proteins) activates the catalytic subunits; reassociation once again suppresses activity (Figure 15.7). **Phosphoprotein phosphatase inhibitor-1 (PPI-1)** is another example of a modulator protein. When PPI-1 is phosphorylated on one of its serine residues, it binds to *phosphoprotein phosphatase* (Figure 15.2), inhibiting its phosphatase activity. The result is an increased phosphorylation of the interconvertible enzyme targeted by the protein kinase/phosphoprotein phosphatase cycle (Figure 15.2). We will meet other important representatives of this class as the processes of metabolism unfold in subsequent chapters. For now, let us focus our attention on the fascinating kinetics of allosteric enzymes.

15.3 • The Allosteric Regulation of Enzyme Activity

Allosteric regulation acts to modulate enzymes situated at key steps in metabolic pathways. Consider as an illustration the following pathway, where A is the precursor for formation of an end product, F, in a sequence of five enzyme-catalyzed reactions:

$$A \xrightarrow{\text{enz 1}} B \xrightarrow{\text{enz 2}} C \xrightarrow{\text{enz 3}} D \xrightarrow{\text{enz 4}} E \xrightarrow{\text{enz 5}} F$$
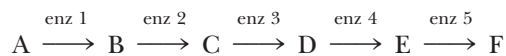
In this scheme, F symbolizes an essential metabolite, such as an amino acid or a nucleotide. In such systems, F, the essential end product, inhibits *enzyme 1,* the *first step* in the pathway. Therefore, when sufficient F is synthesized, it blocks further synthesis of itself. This phenomenon is called **feedback inhibition** or **feedback regulation.**
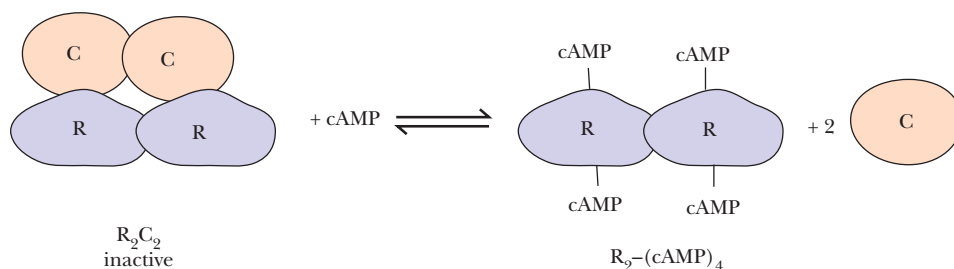
FIGURE 15.7 • Cyclic AMP–dependent protein kinase (also known as *PKA*) is a 150- to 170-kD R_2C_2 tetramer in mammalian cells. The two R (regulatory) subunits bind cAMP ($K_D = 3 \times 10^{-8}$ *M*); cAMP binding releases the R subunits from the C (catalytic) subunits. C subunits are enzymatically active as monomers.

General Properties of Regulatory Enzymes

Enzymes such as enzyme 1, which are subject to feedback regulation, represent a distinct class of enzymes, the **regulatory enzymes.** As a class, these enzymes have certain exceptional properties:

1. Their kinetics do not obey the Michaelis–Menten equation. Their v versus [S] plots yield **sigmoid-** or **S-shaped** curves rather than rectangular hyperbolas (Figure 15.8). Such curves suggest a second-order (or higher) relationship between v and [S]; that is, v is proportional to $[S]^n$, where $n > 1$. A qualitative description of the mechanism responsible for the S-shaped curves is that binding of one S to a protein molecule makes it easier for additional substrate molecules to bind to the same protein molecule. In the jargon of allostery, substrate binding is **cooperative.**

2. Inhibition of a regulatory enzyme by a feedback inhibitor does not conform to any normal inhibition pattern, and the feedback inhibitor F bears little structural similarity to A, the substrate for the regulatory enzyme. F apparently acts at a binding site distinct from the substrate-binding site. The term *allosteric* is apt, because F is sterically dissimilar and, moreover, acts at a site other than the site for S. Its effect is called **allosteric inhibition.**

3. Regulatory or allosteric enzymes like enzyme 1 are, in some instances, regulated by activation. That is, whereas some effector molecules such as F exert negative effects on enzyme activity, other effectors show stimulatory, or positive, influences on activity.

4. Allosteric enzymes have an oligomeric organization. They are composed of more than one polypeptide chain (subunit) and have more than one S-binding site per enzyme molecule.

5. The working hypothesis is that, by some means, interaction of an allosteric enzyme with effectors alters the distribution of conformational possibilities or subunit interactions available to the enzyme. That is, the regulatory effects exerted on the enzyme's activity are achieved by conformational changes occurring in the protein when effector metabolites bind.

In addition to enzymes, noncatalytic proteins may exhibit many of these properties; hemoglobin is the classic example. The allosteric properties of hemoglobin are the subject of a Special Focus beginning on page 480.
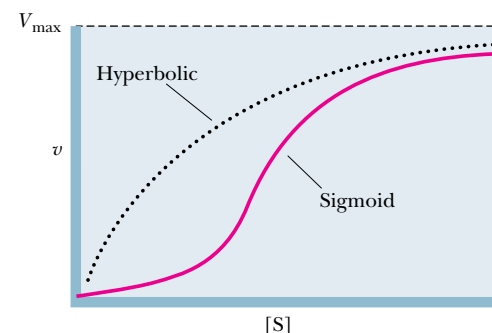
FIGURE 15.8 • Sigmoid v versus [S] plot. The dotted line represents the hyperbolic plot characteristic of normal Michaelis–Menten-type enzyme kinetics.

15.4 • Models for the Allosteric Behavior of Proteins

The Symmetry Model of Monod, Wyman, and Changeux

In 1965, Jacques Monod, Jeffries Wyman, and Jean-Pierre Changeux proposed a theoretical model of allosteric transitions based on the observation that allosteric proteins are oligomers. They suggested that allosteric proteins can exist in (at least) two conformational states, designated **R,** signifying "relaxed," and **T,** or "taut," and that, in each protein molecule, all of the subunits have the same conformation (either R or T). That is, molecular symmetry is conserved. Molecules of mixed conformation (having subunits of both R and T states) are not allowed by this model.

In the absence of ligand, the two states of the allosteric protein are in equilibrium:

$$R_0 \Longrightarrow T_0$$

(Note that the subscript "0" signifies "in the absence of ligand.") The equilibrium constant is termed L: $L = T_0/R_0$. L is assumed to be large; that is, the

(a) A dimeric protein can exist in either of two conformational states at equilibrium.

R_0 T_0
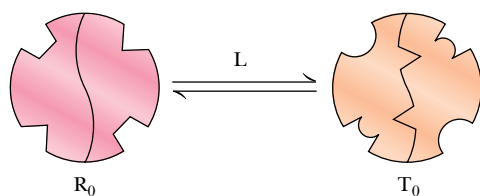
$$L = \frac{T_0}{R_0} \qquad L \text{ is large. } (T_0 >> R_0)$$

(b) Substrate binding shifts equilibrium in favor of R.

F_R S_T

S_R F_T
(substrate   (effector or
binding site) allosteric
              binding site)

Substrate

Substrate bound
R_1
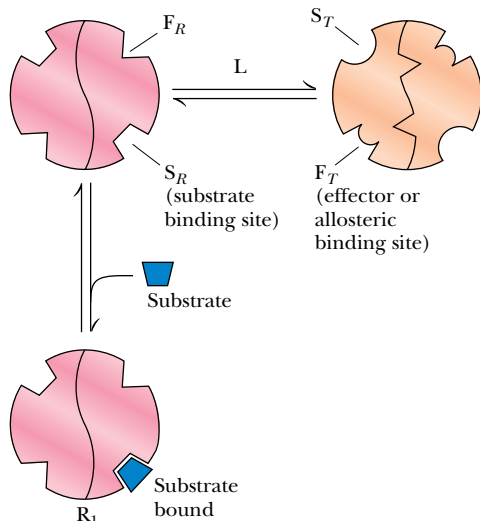
FIGURE 15.9 • Monod–Wyman–Changeux (MWC) model for allosteric transitions. Consider a dimeric protein that can exist in either of two conformational states, R or T. Each subunit in the dimer has a binding site for substrate S and an allosteric effector site, F. The promoters are symmetrically related to one another in the protein, and symmetry is conserved regardless of the conformational state of the protein. The different states of the protein, with or without bound ligand, are linked to one another through the various equilibria. Thus, the relative population of protein molecules in the R or T state is a function of these equilibria and the concentration of the various ligands, substrate (S), and effectors (which bind at F_R or F_T). As [S] is increased, the T/R equilibrium shifts in favor of an increased proportion of R-conformers in the total population (that is, more protein molecules in the R conformational state).

amount of the protein in the T conformational state is much greater than the amount in the R conformation. Let us suppose that $L = 10^4$.

The affinities of the two states for substrate, S, are characterized by the respective dissociation constants, K_R and K_T. The model supposes that $K_T >> K_R$. That is, the affinity of R_0 for S is much greater than the affinity of T_0 for S. Let us choose the extreme where $K_R/K_T = 0$ (that is, K_T is infinitely greater than K_R). In effect, we are picking conditions where S binds only to R. (If K_T is infinite, T does not bind S.)

Given these parameters, consider what happens when S is added to a solution of the allosteric protein at conformational equilibrium (Figure 15.9). Although the relative $[R_0]$ concentration is small, S will bind "only" to R_0, forming R_1. This depletes the concentration of R_0, perturbing the T_0/R_0 equilibrium. To restore equilibrium, molecules in the T_0 conformation undergo a transition to R_0. This shift renders more R_0 available to bind S, yielding R_1, diminishing $[R_0]$, perturbing the T_0/R_0 equilibrium, and so on. Thus, these linked equilibria (Figure 15.9) are such that S-binding by the R_0 state of the allosteric protein perturbs the T_0/R_0 equilibrium with the result that S-binding drives the conformational transition, $T_0 \rightarrow R_0$.

In just this simple system, *cooperativity* is achieved because each subunit has a binding site for S, and thus, *each protein molecule has more than one binding site for S*. Therefore, the increase in the population of R conformers gives a progressive increase in the number of sites available for S. The extent of cooperativity depends on the relative T_0/R_0 ratio and the relative affinities of R and T for S. If L is large (that is, the equilibrium lies strongly in favor of T_0) and if $K_T >> K_R$, as in the example we have chosen, cooperativity is great (Figure 15.10). Ligands such as S here that bind in a cooperative manner, so that binding of one equivalent enhances the binding of additional equivalents of S to the same protein molecule, are termed **positive homotropic effectors.** (The prefix "homo" indicates that the ligand influences the binding of like molecules.)
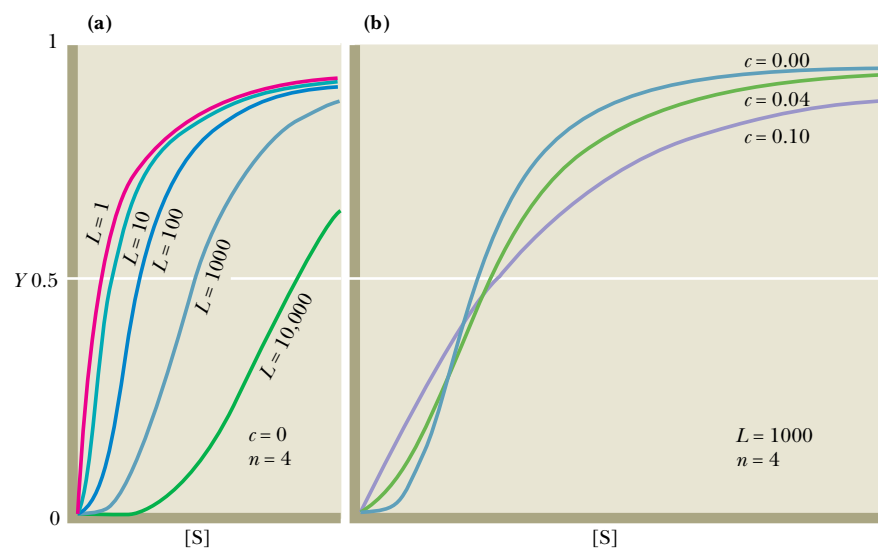
FIGURE 15.10 • The Monod–Wyman–Changeux model. Graphs of allosteric effects for a tetramer ($n = 4$) in terms of Y, the saturation function, versus [S]. Y is defined as [ligand-binding sites that are occupied by ligand]/[total ligand-binding sites]. (a) A plot of Y as a function of [S], at various L values. (b) Y as a function of [S], at different c, where $c = K_R/K_T$. (When $c = 0$, K_T is infinite.) *(Adapted from Monod, J., Wyman, J., and Changeux, J.-P., 1965. On the nature of allosteric transitions: A plausible model.* Journal of Molecular Biology **12**:92.)

Heterotropic Effectors

This simple system also provides an explanation for the more complex substrate-binding responses to positive and negative effectors. Effectors that influence the binding of something other than themselves are termed **heterotropic effectors.** For example, effectors that promote S binding are termed **positive heterotropic effectors** or **allosteric activators.** Effectors that diminish S binding are **negative heterotropic effectors** or **allosteric inhibitors.** Feedback inhibitors fit this class. Consider a protein composed of two subunits, each of which has two binding sites: one for the substrate, S, and one to which allosteric effectors bind, the *allosteric site.* Assume that S binds preferentially ("only") to the R conformer; further assume that the *positive heterotropic effector,* A, binds to the allosteric site only when the protein is in the R conformation, and the *negative allosteric effector,* I, binds at the allosteric site only if the protein is in the T conformation. Thus, with respect to binding at the allosteric site, A and I are competitive with each other.

Positive Effectors

If A binds to R_0, forming the new species $R_{1(A)}$, the relative concentration of R_0 is decreased and the T_0/R_0 equilibrium is perturbed (Figure 15.11). As a consequence, a relative $T_0 \rightarrow R_0$ shift occurs in order to restore equilibrium. The net effect is an increase in the number of R conformers in the presence of A, meaning that more binding sites for S are available. For this reason, A

A dimeric protein which can exist in either of two states R_0 and T_0. This protein can bind 3 ligands:

1) Substrate (S) ▢ : A positive homotropic effector that binds only to R at site S

2) Activator (A) ◣ : A positive heterotropic effector that binds only to R at site F

3) Inhibitor (I) ◥ : A negative heterotropic effector that binds only to T at site F

Effects of A:
$A + R_0 \rightarrow R_{1(A)}$
Increase in number of R-conformers shifts $R_0 \rightleftharpoons T_0$ so that $T_0 \rightarrow R_0$

1) More binding sites for S made available

2) Decrease in cooperativity of substrate saturation curve. Effector A lowers the apparent value of L.

Effects of I:
$I + T_0 \rightarrow T_{1(I)}$
Increase in number of T-conformers (decrease in R_0 as $R_0 \rightarrow T_0$ to restore equilibrium).

Thus, I inhibits association of S and A with R by lowering R_0 level. I increases cooperativity of substrate saturation curve. I raises the apparent value of L.

FIGURE 15.11 • Heterotropic allosteric effects: A and I binding to R and T, respectively. The linked equilibria lead to changes in the relative amounts of R and T and, therefore, shifts in the substrate saturation curve. This behavior, depicted by the graph, defines an allosteric "K" system. The parameters of such a system are: (1) S and A (or I) have different affinities for R and T and (2) A (or I) modifies the apparent $K_{0.5}$ for S by shifting the relative R versus T population.

An Alternative Allosteric Model: The Sequential Allosteric Model of Koshland, Nemethy, and Filmer

Daniel Koshland has championed the idea that proteins are inherently flexible molecules whose conformations are altered when ligands bind. This notion serves as the fundamental tenet of the "induced-fit hypothesis" discussed earlier. Because this is so, ligand binding can potentially cause conformational changes in the protein. Depending on the nature of these conformational changes, virtually any sort of allosteric interaction is possible. That is, the binding of one ligand could result in conformational transitions in the protein that make it easier or harder for other ligands (of the same or different kinds) to bind. In 1966, Koshland and his colleagues proposed an allosteric model in which ligand-induced conformational changes caused transition to a conformational state with altered affinities. Because ligand binding and conformational transitions were distinct steps in a sequential pathway, the Koshland, Nemethy, Filmer (or KNF) model is dubbed the **sequential model** for allosteric transitions. The figure depicts the essential features of this model in a hypothetical dimeric protein. Binding of the ligand S induces a conformational change in the subunit to which it binds. Note that there is no requirement for conservation of symmetry here; the two subunits can assume different conformations (represented as a square and a circle). If the *subunit interactions are tightly coupled,* then binding of S to one subunit could cause the other subunit(s) to assume a conformation having a greater, or a lesser, affinity for S (or some other ligand). The underlying mechanism rests on the fact that the ligand-induced conformational change in one subunit can transmit its effects to neighboring subunits by changing the interactions and alignments of amino acid residues at the interface between subunits. Depending on the relative ligand affinity of the conformation adopted by the neighboring subunit, the overall effect for further ligand binding may be positive, negative, or neutral (figure).

(**a**) Binding of S induces a conformational change.

Symmetric protein dimer → Asymmetric protein dimer
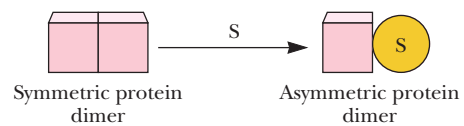
(**b**)

Transmitted conformational change
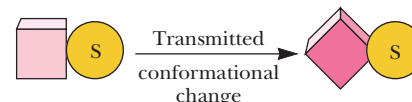
If the relative affinities of the various conformations for S are:

□ < ◆ ≤ S

positive homotropic effects ensue.

If the relative affinities of the various conformations for S are:

◆ < □ < S
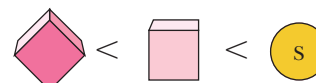
negative homotropic effects are seen.

The Koshland–Nemethy–Filmer sequential model for allosteric behavior. (a) S-binding can, by induced fit, cause a conformational change in the subunit to which it binds. (b) If subunit interactions are tightly coupled, binding of S to one subunit may cause the other subunit to assume a conformation having a greater (positive homotropic) or lesser (negative homotropic) affinity for S. That is, the ligand-induced conformational change in one subunit can affect the adjoining subunit. Such effects could be transmitted between neighboring peptide domains by changing alignments of nonbonded amino acid residues.

leads to a decrease in the cooperativity of the substrate saturation curve, as seen by a shift of this curve to the left (Figure 15.11). Effectively, the presence of A lowers the apparent value of *L*.

Negative Effectors

The converse situation applies in the presence of I, which binds "only" to T. I-binding will lead to an increase in the population of T conformers, at the expense of R_0 (Figure 15.11). The decline in $[R_0]$ means that it is less likely for S (or A) to bind. Consequently, the presence of I increases the cooperativity (that is, the sigmoidicity) of the substrate saturation curve, as evidenced by the shift of this curve to the right (Figure 15.11). The presence of I raises the apparent value of *L*.

K Systems and *V* Systems

The allosteric model just presented is called a ***K* system** because the concentration of substrate giving half-maximal velocity, defined as $K_{0.5}$, changes in response to effectors (Figure 15.11). Note that V_{max} is constant in this system.

An allosteric situation where $K_{0.5}$ is constant but the apparent V_{max} changes in response to effectors is termed a ***V* system.** In a *V* system, all *v* versus S plots are hyperbolic rather than sigmoid (Figure 15.12). The positive heterotropic effector A activates by raising V_{max}, whereas I, the negative heterotropic effector, decreases it. Note that neither A nor I affects $K_{0.5}$. This situation arises if R and T have the *same* affinity for the substrate, S, but differ in their catalytic ability and their affinities for A and I. A and I thus can shift the relative T/R distribution. Acetyl-coenzyme A carboxylase, the enzyme catalyzing the committed step in the fatty acid biosynthetic pathway, behaves as a *V* system in response to its allosteric activator, citrate (see Chapter 25).

K Systems and *V* Systems Fill Different Biological Roles

The *K* and *V* systems have design features that mean they work best under different physiological situations. "*K* system" enzymes are adapted to conditions in which the prevailing substrate concentration is rate-limiting, as when [S] *in vivo* ≈ $K_{0.5}$. On the other hand, when the physiological conditions are such that [S] is usually saturating for the regulatory enzyme of interest, the enzyme conforms to the "*V* system" mode in order to have an effective regulatory response.

15.5 • Glycogen Phosphorylase: Allosteric Regulation and Covalent Modification

The Glycogen Phosphorylase Reaction

The cleavage of glucose units from the nonreducing ends of glycogen molecules is catalyzed by **glycogen phosphorylase,** an allosteric enzyme. The enzymatic reaction involves phosphorolysis of the bond between C-1 of the departing glucose unit and the glycosidic oxygen, to yield *glucose-1-phosphate* and a glycogen molecule that is shortened by one residue (Figure 15.13). (Because

FIGURE 15.12 • *v* versus [S] curves for an allosteric "V" system. The V system fits the model of Monod, Wyman, and Changeux, given the following conditions: (1) R and T have the *same* affinity for the substrate, S. (2) The effectors A and I have different affinities for R and T and thus can shift the relative T/R distribution. (That is, A and I change the apparent value of *L*.) Assume as before that A binds "only" to the R state and I binds "only" to the T state. (3) R and T differ in their catalytic ability. Assume that R is the enzymatically active form, whereas T is inactive. Because A perturbs the T/R equilibrium in favor of more R, A increases the apparent V_{max}. I favors transition to the inactive T state.

FIGURE 15.13 • The glycogen phosphorylase reaction.

FIGURE 15.14 • The phosphoglucomutase reaction.

Glucose-1-phosphate   Glucose-6-phosphate
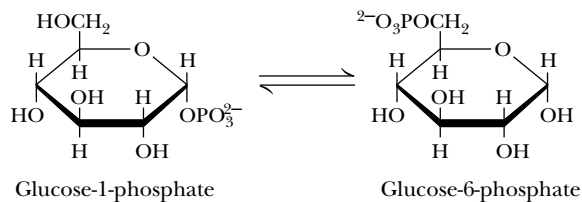
the reaction involves attack by phosphate instead of H_2O, it is referred to as a **phosphorolysis** rather than a hydrolysis.) Phosphorolysis produces a phosphorylated sugar product, glucose-1-P, which is converted to the glycolytic substrate, glucose-6-P, by *phosphoglucomutase* (Figure 15.14). In muscle, glucose-6-P proceeds into glycolysis, providing needed energy for muscle contraction. In liver, hydrolysis of glucose-6-P yields glucose, which is exported to other tissues via the circulatory system.

The Structure of Glycogen Phosphorylase

Muscle glycogen phosphorylase is a dimer of two identical subunits (842 residues, 97.44 kD). Each subunit contains a pyridoxal phosphate cofactor, covalently linked as a Schiff base to Lys^{680}. Each subunit contains an active site (at the center of the subunit) and an allosteric effector site near the subunit interface (Figure 15.15). In addition, a regulatory phosphorylation site is located at Ser^{14} on each subunit. A glycogen-binding site on each subunit facilitates prior association of glycogen phosphorylase with its substrate and also exerts regulatory control on the enzymatic reaction.
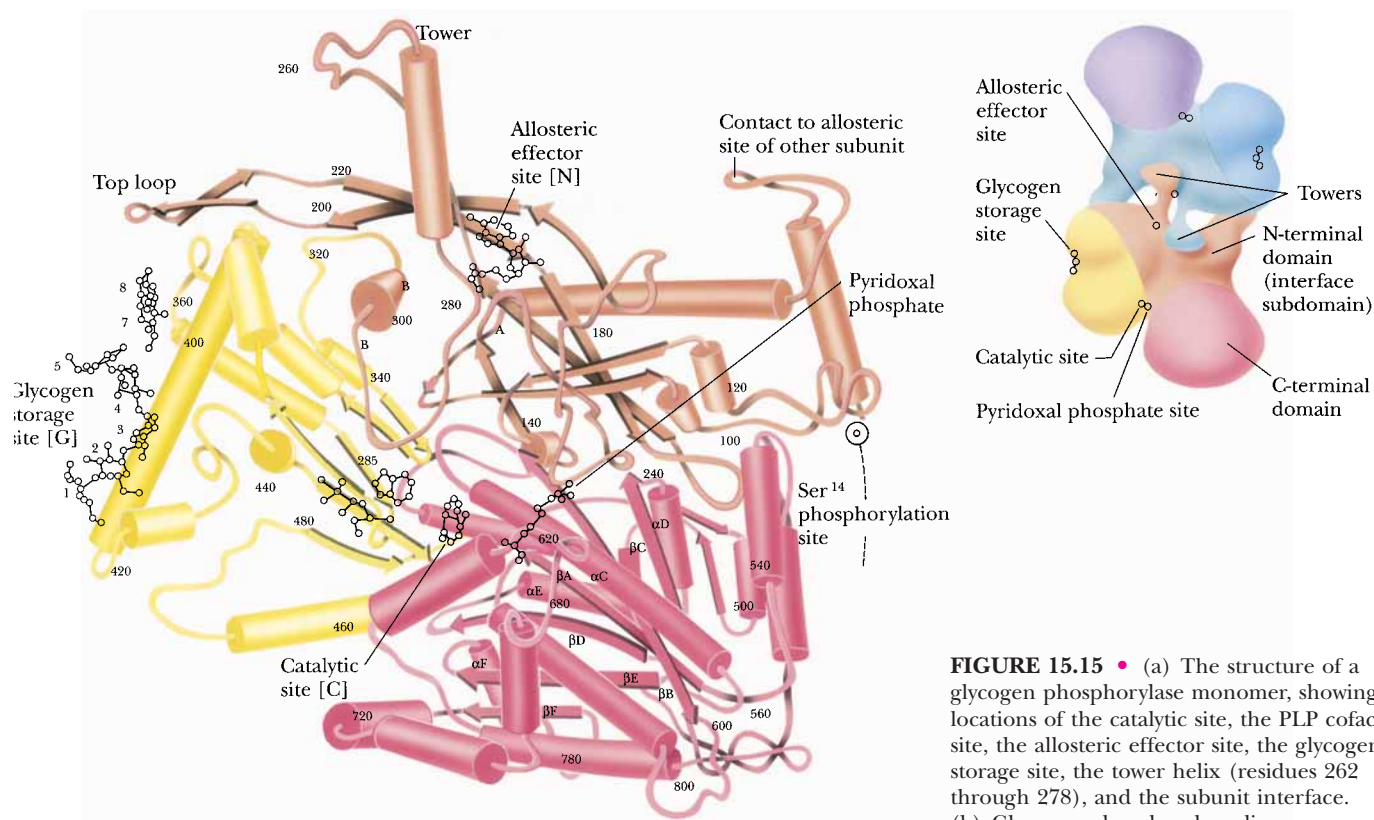
FIGURE 15.15 • (a) The structure of a glycogen phosphorylase monomer, showing the locations of the catalytic site, the PLP cofactor site, the allosteric effector site, the glycogen storage site, the tower helix (residues 262 through 278), and the subunit interface. (b) Glycogen phosphorylase dimer.

Each subunit contributes a tower helix (residues 262 to 278) to the sub-unit–subunit contact interface in glycogen phosphorylase. In the phosphory-lase dimer, the tower helices extend from their respective subunits and pack against each other in an antiparallel manner.

Regulation of Glycogen Phosphorylase by Allosteric Effectors

Muscle Glycogen Phosphorylase Shows Cooperativity in Substrate Binding

The binding of the substrate *inorganic phosphate* (P_i) to muscle glycogen phos-phorylase is highly cooperative (Figure 15.16a), which allows the enzyme activ-ity to increase markedly over a rather narrow range of substrate concentration. P_i is a *positive homotropic effector* with regard to its interaction with glycogen phos-phorylase.

ATP and Glucose-6-P Are Allosteric Inhibitors of Glycogen Phosphorylase

ATP can be viewed as the "end product" of glycogen phosphorylase action, in that the glucose-1-P liberated by glycogen phosphorylase is degraded in mus-cle via metabolic pathways whose purpose is energy (ATP) production. Glucose-1-P is readily converted into glucose-6-P to feed such pathways. (In the liver, glucose-1-P from glycogen is converted to glucose and released into the blood-stream to raise blood glucose levels.) Thus, feedback inhibition of glycogen phosphorylase by ATP and glucose-6-P provides a very effective way to regu-late glycogen breakdown. Both ATP and glucose-6-P act by decreasing the affin-ity of glycogen phosphorylase for its substrate P_i (Figure 15.16b). Because the binding of ATP or glucose-6-P has a negative effect on substrate binding, these substances act as *negative heterotropic effectors*. Note in Figure 15.16b that the sub-strate saturation curve is displaced to the right in the presence of ATP or glu-cose-6-P, and a higher substrate concentration is needed to achieve half-maxi-mal velocity ($V_{max}/2$). When concentrations of ATP or glucose-6-P accumulate to high levels, glycogen phosphorylase is inhibited; when [ATP] and [glucose-6-P] are low, the activity of glycogen phosphorylase is regulated by availability of its substrate, P_i.

AMP Is an Allosteric Activator of Glycogen Phosphorylase

AMP also provides a regulatory signal to glycogen phosphorylase. It binds to the same site as ATP, but it stimulates glycogen phosphorylase rather than inhibiting it (Figure 15.16c). AMP acts as a *positive heterotropic effector,* meaning that it enhances the binding of substrate to glycogen phosphorylase. Significant levels of AMP indicate that the energy status of the cell is low and that more

FIGURE 15.16 • *v* versus S curves for glyco-gen phosphorylase. (a) The sigmoid response of glycogen phosphorylase to the concentration of the substrate phosphate (P_i) shows strong positive cooperativity. (b) ATP is a feedback inhibitor that affects the affinity of glycogen phosphorylase for its substrates but does not affect V_{max}. (Glucose-6-P shows similar effects on glycogen phosphorylase.) (c) AMP is a posi-tive heterotropic effector for glycogen phos-phorylase. It binds at the same site as ATP. AMP and ATP are competitive. Like ATP, AMP affects the affinity of glycogen phosphorylase for its substrates, but does not affect V_{max}.

(a)

(b)
+ ATP

(c)
+ AMP
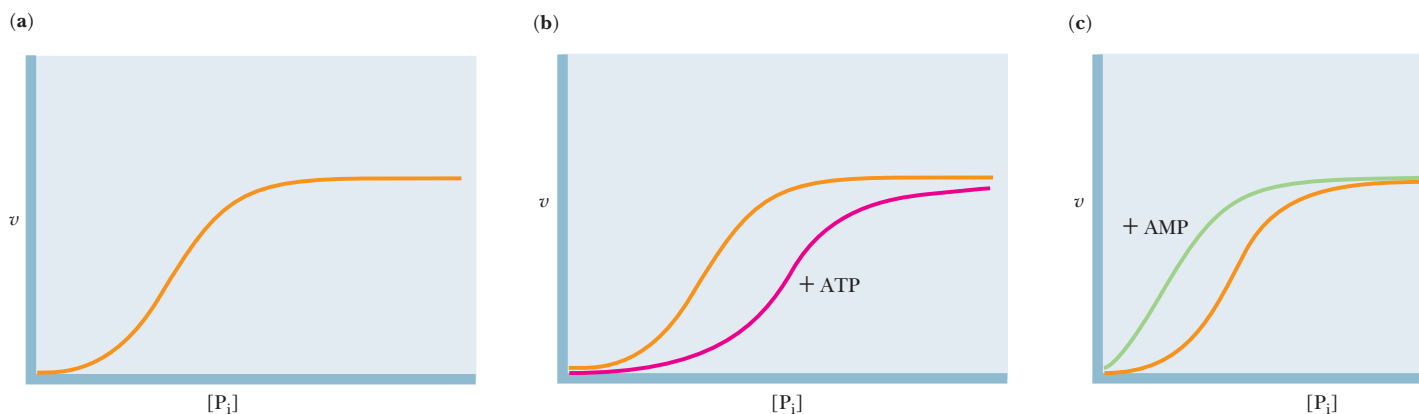
energy (ATP) should be produced. Reciprocal changes in the cellular concentrations of ATP and AMP and their competition for binding to the same site (the *allosteric site*) on glycogen phosphorylase, with opposite effects, allow these two nucleotides to exert *rapid and reversible control* over glycogen phosphorylase activity. Such reciprocal regulation ensures that the production of energy (ATP) is commensurate with cellular needs.

To summarize, muscle glycogen phosphorylase is allosterically activated by AMP and inhibited by ATP and glucose-6-P; caffeine can also act as an allosteric inhibitor (Figure 15.17). When ATP and glucose-6-P are abundant, glycogen breakdown is inhibited. When cellular energy reserves are low (i.e., high [AMP] and low [ATP] and [G-6-P]), glycogen catabolism is stimulated.

Glycogen phosphorylase conforms to the Monod–Wyman–Changeux model of allosteric transitions, with the active form of the enzyme designated the **R state** and the inactive form denoted as the **T state** (Figure 15.17). Thus, AMP promotes the conversion to the active R state, whereas ATP, glucose-6-P, and caffeine favor conversion to the inactive T state.

X-ray diffraction studies of glycogen phosphorylase in the presence of allosteric effectors have revealed the molecular basis for the T $\Longleftrightarrow$ R conversion. Although the structure of the central core of the phosphorylase subunits is identical in the T and R states, a significant change occurs at the subunit interface between the T and R states. This conformation change at the subunit interface is linked to a structural change at the active site that is important for catalysis. In the T state, the negatively charged carboxyl group of Asp^{283} faces the active site, so that binding of the anionic substrate phosphate is unfavorable. In the conversion to the R state, Asp^{283} is displaced from the active site and replaced by Arg^{569}. The exchange of negatively charged aspartate for positively charged arginine at the active site provides a favorable binding site for phosphate. These allosteric controls serve as a mechanism for adjusting the activity of glycogen phosphorylase to meet normal metabolic demands. However, in crisis situations in which abundant energy (ATP) is needed imme-

FIGURE 15.17 • The mechanism of covalent modification and allosteric regulation of glycogen phosphorylase. The T states are blue and the R states blue-green.
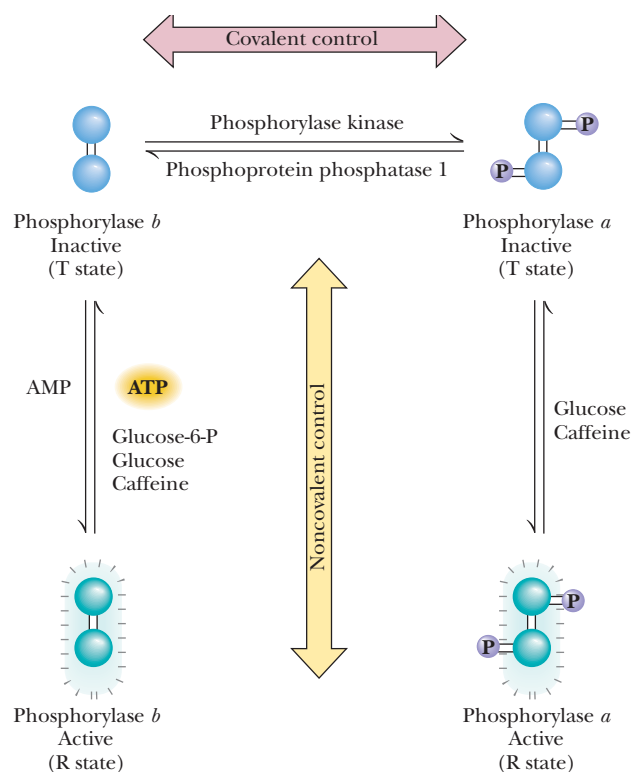
diately, these controls can be overridden by covalent modification of glycogen phosphorylase. Covalent modification through phosphorylation of Ser^{14} in glycogen phosphorylase converts the enzyme from a less active, allosterically regulated form (the *b* form) to a more active, allosterically unresponsive form (the *a* form). Covalent modification is like a "permanent" allosteric transition that is independent of [allosteric effector], such as AMP.

Regulation of Glycogen Phosphorylase by Covalent Modification

As early as 1938, it was known that glycogen phosphorylase existed in two forms: the less active **phosphorylase *b*** and the more active **phosphorylase *a*.** In 1956, Edwin Krebs and Edmond Fischer reported that a "converting enzyme" could convert phosphorylase *b* to phosphorylase *a.* Three years later, Krebs and Fischer demonstrated that the conversion of phosphorylase *b* to phosphorylase *a* involved covalent phosphorylation, as in Figure 15.17.

Phosphorylation of Ser^{14} causes a dramatic conformation change in phosphorylase. Upon phosphorylation, the amino-terminal end of the protein (including residues 10 through 22) swings through an arc of 120°, moving into the subunit interface (Figure 15.18). This conformation change moves Ser^{14} by more than 3.6 nm.
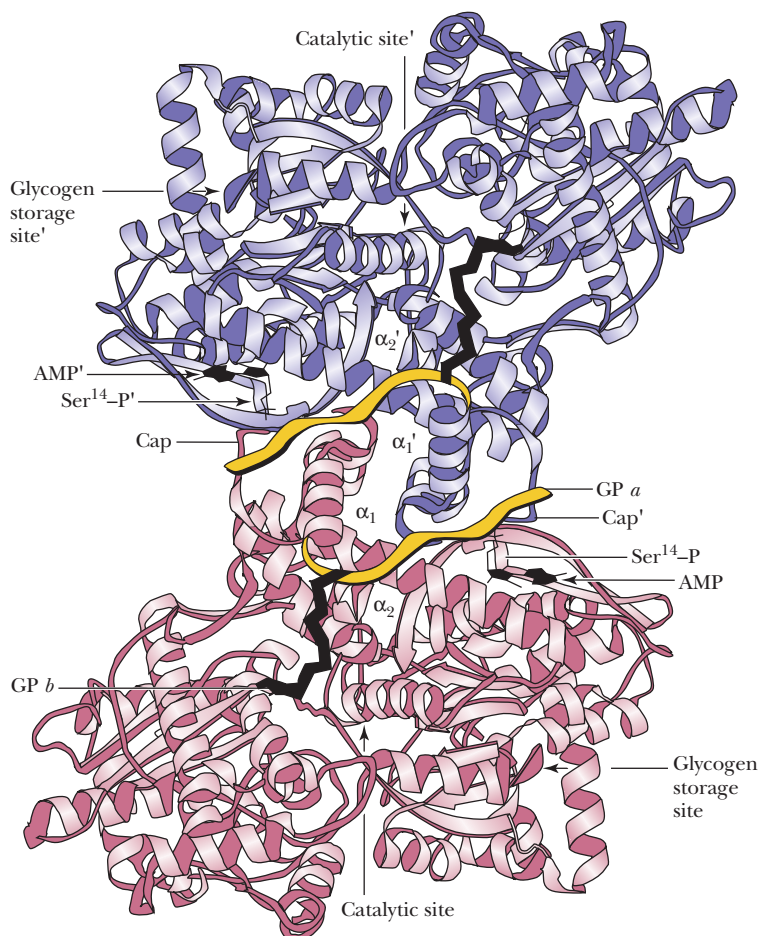
FIGURE 15.18 • In this diagram of the glycogen phosphorylase dimer, the phosphorylation site (Ser^{14}) and the allosteric (AMP) site face the viewer. Access to the catalytic site is from the opposite side of the protein. The diagram shows the major conformational change that occurs in the N-terminal residues upon phosphorylation of Ser^{14}. The solid black line shows the conformation of residues 10 to 23 in the *b,* or unphosphorylated, form of glycogen phosphorylase. The conformational change in the location of residues 10 to 23 upon phosphorylation of Ser^{14} to give the *a* (phosphorylated) form of glycogen phosphorylase is shown in yellow. Note that these residues move from intrasubunit contacts into intersubunit contacts at the subunit interface. (Sites on the two respective subunits are denoted, with those of the upper subunit designated by primes (′).) *(Adapted from Johnson, L. N., and Barford, D., 1993. The effects of phosphorylation on the structure and function of proteins.* Annual Review of Biophysics and Biomolecular Structure **22**:199–232.)
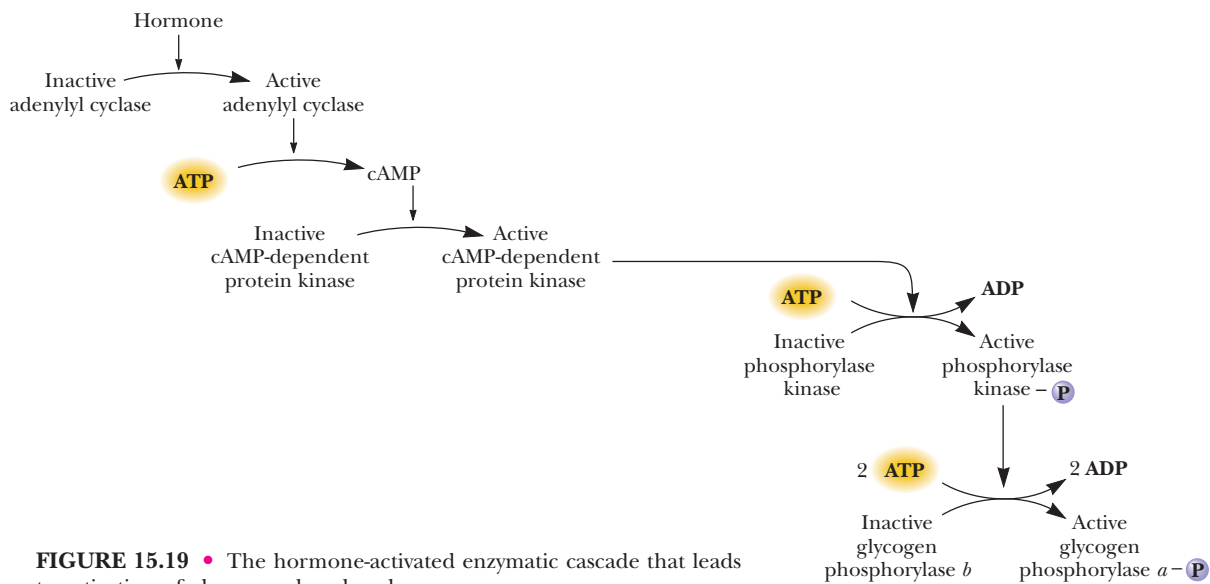
FIGURE 15.19 • The hormone-activated enzymatic cascade that leads to activation of glycogen phosphorylase.

Dephosphorylation of glycogen phosphorylase is carried out by **phospho-protein phosphatase 1.** The action of phosphoprotein phosphatase 1 inactivates glycogen phosphorylase.

Enzyme Cascades Regulate Glycogen Phosphorylase

The phosphorylation reaction that activates glycogen phosphorylase is mediated by an **enzyme cascade** (Figure 15.19). The first part of the cascade leads to hormonal stimulation (described in the next section) of **adenylyl cyclase,** a membrane-bound enzyme that converts ATP to *adenosine-3′,5′-cyclic monophosphate,* denoted as *cyclic AMP* or simply *cAMP* (Figure 15.20). This regulatory molecule is found in all eukaryotic cells and acts as an intracellular messenger molecule, controlling a wide variety of processes. Cyclic AMP is known as a **second messenger** because it is the intracellular agent of a hormone (the "first messenger"). (The myriad cellular roles of cyclic AMP are described in detail in Chapter 34.)
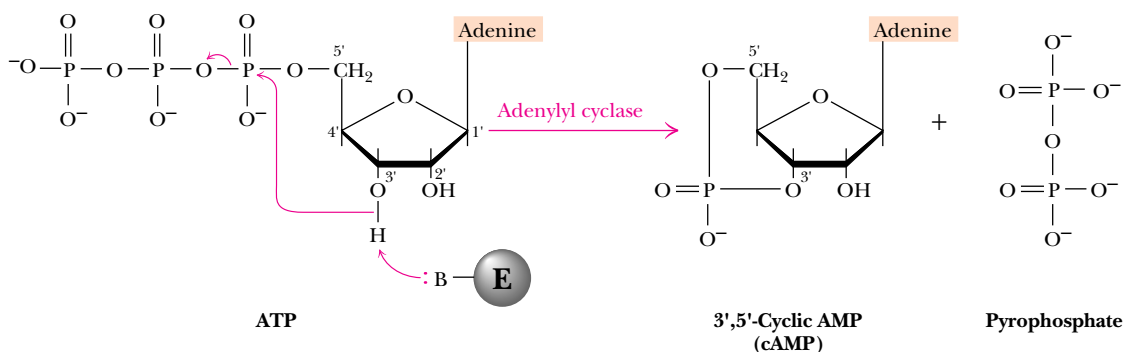
FIGURE 15.20 • The adenylyl cyclase reaction yields 3′,5′-cyclic AMP and pyrophosphate. The reaction is driven forward by subsequent hydrolysis of pyrophosphate by the enzyme inorganic pyrophosphatase.

The hormonal stimulation of adenylyl cyclase is effected by a transmembrane signaling pathway consisting of three components, all membrane-associated. Binding of hormone to the external surface of a hormone receptor causes a conformational change in this transmembrane protein, which in turn stimulates a **GTP-binding protein** (abbreviated **G protein**). G proteins are heterotrimeric proteins consisting of α- (45–47 kD), β- (35 kD), and γ- (7–9 kD) subunits. The α-subunit binds GDP or GTP and has an intrinsic, slow GTPase activity. In the inactive state, the $G_{\alpha\beta\gamma}$ complex has GDP at the nucleotide site. When a G protein is stimulated by a hormone-receptor complex, GDP dissociates and GTP binds to G_{α}, causing it to dissociate from $G_{\beta\gamma}$ and to associate with adenylyl cyclase (Figure 15.21). *Binding of G_{α}(GTP) activates adenylyl cyclase to form cAMP from ATP.* However, the intrinsic GTPase activity of G_{α} eventually hydrolyzes GTP to GDP, leading to dissociation of G_{α}(GDP) from adenylyl cyclase and reassociation with $G_{\beta\gamma}$ to form the inactive $G_{\alpha\beta\gamma}$ complex. This cascade amplifies the hormonal signal because a single hormone-receptor complex can activate many G proteins before the hormone dissociates from the receptor, and because the G_{α}-activated adenylyl cyclase can synthesize many cAMP molecules before bound GTP is hydrolyzed by G_{α}. More than 100 different G protein–coupled receptors and at least 21 distinct G_{α} proteins are known (Chapter 34).

Cyclic AMP is an essential activator of *cAMP-dependent protein kinase (PKA)*. This enzyme is normally inactive because its two catalytic subunits (C) are strongly associated with a pair of regulatory subunits (R), which serve to block activity. Binding of cyclic AMP to the regulatory subunits induces a conformation change that causes the dissociation of the C monomers from the R dimer (Figure 15.7). The free C subunits are active and can phosphorylate other proteins. One of the many proteins phosphorylated by PKA is *phosphorylase kinase* (Figure 15.19). Phosphorylase kinase is inactive in the unphosphorylated state and active in the phosphorylated form. As its name implies, phosphorylase kinase functions to phosphorylate (and activate) glycogen phosphorylase. Thus, stimulation of adenylyl cyclase leads to activation of glycogen breakdown.
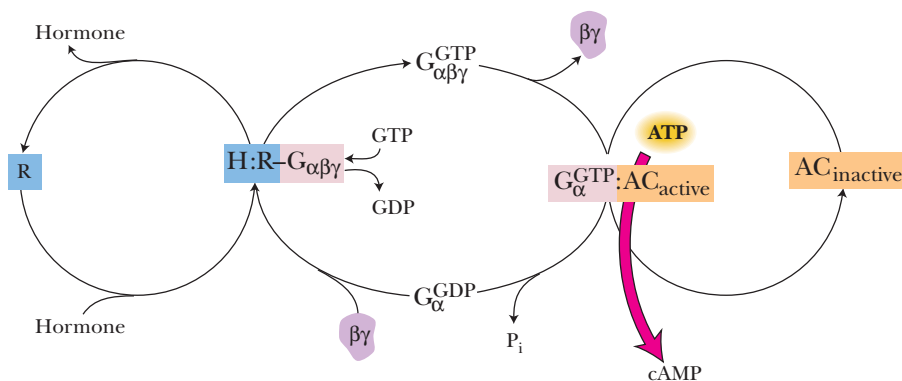
FIGURE 15.21 • Hormone (H) binding to its receptor (R) creates a hormone:receptor complex (H:R) that catalyzes GDP-GTP exchange on the α-subunit of the heterotrimer G protein ($G_{\alpha\beta\gamma}$), replacing GDP with GTP. The G_{α}-subunit with GTP bound dissociates from the $\beta\gamma$-subunits and binds to adenylyl cyclase (AC). AC becomes active upon association with G_{α}:GTP and catalyzes the formation of cAMP from ATP. With time, the intrinsic GTPase activity of the G_{α}-subunit hydrolyzes the bound GTP, forming GDP; this leads to dissociation of G_{α}:GDP from AC, reassociation of G_{α} with the $\beta\gamma$ subunits, and cessation of AC activity. AC and the hormone receptor H are integral plasma membrane proteins; G_{α} and $G_{\beta\gamma}$ are membrane-anchored proteins.

Hemoglobin and Myoglobin—Paradigms of Protein Structure and Function

Ancient life forms evolved in the absence of oxygen and were capable only of anaerobic metabolism. As the earth's atmosphere changed over time, so too did living things. Indeed, the production of O_2 by photosynthesis was a major factor in altering the atmosphere. Evolution to an oxygen-based metabolism was highly beneficial. Aerobic metabolism of sugars, for example, yields far more energy than corresponding anaerobic processes. Two important oxygen-binding proteins appeared in the course of evolution so that aerobic metabolic processes were no longer limited by the solubility of O_2 in water. These proteins are represented in animals as **hemoglobin (Hb)** in blood and **myoglobin (Mb)** in muscle. Because hemoglobin and myoglobin are two of the most-studied proteins in nature, they have become paradigms of protein structure and function. Moreover, hemoglobin is a model for protein quaternary structure and allosteric function. The binding of O_2 by hemoglobin, and its modulation by effectors such as protons, CO_2, and 2,3-bisphosphoglycerate, depend on interactions between subunits in the Hb tetramer. Subunit–subunit interactions in Hb reveal much about the functional significance of quaternary associations and allosteric regulation.

The Comparative Biochemistry of Myoglobin and Hemoglobin

A comparison of the properties of hemoglobin and myoglobin offers insights into allosteric phenomena, even though these proteins are *not* enzymes. Hemoglobin displays sigmoid-shaped O_2-binding curves (Figure 15.22). The unusual shape of these curves was once a great enigma in biochemistry. Such curves closely resemble allosteric enzyme:substrate saturation graphs (see Figure 15.8). In contrast, myoglobin's interaction with oxygen obeys classical Michaelis–Menten-type substrate saturation behavior.

Before examining myoglobin and hemoglobin in detail, let us first encapsulate the lesson: Myoglobin is a compact globular protein composed of a single polypeptide chain 153 amino acids in length; its molecular mass is 17.2 kD (Figure 15.23). It contains **heme,** a porphyrin ring system complexing an iron ion, as its prosthetic group (see Figure 5.15). Oxygen binds to Mb via its heme. Hemoglobin (Hb) is also a compact globular protein, but Hb is a tetramer. It consists of four polypeptide chains, each of which is very similar structurally

FIGURE 15.22 • O_2-binding curves for hemoglobin and myoglobin.
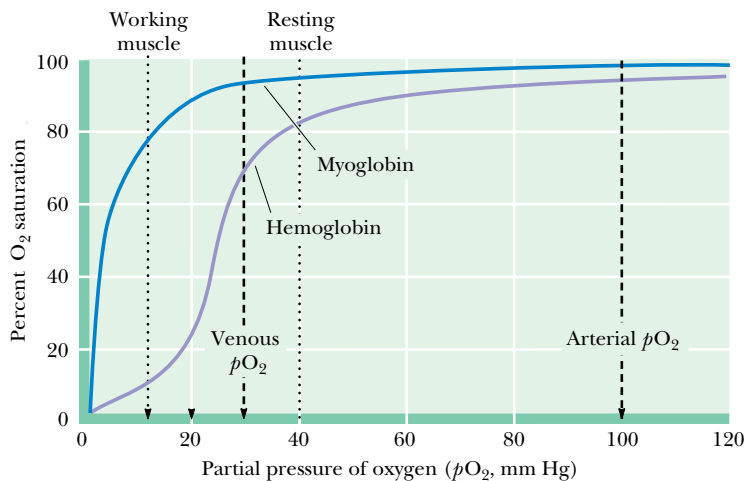
to the myoglobin polypeptide chain, and each bears a heme group. Thus, a hemoglobin molecule can bind four O_2 molecules. In adult human Hb, there are two identical chains of 141 amino acids, the α-chains, and two identical β-chains, each of 146 residues. The human Hb molecule is an $\alpha_2\beta_2$-type tetramer of molecular mass 64.45 kD. The tetrameric nature of Hb is crucial to its biological function: *When a molecule of O_2 binds to a heme in Hb, the heme Fe ion is drawn into the plane of the porphyrin ring. This slight movement sets off a chain of conformational events that are transmitted to adjacent subunits, dramatically enhancing the affinity of their heme groups for O_2.* That is, the binding of O_2 to one heme of Hb makes it easier for the Hb molecule to bind additional equivalents of O_2. Hemoglobin is a marvelously constructed molecular machine. Let us dissect its mechanism, beginning with its monomeric counterpart, the myoglobin molecule.

Myoglobin

Myoglobin is the oxygen-storage protein of muscle. The muscles of diving mammals such as seals and whales are especially rich in this protein, which serves as a store for O_2 during the animal's prolonged periods underwater. Myoglobin is abundant in skeletal and cardiac muscle of nondiving animals as well. Myoglobin is the cause of the characteristic red color of muscle.

The Mb Polypeptide Cradles the Heme Group

The myoglobin polypeptide chain is folded to form a cradle ($4.4 \times 4.4 \times 2.5$ nm) that nestles the heme prosthetic group (Figure 15.24). O_2 binding depends on the heme's oxidation state. The iron ion in the heme of myoglobin is in the $+2$ oxidation state, that is, the *ferrous* form. This is the form that binds O_2. Oxidation of the ferrous form to the $+3$ *ferric* form yields **metmyoglobin,** which will not bind O_2. It is interesting to note that free heme in solution will readily interact with O_2 also, but the oxygen quickly oxidizes the iron atom to the ferric state. Fe^{3+}:protoporphyrin IX is referred to as **hematin.** Thus, the
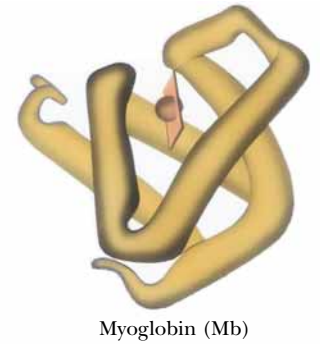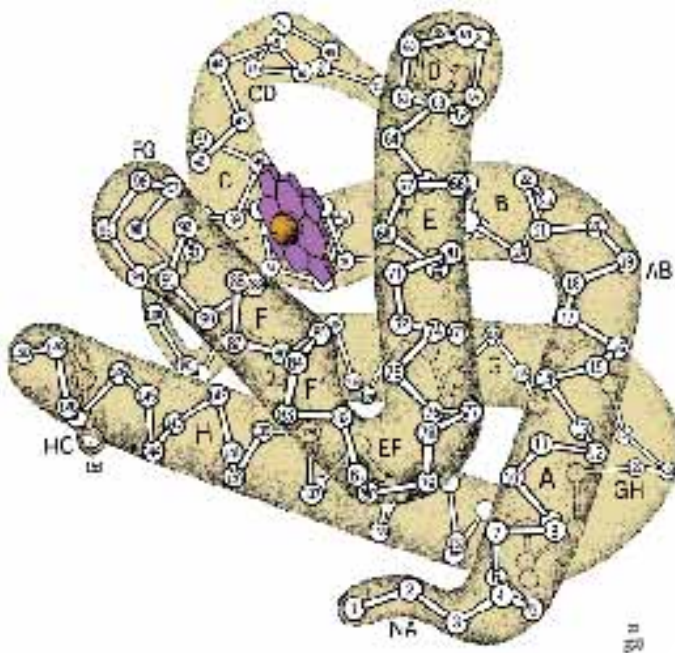
Myoglobin (Mb)
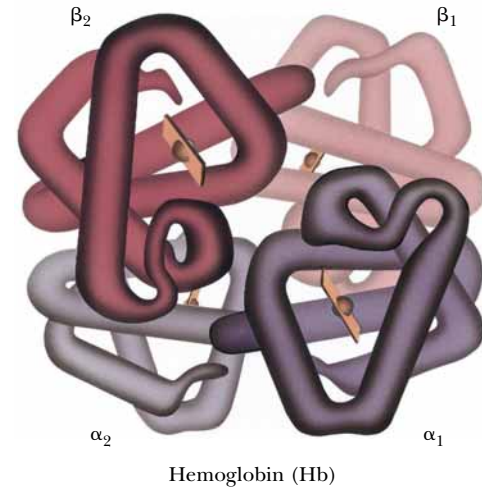
Hemoglobin (Hb)

FIGURE 15.23 • The myoglobin and hemoglobin molecules. *Myoglobin* (sperm whale): one polypeptide chain of 153 aa residues (mass = 17.2 kD) has one heme (mass = 652 D) and binds one O_2. *Hemoglobin* (human): four polypeptide chains, two of 141 aa residues (α) and two of 146 residues (β); mass = 64.45 kD. Each polypeptide has a heme; the Hb tetramer binds four O_2. *(Irving Geis)*

FIGURE 15.24 • Detailed structure of the myoglobin molecule. The myoglobin polypeptide chain consists of eight helical segments, designated by the letters A through H, counting from the N-terminus. These helices, ranging in length from 7 to 26 residues, are linked by short, unordered regions that are named for the helices they connect, as in the AB region or the EF region. The individual amino acids in the polypeptide are indicated according to their position within the various segments, as in His F8, the eighth residue in helix F, or Phe CD1, the first amino acid in the interhelical CD region. Occasionally, amino acids are specified in the conventional way, that is, by the relative position in the chain, as in Gly[153]. The heme group is cradled within the folded polypeptide chain. *(Irving Geis)*

polypeptide of myoglobin may be viewed as serving three critical functions: it cradles the heme group, it protects the heme iron atom from oxidation, and it provides a pocket into which the O_2 can fit.

O_2 Binding to Mb

Iron ions, whether ferrous or ferric, prefer to interact with six ligands, four of which share a common plane. The fifth and sixth ligands lie above and below this plane (see Figure 15.25). In heme, four of the ligands are provided by the nitrogen atoms of the four pyrroles. A fifth ligand is donated by the imidazole side chain of amino acid residue His F8. When myoglobin binds O_2 to become **oxymyoglobin,** the O_2 molecule adds to the heme iron ion as the sixth ligand (Figure 15.25). O_2 adds end on to the heme iron, but it is not oriented perpendicular to the plane of the heme. Rather, it is tilted about 60° with respect to the perpendicular. In **deoxymyoglobin,** the sixth ligand position is vacant, and in metmyoglobin, a water molecule fills the O_2 site and becomes the sixth ligand for the ferric atom. On the oxygen-binding side of the heme lies another histidine residue, His E7. While its imidazole function lies too far away to interact with the Fe atom, it is close enough to contact the O_2. Therefore, the O_2-binding site is a sterically hindered region. Biologically important properties stem from this hindrance. For example, the affinity of *free heme* in solution for carbon monoxide (CO) is 25,000 times greater than its affinity for O_2. But CO only binds 250 times more tightly than O_2 to the heme of myoglobin, because His E7 forces the CO molecule to tilt away from a preferred perpendicular alignment with the plane of the heme (Figure 15.26). This diminished affinity of myoglobin for CO guards against the possibility that traces of CO produced during metabolism might occupy all of the heme sites, effectively preventing O_2 from binding. Nevertheless, CO is a potent poison and can cause death by asphyxiation.

O_2 Binding Alters Mb Conformation

What happens when the heme group of myoglobin binds oxygen? X-ray crystallography has revealed that a crucial change occurs in the position of the iron atom relative to the plane of the heme. In deoxymyoglobin, the ferrous ion has but five ligands, and it lies 0.055 nm above the plane of the heme, in the direction of His F8. The iron:porphyrin complex is therefore dome-shaped.
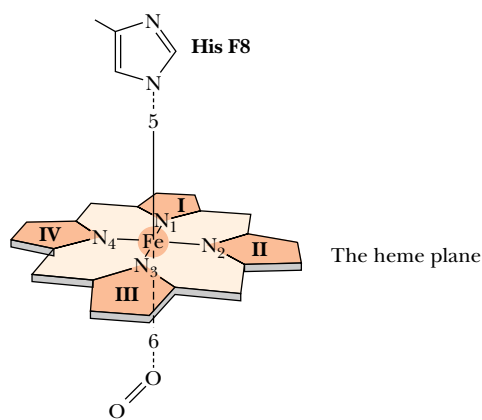
FIGURE 15.25 • The six liganding positions of an iron ion. Four ligands lie in the same plane; the remaining two are, respectively, above and below this plane. In myoglobin, His F8 is the fifth ligand; in oxymyoglobin, O_2 becomes the sixth.

FIGURE 15.26 • Oxygen and carbon monoxide binding to the heme group of myoglobin.

(a) Free heme with imidazole

(b) Mb:CO complex
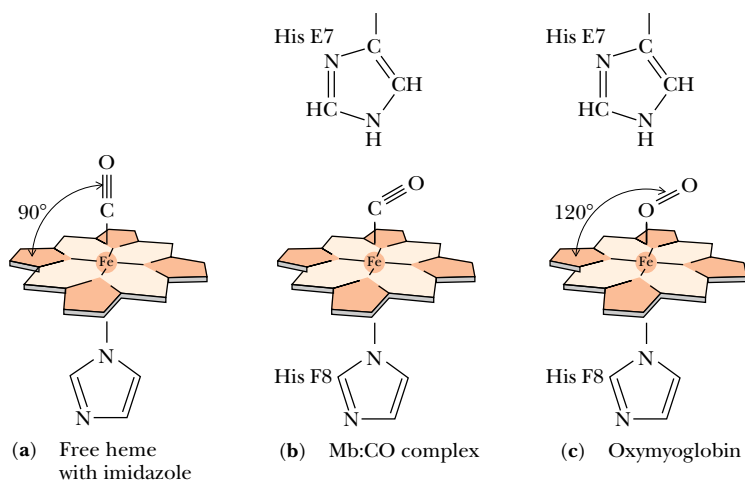
(c) Oxymyoglobin

When O_2 binds, the iron atom is pulled back toward the porphyrin plane and is now displaced from it by only 0.026 nm (Figure 15.27). The consequences of this small motion are trivial as far as the biological role of myoglobin is concerned. However, as we shall soon see, this slight movement profoundly affects the properties of hemoglobin. Its action on His F8 is magnified through changes in polypeptide conformation that alter subunit interactions in the Hb tetramer. These changes in subunit relationships are the fundamental cause of the allosteric properties of hemoglobin.

The Physiological Significance of Cooperative Binding of Oxygen by Hemoglobin

The oxygen-binding equations for myoglobin and hemoglobin are described in detail in the Appendix at the end of this chapter. The relative oxygen affinities of hemoglobin and myoglobin reflect their respective physiological roles (see Figure 15.22). Myoglobin, as an oxygen storage protein, has a greater affinity for O_2 than hemoglobin at all oxygen pressures. Hemoglobin, as the oxygen carrier, becomes saturated with O_2 in the lungs, where the partial pressure of O_2 (pO_2) is about 100 torr.[1] In the capillaries of tissues, pO_2 is typically 40 torr, and oxygen is released from Hb. In muscle, some of it can be bound by myoglobin, to be stored for use in times of severe oxygen deprivation, such as during strenuous exercise.

The Structure of the Hemoglobin Molecule

As noted, hemoglobin is an $\alpha_2\beta_2$ tetramer. Each of the four subunits has a conformation virtually identical to that of myoglobin. Two different types of subunits, α and β, are necessary to achieve cooperative O_2-binding by Hb. The β-chain at 146 amino acid residues is shorter than the myoglobin chain (153 residues), mainly because its final helical segment (the H helix) is shorter. The α-chain (141 residues) also has a shortened H helix and lacks the D helix as well (Figure 15.28). Max Perutz, who has devoted his life to elucidating the atomic structure of Hb, noted very early in his studies that the molecule was
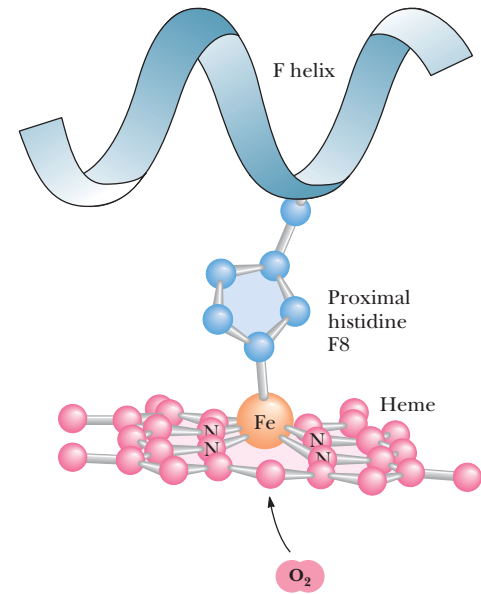
FIGURE 15.27 • The displacement of the Fe ion of the heme of deoxymyoglobin from the plane of the porphyrin ring system by the pull of His F8. In oxymyoglobin, the bound O_2 counteracts this effect.

FIGURE 15.28 • Conformational drawings of the α- and β-chains of Hb and the myoglobin chain. *(Irving Geis)*

Myoglobin (Mb) α-Globin (Hbα) β-Globin (Hbβ)
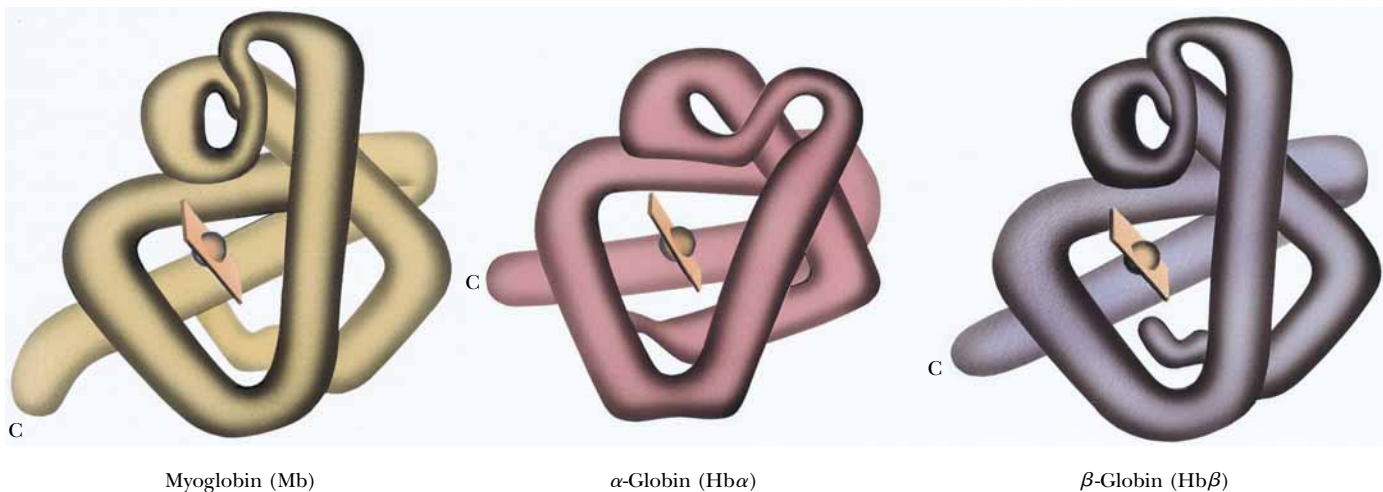
[1]The **torr** is a unit of pressure named for Torricelli, inventor of the barometer. 1 torr corresponds to 1 mm Hg (1/760th of an atmosphere).

(a) Front view

(b) Side view
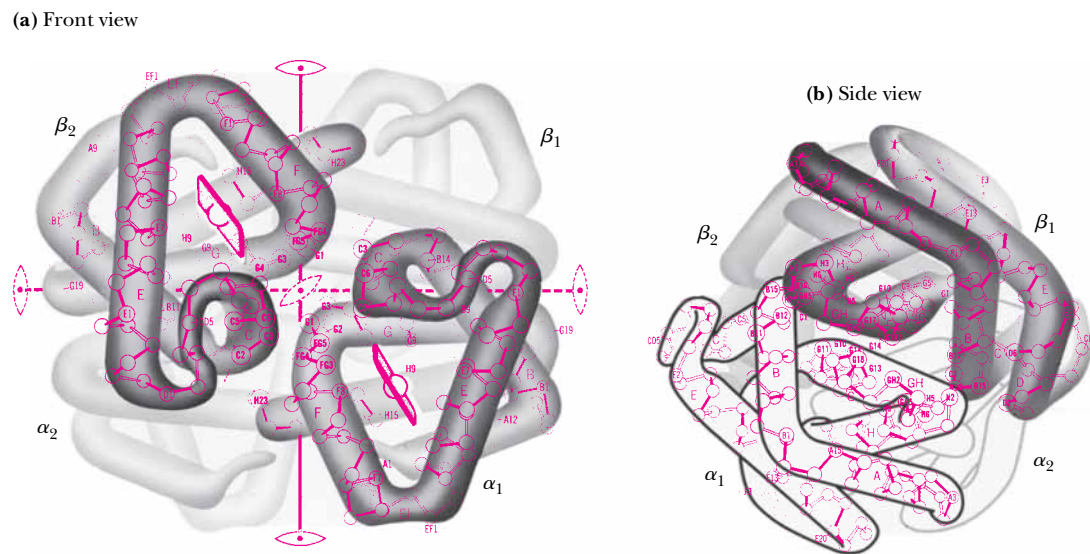
FIGURE 15.29 • The arrangement of subunits in horse methemoglobin, the first hemo-globin whose structure was determined by X-ray diffraction. The iron atoms on metHb are in the oxidized, ferric (Fe^{3+}) state. *(Irving Geis)*

highly symmetrical. The actual arrangement of the four subunits with respect to one another is shown in Figure 15.29 for horse methemoglobin. All verte-brate hemoglobins show a three-dimensional structure essentially the same as this. The subunits pack in a tetrahedral array, creating a roughly spherical mole-cule $6.4 \times 5.5 \times 5.0$ nm. The four heme groups, nestled within the easily rec-ognizable cleft formed between the E and F helices of each polypeptide, are exposed at the surface of the molecule. The heme groups are quite far apart; 2.5 nm separates the closest iron ions, those of hemes α_1 and β_2, and those of hemes α_2 and β_1. The subunit interactions are mostly between dissimilar chains: each of the α-chains is in contact with both β-chains, but there are few α–α or β–β interactions.

$\mathcal{A}$ DEEPER LOOK

The Physiological Significance of the Hb:O_2 Interaction

We can determine quantitatively the physiological significance of the sigmoid nature of the hemoglobin oxygen-binding curve, or, in other words, the biological importance of cooperativity. The equation

$$\frac{Y}{(1 - Y)} = \left(\frac{pO_2}{P_{50}}\right)^n$$

describes the relationship between pO_2, the affinity of hemoglo-bin for O_2 (defined as P_{50}, the partial pressure of O_2 giving half-maximal saturation of Hb with O_2), and the fraction of hemo-globin with O_2 bound, Y, versus the fraction of Hb with no O_2 bound, $(1 - Y)$ (see Appendix Equation [A15.16]). The coeffi-cient n is the *Hill coefficient,* an index of the cooperativity (sig-moidicity) of the hemoglobin oxygen-binding curve (see

Appendix for details). Taking pO_2 in the lungs as 100 torr, P_{50} as 26 torr, and n as 2.8, Y, the fractional saturation of the hemo-globin heme groups with O_2, is 0.98. If pO_2 were to fall to 10 torr within the capillaries of an exercising muscle, Y would drop to 0.06. The oxygen delivered under these conditions would be pro-portional to the difference, $Y_{lungs} - Y_{muscle}$, which is 0.92. That is, virtually all the oxygen carried by Hb would be released. Suppose instead that hemoglobin binding of O_2 were not coop-erative; in that case, the hemoglobin oxygen-binding curve would be hyperbolic, and $n = 1.0$. Then Y in the lungs would be 0.79 and Y in the capillaries, 0.28, and the difference in Y values would be 0.51. Thus, under these conditions, the cooperativity of oxy-gen binding by Hb means that 0.92/0.51 or 1.8 times as much O_2 can be delivered.

Oxygenation Markedly Alters the Quaternary Structure of Hb

Crystals of deoxyhemoglobin shatter when exposed to O_2. Further, X-ray crystallographic analysis reveals that oxy- and deoxyhemoglobin differ markedly in quaternary structure. In particular, specific $\alpha\beta$-subunit interactions change. The $\alpha\beta$ contacts are of two kinds. The $\alpha_1\beta_1$ and $\alpha_2\beta_2$ contacts involve helices B, G, and H and the GH corner. These contacts are extensive and important to subunit packing; they remain unchanged when hemoglobin goes from its deoxy to its oxy form. The $\alpha_1\beta_2$ and $\alpha_2\beta_1$ contacts are called **sliding contacts.** They principally involve helices C and G and the FG corner (Figure 15.30). When hemoglobin undergoes a conformational change as a result of ligand binding to the heme, these contacts are altered (Figure 15.31). Hemoglobin, as a conformationally dynamic molecule, consists of two dimeric halves, an $\alpha_1\beta_1$-subunit pair and an $\alpha_2\beta_2$-subunit pair. Each $\alpha\beta$ dimer moves as a rigid body, and the two halves of the molecule slide past each other upon oxygenation of the heme. The two halves rotate some $15°$ about an imaginary pivot passing through the $\alpha\beta$-subunits; some atoms at the interface between $\alpha\beta$ dimers are relocated by as much as 0.6 nm.

Movement of the Heme Iron by Less Than 0.04 nm Induces the Conformational Change in Hemoglobin

In deoxyhemoglobin, histidine F8 is liganded to the heme iron ion, but steric constraints force the Fe^{2+}:His-N bond to be tilted about $8°$ from the perpendicular to the plane of the heme. Steric repulsion between histidine F8 and the nitrogen atoms of the porphyrin ring system, combined with electrostatic repulsions between the electrons of Fe^{2+} and the porphyrin π-electrons, forces the iron atom to lie out of the porphyrin plane by about 0.06 nm. Changes in electronic and steric factors upon heme oxygenation allow the Fe^{2+} atom to move about 0.039 nm closer to the plane of the porphyrin, so now it is displaced only 0.021 nm above the plane. It is as if the O_2 were drawing the heme Fe^{2+} into the porphyrin plane (Figure 15.32). This modest displacement of 0.039 nm seems a trivial distance, but its biological consequences are far-reaching. As the iron atom moves, it drags histidine F8 along with it, causing helix
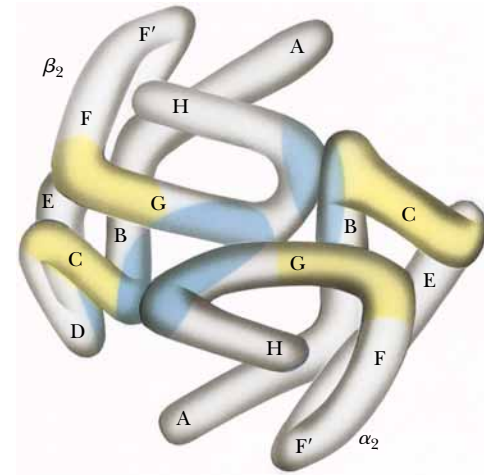
FIGURE 15.30 • Side view of one of the two $\alpha\beta$ dimers in Hb, with packing contacts indicated in blue. The sliding contacts made with the other dimer are shown in yellow. The changes in these sliding contacts are shown in Figure 15.31. *(Irving Geis)*
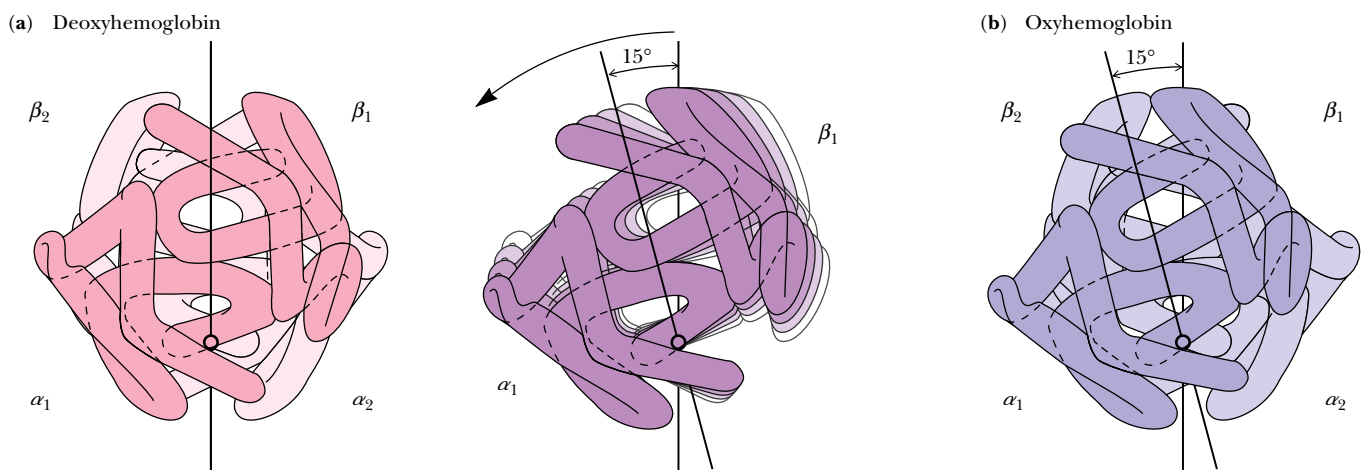
FIGURE 15.31 • Subunit motion in hemoglobin when the molecule goes from the (a) deoxy to the (b) oxy form. *(Irving Geis)*
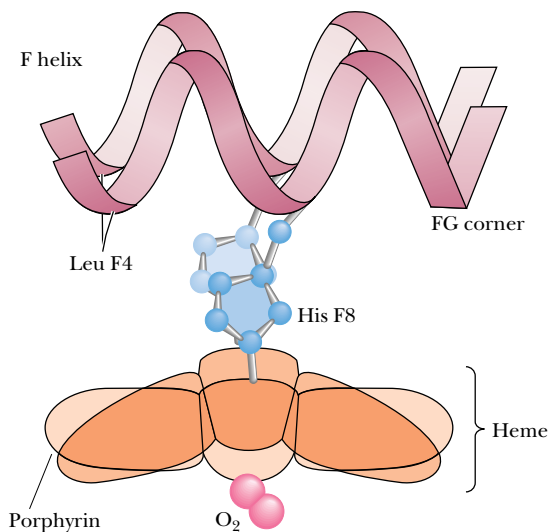
FIGURE 15.32 • Changes in the position of the heme iron atom upon oxygenation lead to conformational changes in the hemoglobin molecule.

F, the EF corner, and the FG corner to follow. These shifts are transmitted to the subunit interfaces, where they trigger conformational readjustments that lead to the rupture of interchain salt links.

The Oxy and Deoxy Forms of Hemoglobin Represent Two Different Conformational States

Hemoglobin resists oxygenation (see Figure 15.22) because the deoxy form is stabilized by specific hydrogen bonds and salt bridges (ion-pair bonds). All of these interactions are broken in oxyhemoglobin, as the molecule stabilizes into a new conformation. A crucial H bond in this transition involves a particular tyrosine residue. Both α- and β-subunits have Tyr as the penultimate C-terminal residue (Tyr α140 = Tyr HC2; Tyr β145 = Tyr HC2, respectively[2]). The phenolic —OH groups of these Tyr residues form intrachain H bonds to the peptide C=O function contributed by Val FG5 in deoxyhemoglobin. (Val FG5 is α93 and β98, respectively.) The shift in helix F upon oxygenation leads to rupture of this Tyr HC2:Val FG5 hydrogen bond. Further, eight salt bridges linking the polypeptide chains are broken as hemoglobin goes from the deoxy to the oxy form (Figure 15.33). Six of these salt links are between different subunits. Four of these six involve either carboxyl-terminal or amino-terminal amino acids in the chains; two are between the amino termini and the carboxyl termini of the α-chains, and two join the carboxyl termini of the β-chains to the ϵ-NH$_3^+$ groups of the two Lys α140 residues. The other two interchain electrostatic bonds link Arg and Asp residues in the two α-chains. In addition, ionic interactions between Asp β94 and His β146 form an intrachain salt bridge in each β-subunit. In deoxyhemoglobin, with all of these interactions intact, the C-termini of the four subunits are restrained, and this conformational state is termed **T,** the **tense** or **taut form.** In oxyhemoglobin, these C-termini have almost complete freedom of rotation, and the molecule is now in its **R,** or **relaxed, form.**

---

[2]C here designates the C-terminus; the H helix is C-terminal in these polypeptides. "C2" symbolizes the next-to-last residue.

(a)

(b)

(c)
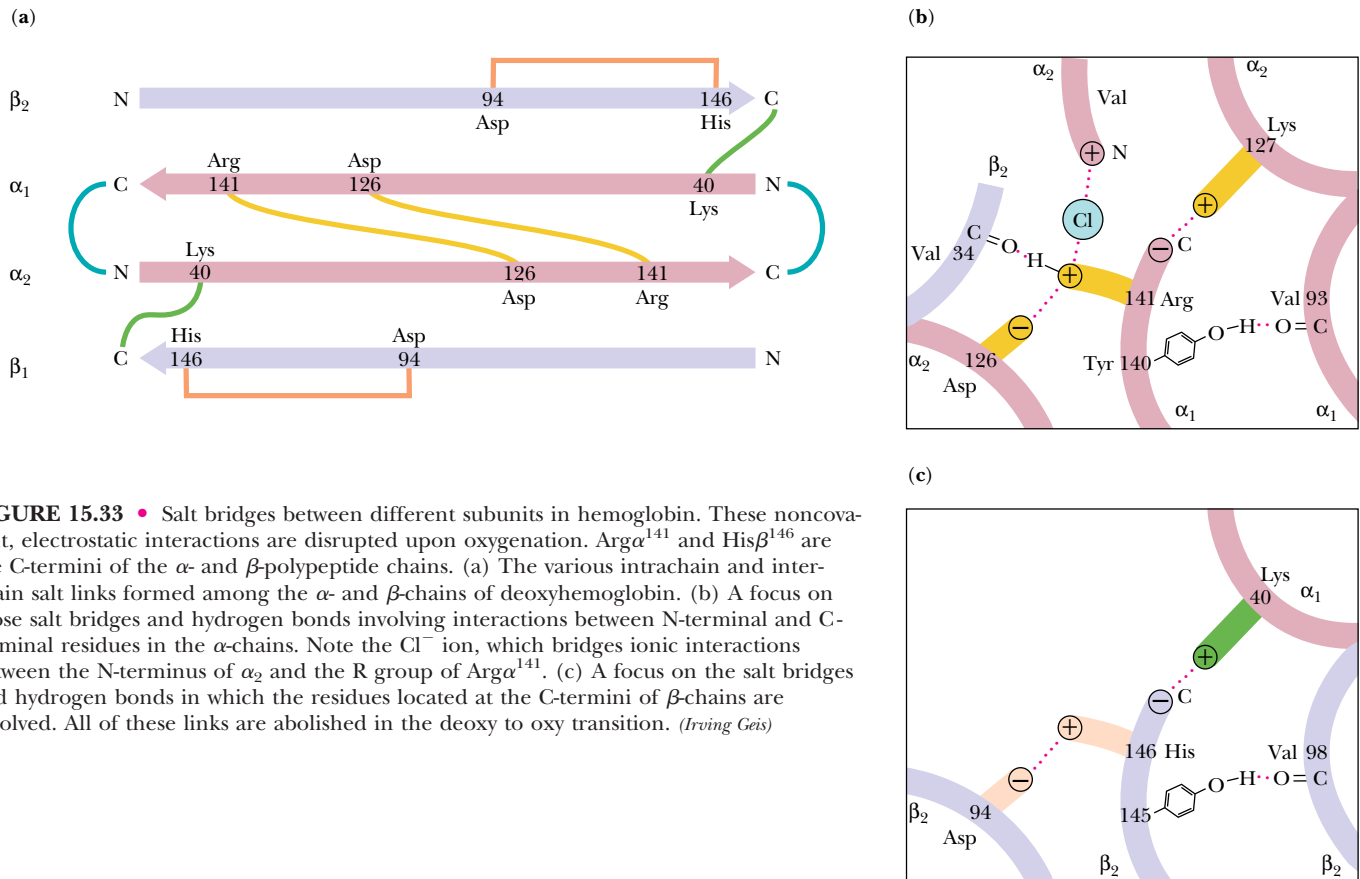
FIGURE 15.33 • Salt bridges between different subunits in hemoglobin. These noncovalent, electrostatic interactions are disrupted upon oxygenation. Argα^{141} and Hisβ^{146} are the C-termini of the α- and β-polypeptide chains. (a) The various intrachain and interchain salt links formed among the α- and β-chains of deoxyhemoglobin. (b) A focus on those salt bridges and hydrogen bonds involving interactions between N-terminal and C-terminal residues in the α-chains. Note the Cl$^-$ ion, which bridges ionic interactions between the N-terminus of α_2 and the R group of Argα^{141}. (c) A focus on the salt bridges and hydrogen bonds in which the residues located at the C-termini of β-chains are involved. All of these links are abolished in the deoxy to oxy transition. *(Irving Geis)*

A Model for the Allosteric Behavior of Hemoglobin

A model for the allosteric behavior of hemoglobin is based on recent observations that oxygen is accessible only to the heme groups of the α-chains when hemoglobin is in the T conformational state. Perutz has pointed out that the heme environment of β-chains in the T state is virtually inaccessible because of steric hindrance by amino acid residues in the E helix. This hindrance dis-

---

$\mathcal{A}$ **D E E P E R   L O O K**

Changes in the Heme Iron upon O_2 Binding

In deoxyhemoglobin, the six d electrons of the heme Fe^{2+} exist as four unpaired electrons and one electron pair, and five ligands can be accommodated: the four N-atoms of the porphyrin ring system and histidine F8. In this electronic configuration, the iron atom is paramagnetic and in the **high-spin state.** When the heme binds O_2 as a sixth ligand, these electrons are rearranged into three e^- pairs and the iron changes to the **low-spin state** and is diamagnetic. This change in spin state allows the bond between the Fe^{2+} ion and histidine F8 to become perpendicular to the heme plane and to shorten. In addition, interactions between the porphyrin N-atoms and the iron strengthen. Also, high-spin Fe^{2+} has a greater atomic volume than low-spin Fe^{2+} because its four unpaired e^- occupy four orbitals rather than two when the electrons are paired in low-spin Fe^{2+}. So, low-spin iron is less sterically hindered and able to move nearer to the porphyrin plane.

appears when the hemoglobin molecule undergoes transition to the R conformational state. Binding of O_2 to the β-chains is thus dependent on the T to R conformational shift, and this shift is triggered by the subtle changes that occur when O_2 binds to the α-chain heme groups.

H^+ Promotes the Dissociation of Oxygen from Hemoglobin

Protons, carbon dioxide, and chloride ions, as well as the metabolite *2,3-bisphosphoglycerate* (or *BPG*), all affect the binding of O_2 by hemoglobin. Their effects have interesting ramifications, which we shall see as we discuss them in turn. Deoxyhemoglobin has a higher affinity for protons than oxyhemoglobin. Thus, as the pH decreases, dissociation of O_2 from hemoglobin is enhanced. In simple symbolism, ignoring the stoichiometry of O_2 or H^+ involved:

$$HbO_2 + H^+ \rightleftharpoons HbH^+ + O_2$$

Expressed another way, H^+ is an antagonist of oxygen binding by Hb, and the saturation curve of Hb for O_2 is displaced to the right as acidity increases (Figure 15.34). This phenomenon is called the **Bohr effect,** after its discoverer, the Danish physiologist Christian Bohr (the father of Niels Bohr, the atomic physicist). The effect has important physiological significance because actively metabolizing tissues produce acid, promoting O_2 release where it is most needed. About two protons are taken up by deoxyhemoglobin. The N-termini of the two α-chains and the His $\beta146$ residues have been implicated as the major players in the Bohr effect. (The pK_a of a free amino terminus in a protein is about 8.0, but the pK_a of a protein histidine imidazole is around 6.5.) Neighboring carboxylate groups of Asp $\beta94$ residues help to stabilize the protonated state of the His $\beta146$ imidazoles that occur in deoxyhemoglobin. However, when Hb binds O_2, changes in the conformation of β-chains upon Hb oxygenation move the negative Asp function away, and dissociation of the imidazole protons is favored.
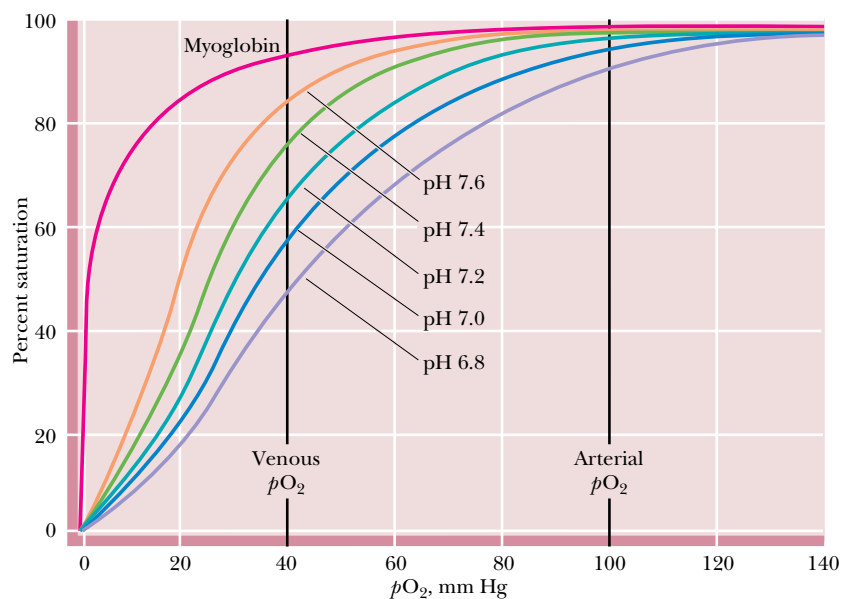
FIGURE 15.34 • The oxygen saturation curves for myoglobin and for hemoglobin at five different pH values: 7.6, 7.4, 7.2, 7.0, and 6.8.

CO$_2$ Also Promotes the Dissociation of O$_2$ from Hemoglobin

Carbon dioxide has an effect on O$_2$ binding by Hb that is similar to that of H$^+$, partly because it produces H$^+$ when it dissolves in the blood:

$$CO_2 + H_2O \underset{}{\overset{\text{carbonic anhydrase}}{\rightleftharpoons}} \underset{\text{carbonic acid}}{H_2CO_3} \rightleftharpoons H^+ + \underset{\text{bicarbonate}}{HCO_3^-}$$
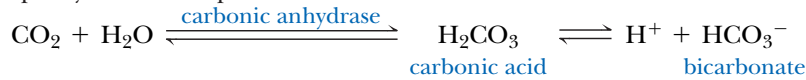
The enzyme *carbonic anhydrase* promotes the hydration of CO$_2$. Many of the protons formed upon ionization of carbonic acid are picked up by Hb as O$_2$ dissociates. The bicarbonate ions are transported with the blood back to the lungs. When Hb becomes oxygenated again in the lungs, H$^+$ is released and reacts with HCO$_3^-$ to re-form H$_2$CO$_3$, from which CO$_2$ is liberated. The CO$_2$ is then exhaled as a gas.

In addition, some CO$_2$ is directly transported by hemoglobin in the form of *carbamate* (—NHCOO$^-$). Free α-amino groups of Hb react with CO$_2$ reversibly:

$$R—NH_2 + CO_2 \rightleftharpoons R—NH—COO^- + H^+$$
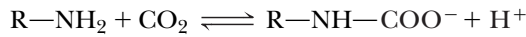
This reaction is driven to the right in tissues by the high CO$_2$ concentration; the equilibrium shifts the other way in the lungs where [CO$_2$] is low. Thus, carbamylation of the N-termini converts them to anionic functions, which then form salt links with the cationic side chains of Arg α141 that stabilize the deoxy or T state of hemoglobin.

In addition to CO$_2$, Cl$^-$ and BPG also bind better to deoxyhemoglobin than to oxyhemoglobin, causing a shift in equilibrium in favor of O$_2$ release. These various effects are demonstrated by the shift in the oxygen saturation curves for Hb in the presence of one or more of these substances (Figure 15.35). Note that the O$_2$-binding curve for Hb + BPG + CO$_2$ fits that of whole blood very well.

2,3-Bisphosphoglycerate Is an Important Allosteric Effector for Hemoglobin

The binding of 2,3-bisphosphoglycerate (BPG) to Hb promotes the release of O$_2$ (Figure 15.35). Erythrocytes (red blood cells) normally contain about 4.5 mM BPG, a concentration equivalent to that of tetrameric hemoglobin molecules. Interestingly, this equivalence is maintained in the Hb:BPG binding stoichiometry because the tetrameric Hb molecule has but one binding site for BPG. This site is situated within the central cavity formed by the association of the four subunits. The strongly negative BPG molecule (Figure 15.36) is electrostatically bound via interactions with the positively charged functional
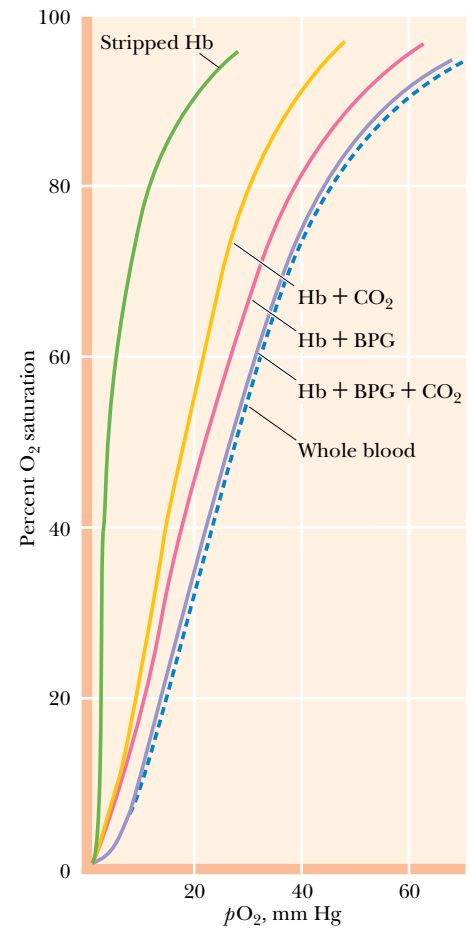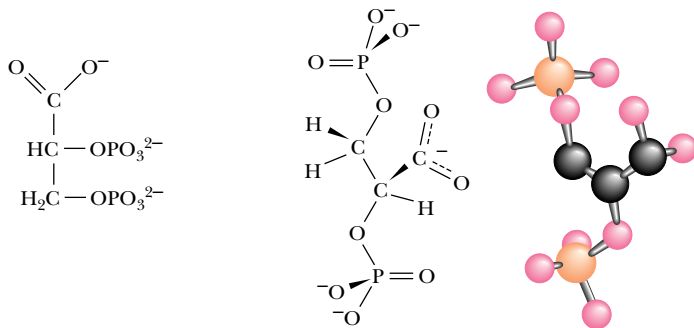
FIGURE 15.35 • Oxygen-binding curves of blood and of hemoglobin in the absence and presence of CO$_2$ and BPG. From left to right: stripped Hb, Hb + CO$_2$, Hb + BPG, Hb + BPG + CO$_2$, and whole blood.

FIGURE 15.36 • The structure, in ionic form, of BPG or 2,3-bisphosphoglycerate, an important allosteric effector for hemoglobin.
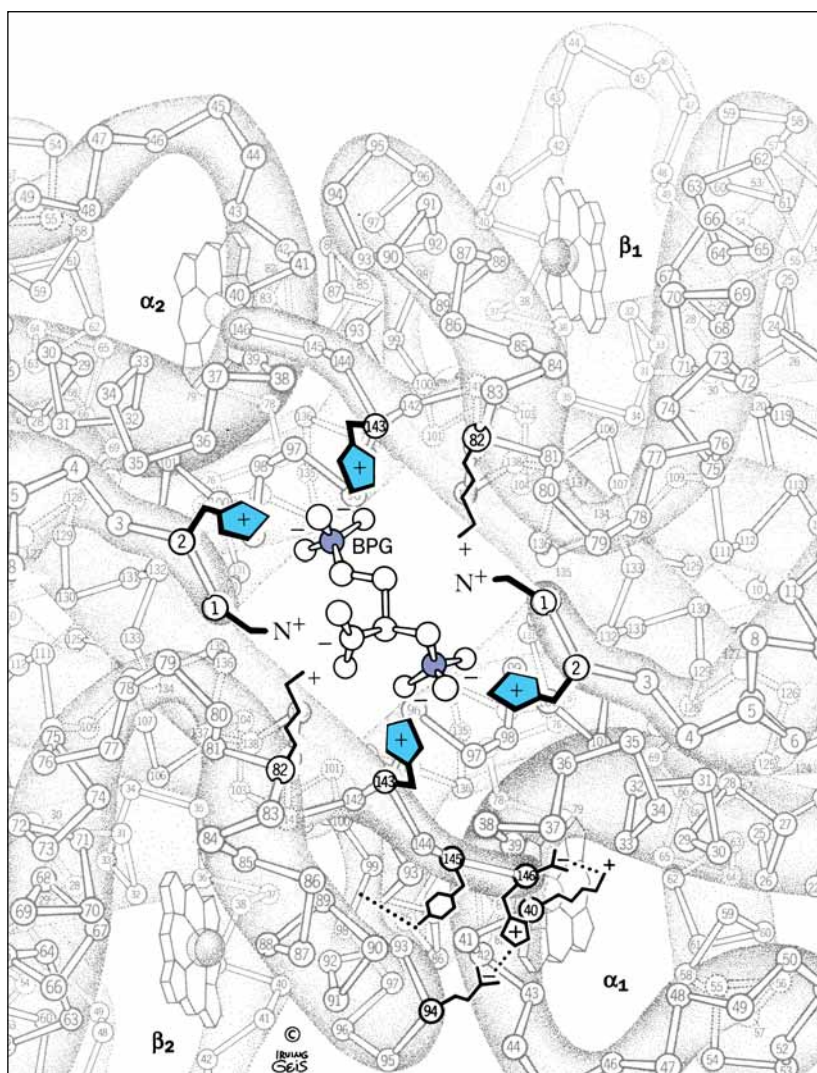
FIGURE 15.37 • The ionic binding of BPG to the two β-subunits of Hb. *(Irving Geis)*

groups of each Lys β82, His β2, His β143, and the NH_3^+-terminal group of each β-chain. These positively charged residues are arranged to form an electrostatic pocket complementary to the conformation and charge distribution of BPG (Figure 15.37). In effect, BPG cross-links the two β-subunits. The ionic bonds between BPG and the two β-chains aid in stabilizing the conformation of Hb in its deoxy form, thereby favoring the dissociation of oxygen. In oxyhemoglobin, this central cavity is too small for BPG to fit. Or, to put it another way, the conformational changes in the Hb molecule that accompany O_2-binding perturb the BPG-binding site so that BPG can no longer be accommodated. Thus, BPG and O_2 are mutually exclusive allosteric effectors for Hb, even though their binding sites are physically distinct.

The Physiological Significance of BPG Binding

The importance of the BPG effect is evident in Figure 15.35. Hemoglobin stripped of BPG is virtually saturated with O_2 at a pO_2 of only 20 torr, and it cannot release its oxygen within tissues, where the pO_2 is typically 40 torr. BPG shifts the oxygen saturation curve of Hb to the right, making the Hb an O_2

delivery system eminently suited to the needs of the organism. BPG serves this vital function in humans, most primates, and a number of other mammals. However, the hemoglobins of cattle, sheep, goats, deer, and other animals have an intrinsically lower affinity for O_2, and these Hbs are relatively unaffected by BPG. In fish, whose erythrocytes contain mitochondria, the regulatory role of BPG is filled by ATP or GTP. In reptiles and birds, a different organophosphate serves, namely inositol pentaphosphate (IPP) or inositol hexaphosphate (IHP) (Figure 15.38).

Inositol pentaphosphate (IPP)   **Inositol hexaphosphate (IHP)**

FIGURE 15.38 • The structures of inositol pentaphosphate and inositol hexaphosphate, the functional analogs of BPG in birds and reptiles.

Fetal Hemoglobin Has a Higher Affinity for O_2 Because It Has a Lower Affinity for BPG

The fetus depends on its mother for an adequate supply of oxygen, but its circulatory system is entirely independent. Gas exchange takes place across the placenta. Ideally then, fetal Hb should be able to absorb O_2 better than maternal Hb so that an effective transfer of oxygen can occur. Fetal Hb differs from adult Hb in that the β-chains are replaced by very similar, but not identical, 146-residue subunits called γ-chains (gamma chains). Fetal Hb is thus $\alpha_2\gamma_2$. Recall that BPG functions through its interaction with the β-chains. BPG binds less effectively with the γ-chains of fetal Hb (also called Hb F). (Fetal γ-chains have Ser instead of His at position 143, and thus lack two of the positive charges in the central BPG-binding cavity.) Figure 15.39 compares the relative affinities of adult Hb (also known as Hb A) and Hb F for O_2 under similar conditions of pH and [BPG]. Note that Hb F binds O_2 at pO_2 values where most of the oxygen has dissociated from Hb A. Much of the difference can be attributed to the diminished capacity of Hb F to bind BPG (compare Figures 15.35 and 15.39); Hb F thus has an intrinsically greater affinity for O_2, and oxygen transfer from mother to fetus is ensured.

Sickle-Cell Anemia

In 1904, a Chicago physician treated a 20-year-old black college student complaining of headache, weakness, and dizziness. The blood of this patient revealed serious anemia—only half the normal number of red cells were pre-

FIGURE 15.39 • Comparison of the oxygen saturation curves of Hb A and Hb F under similar conditions of pH and [BPG].
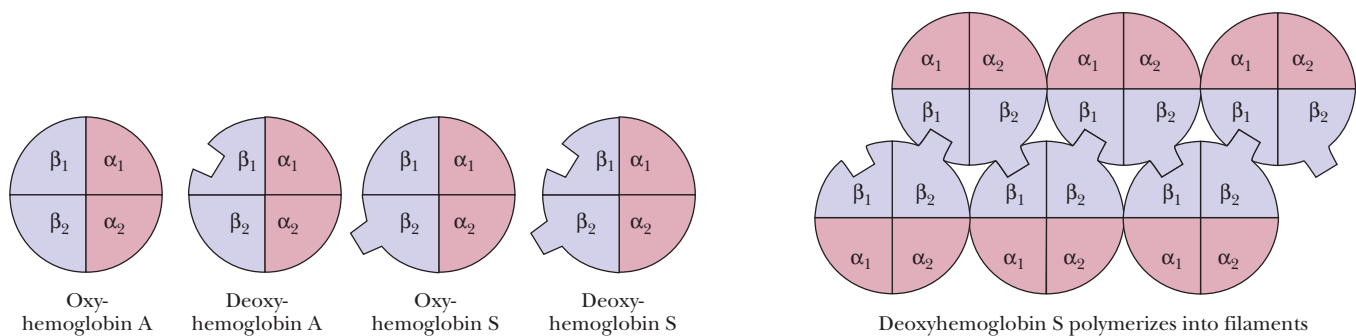
FIGURE 15.40 • The polymerization of Hb S via the interactions between the hydrophobic Val side chains at position $\beta 6$ and the hydrophobic pockets in the EF corners of β-chains in neighboring Hb molecules. The protruding "block" on Oxy S represents the Val hydrophobic protrusion. The complementary hydrophobic pocket in the EF corner of the β-chains is represented by a square-shaped indentation. (This indentation is probably present in Hb A also.) Only the β_2 Val protrusions and the β_1 EF pockets are shown. (The β_1 Val protrusions and the β_2 EF pockets are not involved, although they are present.)

sent. Many of these cells were abnormally shaped; in fact, instead of the characteristic disc shape, these erythrocytes were elongate and crescentlike in form, a feature that eventually gave name to the disease **sickle-cell anemia.** These sickle cells pass less freely through the capillaries, impairing circulation and causing tissue damage. Further, these cells are more fragile and rupture more easily than normal red cells, leading to anemia.

Sickle-Cell Anemia Is a Molecular Disease

A single amino acid substitution in the β-chains of Hb causes sickle-cell anemia. Replacement of the glutamate residue at position 6 in the β-chain by a valine residue marks the only chemical difference between Hb A and sickle-cell hemoglobin, Hb S. The amino acid residues at position $\beta 6$ lie at the surface of the hemoglobin molecule. In Hb A, the ionic R groups of the Glu residues fit this environment. In contrast, the aliphatic side chains of the Val residues in Hb S create hydrophobic protrusions where none existed before. To the detriment of individuals who carry this trait, a hydrophobic pocket forms in the EF corner of each β-chain of Hb when it is in the deoxy state, and this pocket nicely accommodates the Val side chain of a neighboring Hb S molecule (Figure 15.40). This interaction leads to the aggregation of Hb S molecules into long, chainlike polymeric structures. The obvious consequence is that deoxyHb S is less soluble than deoxyHb A. The concentration of hemoglobin in red blood cells is high (about 150 mg/mL), so that even in normal circumstances it is on the verge of crystallization. The formation of insoluble deoxyHb S fibers distorts the red cell into the elongated sickle shape characteristic of the disease.[3]

[3]In certain regions of Africa, the sickle-cell trait is found in 20% of the people. Why does such a deleterious heritable condition persist in the population? For reasons as yet unknown, individuals with this trait are less susceptible to the most virulent form of malaria. The geographic distribution of malaria and the sickle-cell trait are positively correlated.

$\mathcal{H}$UMAN BIOCHEMISTRY

Hemoglobin and Nitric Oxide

Nitric oxide (NO ·) is a simple gaseous molecule whose many remarkable physiological functions are still being discovered. For example, NO · is known to act as a neurotransmitter and as a second messenger in signal transduction (see Chapter 34). Further, **endothelial relaxing factor** (ERF, also known as endothelium-derived relaxing factor, or EDRF), an elusive hormonelike agent that acts to relax the musculature of the walls (**endothelium**) of blood vessels and lower blood pressure, has been identified as NO ·. It has long been known that NO · is a high-affinity ligand for Hb, binding to its heme-Fe^{2+} atom with an affinity 10,000 times greater than that of O_2. An enigma thus arises: Why is NO · not instantaneously bound by Hb within human erythrocytes and prevented from exerting its vasodilation properties?

The reason that Hb doesn't block the action of NO · is due to a unique interaction between Cys93β of Hb and NO · recently described by Li Jia, Celia and Joseph Bonaventura, and Johnathan Stamler at Duke University. Nitric oxide reacts with the sulfhydryl group of Cys93β, forming an S-nitroso derivative:

$$-CH_2-S-N=O$$
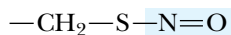
This S-nitroso group is in equilibrium with other S-nitroso compounds formed by reaction of NO · with small-molecule thiols such as free cysteine or glutathione (an isoglutamylcysteinylglycine tripeptide):

S-nitrosoglutathione
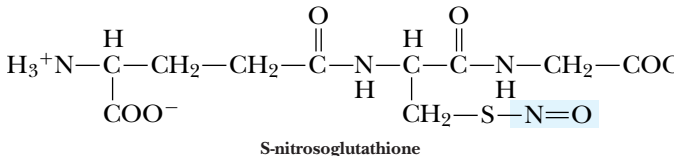
These small-molecule thiols serve to transfer NO · from erythrocytes to endothelial receptors, where it acts to relax vascular tension. NO · itself is a reactive free-radical compound whose biological half-life is very short (1–5 sec). S-nitrosoglutathione has a half-life of several hours.

The reactions between Hb and NO · are complex. NO · forms a ligand with the heme-Fe^{2+} that is quite stable in the absence of O_2. However, in the presence of O_2, NO · is oxidized to NO_3^- and the heme-Fe^{2+} of Hb is oxidized to Fe^{3+}, forming methemoglobin. Fortunately, the interaction of Hb with NO · is controlled by the allosteric transition between R-state Hb (oxyHb) and T-state Hb (deoxyHb). Cys93β is more exposed and reactive in R-state Hb than in T-state Hb, and binding of NO · to Cys93β precludes reaction of NO · with heme iron. Upon release of O_2 from Hb in tissues, Hb shifts conformation from R state to T state, and binding of NO · at Cys93β is no longer favored. Consequently, NO · is released from Cys93β and transferred to small-molecule thiols for delivery to endothelial receptors, causing capillary vasodilation. This mechanism also explains the puzzling observation that free Hb produced by recombinant DNA methodology for use as a whole blood substitute causes a transient rise of 10 to 12 mm Hg in diastolic blood pressure in experimental clinical trials. (Conventional whole blood transfusion has no such effect.) It is now apparent that the "synthetic" Hb, which has no bound NO ·, is binding NO · in the blood and preventing its vasoregulatory function.

In the course of hemoglobin evolution, the only invariant amino acid residues in globin chains are HisF8 (the obligatory heme ligand) and a Phe residue acting to wedge the heme into its pocket. However, in mammals and birds, Cys93β is also invariant, no doubt due to its vital role in NO · delivery.

Adapted from Jia, L., et al., 1996. S-Nitrosohaemoglobin: A dynamic activity of blood involved in vascular control. *Nature* **380:**221–226.

PROBLEMS

1. List six general ways in which enzyme activity is controlled.

2. Why do you suppose proteolytic enzymes are often synthesized as inactive zymogens?

3. First draw both Lineweaver–Burk plots and Hanes–Woolf plots for the following: a Monod–Wyman–Changeux allosteric *K* enzyme system, showing separate curves for the kinetic response in (1) the absence of any effectors; (2) the presence of allosteric activator A; and (3) the presence of allosteric inhibitor I. Then draw a similar set of curves for a Monod–Wyman–Changeux allosteric *V* enzyme system.

4. In the Monod–Wyman–Changeux model for allosteric regulation, what values of *L* and relative affinities of R and T for A will lead activator A to exhibit positive homotropic effects? (That is, under what conditions will the binding of A enhance further A-binding, in the same manner that S-binding shows positive coop-

erativity?) Similarly, what values of *L* and relative affinities of R and T for I will lead inhibitor I to exhibit positive homotropic effects? (That is, under what conditions will the binding of I promote further I-binding?)

5. The equation $\dfrac{Y}{(1-Y)} = \left(\dfrac{pO_2}{P_{50}}\right)^n$ allows the calculation of Y (the fractional saturation of hemoglobin with O_2), given P_{50} and n (see Box on page 484). Let $P_{50} = 26$ torr and $n = 2.8$. Calculate Y in the lungs where $pO_2 = 100$ torr, and Y in the capillaries where $pO_2 = 40$ torr. What is the efficiency of O_2 delivery under these conditions (expressed as $Y_{lungs} - Y_{capillaries}$)? Repeat the calculations, but for $n = 1$. Compare the values for $Y_{lungs} - Y_{capillaries}$ for $n = 2.8$ versus $Y_{lungs} - Y_{capillaries}$ for $n = 1$ to determine the effect of cooperative O_2 binding on oxygen delivery by hemoglobin.

6. The cAMP formed by adenylyl cyclase (Figure 15.20) does not persist because 5′-phosphodiesterase activity prevalent in cells hydrolyzes cAMP to give 5′-AMP. Caffeine inhibits 5′-phosphodiesterase activity. Describe the effects on glycogen phosphorylase activity that arise as a consequence of drinking lots of caffeinated coffee.

7. If no precautions are taken, blood that has been stored for some time becomes depleted in 2,3-BPG. What happens if such blood is used in a transfusion?

8. Enzymes have evolved such that their K_m values (or $K_{0.5}$ values) for substrate(s) are roughly equal to the *in vivo* concentration(s) of the substrate(s). Assume that glycogen phosphorylase is assayed at $[P_i] \approx K_{0.5}$ in the absence and presence of AMP or ATP. Estimate from Figure 15.15 the relative glycogen phosphorylase activity when (a) neither AMP or ATP is present, (b) AMP is present, and (c) ATP is present.

FURTHER READING

Creighton, T. E., 1984. *Proteins: Structure and Molecular Properties.* New York: W. H. Freeman and Co. An advanced textbook on the structure and function of proteins.

Dickerson, R. E., and Geis, I., 1983. *Hemoglobin: Structure, Function, Evolution and Pathology.* Menlo Park, CA: Benjamin/Cummings.

Gill, S. J., et al., 1988. New twists on an old story: Hemoglobin. *Trends in Biochemical Sciences* **13:**465–467.

Johnson, L. N., and Barford, D., 1993. The effects of phosphorylation on the structure and function of proteins. *Annual Review of Biophysics and Biomolecular Structure* **22:**199–232. A review of protein phosphorylation and its role in regulation of enzymatic activity, with particular emphasis on glycogen phosphorylase.

Johnson, L. N., and Barford, D., 1994. Electrostatic effects in the control of glycogen phosphorylase by phosphorylation. *Protein Science* **3:**1726–1730. Discussion of the phosphate group's ability to deliver two negative charges to a protein, a property that no amino acid side chain can provide.

Koshland, D. E., Jr., Nemethy, G., and Filmer, D., 1966. Comparison of experimental binding data and theoretical models in proteins containing subunits. *Biochemistry* **5:**365–385. The KNF model.

Lin, K., et al., 1996. Comparison of the activation triggers in yeast and muscle glycogen phosphorylase. *Science* **273:**1539–1541. Despite structural and regulatory differences between yeast and muscle glyogen phosphorylases, both are activated through changes in their intersubunit interface.

Lin, K., et al., 1997. Distinct phosphorylation signals converge at the catalytic center in glycogen phosphorylases. *Structure* **5:**1511–1523.

Monod, J., Wyman, J., and Changeux, J.-P., 1965. On the nature of allosteric transitions: A plausible model. *Journal of Molecular Biology* **12:**88–118. The classic paper that provided the first theoretical analysis of allosteric regulation.

Rath, V. L., et al., 1996. The evolution of an allosteric site in phosphorylase. *Structure* **4:**463–473.

Schachman, H. K., 1990. Can a simple model account for the allosteric transition of aspartate transcarbamoylase? *Journal of Biological Chemistry* **263:**18583–18586. Tests of the postulates of the allosteric models through experiments on aspartate transcarbamoylase.

Weiss, J. N., 1997. The Hill equation revisited: Uses and abuses. *The FASEB Journal* **11:**835–841.

$\mathcal{A}$ppendix to Chapter 15

The Oxygen-Binding Curves of Myoglobin and Hemoglobin

Myoglobin

The reversible binding of oxygen to myoglobin,
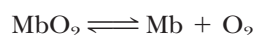
$$MbO_2 \rightleftharpoons Mb + O_2$$

can be characterized by the equilibrium dissociation constant, K.

$$K = \frac{[Mb][O_2]}{[MbO_2]} \tag{A15.1}$$

If Y is defined as the **fractional saturation** of myoglobin with O_2, that is, the fraction of myoglobin molecules having an oxygen molecule bound, then

$$Y = \frac{[MbO_2]}{[MbO_2] + [Mb]} \tag{A15.2}$$

The value of Y ranges from 0 (no myoglobin molecules carry an O_2) to 1.0 (all myoglobin molecules have an O_2 molecule bound). Substituting from Equation (A15.1), $([Mb][O_2])/K$ for $[MbO_2]$ gives

$$Y = \frac{\left(\dfrac{[Mb][O_2]}{K}\right)}{\left(\dfrac{[Mb][O_2]}{K} + [Mb]\right)} = \frac{\left(\dfrac{[O_2]}{K}\right)}{\left(\dfrac{[O_2]}{K} + 1\right)} = \frac{[O_2]}{[O_2] + K} \tag{A15.3}$$

and, if the concentration of O_2 is expressed in terms of the partial pressure (in torr) of oxygen gas in equilibrium with the solution of interest, then

$$Y = \frac{pO_2}{pO_2 + K} \tag{A15.4}$$

(In this form, K has the units of torr.) The relationship defined by Equation (A15.4) plots as a hyperbola. That is, the MbO_2 saturation curve resembles an enzyme:substrate saturation curve. For myoglobin, a partial pressure of 1 torr for pO_2 is sufficient for half-saturation (Figure A15.1). We can define P_{50} as the partial pressure of O_2 at which 50% of the myoglobin molecules have a molecule of O_2 bound (that is, $Y = 0.5$), then

$$0.5 = \frac{pO_2}{pO_2 + P_{50}} \tag{A15.5}$$

(Note from Equation (A15.1) that when $[MbO_2] = [Mb]$, $K = [O_2]$, which is the same as saying when $Y = 0.5$, $K = P_{50}$.) The general equation for O_2 binding to Mb becomes

$$Y = \frac{pO_2}{pO_2 + P_{50}} \tag{A15.6}$$

The ratio of the fractional saturation of myoglobin, Y, to free myoglobin, $1 - Y$, depends on pO_2 and K according to the equation
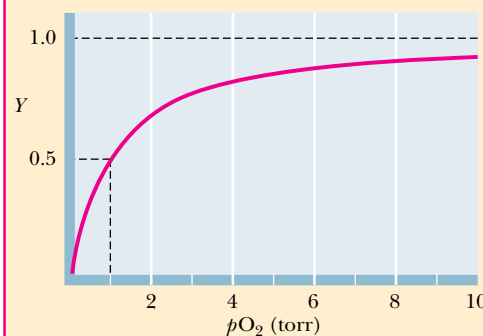
FIGURE A15.1 • Oxygen saturation curve for myoglobin in the form of Y versus pO_2 showing P_{50} is at a pO_2 of 1 torr (1 mm Hg).

495

$$\frac{Y}{1 - Y} = \frac{pO_2}{K} \tag{A15.7}$$

Taking the logarithm yields

$$\log\left(\frac{Y}{1 - Y}\right) = \log pO_2 - \log K \tag{A15.8}$$

A graph of $\log (Y/(1 - Y))$ versus $\log pO_2$ is known as a **Hill plot** (in honor of Archibald Hill, a pioneer in the study of O_2 binding by hemoglobin). A Hill plot for myoglobin (Figure A15.2) gives a straight line. At half-saturation, defined as $Y = 0.5$, $Y/(1 - Y) = 1$, and $\log (Y/(1 - Y)) = 0$. At this value of $\log (Y/(1 - Y))$, the value for $pO_2 = K = P_{50}$. The slope of the Hill plot at the point where $\log (Y/(1 - Y)) = 0$, the midpoint of binding, is known as the **Hill coefficient.** The Hill coefficient for myoglobin is 1.0. A Hill coefficient of 1.0 means that O_2 molecules bind independently of one another to myoglobin, a conclusion entirely logical because each Mb molecule can bind only one O_2.

FIGURE A15.2 • Hill plot for the binding of O_2 to myoglobin. The slope of the line is the **Hill coefficient.** For Mb, the Hill coefficient is 1.0. At $\log(Y/(1 - Y)) = 0$, $\log pO_2 = \log P_{50}$.

Hemoglobin

New properties emerge when four heme-containing polypeptides come together to form a tetramer. The O_2-binding curve of hemoglobin is sigmoid rather than hyperbolic (see Figure 15.21), and Equation (A15.4) does not describe such curves. Of course, each hemoglobin molecule has four hemes and can bind up to four oxygen molecules. Suppose for the moment the O_2 binding to hemoglobin is an "all-or-none" phenomenon, where Hb exists either free of O_2 or with four O_2 molecules bound. This supposition represents the extreme case for cooperative binding of a ligand by a protein with multiple binding sites. In effect, it says that if one ligand binds to the protein molecule, then all other sites are immediately occupied by ligand. Or, to say it another way for the case in hand, suppose that four O_2 molecules bind to Hb simultaneously:

$$Hb + 4\,O_2 \rightleftharpoons Hb(O_2)_4$$
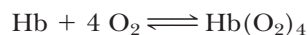
Then the *dissociation* constant, K, would be

$$K = \frac{[Hb][O_2]^4}{[Hb(O_2)_4]} \tag{A15.9}$$

By analogy with Equation (A15.4), the equation for fractional saturation of Hb is given by

$$Y = \frac{[pO_2]^4}{[pO_2]^4 + K} \tag{A15.10}$$

A plot of Y versus pO_2 according to Equation (A15.10) is presented in Figure A15.3. This curve has the characteristic sigmoid shape seen for O_2 binding by Hb. Half-saturation is set to be a pO_2 of 26 torr. Note that, when pO_2 is low, the fractional saturation, Y, changes very little as pO_2 increases. The interpretation is that Hb has little affinity for O_2 at these low partial pressures of O_2. However, as pO_2 reaches some threshold value and the first O_2 is bound, Y, the fractional saturation, increases rapidly. Note that the slope of the curve is steepest in the region where $Y = 0.5$. The sigmoid character of this curve is diagnostic of the fact that the binding of O_2 to one site on Hb strongly enhances binding of additional O_2 molecules to the remaining vacant sites on the same Hb molecule, a phenomenon aptly termed **cooperativity.** (If each O_2 bound independently, exerting no influence on the affinity of Hb for more O_2 binding, this plot would be hyperbolic.)
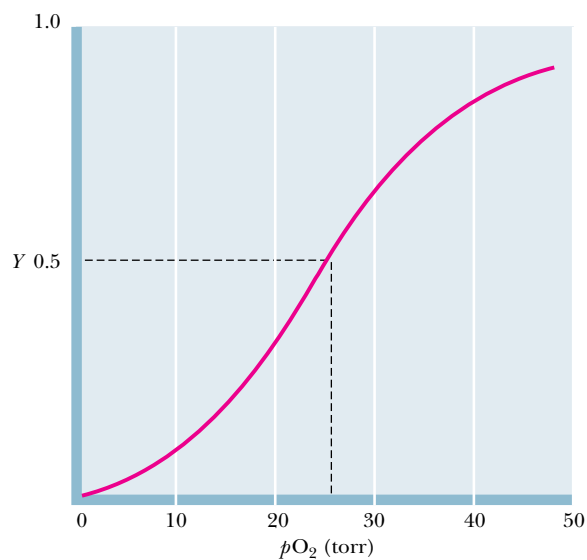
FIGURE A15.3 • Oxygen saturation curve for Hb in the form of Y versus pO_2, assuming $n = 4$, and $P_{50} = 26$ torr. The graph has the characteristic experimentally observed sigmoid shape.

The experimentally observed oxygen-binding curve for Hb does not fit the graph given in Figure A15.3 exactly. If we generalize Equation (A15.10) by replacing the exponent 4 by n, we can write the equation as

$$Y = \frac{[pO_2]^n}{[pO_2]^n + K} \tag{A15.11}$$

Rearranging yields

$$\frac{Y}{1 - Y} = \frac{[pO_2]^n}{K} \tag{A15.12}$$

This equation states that the ratio of oxygenated heme groups (Y) to O_2-free heme $(1 - Y)$ is equal to the nth power of the pO_2 divided by the apparent dissociation constant, K.

Archibald Hill demonstrated in 1913, well before any knowledge about the molecular organization of Hb existed, that the O_2-binding behavior of Hb could be described by Equation (A15.12). If a value of 2.8 is taken for n, Equation (A15.12) fits the experimentally observed O_2-binding curve for Hb very well (Figure A15.4). If the binding of O_2 to Hb were an all-or-none phenomenon,
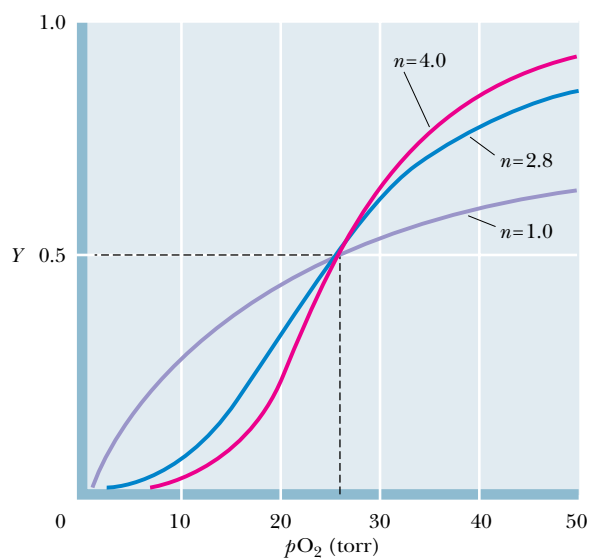
FIGURE A15.4 • A comparison of the experimentally observed O_2 curve for Hb yielding a value for n of 2.8, the hypothetical curve if $n = 4$, and the curve if $n = 1$ (noninteracting O_2-binding sites).

n would equal 4, as discussed above. If the O_2-binding sites on Hb were completely noninteracting, that is, if the binding of one O_2 to Hb had no influence on the binding of additional O_2 molecules to the same Hb, n would equal 1. Figure A15.4 compares these extremes. Obviously, the real situation falls between the extremes of $n = 1$ or 4. The qualitative answer is that O_2 binding by Hb is highly cooperative, and the binding of the first O_2 markedly enhances the binding of subsequent O_2 molecules. However, this binding is not quite an all-or-none phenomenon.

If we take the logarithm of both sides of Equation (A15.12):

$$\log \left(\frac{Y}{1 - Y} \right) = n(\log pO_2) - \log K \qquad (A15.13)$$

this expression is, of course, the generalized form of Equation (A15.8), the *Hill equation*, and a plot of $\log(Y/(1 - Y))$ versus $(\log pO_2)$ *approximates* a straight line in the region around $\log(Y/(1 - Y)) = 0$. Figure A15.5 represents a *Hill plot* comparing hemoglobin and myoglobin.

Because the binding of oxygen to hemoglobin is cooperative, the Hill plot is actually sigmoid (Figure A15.6). Cooperativity is a manifestation of the fact that the dissociation constant for the *first O_2*, K_1, is very different from the dissociation constant for the *last O_2 bound, K_4*. The tangent to the lower asymptote of the Hill plot, when extrapolated to the $\log(Y/(1 - Y)) = 0$ axis, gives the dissociation constant, K_1, for the binding of the first O_2 by Hb. Note that the value of K_1 is quite large ($> 10^2$ torr), indicating a low affinity of Hb for this first O_2 (or conversely, a ready dissociation of the Hb $(O_2)_1$ complex). By a similar process, the tangent to the upper asymptote gives K_4, the dissociation constant for the last O_2 to bind. K_4 has a value of less than 1 torr. The K_1/K_4 ratio exceeds 100, meaning the affinity of Hb for binding the fourth O_2 is over 100 times greater than for binding the first oxygen.

The value P_{50} has been defined above for myoglobin as the pO_2 that gives 50% saturation of the oxygen-binding protein with oxygen. Noting that at 50% saturation, $Y = (1 - Y)$, then we have from Equation (A15.13).

FIGURE A15.5 • Hill plot $(\log(Y/(1 - Y))$ versus $\log pO_2)$ for Mb and Hb, showing that at $\log(Y/(1 - Y)) = 0$, that is, $Y = (1 - Y)$, the slope for Mb is 1.0 and for Hb is 2.8. The plot for Hb only approximates a straight line.
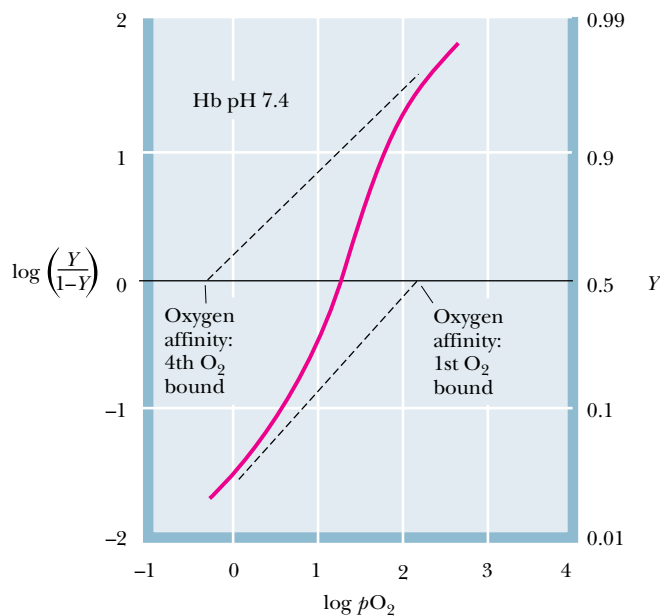
FIGURE A15.6 • Hill plot of Hb showing its nonlinear nature and the fact that its asymptotes can be extrapolated to yield the dissociation constants, K_1 and K_4, for the first and fourth oxygens.

$$0 = n(\log pO_2) - \log K = n(\log P_{50}) - \log K \qquad \text{(A15.14)}$$

$$\log K = n(\log P_{50}) \ or \ K = (P_{50})^n \qquad \text{(A15.15)}$$

That is, the situations for myoglobin and hemoglobin differ; therefore, P_{50} and K cannot be equated for Hb because of its multiple, interacting, O_2-binding sites. The relationship between pO_2 and P_{50} for hemoglobin, by use of Equation (A15.12), becomes

$$\frac{Y}{1 - Y} = \left(\frac{pO_2}{P_{50}}\right)^n \qquad \text{(A15.16)}$$

No single thing abides but all things flow.
Fragment to fragment clings and thus they
  grow
Until we know them by name.
Then by degrees they change and are no
  more the things we know.

LUCRETIUS (ca. 94 B.C.–50 B.C.)

Chapter 16

Mechanisms of Enzyme Action

Like the workings of an ancient clock, the details of enzyme mechanisms are at once complex and simple. (David Parker/Science Photo Library/Photo Researchers, Inc.)

Although the catalytic properties of enzymes may seem almost magical, it is simply chemistry—the breaking and making of bonds—that gives enzymes their prowess. This chapter will explore the unique features of this chemistry. The mechanisms of hundreds of enzymes have been studied in at least some detail. In this chapter, it will be possible to examine only a few of these. Nonetheless, the chemical principles that influence the mechanisms of these few enzymes are universal, and many other cases are understandable in light of the knowledge gained from these examples.

16.1 • The Basic Principle—Stabilization of the Transition State

In all chemical reactions, the reacting atoms or molecules pass through a state that is intermediate in structure between the reactant(s) and the product(s). Consider the transfer of a proton from a water molecule to a chloride anion:

$$\text{H—O—H} + \text{Cl}^- \rightleftharpoons \text{H—O}^{\delta-}\cdots\text{H}\cdots\text{Cl}^{\delta-} \rightleftharpoons \text{HO}^- + \text{H—Cl}$$

$$\textbf{Reactants} \qquad\qquad \textbf{Transition state} \qquad\qquad \textbf{Products}$$
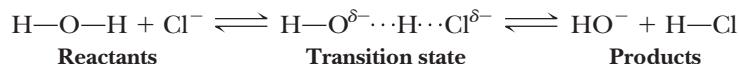
In the middle structure, the proton undergoing transfer is shared equally by the hydroxyl and chloride anions. This structure represents, as nearly as possible, the transition between the reactants and products, and it is known as the **transition state.**[1]

Chemical reactions in which a substrate (S) is converted to a product (P) can be pictured as involving a transition state (which we henceforth denote as $X^{\ddagger}$), a species intermediate in structure between S and P (Figure 16.1). As seen in Chapter 14, the catalytic role of an enzyme is to reduce the energy barrier between substrate and transition state. This is accomplished through the formation of an **enzyme–substrate complex** (ES). This complex is converted to product by passing through a transition state, $EX^{\ddagger}$ (Figure 16.1). As shown, the energy of $EX^{\ddagger}$ is clearly lower than $X^{\ddagger}$. One might be tempted to conclude that this decrease in energy explains the rate acceleration achieved by the enzyme, but there is more to the story.

The energy barrier for the uncatalyzed reaction (Figure 16.1) is of course the difference in energies of the S and $X^{\ddagger}$ states. Similarly, the energy barrier to be surmounted in the enzyme-catalyzed reaction, assuming that E is saturated with S, is the energy difference between ES and $EX^{\ddagger}$. *Reaction rate acceleration by an enzyme means simply that the energy barrier between ES and $EX^{\ddagger}$ is less than the energy barrier between S and $X^{\ddagger}$.* In terms of the free energies of activation, $\Delta G_{\text{e}}^{\ddagger} < \Delta G_{\text{u}}^{\ddagger}$.

(a)

(b)
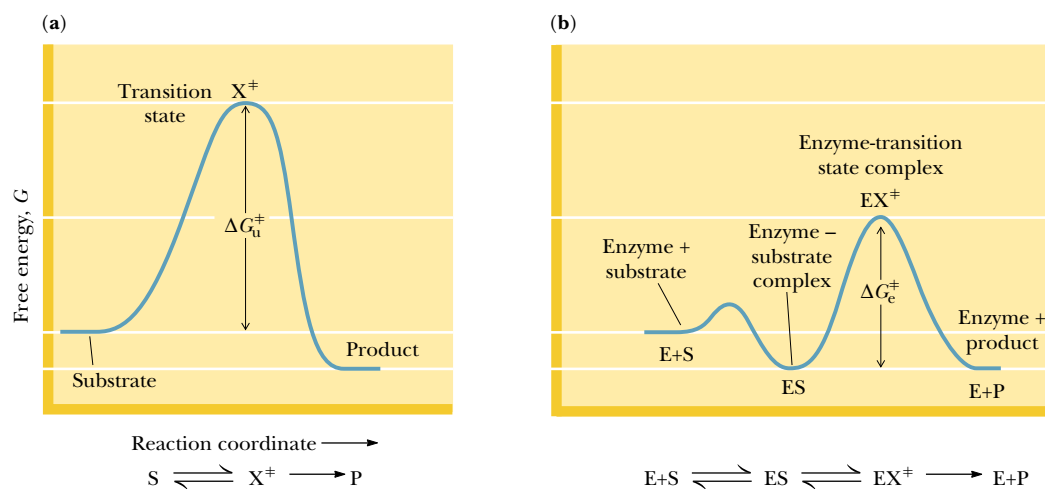
FIGURE 16.1 • Enzymes catalyze reactions by lowering the activation energy. Here the free energy of activation for (a) the uncatalyzed reaction, $\Delta G_{\text{u}}^{\ddagger}$, is larger than that for (b) the enzyme–catalyzed reaction, $\Delta G_{\text{e}}^{'\ddagger}$.

[1]It is important here to distinguish **transition states** from **intermediates.** A transition state is envisioned as an extreme distortion of a bond, and thus the lifetime of a typical transition state is viewed as being on the order of the lifetime of a bond vibration, typically 10^{-13} sec. Intermediates, on the other hand, are longer-lived, with lifetimes in the range of 10^{-13} sec to 10^{-3} sec.

$\mathcal{A}$ D E E P E R L O O K

What Is the Rate Enhancement of an Enzyme?

Enigmas abound in the world of enzyme catalysis. One of these surrounds the discussion of how the rate enhancement by an enzyme can be best expressed. Notice that the uncatalyzed conversion of a substrate S to a product P is usually a simple first-order process, described by a first-order rate constant k_u:

$$v_u = k_u[S]$$

On the other hand, for an enzyme that obeys Michaelis–Menten kinetics, the reaction is viewed as being first-order in S at low S and zero-order in S at high S. (See Chapter 14, where this distinction is discussed.)

$$v_e = \frac{k_{cat}[E_T][S]}{K_m + [S]}$$

If the "rate enhancement" effected by the enzyme is defined as

$$\text{rate enhancement} = v_e/v_u$$

then we can write:

$$\text{rate enhancement} = \frac{k_{cat}}{k_u}\left(\frac{[E_T]}{K_m + [S]}\right)$$

Depending on the relative sizes of K_m and $[S]$, there are two possible results:

Case 1: When $[S]$ is large compared to K_m, the enzyme is saturated with S and the kinetics are zero-order in S.

$$\text{rate enhancement} = \frac{k_{cat}}{k_u}\left(\frac{[E_T]}{[S]}\right)$$

where $[E_T]/[S]$ is the fraction of the total S that is in the ES complex. Note here that defining the rate enhancement in terms of k_{cat}/k_u is equivalent to comparing the quantities $\Delta G_e^\ddagger$ and $\Delta G_u^\ddagger$ in the figure at right.

Case 2: When $[S]$ is small compared to K_m, not all the enzyme molecules have S bound, and the kinetics are first order in S.

$$\text{rate enhancement} = \frac{k_{cat}}{k_u}\left(\frac{[E_T]}{K_m}\right)$$

Here, defining the rate enhancement in terms of $\dfrac{k_{cat}}{k_u K_m}$ is equivalent to comparing the quantities $\Delta G_{e'}^\ddagger$, and $\Delta G_u^\ddagger$ in the figure below. Moreover, to the extent that K_m is approximated by K_S (see Equation 16.1), this rate enhancement can be rewritten as

$$\text{rate enhancement} = \frac{[E_T]}{K_T}$$

where K_T is the dissociation constant for the $EX^\ddagger$ complex (see Equation 16.2).

Viewed in this way, the best definition of "rate enhancement" depends upon the relationship between enzyme and substrate concentrations and the enzyme's kinetic parameters.

Reaction Coordinate
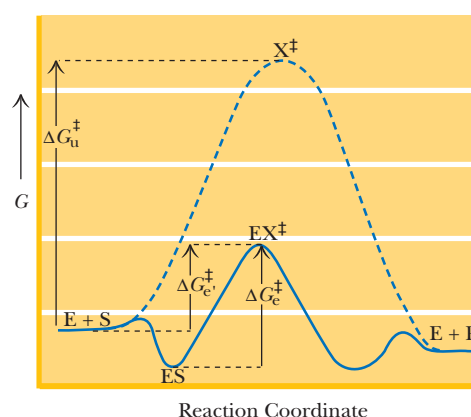
There are important consequences for this statement. The enzyme must stabilize the transition-state complex, $EX^\ddagger$, more than it stabilizes the substrate complex, ES. Put another way, enzymes are "designed" by nature to bind the transition-state structure more tightly than the substrate (or the product). The dissociation constant for the enzyme-substrate complex is

$$K_S = \frac{[E][S]}{[ES]} \tag{16.1}$$

and the corresponding dissociation constant for the transition-state complex is

$$K_T = \frac{[E][X^\ddagger]}{[EX^\ddagger]} \tag{16.2}$$

Enzyme catalysis requires that $K_T < K_S$. According to **transition-state theory** (see references at end of chapter), the rate constants for the enzyme-catalyzed (k_e) and uncatalyzed (k_u) reactions can be related to K_S and K_T by:

$$k_e/k_u \cong K_S/K_T \tag{16.3}$$

Thus, the enzymatic rate acceleration is approximately equal to the ratio of the dissociation constants of the enzyme–substrate and enzyme–transition-state complexes, at least when E is saturated with S.

16.2 • Enzymes Provide Enormous Rate Accelerations

Enzymes are powerful catalysts. Enzyme-catalyzed reactions are typically 10^7 to 10^{14} times faster than their uncatalyzed counterparts (Table 16.1). (There is even a report of a rate acceleration of $>10^{16}$ for the alkaline phosphatase-catalyzed hydrolysis of methylphosphate!)

These large rate accelerations correspond to substantial changes in the free energy of activation for the reaction in question. The urease reaction, for example,

$$\text{H}_2\text{N}-\overset{\displaystyle \overset{O}{\|}}{\text{C}}-\text{NH}_2 + 2\,\text{H}_2\text{O} + \text{H}^+ \longrightarrow 2\,\text{NH}_4{}^+ + \text{HCO}_3{}^-$$
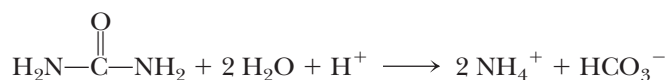
shows an energy of activation some 84 kJ/mol smaller than the corresponding uncatalyzed reaction. To fully understand any enzyme reaction, it is important to account for the rate acceleration in terms of the structure of the enzyme and its mechanism of action. There are a limited number of catalytic mechanisms or factors that contribute to the remarkable performance of enzymes.

Table 16.1

A Comparison of Enzyme-Catalyzed Reactions and Their Uncatalyzed Counterparts

Reaction	Enzyme	Uncatalyzed Rate, v_u (sec^{-1})	Catalyzed Rate, v_e (sec^{-1})	v_e/v_u
$\text{CH}_3-\text{O}-\text{PO}_3{}^{2-} + \text{H}_2\text{O} \longrightarrow \text{CH}_3\text{OH} + \text{HPO}_4{}^{2-}$	Alkaline phosphatase	1×10^{-15}	14	1.4×10^{16}
$\text{H}_2\text{N}-\overset{\overset{O}{\|}}{\text{C}}-\text{NH}_2 + 2\,\text{H}_2\text{O} + \text{H}^+ \longrightarrow 2\,\text{NH}_4{}^+ + \text{HCO}_3{}^-$	Urease	3×10^{-10}	3×10^4	1×10^{14}
$\text{R}-\overset{\overset{O}{\|}}{\text{C}}-\text{O}-\text{CH}_2\text{CH}_3 + \text{H}_2\text{O} \longrightarrow \text{RCOOH} + \text{HOCH}_2\text{CH}_3$	Chymotrypsin	1×10^{-10}	1×10^2	1×10^{12}
Glycogen + $\text{P}_i \longrightarrow$ Glycogen + Glucose-1-P $\quad(n)\qquad\qquad\qquad (n-1)$	Glycogen phosphorylase	$<5 \times 10^{-15}$	1.6×10^{-3}	$>3.2 \times 10^{11}$
Glucose + ATP $\longrightarrow$ Glucose-6-P + ADP	Hexokinase	$<1 \times 10^{-13}$	1.3×10^{-3}	$>1.3 \times 10^{10}$
$\text{CH}_3\text{CH}_2\text{OH} + \text{NAD}^+ \longrightarrow \text{CH}_3\overset{\overset{O}{\|}}{\text{C}}\text{H} + \text{NADH} + \text{H}^+$	Alcohol dehydrogenase	$<6 \times 10^{-12}$	2.7×10^{-5}	$>4.5 \times 10^6$
$\text{CO}_2 + \text{H}_2\text{O} \longrightarrow \text{HCO}_3{}^- + \text{H}^+$	Carbonic anhydrase	10^{-2}	10^5	1×10^7
Creatine + ATP $\longrightarrow$ Cr-P + ADP	Creatine kinase	$<3 \times 10^{-9}$	4×10^{-5}	$>1.33 \times 10^4$

Adapted from Koshland, D., 1956. *Journal of Cellular Comparative Physiology,* Supp. 1, **47:**217.

These include the following:

1. Entropy loss in ES formation
2. Destabilization of ES due to strain, desolvation, or electrostatic effects
3. Covalent catalysis
4. General acid or base catalysis
5. Metal ion catalysis
6. Proximity and orientation

Any or all of these mechanisms may contribute to the net rate acceleration of an enzyme-catalyzed reaction relative to the uncatalyzed reaction. A thorough understanding of any enzyme would require that the net acceleration be accounted for in terms of contributions from one or (usually) more of these mechanisms. Each of these will be discussed in detail in this chapter, but first it is important to appreciate how the formation of the enzyme-substrate (ES) complex makes all these mechanisms possible.

16.3 • The Binding Energy of ES Is Crucial to Catalysis

How is it that $X^{\ddagger}$ is stabilized more than S at the enzyme active site? To understand this, we must dissect and analyze the formation of the enzyme-substrate complex, ES. There are a number of important contributions to the free energy difference between the uncomplexed enzyme and substrate (E + S) and the ES complex (Figure 16.2). The favorable interactions between the substrate and amino acid residues on the enzyme account for the **intrinsic binding energy, ΔG_b**. The intrinsic binding energy ensures the favorable formation of the ES complex, but, if uncompensated, it makes the activation energy for the enzyme-catalyzed reaction unnecessarily large and wastes some of the catalytic power of the enzyme.

Compare the two cases in Figure 16.3. Because the enzymatic reaction rate is determined by the difference in energies between ES and $EX^{\ddagger}$, the smaller

FIGURE 16.2 • The intrinsic binding energy of the enzyme-substrate (ES) complex (ΔG_b) is compensated to some extent by entropy loss due to the binding of E and S (TΔS) and by destabilization of ES (ΔG_d) by strain, distortion, desolvation, and similar effects. If ΔG_b were not compensated by TΔS and ΔG_d, the formation of ES would follow the dashed line.
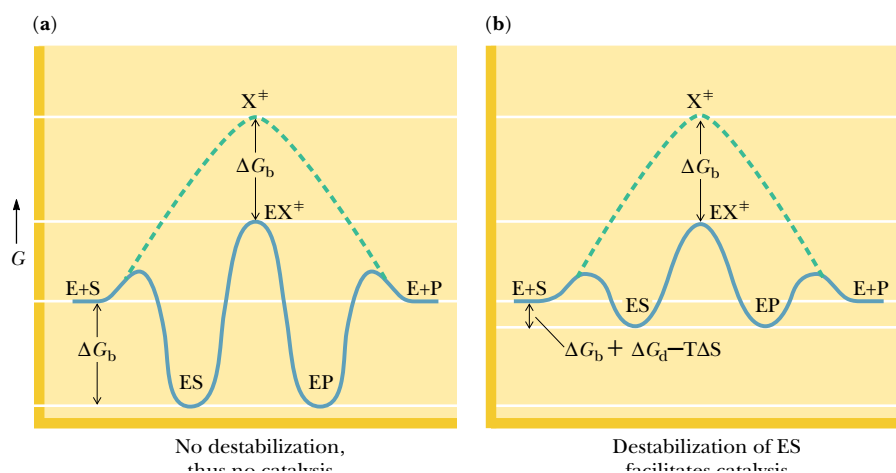
FIGURE 16.3 • (a) Catalysis does not occur if the ES complex and the transition state for the reaction are stabilized to equal extents. (b) Catalysis *will* occur if the transition state is stabilized to a greater extent than the ES complex (*right*). Entropy loss and destabilization of the ES complex ΔG_d ensure that this will be the case.

this difference, the faster the enzyme-catalyzed reaction. Tight binding of the substrate deepens the energy well of the ES complex and actually lowers the rate of the reaction.

16.4 • Entropy Loss and Destabilization of the ES Complex

The message of Figure 16.3 is that raising the energy of ES will increase the enzyme-catalyzed reaction rate. This is accomplished in two ways: (a) **loss of entropy** due to the binding of S to E, and (b) **destabilization of ES** by strain, distortion, desolvation, or other similar effects. The entropy loss arises from the fact that the ES complex (Figure 16.4) is a highly organized (low-entropy) entity compared to E + S in solution (a disordered, high-entropy situation). The entry of the substrate into the active site brings all the reacting groups and coordinating residues of the enzyme together with the substrate in just the proper position for reaction, with a net loss of entropy. The substrate and enzyme both possess **translational entropy,** the freedom to move in three dimensions, as well as **rotational entropy,** the freedom to rotate or tumble about any axis through the molecule. Both types of entropy are lost to some extent when two molecules (E and S) interact to form one molecule (the ES complex). Because ΔS is negative for this process, the term $-T\Delta S$ is a positive quantity, and *the intrinsic binding energy of ES is compensated to some extent by the entropy loss that attends the formation of the complex.*

Destabilization of the ES complex can involve **structural strain, desolvation,** or **electrostatic effects.** Destabilization by strain or distortion is usually just a consequence of the fact (noted previously) that *the enzyme is designed to bind the transition state more strongly than the substrate.* When the substrate binds, the imperfect nature of the "fit" results in distortion or strain in the substrate, the enzyme, or both. This means that the amino acid residues that make up the active site are oriented to coordinate the transition-state structure precisely, but will interact with the substrate or product less effectively.

Destabilization may also involve desolvation of charged groups on the substrate upon binding in the active site. Charged groups are highly stabilized in

Substrate (and enzyme) are free
to undergo translational motion.
A disordered, high-entropy situation

The highly ordered, low-entropy complex
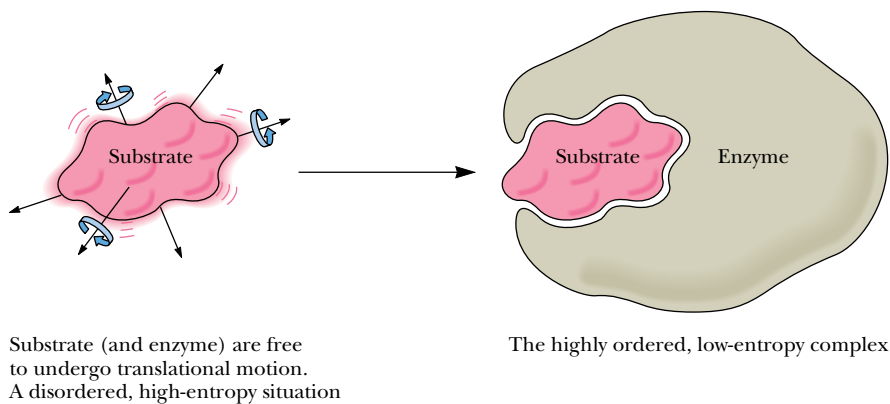
FIGURE 16.4 • Formation of the ES complex results in a loss of entropy. Prior to binding, E and S are free to undergo translational and rotational motion. By comparison, the ES complex is a more highly ordered, low-entropy complex.
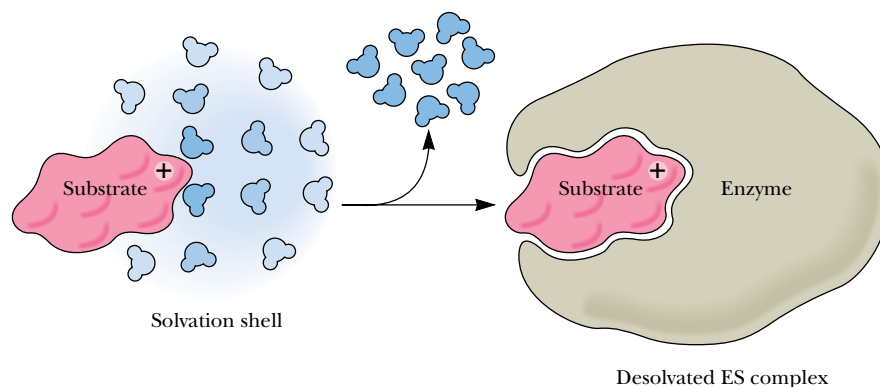
FIGURE 16.5 • Substrates typically lose waters of hydration in the formation of the ES complex. Desolvation raises the energy of the ES complex, making it more reactive.

water. For example, the transfer of Na^+ and Cl^- from the gas phase to aqueous solution is characterized by an **enthalpy of solvation, ΔH_{solv},** of -775 kJ/mol. (Energy is given off and the ions become more stable.) When charged groups on a substrate move from water into an enzyme active site (Figure 16.5), they are often desolvated to some extent, becoming less stable and therefore more reactive.

When a substrate enters the active site, charged groups may be forced to interact (unfavorably) with charges of like sign, resulting in **electrostatic destabilization** (Figure 16.6). The reaction pathway acts in part to remove this stress. If the charge on the substrate is diminished or lost in the course of reaction, electrostatic destabilization can result in rate acceleration.

Whether by strain, desolvation, or electrostatic effects, destabilization raises the energy of the ES complex, and this increase is summed in the term ΔG_d, the free energy of destabilization. As noted in Figure 16.2, the net energy difference between $E + S$ and the ES complex is the sum of the intrinsic binding energy, ΔG_b; the entropy loss on binding, $-T\Delta S$; and the distortion energy, ΔG_d. ES is destabilized (raised in energy) by the amount $\Delta G_d - T\Delta S$. The transition state is subject to no such destabilization, and the difference between the energies of $X^{\ddagger}$ and $EX^{\ddagger}$ is essentially ΔG_b, the full intrinsic binding energy.
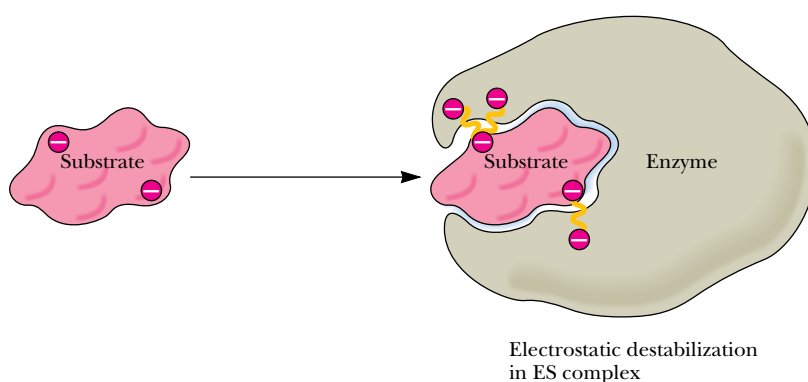
FIGURE 16.6 • Electrostatic destabilization of a substrate may arise from juxtaposition of like charges in the active site. If such charge repulsion is relieved in the course of the reaction, electrostatic destabilization can result in a rate increase.

16.5 • Transition-State Analogs Bind Very Tightly to the Active Site

Although not apparent at first, there are other important implications of Equation 16.3. It is important to consider the magnitudes of K_S and K_T. The ratio k_e/k_u may even exceed 10^{16}, as noted previously. Given a typical ratio of 10^{12} and a typical K_S of 10^{-3} M, the value of K_T should be 10^{-15} M! This is the dissociation constant for the transition-state complex from the enzyme, and this very low value corresponds to very tight binding of the transition state by the enzyme.

It is unlikely that such tight binding in an enzyme transition state will ever be measured experimentally, however, because the transition state itself is a "moving target." It exists only for about 10^{-14} to 10^{-13} sec, less than the time required for a bond vibration. The nature of the elusive transition state can be explored, on the other hand, using **transition-state analogs,** stable molecules that are chemically and structurally similar to the transition state. Such molecules should bind more strongly than a substrate and more strongly than competitive inhibitors that bear no significant similarity to the transition state. Hundreds of examples of such behavior have been reported. For example, Robert Abeles studied a series of inhibitors of **proline racemase** (Figure 16.7) and found that *pyrrole-2-carboxylate* bound to the enzyme 160 times more tightly than L-proline, the normal substrate. This analog binds so tightly because it is planar and is similar in structure to the planar transition state for the racemization of proline. Two other examples of transition-state analogs are shown in Figure 16.8. *Phosphoglycolohydroxamate* binds 40,000 times more tightly to yeast aldolase than the substrate dihydroxyacetone phosphate. Even more remarkable, the 1,6-hydrate of *purine ribonucleoside* has been estimated to bind to adenosine deaminase with a K_i of 3×10^{-13} M!

It should be noted that transition-state analogs are only approximations of the transition state itself and will never bind as tightly as would be expected for the true transition state. These analogs are, after all, stable molecules and cannot be expected to resemble a true transition state too closely.
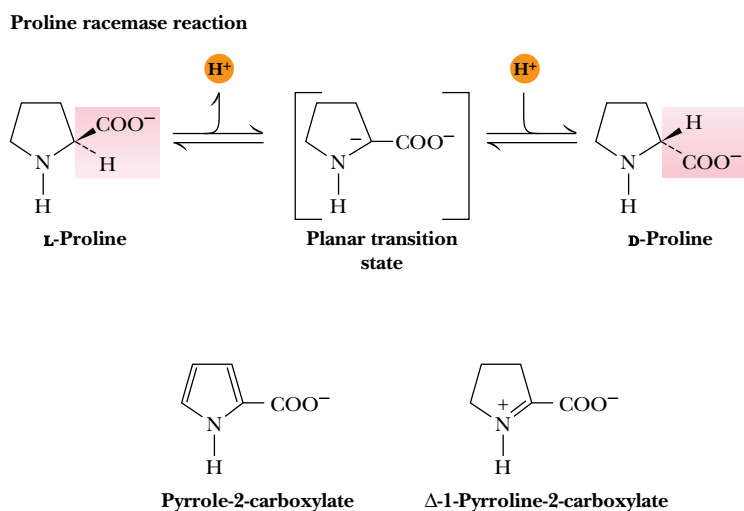
FIGURE 16.7 • The proline racemase reaction. Pyrrole-2-carboxylate and Δ-1-pyrroline-2-carboxylate mimic the planar transition state of the reaction.

(a) Yeast aldolase reaction

Enediolate
(Transition-state intermediate)

$K_m = 4 \times 10^{-4} M$

Phosphoglycolohydroxamate

$K_i = 1 \times 10^{-8} M$

**Fructose-1,6-
bisphosphate**

$\dfrac{K_m}{K_i} = 4 \times 10^4$

(b) Calf intestinal adenosine deaminase reaction

Adenosine
$K_m = 3 \times 10^{-5} M$

**Transition-state
intermediate**

Inosine

**Hydrated form of
purine ribonucleoside**
$K_i = 3 \times 10^{-13} M$

$\dfrac{K_m}{K_i} = 1 \times 10^8$
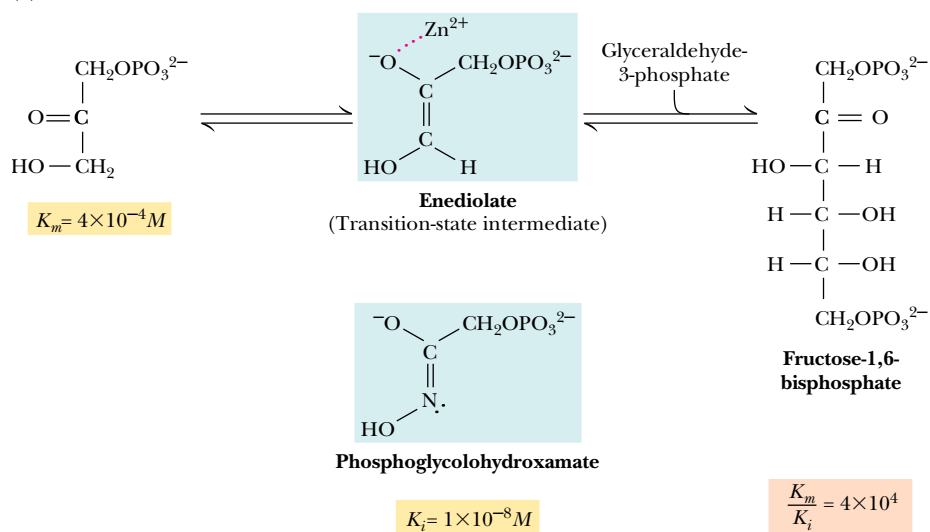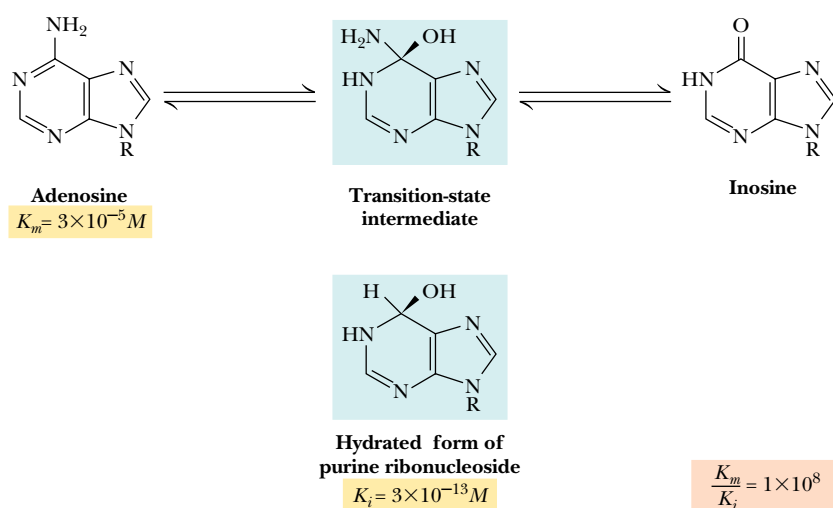
FIGURE 16.8 • (a) Phosphoglycolohydroxamate is an analog of the enediolate transition state of the yeast aldolase reaction. (b) Purine riboside, a potent inhibitor of the calf intestinal adenosine deaminase reaction, binds to adenosine deaminase as the 1,6-hydrate. The hydrated form of purine riboside is an analog of the proposed transition state for the reaction.

16.6 • Covalent Catalysis

Some enzyme reactions derive much of their rate acceleration from the formation of **covalent bonds** between enzyme and substrate. Consider the reaction:

$$BX + Y \longrightarrow BY + X$$

and an enzymatic version of this reaction involving formation of a **covalent intermediate:**

$$BX + Enz \longrightarrow E:B + X + Y \longrightarrow Enz + BY$$
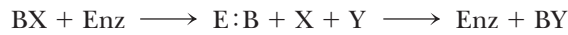
If the enzyme-catalyzed reaction is to be faster than the uncatalyzed case, the acceptor group on the enzyme must be a better attacking group than Y and a better leaving group than X. Note that most enzymes that carry out covalent catalysis have ping-pong kinetic mechanisms.

The side chains of amino acids in proteins offer a variety of **nucleophilic** centers for catalysis, including amines, carboxylates, aryl and alkyl hydroxyls, imidazoles, and thiol groups. These groups readily attack electrophilic centers of substrates, forming covalently bonded enzyme-substrate intermediates. Typical electrophilic centers in substrates include phosphoryl groups, acyl groups, and glycosyl groups (Figure 16.9). The covalent intermediates thus formed can be attacked in a subsequent step by a water molecule or a second substrate, giving the desired product. **Covalent electrophilic catalysis** is also observed, but usually involves coenzyme adducts that generate electrophilic centers. Well over 100 enzymes are now known to form covalent intermediates during catalysis. Table 16.2 lists some typical examples, including that of glyceraldehyde-3-phosphate dehydrogenase, which catalyzes the reaction:

Glyceraldehyde-3-P $+$ NAD$^+$ $+$ P$_i$ $\longrightarrow$

1,3-Bisphosphoglycerate $+$ NADH $+$ H$^+$
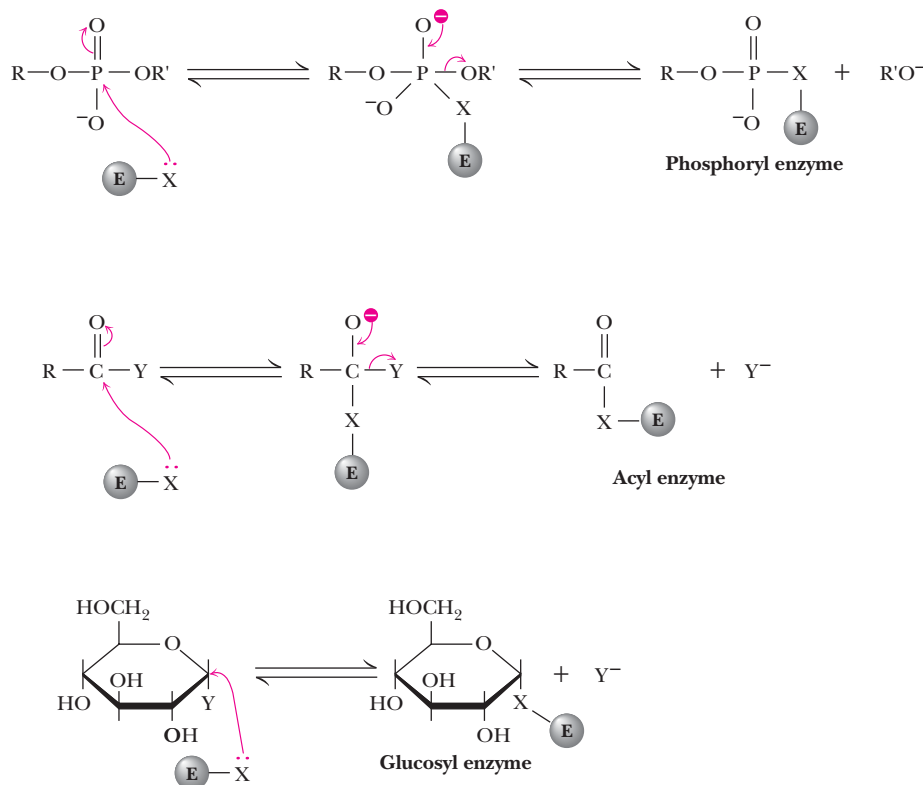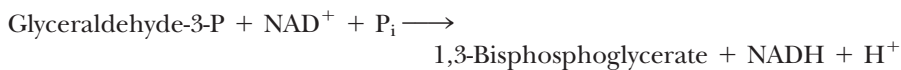
FIGURE 16.9 • Examples of covalent bond formation between enzyme and substrate. In each case, a nucleophilic center (X:) on an enzyme attacks an electrophilic center on a substrate.

Table 16.2

Enzymes That Form Covalent Intermediates

Enzymes	Reacting Group	Covalent Intermediate
1. Chymotrypsin Elastase Esterases Subtilisin Thrombin Trypsin	CH₂ CH OH (Ser)	CH₂ CH O—C—R O (Acyl-Ser)
2. Glyceraldehyde-3-phosphate dehydrogenase Papain	CH₂ CH SH (Cys)	CH₂ CH S—C—R O (Acyl-Cys)
3. Alkaline phosphatase Phosphoglucomutase	CH₂ CH OH (Ser)	CH₂ CH O—PO₃²⁻ (Phosphoserine)
4. Phosphoglycerate mutase Succinyl-CoA synthetase	—CH₂ HN N (His)	—CH₂ O ⁻O—P—N N O⁻ (Phosphohistidine)
5. Aldolase Decarboxylases Pyridoxal phosphate–dependent enzymes	R—NH₃⁺ (Amino)	R—N=C (Schiff base)

As shown in Figure 16.10, this reaction mechanism involves nucleophilic attack by —SH on the substrate glyceraldehyde-3-P to form a covalent *acylcysteine* (or *hemithioacetal*) intermediate. Hydride transfer to NAD⁺ generates a *thioester* intermediate. Nucleophilic attack by phosphate yields the desired mixed carboxylic–phosphoric anhydride product, 1,3-bisphosphoglycerate. Several examples of covalent catalysis will be discussed in detail in later chapters.
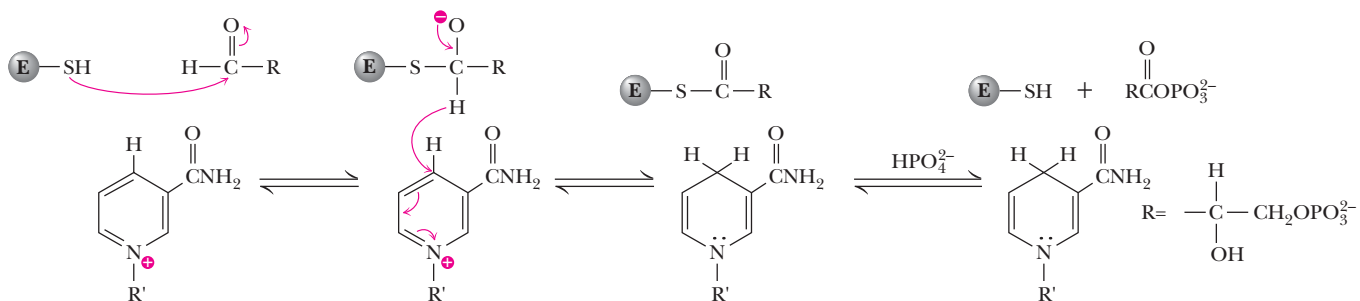
FIGURE 16.10 • Formation of a covalent intermediate in the glyceraldehyde-3-phosphate dehydrogenase reaction. Nucleophilic attack by a cysteine —SH group forms a covalent acylcysteine intermediate. Following hydride transfer to NAD⁺, nucleophilic attack by phosphate yields the product, 1,3-bisphosphoglycerate.

16.7 • General Acid–Base Catalysis

Nearly all enzyme reactions involve some degree of acid or base catalysis. There are two types of acid–base catalysis: (1) **specific acid–base catalysis,** in which H^+ or OH^- accelerates the reaction, and (2) **general acid–base catalysis,** in which an acid or base other than H^+ or OH^- accelerates the reaction. For ordinary solution reactions, these two cases can be distinguished on the basis of simple experiments. As shown in Figure 16.11, in specific acid or base catalysis, the buffer concentration has no effect. In general acid or base catalysis, however, the buffer may donate or accept a proton in the transition state and thus affect the rate. *By definition, general acid–base catalysis is catalysis in which a proton is transferred in the transition state.* Consider the hydrolysis of *p*-nitrophenylacetate with imidazole acting as a general base (Figure 16.12). Proton transfer apparently stabilizes the transition state here. The water has been made more nucleophilic without generation of a high concentration of OH^- or without the formation of unstable, high-energy species. General acid or general base catalysis may increase reaction rates 10- to 100-fold. In an enzyme, ionizable groups on the protein provide the H^+ transferred in the transition state. Clearly, an ionizable group will be most effective as a H^+ transferring agent at or near its pK_a. Because the pK_a of the histidine side chain is near 7, histidine is often the most effective general acid or base. Descriptions of several cases of general acid–base catalysis in typical enzymes follow.

16.8 • Metal Ion Catalysis

Many enzymes require metal ions for maximal activity. If the enzyme binds the metal very tightly or requires the metal ion to maintain its stable, native state, it is referred to as a **metalloenzyme.** Enzymes that bind metal ions more weakly, perhaps only during the catalytic cycle, are referred to as **metal activated.** One role for metals in metal-activated enzymes and metalloenzymes is to act as electrophilic catalysts, stabilizing the increased electron density or negative charge that can develop during reactions. Among the enzymes that function in this

(a)

k_{obs}

pH 8
pH 7
pH 6

Buffer concentration

(b)

pH 8
pH 7
pH 6

Buffer concentration
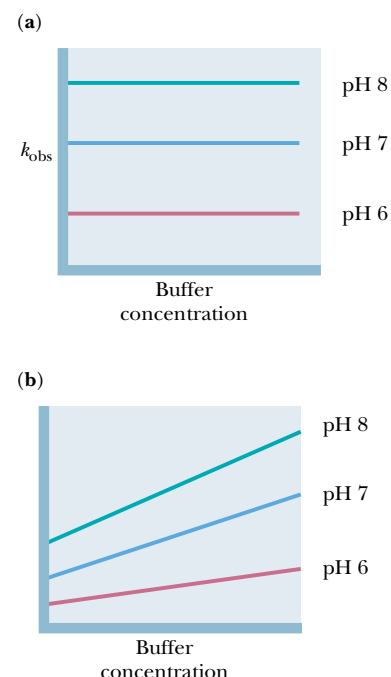
FIGURE 16.11 • Specific and general acid–base catalysis of simple reactions in solution may be distinguished by determining the dependence of observed reaction rate constants (k_{obs}) on pH and buffer concentration. (a) In specific acid–base catalysis, H^+ or OH^- concentration affects the reaction rate, k_{obs} is pH-dependent, but buffers (which accept or donate H^+/OH^-) have no effect. (b) In general acid–base catalysis, in which an ionizable buffer may donate or accept a proton in the transition state, k_{obs} is dependent on buffer concentration.

Reaction
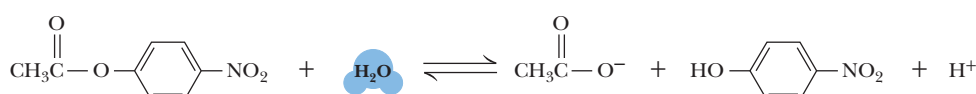
Mechanism
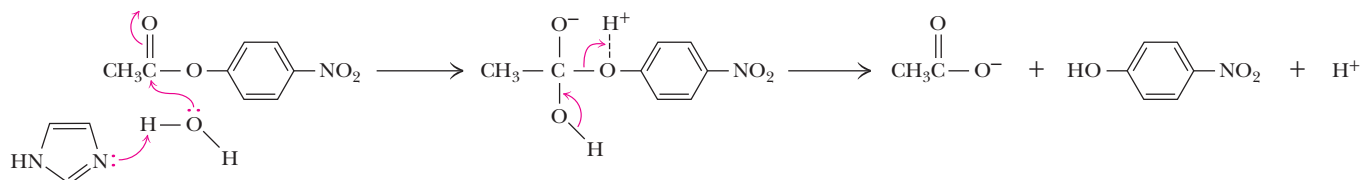
FIGURE 16.12 • Catalysis of *p*-nitrophenylacetate hydrolysis by imidazole—an example of general base catalysis. Proton transfer to imidazole in the transition state facilitates hydroxyl attack on the substrate carbonyl carbon.
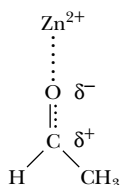
FIGURE 16.13 • Liver alcohol dehydrogenase catalyzes the transfer of a hydride ion $(H:^-)$ from NADH to acetaldehyde (CH_3CHO), forming ethanol (CH_3CH_2OH). An active-site zinc ion stabilizes negative charge development on the oxygen atom of acetaldehyde, leading to an induced partial positive charge on the carbonyl C atom. Transfer of the negatively charged hydride ion to this carbon forms ethanol.

manner (Figure 16.13) is liver alcohol dehydrogenase. Another potential function of metal ions is to provide a powerful nucleophile at neutral pH. Coordination to a metal ion can increase the acidity of a nucleophile with an ionizable proton:

$$M^{2+} + NucH \rightleftharpoons M^{2+}(NucH) \rightleftharpoons M^{2+}(Nuc^-) + H^+$$

The reactivity of the coordinated, deprotonated nucleophile is typically intermediate between that of the un-ionized and ionized forms of the nucleophile. Carboxypeptidase (Chapter 5) contains an active site Zn^{2+}, which facilitates deprotonation of a water molecule in this manner.

16.9 • Proximity

Chemical reactions go faster when the reactants are *in proximity*, that is, near each other. In solution or in the gas phase, this means that increasing the concentrations of reacting molecules, which raises the number of collisions, causes higher rates of reaction. Enzymes, which have specific binding sites for particular reacting molecules, essentially take the reactants out of dilute solution and hold them close to each other. This proximity of reactants is said to raise the "effective" concentration over that of the substrates in solution, and leads to an increased reaction rate. In order to measure proximity effects in enzyme reactions, enzymologists have turned to model studies comparing intermolecular reaction rates with corresponding or similar intramolecular reaction rates. A typical case is the imidazole-catalyzed hydrolysis of *p*-nitrophenylacetate (Figure 16.14a). Under certain conditions the rate constant for this bimolecular reaction is 35 M^{-1} min^{-1}. By comparison, the first-order rate constant for the analogous but intramolecular reaction shown in Figure 16.14b is 839 min^{-1}. The ratio of these two rate constants

$$(839 \ min^{-1})/(35 \ M^{-1} \ min^{-1}) = 23.97 \ M$$

has the units of concentration and can be thought of as an effective concentration of imidazole in the intramolecular reaction. Put another way, a concentration of imidazole of 23.9 M would be required in the intermolecular reaction to make it proceed as fast as the intramolecular reaction.

There is more to this story, however. Enzymes not only bring substrates and catalytic groups close together, they orient them in a manner suitable for catalysis as well. Comparison of the rates of reaction of the molecules shown
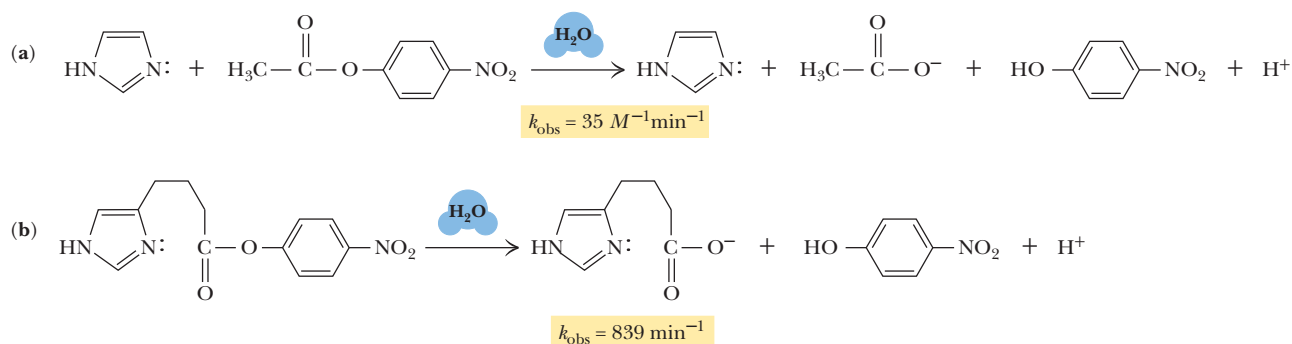
FIGURE 16.14 • An example of proximity effects in catalysis. (a) The imidazole-catalyzed hydrolysis of *p*-nitrophenylacetate is slow, but the corresponding intramolecular reaction is 24-fold faster (assuming [imidazole] = 1 M in [a]).
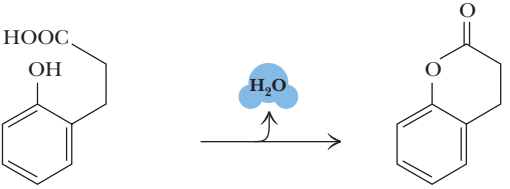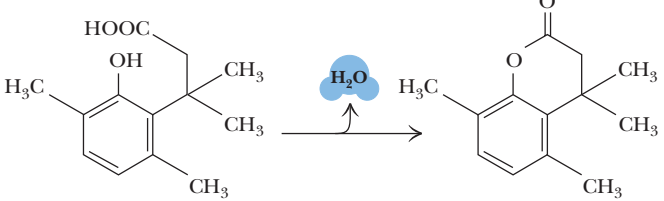
Reaction	Rate const. $(M^{-1}sec^{-1})$	Ratio
	5.9×10^{-6}	
	1.5×10^{6}	2.5×10^{11}

FIGURE 16.15 • Orientation effects in intramolecular reactions can be dramatic. Steric crowding by methyl groups provides a rate acceleration of 2.5×10^{11} for the lower reaction compared to the upper reaction. (*Adapted from Milstien, S., and Cohen, L. A., 1972. Stereopopulation control I. Rate enhancements in the lactonization of o-hydroxyhydrocinnamic acid. Journal of the American Chemical Society **94**:9158–9165.*)

in Figure 16.15 makes it clear that the bulky methyl groups force an orientation on the alkyl carboxylate and the aromatic hydroxyl groups that makes them approximately 250 billion times more likely to react. Enzymes function similarly by placing catalytically functional groups (from the protein side chains or from another substrate) in the proper position for reaction.

Clearly, proximity and orientation play a role in enzyme catalysis, but there is a problem with each of the above comparisons. In both cases, it is impossible to separate true proximity and orientation effects from the effects of entropy loss when molecules are brought together (described the Section 16.4). The actual rate accelerations afforded by proximity and orientation effects in Figures 16.14 and 16.15, respectively, are much smaller than the values given in these figures. Simple theories based on probability and nearest-neighbor models, for example, predict that proximity effects may actually provide rate increases of only 5- to 10-fold. For any real case of enzymatic catalysis, it is nonetheless important to remember that proximity and orientation effects are significant.

16.10 • Typical Enzyme Mechanisms

The balance of this chapter will be devoted to several classic and representative enzyme mechanisms. These particular cases are well understood, because the three-dimensional structures of the enzymes and the bound substrates are known at atomic resolution, and because great efforts have been devoted to kinetic and mechanistic studies. They are important because they represent reaction types that appear again and again in living systems, and because they demonstrate many of the catalytic principles cited above. Enzymes are the catalytic machines that sustain life, and what follows is an intimate look at the inner workings of the machinery.

16.11 • Serine Proteases

Serine proteases are a class of proteolytic enzymes whose catalytic mechanism is based on an active-site serine residue. Serine proteases are one of the best-characterized families of enzymes. This family includes *trypsin, chymotrypsin, elastase, thrombin, subtilisin, plasmin, tissue plasminogen activator,* and other related enzymes. The first three of these are digestive enzymes and are synthesized in the pancreas and secreted into the digestive tract as inactive **proenzymes,** or **zymogens.** Within the digestive tract, the zymogen is converted into the active enzyme form by cleaving off a portion of the peptide chain. Thrombin is a crucial enzyme in the blood-clotting cascade, subtilisin is a bacterial protease, and plasmin breaks down the fibrin polymers of blood clots. Tissue plasminogen activator (TPA) specifically cleaves the proenzyme *plasminogen,* yielding plasmin. Owing to its ability to stimulate breakdown of blood clots, TPA can minimize the harmful consequences of a heart attack, if administered to a patient within 30 minutes of onset. Finally, although not itself a protease, *acetylcholinesterase is a serine esterase* and is related mechanistically to the serine proteases. It degrades the neurotransmitter acetylcholine in the synaptic cleft between neurons.

The Digestive Serine Proteases

Trypsin, chymotrypsin, and elastase all carry out the same reaction—the cleavage of a peptide chain—and although their structures and mechanisms are quite similar, they display very different specificities. Trypsin cleaves peptides

FIGURE 16.16 • Comparison of the amino acid sequences of chymotrypsinogen, trypsinogen, and elastase. Each circle represents one amino acid. Numbering is based on the sequence of chymotrypsinogen. Filled circles indicate residues that are identical in all three proteins. Disulfide bonds are indicated in yellow. The positions of the three catalytically important active-site residues (His[57], Asp[102], and Ser[195]) are indicated.
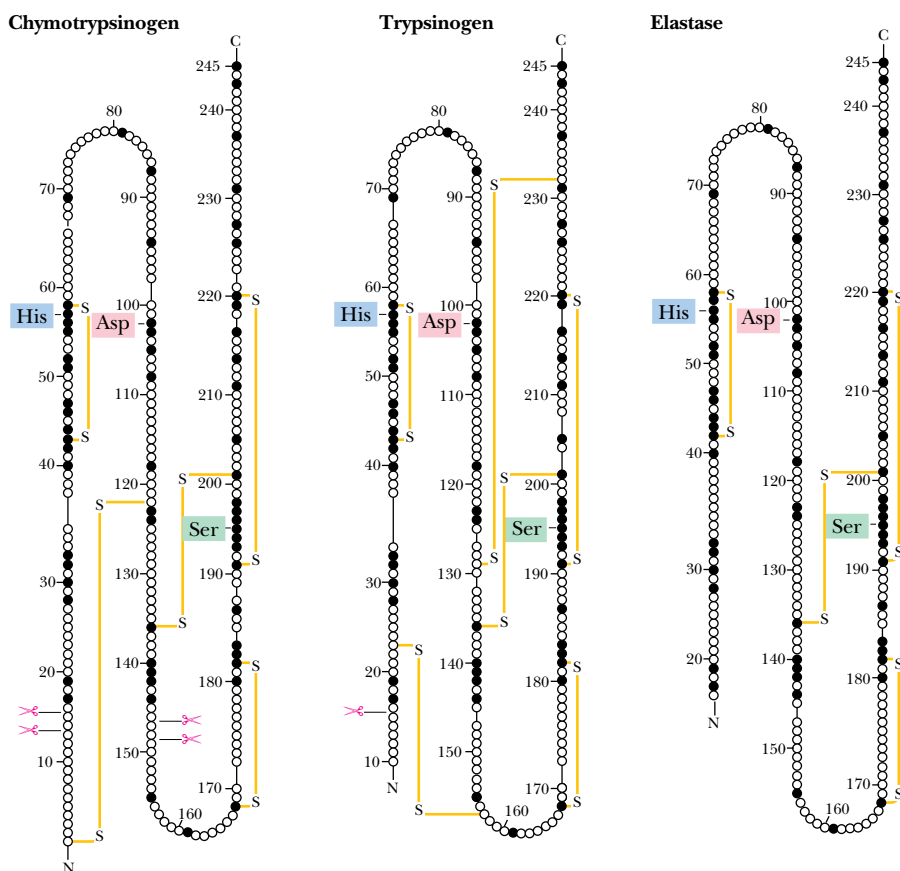
on the carbonyl side of the basic amino acids, arginine or lysine (see Table 5.6). Chymotrypsin prefers to cleave on the carbonyl side of aromatic residues, such as phenylalanine and tyrosine. Elastase is not as specific as the other two; it mainly cleaves peptides on the carbonyl side of small, neutral residues. These three enzymes all possess molecular weights in the range of 25,000, and all have similar sequences (Figure 16.16) and three-dimensional structures. The structure of chymotrypsin is typical (Figure 16.17). The molecule is ellipsoidal in shape and contains an α-helix at the C-terminal end (residues 230 to 245) and several β-sheet domains. Most of the aromatic and hydrophobic residues are buried in the interior of the protein, and most of the charged or hydrophilic residues are on the surface. Three polar residues—His[57], Asp[102], and Ser[195]—form what is known as a **catalytic triad** at the active site (Figure 16.18). These three residues are conserved in trypsin and elastase as well. The active site in this case is actually a depression on the surface of the enzyme, with a small pocket that the enzyme uses to identify the residue for which it is specific (Figure 16.19). Chymotrypsin, for example, has a pocket surrounded by hydrophobic residues and large enough to accommodate an aromatic side chain. The pocket in trypsin has a negative charge (Asp[189]) at its bottom, facilitating the binding of positively charged arginine and lysine residues. Elastase, on the other hand, has a shallow pocket with bulky threonine and valine residues at the opening. Only small, nonbulky residues can be accommodated in its pocket. The backbone of the peptide substrate is hydrogen-bonded in antiparallel fashion to residues 215 to 219 and bent so that the peptide bond to be cleaved is bound close to His[57] and Ser[195].

The Chymotrypsin Mechanism in Detail: Kinetics

Much of what is known about the chymotrypsin mechanism is based on studies of the hydrolysis of artificial substrates—simple organic esters, such as *p*-nitrophenylacetate, and methyl esters of amino acid analogs, such as

FIGURE 16.17 • Structure of chymotrypsin (white) in a complex with eglin C (blue ribbon structure), a target protein. The residues of the catalytic triad (His[57], Asp[102], and Ser[195]) are highlighted. His[57] (blue) is flanked above by Asp[102] (red) and on the right by Ser[195] (yellow). The catalytic site is filled by a peptide segment of eglin. Note how close Ser[195] is to the peptide that would be cleaved in a chymotrypsin reaction.

FIGURE 16.18 • The catalytic triad of chymotrypsin.

FIGURE 16.19 • The substrate-binding pockets of trypsin, chymotrypsin, and elastase. (*Irving Geis*)

p-Nitrophenylacetate   **Acetylphenylalanine methyl ester**   **Formylphenylalanine methyl ester**   **Benzoylalanine methyl ester**
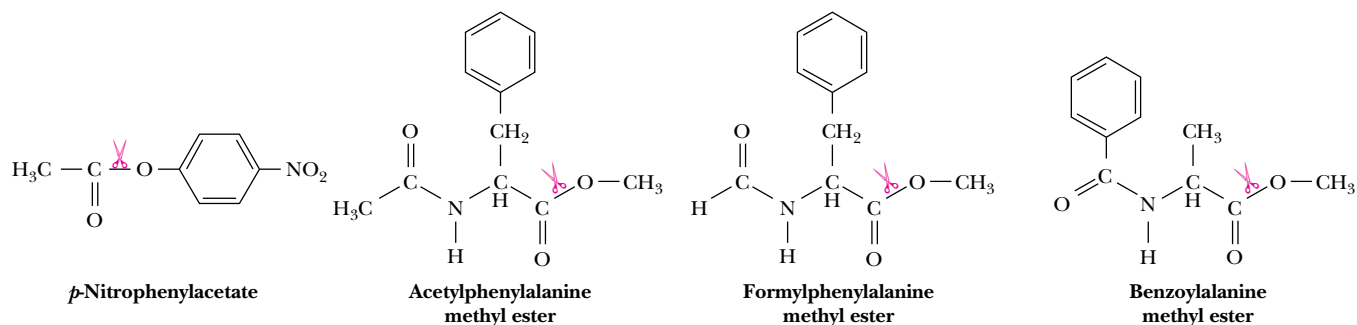
FIGURE 16.20 • Artificial substrates used in studies of the mechanism of chymotrypsin.
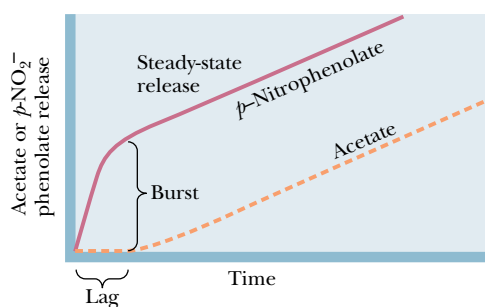
FIGURE 16.21 • Burst kinetics observed in the chymotrypsin reaction. A burst of nitrophenolate production is followed by a slower, steady-state release. After an initial lag period, acetate release is also observed. This kinetic pattern is consistent with rapid formation of an acyl-enzyme intermediate (and the burst of nitrophenolate). The slower, steady-state release of products corresponds to rate-limiting breakdown of the acyl-enzyme intermediate.

formylphenylalanine methyl ester and acetylphenylalanine methyl ester (Figure 16.20). *p*-Nitrophenylacetate is an especially useful model substrate, because the nitrophenolate product is easily observed, owing to its strong absorbance at 400 nm. When large amounts of chymotrypsin are used in kinetic studies with this substrate, a **rapid initial burst** of *p*-nitrophenolate is observed (in an amount approximately equal to the enzyme concentration), followed by a much slower, linear rate of nitrophenolate release (Figure 16.21). Observation of a burst, followed by slower, steady-state product release, is strong evidence for a multistep mechanism, with a fast first step and a slower second step.

In the chymotrypsin mechanism, the nitrophenylacetate combines with the enzyme to form an ES complex. This is followed by a rapid second step in which an **acyl-enzyme intermediate** is formed, with the acetyl group covalently bound to the very reactive Ser^{195}. The nitrophenyl moiety is released as nitrophenolate (Figure 16.22), accounting for the burst of nitrophenolate product. Attack of a water molecule on the acyl-enzyme intermediate yields acetate as the second product in a subsequent, slower step. The enzyme is now free to bind another molecule of *p*-nitrophenylacetate, and the *p*-nitrophenolate product produced at this point corresponds to the slower, steady-state formation of product in the upper right portion of Figure 16.21. In this mechanism, the release of acetate is the **rate-limiting step,** and accounts for the observation of **burst kinetics**—the pattern shown in Figure 16.21.

Serine proteases like chymotrypsin are susceptible to inhibition by **organic fluorophosphates,** such as *diisopropylfluorophosphate (DIFP,* Figure 16.23). DIFP
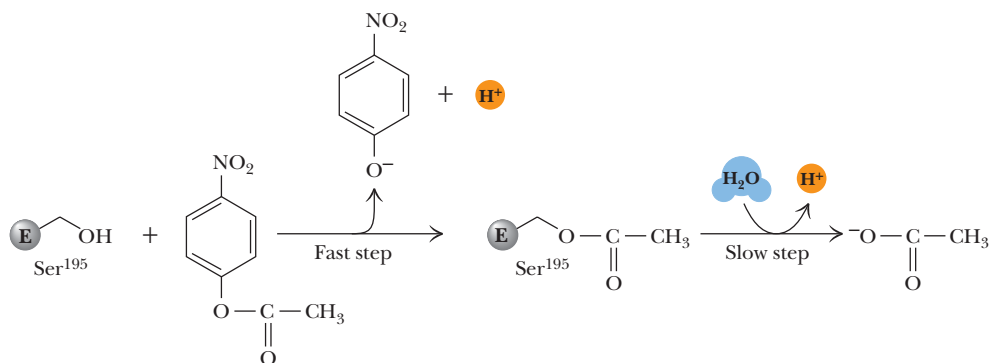
FIGURE 16.22 • Rapid formation of the acyl-enzyme intermediate is followed by slower product release.
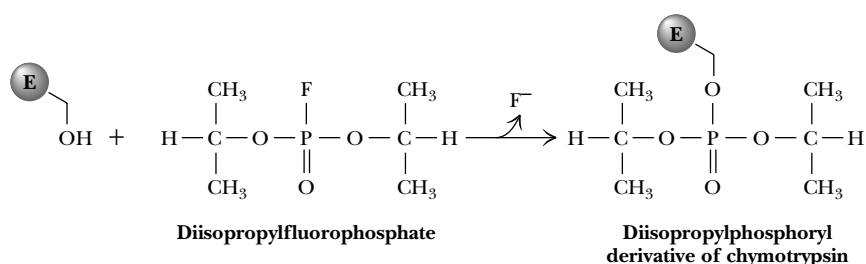
FIGURE 16.23 • Diisopropylfluorophosphate (DIFP) reacts with active-site serine residues of serine proteases (and esterases), causing permanent inactivation.

reacts rapidly with active-site serine residues, such as Ser^{195} of chymotrypsin and the other serine proteases (but not with any of the other serines in these proteins), to form a DIP-enzyme. This covalent enzyme-inhibitor complex is extremely stable, and chymotrypsin is thus permanently inactivated by DIFP.

The Serine Protease Mechanism in Detail: Events at the Active Site

A likely mechanism for peptide hydrolysis is shown in Figure 16.24. As the backbone of the substrate peptide binds adjacent to the catalytic triad, the specific side chain fits into its pocket. Asp^{102} of the catalytic triad positions His^{57} and immobilizes it through a hydrogen bond as shown. In the first step of the reaction, His^{57} acts as a general base to withdraw a proton from Ser^{195}, facilitating nucleophilic attack by Ser^{195} on the carbonyl carbon of the peptide bond to be cleaved. This is probably a *concerted step,* because proton transfer prior to Ser^{195} attack on the acyl carbon would leave a relatively unstable negative charge on the serine oxygen. In the next step, donation of a proton from His^{57} to the peptide's amide nitrogen creates a protonated amine on the covalent, tetrahedral intermediate, facilitating the subsequent bond breaking and dissociation of the amine product. The negative charge on the peptide oxygen is unstable; the tetrahedral intermediate is short-lived and rapidly breaks down to expel the amine product. The acyl-enzyme intermediate that results is reasonably stable; it can even be isolated using substrate analogs for which further reaction cannot occur. With normal peptide substrates, however, subsequent nucleophilic attack at the carbonyl carbon by water generates another transient tetrahedral intermediate (Figure 16.24). His^{57} acts as a general base in this step, accepting a proton from the attacking water molecule. The subsequent collapse of the tetrahedral intermediate is assisted by proton donation from His^{57} to the serine oxygen in a concerted manner. Deprotonation of the carboxyl group and its departure from the active site complete the reaction as shown.

Until recently, the catalytic role of Asp^{102} in trypsin and the other serine proteases had been surmised on the basis of its proximity to His^{57} in structures obtained from X-ray diffraction studies, but it had never been demonstrated with certainty in physical or chemical studies. As can be seen in Figure 16.17, Asp^{102} is buried at the active site and is normally inaccessible to chemical modifying reagents. In 1987, however, Charles Craik, William Rutter, and their colleagues used site-directed mutagenesis (see Chapter 13) to prepare a mutant trypsin with an asparagine in place of Asp^{102}. This mutant trypsin possessed a hydrolytic activity with ester substrates only 1/10,000 that of native trypsin, demonstrating that Asp^{102} is indeed essential for catalysis and that its ability to immobilize and orient His^{57} is crucial to the function of the catalytic triad.

(a)

(b)

Binding of substrate

Formation of covalent ES complex

(c)

(d)

Proton donation by His 57

C—N bond cleavage

(e)

Release of amino product

(f)

Nucleophilic attack by water

(g)

Collapse of tetrahedral intermediate

(h)

Carboxyl product release

(i)
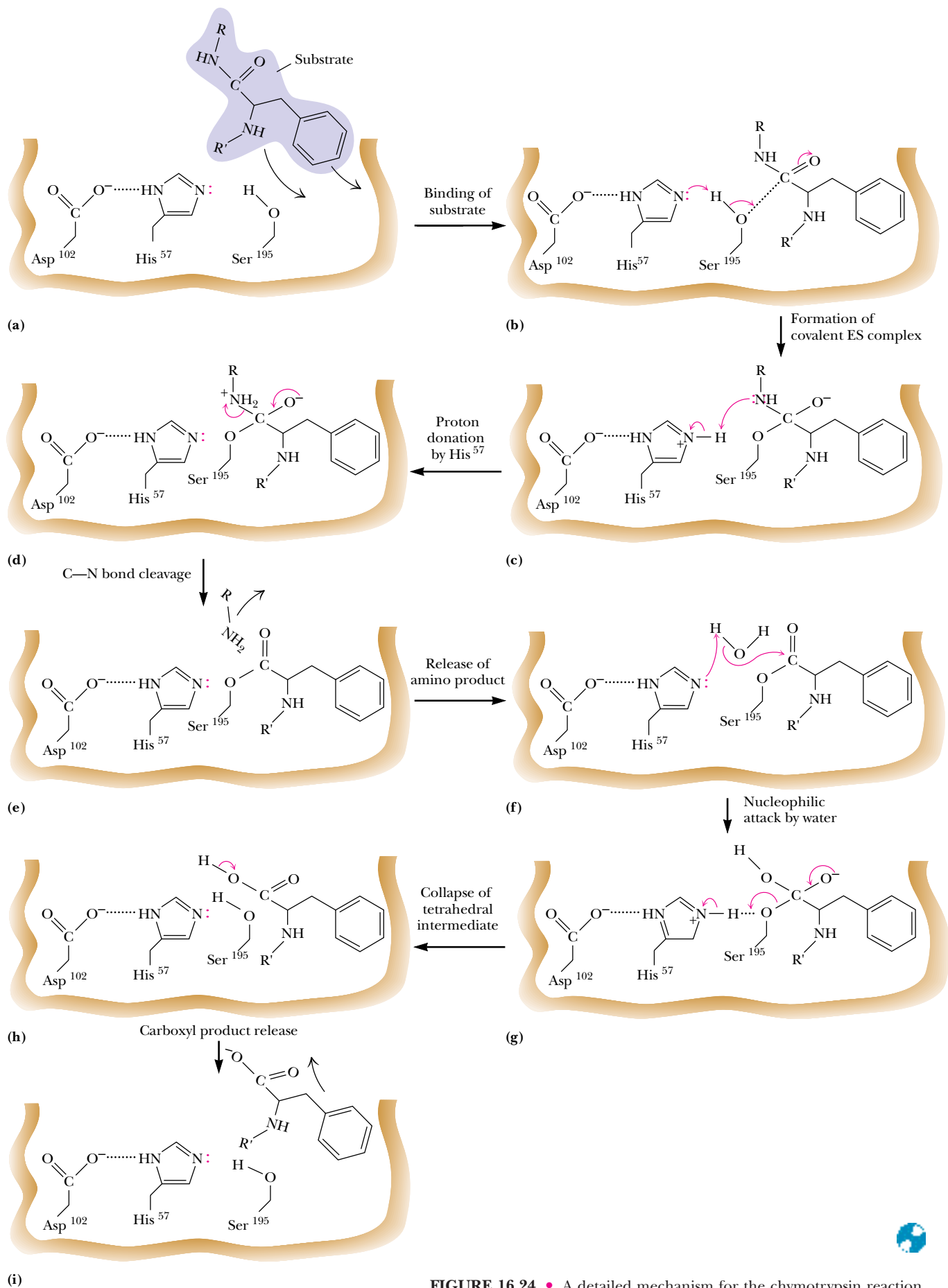
FIGURE 16.24 • A detailed mechanism for the chymotrypsin reaction.

518

Transition-State Stabilization in the Serine Proteases

X-ray crystallographic studies of serine protease complexes with transition-state analogs have shown how chymotrypsin stabilizes the **tetrahedral oxyanion transition states** (structures (c) and (g) in Figure 16.24) of the protease reaction. The amide nitrogens of Ser[195] and Gly[193] form an "oxyanion hole" in which the substrate carbonyl oxygen is hydrogen-bonded to the amide N-H groups.

Formation of the tetrahedral transition state increases the interaction of the carbonyl oxygen with the amide N-H groups in two ways. Conversion of the carbonyl double bond to the *longer* tetrahedral single bond brings the oxygen atom closer to the amide hydrogens. Also, the hydrogen bonds between the charged oxygen and the amide hydrogens are significantly stronger than the hydrogen bonds with the uncharged carbonyl oxygen.

Transition-state stabilization in chymotrypsin also involves the side chains of the substrate. The side chain of the departing amine product forms stronger interactions with the enzyme upon formation of the tetrahedral intermediate. When the tetrahedral intermediate breaks down (Figure 16.24d and e), steric repulsion between the product amine group and the carbonyl group of the acyl-enzyme intermediate leads to departure of the amine product.
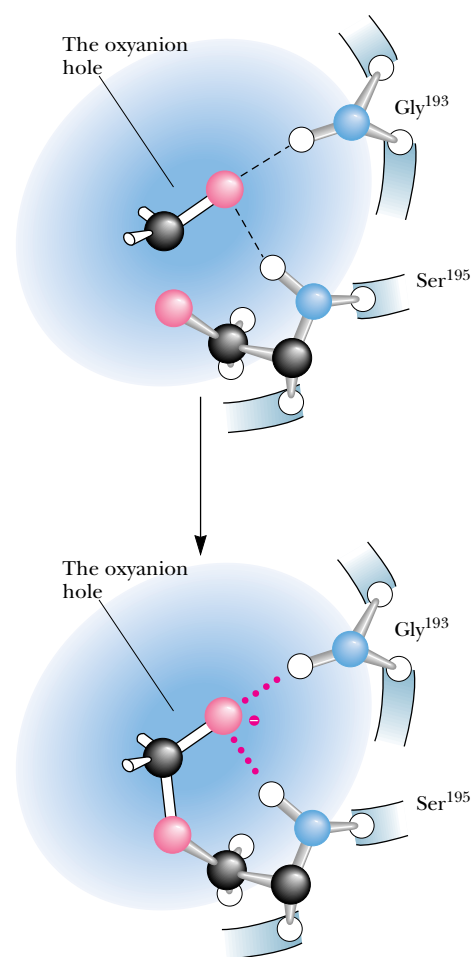
The "oxyanion hole" of chymotrypsin stabilizes the tetrahedral oxyanion transition states of the mechanism in Figure 16.24.

16.12 • The Aspartic Proteases

Mammals, fungi, and higher plants produce a family of proteolytic enzymes known as **aspartic proteases.** These enzymes are active at acidic (or sometimes neutral) pH, and each possesses two aspartic acid residues at the active site. Aspartic proteases carry out a variety of functions (Table 16.3), including digestion (*pepsin* and *chymosin*), lysosomal protein degradation (*cathepsin D* and *E*), and regulation of blood pressure (*renin* is an aspartic protease involved in the production of *angiotensin,* a hormone that stimulates smooth muscle contraction and reduces excretion of salts and fluid). The aspartic proteases display a variety of substrate specificities, but normally they are most active in the cleavage of peptide bonds between two hydrophobic amino acid residues. The preferred substrates of pepsin, for example, contain aromatic residues on both sides of the peptide bond to be cleaved.

Most aspartic proteases are composed of 323 to 340 amino acid residues, with molecular weights near 35,000. Aspartic protease polypeptides consist of

Table 16.3

Some Representative Aspartic Proteases

Name	Source	Function
Pepsin*	Animal stomach	Digestion of dietary protein
Chymosin[†]	Animal stomach	Digestion of dietary protein
Cathepsin D	Spleen, liver, and many other animal tissues	Lysosomal digestion of proteins
Renin[‡]	Kidney	Conversion of angiotensinogen to angiotensin I; regulation of blood pressure
HIV-protease[§]	AIDS virus	Processing of AIDS virus proteins

*The second enzyme to be crystallized (by John Northrup in 1930). Even more than urease before it, pepsin study by Northrup established that enzyme activity comes from proteins.
†Also known as rennin, it is the major pepsinlike enzyme in gastric juice of fetal and newborn animals.
‡A drop in blood pressure causes release of renin from the kidneys, which converts more angiotensinogen to angiotensin.
§A dimer of identical monomers, homologous to pepsin.
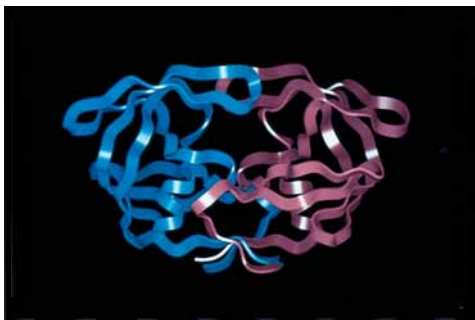
(a)

(b)

FIGURE 16.25 • Structures of (a) HIV-1 protease, a dimer, and (b) pepsin (a monomer). Pepsin's N-terminal half is shown in red; C-terminal half is shown in blue.

two homologous domains that fold to produce a tertiary structure composed of two similar lobes, with approximate twofold symmetry (Figure 16.25). Each of these lobes or domains consists of two β-sheets and two short α-helices. The two domains are bridged and connected by a six-stranded, antiparallel β-sheet. The active site is a deep and extended cleft, formed by the two juxtaposed domains and large enough to accommodate about seven amino acid residues. The two catalytic aspartate residues, residues 32 and 215 in porcine pepsin, for example, are located deep in the center of the active site cleft. The N-terminal domain forms a "flap" that extends over the active site, which may help to immobilize the substrate in the active site.

On the basis, in part, of comparisons with chymotrypsin, trypsin, and the other serine proteases, it was hypothesized that aspartic proteases might function by formation of covalent enzyme-substrate intermediates involving the active-site aspartate residues. Two possibilities were proposed: an acyl-enzyme intermediate involving an acid anhydride bond and an amino-enzyme intermediate involving an amide (peptide) bond (Figure 16.26). All attempts to trap or isolate a covalent intermediate failed, and a mechanism (see following paragraph) favoring noncovalent enzyme-substrate intermediates and general acid–general base catalysis is now favored for aspartic proteases.

The Mechanism of Action of Aspartic Proteases

A crucial datum supporting the general acid–general base model is the pH dependence of protease activity (see Critical Developments in Biochemistry: *The pH Dependence of Aspartic Proteases and HIV-1 Protease,* page 525). Enzymologists hypothesize that the aspartate carboxyl groups function alternately as general acid and general base. This model requires that one of the aspartate carboxyls be protonated and one be deprotonated when substrate binds. X-ray diffraction data on aspartic proteases show that the active-site structure in the vicinity of the two aspartates is highly symmetric. The two aspartates appear to act as a "catalytic dyad" (analogous to the catalytic triad of the serine proteases). The dyad proton may thus be covalently bound to either of
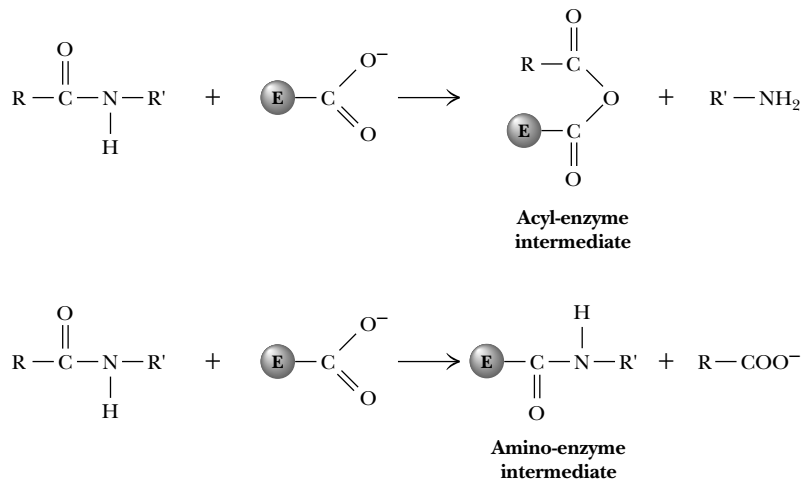
FIGURE 16.26 • Acyl-enzyme and amino-enzyme intermediates originally proposed for aspartic proteases were modeled after the acyl-enzyme intermediate of the serine proteases.

the aspartate groups in the free enzyme or in the enzyme-substrate complex. Thus, in pepsin, for example, Asp^{32} may be deprotonated while Asp^{215} is protonated, or vice versa.

In the most widely accepted mechanism (Figure 16.27), substrate binding is followed by a step in which two concerted proton transfers facilitate nucleophilic attack on the carbonyl carbon of the substrate by water. In the mechanism shown, Asp^{32} acts as a general base, accepting a proton from an active-site water molecule, whereas Asp^{215} acts a general acid, donating a proton to the oxygen of the peptide carbonyl group. *By virtue of these two proton transfers, nucleophilic attack occurs without explicit formation of hydroxide ion at the active site.* The resulting intermediate is termed an **amide dihydrate.** Note that the protonation states of the two aspartate residues are now opposite to those in the free enzyme (Figure 16.27).

Breakdown of the amide dihydrate occurs by a mechanism similar to its formation. The ionized aspartate carboxyl (Asp^{32} in Figure 16.27) acts as a general base to accept a proton from one of the hydroxyl groups of the amide dihydrate, while the protonated carboxyl of the other asparate (Asp^{215} in this case) simultaneously acts as a general acid to donate a proton to the nitrogen atom of one of the departing peptide products.
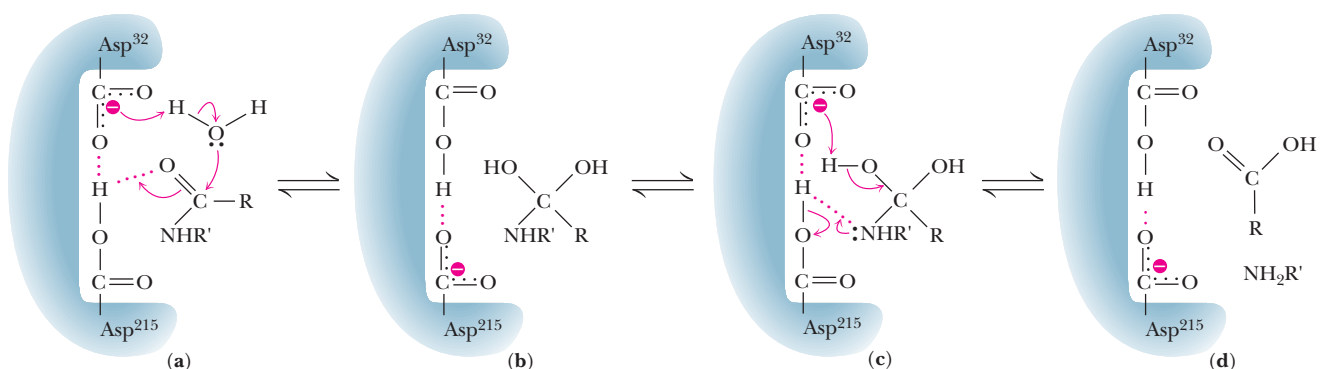
FIGURE 16.27 • A mechanism for the aspartic proteases. In the first step, two concerted proton transfers facilitate nucleophilic attack of water on the substrate carbonyl carbon. In the third step, one aspartate residue (Asp^{32} in pepsin) accepts a proton from one of the hydroxyl groups of the amine dihydrate, and the other aspartate (Asp^{215}) donates a proton to the nitrogen of the departing amine.

The AIDS Virus HIV-1 Protease Is an Aspartic Protease

Recent research on acquired immune deficiency syndrome (AIDS) and its causative viral agent, the human immunodeficiency virus (HIV-1), has brought a new aspartic protease to light. **HIV-1 protease** cleaves the polyprotein products of the HIV-1 genome, producing several proteins necessary for viral growth and cellular infection. HIV-1 protease cleaves several different peptide linkages in the HIV-1 polyproteins, including those shown in Figure 16.28. For example, the protease cleaves between the Tyr and Pro residues of the sequence Ser-Gln-Asn-Tyr-Pro-Ile-Val, which joins the p17 and p24 HIV-1 proteins.

The HIV-1 protease is a remarkable viral imitation of mammalian aspartic proteases: It is a **dimer of identical subunits** that mimics the two-lobed monomeric structure of pepsin and other aspartic proteases. The HIV-1 protease subunits are 99-residue polypeptides that are homologous with the individual domains of the monomeric proteases. Structures determined by X-ray diffraction studies reveal that the active site of HIV-1 protease is formed at the interface of the homodimer and consists of two aspartate residues, designated Asp^{25} and $Asp^{25'}$, one contributed by each subunit (Figure 16.29). In the homodimer, the active site is covered by two identical "flaps," one from each subunit, in contrast to the monomeric aspartic proteases, which possess only a single active-site flap.

Enzyme kinetic measurements by Thomas Meek and his collaborators at SmithKline Beecham Pharmaceuticals have shown that the mechanism of HIV-1 protease is very similar to those of other aspartic proteases (Figure 16.30). Two concerted proton transfers by the aspartate carboxyls facilitate nucleophilic attack by water on the carbonyl carbon of the peptide substrate. If the protease-substrate complex is incubated with $H_2^{18}O$, incorporation of ^{18}O into the peptide carbonyl group can be measured. *Thus, not only is the formation of the amide dihydrate reversible, and the two hydroxyl groups of the dihydrate equivalent, but the protonation states of the active-site carboxyl groups must interchange* (Figure 16.30). The simplest model would involve direct proton exchange across the Asp-Asp dyad as shown. The symmetrical nature of the active-site aspartyl groups is consistent with the idea of facile exchange of the proton between the two Asp residues.

The observation that ^{18}O can accumulate in the substrate from $H_2^{18}O$ also implies that formation and reversal of the amide dihydrate must be faster than

FIGURE 16.28 • HIV mRNA provides the genetic information for synthesis of a polyprotein. Proteolytic cleavage of this polyprotein by HIV protease produces the individual proteins required for viral growth and cellular infection.
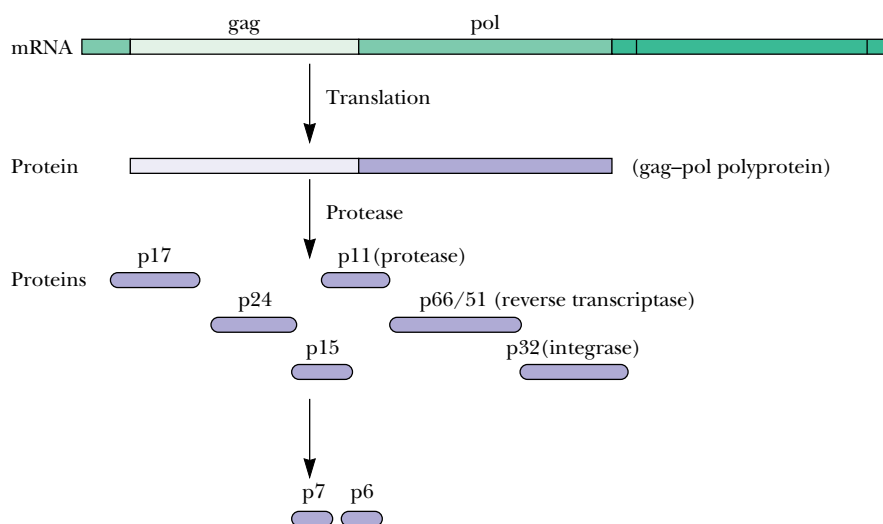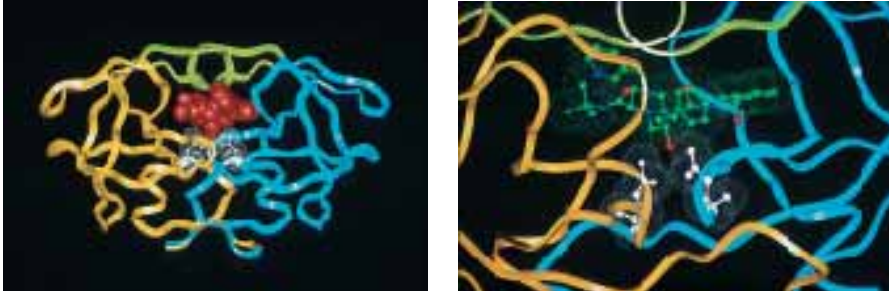
its breakdown to form product. Kinetic studies by Meek and his coworkers are consistent with a model in which breakdown of the dihydrate intermediate is the rate-determining step for the protease reaction. These studies also show that the transition state of this step involves two proton transfers—with one aspartate acting as a general acid to donate a proton to the departing proline and the other aspartate acting as a general base to abstract a proton from one of the hydroxyl groups, facilitating collapse of the dihydrate to a carboxyl group. Note that the events of the breakdown to form product are simply the reversal of the steps that formed the intermediate.
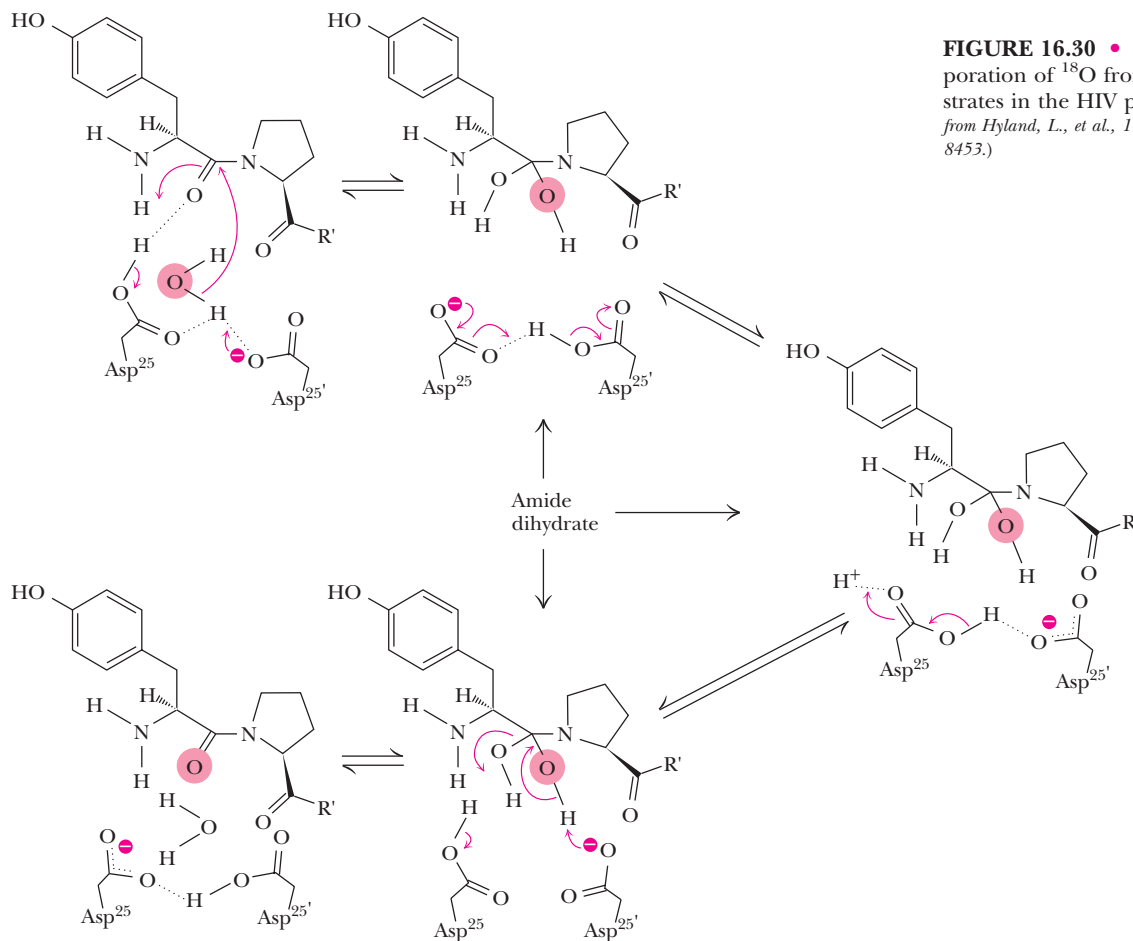
FIGURE 16.30 • A mechanism for the incorporation of ^{18}O from $H_2{}^{18}O$ into peptide substrates in the HIV protease reaction. (*Adapted from Hyland, L., et al., 1991.* Biochemistry **30**:*8441–8453*.)

$\mathcal{H}$UMAN BIOCHEMISTRY

Protease Inhibitors Give Life to AIDS Patients

Infection by HIV was once considered a death sentence, but the emergence of a new family of drugs called protease inhibitors has made it possible for some AIDS patients to improve their overall health and extend their lives. These drugs are all specific inhibitors of the HIV protease. By inhibiting the protease, they prevent the development of new virus particles in the cells of infected patients. Clinical testing has shown that a combination of drugs—including a protease inhibitor together with a reverse transcriptase inhibitor like AZT—can reduce the human immunodeficiency virus (HIV) to undetectable levels in about 40 to 50% of infected individuals. Patients who respond successfully to this combination therapy have experienced dramatic improvement in their overall health and a substantially lengthened lifespan.

Four of the protease inhibitors approved for use in humans by the U.S. Food and Drug Administration are shown below: Crixivan® by Merck, Invirase® by Hoffman-LaRoche, Norvir® by Abbott, and Viracept® by Agouron. These drugs were all developed from a "structure-based" design strategy; that is, the drug molecules were designed to bind tightly to the active site of the HIV-1 protease. The backbone OH-group in all these substances inserts between the two active-site carboxyl groups of the protease.

In the development of an effective drug, it is not sufficient merely to show that a candidate compound can cause the desired biochemical effect. It must also be demonstrated that the drug can be effectively delivered in sufficient quantities to the desired site(s) of action in the organism, and that the drug does not cause undesirable side effects. The HIV-1 protease inhibitors shown here fulfill all of these criteria. Other drug candidates have been found that are even better inhibitors of HIV-1 protease in cell cultures, but many of these fail the test of bioavailability—the ability of a drug to be delivered to the desired site of action in the organism.

Candidate protease inhibitor drugs must be relatively specific for the HIV-1 protease. Many other aspartic proteases exist in the human body and are essential to a variety of body functions, including digestion of food and processing of hormones. An ideal drug thus must strongly inhibit the HIV-1 protease, must be delivered effectively to the lymphocytes where the protease must be blocked, and should not adversely affect the activities of the essential human aspartic proteases.

A final but important consideration is viral mutation. Certain mutant HIV strains are resistant to one or more of the protease inhibitors, and even for patients who respond initially to protease inhibitors it is possible that mutant viral forms may eventually thrive in the infected individual. The search for new and more effective protease inhibitors is ongoing.
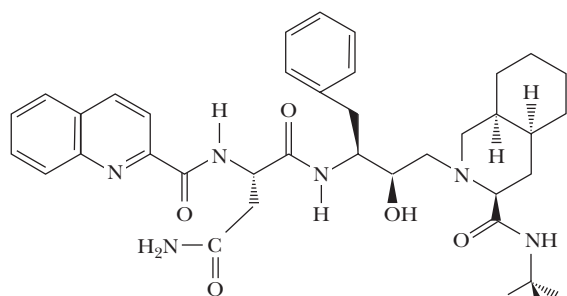
Invirase (Saquinavir)
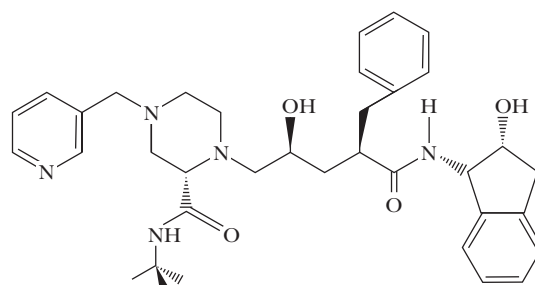
Crixivan (Indinavir)
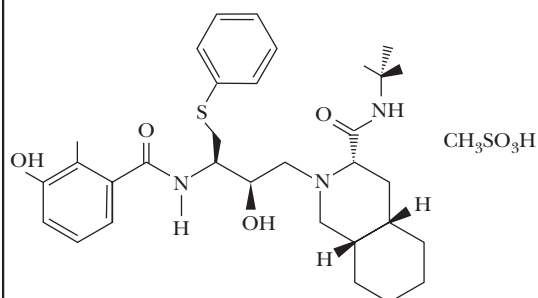
Viracept (Nelfinavir mesylate)
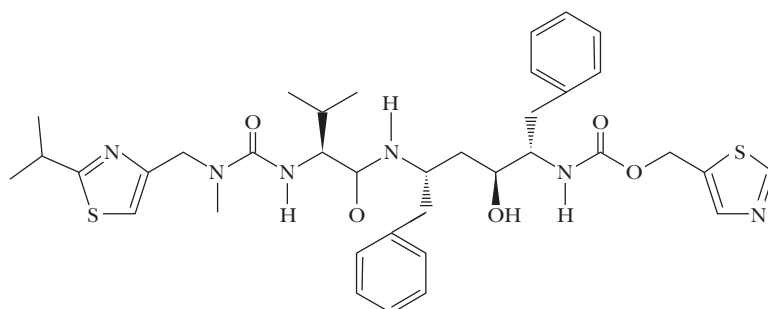
Norvir (Ritonavir)

The pH Dependence of Aspartic Proteases and HIV-1 Protease

The first hint that two active-site carboxyl groups—one protonated and one ionized—might be involved in the catalytic activity of the aspartic proteases came from studies of the pH dependence of enzymatic activity. If an ionizable group in an enzyme active site is essential for activity, a plot of enzyme activity versus pH may look like one of the plots at right.

If activity increases dramatically as pH is increased, catalysis may depend on a deprotonated group that may normally act as a general base, accepting a proton from the substrate or a water molecule, for example (a). Protonation of this group at lower pH prevents it from accepting another proton (from the substrate or water, for example).

On the other hand, if activity decreases sharply as pH is raised, activity may depend on a protonated group, which may act as a general acid, donating a proton to the substrate or a catalytic water molecule (b). At high pH, the proton dissociates and is not available in the catalytic events.

The bell-shaped curve in part (c) of the figure combines both of these behaviors, so that activity first increases, then decreases, as pH is increased. This is consistent with the involvement of two ionizable groups—one with a low pK_a that acts as a base above its pK_a, and a second group with a higher pK_a that acts as an acid below its pK_a.

Kinetic studies with pepsin have produced bell-shaped curves for a variety of substrate peptides; see below, (a).

As such data are fitted to calculated curves, dissociation constants can be estimated for the ionizable groups at the active site. In pepsin, the general base exhibits a pK_a of approximately 1.4, whereas the general acid displays a pK_a of about 4.3. Compare these values with the expected pK_a for an aspartate carboxyl group in a protein of 4.2 to 4.6. The value for the aspartyl group acting as a general acid in pepsin is typical, but that for the aspartyl group acting as a general base is unusually low.

The pH dependence of HIV-1 protease has been assessed by measuring the apparent inhibition constant for a synthetic substrate analog (b). The data are consistent with the catalytic involvement of ionizable groups with pK_a values of 3.3 and 5.3. Maximal enzymatic activity occurs in the pH range between these two values. On the basis of the accumulated kinetic and structural data on HIV-1 protease, these pK_a values have been ascribed to the two active-site aspartate carboxyl groups. Note that the value of 3.3 is somewhat low for an aspartate side chain in a protein, whereas the value of 5.3 is somewhat high.

(a)

(b)

(c)
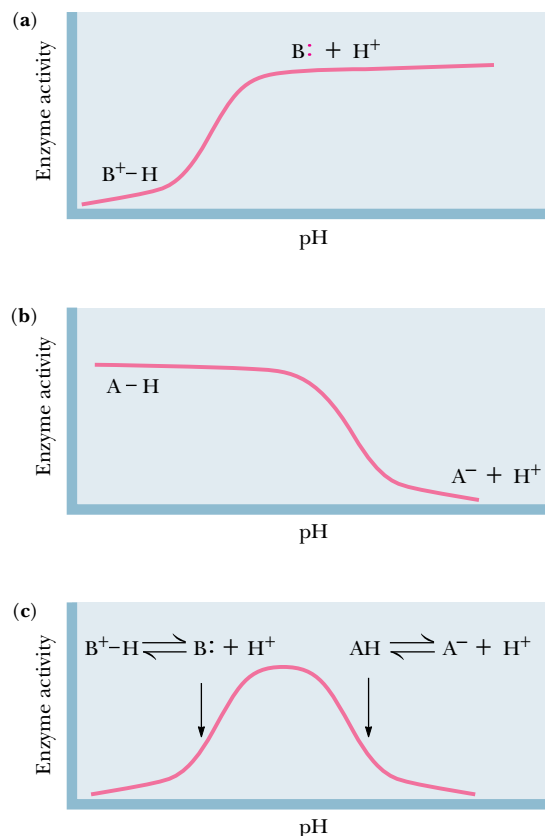
Bell-shaped activity versus pH profiles arise from two separate active-site ionizations. (a) Enzyme activity increases upon deprotonation of B^+-H. (b) Enzyme activity decreases upon deprotonation of A-H. (c) Enzyme activity is maximal in the pH range where one ionizable group is deprotonated (as B:) and the other group is protonated (as A-H).

(a)

(b)
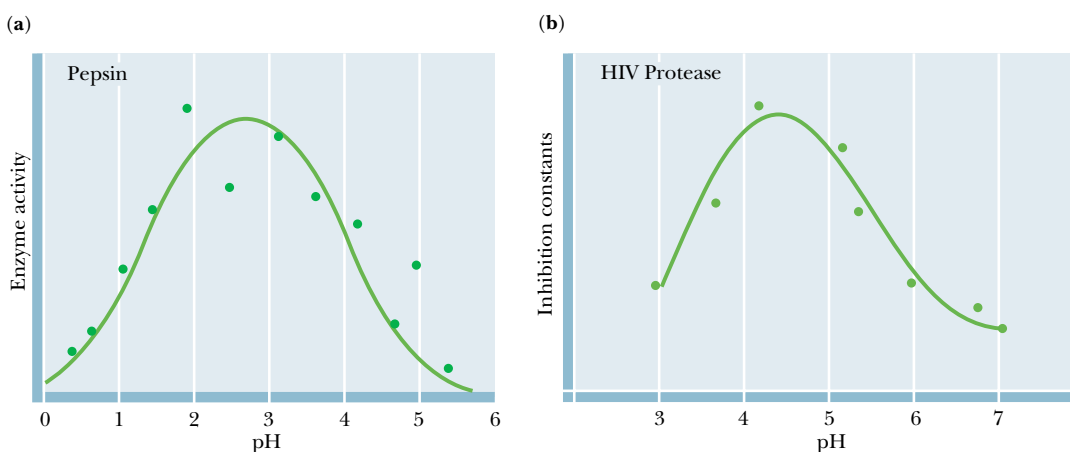
pH-rate profiles for (a) pepsin and (b) HIV protease. (*Adapted from Denburg, J., et al., 1968.* Journal of the American Chemical Society **90:**479–486, *and Hyland, J., et al., 1991.* Biochemistry **30:**8454–8463.)

16.13 • **Lysozyme**

Lysozyme is an enzyme that hydrolyzes polysaccharide chains. It ruptures certain bacterial cells by cleaving the polysaccharide chains that make up their cell wall. Lysozyme is found in many body fluids, but the most thoroughly studied form is from hen egg whites. The Russian scientist P. Laschtchenko first described the bacteriolytic properties of hen egg white lysozyme in 1909. In 1922, Alexander Fleming, the London bacteriologist who later discovered penicillin, gave the name *lysozyme* to the agent in mucus and tears that destroyed certain bacteria, because it was an en*zyme* that caused bacterial *lysis*.

As seen in Chapter 9, bacterial cells are surrounded by a rigid, strong wall of peptidoglycan, a copolymer of two sugar units, *N*-acetylmuramic acid (NAM) and *N*-acetylglucosamine (NAG). Both of these sugars are *N*-acetylated analogs of glucosamine, and in bacterial cell wall polysaccharides, they are joined in $\beta(1 \rightarrow 4)$ glycosidic linkages (Figure 16.31). Lysozyme hydrolyzes the glycosidic bond between C-1 of NAM and C-4 of NAG, as shown in Figure 16.31, but does not act on the $\beta(1 \rightarrow 4)$ linkages between NAG and NAM.

Lysozyme is a small globular protein composed of 129 amino acids (14 kD) in a single polypeptide chain. It has eight cysteine residues linked in four disulfide bonds. The structure of this very stable protein was determined by X-ray crystallographic methods in 1965 by David Phillips (Figure 16.32). Although X-ray structures had previously been reported for proteins (hemoglobin and myoglobin), lysozyme was the first enzyme structure to be solved by crystallographic (or any other) methods. Although the location of the active site was not obvious from the X-ray structure of the protein alone, X-ray studies of lysozyme-inhibitor complexes soon revealed the location and nature of the active site. Since it is an enzyme, lysozyme cannot form stable ES complexes for structural studies, because the substrate is rapidly transformed into products. On the other hand, several substrate analogs have proven to be good com-
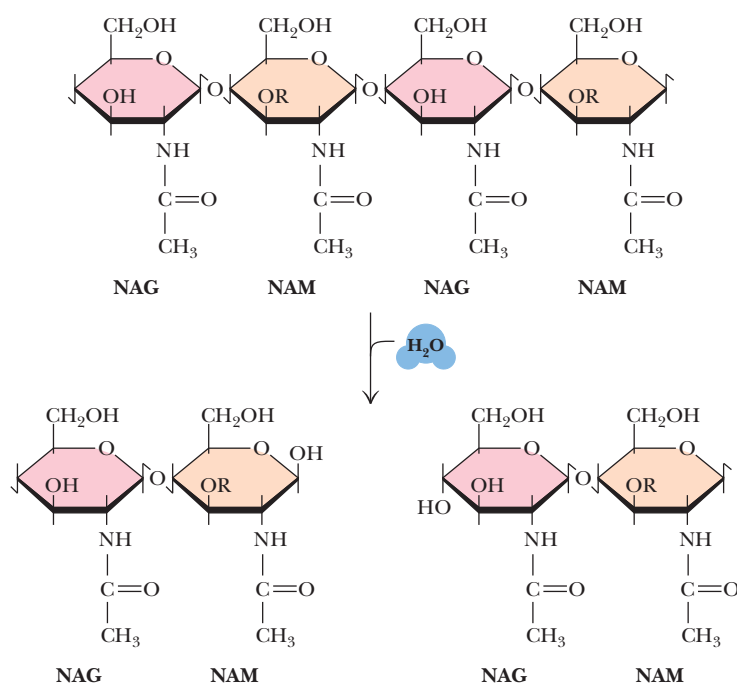
FIGURE 16.31 • The lysozyme reaction.

petitive inhibitors of lysozyme that can form complexes with the enzyme stable enough to be characterized by X-ray crystallography and other physical techniques. One of the best is a trimer of *N*-acetylglucosamine, $(NAG)_3$ (Figure 16.33), which is hydrolyzed by lysozyme at a rate only 1/60,000 that of the native substrate (Table 16.4). $(NAG)_3$ binds at the enzyme active site by forming five hydrogen bonds with residues located in one-half of a depression or crevice that spans the surface of the enzyme (Figure 16.34). The few hydrophobic residues that exist on the surface of lysozyme are located in this depression, and they may participate in hydrophobic and van der Waals interactions with $(NAG)_3$, as well as the normal substrate. The absence of charged groups on $(NAG)_3$ precludes the involvement of electrostatic interactions with the enzyme. Comparisons of the X-ray structures of the native lysozyme and the lysozyme-$(NAG)_3$ complex reveal that several amino acid residues at the active site move slightly upon inhibitor binding, including Trp^{62}, which moves about 0.75 Å to form a hydrogen bond with a hydroxymethyl group (Figure 16.35).

Model Studies Reveal a Strain-Induced Destabilization of a Bound Substrate on Lysozyme

One of the premises of lysozyme models is that the native substrate would occupy the rest of the crevice or depression running across the surface of the enzyme, because there is room to fit three more sugar residues into the crevice and because the hexamer $(NAG)_6$ is in fact a good substrate for lysozyme (Table 16.4). The model building studies refer to the six sugar residue-binding subsites in the crevice with the letters A through F, with A, B, and C representing the part of the crevice occupied by the $(NAG)_3$ inhibitor (Figure 16.35). Modeling studies clearly show that NAG residues fit nicely into subsites A, B, C, E, and F of the crevice, but that fitting a residue of the $(NAG)_6$ hexamer into site D requires a substantial distortion of the sugar (out of its preferred chair conformation) to prevent steric crowding and overlap between atoms C-6 and O-6 of the sugar at the D site and Ile^{98} of the enzyme. This distorted sugar residue is adjacent to the glycosidic bond to be cleaved (between sites D and E), and the inference is made that this distortion or strain brings the substrate closer to the transition state for hydrolysis. This is a good example of strain-induced destabilization of an otherwise favorably binding substrate (Section 16.4). Thus, the overall binding interaction of the rest of the sugar substrate would be favorable ($\Delta G < 0$), but distortion of the ring at the D site uses some of this binding energy to raise the substrate closer to the transition state for hydrolysis, *an example of stabilization of a transition state (relative to the simple enzyme-substrate complex)*. As noted in Section 16.4, distortion is one of the molecular mechanisms that can lead to such transition-state stabilization.

FIGURE 16.32 • The structure of lysozyme. Glu^{35} and Asp^{52} are shown in white.

Table 16.4

Hydrolysis Rate Constants for Model Oligosaccharides with Lysozyme	
Oligosaccharide	Rate Constant, $k_{cat}(s^{-1})$
$(NAG-NAM)_3$	0.5
$(NAG)_6$	0.25
$(NAG)_5$	0.033
$(NAG)_4$	7×10^{-5}
$(NAG)_3$	8×10^{-6}
$(NAG)_2$	2.5×10^{-8}
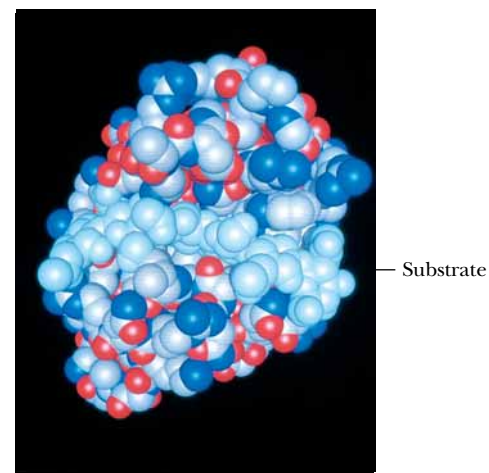
— Substrate

FIGURE 16.34 • The lysozyme-enzyme-substrate complex. (*Photo courtesy of John Rupley, University of Arizona*)

FIGURE 16.33 • $(NAG)_3$, a substrate analog, forms stable complexes with lysozyme.

FIGURE 16.35 ...
tions at the six ...
the lysozyme a...
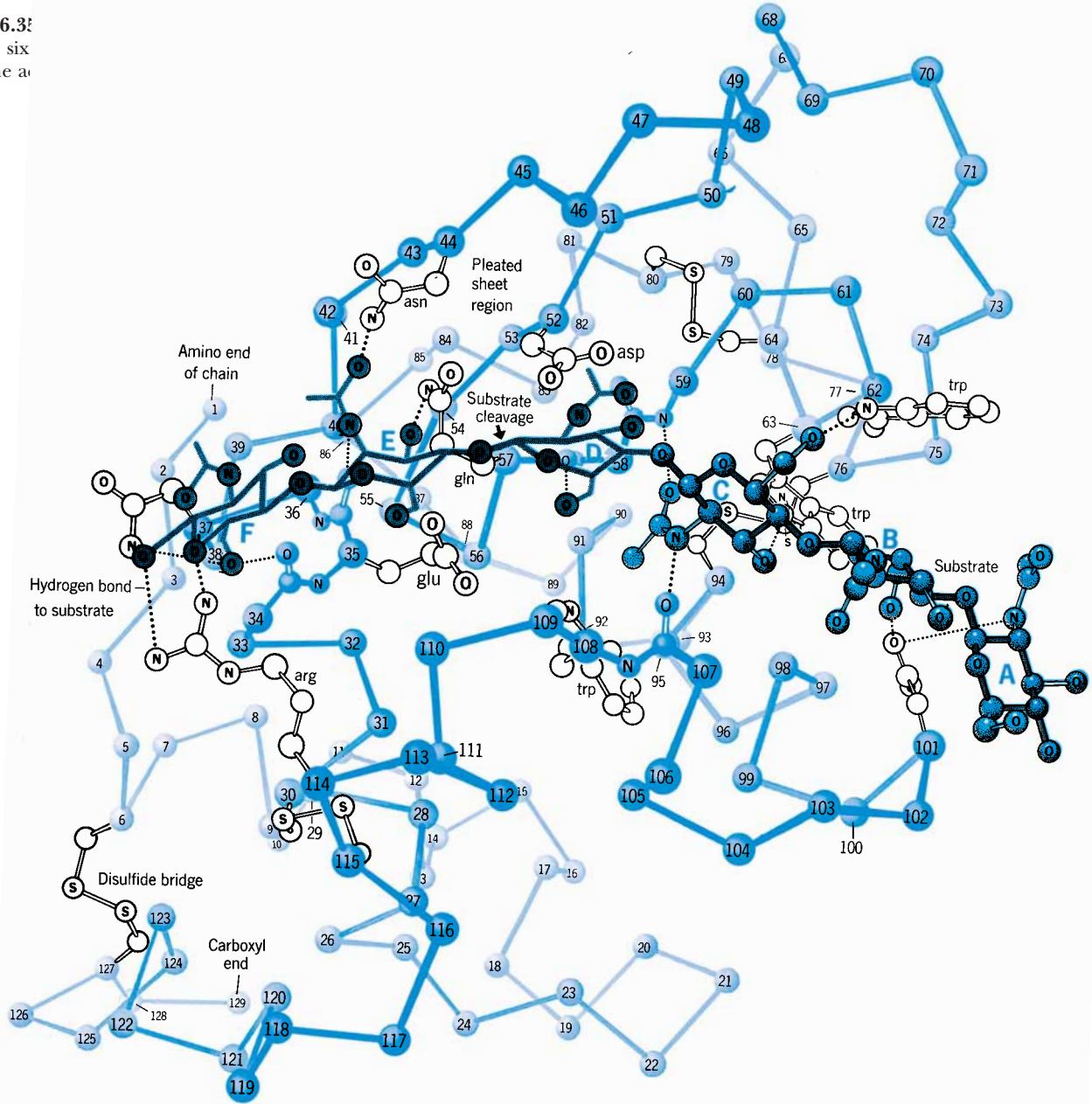
Lysozyme
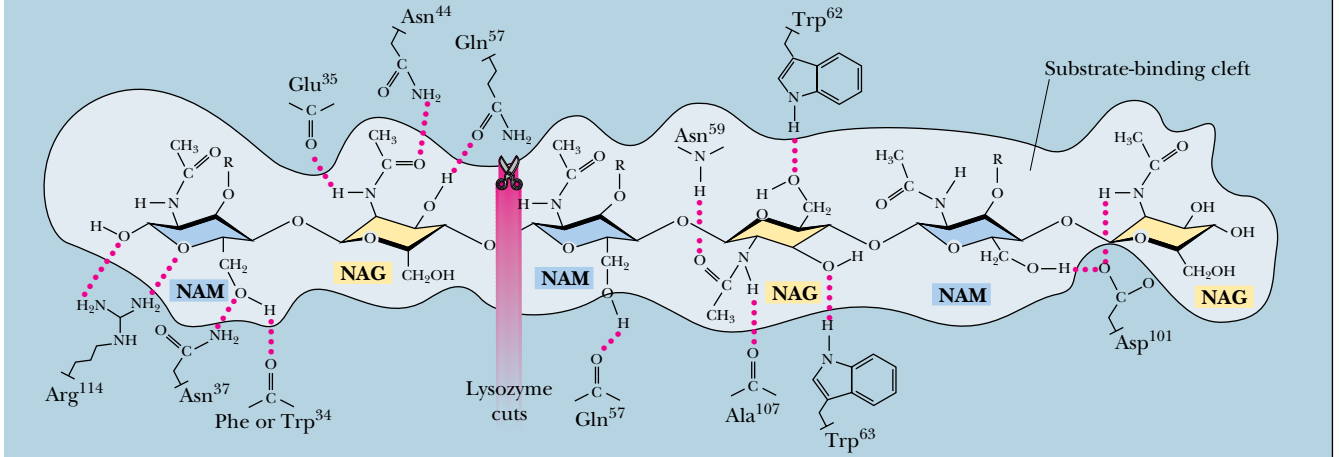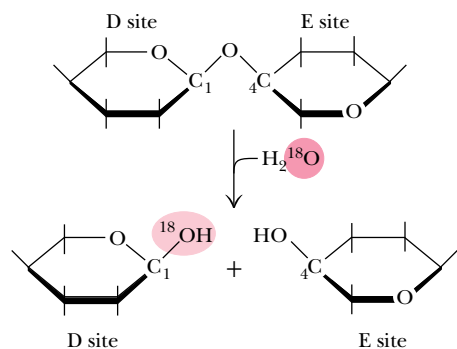
FIGURE 16.36 • The C_1–O bond, not the O–C_4 bond, is cleaved in the lysozyme reaction. ^{18}O from $H_2^{18}O$ is thus incorporated at the C_1 position.

The Lysozyme Mechanism Involves General Acid–Base Catalysis

The mechanism of the lysozyme reaction is shown in Figures 16.36 and 16.37. Studies using ^{18}O-enriched water showed that the C_1—O bond is cleaved on the substrate between the D and E sites. Hydrolysis under these conditions incorporates ^{18}O into the C_1 position of the sugar at the D site, not into the oxygen at C_4 at the E site (Figure 16.36). Model building studies place the cleaved bond approximately between protein residues Glu[35] and Asp[52]. Glu[35] is in a nonpolar or hydrophobic region of the protein, whereas Asp[52] is located in a much more polar environment. Glu[35] is protonated, but Asp[52] is ionized (Figure 16.37). Glu[35] may thus act as a general acid, donating a proton to the oxygen atom of the glycosidic bond and accelerating the reaction. Asp[52], on the other hand, probably stabilizes the carbonium ion generated at the D site upon bond cleavage. Formation of the carbonium ion may also be enhanced by the strain on the ring at the D site. Following bond cleavage, the product formed at the E site diffuses away, and the carbonium ion intermediate can then react with H_2O from the solution. Glu[35] can now act as a general base, accepting a proton from the attacking water. The tetramer of NAG thus formed at sites A through D can now be dissociated from the enzyme.

On the basis of the above, the rate acceleration afforded by lysozyme appears to be due to (a) general acid catalysis by Glu[35]; (b) distortion of the sugar ring at the D site, which may stabilize the carbonium ion (*and the transition state*); and (c) electrostatic stabilization of the carbonium ion by nearby Asp[52]. The overall k_{cat} for lysozyme is about 0.5/sec, which is quite slow (Table
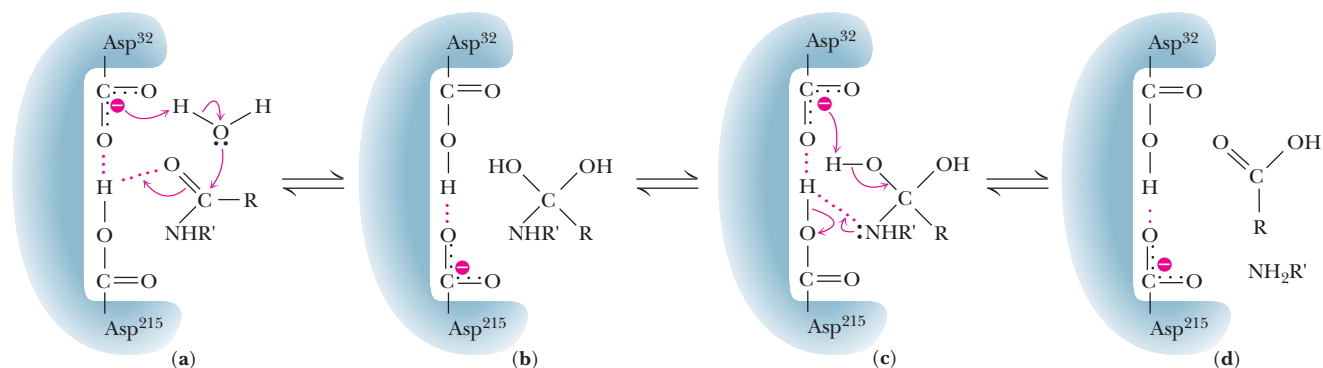
FIGURE 16.37 • A mechanism for the lysozyme reaction.

14.4) compared with that for other enzymes. On the other hand, the destruction of a bacterial cell wall may only require hydrolysis of a few polysaccharide chains. The high osmotic pressure of the cell ensures that cell rupture will follow rapidly. Thus, lysozyme can accomplish cell lysis without a particularly high k_{cat}.

PROBLEMS

1. Tosyl-L-phenylalanine chloromethyl ketone (TPCK) specifically inhibits chymotrypsin by covalently labeling His[57].
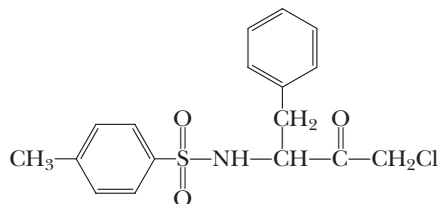
Tosyl-L-phenylalanine chloromethyl ketone (TPCK)

a. Propose a mechanism for the inactivation reaction, indicating the structure of the product(s).
b. State why this inhibitor is specific for chymotrypsin.
c. Propose a reagent based on the structure of TPCK that might be an effective inhibitor of trypsin.
2. In this chapter, the experiment in which Craik and Rutter replaced Asp[102] with Asn in trypsin (reducing activity 10,000-fold) was discussed.

a. On the basis of your knowledge of the catalytic triad structure in trypsin, suggest a structure for the "uncatalytic triad" of Asn-His-Ser in this mutant enzyme.
b. Explain why the structure you have proposed explains the reduced activity of the mutant trypsin.
c. See the original journal articles (Sprang, et al., 1987. *Science* **237**:905–909 and Craik, et al., 1987. *Science* **237**:909–913) to see what Craik and Rutter's answer to this question was.

3. Pepstatin (see page 531) is an extremely potent inhibitor of the monomeric aspartic proteases, with K_I values of less than 1 n*M*.
a. On the basis of the structure of pepstatin, suggest an explanation for the strongly inhibitory properties of this peptide.
b. Would pepstatin be expected to also inhibit the HIV-1 protease? Explain your answer.

4. The k_{cat} for alkaline phosphatase–catalyzed hydrolysis of methylphosphate is approximately 14/sec at pH 8 and 25°C. The rate constant for the uncatalyzed hydrolysis of methylphosphate under the same conditions is approximately 1×10^{-15}/sec. What is the difference in the free energies of activation of these two reactions?
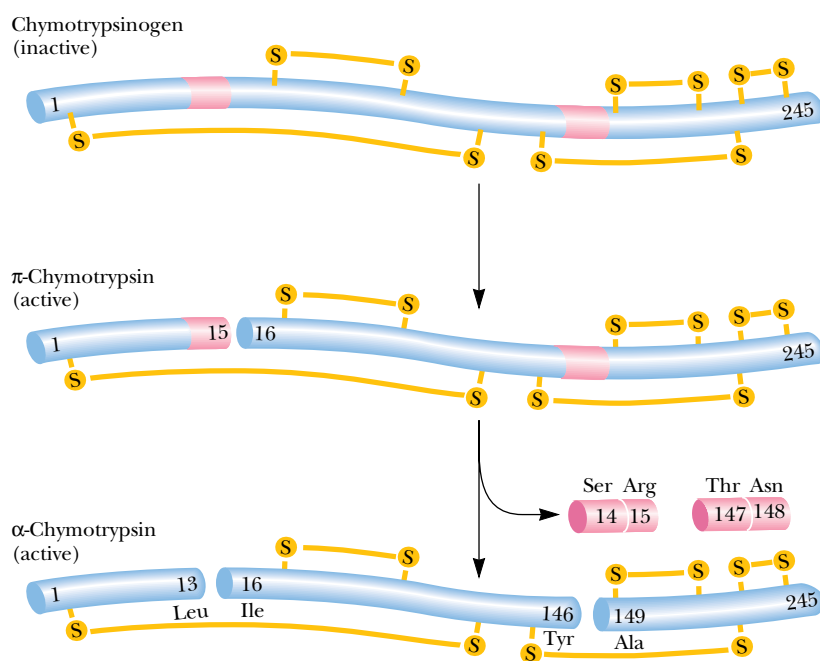
5. Active α-chymotrypsin is produced from chymotrypsinogen, an inactive precursor, as shown in the color figure on page 530.

The first intermediate—π-chymotrypsin—displays chymotrypsin activity. Suggest proteolytic enzymes that might carry out these cleavage reactions effectively.
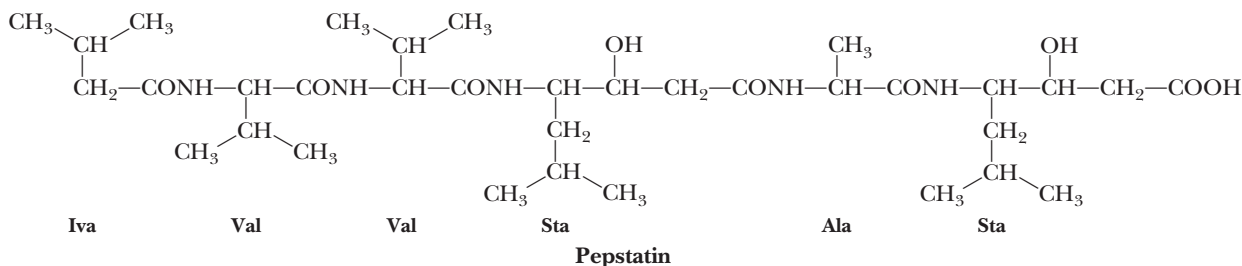
6. Based on the reaction scheme shown below, derive an expression for k_e/k_u, the ratio of the rate constants for the catalyzed and uncatalyzed reactions, respectively, in terms of the free energies of activation for the catalyzed ($\Delta G_e^\ddagger$) and the uncatalyzed ($\Delta G_u^\ddagger$) reactions.

Pepstatin
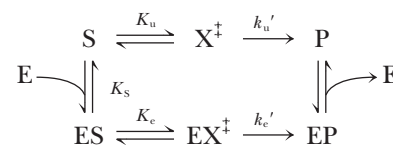
FURTHER READING

General

Cannon, W. R., Singleton, S. F., and Benkovic, S. J., 1997. A perspective on biological catalysis. *Nature Structural Biology* **3:**821–833.

Eigen, M., 1964. Proton transfer, acid–base catalysis, and enzymatic hydrolysis. *Angewandte Chemie, Int. Ed.* **3:**1–72.

Fersht, A., 1985. *Enzyme Structure and Mechanism,* 2nd ed. New York: W. H. Freeman and Company.

Gerlt, J. A., Kreevoy, M. M., Cleland, W. W., and Frey, P. A., 1997. Understanding enzymic catalysis: The importance of short, strong hydrogen bonds. *Chemistry and Biology* **4:**259–267.

Jencks, W. P., 1969. *Catalysis in Chemistry and Enzymology.* New York: McGraw-Hill.

Jencks, W., 1997. From chemistry to biochemistry to catalysis to movement. *Annual Review of Biochemistry* **66:**1–18.

Page, M. I., and Williams, A., eds., 1987. *Enzyme Mechanisms.* London, England: Royal Society of London.

Radzicka, A., and Wolfenden, R., 1995. A proficient enzyme. *Science* **267:**90–93.

Simopoulos, T. T., and Jencks, W. P., 1994. Alkaline phosphatase is an almost perfect enzyme. *Biochemistry* **33:**10375–10380.

Smithrud, D. B., and Benkovic, S. J., 1997. The state of antibody catalysis. *Current Opinions in Biotechnology* **8:**459–466.

Walsh, C., 1979. *Enzymatic Reaction Mechanisms.* San Francisco: W. H. Freeman and Company.

Transition-State Stabilization and Transition-State Analogs

Bearne, S. L., and Wolfenden, R., 1997. Mandelate racemase in pieces: Effective concentrations of enzyme functional groups in the transition state. *Biochemistry* **36:**1646–1656.

Kraut, J., 1988. How do enzymes work? *Science* **242:**533–540.

Kreevoy, M., and Truhlar, D. G., 1986. Transition-state theory. Chapter 1 in *Investigations of Rates and Mechanisms of Reactions,* Vol. 6, Part 1, edited by C. F. Bernasconi. New York: John Wiley & Sons.

Lolis, E., and Petsko, G., 1990. Transition-state analogues in protein crystallography: Probes of the structural source of enzyme catalysis. *Annual Review of Biochemistry* **59:**597–630.

Radzicka, A., and Wolfenden, R., 1995. Transition state and multisubstrate analog inhibitors. *Methods in Enzymology* **249:**284–312.

Wolfenden, R., 1972. Analogue approaches to the structure of the transition state in enzyme reactions. *Accounts of Chemical Research* **5:**10–18.

Wolfenden, R., and Frick, L., 1987. Transition state affinity and the design of enzyme inhibitors. Chapter 7 in *Enzyme Mechanisms,* edited by M. I. Page and A. Williams. London, England: Royal Society of London.

Wolfenden, R., and Kati, W. M., 1991. Testing the limits of protein-ligand binding discrimination with transition-state analogue inhibitors. *Accounts of Chemical Research* **24:**209–215.

Serine Proteases

Cassidy, C. S., Lin, J., and Frey, P. A., 1997. A new concept for the mechanism of action of chymotrypsin: The role of the low-barrier hydrogen bond. *Biochemistry* **36:**4576–4584.

Craik, C. S., et al., 1987. The catalytic role of the active site aspartic acid in serine proteases. *Science* **237:**909–919.

Lesk, A. M., and Fordham, W. D., 1996. Conservation and variability in the structures of serine proteinases of the chymotrypsin family. *Journal of Molecular Biology* **258:**501–537.

Plotnick, M. I., Mayne, L., Schechter, N. M., and Rubin, H., 1996. Distortion of the active site of chymotrypsin complexed with a serpin. *Biochemistry* **35:**7586–7590.

Renatus, M., Engh, R. A., Stubbs, M. T., et al., 1997. Lysine-156 promotes the anomalous proenzyme activity of tPA: X-ray crystal structure of single-chain human tPA. *EMBO Journal* **16:**4797–4805.

Sprang, S., et al., 1987. The three-dimensional structure of Asn[102] mutant of trypsin: Role of Asp[102] in serine protease catalysis. *Science* **237:**905–909.

Stavridi, E. S., O'Malley, K., Lukacs, C. M., et al., 1996. Structural change in α-chymotrypsin induced by complexation with α1-antitrypsin as seen by enhanced sensitivity to proteolysis. *Biochemistry* **35:**10608–10615.

Steitz, T., and Shulman, R., 1982. Crystallographic and NMR studies of the serine proteases. *Annual Review of Biophysics and Bioengineering* **11:**419–444.

Tsukada, H., and Blow, D., 1985. Structure of α-chymotrypsin refined at 1.68 Å resolution. *Journal of Molecular Biology* **184:**703–711.

Aspartic Proteases

Fruton, J., 1976. The mechanism of the catalytic action of pepsin and related acid proteinases. *Advances in Enzymology* **44:**1–36.

Oldziej, S., and Ciarkowski, J., 1996. Mechanism of action of aspartic proteinases: Application of transition-state analogue theory. *Journal of Computer-Aided Molecular Design* **10:**583–588.

Polgar, L., 1987. The mechanism of action of aspartic proteases involves "push-pull" catalysis. *FEBS Letters* **219:**1–4.

HIV-1 Protease

Bardi, J. S., Luque, I., and Friere, E., 1997. Structure-based thermodynamic analysis of HIV-1 protease inhibitors. *Biochemistry* **36:**6588–6596.

Beaulieu, P. L., Wernic, D., Abraham, A., et al., 1997. Potent HIV protease inhibitors containing a novel (hydroxyethyl)amide isostere. *Journal of Medicinal Chemistry* **40:**2164–2176.

Blundell, T., et al., 1990. The 3-D structure of HIV-1 proteinase and the design of antiviral agents for the treatment of AIDS. *Trends in Biochemical Sciences* **15:**425–430.

Carr, A., and Cooper, D. A., 1996. HIV protease inhibitors. *AIDS* **10:**S151–S157.

Chen, Z., Li, Y., Chen, E., et al., 1994. Crystal structure at 1.9-Å resolution of human immunodeficiency virus (HIV) II protease complexed with L-735,524, an orally bioavailable inhibitor of the HIV proteases. *Journal of Biological Chemistry* **269:**26344–26348.

Chen, Z., Li, Y., Schock, H. B., et al., 1995. Three-dimensional structure of a mutant HIV-1 protease displaying cross-resistance to all protease inhibitors in clinical trials. *Journal of Biological Chemistry* **270:**21433–21436.

Hyland, L., et al., 1991. Human immunodeficiency virus-1 protease 1: Initial velocity studies and kinetic characterization of reaction intermediates by [18]O isotope exchange. *Biochemistry* **30:**8441–8453.

Hyland, L., Tomaszek, T., and Meek, T., 1991. Human immunodeficiency virus-1 protease 2: Use of pH rate studies and solvent isotope effects to elucidate details of chemical mechanism. *Biochemistry* **30:**8454–8463.

Korant, B., Lu, Z., Strack, P., and Rizzo, C., 1996. HIV protease mutations leading to reduced inhibitor susceptibility. *Advances in Experimental Medicine and Biology* **389:**241–245.

Rose, R. B., Craik, C. S., Douglas, N. L., and Stroud, R. M., 1996. Three-dimensional structures of HIV-1 and SIV protease product complexes. *Biochemistry* **35:**12933–12944.

Vondrasek, J., and Wlodawer, A., 1997. Database of HIV proteinase structures. *Trends in Biochemical Sciences* **22:**183.

Wang, Y. X., Freedberg, D. I., Yamazaki, T., et al., 1997. Solution NMR evidence that the HIV-1 protease catalytic aspartyl groups have different ionization states in the complex formed with the asymmetric drug KNI-272. *Biochemistry* **35:**9945–9950.

Lysozyme

Chipman, D., and Sharon, N., 1969. Mechanism of lysozyme action. *Science* **165:**454–465.

Ford, L., et al., 1974. Crystal structure of a lysozyme-tetrasaccharide lactone complex. *Journal of Molecular Biology* **88:**349–371.

Kirby, A., 1987. Mechanism and stereoelectronic effects in the lysozyme reaction. *CRC Critical Reviews in Biochemistry* **22:**283–315.

Phillips, D., 1966. The three-dimensional structure of an enzyme molecule. *Scientific American* **215:**75–80.

$\mathcal{C}$hapter 17

Molecular Motors
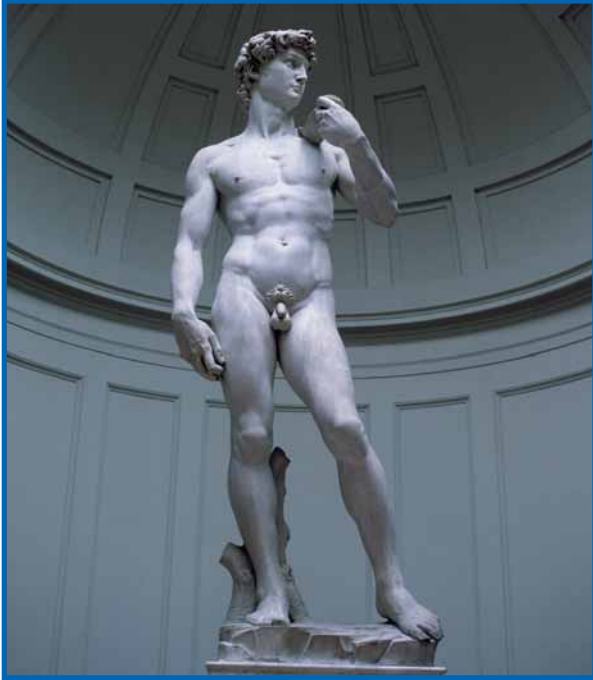
Michaelangelo's "David" epitomizes the musculature of the human form. (The Firenze Academia/photo by Stephanie Colasanti/Corbis)

Movement is an intrinsic property associated with all living things. Within cells, molecules undergo coordinated and organized movements, and cells themselves may move across a surface. At the tissue level, **muscle contraction** allows higher organisms to carry out and control crucial internal functions, such as peristalsis in the gut and the beating of the heart. Muscle contraction also enables the organism to carry out organized and sophisticated movements, such as walking, running, flying, and swimming.

17.1 • Molecular Motors

Motor proteins, also known as **molecular motors,** use chemical energy (ATP) to orchestrate all these movements, transforming ATP energy into the mechanical energy of motion. In all cases, ATP hydrolysis is presumed to drive and

533

control protein conformational changes that result in sliding or walking movements of one molecule relative to another. To carry out directed movements, molecular motors must be able to associate and dissociate reversibly with a polymeric protein array, a surface or substructure in the cell. ATP hydrolysis drives the process by which the motor protein ratchets along the protein array or surface. As fundamental and straightforward as all this sounds, elucidation of these basically simple processes has been extremely challenging for biochemists, involving the application of many sophisticated chemical and physical methods in many different laboratories. This chapter describes the structures and chemical functions of molecular motor proteins and some of the experiments by which we have come to understand them.

17.2 • Microtubules and Their Motors

One of the simplest self-assembling structures found in biological systems is the *microtubule,* one of the fundamental components of the eukaryotic *cytoskeleton* and the primary structural element of cilia and flagella (Figure 17.1). **Microtubules** are hollow, cylindrical structures, approximately 30 nm in diameter, formed from **tubulin,** a dimeric protein composed of two similar 55-kD subunits known as *α-tubulin* and *β-tubulin*. Eva Nogales, Sharon Wolf, and Kenneth Downing have determined the structure of the bovine tubulin $\alpha\beta$ dimer to 3.7 Å resolution (Figure 17.2a). Tubulin dimers polymerize as shown in Figure 17.2b to form microtubules, which are essentially helical structures, with 13 tubulin monomer "residues" per turn. Microtubules grown *in vitro* are dynamic structures that are constantly being assembled and disassembled.
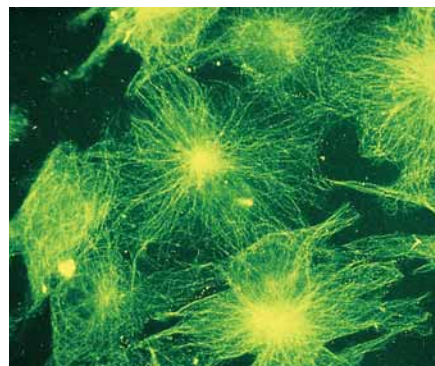
(a)
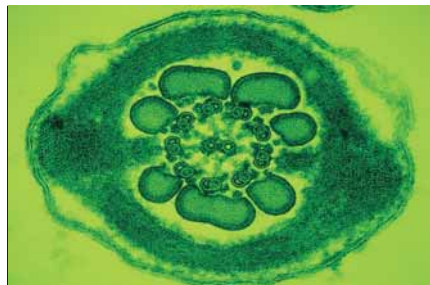
(b)

(c)
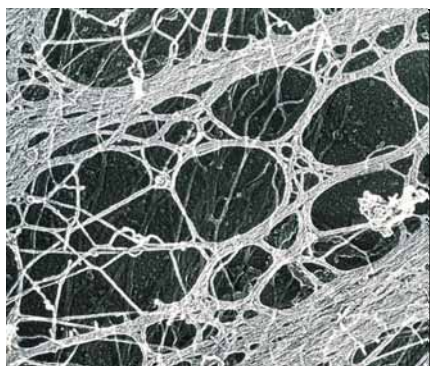
(d)

(e)
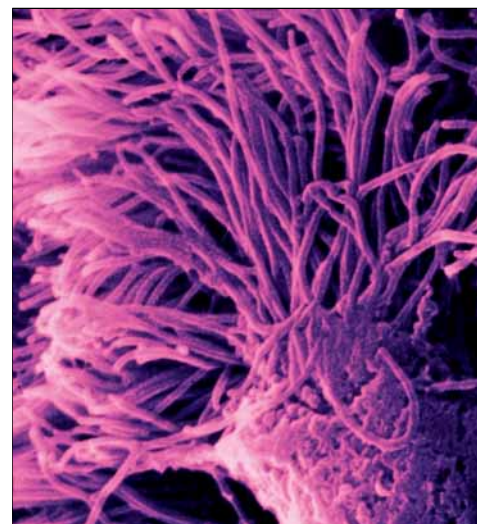
(f)

FIGURE 17.1 • Micrographs and electron micrographs of cytoskeletal elements, cilia, and flagella: (a) microtubules, (b) rat sperm tail microtubules (cross-section), (c) *Stylonychia,* a ciliated protozoan (undergoing division), (d) cytoskeleton of a eukaryotic cell, (e) *Pseudomonas fluorescens* (aerobic soil bacterium), showing flagella, (f) nasal cilia. *(a, K. G. Murti/Visuals Unlimited; b, David Phillips/Visuals Unlimited; c, Eric Grave/Phototake; d, Fawcett and Heuser/Photo Researchers, Inc.; e, Dr. Tony Brain/Custom Medical Stock; f, Veronika Burmeister, Visuals Unlimited)*
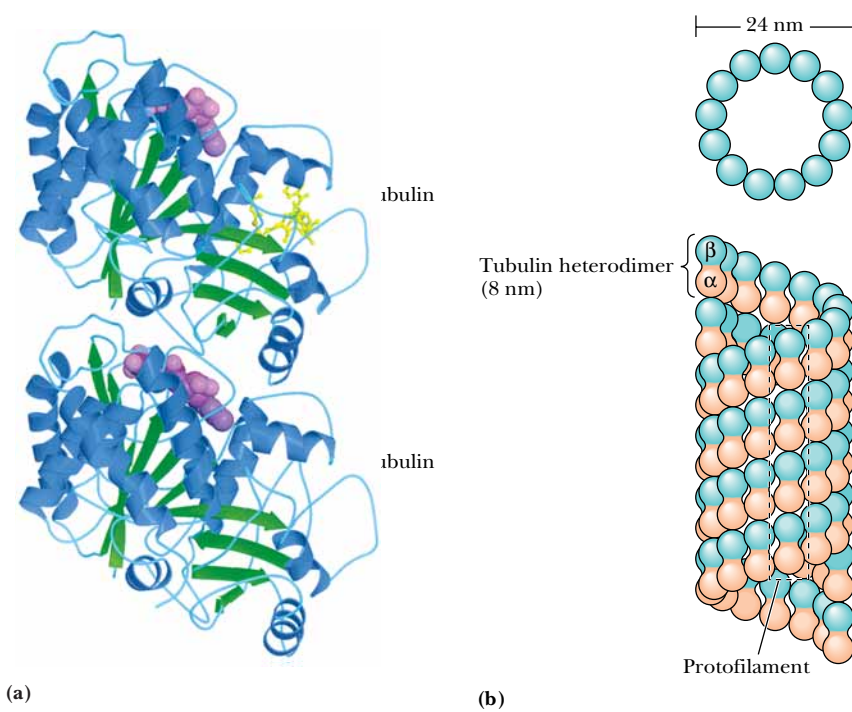
(a)   **(b)**

Because all tubulin dimers in a microtubule are oriented similarly, microtubules are polar structures. The end of the microtubule at which growth occurs is the **plus end,** and the other is the **minus end.** Microtubules *in vitro* carry out a GTP-dependent process called **treadmilling,** in which tubulin dimers are added to the plus end at about the same rate at which dimers are removed from the minus end (Figure 17.3).

Microtubules Are Constituents of the Cytoskeleton

Although composed only of 55-kD tubulin subunits, microtubules can grow sufficiently large to span a eukaryotic cell or to form large structures such as cilia and flagella. Inside cells, networks of microtubules play many functions, including formation of the mitotic spindle that segregates chromosomes during cell division, the movement of organelles and various vesicular structures through the cell, and the variation and maintenance of cell shape. Microtubules are, in fact, a significant part of the **cytoskeleton,** a sort of intracellular scaffold formed of microtubules, *intermediate filaments,* and *microfilaments* (Figure 17.4). In most cells, microtubules are oriented with their minus ends toward the centrosome and their plus ends toward the cell periphery. This consistent orientation is important for mechanisms of intracellular transport.

Microtubules Are the Fundamental Structural Units of Cilia and Flagella

As already noted, microtubules are also the fundamental building blocks of cilia and flagella. **Cilia** are short, cylindrical, hairlike projections on the surfaces of the cells of many animals and lower plants. The beating motion of cilia functions either to move cells from place to place or to facilitate the movement of extracellular fluid over the cell surface. Flagella are much longer structures found singly or a few at a time on certain cells (such as sperm cells). They pro-
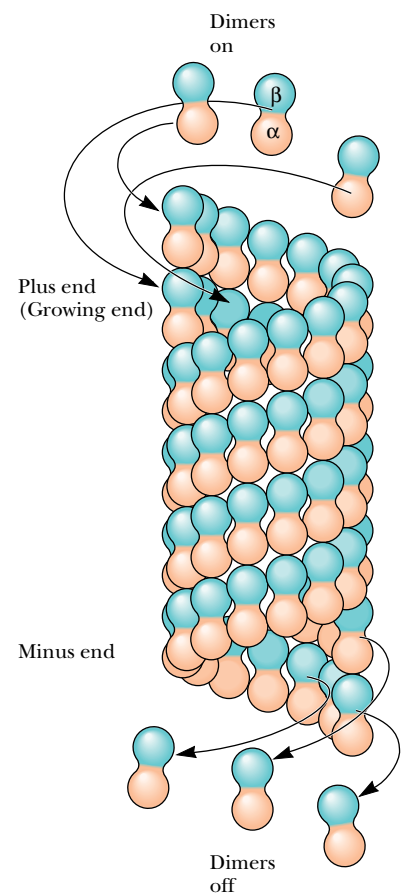
(a)

(b)
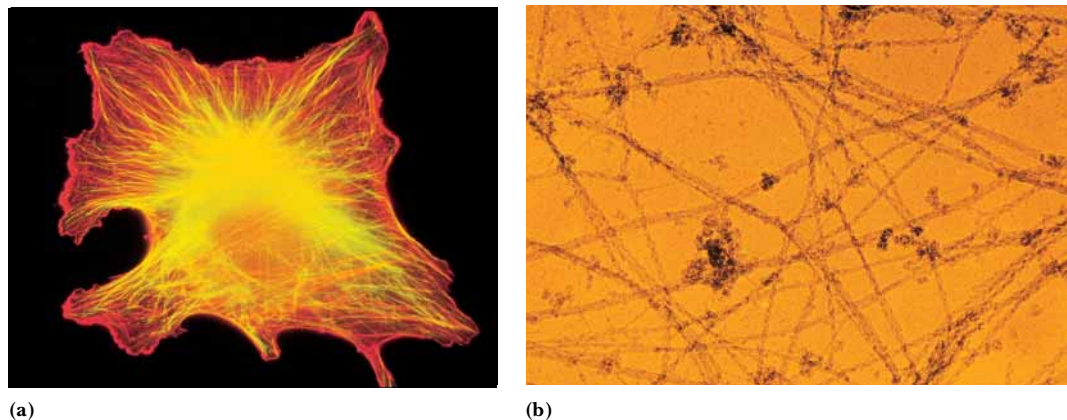
FIGURE 17.4 • Intermediate filaments have diameters of approximately 7 to 12 nm, whereas microfilaments, which are made from actin, have diameters of approximately 7 nm. The intermediate filaments appear to play only a structural role (maintaining cell shape), but the microfilaments and microtubules play more dynamic roles. Microfilaments are involved in cell motility, whereas microtubules act as long filamentous tracks, along which cellular components may be rapidly transported by specific mechanisms. (a) Cytoskeleton, double-labeled with actin in red and tubulin in green. (b) Cytoskeletal elements in a eukaryotic cell, including microtubules (thickest strands), intermediate filaments, and actin microfilaments (smallest strands). *(a, b, M. Schliwa/Visuals Unlimited)*
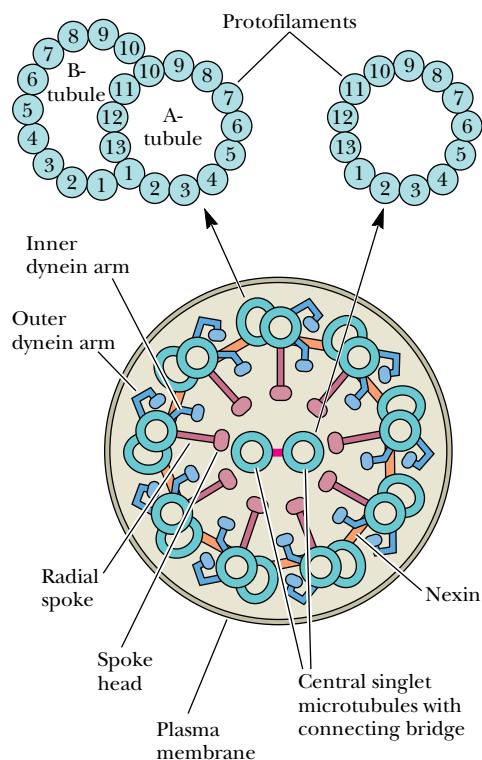
FIGURE 17.5 • The structure of an axoneme. Note the manner in which two microtubules are joined in the nine outer pairs. The smaller-diameter tubule of each pair, which is a true cylinder, is called the A-tubule and is joined to the center sheath of the axoneme by a spoke structure. Each outer pair of tubules is joined to adjacent pairs by a nexin bridge. The A-tubule of each outer pair possesses an outer dynein arm and an inner dynein arm. The larger-diameter tubule is known as the B-tubule.

pel cells through fluids. Cilia and flagella share a common design (Figure 17.5). The **axoneme** is a complex bundle of microtubule fibers that includes two central, separated microtubules surrounded by nine pairs of joined microtubules. The axoneme is surrounded by a plasma membrane that is continuous with the plasma membrane of the cell. Removal of the plasma membrane by detergent and subsequent treatment of the exposed axonemes with high concentrations of salt releases the **dynein** molecules (Figure 17.6), which form the *dynein arms.*

The Mechanism of Ciliary Motion

The motion of cilia results from the ATP-driven sliding or walking of dyneins along one microtubule while they remain firmly attached to an adjacent microtubule. The flexible stems of the dyneins remain permanently attached to A-tubules (Figure 17.6). However, the projections on the globular heads form transient attachments to adjacent B-tubules. Binding of ATP to the dynein heavy chain causes dissociation of the projections from the B-tubules. These projections then reattach to the B-tubules at a position closer to the minus end. Repetition of this process causes the sliding of A-tubules relative to B-tubules. The cross-linked structure of the axoneme dictates that this sliding motion will occur in an asymmetric fashion, resulting in a bending motion of the axoneme, as shown in Figure 17.7

Microtubules Also Mediate Intracellular Motion of Organelles and Vesicles

The ability of dyneins to effect **mechano-chemical coupling**—i.e., motion coupled with a chemical reaction—is also vitally important *inside* eukaryotic cells, which, as already noted, contain microtubule networks as part of the cytoskeleton. The mechanisms of intracellular, microtubule-based transport of organelles and vesicles were first elucidated in studies of **axons,** the long pro-
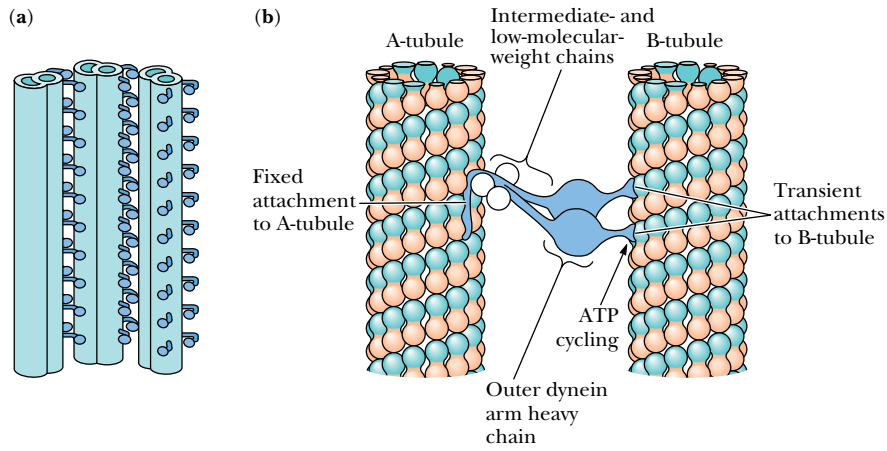
FIGURE 17.6 • (a) Diagram showing dynein interactions between adjacent microtubule pairs. (b) Detailed views of dynein crosslinks between the A-tubule of one microtubule pair and the B-tubule of a neighboring pair. (The B-tubule of the first pair and the A-tubule of the neighboring pair are omitted for clarity.) Isolated axonemal dyneins, which possess ATPase activity, consist of two or three "heavy chains" with molecular masses of 400 to 500 kD, referred to as α and β (and γ when present), as well as several chains with intermediate (40 to 120 kD) and low (15 to 25 kD) molecular masses. Each outer-arm heavy chain consists of a globular domain with a flexible stem on one end and a shorter projection extending at an angle with respect to the flexible stem. In a dynein arm, the flexible stems of several heavy chains are joined in a common base, where the intermediate- and low-molecular-weight proteins are located.
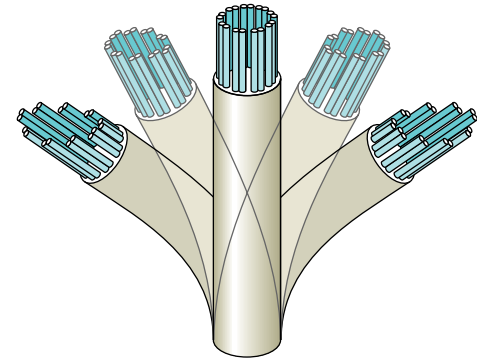
FIGURE 17.7 • A mechanism for ciliary motion. The sliding motion of dyneins along one microtubule while attached to an adjacent microtubule results in a bending motion of the axoneme.

jections of neurons that extend great distances away from the body of the cell. In these cells, it was found that subcellular organelles and vesicles could travel at surprisingly fast rates—as great as 2 to 5 μm/sec—in either direction. Unraveling the molecular mechanism for this rapid transport turned out to be a challenging biochemical problem. The early evidence that these movements occur by association with specialized proteins on the microtubules was met with some resistance, for two reasons. First, the notion that a network of microtubules could mediate transport was novel and, like all novel ideas, difficult to accept. Second, many early attempts to isolate dyneins from neural tissue were unsuccessful, and the dynein-like proteins that were first isolated from cytosolic fractions were thought to represent contaminations from axoneme structures. However, things changed dramatically in 1985 with a report by Michael Sheetz and his coworkers of a new ATP-driven, force-generating protein, different from myosin and dynein, which they called *kinesin*. Then, in 1987, Richard McIntosh and Mary Porter described the isolation of *cytosolic dynein* proteins from *Caenorhabditis elegans*, a nematode worm that never makes motile axonemes at any stage of its life cycle. Kinesins have now been found in many eukaryotic cell types, and similar cytosolic dyneins have been found in fruit flies, amoebae, and slime molds; in vertebrate brain and testes; and in HeLa cells (a unique human tumor cell line).

Dyneins Move Organelles in a Plus-to-Minus Direction; Kinesins, in a Minus-to-Plus Direction

The cytosolic dyneins bear many similarities to axonemal dynein. The protein isolated from *C. elegans* includes a "heavy chain" with a molecular mass of approximately 400 kD, as well as smaller peptides with molecular mass ranging from 53 kD to 74 kD. The protein possesses a microtubule-activated ATPase

CRITICAL DEVELOPMENTS IN BIOCHEMISTRY

Effectors of Microtubule Polymerization as Therapeutic Agents

Microtubules in eukaryotic cells are important for the maintenance and modulation of cell shape and the disposition of intracellular elements during the growth cycle and mitosis. It may thus come as no surprise that the *inhibition of microtubule polymerization* can block many normal cellular processes. The alkaloid **colchicine** (see figure), a constituent of the swollen, underground stems of the autumn crocus (*Colchicum autumnale*) and meadow saffron, inhibits the polymerization of tubulin into microtubules. This effect blocks the mitotic cycle of plants and animals. Colchicine also inhibits cell motility and intracellular transport of vesicles and organelles (which in turn blocks secretory processes of cells). Colchicine has been used for hundreds of years to alleviate some of the acute pain of gout and rheumatism. In gout, white cell lysosomes surround and engulf small crystals of uric acid. The subsequent rupture of the lysosomes and the attendant lysis of the white cells initiate an inflammatory response that causes intense pain. The mechanism of pain alleviation by colchicine is not known for certain, but appears to involve inhibition of white cell movement in tissues. Interestingly, colchicine's ability to inhibit mitosis has given it an important role in the commercial development of new varieties of agricultural and ornamental plants. When mitosis is blocked by colchicine, the treated cells may be left with an extra set of chromosomes. Plants with extra sets of chromosomes are typically larger and more vigorous than normal plants. Flowers developed in this way may grow with double the normal number of petals, and fruits may produce much larger amounts of sugar.

Another class of alkaloids, the **vinca alkaloids** from *Vinca rosea,* the Madagascar periwinkle, can also bind to tubulin and inhibit microtubule polymerization. **Vinblastine** and **vincristine** are used as potent agents for cancer chemotherapy, owing to their ability to inhibit the growth of fast-growing tumor cells. For reasons that are not well understood, colchicine is not an effective chemotherapeutic agent, though it appears to act similarly to the vinca alkaloids in inhibiting tubulin polymerization.

A new antitumor drug, **taxol,** has been isolated from the bark of *Taxus brevifolia,* the Pacific yew tree. Like vinblastine and colchicine, taxol inhibits cell replication by acting on microtubules. Unlike these other antimitotic drugs, however, taxol stimulates microtubule polymerization and stabilizes microtubules. The remarkable success of taxol in treatment of breast and ovarian cancers stimulated research efforts to synthesize taxol directly and to identify new antimitotic agents that, like taxol, stimulate microtubule polymerization.

Vinblastine: R = CH₃
Vincristine: R = CHO
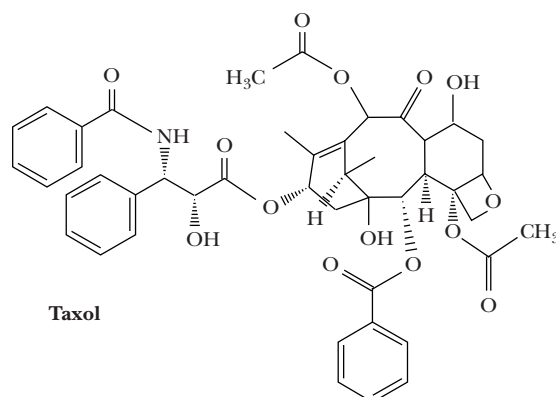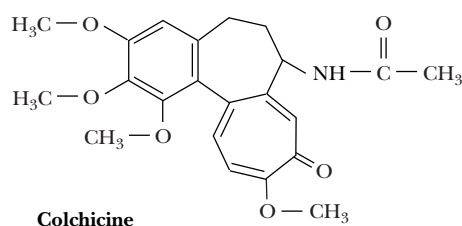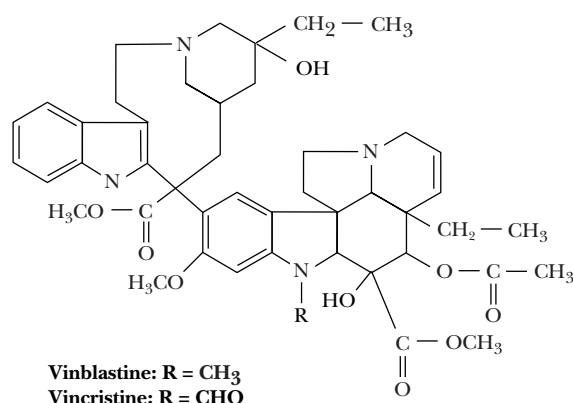
Colchicine

Taxol

The structures of vinblastine, vincristine, colchicine, and taxol.

activity, and, when anchored to a glass surface *in vitro,* these proteins, in the presence of ATP, can bind microtubules and move them through the solution. In the cell, cytosolic dyneins specifically move organelles and vesicles from the plus end of a microtubule to the minus end. Thus, as shown in Figure 17.8, dyneins move vesicles and organelles from the cell periphery toward the centrosome (or, in an axon, from the synaptic termini toward the cell body). The

(a)

(b)
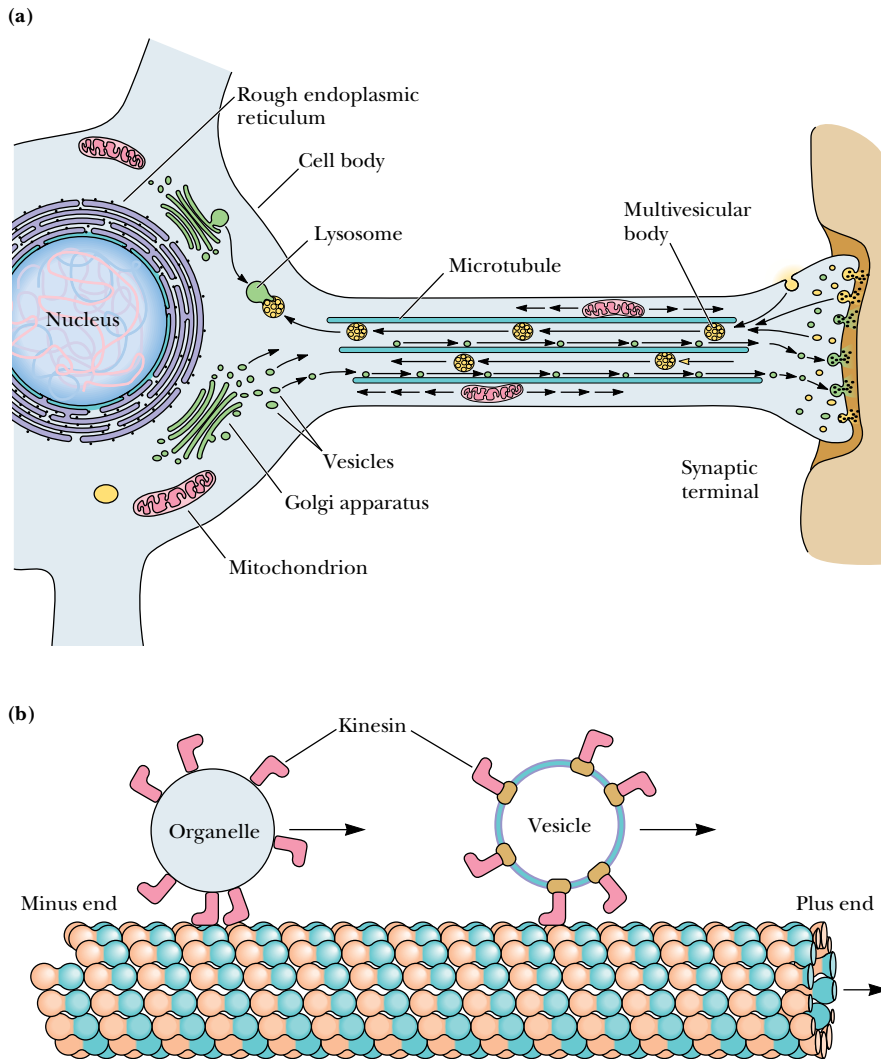
FIGURE 17.8 • (a) Rapid axonal transport along microtubules permits the exchange of material between the synaptic terminal and the body of the nerve cell. (b) Vesicles, multivesicular bodies, and mitochondria are carried through the axon by this mechanism.
(Adapted from a drawing by Ronald Vale)

kinesins, on the other hand, assist the movement of organelles and vesicles from the minus end to the plus end of microtubules, resulting in outward movement of organelles and vesicles. Kinesin is similar to cytosolic dyneins but smaller in size (360 kD), and contains subunits of 110 kD and 65 to 70 kD. Its length is 100 nm. Like dyneins, kinesins possess ATPase activity in their globular heads, and it is the free energy of ATP hydrolysis that drives the movement of vesicles along the microtubules.

The N-terminal domain of the kinesin heavy chain (38 kD, approximately 340 residues) contains the ATP- and microtubule-binding sites and is the domain responsible for movement. Electron microscopy and image analysis of tubulin–kinesin complexes reveals (Figure 17.9) that the kinesin head domain is compact and primarily contacts a single tubulin subunit on a microtubule surface, inducing a conformational change in the tubulin subunit. Optical trapping experiments (see page 554) demonstrate that kinesin heads move in 8-nm (80-Å) steps along the long axis of a microtubule. Kenneth Johnson and his coworkers have shown that the ability of a single kinesin tetramer to move unidirectionally for long distances on a microtubule depends upon cooperative interactions between the two mechanochemical head domains of the protein.

FIGURE 17.9 • The structure of the tubulin–kinesin complex, as revealed by image analysis of cryoelectron microscopy data. (a) The computed, three-dimensional map of a microtubule, (b) the kinesin globular head domain–microtubule complex, (c) a contour plot of a horizontal section of the kinesin–microtubule complex, and (d) a contour plot of a vertical section of the same complex. *(Taken from Kikkawa et al., 1995.* Nature *376:274–277. Photo courtesy of Nobutaka Hirokawa.)*
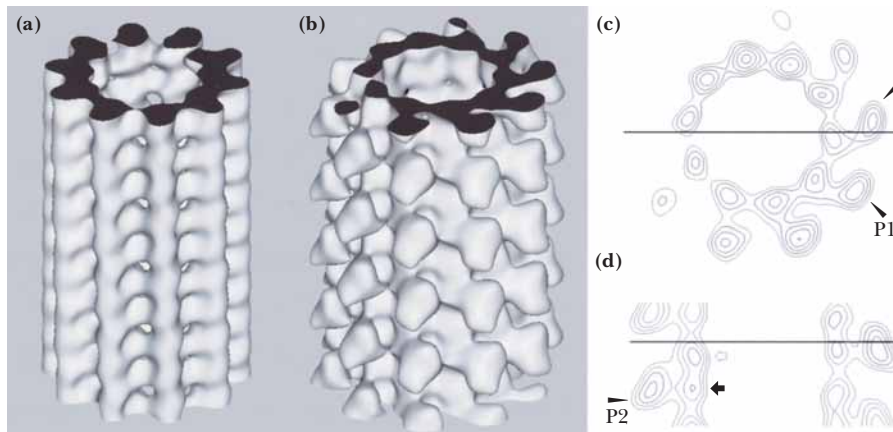
17.3 • Skeletal Muscle Myosin and Muscle Contraction

The Morphology of Muscle

Four different kinds of muscle are found in animals (Figure 17.10). They are **skeletal** muscle, **cardiac (heart)** muscle, **smooth** muscle, and **myoepithelial cells.** The cells of the latter three types contain only a single nucleus and are called **myocytes.** The cells of skeletal muscle are long and multinucleate and are referred to as **muscle fibers.** At the microscopic level, skeletal muscle and cardiac muscle display alternating light and dark bands, and for this reason are often referred to as **striated** muscles. The different types of muscle cells vary widely in structure, size, and function. In addition, the times required for contractions and relaxations by various muscle types vary considerably. The fastest responses (on the order of milliseconds) are observed for **fast-twitch** skeletal

(a) Part of a skeletal muscle cell   (b) Heart muscle cells   (c) Smooth muscle cells   (d) Myoepithelial cell
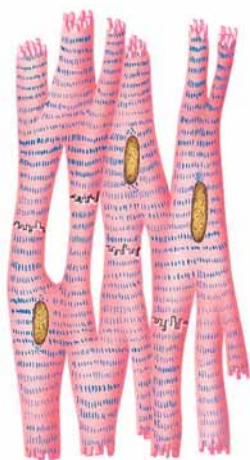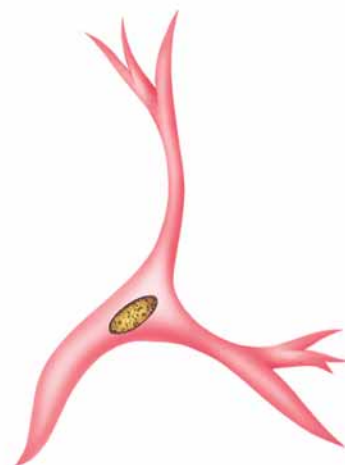
FIGURE 17.10 • The four classes of muscle cells in mammals. Skeletal muscle and cardiac muscle are striated. Cardiac muscle, smooth muscle, and myoepithelial cells are mononucleate, whereas skeletal muscle is multinucleate.

muscle, and the slowest responses (on the order of seconds) are found in smooth muscle. **Slow-twitch** skeletal muscle tissue displays an intermediate response time.

Structural Features of Skeletal Muscle

Skeletal muscles in higher animals consist of 100-μm-diameter **fiber bundles,** some as long as the muscle itself. Each of these muscle fibers contains hundreds of **myofibrils** (Figure 17.11), each of which spans the length of the fiber and is about 1 to 2 μm in diameter. Myofibrils are linear arrays of cylindrical **sarcomeres,** the basic structural units of muscle contraction. The sarcomeres are surrounded on each end by a membrane system that is actually an elaborate extension of the muscle fiber plasma membrane or **sarcolemma.** These extensions of the sarcolemma, which are called **transverse tubules** or **t-tubules,** enable the sarcolemmal membrane to contact the ends of each myofibril in the muscle fiber (Figure 17.11). This topological feature is crucial to the initiation of contractions. In between the t-tubules, the sarcomere is covered with a specialized endoplasmic reticulum called the **sarcoplasmic reticulum,** or **SR.** The SR contains high concentrations of Ca^{2+}, and the release of Ca^{2+} from the SR and its interactions within the sarcomeres trigger muscle contraction, as we will see. Each SR structure consists of two domains. **Longitudinal tubules** run the length of the sarcomere and are capped on either end by the **terminal cisternae** (Figure 17.11). The structure at the end of each sarcomere, which consists of a t-tubule and two apposed terminal cisternae, is called a **triad,** and the intervening gaps of approximately 15 nm are called **triad junctions.** The junctional face of each terminal cisterna is joined to its respective t-tubule by a **foot structure.** Skeletal muscle contractions are initiated by nerve stimuli that act directly on the muscle. Nerve impulses produce an electrochemical signal
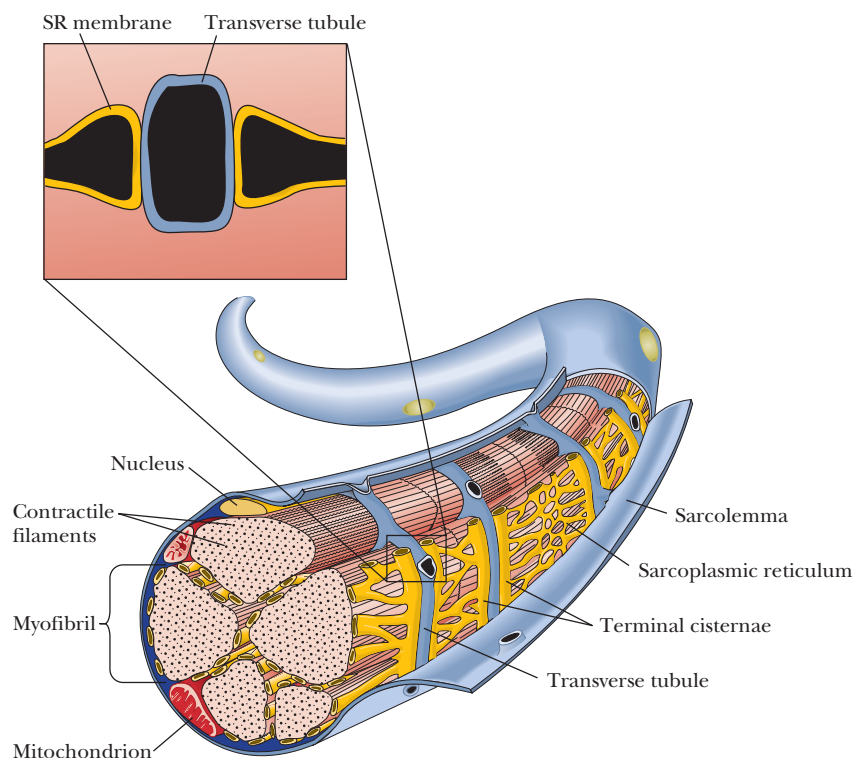
FIGURE 17.11 • The structure of a skeletal muscle cell, showing the manner in which t-tubules enable the sarcolemmal membrane to contact the ends of each myofibril in the muscle fiber. The foot structure is shown in the box.

(see Chapter 34) called an action potential that spreads over the sarcolemmal membrane and into the fiber along the t-tubule network. This signal is passed across the triad junction and induces the release of Ca^{2+} ions from the SR. These Ca^{2+} ions bind to the muscle fibers and induce contraction.

The Molecular Structure of Skeletal Muscle

Examination of myofibrils in the electron microscope reveals a banded or striated structure. The bands are traditionally identified by letters (Figure 17.12). Regions of high electron density, denoted **A bands,** alternate with regions of low electron density, the **I bands.** Small, dark **Z lines** lie in the middle of the I bands, marking the ends of the sarcomere. Each A band has a central region of slightly lower electron density called the **H zone,** which contains a central **M disk** (also called an **M line**). Electron micrographs of cross-sections of each of these regions reveal molecular details. The H zone shows a regular, hexagonally arranged array of **thick filaments** (15 nm diameter), whereas the I band shows a regular, hexagonal array of **thin filaments** (7 nm diameter). In the dark regions at the ends of each A band, the thin and thick filaments interdigitate, as shown in Figure 17.12. The thin filaments are composed primarily of three proteins called **actin, troponin,** and **tropomyosin.** The thick filaments consist mainly of a protein called **myosin.** The thin and thick filaments are joined by **cross-bridges.** These cross-bridges are actually extensions of the myosin molecules, and muscle contraction is accomplished by the sliding of the cross-bridges along the thin filaments, a mechanical movement driven by the free energy of ATP hydrolysis.

FIGURE 17.12 • Electron micrograph of a skeletal muscle myofibril (in longitudinal section). The length of one sarcomere is indicated, as are the A and I bands, the H zone, the M disk, and the Z lines. Cross-sections from the H zone show a hexagonal array of thick filaments, whereas the I band cross-section shows a hexagonal array of thin filaments. *(Photo courtesy of Hugh Huxley, Brandeis University)*
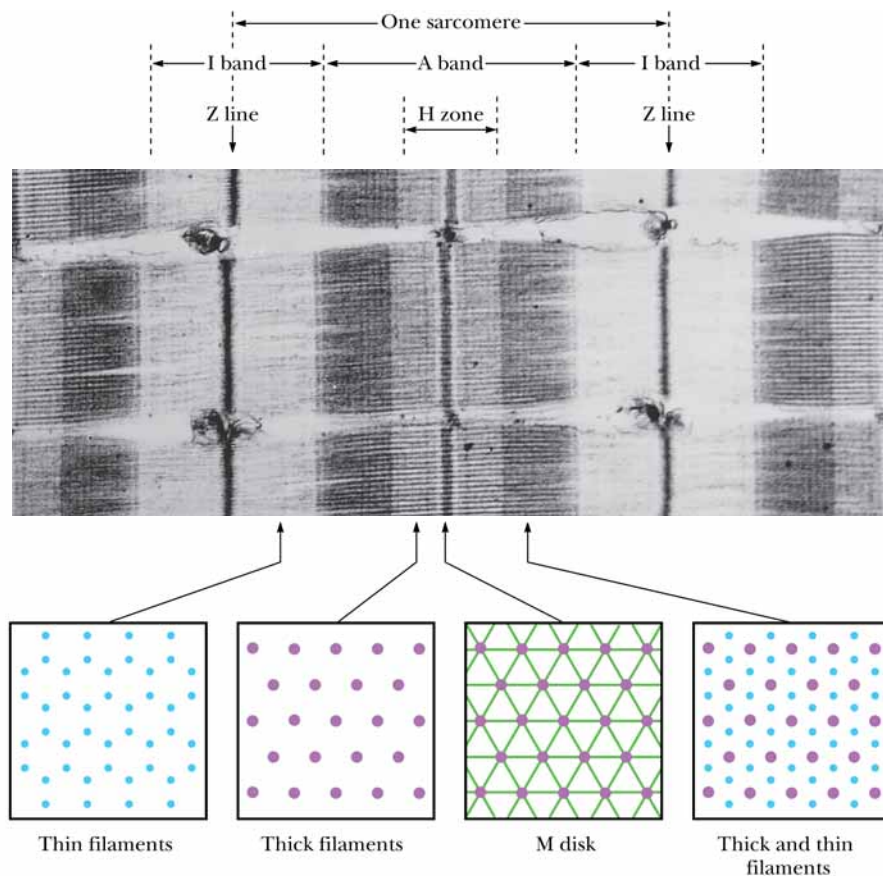
The Composition and Structure of Thin Filaments

Actin, the principal component of thin filaments, can be isolated in two forms. Under conditions of low ionic strength, actin exists as a 42-kD globular protein, denoted **G-actin.** G-actin consists of two principal lobes or domains (Figure 17.13). Under physiological conditions (higher ionic strength), G-actin polymerizes to form a *fibrous* form of actin, called **F-actin.** As shown in Figure 17.14, F-actin is a right-handed helical structure, with a helix pitch of about 72 nm per turn. The F-actin helix is the core of the thin filament, to which *tropomyosin* and the **troponin complex** also add. Tropomyosin is a dimer of homologous but nonidentical 33-kD subunits. These two subunits form long α-helices that intertwine, creating 38- to 40-nm-long coiled coils, which join in head-to-tail fashion to form long rods. These rods bind to the F-actin polymer and lie almost parallel to the long axis of the F-actin helix (Figure 17.15a–c). Each tropomyosin heterodimer contacts approximately seven actin subunits. The troponin complex consists of three different proteins: **troponin T,** or **TnT** (37 kD); **troponin I,** or **TnI** (24 kD); and **troponin C,** or **TnC** (18 kD). TnT binds to tropomyosin, specifically at the head-to-tail junction. Troponin I binds both to tropomyosin and to actin. Troponin C is a Ca^{2+}-binding protein that binds to TnI. TnC shows 70% homology with the important Ca^{2+} signaling protein, calmodulin (Chapter 34). The release of Ca^{2+} from the SR, which signals a contraction, raises the cytosolic Ca^{2+} concentration high enough to saturate the Ca^{2+} sites on TnC. Ca^{2+} binding induces a conformational change in the amino-terminal domain of TnC, which in turn causes a rearrangement of the troponin complex and tropomyosin with respect to the actin fiber.
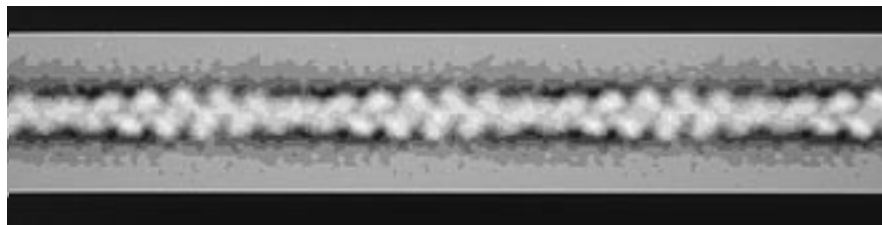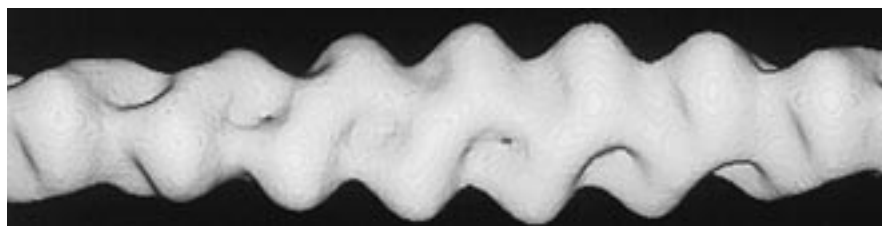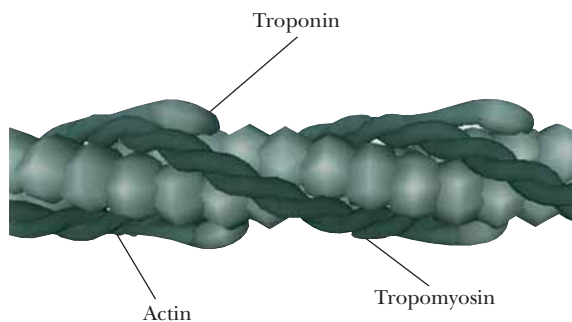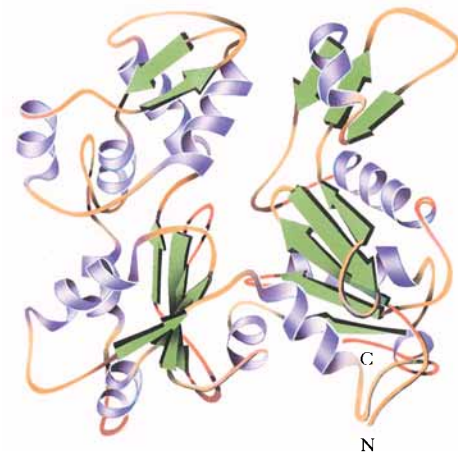
FIGURE 17.13 • The three-dimensional structure of an actin monomer from skeletal muscle. This view shows the two domains *(left and right)* of actin.

(a)

(b)

(c)   Actin   Tropomyosin

Troponin
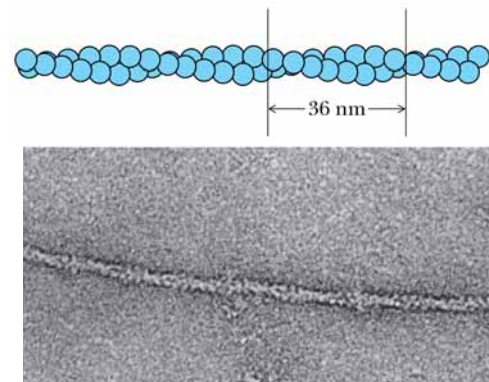
FIGURE 17.14 • The helical arrangement of actin monomers in F-actin. The F-actin helix has a pitch of 72 nm and a repeat distance of 36 nm. *(Electron micrograph courtesy of Hugh Huxley, Brandeis University)*

FIGURE 17.15 • (a) An electron micrograph of a thin filament, (b) a corresponding image reconstruction, and (c) a schematic drawing based on the images in (a) and (b). The tropomyosin coiled coil winds around the actin helix, each tropomyosin dimer interacting with seven consecutive actin monomers. Troponin T binds to tropomyosin at the head-to-tail junction. *(a and b, courtesy of Linda Rost and David DeRosier, Brandeis University; c, courtesy of George Phillips, Rice University)*

The Composition and Structure of Thick Filaments

Myosin, the principal component of muscle thick filaments, is a large protein consisting of six polypeptides, with an aggregate molecular weight of approximately 540 kD. As shown in Figure 17.16, the six peptides include two 230-kD **heavy chains,** as well as two pairs of different 20-kD **light chains,** denoted **LC1** and **LC2.** The heavy chains consist of globular amino-terminal **myosin heads,** joined to long α-helical carboxy-terminal segments, the **tails.** These tails are intertwined to form a left-handed coiled coil approximately 2 nm in diameter and 130 to 150 nm long. Each of the heads in this dimeric structure is associated with an LC1 and an LC2. The myosin heads exhibit **ATPase activity,** and hydrolysis of ATP by the myosin heads drives muscle contraction. LC1 is also known as the **essential light chain,** and LC2 is designated the **regulatory light chain.** Both light chains are homologous to calmodulin and TnC. Dissociation of LC1 from the myosin heads by alkali cations results in loss of the myosin ATPase activity.

FIGURE 17.16 • (a) An electron micrograph of a myosin molecule and a corresponding schematic drawing. The tail is a coiled coil of intertwined α-helices extending from the two globular heads. One of each of the myosin light chain proteins, LC1 and LC2, is bound to each of the globular heads. (b) A ribbon diagram shows the structure of the S1 myosin head (green, red, and purple segments) and its associated essential (yellow) and regulatory (magenta) light chains. *(a, Electron micrograph courtesy of Henry Slayter, Harvard Medical School; b, courtesy of Ivan Rayment and Hazel M. Holden, University of Wisconsin, Madison)*
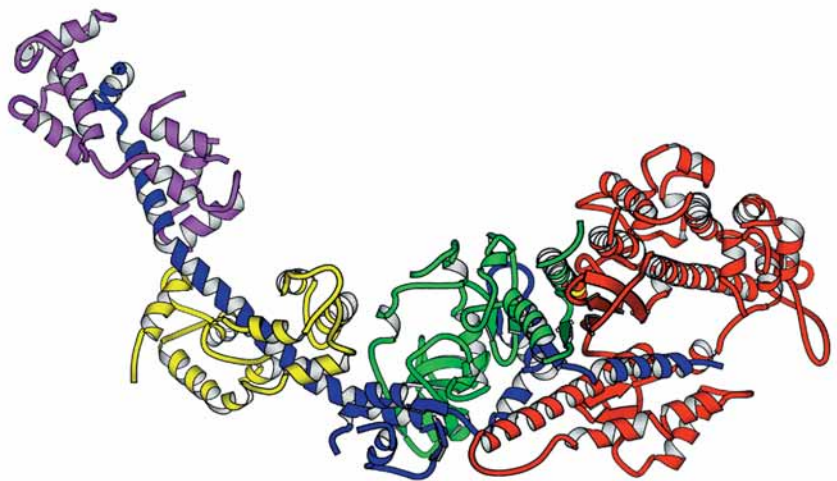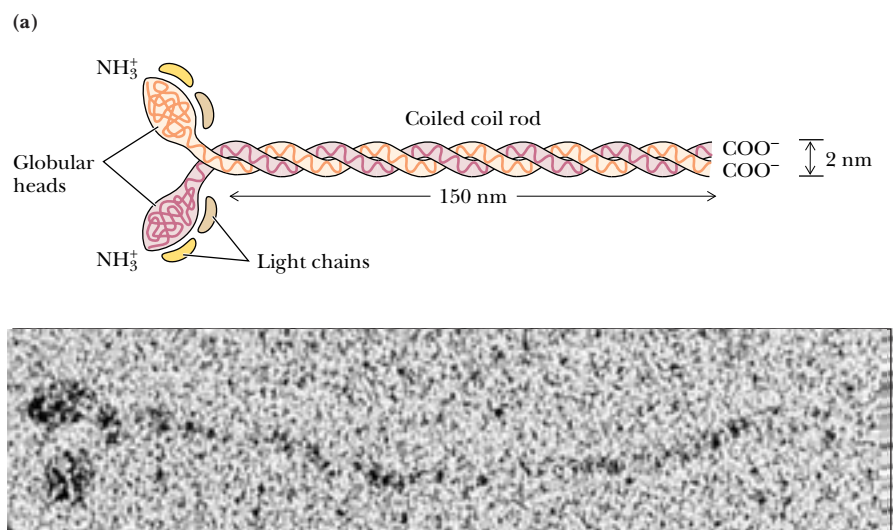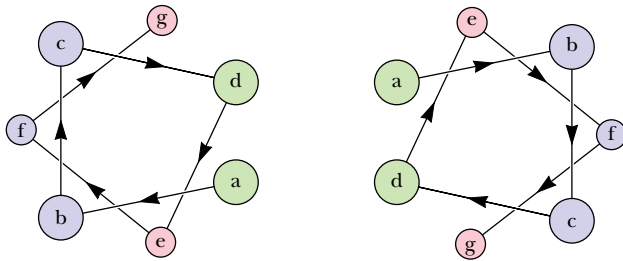
FIGURE 17.17 • An axial view of the two-stranded, α-helical coiled coil of a myosin tail. Hydrophobic residues a and d of the seven-residue repeat sequence align to form a hydrophobic core. Residues b, c, and f face the outer surface of the coiled coil and are typically ionic.

Approximately 500 of the 820 amino acid residues of the myosin head are highly conserved between various species. One conserved region, located approximately at residues 170 to 214, constitutes part of the ATP-binding site. Whereas many ATP-binding proteins and enzymes employ a β-sheet–α-helix–β-sheet motif, this region of myosin forms a related α-β-α structure, beginning with an Arg at (approximately) residue 192. The β-sheet in this region of all myosins includes the amino acid sequence

<div align="center">Gly-Glu-Ser-Gly-Ala-Gly-Lys-Thr</div>
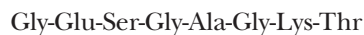
The Gly-X-X-Gly-X-Gly found in this segment is found in many ATP- and nucleotide-binding enzymes. The Lys of this segment is thought to interact with the α-phosphate of bound ATP.

Repeating Structural Elements Are the Secret of Myosin's Coiled Coils

Myosin tails show less homology than the head regions, but several key features of the tail sequence are responsible for the α-helical coiled coils formed by myosin tails. *Several orders of repeating structure* are found in all myosin tails, including 7-residue, 28-residue, and 196-residue repeating units. Large stretches of the tail domain are composed of 7-residue repeating segments. The first and fourth residues of these 7-residue units are generally small, hydrophobic amino acids, whereas the second, third, and sixth are likely to be charged residues. The consequence of this arrangement is shown in Figure 17.17. Seven residues form two turns of an α-helix, and, in the coiled coil structure of the myosin tails, the first and fourth residues face the interior contact region of the coiled coil. Residues b, c, and f (2, 3, and 6) of the 7-residue repeat face the periphery, where charged residues can interact with the water solvent. Groups of four 7-residue units with distinct patterns of alternating side-chain charge form 28-residue repeats that establish alternating regions of positive and negative charge on the surface of the myosin coiled coil. These alternating charged regions interact with similar regions in the tails of adjacent myosin molecules to assist in stabilizing the thick filament.

At a still higher level of organization, groups of seven of these 28-residue units—a total of 196 residues—also form a repeating pattern, and this large-scale repeating motif contributes to the packing of the myosin molecules in the thick filament. The myosin molecules in thick filaments are offset (Figure 17.18) by approximately 14 nm, a distance that corresponds to 98 residues of a coiled coil, or exactly half the length of the 196-residue repeat. Thus, several layers of repeating structure play specific roles in the formation and stabilization of the myosin coiled coil and the thick filament formed from them.
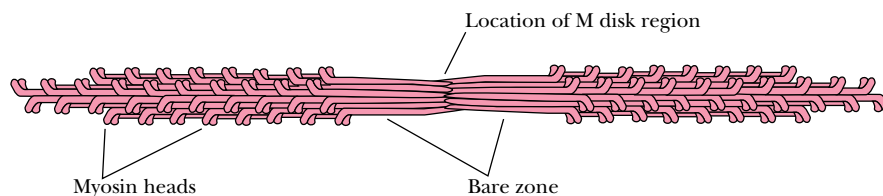
FIGURE 17.18 • The packing of myosin molecules in a thick filament. Adjoining molecules are offset by approximately 14 nm, a distance corresponding to 98 residues of the coiled coil.

The Associated Proteins of Striated Muscle

In addition to the major proteins of striated muscle (myosin, actin, tropomyosin, and the troponins), numerous other proteins play important roles in the maintenance of muscle structure and the regulation of muscle contraction. Myosin and actin together account for 65% of the total muscle protein, and tropomyosin and the troponins each contribute an additional 5% (Table 17.1). The other regulatory and structural proteins thus comprise approximately 25% of the myofibrillar protein. The regulatory proteins can be classified as either **myosin-associated proteins** or **actin-associated proteins.**

The myosin-associated proteins include three proteins found in the M disks. The M disks consist primarily of **M protein** (165 kD), **myomesin** (185 kD), and **creatine kinase** (a dimer of 42-kD subunits). Creatine kinase facilitates rapid regeneration of the ATP consumed during muscle contraction. The association of M protein, myomesin, and creatine kinase in the M disk maintains the structural integrity of the myosin filaments. Several other myosin-associated proteins have also been identified, including **C protein** (135 kD), **F protein** (121 kD), **H protein** (74 kD), and **I protein** (50 kD). The C protein is localized to several regularly spaced stripes in the A band. C protein inhibits myosin ATPase activity at low ionic strength but activates it at physiological ionic strength. The roles of F, H, and I proteins are not yet understood.

Actin-associated proteins (other than tropomyosin and the troponins) include **α-actinin** (a homodimer of 95-kD subunits), **β-actinin** (a heterodimer of 37-kD and 34-kD subunits), **γ-actinin** (a 35-kD monomer), and **paratropomyosin** (a homodimer of 34-kD subunits). α-Actinin is found in the Z lines and activates contraction of actomyosin. It is thought to play a role in attachment of actin to the Z lines. α-Actinin consists of three domains: an N-terminal, actin-binding domain; a central domain consisting of four repeats of a 122-residue sequence; and a C-terminal domain that contains two EF-hand, calcium-binding domains (Figure 17.19). The four central repeats in α-actinin are highly homologous with the 106-residue repeat sequences of **spectrin,** the major structural protein of the red blood cell cytoskeleton. The repeating segments of both α-actinin and spectrin are thought to consist of bundles of four α-helices (Figure 17.20). β-Actinin acts as an actin-capping protein, specifically binding to the end of an actin filament. γ-Actinin also inhibits actin polymerization, but its location in thin filaments is not known with certainty. Paratropomyosin is similar to tropomyosin, but appears to be located only at the A band–I band junction.

Two cytoskeletal proteins, **titin** (also known as **connectin**) and **nebulin,** account for 15% of the total protein in the myofibril. Together these proteins form a flexible filamentous network that surrounds the myofibrils. Titin is an **elastic protein** and can stretch under tension. Its discovery and characteriza-
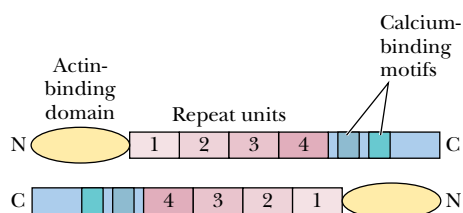
FIGURE 17.19 • α-Actinin exists as a homodimer of antiparallel subunits, illustrated here in terms of their primary structure. The N-terminal, actin-binding domain and the C-terminal, EF-hand domains are separated by a central domain consisting of four repeats of a 122-residue sequence.

Table 17.1

Myofibrillar Structural Proteins of Rabbit Skeletal Muscle

Protein	Molecular Mass (kD)	Content (wt %)	Localization	Function
Contractile proteins				
Myosin	520	43	A band	Contracts with actin
Actin	42	22	I band	Contracts with myosin
Regulatory proteins				
Major				
Tropomyosin	33 × 2	5	I band	Binds to actin and locates troponin
Troponin	70	5	I band	Ca regulation
Troponin C	18			Ca binding
Troponin I	21			Inhibits actin–myosin interaction
Troponin T	31			Binds to tropomyosin
Minor				
M protein	165	2	M line	Binds to myosin
Myomesin	185	<1	M line	Binds to myosin
Creatine kinase	42	<1	M line	Binds to myosin
C protein	135	2	A band	Binds to myosin
F protein	121	<1	A band	Binds to myosin
H protein	74	<1	Near M line	Binds to myosin
I protein	50	<1	A band	Inhibits actin–myosin interaction
α-Actinin	95 × 2	2	Z line	Gelates actin filaments
β-Actinin	37 + 34	<1	Free end of actin filament	Caps actin filaments
γ-Actinin	35	<1	?	Inhibits actin polymerization
eu-Actinin	42	<1	Z line	Binds to actin
ABP (filamin)	240 × 2	<1	Z line	Gelates actin filaments
Paratropomyosin	34 × 2	<1	A–I junction	Inhibits actin–myosin interaction
Cytoskeletal proteins				
Titin 1	2800	10	A–I	Links myosin filament to Z line
Titin 2	2100			
Nebulin	800	5	N_2 line*	
Vinculin	130	<1	Under sarcolemma	
Desmin (skeletin)	53	<1	Periphery of Z line	Intermediate filament
Vimentin	55	<1	Periphery of Z line	Intermediate filament
Synemin	220	<1	Z line	
Z protein	50	<1	Z line	Forms lattice structure
Z-nin	400	<1	Z line	

*A structure within the I band.

Adapted from Ohtsuki, I., Maruyama, K., and Ebashi, S., 1986. Regulatory and cytoskeletal proteins of vertebrate skeletal muscle. *Advances in Protein Chemistry* **38:**1–67.

$\mathcal{H}$UMAN BIOCHEMISTRY

The Molecular Defect in Duchenne Muscular Dystrophy Involves an Actin-Anchoring Protein

Discovery of a new actinin/spectrin–like protein has provided insights into the molecular basis for at least one form of muscular dystrophy. Duchenne muscular dystrophy is a degenerative and fatal disorder of muscle affecting approximately 1 in 3500 boys. Victims of Duchenne dystrophy show early abnormalities in walking and running. By the age of five, the victim cannot run and has difficulty standing, and by early adolescence, walking is difficult or impossible. The loss of muscle function progresses upward in the body, affecting next the arms and the diaphragm. Respiratory problems or infections usually result in death by the age of 30. Louis Kunkel and his coworkers identified the Duchenne muscular dystrophy gene in 1986. This gene produces a protein called **dystrophin,** which is highly homologous to α-actinin and spectrin. A defect in dystrophin is responsible for the muscle degeneration of Duchenne dystrophy.

Dystrophin is located on the cytoplasmic face of the muscle plasma membrane, linked to the plasma membrane via an integral membrane glycoprotein. Dystrophin has a high molecular mass (427 kD), but constitutes less than 0.01% of the total muscle protein. It folds into four principal domains (figure, part a), including an N-terminal domain similar to the actin-binding domains of actinin and spectrin, a long repeat domain, a cysteine-rich domain, and a C-terminal domain that is unique to dystrophin. The repeat domain consists of 24 repeat units of approximately 109 residues each. "Spacer sequences" high in proline content, which do not align with the repeat consensus sequence, occur at the beginning and end of the repeat domain. Spacer segments are found between repeat elements 3 and 4 and 19 and 20. The high proline content of the spacers suggests that they may represent hinge domains. The spacer/hinge segments are sensitive to proteolytic enzymes, indicating that they may represent more exposed regions of the polypeptide.

(a)
Dystrophin

A comparison of the amino acid sequences of dystrophin, α-actinin, and spectrin. The potential hinge segments in the dystrophin structure are indicated.
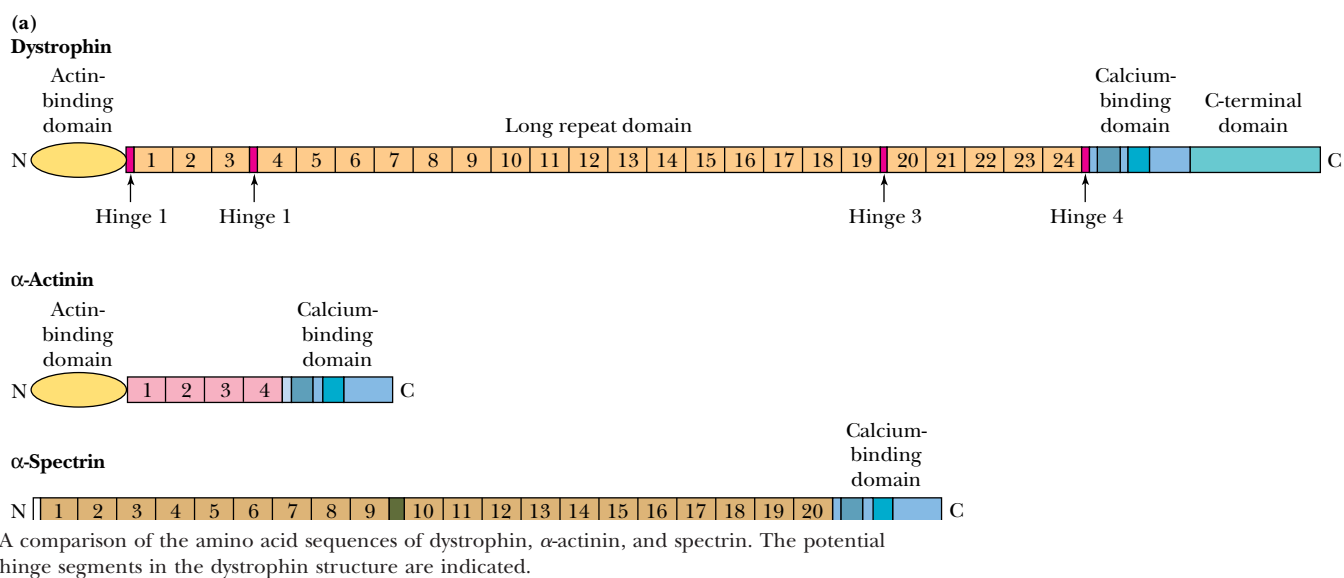
FIGURE 17.20 • A schematic drawing of the four-helix cluster model for α-actinin and spectrin. Helix 1 is long and is postulated to lie at an angle with respect to the long axis of the repeated domain.
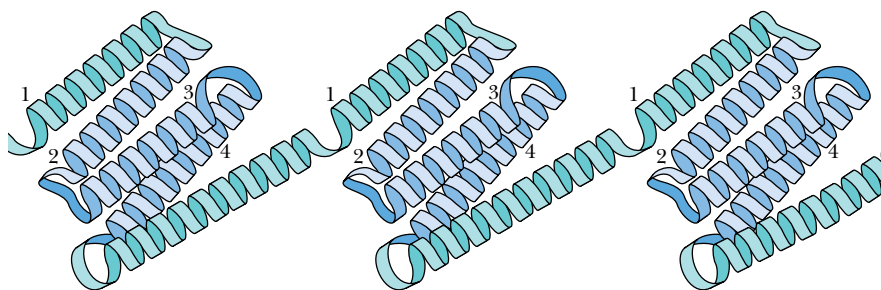
Dystrophin itself appears to be part of an elaborate protein/glycoprotein complex that bridges the inner cytoskeleton (actin filaments) and the extracellular matrix (via a matrix protein called laminin (see figure)). It is now clear that defects in one or more of the proteins in this complex are responsible for many of the other forms of muscular dystrophy. The glycoprotein complex is composed of two subcomplexes, the dystroglycan complex and the sarcoglycan complex. The dystroglycan complex consists of α-dystroglycan, an extracellular protein that binds to merosin, a laminin subunit and component of the extracellular matrix, and β-dystroglycan, a transmembrane protein that binds the C-terminal domain of dystrophin inside the cell (see figure). The sarcoglycan complex is composed of α-, β-, and γ-sarcoglycans, all of which are transmembrane glycoproteins. Alterations of the sarcoglycan proteins are linked to limb-girdle muscular dystrophy and autosomal recessive muscular dystrophy. Mutations in the gene for merosin, which binds to α-dystroglycan, are linked to severe congenital muscular dystrophy, yet another form of the disease.

(b)
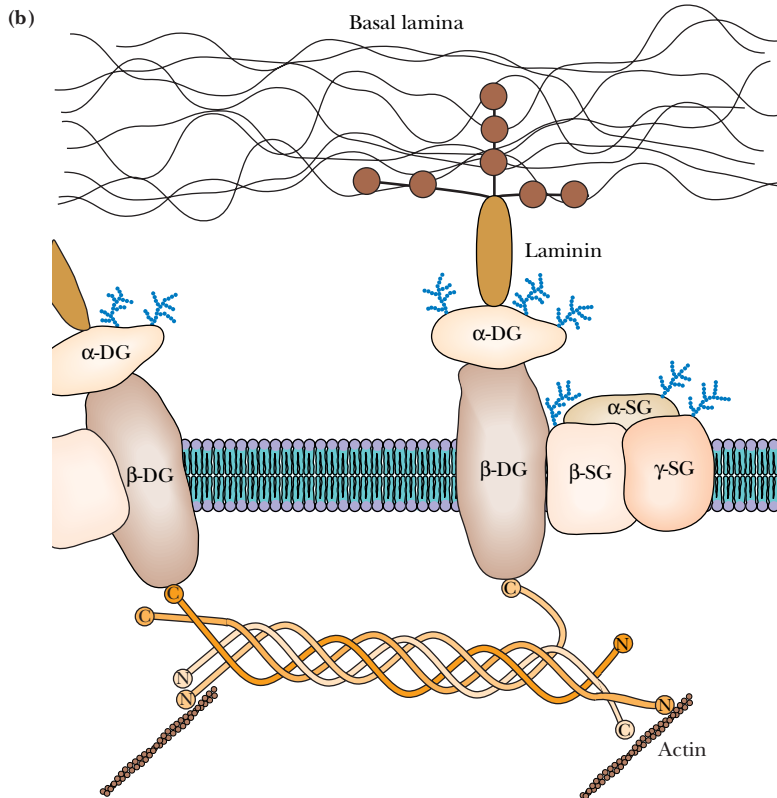
A model for the actin–dystrophin–glycoprotein complex in skeletal muscle. Dystrophin is postulated to form tetramers of antiparallel monomers that bind actin at their N-termini and a family of dystrophin-associated glycoproteins at their C-termini. This dystrophin-anchored complex may function to stabilize the sarcolemmal membrane during contraction–relaxation cycles, link the contractile force generated in the cell (fiber) with the extracellular environment, or maintain local organization of key proteins in the membrane. The dystrophin-associated membrane proteins (dystroglycans and sarcoglycans) range from 25 to 154 kD. *(Adapted from Ahn, A. H., and Kunkel, L. M., 1993.* Nature Genetics **3**:283–291, and Worton, R., 1995. Science **270**:755–756.)*

tion ended a century-long debate over the possible existence of an elastic component in muscle.

Titin is the largest known protein, consisting of nearly 27,000 amino acids and having a molecular mass of 2,993 kD. The sequencing of titin was accomplished by Siegfried Labeit and Bernhard Kolmerer in 1995. (To accomplish this prodigious feat, Labeit and Kolmerer pieced together the full sequence from 50 overlapping cDNA fragments!) Titin's sequence is composed mainly (90%) of 244 repeats of the immunoglobulin (Ig) and fibronectin 3 (FN3) domains. In the center of the titin molecule is a novel protein motif (not known in other proteins), consisting of repeats of the sequence **PEVK** (proline-gluta-

mate-valine-lysine). PEVK motifs may act as spring devices to pull muscles back into shape after they have been stretched and may also play a role in regulating the stiffness and elasticity of muscle fibers. In characteristically stiff muscles, such as cardiac muscle, the PEVK region is only 163 residues in length, whereas in the more elastic skeletal muscle the PEVK domain is over 2000 residues in length.

Titin forms long, flexible, thin filaments in muscle fibers. A single titin filament spans 1000 nm in its relaxed state, and a titin filament under tension can stretch to a length of over 3000 nm! Titin filaments in muscle originate at the periphery of the M band and extend along the myosin filaments all the way to the Z line (Figure 17.21). They appear to function by linking the myosin filaments to the Z lines and by acting as a template to regulate the assembly of myosin filaments and the spacing of myosin monomers in the filaments. When myofibrils are stretched beyond the overlap of the thick and thin filaments, titin filaments passively generate tension. This effect is provided by a relatively small number of titin molecules. The ratio of myosin to titin filaments is approximately 24 to 1. With 300 myosin molecules per thick filament, only 6 or so titin filaments are present in each half of a myosin thick filament.

The Mechanism of Muscle Contraction

When muscle fibers contract, the thick myosin filaments slide or walk along the thin actin filaments. The basic elements of the **sliding filament model** were first described in 1954 by two different research groups, Hugh Huxley and his colleague Jean Hanson, and the physiologist Andrew Huxley and his colleague Ralph Niedergerke. Several key discoveries paved the way for this model. Electron microscopic studies of muscle revealed that sarcomeres decreased in length during contraction, and that this decrease was due to decreases in the width of both the I band and the H zone (Figure 17.22). At the same time, the width of the A band (which is the length of the thick filaments) and the distance from the Z disks to the nearby H zone (that is, the length of the thin filaments) did not change. These observations made it clear that the lengths of both the thin and thick filaments were constant during contraction. This conclusion was consistent with a sliding filament model.

The Sliding Filament Model

The shortening of a sarcomere (Figure 17.22) involves sliding motions in opposing directions at the two ends of a myosin thick filament. Net sliding motions in a specific direction occur because the thin and thick filaments both have
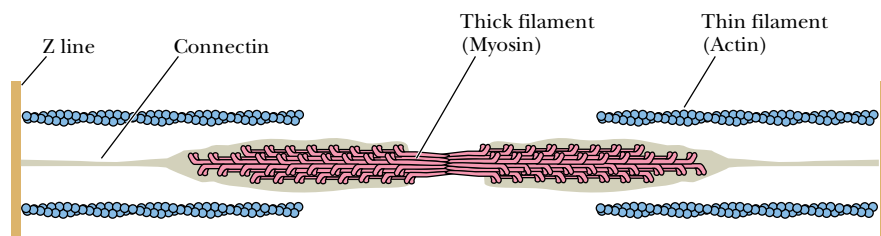
FIGURE 17.21 • A drawing of the arrangement of the elastic protein titin in the skeletal muscle sarcomere. Titin filaments originate at the periphery of the M band and extend along the myosin filaments to the Z lines. These titin filaments produce the passive tension existing in myofibrils that have been stretched so that the thick and thin filaments no longer overlap and cannot interact. *(Adapted from Ohtsuki, I., Maruyama, K., and Ebashi, S., 1986. Advances in Protein Chemistry **38**:1–67.)*
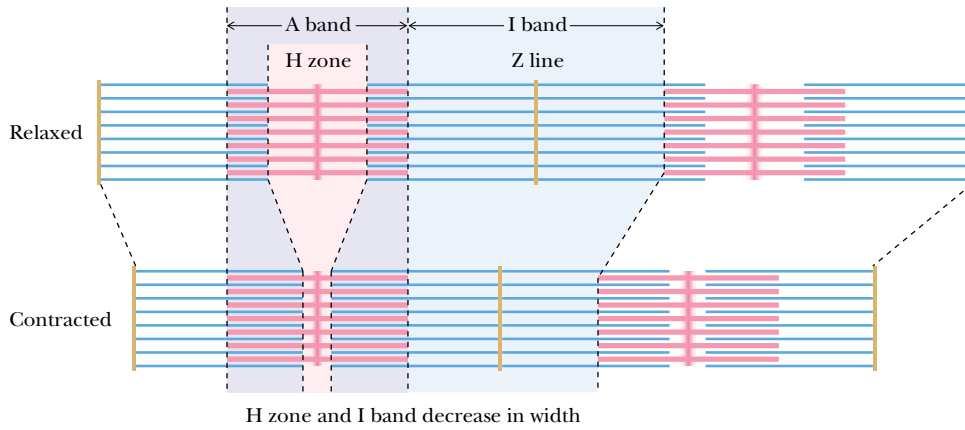
FIGURE 17.22 • The sliding filament model of skeletal muscle contraction. The decrease in sarcomere length is due to decreases in the width of the I band and H zone, with no change in the width of the A band. These observations mean that the lengths of both the thick and thin filaments do not change during contraction. Rather, the thick and thin filaments slide along one another.

directional character. The organization of the thin and thick filaments in the sarcomere takes particular advantage of this directional character. Actin filaments always extend outward from the Z lines in a uniform manner. Thus, between any two Z lines, the two sets of actin filaments point in opposing directions. The myosin thick filaments, on the other hand, also assemble in a directional manner. The polarity of myosin thick filaments reverses at the M disk. The nature of this reversal is not well understood, but presumably involves structural constraints provided by proteins in the M disk, such as the M protein and myomesin described above. The reversal of polarity at the M disk means that actin filaments on either side of the M disk are pulled toward the M disk during contraction by the sliding of the myosin heads, causing net shortening of the sarcomere.

Albert Szent-Györgyi's Discovery of the Effects of Actin on Myosin

The molecular events of contraction are powered by the ATPase activity of myosin. Much of our present understanding of this reaction and its dependence on actin can be traced to several key discoveries by Albert Szent-Györgyi at the University of Szeged in Hungary in the early 1940s. Szent-Györgyi showed that solution viscosity is dramatically increased when solutions of myosin and actin are mixed. Increased viscosity is a manifestation of the formation of an **actomyosin complex.**

𝒜 **D E E P E R   L O O K**

Viscous Solutions Reflect Long-Range Molecular Interactions

High viscosity in an aqueous solution is a sign of long-range molecular interactions, defined as interactions that extend through and connect many molecules. Concentrated sugar solutions (molasses, for example) are viscous because of the extensive hydrogen-bonding networks established by the multiple hydroxyl groups of sugar molecules. Solutions of DNA are highly viscous because isolated DNA fibers are extremely long (often in the millimeter size range) and highly hydrated. As Szent-Györgyi discovered, the extensive aggregates formed by myosin and actin also produce highly viscous solutions.

Szent-Györgyi further showed that the viscosity of an actomyosin solution was lowered by the addition of ATP, indicating that ATP decreases myosin's affinity for actin. Kinetic studies demonstrated that myosin ATPase activity was increased substantially by actin. (For this reason, Szent-Györgyi gave the name **actin** to the thin filament protein.) The ATPase turnover number of pure myosin is 0.05/sec. In the presence of actin, however, the turnover number increases to about 10/sec, a number more like that of intact muscle fibers.

The specific effect of actin on myosin ATPase becomes apparent if the *product release* steps of the reaction are carefully compared. In the absence of actin, the addition of ATP to myosin produces a rapid release of H^+, one of the products of the ATPase reaction:

$$ATP^{4-} + H_2O \longrightarrow ADP^{3-} + P_i^{2-} + H^+$$
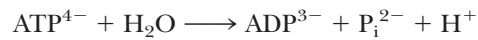
However, release of ADP and P_i from myosin is much slower. Actin activates myosin ATPase activity by stimulating the release of P_i and then ADP. Product release is followed by the binding of a new ATP to the actomyosin complex, which causes actomyosin to dissociate into free actin and myosin. The cycle of ATP hydrolysis then repeats, as shown in Figure 17.23a. The crucial point of this model is that *ATP hydrolysis and the association and dissociation of actin and myosin are coupled.* It is this coupling that enables ATP hydrolysis to power muscle contraction.

The Coupling Mechanism: ATP Hydrolysis Drives Conformation Changes in the Myosin Heads

The only remaining piece of the puzzle is this: How does the close coupling of actin-myosin binding and ATP hydrolysis result in the shortening of myofibrils? Put another way, how are the model for ATP hydrolysis and the sliding filament model related? The answer to this puzzle is shown in Figure 17.23b. The free energy of ATP hydrolysis is translated into a conformation change in the myosin head, so that dissociation of myosin and actin, hydrolysis of ATP, and rebinding of myosin and actin occur with stepwise movement of the myosin S1 head along the actin filament. The conformation change in the myosin head is driven by the hydrolysis of ATP.

As shown in the cycle in Figure 17.23a, the myosin heads—with the hydrolysis products ADP and P_i bound—are mainly dissociated from the actin filaments in resting muscle. When the signal to contract is presented (see following discussion), the myosin heads move out from the thick filaments to bind to actin on the thin filaments (Step 1). Binding to actin stimulates the release of phosphate, and this is followed by the crucial conformational change by the S1 myosin heads—the so-called **power stroke**—and ADP dissociation. In this step (Step 2), the thick filaments *move* along the thin filaments as the myosin heads relax to a lower energy conformation. In the power stroke, the myosin heads tilt by approximately 45 degrees and the conformational energy of the myosin heads is lowered by about 29 kJ/mol. This moves the thick filament approximately 10 nm along the thin filament (Step 3). Subsequent binding (Step 4) and hydrolysis (Step 5) of ATP cause dissociation of the heads from the thin filaments and also cause the myosin heads to shift back to their high-energy conformation with the heads' long axis nearly perpendicular to the long axis of the thick filaments. The heads may then begin another cycle by binding to actin filaments. This cycle is repeated at rates up to 5/sec in a typical skeletal muscle contraction. The conformational changes occurring in this cycle are the secret of the energy coupling that allows ATP binding and hydrolysis to drive muscle contraction.

The conformation change in the power stroke has been studied in two ways: (1) cryoelectron microscopy together with computerized image analysis

(a)

Actin

Myosin

ADP
P

H_2O ⑤

Conformation change-
cocking of the
myosin head

① Formation of
crossbridge

Crossbridge — ADP
P

ATP

ATP binding causes
dissociation of
myosin from actin

④

②

Low-energy conformation
of the myosin head

Power stroke

ADP and P_i
are released

ADP +
P

③

(b)

Actin filament
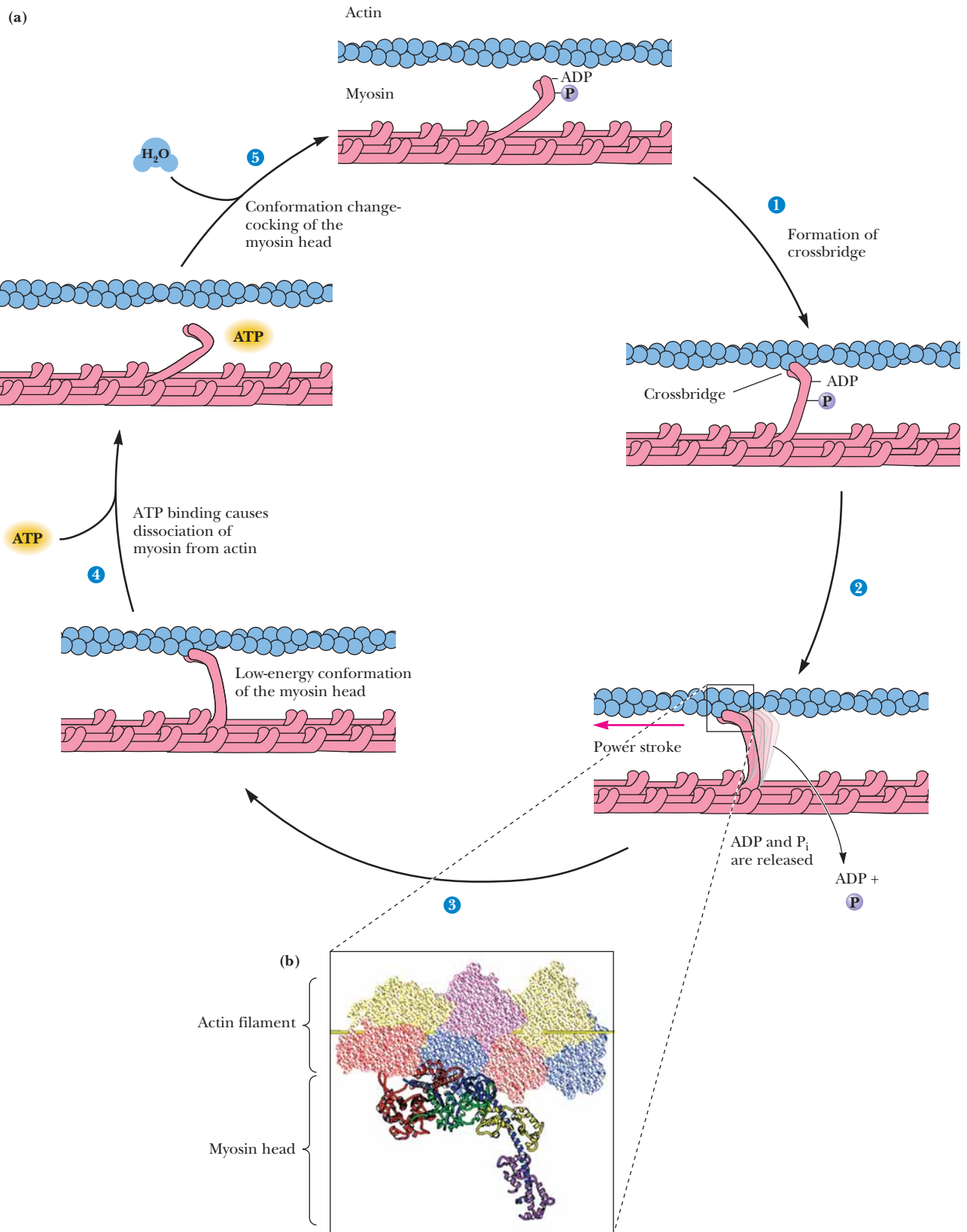
Myosin head

FIGURE 17.23 • The mechanism of skeletal muscle contraction. The free energy of ATP
hydrolysis drives a conformational change in the myosin head, resulting in net movement
of the myosin heads along the actin filament. (*Inset*) A ribbon and space-filling representa-
tion of the actin–myosin interaction. (*S1 myosin image courtesy of Ivan Rayment and Hazel M. Holden,
University of Wisconsin, Madison.*)

has yielded low-resolution images of S1-decorated actin in the presence and absence of MgADP (corresponding approximately to the states before and after the power stroke), and (2) feedback-enhanced laser optical trapping experiments have measured the movements and forces exerted during single turnovers of single myosin molecules along an actin filament. The images of myosin, when compared with the X-ray crystal structure of myosin S1, show that the long α-helix of S1 that binds the light chains (ELC and RLC) may behave as a lever arm, and that this arm swings through an arc of 23 degrees upon release of ADP. (A glycine residue at position 770 in the S1 myosin head lies at the N-terminal end of this helix/lever arm and may act as a hinge.) *This results in a 3.5-nm (35-Å) movement of the last myosin heavy chain residue of the X-ray structure in a direction nearly parallel to the actin filament.* These two imaging "snapshots" of the myosin S1 conformation may represent only part of the working power stroke of the contraction cycle, and the total movement of a myosin head with respect to the apposed actin filament may thus be more than 3.5 nm.

CRITICAL DEVELOPMENTS IN BIOCHEMISTRY

Molecular "Tweezers" of Light Take the Measure of a Muscle Fiber's Force

The optical trapping experiment involves the attachment of myosin molecules to silica beads that are immobilized on a microscope coverslip (see figure). Actin filaments are then prepared such that a polystyrene bead is attached to each end of the filament. These beads can be "caught" and held in place in solution by a pair of "optical traps"—two high-intensity infrared laser beams, one focused on the polystyrene bead at one end of the actin filament and the other focused on the bead at the other end of the actin filament. The force acting on each bead in such a trap is proportional to the position of the bead in the "trap," so that displacement and forces acting on the bead (and thus on the actin filament) can both be measured. When the "trapped" actin filament is brought close to the silica bead, one or a few myosin molecules may interact with sites on the actin, and ATP-induced interactions of individual myosin molecules with the trapped actin filament can be measured and quantitated. Such optical trapping experiments have shown that *a single cycle or turnover of a single myosin molecule along an actin filament involves an average movement of 4 to 11 nm (40–110 Å) and generates an average force of 1.7 to 4×10^{-12} newton (1.7–4 piconewtons (pN)).*

The magnitudes of the movements observed in the optical trapping experiments are consistent with the movements predicted by the cryoelectron microscopy imaging data. Can the movements and forces detected in a single contraction cycle by optical trapping also be related to the energy available from hydrolysis of a single ATP molecule? The energy required for a contraction cycle is defined by the "work" accomplished by contraction, and work (w) is defined as force (F) times distance (d):

$$w = F \cdot d$$

For a movement of 4 nm against a force of 1.7 pN, we have

$$w = (1.7 \text{ pN}) \cdot (4 \text{ nm}) = 0.68 \times 10^{-20} \text{ J}$$

For a movement of 11 nm against a force of 4 pN, the energy requirement is larger:

$$w = (4 \text{ pN}) \cdot (11 \text{ nm}) = 4.4 \times 10^{-20} \text{ J}$$

If the cellular free energy of hydrolysis of ATP is taken as −50 kJ/mol, the free energy available from the hydrolysis of a single ATP molecule is

$$\Delta G = (-50 \text{ kJ/mol})/6.02 \times 10^{23} \text{ molecules/mol} = 8.3 \times 10^{-20} \text{ J}$$

Thus, *the free energy of hydrolysis of a single ATP molecule is sufficient to drive the observed movements against the forces that have been measured.*
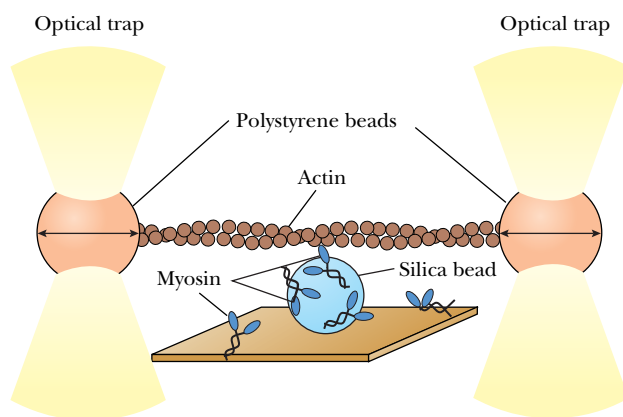
Movements of single myosin molecules along an actin filament can be measured by means of an optical trap consisting of laser beams focused on polystyrene beads attached to the ends of actin molecules. *(Adapted from Finer et al., 1994. Nature **368**:113 – 119. See also Block, 1995. Nature **378**:132–133.)*

Control of the Contraction–Relaxation Cycle by Calcium Channels and Pumps

The trigger for all muscle contraction is an increase in Ca^{2+} concentration in the vicinity of the muscle fibers of skeletal muscle or the myocytes of cardiac and smooth muscle. In all these cases, this increase in Ca^{2+} is due to the flow of Ca^{2+} through **calcium channels** (Figure 17.24). A muscle contraction ends when the Ca^{2+} concentration is reduced by specific calcium pumps (such as the SR Ca^{2+}-ATPase, Chapter 10). The sarcoplasmic reticulum, t-tubule, and sarcolemmal membranes all contain Ca^{2+} channels. As we shall see, the Ca^{2+} channels of the SR function together with the t-tubules in a remarkable coupled process.

Ca^{2+} release in skeletal and heart muscle has been characterized through the use of specific antagonist molecules that block Ca^{2+} channel activity. The **dihydropyridine (DHP) receptors** of t-tubules, for example, are blocked by **dihydropyridine** derivatives, such as **nifedipine** (Figure 17.25). The purified DHP receptor of heart muscle can be incorporated into liposomes, whereupon it shows calcium channel activity. The channel displays voltage-dependent gating and is selective for divalent cations over monovalent cations. *Thus, the heart muscle DHP receptor is a voltage-dependent Ca^{2+} channel.* Other evidence suggests that the skeletal muscle DHP receptor is a voltage-sensing protein; it presumably undergoes voltage-dependent conformation changes.

The DHP receptor from t-tubules consists of five different polypeptides, designated α_1 (150 to 173 kD), α_2 (120 to 150 kD), β (50 to 65 kD), γ (30 to 35 kD), and δ (22 to 27 kD). The α_2- and δ-subunits are linked by a disulfide bond. The α_1, α_2-δ, β, and γ stoichiometry is 1:1:1:1. The α_2-subunit is glycosylated, but α_1 is not. α_1 is homologous with the α-subunit of the voltage-sensitive sodium channel (Chapter 34). The sequence of α_1 contains four internal sequence repeats, each containing six transmembrane helices, one of which is positively charged and is believed to be a voltage sensor (Figure 17.26). The loop between helices 5 and 6 contributes to the pore. These six segments share many similarities with the corresponding segments of the sodium channel. The α_1-subunit of the DHP receptor in heart muscle is implicated in channel formation and voltage-dependent gating.

The Ca^{2+}-release channel from the terminal cisternae of sarcoplasmic reticulum has been identified by virtue of its high affinity for **ryanodine,** a toxic alkaloid (Figure 17.25). The purified receptor consists of oligomers, containing four or more subunits of a single large polypeptide (565 kD). Electron microscopy reveals that the purified ryanodine receptor (Figure 17.27) is in fact the **foot structure** observed in native muscle tissue. Image reconstructions reveal that the receptor is a square structure with fourfold symmetry, containing a central pore with four radially extending canals (Figure 17.28). These
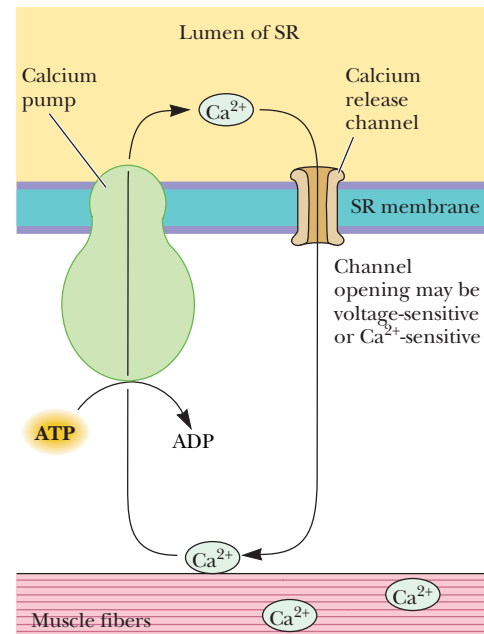
FIGURE 17.24 • Ca^{2+} is the trigger signal for muscle contraction. Release of Ca^{2+} through voltage- or Ca^{2+}-sensitive channels activates contraction. Ca^{2+} pumps induce relaxation by reducing the concentration of Ca^{2+} available to the muscle fibers.

Nifedipine   **Ryanodine**
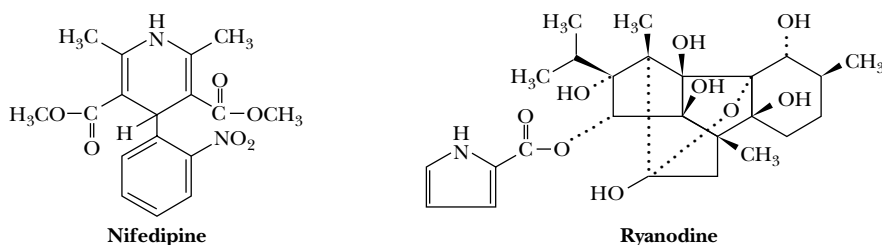
FIGURE 17.25 • The structures of nifedipine and ryanodine. Nifedipine binds with high affinity to the Ca^{2+}-release channels of t-tubules. Ryanodine binds with high affinity to the Ca^{2+} channels of SR terminal cisternae.

DHP-sensitive calcium channel
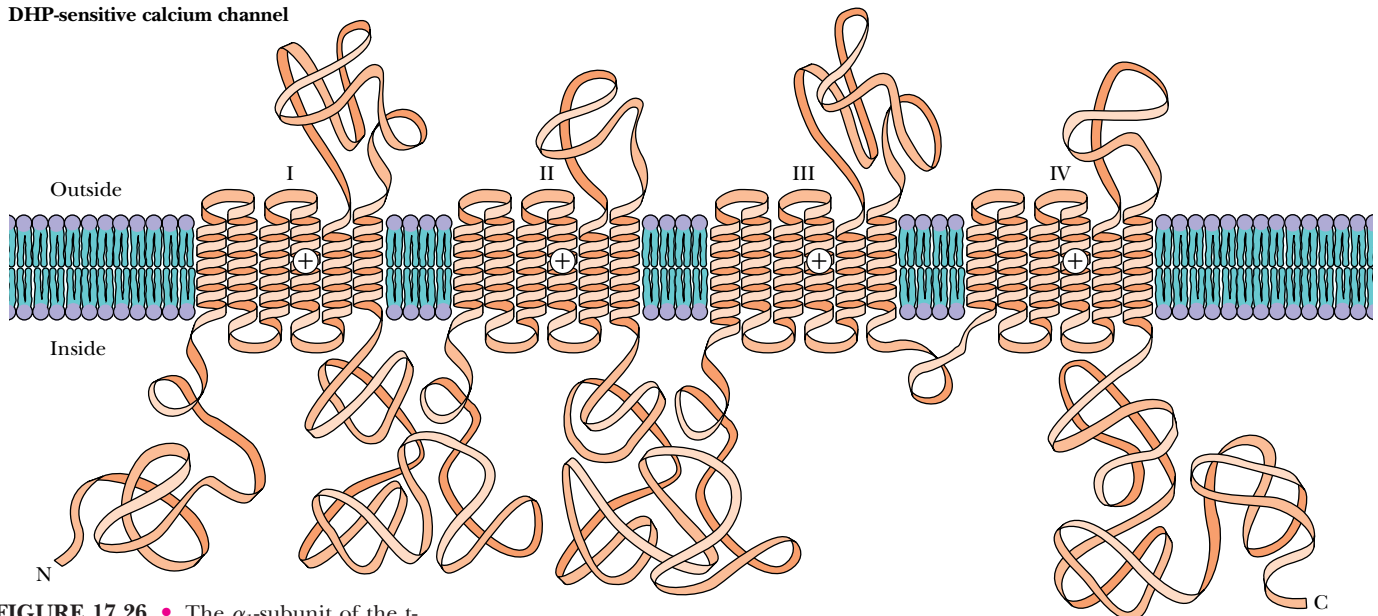
FIGURE 17.26 • The α_1-subunit of the t-tubule Ca^{2+} channel/DHP receptor contains six peptide segments that may associate to form the Ca^{2+} channel. This Ca^{2+} channel polypeptide is homologous with the voltage-sensitive Na^+ channel of neuronal tissue.
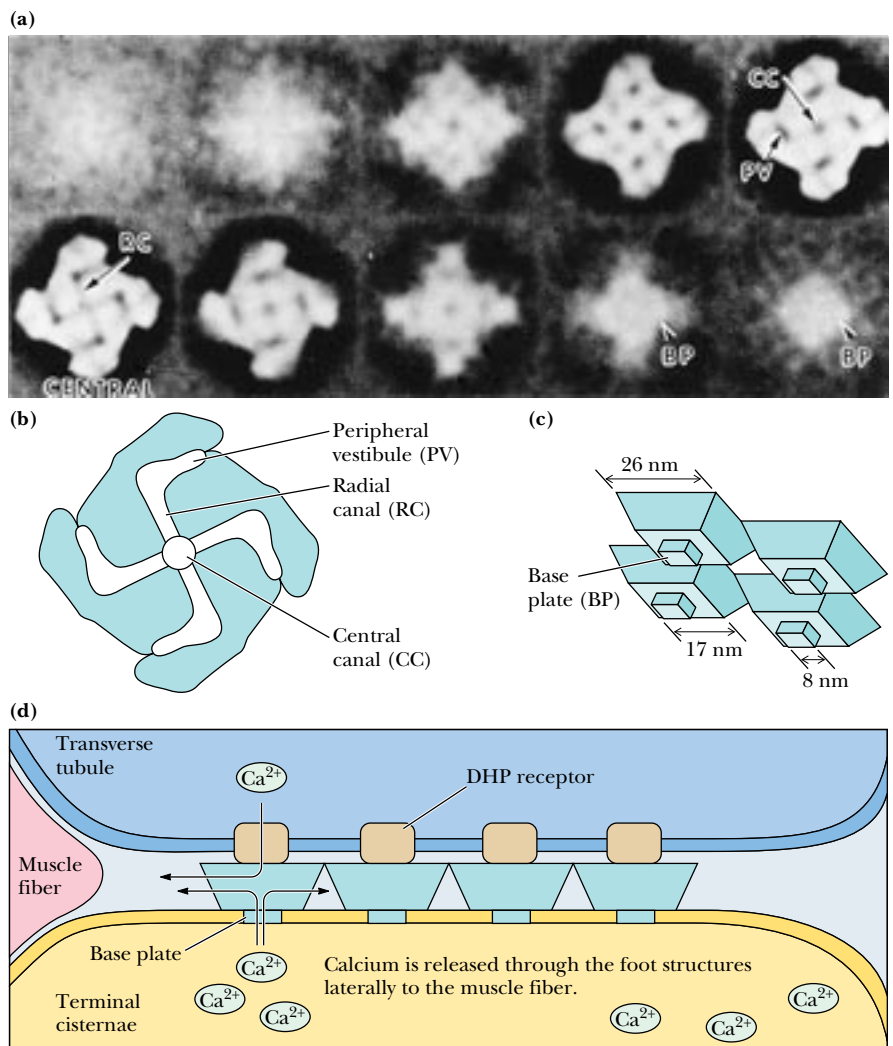
FIGURE 17.27 • (a) Electron micrograph images of foot structures of terminal cisternae. (b, c) Foot structures appear as trapezoids and diamonds on the surface of the membrane. The central canal (CC), radial canals (RC), and peripheral vestibules (PV) are indicated. (d) The relationship between the foot structures, t-tubule, terminal cisternae, and muscle fiber. *(Photo courtesy of Sidney Fleischer, Vanderbilt University)*

FIGURE 17.28 • Image reconstructions of the junctional channel complex of a foot structure. *(Photo courtesy of Sidney Fleischer, Vanderbilt University)*

radial canals each extend to openings in the periphery of the structure and are therefore contiguous with the myoplasm.

So how do the foot structures effect the release of Ca^{2+} from the terminal cisternae of the SR? The feet that join the t-tubules and the terminal cisternae of the SR are approximately 16 nm thick. The feet apparently function by first sensing either a voltage-dependent conformation change (skeletal muscle) or the transport of Ca^{2+} across the voltage-sensitive Ca^{2+} channel (heart muscle) of the t-tubule and then facilitating the release of large amounts of Ca^{2+} through the foot structure from the SR. The reconstructed image (Figure 17.28) for the foot structure suggests a possible pathway for Ca^{2+} transport from the lumen of the SR to the myoplasm via the ryanodine receptor. A Ca^{2+}- or voltage-dependent conformation change may serve to gate open the central canal of the foot structure. On entering the central canal, calcium ions move outward through the radial canals to the outer vestibule regions and into the myoplasm adjacent to the triad junctions, where binding to the muscle fibers induces contraction.

Regulation of Contraction by Ca^{2+}

Early in this chapter, the importance of Ca^{2+} ion as the triggering signal for muscle contraction was described. Ca^{2+} is the intermediary signal that allows striated muscle to respond to motor nerve impulses (Figure 17.24). The importance of Ca^{2+} as a contraction signal was understood in the 1940s, but it remained for Setsuro Ebashi, a pioneer of muscle research, to show in the early 1960s that the Ca^{2+} signal is correctly interpreted by muscle only when tropomyosin and the troponins are present. Specifically, actomyosin prepared from pure preparations of actin and myosin (thus containing no tropomyosin and troponins) was observed to contract when ATP was added, even in the absence of Ca^{2+}. However, actomyosin prepared directly from whole muscle would contract in the presence of ATP only when Ca^{2+} was added. Clearly the muscle extracts contained a factor that conferred normal Ca^{2+} sensitivity to actomyosin. The factor turned out to be the tropomyosin–troponin complex.

Actin thin filaments consist of actin, tropomyosin, and the troponins in a 7:1:1 ratio (Figure 17.15). Each tropomyosin molecule spans seven actin molecules, lying along the thin filament groove, between pairs of actin monomers. As shown in a cross-section view in Figure 17.29, in the absence of Ca^{2+}, troponin I is thought to interact directly with actin to prevent the interaction of actin with myosin S1 heads. Troponin I and troponin T interact with tropomyosin to keep tropomyosin away from the groove between adjacent actin
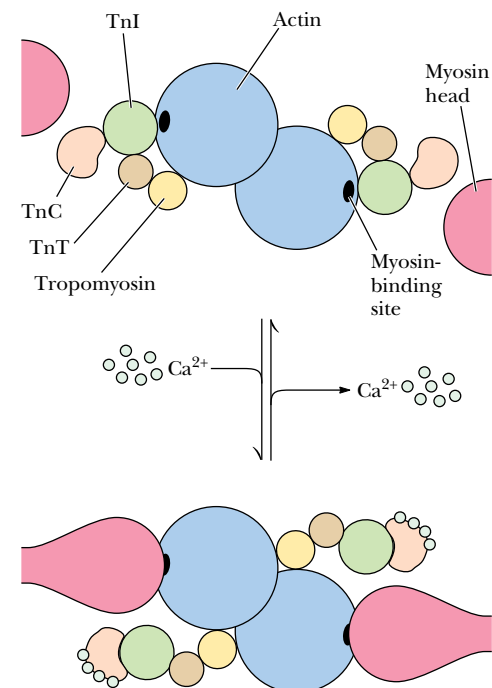
FIGURE 17.29 • A drawing of the thick and thin filaments of skeletal muscle in cross-section showing the changes that are postulated to occur when Ca^{2+} binds to troponin C.

monomers. However, the binding of Ca^{2+} ions to troponin C appears to increase the binding of troponin C to troponin I, simultaneously decreasing the interaction of troponin I with actin. As a result, tropomyosin slides deeper into the actin-thin filament groove, exposing myosin-binding sites on actin, and initiating the muscle contraction cycle (Figure 17.23). Because the troponin complexes can interact only with every seventh actin in the thin filament, the conformational changes that expose myosin-binding sites on actin may well be cooperative. Binding of an S1 head to an actin may displace tropomyosin and the troponin complex from myosin-binding sites on adjacent actin subunits.

The Interaction of Ca²⁺ with Troponin C

There are four Ca^{2+}-binding sites on troponin C—two high-affinity sites on the carboxy-terminal end of the molecule, labeled III and IV in Figure 17.30, and two low-affinity sites on the amino-terminal end, labeled I and II. Ca^{2+} binding to sites III and IV is sufficiently strong ($K_D = 0.1 \ \mu M$) that these sites are presumed to be filled under resting conditions. Sites I and II, however, where the K_D is approximately 10 μM, are empty in resting muscle. The rise of Ca^{2+} levels when contraction is signaled leads to the filling of sites I and II, causing a conformation change in the amino-terminal domain of TnC. This conformational change apparently facilitates a more intimate binding of TnI to TnC that involves the C helix, and also possibly the E helix of TnC. The increased interaction between TnI and TnC results in a decreased interaction between TnI and actin.

FIGURE 17.30 • (a) A ribbon diagram and (b) a molecular graphic showing two slightly different views of the structure of troponin C. Note the long α-helical domain connecting the N-terminal and C-terminal lobes of the molecule.
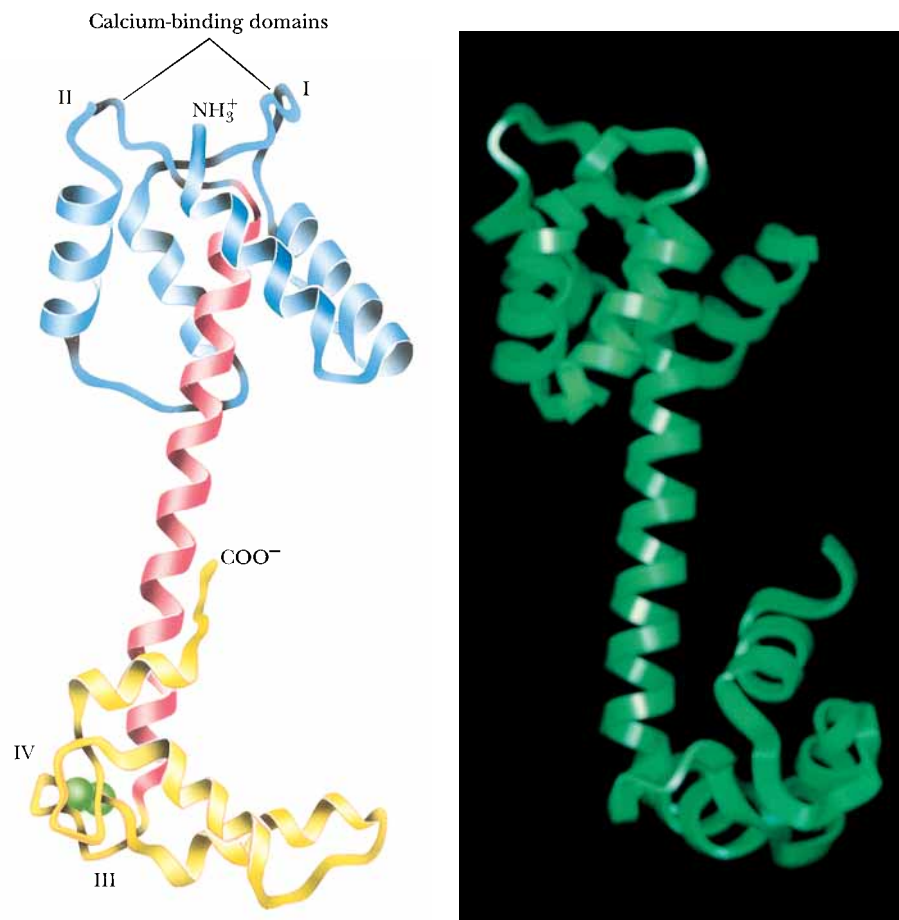
The Structure of Cardiac and Smooth Muscle

The structure of heart myocytes is different from that of skeletal muscle fibers. Heart myocytes are approximately 50 to 100 μm long and 10 to 20 μm in diameter. The t-tubules found in heart tissue have a fivefold larger diameter than those of skeletal muscle. The number of t-tubules found in cardiac muscle differs from species to species. Terminal cisternae of mammalian cardiac muscle can associate with other cellular elements to form **dyads** as well as triads. The association of terminal cisternae with the sarcolemma membrane in a dyad structure is called a **peripheral coupling.** The terminal cisternae may also form dyad structures with t-tubules that are called **internal couplings** (Figure 17.31). As with skeletal muscle, foot structures form the connection between the terminal cisternae and t-tubule membranes.

In higher animals, large percentages of the terminal cisternae of cardiac muscle are not associated with t-tubules at all. For SR of this type, Ca^{2+} release must occur by a different mechanism from that found in skeletal muscle. In this case, it appears that Ca^{2+} leaking through sarcolemmal Ca^{2+} channels can trigger the release of even more Ca^{2+} from the SR. This latter process is called **Ca^{2+}-induced Ca^{2+} release** (abbreviated **CICR**).

The Structure of Smooth Muscle Myocytes

The myocytes of smooth muscle are approximately 100 to 500 μm in length and only 2 to 6 μm in diameter. Smooth muscle contains very few t-tubules and much less SR than skeletal muscle. The Ca^{2+} that stimulates contraction in smooth muscle cells is predominantly extracellular in origin. This Ca^{2+} enters the cell through Ca^{2+} channels in the sarcolemmal membrane that can be opened by electrical stimulation, or by the binding of hormones or drugs. The contraction response time of smooth muscle cells is very slow compared with that of skeletal and cardiac muscle.

The Mechanism of Smooth Muscle Contraction

Vertebrate organisms employ smooth muscle myocytes for long, slow, and involuntary contractions in various organs, including large blood vessels; intestinal walls; and, in the female, the uterus. Smooth muscle contains no troponin complex; thin filaments consist only of actin and tropomyosin. Despite the absence of troponins, smooth muscle contraction *is* dependent on Ca^{2+}, which activates **myosin light chain kinase (MLCK),** an enzyme that phosphorylates LC2, the regulatory light chain of myosin. Contraction of smooth muscle is initiated by phosphorylation of LC2, and dephosphorylation causes relaxation of smooth muscle tissue.
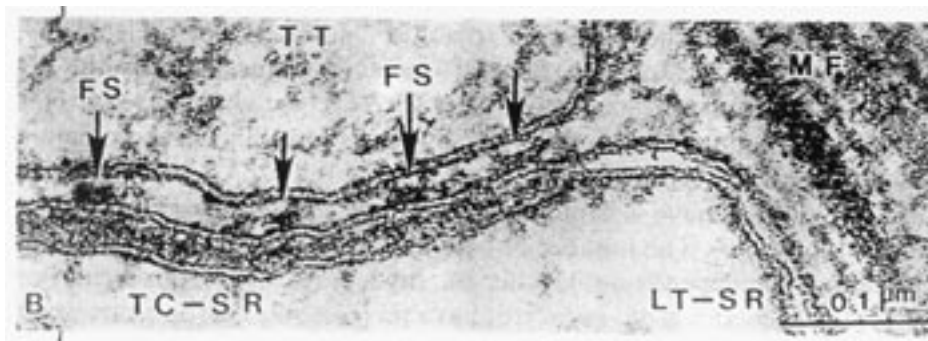
FIGURE 17.31 • Electron micrograph of a dog heart muscle. The terminal cisterna of the SR (TC-SR) is associated with the t-tubule (TT) by means of foot structures (FS), forming a dyad junction. MF indicates the location of myofilaments. LT-SR signifies the longitudinal tubule of the SR. *(From Fleischer, S., and Inui, M., 1989. Annual Review of Biophysics and Biophysical Chemistry* **18:***333–364.)*
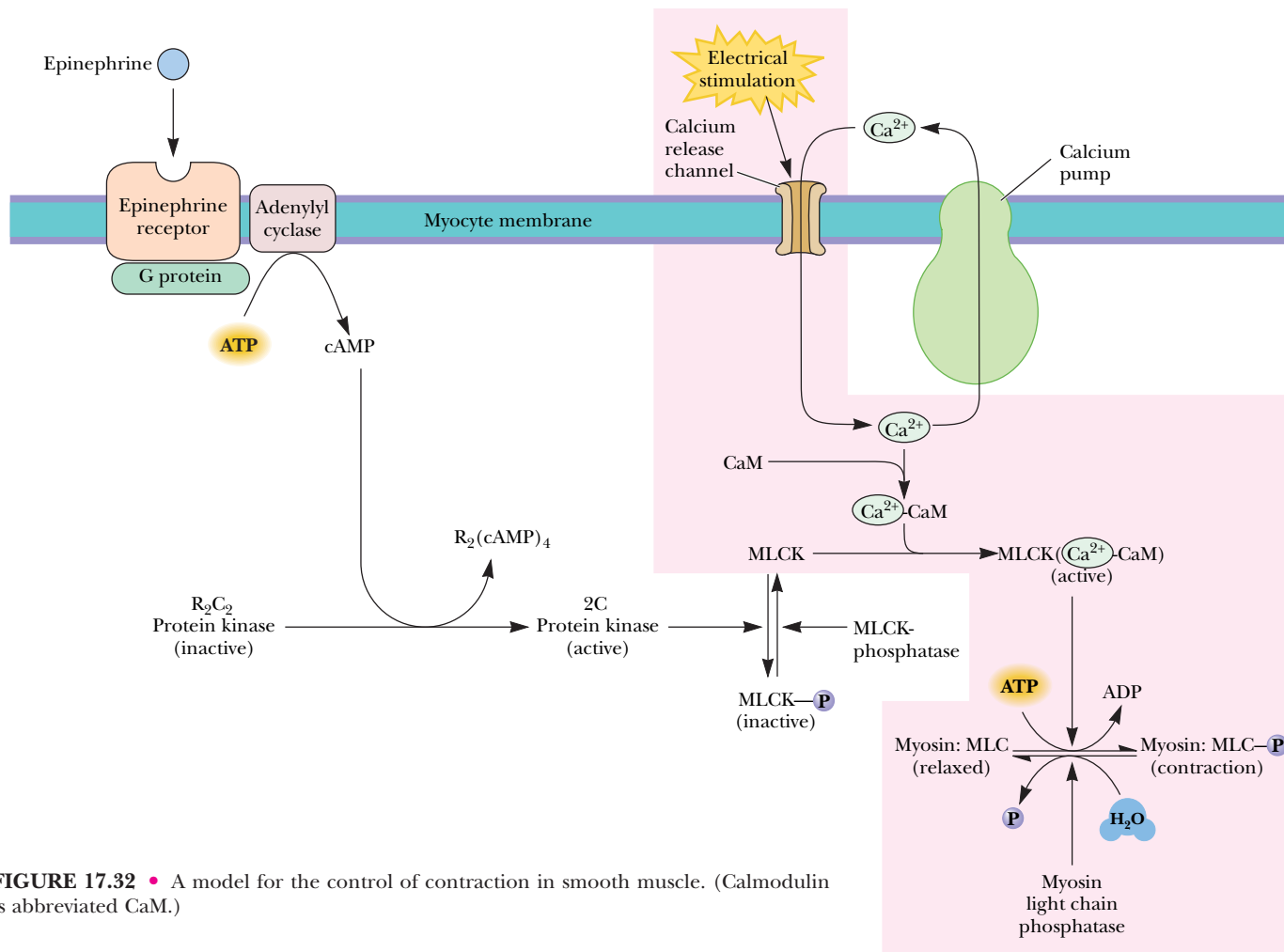
FIGURE 17.32 • A model for the control of contraction in smooth muscle. (Calmodulin is abbreviated CaM.)

The mechanism of this contraction process is shown in Figure 17.32. Smooth muscle myocytes have a resting $[Ca^{2+}]$ of approximately 0.1 μM. Electrical stimulation (by the autonomic or involuntary nervous system) opens Ca^{2+} channels in the sarcolemmal membrane, allowing $[Ca^{2+}]$ to rise to about 10 μM, a concentration at which Ca^{2+} binds readily to **calmodulin** (see Chapter 34). Binding of the Ca^{2+}-calmodulin complex to MLCK activates the kinase reaction, phosphorylating LC2 and stimulating smooth muscle contraction. Export of Ca^{2+} by the plasma membrane Ca^{2+}-ATPase returns Ca^{2+} to its resting level, deactivating MLCK. Smooth muscle relaxation then occurs through the action of **myosin light chain phosphatase,** which dephosphorylates LC2. This reaction is relatively slow, and smooth muscle contractions are typically more sustained and dissipate more slowly than those of striated muscle.

Smooth muscle contractions are subject to the actions of hormones and related agents. As shown in Figure 17.32, binding of the hormone **epinephrine** to smooth muscle receptors activates an intracellular **adenylyl cyclase** reaction that produces cyclic AMP (cAMP). The cAMP serves to activate a protein kinase that phosphorylates the myosin light chain kinase. The phosphorylated MLCK has a lower affinity for the Ca^{2+}-calmodulin complex and thus is physiologically inactive. Reversal of this inactivation occurs via **myosin light chain kinase phosphatase.**

ℋUMAN BIOCHEMISTRY

Smooth Muscle Effectors Are Useful Drugs

The action of epinephrine and related agents forms the basis of therapeutic control of smooth muscle contraction. Breathing disorders, including asthma and various allergies, can result from excessive contraction of bronchial smooth muscle tissue. Treatment with epinephrine, whether by tablets or aerosol inhalation, inhibits MLCK and relaxes bronchial muscle tissue. More specific **bronchodilators,** such as **albuterol** (see figure), act more selec-

tively on the lungs and avoid the undesirable side effects of epinephrine on the heart. Albuterol is also used to prevent premature labor in pregnant women, owing to its relaxing effect on uterine smooth muscle. Conversely, **oxytocin,** known also as **pitocin,** stimulates contraction of uterine smooth muscle. This natural secretion of the pituitary gland is often administered to induce labor.

Albuterol

$H_3\overset{+}{N}$ — Gly — Leu — Pro — Cys — Asn — Gln — Ile — Tyr — Cys — COO⁻
S — S
Oxytocin (Pitocin)
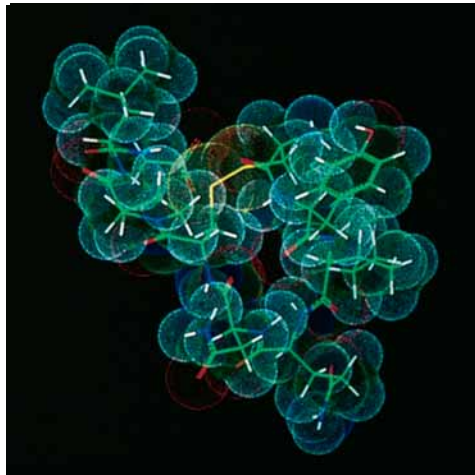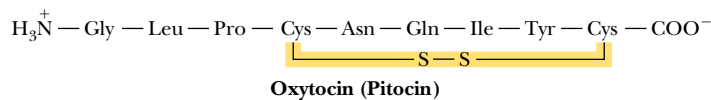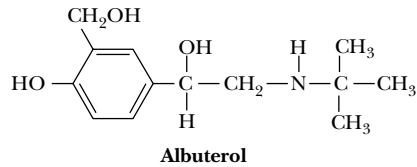
The structure of oxytocin.

17.4 • A Proton Gradient Drives the Rotation of Bacterial Flagella

Bacterial cells swim and move by rotating their flagella. The flagella of *Escherichia coli* are helical filaments about 10,000 nm (10 μm) in length and 15 nm in diameter. The direction of rotation of these filaments affects the movements of the cell. When the half-dozen filaments on the surface of the bacterial cell rotate in a counterclockwise direction, they twist and bundle together and rotate in a concerted fashion, propelling the cell through the medium. (On the other hand, clockwise-rotating flagella cannot bundle together and under such conditions the cell merely tumbles and moves erratically.)

Filament

Hook

Rod

S ring

Periplasmic space

Plasma membrane

Cytosol

M ring

H+

Mot A

H+

Mot B

(a)

Channel complex

Elastic linkage to cell wall

Outside channel

Inside channel

Proton-accepting site on M-ring

i   o

(b)

Proton to inside

Proton from outside

i   o

(c)

Restoring force, f

|←d→| i   o
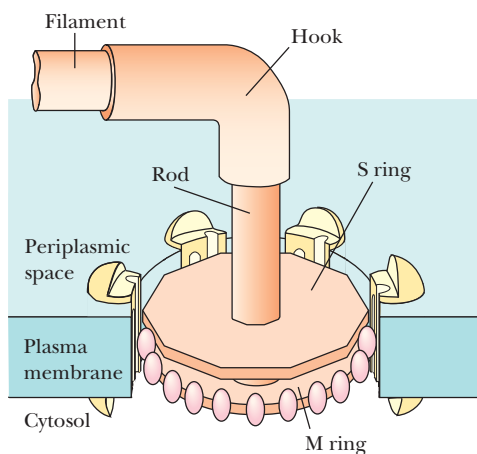
FIGURE 17.33 • A model of the flagellar motor assembly of *Escherichia coli*. The M ring carries an array of about 100 motB proteins at its periphery. These juxtapose with motA proteins in the protein complex that surrounds the ring assembly. Motion of protons through the motA/motB complexes drives the rotation of the rings and the associated rod and helical filament.
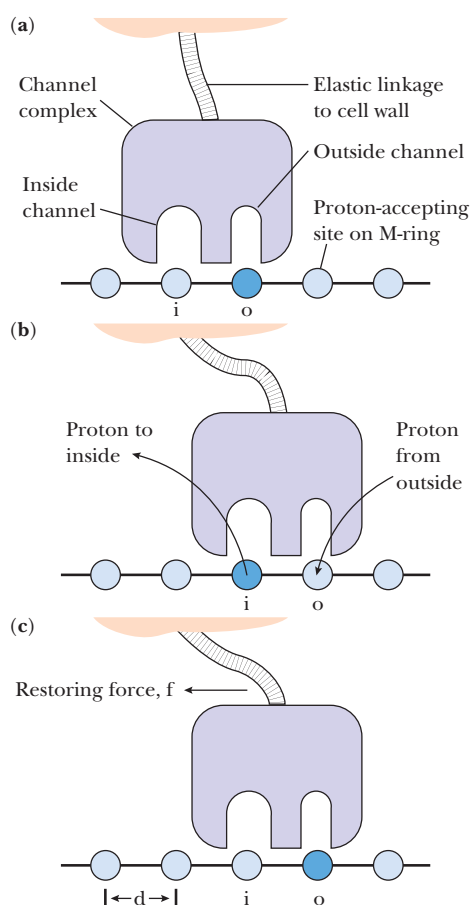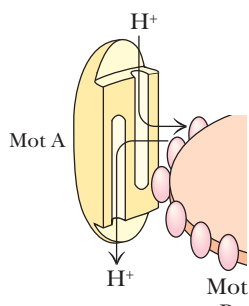
The rotations of bacterial flagellar filaments are the result of the rotation of motor protein complexes in the bacterial plasma membrane. The flagellar motor consists of at least two rings (including the M ring and the S ring) with diameters of about 25 nm assembled around and connected rigidly to a rod attached in turn to the helical filament (Figure 17.33). The rings are surrounded by a circular array of membrane proteins. In all, at least 40 genes appear to code for proteins involved in this magnificent assembly. One of these, the motB protein, lies on the edge of the M ring, where it interacts with the motA protein, located in the membrane protein array and facing the M ring.

In contrast to the many other motor proteins described in this chapter, a proton gradient, not ATP hydrolysis, drives the flagellar motor. The concentration of protons, $[H^+]$, outside the cell is typically higher than that inside the cell. Thus, there is a thermodynamic tendency for protons to move into the cell. The motA and motB proteins together form a proton shuttling device that is coupled to motion of the motor disks. Proton movement into the cell through this protein complex or "channel" drives the rotation of the flagellar motor. A model for this coupling has been proposed by Howard Berg and his coworkers (Figure 17.34). In this model, the motB proteins possess proton exchanging sites—for example, carboxyl groups on aspartate or glutamate residues or imidazole moieties on histidine residues. The motA proteins, on the other hand, possess a pair of "half-channels," with one half-channel facing the inside of the cell and the other facing the outside. In Berg's model, the outside edges of the motA channel protein cannot move past a proton-exchanging site on motB when that site has a proton bound, and the center of the channel protein cannot move past an exchange site when that site is empty. As shown in Figure 17.34, these constraints lead to coupling between proton translocation and rotation of the flagellar filament. For example, imagine that a proton has entered the outside channel of motA and is bound to an exchange site on motB (Figure 17.34a). An oscillation by motA, linked elastically to the cell wall, can then position the inside channel over the proton at the exchange site (Figure 17.34b), whereupon the proton can travel through the inside channel and into the cell, while another proton travels up the outside channel to bind to an adjacent exchange site. The restoring force acting on the channel protein then pulls the motA/motB complex to the left as shown (Figure 17.34c), leading to counterclockwise rotation of the disk, rod, and helical filament. The flagellar motor is driven entirely by the proton gradient. Thus, a reversal of the proton gradient (which would occur, for example, if the external medium became alkaline) would drive the flagellar filaments in a clockwise direction. Extending this picture of a single motA/motB complex to the

FIGURE 17.34 • Howard Berg's model for coupling between transmembrane proton flow and rotation of the flagellar motor. A proton moves through an outside channel to bind to an exchange site on the M ring. When the channel protein slides one step around the ring, the proton is released and flows through an inside channel and into the cell, while another proton flows into the outside channel to bind to an adjacent exchange site. When the motA channel protein returns to its original position under an elastic restoring force, the associated motB protein moves with it, causing a counterclockwise rotation of the ring, rod, and helical filament. *(Adapted from Meister, M., Caplan, S. R., and Berg, H. C., 1989. Dynamics of a tightly coupled mechanism for flagellar rotation.* Biophysical Journal **55:**905–914)

whole motor disk array, one can imagine the torrent of protons that pass through the motor assembly to drive flagellar rotation at a typical speed of 100 rotations per second. Berg estimates that the M ring carries 100 motB proton-exchange sites, and various models predict that 800 to 1200 protons must flow through the complex during a single rotation of the flagellar filament!

PROBLEMS

1. The cheetah is generally regarded as nature's fastest mammal, but another amazing athlete in the animal kingdom (and almost as fast as the cheetah) is the pronghorn antelope, which roams the plains of Wyoming. Whereas the cheetah can maintain its top speed of 70 mph for only a few seconds, the pronghorn antelope can run at 60 mph for about an hour! (It is thought to have evolved to do so in order to elude now-extinct ancestral cheetahs that lived in North America.) What differences would you expect in the muscle structure and anatomy of pronghorn antelopes that could account for their remarkable speed and endurance?

2. An ATP analog, β,γ-methylene-ATP, in which a —CH_2— group replaces the oxygen atom between the β- and γ-phosphorus atoms, is a potent inhibitor of muscle contraction. At which step in the contraction cycle would you expect β,γ-methylene-ATP to block contraction?

3. ATP stores in muscle are augmented or supplemented by stores of phosphocreatine. During periods of contraction, phosphocreatine is hydrolyzed to drive the synthesis of needed ATP in the creatine kinase reaction:

$$\text{phosphocreatine} + \text{ADP} \rightleftharpoons \text{creatine} + \text{ATP}$$

Muscle cells contain two different isozymes of creatine kinase, one in the mitochondria and one in the sarcoplasm. Explain.

4. *Rigor* is a muscle condition in which muscle fibers, depleted of ATP and phosphocreatine, develop a state of extreme rigidity and cannot be easily extended. (In death, this state is called *rigor mortis,* the rigor of death.) From what you have learned about muscle contraction, explain the state of rigor in molecular terms.

5. Skeletal muscle can generate approximately 3 to 4 kg of tension or force per square centimeter of cross-sectional area. This number is roughly the same for all mammals. Because many human muscles have large cross-sectional areas, the force that these muscles can (and must) generate is prodigious. The gluteus maximus (on which you are probably sitting as you read this) can generate a tension of 1200 kg! Estimate the cross-sectional area of all of the muscles in your body and the total force that your skeletal muscles could generate if they all contracted at once.

FURTHER READING

Ahn, A. H., and Kunkel, L. M., 1993. The structural and functional diversity of dystrophin. *Nature Genetics* **3:**283–291.

Allen, B., and Walsh, M., 1994. The biochemical basis of the regulation of smooth-muscle contraction. *Trends in Biochemical Sciences* **19:**362–368.

Amos, L., 1985. Structure of muscle filaments studied by electron microscopy. *Annual Review of Biophysics and Biophysical Chemistry* **14:**291–313.

Astumian, R. D., and Bier, M., 1996. Mechanochemical coupling of the motion of molecular motors to ATP hydrolysis. *Biophysical Journal* **70:**637–653.

Berliner, E., Young, E., Anderson, K., et al., 1995. Failure of a single-headed kinesin to track parallel to microtubule protofilaments. *Nature* **373:**718–721.

Blake, D., Tinsley, J., Davies, K., et al., 1995. Coiled-coil regions in the carboxy-terminal domains of dystrophin and related proteins: Potentials for protein–protein interactions. *Trends in Biochemical Sciences* **20:**133–135.

Blanchard, A., Ohanian, V., and Critchley, D., 1989. The structure and function of α-actinin. *Journal of Muscle Research and Cell Motility* **10:**280–289.

Block, S. M., 1998. Kinesin: What gives? *Cell* **93:**5–8.

Bork, P., and Sudol, M., 1994. The WW domain: A signaling site in dystrophin. *Trends in Biochemical Sciences* **19:**531–533.

Boyer, P. D., 1997. The ATP synthase—A splendid molecular machine. *Annual Review of Biochemistry* **66:**717–749.

Cooke, R., 1995. The actomyosin engine. *The FASEB Journal* **9:**636–642.

Cooke, R., 1986. The mechanism of muscle contraction. *CRC Critical Reviews in Biochemistry* **21:**53–118.

Coppin, C. M., Finer, J. T., Spudich, J. A., and Vale, R. D., 1996. Detection of sub-8-nm movements of kinesin by high-resolution optical-trap microscopy. *Proceedings of the National Academy of Sciences* **93:**1913–1917.

Davison, M., and Critchley, D., 1988. α-Actinin and the DMD protein contain spectrin-like repeats. *Cell* **52:**159–160.

Davison, M., et al., 1989. Structural analysis of homologous repeated domains in α-actinin and spectrin. *International Journal of Biological Macromolecules* **11:**81–90.

DeRosier, D. J., 1998. The turn of the screw: The bacterial flagellar motor. *Cell* **93:**17–20.

Eden, D., Luu, B. Q., Zapata, D. J., et al., 1995. Solution structure of two molecular motor domains: Nonclaret disjunctional and kinesin. *Biophysical Journal* **68:**59S–64S.

Engel, A., 1997. A closer look at a molecular motor by atomic force microscopy. *Biophysical Journal* **72:**988.

Farah, C., and Reinach, F., 1995. The troponin complex and regulation of muscle contraction. *The FASEB Journal* **9:**755–767.

Finer, J. T., Simmons, R. M., and Spudich, J. A., 1994. Single myosin molecule mechanics: Piconewton forces and nanometer steps. *Nature* **368:**113–119.

Fisher, A., Smith, C., Thoden, J., et al., 1995. Structural studies of myosin:nucleotide complexes: A revised model for the molecular basis of muscle contraction. *Biophysical Journal* **68:**19S–26S.

Fisher, A., Smith, C., Thoden, J., et al., 1995. X-ray structures of the myosin motor domain of *Dictyostelium discoideum* complexed with MgADP·BeF$_x$ and MgADP·A1F$_4^-$. *Biochemistry* **34:**8960–8972.

Fleischer, S., and Inui, M., 1989. Biochemistry and biophysics of excitation–contraction coupling. *Annual Review of Biophysics and Biophysical Chemistry* **18:**333–364.

Funatsu, T., Harada, Y., Tokunaga, M., et al., 1995. Imaging of single fluorescent molecules and individual ATP turnovers by single myosin molecules in aqueous solution. *Nature* **374:**555–559.

Gilbert, S., Webb, M., Brune, M., and Johnson, K., 1995. Pathway of processive ATP hydrolysis by kinesin. *Nature* **373:**671–676.

Goldman, Y. E., 1998. Wag the tail: Structural dynamics of actomyosin. *Cell* **93:**1–4.

Gopal, D., Pavlov, D. I., Levitsky, D. I., et al., 1996. Chemomechanical transduction in the actomyosin molecular motor by 2′,3′-dideoxydidehydro-ATP and characterization of its interaction with myosin subfragment 1 in the presence and absence of actin. *Biochemistry* **35:**10149–10157.

Henningsen, U., and Schliwa, M., 1997. Reversal in the direction of movement of a molecular motor. *Nature* **389:**93–96.

Hirose, K., Lockhart, A., Cross, R., and Amos, L., 1995. Nucleotide-dependent angular change in kinesin motor domain bound to tubulin. *Nature* **376:**277–279.

Hoenger, A., Sablin, E., Vale, R., et al., 1995. Three-dimensional structure of a tubulin-motor-protein complex. *Nature* **376:**271–274.

Howard, J., 1996. The movement of kinesin along microtubules. *Annual Review of Physiology* **58:**703–729.

Kabsch, W., and Holmes, K., 1995. The actin fold. *The FASEB Journal* **9:**167–174.

Kabsch, W., et al., 1990. Atomic structure of the actin:DNase I complex. *Nature* **347:**37–43.

Kikkawa, J., Ishikawa, T., Wakabayashi, T., and Hirokawa, N., 1995. Three-dimensional structure of the kinesin head–microtubule complex. *Nature* **376:**274–277.

Kinosita, K., Jr., Yasuda, R., Noji, H., et al., 1998. F$_1$-ATPase: A rotary motor made of a single molecule. *Cell* **93:**21–24.

Koenig, M., and Kunkel, L., 1990. Detailed analysis of the repeat domain of dystrophin reveals four potential hinge segments that may confer flexibility. *Journal of Biological Chemistry* **265:**4560–4566.

Kull, F. J., Sablin, E. P., Lau, R., et al., 1996. Crystal structure of the kinesin motor domain reveals a structural similarity to myosin. *Nature* **380:**550–555.

Labeit, S., and Kolmerer, B., 1995. Titins: Giant proteins in charge of muscle ultrastructure and elasticity. *Science* **270:**293–296.

Lohman, T. M., Thorn, K., and Vale, R. D., 1998. Staying on track: Common features of DNA helicases and microtubule motors.. *Cell* **93:**9–12.

Löwe, J., and Amos, L., 1998. Crystal structure of the bacterial cell-division protein FtsZ. *Nature* **391:**203–206.

Macnab, R. M., and Parkinson, J. S., 1991. Genetic analysis of the bacterial flagellum. *Trends in Genetics* **7:**196–200.

McLachlan, A., 1984. Structural implications of the myosin amino acid sequence. *Annual Review of Biophysics and Bioengineering* **13:**167–189.

Meister, M., Caplan, S. R., and Berg, H., 1989. Dynamics of a tightly coupled mechanism for flagellar rotation. *Biophysical Journal* **55:**905–914.

Meyhofer, E., and Howard, J., 1995. The force generated by a single kinesin molecule against an elastic load. *Proceedings of the National Academy of Sciences* **92:**574–578.

Molloy, J., Burns, J., Kendrick-Jones, J., et al., 1995. Movement and force produced by a single myosin head. *Nature* **378:**209–213.

Nogales, E., Wolf, S., and Downing, K. H., 1998. Structure of the $\alpha\beta$ tubulin dimer by electron crystallography. *Nature* **391:**199–203.

Ohtsuki, I., Maruyama, K., and Ebashi, S., 1986. Regulatory and cytoskeletal proteins of vertebrate skeletal muscle. *Advances in Protein Chemistry* **38:**1–67.

Rayment, I., 1996. Kinesin and myosin: Molecular motors with similar engines. *Structure* **4:**501–504.

Rayment, I., and Holden, H., 1994. The three-dimensional structure of a molecular motor. *Trends in Biochemical Sciences* **19:**129–134.

Saito, A., et al., 1988. Ultrastructure of the calcium release channel of sarcoplasmic reticulum. *Journal of Cell Biology* **107:**211–219.

Smith, C., and Rayment, I., 1995. X-ray structure of the magnesium(II)–pyrophosphate complex of the truncated head in *Dictyostelium discoideum* myosin to 2.7 Å resolution. *Biochemistry* **34:**8973–8981.

Spudich, J., 1994. How molecular motors work. *Nature* **372:**515–518.

Svoboda, K., Schmidt, C., Schnapp, B., and Block, S., 1993. Direct observation of kinesin stepping by optical trapping interferometry. *Nature* **365:**721–727.

Thomas, D., 1987. Spectroscopic probes of muscle crossbridge rotation. *Annual Review of Physiology* **49:**691–709.

Trinick, J., 1994. Titin and nebulin: Protein rulers in muscles? *Trends in Biochemical Sciences* **19:**405–409.

Vallee, R., and Shpetner, H., 1990. Motor proteins of cytoplasmic microtubules. *Annual Review of Biochemistry* **59:**909–932.

Wagenknecht, T., et al., 1989. Three-dimensional architecture of the calcium channel/foot structure of sarcoplasmic reticulum. *Nature* **338:**167–170.

Walker, R., and Sheetz, M., 1993. Cytoplasmic microtubule-associated motors. *Annual Review of Biochemistry* **62:**429–451.

Whittaker, M., Wilson-Kubalek, E., Smith, Jr., et al., 1995. A 35 Å movement of smooth muscle myosin on ADP release. *Nature* **378:**748–753.

Wilson, L., and Jordan, M. A., 1995. Microtubule dynamics: Taking aim at a moving target. *Chemistry and Biology* **2:**569–573.

Worton, R., 1995. Muscular dystrophies: Diseases of the dystrophin–glycoprotein complex. *Science* **270:**755–756.

$\mathcal{P}$art III

Metabolism and Its Regulation
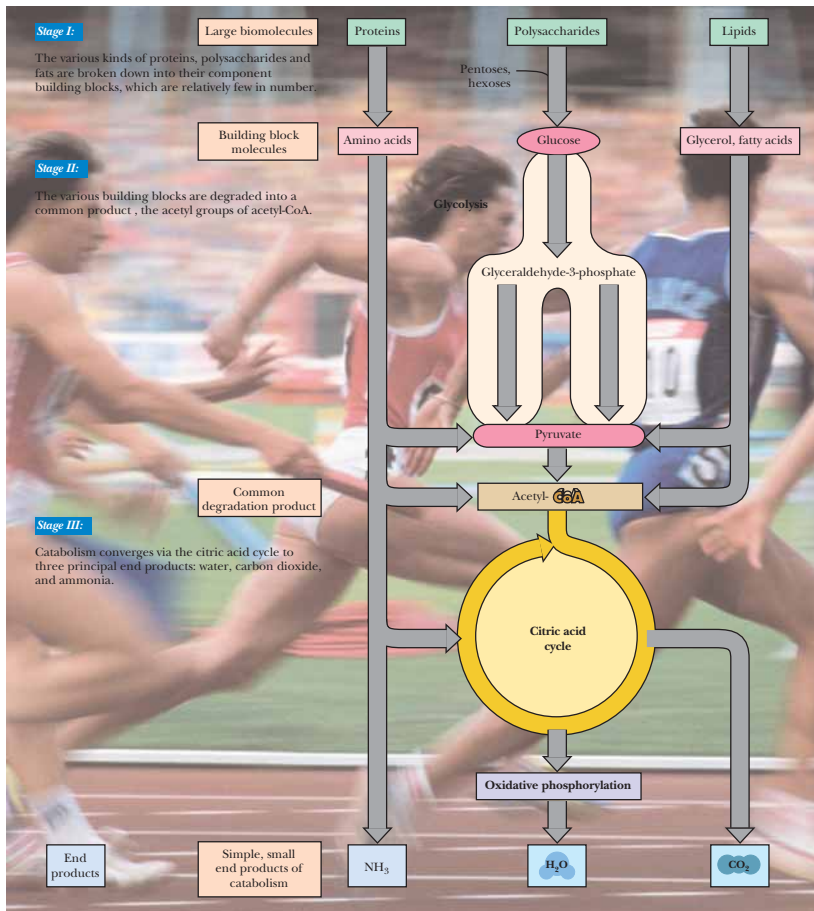
Metabolism accomplishes, among other things, the conversion of food energy into the energy of motion. Regulation of metabolism allows the abrupt transition from a state of rest to the breath-taking power and grace of athletic competition. (European champs by Paul J. Sutton/Duomo; line art by J/B Woolsey Associates)

All is flux, nothing stays still.
Nothing endures but change.

Heraclitus (c. 540–c. 480 b.c.)

Chapter 18

Metabolism—An Overview

Anise swallowtail butterfly (Papilio zelicans) *with its pupal case.*
Metamorphosis of butterflies is a dramatic example of metabolic change.
(© 1986 Peter Bryant/Biological Photo Service)

The word *metabolism* derives from the Greek word for "change." **Metabolism** represents the sum of the chemical changes that convert **nutrients,** the "raw materials" necessary to nourish living organisms, into energy and the chemically complex finished products of cells. Metabolism consists of literally hundreds of enzymatic reactions organized into discrete pathways. These pathways proceed in a stepwise fashion, transforming substrates into end products through many specific chemical **intermediates.** Metabolism is sometimes referred to as **intermediary metabolism** to reflect this aspect of the process. Metabolic maps (Figure 18.1) portray virtually all of the principal reactions of the intermediary metabolism of carbohydrates, lipids, amino acids, nucleotides,

FIGURE 18.1 • A metabolic map, indicating the reactions of intermediary metabolism ▶ and the enzymes that catalyze them. Over 500 different chemical intermediates, or metabolites, and a greater number of enzymes are represented here. *(© 1997 20th edition, designed by and courtesy of D. E. Nicholson, University of Leeds, U. K., and the Sigma Chemical Co.)*
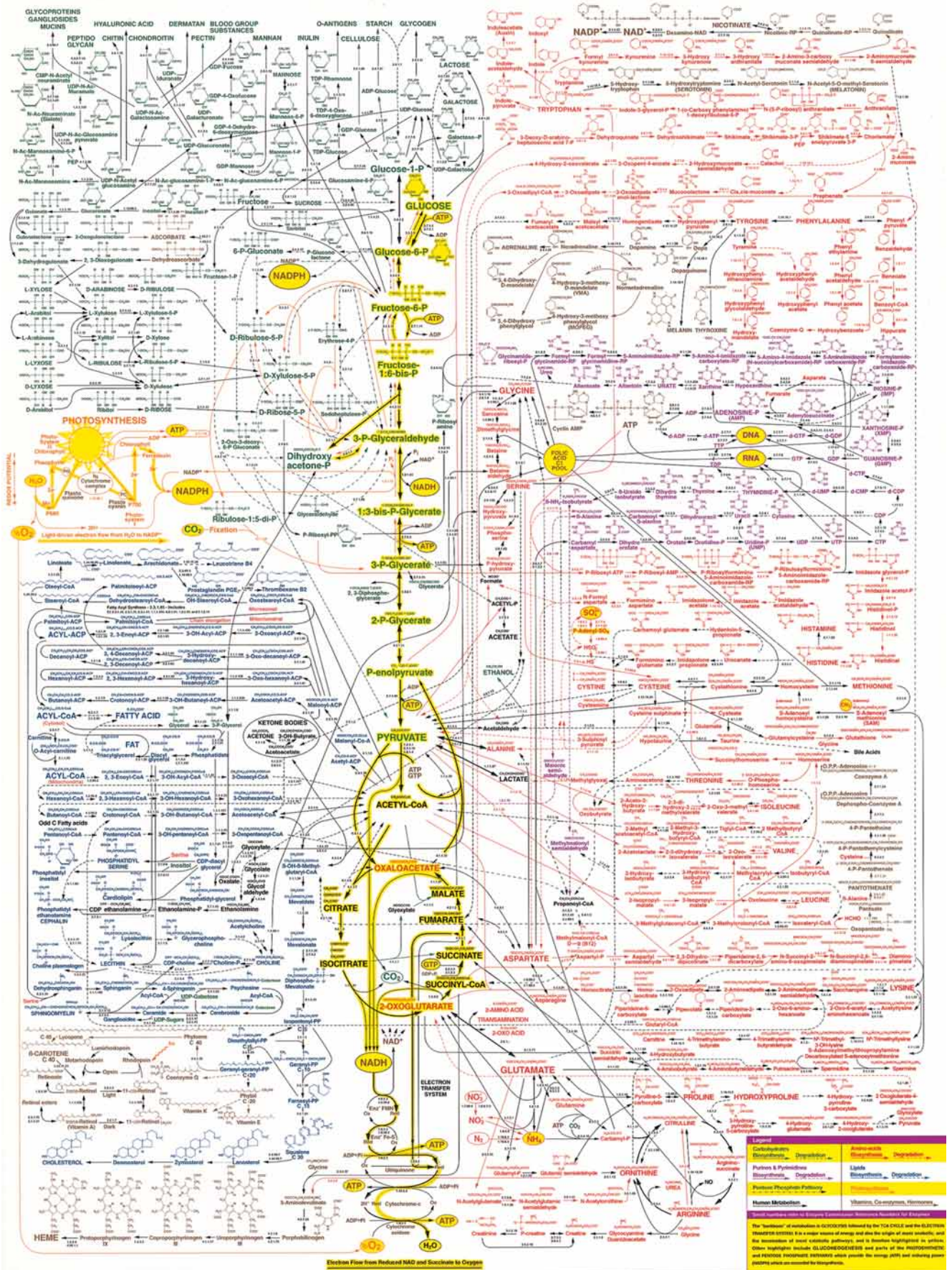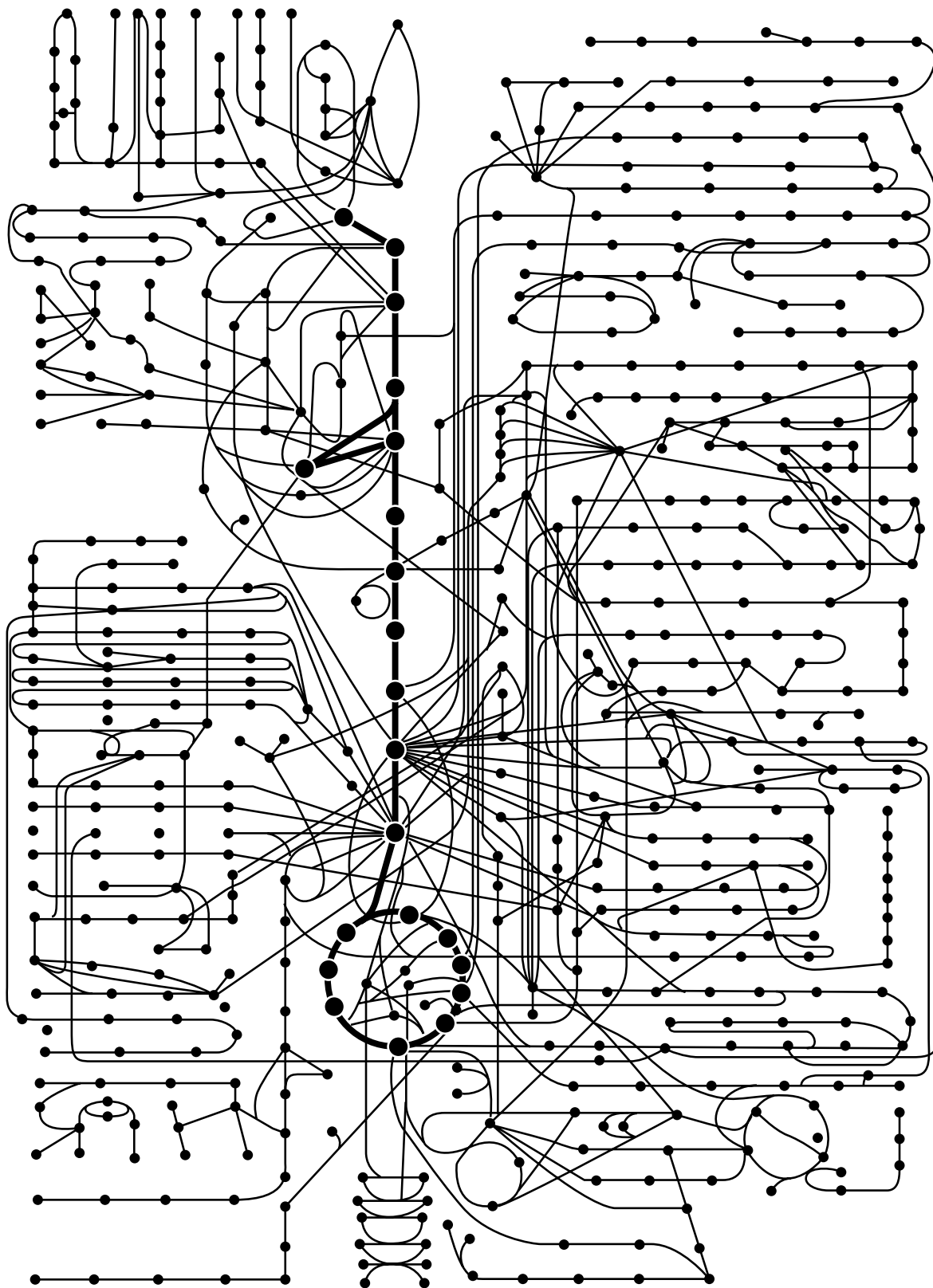
FIGURE 18.2 • The metabolic map as a set of dots and lines. The heavy dots and lines trace the central energy-releasing pathways known as glycolysis and the citric acid cycle. *(Adapted from Alberts, B., et al., 1989.* Molecular Biology of the Cell, *2nd ed. New York: Garland Publishing Co.)*

and their derivatives. These maps are very complex at first glance and seem to be virtually impossible to learn easily. Despite their appearance, these maps become easy to follow once the major metabolic routes are known and their functions are understood. The underlying order of metabolism and the important interrelationships between the various pathways then appear as simple patterns against the seemingly complicated background.

The Metabolic Map as a Set of Dots and Lines

One interesting transformation of the intermediary metabolism map is to represent each intermediate as a black dot and each enzyme as a line (Figure 18.2). Then, the more than 1000 different enzymes and substrates are represented by just two symbols. This chart has about 520 dots (intermediates). Table 18.1 lists the numbers of dots that have one or two or more lines (enzymes) associated with them. Thus, this table classifies intermediates by the number of enzymes that act upon them. A dot connected to just a single line must be either a nutrient, a storage form, an end product, or an excretory product of metabolism. Also, because many pathways tend to proceed in only one direction (that is, they are essentially irreversible under physiological conditions), a dot connected to just two lines is probably an intermediate in only one pathway and has only one fate in metabolism. If three lines are connected to a dot, that intermediate has at least two possible metabolic fates; four lines, three fates; and so on. Note that about 80% of the intermediates connect to only one or two lines and thus have only a limited purpose in the cell. However, many intermediates are subject to a variety of fates. In such instances, the pathway followed is an important regulatory choice. Indeed, whether any substrate is routed down a particular metabolic pathway is the consequence of a regulatory decision made in response to the cell's (or organism's) momentary requirements for energy or nutrition. The regulation of metabolism is an interesting and important subject to which we will return often.

Table 18.1

Number of Dots (Intermediates) in the Metabolic Map of Figure 18.2, and the Number of Lines Associated with Them

Lines	Dots
1 or 2	410
3	71
4	20
5	11
6 or more	8

18.1 • Virtually All Organisms Have the Same Basic Set of Metabolic Pathways

One of the great unifying principles of modern biology is that organisms show marked similarity in their major pathways of metabolism. Given the almost unlimited possibilities within organic chemistry, this generality would appear most unlikely. Yet it's true, and it provides strong evidence that all life has descended from a common ancestral form. All forms of nutrition and almost all metabolic pathways evolved in early prokaryotes prior to the appearance of eukaryotes 1 billion years ago. For example, **glycolysis,** the metabolic pathway by which energy is released from glucose and captured in the form of ATP under anaerobic conditions, is common to almost every cell. It is believed to be the most ancient of metabolic pathways, having arisen prior to the appearance of oxygen in abundance in the atmosphere. All organisms, even those that can synthesize their own glucose, are capable of glucose degradation and ATP synthesis via glycolysis. Other prominent pathways are also virtually ubiquitous among organisms.

Metabolic Diversity

Although most cells have the same basic set of central metabolic pathways, different cells (and, by extension, different organisms) are characterized by the alternative pathways they might express. These pathways offer a wide diversity

of metabolic possibilities. For instance, organisms are often classified according to the major metabolic pathways they exploit to obtain carbon or energy. Classification based on carbon requirements defines two major groups, autotrophs and heterotrophs. **Autotrophs** are organisms that can use just carbon dioxide as their sole source of carbon. **Heterotrophs** require an organic form of carbon, such as glucose, in order to synthesize other essential carbon compounds.

Classification based on energy sources also gives two groups: phototrophs and chemotrophs. **Phototrophs** are *photosynthetic organisms,* which use light as a source of energy. **Chemotrophs** use organic compounds such as glucose or, in some instances, oxidizable inorganic substances such as Fe^{2+}, NO_2^-, NH_4^+, or elemental sulfur as sole sources of energy. Typically, the energy is extracted through oxidation–reduction reactions. Based on these characteristics, every organism falls into one of four categories (Table 18.2).

Metabolic Diversity Among the Five Kingdoms

Prokaryotes (the kingdom Monera—bacteria) show a greater metabolic diversity than all the four eukaryotic kingdoms (Protoctista [previously called Protozoa], Fungi, Plants, and Animals) put together. Prokaryotes are variously chemoheterotrophic, photoautotrophic, photoheterotrophic, or chemoautotrophic. No protoctista are chemoautotrophs; fungi and animals are exclusively chemoheterotrophs; plants are characteristically photoautotrophs, although some are heterotrophic in their mode of carbon acquisition.

The Role of O_2 in Metabolism

A further metabolic distinction among organisms is whether or not they can use oxygen as an electron acceptor in energy-producing pathways. Those that can are called **aerobes** or *aerobic organisms;* others, termed **anaerobes,** can subsist without O_2. Organisms for which O_2 is obligatory for life are called **obligate aerobes;** humans are an example. Some species, the so-called **facultative anaerobes,** can adapt to anaerobic conditions by substituting other electron acceptors for O_2 in their energy-producing pathways; *Escherichia coli* is an exam-

Table 18.2

Metabolic Classification of Organisms According to Their Carbon and Energy Requirements				
Classification	**Carbon Source**	**Energy Source**	**Electron Donors**	**Examples**
Photoautotrophs	CO_2	Light	H_2O, H_2S, S, other inorganic compounds	Green plants, algae, cyanobacteria, photosynthetic bacteria
Photoheterotrophs	Organic compounds	Light	Organic compounds	Nonsulfur purple bacteria
Chemoautotrophs	CO_2	Oxidation–reduction reactions	Inorganic compounds: H_2, H_2S, NH_4^+, NO_2^-, Fe^{2+}, Mn^{2+}	Nitrifying bacteria; hydrogen, sulfur, and iron bacteria
Chemoheterotrophs	Organic compounds	Oxidation–reduction reactions	Organic compounds, e.g., glucose	All animals, most microorganisms, nonphotosynthetic plant tissue such as roots, photosynthetic cells in the dark

Calcium Carbonate—A Biological Sink for CO_2

A major biological sink for CO_2 that is often overlooked is the calcium carbonate shells of corals, molluscs, and crustacea. These invertebrate animals deposit $CaCO_3$ in the form of protective exoskeletons. In some invertebrates, such as the *scleractinians* (hard corals) of tropical seas, photosynthetic dinoflagellates (kingdom Protoctista) known as *zooxanthellae* live within the ani-

mal cells as **endosymbionts.** These phototrophic cells use light to drive the resynthesis of organic molecules from CO_2 released (as bicarbonate ion) by the animal's metabolic activity. In the presence of Ca^{2+}, the photosynthetic CO_2 fixation "pulls" the deposition of $CaCO_3$, as summarized in the following coupled reactions:

$$Ca^{2+} + 2\ HCO_3^{-} \rightleftharpoons CaCO_{3(s)}\downarrow + H_2CO_3$$
$$H_2CO_3 \rightleftharpoons H_2O + CO_2$$
$$H_2O + CO_2 \longrightarrow \text{carbohydrate} + O_2$$
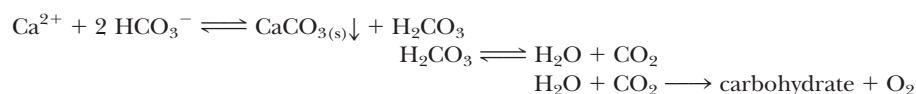
ple. Yet others cannot use oxygen at all and are even poisoned by it; these are the **obligate anaerobes.** *Clostridium botulinum,* the bacterium that produces botulin toxin, is representative.

The Flow of Energy in the Biosphere and the Carbon and Oxygen Cycles Are Intimately Related

The primary source of energy for life is the sun. Photoautotrophs utilize light energy to drive the synthesis of organic molecules, such as carbohydrates, from atmospheric CO_2 and water (Figure 18.3). Heterotrophic cells then use these organic products of photosynthetic cells both as fuels and as building blocks, or precursors, for the biosynthesis of their own unique complement of biomolecules. Ultimately, CO_2 is the end product of heterotrophic carbon metabolism, and CO_2 is returned to the atmosphere for reuse by the photoautotrophs. In effect, solar energy is converted to the chemical energy of organic molecules by photoautotrophs, and heterotrophs recover this energy by metabolizing the organic substances. The flow of energy in the biosphere is thus conveyed within the carbon cycle, and the impetus driving the cycle is light energy.
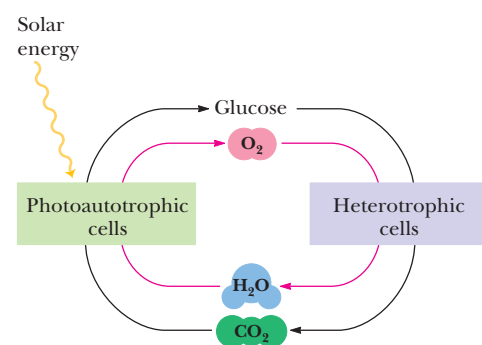
FIGURE 18.3 • The flow of energy in the biosphere is coupled primarily to the carbon and oxygen cycles.

18.2 • Metabolism Consists of Catabolism (Degradative Pathways) and Anabolism (Biosynthetic Pathways)

Metabolism serves two fundamentally different purposes: the generation of energy to drive vital functions and the synthesis of biological molecules. To achieve these ends, metabolism consists largely of two contrasting processes, catabolism and anabolism. *Catabolic pathways are characteristically energy-yielding, whereas anabolic pathways are energy-requiring.* **Catabolism** involves the oxidative degradation of complex nutrient molecules (carbohydrates, lipids, and proteins) obtained either from the environment or from cellular reserves. The breakdown of these molecules by catabolism leads to the formation of simpler molecules such as lactic acid, ethanol, carbon dioxide, urea, or ammonia. Catabolic reactions are usually exergonic, and often the chemical energy released is captured in the form of ATP (Chapter 3). Because catabolism is oxidative for the most part, part of the chemical energy may be conserved as

energy-rich electrons transferred to the coenzymes NAD^+ and $NADP^+$. These two reduced coenzymes have very different metabolic roles: *NAD^+ reduction is part of catabolism; NADPH oxidation is an important aspect of anabolism.* The energy released upon oxidation of NADH is coupled to the phosphorylation of ADP in aerobic cells, and so NADH oxidation back to NAD^+ serves to generate more ATP; in contrast, NADPH is the source of the reducing power needed to drive reductive biosynthetic reactions.

Thermodynamic considerations demand that the energy necessary for biosynthesis of any substance exceed the energy available from its catabolism. Otherwise, organisms could achieve the status of perpetual motion machines: A few molecules of substrate whose catabolism yielded more ATP than required for its resynthesis would allow the cell to cycle this substance and harvest an endless supply of energy.

Anabolism Is Biosynthesis

Anabolism is a synthetic process in which the varied and complex biomolecules (proteins, nucleic acids, polysaccharides, and lipids) are assembled from simpler precursors. Such biosynthesis involves the formation of new covalent bonds, and an input of chemical energy is necessary to drive such endergonic processes. The ATP generated by catabolism provides this energy. Furthermore, NADPH is an excellent donor of high-energy electrons for the reductive reactions of anabolism. Despite their divergent roles, anabolism and catabolism are interrelated in that the products of one provide the substrates of the other (Figure 18.4). Many metabolic intermediates are shared between the two processes, and the precursors needed by anabolic pathways are found among the products of catabolism.

Anabolism and Catabolism Are Not Mutually Exclusive

Interestingly, anabolism and catabolism occur simultaneously in the cell. The conflicting demands of concomitant catabolism and anabolism are managed by cells in two ways. First, the cell maintains tight and separate regulation of both catabolism and anabolism, so that metabolic needs are served in an immediate and orderly fashion. Second, competing metabolic pathways are often

FIGURE 18.4 • Energy relationships between the pathways of catabolism and anabolism. Oxidative, exergonic pathways of catabolism release free energy and reducing power that are captured in the form of ATP and NADPH, respectively. Anabolic processes are endergonic, consuming chemical energy in the form of ATP and using NADPH as a source of high-energy electrons for reductive purposes.
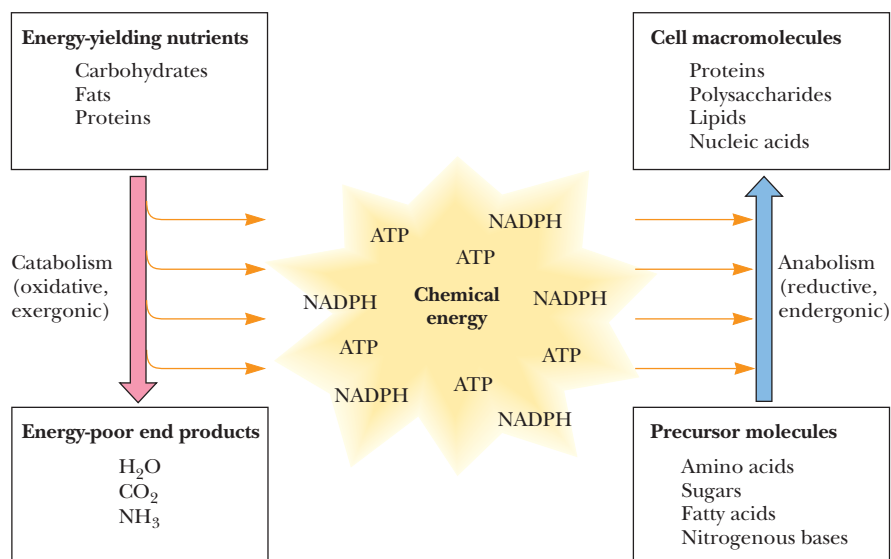
localized within different cellular compartments. Isolating opposing activities within distinct compartments, such as separate organelles, avoids interference between them. For example, the enzymes responsible for catabolism of fatty acids, the *fatty acid oxidation pathway,* are localized within mitochondria. In contrast, *fatty acid biosynthesis* takes place in the cytosol. In subsequent chapters, we shall see that the particular molecular interactions responsible for the regulation of metabolism become important to an understanding and appreciation of metabolic biochemistry.

Modes of Enzyme Organization in Metabolic Pathways

The individual metabolic pathways of anabolism and catabolism consist of sequential enzymatic steps (Figure 18.5). Several types of organization are possible. The enzymes of some multienzyme systems may exist as physically separate, soluble entities, with diffusing intermediates (Figure 18.5a). In other instances, the enzymes of a pathway are collected to form a discrete *multienzyme complex,* and the substrate is sequentially modified as it is passed along from enzyme to enzyme (Figure 18.5b). This type of organization has the advantage that intermediates are not lost or diluted by diffusion. In a third pattern of organization, the enzymes common to a pathway reside together as a *membrane-bound system* (Figure 18.5c). In this case, the enzyme participants (and perhaps the substrates as well) must diffuse in just the two dimensions of the membrane to interact with their neighbors.

As research reveals the ultrastructural organization of the cell in ever greater detail, more and more of the so-called soluble enzyme systems are found to be physically united into functional complexes. Thus, in many (perhaps all) metabolic pathways, the consecutively acting enzymes are associated into stable multienzyme complexes that are sometimes referred to as **metabolons,** a word meaning "units of metabolism."
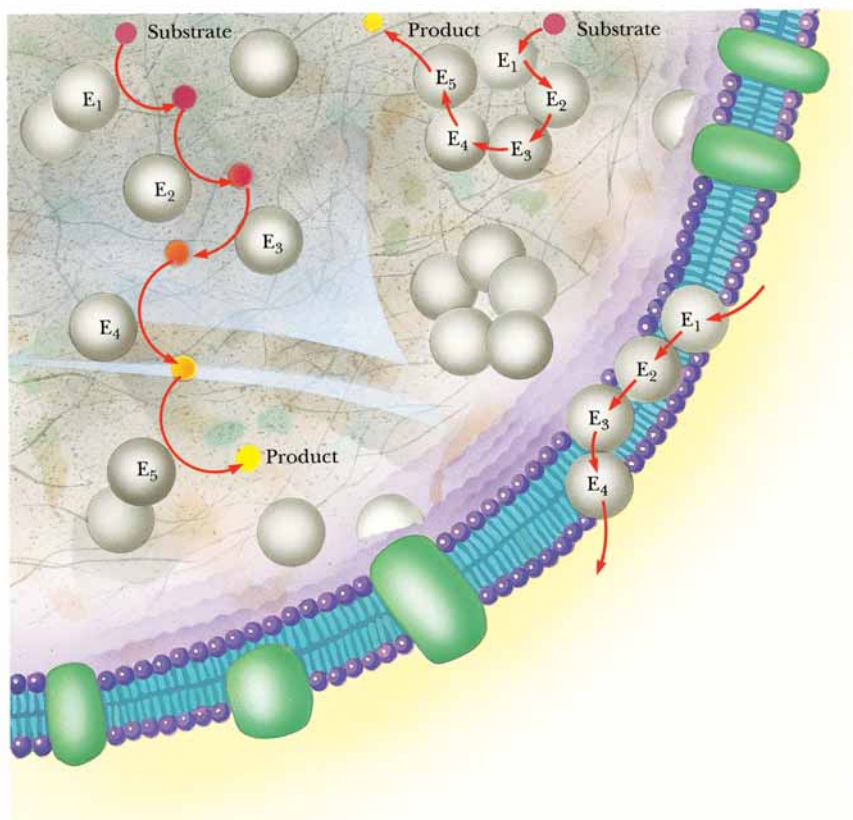
FIGURE 18.5 • Schematic representation of types of multienzyme systems carrying out a metabolic pathway: (a) Physically separate, soluble enzymes with diffusing intermediates. (b) A multienzyme complex. Substrate enters the complex, becomes covalently bound and then sequentially modified by enzymes E_1 to E_5 before product is released. No intermediates are free to diffuse away. (c) A membrane-bound multienzyme system.

The Pathways of Catabolism Converge to a Few End Products

If we survey the catabolism of the principal energy-yielding nutrients (carbohydrates, lipids, and proteins) in a typical heterotrophic cell, we see that the degradation of these substances involves a succession of enzymatic reactions. In the presence of oxygen (*aerobic catabolism*), these molecules are degraded ultimately to carbon dioxide, water, and ammonia. Aerobic catabolism consists of three distinct stages. In **stage 1,** the nutrient macromolecules are broken down into their respective building blocks. Given the great diversity of macromolecules, these building blocks represent a rather limited number of products. Proteins yield up their 20 component amino acids, polysaccharides give rise to carbohydrate units that are convertible to glucose, and lipids are broken down into glycerol and fatty acids (Figure 18.6).

In **stage 2,** the collection of product building blocks generated in stage 1 is further degraded to yield an even more limited set of simpler metabolic intermediates. The deamination of amino acids leaves α-keto acid carbon skeletons. Several of these α-keto acids are citric acid cycle intermediates and are fed directly into stage 3 catabolism via this cycle. Others are converted either to the three-carbon α-keto acid *pyruvate* or to the acetyl groups of *acetyl-coenzyme A* (acetyl-CoA). Glucose and the glycerol from lipids also generate pyruvate, whereas the fatty-acids are broken into two-carbon units that appear as *acetyl-CoA*. Because pyruvate also gives rise to acetyl-CoA, we see that the degradation of macromolecular nutrients converges to a common end product, acetyl-CoA (Figure 18.6).

The combustion of the acetyl groups of acetyl-CoA by the *citric acid cycle* and *oxidative phosphorylation* to produce CO_2 and H_2O represents **stage 3** of catabolism. The end products of the citric acid cycle, CO_2 and H_2O, are the ultimate waste products of aerobic catabolism. As we shall see in Chapter 20, the oxidation of acetyl-CoA during stage 3 metabolism generates most of the energy produced by the cell.

Anabolic Pathways Diverge, Synthesizing an Astounding Variety of Biomolecules from a Limited Set of Building Blocks

A rather limited collection of simple precursor molecules is sufficient to provide for the biosynthesis of virtually any cellular constituent, be it protein, nucleic acid, lipid, or polysaccharide. All of these substances are constructed from appropriate building blocks via the pathways of anabolism. In turn, the building blocks (amino acids, nucleotides, sugars, and fatty acids) can be generated from metabolites in the cell. For example, amino acids can be formed by amination of the corresponding α-keto acid carbon skeletons, and pyruvate can be converted to hexoses for polysaccharide biosynthesis.

Amphibolic Intermediates

Certain of the central pathways of intermediary metabolism, such as the citric acid cycle, and many metabolites of other pathways have dual purposes—they serve in both catabolism and anabolism. This dual nature is reflected in the designation of such pathways as **amphibolic** rather than solely catabolic or anabolic. In any event, in contrast to catabolism—which converges to the common intermediate, acetyl-CoA—the pathways of anabolism diverge from a small group of simple metabolic intermediates to yield a spectacular variety of cellular constituents.

amphi • from the Greek for "on both sides"
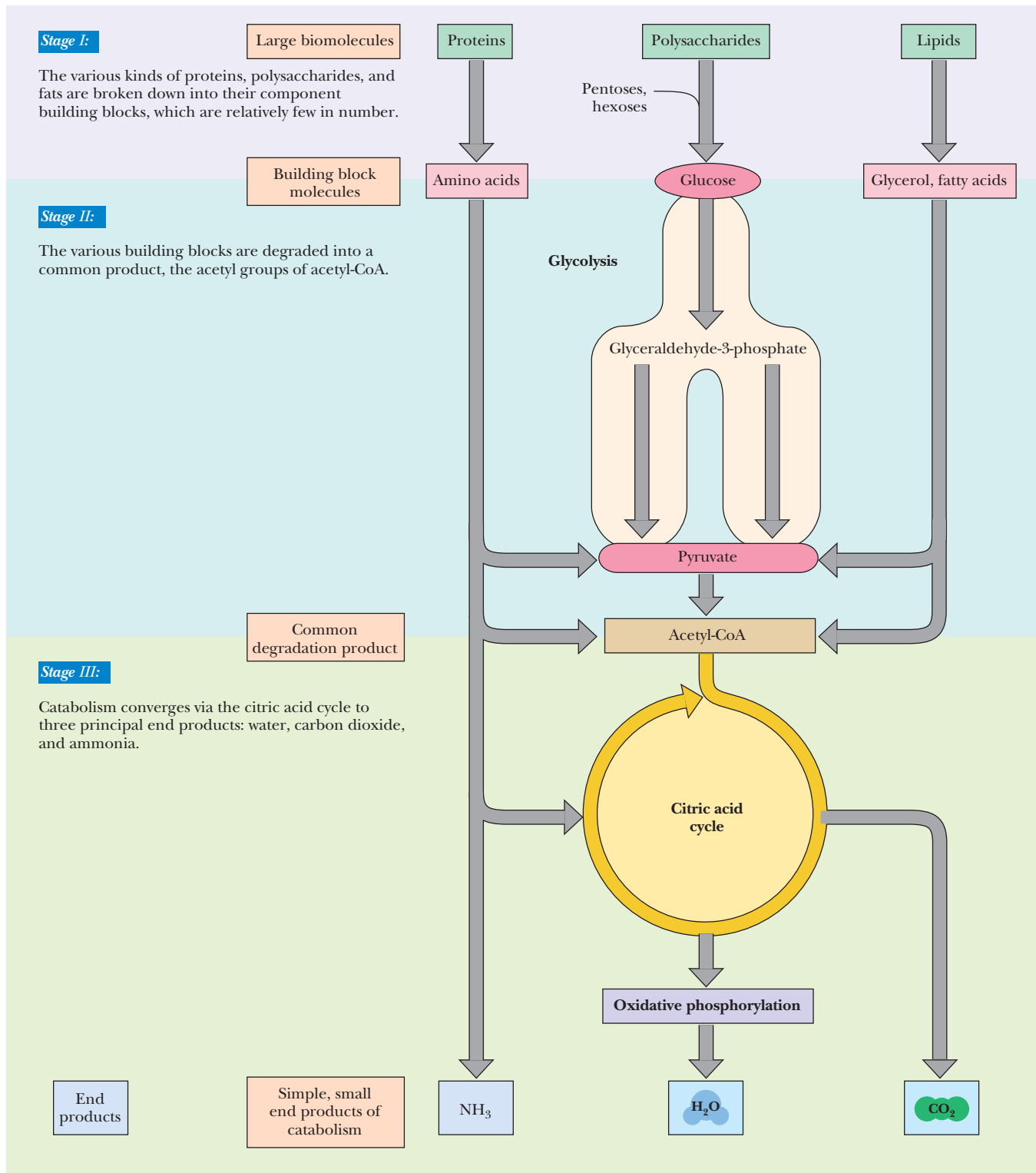
FIGURE 18.6 • The three stages of catabolism. **Stage I:** Proteins, polysaccharides, and lipids are broken down into their component building blocks, which are relatively few in number. **Stage II:** The various building blocks are degraded into the common product, the acetyl groups of acetyl-CoA. **Stage III:** Catabolism converges to three principal end products: water, carbon dioxide, and ammonia.

Corresponding Pathways of Catabolism and Anabolism Differ in Important Ways

The anabolic pathway for synthesis of a given end product usually does not precisely match the pathway used for catabolism of the same substance. Some of the intermediates may be common to steps in both pathways, but different enzymatic reactions and unique metabolites characterize other steps. A good example of these differences is found in a comparison of the catabolism of glucose to pyruvic acid by the pathway of glycolysis and the biosynthesis of glucose from pyruvate by the pathway called *gluconeogenesis*. The glycolytic pathway from glucose to pyruvate consists of 10 enzymes. Although it may seem efficient for glucose synthesis from pyruvate to proceed by a reversal of all 10 steps, gluconeogenesis uses only seven of the glycolytic enzymes in reverse, replacing the remaining three with four enzymes specific to glucose biosynthesis. In similar fashion, the pathway responsible for degrading proteins to amino acids differs from the protein synthesis system, and the oxidative degradation of fatty acids to two-carbon acetyl-CoA groups does not follow the same reaction path as the biosynthesis of fatty acids from acetyl-CoA.

Metabolic Regulation Favors Different Pathways for Oppositely Directed Metabolic Sequences

A second reason for different pathways serving in opposite metabolic directions is that such pathways must be independently regulated. If catabolism and anabolism passed along the same set of metabolic tracks, equilibrium considerations would dictate that slowing the traffic in one direction by inhibiting a particular enzymatic reaction would necessarily slow traffic in the opposite direction. Independent regulation of anabolism and catabolism can be accomplished only if these two contrasting processes move along different routes *or,* in the case of shared pathways, the rate-limiting steps serving as the points of regulation are catalyzed by enzymes that are unique to each opposing sequence (Figure 18.7).
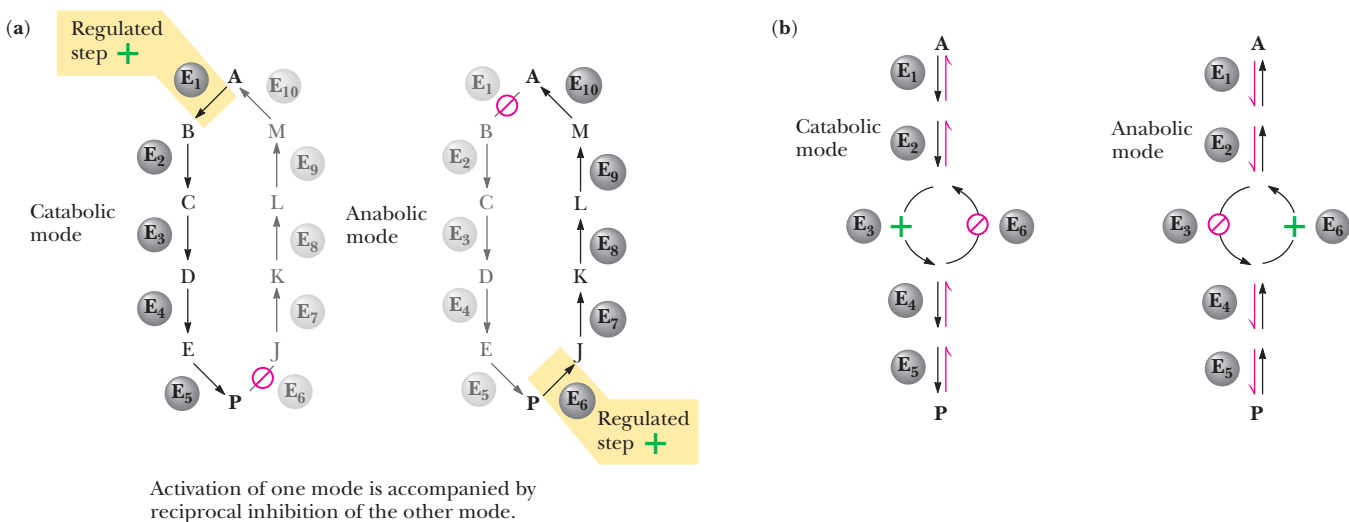
FIGURE 18.7 • Parallel pathways of catabolism and anabolism must differ in at least one metabolic step in order that they can be regulated independently. Shown here are two possible arrangements of opposing catabolic and anabolic sequences between A and P. (a) The parallel sequences proceed via independent routes. (b) Only one reaction has two different enzymes, a catabolic one (E_3) and its anabolic counterpart (E_6). These provide sites for regulation.
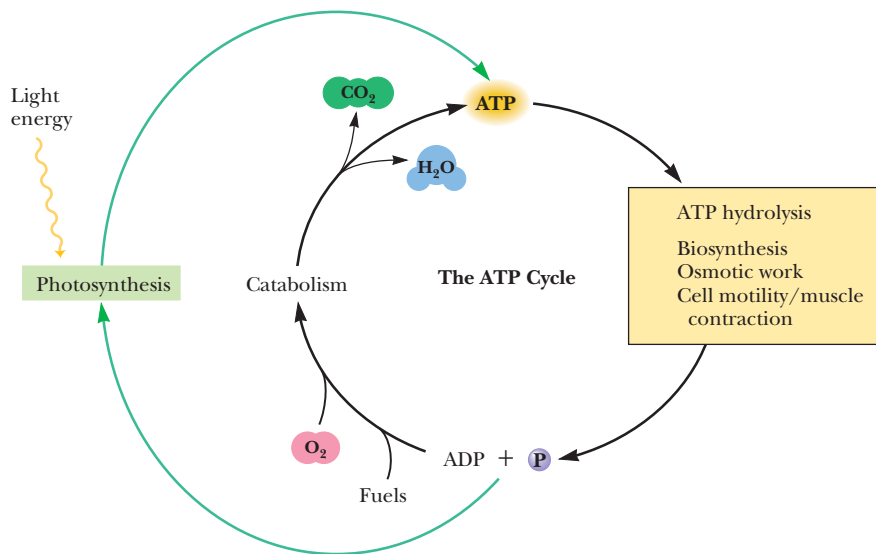
FIGURE 18.8 • The ATP cycle in cells. ATP is formed via photosynthesis in phototrophic cells or catabolism in heterotrophic cells. Energy-requiring cellular activities are powered by ATP hydrolysis, liberating ADP and P_i.

The ATP Cycle

We saw in Chapter 3 that ATP is the energy currency of cells. In phototrophs, ATP is one of the two energy-rich primary products resulting from the transformation of light energy into chemical energy. (The other is NADPH; see the following discussion.) In heterotrophs, the pathways of catabolism have as their major purpose the release of free energy that can be captured in the form of energy-rich phosphoric anhydride bonds in ATP. In turn, ATP provides the energy that drives the manifold activities of all living cells—the synthesis of complex biomolecules, the osmotic work involved in transporting substances into cells, the work of cell motility, the work of muscle contraction. These diverse activities are all powered by energy released in the hydrolysis of ATP to ADP and P_i. Thus, there is an energy cycle in cells where ATP serves as the vessel carrying energy from photosynthesis or catabolism to the energy-requiring processes unique to living cells (Figure 18.8).

NAD^+ Collects Electrons Released in Catabolism

The substrates of catabolism—proteins, carbohydrates, and lipids—are good sources of chemical energy because the carbon atoms in these molecules are in a relatively reduced state (Figure 18.9). In the oxidative reactions of catabolism, reducing equivalents are released from these substrates, often in the form of **hydride ions** (a proton coupled with two electrons, $H:^-$). These hydride ions are transferred in enzymatic **dehydrogenase** reactions from the substrates
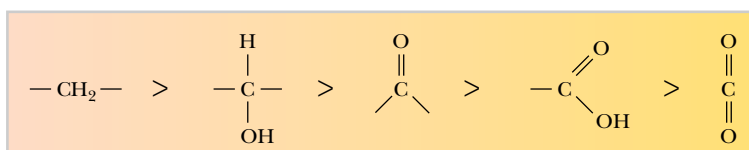
FIGURE 18.9 • Comparison of the state of reduction of carbon atoms in biomolecules: —CH_2— (fats) > —CHOH— (carbohydrates) > —C=O (carbonyls) > —COOH (carboxyls) > CO_2 (carbon dioxide, the final product of catabolism).

to NAD^+ molecules, reducing them to NADH. A second proton accompanies these reactions, appearing in the overall equation as H^+ (Figure 18.10). In turn, NADH is oxidized back to NAD^+ when it transfers its reducing equivalents to electron acceptor systems that are part of the metabolic apparatus of the mitochondria. The ultimate oxidizing agent (e^- acceptor) is O_2, becoming reduced to H_2O.

Oxidation reactions are exergonic, and the energy released is coupled with the formation of ATP in a process called **oxidative phosphorylation.** The NAD^+–NADH system can be viewed as a *shuttle* that carries the electrons released from catabolic substrates to the mitochondria, where they are transferred to O_2, the ultimate electron acceptor in catabolism. In the process, the free energy released is trapped in ATP. The NADH cycle is an important player in the transformation of the chemical energy of carbon compounds into the chemical energy of phosphoric anhydride bonds. Such transformations of energy from one form to another are referred to as **energy transduction.** Oxidative phosphorylation is one cellular mechanism for energy transduction. Chapter 21 is devoted to electron transport reactions and oxidative phosphorylation.

NADPH Provides the Reducing Power for Anabolic Processes

Whereas catabolism is fundamentally an oxidative process, anabolism is, by its contrasting nature, reductive. The biosynthesis of the complex constituents of the cell begins at the level of intermediates derived from the degradative pathways of catabolism; or, less commonly, biosynthesis begins with oxidized substances available in the inanimate environment, such as carbon dioxide. When the hydrocarbon chains of fatty acids are assembled from acetyl-CoA units, activated hydrogens are needed to reduce the carbonyl (C=O) carbon of acetyl-CoA into a —CH_2— at every other position along the chain. When glucose is
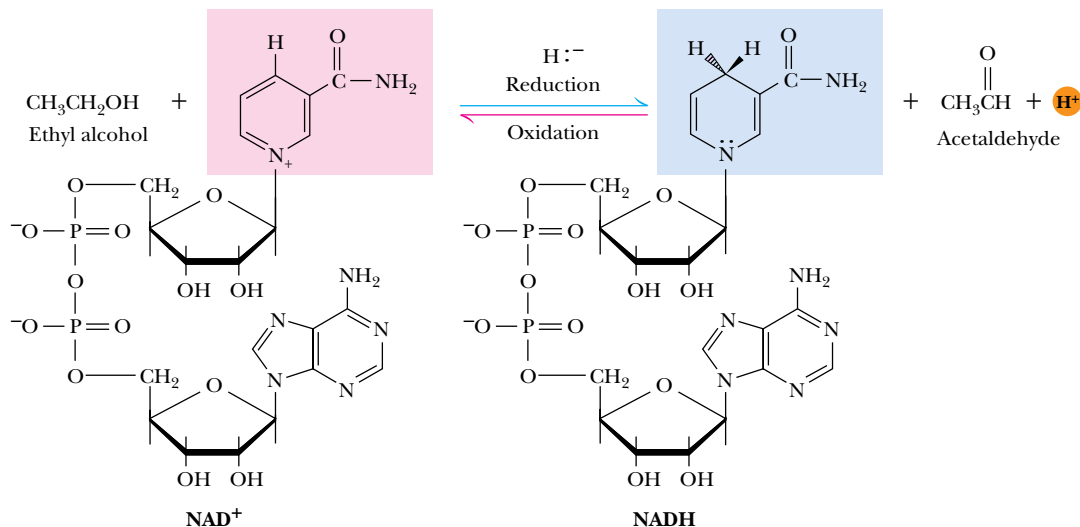
FIGURE 18.10 • Hydrogen and electrons released in the course of oxidative catabolism are transferred as hydride ions to the pyridine nucleotide, NAD^+, to form NADH + H^+ in dehydrogenase reactions of the type

$$AH_2 + NAD^+ \longrightarrow A + NADH + H^+$$
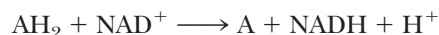
The reaction shown is catalyzed by alcohol dehydrogenase.

synthesized from CO_2 during photosynthesis in plants, reducing power is required. These reducing equivalents are provided by NADPH, the usual source of high-energy hydrogens for reductive biosynthesis. NADPH is generated when $NADP^+$ is reduced with electrons in the form of hydride ions. In heterotrophic organisms, these electrons are removed from fuel molecules by $NADP^+$-specific dehydrogenases. In these organisms, NADPH can be viewed as the carrier of electrons from catabolic reactions to anabolic reactions (Figure 18.11). In photosynthetic organisms, the energy of light is used to pull electrons from water and transfer them to $NADP^+$; O_2 is a by-product of this process.

18.3 • Experimental Methods to Reveal Metabolic Pathways

Armed with the knowledge that metabolism is organized into pathways of successive reactions, we can appreciate by hindsight the techniques employed by early biochemists to reveal their sequence. A major intellectual advance took place at the end of the 19th century when Eduard Buchner showed that the fermentation of glucose to yield ethanol and carbon dioxide can occur in extracts of broken yeast cells. Until this discovery, many thought that metabolism was a vital property, unique to intact cells; even the eminent microbiologist Louis Pasteur, who contributed so much to our understanding of fermentation, was a *vitalist,* one of those who believed that the processes of living substance transcend the laws of chemistry and physics. After Buchner's revelation, biochemists searched for intermediates in the transformation of glucose and soon learned that inorganic phosphate was essential to glucose breakdown. This observation gradually led to the discovery of a variety of phosphorylated organic compounds that serve as intermediates along the fermentative pathway.

An important tool for elucidating the steps in the pathway was the use of *metabolic inhibitors.* Adding an enzyme inhibitor to a cell-free extract caused an accumulation of intermediates in the pathway prior to the point of inhibition (Figure 18.12). Each inhibitor was specific for a particular site in the sequence of metabolic events. As the arsenal of inhibitors was expanded, the individual steps in metabolism were revealed.

FIGURE 18.11 • Transfer of reducing equivalents from catabolism to anabolism via the NADPH cycle.

FIGURE 18.12 • The use of inhibitors to reveal the sequence of reactions in a metabolic pathway. (a) **Control:** Under normal conditions, the steady-state concentrations of a series of intermediates will be determined by the relative activities of the enzymes in the pathway. (b) **Plus inhibitor:** In the presence of an inhibitor (in this case, an inhibitor of *enzyme 4*), intermediates upstream of the metabolic block (B, C, and D) accumulate, revealing themselves as intermediates in the pathway. The concentration of intermediates lying downstream (E and F) will fall.

Mutations Create Specific Metabolic Blocks

Genetics provides an approach to the identification of intermediate steps in metabolism that is somewhat analogous to inhibition. Mutation in a gene encoding an enzyme often results in an inability to synthesize the enzyme in an active form. Such a defect leads to a block in the metabolic pathway at the point where the enzyme acts, and the enzyme's substrate accumulates. Such genetic disorders are lethal if the end product of the pathway is essential or if the accumulated intermediates have toxic effects. In microorganisms, however, it is often possible to manipulate the growth medium so that essential end products are provided. Then the biochemical consequences of the mutation can be investigated. Studies on mutations in genes of the filamentous fungus *Neurospora crassa* led G. W. Beadle and E. L. Tatum to hypothesize in 1941 that genes are units of heredity that encode enzymes (a principle referred to as the "one gene–one enzyme" hypothesis).

Isotopic Tracers as Metabolic Probes

Another widely used approach to the elucidation of metabolic sequences is to "feed" cells a substrate or metabolic intermediate labeled with a particular isotopic form of an element that can be traced. Two sorts of isotopes are useful in this regard: radioactive isotopes, such as ^{14}C, and stable "heavy" isotopes, such as ^{18}O or ^{15}N (Table 18.3). Because the chemical behavior of isotopically labeled compounds is rarely distinguishable from that of their unlabeled counterparts, isotopes provide reliable "tags" for observing metabolic changes. The metabolic fate of a radioactively labeled substance can be traced by determining the presence and position of the radioactive atoms in intermediates derived from the labeled compound (Figure 18.13).

Table 18.3

Properties of Radioactive and Stable "Heavy" Isotopes Used as Tracers in Metabolic Studies

Isotope	Type	Radiation Type	Half-Life	Relative Abundance*
^{2}H	Stable			0.0154%
^{3}H	Radioactive	β^-	12.1 years	
^{13}C	Stable			1.1%
^{14}C	Radioactive	β^-	5700 years	
^{15}N	Stable			0.365%
^{18}O	Stable			0.204%
^{24}Na	Radioactive	β^-, γ	15 hours	
^{32}P	Radioactive	β^-	14.3 days	
^{35}S	Radioactive	β^-	87.1 days	
^{36}Cl	Radioactive	β^-	310,000 years	
^{42}K	Radioactive	β^-	12.5 hours	
^{45}Ca	Radioactive	β^-	152 days	
^{59}Fe	Radioactive	β^-, γ	45 days	
^{131}I	Radioactive	β^-, γ	8 days	

*The relative natural abundance of a stable isotope is important because, in tracer studies, the amount of stable isotope is typically expressed in terms of atoms percent excess over the natural abundance of the isotope.
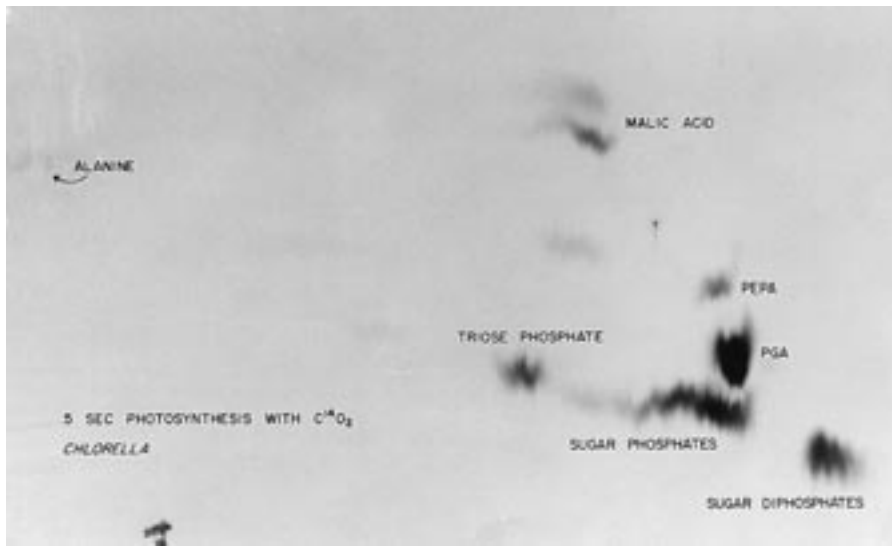
FIGURE 18.13 • One of the earliest experiments using a radioactive isotope as a metabolic tracer. Cells of *Chlorella* (a green alga) synthesizing carbohydrate from carbon dioxide were exposed briefly (5 sec) to ^{14}C-labeled CO_2. The products of CO_2 incorporation were then quickly isolated from the cells, separated by two-dimensional paper chromatography, and observed via autoradiographic exposure of the chromatogram. Such experiments identified radioactive 3-phosphoglycerate (PGA) as the primary product of CO_2 fixation. The 3-phosphoglycerate was labeled in the 1-position (in its carboxyl group). Radioactive compounds arising from the conversion of 3-phosphoglycerate to other metabolic intermediates included phosphoenolpyruvate (PEP), malic acid, triose phosphate, alanine, and sugar phosphates and diphosphates. *(Photograph courtesy of Professor Melvin Calvin, Lawmann Berkeley Laboratory, University of California, Berkeley.)*

Heavy Isotopes

Heavy isotopes endow the compounds in which they appear with slightly greater masses than their unlabeled counterparts. These compounds can be separated and quantitated by mass spectrometry (or density gradient centrifugation, if they are macromolecules). For example, ^{18}O was used in separate experiments as a tracer of the fate of the oxygen atoms in water and carbon dioxide to determine whether the atmospheric oxygen produced in photosynthesis arose from H_2O, CO_2, or both:

$$CO_2 + H_2O \longrightarrow (CH_2O) + O_2$$
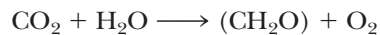
If ^{18}O-labeled CO_2 was presented to a green plant carrying out photosynthesis, none of the ^{18}O was found in O_2. Curiously, it was recovered as $H_2^{18}O$. In contrast, when plants fixing CO_2 were equilibrated with $H_2^{18}O$, $^{18}O_2$ was evolved. These latter labeling experiments established that photosynthesis is best described by the equation

$$C^{16}O_2 + 2 H_2^{18}O \longrightarrow (CH_2^{16}O) + {}^{18}O_2 + H_2^{16}O$$

That is, in the process of photosynthesis, the two oxygen atoms in O_2 come from two H_2O molecules. One O is lost from CO_2 and appears in H_2O, and the other O of CO_2 is retained in the carbohydrate product. Two of the four H atoms are accounted for in (CH_2O), and two reduce the O lost from CO_2 to H_2O.

NMR as a Metabolic Probe

A technology analogous to isotopic tracers is provided by **nuclear magnetic resonance (NMR) spectroscopy.** The atomic nuclei of certain isotopes, such as the naturally occurring isotope of phosphorus, ^{31}P, have *magnetic moments*. The resonance frequency of a magnetic moment is influenced by the local chemical environment. That is, the NMR signal of the nucleus is influenced in an identifiable way by the chemical nature of its neighboring atoms in the compound. In many ways, these nuclei are ideal tracers because their signals contain a great deal of structural information about the environment around the atom, and thus the nature of the compound containing the atom. Transformations of sub-

strates and metabolic intermediates labeled with magnetic nuclei can be traced by following changes in NMR spectra. Furthermore, NMR spectroscopy is a noninvasive procedure. Whole-body NMR spectrometers are being used today in hospitals to directly observe the metabolism (and clinical condition) of living subjects (Figure 18.14). NMR promises to be a revolutionary tool for clinical diagnosis and for the investigation of metabolism *in situ* (literally "in site," meaning, in this case, "where and as it happens").

Metabolic Pathways Are Compartmentalized Within Cells

Although the interior of a prokaryotic cell is not subdivided into compartments by internal membranes, the cell still shows some segregation of metabolism. For example, certain metabolic pathways, such as phospholipid synthesis and oxidative phosphorylation, are localized in the plasma membrane. Also, protein biosynthesis is carried out on ribosomes.

In contrast, eukaryotic cells are extensively compartmentalized by an endomembrane system. Each of these cells has a true nucleus bounded by a double membrane called the *nuclear envelope*. The nuclear envelope is continuous with the endomembrane system, which is composed of differentiated regions: the endoplasmic reticulum; the Golgi complex; various membrane-bounded vesicles such as lysosomes, vacuoles, and microbodies; and, ultimately, the plasma membrane itself. Eukaryotic cells also possess mitochondria and, if they are photosynthetic, chloroplasts. Disruption of the cell membrane and fractionation of the cell contents into the component organelles have allowed an analysis of their respective functions (Figure 18.15). Each compartment is dedicated to specialized metabolic functions, and the enzymes appropriate to these specialized functions are confined together within the organelle. In many instances, the enzymes of a metabolic sequence occur together within the organellar membrane. Thus, *the flow of metabolic intermediates in the cell is spa-*
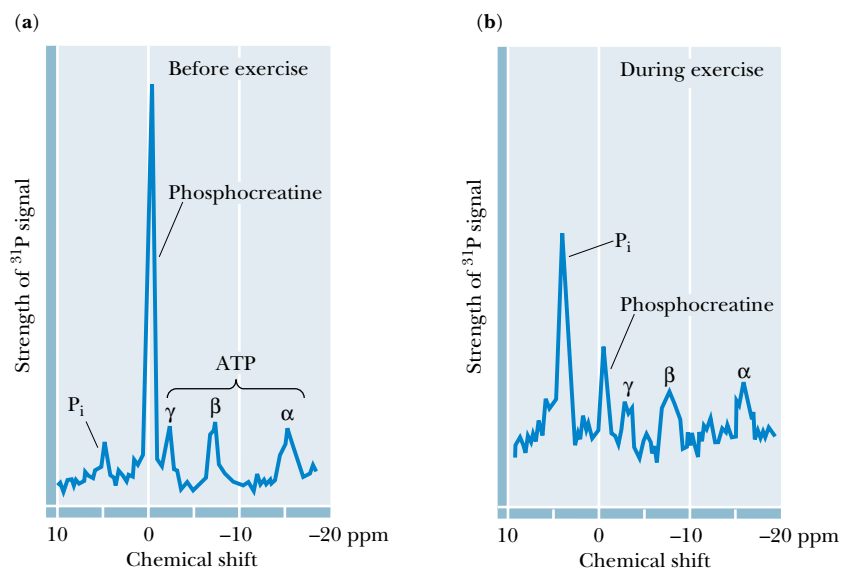
FIGURE 18.14 • With NMR spectroscopy one can observe the metabolism of a living subject in real time. These NMR spectra show the changes in ATP, creatine-P (phosphocreatine), and P_i levels in the forearm muscle of a human subjected to 19 minutes of exercise. Note that the three P atoms of ATP (α, β, and γ) have different chemical shifts, reflecting their different chemical environments.

600rpm

Tube is
moved
slowly up
and down
as pestle
rotates.

Teflon
pestle

Tissue–sucrose homogenate
(minced tissue + 0.25*M*
sucrose buffer)

Strain homogenate
to remove connective
tissue and blood vessels.

Centrifuge homogenate
at 600g × 10 min.

Supernatant 1

Centrifuge supernatant 1
at 15,000g × 5 min.

Nuclei and any
unbroken cells

Supernatant 2

Centrifuge
supernatant 2 at
100,000g × 60 min.

Mitochondria,
lysosomes,
and microbodies

Supernatant 3:
Soluble fraction
of cytoplasm
(cytosol)

Ribosomes and microsomes,
consisting of endoplasmic
reticulum, Golgi, and plasma
membrane fragments

FIGURE 18.15 • Fractionation of a cell extract by differential centrifugation. It is possible to separate organelles and subcellular particles in a centrifuge because their inherent size and density differences give them different rates of sedimentation in an applied centrifugal field. Nuclei are pelleted in relatively weak centrifugal fields, mitochondria in somewhat stronger fields, whereas very strong centrifugal fields are necessary to pellet ribosomes and fragments of the endomembrane system.
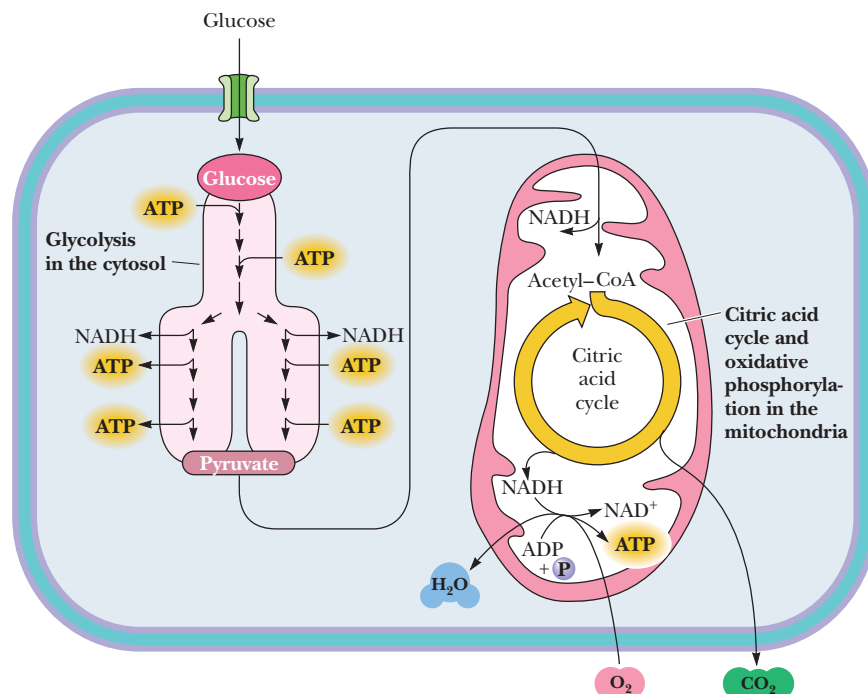
FIGURE 18.16 • Compartmentalization of glycolysis, the citric acid cycle, and oxidative phosphorylation.

tially as well as chemically segregated. For example, the 10 enzymes of glycolysis are found in the cytosol, but pyruvate, the product of glycolysis, is fed into the mitochondria. These organelles contain the citric acid cycle enzymes, which oxidize pyruvate to CO_2. The great amount of energy released in the process is captured by the oxidative phosphorylation system of mitochondrial membranes and used to drive the formation of ATP (Figure 18.16).

18.4 • Nutrition

The use of foods by organisms is termed **nutrition.** The ability of an organism to use a particular food material depends upon its chemical composition and upon the metabolic pathways available to the organism. In addition to essential fiber, food includes the macronutrients—protein, carbohydrate, and lipid—and the micronutrients—including vitamins and minerals.

Protein

Higher organisms must consume protein in order to make new proteins. Dietary protein is a rich source of nitrogen, and certain amino acids—the so-called **essential amino acids**—cannot be synthesized by higher organisms and can be obtained only in the diet. The average adult in the United States consumes far more protein than required for synthesis of essential proteins. Excess dietary protein is then merely a source of metabolic energy. Some of the amino acids (termed **glucogenic**) can be converted into glucose, whereas others, the **ketogenic** amino acids, can be converted to fatty acids and/or keto acids. If fat and carbohydrate are already adequate for the energy needs of the organism, then both kinds of amino acids will be converted to triacylglycerol and stored in adipose tissue.

A certain percentage of an organism's own protein undergoes a constant process of degradation and resynthesis. Together with dietary protein, this recycled protein material participates in a nitrogen equilibrium or **nitrogen balance.** A positive nitrogen balance occurs whenever there is a net increase in the organism's protein content, such as during periods of growth. A negative nitrogen balance exists when dietary intake of nitrogen is insufficient.

Carbohydrate

The principal purpose of carbohydrate in the diet is production of metabolic energy. Simple sugars are metabolized in the glycolytic pathway (see Chapter 19). Complex carbohydrates are degraded into simple sugars, which then can enter the glycolytic pathway. Carbohydrates are also essential components of nucleotides, nucleic acids, glycoproteins, and glycolipids. Human metabolism can adapt to a wide range of dietary carbohydrate levels, but the brain requires glucose for fuel. When dietary carbohydrate consumption exceeds the energy needs of the organism, excess carbohydrate is converted to triacylglycerols and glycogen for long-term energy storage. On the other hand, when dietary carbohydrate intake is low, **ketone bodies** are formed from acetate units to provide metabolic fuel for the brain.

Lipid

Fatty acids and triacylglycerols can be used as fuel by many tissues in the human body, and phospholipids are essential components of all biological membranes. Even though the human body can tolerate a wide range of fat intake levels, there are disadvantages in either extreme. Excess dietary fat is stored as triacylglycerols in adipose tissue, but high levels of dietary fat can also increase the risk of atherosclerosis and heart disease. Moreover, high dietary fat levels are also correlated with increased risk for colon, breast, and prostate cancers. When dietary fat consumption is low, there is a risk of **essential fatty acid** deficiencies. As seen in Chapter 25, the human body cannot synthesize linoleic and linolenic acids, so these must be acquired in the diet. Additionally, arachidonic

---

$\mathcal{A}$ **D E E P E R   L O O K**

A Fad Diet—Low Carbohydrates, High Protein, High Fat

Possibly the most serious nutrition problem in the United States is excessive food consumption, and many people have experimented with fad diets in the hope of losing excess weight. One of the most popular of the fad diets has been the high-protein, high-fat (low-carbohydrate) diet. The premise for such diets is tantalizing: because the tricarboxylic acid (TCA) cycle (see Chapter 20) is the primary site of fat metabolism, and because glucose is usually needed to replenish intermediates in the TCA cycle, if carbohydrates are restricted in the diet, dietary fat should merely be converted to ketone bodies and excreted. This so-called diet appears to work at first because a low-carbohydrate diet results in an initial water (and weight) loss. This occurs because glycogen reserves are depleted by the diet and because about 3 grams of water of hydration are lost for every gram of glycogen.

However, the long-term results of this diet are usually disappointing for several reasons. First, ketone body excretion by the human body usually does not exceed 20 grams (400 kJ) per day. Second, amino acids can function effectively to replenish TCA cycle intermediates, making the reduced carbohydrate regimen irrelevant. Third, the typical fare in a high-protein, high-fat, low-carbohydrate diet is expensive but not very tasty, and it is thus difficult to maintain. Finally, a high-fat diet is a high risk factor for atherosclerosis and coronary artery disease.

acid can by synthesized in humans only from linoleic acid, so it too is classified as essential. The essential fatty acids are key components of biological membranes, and arachidonic acid is the precursor to prostaglandins, which mediate a variety of processes in the body.

Fiber

The components of food materials that cannot be broken down by human digestive enzymes are referred to as **dietary fiber.** There are several kinds of dietary fiber, each with its own chemical and biological properties. **Cellulose** and **hemicellulose** are insoluble fiber materials that stimulate regular function of the colon. They may play a role in reducing the risk of colon cancer. **Lignins** make up another class of insoluble fibers which absorb organic molecules in the digestive system. Lignins bind cholesterol and clear it from the digestive system, reducing the risk of heart disease. Pectins and gums are water-soluble fiber materials that form viscous gel-like suspensions in the digestive system, slowing the rate of absorption of many nutrients, including carbohydrates, and lowering serum cholesterol in many cases. The insoluble fibers are prevalent in vegetable grains. Water-soluble fiber is a component of fruits, legumes, and oats.

SPECIAL FOCUS:
VITAMINS

Vitamins are essential nutrients that are required in the diet, usually in trace amounts, because they cannot be synthesized by the organism itself. The requirement for any given vitamin depends on the organism. Not all "vitamins" are required by all organisms. Vitamins required in the human diet are listed in Table 18.4. These important substances are traditionally distinguished as being either water-soluble or fat-soluble. Except for vitamin C (ascorbic acid), the water-soluble vitamins are all components or precursors of important biological substances known as **coenzymes.** These are low-molecular-weight molecules that bring unique chemical functionality to certain enzyme reactions. Coenzymes may also act as *carriers* of specific functional groups, such as methyl groups and acyl groups. The side chains of the common amino acids provide only a limited range of chemical reactivities and carrier properties. Coenzymes, acting in concert with appropriate enzymes, provide a broader range of catalytic properties for the reactions of metabolism. Coenzymes are typically modified by these reactions and are then converted back to their original forms by other enzymes, so that small amounts of these substances can be used repeatedly. The coenzymes derived from the water-soluble vitamins are listed in Table 18.4. Each of these will be discussed in this chapter. The fat-soluble vitamins are not directly related to coenzymes, but they play essential roles in a variety of critical biological processes, including vision, maintenance of bone structure, and blood coagulation. The mechanisms of action of fat-soluble vitamins are not as well understood as their water-soluble counterparts, but modern research efforts are gradually closing this gap.

Vitamin B$_1$: Thiamine and Thiamine Pyrophosphate

As shown in Figure 18.17, thiamine is composed of a substituted *thiazole* ring joined to a substituted pyrimidine by a methylene bridge. It is the precursor of **thiamine pyrophosphate (TPP),** a coenzyme involved in reactions of carbo-

Table 18.4

Vitamins and Coenzymes	
Vitamin	Coenzyme Form
Water-Soluble	
Thiamine (vitamin B_1)	Thiamine pyrophosphate
Niacin (nicotinic acid)	Nicotinamide adenine dinucleotide (NAD^+)
	Nicotinamide adenine dinucleotide phosphate ($NADP^+$)
Riboflavin (vitamin B_2)	Flavin adenine dinucleotide (FAD)
	Flavin mononucleotide (FMN)
Pantothenic acid	Coenzyme A
Pyridoxal, pyridoxine, pyridoxamine (vitamin B_6)	Pyridoxal phosphate
Cobalamin (vitamin B_{12})	5′-Deoxyadenosylcobalamin
	Methylcobalamin
Biotin	Biotin-lysine complexes (biocytin)
Lipoic acid	Lipoyl-lysine complexes (lipoamide)
Folic acid	Tetrahydrofolate
Fat-Soluble	
Retinol (vitamin A)	
Ergocalciferol (vitamin D_2)	
Cholecalciferol (vitamin D_3)	
α-Tocopherol (vitamin E)	
Vitamin K	

hydrate metabolism in which bonds to carbonyl carbons (aldehydes or ketones) are synthesized or cleaved. In particular, the *decarboxylations of α-keto acids and the formation and cleavage of α-hydroxyketones* depend on thiamine pyrophosphate. The first of these is illustrated in Figure 18.18 by (a) the decarboxylation of pyruvate by **yeast pyruvate decarboxylase** to yield carbon dioxide and acetaldehyde. An example of the formation and cleavage of α-hydroxyketones is presented in Figure 18.18 (b) the condensation of two molecules of pyruvate in the **acetolactate synthase** reaction. Another example is provided by a reaction from the pentose phosphate pathway (Chapters 22 and 23) called the **transketolase** reaction. This latter reaction is referred to as an **α-ketol transfer** for obvious reasons.

Thiamine (vitamin B_1)

Thiamine pyrophosphate (TPP)
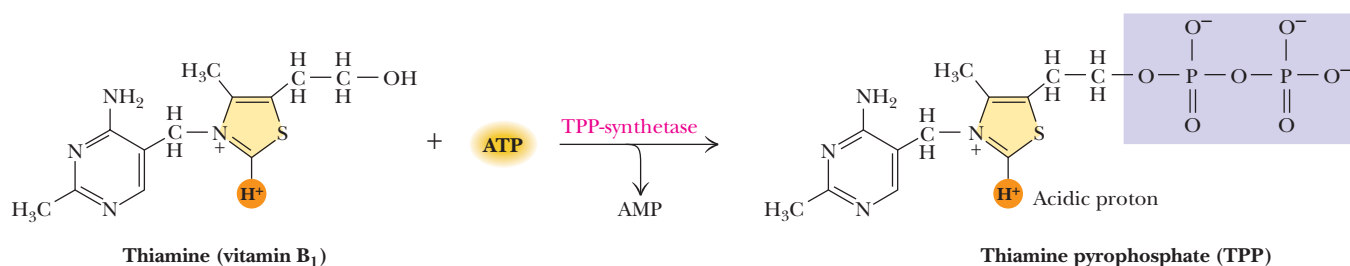
FIGURE 18.17 • Thiamine pyrophosphate (TPP), the active form of vitamin B_1, is formed by the action of TPP-synthetase.

(a)

An α-cleavage reaction

$$CH_3-\overset{\overset{\displaystyle O}{\|}}{C}-\boxed{COO^-} \xrightarrow[\text{decarboxylase}]{\text{Pyruvate}} CH_3-\overset{\overset{\displaystyle O}{\|}}{C}-H \ + \ CO_2$$

(b)

An α-condensation reaction

$$CH_3-\overset{\overset{\displaystyle O}{\|}}{C}-\boxed{COO^-} \ + \ CH_3-\overset{\overset{\displaystyle O}{\|}}{C}-COO^- \xrightarrow[\text{synthase}]{\text{Acetolactate}} CH_3-\overset{\overset{\displaystyle O}{\|}}{C}-\overset{\overset{\displaystyle OH}{|}}{\underset{\underset{\displaystyle CH_3}{|}}{C}}-COO^- \ + \ CO_2$$
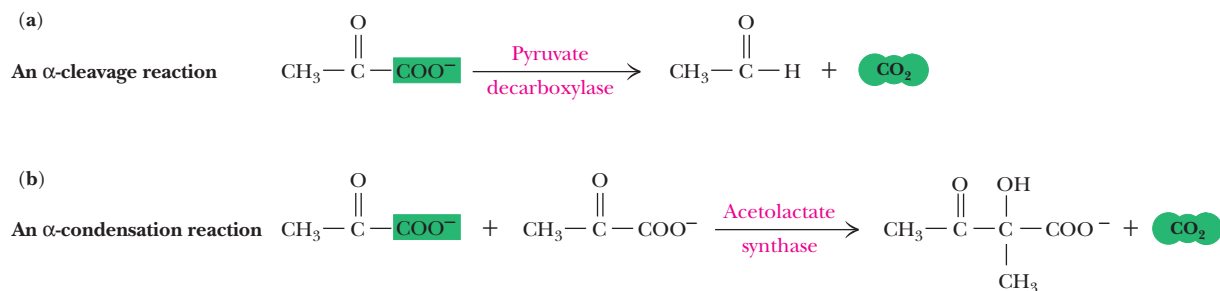
FIGURE 18.18 • Thiamine pyrophosphate participates in (a) the decarboxylation of α-keto acids and (b) the formation and cleavage of α-hydroxyketones.

Vitamins Containing Adenine Nucleotides

Several classes of vitamins are related to, or are precursors of, coenzymes that contain adenine nucleotides as part of their structure. These coenzymes include the flavin dinucleotides, the pyridine dinucleotides, and coenzyme A. The adenine nucleotide portion of these coenzymes does not participate actively in the reactions of these coenzymes; rather, it enables the proper enzymes to recognize the coenzyme. Specifically, the adenine nucleotide greatly increases both the *affinity* and the *specificity* of the coenzyme for its site on the enzyme, owing to its numerous sites for hydrogen bonding, and also the hydrophobic and ionic bonding possibilities it brings to the coenzyme structure.

Nicotinic Acid and the Nicotinamide Coenzymes

Nicotinamide is an essential part of two important coenzymes: **nicotinamide adenine dinucleotide (NAD$^+$)** and **nicotinamide adenine dinucleotide phosphate (NADP$^+$)** (Figure 18.19). The reduced forms of these coenzymes are NADH and NADPH. *The nicotinamide coenzymes (also known as pyridine nucleotides) are **electron carriers**.* They play vital roles in a variety of enzyme-catalyzed oxidation–reduction reactions. (NAD$^+$ is an electron acceptor in oxidative (catabolic) pathways and NADPH is an electron donor in reductive (biosynthetic) pathways.) These reactions involve direct transfer of hydride anion either to NAD(P)$^+$ or from NAD(P)H. The enzymes that facilitate such

$\mathcal{H}$UMAN BIOCHEMISTRY

Thiamine and Beriberi

Thiamine, whose structure is shown in Figure 18.17, is known as vitamin B$_1$ and is essential for the prevention of **beriberi,** a nervous system disease that has occurred in the Far East for centuries and has resulted in considerable sickness and death in these countries. (As recently as 1958, it was the fourth leading cause of death in the Philippine Islands.) It was shown in 1882 by the director-general of the medical department of the Japanese navy that beriberi could be prevented by dietary modifications. Ten years later, Christiaan Eijkman, a Dutch medical scientist working in Java, began research that eventually showed that thiamine was the

"anti-beriberi" substance. He found that chickens fed polished rice exhibited paralysis and head retractions and that these symptoms could be reversed if the rice polishings (the outer layers and embryo of the rice kernel) were fed to the birds. In 1911, Casimir Funk prepared a crystalline material from rice bran that cured beriberi in birds. He named it **beriberi vitamine,** because he viewed it as a "vital amine," and thus he is credited with coining the word *vitamin.* The American biochemist R. R. Williams and his research group were the first to establish the structure of thiamine (in 1935) and a route for its synthesis.
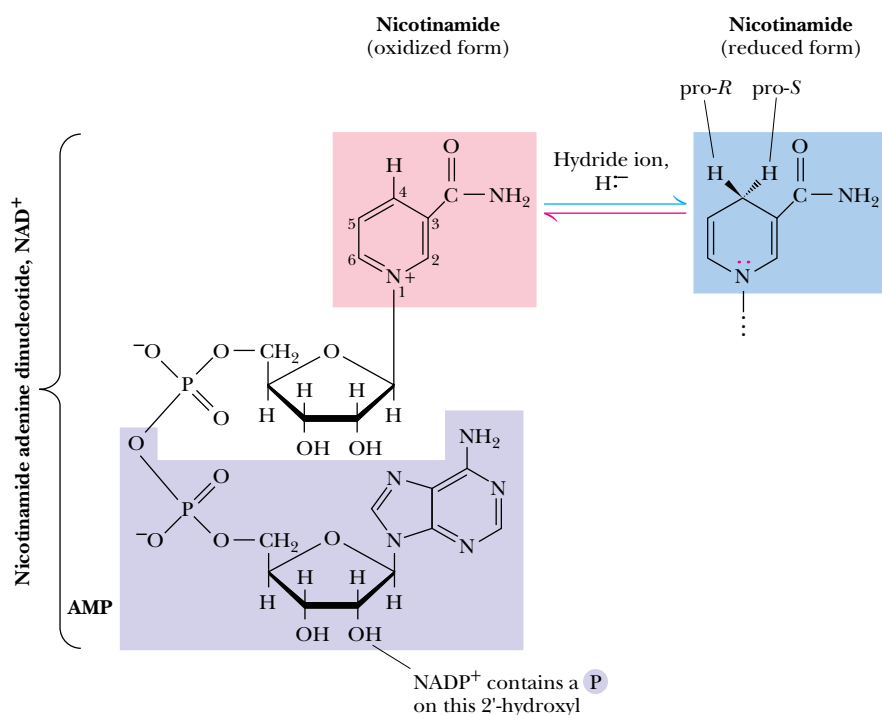
FIGURE 18.19 • The structures and redox states of the nicotinamide coenzymes. Hydride ion ($H:^-$, a proton with two electrons) transfers to NAD^+ to produce NADH.

transfers are thus known as **dehydrogenases.** The hydride anion contains two electrons, and thus NAD^+ and $NADP^+$ act exclusively as **two-electron carriers.** The C-4 position of the pyridine ring, which can either accept or donate hydride ion, is the reactive center of both NAD and NADP. The quaternary nitrogen of the nicotinamide ring functions as an electron sink to facilitate hydride transfer to NAD^+, as shown in Figure 18.20. The adenine portion of the molecule is not directly involved in redox processes.
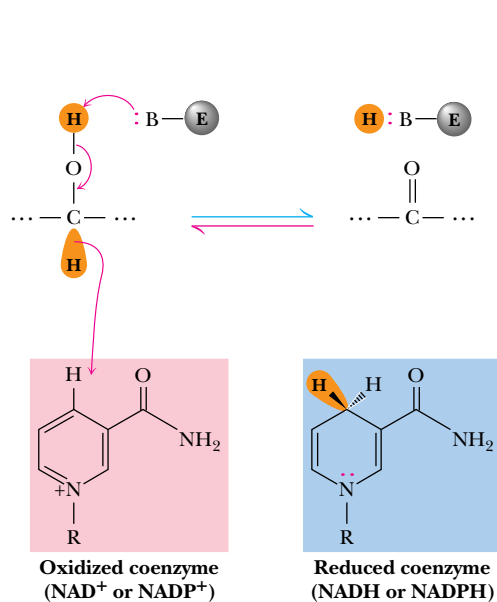
FIGURE 18.20 • NAD^+ and $NADP^+$ participate exclusively in two-electron transfer reactions. For example, alcohols can be oxidized to ketones or aldehydes via hydride transfer to $NAD(P)^+$.

ℋUMAN BIOCHEMISTRY

Niacin and Pellegra

Pellegra, a disease characterized by dermatitis, diarrhea, and dementia, has been known for centuries. It was once prevalent in the southern part of the United States and is still a common problem in some parts of Spain, Italy, and Romania. Pellegra was once thought to be an infectious disease, but Joseph Goldberger showed early in this century that it could be cured by dietary actions. Soon thereafter, it was found that brewer's yeast would prevent pellegra in humans. Studies of a similar disease in dogs, called **blacktongue,** eventually led to the identification of **nicotinic acid** as the relevant dietary factor. Elvehjem and his colleagues at the University of Wisconsin in 1937 isolated **nicotinamide** from liver, and showed that it and nicotinic acid could prevent and cure blacktongue in dogs. That same year, nicotin-

amide and nicotinic acid were both shown to be able to cure pellegra in humans. Interestingly, plants and many animals can synthesize nicotinic acid from tryptophan and other precursors, and nicotinic acid is thus not a true vitamin for these species. However, if dietary intake of tryptophan is low, nicotinic acid is required for optimal health. Nicotinic acid, which is beneficial to humans and animals, is structurally related to **nicotine,** a highly toxic tobacco alkaloid. In order to avoid confusion of nicotinic acid and nicotinamide with nicotine itself, **niacin** was adopted as a common name for nicotinic acid. Cowgill, at Yale University, suggested the name from the letters of three words—*ni*cotinic, *ac*id, and vitam*in*.
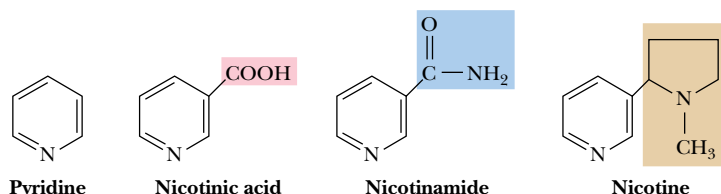
The structures of pyridine, nicotinic acid, nicotinamide, and nicotine.

Examination of the structures of NADH and NADPH reveals that the 4-position of the nicotinamide ring is **pro-chiral,** meaning that while this carbon is not chiral, it *would* be if either of its hydrogens were replaced by something else. As shown in Figure 18.20, the hydrogen "projecting" out of the page toward you is the "pro-*R*" hydrogen because, if a deuterium is substituted at this position, the molecule would have the *R*-configuration. Substitution of the other hydrogen would yield an *S*-configuration. An interesting aspect of the enzymes that require nicotinamide coenzymes is that they are **stereospecific** and withdraw hydrogen from either the pro-*R* or the pro-*S* position selectively. This stereospecificity arises from the fact that enzymes (and the active sites of enzymes) are inherently asymmetric structures. These same enzymes are stereospecific with respect to the substrates as well.

The NAD- and NADP-dependent dehydrogenases catalyze at least six different types of reactions: simple hydride transfer, deamination of an amino acid to form an α-keto acid, oxidation of β-hydroxy acids followed by decarboxylation of the β-keto acid intermediate, oxidation of aldehydes, reduction of isolated double bonds, and the oxidation of carbon–nitrogen bonds (as with dihydrofolate reductase).

Riboflavin and the Flavin Coenzymes

Riboflavin, or **vitamin B$_2$,** is a constituent and precursor of both **riboflavin 5′-phosphate,** also known as **flavin mononucleotide (FMN),** and **flavin adenine dinucleotide (FAD).** The name *riboflavin* is a synthesis of the names for the molecule's component parts, **ribitol** and **flavin.** The structures of riboflavin,
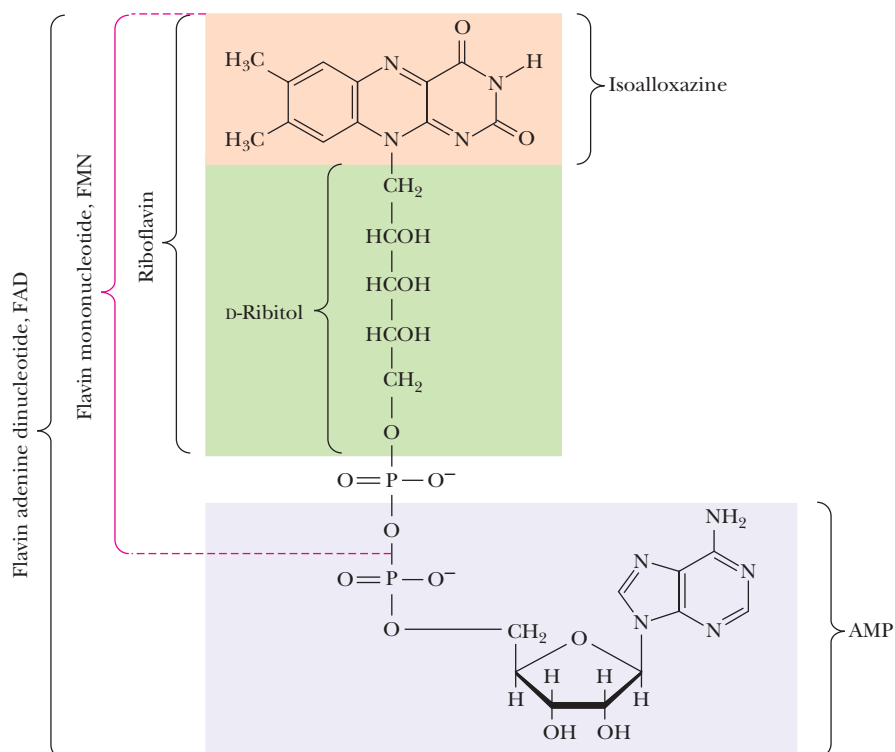
FIGURE 18.21 • The structures of riboflavin, flavin mononucleotide (FMN), and flavin adenine dinucleotide (FAD). Flavin coenzymes bind tightly to the enzymes that use them, with typical dissociation constants in the range of 10^{-8} to 10^{-11} *M,* so that only very low levels of free flavin coenzymes occur in most cells. Even in organisms that rely on the nicotinamide coenzymes (NADH and NADPH) for many of their oxidation–reduction cycles, the flavin coenzymes fill essential roles. Flavins are stronger oxidizing agents than NAD^+ and $NADP^+$. They can be reduced by both one-electron and two-electron pathways and can be reoxidized easily by molecular oxygen. Enzymes that use flavins to carry out their reactions—*flavoenzymes*—are involved in many kinds of oxidation–reduction reactions.

FMN, and FAD are shown in Figure 18.21. The *isoalloxazine ring* is the core structure of the various flavins. Because the ribityl group is not a true pentose sugar (it is a sugar alcohol) and is not joined to riboflavin in a glycosidic bond, the molecule is not truly a "nucleotide," and the terms *flavin mononucleotide* and *dinucleotide* are incorrect. Nonetheless, these designations are so deeply ingrained in common biochemical usage that the erroneous nomenclature persists. The flavins have a characteristic bright yellow color and take their name from the Latin *flavus* for "yellow." As shown in Figure 18.22, the oxidized form of the isoalloxazine structure absorbs light around 450 nm (in the visible region) and also at 350 to 380 nm. The color is lost, however, when the ring is reduced or "bleached." Similarly, the enzymes that bind flavins, known as **flavoenzymes,** can be yellow, red, or green in their oxidized states. Nevertheless, these enzymes also lose their color on reduction of the bound flavin group.

Flavin coenzymes can exist in any of three different redox states. Fully oxidized flavin is converted to a **semiquinone** by a one-electron transfer, as shown in Figure 18.22. At physiological pH, the semiquinone is a neutral radical, blue in color, with a λ_{max} of 570 nm. The semiquinone possesses a pK_a of about 8.4. When it loses a proton at higher pH values, it becomes a radical anion, displaying a red color with a λ_{max} of 490 nm. The semiquinone radical is particularly stable, owing to extensive delocalization of the unpaired electron across the π-electron system of the isoalloxazine. A second one-electron transfer converts the semiquinone to the completely reduced dihydroflavin as shown in Figure 18.22.

Access to three different redox states allows flavin coenzymes to participate in *one-electron transfer* and *two-electron transfer reactions*. Partly because of this, flavoproteins catalyze many different reactions in biological systems and work together with many different electron acceptors and donors. These include two-electron acceptor/donors, such as NAD^+ and $NADP^+$, one- or two-elec-

Oxidized form
$\lambda_{max} = 450$ nm
(yellow)

Reduced form
(colorless)

FAD or FMN

FADH$_2$ or FMNH$_2$

Semiquinone form
$\lambda_{max} = 570$ nm
(blue)

Semiquinone anion
$\lambda_{max} = 490$ nm
(red)

FADH or FMNH

$pK_a \cong 8.4$
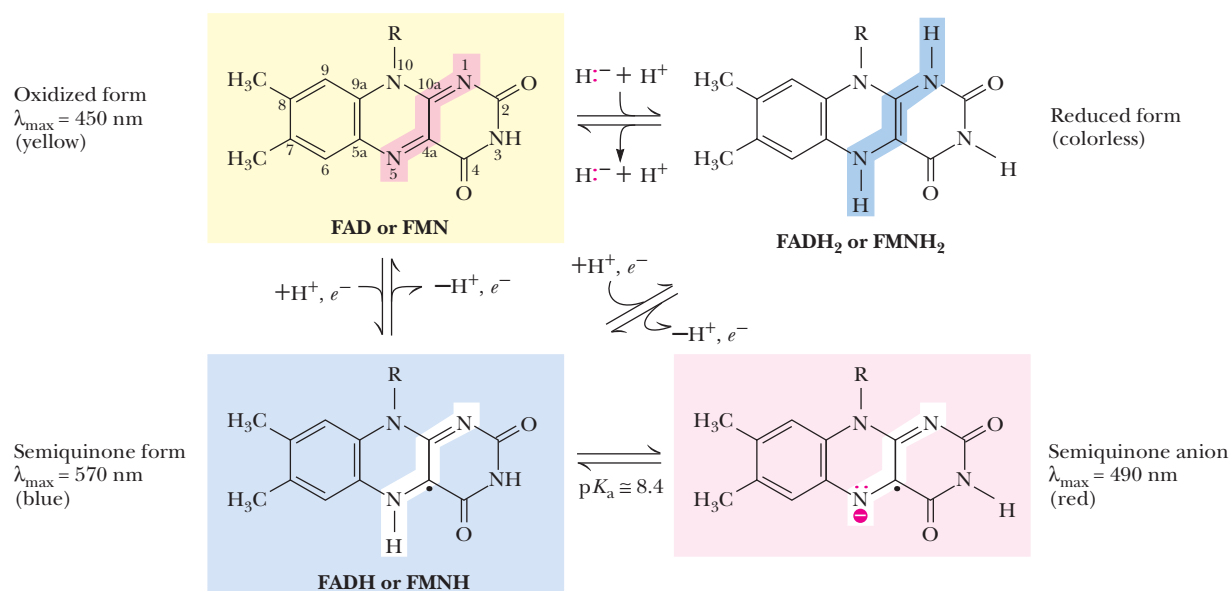
FIGURE 18.22 • The redox states of FAD and FMN. The boxes correspond to the colors of each of these forms. The atoms primarily involved in electron transfer are indicated by red shading in the oxidized form, white in the semiquinone form, and blue in the reduced form.

tron carriers, such as quinones, and a variety of one-electron acceptor/donors, such as cytochrome proteins. Many of the components of the respiratory electron transport chain are one-electron acceptor/donors. The stability of the flavin semiquinone state allows flavoproteins to function as effective electron carriers in respiration processes (Chapter 21).

𝒜 D E E P E R   L O O K

Riboflavin and Old Yellow Enzyme

Riboflavin was first isolated from whey in 1879 by Blyth, and the structure was determined by Kuhn and coworkers in 1933. For the structure determination, this group isolated 30 mg of pure riboflavin from the whites of about 10,000 eggs. The discovery of the actions of riboflavin in biological systems arose from the work of Otto Warburg in Germany and Hugo Theorell in Sweden, both of whom identified yellow substances bound to a yeast enzyme involved in the oxidation of pyridine nucleotides. Theorell showed that riboflavin 5′-phosphate was the source of the yellow color in this *old yellow enzyme.* By 1938, Warburg had identified FAD, the second common form of riboflavin, as the coenzyme in D-amino acid oxidase, another yellow protein. Riboflavin deficiencies are not at all common. Humans require only about 2 mg per day, and the vitamin is prevalent in many foods. This vitamin

is extremely light sensitive, and it is degraded in foods (milk, for example) left in the sun.

The milling and refining of wheat, rice, and other grains causes a loss of riboflavin and other vitamins. In order to correct and prevent dietary deficiencies, the Committee on Food and Nutrition of the National Research Council began in the 1940s to recommend enrichment of cereal grains sold in the United States. Thiamine, riboflavin, niacin, and iron were the first nutrients originally recommended for enrichment by this group. As a result of these actions, generations of American children have become accustomed to reading (on their cereal boxes and bread wrappers) that their foods contain certain percentages of the "U.S. Recommended Daily Allowance" of various vitamins and nutrients.

FIGURE 18.23 • The structure of coenzyme A. Acyl groups form thioester linkages with the —SH group of the β-mercaptoethylamine moiety.

Pantothenic Acid and Coenzyme A

Pantothenic acid, sometimes called vitamin B_3, is a vitamin that makes up one part of a complex coenzyme called **coenzyme A (CoA)** (Figure 18.23). Pantothenic acid is also a constituent of **acyl carrier proteins.** Coenzyme A consists of 3′,5′-adenosine bisphosphate joined to 4-phosphopantetheine in a phosphoric anhydride linkage. Phosphopantetheine in turn consists of three parts: β-mercaptoethylamine linked to β-alanine, which makes an amide bond with a branched-chain dihydroxy acid. As was the case for the nicotinamide and flavin coenzymes, the adenine nucleotide moiety of CoA acts as a recognition site, increasing the affinity and specificity of CoA binding to its enzymes.

The two main functions of coenzyme A are

   (a) *activation of acyl groups for transfer by nucleophilic attack* and
   (b) *activation of the α-hydrogen of the acyl group for abstraction as a proton.*

Both of these functions are mediated by the reactive sulfhydryl group on CoA, which forms **thioester** linkages with acyl groups.

The activation of acyl groups for transfer by CoA can be appreciated by comparing the hydrolysis of the thioester bond of acetyl-CoA with hydrolysis of a simple oxygen ester:

$$\text{Ethyl acetate} + H_2O \longrightarrow \text{acetate} + \text{ethanol} + H^+ \quad \Delta G^{\circ\prime} = -20.0 \text{ kJ/mol}$$

$$\text{Acetyl-SCoA} + H_2O \longrightarrow \text{acetate} + \text{CoA-SH} + H^+ \quad \Delta G^{\circ\prime} = -31.5 \text{ kJ/mol}$$

Hydrolysis of the thioester is more favorable than that of oxygen esters, presumably because the carbon–sulfur bond has less double bond character than the corresponding carbon–oxygen bond. This means that transfer of the acetyl group from acetyl-CoA to a given nucleophile (Figure 18.24) will be more spontaneous than transfer of an acetyl group from an oxygen ester. For this reason, acetyl-CoA is said to have a high group-transfer potential.

The 4-phosphopantetheine group of CoA is also utilized (for essentially the same purposes) in **acyl carrier proteins (ACPs)** involved in fatty acid biosynthesis (see Chapter 25). In acyl carrier proteins, the 4-phosphopantetheine is covalently linked to a serine hydroxyl group. Pantothenic acid is an essential factor for the metabolism of fat, protein, and carbohydrates in the tricarboxylic acid cycle and other pathways. In view of its universal importance in metabolism, it is surprising that pantothenic acid deficiencies are not a more serious problem in humans, but this vitamin is abundant in almost all foods, so that deficiencies are rarely observed.
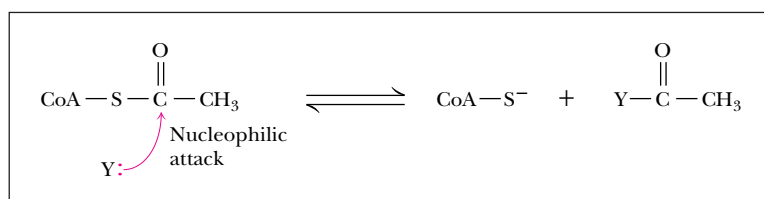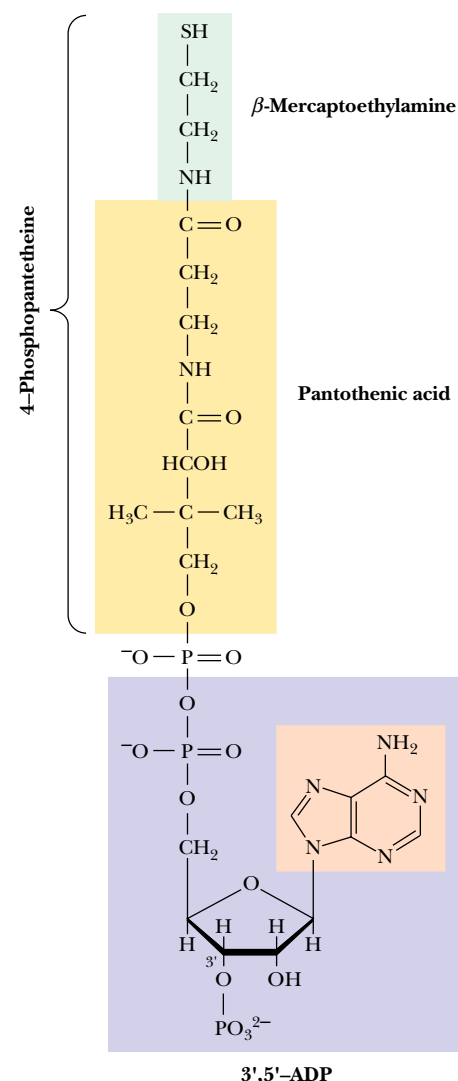
FIGURE 18.24 • Acyl transfer from acyl-CoA to a nucleophile is more favorable than transfer of an acyl group from an oxygen ester.

$\mathscr{A}$ DEEPER LOOK

Fritz Lipmann and Coenzyme A

Pantothenic acid is found in extracts from nearly all plants, bacteria, and animals, and the name derives from the Greek *pantos,* meaning "everywhere." It is required in the diet of all vertebrates, but some microorganisms produce it in the rumens of animals such as cattle and sheep. This vitamin is widely distributed in foods common to the human diet, and deficiencies are only observed in cases of severe malnutrition. The eminent German–born biochemist Fritz Lipmann was the first to show that a coenzyme was required to facilitate biological acetylation reactions. (The "A" in

coenzyme A in fact stands for *acetylation*.) In studies of acetylation of sulfanilic acid (chosen because of a favorable colorimetric assay) by liver extracts, Lipmann found that a heat-stable cofactor was required. Eventually Lipmann isolated and purified the required cofactor—coenzyme A—from both liver and yeast. For his pioneering work in elucidating the role of this important coenzyme, Fritz Lipmann received the Nobel Prize in physiology or medicine in 1953.

Vitamin B_6: Pyridoxine and Pyridoxal Phosphate

The biologically active form of vitamin B_6 is **pyridoxal-5-phosphate (PLP),** a coenzyme that exists under physiological conditions in two tautomeric forms (Figure 18.25). PLP participates in the catalysis of a wide variety of reactions involving amino acids, including transaminations, α- and β-decarboxylations, β- and γ-eliminations, racemizations, and aldol reactions (Figure 18.26). Note that these reactions include cleavage of any of the bonds to the amino acid alpha carbon, as well as several bonds in the side chain. The remarkably versatile chemistry of PLP is due to its ability to

(a) *form stable Schiff base (aldimine) adducts with α-amino groups of amino acids,* and

(b) *act as an effective electron sink to stabilize reaction intermediates.*

The Schiff base formed by PLP and its role as an electron sink are illustrated in Figure 18.27. In nearly all PLP-dependent enzymes, PLP in the absence of substrate is bound in a Schiff base linkage with the ϵ-NH_2 group of an active site lysine. Rearrangement to a Schiff base with the arriving substrate is a **transaldiminization** reaction. One key to PLP chemistry is the protonation of the Schiff base, which is stabilized by H bonding to the ring oxygen, increasing the acidity of the C_α proton [as shown in (3) of Figure 18.27]. The carbanion formed by loss of the C_α proton is stabilized by electron delocalization into the pyridinium ring, with the positively charged ring nitrogen acting as an electron sink. Another important intermediate is formed by protonation of the aldehyde carbon of PLP. As shown, this produces a new substrate–PLP Schiff base, which plays a role in transamination reactions and increases the acidity of the proton at C_β, a feature important in γ-elimination reactions.

The versatile chemistry of pyridoxal phosphate offers a rich learning experience for the student of mechanistic chemistry. William Jencks, in his classic text, *Catalysis in Chemistry and Enzymology,* writes:

> It has been said that God created an organism especially adapted to help the biologist find an answer to every question about the physiology of living systems; if this is so it must be concluded that pyridoxal phosphate was created to provide satisfaction and enlightenment to those enzymologists and chemists who enjoy pushing electrons, for no other coenzyme is involved in such a wide variety of reactions, in both enzyme and model systems, which can be reasonably interpreted in terms of the chemical properties of the coenzyme. Most of
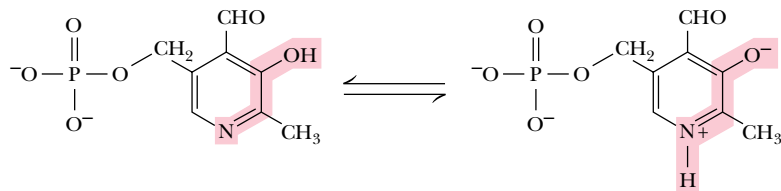
FIGURE 18.25 • The tautomeric forms of pyridoxal-5-phosphate (PLP).
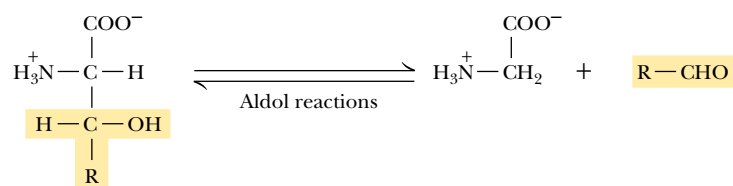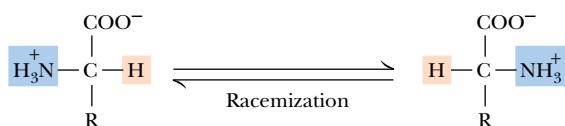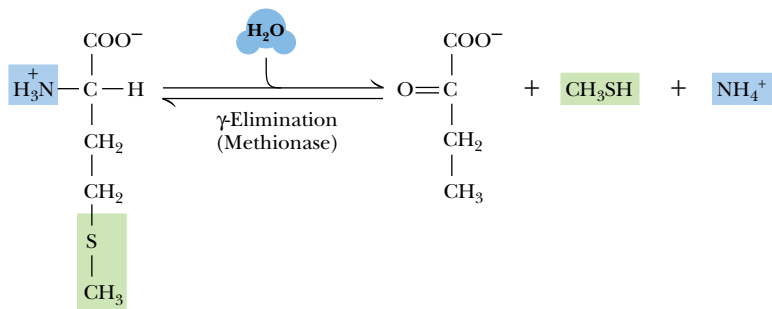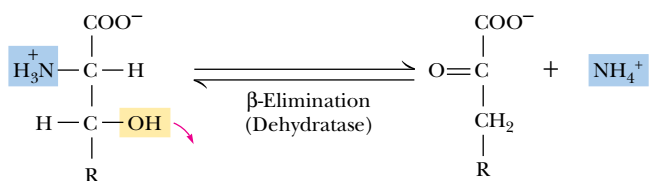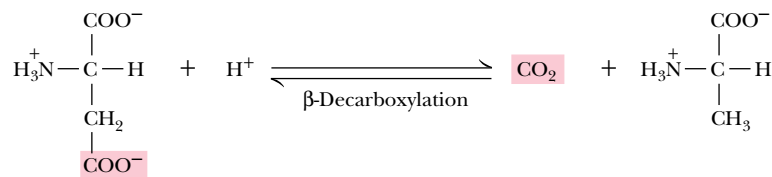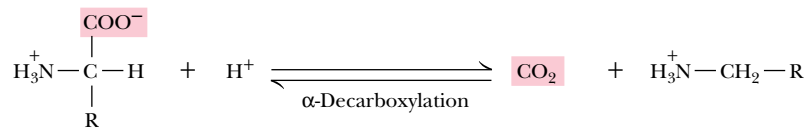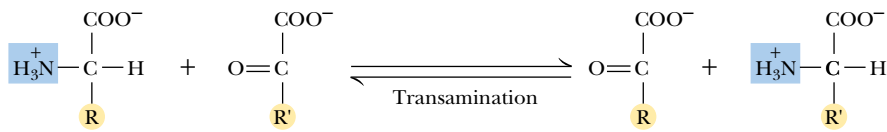
FIGURE 18.26 • The seven classes of reactions catalyzed by pyridoxal-5-phosphate.
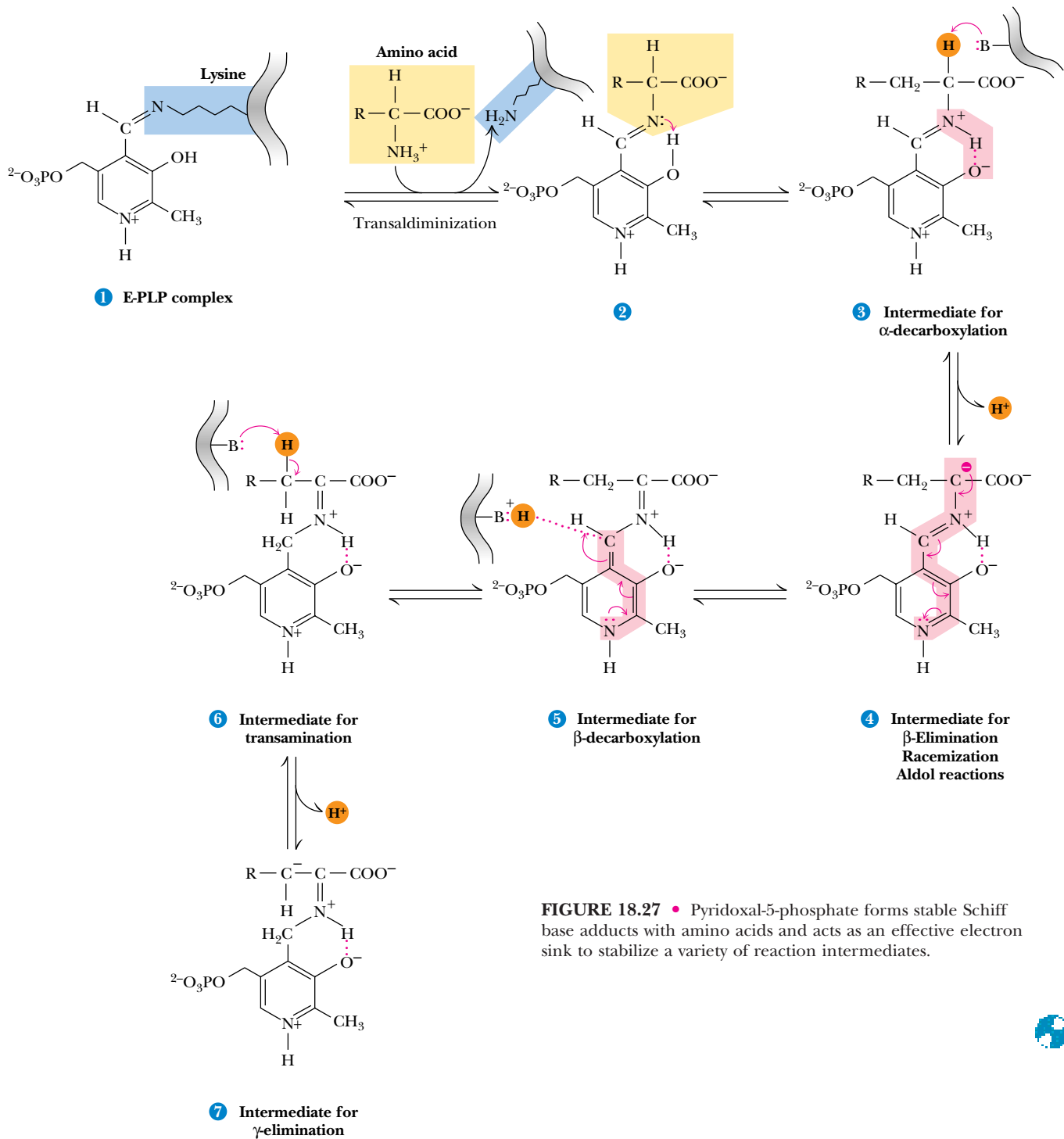
FIGURE 18.27 • Pyridoxal-5-phosphate forms stable Schiff base adducts with amino acids and acts as an effective electron sink to stabilize a variety of reaction intermediates.

these reactions are made possible by a common structural feature. That is, electron withdrawal toward the cationic nitrogen atom of the imine and into the electron sink of the pyridoxal ring from the α carbon atom of the attached amino acid activates all three of the substituents on this carbon atom for reactions which require electron withdrawal from this atom.[1]

[1]Jencks, William P., 1969. *Catalysis in Chemistry and Enzymology.* New York: McGraw-Hill.

𝒜 D E E P E R   L O O K

Vitamin B₆

Goldberger and Lillie in 1926 found that rats fed certain nutritionally deficient diets developed **dermatitis acrodynia,** a skin disorder characterized by edema and lesions of the ears, paws, nose, and tail. Szent-Györgyi later found that a factor he had isolated prevented these skin lesions in the rat. He proposed the name **vitamin B₆** for his factor. **Pyridoxine,** a form of this vitamin found in plants (and the form of B₆ sold commercially), was isolated in 1938 by three research groups working independently. **Pyridoxal** and **pyridoxamine,** the forms that predominate in animals, were identified in 1945. A metabolic role for pyridoxal was postulated by Esmond Snell, who had shown that when pyridoxal was heated with glutamate (in the absence of any enzymes), the amino group of glutamate was transferred to pyridoxal, forming pyridoxamine. Snell postulated (correctly) that pyridoxal might be a component of a coenzyme needed for transamination reactions in which the α-amino group of an amino acid is transferred to the α-carbon of an α-keto acid.
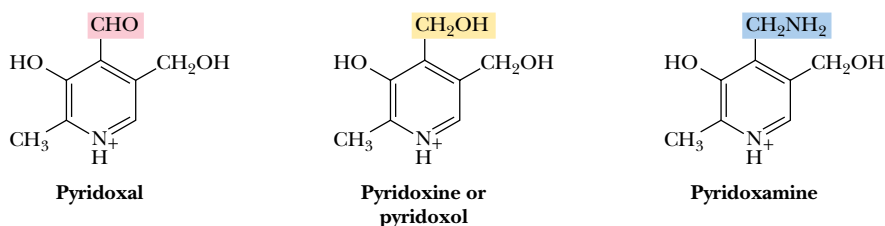
The structures of pyridoxal, pyridoxine, and pyridoxamine.

Vitamin B₁₂: Cyanocobalamin

Vitamin B₁₂, or **cyanocobalamin,** is converted in the body into two coenzymes. The predominant coenzyme form is **5′-deoxyadenosylcobalamin** (Figure 18.28), but smaller amounts of **methylcobalamin** also exist in liver, for example. The crystal structure of 5′-deoxyadenosylcobalamin was determined by X-ray diffraction in 1961 by Dorothy Hodgkin and coworkers in England. The structure consists of a *corrin ring* with a *cobalt ion* in the center. The corrin ring, with four *pyrrole groups,* is similar to the heme prophyrin ring, except that two of the pyrrole rings are linked directly. Methylene bridges form the other pyrrole–pyrrole linkages, as for porphyrin. The cobalt is coordinated to the four (planar) pyrrole nitrogens. One of the axial cobalt ligands is a nitrogen of the dimethylbenzimidazole group. The other axial cobalt ligand may be —CN, —CH₃, —OH, or the 5′-carbon of a 5′-deoxyadenosyl group, depending on the form of the coenzyme. The most striking feature of Hodgkin's structure of 5′-deoxyadenosylcobalamin is the cobalt–carbon bond distance of 0.205 nm. *This bond is predominantly covalent* and the structure is actually an **alkyl cobalt.** Such alkyl cobalts were thought to be highly unstable until Hodgkin's pioneering X-ray study. The Co–carbon–carbon bond angle of 130 degrees indicates partial ionic character.

The B₁₂ coenzymes participate in three types of reactions (Figure 18.29):

1. *Intramolecular rearrangements*
2. *Reductions of ribonucleotides to deoxyribonucleotides* (in certain bacteria)
3. *Methyl group transfers*

FIGURE 18.28 • The structure of cyanocobalamin *(top)* and simplified structures showing several coenzyme forms of vitamin B$_{12}$. The Co—C bond of 5′-deoxyadenosylcobalamin is predominantly covalent (note the short bond length of 0.205 nm) but with some ionic character. Note that the convention of writing the cobalt atom as Co^{3+} attributes the electrons of the Co—C and Co—N bonds to carbon and nitrogen, respectively.

Dimethylbenzimidazole (DMBz)

Cyanocobalamin

Cyanocobalamin
Vitamin B$_{12}$

5′-Deoxyadenosylcobalamin

Methylcobalamin

Hydroxocobalamin
Vitamin B$_{12b}$

Coenzyme Forms
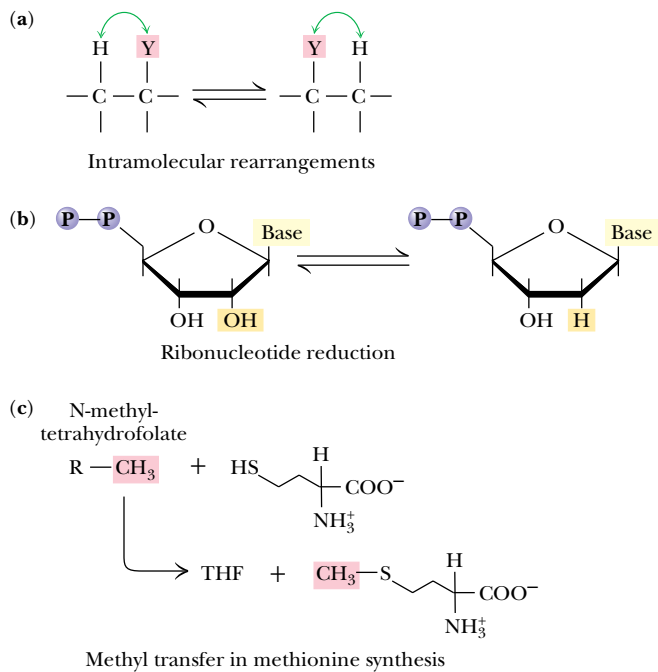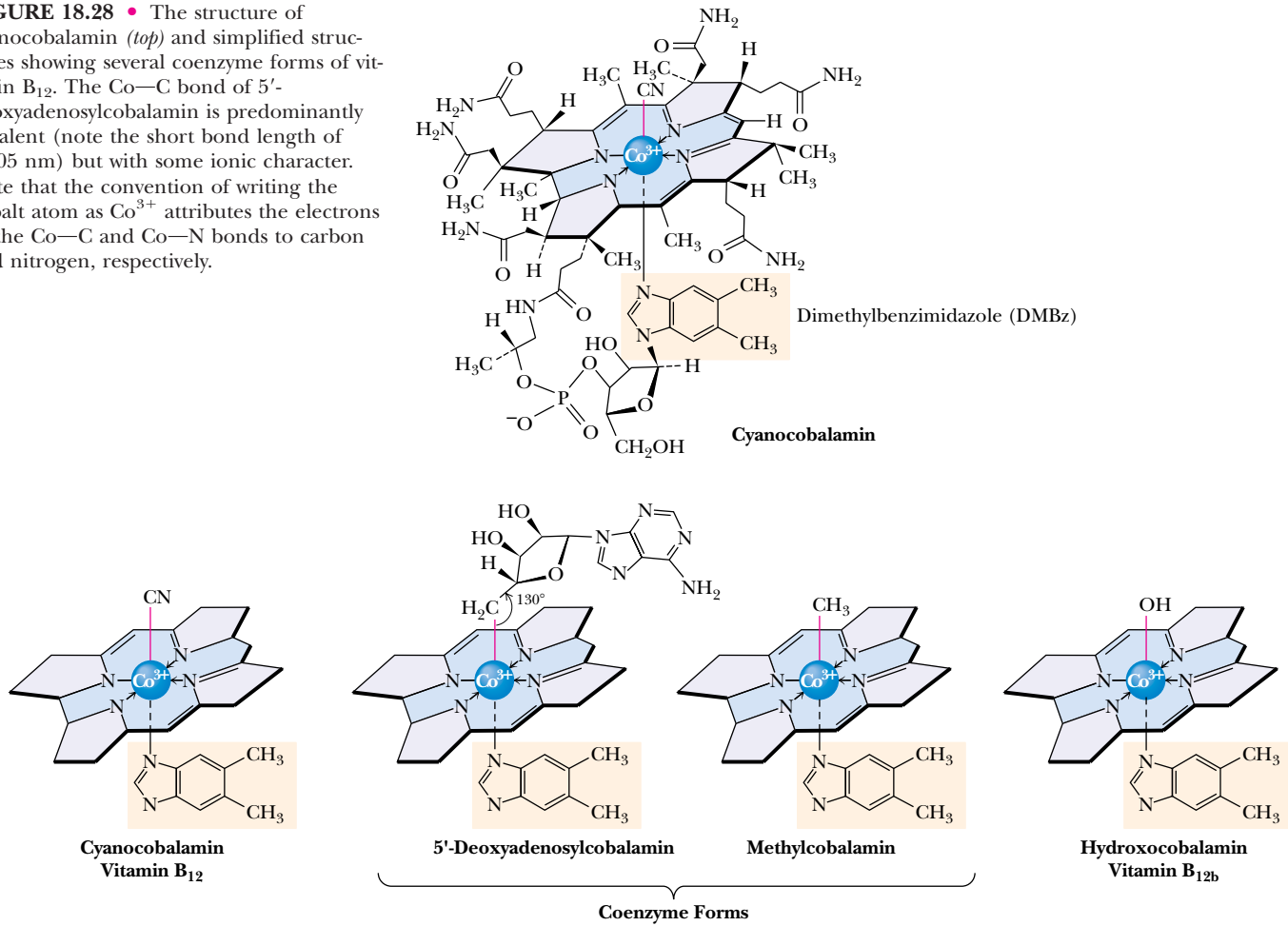
FIGURE 18.29 • Vitamin B$_{12}$ functions as a coenzyme in intramolecular rearrangements, reduction of ribonucleotides, and methyl group transfers.

(a)

Intramolecular rearrangements

(b)

Ribonucleotide reduction

(c)   N-methyl-tetrahydrofolate

Methyl transfer in methionine synthesis

$\mathcal{H}$UMAN BIOCHEMISTRY

Vitamin B$_{12}$ and Pernicious Anemia

The most potent known vitamin (that is, the one needed in the smallest amounts) was the last to be discovered. Vitamin B$_{12}$ is best known as the vitamin that prevents **pernicious anemia.** Minot and Murphy in 1926 demonstrated that such anemia could be prevented by eating large quantities of liver, but the active agent was not identified for many years. In 1948, Rickes and coworkers (in the United States) and Smith (in England) both reported the first successful isolation of vitamin B$_{12}$. West showed that injections of the vitamin induced dramatic beneficial responses in pernicious anemia patients. Eventually, two different crystalline preparations of the vitamin were distinguished. The first appeared to be true cyanocobalamin. The second showed the same biological activity as a cyanocobalamin, but had a different spectrum and was named **vitamin B$_{12b}$** and also **hydroxocobalamin.** It was eventually found that the cyanide group in cyanocobalamin originated from the charcoal used in the purification process!

Vitamin B$_{12}$ is not synthesized by animals or by plants. Only a few species of bacteria synthesize this complex substance. Carnivorous animals easily acquire sufficient amounts of B$_{12}$ from meat in their diet, but herbivorous creatures typically depend on intestinal bacteria to synthesize B$_{12}$ for them. This is sometimes not sufficient, and certain animals, including rabbits, occasionally eat their feces in order to accumulate the necessary quantities of B$_{12}$.

The nutritional requirement for vitamin B$_{12}$ is low. Adult humans require only about 3 micrograms per day, an amount easily acquired with normal eating habits. However, because plants do not synthesize vitamin B$_{12}$, pernicious anemia symptoms are sometimes observed in strict vegetarians.

The first two of these are mediated by 5′-deoxyadenosylcobalamin, whereas methyl transfers are effected by methylcobalamin. The mechanism of ribonucleotide reductase is discussed in Chapter 27. Methyl group transfers that employ *tetrahydrofolate* as a coenzyme are described later in this chapter.

Vitamin C: Ascorbic Acid

L-Ascorbic acid, better known as **vitamin C,** has the simplest chemical structure of all the vitamins (Figure 18.30). It is widely distributed in the animal and plant kingdoms, and only a few vertebrates—humans and other primates, guinea pigs, fruit-eating bats, certain birds, and some fish (rainbow trout, carp, and Coho salmon, for example)—are unable to synthesize it. In all these organisms, the inability to synthesize ascorbic acid stems from a lack of a liver enzyme, L-gulono-γ-lactone oxidase.

Ascorbic acid is a reasonably strong reducing agent. The biochemical and physiological functions of ascorbic acid most likely derive from its reducing properties—it functions as an electron carrier. Loss of one electron due to interactions with oxygen or metal ions leads to **semidehydro-L-ascorbate,** a reactive free radical (Figure 18.30) that can be reduced back to L-ascorbic acid by various enzymes in animals and plants. A characteristic reaction of ascorbic acid is its oxidation to *dehydro-L-ascorbic acid*. Ascorbic acid and dehydroascorbic acid form an effective redox system.

In addition to its role in preventing scurvy (see *Human Biochemistry box: Ascorbic Acid and Scurvy* and also Chapter 6), ascorbic acid also plays important roles in the brain and nervous system. It also mobilizes iron in the body, prevents anemia, ameliorates allergic responses, and stimulates the immune system.

L-Ascorbate free radical
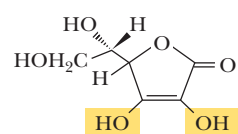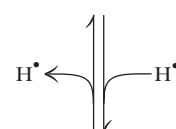
Ascorbic acid (Vitamin C)

Dehydro-L-ascorbic acid
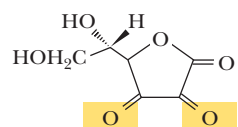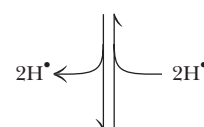
FIGURE 18.30 • The physiological effects of ascorbic acid (vitamin C) are the result of its action as a reducing agent. A two-electron oxidation of ascorbic acid yields dehydroascorbic acid.

$\mathscr{H}$UMAN BIOCHEMISTRY

Ascorbic Acid and Scurvy

Ascorbic acid is effective in the treatment and prevention of **scurvy,** a potentially fatal disorder characterized by anemia, alteration of protein metabolism, and weakening of collagenous structures in bone, cartilage, teeth, and connective tissues (see Chapter 6). Western world diets are now routinely so rich in vitamin C that it is easy to forget that scurvy affected many people in ancient Egypt, Greece, and Rome, and that, in the Middle Ages, it was endemic in northern Europe in winter when fresh fruits and vegetables were scarce. Ascorbic acid is a vitamin that has routinely altered the course of history, ending ocean voyages and military campaigns when food supplies became depleted of vitamin C and fatal outbreaks of scurvy occurred.

The isolation of ascorbic acid was first reported by Albert Szent-Györgyi (who called it *hexuronic acid*) in 1928. The structure was determined by Hirst and Haworth in 1933, and, simultaneously, Reichstein reported its synthesis. Haworth and Szent-Györgyi, who together suggested that the name be changed to L-ascorbic acid to describe its **antiscorbutic** (antiscurvy) activity, were awarded the Nobel Prize in 1937 for their studies of vitamin C.
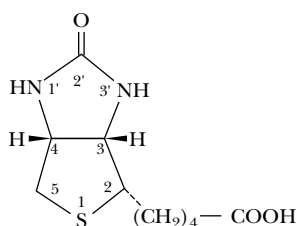
FIGURE 18.31 • The structure of biotin.

Biotin

Biotin (Figure 18.31) acts as a **mobile carboxyl group carrier** in a variety of enzymatic carboxylation reactions. In each of these, biotin is bound covalently to the enzyme as a prosthetic group via the ϵ-amino group of a lysine residue on the protein (Figure 18.32). The biotin-lysine function is referred to as a **biocytin** residue. The result is that *the biotin ring system is tethered to the protein by a long, flexible chain*. The 10 atoms in this chain separate the biotin ring and the lysine α-carbon by approximately 1.5 nm. This chain allows biotin to acquire carboxyl groups at one subsite of the enzyme active site and deliver them to a substrate acceptor at another subsite.

Most biotin-dependent carboxylations (Table 18.5) use *bicarbonate* as the carboxylating agent and transfer the carboxyl group to a *substrate carbanion*. Bicarbonate is plentiful in biological fluids, but it is a poor electrophile at carbon and must be "activated" for attack by the substrate carbanion.

Table 18.5

Principal Biotin-Dependent Carboxylations
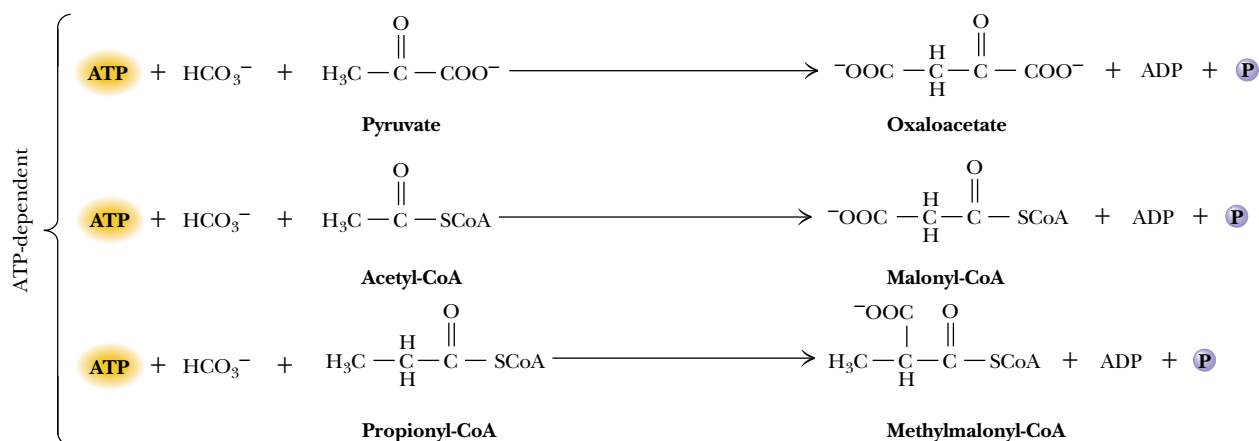
Biotin

Early in the 1900s, it was observed that certain strains of yeast required a material called **bios** for growth. Bios was eventually found to contain four different substances: myoinositol, β-alanine, pantothenic acid, and a compound later shown to be *biotin*. Kögl and Tönnis first isolated biotin from egg yolk in 1936. Boas, in 1927, and Szent-György, in 1931, found substances in liver that were capable of curing and preventing the dermatitis, loss of hair, and paralysis that occurred in rats fed large amounts of raw egg whites (a condition known as *egg white injury*). Boas called the factor "protective factor X" and Szent-György named the substance *vitamin H* (from the German *haut,* meaning "skin"), but both were

soon shown to be identical to biotin. It is now known that egg white contains a basic protein called **avidin,** which has an extremely high affinity for biotin ($K_D = 10^{-15}$ M). The sequestering of biotin by avidin is the cause of the egg white injury condition.

The structure of biotin was determined in the early 1940s by Kögl in Europe and by du Vigneaud and coworkers in the United States. Interestingly, the biotin molecule contains three asymmetric carbon atoms, and biotin could thus exist as eight different stereoisomers. Only one of these shows biological activity.

Lipoic Acid

Lipoic acid exists as a mixture of two structures: a closed-ring disulfide form and an open–chain reduced form (Figure 18.33). Oxidation–reduction cycles interconvert these two species. As is the case for biotin, lipoic acid does not often occur free in nature, but rather is covalently attached in amide linkage with lysine residues on enzymes. The enzyme that catalyzes the formation of the *lipoamide* linkage requires ATP and produces lipoamide-enzyme conjugates, AMP, and pyrophosphate as products of the reaction.

Lipoic acid is an **acyl group carrier.** It is found in *pyruvate dehydrogenase* and *α-ketoglutarate dehydrogenase,* two multienzyme complexes involved in carbohydrate metabolism (Figure 18.34). *Lipoic acid functions to couple acyl-group transfer and electron transfer during oxidation and decarboxylation of α-keto acids.*

The special properties of lipoic acid arise from the ring strain experienced by oxidized lipoic acid. The closed ring form is approximately 20 kJ higher in energy than the open-chain form, and this results in a strong negative reduction potential of about -0.30 V. The oxidized form readily oxidizes cyanides to isothiocyanates and sulfhydryl groups to mixed disulfides.

The biotin-lysine (biocytin) complex
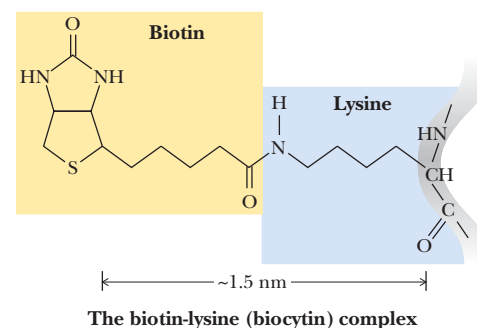
FIGURE 18.32 • Biotin is covalently linked to a protein via the ε-amino group of a lysine residue. The biotin ring is thus tethered to the protein by a 10-atom chain. It functions by carrying carboxyl groups between distant sites on biotin-dependent enzymes.

Lipoic Acid

Lipoic acid (6,8-dithiooctanoic acid) was isolated and characterized in 1951 in studies that showed that it was required for the growth of certain bacteria and protozoa. This accomplishment was one of the most impressive feats of isolation in the early history of biochemistry. Eli Lilly and Co., in cooperation with Lester J. Reed at the University of Texas and I. C. Gunsalus at the

University of Illinois, isolated just 30 mg of lipoic acid from approximately 10 tons of liver! No evidence exists of a dietary lipoic acid requirement by humans; strictly speaking, it is not considered a vitamin. Nevertheless, it is an essential component of several enzymes of intermediary metabolism and is present in body tissues in small amounts.

(a)

Lipoic acid, oxidized form

(b)

Reduced form

(c)
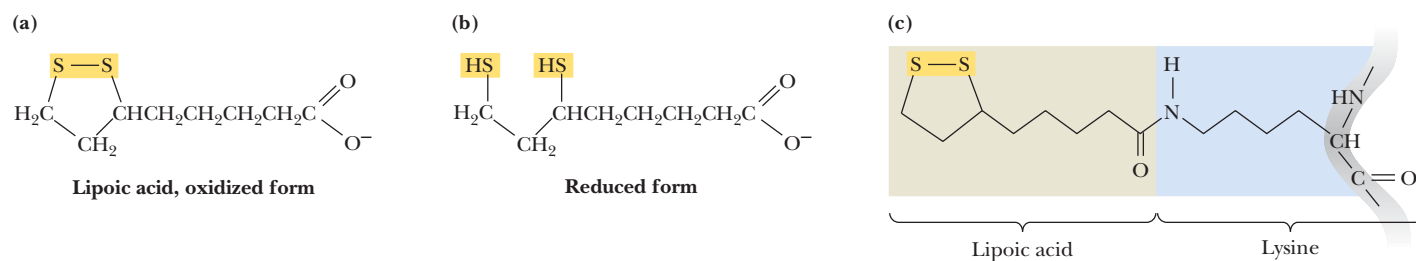
Lipoic acid   Lysine

FIGURE 18.33 • The oxidized and reduced forms of lipoic acid and the structure of the lipoic acid–lysine conjugate.

Folic Acid

Folic acid derivatives (folates) are acceptors and donors of one-carbon units for all oxidation levels of carbon except that of CO_2 (where biotin is the relevant carrier). The active coenzyme form of folic acid is **tetrahydrofolate (THF).** THF is formed via two successive reductions of folate by *dihydrofolate reductase* (Figure 18.35). One-carbon units in three different oxidation states may be bound to tetrahydrofolate at the N^5 and/or N^{10} nitrogens (Table 18.6). These one-carbon units

---

𝒜 D E E P E R   L O O K

Folic Acid, Pterins, and Insect Wings

Folic acid is a member of the vitamin B complex found in green plants, fresh fruit, yeast, and liver. Folic acid takes its name from *folium,* Latin for "leaf." Pterin compounds are named from the Greek word for "wing" because these substances were first identified in insect wings. Two pterins are familiar to any child who has seen (and chased) the common yellow sulfur butterfly and its white counterpart, the cabbage butterfly. *Xanthopterin* and *leu-*

copterin are the respective pigments in these butterflies' wings. Mammalian organisms cannot synthesize pterins; they derive folates from their diet or from microorganisms active in the intestines. Folic acid derives its name from *folium,* Latin for "leaf." Pterin compounds are named from the Greek πτέρυξ, for "wing," since these substances were first identified in insect wings.

Folic acid

Pterin
(2-amino-4-oxopteridine)

p-Aminobenzoic
acid
(PABA)

Glutamates

Pteridine

Pterin: 2-amino-4-
oxopteridine

Xanthopterin (yellow)   Leucopterin (white)

$$\text{Pyruvate} + \text{CoA} + \text{NAD}^+ \xrightarrow[\substack{\text{Pyruvate} \\ \text{dehydrogenase}}]{} \text{Acetyl-CoA} + \text{CO}_2 + \text{NADH} + \text{H}^+$$

$$\alpha\text{-Ketoglutarate} + \text{CoA} + \text{NAD}^+ \xrightarrow[\substack{\alpha\text{-Ketoglutarate} \\ \text{dehydrogenase}}]{} \text{Succinyl-CoA} + \text{CO}_2 + \text{NADH} + \text{H}^+$$
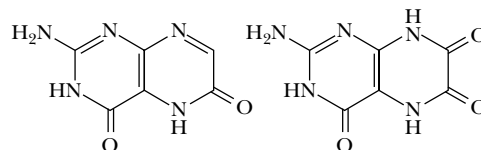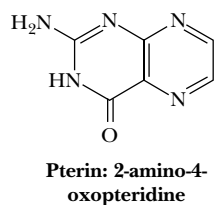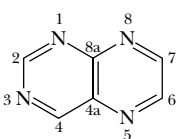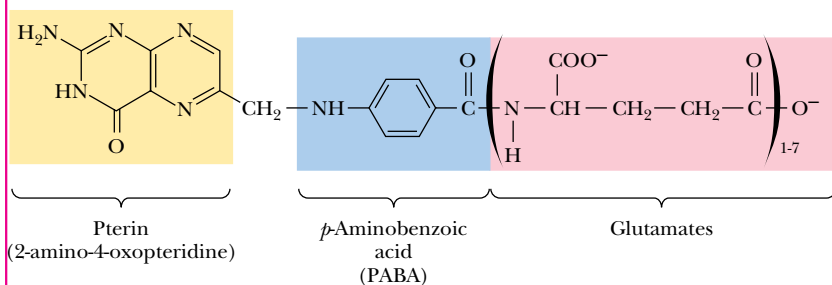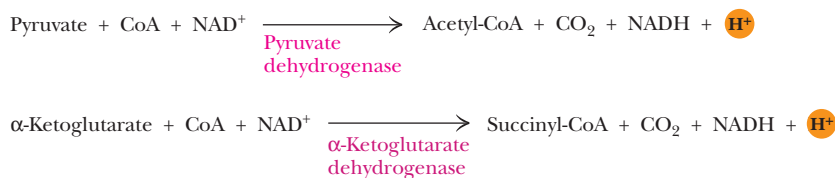
FIGURE 18.34 • The enzyme reactions catalyzed by lipoic acid.

may exist at the oxidation levels of methanol, formaldehyde, or formate (carbon atom oxidation states of –2, 0, and 2, respectively). The biosynthetic pathways for methionine and homocysteine (Chapter 26), purines (Chapter 27), and the pyrimidine thymine (Chapter 27) rely on the incorporation of one-carbon units from THF derivatives.

The Vitamin A Group

Vitamin A or **retinol** (Figure 18.36) often occurs in the form of esters, called **retinyl esters.** The aldehyde form is called **retinal** or **retinaldehyde.** Like all the fat-soluble vitamins, retinol is an *isoprenoid* molecule and is biosynthesized from isoprene building blocks (Chapter 8). Retinol can be absorbed in the diet from animal sources or synthesized from β-carotene from plant sources. The absorption by the body of fat-soluble vitamins proceeds by mechanisms different from those of the water-soluble vitamins. Once ingested, preformed vitamin A or β-carotene and its analogs are released from proteins by the action of proteolytic enzymes in the stomach and small intestine. The free carotenoids and retinyl esters aggregate in fatty globules that enter the duodenum. The detergent actions of bile salts break these globules down into small aggregates that can be digested by pancreatic lipase, cholesteryl ester hydrolase, retinyl ester hydrolase, and similar enzymes. The product compounds form *mixed micelles* (see Chapter 8) containing the retinol, carotenoids, and other lipids, which are absorbed into mucosal cells in the upper half of the intestinal tract. Retinol is esterified (usually with palmitic acid) and transported to the liver in a lipoprotein complex.

The retinol that is delivered to the retinas of the eyes in this manner is accumulated by **rod** and **cone cells.** In the rods (which are the better characterized of the two cell types), retinol is oxidized by a specific **retinol dehydrogenase** to become all-*trans* retinal and then converted to 11-*cis* retinal by **reti-**

Table 18.6

Oxidation States of Carbon in 1-Carbon Units Carried by Tetrahydrofolate

Oxidation Number*	Oxidation Level	One-Carbon Form†	Tetrahydrofolate Form
−2	Methanol (most reduced)	$-\text{CH}_3$	N^5-Methyl-THF
0	Formaldehyde	$-\text{CH}_2-$	N^5,N^{10}-Methylene-THF
2	Formate (most oxidized)	$-\text{CH}{=}\text{O}$	N^5-Formyl-THF
		$-\text{CH}{=}\text{O}$	N^{10}-Formyl-THF
		$-\text{CH}{=}\text{NH}$	N^5-Formimino-THF
		$-\text{CH}{=}$	N^5,N^{10}-Methenyl-THF

*Calculated by assigning valence bond electrons to the more electronegative atom and then counting the charge on the quasi ion. A carbon assigned four valence electrons would have an oxidation number of 0. The carbon in N^5-methyl-THF is assigned six electrons from the three C—H bonds and thus has an oxidation number of −2.

† Note: All vacant bonds in the structures shown are to atoms more electronegative than C.
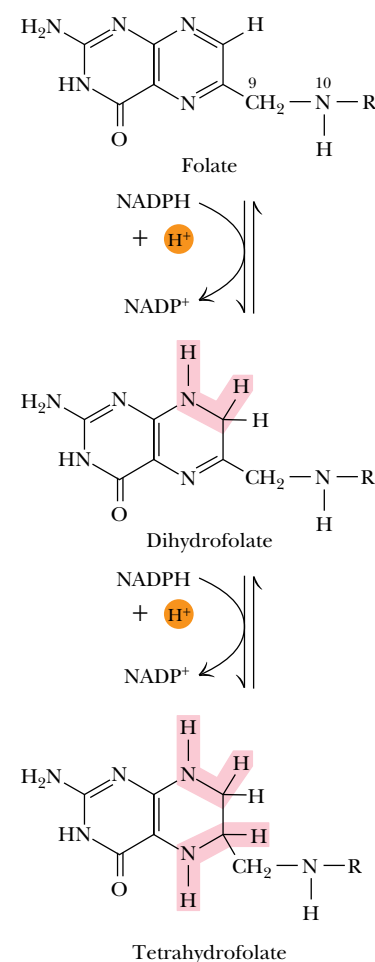
FIGURE 18.35 • Formation of THF from folic acid by the dihydrofolate reductase reaction. The R group on these folate molecules symbolizes the one to seven (or more) glutamate units that folates characteristically contain. All of these glutamates are bound in γ-carboxyl amide linkages (as in the folic acid structure shown in the box *A Deeper Look: Folic Acid, Pterins, and Insect Wings*).The one-carbon units carried by THF are bound at N^5, or at N^{10}, or as a single carbon attached to both N^5 and N^{10}.

β-Carotene and Vision

Night blindness was probably the first disorder to be ascribed to a nutritional deficiency. The ancient Egyptians left records as early as 1500 B.C. of recommendations that the juice squeezed from cooked liver could cure night blindness if applied topically, and the method may have been known much earlier. Frederick Gowland Hopkins, working in England in the early 1900s, found that alcoholic extracts of milk contained a growth-stimulating fac-

tor. Marguerite Davis and Elmer McCollum at Wisconsin showed that egg yolk and butter contain a similar growth-stimulating lipid, which, in 1915, they called "fat soluble A." Moore in England showed that **β-carotene,** the plant pigment, could be converted to the colorless form of the liver-derived vitamin. In 1935, George Wald of Harvard showed that *retinene* found in visual pigments of the eye was identical with *retinaldehyde,* a derivative of vitamin A.

nal isomerase (Figure 18.36). The aldehyde group of retinal forms a Schiff base with a lysine on **opsin,** to form light-sensitive **rhodopsin.**

The Vitamin D Group

The two most prominent members of the **vitamin D** family are **ergocalciferol** (known as vitamin D_2) and **cholecalciferol** (vitamin D_3). Cholecalciferol is produced in the skin of animals by the action of ultraviolet light (sunlight, for example) on its precursor molecule, 7-dehydrocholesterol (Figure 18.37). The absorption of light energy induces a photoisomerization via an excited singlet state, which results in breakage of the 9,10 carbon bond and formation of **previtamin D_3.** The next step is a spontaneous isomerization to yield vitamin D_3, cholecalciferol. Ergocalciferol, which differs from cholecalciferol only in the side-chain structure, is similarly produced by the action of sunlight on the plant sterol **ergosterol.** (Ergosterol is so named because it was first isolated from
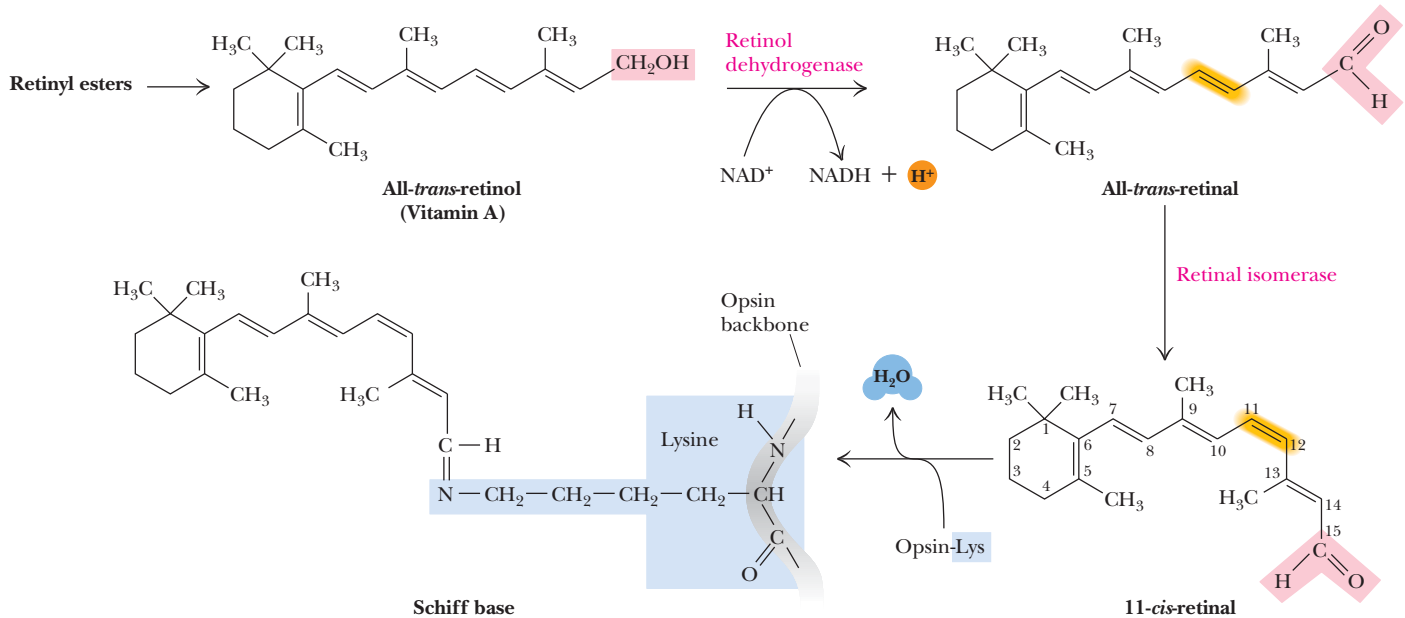
FIGURE 18.36 • The incorporation of retinal into the light-sensitive protein rhodopsin involves several steps. All-*trans*-retinol is oxidized by retinol dehydrogenase and then isomerized to 11-*cis*-retinal, which forms a Schiff base linkage with opsin to form light-sensitive rhodopsin.
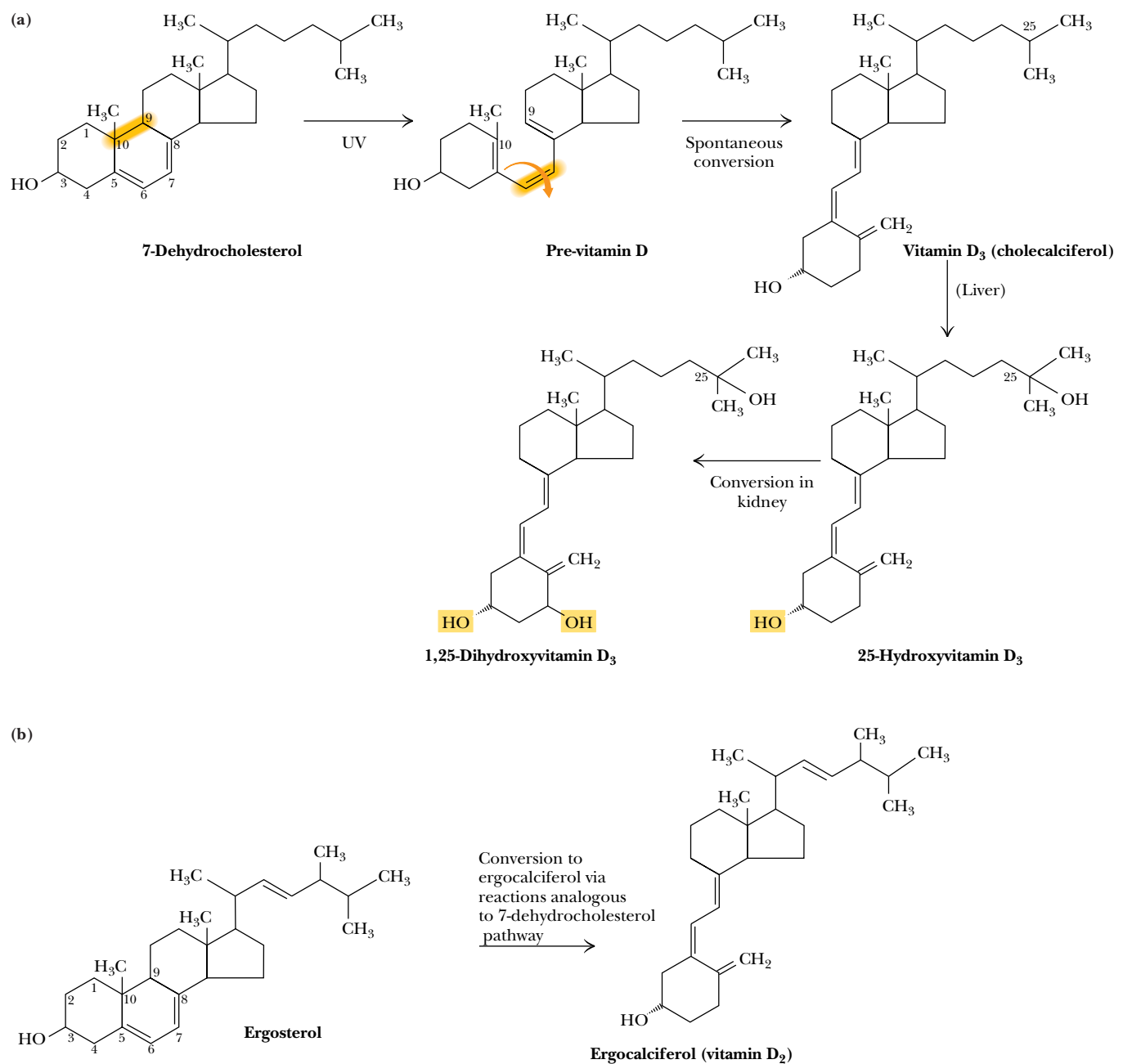
FIGURE 18.37 • (a) Vitamin D_3 (cholecalciferol) is produced in the skin by the action of sunlight on 7-dehydrocholesterol. The successive action of mixed-function oxidases in the liver and kidney produces 1,25-dihydroxyvitamin D_3, the active form of vitamin D. (b) Ergocalciferol is produced in analogous fashion from ergosterol.

$\mathcal{H}$UMAN BIOCHEMISTRY

Vitamin D and Rickets

Vitamin D is a family of closely related molecules that prevent **rickets,** a childhood disease characterized by inadequate intestinal absorption and kidney reabsorption of calcium and phosphate. These inadequacies eventually lead to the demineralization of bones. The symptoms of rickets include bowlegs, knock-knees, curvature of the spine, and pelvic and thoracic deformities, the results of normal mechanical stresses on demineralized bones. Vitamin D deficiency in adults leads to a weakening of bones and cartilage known as **osteomalacia.**

Vitamin E

In a study of the effect of nutrition on reproduction in the rat in the 1920s, Herbert Evans and Katherine Bishop found that rats failed to reproduce on a diet of rancid lard, unless lettuce or whole wheat was added to the diet. The essential factor was traced to a vitamin in the wheat germ oil. Named *vitamin E* by Evans (using the next available letter following on the discovery of vita-

min D), the factor was purified by Emerson, who named it *tocopherol,* from the Greek *tokos* for "childbirth," and *pherein,* for "to bring forth." Vitamin E is now recognized as a generic term for a family of substances, all of them similar in structure to the most active form, *α-tocopherol.*

ergot, a rye fungus.) Because humans can produce vitamin D_3 from 7–dehydrocholesterol by the action of sunlight on the skin, "vitamin D" is not strictly speaking a vitamin at all.

On the basis of its mechanism of action in the body, cholecalciferol should be called a **prohormone,** a hormone precursor. Dietary forms of vitamin D are absorbed through the aid of bile salts in the small intestine. Whether absorbed in the intestine or photosynthesized in the skin, cholecalciferol is then transported to the liver by a specific **vitamin D–binding protein (DBP),** also known as **transcalciferin.** In the liver, cholecalciferol is hydroxylated at the C-25 position by a mixed-function oxidase to form *25-hydroxyvitamin D* (that is, *25-hydroxycholecalciferol*). Although this is the major circulating form of vitamin D in the body, 25-hydroxyvitamin D possesses far less biological activity than the final active form. To form this latter species, 25-hydroxyvitamin D is returned to the circulatory system and transported to the kidneys. There it is hydroxylated at the C-1 position by a mitochondrial mixed-function oxidase to form *1,25-dihydroxyvitamin D_3* (that is, *1,25-dihydroxycholecalciferol*), the active form of vitamin D. 1,25-Dihydroxycholecalciferol is then transported to target tissues, where it acts like a hormone to regulate calcium and phosphate metabolism.

1,25-Dihydroxyvitamin D_3, together with two peptide hormones, *calcitonin* and *parathyroid hormone (PTH),* functions to regulate calcium homeostasis and plays a role in phosphorus homeostasis. As described elsewhere in this text, calcium is important for many processes, including muscle contraction, nerve impulse transmission, blood clotting, and membrane structure. Phosphorus, of course, is of critical importance to DNA, RNA, lipids, and many metabolic processes. Phosphorylation of proteins is an important regulatory signal for many biological processes. Phosphorus and calcium are also critically important for the formation of bones. Any disturbance of normal serum phosphorus and calcium levels will result in alterations of bone structure, as in rickets. The mechanism of calcium homeostasis involves precise coordination of calcium (a) absorption in the intestine, (b) deposition in the bones, and (c) excretion by the kidneys. If a decrease in serum calcium occurs, vitamin D is converted to its active form, which acts in the intestine to increase calcium absorption. PTH and vitamin D act on bones to enhance absorption of calcium, and PTH acts on the kidney to cause increased calcium reabsorption. If serum calcium levels get too high, calcitonin induces calcium excretion from the kidneys and inhibits calcium mobilization from bone, while inhibiting vitamin D metabolism and PTH secretion.

Vitamin E: Tocopherol

The structure of **vitamin E** in its most active form, **α-tocopherol,** is shown in Figure 18.38. α-Tocopherol is a potent antioxidant, and its function in animals and humans is often ascribed to this property. On the other hand, the molecular details of its function are almost entirely unknown. One possible role for
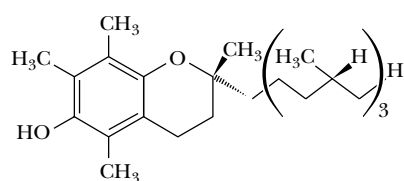
Vitamin E (α-tocopherol)

FIGURE 18.38 • The structure of vitamin E (α-tocopherol).

Vitamin K₁
(phylloquinone)
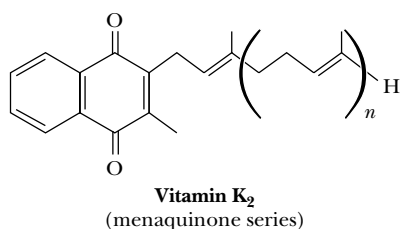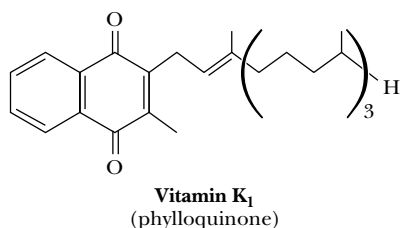
FIGURE 18.39 • The structures of the K vitamins.

Vitamin K₂
(menaquinone series)

**γ-Carboxyglutamic acid
in a protein**

FIGURE 18.40 • The glutamyl carboxylase reaction is vitamin K–dependent. This enzyme activity is essential for the formation of γ-carboxyglutamyl residues in several proteins of the blood-clotting cascade (Figure 15.5), accounting for the vitamin K dependence of coagulation.

vitamin E may relate to the protection of unsaturated fatty acids in membranes because these fatty acids are particularly susceptible to oxidation. When human plasma levels of α-tocopherol are low, red blood cells are increasingly subject to oxidative hemolysis. Infants, especially premature infants, are deficient in vitamin E. When low-birth-weight infants are exposed to high oxygen levels for the purpose of alleviating respiratory distress, the risk of oxygen-induced retina damage can be reduced with vitamin E administration. The mechanism(s) of action of vitamin E remain obscure.

Vitamin K: Naphthoquinone

The function of **vitamin K** (Figure 18.39) in the activation of blood clotting was not elucidated until the early 1970s, when it was found that animals and humans treated with coumarin-type anticoagulants contained an inactive form of **prothrombin** (an essential protein in the coagulation cascade). It was soon shown that a post-translational modification of prothrombin is essential to its function. In this modification, 10 glutamic acid residues on the amino terminal end of prothrombin are carboxylated to form γ-carboxyglutamyl residues. These residues are effective in the coordination of calcium, which is required for the coagulation process. The enzyme responsible for this modification, a liver microsomal *glutamyl carboxylase,* requires vitamin K for its activity (Figure 18.40). Not only prothrombin (called "factor II" in the clotting pathway) but also clotting factors VII, IX, and X and several plasma proteins—proteins C, M, S, and Z—contain γ-carboxyglutamyl residues in a manner similar to prothrombin. Other examples of γ-carboxyglutamyl residues in proteins are known.
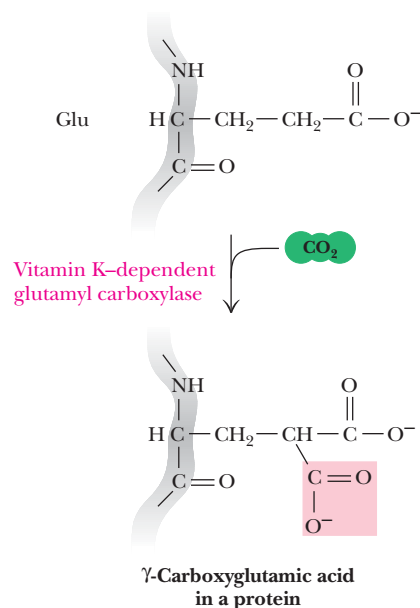
$\mathscr{H}$UMAN BIOCHEMISTRY

Vitamin K and Blood Clotting

In studies in Denmark in the 1920s, Henrik Dam noticed that chicks fed a diet extracted with nonpolar solvents developed hemorrhages. Moreover, blood taken from such animals clotted slowly. Further studies by Dam led him to conclude in 1935 that the antihemorrhage factor was a new fat-soluble vitamin, which he called *vitamin K* (from *koagulering,* the Danish word for "coagulation").

Dam, along with Karrar of Zurich, isolated the pure vitamin from alfalfa as a yellow oil. Another form, which was crystalline at room temperature, was soon isolated from fish meal. These two compounds were named *vitamins K₁* and *K₂*. Vitamin K₂ can actually occur as a family of structures with different chain lengths at the C-3 position.

PROBLEMS

1. If 3×10^{14} kg of CO_2 are cycled through the biosphere annually, how many human equivalents (70-kg persons composed of 18% carbon by weight) could be produced each year from this amount of CO_2?

2. Define the differences in carbon and energy metabolism between *photoautotrophs* and *photoheterotrophs,* and between *chemoautotrophs* and *chemoheterotrophs.*

3. Name three principal inorganic sources of oxygen atoms that are commonly available in the inanimate environment and readily accessible to the biosphere.

4. What are the features that generally distinguish pathways of catabolism from pathways of anabolism?

5. Name the three principal modes of enzyme organization in metabolic pathways.

6. Why do metabolic pathways have so many different steps?

7. Why is the pathway for the biosynthesis of a biomolecule at least partially different from the pathway for its catabolism? Why is the pathway for the biosynthesis of a biomolecule inherently more complex than the pathway for its degradation?

8. What are the metabolic roles of ATP, NAD^+, and NADPH?

9. Metabolic regulation is achieved via regulating enzyme activity in three prominent ways: allosteric regulation, covalent modification, and enzyme synthesis and degradation. Which of these three modes of regulation is likely to be the quickest; which the slowest? For each of these general enzyme regulatory mechanisms, cite conditions in which cells might employ that mode in preference to either of the other two.

10. What are the advantages of compartmentalizing particular metabolic pathways within specific organelles?

11. Maple-syrup urine disease (MSUD) is an autosomal recessive genetic disease characterized by progressive neurological dysfunction and a sweet, burnt-sugar or maple-syrup smell in the urine. Affected individuals carry high levels of branched-chain amino acids (leucine, isoleucine, and valine) and their respective branched-chain α-keto acids in cells and body fluids. The genetic defect has been traced to the mitochondrial branched-chain α-keto acid dehydrogenase (BCKD). Affected individuals exhibit mutations in their BCKD, but these mutant enzymes exhibit normal levels of activity. Nonetheless, treatment of MSUD patients with substantial doses of thiamine can alleviate the symptoms of the disease. Suggest an explanation for the symptoms described and for the role of thiamine in ameliorating the symptoms of MSUD.

FURTHER READING

Atkinson, D. E., 1977. *Cellular Energy Metabolism and Its Regulation.* New York: Academic Press. A monograph on energy metabolism that is filled with novel insights regarding the ability of cells to generate energy in a carefully regulated fashion while contending with the thermodynamic realities of life.

Boyer, P. D., 1970. *The Enzymes,* 3rd ed. New York: Academic Press. A good reference source for the mechanisms of action of vitamins and coenzymes.

Boyer, P. D., 1970. *The Enzymes,* Vol. 6. New York: Academic Press. See discussion of carboxylation and decarboxylation involving TPP, PLP, lipoic acid, and biotin; B_{12}-dependent mutases.

Boyer, P. D., 1972. *The Enzymes,* Vol. 7. New York: Academic Press. See especially elimination reactions involving PLP.

Boyer, P. D., 1974. *The Enzymes,* Vol. 10. New York: Academic Press. See discussion of pyridine nucleotide-dependent enzymes.

Boyer, P. D., 1976. *The Enzymes,* Vol. 13. New York: Academic Press. See discussion of flavin-dependent enzymes.

Cooper, T. G., 1977. *The Tools of Biochemistry.* New York: Wiley-Interscience. Chapter 3, "Radiochemistry," discusses techniques for using radioisotopes in biochemistry.

DeLuca, H., and Schnoes, H., 1983. Vitamin D: Recent advances. *Annual Review of Biochemistry* **52:**411–439.

Jencks, W. P., 1969. *Catalysis in Chemistry and Enzymology.* New York: McGraw-Hill.

Knowles, J. R., 1989. The mechanism of biotin-dependent enzymes. *Annual Review of Biochemistry* **58:**195–221.

Page, M. I., and Williams, A., eds., 1987. *Enzyme Mechanisms.* London: Royal Society of London.

Reed, L., 1974. Multienzyme complexes. *Accounts of Chemical Research* **7:**40–46.

Srere, P. A., 1987. Complexes of sequential metabolic enzymes. *Annual Review of Biochemistry* **56:**89–124. A review of how enzymes in some metabolic pathways are organized into complexes.

Walsh, C. T., 1979. *Enzymatic Reaction Mechanisms.* San Francisco: W. H. Freeman.

$\mathcal{C}$hapter 19

Glycolysis
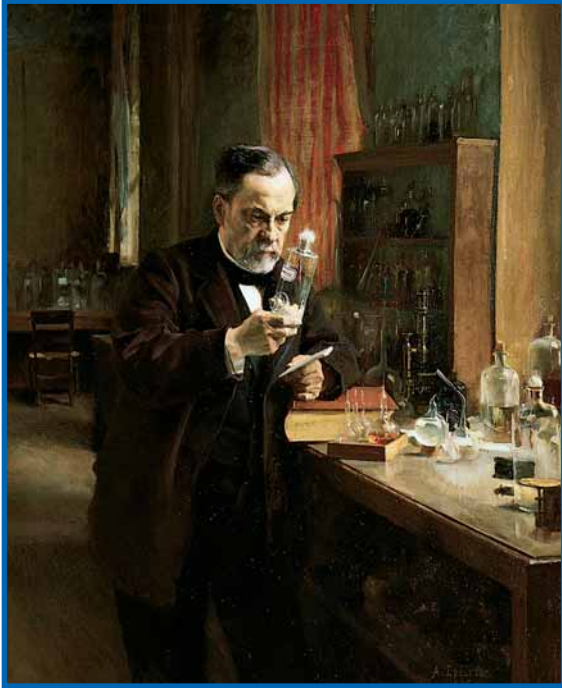
Louis Pasteur in his laboratory. Pasteur's scientific investigations into fermentation of sugar were sponsored by the French wine industry. (Albert Edelfelt, Musee d'Orsay, Paris; Giraudon/Art Resource, New York)

Living organisms, like machines, conform to the law of conservation of energy, and must pay for all their activities in the currency of catabolism.

ERNEST BALDWIN, *Dynamic Aspects of Biochemistry* (1952)

Nearly every living cell carries out a catabolic process known as **glycolysis—** the stepwise degradation of glucose (and other simple sugars). Glycolysis is a paradigm of metabolic pathways. Carried out in the cytosol of cells, it is basically an anaerobic process; its principal steps occur with no requirement for oxygen. Living things first appeared in an environment lacking O_2, and glycolysis was an early and important pathway for extracting energy from nutrient molecules. It played a central role in anaerobic metabolic processes during the first 2 billion years of biological evolution on earth. Modern organisms still employ glycolysis to provide precursor molecules for aerobic catabolic pathways (such as the tricarboxylic acid cycle) and as a short-term energy source when oxygen is limiting.

glycolysis • from the Greek *glyk-,* sweet, and *lysis,* splitting

609
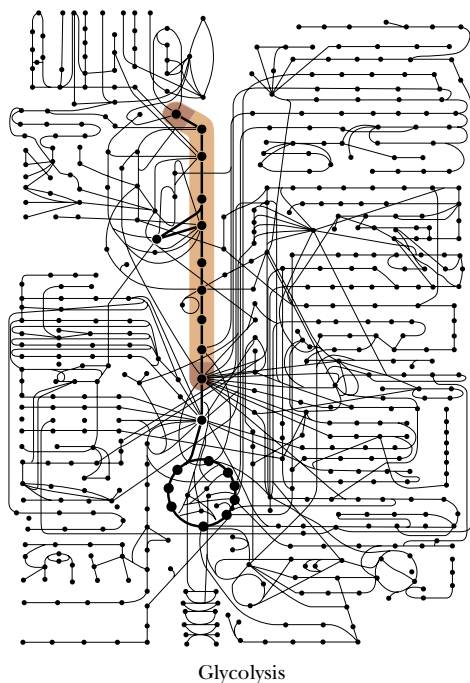
Glycolysis

19.1 • Overview of Glycolysis

An overview of the glycolytic pathway is presented in Figure 19.1. Most of the details of this pathway (the first metabolic pathway to be elucidated) were worked out in the first half of the 20th century by the German biochemists Otto Warburg, G. Embden, and O. Meyerhof. In fact, the sequence of reactions in Figure 19.1 is often referred to as the **Embden–Meyerhof pathway.**

Glycolysis consists of two phases. In the first, a series of five reactions, glucose is broken down to two molecules of glyceraldehyde-3-phosphate. In the second phase, five subsequent reactions convert these two molecules of glyceraldehyde-3-phosphate into two molecules of pyruvate. Phase 1 consumes two molecules of ATP (Figure 19.2). The later stages of glycolysis result in the production of four molecules of ATP. The net is $4 - 2 = 2$ molecules of ATP produced per molecule of glucose.

Rates and Regulation of Glycolytic Reactions Vary Among Species

Microorganisms, plants, and animals (including humans) carry out the 10 reactions of glycolysis in more or less similar fashion, although the rates of the individual reactions and the means by which they are regulated differ from species to species. The most significant difference among species, however, is the way in which the product pyruvate is utilized. The three possible paths for pyruvate are shown in Figure 19.1. In aerobic organisms, including humans, pyruvate is oxidized (with loss of the carboxyl group as CO_2), and the remaining two-carbon unit becomes the acetyl group of acetyl-coenzyme A. This acetyl group is metabolized by the tricarboxylic acid cycle (and fully oxidized) to yield CO_2. The electrons removed in this oxidation process are subsequently passed through the mitochondrial electron transport system and used to generate molecules of ATP by oxidative phosphorylation, thus capturing most of the metabolic energy available in the original glucose molecule.

19.2 • The Importance of Coupled Reactions in Glycolysis

The process of glycolysis converts some, but not all, of the metabolic energy of the glucose molecule into ATP. The free energy change for the conversion of glucose to two molecules of lactate (the anaerobic route shown in Figure 19.1) is -183.6 kJ/mol:

$$C_6H_{12}O_6 \longrightarrow 2H_3C\text{—}CHOH\text{—}COO^- + 2H^+ \tag{19.1}$$
$$\Delta G^{\circ\prime} = -183.6 \text{ kJ/mol}$$
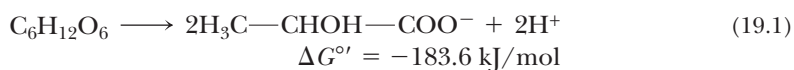
This process occurs with no net oxidation or reduction. Although several individual steps in the pathway involve oxidation or reduction, these steps compensate each other exactly. Thus, the conversion of a molecule of glucose to two molecules of lactate involves simply a rearrangement of bonds, with no net loss or gain of electrons. The energy made available through this rearrangement into a more stable (lower energy) form is a relatively small part of the total energy obtainable from glucose.

The production of two molecules of ATP in glycolysis is an energy-requiring process:

$$2ADP + 2P_i \longrightarrow 2ATP + 2H_2O \tag{19.2}$$
$$\Delta G^{\circ\prime} = 2 \times 30.5 \text{ kJ/mol} = 61.0 \text{ kJ/mol}$$
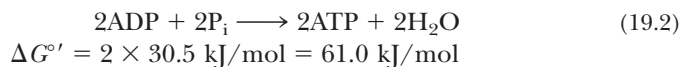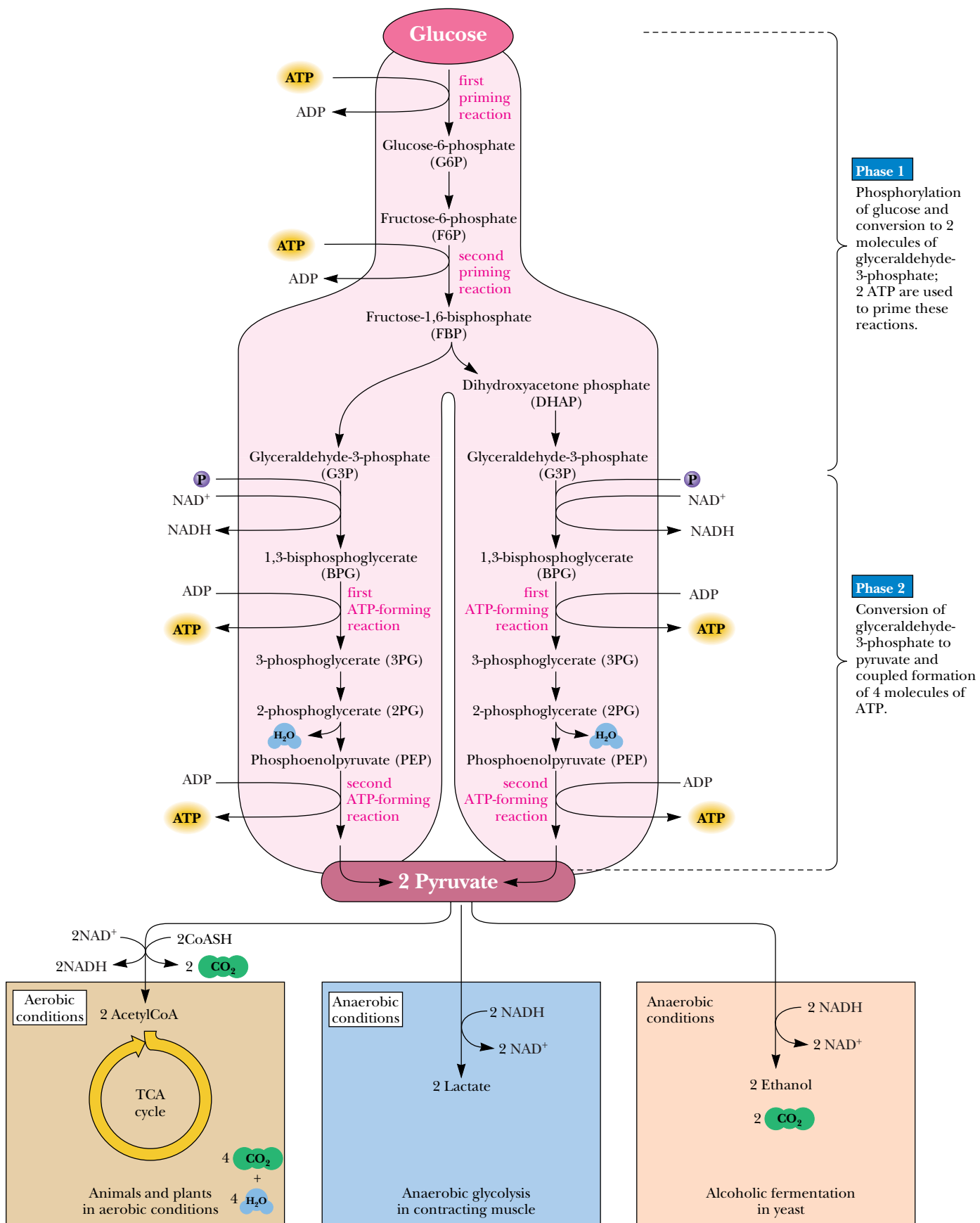
FIGURE 19.1 • The glycolytic pathway.
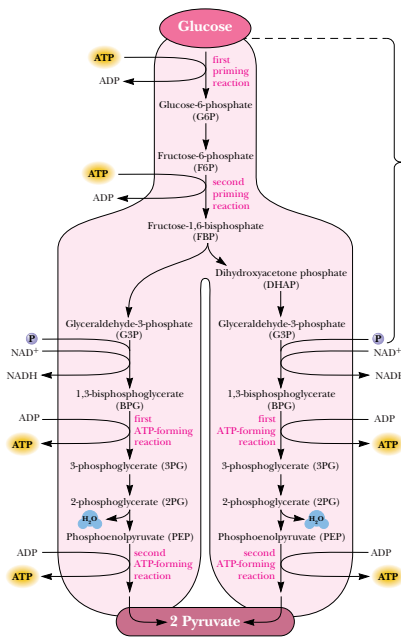
In the first five steps of glycolysis, one six-carbon molecule of glucose is split into two 3-carbon compounds.

2 molecules of ATP are required to prime these reactions.
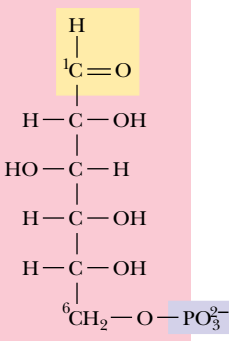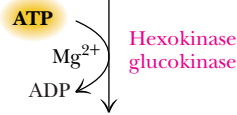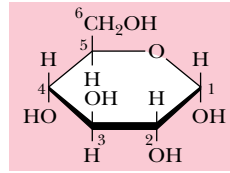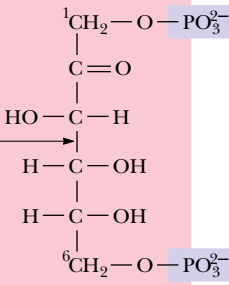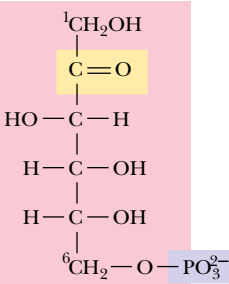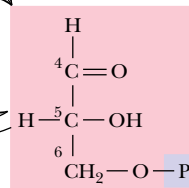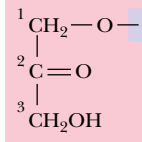
FIGURE 19.2 • In the first phase of glycolysis, five reactions convert a molecule of glucose to two molecules of glyceraldehyde-3-phosphate.

Glycolysis couples these two reactions:

$$\text{Glucose} + 2\text{ADP} + 2\text{P}_i \longrightarrow 2 \text{ lactate} + 2\text{ATP} + 2\text{H}^+ + 2\text{H}_2\text{O} \qquad (19.3)$$
$$\Delta G^{\circ}{}' = -183.6 + 61 = -122.6 \text{ kJ/mol}$$
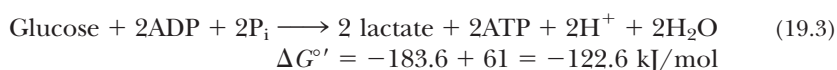
Thus, under standard-state conditions, $(61/183.6) \times 100\%$, or 33%, of the free energy released is preserved in the form of ATP in these reactions. However, as we discussed in Chapter 3, the various solution conditions, such as pH, concentration, ionic strength, and presence of metal ions, can substantially alter the free energy change for such reactions. Under actual cellular conditions, the free energy change for the synthesis of ATP (Equation 19.2) is much larger, and approximately 50% of the available free energy is converted into ATP. Clearly, then, more than enough free energy is available in the conversion of glucose into lactate to drive the synthesis of two molecules of ATP.

19.3 • The First Phase of Glycolysis

One way to synthesize ATP using the metabolic free energy contained in the glucose molecule would be to convert glucose into one (or more) of the high-energy phosphates in Table 3.3 that have standard-state free energies of hydrolysis more negative than that of ATP. Those molecules in Table 3.3 that can be synthesized easily from glucose are phosphoenolpyruvate, 1,3-bisphosphoglycerate, and acetyl phosphate. In fact, in the first stage of glycolysis, glucose is converted into two molecules of glyceraldehyde-3-phosphate. Energy released from this high-energy molecule in the second phase of glycolysis is then used to synthesize ATP.

Reaction 1: Phosphorylation of Glucose by Hexokinase or Glucokinase—The First Priming Reaction

The initial reaction of the glycolysis pathway involves phosphorylation of glucose at carbon atom 6 by either hexokinase or glucokinase. The formation of such a phosphoester is thermodynamically unfavorable and requires energy input to operate in the forward direction (Chapter 3). The energy comes from ATP, a requirement that at first seems counterproductive. Glycolysis is designed to *make* ATP, not consume it. However, the hexokinase, glucokinase reaction (Figure 19.2) is one of two **priming reactions** in the cycle. Just as old-fashioned, hand-operated water pumps (Figure 19.3) have to be primed with a small amount of water to deliver more water to the thirsty pumper, the glycolysis pathway requires two priming ATP molecules to start the sequence of reactions and delivers four molecules of ATP in the end.

The complete reaction for the first step in glycolysis is

$$\alpha\text{-D-Glucose} + \text{ATP}^{4-} \longrightarrow \alpha\text{-D-glucose-6-phosphate}^{2-} + \text{ADP}^{3-} + \text{H}^+ \quad (19.4)$$
$$\Delta G^{\circ}{}' = -16.7 \text{ kJ/mol}$$
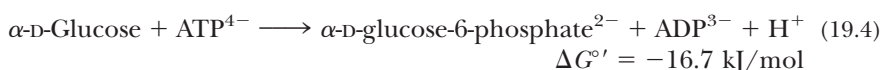
The hydrolysis of ATP makes 30.5 kJ/mol available in this reaction, and the phosphorylation of glucose "costs" 13.8 kJ/mol (see Table 19.1). Thus, the reaction liberates 16.7 kJ/mol under standard-state conditions ($1M$ concentrations), and the equilibrium of the reaction lies far to the right ($K_{\text{eq}} = 850$ at 25°C; see Table 19.1).

Under cellular conditions, this first reaction of glycolysis is even more favorable than at standard state. As pointed out in Chapter 3, the free energy change for any reaction depends on the concentrations of reactants and products.

FIGURE 19.3 • Just as a water pump must be "primed" with water to get more water out, the glycolytic pathway is primed with ATP in steps 1 and 3 in order to achieve net production of ATP in the second phase of the pathway.
(Michelle Sassi/The Stock Market)

Table 19.1

Reactions and Thermodynamics of Glycolysis

Reaction	Enzyme
α-D-Glucose + ATP^{4-} $\rightleftharpoons$ glucose-6-phosphate^{2-} + ADP^{3-} + H$^+$	Hexokinase
	Hexokinase
	Glucokinase
Glucose-6-phosphate^{2-} $\rightleftharpoons$ fructose-6-phosphate^{2-}	Phosphoglucoisomerase
Fructose-6-phosphate^{2-} + ATP^{4-} $\rightleftharpoons$ fructose-1,6-bisphosphate^{4-} + ADP^{3-} + H$^+$	Phosphofructokinase
Fructose-1,6-bisphosphate^{4-} $\rightleftharpoons$ dihydroxyacetone-P^{2-} + glyceraldehyde-3-P^{2-}	Fructose bisphosphate aldolase
Dihydroxyacetone-P^{2-} $\rightleftharpoons$ glyceraldehyde-3-P^{2-}	Triose phosphate isomerase
Glyceraldehyde-3-P^{2-} + P$_i$$^{2-}$ + NAD$^+$ $\rightleftharpoons$ 1,3-bisphosphoglycerate^{4-} + NADH + H$^+$	Glyceraldehyde-3-P dehydrogenase
1,3-Bisphosphoglycerate^{4-} + ADP^{3-} $\rightleftharpoons$ 3-P-glycerate^{3-} + ATP^{4-}	Phosphoglycerate kinase
3-Phosphoglycerate^{3-} $\rightleftharpoons$ 2-phosphoglycerate^{3-}	Phosphoglycerate mutase
2-Phosphoglycerate^{3-} $\rightleftharpoons$ phosphoenolpyruvate^{3-} + H$_2$O	Enolase
Phosphoenolpyruvate^{3-} + ADP^{3-} + H$^+$ $\rightleftharpoons$ pyruvate$^-$ + ATP^{4-}	Pyruvate kinase
Pyruvate$^-$ + NADH + H$^+$ $\rightleftharpoons$ lactate$^-$ + NAD$^+$	Lactate dehydrogenase

Table 19.2

Steady-State Concentrations of Glycolytic Metabolites in Erythrocytes

Metabolite	mM
Glucose	5.0
Glucose-6-phosphate	0.083
Fructose-6-phosphate	0.014
Fructose-1,6-bisphosphate	0.031
Dihydroxyacetone phosphate	0.14
Glyceraldehyde-3-phosphate	0.019
1,3-Bisphosphoglycerate	0.001
2,3-Bisphosphoglycerate	4.0
3-Phosphoglycerate	0.12
2-Phosphoglycerate	0.030
Phosphoenolpyruvate	0.023
Pyruvate	0.051
Lactate	2.9
ATP	1.85
ADP	0.14
P$_i$	1.0

Equation 3.12 in Chapter 3 and the data in Table 19.2 can be used to calculate a value for ΔG for the hexokinase, glucokinase reaction in erythrocytes:

$$\Delta G = \Delta G^{\circ\prime} + RT \ln \left(\frac{[\text{G-6-P}][\text{ADP}]}{[\text{Glu}][\text{ATP}]} \right) \tag{19.5}$$

$$\Delta G = -16.7 \text{ kJ/mol} + (8.314 \text{ J/mol} \cdot \text{K})(310 \text{ K}) \ln \left(\frac{[0.083][0.14]}{[5.0][1.85]} \right)$$

$$\Delta G = -33.9 \text{ kJ/mol}$$

Thus, ΔG is even more favorable under cellular conditions than at standard state. As we will see later in this chapter, the hexokinase, glucokinase reaction is one of several that drive glycolysis forward.

The Cellular Advantages of Phosphorylating Glucose

The incorporation of a phosphate into glucose in this energetically favorable reaction is important for several reasons. First, phosphorylation keeps the substrate in the cell. Glucose is a neutral molecule and could diffuse across the cell membrane, but phosphorylation confers a negative charge on glucose, and the plasma membrane is essentially impermeable to glucose-6-phosphate (Figure 19.4). Moreover, rapid conversion of glucose to glucose-6-phosphate keeps the *intracellular* concentration of glucose low, favoring diffusion of glucose *into* the cell. In addition, because regulatory control can be imposed only on reactions not at equilibrium, the favorable thermodynamics of this first reaction makes it an important site for regulation.

Hexokinase

In most animal, plant, and microbial cells, the enzyme that phosphorylates glucose is **hexokinase.** Magnesium ion (Mg^{2+}) is required for this reaction, as for the other kinase enzymes in the glycolytic pathway. The true substrate for the hexokinase reaction is MgATP^{2-}. The apparent K_m for glucose of the animal

Table 19.1

Source	Subunit Molecular Weight (M_r)	Oligomeric Composition	$\Delta G°'$ (kJ/mol)	K_{eq} at 25°C	ΔG (kJ/mol)
Mammals	100,000	Monomer	−16.7	850	−33.9*
Yeast	55,000	Dimer			
Mammalian liver	50,000	Monomer			
Human	65,000	Dimer	+1.67	0.51	−2.92
Rabbit muscle	78,000	Tetramer	−14.2	310	−18.8
Rabbit muscle	40,000	Tetramer	+23.9	6.43×10^{-5}	−0.23
Chicken muscle	27,000	Dimer	+7.56	0.0472	+2.41
Rabbit muscle	37,000	Tetramer	+6.30	0.0786	−1.29
Rabbit muscle	64,000	Monomer	−18.9	2060	+0.1
Rabbit muscle	27,000	Dimer	+4.4	0.169	+0.83
Rabbit muscle	41,000	Dimer	+1.8	0.483	+1.1
Rabbit muscle	57,000	Tetramer	−31.7	3.63×10^5	−23.0
Rabbit muscle	35,000	Tetramer	−25.2	2.63×10^4	−14.8

*ΔG values calculated for 310 K (37°C) using the data in Table 19.2 for metabolite concentrations in erythrocytes. $\Delta G°'$ values are assumed to be the same at 25°C and 37°C.

skeletal muscle enzyme is approximately 0.1 mM, and the enzyme thus operates efficiently at normal blood glucose levels of 4 mM or so. Different body tissues possess different isozymes of hexokinase, each exhibiting somewhat different kinetic properties. The animal enzyme is allosterically inhibited by the product, glucose-6-phosphate. High levels of glucose-6-phosphate inhibit hexokinase activity until consumption by glycolysis lowers its concentration. The hexokinase reaction is one of three points in the glycolysis pathway that are *regulated*. As the generic name implies, hexokinase can phosphorylate a variety of hexose sugars, including glucose, mannose, and fructose.

Glucokinase

Liver contains an enzyme called **glucokinase,** which also carries out the reaction in Figure 19.4 but is highly specific for D-glucose, has a much higher K_m for glucose (approximately 10.0 mM), and is not product-inhibited. With such

FIGURE 19.4 • Phosphorylation of glucose to glucose-6-phosphate by ATP creates a charged molecule that cannot easily cross the plasma membrane.

a high K_m for glucose, glucokinase becomes important metabolically only when liver glucose levels are high (for example, when the individual has consumed large amounts of sugar). When glucose levels are low, hexokinase is primarily responsible for phosphorylating glucose. However, when glucose levels are high, glucose is converted by glucokinase to glucose-6-phosphate and is eventually stored in the liver as glycogen. Glucokinase is an *inducible* enzyme—the amount present in the liver is controlled by *insulin* (secreted by the pancreas). (Patients with **diabetes mellitus** produce insufficient insulin. They have low levels of glucokinase, cannot tolerate high levels of blood glucose, and produce little liver glycogen.) Because glucose-6-phosphate is common to several metabolic pathways (Figure 19.5), it occupies a branch point in glucose metabolism.

Reaction 2: Phosphoglucoisomerase Catalyzes the Isomerization of Glucose-6-Phosphate

The second step in glycolysis is a common type of metabolic reaction: the isomerization of a sugar. In this particular case, the carbonyl oxygen of glucose-6-phosphate is shifted from C-1 to C-2. This amounts to isomerization of an aldose (glucose-6-phosphate) to a ketose—fructose-6-phosphate (Figure 19.6). The reaction is necessary for two reasons. First, the next step in glycolysis is phosphorylation at C-1, and the hemiacetal —OH of glucose would be more difficult to phosphorylate than a simple primary hydroxyl. Second, the isomerization to fructose (with a carbonyl group at position 2 in the linear form) activates carbon C-3 for cleavage in the fourth step of glycolysis. The enzyme responsible for this isomerization is **phosphoglucoisomerase,** also known as **glucose phosphate isomerase.** In humans, the enzyme requires Mg^{2+} for activity and is highly specific for glucose-6-phosphate. The $\Delta G°'$ is 1.67 kJ/mol, and the value of ΔG under cellular conditions (Table 19.1) is -2.92 kJ/mol. This small value means that the reaction operates near equilibrium in the cell and is readily reversible. Phosphoglucoisomerase proceeds through an *enediol* intermediate, as shown in Figure 19.6. Although the predominant forms of glucose-6-phosphate and fructose-6-phosphate in solution are the ring forms (Figure 19.6), the isomerase interconverts the open-chain form of G-6-P with the open-chain form of F-6-P. The first reaction catalyzed by the isomerase is the opening of the pyranose ring (Figure 19.6, Step A). In the next step, the C-2 proton is removed from the substrate by a basic residue on the enzyme, facilitating formation of the enediol intermediate (Figure 19.6, Step B). This process then

FIGURE 19.5 • Glucose-6-phosphate is the branch point for several metabolic pathways.

FIGURE 19.6 • The phosphoglucoisomerase mechanism involves opening of the pyranose ring (Step A), proton abstraction leading to enediol formation (Step B), and proton addition to the double bond, followed by ring closure (Step C).

operates somewhat in reverse (Figure 19.6, Step C), creating a carbonyl group at C-2 to complete the formation of fructose-6-phosphate. The furanose form of the product is formed in the usual manner by attack of the C-5 hydroxyl on the carbonyl group, as shown.

Reaction 3: Phosphofructokinase—The Second Priming Reaction

The action of phosphoglucoisomerase, "moving" the carbonyl group from C-1 to C-2, creates a new primary alcohol function at C-1 (see Figure 19.5). The next step in the glycolytic pathway is the phosphorylation of this group by **phosphofructokinase.** Once again, the substrate that provides the phosphoryl group is ATP. Like the hexokinase, glucokinase reaction, the phosphorylation of fructose-6-phosphate is a priming reaction and is endergonic:

$$\text{Fructose-6-P} + \text{P}_i \longrightarrow \text{fructose-1,6-bisphosphate} \qquad (19.6)$$
$$\Delta G°' = 16.3 \text{ kJ/mol}$$

When coupled (by phosphofructokinase) with the hydrolysis of ATP, the overall reaction (Figure 19.7) is strongly exergonic:

$$\text{Fructose-6-P} + \text{ATP} \longrightarrow \text{fructose-1,6-bisphosphate} + \text{ADP} \qquad (19.7)$$
$$\Delta G°' = -14.2 \text{ kJ/mol}$$
$$\Delta G \text{ (in erythrocytes)} = -18.8 \text{ kJ/mol}$$

At pH 7 and 37°C, the phosphofructokinase reaction equilibrium lies far to the right. Just as the hexokinase reaction commits the cell to taking up glucose, *the phosphofructokinase reaction commits the cell to metabolizing glucose* rather than converting it to another sugar or storing it. Similarly, just as the large free energy change of the hexokinase reaction makes it a likely candidate for regulation, so the phosphofructokinase reaction is an important site of regulation—indeed, the most important site in the glycolytic pathway.

Phosphofructokinase with ADP shown in white and fructose-6-P in red.

Fructose-6-phosphate   **Fructose-1,6-bisphosphate**

$$\Delta G^{\circ\prime} = -14.2 \text{ kJ/mol}$$
$$\Delta G_{erythrocyte} = -18.8 \text{ kJ/mol}$$

FIGURE 19.7 • The phosphofructokinase reaction.

[Fructose-6-phosphate]

FIGURE 19.8 • At high [ATP], phosphofructokinase (PFK) behaves cooperatively, and the plot of enzyme activity versus [fructose-6-phosphate] is sigmoid. High [ATP] thus inhibits PFK, decreasing the enzyme's affinity for fructose-6-phosphate.

Regulation of Phosphofructokinase

Phosphofructokinase is the "valve" controlling the rate of glycolysis. ATP is an allosteric inhibitor of this enzyme. In the presence of high ATP concentrations, phosphofructokinase behaves cooperatively, plots of enzyme activity versus fructose-6-phosphate are sigmoid, and the K_m for fructose-6-phosphate is increased (Figure 19.8). Thus, when ATP levels are sufficiently high in the cytosol, glycolysis "turns off." Under most cellular conditions, however, the ATP concentration does not vary over a large range. The ATP concentration in muscle during vigorous exercise, for example, is only about 10% lower than that during the resting state. The rate of glycolysis, however, varies much more. A large range of glycolytic rates cannot be directly accounted for by only a 10% change in ATP levels.

AMP reverses the inhibition due to ATP, and AMP levels in cells *can* rise dramatically when ATP levels decrease, due to the action of the enzyme *adenylate kinase*, which catalyzes the reaction

$$\text{ADP} + \text{ADP} \rightleftharpoons \text{ATP} + \text{AMP}$$

with the equilibrium constant:

$$K_{eq} = \frac{[\text{ATP}][\text{AMP}]}{[\text{ADP}]^2} = 0.44 \tag{19.8}$$

Adenylate kinase rapidly interconverts ADP, ATP, and AMP to maintain this equilibrium. ADP levels in cells are typically 10% of ATP levels, and AMP levels are often less than 1% of the ATP concentration. Under such conditions, a small net change in ATP concentration due to ATP hydrolysis results in a much larger relative increase in the AMP levels because of adenylate kinase activity.

EXAMPLE

Calculate the change in concentration in AMP that would occur if 8% of the ATP in an erythrocyte (red blood cell) were suddenly hydrolyzed to ADP. In erythrocytes (Table 19.2), the concentration of ATP is typically 1850 μM, the concentration of ADP is 145 μM, and the concentration of AMP is 5 μM. The total adenine nucleotide concentration is 2000 μM.

SOLUTION

The problem can be solved using the equilibrium expression for the adenylate kinase reaction:

$$K_{eq} = 0.44 = \frac{[\text{ATP}][\text{AMP}]}{[\text{ADP}]^2}$$

If 8% of the ATP is hydrolyzed to ADP, then [ATP] becomes $1850(0.92) =$ 1702 μM, and [AMP] + [ADP] becomes $2000 - 1702 = 298$ μM, and [AMP] may be calculated from the adenylate kinase equilibrium:

$$0.44 = \frac{[1702 \ \mu M][\text{AMP}]}{[\text{ADP}]^2}$$

Since [AMP] = 298 $\mu M -$ [ADP],

$$0.44 = \frac{1702(298 - [\text{ADP}])}{[\text{ADP}]^2}$$

$$[\text{ADP}] = 278 \ \mu M$$

$$[\text{AMP}] = 20 \ \mu M$$

Thus, an 8% decrease in [ATP] results in a 20/5 or *fourfold increase in the concentration of AMP.*

FIGURE 19.9 • Fructose-2,6-bisphosphate activates phosphofructokinase, increasing the affinity of the enzyme for fructose-6-phosphate and restoring the hyperbolic dependence of enzyme activity on substrate.

Clearly, the activity of phosphofructokinase depends both on ATP and AMP levels and is a function of the cellular energy status. Phosphofructokinase activity is increased when the energy status falls and is decreased when the energy status is high. The rate of glycolysis activity thus decreases when ATP is plentiful and increases when more ATP is needed.

Glycolysis and the citric acid cycle (to be discussed in Chapter 20) are coupled via phosphofructokinase, because *citrate,* an intermediate in the citric acid cycle, is an allosteric inhibitor of phosphofructokinase. When the citric acid cycle reaches saturation, glycolysis (which "feeds" the citric acid cycle under aerobic conditions) slows down. The citric acid cycle directs electrons into the electron transport chain (for the purpose of ATP synthesis in oxidative phosphorylation) and also provides precursor molecules for biosynthetic pathways. Inhibition of glycolysis by citrate ensures that glucose will not be committed to these activities if the citric acid cycle is already saturated.

Phosphofructokinase is also regulated by **β-D-fructose-2,6-bisphosphate,** a potent allosteric activator that increases the affinity of phosphofructokinase for the substrate fructose-6-phosphate (Figure 19.9). Stimulation of phosphofructokinase is also achieved by decreasing the inhibitory effects of ATP (Figure 19.10). Fructose-2,6-bisphosphate increases the net flow of glucose through glycolysis by stimulating phosphofructokinase and, as we shall see in Chapter 23, by inhibiting fructose-1,6-bisphosphatase, the enzyme that catalyzes this reaction in the opposite direction.

FIGURE 19.10 • Fructose-2,6-bisphosphate decreases the inhibition of phosphofructokinase due to ATP.

Reaction 4: Cleavage of Fructose-1,6-bisP by Fructose Bisphosphate Aldolase

Fructose bisphosphate aldolase cleaves fructose-1,6-bisphosphate between the C-3 and C-4 carbons to yield two triose phosphates. The products are dihydroxyacetone phosphate (DHAP) and glyceraldehyde-3-phosphate. The reaction (Figure 19.11) has an equilibrium constant of approximately 10^{-4} M, and a corresponding $\Delta G^{\circ\prime}$ of +23.9 kJ/mol. These values might imply that the reaction does not proceed effectively from left to right as written. However, the reaction makes two molecules (glyceraldehyde-3-P and dihydroxyacetone-P) from one molecule (fructose-1,6-bisphosphate), and the equilibrium is thus greatly influenced by concentration. The value of ΔG in erythrocytes is actually −0.23 kJ/mol (see Table 19.1). At physiological concentrations, the reaction is essentially at equilibrium.

Fructose-2,6-bisphosphate

$$\Delta G°' = 23.9 \text{ kJ/mol}$$

FIGURE 19.11 • The fructose-1,6-bisphosphate aldolase reaction.

R'= H (aldehyde)
R'= alkyl, etc. (ketone)

FIGURE 19.12 • An aldol condensation reaction.

Two classes of aldolase enzymes are found in nature. Animal tissues produce a Class I aldolase, characterized by the formation of a covalent Schiff base intermediate between an active-site lysine and the carbonyl group of the substrate. Class I aldolases do not require a divalent metal ion (and thus are not inhibited by EDTA) but are inhibited by sodium borohydride, $NaBH_4$, in the presence of substrate (see A Deeper Look, page 622). Class II aldolases are produced mainly in bacteria and fungi and are not inhibited by borohydride, but do contain an active-site metal (normally zinc, Zn^{2+}) and are inhibited by EDTA. Cyanobacteria and some other simple organisms possess both classes of aldolase.

The aldolase reaction is merely the reverse of the **aldol condensation** well known to organic chemists. The latter reaction involves an attack by a nucleophilic enolate anion of an aldehyde or ketone on the carbonyl carbon of an aldehyde (Figure 19.12). The opposite reaction, aldol cleavage, begins with removal of a proton from the β-hydroxyl group, which is followed by the elimination of the enolate anion. A mechanism for the aldol cleavage reaction of fructose-1,6-bisphosphate in the Class I–type aldolases is shown in Figure 19.13a. In Class II aldolases, an active-site metal such as Zn^{2+} behaves as an electrophile, polarizing the carbonyl group of the substrate and stabilizing the enolate intermediate (Figure 19.13b).

Reaction 5: Triose Phosphate Isomerase

Of the two products of the aldolase reaction, only glyceraldehyde-3-phosphate goes directly into the second phase of glycolysis. The other triose phosphate, dihydroxyacetone phosphate, must be converted to glyceraldehyde-3-phosphate by the enzyme **triose phosphate isomerase** (Figure 19.14). This reaction thus permits both products of the aldolase reaction to continue in the glycolytic pathway, and in essence makes the C-1, C-2, and C-3 carbons of the starting glucose molecule equivalent to the C-6, C-5, and C-4 carbons, respectively. The reaction mechanism involves an enediol intermediate that can donate either of its hydroxyl protons to a basic residue on the enzyme and thereby become either dihydroxyacetone phosphate or glyceraldehyde-3-phosphate (Figure 19.15). Triose phosphate isomerase is one of the enzymes that have evolved to a state of "catalytic perfection," with a turnover number near the diffusion limit (Chapter 14, Table 14.5).

The triose phosphate isomerase reaction completes the first phase of glycolysis, each glucose that passes through being converted to two molecules of glyceraldehyde-3-phosphate. Although the last two steps of the pathway are

Triose phosphate isomerase with substrate analog 2-phosphoglycerate shown in red.

FIGURE 19.13 • (a) A mechanism for the fructose-1,6-bisphosphate aldolase reaction. The Schiff base formed between the substrate carbonyl and an active-site lysine acts as an electron sink, increasing the acidity of the β-hydroxyl group and facilitating cleavage as shown. (B) In class II aldolases, an active-site Zn^{2+} stabilizes the enolate intermediate, leading to polarization of the substrate carbonyl group.

energetically unfavorable, the overall five-step reaction sequence has a net $\Delta G^{\circ\prime}$ of +2.2 kJ/mol ($K_{eq} \approx 0.43$). It is the free energy of hydrolysis from the two priming molecules of ATP that brings the overall equilibrium constant close to 1 under standard-state conditions. The net ΔG under cellular conditions is quite negative (-53.4 kJ/mol in erythrocytes).

FIGURE 19.14 • The triose phosphate isomerase reaction.

FIGURE 19.15 • A reaction mechanism for triose phosphate isomerase.

𝒜 D E E P E R   L O O K

The Chemical Evidence for the Schiff Base Intermediate in Class I Aldolases

Fructose bisphosphate aldolase of animal muscle is a Class I aldolase, which forms a Schiff base or *imine* intermediate between the substrate (fructose-1,6-bisP or dihydroxyacetone-P) and a lysine amino group at the enzyme active site. The chemical evidence for this intermediate comes from studies with the aldolase and the reducing agent sodium borohydride, $NaBH_4$. Incubation of fructose bisphosphate aldolase with dihydroxyacetone-P and $NaBH_4$ inactivates the enzyme. Interestingly, no inactivation is observed if $NaBH_4$ is added to the enzyme in the absence of substrate.

These observations are explained by the mechanism shown in the figure. $NaBH_4$ inactivates Class I aldolases by transfer of a hydride ion ($H:^-$) to the imine carbon atom of the enzyme–substrate adduct. The resulting secondary amine is stable to hydrolysis, and the active-site lysine is thus permanently modified and inactivated. $NaBH_4$ inactivates Class I aldolases in the presence of either dihydroxyacetone-P or fructose-1,6-bisP, but inhibition doesn't occur in the presence of glyceraldehyde-3-P.

Definitive identification of lysine as the modified active-site residue has come from radioisotope-labeling studies. $NaBH_4$ reduction of the aldolase Schiff base intermediate formed from ^{14}C-labeled dihydroxyacetone-P yields an enzyme covalently labeled with [14]C. Acid hydrolysis of the inactivated enzyme liberates a novel ^{14}C-labeled amino acid, N^6-*dihydroxypropyl-L-lysine.* This is the product anticipated from reduction of the Schiff base formed between a lysine residue and the ^{14}C-labeled dihydroxyacetone-P. (The phosphate group is lost during acid hydrolysis of the inactivated enzyme.) The use of ^{14}C labeling in a case such as this facilitates the separation and identification of the telltale amino acid.

Formation of Schiff base intermediate

Borohydride reduction of Schiff base intermediate

Stable (trapped) E–S derivative

Degradation of enzyme (acid hydrolysis)

N^6-dihydroxypropyl-L-lysine

19.4 • The Second Phase of Glycolysis

The second half of the glycolytic pathway involves the reactions that convert the metabolic energy in the glucose molecule into ATP. Altogether, four new ATP molecules are produced. If two are considered to offset the two ATPs consumed in phase 1, a net yield of 2 ATPs per glucose is realized. Phase II starts with the oxidation of glyceraldehyde-3-phosphate, a reaction with a large

FIGURE 19.16 • The second phase of glycolysis. Carbon atoms are numbered to show their original positions in glucose.

enough energy "kick" to produce a high-energy phosphate, namely, 1,3-bis-phosphoglycerate (Figure 19.16). Phosphoryl transfer from 1,3-BPG to ADP to make ATP is highly favorable. The product, 3-phosphoglycerate, is converted via several steps to phosphoenolpyruvate (PEP), another high-energy phosphate. PEP readily transfers its phosphoryl group to ADP in the pyruvate kinase reaction to make another ATP.

Reaction 6: Glyceraldehyde-3-Phosphate Dehydrogenase

In the first glycolytic reaction to involve oxidation–reduction, glyceraldehyde-3-phosphate is oxidized to 1,3-bisphosphoglycerate by **glyceraldehyde-3-phosphate dehydrogenase.** Although the oxidation of an aldehyde to a carboxylic acid is a highly exergonic reaction, the overall reaction (Figure 19.17) involves both formation of a carboxylic-phosphoric anhydride and the reduction of NAD^+ to NADH and is therefore slightly endergonic at standard state, with a $\Delta G^{\circ\prime}$ of +6.30 kJ/mol. The free energy that might otherwise be released as heat in this reaction is directed into the formation of a high-energy phosphate compound, 1,3-bisphosphoglycerate, and the reduction of NAD^+. The reaction mechanism involves nucleophilic attack by a cysteine —SH group on the carbonyl carbon of glyceraldehyde-3-phosphate to form a hemithioacetal (Figure 19.18). The hemithioacetal intermediate decomposes by hydride $(H:^-)$ transfer to NAD^+ to form a high-energy thioester. Nucleophilic attack by phosphate displaces the product, 1,3-bisphosphoglycerate, from the enzyme. The enzyme can be inactivated by reaction with iodoacetate, which reacts with and blocks the essential cysteine sulfhydryl.

The glyceraldehyde-3-phosphate dehydrogenase reaction is the site of action of *arsenate (AsO_4^{3-}),* an anion analogous to phosphate. Arsenate is an effective substrate in this reaction, forming *1-arseno-3-phosphoglycerate* (Figure 19.19), but acyl arsenates are quite unstable and are rapidly hydrolyzed. 1-Arseno-3-phosphoglycerate breaks down to yield *3-phosphoglycerate,* the product of the seventh reaction of glycolysis. The result is that glycolysis continues in the presence of arsenate, but the molecule of ATP formed in reaction 7 (phosphoglycerate kinase) is not made because this step has been bypassed. The lability of 1-arseno-3-phosphoglycerate effectively uncouples the oxidation and phosphorylation events, which are normally tightly coupled in the glyceraldehyde-3-phosphate dehydrogenase reaction.

Reaction 7: Phosphoglycerate Kinase

The glycolytic pathway breaks even in terms of ATPs consumed and produced with this reaction. The enzyme **phosphoglycerate kinase** transfers a phosphoryl group from 1,3-bisphosphoglycerate to ADP to form an ATP (Figure 19.20). Because each glucose molecule sends two molecules of glyceraldehyde-3-phosphate into the second phase of glycolysis and because two ATPs were consumed per glucose in the first-phase reactions, the phosphoglycerate kinase reaction "pays off" the ATP debt created by the priming reactions. As might be expected for a phosphoryl transfer enzyme, Mg^{2+} ion is required for activity, and the true nucleotide substrate for the reaction is $MgADP^-$. It is appropriate to view the sixth and seventh reactions of glycolysis as a coupled pair, with 1,3-bis-

$$\Delta G^{\circ\prime} = +6.3 \text{ kJ/mol}$$

FIGURE 19.17 • The glyceraldehyde-3-phosphate dehydrogenase reaction.

FIGURE 19.18 • A mechanism for the glyceraldehyde-3-phosphate dehydrogenase reaction. Reaction of an enzyme sulfhydryl with the carbonyl carbon of glyceraldehyde-3-P forms a thiohemiacetal, which loses a hydride to NAD^+ to become a thioester. Phosphorolysis of this thioester releases 1,3-bisphosphoglycerate.

phosphoglycerate as an intermediate. The phosphoglycerate kinase reaction is sufficiently exergonic at standard state to pull the G-3-P dehydrogenase reaction along. (In fact, the aldolase and triose phosphate isomerase are also pulled forward by phosphoglycerate kinase.) The net result of these coupled reactions is

Glyceraldehyde-3-phosphate + ADP + P_i + NAD^+ $\longrightarrow$
$$\text{3-phosphoglycerate} + \text{ATP} + \text{NADH} + H^+$$
$$\Delta G^{\circ\prime} = -12.6 \text{ kJ/mol} \quad (19.9)$$

1-Arseno-3-phosphoglycerate

FIGURE 19.19

$$\Delta G^{\circ\prime} = -18.9 \text{ kJ/mol}$$

FIGURE 19.20 • The phosphoglycerate kinase reaction.

FIGURE 19.21 • Formation and decomposition of 2,3-bisphosphoglycerate.

Another reflection of the coupling between these reactions lies in their values of ΔG under cellular conditions (Table 19.1). In spite of its strongly negative $\Delta G°'$, the phosphoglycerate kinase reaction operates at equilibrium in the erythrocyte ($\Delta G = 0.1$ kJ/mol). In essence, the free energy available in the phosphoglycerate kinase reaction is used to bring the three previous reactions closer to equilibrium. Viewed in this context, it is clear that ADP has been phosphorylated to form ATP at the expense of a substrate, namely, glyceraldehyde-3-phosphate. This is an example of **substrate-level phosphorylation,** a concept that will be encountered again. (The other kind of phosphorylation, *oxidative phosphorylation,* is driven energetically by the transport of electrons from appropriate coenzymes and substrates to oxygen. Oxidative phosphorylation will be covered in detail in Chapter 21). Even though the coupled reactions exhibit a very favorable $\Delta G°'$, there are conditions (i.e., high ATP and 3-phosphoglycerate levels) under which Equation 19.9 can be reversed, so that 3-phosphoglycerate is phosphorylated from ATP.

An important regulatory molecule, *2,3-bisphosphoglycerate,* is synthesized and metabolized by a pair of reactions that make a detour around the phosphoglycerate kinase reaction. 2,3-BPG, which stabilizes the deoxy form of hemoglobin and is primarily responsible for the cooperative nature of oxygen binding by hemoglobin (see Chapter 15), is formed from 1,3-bisphosphoglycerate by **bisphosphoglycerate mutase** (Figure 19.21). Interestingly, 3-phosphoglycerate is required for this reaction, which involves phosphoryl transfer from the C-1 position of 1,3-bisphosphoglycerate to the C-2 position of 3-phosphoglycerate (Figure 19.22). Hydrolysis of 2,3-BPG is carried out by *2,3-bisphosphoglycerate phosphatase.* Although other cells contain only a trace of 2,3-BPG, erythrocytes typically contain 4 to 5 mM 2,3-BPG.

Reaction 8: Phosphoglycerate Mutase

The remaining steps in the glycolytic pathway prepare for synthesis of the second ATP equivalent. This begins with the **phosphoglycerate mutase** reaction (Figure 19.23), in which the phosphoryl group of 3-phosphoglycerate is moved

FIGURE 19.22 • The mutase that forms 2,3-BPG from 1,3-BPG requires 3-phosphoglycerate. The reaction is actually an intermolecular phosphoryl transfer from C-1 of 1,3-BPG to C-2 of 3-PG.

from C-3 to C-2. (The term *mutase* is applied to enzymes that catalyze migration of a functional group within a substrate molecule.) The free energy change for this reaction is very small under cellular conditions ($\Delta G = 0.83$ kJ/mol in erythrocytes). Phosphoglycerate mutase enzymes isolated from different sources exhibit different reaction mechanisms. As shown in Figure 19.24, the

$$\Delta G^{\circ'} = +4.4 \text{ kJ/mol}$$

FIGURE 19.23 • The phosphoglycerate mutase reaction.

3-Phosphoglycerate (3-PG)

2,3-Bisphosphoglycerate intermediate

2-Phosphoglycerate (2-PG)

FIGURE 19.24 • A mechanism for the phosphoglycerate mutase reaction in rabbit muscle and in yeast. Zelda Rose of the Institute for Cancer Research in Philadelphia showed that the enzyme requires a small amount of 2,3-BPG to phosphorylate the histidine residue before the mechanism can proceed. Prior to her work, the role of the phosphohistidine in this mechanism was not understood.

FIGURE 19.25 • The phosphoglycerate mutase of wheat germ catalyzes an intramolecular phosphoryl transfer.

enzymes isolated from yeast and from rabbit muscle form *phosphoenzyme* intermediates, use *2,3-bisphosphoglycerate* as a cofactor, and undergo *inter*molecular phosphoryl group transfers (in which the phosphate of the product 2-phosphoglycerate is not that from the 3-phosphoglycerate substrate). The prevalent form of phosphoglycerate mutase is a *phosphoenzyme,* with a phosphoryl group covalently bound to a histidine residue at the active site. This phosphoryl group is transferred to the C-2 position of the substrate to form a transient, enzyme-bound 2,3-bisphosphoglycerate, which then decomposes by a second phosphoryl transfer from the C-3 position of the intermediate to the histidine residue on the enzyme. About once in every 100 enzyme turnovers, the intermediate, 2,3-bisphosphoglycerate, dissociates from the active site, leaving an inactive, unphosphorylated enzyme. The unphosphorylated enzyme can be reactivated by binding 2,3-BPG. For this reason, maximal activity of phosphoglycerate mutase requires the presence of small amounts of 2,3-BPG.

A different mechanism operates in the wheat germ enzyme. 2,3-Bisphosphoglycerate is not a cofactor. Instead, the enzyme carries out *intra*molecular phosphoryl group transfer (Figure 19.25). The C-3 phosphate is transferred to an active-site residue and then to the C-2 position of the original substrate molecule to form the product, 2-phosphoglycerate.

Reaction 9: Enolase

Recall that, prior to synthesizing ATP in the phosphoglycerate kinase reaction, it was necessary to first make a substrate having a high-energy phosphate. Reaction 9 of glycolysis similarly makes a high-energy phosphate in preparation for ATP synthesis. **Enolase** catalyzes the formation of *phosphoenolpyruvate* from 2-phosphoglycerate (Figure 19.26). The reaction in essence involves a dehydration—the removal of a water molecule—to form the enol structure of PEP. The $\Delta G^{\circ}{}'$ for this reaction is relatively small at 1.8 kJ/mol ($K_{eq} = 0.5$); and, under cellular conditions, ΔG is very close to zero. In light of this condition, it may be difficult at first to understand how the enolase reaction transforms a substrate with a relatively low free energy of hydrolysis into a product (PEP) with a very high free energy of hydrolysis. This puzzle is clarified by real-

$\Delta G^{\circ}{}' = +1.8$ kJ/mol

FIGURE 19.26 • The enolase reaction.

FIGURE 19.27 • The pyruvate kinase reaction.

izing that 2-phosphoglycerate and PEP contain about the same amount of *potential* metabolic energy, with respect to decomposition to P_i, CO_2, and H_2O. What the enolase reaction does is rearrange the substrate into a form from which more of this potential energy can be released upon hydrolysis. The enzyme is strongly inhibited by fluoride ion in the presence of phosphate. Inhibition arises from the formation of *fluorophosphate (FPO_3^{2-})*, which forms a complex with Mg^{2+} at the active site of the enzyme.

Reaction 10: Pyruvate Kinase

The second ATP-synthesizing reaction of glycolysis is catalyzed by **pyruvate kinase,** which brings the pathway at last to its pyruvate branch point. Pyruvate kinase mediates the transfer of a phosphoryl group from phosphoenolpyruvate to ADP to make ATP and pyruvate (Figure 19.27). The reaction requires Mg^{2+} ion and is stimulated by K^+ and certain other monovalent cations.

$$\begin{array}{lr} & \Delta G°' \text{ (kJ/mol)} \\ \text{Phosphoenolpyruvate}^{3-} + H_2O \longrightarrow \text{pyruvate}^- + HPO_4^{2-} & -62.2 \\ \underline{ADP^{3-} + HPO_4^{2-} + H^+ \longrightarrow ATP^{4-} + H_2O \qquad\qquad} & \underline{+30.5} \\ \text{Phosphoenolpyruvate}^{3-} + ADP^{3-} + H^+ \longrightarrow \text{pyruvate}^- + ATP^{4-} & -31.7 \end{array}$$

The corresponding K_{eq} at 25°C is 3.63×10^5, and it is clear that the pyruvate kinase reaction equilibrium lies very far to the right. Concentration effects reduce the magnitude of the free energy change somewhat in the cellular environment, but the ΔG in erythrocytes is still quite favorable at -23.0 kJ/mol. The high free energy change for the conversion of PEP to pyruvate is due largely to the highly favorable and spontaneous conversion of the enol tautomer of pyruvate to the more stable keto form (Figure 19.28) following the phosphoryl group transfer step.

FIGURE 19.28 • The conversion of phosphoenolpyruvate (PEP) to pyruvate may be viewed as involving two steps: phosphoryl transfer followed by an enol-keto tautomerization. The tautomerization is spontaneous ($\Delta G°' \approx -35-40$ kJ/mol) and accounts for much of the free energy change for PEP hydrolysis.

The large negative ΔG of this reaction makes pyruvate kinase a suitable target site for regulation of glycolysis. For each glucose molecule in the glycolysis pathway, two ATPs are made at the pyruvate kinase stage (because two triose molecules were produced per glucose in the aldolase reaction). Because the pathway broke even in terms of ATP at the phosphoglycerate kinase reaction (two ATPs consumed and two ATPs produced), the two ATPs produced by pyruvate kinase represent the "payoff" of glycolysis—a net yield of two ATP molecules.

Pyruvate kinase possesses allosteric sites for numerous effectors. It is activated by AMP and fructose-1,6-bisphosphate and inhibited by ATP, acetyl-CoA, and alanine. (Note that alanine is the α-amino acid counterpart of the α-keto acid, pyruvate.) Furthermore, liver pyruvate kinase is regulated by covalent modification. Hormones such as *glucagon* activate a cAMP-dependent protein kinase, which transfers a phosphoryl group from ATP to the enzyme. The phosphorylated form of pyruvate kinase is more strongly inhibited by ATP and alanine and has a higher K_m for PEP, so that, in the presence of physiological levels of PEP, the enzyme is inactive. Then PEP is used as a substrate for glucose synthesis in the *gluconeogenesis* pathway (to be described in Chapter 23), instead of going on through glycolysis and the citric acid cycle (or fermentation routes). A suggested active-site geometry for pyruvate kinase, based on NMR and EPR studies by Albert Mildvan and colleagues, is presented in Figure 19.29. The carbonyl oxygen of pyruvate and the γ-phosphorus of ATP lie within 0.3 nm of each other at the active site, consistent with direct transfer of the phosphoryl group without formation of a phosphoenzyme intermediate.

FIGURE 19.29 • A mechanism for the pyruvate kinase reaction, based on NMR and EPR studies by Albert Mildvan and colleagues. Phosphoryl transfer from phosphoenolpyruvate (PEP) to ADP occurs in four steps: (a) a water on the Mg^{2+} ion coordinated to ADP is replaced by the phosphoryl group of PEP; (b) Mg^{2+} dissociates from the α-P of ADP; (c) the phosphoryl group is transferred; and (d) the enolate of pyruvate is protonated. *(Adapted from Mildvan, A., 1979. Advances in Enzymology **49**:103–126.)*

19.5 • The Metabolic Fates of NADH and Pyruvate— The Products of Glycolysis

In addition to ATP, the products of glycolysis are NADH and pyruvate. Their processing depends upon other cellular pathways. NADH must be recycled to NAD^+, lest NAD^+ become limiting in glycolysis. NADH can be recycled by both aerobic and anaerobic paths, either of which results in further metabolism of pyruvate. What a given cell does with the pyruvate produced in glycolysis depends in part on the availability of oxygen. Under aerobic conditions, pyruvate can be sent into the citric acid cycle (also known as the tricarboxylic acid cycle; see Chapter 20), where it is oxidized to CO_2 with the production of additional NADH (and $FADH_2$). Under aerobic conditions, the NADH produced in glycolysis and the citric acid cycle is reoxidized to NAD^+ in the mitochondrial electron transport chain (Chapter 21).

19.6 • Anaerobic Pathways for Pyruvate

Under anaerobic conditions, the pyruvate produced in glycolysis is processed differently. In yeast, it is reduced to ethanol; in other microorganisms and in animals, it is reduced to lactate. These processes are examples of **fermentation** —the production of ATP energy by reaction pathways in which organic molecules function as donors and acceptors of electrons. In either case, reduction of pyruvate provides a means of reoxidizing the NADH produced in the glyceraldehyde-3-phosphate dehydrogenase reaction of glycolysis (Figure 19.30). In yeast, **alcoholic fermentation** is a two-step process. Pyruvate is decarboxylated to acetaldehyde by **pyruvate decarboxylase** in an essentially irreversible reaction. Thiamine pyrophosphate is a required cofactor for this enzyme. The second step, the reduction of acetaldehyde to ethanol by NADH, is catalyzed

FIGURE 19.30 • (a) Pyruvate reduction to ethanol in yeast provides a means for regenerating NAD^+ consumed in the glyceraldehyde-3-P dehydrogenase reaction. (b) In oxygen-depleted muscle, NAD^+ is regenerated in the lactate dehydrogenase reaction.

by **alcohol dehydrogenase** (Figure 19.30). At pH 7, the reaction equilibrium strongly favors ethanol. The end products of alcoholic fermentation are thus ethanol and carbon dioxide. Alcoholic fermentations are the basis for the brewing of beers and the fermentation of grape sugar in wine making. Lactate produced by anaerobic microorganisms during **lactic acid fermentation** is responsible for the taste of sour milk and for the characteristic taste and fragrance of sauerkraut, which in reality is fermented cabbage.

Lactate Accumulates Under Anaerobic Conditions in Animal Tissues

In animal tissues experiencing anaerobic conditions, pyruvate is reduced to lactate. Pyruvate reduction occurs in tissues that normally experience minimal access to blood flow (e.g., the cornea of the eye) and also in rapidly contracting skeletal muscle. When skeletal muscles are exercised strenuously, the available tissue oxygen is consumed, and the pyruvate generated by glycolysis can no longer be oxidized in the TCA cycle. Instead, excess pyruvate is reduced to lactate by **lactate dehydrogenase** (Figure 19.30). In anaerobic muscle tissue, lactate represents the end of glycolysis. Anyone who exercises to the point of consuming all available muscle oxygen stores knows the cramps and muscle fatigue associated with the buildup of lactic acid in the muscle. Most of this lactate must be carried out of the muscle by the blood and transported to the liver, where it can be resynthesized into glucose in gluconeogenesis. Moreover, because glycolysis generates only a fraction of the total energy available from the breakdown of glucose (the rest is generated by the TCA cycle and oxidative phosphorylation), the onset of anaerobic conditions in skeletal muscle also means a reduction in the energy available from the breakdown of glucose.

19.7 • The Energetic Elegance of Glycolysis

The elegance of nature's design for the glycolytic pathway may be appreciated through an examination of Figure 19.31. The standard-state free energy changes for the 10 reactions of glycolysis and the lactate dehydrogenase reaction (Figure 19.31a) are variously positive and negative and, taken together, offer little insight into the coupling that occurs in the cellular milieu. On the other hand, the values of ΔG under cellular conditions (Figure 19.31b) fall into two distinct classes. For reactions 2 and 4 through 9, ΔG is very close to zero, so that these reactions operate essentially at equilibrium. Small changes

FIGURE 19.31 • A comparison of free energy changes for the reactions of glycolysis (step 1 = hexokinase) under (a) standard-state conditions and (b) actual intracellular conditions in erythrocytes. The values of $\Delta G°'$ provide little insight into the actual free energy changes that occur in glycolysis. On the other hand, under intracellular conditions, seven of the glycolytic reactions operate near equilibrium (with ΔG near zero). The driving force for glycolysis lies in the hexokinase (1), phosphofructokinase (3), and pyruvate kinase (10) reactions. The lactate dehydrogenase (step 11) reaction also exhibits a large negative ΔG under cellular conditions.

(a) ΔG at standard state ($\Delta G°'$)

(b) ΔG in erythrocytes (ΔG)

in the concentrations of reactants and products could "push" any of these reactions either forward or backward. By contrast, the hexokinase, phosphofructokinase, and pyruvate kinase reactions all exhibit large negative ΔG values under cellular conditions. These reactions are thus the sites of glycolytic regulation. When these three enzymes are active, glycolysis proceeds and glucose is readily metabolized to pyruvate or lactate. Inhibition of the three key enzymes by allosteric effectors brings glycolysis to a halt. When we consider **gluconeogenesis**—the biosynthesis of glucose—in Chapter 23, we will see that different enzymes are used to carry out reactions 1, 3, and 10 in reverse, effecting the net synthesis of glucose. The maintenance of reactions 2 and 4 through 9 at or near equilibrium permits these reactions (and their respective enzymes!) to operate effectively in *either* the forward or reverse direction.

19.8 • Utilization of Other Substrates in Glycolysis

The glycolytic pathway described in this chapter begins with the breakdown of glucose, but other sugars, both simple and complex, can enter the cycle if they can be converted by appropriate enzymes to one of the intermediates of glycolysis. Figure 19.32 shows the mechanisms by which several simple metabolites can enter the glycolytic pathway. **Fructose,** for example, which is pro-

FIGURE 19.32 • Mannose, galactose, fructose, and other simple metabolites can enter the glycolytic pathway.

duced by breakdown of sucrose, may participate in glycolysis by at least two different routes. In the liver, fructose is phosphorylated at C-1 by the enzyme **fructokinase:**

$$\text{D-Fructose} + \text{ATP}^{4-} \longrightarrow \text{D-fructose-1-phosphate}^{2-} + \text{ADP}^{3-} + \text{H}^+ \qquad (19.10)$$

Subsequent action by **fructose-1-phosphate aldolase** cleaves fructose-1-P in a manner like the fructose bisphosphate aldolase reaction to produce dihydroxyacetone phosphate and D-glyceraldehyde:

$$\text{D-Fructose-1-P}^{2-} \longrightarrow \text{D-glyceraldehyde} + \text{dihydroxyacetone phosphate}^{2-}$$
$$(19.11)$$

Dihydroxyacetone phosphate is of course an intermediate in glycolysis. D-Glyceraldehyde can be phosphorylated by **triose kinase** in the presence of ATP to form D-glyceraldehyde-3-phosphate, another glycolytic intermediate.

In the kidney and in muscle tissues, fructose is readily phosphorylated by hexokinase, which, as pointed out above, can utilize several different hexose substrates. The free energy of hydrolysis of ATP drives the reaction forward:

$$\text{D-Fructose} + \text{ATP}^{4-} \longrightarrow \text{D-fructose-6-phosphate}^{2-} + \text{ADP}^{3-} + \text{H}^+ \qquad (19.12)$$

Fructose-6-phosphate generated in this way enters the glycolytic pathway directly in step 3, the second priming reaction. This is the principal means for channeling fructose into glycolysis in adipose tissue, which contains high levels of fructose.

The Entry of Mannose into Glycolysis

Another simple sugar that enters glycolysis at the same point as fructose is **mannose,** which occurs in many glycoproteins, glycolipids, and polysaccharides (Chapter 7). Mannose is also phosphorylated from ATP by hexokinase, and the mannose-6-phosphate thus produced is converted to fructose-6-phosphate by **phosphomannoisomerase.**

$$\text{D-Mannose} + \text{ATP}^{4-} \longrightarrow \text{D-mannose-6-phosphate}^{2-} + \text{ADP}^{3-} + \text{H}^+ \qquad (19.13)$$

$$\text{D-Mannose-6-phosphate}^{2-} \longrightarrow \text{D-fructose-6-phosphate}^{2-} \qquad (19.14)$$

The Special Case of Galactose

A somewhat more complicated route into glycolysis is followed by **galactose,** another simple hexose sugar. The process, called the **Leloir pathway** after Luis Leloir, its discoverer, begins with phosphorylation from ATP at the C-1 position by **galactokinase:**

$$\text{D-Galactose} + \text{ATP}^{4-} \longrightarrow \text{D-galactose-1-phosphate}^{2-} + \text{ADP}^{3-} + \text{H}^+ \qquad (19.15)$$

Galactose-1-phosphate is then converted into *UDP-galactose* (a sugar nucleotide) by **galactose-1-phosphate uridylyltransferase** (Figure 19.33), with concurrent production of glucose-1-phosphate and consumption of a molecule of UDP-glucose. The uridylyltransferase reaction proceeds via a "ping-pong" mechanism (Figure 19.34) with a covalent enzyme-UMP intermediate. The glucose-1-phosphate produced by the transferase reaction is a substrate for the **phosphoglucomutase** reaction (Figure 19.33), which produces glucose-6-phosphate, a glycolytic substrate. The other transferase product, UDP-galactose, is converted to UDP-glucose by **UDP-glucose-4-epimerase.** The combined action of the uridylyltransferase and epimerase thus produces glucose-1-P from galactose-1-P, with regeneration of UDP-glucose.

A rare hereditary condition known as **galactosemia** involves defects in galactose-1-P uridylyltransferase that render the enzyme inactive. Toxic levels of

FIGURE 19.33 • Galactose metabolism via the Leloir pathway.

galactose accumulate in afflicted individuals, causing cataracts and permanent neurological disorders. These problems can be prevented by removing galactose and lactose from the diet. In adults, the toxicity of galactose appears to be less severe, due in part to the metabolism of galactose-1-P by **UDP-glucose pyrophosphorylase,** which apparently can accept galactose-1-P in place of glucose-1-P (Figure 19.35). The levels of this enzyme may increase in galactosemic individuals, in order to accommodate the metabolism of galactose.

FIGURE 19.34 • The galactose-1-phosphate uridylyltransferase reaction involves a "ping-pong" kinetic mechanism.

FIGURE 19.35 • The UDP–glucose pyrophosphorylase reaction.

Lactose Intolerance

A much more common metabolic disorder, **lactose intolerance,** occurs commonly in most parts of the world (notable exceptions being some parts of Africa and northern Europe). Lactose intolerance is an inability to digest lactose because of the absence of the enzyme **lactase** in the intestines of adults. The symptoms of this disorder, which include diarrhea and general discomfort, can be relieved by eliminating milk from the diet.

Glycerol Can Also Enter Glycolysis

Glycerol is the last important simple substance whose ability to enter the glycolytic pathway must be considered. This metabolite, which is produced in substantial amounts by the decomposition of *triacylglycerols* (see Chapter 24) can be converted to glycerol-3-phosphate by the action of **glycerol kinase** and then oxidized to dihydroxyacetone phosphate by the action of **glycerol phosphate dehydrogenase,** with NAD^+ as the required coenzyme (Figure 19.36). The dihydroxyacetone phosphate thereby produced enters the glycolytic pathway as a substrate for triose phosphate isomerase.

FIGURE 19.36

PROBLEMS

1. List the reactions of glycolysis that

a. are energy-consuming (under standard-state conditions).

b. are energy-yielding (under standard-state conditions).

c. consume ATP.

d. yield ATP.

e. are strongly influenced by changes in concentration of substrate and product because of their molecularity.

f. are at or near equilibrium in the erythrocyte (see Table 19.2).

2. Determine the anticipated location in pyruvate of labeled carbons if glucose molecules labeled (in separate experiments) with ^{14}C at each position of the carbon skeleton proceed through the glycolytic pathway.

3. In an erythrocyte undergoing glycolysis, what would be the effect of a sudden increase in the concentration of

a. ATP?   **b.** AMP?   **c.** fructose-1,6-bisphosphate?

d. fructose-2,6-bisphosphate?   **e.** citrate?

f. glucose-6-phosphate?

4. Discuss the cycling of NADH and NAD$^+$ in glycolysis and the related fermentation reactions.

5. For each of the following reactions, name the enzyme that carries out this reaction in glycolysis and write a suitable mechanism for the reaction.

$$
\begin{array}{c}
\mathrm{CH_2OPO_3^{2-}} \\
|\ \\
\mathrm{C}{=}\mathrm{O} \\
|\ \\
\mathrm{HOCH} \\
|\ \\
\mathrm{HCOH} \\
|\ \\
\mathrm{HCOH} \\
|\ \\
\mathrm{CH_2OPO_3^{2-}}
\end{array}
\rightleftharpoons
\begin{array}{c}
\mathrm{CH_2OPO_3^{2-}} \\
|\ \\
\mathrm{C}{=}\mathrm{O} \\
|\ \\
\mathrm{CH_2OH}
\end{array}
+
\begin{array}{c}
\mathrm{CHO} \\
|\ \\
\mathrm{HCOH} \\
|\ \\
\mathrm{CH_2OPO_3^{2-}}
\end{array}
$$

$$
\begin{array}{c}
\mathrm{CHO} \\
|\ \\
\mathrm{HCOH} \\
|\ \\
\mathrm{CH_2OPO_3^{2-}}
\end{array}
\rightleftharpoons
\begin{array}{c}
\mathrm{O}\ \diagdown \ \mathrm{OPO_3^{2-}} \\
\mathrm{C} \\
|\ \\
\mathrm{HCOH} \\
|\ \\
\mathrm{CH_2OPO_3^{2-}}
\end{array}
$$

6. Write the reactions that permit galactose to be utilized in glycolysis. Write a suitable mechanism for one of these reactions.

7. How might iodoacetic acid affect the glyceraldehyde-3-phosphate dehydrogenase reaction in glycolysis? Justify your answer.

8. If ^{32}P-labeled inorganic phosphate were introduced to erythrocytes undergoing glycolysis, would you expect to detect ^{32}P in glycolytic intermediates? If so, describe the relevant reactions and the ^{32}P incorporation you would observe.

9. Sucrose can enter glycolysis by either of two routes:

Sucrose phosphorylase:
Sucrose + P$_i$ $\rightleftharpoons$ fructose + glucose-1-phosphate

Invertase:
Sucrose + H$_2$O $\rightleftharpoons$ fructose + glucose

Would either of these reactions offer an advantage over the other in the preparation of hexoses for entry into glycolysis?

10. What would be the consequences of a Mg^{2+} ion deficiency for the reactions of glycolysis?

11. Triose phosphate isomerase catalyzes the conversion of dihydroxyacetone-P to glyceraldehyde-3-P. The standard free energy change, $\Delta G^{\circ\prime}$, for this reaction is $+7.6$ kJ/mol. However, the observed free energy change (ΔG) for this reaction in erythrocytes is $+2.4$ kJ/mol.

a. Calculate the ratio of [dihydroxyacetone-P]/[glyceraldehyde-3-P] in erythrocytes from ΔG.

b. If [dihydroxyacetone-P] = 0.2 mM, what is [glyceraldehyde-3-P]?

12. Enolase catalyzes the conversion of 2-phosphoglycerate to phosphoenolpyruvate + H$_2$O. The standard free energy change, $\Delta G^{\circ\prime}$, for this reaction is $+1.8$ kJ/mol. If the concentration of 2-phosphoglycerate is 0.045 mM and the concentration of phosphoenolpyruvate is 0.034 mM, what is ΔG, the free energy change for the enolase reaction, under these conditions?

13. The standard free energy change ($\Delta G^{\circ\prime}$) for hydrolysis of phosphoenolpyruvate (PEP) is -61.9 kJ/mol. The standard free energy change ($\Delta G^{\circ\prime}$) for ATP hydrolysis is -30.5 kJ/mol.

a. What is the standard free energy change for the pyruvate kinase reaction:

$$\mathrm{ADP + phosphoenolpyruvate \longrightarrow ATP + pyruvate}$$

b. What is the equilibrium constant for this reaction?

c. Assuming the intracellular concentrations of [ATP] and [ADP] remain fixed at 8 mM and 1 mM, respectively, what will be the ratio of [pyruvate]/[phosphoenolpyruvate] when the pyruvate kinase reaction reaches equilibrium?

14. The standard free energy change ($\Delta G^{\circ\prime}$) for hydrolysis of fructose-1,6-bisphosphate (FBP) to fructose-6-phosphate (F-6-P) and P$_i$ is -16.7 kJ/mol:

$$\mathrm{FBP + H_2O \longrightarrow fructose\text{-}6\text{-}P + P_i}$$

The standard free energy change ($\Delta G^{\circ\prime}$) for ATP hydrolysis is -30.5 kJ/mol:

$$\mathrm{ATP + H_2O \longrightarrow ADP + P_i}$$

a. What is the standard free energy change for the phosphofructokinase reaction:

$$\mathrm{ATP + fructose\text{-}6\text{-}P \longrightarrow ADP + FBP}$$

b. What is the equilibrium constant for this reaction?

c. Assuming the intracellular concentrations of [ATP] and [ADP] are maintained constant at 4 mM and 1.6 mM, respectively, in a rat liver cell, what will be the ratio of [FBP]/[fructose-6-P] when the phosphofructokinase reaction reaches equilibrium?

15. The standard free energy change ($\Delta G^{\circ\prime}$) for hydrolysis of 1,3-bisphosphoglycerate (1,3-BPG) to 3-phosphoglycerate (3-PG) and P$_i$ is -49.6 kJ/mol:

$$\mathrm{1,3\text{-}BPG + H_2O \longrightarrow 3\text{-}PG + P_i}$$

The standard free energy change ($\Delta G^{\circ\prime}$) for ATP hydrolysis is -30.5 kJ/mol:

$$ATP + H_2O \longrightarrow ADP + P_i$$

a. What is the standard free energy change for the phosphoglycerate kinase reaction:

$$ADP + 1,3\text{-BPG} \longrightarrow ATP + 3\text{-PG}$$

b. What is the equilibrium constant for this reaction?

c. If the steady-state concentrations of [1,3-BPG] and [3-PG] in an erythrocyte are 1 μM and 120 μM, respectively, what will be the ratio of [ATP]/[ADP], assuming the phosphoglycerate kinase reaction is at equilibrium?

FURTHER READING

Arkin, A., Shen, P., and Ross, J., 1997. A test case of correlation metric construction of a reaction pathway from measurements. *Science* **277:**1275–1279.

Beitner, R., 1985. *Regulation of Carbohydrate Metabolism.* Boca Raton, FL: CRC Press.

Bioteux, A., and Hess, A., 1981. Design of glycolysis. *Philosophical Transactions, Royal Society of London B* **293:**5–22.

Bodner, G. M., 1986. Metabolism: Part I, Glycolysis. *Journal of Chemical Education* **63:**566–570.

Bosca, L., and Corredor, C., 1984. Is phosphofructokinase the rate-limiting step of glycolysis? *Trends in Biochemical Sciences* **9:**372–373.

Boyer, P. D., 1972. *The Enzymes,* 3rd ed., vols. 5–9. New York: Academic Press.

Braun, L., Puskas, F., Csala, M., et al., 1997. Ascorbate as a substrate for glycolysis or gluconeogenesis: Evidence for an interorgan ascorbate cycle. *Free Radical Biology and Medicine* **23:**804–808.

Conley, K. E., Blei, M. L., Richards, T. L., et al., 1997. Activation of glycolysis in human muscle *in vivo. American Journal of Physiology* **273:**C306–C315.

Fothergill-Gilmore, L., 1986. The evolution of the glycolytic pathway. *Trends in Biochemical Sciences* **11:**47–51.

Goncalves, P. M., Giffioen, G., Bebelman, J. P., and Planta, R. J., 1997. Signalling pathways leading to transcriptional regulation of genes involved in the activation of glycolysis in yeast. *Molecular Microbiology* **25:**483–493.

Green, H. J., 1997. Mechanisms of muscle fatigue in intense exercise. *Journal of Sports Sciences* **15:**247–256.

Jucker, B. M., Rennings, A. J., Cline, G. W., et al., 1997. *In vivo* NMR investigation of intramuscular glucose metabolism in conscious rats. *American Journal of Physiology* **273:**E139–E148.

Knowles, J., and Albery, W., 1977. Perfection in enzyme catalysis: The energetics of triose phosphate isomerase. *Accounts of Chemical Research* **10:**105–111.

Luczak-Szczurek, A., and Flisinska-Bojanowska, A., 1977. Effect of high-protein diet on glycolytic processes in skeletal muscles of exercising rats. *Journal of Physiology and Pharmacology* **48:**119–126.

Newsholme, E., Challiss, R., and Crabtree, B., 1984. Substrate cycles: Their role in improving sensitivity in metabolic control. *Trends in Biochemical Sciences* **9:**277–280.

Pilkus, S., and El-Maghrabi, M., 1988. Hormonal regulation of hepatic gluconeogenesis and glycolysis. *Annual Review of Biochemistry* **57:**755–783.

Saier, M., Jr., 1987. *Enzymes in Metabolic Pathways.* New York: Harper and Row.

Sparks, S., 1997. The purpose of glycolysis. *Science* **277:**459–460.

Vertessy, B. G., Orosz, F., Kovacs, J., and Ovadi, J., 1997. Alternative binding of two sequential glycolytic enzymes to microtubules. Molecular studies in the phosphofructokinase/aldolase/microtubule system. *Journal of Biological Chemistry* **272:**25542–25546.

Wackerhage, H., Mueller, K., Hoffmann, U., et al., 1996. Glycolytic ATP production estimated from ^{31}P magnetic resonance spectroscopy measurements during ischemic exercise *in vivo. Magma* **4:**151–155.

Waddell, T. G., et al., 1997. Optimization of glycolysis: A new look at the efficiency of energy coupling. *Biochemical Education* **25:**204–205.

Walsh, C. T., 1979. *Enzymatic Reaction Mechanisms.* San Francisco: W. H. Freeman.

$\mathcal{C}$hapter 20

The Tricarboxylic Acid Cycle

Thus times do shift, each thing his turn does hold;

New things succeed, as former things grow old.

ROBERT HERRICK (*Hesperides* [1648], "Ceremonies for Christmas Eve")

A time-lapse photograph of a ferris wheel at night. Aerobic cells use a metabolic wheel—the tricarboxylic acid cycle—to generate energy by acetyl-CoA oxidation.
(Ferns Wheel, DelMar Fair © Corbis/Richard Cummins)

$\mathbf{T}$he glycolytic pathway converts glucose to pyruvate and produces two molecules of ATP per glucose—only a small fraction of the potential energy available from glucose. Under anaerobic conditions, pyruvate is reduced to lactate in animals and to ethanol in yeast, and much of the potential energy of the glucose molecule remains untapped. *In the presence of oxygen,* however, a much more interesting and thermodynamically complete story unfolds. Under aerobic conditions, NADH is oxidized in the electron transport chain, rather than becoming oxidized through reduction of pyruvate to lactate or acetaldehyde to ethanol, for example. Further, pyruvate is converted to *acetyl-coenzyme A* and oxidized to CO_2 in the **tricarboxylic acid (TCA) cycle** (also called the **citric acid**

639

FIGURE 20.1 • Pyruvate produced in glycolysis is oxidized in the tricarboxylic acid (TCA) cycle. Electrons liberated in this oxidation flow through the electron transport chain and drive the synthesis of ATP in oxidative phosphorylation. In eukaryotic cells, this overall process occurs in mitochondria.

cycle). The electrons liberated by this oxidative process are then passed through an elaborate, membrane-associated **electron transport pathway** to O_2, the final electron acceptor. Electron transfer is coupled to creation of a proton gradient across the membrane. Such a gradient represents an energized state, and the energy stored in this gradient is used to drive the synthesis of many equivalents of ATP.

ATP synthesis as a consequence of electron transport is termed **oxidative phosphorylation;** the complete process is diagrammed in Figure 20.1. *Aerobic pathways* permit the production of 30 to 38 molecules of ATP per glucose oxidized. Athough two molecules of ATP come from glycolysis and two more directly out of the TCA cycle, most of the ATP arises from oxidative phosphorylation. Specifically, reducing equivalents released in the oxidative reactions of glycolysis, pyruvate decarboxylation, and the TCA cycle are captured in the form of NADH and enzyme-bound $FADH_2$, and these reduced coenzymes fuel the electron transport pathway and oxidative phosphorylation. The path to oxidative phosphorylation winds through the TCA cycle, and we will examine this cycle in detail in this chapter.

20.1 • Hans Krebs and the Discovery of the TCA Cycle

Within the orderly and logical confines of a textbook, it is difficult to appreciate the tortuous path of the research scientist through the labyrinth of scientific discovery, the patient sifting and comparing of hypotheses, and the often plodding progress toward new information. The elucidation of the TCA cycle in this century is a typical case, and one worth recounting. Armed with accumulated small contributions—pieces of the puzzle—from many researchers over many years, Hans Krebs, in a single, seminal inspiration, put the pieces together and finally deciphered the cyclic nature of pyruvate oxidation. In his honor, the TCA cycle is often referred to as the **Krebs cycle.**

In 1932 Krebs was studying the rates of oxidation of small organic acids by kidney and liver tissue. Only a few substances were active in these experiments —notably succinate, fumarate, acetate, malate, and citrate (Figure 20.2). Later it was found that oxaloacetate could be made from pyruvate in such tissues, and that it could be further oxidized like the other dicarboxylic acids.

In 1935 in Hungary, a crucial discovery was made by Albert Szent-Györgyi, who was studying the oxidation of similar organic substrates by pigeon breast muscle, an active flight muscle with very high rates of oxidation and metabolism. Carefully measuring the amount of oxygen consumed, he observed that addition of any of three four-carbon dicarboxylic acids—fumarate, succinate, or malate—caused the consumption of much more oxygen than was required for the oxidation of the added substance itself. He concluded that these substances were limiting in the cell and, when provided, stimulated oxidation of endogenous glucose and other carbohydrates in the tissues. He also found that **malonate,** a competitive inhibitor of succinate dehydrogenase (Chapter 14), inhibited these oxidative processes; this finding suggested that succinate oxidation is a crucial step. Szent-Györgyi hypothesized that these dicarboxylic acids were linked by an enzymatic pathway that was important for aerobic metabolism.

Tricarboxylic
Acid Cycle

FIGURE 20.2 • The organic acids observed by Krebs to be oxidized in suspensions of liver and kidney tissue. These substances were the pieces in the TCA puzzle that Krebs and others eventually solved.

Citrate

↓

Isocitrate

↓

α-Ketoglutarate

↓

Succinyl-CoA

↓

Succinate

↓

Fumarate

↓

Malate

↓

Oxaloacetate

FIGURE 20.3 • Martius and Knoop's observation that citrate could be converted to isocitrate and then α-ketoglutarate provided a complete pathway from citrate to oxaloacetate.

Another important piece of the puzzle came from the work of Carl Martius and Franz Knoop, who showed that citric acid could be converted to isocitrate and then to α-ketoglutarate. This finding was significant because it was already known that α-ketoglutarate could be enzymatically oxidized to succinate. At this juncture, the pathway from citrate to oxaloacetate seemed to be as shown in Figure 20.3. Whereas the pathway made sense, the *catalytic* effect of succinate and the other dicarboxylic acids from Szent-Györgyi's studies remained a puzzle.

In 1937 Krebs found that citrate could be formed in muscle suspensions if oxaloacetate and either pyruvate or acetate were added. He saw that he now had a cycle, not a simple pathway, and that addition of any of the intermediates could generate all of the others. The existence of a cycle, together with the entry of pyruvate into the cycle in the synthesis of citrate, provided a clear explanation for the accelerating properties of succinate, fumarate, and malate. If all these intermediates led to oxaloacetate, which combined with pyruvate from glycolysis, they could stimulate the oxidation of many substances besides themselves. (Kreb's conceptual leap to a cycle was not his first. Together with medical student Kurt Henseleit, he had already elucidated the details of the *urea cycle* in 1932.) The complete tricarboxylic acid (Krebs) cycle, as it is now understood, is shown in Figure 20.4.

20.2 • The TCA Cycle—A Brief Summary

The entry of new carbon units into the cycle is through acetyl-CoA. This entry metabolite can be formed either from pyruvate (from glycolysis) or from oxidation of fatty acids (discussed in Chapter 25). Transfer of the two-carbon acetyl group from acetyl-CoA to the four-carbon oxaloacetate to yield six-carbon citrate is catalyzed by *citrate synthase*. A dehydration–rehydration rearrangement of citrate yields isocitrate. Two successive decarboxylations produce α-ketoglutarate and then succinyl-CoA, a CoA conjugate of a four-carbon unit. Several steps later, oxaloacetate is regenerated and can combine with another two-carbon unit of acetyl-CoA. Thus, carbon enters the cycle as acetyl-CoA and exits as CO_2. In the process, metabolic energy is captured in the form of ATP, NADH, and enzyme-bound $FADH_2$ (symbolized as $[FADH_2]$).

The Chemical Logic of the TCA Cycle

The cycle shown in Figure 20.4 at first appears to be a complicated way to oxidize acetate units to CO_2, but there is a chemical basis for the apparent complexity. Oxidation of an acetyl group to a pair of CO_2 molecules requires C—C cleavage:

$$CH_3COO^- \longrightarrow CO_2 + CO_2$$

In many instances, C—C cleavage reactions in biological systems occur between carbon atoms α- and β- to a carbonyl group:

$$-\overset{\overset{\textstyle O}{\|}}{C}-C_\alpha-C_\beta-$$

↑

Cleavage

A good example of such a cleavage is the fructose bisphosphate aldolase reaction (see Chapter 19, Figure 19.14a).

FIGURE 20.4 • The tricarboxylic acid cycle.

Another common type of C—C cleavage is α-cleavage of an α-hydroxy-ketone:

$$-\overset{\overset{\textstyle O}{\|}}{C}-C_\alpha-C_\beta-$$
$$\uparrow$$
Cleavage

(We see this type of cleavage in the *transketolase* reaction described in Chapter 23.)

Neither of these cleavage strategies is suitable for acetate. It has no β-carbon, and the second method would require hydroxylation—not a favorable reaction for acetate. Instead, living things have evolved the clever chemistry of condensing acetate with oxaloacetate and *then* carrying out a β-cleavage. *The TCA cycle combines this β-cleavage reaction with oxidation to form CO_2, regenerate oxaloacetate, and capture the liberated metabolic energy in NADH and ATP.*

20.3 • The Bridging Step: Oxidative Decarboxylation of Pyruvate

Pyruvate produced by glycolysis is a significant source of acetyl-CoA for the TCA cycle. Because, in eukaryotic cells, glycolysis occurs in the cytoplasm, whereas the TCA cycle reactions and all subsequent steps of aerobic metabolism take place in the mitochondria, pyruvate must first enter the mitochondria to enter the TCA cycle. The oxidative decarboxylation of pyruvate to acetyl-CoA,

$$\text{Pyruvate} + \text{CoA} + \text{NAD}^+ \longrightarrow \text{acetyl-CoA} + CO_2 + \text{NADH} + \text{H}^+$$

is the connecting link between glycolysis and the TCA cycle. The reaction is catalyzed by pyruvate dehydrogenase, a multienzyme complex.

The **pyruvate dehydrogenase complex (PDC)** is a noncovalent assembly of three different enzymes operating in concert to catalyze successive steps in the conversion of pyruvate to acetyl-CoA. The active sites of all three enzymes are not far removed from one another, and the product of the first enzyme is passed directly to the second enzyme and so on, without diffusion of substrates and products through the solution. The overall reaction (see *A Deeper Look:* "Reaction Mechanism of the Pyruvate Dehydrogenase Complex") involves a total of five coenzymes: thiamine pyrophosphate, coenzyme A, lipoic acid, NAD^+, and FAD.

20.4 • Entry into the Cycle: The Citrate Synthase Reaction

The first reaction within the TCA cycle, the one by which carbon atoms are introduced, is the **citrate synthase reaction** (Figure 20.5). Here acetyl-CoA reacts with oxaloacetate in a **Perkin condensation** (a carbon–carbon condensation between a ketone or aldehyde and an ester). The acyl group is activated in two ways in an acyl-CoA molecule: the carbonyl carbon is activated for attack by nucleophiles, and the C_α carbon is more acidic and can be deprotonated to form a carbanion. The citrate synthase reaction depends upon the latter mode of activation. As shown in Figure 20.5, a general base on the enzyme accepts a proton from the methyl group of acetyl-CoA, producing a stabilized α-carbanion of acetyl-CoA. This strong nucleophile attacks the α-carbonyl of oxaloacetate, yielding citryl-CoA. This part of the reaction has an equilibrium constant

FIGURE 20.5 • Citrate is formed in the citrate synthase reaction from oxaloacetate and acetyl-CoA. The mechanism involves nucleophilic attack by the carbanion of acetyl-CoA on the carbonyl carbon of oxaloacetate, followed by thioester hydrolysis.

near 1, but the overall reaction is driven to completion by the subsequent hydrolysis of the high-energy thioester to citrate and free CoA. The overall $\Delta G^{\circ\prime}$ is -31.4 kJ/mol, and under standard conditions the reaction is essentially irreversible. Although the mitochondrial concentration of oxaloacetate is very low (much less than 1 μM—see example in Section 20.11), the strong, negative $\Delta G^{\circ\prime}$ drives the reaction forward.

The Structure of Citrate Synthase

Citrate synthase in mammals is a dimer of 49-kD subunits (Table 20.1). On each subunit, oxaloacetate and acetyl-CoA bind to the active site, which lies in a cleft between two domains and is surrounded mainly by α-helical segments (Figure 20.6). Binding of oxaloacetate induces a conformational change that facilitates the binding of acetyl-CoA and closes the active site, so that the reactive carbanion of acetyl-CoA is protected from protonation by water.

Regulation of Citrate Synthase

Citrate synthase is the first step in this metabolic pathway, and as stated the reaction has a large negative $\Delta G^{\circ\prime}$. As might be expected, it is a highly regulated enzyme. NADH, a product of the TCA cycle, is an allosteric inhibitor of citrate synthase, as is succinyl-CoA, the product of the fifth step in the cycle (and an acetyl-CoA analog).

FIGURE 20.6 • Citrate synthase. In the monomer shown here, citrate is shown in green, and CoA is pink.

Reaction Mechanism of the Pyruvate Dehydrogenase Complex

The mechanism of the pyruvate dehydrogenase reaction is a *tour de force* of mechanistic chemistry, involving as it does a total of three enzymes (a) and five different coenzymes—thiamine pyrophosphate, lipoic acid, coenzyme A, FAD, and NAD^+ (b).

The first step of this reaction, decarboxylation of pyruvate and transfer of the acetyl group to lipoic acid, depends on accumulation of negative charge on the carbonyl carbon of pyruvate. This is facilitated by the quaternary nitrogen on the *thiazolium* group of thiamine pyrophosphate. As shown in (c), this cationic

imine nitrogen plays two distinct and important roles in TPP-catalyzed reactions:

1. It provides electrostatic stabilization of the carbanion formed upon removal of the C-2 proton. (The sp^2 hybridization and the availability of vacant d orbitals on the adjacent sulfur probably also facilitate proton removal at C-2.)
2. TPP attack on pyruvate leads to decarboxylation. The TPP cationic imine nitrogen can act as an effective electron sink to stabilize the negative charge that must develop on the carbon

(a)

(a) The structure of the pyruvate dehydrogenase complex. This complex consists of three enzymes: pyruvate dehydrogenase (PDH), dihydrolipoyl transacetylase (TA), and dihydrolipoyl dehydrogenase (DLD). (i) 24 dihydrolipoyl transacetylase subunits form a cubic core structure. (ii) 24 $\alpha\beta$ dimers of pyruvate dehydrogenase are added to the cube (two per edge). (iii) Addition of 12 dihydrolipoyl dehydrogenase subunits (two per face) completes the complex.

(b)

(b) The reaction mechanism of the pyruvate dehydrogenase complex. Decarboxylation of pyruvate occurs with formation of hydroxyethyl-TPP (Step 1). Transfer of the two-carbon unit to lipoic acid in Step 2 is followed by formation of acetyl-CoA in Step 3. Lipoic acid is reoxidized in Step 4 of the reaction.

that has been attacked. This stabilization takes place by resonance interaction through the double bond to the nitrogen atom.

This resonance-stabilized intermediate can be protonated to give **hydroxyethyl-TPP.** This well-characterized intermediate was once thought to be so unstable that it could not be synthesized or isolated. However, its synthesis and isolation are actually routine. (In fact, a substantial amount of the thiamine pyrophosphate in living things exists as the hydroxyethyl form.)

The reaction of hydroxyethyl-TPP with the oxidized form of lipoic acid yields the energy-rich thiol ester of reduced lipoic acid and results in oxidation of the hydroxyl-carbon of the two-carbon substrate unit (c). This is followed by nucleophilic attack by coenzyme A on the carbonyl-carbon (a characteristic feature of CoA chemistry). The result is transfer of the acetyl group from lipoic acid to CoA. The subsequent oxidation of lipoic acid is catalyzed by the FAD–dependent dihydrolipoyl dehydrogenase and NAD^+ is reduced.

(**c**)

Pyruvate

Resonance-stabilized carbanion on substrate

H^+

Hydroxyethyl-TPP

CO_2

(c) The mechanistic details of the first three steps of the pyruvate dehydrogenase complex reaction.

H^+

Table 20.1

The Enzymes and Reactions of the TCA Cycle

Reaction	Enzyme
1. Acetyl-CoA + oxaloacetate + $H_2O \rightleftharpoons$ CoASH + citrate	Citrate synthase
2. Citrate $\rightleftharpoons$ isocitrate	Aconitase
3. Isocitrate + $NAD^+ \rightleftharpoons$ α-ketoglutarate + NADH + CO_2 + H^+	Isocitrate dehydrogenase
4. α-Ketoglutarate + CoASH + $NAD^+ \rightleftharpoons$ succinyl-CoA + NADH + CO_2 + H^+	α-Ketoglutarate dehydrogenase complex
5. Succinyl-CoA + GDP + $P_i \rightleftharpoons$ succinate + GTP + CoASH	Succinyl-CoA synthetase
6. Succinate + [FAD] $\rightleftharpoons$ fumarate + [$FADH_2$]	Succinate dehydrogenase
7. Fumarate + $H_2O \rightleftharpoons$ L-malate	Fumarase
8. L-Malate + $NAD^+ \rightleftharpoons$ oxaloacetate + NADH + H^+	Malate dehydrogenase

Net for reactions 1–8:

Acetyl-CoA + 3 NAD^+ + [FAD] + GDP + P_i + 2 $H_2O \rightleftharpoons$ CoASH + 3 NADH + [$FADH_2$] + GTP + 2 CO_2 + 3 H^+

Simple combustion of acetate: Acetate + 2 O_2 + $H^+ \rightleftharpoons$ 2 CO_2 + 2 H_2O

20.5 • The Isomerization of Citrate by Aconitase

Citrate itself poses a problem: it is a poor candidate for further oxidation because it contains a tertiary alcohol, which could be oxidized only by breaking a carbon–carbon bond. An obvious solution to this problem is to isomerize the tertiary alcohol to a secondary alcohol, which the cycle proceeds to do in the next step.

Citrate is isomerized to isocitrate by **aconitase** in a two-step process involving aconitate as an intermediate (Figure 20.7). In this reaction, the elements

Aconitase removes the pro-*R* H of the pro-*R* arm of citrate

FIGURE 20.7 • (a) The aconitase reaction converts citrate to *cis*-aconitate and then to isocitrate. Aconitase is stereospecific and removes the pro-*R* hydrogen from the pro-*R* arm of citrate. (b) The active site of aconitase. The iron-sulfur cluster (red) is coordinated by cysteines (yellow) and isocitrate (white).

Table 20.1

Subunit M_r	Oligomeric Composition	$\Delta G°'$ (kJ/mol)	K_{eq} at 25°C	ΔG (kJ/mol)
49,000*	Dimer	−31.4	3.2×10^5	−53.9
44,500	Dimer	+6.7	0.067	+0.8
	$\alpha_2\beta\gamma$	−8.4	29.7	−17.5
E_1 96,000	Dimer			
E_2 70,000	24-mer	−30	1.8×10^5	−43.9
E_3 56,000	Dimer			
α 34,500	$\alpha\beta$	−3.3	3.8	≈0
β 42,500				
α 70,000	$\alpha\beta$	+0.4	0.85	≠0
β 27,000				
48,500	Tetramer	−3.8	4.6	≈0
35,000	Dimer	+29.7	6.2×10^{-6}	≈0
		−40		≈(−115)
		−849		

*CS in mammals, A in pig heart, αKDC in *E. coli,* S-CoA S in pig heart, SD in bovine heart, F in pig heart, MD in pig heart. ΔG values from Newsholme, E. A., and Leech, A. R., 1983. *Biochemistry for the Medical Sciences.* New York: Wiley.

of water are first abstracted from citrate to yield aconitate, which is then rehydrated with H— and HO— adding back in opposite positions to produce isocitrate. The net effect is the conversion of a tertiary alcohol (citrate) to a secondary alcohol (isocitrate). Oxidation of the secondary alcohol of isocitrate involves breakage of a C—H bond, a simpler matter than the C—C cleavage required for the direct oxidation of citrate.

Inspection of the citrate structure shows a total of four chemically equivalent hydrogens, but only one of these—the pro-*R* H atom of the pro-*R* arm of citrate—is abstracted by aconitase, which is quite stereospecific. Formation of the double bond of aconitate following proton abstraction requires departure of hydroxide ion from the C-3 position. Hydroxide is a relatively poor leaving group, and its departure is facilitated in the aconitase reaction by coordination with an iron atom in an iron–sulfur cluster.

Aconitase Utilizes an Iron–Sulfur Cluster

Aconitase contains an **iron–sulfur cluster** consisting of three iron atoms and four sulfur atoms in a near-cubic arrangement (Figure 20.8). This cluster is bound to the enzyme via three cysteine groups from the protein. One corner of the cube is vacant and binds Fe^{2+}, which activates aconitase. The iron atom in this position can coordinate the C-3 carboxyl and hydroxyl groups of citrate. This iron atom thus acts as a Lewis acid, accepting an unshared pair of electrons from the hydroxyl, making it a better leaving group. The equilibrium for the aconitase reaction favors citrate, and an equilibrium mixture typically contains about 90% citrate, 4% *cis*-aconitate, and 6% isocitrate. The $\Delta G°'$ is +6.7 kJ/mol.

FIGURE 20.8 • The iron–sulfur cluster of aconitase. Binding of Fe^{2+} to the vacant position of the cluster activates aconitase. The added iron atom coordinates the C-3 carboxyl and hydroxyl groups of citrate and acts as a Lewis acid, accepting an electron pair from the hydroxyl group and making it a better leaving group.

Fluoroacetate Blocks the TCA Cycle

Fluoroacetate is an extremely poisonous agent that blocks the TCA cycle *in vivo, although it has no apparent effect on any of the isolated enzymes.* Its LD_{50}, the *le*thal *do*se for 50% of animals consuming it, is 0.2 mg per kilogram of body weight; it has been used as a rodent poison. The action of fluoroacetate has been traced to aconitase, which is inhibited *in vivo* by *fluorocitrate,* which is formed from fluoroacetate in two steps (Figure 20.9). Fluoroacetate readily crosses both the cellular and mitochondrial membranes, and in mitochondria it is converted to fluoroacetyl-CoA by *acetyl-CoA synthetase.* Fluoroacetyl-CoA is a substrate for citrate synthase, which condenses it with oxaloacetate to form fluorocitrate. Fluoroacetate may thus be viewed as a **trojan horse inhibitor.** Analogous to the giant Trojan Horse of legend—which the soldiers of Troy took into their city, not knowing that Greek soldiers were hidden inside it and waiting to attack—fluoroacetate enters the TCA cycle innocently enough, in the citrate synthase reaction. Citrate synthase converts fluoroacetate to inhibitory fluorocitrate for its TCA cycle partner, aconitase, blocking the cycle.

FIGURE 20.9 • The conversion of fluoroacetate to fluorocitrate.

20.6 • Isocitrate Dehydrogenase—The First Oxidation in the Cycle

In the next step of the TCA cycle, isocitrate is oxidatively decarboxylated to yield α-ketoglutarate, with concomitant reduction of NAD^+ to NADH in the isocitrate dehydrogenase reaction (Figure 20.10). The reaction has a net $\Delta G^{\circ\prime}$ of -8.4 kJ/mol, and it is sufficiently exergonic to pull the aconitase reaction forward. This two-step reaction involves (1) oxidation of the C-2 alcohol of isocitrate to form oxalosuccinate, followed by (2) a β-decarboxylation reaction that expels the central carboxyl group as CO_2, leaving the product α-ketoglutarate. Oxalosuccinate, the β-keto acid produced by the initial dehydrogenation reaction, is unstable and thus is readily decarboxylated.

Isocitrate Dehydrogenase Links the TCA Cycle and Electron Transport

Isocitrate dehydrogenase provides the first connection between the TCA cycle and the electron transport pathway and oxidative phosphorylation, via its production of NADH. As a connecting point between two metabolic pathways, isocitrate dehydrogenase is a regulated reaction. NADH and ATP are allosteric inhibitors, whereas ADP acts as an allosteric activator, lowering the K_m for isocitrate by a factor of 10. The enzyme is virtually inactive in the absence of ADP. Also, the product, α-ketoglutarate, is a crucial α-keto acid for aminotransferase reactions (see Chapters 14 and 27), connecting the TCA cycle (that is, carbon metabolism) with nitrogen metabolism.

FIGURE 20.10 • (a) The isocitrate dehydrogenase reaction. (b) The active site of isocitrate dehydrogenase. Isocitrate is shown in green, $NADP^+$ is shown in gold, with Ca^{2+} in red.

20.7 • α-Ketoglutarate Dehydrogenase—A Second Decarboxylation

A second oxidative decarboxylation occurs in the **α-ketoglutarate dehydrogenase reaction** (Figure 20.11). Like the pyruvate dehydrogenase complex, α-ketoglutarate dehydrogenase is a multienzyme complex—consisting of *α-ketoglutarate dehydrogenase, dihydrolipoyl transsuccinylase,* and *dihydrolipoyl dehydrogenase*—that employs five different coenzymes (Table 20.2). The dihydrolipoyl dehydrogenase in this reaction is identical to that in the pyruvate dehydrogenase reaction. The mechanism is analogous to that of pyruvate dehydrogenase, and the free energy changes for these reactions are -29 to -33.5 kJ/mol. As with the pyruvate dehydrogenase reaction, this reaction produces NADH and a thioester product—in this case, succinyl-CoA. Succinyl-CoA and NADH products are energy-rich species that are important sources of metabolic energy in subsequent cellular processes.

20.8 • Succinyl-CoA Synthetase—A Substrate-Level Phosphorylation

The NADH produced in the foregoing steps can be routed through the electron transport pathway to make high-energy phosphates via oxidative phosphorylation. However, succinyl-CoA is itself a high-energy intermediate and is utilized in the next step of the TCA cycle to drive the phosphorylation of GDP to GTP (in mammals) or ADP to ATP (in plants and bacteria). The reaction (Figure 20.12) is catalyzed by **succinyl-CoA synthetase,** sometimes called **succinate thiokinase.** The free energies of hydrolysis of succinyl-CoA and GTP or ATP are similar, and the net reaction has a $\Delta G^{\circ\prime}$ of -3.3 kJ/mol. Succinyl-CoA synthetase provides another example of a **substrate-level phosphorylation** (Chapter 19), in which a substrate, rather than an electron transport chain or proton gradient, provides the energy for phosphorylation. It is the only such reaction in the TCA cycle. The GTP produced by mammals in this reaction can exchange its terminal phosphoryl group with ADP via the **nucleoside diphosphate kinase reaction:**

$$\text{GTP} + \text{ADP} \xrightleftharpoons[\text{kinase}]{\text{Nucleoside diphosphate}} \text{ATP} + \text{GDP}$$

FIGURE 20.11 • The α-ketoglutarate dehydrogenase reaction.

Table 20.2

Composition of the α-Ketoglutarate Dehydrogenase Complex from *E. coli*

Enzyme	Coenzyme	Enzyme M_r	Number of Subunits	Subunit M_r	Number of Subunits per Complex
α-Ketoglutarate dehydrogenase	Thiamine pyrophosphate	192,000	2	96,000	24
Dihydrolipoyl transsuccinylase	Lipoic acid, CoASH	1,700,000	24	70,000	24
Dihydrolipoyl dehydrogenase	FAD, NAD$^+$	112,000	2	56,000	12

The Mechanism of Succinyl-CoA Synthetase

The mechanism of succinyl-CoA synthetase is postulated to involve displacement of CoA by phosphate, forming succinyl phosphate at the active site, followed by transfer of the phosphoryl group to an active-site histidine (making a *phosphohistidine* intermediate) and release of succinate. The phosphoryl moiety is then transferred to GDP to form GTP (Figure 20.13). This sequence of steps "preserves" the energy of the thioester bond of succinyl-CoA in a series of high-energy intermediates that lead to a molecule of ATP:

$$\text{Thioester} \longrightarrow [\text{succinyl-P}] \longrightarrow [\text{phosphohistidine}] \longrightarrow \text{GTP} \longrightarrow \text{ATP}$$

The First Five Steps of the TCA Cycle Produce NADH, CO$_2$, GTP (ATP), and Succinate

This is a good point to pause in our trip through the TCA cycle and see what has happened. A two-carbon acetyl group has been introduced as acetyl-CoA and linked to oxaloacetate, and two CO$_2$ molecules have been liberated. The cycle has produced two molecules of NADH and one of GTP or ATP, and has left a molecule of succinate.

The TCA cycle can now be completed by converting succinate to oxaloacetate. This latter process represents a net oxidation. The TCA cycle breaks it down into (consecutively) an oxidation step, a hydration reaction, and a second oxidation step. The oxidation steps are accompanied by the reduction of an [FAD] and an NAD$^+$. The reduced coenzymes, [FADH$_2$] and NADH, subsequently provide reducing power in the electron transport chain. (We see in Chapter 24 that virtually the same chemical strategy is used in β-oxidation of fatty acids.)

FIGURE 20.12 • The succinyl-CoA synthetase reaction.

FIGURE 20.13 • The mechanism of the succinyl-CoA synthetase reaction.

FIGURE 20.14 • The succinate dehydrogenase reaction. Oxidation of succinate occurs with reduction of [FAD]. Reoxidation of [FADH$_2$] transfers electrons to coenzyme Q.

FIGURE 20.15 • The covalent bond between FAD and succinate dehydrogenase involves the C-8a methylene group of FAD and the N-3 of a histidine residue on the enzyme.

FIGURE 20.16 • The Fe$_2$S$_2$ cluster of succinate dehydrogenase.

20.9 • Succinate Dehydrogenase—An Oxidation Involving FAD

The oxidation of succinate to fumarate (Figure 20.14) is carried out by **succinate dehydrogenase,** a membrane-bound enzyme that is actually part of the electron transport chain. As will be seen in Chapter 21, succinate dehydrogenase is part of the succinate–coenzyme Q reductase of the electron transport chain. In contrast with all of the other enzymes of the TCA cycle, which are soluble proteins found in the mitochondrial matrix, succinate dehydrogenase is an integral membrane protein tightly associated with the inner mitochondrial membrane. Succinate oxidation involves removal of H atoms across a C—C bond, rather than a C—O or C—N bond, and produces the *trans*-unsaturated fumarate. This reaction (the oxidation of an alkane to an alkene) is not sufficiently exergonic to reduce NAD$^+$, but it does yield enough energy to reduce [FAD]. (By contrast, oxidations of alcohols to ketones or aldehydes are more energetically favorable and provide sufficient energy to reduce NAD$^+$.) This important point is illustrated and clarified in an example in Chapter 21.

Succinate dehydrogenase is a dimeric protein, with subunits of molecular masses 70 kD and 27 kD (see Table 20.1). FAD is covalently bound to the larger subunit; the bond involves a methylene group of C-8a of FAD and N-3 of a histidine on the protein (Figure 20.15). Succinate dehydrogenase also contains three different iron–sulfur clusters (Figure 20.16). Viewed from either end of the succinate molecule, the reaction involves dehydrogenation α,β to a carbonyl (actually, a carboxyl) group. The dehydrogenation is stereospecific (Figure 20.14), with the pro-*S* hydrogen removed from one carbon atom and the pro-*R* hydrogen removed from the other. The electrons captured by [FAD] in this reaction are passed directly into the iron–sulfur clusters of the enzyme and on to *coenzyme Q(UQ)*. The covalently bound FAD is first reduced to [FADH$_2$] and then reoxidized to form [FAD] and the reduced form of coenzyme Q, UQH_2. Electrons captured by UQH_2 then flow through the rest of the electron transport chain in a series of events that is discussed in detail in Chapter 21.

Note that flavin coenzymes can carry out either one-electron or two-electron transfers. The succinate dehydrogenase reaction represents a net two-electron reduction of FAD.

20.10 • Fumarase Catalyzes *Trans*-Hydration of Fumarate

Fumarate is hydrated in a stereospecific reaction by fumarase to give L-malate (Figure 20.17). The reaction involves *trans*-addition of the elements of water across the double bond. Recall that aconitase carries out a similar reaction,

FIGURE 20.17 • The fumarase reaction.

Carbonium ion mechanism

FIGURE 20.18 • Two possible mechanisms for the fumarase reaction.

and that *trans*-addition of —H and —OH occurs across the double bond of *cis*-aconitate. Though the exact mechanism is uncertain, it may involve protonation of the double bond to form an intermediate carbonium ion (Figure 20.18) or possibly attack by water or OH^- anion to produce a carbanion, followed by protonation.

20.11 • Malate Dehydrogenase—Completing the Cycle

In the last step of the TCA cycle, L-malate is oxidized to oxaloacetate by **malate dehydrogenase** (Figure 20.19). This reaction is very endergonic, with a $\Delta G°'$ of +30 kJ/mol. Consequently, the concentration of oxaloacetate in the mitochondrial matrix is usually quite low (see the following example). The reaction, however, is pulled forward by the favorable citrate synthase reaction. Oxidation of malate is coupled to reduction of yet another molecule of NAD^+, the third one of the cycle. Counting the [FAD] reduced by succinate dehydrogenase, this makes the fourth coenzyme reduced through oxidation of a single acetate unit.

FIGURE 20.19 • The malate dehydrogenase reaction.

A D E E P E R   L O O K

Steric Preferences in NAD⁺-Dependent Dehydrogenases

As noted in Chapter 18, the enzymes that require nicotinamide coenzymes are stereospecific and transfer hydride to either the pro-*R* or the pro-*S* positions selectively. The table (facing page) lists the preferences of several dehydrogenases.

What accounts for this stereospecificity? It arises from the fact that the enzymes (and especially the active sites of enzymes) are inherently asymmetric structures. The nicotinamide coenzyme (and the substrate) fit the active site in only one way. Malate

dehydrogenase, the citric acid cycle enzyme, transfers hydride to the H_R position of NADH, but glyceraldehyde-3-P dehydrogenase in the glycolytic pathway transfers hydride to the H_S position, as shown in the accompanying table. Dehydrogenases are stereospecific with respect to the substrates as well. Note that alcohol dehydrogenase removes hydrogen from the pro-*R* position of ethanol and transfers it to the pro-*R* position of NADH.

NAD(P)⁺-dependent enzymes are stereospecific. Malate dehydrogenase, for example, transfers a hydride to the pro-*R* position of NADH, whereas glyceraldehyde-3-phosphate dehydrogenase transfers a hydride to the pro-*S* position of the nicotinamide. Alcohol dehydrogenase removes a hydride from the pro-*R* position of ethanol and transfers it to the pro-*R* position of NADH.

Steric Specificity for NAD of Various Pyridine Nucleotide-Linked Enzymes

Dehydrogenase	Source	Steric Specificity
Alcohol (with ethanol)	Yeast, *Pseudomonas,* liver, wheat germ	
Alcohol (with isopropyl alcohol)	Yeast	
Acetaldehyde	Liver	
L-Lactate	Heart muscle, *Lactobacillus*	H_R
L-Malate	Pig heart, wheat germ	
D-Glycerate	Spinach	
Dihydroorotate	*Zymobacterium oroticum*	
α-Glycerophosphate	Muscle	
Glyceraldehyde-3-P	Yeast, muscle	
L-Glutamate	Liver	
D-Glucose	Liver	
β-Hydroxysteroid	*Pseudomonas*	
NADH cytochrome *c* reductase	Rat liver mitochondria, pig heart	H_S
NADPH transhydrogenase	*Pseudomonas*	
NADH diaphorase	Pig heart	
L-β-Hydroxybutyryl-CoA	Heart muscle	

The stereospecificity of hydride transfer in dehydrogenases is a consequence of the asymmetric nature of the active site.

EXAMPLE

A typical intramitochondrial concentration of malate is 0.22 mM. If the $[NAD^+]/[NADH]$ ratio in mitochondria is 20 and if the malate dehydrogenase reaction is at equilibrium, calculate the intramitochondrial concentration of oxaloacetate at 25°C.

SOLUTION

For the malate dehydrogenase reaction,

$$\text{Malate} + NAD^+ \rightleftharpoons \text{oxaloacetate} + NADH + H^+$$

with the value of $\Delta G°'$ being +30 kJ/mol. Then

$$\Delta G°' = -RT \ln K_{eq}$$

$$= -(8.314 \text{ J/mol·K}) (298) \ln \left(\frac{[1] x}{[20][2.2 \times 10^{-4}]} \right)$$

$$\frac{-30,000 \text{ J/mol}}{2478 \text{ J/mol}} = \ln (x/4.4 \times 10^{-3})$$

$$-12.1 = \ln (x/4.4 \times 10^{-3})$$

$$x = (5.6 \times 10^{-6})(4.4 \times 10^{-3})$$

$$x = [\text{oxaloacetate}] = 0.024 \ \mu M$$

Malate dehydrogenase is structurally and functionally similar to other dehydrogenases, notably lactate dehydrogenase (Figure 20.20). Both consist of alternating β-sheet and α-helical segments. Binding of NAD^+ causes a conformational change in the 20-residue segment that connects the D and E strands of the β-sheet. The change is triggered by an interaction between the adenosine phosphate moiety of NAD^+ and an arginine residue in this loop region. Such a conformational change is consistent with an ordered single-displacement mechanism for NAD^+-dependent dehydrogenases (Chapter 14).

FIGURE 20.20 • (a) The structure of malate dehydrogenase. (b) The active site of malate dehydrogenase. Malate is shown in red; NAD^+ is blue.

20.12 • A Summary of the Cycle

The net reaction accomplished by the TCA cycle, as follows, shows two molecules of CO_2, one ATP, and four reduced coenzymes produced per acetate group oxidized. The cycle is exergonic, with a net $\Delta G°'$ for one pass around the cycle of approximately -40 kJ/mol. Table 20.1 compares the $\Delta G°'$ values for the individual reactions with the overall $\Delta G°'$ for the net reaction.

$$\text{Acetyl-CoA} + 3\text{ NAD}^+ + [\text{FAD}] + \text{ADP} + \text{P}_i + 2\text{ H}_2\text{O} \rightleftharpoons$$
$$2\text{ CO}_2 + 3\text{ NADH} + 3\text{ H}^+ + [\text{FADH}_2] + \text{ATP} + \text{CoASH}$$
$$\Delta G°' = -40\text{ kJ/mol}$$

Glucose metabolized via glycolysis produces two molecules of pyruvate and thus two molecules of acetyl-CoA, which can enter the TCA cycle. Combining glycolysis and the TCA cycle gives the net reaction shown:

$$\text{Glucose} + 2\text{ H}_2\text{O} + 10\text{ NAD}^+ + 2\text{ [FAD]} + 4\text{ ADP} + 4\text{ P}_i \rightleftharpoons$$
$$6\text{ CO}_2 + 10\text{ NADH} + 10\text{ H}^+ + 2\text{ [FADH}_2] + 4\text{ ATP}$$

All six carbons of glucose are liberated as CO_2, and a total of four molecules of ATP are formed thus far in substrate-level phosphorylations. The 12 reduced coenzymes produced up to this point can eventually produce a maximum of 34 molecules of ATP in the electron transport and oxidative phosphorylation pathways. A stoichiometric relationship for these subsequent processes is

$$\text{NADH} + \text{H}^+ + \tfrac{1}{2}\text{O}_2 + 3\text{ ADP} + 3\text{ P}_i \rightleftharpoons \text{NAD}^+ + 3\text{ ATP} + 4\text{ H}_2\text{O}$$
$$[\text{FADH}_2] + \tfrac{1}{2}\text{O}_2 + 2\text{ ADP} + 2\text{ P}_i \rightleftharpoons [\text{FAD}] + 2\text{ ATP} + 3\text{ H}_2\text{O}$$

Thus, a total of 3 ATP per NADH and 2 ATP per $FADH_2$ may be produced through the processes of electron transport and oxidative phosphorylation.

The Fate of the Carbon Atoms of Acetyl-CoA in the TCA Cycle

It is instructive to consider how the carbon atoms of a given acetate group are routed through several turns of the TCA cycle. As shown in Figure 20.21, neither of the carbon atoms of a labeled acetate unit is lost as CO_2 in the first turn of the cycle. The CO_2 evolved in any turn of the cycle derives from the carboxyl groups of the oxaloacetate acceptor (from the previous turn), not from incoming acetyl-CoA. On the other hand, succinate labeled on one end from the original labeled acetate forms two different labeled oxaloacetates. The carbonyl carbon of acetyl-CoA is evenly distributed between the two carboxyl carbons of oxaloacetate, and the labeled methyl carbon of incoming acetyl-CoA ends up evenly distributed between the methylene and carbonyl carbons of oxaloacetate.

When these labeled oxaloacetates enter a second turn of the cycle, both of the carboxyl carbons are lost as CO_2, but the methylene and carbonyl carbons survive through the second turn. Thus, the methyl carbon of a labeled acetyl-CoA survives two full turns of the cycle. In the third turn of the cycle, one-half of the carbon from the original methyl group of acetyl-CoA has become one of the carboxyl carbons of oxaloacetate and is thus lost as CO_2. In the fourth turn of the cycle, further "scrambling" results in loss of half of the remaining labeled carbon (one-fourth of the original methyl carbon label of acetyl-CoA), and so on.

It can be seen that the carbonyl and methyl carbons of labeled acetyl-CoA have very different fates in the TCA cycle. The carbonyl carbon survives the first turn intact but is completely lost in the second turn. The methyl carbon

(a) Fate of the carboxyl carbon of acetate unit

All labelled carboxyl carbon removed by these two steps

(b) Fate of methyl carbon of acetate unit

survives two full turns, then undergoes a 50% loss through each succeeding turn of the cycle.

It is worth noting that the carbon–carbon bond cleaved in the TCA pathway entered as an acetate unit in the previous turn of the cycle. Thus, the oxidative decarboxylations that cleave this bond are just a cleverly disguised acetate C—C cleavage and oxidation.

20.13 • The TCA Cycle Provides Intermediates for Biosynthetic Pathways

Until now we have viewed the TCA cycle as a catabolic process because it oxidizes acetate units to CO_2 and converts the liberated energy to ATP and reduced coenzymes. The TCA cycle is, after all, the end point for breakdown of food materials, at least in terms of carbon turnover. However, as shown in Figure 20.22, four-, five-, and six-carbon species produced in the TCA cycle also fuel a variety of **biosynthetic processes.** α-Ketoglutarate, succinyl-CoA, fumarate, and oxaloacetate are all precursors of important cellular species. (In order to par-

FIGURE 20.21 • The fate of the carbon atoms of acetate in successive TCA cycles. (a) The carbonyl carbon of acetyl-CoA is fully retained through one turn of the cycle but is lost completely in a second turn of the cycle. (b) The methyl carbon of a labeled acetyl-CoA survives two full turns of the cycle but becomes equally distributed among the four carbons of oxaloacetate by the end of the second turn. In each subsequent turn of the cycle, one-half of this carbon (the original labeled methyl group) is lost.

FIGURE 20.22 • The TCA cycle provides intermediates for numerous biosynthetic processes in the cell.

ticipate in eukaryotic biosynthetic processes, however, they must first be transported out of the mitochondria.) A transamination reaction converts α-ketoglutarate directly to glutamate, which can then serve as a versatile precursor for proline, arginine, and glutamine (as described in Chapter 26). Succinyl-CoA provides most of the carbon atoms of the porphyrins. Oxaloacetate can be transaminated to produce aspartate. Aspartic acid itself is a precursor of the pyrimidine nucleotides and, in addition, is a key precursor for the synthesis of asparagine, methionine, lysine, threonine, and isoleucine. Oxaloacetate can also be decarboxylated to yield PEP, which is a key element of several pathways, namely (1) synthesis (in plants and microorganisms) of the aromatic amino acids phenylalanine, tyrosine, and tryptophan; (2) formation of 3-phospho-glycerate and conversion to the amino acids serine, glycine, and cysteine; and (3) *gluconeogenesis*, which, as we will see in Chapter 23, is the pathway that synthesizes new glucose and many other carbohydrates.

Finally, citrate can be exported from the mitochondria and then broken down by **ATP-citrate lyase** to yield oxaloacetate and acetyl-CoA, a precursor of fatty acids (Figure 20.23). Oxaloacetate produced in this reaction is rapidly reduced to malate, which can then be processed in either of two ways: it may be transported into mitochondria, where it is reoxidized to oxaloacetate, or it may be oxidatively decarboxylated to pyruvate by **malic enzyme,** with subse-

FIGURE 20.23 • Export of citrate from mitochondria and cytosolic breakdown produces oxaloacetate and acetyl-CoA. Oxaloacetate is recycled to malate or pyruvate, which re-enters the mitochondria. This cycle provides acetyl-CoA for fatty acid synthesis in the cytosol.

quent mitochondrial uptake of pyruvate. This cycle permits citrate to provide acetyl-CoA for biosynthetic processes, with return of the malate and pyruvate by-products to the mitochondria.

20.14 • The Anaplerotic, or "Filling Up," Reactions

In a sort of reciprocal arrangement, the cell also feeds many intermediates back into the TCA cycle from other reactions. Since such reactions replenish the TCA cycle intermediates, Hans Kornberg proposed that they be called **anaplerotic reactions** (literally, the "filling up" reactions). Thus, **PEP carboxylase** and **pyruvate carboxylase** synthesize oxaloacetate from pyruvate (Figure 20.24).

Pyruvate carboxylase is the most important of the anaplerotic reactions. It exists in the mitochondria of animal cells but not in plants, and it provides a direct link between glycolysis and the TCA cycle. The enzyme is tetrameric and contains covalently bound biotin and an Mg^{2+} site on each subunit. (It is examined in greater detail in our discussion of gluconeogenesis in Chapter 23.) Pyruvate carboxylase has an absolute allosteric requirement for acetyl-CoA. Thus, when acetyl-CoA levels exceed the oxaloacetate supply, allosteric activation of pyruvate carboxylase by acetyl-CoA raises oxaloacetate levels, so that the excess acetyl-CoA can enter the TCA cycle.

FIGURE 20.24 • Phosphoenolpyruvate (PEP) carboxylase, pyruvate carboxylase, and malic enzyme catalyze anaplerotic reactions, replenishing TCA cycle intermediates.

$\mathscr{A}$ D E E P E R L O O K

Fool's Gold and the Reductive Citric Acid Cycle—The First Metabolic Pathway?

How did life arise on the planet Earth? It was once supposed that a reducing atmosphere, together with random synthesis of organic compounds, gave rise to a prebiotic "soup," in which the first living things appeared. However, certain key compounds, such as arginine, lysine, and histidine, the straight-chain fatty acids, porphyrins, and essential coenzymes, have not been convincingly synthesized under simulated prebiotic conditions. This and other problems have led researchers to consider other models for the evolution of life.

One of these alternate models, postulated by Günter Wächtershäuser, involves an archaic version of the TCA cycle running in the reverse (reductive) direction. Reversal of the TCA cycle results in assimilation of CO_2 and fixation of carbon as shown. For each turn of the reversed cycle, two carbons are fixed in the formation of isocitrate and two more are fixed in the reductive transformation of acetyl-CoA to oxaloacetate. Thus, for every succinate that enters the reversed cycle, two succinates are returned, making the cycle highly autocatalytic. Because TCA cycle intermediates are involved in many biosynthetic pathways (see Section 20.13), a reversed TCA cycle would be a bountiful and broad source of metabolic substrates.

A reversed, reductive TCA cycle would require energy input to drive it. What might have been the thermodynamic driving force for such a cycle? Wächtershäuser hypothesizes that the anaerobic reaction of FeS and H_2S to form insoluble FeS_2 (pyrite, also known as fool's gold) in the prebiotic milieu could have been the driving reaction:

$$FeS + H_2S \longrightarrow FeS_2 \text{ (pyrite) } \downarrow + H_2$$

This reaction is highly exergonic, with a standard-state free energy change ($\Delta G°'$) of -38 kJ/mol. Under the conditions that might have existed in a prebiotic world, this reaction would have been sufficiently exergonic to drive the reductive steps of a reversed TCA cycle. In addition, in an H_2S-rich prebiotic environment, organic compounds would have been in equilibrium with their thio-organic counterparts. High-energy thioesters formed in this way may have played key roles in the energetics of early metabolic pathways.

Wächtershäuser has also suggested that early metabolic processes first occurred on the surface of pyrite and other related mineral materials. The iron–sulfur chemistry that prevailed on these mineral surfaces may have influenced the evolution of the iron–sulfur proteins that control and catalyze many reactions in modern pathways (including the succinate dehydrogenase and aconitase reactions of the TCA cycle).

A Reductive, Reversed TCA Cycle

FIGURE 20.25 • The phosphoenolpyruvate carboxykinase reaction.

PEP carboxylase occurs in yeast, bacteria, and higher plants, but not in animals. The enzyme is specifically inhibited by aspartate, which is produced by transamination of oxaloacetate. Thus, organisms utilizing this enzyme control aspartate production by regulation of PEP carboxylase. Malic enzyme is found in the cytosol or mitochondria of many animal and plant cells and is an NADPH-dependent enzyme.

It is worth noting that the reaction catalyzed by **PEP carboxykinase** (Figure 20.25) could also function as an anaplerotic reaction, were it not for the particular properties of the enzyme. CO_2 binds weakly to PEP carboxykinase, whereas oxaloacetate binds very tightly ($K_D = 2 \times 10^{-6}$ M), and, as a result, the enzyme favors formation of PEP from oxaloacetate.

The catabolism of amino acids provides pyruvate, acetyl-CoA, oxaloacetate, fumarate, α-ketoglutarate, and succinate, all of which may be oxidized by the TCA cycle. In this way, proteins may serve as excellent sources of nutrient energy, as seen in Chapter 26.

20.15 • Regulation of the TCA Cycle

Situated as it is between glycolysis and the electron transport chain, the TCA cycle must be carefully controlled by the cell. If the cycle were permitted to run unchecked, large amounts of metabolic energy could be wasted in over-production of reduced coenzymes and ATP; conversely, if it ran too slowly, ATP would not be produced rapidly enough to satisfy the needs of the cell. Also, as just seen, the TCA cycle is an important source of precursors for biosynthetic processes and must be able to provide them as needed.

What are the sites of regulation in the TCA cycle? Based upon our experience with glycolysis (Figure 19.31), we might anticipate that some of the reactions of the TCA cycle would operate near equilibrium under cellular conditions (with $\Delta G \approx 0$), whereas others—the sites of regulation—would be characterized by large, negative ΔG values. Estimates for the values of ΔG in mitochondria, based on mitochondrial concentrations of metabolites, are summarized in Table 20.1. Three reactions of the cycle—citrate synthase, isocitrate dehydrogenase, and α-ketoglutarate dehydrogenase—operate with large, negative ΔG values under mitochondrial conditions and are thus the primary sites of regulation in the cycle.

The regulatory actions that control the TCA cycle are shown in Figure 20.26. As one might expect, the principal regulatory "signals" are the concentrations of acetyl-CoA, ATP, NAD^+, and NADH, with additional effects provided by several other metabolites. The main sites of regulation are pyruvate dehydrogenase, citrate synthase, isocitrate dehydrogenase, and α-ketoglutarate dehydrogenase. All of these enzymes are inhibited by NADH, so that when the cell has produced all the NADH that can conveniently be turned into ATP, the cycle shuts down. For similar reasons, ATP is an inhibitor of pyruvate dehydrogenase and isocitrate dehydrogenase. The TCA cycle is turned on, however, when either the ADP/ATP or NAD^+/NADH ratio is high, an indication that the cell has run low on ATP or NADH. Regulation of the TCA cycle by NADH,

FIGURE 20.26 • Regulation of the TCA cycle.

NAD^+, ATP, and ADP thus reflects the energy status of the cell. On the other hand, succinyl-CoA is an *intracycle regulator,* inhibiting citrate synthase and α-ketoglutarate dehydrogenase. Acetyl-CoA acts as a signal to the TCA cycle that glycolysis or fatty acid breakdown is producing two-carbon units. Acetyl-CoA activates pyruvate carboxylase, the anaplerotic reaction that provides oxaloacetate, the acceptor for increased flux of acetyl-CoA into the TCA cycle.

Regulation of Pyruvate Dehydrogenase

As we shall see in Chapter 23, most organisms can synthesize sugars such as glucose from pyruvate. However, animals cannot synthesize glucose from acetyl-CoA. For this reason, the pyruvate dehydrogenase complex, which converts pyruvate to acetyl-CoA, plays a pivotal role in metabolism. Conversion to acetyl-CoA commits nutrient carbon atoms either to oxidation in the TCA cycle or to fatty acid synthesis (see Chapter 25). Because this choice is so crucial to the organism, pyruvate dehydrogenase is a carefully regulated enzyme. It is subject to product inhibition and is further regulated by nucleotides. Finally, activity of pyruvate dehydrogenase is regulated by phosphorylation and dephosphorylation of the enzyme complex itself.

High levels of either product, acetyl-CoA or NADH, allosterically inhibit the pyruvate dehydrogenase complex. Acetyl-CoA specifically blocks dihydrolipoyl transacetylase, and NADH acts on dihydrolipoyl dehydrogenase. The mammalian pyruvate dehydrogenase is also regulated by covalent modifications. As shown in Figure 20.27, a Mg^{2+}-dependent **pyruvate dehydrogenase kinase** is associated with the enzyme in mammals. This kinase is allosterically activated by NADH and acetyl-CoA, and when levels of these metabolites rise in the mitochondrion, they stimulate phosphorylation of a serine residue on the pyruvate dehydrogenase subunit, blocking the first step of the pyruvate dehydrogenase reaction, the decarboxylation of pyruvate. Inhibition of the dehydrogenase in this manner eventually lowers the levels of NADH and acetyl-CoA in the matrix of the mitochondrion. Reactivation of the enzyme is carried out by **pyruvate dehydrogenase phosphatase,** a Ca^{2+}-activated enzyme that binds to the dehydrogenase complex and hydrolyzes the phosphoserine moiety on the dehydrogenase subunit. At low ratios of NADH to NAD^+ and low acetyl-CoA levels, the phosphatase maintains the dehydrogenase in an activated state, but a high level of acetyl-CoA or NADH once again activates the kinase and leads to the inhibition of the dehydrogenase. Insulin and Ca^{2+} ions activate dephosphorylation, and pyruvate inhibits the phosphorylation reaction.

Pyruvate dehydrogenase is also sensitive to the energy status of the cell. AMP activates pyruvate dehydrogenase, whereas GTP inhibits it. High levels of AMP are a sign that the cell may become energy-poor. Activation of pyruvate dehydrogenase under such conditions commits pyruvate to energy production.

Regulation of Isocitrate Dehydrogenase

The mechanism of regulation of isocitrate dehydrogenase is in some respects the reverse of pyruvate dehydrogenase. The mammalian isocitrate dehydrogenase is subject only to allosteric activation by ADP and NAD^+ and to inhibition by ATP and NADH. Thus, high NAD^+/NADH and ADP/ATP ratios stimulate isocitrate dehydrogenase and TCA cycle activity. The *Escherichia coli* enzyme, on the other hand, is regulated by covalent modification. Serine residues on each subunit of the dimeric enzyme are phosphorylated by a protein kinase, causing inhibition of the isocitrate dehydrogenase activity. Activity is restored by the action of a specific phosphatase. When TCA cycle and glycolytic intermediates—such as isocitrate, 3-phosphoglycerate, pyruvate, PEP, and oxaloacetate—are high, the kinase is inhibited, the phosphatase is acti-

FIGURE 20.27 • Regulation of the pyruvate dehydrogenase reaction.

vated, and the TCA cycle operates normally. When levels of these intermediates fall, the kinase is activated, isocitrate dehydrogenase is inhibited, and isocitrate is diverted to the *glyoxylate pathway,* as explained in the next section.

It may seem surprising that isocitrate dehydrogenase is strongly regulated, because it is not an apparent branch point within the TCA cycle. However, the citrate/isocitrate ratio controls the rate of production of cytosolic acetyl-CoA, because acetyl-CoA in the cytosol is derived from citrate exported from the mitochondrion. (Breakdown of cytosolic citrate produces oxaloacetate and acetyl-CoA, which can be used in a variety of biosynthetic processes.) Thus, isocitrate dehydrogenase activity in the mitochondrion favors catabolic TCA cycle activity over anabolic utilization of acetyl-CoA in the cytosol.

20.16 • The Glyoxylate Cycle of Plants and Bacteria

Plants (particularly seedlings, which cannot yet accomplish efficient photosynthesis), as well as some bacteria and algae, can use acetate as the *only* source of carbon for all the carbon compounds they produce. Although we saw that the TCA cycle can supply intermediates for some biosynthetic processes, the

cycle gives off 2 CO_2 for every two-carbon acetate group that enters and cannot effect the *net synthesis* of TCA cycle intermediates. Thus, it would not be possible for the cycle to produce the massive amounts of biosynthetic intermediates needed for acetate-based growth unless alternative reactions were available. In essence, the TCA cycle is geared primarily to energy production, and it "wastes" carbon units by giving off CO_2. Modification of the cycle to support acetate-based growth would require eliminating the CO_2-producing reactions and enhancing the net production of four-carbon units (i.e., oxaloacetate). Plants and bacteria employ a modification of the TCA cycle called the **glyoxylate cycle** to produce four-carbon dicarboxylic acids (and eventually even sugars) from two-carbon acetate units. The glyoxylate cycle bypasses the two oxidative decarboxylations of the TCA cycle, and instead routes isocitrate through the **isocitrate lyase** and **malate synthase** reactions (Figure 20.28). *Glyoxylate* produced by isocitrate lyase reacts with a second molecule of acetyl-

FIGURE 20.28 • The glyoxylate cycle. The first two steps are identical to TCA cycle reactions. The third step bypasses the CO_2-evolving steps of the TCA cycle to produce succinate and glyoxylate. The malate synthase reaction forms malate from glyoxylate and another acetyl-CoA. The result is that one turn of the cycle consumes one oxaloacetate and two acetyl-CoA molecules but produces two molecules of oxaloacetate. The net for this cycle is one oxaloacetate from two acetyl-CoA molecules.

CoA to form L-malate. The net effect is to conserve carbon units, using two acetyl-CoA molecules per cycle to generate oxaloacetate. Some of this is converted to PEP and then to glucose by pathways discussed in Chapter 23.

The Glyoxylate Cycle Operates in Specialized Organelles

The enzymes of the glyoxylate cycle in plants are contained in **glyoxysomes,** organelles devoted to this cycle. Yeast and algae carry out the glyoxylate cycle in the cytoplasm. The enzymes common to both the TCA and glyoxylate pathways exist as isozymes, with spatially and functionally distinct enzymes operating independently in the two cycles.

Isocitrate Lyase Short-Circuits the TCA Cycle by Producing Glyoxylate and Succinate

The **isocitrate lyase** reaction (Figure 20.29) produces succinate, a four-carbon product of the cycle, as well as glyoxylate, which can then combine with a second molecule of acetyl-CoA. Isocitrate lyase catalyzes an aldol cleavage and is similar to the reaction mediated by aldolase in glycolysis. The **malate synthase** reaction (Figure 20.30), a Claisen condensation of acetyl-CoA with the aldehyde of glyoxylate to yield malate, is quite similar to the citrate synthase reaction. Compared with the TCA cycle, the glyoxylate cycle (a) contains only five steps (as opposed to eight), (b) lacks the CO_2-liberating reactions, (c) consumes two molecules of acetyl-CoA per cycle, and (d) produces four-carbon units (oxaloacetate) as opposed to one-carbon units.

The Glyoxylate Cycle Helps Plants Grow in the Dark

The existence of the glyoxylate cycle explains how certain seeds grow underground (or in the dark), where photosynthesis is impossible. Many seeds (peanuts, soybeans, and castor beans, for example) are rich in lipids; and, as we see in Chapter 24, most organisms degrade the fatty acids of lipids to acetyl-CoA. Glyoxysomes form in seeds as germination begins, and the glyoxylate cycle uses the acetyl-CoA produced in fatty acid oxidation to provide large amounts of oxaloacetate and other intermediates for carbohydrate synthesis. Once the growing plant begins photosynthesis and can fix CO_2 to produce carbohydrates (see Chapter 22), the glyoxysomes disappear.

Glyoxysomes Must Borrow Three Reactions from Mitochondria

Glyoxysomes do not contain all the enzymes needed to run the glyoxylate cycle; succinate dehydrogenase, fumarase, and malate dehydrogenase are absent. Consequently, glyoxysomes must cooperate with mitochondria to run their cycle (Figure 20.31). Succinate travels from the glyoxysomes to the mitochondria, where it is converted to oxaloacetate. Transamination to aspartate follows

FIGURE 20.29 • The isocitrate lyase reaction.

FIGURE 20.30 • The malate synthase reaction.

because oxaloacetate cannot be transported out of the mitochondria. Aspartate formed in this way then moves from the mitochondria back to the glyoxysomes, where a reverse transamination with α-ketoglutarate forms oxaloacetate, completing the shuttle. Finally, to balance the transaminations, glutamate shuttles from glyoxysomes to mitochondria.

FIGURE 20.31 • Glyoxysomes lack three of the enzymes needed to run the glyoxylate cycle. Succinate dehydrogenase, fumarase, and malate dehydrogenase are all "borrowed" from the mitochondria in a shuttle in which succinate and glutamate are passed to the mitochondria, and α-ketoglutarate and aspartate are passed to the glyoxysome.

PROBLEMS

1. Describe the labeling pattern that would result from the introduction into the TCA cycle of glutamate labeled at C_γ with ^{14}C.

2. Describe the effect on the TCA cycle of (a) increasing the concentration of NAD^+, (b) reducing the concentration of ATP, and (c) increasing the concentration of isocitrate.

3. The serine residue of isocitrate dehydrogenase that is phosphorylated by protein kinase lies within the active site of the enzyme. This situation contrasts with most other examples of covalent modification by protein phosphorylation, where the phosphorylation occurs at a site remote from the active site. What direct effect do you think such active-site phosphorylation might have on the catalytic activity of isocitrate dehydrogenase? (See Barford, D., 1991. Molecular mechanisms for the control of enzymic activity by protein phosphorylation. *Biochimica et Biophysica Acta* **1133:**55–62.)

4. The first step of the α-ketoglutarate dehydrogenase reaction involves decarboxylation of the substrate and leaves a covalent TPP intermediate. Write a reasonable mechanism for this reaction.

5. In a tissue where the TCA cycle has been inhibited by fluoroacetate, what difference in the concentration of each TCA cycle metabolite would you expect, compared with a normal, uninhibited tissue?

6. On the basis of the description in Chapter 18 of the physical properties of FAD and $FADH_2$, suggest a method for the measurement of the enzyme activity of succinate dehydrogenase.

7. Starting with citrate, isocitrate, α-ketoglutarate, and succinate, state which of the individual carbons of the molecule undergo oxidation in the next step of the TCA cycle. Which molecules undergo a net oxidation?

8. In addition to fluoroacetate, consider whether other analogs of TCA cycle metabolites or intermediates might be introduced to inhibit other, specific reactions of the cycle. Explain your reasoning.

9. Based on the action of thiamine pyrophosphate in catalysis of the pyruvate dehydrogenase reaction, suggest a suitable chemical mechanism for the pyruvate decarboxylase reaction in yeast:

$$\text{pyruvate} \longrightarrow \text{acetaldehyde} + CO_2$$

10. Aconitase catalyzes the citric acid cycle reaction:

$$\text{citrate} \rightleftharpoons \text{isocitrate}$$

The standard free energy change, $\Delta G^{\circ\prime}$, for this reaction is $+6.7$ kJ/mol. However, the observed free energy change (ΔG) for this reaction in pig heart mitochondria is $+0.8$ kJ/mol. What is the ratio of [isocitrate]/[citrate] in these mitochondria? If [isocitrate] $= 0.03$ *mM*, what is [citrate]?

FURTHER READING

Akiyama, S. K., and Hammes, G. G., 1980. Elementary steps in the reaction mechanism of the pyruvate dehydrogenase multienzyme complex from *Escherichia coli:* Kinetics of acetylation and deacetylation. *Biochemistry* **19:**4208–4213.

Akiyama, S. K., and Hammes, G. G., 1981. Elementary steps in the reaction mechanism of the pyruvate dehydrogenase multienzyme complex from *Escherichia coli:* Kinetics of flavin reduction. *Biochemistry* **20:**1491–1497.

Atkinson, D. E., 1977. *Cellular Energy Metabolism and Its Regulation.* New York: Academic Press.

Bodner, G. M., 1986. The tricarboxylic acid (TCA), citric acid or Krebs cycle. *Journal of Chemical Education* **63:**673–677.

Frey, P. A., 1982. Mechanism of coupled electron and group transfer in *Escherichia coli* pyruvate dehydrogenase. *Annals of the New York Academy of Sciences* **378:**250–264.

Gibble, G.W., 1973. Fluoroacetate toxicity. *Journal of Chemical Education* **50:**460–462.

Hansford, R. G., 1980. Control of mitochondrial substrate oxidation. In *Current Topics in Bioenergetics,* vol. 10, pp. 217–278. New York: Academic Press.

Hawkins, R. A., and Mans, A. M., 1983. Intermediary metabolism of carbohydrates and other fuels. In *Handbook of Neurochemistry,* 2nd ed., Lajtha, A., ed., pp. 259–294. New York: Plenum Press.

Kelly, R. M., and Adams, M. W., 1994. Metabolism in hyperthermophilic microorganisms. *Antonie van Leeuwenhoek* **66:**247–270.

Krebs, H. A., 1970. The history of the tricarboxylic acid cycle. *Perspectives in Biology and Medicine* **14:**154–170.

Krebs, H. A., 1981. *Reminiscences and Reflections.* Oxford, England: Oxford University Press.

Lowenstein, J. M., 1967. The tricarboxylic acid cycle. In *Metabolic Pathways,* 3rd ed., Greenberg, D., ed,. vol. 1, pp. 146–270. New York: Academic Press.

Lowenstein, J. M., ed., 1969. *Citric Acid Cycle: Control and Compartmentation.* New York: Marcel Dekker.

Maden, B. E., 1995. No soup for starters? Autotrophy and the origins of metabolism. *Trends in Biochemical Sciences* **20:**337–341.

Newsholme, E. A., and Leech, A. R., 1983. *Biochemistry for the Medical Sciences.* New York: John Wiley & Sons.

Srere, P. A., 1975. The enzymology of the formation and breakdown of citrate. *Advances in Enzymology* **43:**57–101.

Srere, P. A., 1987. Complexes of sequential metabolic enzymes. *Annual Review of Biochemistry* **56:**89–124.

Walsh, C., 1979. *Enzymatic Reaction Mechanisms.* San Francisco: W. H. Freeman.

Wiegand, G., and Remington, S. J., 1986. Citrate synthase: Structure, control and mechanism. *Annual Review of Biophysics and Biophysical Chemistry* **15:**97–117.

Williamson, J. R., 1980. Mitochondrial metabolism and cell regulation. In *Mitochondria: Bioenergetics, Biogenesis and Membrane Structure,* Packer, L., and Gomez-Puyou, A., eds. New York: Academic Press.

Chapter 21

Electron Transport and Oxidative Phosphorylation

Wall Piece #*IV (1985), a kinetic sculpture by George Rhoads. This complex mechanical art form can be viewed as a metaphor for the molecular apparatus underlying electron transport and ATP synthesis by oxidative phosphorylation.* (1985 by George Rhoads)

In all things of nature there is something of the marvelous.

ARISTOTLE (384–322 B.C.)

Living cells save up metabolic energy predominantly in the form of fats and carbohydrates, and they "spend" this energy for biosynthesis, membrane transport, and movement. In both directions, energy is exchanged and transferred in the form of ATP. In Chapters 19 and 20 we saw that glycolysis and the TCA cycle convert some of the energy available from stored and dietary sugars directly to ATP. However, most of the metabolic energy that is obtainable from substrates entering glycolysis and the TCA cycle is funneled via oxidation–reduction reactions into NADH and reduced flavoproteins, the latter symbolized by [$FADH_2$]. We now embark on the discovery of how cells convert the stored metabolic energy of NADH and [$FADH_2$] into ATP.

Whereas ATP made in glycolysis and the TCA cycle is the result of substrate-level phosphorylation, NADH-dependent ATP synthesis is the result of **oxidative phosphorylation.** Electrons stored in the form of the reduced coenzymes, NADH or [$FADH_2$], are passed through an elaborate and highly orga-

673

Electron Transport and
Oxidative Phosphorylation

nized chain of proteins and coenzymes, the so-called **electron transport chain,** finally reaching O_2 (molecular oxygen), the terminal electron acceptor. Each component of the chain can exist in (at least) two oxidation states, and each component is successively reduced and reoxidized as electrons move through the chain from NADH (or [FADH$_2$]) to O_2. In the course of electron transport, a proton gradient is established across the inner mitochondrial membrane. It is the energy of this proton gradient that drives ATP synthesis.

21.1 • Electron Transport and Oxidative Phosphorylation Are Membrane-Associated Processes

The processes of electron transport and oxidative phosphorylation are **membrane-associated.** Bacteria are the simplest life form, and bacterial cells typically consist of a single cellular compartment surrounded by a plasma membrane and a more rigid cell wall. In such a system, the conversion of energy from NADH and [FADH$_2$] to the energy of ATP via electron transport and oxidative phosphorylation is carried out at (and across) the plasma membrane. In eukaryotic cells, electron transport and oxidative phosphorylation are localized in mitochondria, which are also the sites of TCA cycle activity and (as we shall see in Chapter 24) fatty acid oxidation. Mammalian cells contain from 800 to 2500 mitochondria; other types of cells may have as few as one or two or as many as half a million mitochondria. Human erythrocytes, whose purpose is simply to transport oxygen to tissues, contain *no* mitochondria at all. The typical mitochondrion is about 0.5 ± 0.3 microns in diameter and from 0.5 micron to several microns long; its overall shape is sensitive to metabolic conditions in the cell.

Mitochondria are surrounded by a simple **outer membrane** and a more complex **inner membrane** (Figure 21.1). The space between the inner and outer membranes is referred to as the **intermembrane space.** Several enzymes that utilize ATP (such as creatine kinase and adenylate kinase) are found in the intermembrane space. The smooth outer membrane is about 30 to 40% lipid and 60 to 70% protein, and has a relatively high concentration of phosphatidylinositol. The outer membrane contains significant amounts of **porin** —a transmembrane protein, rich in β-sheets, that forms large channels across the membrane, permitting free diffusion of molecules with molecular weights of about 10,000 or less. Apparently, the outer membrane functions mainly to

(a)   **(b)**

FIGURE 21.1 • (a) An electron micrograph of a mitochondrion. (b) A drawing of a mitochondrion with components labelled. *(a, B. King/BPS)*

maintain the shape of the mitochondrion. The inner membrane is richly packed with proteins, which account for nearly 80% of its weight; thus, its density is higher than that of the outer membrane. The fatty acids of inner membrane lipids are highly unsaturated. Cardiolipin and diphosphatidylglycerol (Chapter 8) are abundant. The inner membrane lacks cholesterol and is quite impermeable to molecules and ions. Species that must cross the mitochondrial inner membrane—ions, substrates, fatty acids for oxidation, and so on—are carried by specific transport proteins in the membrane. Notably, the inner membrane is extensively folded (Figure 21.1). The folds, known as **cristae,** provide the inner membrane with a large surface area in a small volume. During periods of active respiration, the inner membrane appears to shrink significantly, leaving a comparatively large intermembrane space.

The Mitochondrial Matrix Contains the Enzymes of the TCA Cycle

The space inside the inner mitochondrial membrane is called the **matrix,** and it contains most of the enzymes of the TCA cycle and fatty acid oxidation. (An important exception, succinate dehydrogenase of the TCA cycle, is located in the inner membrane itself.) In addition, mitochondria contain circular DNA molecules, along with ribosomes and the enzymes required to synthesize proteins coded within the mitochondrial genome. Although some of the mitochondrial proteins are made this way, most are encoded by nuclear DNA and synthesized by cytosolic ribosomes.

21.2 • Reduction Potentials—An Accounting Device for Free Energy Changes in Redox Reactions

On numerous occasions in earlier chapters, we have stressed that NADH and reduced flavoproteins ($[FADH_2]$) are forms of metabolic energy. These reduced coenzymes have a strong tendency to be oxidized—that is, to transfer electrons to other species. The electron transport chain converts the energy of electron transfer into the energy of phosphoryl transfer stored in the phosphoric anhydride bonds of ATP. Just as the *group transfer potential* was used in Chapter 3 to quantitate the energy of phosphoryl transfer, the **standard reduction potential,** denoted by $\mathcal{E}_\circ'$, quantitates the tendency of chemical species to be reduced or oxidized. The standard reduction potential describing electron transfer between two species,

$$
\begin{array}{ll}
\text{Reduced donor} & \text{Oxidized acceptor} \\
& ne^- \\
\text{Oxidized donor} & \text{Reduced acceptor}
\end{array}
\qquad (21.1)
$$

is related to the free energy change for the process by

$$\Delta G^{\circ\prime} = -n\mathcal{F}\Delta\mathcal{E}_\circ' \qquad (21.2)$$

where n represents the number of electrons transferred; $\mathcal{F}$ is Faraday's constant, 96,485 $J/V \cdot mol$; and $\Delta\mathcal{E}_\circ'$ is the difference in reduction potentials between the donor and acceptor. This relationship is straightforward, but it depends on a *standard* of reference by which reduction potentials are defined.

Measurement of Standard Reduction Potentials

Standard reduction potentials are determined by measuring the voltages generated in **reaction half-cells** (Figure 21.2). A half-cell consists of a solution containing 1 M concentrations of both the oxidized and reduced forms of the substance whose reduction potential is being measured, and a simple electrode.

(a) Ethanol ⟶ acetaldehyde
−0.197v

(b) Fumarate ⟶ succinate
+0.031v

(c) Fe^{3+} ⟶ Fe^{2+}
+0.771v

FIGURE 21.2 • Experimental apparatus used to measure the standard reduction potential of the indicated redox couples: (a) the acetaldehyde/ethanol couple, (b) the fumarate/succinate couple, (c) the Fe^{3+}/Fe^{2+} couple.

(Together, the oxidized and reduced forms of the substance are referred to as a **redox couple.**) Such a **sample half-cell** is connected to a **reference half-cell** and electrode via a conductive bridge (usually a salt-containing agar gel). A sensitive potentiometer (voltmeter) connects the two electrodes so that the electrical potential (voltage) between them can be measured. The reference half-cell normally contains 1 M H^+ in equilibrium with H_2 gas at a pressure of 1 atm. The H^+/H_2 reference half-cell is arbitrarily assigned a standard reduction potential of 0.0 V. The standard reduction potentials of all other redox couples are defined relative to the H^+/H_2 reference half-cell on the basis of the sign and magnitude of the voltage (electromotive force, emf) registered on the potentiometer (Figure 21.2).

If electron flow between the electrodes is toward the sample half-cell, reduction occurs spontaneously in the sample half-cell, and the reduction potential is said to be positive. If electron flow between the electrodes is away from the sample half-cell and toward the reference cell, the reduction potential is said to be negative because electron loss (oxidation) is occurring in the sample half-cell. Strictly speaking, the standard reduction potential, $\mathscr{E}_o'$, is the electromotive force generated at 25°C and pH 7.0 by a sample half-cell (containing 1 M concentrations of the oxidized and reduced species) with respect to a reference half-cell. (Note that the reduction potential of the hydrogen half-cell is pH-dependent. The standard reduction potential, 0.0 V, assumes 1 M H^+. The hydrogen half-cell measured at pH 7.0 has an $\mathscr{E}_o'$ of -0.421 V.)

Several Examples

Figure 21.2a shows a sample/reference half-cell pair for measurement of the standard reduction potential of the acetaldehyde/ethanol couple. Because electrons flow toward the reference half-cell and away from the sample half-cell, the standard reduction potential is negative, specifically -0.197 V. In contrast, the fumarate/succinate couple and the Fe^{3+}/Fe^{2+} couple both cause electrons to flow from the reference half-cell to the sample half-cell; that is, reduction occurs spontaneously in each system, and the reduction potentials of both are thus positive. The standard reduction potential for the Fe^{3+}/Fe^{2+} half-cell is much larger than that for the fumarate/succinate half-cell, with values of $+0.771$ V and $+0.031$ V, respectively. For each half-cell, a **half-cell reaction** describes the reaction taking place. For the fumarate/succinate half-cell coupled to a H^+H_2 reference half-cell, the reaction occurring is indeed a reduction of fumarate.

$$\text{Fumarate} + 2\ H^+ + 2\ e^- \longrightarrow \text{succinate} \qquad \mathscr{E}_o' = +0.031\ \text{V} \qquad (21.3)$$

Similarly, for the Fe^{3+}/Fe^{2+} half-cell,

$$Fe^{3+} + e^- \longrightarrow Fe^{2+} \qquad \mathscr{E}_o' = +0.771\ \text{V} \qquad\qquad (21.4)$$

However, the reaction occurring in the acetaldehyde/ethanol half-cell is the oxidation of ethanol:

$$\text{Ethanol} \longrightarrow \text{acetaldehyde} + 2\ H^+ + 2\ e^- \qquad \mathscr{E}_o' = -0.197\ \text{V} \quad (21.5)$$

The Significance of $\mathscr{E}_o'$

Some typical half-cell reactions and their respective standard reduction potentials are listed in Table 21.1. Whenever reactions of this type are tabulated, they are uniformly written as *reduction* reactions, regardless of what occurs in the given half-cell. The sign of the standard reduction potential indicates which reaction really occurs when the given half-cell is combined with the reference hydrogen half-cell. Redox couples that have large positive reduction potentials

Table 21.1

Standard Reduction Potentials for Several Biological Reduction Half-Reactions	
Reduction Half-Reaction	$\mathscr{E}_o{}'$ **(V)**
$\frac{1}{2} O_2 + 2 H^+ + 2 e^- \longrightarrow H_2O$	0.816
$Fe^{3+} + e^- \longrightarrow Fe^{2+}$	0.771
Photosystem P700	0.430
$NO_3^- + 2 H^+ + 2 e^- \longrightarrow NO_2^- + H_2O$	0.421
Cytochrome $f(Fe^{3+}) + e^- \longrightarrow$ cytochrome $f(Fe^{2+})$	0.365
Cytochrome $a_3(Fe^{3+}) + e^- \longrightarrow$ cytochrome $a_3(Fe^{2+})$	0.350
Cytochrome $a(Fe^{3+}) + e^- \longrightarrow$ cytochrome $a(Fe^{2+})$	0.290
Rieske Fe-S$(Fe^{3+}) + e^- \longrightarrow$ Rieske Fe-S(Fe^{2+})	0.280
Cytochrome $c(Fe^{3+}) + e^- \longrightarrow$ cytochrome $c(Fe^{2+})$	0.254
Cytochrome $c_1(Fe^{3+}) + e^- \longrightarrow$ cytochrome $c_1(Fe^{2+})$	0.220
$UQH \cdot + H^+ + e^- \longrightarrow UQH_2$ (UQ = coenzyme Q)	0.190
$UQ + 2 H^+ + 2 e^- \longrightarrow UQH_2$	0.060
Cytochrome $b_H(Fe^{3+}) + e^- \longrightarrow$ cytochrome $b_H(Fe^{2+})$	0.050
Fumarate $+ 2 H^+ + 2 e^- \longrightarrow$ succinate	0.031
$UQ + H^+ + e^- \longrightarrow UQH \cdot$	0.030
Cytochrome $b_5(Fe^{3+}) + e^- \longrightarrow$ cytochrome b_5 (Fe^{2+})	0.020
$[FAD] + 2 H^+ + 2 e^- \longrightarrow [FADH_2]$	0.003–0.091*
Cytochrome $b_L(Fe^{3+}) + e^- \longrightarrow$ cytochrome $b_L(Fe^{2+})$	−0.100
Oxaloacetate $+ 2 H^+ + 2 e^- \longrightarrow$ malate	−0.166
Pyruvate $+ 2 H^+ + 2 e^- \longrightarrow$ lactate	−0.185
Acetaldehyde $+ 2 H^+ + 2 e^- \longrightarrow$ ethanol	−0.197
$FMN + 2 H^+ + 2 e^- \longrightarrow FMNH_2$	−0.219
$FAD + 2 H^+ + 2 e^- \longrightarrow FADH_2$	−0.219
Glutathione (oxidized) $+ 2 H^+ + 2 e^- \longrightarrow$ 2 glutathione (reduced)	−0.230
Lipoic acid $+ 2 H^+ + 2 e^- \longrightarrow$ dihydrolipoic acid	−0.290
1,3-Bisphosphoglycerate $+ 2 H^+ + 2 e^- \longrightarrow$ glyceraldehyde-3-phosphate $+ P_i$	−0.290
$NAD^+ + 2 H^+ + 2 e^- \longrightarrow NADH + H^+$	−0.320
$NADP^+ + 2 H^+ + 2 e^- \longrightarrow NADPH + H^+$	−0.320
Lipoyl dehydrogenase $[FAD] + 2 H^+ + 2 e^- \longrightarrow$ lipoyl dehydrogenase $[FADH_2]$	−0.340
α-Ketoglutarate $+ CO_2 + 2 H^+ + 2 e^- \longrightarrow$ isocitrate	−0.380
$2 H^+ + 2 e^- \longrightarrow H_2$	−0.421
Ferredoxin (spinach) $(Fe^{3+}) + e^- \longrightarrow$ ferredoxin (spinach) (Fe^{2+})	−0.430
Succinate $+ CO_2 + 2 H^+ + 2 e^- \longrightarrow \alpha$-ketoglutarate $+ H_2O$	−0.670

*Typical values for reduction of bound FAD in flavoproteins such as succinate dehydrogenase (see Bonomi, F., Pagani, S., Cerletti, P., and Giori, C., 1983. *European Journal of Biochemistry* **134:**439–445).

have a strong tendency to accept electrons, and the oxidized form of such a couple (O_2, for example) is a strong oxidizing agent. Redox couples with large negative reduction potentials have a strong tendency to undergo oxidation (that is, donate electrons), and the reduced form of such a couple (NADPH, for example) is a strong reducing agent.

Coupled Redox Reactions

The half-reactions and reduction potentials in Table 21.1 can be used to analyze energy changes in redox reactions. The oxidation of NADH to NAD^+ can be coupled with the reduction of α-ketoglutarate to isocitrate:

$$NAD^+ + \text{isocitrate} \longrightarrow NADH + H^+ + \alpha\text{-ketoglutarate} + CO_2 \quad (21.6)$$

This is the isocitrate dehydrogenase reaction of the TCA cycle. Writing the two half-cell reactions, we have

$$NAD^+ + 2\,H^+ + 2\,e^- \longrightarrow NADH + H^+$$
$$\mathcal{E}_\circ{}' = -0.32\,\text{V} \quad (21.7)$$

$$\alpha\text{-Ketoglutarate} + CO_2 + 2\,H^+ + 2\,e^- \longrightarrow \text{isocitrate}$$
$$\mathcal{E}_\circ{}' = -0.38\,\text{V} \quad (21.8)$$

In a spontaneous reaction, electrons are donated by (flow away from) the half–reaction with the more negative reduction potential and are accepted by (flow toward) the half–reaction with the more positive reduction potential. Thus, in the present case, isocitrate donates electrons and NAD^+ accepts electrons. The convention defines $\Delta\mathcal{E}_\circ{}'$ as

$$\Delta\mathcal{E}_\circ{}' = \mathcal{E}_\circ{}'(\text{acceptor}) - \mathcal{E}_\circ{}'(\text{donor}) \quad (21.9)$$

In the present case, isocitrate is the donor and NAD^+ the acceptor, so we write

$$\Delta\mathcal{E}_\circ{}' = -0.32\,\text{V} - (-0.38\,\text{V}) = +0.06\,\text{V} \quad (21.10)$$

From Equation 21.2, we can now calculate $\Delta G^{\circ\prime}$ as

$$\Delta G^{\circ\prime} = -(2)(96.485\,\text{kJ/V} \cdot \text{mol})(0.06\,\text{V}) \quad (21.11)$$

$$\Delta G^{\circ\prime} = -11.58\,\text{kJ/mol}$$

Note that a reaction with a net positive $\Delta\mathcal{E}_\circ{}'$ yields a negative $\Delta G^{\circ\prime}$, indicating a spontaneous reaction.

The Dependence of the Reduction Potential on Concentration

We have already noted that the standard free energy change for a reaction, $\Delta G^{\circ\prime}$, does not reflect the actual conditions in a cell, where reactants and products are not at standard-state concentrations (1 M). Equation 3.12 was introduced to permit calculations of actual free energy changes under non–standard-state conditions. Similarly, standard reduction potentials for redox couples must be modified to account for the actual concentrations of the oxidized and reduced species. For any redox couple,

$$\text{ox} + ne^- \rightleftharpoons \text{red} \quad (21.12)$$

the actual reduction potential is given by

$$\mathcal{E} = \mathcal{E}_\circ{}' + (RT/n\mathscr{F}) \ln \frac{[\text{ox}]}{[\text{red}]} \quad (21.13)$$

Reduction potentials can also be quite sensitive to molecular environment. The influence of environment is especially important for flavins, such as $FAD/FADH_2$ and $FMN/FMNH_2$. These species are normally bound to their respective flavoproteins; the reduction potential of bound FAD, for example, can be very different from the value shown in Table 21.1 for the free FAD–$FADH_2$ couple of -0.219 V. A problem at the end of the chapter addresses this case.

21.3 • The Electron Transport Chain—An Overview

As we have seen, the metabolic energy from oxidation of food materials—sugars, fats, and amino acids—is funneled into formation of reduced coenzymes (NADH) and reduced flavoproteins ([FADH$_2$]). The electron transport chain reoxidizes the coenzymes, and channels the free energy obtained from these reactions into the synthesis of ATP. This reoxidation process involves the removal of both protons and electrons from the coenzymes. Electrons move from NADH and [FADH$_2$] to molecular oxygen, O$_2$, which is the terminal acceptor of electrons in the chain. The reoxidation of NADH,

$$\text{NADH(reductant)} + \text{H}^+ + \tfrac{1}{2}\,\text{O}_2(\text{oxidant}) \longrightarrow \text{NAD}^+ + \text{H}_2\text{O} \quad (21.14)$$

involves the following half-reactions:

$$\text{NAD}^+ + 2\,\text{H}^+ + 2\,e^- \longrightarrow \text{NADH} + \text{H}^+ \qquad \mathscr{E}_\circ{}' = -0.32\ \text{V} \quad (21.15)$$

$$\tfrac{1}{2}\,\text{O}_2 + 2\,\text{H}^+ + 2\,e^- \longrightarrow \text{H}_2\text{O} \qquad\qquad \mathscr{E}_\circ{}' = +0.816\ \text{V} \quad (21.16)$$

Here, half-reaction (21.16) is the electron acceptor and half-reaction (21.15) is the electron donor. Then

$$\Delta\mathscr{E}_\circ{}' = 0.816 - (-0.32) = 1.136\ \text{V}$$

and, according to Equation (21.2), the standard-state free energy change, $\Delta G^\circ{}'$, is -219 kJ/mol. Molecules along the electron transport chain have reduction potentials between the values for the NAD$^+$/NADH couple and the oxygen/H$_2$O couple, so that electrons move down the energy scale toward progressively more positive reduction potentials (Figure 21.3).

FIGURE 21.3 • $\mathscr{E}_\circ{}'$ and $\mathscr{E}$ values for the components of the mitochondrial electron transport chain. Values indicated are consensus values for animal mitochondria. Black bars represent $\mathscr{E}_\circ{}'$; red bars, $\mathscr{E}'$.

Although electrons move from more negative to more positive reduction potentials in the electron transport chain, it should be emphasized that the electron carriers do not operate in a simple linear sequence. This will become evident when the individual components of the electron transport chain are discussed in the following paragraphs.

The Electron Transport Chain Can Be Isolated in Four Complexes

The electron transport chain involves several different molecular species, including:

(a) **Flavoproteins,** which contain tightly bound FMN or FAD as prosthetic groups, and which (as noted in Chapter 20) may participate in one- or two-electron transfer events.

(b) **Coenzyme Q,** also called **ubiquinone** (and abbreviated **CoQ** or **UQ**) (Figure 8.18), which can function in either one- or two-electron transfer reactions.

(c) Several **cytochromes** (proteins containing heme prosthetic groups [see Chapter 5], which function by carrying or transferring electrons), including cytochromes b, c, c_1, a, and a_3. Cytochromes are one-electron transfer agents, in which the heme iron is converted from Fe^{2+} to Fe^{3+} and back.

(d) A number of **iron–sulfur proteins,** which participate in one-electron transfers involving the Fe^{2+} and Fe^{3+} states.

(e) Protein-bound **copper,** a one-electron transfer site, which converts between Cu^+ and Cu^{2+}.

All these intermediates except for cytochrome c are membrane-associated (either in the mitochondrial inner membrane of eukaryotes or in the plasma membrane of prokaryotes). All three types of proteins involved in this chain—flavoproteins, cytochromes, and iron–sulfur proteins—possess electron-transferring **prosthetic groups.**

FIGURE 21.4 • An overview of the complexes and pathways in the mitochondrial electron transport chain. *(Adapted from Nicholls, D. G., and Ferguson, S. J., 1992. Bioenergetics 2. London: Academic Press.)*

The components of the electron transport chain can be purified from the mitochondrial inner membrane. Solubilization of the membranes containing the electron transport chain results in the isolation of four distinct protein complexes, and the complete chain can thus be considered to be composed of four parts: (I) **NADH–coenzyme Q reductase,** (II) **succinate–coenzyme Q reductase,** (III) **coenzyme Q–cytochrome c reductase,** and (IV) **cytochrome c oxidase** (Figure 21.4). Complex I accepts electrons from NADH, serving as a link between glycolysis, the TCA cycle, fatty acid oxidation, and the electron transport chain. Complex II includes succinate dehydrogenase and thus forms a direct link between the TCA cycle and electron transport. Complexes I and II produce a common product, reduced coenzyme Q (UQH_2), which is the substrate for coenzyme Q–cytochrome *c* reductase (Complex III). As shown in Figure 21.4, there are two other ways to feed electrons to UQ: the **electron-transferring flavoprotein,** which transfers electrons from the flavoprotein-linked step of fatty acyl-CoA dehydrogenase, and ***sn*-glycerophosphate dehydrogenase.** Complex III oxidizes UQH_2 while reducing cytochrome *c*, which in turn is the substrate for Complex IV, cytochrome *c* oxidase. Complex IV is responsible for reducing molecular oxygen. Each of the complexes shown in Figure 21.4 is a large multisubunit complex embedded within the inner mitochondrial membrane.

21.4 • Complex I: NADH–Coenzyme Q Reductase

As its name implies, this complex transfers a pair of electrons from NADH to coenzyme Q, a small, hydrophobic, yellow compound. Another common name for this enzyme complex is *NADH dehydrogenase.* The complex (with an estimated mass of 850 kD) involves more than 30 polypeptide chains, one molecule of flavin mononucleotide (FMN), and as many as seven Fe-S clusters, together containing a total of 20 to 26 iron atoms (Table 21.2). By virtue of its dependence on FMN, NADH–UQ reductase is a *flavoprotein.*

Table 21.2

Protein Complexes of the Mitochondrial Electron-Transport Chain

Complex	Mass (kD)	Subunits	Prosthetic Group	Binding Site for:
NADH–UQ reductase	850	>30	FMN Fe-S	NADH (matrix side) UQ (lipid core)
Succinate–UQ reductase	140	4	FAD Fe-S	Succinate (matrix side) UQ (lipid core)
UQ–Cyt *c* reductase	250	9–10	Heme b_L Heme b_H Heme c_1 Fe-S	Cyt *c* (intermembrane space side)
Cytochrome *c*	13	1	Heme *c*	Cyt c_1 Cyt *a*
Cytochrome *c* oxidase	162	>10	Heme *a* Heme a_3 Cu_A Cu_B	Cyt *c* (intermembrane space side)

Adapted from: Hatefi, Y., 1985. The mitochondrial electron transport chain and oxidative phosphorylation system. *Annual Review of Biochemistry* **54:**1015–1069; and DePierre, J., and Ernster, L., 1977. Enzyme topology of intracellular membranes. *Annual Review of Biochemistry* **46:**201–262.

Although the precise mechanism of the NADH–UQ reductase is not known, the first step involves binding of NADH to the enzyme on the *matrix* side of the inner mitochondrial membrane, and transfer of electrons from NADH to tightly bound FMN:

$$NADH + [FMN] + H^+ \longrightarrow [FMNH_2] + NAD^+ \qquad (21.17)$$

The second step involves the transfer of electrons from the reduced [FMNH$_2$] to a series of Fe-S proteins, including both 2Fe-2S and 4Fe-4S clusters (see Figures 20.8 and 20.16). The unique redox properties of the flavin group of FMN are probably important here. NADH is a two-electron donor, whereas the Fe-S proteins are one-electron transfer agents. The flavin of FMN has three redox states—the oxidized, semiquinone, and reduced states. It can act as *either* a one-electron *or* a two-electron transfer agent and may serve as a critical link between NADH and the Fe-S proteins.

The final step of the reaction involves the transfer of two electrons from iron–sulfur clusters to coenzyme Q. Coenzyme Q is a **mobile electron carrier.** Its isoprenoid tail makes it highly hydrophobic, and it diffuses freely in the hydrophobic core of the inner mitochondrial membrane. As a result, it shuttles electrons from Complexes I and II to Complex III. The redox cycle of UQ is shown in Figure 21.5, and the overall scheme is shown schematically in Figure 21.6.

Complex I Transports Protons from the Matrix to the Cytosol

The oxidation of one NADH and the reduction of one UQ by NADH–UQ reductase results in the net transport of protons from the matrix side to the cytosolic side of the inner membrane. The cytosolic side, where H$^+$ accumulates, is referred to as the **P** (for *positive*) face; similarly, the matrix side is the **N** (for *negative*) face. Some of the energy liberated by the flow of electrons

FIGURE 21.5 • (a) The three oxidation states of coenzyme Q. (b) A space-filling model of coenzyme Q.

FIGURE 21.6 • Proposed structure and electron transport pathway for Complex I. Three protein complexes have been isolated, including the **flavoprotein (FP), iron–sulfur protein (IP),** and **hydrophobic protein (HP).** FP contains three peptides (of mass 51, 24, and 10 kD) and bound FMN and has 2 Fe-S centers (a 2Fe-2S center and a 4Fe-4S center). IP contains six peptides and at least 3 Fe-S centers. HP contains at least seven peptides and one Fe-S center.

through this complex is used in a *coupled process* to drive the transport of protons across the membrane. (This is an example of *active transport,* a phenomenon examined in detail in Chapter 10.) Available experimental evidence suggests a stoichiometry of four H^+ transported per two electrons passed from NADH to UQ.

21.5 • Complex II: Succinate–Coenzyme Q Reductase

Complex II is perhaps better known by its other name—**succinate dehydrogenase,** the only TCA cycle enzyme that is an integral membrane protein in the inner mitochondrial membrane. This enzyme has a mass of approximately 100 to 140 kD and is composed of four subunits: two Fe-S proteins of masses 70 kD and 27 kD, and two other peptides of masses 15 kD and 13 kD. Also known as *flavoprotein 2 (FP₂),* it contains an FAD covalently bound to a histidine residue (see Figure 20.15), and three Fe-S centers: a 4Fe-4S cluster, a 3Fe-4S cluster, and a 2Fe-2S cluster. When succinate is converted to fumarate in the TCA cycle, concomitant reduction of bound FAD to $FADH_2$ occurs in succinate dehydrogenase. This $FADH_2$ transfers its electrons immediately to Fe-S centers, which pass them on to UQ. Electron flow from succinate to UQ,

$$\text{Succinate} \longrightarrow \text{fumarate} + 2\ H^+ + 2\ e^- \qquad (21.18)$$

$$\text{UQ} + 2\ H^+ + 2\ e^- \longrightarrow \text{UQH}_2 \qquad (21.19)$$

FIGURE 21.7 • The fatty acyl-CoA dehydrogenase reaction, emphasizing that the reaction involves reduction of enzyme-bound FAD (indicated by brackets).

$$\text{Net rxn:} \quad \text{Succinate} + \text{UQ} \longrightarrow \text{fumarate} + \text{UQH}_2 \; \Delta\mathcal{E}_o{}' = 0.029\text{V} \quad (21.20)$$
$$\Delta G°' = -5.6 \text{ kJ/mol}$$

yields a net reduction potential of 0.029 V. (Note that the first half-reaction is written in the direction of the e^- flow. As always, $\Delta\mathcal{E}_o'$ is calculated according to Equation 21.9.) The small free energy change of this reaction is not sufficient to drive the transport of protons across the inner mitochondrial membrane.

This is a crucial point because (as we will see) proton transport is coupled with ATP synthesis. Oxidation of one FADH_2 in the electron transport chain results in synthesis of approximately two molecules of ATP, compared with the approximately three ATPs produced by the oxidation of one NADH. Other enzymes can also supply electrons to UQ, including mitochondrial *sn*-glycerophosphate dehydrogenase, an inner membrane–bound shuttle enzyme, and the fatty acyl–CoA dehydrogenases, three soluble matrix enzymes involved in fatty acid oxidation (Figure 21.7; also see Chapter 24). The path of electrons from succinate to UQ is shown in Figure 21.8.

FIGURE 21.8 • A probable scheme for electron flow in Complex II. Oxidation of succinate occurs with reduction of [FAD]. Electrons are then passed to Fe-S centers and then to coenzyme Q (UQ). Proton transport does not occur in this complex.

21.6 • Complex III: Coenzyme Q–Cytochrome *c* Reductase

In the third complex of the electron transport chain, reduced coenzyme Q (UQH_2) passes its electrons to cytochrome *c* via a unique redox pathway known as the **Q cycle.** *UQ–cytochrome c reductase* (UQ–cyt *c* reductase), as this complex is known, involves three different cytochromes and an Fe-S protein. In the cytochromes of these and similar complexes, the iron atom at the center of the porphyrin ring cycles between the reduced Fe^{2+} (ferrous) and oxidized Fe^{3+} (ferric) states.

Cytochromes were first named and classified on the basis of their absorption spectra (Figure 21.9), which depend upon the structure and environment of their heme groups. The ***b* cytochromes** contain *iron–protoporphyrin IX* (Figure 21.10), the same heme found in hemoglobin and myoglobin. The ***c* cytochromes** contain *heme c,* derived from iron–protoporphyrin IX by the covalent attachment of cysteine residues from the associated protein. UQ–cyt *c*

Iron protoporphyrin IX
(found in cytochrome *b*, myoglobin, and hemoglobin)

Heme C
(found in cytochrome *c*)

(a) Cytochrome *c*: reduced spectrum

(b) Cytochrome *c*: oxidized spectrum

(c) Cytochrome *c*: reduced spectrum minus oxidized spectrum

(d) Submitochondrial particles (room temperature): reduced spectrum minus oxidized spectrum

(e) Submitochondrial particles (77K): reduced spectrum minus oxidized spectrum

FIGURE 21.9 • Typical visible absorption spectra of cytochromes. (a) Cytochrome *c*, reduced spectrum; (b) cytochrome *c*, oxidized spectrum; (c) the difference spectrum: (a) minus (b); (d) beef heart mitochondrial particles: room temperature difference (reduced minus oxidized) spectrum; (e) beef heart submitochondrial particles: same as (d) but at 77 K. α- and β- bands are labeled, and in (d) and (e) the bands for cytochromes *a*, *b* and *c* are indicated.

Heme A
(found in cytochrome *a*)

FIGURE 21.10 • The structures of iron protoporphyrin IX, heme *c*, and heme *a*.

FIGURE 21.11 • The structure of UQ-cyt *c* reductase, also known as the cytochrome bc_1 complex. The alpha helices of cytochrome b (pale green) define the transmembrane domain of the protein. The bottom of the structure as shown extends approximately 75 Å into the mitochondrial matrix, and the top of the structure as shown extends about 38 Å into the intermembrane space. *(Photograph kindly provided by Di Xia and Johann Deisenhofer [From Xia, D., Yu, C.-A., Kim, H., Xia, J.-Z., Kachurin, A. M., Zhang, L., Yu, L., and Deisenhofer, J., 1997. The crystal structure of the cytochrome bc_1 complex from bovine heart mitochondria.* Science **277**:60–66.*])*

reductase contains a *b*-type cytochrome, of 30 to 40 kD, with two different heme sites (Figure 21.11) and one *c*-type cytochrome. (One other variation, heme *a*, contains a 15-carbon isoprenoid chain on a modified vinyl group, and a formyl group in place of one of the methyls [see Figure 21.10]. **Cytochrome *a*** is found in two forms in Complex IV of the electron transport chain, as we shall see.) The two hemes on the *b* cytochrome polypeptide in UQ–cyt *c* reductase are distinguished by their reduction potentials and the wavelength (λ_{max}) of the so-called **α band** (see Figure 21.9). One of these hemes, known as b_L or b_{566}, has a standard reduction potential, $\mathscr{E}_o{}'$, of -0.100 V and a wavelength of maximal absorbance (λ_{max}) of 566 nm. The other, known as b_H or b_{562}, has a standard reduction potential of $+0.050$ V and a λ_{max} of 562 nm. (*H* and *L* here refer to *high* and *low* reduction potential.)

The structure of the UQ–cyt *c* reductase, also known as the cytochrome bc_1 complex, has been determined by Johann Deisenhofer and his colleagues. (Deisenhofer was a co-recipient of the Nobel Prize in Chemistry for his work on the structure of a photosynthetic reaction center [see Chapter 22]). The complex is a dimer, with each monomer consisting of 11 protein subunits and 2165 amino acid residues (monomer mass, 248 kD). The dimeric structure is pear-shaped and consists of a large domain that extends 75 Å into the mito-

chondrial matrix, a transmembrane domain consisting of 13 transmembrane α-helices in each monomer and a small domain that extends 38 Å into the intermembrane space (Figure 21.11). Most of the **Rieske protein** (an Fe-S protein named for its discoverer) is mobile in the crystal (only 62 of 196 residues are shown in the structure in Figure 21.11), and Deisenhofer has postulated that mobility of this subunit could be required for electron transfer in the function of this complex.

Complex III Drives Proton Transport

As with Complex I, passage of electrons through the Q cycle of Complex III is accompanied by proton transport across the inner mitochondrial membrane. The postulated pathway for electrons in this system is shown in Figure 21.12. A large pool of UQ and UQH_2 exists in the inner mitochondrial membrane. The Q cycle is initiated when a molecule of UQH_2 from this pool diffuses to a site (called Q_p) on Complex III near the cytosolic face of the membrane.

Oxidation of this UQH_2 occurs in two steps. First, an electron from UQH_2 is transferred to the Rieske protein and then to cytochrome c_1. This releases two H^+ to the cytosol and leaves $UQ \cdot^-$, a semiquinone anion form of UQ, at the Q_p site. The second electron is then transferred to the b_L heme, converting $UQ \cdot^-$ to UQ. The Rieske protein and cytochrome c_1 are similar in structure; each has a globular domain and is anchored to the inner membrane by

(a) First half of Q cycle

(b) Second half of Q cycle

Net
$$UQH_2 + 2\,H_{in}^+ + 2\,Cyt\ c_{ox} \xrightarrow{2e^-} 4\,H_{out}^+ + 2\,Cyt\ c_{red} + UQ$$

FIGURE 21.12 • The Q cycle in mitochondria. (a) The electron transfer pathway following oxidation of the first UQH_2 at the Q_p site near the cytosolic face of the membrane. (b) The pathway following oxidation of a second UQH_2.

a hydrophobic segment. However, the hydrophobic segment is N-terminal in the Rieske protein and C-terminal in cytochrome c_1.

The electron on the b_L heme facing the cytosolic side of the membrane is now passed to the b_H heme on the matrix side of the membrane. This electron transfer occurs against a membrane potential of 0.15 V and is driven by the loss of redox potential as the electron moves from b_L ($\mathscr{E}_\circ' = -0.100$V) to b_H ($\mathscr{E}_\circ' = +0.050$V). The electron is then passed from b_H to a molecule of UQ at a second quinone-binding site, Q_n, converting this UQ to $UQ \cdot^-$. The resulting $UQ \cdot^-$ remains firmly bound to the Q_n site. This completes the first half of the Q cycle (Figure 21.12a).

The second half of the cycle (Figure 21.12b) is similar to the first half, with a second molecule of UQH_2 oxidized at the Q_p site, one electron being passed to cytochrome c_1 and the other transferred to heme b_L and then to heme b_H. In this latter half of the Q cycle, however, the b_H electron is transferred to the semiquinone anion, $UQ \cdot^-$, at the Q_n site. With the addition of two H^+ from the mitochondrial matrix, this produces a molecule of UQH_2, which is released from the Q_n site and returns to the coenzyme Q pool, completing the Q cycle.

The Q Cycle Is an Unbalanced Proton Pump

Why has nature chosen this rather convoluted path for electrons in Complex III? First of all, Complex III takes up two protons on the matrix side of the inner membrane and releases four protons on the cytoplasmic side for each pair of electrons that passes through the Q cycle. The apparent imbalance of *two protons in* for *four protons out* is offset by proton translocations in Complex IV, the cytochrome oxidase complex. The other significant feature of this mechanism is that it offers a convenient way for a two-electron carrier, UQH_2, to interact with the b_L and b_H hemes, the Rieske protein Fe-S cluster, and cytochrome c_1, all of which are one-electron carriers.

Cytochrome *c* Is a Mobile Electron Carrier

Electrons traversing Complex III are passed through cytochrome c_1 to cytochrome c. Cytochrome c is the only one of the cytochromes that is water-soluble. Its structure, determined by X-ray crystallography (Figure 21.13), is globular; the planar heme group lies near the center of the protein, surrounded predominantly by hydrophobic protein residues. The iron in the porphyrin ring is coordinated both to a histidine nitrogen and to the sulfur atom of a methionine residue. Coordination with ligands in this manner on both sides of the porphyrin plane precludes the binding of oxygen and other ligands, a feature that distinguishes the cytochromes from hemoglobin (Chapter 15).

Cytochrome c, like UQ, is a mobile electron carrier. It associates loosely with the inner mitochondrial membrane (in the *intermembrane space* on the cytosolic side of the inner membrane) to acquire electrons from the Fe-S–cyt c_1 aggregate of Complex III, and then it migrates along the membrane surface in the reduced state, carrying electrons to *cytochrome c oxidase*, the fourth complex of the electron transport chain.

FIGURE 21.13 • The structure of mitochondrial cytochrome *c*. The heme is shown at the center of the structure, covalently linked to the protein via its two sulfur atoms (yellow). A third sulfur from a methionine residue coordinates the iron.

21.7 • Complex IV: Cytochrome *c* Oxidase

Complex IV is called cytochrome *c* oxidase because it accepts electrons from cytochrome *c* and directs them to the four-electron reduction of O_2 to form H_2O:

$$4 \text{ cyt } c \text{ (Fe}^{2+}) + 4 \text{ H}^+ + O_2 \longrightarrow 4 \text{ cyt } c \text{ (Fe}^{3+}) + 2 \text{ H}_2O \qquad (21.21)$$

FIGURE 21.14 • An electrophoresis gel showing the complex subunit structure of bovine heart cytochrome *c* oxidase. The three largest subunits, I, II, and III, are coded for by mitochondrial DNA. The others are encoded by nuclear DNA. *(Photo kindly provided by Professor Roderick Capaldi)*

Thus, O_2 and cytochrome *c* oxidase are the final destination for the electrons derived from the oxidation of food materials. In concert with this process, cytochrome *c* oxidase also drives transport of protons across the inner mitochondrial membrane. These important functions are carried out by a transmembrane protein complex consisting of more than 10 subunits (Table 21.2).

An electrophoresis gel of the bovine heart complex is shown in Figure 21.14. The total mass of the protein in the complex, composed of 13 subunits, is 204 kD. Subunits I through III, the largest ones, are encoded by mitochondrial DNA, synthesized in the mitochondrion, and inserted into the inner membrane from the matrix side. The smaller subunits are coded by nuclear DNA and synthesized in the cytosol.

The structure of cytochrome *c* oxidase has been solved. The essential Fe and Cu sites are contained entirely within the structures of subunits I, II, and III. None of the 10 nuclear DNA–derived subunits directly impinges on the essential metal sites. The implication is that subunits I to III actively participate in the events of electron transfer, but that the other 10 subunits play regulatory roles in this process. Subunit I is cylindrical in shape and consists of 12 transmembrane helices, without any significant extramembrane parts (Figure 21.15). Hemes *a* and a_3, which lie perpendicular to the membrane plane, are cradled by the helices of subunit I. Subunits II and III lie on opposite sides of subunit I and do not contact each other. Subunit II has an extramembrane domain on the cytosolic face of the mitochondrial membrane. This domain consists of a 10-strand β-barrel that holds Cu_A 7 Å from the nearest surface atom of the subunit. Subunit III consists of 7 transmembrane helices with no significant extramembrane domains. Figure 21.16 presents a molecular graphic image of cytochrome *c* oxidase.

FIGURE 21.16 • Molecular graphic image of cytochrome *c* oxidase. Seven of the 10 nuclear DNA–derived subunits (IV, VIa, VIc, VIIa, VIIb, VIIc, and VIII) possess transmembrane segments. Three (Va, Vb, and VIb) do not. Subunits IV and VIc are transmembrane and dumbbell-shaped. Subunit Va is globular and bound to the matrix side of the complex, whereas VIb is a globular subunit on the cytosolic side of the membrane complex. Vb is globular and matrix-side associated as well, but it has an N-terminal extended domain. VIa has a transmembrane helix and a small globular domain. Subunit VIIa consists of a tilted transmembrane helix, with another short helical segment on the matrix side of the membrane. Subunits VIIa, VIIb, and VIII consist of transmembrane segments with short extended regions outside the membrane.

FIGURE 21.15 • Molecular graphic image of subunits I, II, and III of cytochrome *c* oxidase.

FIGURE 21.17 • The electron transfer pathway for cytochrome oxidase. Cytochrome *c* binds on the cytosolic side, transferring electrons through the copper and heme centers to reduce O_2 on the matrix side of the membrane.

Electron Transfer in Complex IV Involves Two Hemes and Two Copper Sites

Cytochrome *c* oxidase contains two heme centers (cytochromes *a* and a_3) as well as two copper atoms (Figure 21.17). The copper sites, Cu_A and Cu_B, are associated with cytochromes *a* and a_3, respectively. The copper sites participate in electron transfer by cycling between the reduced *(cuprous)* Cu^+ state and the oxidized *(cupric)* Cu^{2+} state. (Remember, the cytochromes and copper sites are one-electron transfer agents.) Reduction of one oxygen molecule requires passage of four electrons through these carriers—one at a time (Figure 21.17).

Electrons from cytochrome *c* are transferred to Cu_A sites and then passed to the heme iron of cytochrome *a*. Cu_A is liganded by two cysteines and two histidines (Figure 21.18). The heme of cytochrome *a* is liganded by imidazole rings of histidine residues (Figure 21.18). The Cu_A and the Fe of cytochrome *a* are within 1.5 nm of each other.

Cu_B and the iron atom of cytochrome a_3 are also situated close to each other and are thought to share a ligand, which may be a cysteine sulfur (Figure 21.19). This closely associated pair of metal ions is referred to as a **binuclear center.**

As shown in Figure 21.20, the electron pathway through Complex IV continues as Cu_B accepts a single electron from cytochrome *a* (state O → state H). A second electron then reduces the iron center to Fe^{2+} (H → R), leading to the binding of O_2 (R → A) and the formation of a peroxy bridge between heme a_3 and Cu_B (A → P). *This amounts to the transfer of two electrons from the binuclear center to the bound O_2.* The next step involves uptake of two H^+ and a third electron (P → F), which leads to cleavage of the O—O bond and generation of Fe^{4+} at the heme. Uptake of a fourth e^- facilitates formation of ferric hydroxide at the heme center (F → O'). In the final step of the cycle (O' → O), protons from the mitochondrial matrix are accepted by the coordinated hydroxyl groups, and the resulting water molecules dissociate from the binuclear center.

Complex IV Also Transports Protons Across the Inner Mitochondrial Membrane

The reduction of oxygen in Complex IV is accompanied by transport of protons across the inner mitochondrial membrane. Transfer of four electrons through this complex drives the transport of approximately four protons. The mechanism of proton transport is unknown but is thought to involve the steps from state P to state O (Figure 21.20). Four protons are taken up on the matrix side for every two protons transported to the cytoplasm (see Figure 21.17).

FIGURE 21.18 • (a) The Cu_A site of cytochrome oxidase. Copper ligands include two histidine imidazole groups and two cysteine side chains from the protein. (b) The coordination of histidine imidazole ligands to the iron atom in the heme *a* center of cytochrome oxidase.

Independence of the Four Carrier Complexes

It should be emphasized here that the four major complexes of the electron transport chain operate quite independently in the inner mitochondrial membrane. Each is a multiprotein aggregate maintained by numerous strong associations between peptides of the complex, but there is no evidence that the complexes associate with one another in the membrane. Measurements of the lateral diffusion rates of the four complexes, of coenzyme Q, and of cytochrome *c* in the inner mitochondrial membrane show that the rates differ considerably, indicating that these complexes do not move together in the membrane. Kinetic studies with reconstituted systems show that electron transport does not operate by means of connected sets of the four complexes.

A Dynamic Model of Electron Transport

The model that emerges for electron transport is shown in Figure 21.21. The four complexes are independently mobile in the membrane. Coenzyme Q collects electrons from NADH–UQ reductase and succinate–UQ reductase and delivers them (by diffusion through the membrane core) to UQ–cyt *c* reductase. Cytochrome *c* is water-soluble and moves freely, carrying electrons from UQ–cyt *c* reductase to cytochrome *c* oxidase. In the process of these electron transfers, protons are driven across the inner membrane (from the matrix side to the intermembrane space). The proton gradient generated by electron transport represents an enormous source of potential energy. As seen in the next section, this potential energy is used to synthesize ATP as protons flow back into the matrix.

The $H^+/2e^-$ Ratio for Electron Transport Is Uncertain

In 1961, Peter Mitchell, a British biochemist, proposed that the energy stored in a proton gradient across the inner mitochondrial membrane by electron transport drives the synthesis of ATP in cells. The proposal became known as

FIGURE 21.19 • The binuclear center of cytochrome oxidase. A ligand, L (probably a cysteine S), is shown bridging the Cu_B and Fe_{a_3} metal sites.

FIGURE 21.20 • A model for the mechanism of O_2 reduction by cytochrome oxidase. *(Adapted from Nicholls, D. G., and Ferguson, S. J., 1992.* Bioenergetics 2. *London: Academic Press; and Babcock, G. T., and Wikström, M., 1992.* Nature ***356:**301–309.)*

FIGURE 21.21 • A model for the electron transport pathway in the mitochondrial inner membrane. UQ/UQH_2 and cytochrome c are mobile electron carriers and function by transferring electrons between the complexes. The proton transport driven by Complexes I, III, and IV is indicated.

Mitchell's chemiosmotic hypothesis. The ratio of protons transported per pair of electrons passed through the chain—the so-called **$H^+/2\,e^-$ ratio**—has been an object of great interest for many years. Nevertheless, the ratio has remained extremely difficult to determine. The consensus estimate for the electron transport pathway from succinate to O_2 is 6 $H^+/2\ e^-$. The ratio for Complex I by itself remains uncertain, but recent best estimates place it as high as 4 $H^+/2\ e^-$. On the basis of this value, the stoichiometry of transport for the pathway from NADH to O_2 is 10 $H^+/2\ e^-$. Although this is the value assumed in Figure 21.21, it is important to realize that this represents a consensus drawn from many experiments.

21.8 • The Thermodynamic View of Chemiosmotic Coupling

Peter Mitchell's chemiosmotic hypothesis revolutionized our thinking about the energy coupling that drives ATP synthesis by means of an electrochemical gradient. How much energy is stored in this electrochemical gradient? For the transmembrane flow of protons across the inner membrane (from inside [matrix] to outside), we could write

$$H^+{}_{in} \longrightarrow H^+{}_{out} \tag{21.26}$$

The free energy difference for protons across the inner mitochondrial membrane includes a term for the concentration difference and a term for the electrical potential. This is expressed as

$$\Delta G = RT \ln \frac{[c_2]}{[c_1]} + Z\mathscr{F}\Delta\Psi \tag{21.27}$$

Oxidative Phosphorylation—The Clash of Ideas and Energetic Personalities

For many years, the means by which electron transport and ATP synthesis are coupled was unknown. It is no exaggeration to say that the search for the coupling mechanism was one of the largest, longest, most bitter fights in the history of biochemical research. Since 1777, when the French chemist Lavoisier determined that foods undergo oxidative combustion in the body, chemists and biochemists have wondered how energy from food is captured by living things. A piece of the puzzle fell into place in 1929, when Fiske and Subbarow first discovered and studied adenosine 5′-triphosphate in muscle extracts. Soon it was understood that ATP hydrolysis provides the energy for muscle contraction and other processes.

Engelhardt's experiments in 1930 led to the notion that ATP is synthesized as the result of electron transport, and, by 1940, Severo Ochoa had carried out a measurement of the **P/O ratio,** the number of molecules of ATP generated per atom of oxygen consumed in the electron transport chain. Because two electrons are transferred down the chain per oxygen atom reduced, the P/O ratio also reflects the ratio of ATPs synthesized per pair of electrons consumed. After many tedious and careful measurements, scientists decided that the P/O ratio was 3 for NADH oxidation and 2 for succinate (that is, [FADH$_2$]) oxidation. Electron flow and ATP synthesis are very tightly coupled in the sense that, in normal mitochondria, neither occurs without the other.

A High-Energy Chemical Intermediate Coupling Oxidation and Phosphorylation Proved Elusive

Many models were proposed to account for the coupling of electron transport and ATP synthesis. A persuasive model, advanced by E. C. Slater in 1953, proposed that energy derived from electron transport was stored in a **high-energy intermediate** (symbolized as X~P). This chemical species—in essence an activated form of phosphate—functioned according to certain relations according to Equations (21.22)–(21.25) (see below) to drive ATP synthesis.

This hypothesis was based on the model of substrate-level phosphorylation in which a high-energy substrate intermediate is a precursor to ATP. A good example is the 3-phosphoglycerate kinase reaction of glycolysis, where 1,3-bisphosphoglycerate serves as a high-energy intermediate leading to ATP. Literally hundreds of attempts were made to isolate the high-energy intermediate, X~P. Among the scientists involved in the research, rumors that one group or another had isolated X~P circulated frequently, but none was substantiated. Eventually it became clear that the intermediate could not be isolated because it did not exist.

Peter Mitchell's Chemiosmotic Hypothesis

In 1961, Peter Mitchell proposed a novel coupling mechanism involving a proton gradient across the inner mitochondrial membrane. In Mitchell's **chemiosmotic hypothesis,** protons are driven across the membrane from the matrix to the intermembrane space and cytosol by the events of electron transport. This mechanism stores the energy of electron transport in an **electrochemical potential.** As protons are driven out of the matrix, the pH rises and the matrix becomes negatively charged with respect to the cytosol (Figure 21.22). Proton pumping thus creates a pH gradient and an electrical gradient across the inner membrane, both of which tend to attract protons back into the matrix from the cytoplasm. Flow of protons down this electrochemical gradient, an energetically favorable process, then drives the synthesis of ATP.

Paul Boyer and the Conformational Coupling Model

Another popular model invoked what became known as **conformational coupling.** If the energy of electron transport was not stored in some high-energy intermediate, perhaps it was stored in a **high-energy protein conformation.** Proposed by Paul Boyer, this model suggested that reversible conformation changes transferred energy from proteins of the electron transport chain to the enzymes involved in ATP synthesis. This model was consistent with some of the observations made by others, and it eventually evolved into the **binding change mechanism** (the basis for the model in Figure 21.28). Boyer's model is supported by a variety of binding experiments and is essentially consistent with Mitchell's chemiosmotic hypothesis.

Electron transport drives H$^+$ out and creates an electrochemical gradient

Low [H$^+$]

High [H$^+$]

Higher pH, lower [H$^+$] in matrix

Lower pH, higher [H$^+$] in intermembrane space

FIGURE 21.22 • The proton and electrochemical gradients existing across the inner mitochondrial membrane. The electrochemical gradient is generated by the transport of protons across the membrane.

$$\text{NADH} + \text{H}^+ + \text{FMN} + \text{X} \longrightarrow \text{NAD}^+\!\!-\!\!\text{X} + \text{FMNH}_2 \qquad (21.22)$$
$$\text{NAD}^+\!\!-\!\!\text{X} + \text{P}_i \longrightarrow \text{NAD}^+ + \text{X}\!\sim\!\text{P} \qquad (21.23)$$
$$\text{X}\!\sim\!\text{P} + \text{ADP} \longrightarrow \text{X} + \text{ATP} + \text{H}_2\text{O} \qquad (21.24)$$

Net reaction:
$$\text{NADH} + \text{H}^+ + \text{FMN} + \text{ADP} + \text{P}_i \longrightarrow \text{NAD}^+ + \text{FMNH}_2 + \text{ATP} + \text{H}_2\text{O} \quad (21.25)$$

where c_1 and c_2 are the proton concentrations on the two sides of the membrane, Z is the charge on a proton, $\mathscr{F}$ is Faraday's constant, and $\Delta\Psi$ is the potential difference across the membrane. For the case at hand, this equation becomes

$$\Delta G = RT \ln \frac{[\text{H}^+_{\text{out}}]}{[\text{H}^+_{\text{in}}]} + \mathscr{F}\Delta\Psi \tag{21.28}$$

In terms of the matrix and cytoplasm pH values, the free energy difference is

$$\Delta G = -2.303RT(\text{pH}_{\text{out}} - \text{pH}_{\text{in}}) + \mathscr{F}\Delta\Psi \tag{21.29}$$

Reported values for $\Delta\Psi$ and ΔpH vary, but the membrane potential is always found to be positive outside and negative inside, and the pH is always more acidic outside and more basic inside. Taking typical values of $\Delta\Psi = 0.18$ V and ΔpH = 1 unit, the free energy change associated with the movement of one mole of protons from inside to outside is

$$\Delta G = 2.3RT + \mathscr{F}(0.18 \text{ V}) \tag{21.30}$$

With $\mathscr{F} = 96.485$ kJ/V·mol, the value of ΔG at 37°C is

$$\Delta G = 5.9 \text{ kJ} + 17.4 \text{ kJ} = 23.3 \text{ kJ} \tag{21.31}$$
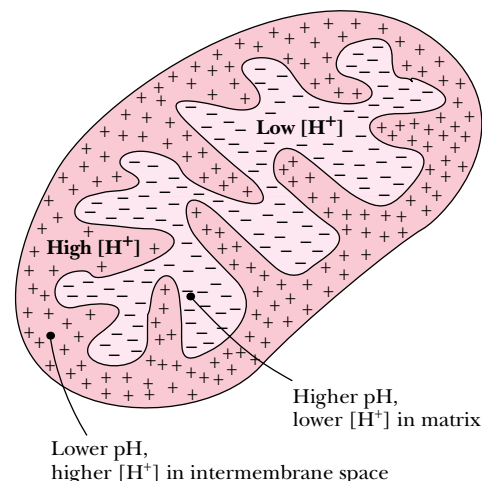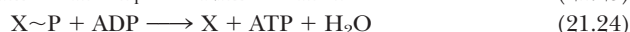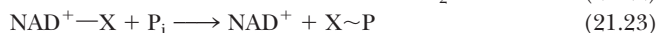
which is the free energy change for movement of a mole of protons across a typical inner membrane. Note that the free energy terms for *both* the pH difference and the potential difference are unfavorable for the outward transport of protons, with the latter term making the greater contribution. On the other hand, the ΔG for *inward* flow of protons is -23.3 kJ/mol. It is this energy that drives the synthesis of ATP, in accord with Mitchell's model. Peter Mitchell was awarded the Nobel Prize in chemistry in 1978.

FIGURE 21.23 • Electron micrograph of submitochondrial particles showing the 8.5-nm projections or particles on the inner membrane, eventually shown to be F_1–ATP synthase. *(Parsons, D. F., 1963.* Science ***140:**985)*

21.9 • ATP Synthase

The mitochondrial complex that carries out ATP synthesis is called **ATP synthase** or sometimes **F_1F_0–ATPase** (for the reverse reaction it catalyzes). ATP synthase was observed in early electron micrographs of submitochondrial particles (prepared by sonication of inner membrane preparations) as round, 8.5-nm-diameter projections or particles on the inner membrane (Figure 21.23). In micrographs of native mitochondria, the projections appear on the matrix-facing surface of the inner membrane. Mild agitation removes the particles from isolated membrane preparations, and the isolated spherical particles catalyze ATP hydrolysis, the reverse reaction of the ATP synthase. Stripped of these particles, the membranes can still carry out electron transfer but cannot synthesize ATP. In one of the first *reconstitution* experiments with membrane proteins, Efraim Racker showed that adding the particles back to stripped membranes restored electron transfer–dependent ATP synthesis.

ATP Synthase Consists of Two Complexes—F_1 and F_0

ATP synthase actually consists of two principal complexes. The spheres observed in electron micrographs make up the **F_1 unit,** which catalyzes ATP synthesis. These F_1 spheres are attached to an integral membrane protein aggregate called the **F_0 unit.** F_1 consists of five polypeptide chains named α, β, γ, δ, and ϵ, with a subunit stoichiometry $\alpha_3\beta_3\gamma\delta\epsilon$ (Table 21.3). F_0 consists of three hydrophobic subunits denoted by a, b, and c, with an apparent stoichiometry of $a_1b_2c_{9-12}$. F_0 forms the transmembrane pore or channel through which protons move to drive ATP synthesis. The α, β, γ, δ, and ϵ subunits of F_1 contain 510, 482, 272, 146, and 50 amino acids, respectively, with a total molecular mass

Table 21.3

Escherichia coli F_1F_0 ATP Synthase Subunit Organization

Complex	Protein Subunit	Mass (kD)	Stoichiometry
F_1	α	55	3
	β	52	3
	γ	30	1
	δ	15	1
	ϵ	5.6	1
F_0	a	30	1
	b	17	2
	c	8	9–12

(a)

(b)

FIGURE 21.24 • Molecular graphic images (a) side view and (b) top view of the F_1–ATP synthase showing the individual component peptides. The γ-subunit is the pink structure visible in the center of view (b).

for F_1 of 371 kD. The α and β subunits are homologous, and each of these subunits bind a single ATP. The catalytic sites are in the β subunits; the function of the ATP sites in the α subunits is unknown (deletion of the sites does not affect activity).

John Walker and his colleagues have determined the structure of the F_1 complex (Figure 21.24). The F_1–ATPase is an inherently asymmetrical structure, with the three β subunits having three different conformations. In the structure solved by Walker, one of the β-subunit ATP sites contains AMP-PNP (a nonhydrolyzable analog of ATP), and another contains ADP, with the third site being empty. This state is consistent with the **binding change mechanism** for ATP synthesis proposed by Paul Boyer, in which three reaction sites cycle concertedly through the three intermediate states of ATP synthesis (take a look at Figure 21.28 on page 697).

How might such cycling occur? Important clues have emerged from several experiments that show that the γ subunit rotates with respect to the $\alpha\beta$ complex. How such rotation might be linked to transmembrane proton flow and ATP synthesis is shown in Figure 21.25. In this model, the c subunits of F_0

FIGURE 21.25 • A model of the F_1 and F_0 components of the ATP synthase, a rotating molecular motor. The a, b, α, β, and δ subunits constitute the stator of the motor, and the c, γ, and ϵ subunits form the rotor. Flow of protons through the structure turns the rotor and drives the cycle of conformational changes in α and β that synthesize ATP.

are arranged in a ring. Several lines of evidence suggest that each c subunit consists of a pair of antiparallel transmembrane helices with a short hairpin loop on the cytosolic side of the membrane. A ring of c subunits could form a **rotor** that turns with respect to the a subunit, a **stator** consisting of five transmembrane α-helices with proton access channels on either side of the membrane. The γ subunit is postulated to be the link between F_1 and F_0. Several experiments have shown that γ rotates relative to the $(\alpha\beta)_3$ complex during ATP synthesis. If γ is anchored to the c subunit rotor, then the c rotor–γ complex can rotate together relative to the $(\alpha\beta)_3$ complex. Subunit b possesses a single transmembrane segment and a long hydrophilic head domain, and the complete stator may consist of the b subunits anchored at one end to the a subunit and linked at the other end to the $(\alpha\beta)_3$ complex via the δ subunit, as shown in Figure 21.25.

What, then, is the mechanism for ATP synthesis? The c rotor subunits each carry an essential residue, Asp^{61}. (Changing this residue to Asn abolishes ATP synthase activity.) Rotation of the c rotor relative to the stator may depend upon neutralization of the negative charge on each c subunit Asp^{61} as the rotor turns. Protons taken up from the cytosol by one of the proton access channels in a could protonate an Asp^{61} and then ride the rotor until they reach the other proton access channel on a, from which they would be released into the matrix. Such rotation would cause the γ subunit to turn relative to the three β-subunit nucleotide sites of F_1, changing the conformation of each in sequence, so that ADP is first bound, then phosphorylated, then released, according to Boyer's binding change mechanism. Paul Boyer and John Walker shared in the 1997 Nobel Prize for chemistry for their work on the structure and mechanism of ATP synthase.

Boyer's ^{18}O Exchange Experiment Identified the Energy-Requiring Step

The elegant studies by Paul Boyer of ^{18}O exchange in ATP synthase have provided other important insights into the mechanism of the enzyme. Boyer and his colleagues studied the ability of the synthase to incorporate labeled oxygen from $H_2^{18}O$ into P_i. This reaction (Figure 21.26) occurs via synthesis of ATP from ADP and P_i, followed by hydrolysis of ATP with incorporation of oxygen atoms from the solvent. Although *net production of ATP* requires coupling with a proton gradient, Boyer observed that this *exchange reaction* occurs readily, even in the absence of a proton gradient. His finding indicated that the formation of *enzyme-bound ATP* does not require energy. Indeed, movement of protons through the F_0 channel causes the *release of newly synthesized ATP* from the enzyme. Thus, the energy provided by electron transport creates a proton gradient that drives enzyme conformational changes resulting in the binding of

FIGURE 21.26 • ATP production in the presence of a proton gradient and ATP/ADP exchange in the absence of a proton gradient. Exchange leads to incorporation of ^{18}O in phosphate as shown.

FIGURE 21.27 • The binding change mechanism for ATP synthesis by ATP synthase. This model assumes that F_1 has three interacting and conformationally distinct active sites. The open (O) conformation is inactive and has a low affinity for ligands; the L conformation (with "loose" affinity for ligands) is also inactive; the tight (T) conformation is active and has a high affinity for ligands. Synthesis of ATP is initiated (step 1) by binding of ADP and P_i to an L site. In the second step, an energy-driven conformational change converts the L site to a T conformation and also converts T to O and O to L. In the third step, ATP is synthesized at the T site and released from the O site. Two additional passes through this cycle produce two more ATPs and return the enzyme to its original state.

substrates on ATP synthase, ATP synthesis, and the release of products. The mechanism involves catalytic cooperativity between three interacting sites (Figure 21.27).

Racker and Stoeckenius Confirmed the Mitchell Model in a Reconstitution Experiment

When Mitchell first described his chemiosmotic hypothesis in 1961, little evidence existed to support it, and it was met with considerable skepticism by the scientific community. Eventually, however, considerable evidence accumulated to support this model. It is now clear that the electron transport chain generates a proton gradient, and careful measurements have shown that ATP is synthesized when a pH gradient is applied to mitochondria that cannot carry out electron transport. Even more relevant is a simple but crucial experiment reported in 1974 by Efraim Racker and Walther Stoeckenius, which provided specific confirmation of the Mitchell hypothesis. In this experiment, the bovine mitochondrial *ATP synthase* was reconstituted in simple lipid vesicles with **bacteriorhodopsin,** a light-driven proton pump from *Halobacterium halobium.* As shown in Figure 21.28, upon illumination, bacteriorhodopsin pumped protons
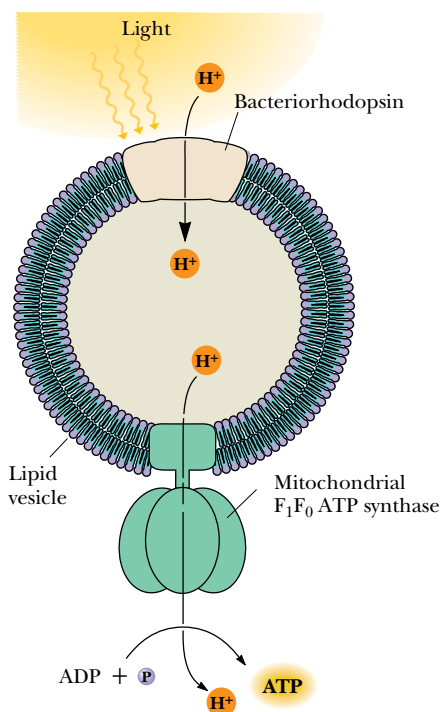
FIGURE 21.28 • The reconstituted vesicles containing ATP synthase and bacteriorhodopsin used by Stoeckenius and Racker to confirm the Mitchell chemiosmotic hypothesis.
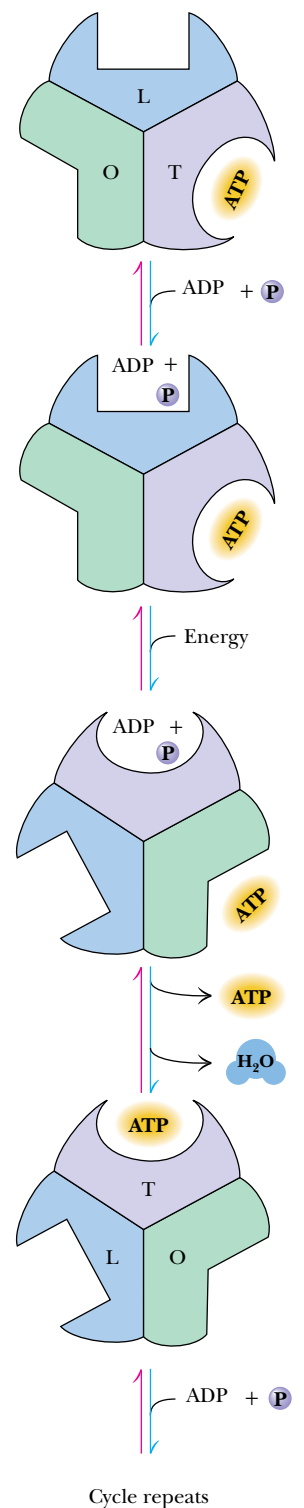
into these vesicles, and the resulting proton gradient was sufficient to drive ATP synthesis by the ATP synthase. Because the only two kinds of proteins present were one that produced a proton gradient and one that used such a gradient to make ATP, this experiment essentially verified Mitchell's chemiosmotic hypothesis.

21.10 • Inhibitors of Oxidative Phosphorylation

The unique properties and actions of an inhibitory substance can often help to identify aspects of an enzyme mechanism. Many details of electron transport and oxidative phosphorylation mechanisms have been gained from studying the effects of particular inhibitors. Figure 21.29 presents the structures of some electron transport and oxidative phosphorylation inhibitors. The sites of inhibition by these agents are indicated in Figure 21.30.

Inhibitors of Complexes I, II, and III Block Electron Transport

Rotenone is a common insecticide that strongly inhibits the NADH–UQ reductase. Rotenone is obtained from the roots of several species of plants. Tribes in certain parts of the world have made a practice of beating the roots of trees along riverbanks to release rotenone into the water, where it paralyzes fish and makes them easy prey. Ptericidin, Amytal, and other barbiturates, mercurial
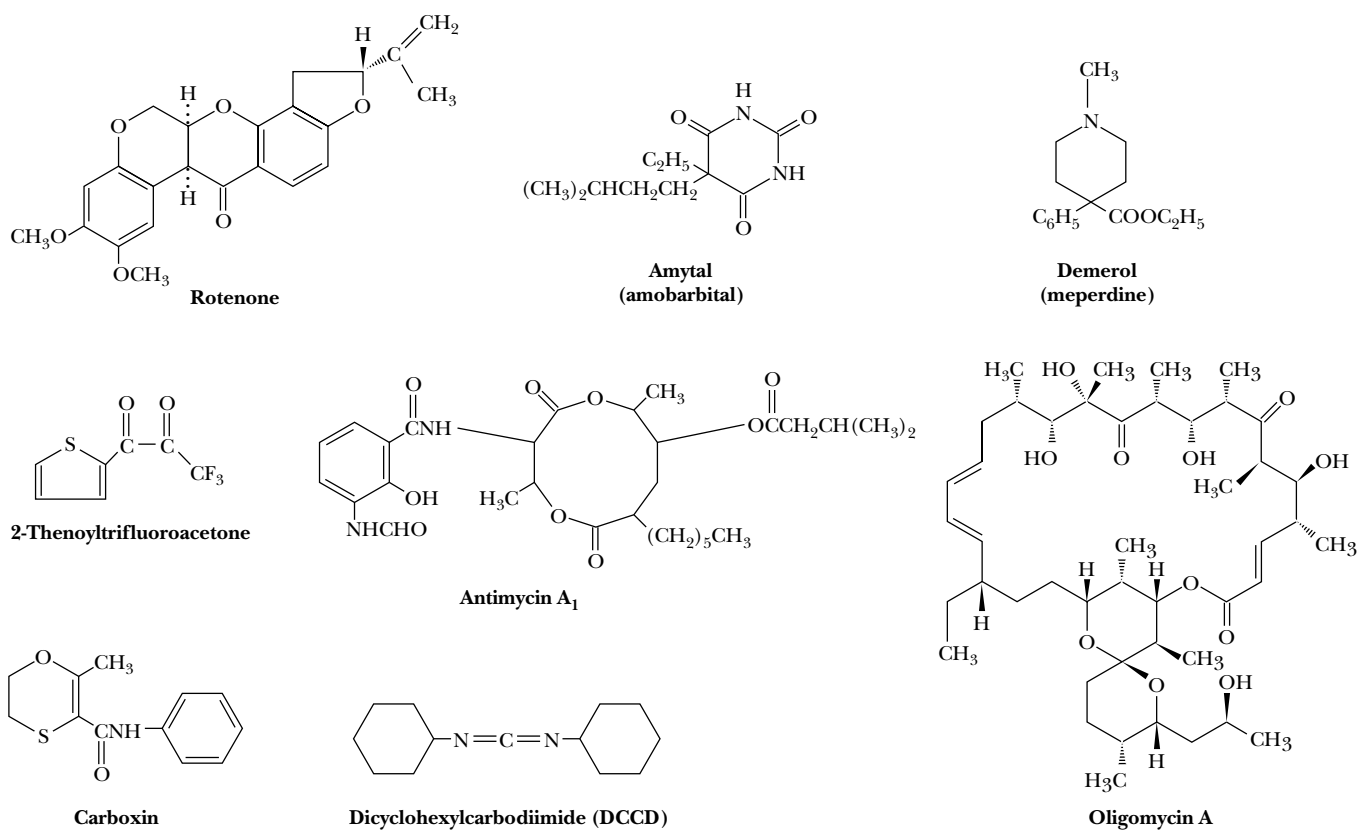
FIGURE 21.29 • The structures of several inhibitors of electron transport and oxidative phosphorylation.
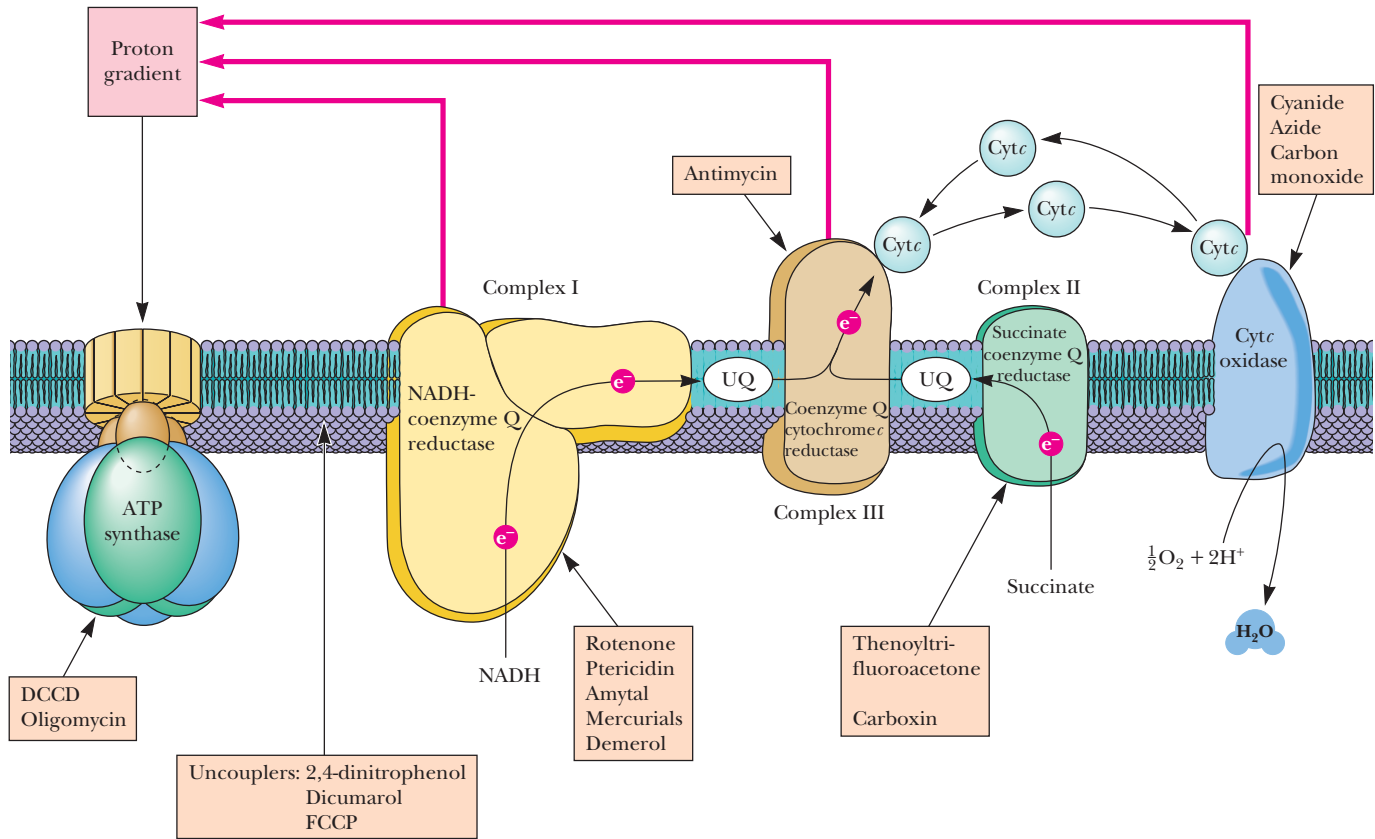
FIGURE 21.30 • The sites of action of several inhibitors of electron transport and/or oxidative phosphorylation.

agents, and the widely prescribed painkiller Demerol also exert inhibitory actions on this enzyme complex. All these substances appear to inhibit reduction of coenzyme Q and the oxidation of the Fe-S clusters of NADH–UQ reductase.

2-Thenoyltrifluoroacetone and carboxin and its derivatives specifically block Complex II, the succinate–UQ reductase. Antimycin, an antibiotic produced by *Streptomyces griseus,* inhibits the UQ–cytochrome *c* reductase by blocking electron transfer between b_H and coenzyme Q in the Q_n site. Myxothiazol inhibits the same complex by acting at the Q_p site.

Cyanide, Azide, and Carbon Monoxide Inhibit Complex IV

Complex IV, the cytochrome *c* oxidase, is specifically inhibited by cyanide (CN^-), azide (N_3^-), and carbon monoxide (CO). Cyanide and azide bind tightly to the ferric form of cytochrome a_3, whereas carbon monoxide binds only to the ferrous form. The inhibitory actions of cyanide and azide at this site are very potent, whereas the principal toxicity of carbon monoxide arises from its affinity for the iron of hemoglobin. Herein lies an important distinction between the poisonous effects of cyanide and carbon monoxide. Because animals (including humans) carry many, many hemoglobin molecules, they must inhale a large quantity of carbon monoxide to die from it. These same organisms, however, possess comparatively few molecules of cytochrome a_3. Consequently, a limited exposure to cyanide can be lethal. The sudden action of cyanide attests to the organism's constant and immediate need for the energy supplied by electron transport.

Oligomycin and DCCD Are ATP Synthase Inhibitors

Inhibitors of ATP synthase include dicyclohexylcarbodiimide (DCCD) and oligomycin (Figure 21.29). DCCD bonds covalently to carboxyl groups in hydrophobic domains of proteins in general, and to a glutamic acid residue of the c subunit of F_0, the proteolipid forming the proton channel of the ATP synthase, in particular. If the c subunit is labeled with DCCD, proton flow through F_0 is blocked and ATP synthase activity is inhibited. Likewise, oligomycin acts directly on the ATP synthase. By binding to a subunit of F_0, oligomycin also blocks the movement of protons through F_0.

21.11 • Uncouplers Disrupt the Coupling of Electron Transport and ATP Synthase

Another important class of reagents affects ATP synthesis, but in a manner that does not involve direct binding to any of the proteins of the electron transport chain or the F_1F_0–ATPase. These agents are known as **uncouplers** because they disrupt the tight coupling between electron transport and the ATP synthase. Uncouplers act by dissipating the proton gradient across the inner mitochondrial membrane created by the electron transport system. Typical examples include 2,4-dinitrophenol, dicumarol, and carbonyl cyanide-*p*-trifluoro-methoxyphenyl hydrazone (perhaps better known as fluorocarbonyl-cyanide phenylhydrazone or FCCP) (Figure 21.31). These compounds share two common features: hydrophobic character and a dissociable proton. As uncouplers, they function by carrying protons across the inner membrane. Their tendency is to acquire protons on the cytosolic surface of the membrane (where the proton concentration is high) and carry them to the matrix side, thereby destroying the proton gradient that couples electron transport and the ATP synthase. In mitochondria treated with uncouplers, electron transport continues, and protons are driven out through the inner membrane. However, they leak back in so rapidly via the uncouplers that ATP synthesis does not occur. Instead, the energy released in electron transport is dissipated as heat.

Endogenous Uncouplers Enable Organisms To Generate Heat

Ironically, certain cold-adapted animals, hibernating animals, and newborn animals generate large amounts of heat by uncoupling oxidative phosphorylation. Adipose tissue in these organisms contains so many mitochondria that it is called *brown adipose tissue* for the color imparted by the mitochondria. The inner membrane of brown adipose tissue mitochondria contains an endogenous protein called **thermogenin** (literally, "heat maker"), or *uncoupling protein,* that creates a passive proton channel through which protons flow from the cytosol to the matrix. Certain plants also use the heat of uncoupled proton transport for a special purpose. Skunk cabbage and related plants contain floral spikes that are maintained as much as 20 degrees above ambient temperature in this way. The warmth of the spikes serves to vaporize odiferous molecules, which attract insects that fertilize the flowers.

Dinitrophenol

Dicumarol

Carbonyl cyanide-p-trifluoro-methoxyphenyl hydrazone
—best known as **FCCP**; for **F**luoro **C**arbonyl **C**yanide **P**henylhydrazone

FIGURE 21.31 • Structures of several uncouplers, molecules that dissipate the proton gradient across the inner mitochondrial membrane and thereby destroy the tight coupling between electron transport and the ATP synthase reaction.

21.12 • ATP Exits the Mitochondria via an ATP–ADP Translocase

ATP, the cellular energy currency, must exit the mitochondria to carry energy throughout the cell, and ADP must be brought into the mitochondria for reprocessing. Neither of these processes occurs spontaneously because the highly charged ATP and ADP molecules do not readily cross biological membranes. Instead, these processes are mediated by a single transport system, the **ATP–ADP translocase.** This protein tightly couples the exit of ATP with the entry of ADP so that the mitochondrial nucleotide levels remain approximately constant. For each ATP transported out, one ADP is transported into the matrix. The translocase, which accounts for approximately 14% of the total mitochondrial membrane protein, is a homodimer of 30-kD subunits. Transport occurs via a single nucleotide-binding site, which alternately faces the matrix and the cytosol (Figure 21.32). It binds ATP on the matrix side, reorients to face the cytosol, and exchanges ATP for ADP, with subsequent movement back to the matrix face of the inner membrane.

Outward Movement of ATP Is Favored over Outward ADP Movement

The charge on ATP at pH 7.2 or so is about -4, and the charge on ADP at the same pH is about -3. Thus, net exchange of an ATP (out) for an ADP (in) results in the net movement of one negative charge from the matrix to the cytosol. (This process is equivalent to the movement of a proton from the cytosol to the matrix.) Recall that the inner membrane is positive outside (see Figure 21.22), and it becomes clear that outward movement of ATP is favored over outward ADP transport, ensuring that ATP will be transported out (Figure 21.32). Inward movement of ADP is favored over inward movement of ATP for the same reason. Thus, the membrane electrochemical potential itself controls the specificity of the ATP–ADP translocase. However, the electrochemical potential is diminished by the ATP–ADP translocase cycle and therefore operates with an energy cost to the cell. The cell must compensate by passing yet more electrons down the electron transport chain.

What is the cost of ATP–ADP exchange relative to the energy cost of ATP synthesis itself? We already noted that moving 1 ATP out and 1 ADP in is the equivalent of one proton moving from the cytosol to the matrix. *Synthesis of an*
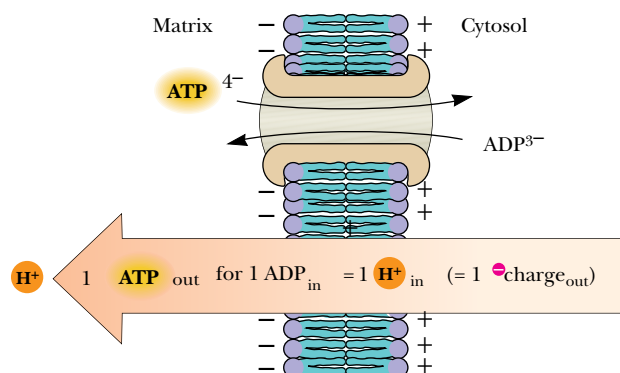
FIGURE 21.32 • Outward transport of ATP (via the ATP/ADP translocase) is favored by the membrane electrochemical potential.

ATP results from the movement of approximately three protons from the cytosol into the matrix through F_O. Altogether this means that approximately four protons are transported into the matrix per ATP synthesized. Thus, approximately one-fourth of the energy derived from the respiratory chain (electron transport and oxidative phosphorylation) is expended as the electrochemical energy devoted to mitochondrial ATP–ADP transport.

21.13 • What Is the P/O Ratio for Mitochondrial Electron Transport and Oxidative Phosphorylation?

The **P/O ratio** is the number of molecules of ATP formed in oxidative phosphorylation per two electrons flowing through a defined segment of the electron transport chain. In spite of intense study of this ratio, its actual value remains a matter of contention. If we accept the value of 10 H^+ transported out of the matrix per 2 e^- passed from NADH to O_2 through the electron transport chain, and also agree (as above) that 4 H^+ are transported into the matrix per ATP synthesized (and translocated), then the mitochondrial P/O ratio is 10/4, or 2.5, for the case of electrons entering the electron transport chain as NADH. This is somewhat lower than earlier estimates, which placed the P/O ratio at 3 for mitochondrial oxidation of NADH. For the portion of the chain from succinate to O_2, the H^+/2 e^- ratio is 6 (as noted above), and the P/O ratio in this case would be 6/4, or 1.5; earlier estimates placed this number at 2. The consensus of experimental measurements of P/O ratios for these two cases has been closer to the more modern values of 2.5 and 1.5. Many chemists and biochemists, accustomed to the integral stoichiometries of chemical and metabolic reactions, have been reluctant to accept the notion of nonintegral P/O ratios. At some point, as we learn more about these complex coupled processes, it may be necessary to reassess the numbers.

21.14 • Shuttle Systems Feed the Electrons of Cytosolic NADH into Electron Transport

$$\left(\frac{1\,\text{ATP}}{4\,\text{H}^+}\right)\left(\frac{10\,\text{H}^+}{2\,e^-\ [\text{NADH} \rightarrow \tfrac{1}{2}\text{O}_2]}\right) = \frac{10}{4} = \frac{\text{P}}{\text{O}}$$

Most of the NADH used in electron transport is produced in the mitochondrial matrix space, an appropriate site because NADH is oxidized by Complex I on the matrix side of the inner membrane. Furthermore, the inner mitochondrial membrane is impermeable to NADH. Recall, however, that NADH is produced in glycolysis by glyceraldehyde-3-P dehydrogenase in the cytosol. If this NADH were not oxidized to regenerate NAD^+, the glycolytic pathway would cease to function due to NAD^+ limitation. Eukaryotic cells have a number of *shuttle systems* that harvest the electrons of cytosolic NADH for delivery to mitochondria without actually transporting NADH across the inner membrane (Figures 21.33 and 21.34).

The Glycerophosphate Shuttle Ensures Efficient Use of Cytosolic NADH

In the **glycerophosphate shuttle,** two different **glycerophosphate dehydrogenases,** one in the cytoplasm and one on the outer face of the mitochondrial inner membrane, work together to carry electrons into the mitochondrial matrix (Figure 21.32). NADH produced in the cytosol transfers its electrons to *dihydroxyacetone phosphate,* thus reducing it to *glycerol-3-phosphate.* This metabolite is reoxidized by the FAD^+-dependent mitochondrial membrane enzyme to
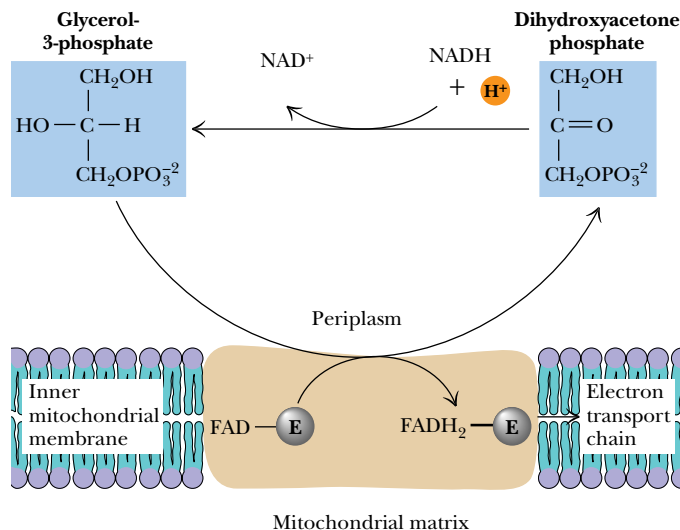
FIGURE 21.33 • The glycerophosphate shuttle (also known as the glycerol phosphate shuttle) couples the cytosolic oxidation of NADH with mitochondrial reduction of [FAD].
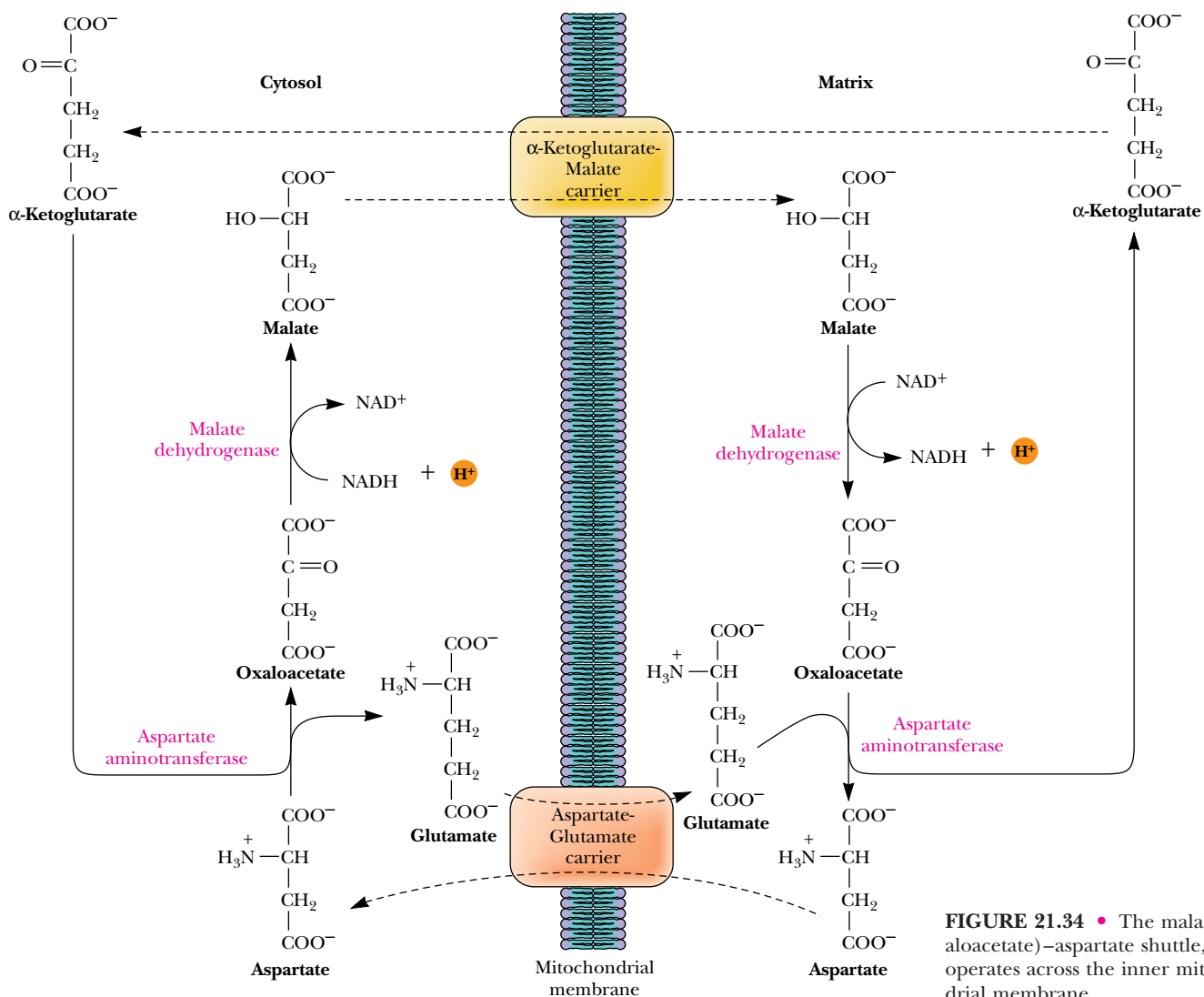
FIGURE 21.34 • The malate (oxaloacetate)–aspartate shuttle, which operates across the inner mitochondrial membrane.

reform dihydroxyacetone phosphate and enzyme-bound $FADH_2$. The two electrons of $[FADH_2]$ are passed directly to UQ, forming UQH_2. Thus, via this shuttle, cytosolic NADH can be used to produce mitochondrial $[FADH_2]$ and, subsequently, UQH_2. As a result, cytosolic NADH oxidized via this shuttle route yields only 1.5 molecules of ATP. The cell "pays" with a potential ATP molecule for the convenience of getting cytosolic NADH into the mitochondria. Although this may seem wasteful, there is an important payoff. The glycerophosphate shuttle is essentially irreversible, and even when NADH levels are very low relative to NAD^+, the cycle operates effectively.

The Malate–Aspartate Shuttle Is Reversible

The second electron shuttle system, called the **malate–aspartate shuttle,** is shown in Figure 21.34. Oxaloacetate is reduced in the cytosol, acquiring the electrons of NADH (which is oxidized to NAD^+). Malate is transported across the inner membrane, where it is reoxidized by malate dehydrogenase, converting NAD^+ to NADH in the matrix. This mitochondrial NADH readily enters the electron transport chain. The oxaloacetate produced in this reaction cannot cross the inner membrane and must be transaminated to form *aspartate, which can be transported* across the membrane to the cytosolic side. Transamination in the cytosol recycles aspartate back to oxaloacetate. In contrast to the glycerol phosphate shuttle, the malate–aspartate cycle is reversible, and it operates as shown in Figure 21.34 only if the $NADH/NAD^+$ ratio in the cytosol is higher than the ratio in the matrix. Because this shuttle produces NADH in the matrix, the full 2.5 ATPs per NADH are recovered.

The Net Yield of ATP from Glucose Oxidation Depends on the Shuttle Used

The complete route for the conversion of the metabolic energy of glucose to ATP has now been described, in Chapters 19 through 21. Assuming appropriate P/O ratios, the number of ATP molecules produced by the complete oxidation of a molecule of glucose can be estimated. Keeping in mind that P/O ratios must be viewed as approximate, for all the reasons previously cited, we will assume the values of 2.5 and 1.5 for the mitochondrial oxidation of NADH and succinate, respectively. In eukaryotic cells, the combined pathways of glycolysis, the TCA cycle, electron transport, and oxidative phosphorylation then yield a net of approximately 30 to 32 molecules of ATP per molecule of glucose oxidized, depending on the shuttle route employed (Table 21.4).

The net stoichiometric equation for the oxidation of glucose, using the glycerol phosphate shuttle, is

$$\text{Glucose} + 6\ O_2 + {\sim}30\ \text{ADP} + {\sim}30\ P_i \longrightarrow$$
$$6\ CO_2 + {\sim}30\ \text{ATP} + {\sim}36\ H_2O \quad \text{(21.32)}$$
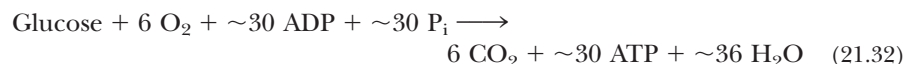
Because the 2 NADH formed in glycolysis are "transported" by the glycerol phosphate shuttle in this case, they each yield only 1.5 ATP, as already described. On the other hand, if these 2 NADH take part in the malate–aspartate shuttle, each yields 2.5 ATP, giving a total (in this case) of 32 ATP formed per glucose oxidized. Most of the ATP—26 out of 30 or 28 out of 32—is produced by oxidative phosphorylation; only 4 ATP molecules result from direct synthesis during glycolysis and the TCA cycle.

The situation in bacteria is somewhat different. Prokaryotic cells need not carry out ATP/ADP exchange. Thus, bacteria have the potential to produce approximately 38 ATP per glucose.

Table 21.4

Yield of ATP from Glucose Oxidation		
Pathway	**ATP Yield per Glucose**	
	Glycerol–Phosphate Shuttle	Malate–Aspartate Shuttle
Glycolysis: glucose to pyruvate (cytosol)		
Phosphorylation of glucose	−1	−1
Phosphorylation of fructose-6-phosphate	−1	−1
Dephosphorylation of 2 molecules of 1,3-BPG	+2	+2
Dephosphorylation of 2 molecules of PEP	+2	+2
Oxidation of 2 molecules of glyceraldehyde-3-phosphate yields 2 NADH		
Pyruvate conversion to acetyl-CoA (mitochondria)		
2 NADH		
Citric acid cycle (mitochondria)		
2 molecules of GTP from 2 molecules of succinyl-CoA	+2	+2
Oxidation of 2 molecules each of isocitrate, α-ketoglutarate, and malate yields 6 NADH		
Oxidation of 2 molecules of succinate yields 2 [FADH$_2$]		
Oxidative phosphorylation (mitochondria)		
2 NADH from glycolysis yield 1.5 ATP each if NADH is oxidized by glycerol-phosphate shuttle; 2.5 ATP by malate-aspartate shuttle	+3	+5
Oxidative decarboxylation of 2 pyruvate to 2 acetyl-CoA: 2 NADH produce 2.5 ATP each	+5	+5
2 [FADH$_2$] from each citric acid cycle produce 1.5 ATP each	+3	+3
6 NADH from citric acid cycle produce 2.5 ATP each	+15	+15
Net Yield	30	32

Note: These P/O ratios of 2.5 and 1.5 for mitochondrial oxidation of NADH and [FADH$_2$] are "consensus values." Because they may not reflect actual values and because these ratios may change depending on metabolic conditions, these estimates of ATP yield from glucose oxidation are approximate.

3.5 Billion Years of Evolution Have Resulted in a System That Is 54% Efficient

Hypothetically speaking, how much energy does a eukaryotic cell extract from the glucose molecule? Taking a value of 50 kJ/mol for the hydrolysis of ATP under cellular conditions (Chapter 3), the production of 32 ATP per glucose oxidized yields 1600 kJ/mol of glucose. The cellular oxidation (combustion) of glucose yields $\Delta G = -2937$ kJ/mol. We can calculate an efficiency for the pathways of glycolysis, the TCA cycle, electron transport, and oxidative phosphorylation of

$$\frac{1600}{2937} \times 100\% = 54\%$$

This is the result of approximately 3.5 billion years of evolution.

PROBLEMS

1. For the following reaction,

$$[FAD] + 2 \text{ cyt } c \text{ (Fe}^{2+}) + 2 \text{ H}^+ \rightleftharpoons [FADH_2] + 2 \text{ cyt } c \text{ (Fe}^{3+})$$
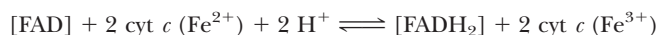
determine which of the redox couples is the electron acceptor and which is the electron donor under standard-state conditions, calculate the value of $\Delta\mathscr{E}_o{}'$, and determine the free energy change for the reaction.

2. Calculate the value of $\Delta\mathscr{E}_o{}'$ for the glyceraldehyde-3-phosphate dehydrogenase reaction, and calculate the free energy change for the reaction under standard-state conditions.

3. For the following redox reaction,

$$NAD^+ + 2 \text{ H}^+ + 2 \text{ } e^- \longrightarrow NADH + H^+$$
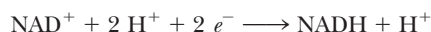
suggest an equation (analogous to Equation 21.13) that predicts the pH dependence of this reaction, and calculate the reduction potential for this reaction at pH 8.

4. Sodium nitrite ($NaNO_2$) is used by emergency medical personnel as an antidote for cyanide poisoning (for this purpose, it must be administered immediately). Based on the discussion of cyanide poisoning in Section 21.10, suggest a mechanism for the life-saving effect of sodium nitrite.

5. A wealthy investor has come to you for advice. She has been approached by a biochemist who seeks financial backing for a company that would market dinitrophenol and dicumarol as weight-loss medications. The biochemist has explained to her that these agents are uncouplers and that they would dissipate metabolic energy as heat. The investor wants to know if you think she should invest in the biochemist's company. How do you respond?

6. Assuming that 3 H^+ are transported per ATP synthesized in the mitochondrial matrix, the membrane potential difference is 0.18 V (negative inside), and the pH difference is 1 unit (acid outside, basic inside), calculate the largest ratio of $[ATP]/[ADP][P_i]$ under which synthesis of ATP can occur.

7. Of the dehydrogenase reactions in glycolysis and the TCA cycle, all but one use NAD^+ as the electron acceptor. The lone exception is the succinate dehydrogenase reaction, which uses covalently bound FAD of a flavoprotein as the electron acceptor. The standard reduction potential for this bound FAD is in the range of 0.003 to 0.091 V (Table 21.1). Compared with the other dehydrogenase reactions of glycolysis and the TCA cycle, what is unique about succinate dehydrogenase? Why is bound FAD a more suitable electron acceptor in this case?

8. a. What is the standard free energy change ($\Delta G^\circ{}'$) for the reduction of coenzyme Q by NADH as carried out by complex I (NADH-coenzyme Q reductase) of the electron transport pathway if $\mathscr{E}_o{}'(NAD^+/NADH + H^+) = -0.320$ volts and $\mathscr{E}_o{}'(CoQ/CoQH_2) = +0.060$ volts.

b. What is the equilibrium constant (K_{eq}) for this reaction?

c. Assume that (1) the actual free energy release accompanying the NADH-coenzyme Q reductase reaction is equal to the amount released under standard conditions (as calculated above), (2) this energy can be converted into the synthesis of ATP with an efficiency = 0.75 (that is, 75% of the energy released upon NADH oxidation is captured in ATP synthesis), and (3) the oxidation of

1 equivalent of NADH by coenzyme Q leads to the phosphorylation of 1 equivalent of ATP.

Under these conditions, what is the maximum ratio of $[ATP]/[ADP]$ attainable by oxidative phosphorylation when $[P_i]$ = 1 mM? (Assume $\Delta G^\circ{}'$ for ATP synthesis = +30.5 kJ/mol.)

9. Consider the oxidation of succinate by molecular oxygen as carried out via the electron transport pathway

$$\text{succinate} + \tfrac{1}{2}O_2 \longrightarrow \text{fumarate} + H_2O$$
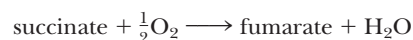
a. What is the standard free energy change ($\Delta G^\circ{}'$) for this reaction if $\mathscr{E}_o{}'(\text{fum/succ}) = +0.031$ volts and $\mathscr{E}_o{}'(\tfrac{1}{2}O_2/H_2O)$ = +0.816 volts.

b. What is the equilibrium constant (K_{eq}) for this reaction?

c. Assume that (1) the actual free energy release accompanying succinate oxidation by the electron transport pathway is equal to the amount released under standard conditions (as calculated above), (2) this energy can be converted into the synthesis of ATP with an efficiency = 0.7 (that is, 70% of the energy released upon succinate oxidation is captured in ATP synthesis), (3) the oxidation of 1 succinate leads to the phosphorylation of 2 equivalents of ATP.

Under these conditions, what is the maximum ratio of $[ATP]/[ADP]$ attainable by oxidative phosphorylation when $[P_i]$ = 1 mM? (Assume $\Delta G^\circ{}'$ for ATP synthesis = +30.5 kJ/mol.)

10. Consider the oxidation of NADH by molecular oxygen as carried out via the electron transport pathway

$$NADH + H^+ + \tfrac{1}{2}O_2 \longrightarrow NAD^+ + H_2O$$
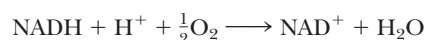
a. What is the standard free energy change ($\Delta G^\circ{}'$) for this reaction if $\Delta\mathscr{E}_o{}'(NAD^+/NADH) = -0.320$ volts and $\Delta\mathscr{E}_o{}'(\tfrac{1}{2}O_2/H_2O)$ = +0.816 volts.

b. What is the equilibrium constant (K_{eq}) for this reaction?

c. Assume that (1) the actual free energy release accompanying NADH oxidation by the electron transport pathway is equal to the amount released under standard conditions (as calculated above), (2) this energy can be converted into the synthesis of ATP with an efficiency = 0.75 (that is, 75% of the energy released upon NADH oxidation is captured in ATP synthesis), and (3) the oxidation of 1 NADH leads to the phosphorylation of 3 equivalents of ATP.

Under these conditions, what is the maximum ratio of $[ATP]/[ADP]$ attainable by oxidative phosphorylation when $[P_i]$ = 2 mM? (Assume $\Delta G^\circ{}'$ for ATP synthesis = +30.5 kJ/mol.)

11. Write a balanced equation for the reduction of molecular oxygen by reduced cytochrome c as carried out by complex IV (cytochrome oxidase) of the electron transport pathway.

a. What is the standard free energy change ($\Delta G^\circ{}'$) for this reaction if

$$\Delta\mathscr{E}_o{}'\text{cyt } c(\text{Fe}^{3+})/\text{cyt } c(\text{Fe}^{2+}) = +0.254 \text{ volts and}$$
$$\Delta\mathscr{E}_o{}'(\tfrac{1}{2}O_2/H_2O) = 0.816 \text{ volts.}$$

b. What is the equilibrium constant (K_{eq}) for this reaction?

c. Assume that (1) the actual free energy release accompanying cytochrome *c* oxidation by the electron transport pathway is equal to the amount released under standard conditions (as calculated in section **a.**), (2) this energy can be converted into the synthesis of ATP with an efficiency = 0.6 (that is, 60% of the energy released upon cytochrome *c* oxidation is captured in ATP synthesis), and (3) the reduction of 1 molecule of O_2 by reduced cytochrome *c* leads to the phosphorylation of 2 equivalents of ATP.

Under these conditions, what is the maximum ratio of [ATP]/[ADP] attainable by oxidative phosphorylation when $[P_i]$ = 3 m*M*? (Assume $\Delta G°'$ for ATP synthesis = +30.5 kJ/mol.)

12. The standard reduction potential for $(NAD^+/NADH)$ is −0.320 volts, and the standard reduction potential for (pyruvate/lactate) is −0.185 volts.

a. What is the standard free energy change, $\Delta G°'$, for the lactate dehydrogenase reaction:

$$NADH + H^+ + pyruvate \rightleftharpoons lactate + NAD^+$$

b. What is the equilibrium constant, K_{eq}, for this reaction?

c. If [pyruvate] = 0.05 m*M* and [lactate] = 2.9 m*M* and ΔG for the lactate dehydrogenase reaction = −15 kJ/mol in erythrocytes, what is the $[NAD^+]/[NADH]$ ratio under these conditions?

13. Assume that the free energy change, ΔG, associated with the movement of one mole of protons from the outside to the inside of a bacterial cell is −23 kJ/mol and 3 H^+ must cross the bacterial plasma membrane per ATP formed by the bacterial F_1F_0–ATP synthase. ATP synthesis thus takes place by the coupled process:

$$3\,H_{out}^+ + ADP + P_i \rightleftharpoons 3\,H_{in}^+ + ATP + H_2O$$
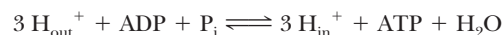
a. If the overall free energy change ($\Delta G_{overall}$) associated with ATP synthesis in these cells by the coupled process is −21 kJ/mol, what is the equilibrium constant, K_{eq}, for the process?

b. What is $\Delta G_{synthesis}$, the free energy change for ATP synthesis, in these bacteria under these conditions?

c. The standard free energy change for ATP hydrolysis, $\Delta G°'_{hydrolysis}$, is −30.5 kJ/mol. If $[P_i]$ = 2 m*M* in these bacterial cells, what is the [ATP]/[ADP] ratio in these cells?

FURTHER READING

Abraham, J. P., Leslie, A. G. W., Lutter, R., and Walker, J. E., 1994. Structure at 2.8 Å resolution of F₁–ATPase from bovine heart mitochondria. *Nature* **370:**621–628.

Babcock, G. T., and Wikström, M., 1992. Oxygen activation and the conservation of energy in cell respiration. *Nature* **356:**301–309.

Bonomi, F., Pagani, S., Cerletti, P., and Giori, C., 1983. Modification of the thermodynamic properties of the electron-transferring groups in mitochondrial succinate dehydrogenase upon binding of succinate. *European Journal of Biochemistry* **134:**439–445.

Boyer, P., et al., 1977. Oxidative phosphorylation and photophosphorylation. *Annual Review of Biochemistry* **46:**955–966.

Boyer, P. D., 1989. A perspective of the binding change mechanism for ATP synthesis. *The FASEB Journal* **3:**2164–2178.

Boyer, P. D., 1997. The ATP synthase—a splendid molecular machine. *Annual Review of Biochemistry* **66:**717–750.

Cross, R. L., 1994. Our primary source of ATP. *Nature* **370:**594–595.

Dickerson, R. E., 1980. Cytochrome *c* and the evolution of energy metabolism. *Scientific American* **242**(3):137–153.

Ernster, L., ed., 1980. *Bioenergetics.* New York: Elsevier Press.

Ferguson-Miller, S., 1996. Mammalian cytochrome *c* oxidase, a molecular monster subdued. *Science* **272:**1125.

Fillingame, R. H., 1980. The proton-translocating pump of oxidative phosphorylation. *Annual Review of Biochemistry* **49:**1079–1113.

Futai, M., Noumi, T., and Maeda, M., 1989. ATP synthase: Results by combined biochemical and molecular biological approaches. *Annual Review of Biochemistry* **58:**111–136.

Harold, F. M., 1986. *The Vital Force: A Study of Bioenergetics.* New York: W. H. Freeman and Company.

Iwata, S., Ostermeier, C., Ludwig, B., and Michel, H., 1995. Structure at 2.8 Å resolution of cytochrome *c* oxidase from *Paracoccus denitrificans. Nature* **376:**660–669.

Junge, W., Lill, H., and Engelbrecht, S., 1997. ATP synthase: An electrochemical transducer with rotatory mechanics. *Trends in Biochemical Sciences* **22:**420–423.

Mitchell, P., 1979. Keilin's respiratory chain concept and its chemiosmotic consequences. *Science* **206:**1148–1159.

Mitchell, P., and Moyle, J., 1965. Stoichiometry of proton translocation through the respiratory chain and adenosine triphosphatase systems of rat mitochondria. *Nature* **208:**147–151.

Moser, C. C., et al. 1992. Nature of biological electron transfer. *Nature* **355:**796–802.

Naqui, A., Chance, B., and Cadenas, E., 1986. Reactive oxygen intermediates in biochemistry. *Annual Review of Biochemistry* **55:**137.

Nicholls, D. G., and Ferguson, S. J., 1992. *Bioenergetics 2.* London: Academic Press.

Nicholls, D. G., and Rial, E., 1984. Brown fat mitochondria. *Trends in Biochemical Sciences* **9:**489–491.

Noji, H., Yasuda, R., Yoshida, M., and Kinosita, K., 1997. Direct observation of the rotation of F₁-ATPase. *Nature* **386:**299–302.

Pedersen, P., and Carafoli, E., 1987. Ion-motive ATPases. I. Ubiquity, properties and significance to cell function. *Trends in Biochemical Sciences* **12:**146–150.

Sabbert, D., Engelbrecht, S., and Junge, W., 1996. Intersubunit rotation in active F₁-ATPase. *Nature* **381:**623–625.

Slater, E. C., 1983. The Q cycle: An ubiquitous mechanism of electron transfer. *Trends in Biochemical Sciences* **8:**239–242.

Trumpower, B. L., 1990. Cytochrome bc_1 complexes of microorganisms. *Microbiological Reviews* **54:**101–129.

Trumpower, B. L., 1990. The protonmotive Q cycle—energy transduction by coupling of proton translocation to electron transfer by the cytochrome bc_1 complex. *Journal of Biological Chemistry* **265:**11409–11412.

Tsukihara, T., Aoyama, H., Yamashita, E., et al., 1996. The whole structure of the 13-subunit oxidized cytochrome *c* oxidase at 2.8 Å. *Science* **272:**1136–1144.

Vignais, P. V., and Lunardi, J., 1985. Chemical probes of mitochondrial ATP synthesis and translocation. *Annual Review of Biochemistry* **54:**977–1014.

von Jagow, G., 1980. *b*-Type cytochromes. *Annual Review of Biochemistry* **49:**281–314.

Walker, J. E., 1992. The NADH:ubiquinone oxidoreductase (Complex I) of respiratory chains. *Quarterly Reviews of Biophysics* **25:**253–324.

Weiss, H., Friedrich, T., Hofhaus, G., and Preis, D., 1991. The respiratory-chain NADH dehydrogenase (Complex I) of mitochondria. *European Journal of Biochemistry* **197:**563–576.

Wilkens, S., Dunn, S. D., Chandler, J., et al., 1997. Solution structure of the N-terminal domain of the δ subunit of the *E. coli* ATP synthase. *Nature Structural Biology* **4:**198–201.

Xia, D., Yu, C-A., Kim, H., et al., 1997. The crystal structure of the cytochrome bc_1 complex from bovine heart mitochondria. *Science* **277:**60–66.

$\mathcal{C}$hapter 22

Photosynthesis

"Sunflowers," by Claude Monet (1840–1926), French, Metropolitan Museum of Art, New York City/Superstock, Inc.

The vast majority of energy consumed by living organisms stems from solar energy captured by the process of photosynthesis. Only chemolithotropic bacteria (Chapter 18) are independent of this energy source. Of the 1.5×10^{22} kJ of energy reaching the earth each day from the sun, 1% is absorbed by photosynthetic organisms and transduced into chemical energy.[1] This energy, in the form of biomolecules, becomes available to other members of the biosphere through food chains. The transduction of solar, or light, energy into chemical energy is often expressed in terms of **carbon dioxide fixation,** in which hexose is formed from carbon dioxide and oxygen is evolved:

$$6 \ CO_2 + 6 \ H_2O \xrightarrow{\text{Light}} C_6H_{12}O_6 + 6 \ O_2 \qquad (22.1)$$
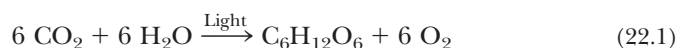
[1]Of the remaining 99%, two-thirds is absorbed by the earth and oceans, thereby heating the planet; the remaining one-third is lost as light reflected back into space.

709

Photosynthesis

Estimates indicate that 10^{11} tons of carbon dioxide are fixed globally per year, of which one-third is fixed in the oceans, primarily by photosynthetic marine microorganisms.

Although photosynthesis is traditionally equated with CO_2 fixation, light energy (or rather the chemical energy derived from it) can be used to drive virtually any cellular process. The assimilation of inorganic forms of nitrogen and sulfur into organic molecules (Chapter 27) represents two other metabolic conversions driven by light energy in green plants. Our previous considerations of aerobic metabolism (Chapters 19 through 21) treated cellular respiration (precisely the reverse of Equation [22.1]) as the central energy-releasing process in life. It necessarily follows that the formation of hexose from carbon dioxide and water, the products of cellular respiration, must be endergonic. The necessary energy comes from light. Note that in the carbon dioxide fixation reaction described, light is used to drive a chemical reaction against its thermodynamic potential.

22.1 • General Aspects of Photosynthesis

Photosynthesis Occurs in Membranes

Organisms capable of photosynthesis are very diverse, ranging from simple prokaryotic forms to the largest organisms of all, *Sequoia gigantea,* the giant redwood trees of California. Despite this diversity, we find certain generalities regarding photosynthesis. An important one is that *photosynthesis occurs in membranes.* In photosynthetic prokaryotes, the photosynthetic membranes fill up the cell interior; in photosynthetic eukaryotes, the photosynthetic membranes are localized in large organelles known as **chloroplasts** (Figures 22.1 and 22.2). Chloroplasts are one member in a family of related plant-specific organelles known as **plastids.** Chloroplasts themselves show a range of diversity, from the single, spiral chloroplast that gives *Spirogyra* its name to the multitude of ellipsoidal plastids typical of higher plant cells (Figure 22.3).

Characteristic of all chloroplasts, however, is the organization of the inner membrane system, the so-called **thylakoid membrane.** The thylakoid membrane

FIGURE 22.1 • Electron micrograph of a representative chloroplast. *(James Dennis/CNRI/Phototake NYC)*
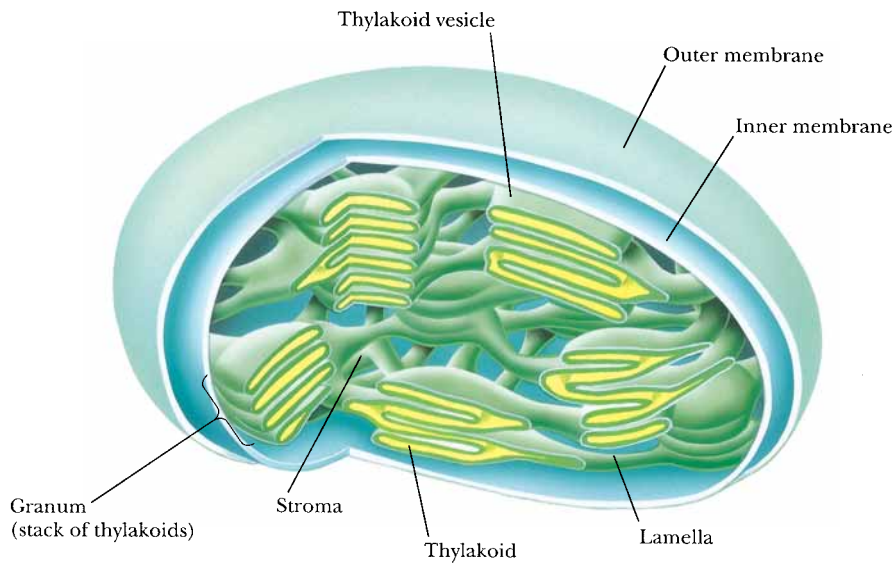
FIGURE 22.2 • Schematic diagram of an idealized chloroplast.

is organized into paired folds that extend throughout the organelle, as in Figure 22.1. These paired folds, or **lamellae,** give rise to flattened sacs or disks, **thylakoid vesicles** (from the Greek *thylakos,* meaning "sack"), which occur in stacks called **grana.** A single stack, or **granum,** may contain dozens of thylakoid vesicles, and different grana are joined by lamellae that run through the soluble portion, or **stroma,** of the organelle. Chloroplasts thus possess three membrane-bound aqueous compartments: the intermembrane space, the stroma, and the interior of the thylakoid vesicles, the so-called **thylakoid space** (also known as the **thylakoid lumen**). As we shall see, this third compartment serves an important function in the transduction of light energy into ATP formation. The thylakoid membrane has a highly characteristic lipid composition and, like the inner membrane of the mitochondrion, is impermeable to most ions and molecules. Chloroplasts, like their mitochondrial counterparts, possess DNA, RNA,
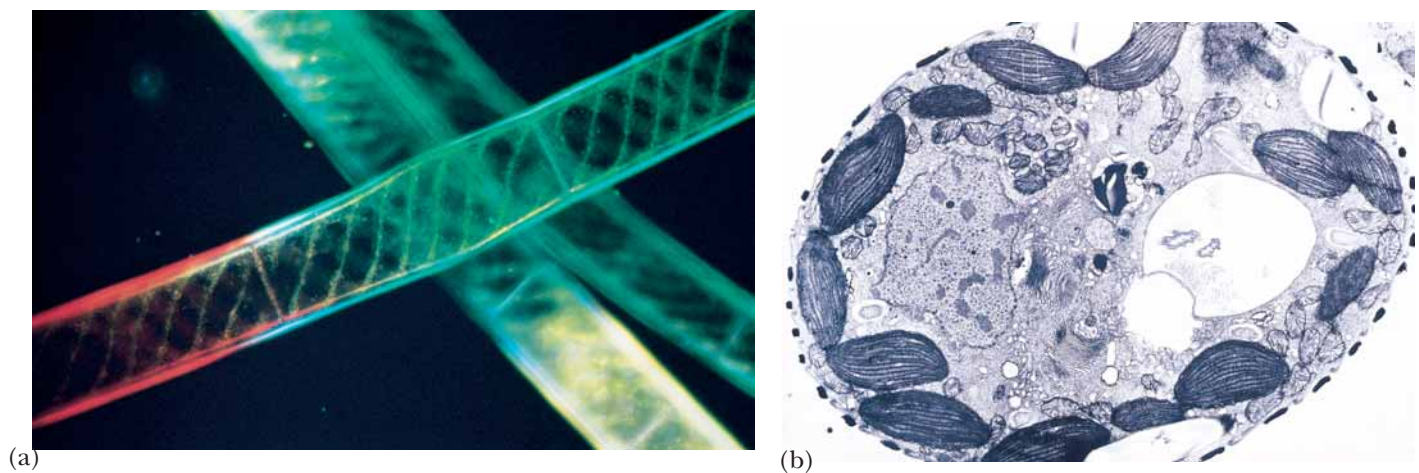
FIGURE 22.3 • (a) *Spirogyra*—a freshwater green alga. (b) A higher plant cell.
(a, Michael Siegel/Phototake NYC; b, Biophoto Associates/Science Source.)

and ribosomes and consequently display a considerable amount of autonomy. However, many critical chloroplast components are encoded by nuclear genes, so autonomy is far from absolute.

Photosynthesis Consists of Both Light Reactions and Dark Reactions

If a chloroplast suspension is illuminated in the absence of carbon dioxide, oxygen is evolved. Furthermore, if the illuminated chloroplasts are now placed in the dark and supplied with CO_2, net hexose synthesis can be observed (Figure 22.4). Thus, the evolution of oxygen can be temporally separated from CO_2 fixation and also has a light dependency that CO_2 fixation lacks. The **light reactions** of photosynthesis, of which O_2 evolution is only one part, are associated with the thylakoid membranes. In contrast, the light-independent reactions, or so-called **dark reactions,** notably CO_2 fixation, are located in the stroma. A concise summary of the photosynthetic process is that radiant electromagnetic energy (light) is transformed by a specific photochemical system located in the thylakoids to yield chemical energy in the form of reducing potential (NADPH) and high-energy phosphate (ATP). NADPH and ATP can then be used to drive the endergonic process of hexose formation from CO_2 by a series of enzymatic reactions found in the stroma (see Equation 22.3, which follows).

temporally • with regard to time

Water Is the Ultimate e^- Donor for Photosynthetic NADP$^+$ Reduction

In green plants, water serves as the ultimate electron donor for the photosynthetic generation of reducing equivalents. The reaction sequence

$$2\,H_2O + 2\,NADP^+ + x\,ADP + x\,P_i \xrightarrow{nh\nu}$$
$$O_2 + 2\,NADPH + 2\,H^+ + x\,ATP + x\,H_2O \quad (22.2)$$
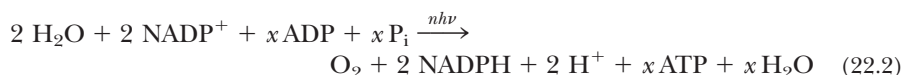
describes the process, where $nh\nu$ symbolizes *light energy* (n is some number of photons of energy $h\nu$, where h is Planck's constant and ν is the frequency of
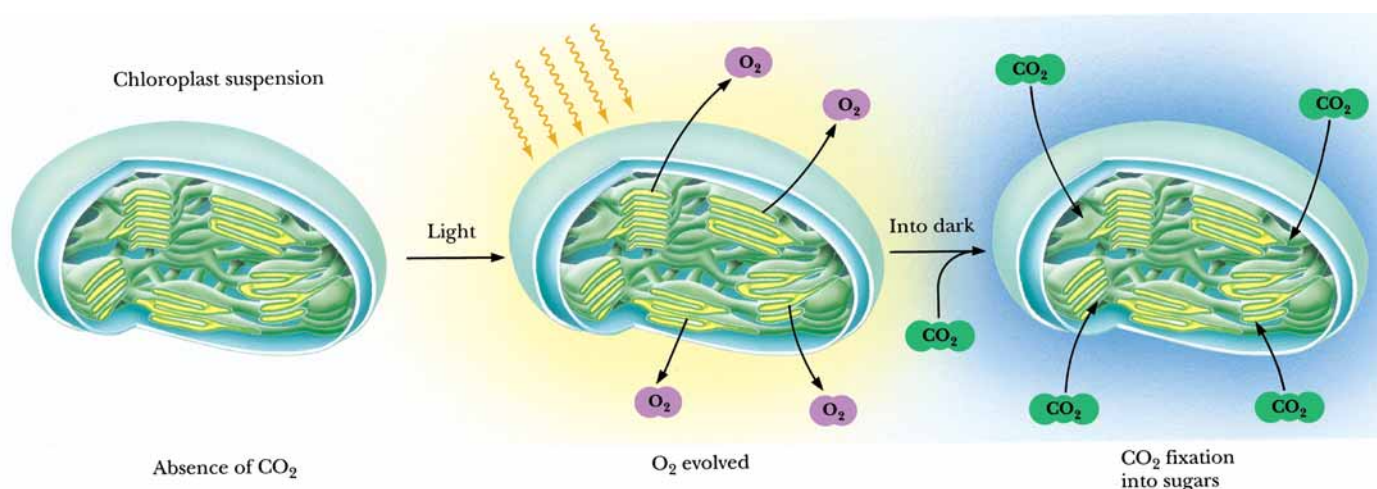
FIGURE 22.4 • The light-dependent and light-independent reactions of photosynthesis. Light reactions are associated with the thylakoid membranes, and light-independent reactions are associated with the stroma.

the light). Light energy is necessary to make the unfavorable reduction of $NADP^+$ by H_2O ($\Delta\mathcal{E}_\circ' = -1.136$ V; $\Delta G^{\circ\prime} = +219$ kJ/mol $NADP^+$) thermodynamically favorable. Thus, the light energy input, $nh\nu$, must exceed 219 kJ/mol $NADP^+$. The stoichiometry of ATP formation depends on the pattern of photophosphorylation operating in the cell at the time and on the ATP yield in terms of the chemiosmotic ratio, ATP/H^+, as we will see later. Nevertheless, the stoichiometry of the metabolic pathway of CO_2 fixation is certain:

$$12 \text{ NADPH} + 12 \text{ H}^+ + 18 \text{ ATP} + 6 \text{ CO}_2 + 12 \text{ H}_2\text{O} \longrightarrow$$
$$C_6H_{12}O_6 + 12 \text{ NADP}^+ + 18 \text{ ADP} + 18 \text{ P}_i \quad (22.3)$$
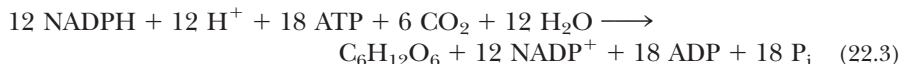
A More Generalized Equation for Photosynthesis

In 1931, comparative study of photosynthesis in bacteria led van Niel to a more general formulation of the overall reaction:

$$\text{CO}_2 \quad + \quad 2 \text{ H}_2\text{A} \quad \xrightarrow{\text{Light}} \quad (\text{CH}_2\text{O}) + \quad 2\text{A} \quad + \text{H}_2\text{O} \quad\quad (22.4)$$

Hydrogen	**Hydrogen**	**Reduced**	**Oxidized**
acceptor	**donor**	**acceptor**	**donor**
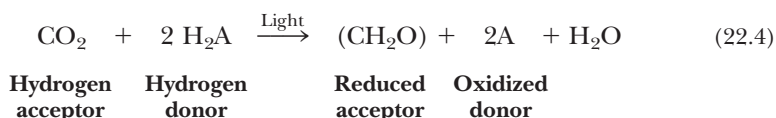
In photosynthetic bacteria, H_2A is variously H_2S (photosynthetic green and purple sulfur bacteria), isopropanol, or some similar oxidizable substrate. [*(CH$_2$O)* symbolizes a carbohydrate unit.]

$$\text{CO}_2 + 2 \text{ H}_2\text{S} \longrightarrow (\text{CH}_2\text{O}) + \text{H}_2\text{O} + 2 \text{ S}$$

$$\text{CO}_2 + 2 \text{ CH}_3\text{—CHOH—CH}_3 \longrightarrow (\text{CH}_2\text{O}) + \text{H}_2\text{O} + 2 \overset{\overset{\textstyle O}{\|}}{\text{CH}_3\text{—C—CH}_3}$$
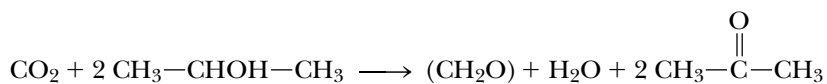
In cyanobacteria and the eukaryotic photosynthetic cells of algae and higher plants, H_2A is H_2O, as implied earlier, and 2 A is O_2. The accumulation of O_2 to constitute 20% of the earth's atmosphere is the direct result of eons of global oxygenic photosynthesis.

22.2 • Photosynthesis Depends on the Photoreactivity of Chlorophyll

Chlorophylls are magnesium-containing substituted tetrapyrroles whose basic structure is reminiscent of heme, the iron-containing porphyrin (Chapters 5 and 21). Chlorophylls differ from heme in a number of properties: magnesium instead of iron is coordinated in the center of the planar conjugated ring structure; a long-chain alcohol, **phytol,** is esterified to a pyrrole ring substituent; and the methine bridge linking pyrroles III and IV is substituted and cross-linked to ring III, leading to the formation of a fifth five-membered ring. The structures of chlorophyll *a* and *b* are shown in Figure 22.5.

Chlorophylls are excellent light absorbers because of their aromaticity. That is, they possess delocalized π electrons above and below the planar ring structure. The energy differences between electronic states in these π orbitals correspond to the energies of visible light photons. When light energy is absorbed, an electron is promoted to a higher orbital, enhancing the potential for transfer of this electron to a suitable acceptor. Loss of such a photo-excited electron to an acceptor is an oxidation–reduction reaction. The net result is the transduction of light energy into the chemical energy of a redox reaction.
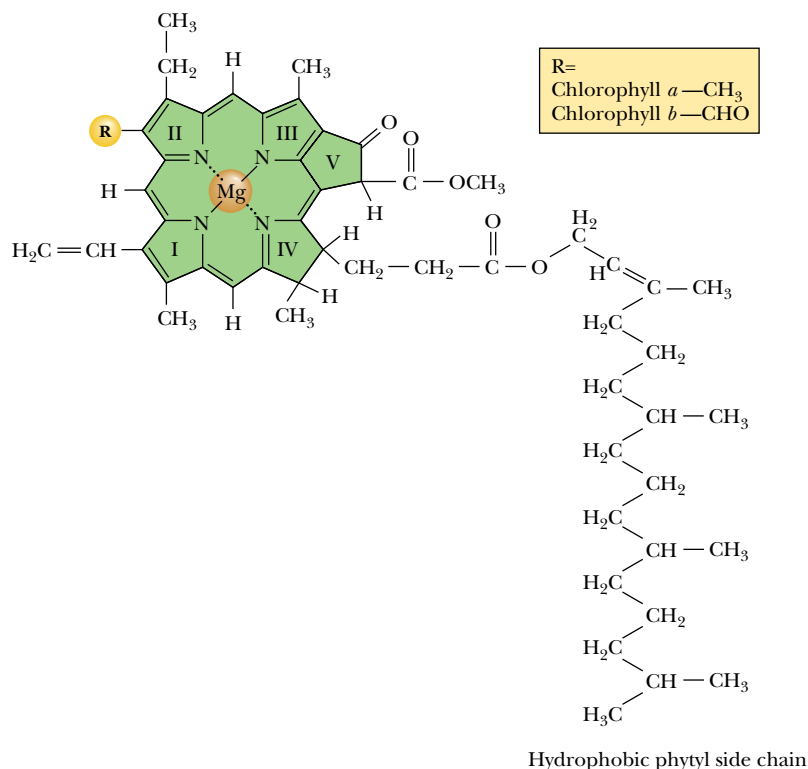
FIGURE 22.5 • Structures of chlorophyll *a* and *b*. Chlorophylls are structurally related to hemes, except Mg^{2+} replaces Fe^{2+} and ring II is more reduced than the corresponding ring of the porphyrins. The chlorophyll tetrapyrrole ring system is known as a chlorin. $R = CH_3$ in chlorophyll *a*; $R = CHO$ in chlorophyll *b*. Note that the aldehyde C=O bond of chlorophyll *b* introduces an additional double bond into conjugation with the double bonds of the tetrapyrrole ring system. Ring V is the additional ring created by interaction of the substituent of the methine bridge between pyrroles III and IV with the side chain of ring III. The phytyl side chain of ring IV provides a hydrophobic tail to anchor the chlorophyll in membrane protein complexes.

Chlorophylls and Accessory Light-Harvesting Pigments

The absorption spectra of chlorophylls *a* and *b* (Figure 22.6) differ somewhat. Plants that possess both chlorophylls can harvest a wider spectrum of incident energy. Other pigments in photosynthetic organisms, so-called **accessory light-harvesting pigments** (Figure 22.7), increase the possibility for absorption of incident light of wavelengths not absorbed by the chlorophylls. These accessory pigments, such as *carotenoids* and *phycobilins,* are also responsible for the magnificent colors of autumn. They persist longer after leaf death than the green chlorophylls, finally imparting their particular hues to the plant. These pigments, like chlorophyll, possess many conjugated double bonds and thus absorb visible light.

The Fate of Light Energy Absorbed by Photosynthetic Pigments

Each photon represents a quantum of light energy. A quantum of light energy absorbed by a photosynthetic pigment has four possible fates (Figure 22.8):

A. Loss as heat. The energy can be dissipated as heat through redistribution into atomic vibrations within the pigment molecule.

B. Loss of light. Energy of excitation reappears as **fluorescence** (light emission); a photon of fluorescence is emitted as the e^- returns to a lower orbital. This fate is common only in saturating light intensities. For thermodynamic reasons, the photon of fluorescence is of longer wavelength and hence lower energy than the quantum of excitation.

C. Resonance energy transfer. The excitation energy can be transferred by resonance energy transfer, a radiationless process, to a neighboring molecule if their energy level difference corresponds to the quantum of excitation energy. In this process, the quantum, or so-called **exciton,** is transferred,

FIGURE 22.6 • Absorption spectra of chlorophylls *a* and *b*.

(**a**)

β-Carotene

(**b**)
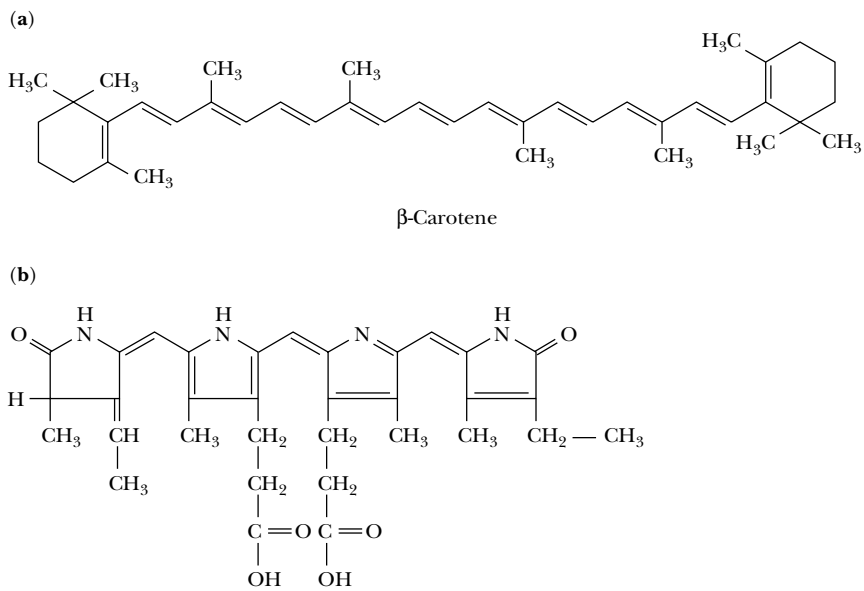
FIGURE 22.7 • Structures of representative accessory light-harvesting pigments in photosynthetic cells. (a) β-Carotene, an accessory light-harvesting pigment in leaves. Note the many conjugated double bonds. (b) Phycocyanobilin, a blue pigment found in cyanobacteria. It is a linear or open pyrrole.

Light energy ($h\nu$)

Pigment molecule (P)

Excited state (P*)

Q_{ox}

Q^-_{red}

Transfer

Thermal dissipation

Fluorescence

Exciton transfer

Oxidized P (P⁺)

Heat

Photon of fluorescence

$h\nu$

P*

Exciton transfer to neighboring P molecule
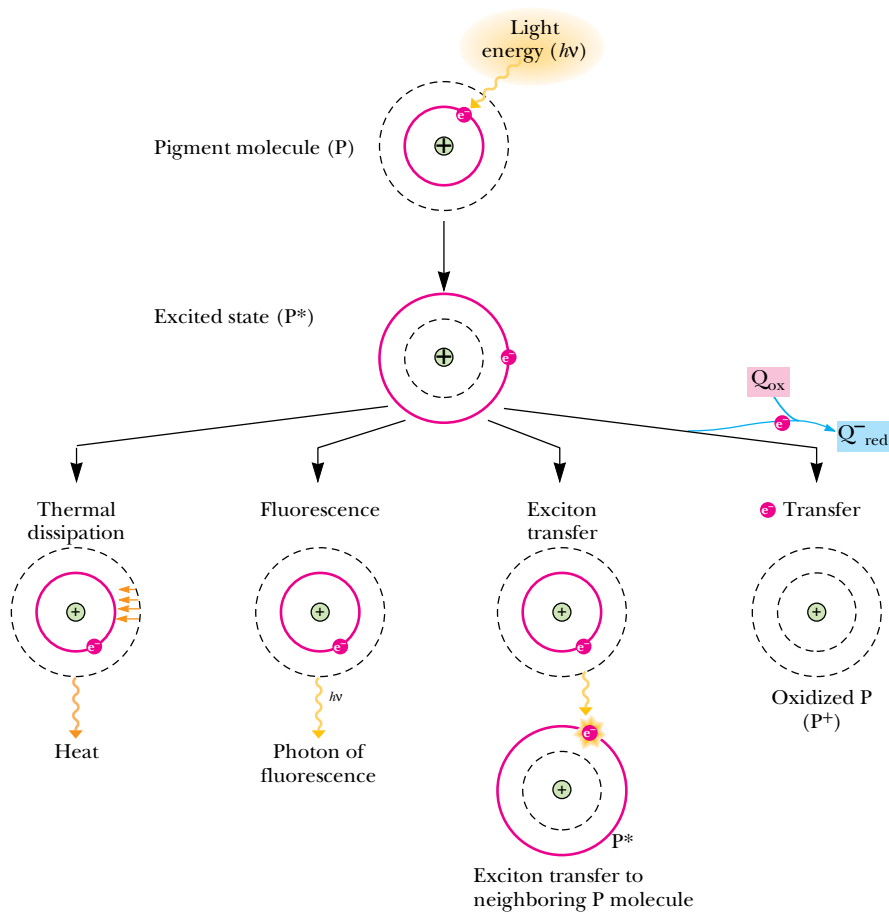
FIGURE 22.8 • Possible fates of the quantum of light energy absorbed by photosynthetic pigments.

raising an electron in the receptor molecule to a higher energy state as the photo-excited e^- in the original absorbing molecule returns to ground state. This so-called *Förster resonance energy transfer* is the mechanism whereby quanta of light falling anywhere within an array of pigment molecules can be transferred ultimately to specific photochemically reactive sites.

D. Energy transduction. The energy of excitation, in raising an electron to a higher energy orbital, dramatically changes the standard reduction potential, $\mathcal{E}_\circ{}'$, of the pigment such that it becomes a much more effective electron donor. That is, the excited-state species, by virtue of having an electron at a higher energy level through light absorption, has become a potent electron donor. Reaction of this excited-state electron donor with an electron acceptor situated in its vicinity leads to the transformation, or **transduction,** of light energy (photons) to chemical energy (reducing power, the potential for electron-transfer reactions). *Transduction of light energy into chemical energy, the photochemical event, is the essence of photosynthesis.*

Photosynthetic Units Consist of Many Chlorophyll Molecules but Only a Single Reaction Center

In the early 1930s, Emerson and Arnold investigated the relationship between the amount of incident light energy, the amount of chlorophyll present, and the amount of oxygen evolved by illuminated algal cells (this relationship is called the **quantum yield of photosynthesis**). Their studies gave an unexpected result: When algae were illuminated with very brief light flashes that could excite every chlorophyll molecule at least once, only one molecule of O_2 was evolved per 2400 chlorophyll molecules. This result implied that not all chlorophyll molecules are photochemically reactive, and it led to the concept that photosynthesis occurs in functionally discrete units. Chlorophyll serves two roles in photosynthesis. It is involved in light harvesting and the transfer of light energy to photoreactive sites by exciton transfer, and it participates directly in the photochemical events whereby light energy becomes chemical energy. A **photosynthetic unit** can be envisioned as an antenna of several hundred light-harvesting chlorophyll molecules plus a special pair of photochemically reactive chlorophyll *a* molecules called the **reaction center.** The purpose of the vast majority of chlorophyll in a photosynthetic unit is to harvest light incident within the unit and funnel it, via resonance energy transfer, to special reaction center chlorophyll molecules that are photochemically active. Most chlorophyll thus acts as a large light-collecting antenna, and it is at the reaction centers that the photochemical event occurs (Figure 22.9). Oxidation of chlorophyll leaves a **cationic free radical,** $Chl\cdot^+$, whose properties as an electron acceptor have important consequences for photosynthesis. Note that the Mg^{2+} ion does not change in valence during these redox reactions.
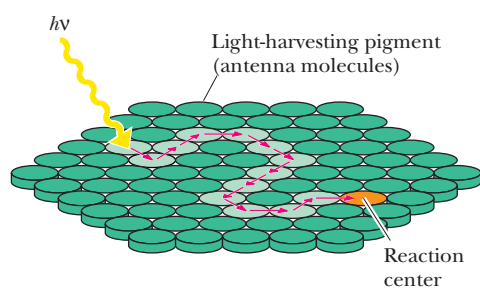
FIGURE 22.9 • Schematic diagram of a photosynthetic unit. The light-harvesting pigments, or antenna molecules *(green)*, absorb and transfer light energy to the specialized chlorophyll dimer that constitutes the reaction center *(orange)*.

22.3 • Eukaryotic Phototrophs Possess Two Distinct Photosystems

The existence of two separate but interacting photosystems in photosynthetic eukaryotes was demonstrated through analysis of the **photochemical action spectrum** of photosynthesis, in which the oxygen-evolving capacity as a function of light wavelength was determined (Figure 22.10).

Although chlorophyll *a* has some capacity to absorb 700-nm light, light of this wavelength is relatively inefficient in driving photosynthesis. However, if light of shorter wavelength (less than 680 nm) is used to supplement 700-nm
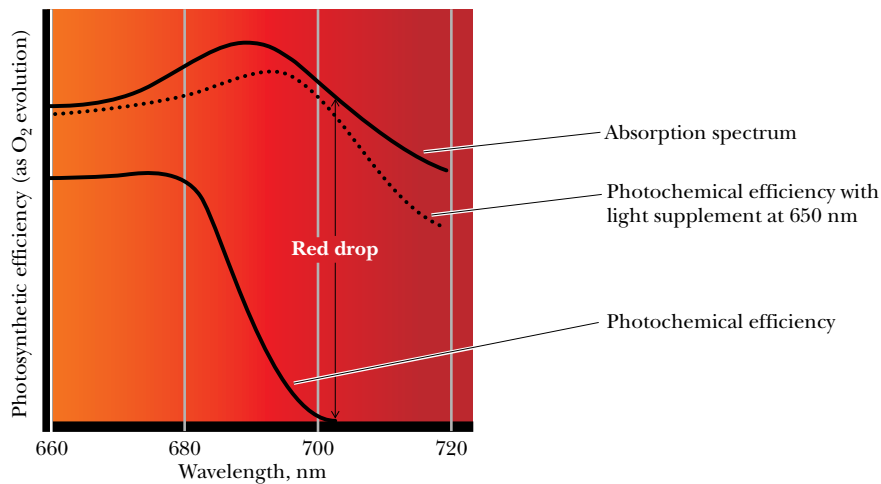
FIGURE 22.10 • The photochemical action spectrum of photosynthesis. The quantum yield of photosynthesis as a function of wavelength of incident light shows an abrupt decrease above 680 nm, the so-called *red drop*.

light, an enhancement of photosynthetic quantum yield, the so-called *Emerson enhancement effect,* is observed. In other words, these two wavelengths are synergistic: When given together, these wavelengths elicit more O_2 evolution than expected from the sum of the amounts when each wavelength of light is given alone. One interpretation is that two light reactions participate in oxygen-evolving photosynthetic cells, one using light of 700 nm and the other using light of wavelength 680 nm or less. The existence of two light reactions established the presence of two photosystems, I and II. **Photosystem I** (PSI) is defined as containing reaction center chlorophylls with maximal red light absorption at 700 nm; PSI is not involved in O_2 evolution. **Photosystem II** (PSII) functions in O_2 evolution, using reaction centers that exhibit maximal red light absorption at 680 nm.

All photosynthetic cells contain some form of photosystem. Photosynthetic bacteria, unlike cyanobacteria and eukaryotic phototrophs, have only one photosystem. Interestingly, bacterial photosystems resemble eukaryotic PSII more than PSI, even though photosynthetic bacteria lack O_2-evolving capacity.

P700 and P680 Are the Reaction Centers of PSI and PSII, Respectively

Precise spectrophotometric measurements showed that a small amount of pigment absorbing 700-nm light **(P700)** is bleached when light of this wavelength is used to illuminate suspensions of eukaryotic photosynthetic cells. Because bleaching, or disappearance, of the 700-nm absorbance can be mimicked by adding an electron acceptor such as ferricyanide, bleaching is correlated with electron loss from P700. The concentration of P700 is small, only 0.25% of the total amount of chlorophyll in plants. However, this low concentration is consistent with the notion of **reaction centers** (specific photoreactive sites). P700 is the reaction center of photosystem I. Similar studies using shorter-wavelength light identified an analogous pigment, **P680,** which constitutes the reaction center of photosystem II. Both P700 and P680 are chlorophyll *a* dimers situated within specialized protein complexes.

Chlorophyll Exists in Plant Membranes in Association with Proteins

Detergent treatment of a suspension of thylakoids dissolves the membranes, releasing complexes containing both chlorophyll and protein. These chlorophyll–protein complexes represent integral components of the thylakoid membrane, and their organization reflects their roles as either **light-harvesting com-**

PS II
"blue" light < 680 nm

PS I
"red" light 700 nm

P680

P700

Strong oxidant $\mathscr{E}_\circ' > +0.8$ V

Weak reductant "Q" $\mathscr{E}_\circ' \approx 0$ V

Weak oxidant $\mathscr{E}_\circ' \approx 0.45$ V

Strong reductant $\mathscr{E}_\circ' < -0.6$ V

H_2O

$\frac{1}{2}$ O_2

ADP + P → ATP

NADP⁺   NADPH
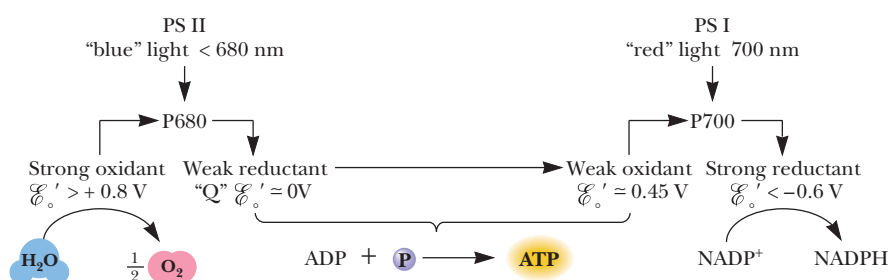
FIGURE 22.11 • Roles of the two photosystems, PSI and PSII.

plexes (LHC), **PSI complexes,** or **PSII complexes.** All chlorophyll is apparently localized within these three macromolecular assemblies.

The Roles of PSI and PSII

What are the roles of the two photosystems, and what is their relationship to each other? Photosystem I provides reducing power in the form of NADPH. Photosystem II splits water, producing O_2, and feeds the electrons released into an electron transport chain that couples PSII to PSI. Electron transfer between PSII and PSI pumps protons for chemiosmotic ATP synthesis. As summarized by Equation (22.2), photosynthesis involves the reduction of NADP⁺, using electrons derived from water and activated by light, $h\nu$. ATP is generated in the process. The standard reduction potential for the NADP⁺/NADPH couple is -0.32 V. Thus, a strong reductant with $\mathscr{E}_\circ'$ more negative than -0.32 V is required to reduce NADP⁺ under standard conditions. By similar reasoning, a very strong oxidant will be required to oxidize water to oxygen because $\mathscr{E}_\circ'(\frac{1}{2}O_2/H_2O)$ is $+0.82$ V. Separation of the oxidizing and reducing aspects of Equation (22.2) is accomplished in nature by devoting PSI to NADP⁺ reduction and PSII to water oxidation. PSI and PSII are linked via an electron transport chain so that the weak reductant generated by PSII can provide an electron to reduce the weak oxidant side of P700 (Figure 22.11). Thus, *electrons flow from H_2O to NADP⁺*, driven by light energy absorbed at the reaction centers. Oxygen is a by-product of the **photolysis,** literally "light-splitting," of water. Accompanying electron flow is production of a proton gradient and ATP synthesis (see Section 22.7). This light-driven phosphorylation is termed **photophosphorylation.**

22.4 • The *Z* Scheme of Photosynthetic Electron Transfer

Photosystems I and II contain unique complements of electron carriers, and these carriers mediate the stepwise transfer of electrons from water to NADP⁺. When the individual redox components of PSI and PSII are arranged as an e^- transport chain according to their standard reduction potentials, the zigzag result resembles the letter *Z* laid sideways (Figure 22.12). The various electron carriers are indicated as follows: "Mn complex" symbolizes the manganese-containing oxygen-evolving complex; D is its e^- acceptor and the immediate e^- donor to P680⁺; Q_A and Q_B represent special plastoquinone molecules (see Figure 22.15) and PQ the plastoquinone pool; Fe-S stands for the Rieske iron–sulfur center, and *cyt f,* cytochrome *f.* PC is the abbreviation for plastocyanin, the immediate e^- donor to P700⁻; and F_A, F_B, and F_X represent the membrane-

associated ferredoxins downstream from A_0 (a specialized Chl a) and A_1 (a specialized PSI quinone). Fd is the soluble ferredoxin pool that serves as the e^- donor to the flavoprotein (Fp), called **ferredoxin–NADP$^+$ reductase,** which catalyzes reduction of NADP$^+$ to NADPH. $Cyt(b_6)_n,(b_6)_p$ symbolizes the cytochrome b_6 moieties functioning to transfer e^- from F_A/F_B back to P700$^+$ during cyclic photophosphorylation (the pathway symbolized by the dashed arrow).

Overall photosynthetic electron transfer is accomplished by three **membrane-spanning supramolecular complexes,** composed of intrinsic and extrinsic polypeptides (shown as shaded boxes bounded by solid black lines in Figure 22.12). These complexes are the PSII complex, the cytochrome b_6/cytochrome f complex, and the PSI complex. The PSII complex is aptly described as a light-driven **water:plastoquinone oxidoreductase;** it is the enzyme system responsible for photolysis of water, and as such, it is also referred to as the **oxygen-evolving complex,** or OEC. Within this complex, a manganese-containing protein is intimately involved in the evolution of oxygen, perhaps through formation of a tetrametallic center consisting of 4 Mn^{2+} coordinating two equivalents of water. Both protons and electrons are abstracted from these water molecules, and O$_2$ is released as P680 undergoes four cycles of oxidation (Figure 22.13).

Oxygen Evolution Requires the Accumulation of Four Oxidizing Equivalents in PSII

When isolated chloroplasts that have been held in the dark are illuminated with very brief flashes of light, O$_2$ evolution reaches a peak on the third flash and every fourth flash thereafter (Figure 22.14a). The oscillation in O$_2$ evolved dampens over repeated flashes and converges to an average value. These data are interpreted to mean that the P680 reaction center complex cycles through five different oxidation states, numbered **S$_0$** to **S$_4$.** One electron and one proton are removed photochemically in each step. When **S$_4$** is attained, an O$_2$ molecule is released (Figure 22.14b) as PSII returns to oxidation state **S$_0$** and two new water molecules bind. The reason the first pulse of O$_2$ release occurred on the third flash (Figure 22.14a) is that the PSII reaction centers in the isolated chloroplasts were already poised at **S$_1$** reduction level.

Light-Driven Electron Flow from H$_2$O Through PSII

The events intervening between H$_2$O and P680 involve D, the name assigned to a specific protein **tyrosine residue** that mediates e^- transfer from H$_2$O via the Mn complex to P680$^+$ (Figure 22.12). The oxidized form of D is a tyrosyl free radical species, $D\cdot^+$. To begin the cycle, an exciton of energy excites P680 to P680*, whereupon P680* donates an electron to a special molecule of **pheophytin,** symbolized by "Pheo" in Figure 22.12. Pheophytin is like chlorophyll a, except 2 H$^+$ replace the centrally coordinated Mg^{2+} ion. This special pheophytin is the direct electron acceptor from P680*. Loss of an electron from P680* creates P680$^+$, the electron acceptor for D. Electrons flow from Pheo via specialized molecules of **plastoquinone,** represented by "Q" in Figure 22.12, to a pool of plastoquinone within the membrane. Because of its lipid nature, plastoquinone is mobile within the membrane and hence serves to shuttle electrons from the PSII supramolecular complex to the cytochrome b_6/cytochrome f complex. Alternate oxidation–reduction of plastoquinone to its hydroquinone form involves the uptake of protons (Figure 22.15). The asymmetry of the thylakoid membrane is designed to exploit this proton uptake and release so that protons (H$^+$) accumulate within the thylakoid vesicle, establishing an electrochemical gradient. Note that plastoquinone is an analog of coenzyme Q, the mitochondrial electron carrier (Chapter 21).

(a)

(b)
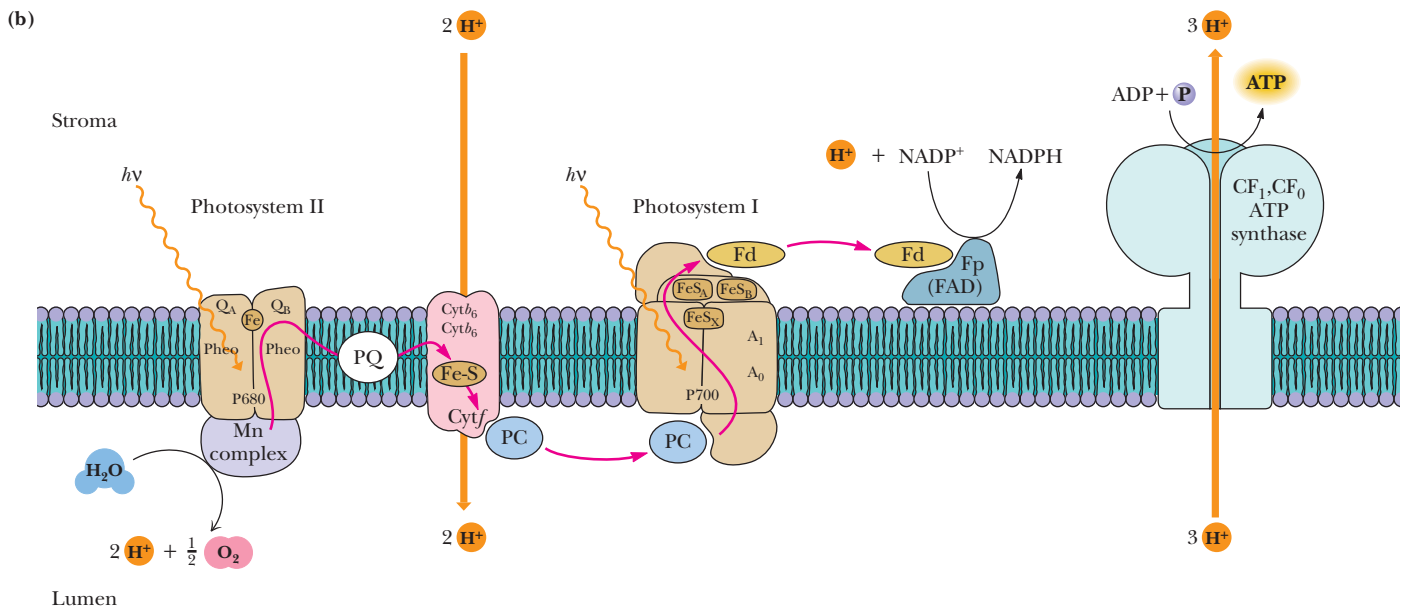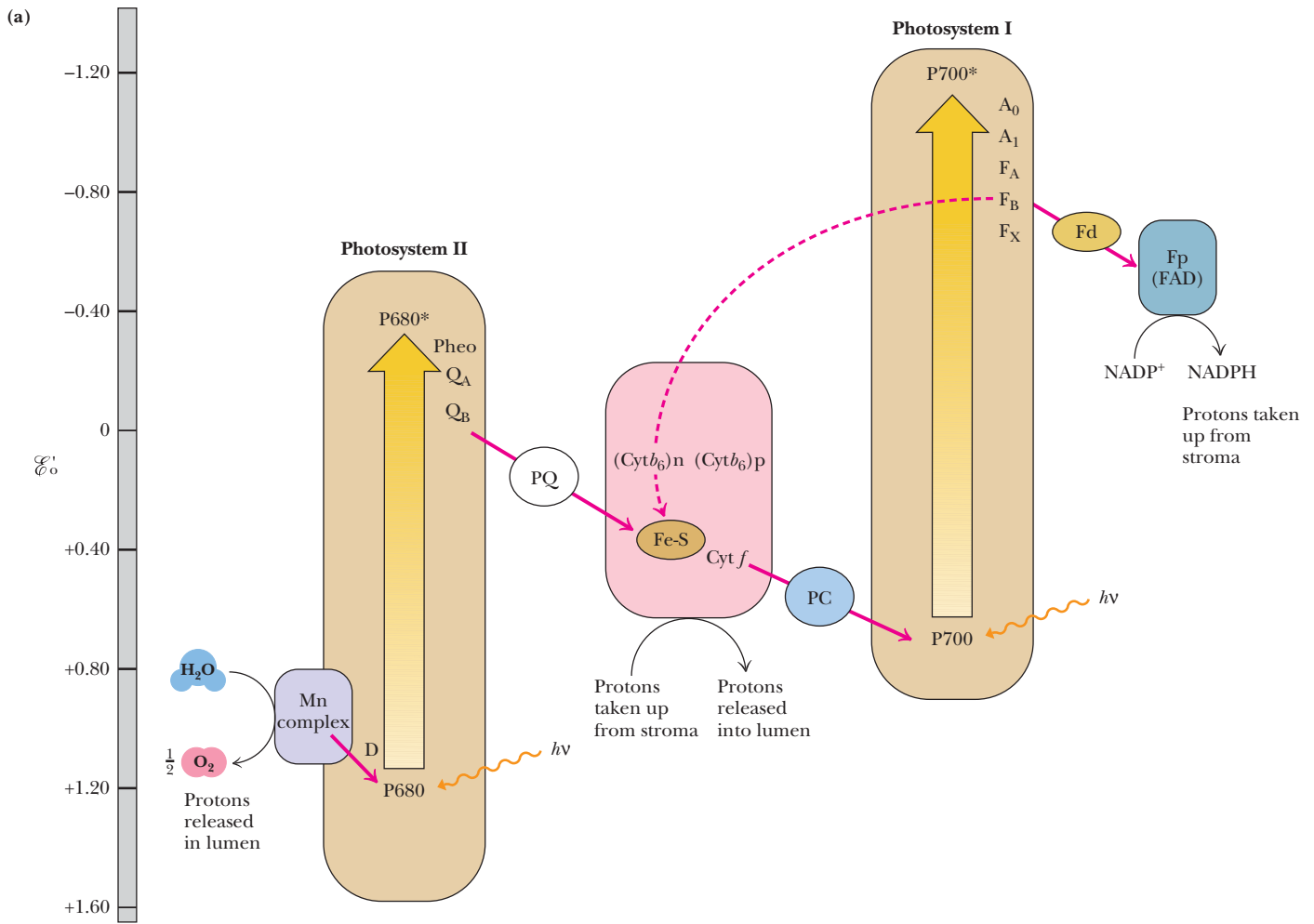
◀ **FIGURE 22.12** • The *Z* scheme of photosynthesis. (a) The *Z* scheme is a diagrammatic representation of photosynthetic electron flow from H_2O to $NADP^+$. The energy relationships can be derived from the $\mathscr{E}_\circ'$ scale beside the *Z* diagram, with lower standard potentials and hence greater energy as you go from bottom to top. Energy input as light is indicated by two broad arrows, one photon appearing in P680 and the other in P700. P680* and P700* represent photoexcited states. Electron loss from P680* and P700* creates $P680^+$ and $P700^+$. The representative components of the three supramolecular complexes (*PSI, PSII,* and the *cytochrome b_6/cytochrome f complex*) are in shaded boxes enclosed by solid black lines. Proton translocations that establish the proton-motive force driving ATP synthesis are illustrated as well. (b) Figure showing the functional relationships among PSII, the cytochrome *b*/cytochrome *f* complex, PSI, and the photosynthetic CF_1CF_0 ATP synthase within the thylakoid membrane. Note that e^- acceptors Q_A (for PSII) and A_1 (for PSI) are at the stromal side of the thylakoid membrane, whereas the e^- donors to $P680^+$ and $P700^+$ are situated at the lumenal side of the membrane. The consequence is charge separation ($-_{\text{stroma}}$, $+_{\text{lumen}}$) across the membrane. Also note that protons are translocated into the thylakoid lumen, giving rise to a chemiosmotic gradient that is the driving force for ATP synthesis by CF_1CF_0 ATP synthase.
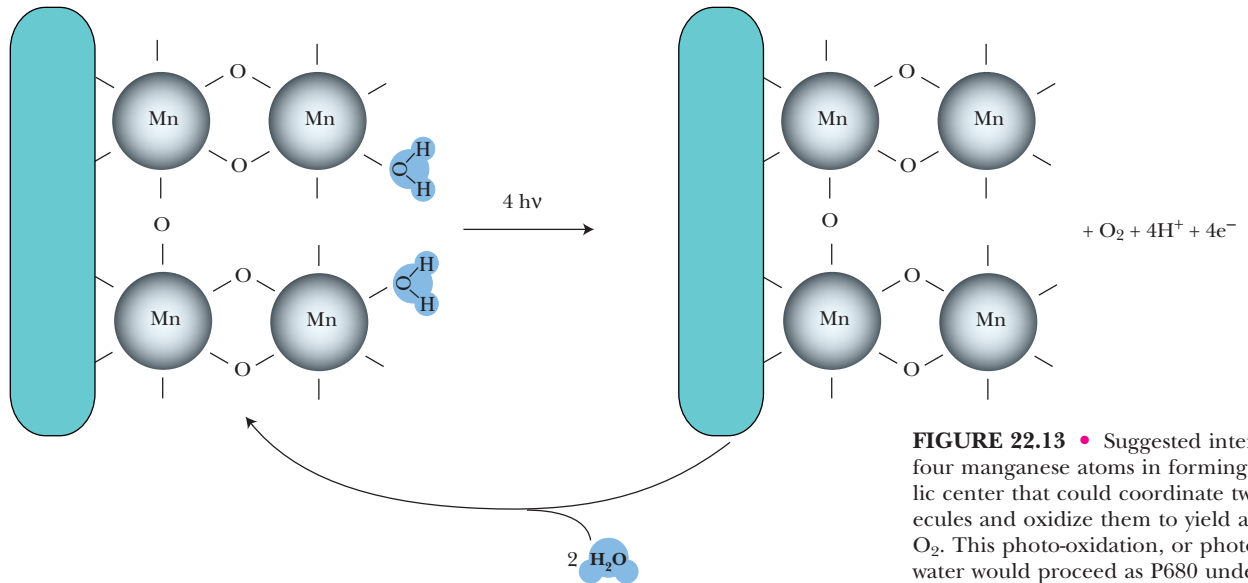
FIGURE 22.13 • Suggested interaction of four manganese atoms in forming a tetra-metallic center that could coordinate two water molecules and oxidize them to yield a molecule of O_2. This photo-oxidation, or photolysis, of water would proceed as P680 undergoes four cycles of light-induced oxidation. The four oxidizing equivalents accumulate in the manganese-containing active site of the O_2-evolving complex. (*Adapted from Hoganson, C. W., and Babcock, G. T., 1997. A metalloradical mechanism for the generation of oxygen in photosynthesis.* Science **277:**1953–1956.)
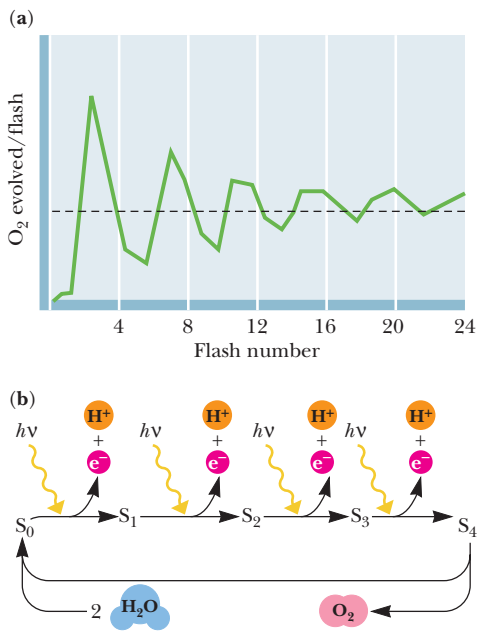
FIGURE 22.14 • Oxygen evolution requires the accumulation of four oxidizing equivalents in PSII. (a) Dark-adapted chloroplasts show little O_2 evolution after two brief light flashes. Oxygen evolution then shows a peak on the third flash and every fourth flash thereafter. The oscillation in O_2 evolution is dampened by repeated flashes and converges to an average value after 20 or so flashes. (b) The oscillation in O_2 evolution per light flash is due to the cycling of the PSII reaction center through five different oxidation states, S_0 to S_4. When S_4 is reached, O_2 is released. One e^- is removed photochemically at each light flash, moving the reaction center successively through S_1, S_2, S_3, and S_4. S_4 decays spontaneously to S_0 by oxidizing 2 H_2O to O_2. The peak of O_2 evolution at flash 3 in part (a) is due to the fact that the isolated chloroplast suspension is already at the S_1 stage.

Plastoquinone A

Plastohydroquinone A
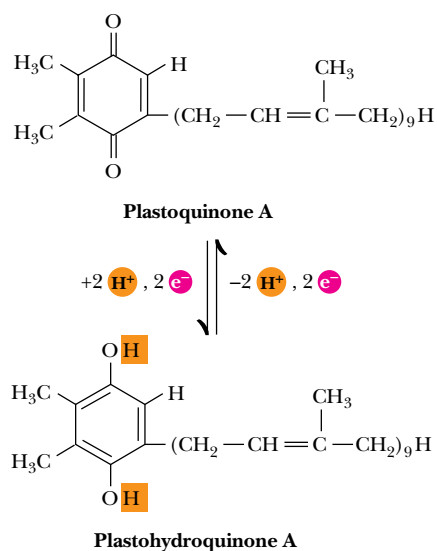
FIGURE 22.15 • The structures of plasto-quinone and its reduced form, plastohydro-quinone (or plastoquinol). The oxidation of the hydroquinone releases 2 H^+ as well as 2 e^-. The form shown (plastoquinone A) has nine isoprene units and is the most abundant plasto-quinone in plants and algae. Other plasto-quinones have different numbers of isoprene units and may vary in the substitutions on the quinone ring.

Electron Transfer Within the Cytochrome b_6/Cytochrome f Complex

The cytochrome b_6/cytochrome f or **plastoquinol:plastocyanin oxidoreductase** is a large (210 kD) multimeric protein possessing 22 to 24 transmembrane α-helices. It includes the two heme-containing electron transfer proteins for which it is named as well as *iron–sulfur clusters* (Chapter 21), which also participate in electron transport. The purpose of this complex is to mediate the transfer of electrons from PSII to PSI and to pump protons across the thylakoid membrane via a plastoquinone-mediated Q cycle, analogous to that found in mitochondrial e^- transport (Chapter 21). Cytochrome f (f from the Latin *folium*, meaning "foliage") is a c-type cytochrome, with an α-absorbance band at 553 nm and a reduction potential of +0.365 V. Cytochrome b_6 apparently does not lie directly on the pathway of electron transfer from PSII to PSI. This cytochrome, whose α-absorbance band lies at 559 nm and whose standard reduction potential is −0.06 V, is thought to participate in an alternative *cyclic e^- transfer pathway.* Under certain conditions, electrons derived from P700* are not passed on to $NADP^+$ but instead cycle down an alternative path via ferredoxins in the PSI complex to cytochrome b_6, plastoquinone, and ultimately back to $P700^+$. This cyclic flow yields no O_2 evolution or $NADP^+$ reduction but can lead to ATP synthesis via so-called *cyclic photophosphorylation,* discussed later.

Electron Transfer from the Cytochrome b_6/Cytochrome f Complex to PSI

Plastocyanin ("PC" in Figure 22.12) is an electron carrier capable of diffusion along the inside of the thylakoid and migration in and out of the membrane, aptly suited to its role in shuttling electrons between the cytochrome b_6/cytochrome f complex and PSI. Plastocyanin is a low-molecular-weight (10.4 kD) protein containing a single copper atom. PC functions as a single-electron carrier ($\mathscr{E}_\circ' = +0.32$ V) as its copper atom undergoes alternate oxidation–reduction between the cuprous (Cu^+) and cupric (Cu^{2+}) states. PSI is a light-driven **plastocyanin:ferredoxin oxidoreductase.** When P700, the specialized chlorophyll a dimer of PSI, is excited by light and oxidized by transferring its e^- to an adjacent chlorophyll a molecule that serves as its immediate e^- acceptor, $P700^+$ is formed. (The standard reduction potential for the $P700^+$/P700 couple lies near +0.45 V.) $P700^+$ readily gains an electron from plastocyanin.

The immediate electron acceptor for P700* is a special molecule of chlorophyll. This unique Chl a (A_0) rapidly passes the electron to a specialized quinone (A_1), which in turn passes the e^- to the first in a series of *membrane-bound ferredoxins* (Fd, Chapter 21). This Fd series ends with a soluble form of ferredoxin, Fd_s, which serves as the immediate electron donor to the flavoprotein (Fp) that catalyzes $NADP^+$ reduction, namely, **ferredoxin:NADP$^+$ reductase.**

The Initial Events in Photosynthesis Are Very Rapid Electron-Transfer Reactions

Electron transfer from P680 to Q and from P700 to Fd occurs on a picosecond-to-microsecond time scale. The necessity for such rapid reaction becomes obvious when one realizes that light-induced Chl excitation followed by electron transfer leads to separation of opposite charges in close proximity, as in $P700^+$:A_0^-. Accordingly, subsequent electron transfer reactions occur rapidly in order to shuttle the electron away quickly, before the wasteful back reaction of charge recombination (and dissipation of excitation energy), as in return to P700:A_0, can happen.

22.5 • The Molecular Architecture of Photosynthetic Reaction Centers

What molecular architecture couples the absorption of light energy to rapid electron-transfer events, in turn coupling these e^- transfers to proton translocations so that ATP synthesis is possible? Part of the answer to this question lies in the membrane-associated nature of the photosystems. Membrane proteins have been difficult to study due to their insolubility in the usual aqueous solvents employed in protein biochemistry. A major breakthrough occurred in 1984 when Johann Deisenhofer, Hartmut Michel, and Robert Huber reported the first X-ray crystallographic analysis of a membrane protein. To the great benefit of photosynthesis research, this protein was the reaction center from the photosynthetic purple bacterium *Rhodopseudomonas viridis*. This research earned these three scientists the 1984 Nobel Prize in chemistry.

Structure of the *R. viridis* Photosynthetic Reaction Center

Rhodopseudomonas viridis is a photosynthetic prokaryote with a single type of photosystem. The reaction center (145 kD) of the *R. viridis* photosystem is localized in the plasma membrane of these photosynthetic bacteria and is composed of four different polypeptides, designated *L* (273 amino acid residues), *M* (323 residues), *H* (258 residues), and *cytochrome* (333 amino acid residues). *L* and *M* each consist of five membrane-spanning α-helical segments; *H* has one such helix, the majority of the protein forming a globular domain in the cytoplasm (Figure 22.16). The cytochrome subunit contains four heme groups; the N-terminal amino acid of this protein is cysteine. This cytochrome is anchored to the periplasmic face of the membrane via the hydrophobic chains of two fatty acid groups that are esterified to a glyceryl moiety joined via a thioether bond to the Cys (Figure 22.16). *L* and *M* each bear two *bacteriochlorophyll* molecules (the bacterial version of Chl) and one *bacteriopheophytin*. *L* also has a bound quinone molecule, Q_A. Together, *L* and *M* coordinate an Fe atom. The photochemically active species of the *R. viridis* reaction center, **P870,** is composed of two bacteriochlorophylls, one contributed by *L* and the other by *M*.

Photosynthetic Electron Transfer in the *R. viridis* Reaction Center

The prosthetic groups of the *R. viridis* reaction center (P870, BChl, BPheo, and the bound quinones) are fixed in a spatial relationship to one another that favors photosynthetic e^- transfer (Figure 22.16). Photoexcitation of P870 (creation of P870*) leads to e^- loss (P870$^+$) via electron transfer to the nearby bacteriochlorophyll (BChl). The e^- is then transferred via the *L* bacteriopheophytin (BPheo) to Q_A, which is also an *L* prosthetic group. The corresponding site on *M* is occupied by a loosely bound quinone, Q_B, and electron transfer from Q_A to Q_B takes place. An interesting aspect of the system is that *no elec-*

Cytochrome with 4 heme groups

$h\nu$

M   L

P870

BChl

BChl

<1ps

20ps

BPheo

BPheo

230ps

Q_A

Fe

Q_B

100μs

H

Note: The cytochrome subunit is membrane-associated via a diacylglycerol moiety on its N-terminal Cys residue:

Membrane anchor

FIGURE 22.16 • Model of the structure and activity of the *R. viridis* reaction center. Four polypeptides (designated *cytochrome, M, L,* and *H*) make up the reaction center, an integral membrane complex. The cytochrome maintains its association with the membrane via a diacylglyceryl group linked to its N-terminal Cys residue by a thioether bond. *M* and *L* both consist of five membrane-spanning α-helices; *H* has a single membrane-spanning α-helix. The prosthetic groups are spatially situated so that rapid e^- transfer from P870* to Q_B is facilitated. Photoexcitation of P870 leads in less than 1 picosecond (psec) to reduction of the *L*-branch BChl only. P870$^+$ is re-reduced via an e^- provided through the heme groups of the cytochrome.

tron transfer occurs through *M*, even though it has components apparently symmetrical to and identical with the *L* e^- transfer pathway.

The reduced quinone formed at the Q_B site is free to diffuse to a neighboring *cytochrome b/cytochrome c_1* membrane complex, where its oxidation is coupled to H^+ translocation (and, hence, ultimately to ATP synthesis) (Figure 22.17). *Cytochrome c_2*, a periplasmic protein, serves to cycle electrons back to $P870^+$ via the four hemes of the reaction center cytochrome subunit. A specific tyrosine residue of *L* (Try^{162}) is situated between P870 and the closest cytochrome heme. This Tyr is the immediate e^- donor to $P870^+$ and completes the light-driven electron transfer cycle. The structure of the *R. viridis* reaction center (derived from X-ray crystallographic data) is modeled in Figure 22.18.

Eukaryotic Reaction Centers: The Molecular Architecture of PSII

PSII of higher plants and green algae contains more than 20 subunits and is considerably more complex than the *R. viridis* reaction center. Nevertheless, the *R. viridis* reaction center is a fairly good model for the core structure of PSII. P680 and its two equivalents of pheophytin (Pheo) are located on a pair of integral membrane proteins designated **D1** (38 kD) and **D2** (39.4 kD) (Figure 22.19). The tyrosine species *D* is Tyr^{161} in the **D1** amino acid sequence. Complexed to **D2** is a tightly bound plastoquinone molecule, Q_A. Electrons flow from P680* to Pheo on **D1** and thence to Q_A on **D2** and then on to a second plastoquinone situated in the Q_B site on **D1.** Electron transfer from Q_A and Q_B is assisted by an iron atom located between them. Each plastoquinone (PQ) that enters the Q_B site accepts two electrons derived from water and two H^+ from the stroma before it is released into the membrane as the hydroquinone, PQH_2. The stoichiometry of the overall reaction catalyzed by PSII is
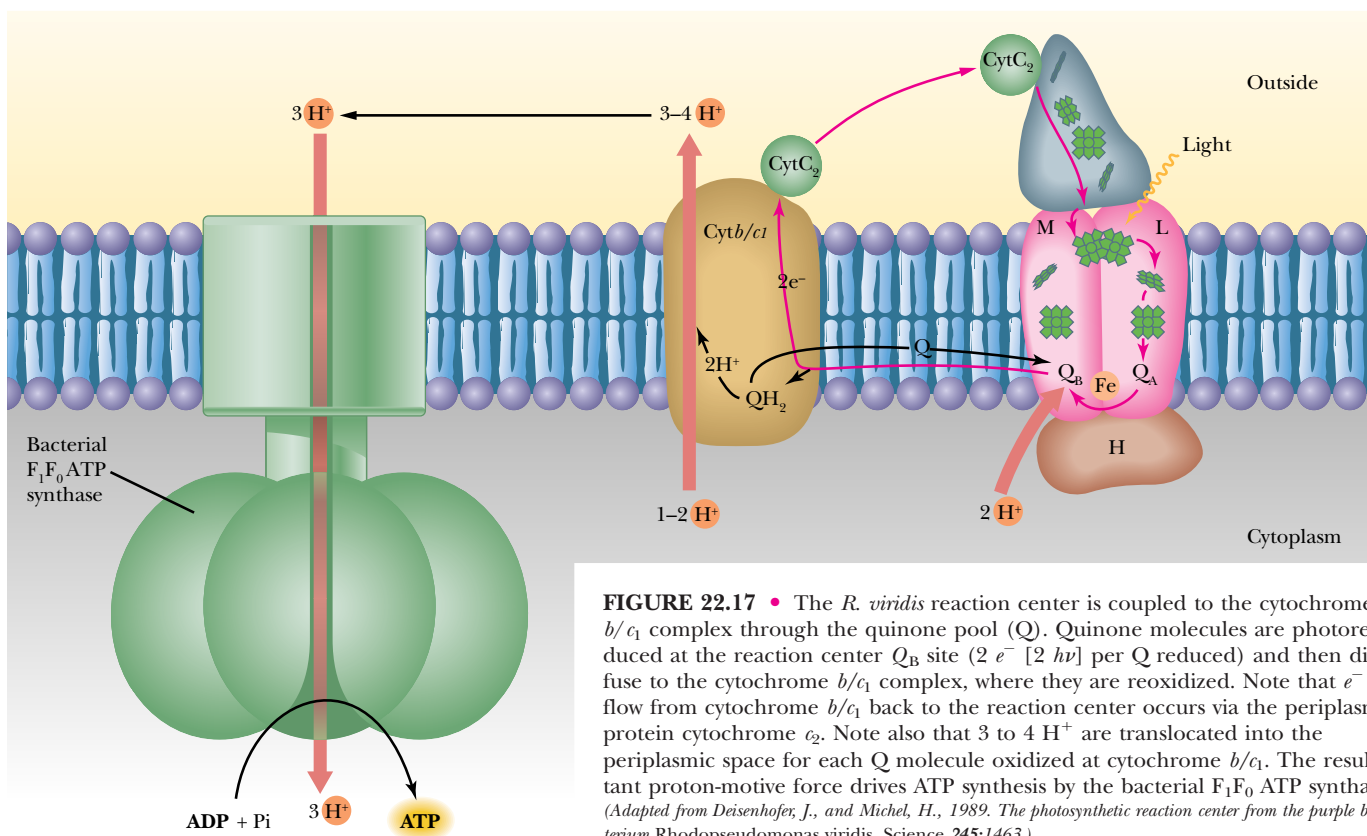
FIGURE 22.17 • The *R. viridis* reaction center is coupled to the cytochrome *b*/c_1 complex through the quinone pool (Q). Quinone molecules are photoreduced at the reaction center Q_B site (2 e^- [2 *hν*] per Q reduced) and then diffuse to the cytochrome *b*/c_1 complex, where they are reoxidized. Note that e^- flow from cytochrome *b*/c_1 back to the reaction center occurs via the periplasmic protein cytochrome c_2. Note also that 3 to 4 H^+ are translocated into the periplasmic space for each Q molecule oxidized at cytochrome *b*/c_1. The resultant proton-motive force drives ATP synthesis by the bacterial F_1F_0 ATP synthase. *(Adapted from Deisenhofer, J., and Michel, H., 1989. The photosynthetic reaction center from the purple bacterium* Rhodopseudomonas viridis. Science **245**:1463.)

(a) (b) (c)
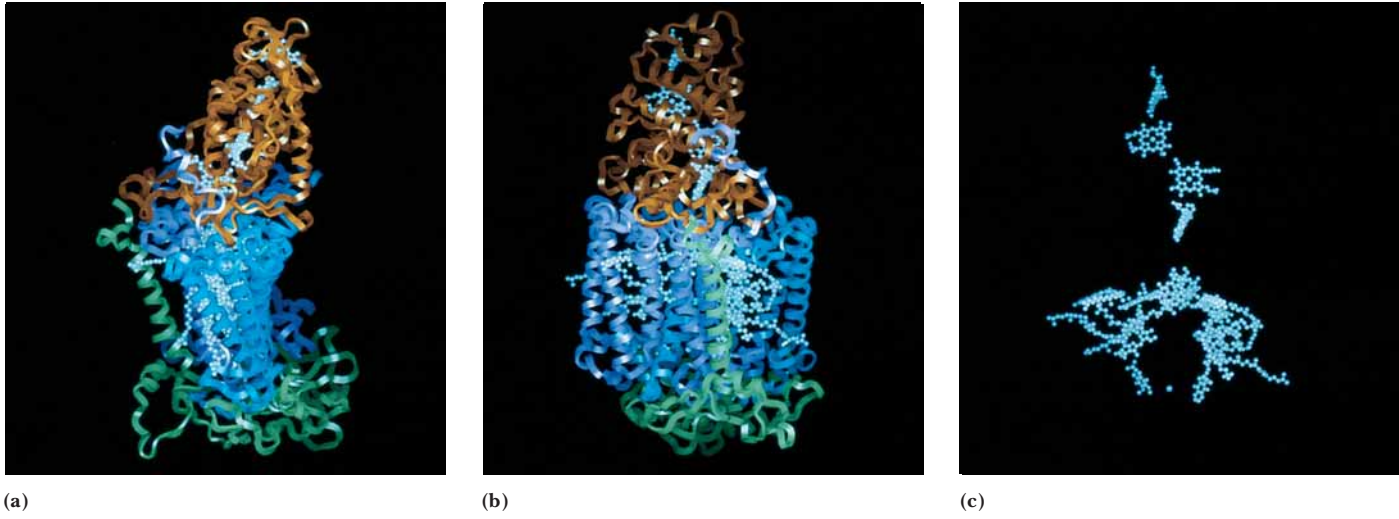
FIGURE 22.18 • Model of the *R. viridis* reaction center. (a, b) Two views of the ribbon diagram of the reaction center. *M* and *L* subunits appear in purple and blue, respectively. Cytochrome subunit is brown; H subunit is green. These proteins provide a scaffold upon which the prosthetic groups of the reaction center are situated for effective photosynthetic electron transfer. Panel (c) shows the spatial relationship between the various prosthetic groups (4 hemes, P870, 2 BChl, 2 BPheo, 2 quinones, and the Fe atom) in the same view as in (b), but with protein chains deleted.

$2\,H_2O + 2\,PQ + 4\,h\nu \rightarrow O_2 + 2\,PQH_2$. A cytochrome species, **cytochrome b_{559},** composed of two polypeptides (4.4 kD and 9.3 kD), is associated with PSII; its function is as yet unclear. Two chlorophyll-binding proteins (47 and 43 kD) harvest light and deliver exciton energy to P680. A Mn-containing extrinsic membrane protein, the **OEC** or **oxygen-evolving complex** (whose principal sub-units are 33-, 23-, and 16-kD polypeptides) is located on the lumenal side of the thylakoid membrane.
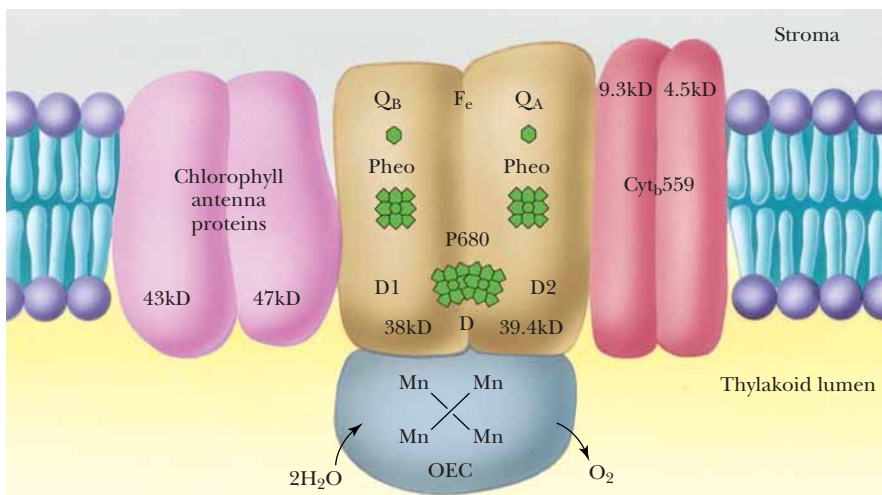
FIGURE 22.19 • The molecular architecture of PSII. The core of the PSII complex con-sists of the two polypeptides (D1 and D2) that bind P680, pheophytin (Pheo), and the quinones, Q_A and Q_B. Additional components of this complex include cytochrome b_{559}, two additional intrinsic proteins (47 and 43 kD) that serve an accessory light-harvesting function, and an extrinsic protein complex that is essential to O_2 evolution.
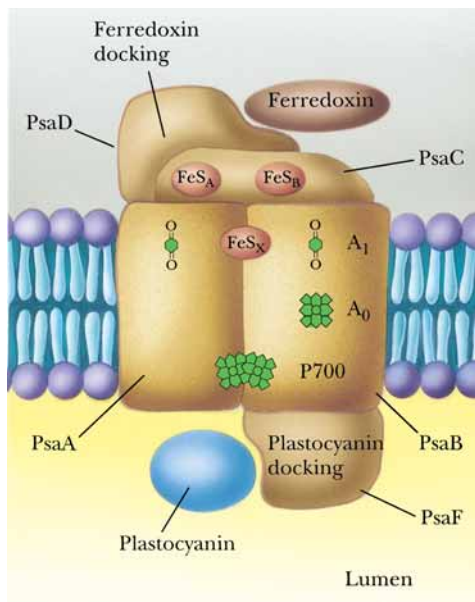
FIGURE 22.20 • The molecular architecture of PSI. PsaA and PsaB constitute the reaction center dimer, an integral membrane complex; P700 is located at the lumenal side of this dimer. PsaC, which bears Fe-S centers F_A and F_B, and PsaD, the interaction site for ferredoxin, are on the stromal side of the thylakoid membrane. PsaF, which provides the plastocyanin interaction site, is on the lumenal side. *(Adapted from Golbeck, J. H., 1992. Annual Review of Plant Physiology and Plant Molecular Biology **43:**293–324.)*

The Molecular Architecture of PSI

The structure of PSI from the cyanobacterium *Synechococcus elongatus* has been solved by X-ray crystallography, and this structure shows strong similarities to the *R. viridis* reaction center and our emerging view of the eukaryotic PSII, both discussed earlier. Because of direct correlations with information about eukaryotic PSI, this cyanobacterial PSI provides a general model for all P700-dependent photosystems (Figure 22.20). Although PSI consists of 11 different protein subunits, all the electron-transferring prosthetic groups essential to PSI function are localized to just three polypeptides. Two of these, **PsaA** and **PsaB** (83 kD each), compose the reaction center heterodimer, a structural pattern that now seems universal in photosynthetic reaction centers. **PsaA** and **PsaB** each have 11 transmembrane α-helices. PSI has approximately 100 chlorophyll molecules, including the two composing P700 and two positioned some 16 Å from P700, one of which functions as A_0, the immediate e^- acceptor for P700 (Figure 22.20). Quinones are found in association with PSI, including one that functions as A_1, an intermediate e^- carrier. The Fe-S center designated F_x bridges **PsaA** and **PsaB.** The third protein, **PsaC** (9 kD), bears two additional Fe-S clusters designated F_A and F_B; **PsaC** (along with two other proteins designated **PsaD** and **PsaE**) lies on the stromal face of the reaction center complex. **PsaD** is the site of ferredoxin binding in eukaryotic PSI systems. **PsaF,** with three transmembrane α-helices, provides the interaction site for plastocyanin (on the lumenal side of the membrane).

The overall structure of *S. elongatus* PSI thus consists of a core reaction center surrounded by and connected to a large Chl-based antenna system. Three equivalents of such PSI complexes occur together to form a trimeric structure. Photochemistry begins with exciton absorption at P700, almost instantaneous electron transfer and charge separation ($P700^+$:A_0^-), followed by transfer of the electron from A_0 to A_1 and on to F_x and then F_A/F_B, where it is used to reduce a ferredoxin molecule at the "stromal" side of the membrane. The positive charge at $P700^+$ and the e^- at F_A/F_B represent a charge separation across the membrane, an energized condition created by light.

22.6 • The Quantum Yield of Photosynthesis

The **quantum yield** of photosynthesis, the amount of product formed per equivalent of light input, has traditionally been expressed as the ratio of CO_2 fixed or O_2 evolved per quantum absorbed. At each reaction center, one photon or quantum yields one electron. Interestingly, an overall stoichiometry of one H^+ translocated into the thylakoid vesicle for each photon has also been observed. Two photons per center would allow a pair of electrons to flow from H_2O to $NADP^+$ (Figure 22.12), resulting in the formation of 1 NADPH and $\frac{1}{2}$ O_2. If one ATP were formed for every 3 H^+ translocated during photosynthetic electron transport, $1\frac{1}{3}$ ATP would be synthesized. More appropriately, 4 $h\nu$ per center (8 quanta total) would drive the evolution of 1 O_2, the reduction of 2 $NADP^+$, and the phosphorylation of $2\frac{2}{3}$ ATP.

The energy of a photon depends on its wavelength, according to the equation $E = h\nu = hc/\lambda$, where E is energy, c is the speed of light, and λ is its wavelength. Expressed in molar terms, an *Einstein* is the amount of energy in Avogadro's number of photons: $E = Nhc/\lambda$. Light of 700-nm wavelength is the longest-wavelength and the lowest-energy light acting in the eukaryotic photosystems discussed here. An Einstein of 700-nm light is equivalent in energy to approximately 170 kJ. Eight Einsteins of this light, 1360 kJ, theoretically generate 2 moles of NADPH, $2\frac{2}{3}$ moles of ATP, and 1 mole of O_2.

Photosynthetic Energy Requirements for Hexose Synthesis

The fixation of carbon dioxide to form hexose, *the dark reactions of photosynthesis,* requires considerable energy. The overall stoichiometry of this process (Eq. 22.3) involves 12 NADPH and 18 ATP. To generate 12 equivalents of NADPH necessitates the consumption of 48 Einsteins of light, minimally 170 kJ each. However, if the preceding ratio of $1\frac{1}{3}$ ATP per NADPH were correct, insufficient ATP for CO_2 fixation would be produced. Six additional Einsteins would provide the necessary two additional ATP. From 54 Einsteins, or 9180 kJ, one mole of hexose would be synthesized. The standard free energy change, $\Delta G°'$, for hexose formation from carbon dioxide and water (the exact reverse of cellular respiration) is +2870 kJ/mol.

22.7 • Light-Driven ATP Synthesis—Photophosphorylation

Light-driven ATP synthesis, termed **photophosphorylation,** is a fundamental part of the photosynthetic process. The conversion of light energy to chemical energy results in electron-transfer reactions leading to the generation of reducing power (NADPH). Coupled with these electron transfers, protons are driven across the thylakoid membranes from the stromal side to the lumenal side. These proton translocations occur in a manner analogous to the proton translocations accompanying mitochondrial electron transport that provide the driving force for oxidative phosphorylation (Chapter 21). Figure 22.12 indicates that proton translocations can occur at a number of sites. For example, protons may be translocated by reactions between H_2O and PSII as a consequence of the photolysis of water. The oxidation–reduction events as electrons pass through the plastoquinone pool and the Q cycle are another source of proton translocations. The proton transfer accompanying $NADP^+$ reduction also can be envisioned as protons being taken from the stromal side of the thylakoid vesicle. The current view is that two protons are translocated for each electron that flows from H_2O to $NADP^+$. Because this electron transfer requires two photons, one falling at PSII and one at PSI, the overall yield is one proton per quantum of light.

The Mechanism of Photophosphorylation Is Chemiosmotic

The thylakoid membrane is asymmetrically organized, or "sided," like the mitochondrial membrane. It also shares the property of being a barrier to the passive diffusion of H^+ ions. Photosynthetic electron transport thus establishes an electrochemical gradient, or proton-motive force, across the thylakoid membrane with the interior, or lumen, side accumulating H^+ ions relative to the stroma of the chloroplast. Like oxidative phosphorylation, the mechanism of photophosphorylation is chemiosmotic.

A proton-motive force of approximately −250 mV is needed to achieve ATP synthesis. This proton-motive force, Δp, is composed of a membrane potential, $\Delta\Psi$, and a pH gradient, ΔpH (Chapter 21). The proton-motive force is defined as the free energy difference, ΔG, divided by $\mathscr{F}$, Faraday's constant:

$$\Delta p = \Delta G/\mathscr{F} = \Delta\Psi - (2.3RT/\mathscr{F})\Delta\text{pH} \tag{22.5}$$

In chloroplasts, the value of $\Delta\Psi$ is typically −50 to −100 mV, and the pH gradient is equivalent to about 3 pH units, so that $-(2.3\ RT/\mathscr{F})\Delta\text{pH} = -200$ mV. This situation contrasts with the mitochondrial proton-motive force, where the membrane potential contributes relatively more to Δp than does the pH gradient.

CRITICAL DEVELOPMENTS IN BIOCHEMISTRY

Experiments with Isolated Chloroplasts Provided the First Direct Evidence for the Chemiosmotic Hypothesis

Experimental proof that the mechanism of photophosphorylation is chemiosmotic was provided in an elegant experiment by Andre Jagendorf and Ernest Uribe in 1966 (see figure). Jagendorf and Uribe reasoned that if photophosphorylation were indeed driven by an electrochemical gradient established by photosynthetic electron transfer reactions, they might artificially generate such a gradient by first incubating chloroplasts in an acid bath in the dark and then quickly raising the pH of the external medium. The resulting inequality in hydrogen ion electrochemical activity across the membrane should mimic the conditions normally found upon illumination of chloroplasts and should provide the energized condition necessary to drive ATP formation. To test this interpretation, Jagendorf and Uribe bathed isolated chloroplasts in a weakly acidic (pH 4) medium for 60 seconds, allowing the pH inside the chloroplasts to equilibrate with the external medium. The pH of the solution was then quickly raised to slightly alkaline pH (pH 8), artificially creating a pH gradient across the thylakoid membranes. When ADP and P_i were added, ATP synthesis was observed as the pH gradient collapsed. This classic experiment was the first real proof of Mitchell's chemiosmotic hypothesis and directed the scientific community to a greater acceptance of Mitchell's interpretations. Mitchell's chemiosmotic hypothesis for ATP synthesis now occupies the position of dogma as the weight of evidence has accumulated in its favor. Photophosphorylation then can be concisely summarized by noting that thylakoid vesicles accumulate H^+ upon illumination and that the electrochemical gradient thus created represents an energized state that can be tapped to drive ATP synthesis. Collapse of the gradient—that is, equilibration of the ion concentration difference across the membrane—is the energy-transducing mechanism: the chemical potential of a concentration difference is transduced into synthesis of ATP.
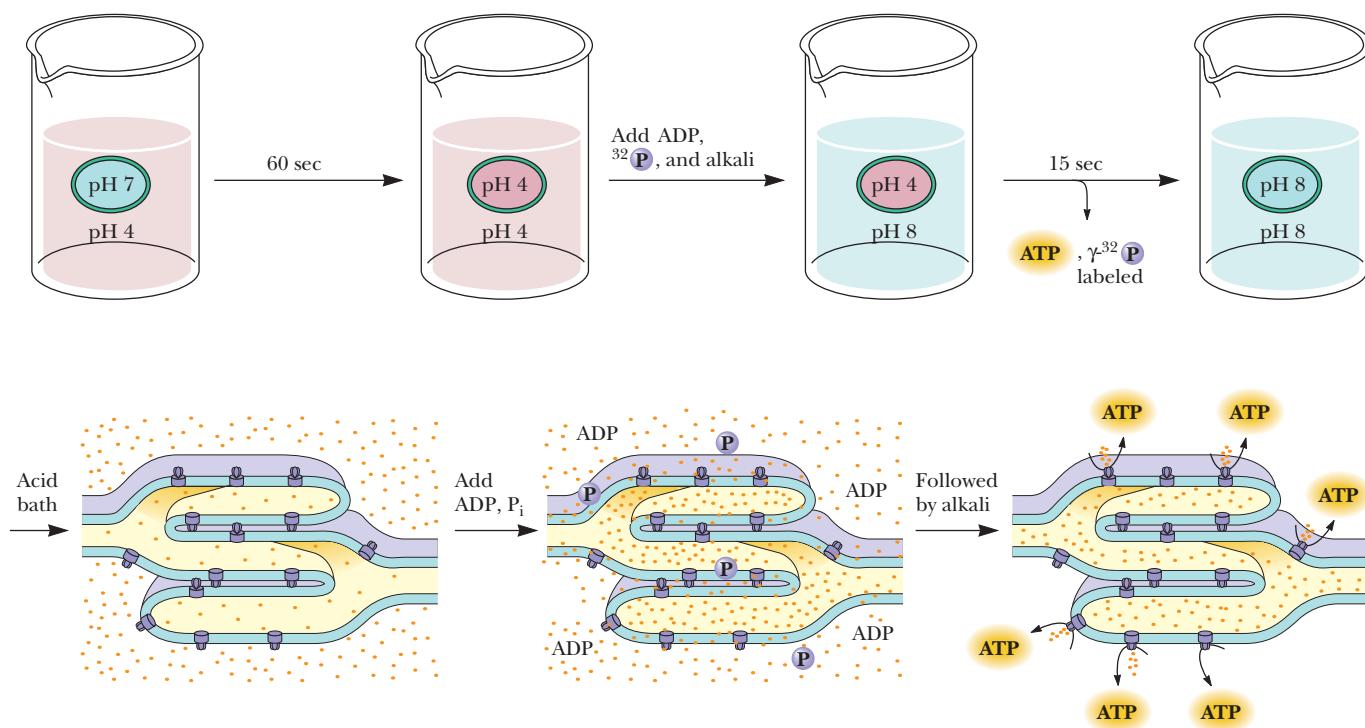
The mechanism of photophosphorylation is chemiosmotic. In 1966, Jagendorf and Uribe experimentally demonstrated for the first time that establishment of an electrochemical gradient across the membrane of an energy-transducing organelle could lead to ATP synthesis. They equilibrated isolated chloroplasts for 60 seconds in a pH 4 bath, adjusted the pH to 8 in the presence of ADP and P_i, and allowed phosphorylation to proceed for 15 seconds. The entire experiment was carried out in the dark.

CF$_1$CF$_0$ ATP Synthase Is the Chloroplast Equivalent of the Mitochondrial F$_1$F$_0$ ATP Synthase

The transduction of the electrochemical gradient into the chemical energy represented by ATP is carried out by the chloroplast ATP synthase, which is highly analogous to the mitochondrial F$_1$F$_0$ ATP synthase. The chloroplast enzyme complex is called **CF$_1$CF$_0$ ATP synthase,** "C" symbolizing chloroplast. Like the mitochondrial complex, CF$_1$CF$_0$ ATP synthase is a heteromultimer of α, β, γ, δ, ϵ, a, b, and c subunits (Chapter 21), consisting of a knoblike structure some 9 nm in diameter (CF$_1$) attached to a stalked base (CF$_0$) embedded in the thylakoid membrane. The mechanism of action of CF$_1$CF$_0$ ATP synthase in coupling ATP synthesis to the collapse of the pH gradient is similar to that of the mitochondrial ATP synthase described in Chapter 21. The mechanism of photophosphorylation is summarized schematically in Figure 22.21.

Cyclic and Noncyclic Photophosphorylation

Photosynthetic electron transport, which pumps H$^+$ into the thylakoid lumen, can occur in two modes, both of which lead to the establishment of a transmembrane proton-motive force. Thus, both modes are coupled to ATP synthesis and are considered alternative mechanisms of photophosphorylation even though they are distinguished by differences in their electron transfer pathways. The two modes are cyclic and noncyclic photophosphorylation.
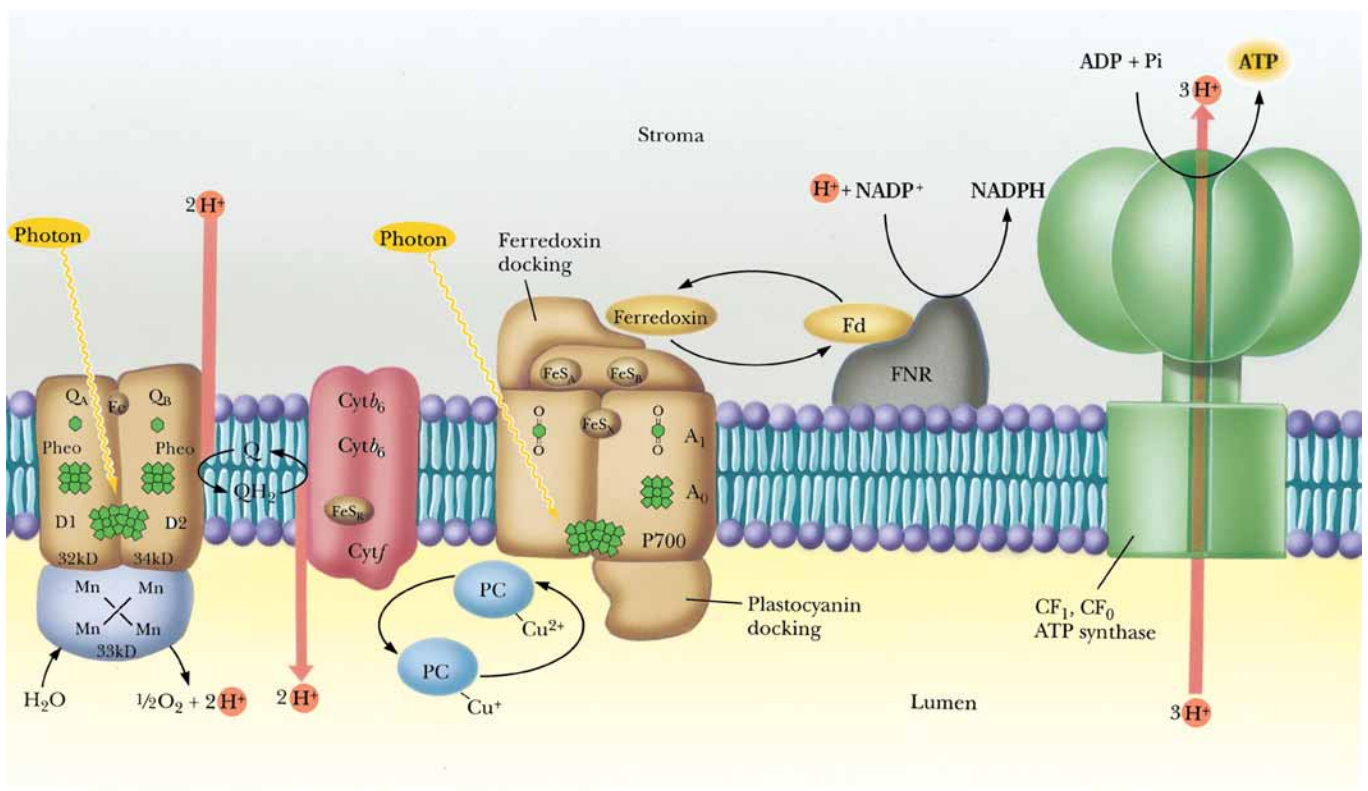
FIGURE 22.21 • The mechanism of photophosphorylation. Photosynthetic electron transport establishes a proton gradient that is tapped by the CF$_1$CF$_0$ ATP synthase to drive ATP synthesis. Critical to this mechanism is the fact that the membrane-bound components of light-induced electron transport and ATP synthesis are asymmetrical with respect to the thylakoid membrane so that vectorial discharge and uptake of H$^+$ ensue, generating the proton-motive force.

Noncyclic photophosphorylation has been the focus of our discussion and is represented by the scheme in Figure 22.21, where electrons activated by quanta at PSII and PSI flow from H_2O to $NADP^+$, with concomitant establishment of the proton-motive force driving ATP synthesis. Note that in noncyclic photophosphorylation, O_2 is evolved and $NADP^+$ is reduced.

Cyclic Photophosphorylation

In **cyclic photophosphorylation,** the "electron hole" in $P700^+$ created by electron loss from P700 is filled *not* by an electron derived from H_2O via PSII but by a cyclic pathway in which the photoexcited electron returns ultimately to $P700^+$. This pathway is schematically represented in Figure 22.12 by the dashed line connecting F_B and cytochrome b_6. Thus, the function of cytochrome b_6 (b_{563}) is to couple the bound ferredoxin carriers of the PSI complex with the cytochrome b_6/cytochrome f complex via the plastoquinone pool. This pathway diverts the activated e^- from $NADP^+$ reduction back through plastocyanin to re-reduce $P700^+$ (Figure 22.22).

Proton translocations accompany these cyclic electron transfer events, so ATP synthesis can be achieved. In cyclic photophosphorylation, ATP is the sole product of energy conversion. No NADPH is generated, and, because PSII is not involved, no oxygen is evolved. The maximal rate of cyclic photophosphorylation is less than 5% of the rate of noncyclic photophosphorylation. Cyclic photophosphorylation depends only on PSI.
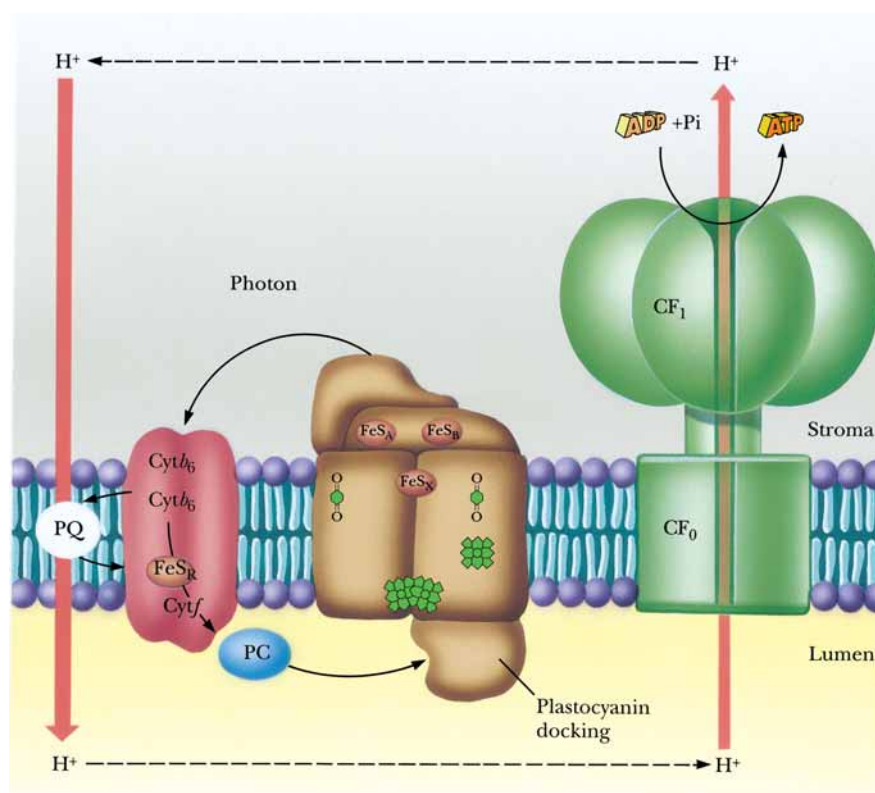
FIGURE 22.22 • The pathway of cyclic photophosphorylation by PSI. *(Adapted from Arnon, D. I., 1984.* Trends in Biochemical Sciences *9:258.)*

22.8 • Carbon Dioxide Fixation

As we began this chapter, we saw that photosynthesis traditionally is equated with the process of CO_2 fixation, that is, the net synthesis of carbohydrate from CO_2. Indeed, the capacity to perform net accumulation of carbohydrate from CO_2 distinguishes the phototrophic (and autotrophic) organisms from heterotrophs. Although animals possess enzymes capable of linking CO_2 to organic acceptors, they cannot achieve a net accumulation of organic material by these reactions. For example, fatty acid biosynthesis is primed by covalent attachment of CO_2 to acetyl-CoA to form malonyl-CoA (Chapter 25). Nevertheless, this "fixed CO_2" is liberated in the very next reaction, so no net CO_2 incorporation occurs.

Elucidation of the pathway of CO_2 fixation represents one of the earliest applications of radioisotope tracers to the study of biology. In 1945, Melvin Calvin and his colleagues at the University of California, Berkeley, were investigating photosynthetic CO_2 fixation in *Chlorella*. Using $^{14}CO_2$, they traced the incorporation of radioactive ^{14}C into organic products and found that the earliest labeled product was **3-phosphoglycerate** (see Figure 18.13). Although this result suggested that the CO_2 acceptor was a two-carbon compound, further investigation revealed that, in reality, two equivalents of 3-phosphoglycerate were formed following addition of CO_2 to a five-carbon (pentose) sugar:

$$CO_2 + \text{5-carbon acceptor} \longrightarrow \text{[6-carbon intermediate]} \longrightarrow$$
$$\text{Two 3-phosphoglycerates}$$

Ribulose-1,5-Bisphosphate Is the CO_2 Acceptor in CO_2 Fixation

The five-carbon CO_2 acceptor was identified as **ribulose-1,5-bisphosphate** (RuBP), and the enzyme catalyzing this key reaction of CO_2 fixation is **ribulose bisphosphate carboxylase/oxygenase,** or, in the jargon used by workers in this field, **rubisco.** The name *ribulose bisphosphate carboxylase/oxygenase* reflects the fact that rubisco catalyzes the reaction of either CO_2 or, alternatively, O_2 with RuBP. Rubisco is found in the chloroplast stroma. It is a very abundant enzyme, constituting more than 15% of the total chloroplast protein. Given the preponderance of plant material in the biosphere, rubisco is probably the world's most abundant protein. Rubisco is large: in higher plants, rubisco is a 550-kD heteromultimeric ($\alpha_8\beta_8$) complex consisting of eight identical large subunits (55 kD) and eight small subunits (15 kD) (Figure 22.23). The large subunit is the catalytic unit of the enzyme. It binds both substrates (CO_2 and RuBP) and Mg^{2+} (a divalent cation essential for enzymatic activity). The small subunit modulates the activity of the enzyme, increasing k_{cat} more than 100-fold.[2]

The Ribulose-1,5-Bisphosphate Carboxylase Reaction

The addition of CO_2 to ribulose-1,5-bisphosphate results in the formation of an enzyme-bound intermediate, **2-carboxy,3-keto-arabinitol** (Figure 22.24). This intermediate arises when CO_2 adds to the enediol intermediate gener-

FIGURE 22.23 • Schematic diagram of the subunit organization of ribulose bisphosphate carboxylase as revealed by X-ray crystallography. The enzyme consists of eight equivalents each of two types of subunits, large *L* (55 kD) and small *S* (15 kD). Clusters of four small subunits are located at each end of the symmetrical octamer formed by four L_2 dimers. *(From Knight, S., Andersson, I., and Branden, C. I., 1990.* Journal of Molecular Biology *215:113–160.)*

[2]The rubisco large subunit is encoded by a gene within the chloroplast DNA, whereas the small subunit is encoded by a multigene family in the nuclear DNA. Assembly of active rubisco heteromultimers occurs within chloroplasts following transit of the small subunit polypeptide across the chloroplast membrane.
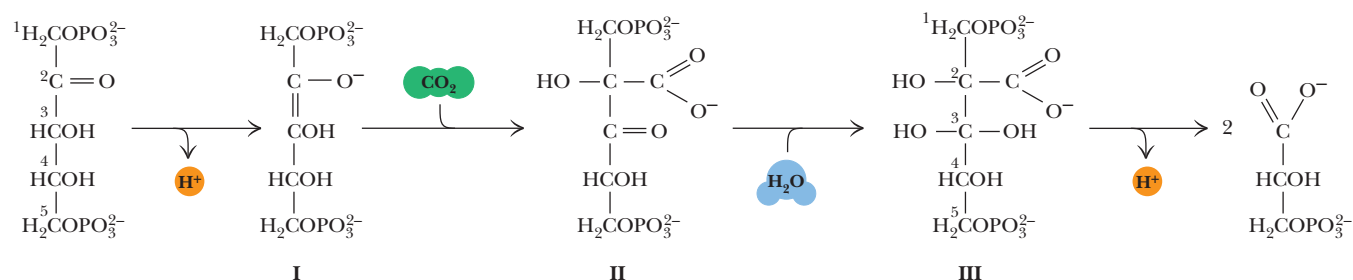
FIGURE 22.24 • The ribulose bisphosphate carboxylase reaction. Enzymatic abstraction of the C-3 proton of RuBP yields a 2,3-enediol intermediate (I), which is stereospecifically carboxylated at C-2 to create the six-carbon β-keto acid intermediate (II) known as 2-carboxy,3-keto-arabinitol. Intermediate II is rapidly hydrated to give the gem-diol form (III). Deprotonation of the C-3 hydroxyl and cleavage yield two 3-phosphoglycerates. Mg^{2+} at the active site aids in stabilizing the 2,3-enediol transition state for CO_2 addition and in facilitating the carbon–carbon bond cleavage that leads to product formation. Note that CO_2, not HCO_3^- (its hydrated form), is the true substrate.

ated from ribulose-1,5-bisphosphate. Hydrolysis of the C_2–C_3 bond of the intermediate generates two molecules of 3-phosphoglycerate. The CO_2 ends up as the carboxyl group of one of the two molecules.

Regulation of Ribulose-1,5-Bisphosphate Carboxylase Activity

Rubisco exists in three forms: an inactive form designated *E;* a carbamylated, but inactive, form designated *EC;* and an active form, *ECM,* which is carbamylated and has Mg^{2+} at its active sites as well. Carbamylation of rubisco takes place by addition of CO_2 to its Lys^{201} ϵ-NH_2 groups (to give ϵ—NH—COO^- derivatives). The CO_2 molecules used to carbamylate Lys residues do not become substrates. The carbamylation reaction is promoted by slightly alkaline pH (pH 8). Carbamylation of rubisco completes the formation of a binding site for the Mg^{2+} that participates in the catalytic reaction. Once Mg^{2+} binds to *EC,* rubisco achieves its active *ECM* form. Activated rubisco displays a K_m for CO_2 of 10 to 20 μM.[3]

Substrate RuBP binds much more tightly to the inactive *E* form of rubisco ($K_D = 20$ nM) than to the active *ECM* form (K_m for RuBP = 20 μM). Thus, RuBP is also a potent inhibitor of rubisco activity. Release of RuBP from the active site of rubisco is mediated by **rubisco activase.** Rubisco activase is a *regulatory protein;* it binds to *E*-form rubisco and, in an ATP-dependent reaction, promotes the release of RuBP. Rubisco then becomes activated by carbamylation and Mg^{2+} binding. Rubisco activase itself is activated in an indirect manner by light. Thus, light is the ultimate activator of rubisco.

22.9 • The Calvin–Benson Cycle

The immediate product of CO_2 fixation, 3-phosphoglycerate, must undergo a series of transformations before the net synthesis of carbohydrate is realized. Among carbohydrates, hexoses (particularly glucose) occupy center stage. Glucose is the building block for both cellulose and starch synthesis. These plant polymers constitute the most abundant organic material in the living world, and thus, the central focus on glucose as the ultimate end product of CO_2 fixation is amply justified. Also, sucrose (α-D-glucopyranosyl-$(1 \rightarrow 2)$-β-D-fructofuranoside) is the major carbon form translocated out of leaves to other plant tissues. In nonphotosynthetic tissues, sucrose is metabolized via glycolysis and the TCA cycle to produce ATP.

---

[3]The relative abundance of CO_2 in the atmosphere is low, about 0.03%. The concentration of CO_2 dissolved in aqueous solutions equilibrated with air is about 10 μM.

The set of reactions that transforms 3-phosphoglycerate into hexose is named the **Calvin–Benson cycle** (often referred to simply as the *Calvin cycle*) for its discoverers. The reaction series is indeed cyclic because not only must carbohydrate appear as an end product, but the 5-carbon acceptor, RuBP, must be regenerated to provide for continual CO_2 fixation. Balanced equations that schematically represent this situation are

$$6(1) + 6(5) \longrightarrow 12(3)$$
$$12(3) \longrightarrow 1(6) + 6(5)$$
$$Net: \quad 6(1) \longrightarrow 1(6)$$
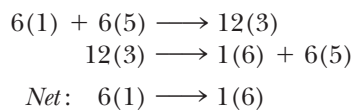
Each number in parentheses represents the number of carbon atoms in a compound, and the number preceding the parentheses indicates the stoichiometry of the reaction. Thus, 6(1), or 6 CO_2, condense with 6(5) or 6 RuBP to give 12 3-phosphoglycerates. These 12(3)s are then rearranged in the Calvin cycle to form one hexose, 1(6), and regenerate the six 5-carbon (RuBP) acceptors.

The Enzymes of the Calvin Cycle

The Calvin cycle enzymes serve three important ends:

1. They constitute the predominant CO_2 fixation pathway in nature.
2. They accomplish the reduction of 3-phosphoglycerate, the primary product of CO_2 fixation, to glyceraldehyde-3-phosphate so that carbohydrate synthesis becomes feasible.
3. They catalyze reactions that transform 3-carbon compounds into 4-, 5-, 6-, and 7-carbon compounds.

Most of the enzymes mediating the reactions of the Calvin cycle also participate in either glycolysis (Chapter 19) or the pentose phosphate pathway (Chapter 23). The aim of the Calvin scheme is to account for hexose formation from 3-phosphoglycerate. In the course of this metabolic sequence, the NADPH and ATP produced in the light reactions are consumed, as indicated earlier in Equation (22.3).

The Calvin cycle of reactions starts with *ribulose bisphosphate carboxylase* catalyzing formation of 3-phosphoglycerate from CO_2 and RuBP and concludes with **ribulose-5-phosphate kinase** (also called *phosphoribulose kinase*), which forms RuBP (Figure 22.25 and Table 22.1). The carbon balance is given at the right side of the table. Several features of the reactions in Table 22.1 merit discussion. Note that the 18 equivalents of ATP consumed in hexose formation are expended in reactions 2 and 15: 12 to form 12 equivalents of 1,3-bisphosphoglycerate from 3-phosphoglycerate by a reversal of the normal glycolytic reaction catalyzed by **3-phosphoglycerate kinase,** and six to phosphorylate Ru-5-P to regenerate 6 RuBP. All 12 NADPH equivalents are used in reaction 3. Plants possess an **NADPH-specific glyceraldehyde-3-phosphate dehydrogenase,** which contrasts with its glycolytic counterpart in its specificity for NADP over NAD and in the direction in which the reaction normally proceeds.

Balancing the Calvin Cycle Reactions To Account for Net Hexose Synthesis

When carbon rearrangements are balanced to account for net hexose synthesis, five of the glyceraldehyde-3-phosphate molecules are converted to dihydroxyacetone phosphate (DHAP). Three of these DHAPs then condense with three glyceraldehyde-3-P via the aldolase reaction to yield 3 hexoses in the form

6 ADP   6 **ATP**   Phosphoribulose kinase

15

Ribulose-1,5-bis-phosphate (RuBP)

$H_2COPO_3^{2-}$
|
C=O
|
HCOH
|
HCOH
|
$H_2COPO_3^{2-}$

6 CO_2 1   6

Ribulose bisphosphate carboxylase

Two 3-Phospho-glycerates (3PG)

$H_2COPO_3^{2-}$
|
HOCH
|
COO⁻
+
COO⁻
|
HCOH
|
$H_2COPO_3^{2-}$

12 **ATP** 12 **ADP**   2   12

Phospho-glycerate kinase

1,3-Bisphospho-glycerate (BPG)

O=C—OPO$_3^{2-}$
|
HCOH
|
$H_2COPO_3^{2-}$

12 **NADPH**   12 **NADP⁺**+ 12 **P**   3   12

Glyceraldehyde-3-phosphate dehydrogenase

Glyceraldehyde-3-phosphate (G3P)

CHO
|
HCOH
|
$H_2COPO_3^{2-}$

6

Ribulose-5-phosphate (Ru5P)

H_2COH
|
C=O
|
HCOH
|
HCOH
|
$H_2COPO_3^{2-}$

12

4   5   **Triose phosphate isomerase**

Dihydroxyacetone phosphate (DHAP)

$H_2COPO_3^{2-}$
|
C=O
|
H_2COH

7

3   3   2

Erythrose-4-phosphate (E4P)

CHO
|
HCOH
|
HCOH
|
$H_2COPO_3^{2-}$

2

Aldolase

10

5   **Aldolase**

Sedoheptulose-1,7-bisphosphate (SBP)

$H_2COPO_3^{2-}$
|
C=O
|
HOCH
|
HCOH
|
HCOH
|
HCOH
|
$H_2COPO_3^{2-}$

11   2

P 2   **Sedoheptulose bisphosphatase**

Sedoheptulose-7-phosphate (S7P)

H_2COH
|
C=O
|
HOCH
|
HCOH
|
HCOH
|
HCOH
|
$H_2COPO_3^{2-}$

2

4

2

Fructose-1,6-bisphosphate (FBP)

$H_2COPO_3^{2-}$
|
C=O
|
HOCH
|
HCOH
|
HCOH
|
$H_2COPO_3^{2-}$

6   **Fructose bisphosphatase**

P 3

Fructose-6-phosphate (F6P)

H_2COH
|
C=O
|
HOCH
|
HCOH
|
HCOH
|
$H_2COPO_3^{2-}$

2

2   2

9   **Transketolase**

2   **Transketolase**   12

Glucose

8   Glucose-6-phosphatase

P

Glucose-6-phosphate (G6P)

CHO
|
HCOH
|
HOCH
|
HCOH
|
HCOH
|
$H_2COPO_3^{2-}$

7   1

Phospho-glucoisomerase

13   Phosphopentose epimerase

Xylulose-5-phosphate (Xu5P)

H_2COH
|
C=O
|
HOCH
|
HCOH
|
$H_2COPO_3^{2-}$

4

4

2

2   Phospho-pentose isomerase   14

Ribose-5-phosphate (R5P)

CHO
|
HCOH
|
HCOH
|
HCOH
|
$H_2COPO_3^{2-}$

2

734

◀ **FIGURE 22.25** • The Calvin–Benson cycle of reactions. The number associated with the arrow at each step indicates the number of molecules reacting in a turn of the cycle that produces one molecule of glucose. Reactions are numbered as in Table 22.1.

of fructose bisphosphate (Figure 22.25). (Recall that the $\Delta G°'$ for the aldolase reaction in the glycolytic direction is $+23.9$ kJ/mol. Thus, the aldolase reaction running "in reverse" in the Calvin cycle would be thermodynamically favored under standard-state conditions.) Taking one FBP to glucose, the desired product of this scheme, leaves 30 carbons, distributed as two fructose-6-phosphates, four glyceraldehyde-3-phosphates, and 2 DHAP. These 30 Cs are reorganized into 6 RuBP by reactions 9 through 15. Step 9 and steps 12 through 14 involve carbohydrate rearrangements like those in the pentose phosphate pathway (see Chapter 23). Reaction 11 is mediated by **sedoheptulose-1,7-bisphosphatase.** This phosphatase is unique to plants; it generates sedoheptulose-7-P, the seven-carbon sugar serving as the transketolase substrate. Likewise, **phosphoribulose kinase** carries out the unique plant function of providing RuBP from Ru-5-P (reaction 15). The net conversion accounts for the fixation of six equivalents of carbon dioxide into one hexose at the expense of 18 ATP and 12 NADPH.

Table 22.1

The Calvin Cycle Series of Reactions

Reactions 1 through 15 constitute the cycle that leads to the formation of one equivalent of glucose. The enzyme catalyzing each step, a concise reaction, and the overall carbon balance is given. Numbers in parentheses show the numbers of carbon atoms in the substrate and product molecules. Prefix numbers indicate in a stoichiometric fashion how many times each step is carried out in order to provide a balanced net reaction.

Reaction	Carbon balance
1. Ribulose bisphosphate carboxylase: $6\ CO_2 + 6\ H_2O + 6\ RuBP \longrightarrow 12\ 3\text{-PG}$	$6(1) + 6(5) \longrightarrow 12(3)$
2. 3-Phosphoglycerate kinase: $12\ 3\text{-PG} + 12\ ATP \longrightarrow 12\ 1,3\text{-BPG} + 12\ ADP$	$12(3) \longrightarrow 12(3)$
3. $NADP^+$-glyceraldehyde-3-P dehydrogenase:	
$12\ 1,3\text{-BPG} + 12\ NADPH \longrightarrow 12\ NADP^+ + 12\ G3P + 12\ P_i$	$12(3) \longrightarrow 12(3)$
4. Triose-P isomerase: $5\ G3P \longrightarrow 5\ DHAP$	$5(3) \longrightarrow 5(3)$
5. Aldolase: $3\ G3P + 3\ DHAP \longrightarrow 3\ FBP$	$3(3) + 3(3) \longrightarrow 3(6)$
6. Fructose bisphosphatase: $3\ FBP + 3\ H_2O \longrightarrow 3\ F6P + 3\ P_1$	$3(6) \longrightarrow 3(6)$
7. Phosphoglucoisomerase: $1\ F6P \longrightarrow 1\ G6P$	$1(6) \longrightarrow 1(6)$
8. Glucose phosphatase: $1\ G6P + 1\ H_2O \longrightarrow 1\ GLUCOSE + 1\ P_i$	$1(6) \longrightarrow 1(6)$
The remainder of the pathway involves regenerating six RuBP acceptors ($= 30$ C) from the leftover two F6P (12 C), four G3P (12 C), and two DHAP (6 C).	
9. Transketolase: $2\ F6P + 2\ G3P \longrightarrow 2\ Xu5P + 2\ E4P$	$2(6) + 2(3) \longrightarrow 2(5) + 2(4)$
10. Aldolase: $2\ E4P + 2\ DHAP \longrightarrow 2$ sedoheptulose-1,7-bisphosphate (SBP)	$2(4) + 2(3) \longrightarrow 2(7)$
11. Sedoheptulose bisphosphatase: $2\ SBP + 2\ H_2O \longrightarrow 2\ S7P + 2\ P_i$	$2(7) \longrightarrow 2(7)$
12. Transketolase: $2\ S7P + 2\ G3P \longrightarrow 2\ Xu5P + 2\ R5P$	$2(7) + 2(3) \longrightarrow 4(5)$
13. Phosphopentose epimerase: $4\ Xu5P \longrightarrow 4\ Ru5P$	$4(5) \longrightarrow 4(5)$
14. Phosphopentose isomerase: $2\ R5P \longrightarrow 2\ Ru5P$	$2(5) \longrightarrow 2(5)$
15. Phosphoribulose kinase: $6\ Ru5P + 6\ ATP \longrightarrow 6\ RuBP + 6\ ADP$	$6(5) \longrightarrow 6(5)$
Net: $6\ CO_2 + 18\ ATP + 12\ NADPH + 12\ H^+ + 12\ H_2O \longrightarrow$	
glucose $+ 18\ ADP + 18\ P_i + 12\ NADP^+$	$6(1) \longrightarrow 1(6)$
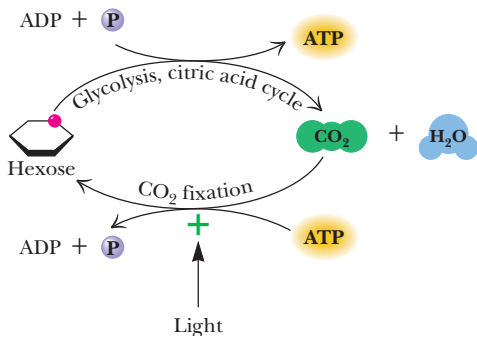
FIGURE 22.26 • Light regulation of CO_2 fixation prevents a substrate cycle between cellular respiration and hexose synthesis by CO_2 fixation. Because plants possess mitochondria and are capable of deriving energy from hexose catabolism (glycolysis and the citric acid cycle), regulation of photosynthetic CO_2 fixation by light activation controls the net flux of carbon between these opposing routes.
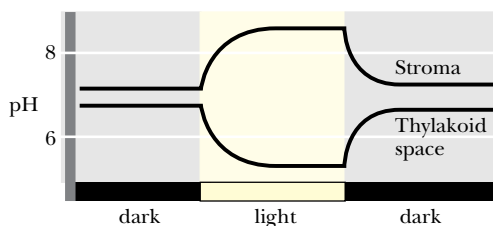
FIGURE 22.27 • Light-induced pH changes in chloroplast compartments. Illumination of chloroplasts leads to proton pumping and pH changes in the chloroplast, such that the pH within the thylakoid space falls and the pH of the stroma rises. These pH changes modulate the activity of key Calvin cycle enzymes.

FIGURE 22.28 • The pathway for light regulation of Calvin cycle enzymes. Light-generated reducing power (Fd_{red} = reduced ferredoxin) provides e^- for reduction of thioredoxin (T) by FTR (ferredoxin–thioredoxin reductase). Several Calvin cycle enzymes have pairs of Cys residues that are involved in the disulfide-sulfhydryl transition between an inactive (—S—S—) form and an active (—SH HS—) form, as shown here. These enzymes include *fructose-1,6-bisphosphatase* (residues Cys^{174} and Cys^{179}), *$NADP^+$-malate dehydrogenase* (residues Cys^{10} and Cys^{15}), and *ribulose-5-P kinase* (residues Cys^{16} and Cys^{55}).

22.10 • Regulation of Carbon Dioxide Fixation

Plant cells contain mitochondria and can carry out cellular respiration (glycolysis, the citric acid cycle, and oxidative phosphorylation) to provide energy in the dark. Futile cycling of carbohydrate to CO_2 by glycolysis and the citric acid cycle in one direction, and CO_2 to carbohydrate by the CO_2 fixation pathway in the opposite direction, is thwarted through regulation of the Calvin cycle (Figure 22.26). In this regulation, the activities of key Calvin cycle enzymes are coordinated with the output of photosynthesis. In effect, these enzymes respond indirectly to *light activation.* Thus, when light energy is available to generate ATP and NADPH for CO_2 fixation, the Calvin cycle proceeds. In the dark, when ATP and NADPH cannot be produced by photosynthesis, fixation of CO_2 ceases. The light-induced changes in the chloroplast which regulate key Calvin cycle enzymes include (1) *changes in stromal pH,* (2) *generation of reducing power,* and (3) *Mg^{2+} efflux from the thylakoid lumen.*

Light-Induced pH Changes in Chloroplast Compartments

As discussed in Section 22.7, illumination of chloroplasts leads to light-driven pumping of protons into the thylakoid lumen, which causes pH changes in both the stroma and the thylakoid lumen (Figure 22.27). The stromal pH rises, typically to pH 8. Because rubisco and rubisco activase are more active at pH 8, CO_2 fixation is activated as stromal pH rises. *Fructose-1,6-bisphosphatase, ribulose-5-phosphate kinase,* and *glyceraldehyde-3-phosphate dehydrogenase* all have alkaline pH optima. Thus, their activities increase as a result of the light-induced pH increase in the stroma.

Light-Induced Generation of Reducing Power

Illumination of chloroplasts initiates photosynthetic electron transport, which generates reducing power in the form of reduced ferredoxin and NADPH. Several enzymes of CO_2 fixation, notably *fructose-1,6-bisphosphatase, sedoheptulose-1,7-bisphosphatase,* and *ribulose-5-phosphate kinase,* are activated upon reduction of specific Cys-Cys disulfide bonds to cysteine sulfhydryls. The reduced form of **thioredoxin** mediates this reaction. Thioredoxin is a small (12 kD) protein possessing in its reduced state a pair of sulfhydryls (—SH HS—), which upon oxidation form a disulfide bridge (—S—S—). Thioredoxin serves as the hydrogen carrier between NADPH or Fd_{red} and enzymes regulated by light (Figure 22.28).

Light-Induced Mg^{2+} Efflux from Thylakoid Vesicles

When light-driven proton pumping across the thylakoid membrane occurs, a concomitant efflux of Mg^{2+} ions from vesicles into the stroma is observed. This efflux of Mg^{2+} somewhat counteracts the charge accumulation due to H^+
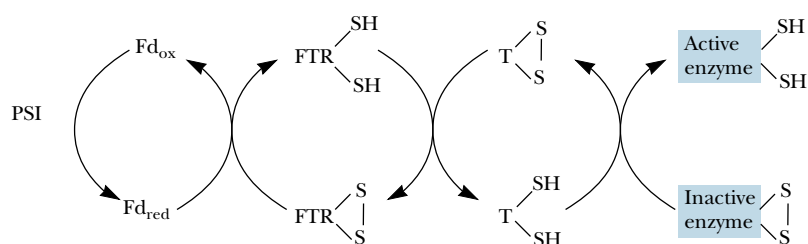
influx and is one reason why the membrane potential change in response to proton pumping is less in chloroplasts than in mitochondria (Eq. 22.5). Both *ribulose bisphosphate carboxylase* and *fructose-1,6-bisphosphatase* are Mg^{2+}-activated enzymes, and Mg^{2+} flux into the stroma as a result of light-driven proton pumping stimulates the CO_2 fixation pathway at these key steps. Activity measurements have indicated that fructose bisphosphatase may be the rate-limiting step in the Calvin cycle. The recurring theme of fructose bisphosphatase as the target of the light-induced changes in the chloroplasts implicates this enzyme as a key point of control in the Calvin cycle.

22.11 • The Ribulose Bisphosphate Oxygenase Reaction: Photorespiration

As indicated, ribulose bisphosphate carboxylase/oxygenase catalyzes an alternative reaction in which O_2 replaces CO_2 as the substrate added to RuBP (Figure 22.29a). The *ribulose-1,5-bisphosphate oxygenase* reaction diminishes plant
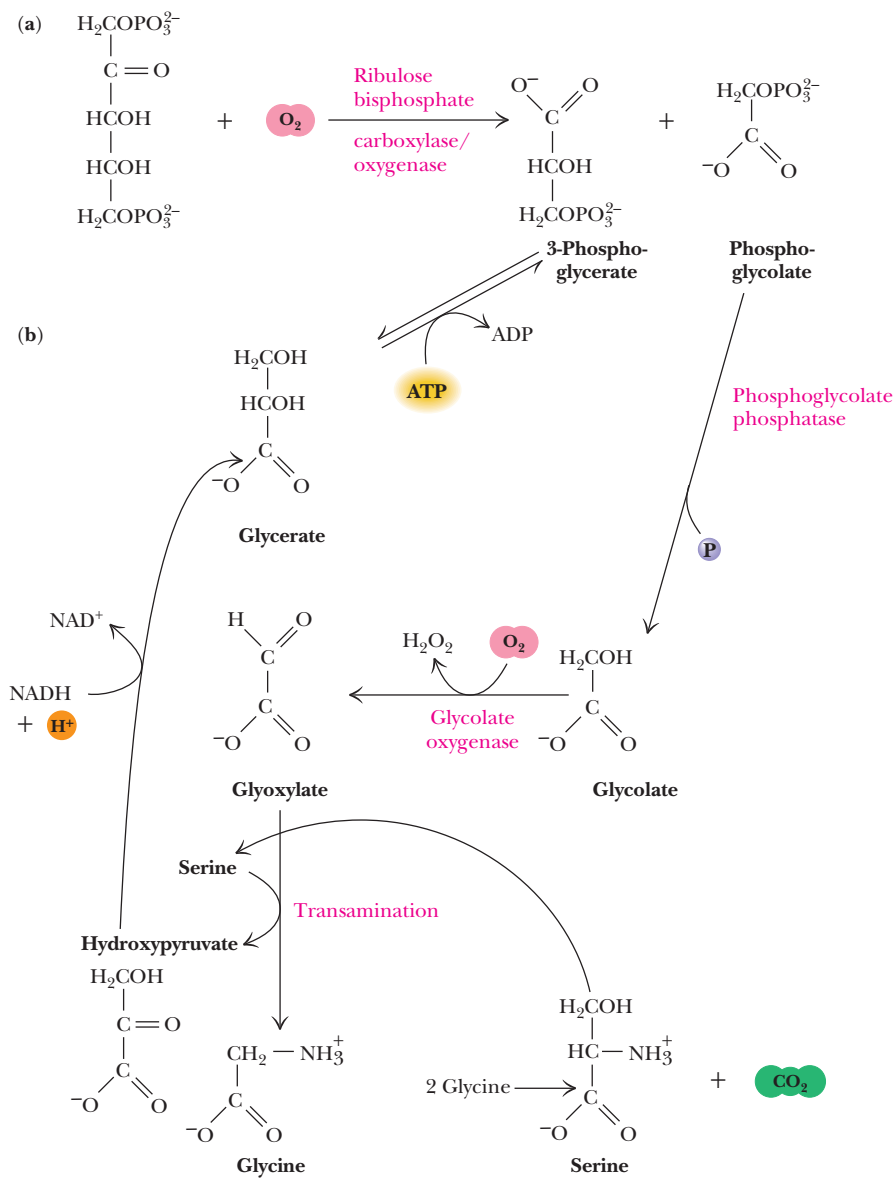
FIGURE 22.29 • The oxygenase reaction of rubisco. (a) The reaction of ribulose bisphosphate carboxylase with O_2 in the presence of ribulose bisphosphate leads to wasteful cleavage of RuBP to yield 3-phosphoglycerate and phosphoglycolate. (b) Conversion of phosphoglycolate to glycine. In mitochondria, two glycines from photorespiration are converted into one serine plus CO_2. This step is the source of the CO_2 evolved in photorespiration. Transamination of glyoxylate to glycine by the product serine yields hydroxypyruvate; reduction of hydroxypyruvate yields glycerate, which can be phosphorylated to 3-phosphoglycerate. 3-Phosphoglycerate can fuel resynthesis of ribulose bisphosphate by the Calvin cycle (Figure 22.25).

productivity because it leads to loss of RuBP, the essential CO_2 acceptor. The K_m for O_2 in this oxygenase reaction is about 200 μM. Given the relative abundance of CO_2 and O_2 in the atmosphere and their relative K_m values in these rubisco-mediated reactions, the ratio of carboxylase to oxygenase activity *in vivo* is about 3 or 4 to 1.

The products of ribulose bisphosphate oxygenase activity are *3-phosphoglycerate* and *phosphoglycolate*. Dephosphorylation and oxidation convert phosphoglycolate to **glyoxylate,** the α-keto acid of glycine (Figure 22.29b). Transamination yields glycine. Other fates of phosphoglycolate are also possible, including oxidation to CO_2, with the released energy being dissipated as heat. Obviously, agricultural productivity is dramatically lowered by this phenomenon, which, because it is a light-related uptake of O_2 *and* release of CO_2, is termed **photorespiration.** As we shall see, certain plants, particularly tropical grasses, have evolved means to circumvent photorespiration. These plants are more efficient users of light for carbohydrate synthesis.

22.12 • The C-4 Pathway of CO_2 Fixation

Tropical grasses are less susceptible to the effects of photorespiration, as noted earlier. Studies employing $^{14}CO_2$ as a tracer indicated that the first organic intermediate labeled in these plants was not a three-carbon compound but a four-carbon compound. Hatch and Slack, two Australian biochemists, first discovered this C-4 product of CO_2 fixation, and the C-4 pathway of CO_2 incorporation is named the *Hatch–Slack pathway* after them. The C-4 pathway is not an alternative to the Calvin cycle series of reactions or even a net CO_2 fixation scheme. Instead, it functions as a *CO_2 delivery system,* carrying carbon dioxide from the relatively oxygen-rich surface of the leaf to interior cells where oxygen is lower in concentration and hence less effective in competing with CO_2 in the rubisco reaction. Thus, the C-4 pathway is a means of avoiding photorespiration by sheltering the rubisco reaction in a cellular compartment away from high [O_2]. The C-4 compounds serving as CO_2 transporters are *malate* or *aspartate*.

Compartmentation of these reactions to prevent photorespiration involves the interaction of two cell types, *mesophyll cells* and *bundle sheath cells.* The mesophyll cells take up CO_2 at the leaf surface, where O_2 is abundant, and use it to carboxylate phosphoenolpyruvate to yield OAA in a reaction catalyzed by **PEP carboxylase** (Figure 22.30). This four-carbon dicarboxylic acid is then either reduced to malate by an **NADPH-specific malate dehydrogenase** or transaminated to give *aspartate* in the mesophyll cells.[4] The 4-C CO_2 carrier (malate or aspartate) then is transported to the bundle sheath cells, where it is decarboxylated to yield CO_2 and a 3-C product. The CO_2 is then fixed into organic carbon by the Calvin cycle localized within the bundle sheath cells, and the 3-C product is returned to the mesophyll cells, where it is reconverted to PEP in preparation to accept another CO_2 (Figure 22.30). Plants that use the C-4 pathway are termed **C4 plants,** in contrast to those plants with the conventional pathway of CO_2 uptake **(C3 plants).**

[4]A number of different biochemical subtypes of C4 plants are known. They differ in whether OAA or malate is the CO_2 carrier to the bundle sheath cell and in the nature of the reaction by which the CO_2 carrier is decarboxylated to regenerate a 3-C product. In all cases, the 3-C product is returned to the mesophyll cell and reconverted to PEP.
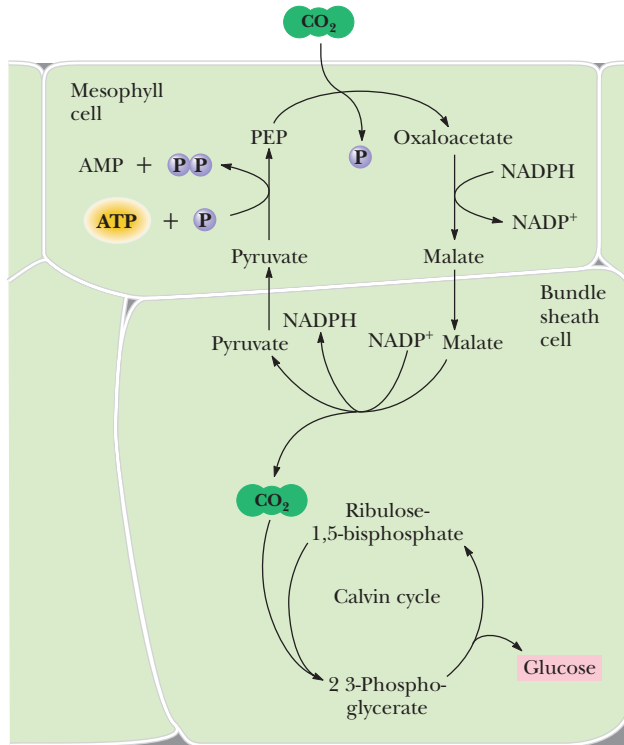
FIGURE 22.30 • Essential features of the compartmentation and biochemistry of the Hatch–Slack pathway of carbon dioxide uptake in C4 plants. Carbon dioxide is fixed into organic linkage by PEP carboxylase of mesophyll cells, forming OAA. Either malate (the reduced form of OAA) or aspartate (the aminated form) serves as the carrier transporting CO_2 to the bundle sheath cells. Within the bundle sheath cells, CO_2 is liberated by decarboxylation of malate or aspartate; the C-3 product is returned to the mesophyll cell. Formation of PEP by pyruvate:P_i dikinase reinitiates the cycle. The CO_2 liberated in the bundle sheath cell is used to synthesize hexose by the conventional rubisco–Calvin cycle series of reactions.

Intercellular Transport of Each CO_2 via a C-4 Intermediate Costs 2 ATP

The transport of each CO_2 requires the expenditure of two high-energy phosphate bonds. The energy of these bonds is expended in the phosphorylation of pyruvate to PEP (phosphoenolpyruvate) by the plant enzyme **pyruvate-P_i dikinase;** the products are PEP, AMP, and pyrophosphate (PP_i). This represents a unique phosphotransferase reaction in that both the β- and γ-phosphates of a single ATP are used to phosphorylate the two substrates, pyruvate and P_i. The reaction mechanism involves an enzyme phosphohistidine intermediate. The γ-phosphate of ATP is transferred to P_i, whereas formation of E-His-P occurs by addition of the β-phosphate from ATP:

$$E\text{—}His + AMP_\alpha\text{—}P_\beta\text{—}P_\gamma + P_i \longrightarrow E\text{—}His\text{—}P_\beta + AMP_\alpha + P_\gamma P_i$$
$$E\text{—}His\text{—}P_\beta + pyruvate \longrightarrow PEP + E\text{—}His$$
$$\textit{Net:} \quad ATP + pyruvate + P_i \longrightarrow AMP + PEP + PP_i$$
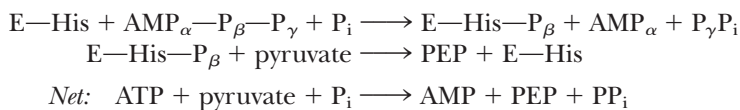
Pyruvate-P_i dikinase is regulated by reversible phosphorylation of a threonine residue, the nonphosphorylated form being active. Interestingly, ADP is the phosphate donor in this interconvertible regulation. Despite the added metabolic expense of two phosphodiester bonds for each equivalent of carbon dioxide taken up, CO_2 fixation is more efficient in C4 plants, provided that light intensities and temperatures are both high. (As temperature rises, photorespiration in C3 plants rises and efficiency of CO_2 fixation falls.) Tropical grasses that are C4 plants include sugarcane, maize, and crabgrass. In terms of photosynthetic efficiency, cultivated fields of sugarcane represent the pinnacle of light-harvesting efficiency. Approximately 8% of the incident light energy on a sugarcane field appears as chemical energy in the form of CO_2 fixed into carbohydrate. This efficiency compares dramatically with the estimated pho-

tosynthetic efficiency of 0.2% for uncultivated plant areas. Research on photorespiration is actively pursued in hopes of enhancing the efficiency of agriculture by controlling this wasteful process. Only 1% of the 230,000 different plant species known are C4 plants; most are in hot climates.

22.13 • Crassulacean Acid Metabolism

In contrast to C4 plants, which have separated CO_2 uptake and fixation into distinct cells in order to minimize photorespiration, succulent plants native to semiarid and tropical environments separate CO_2 uptake and fixation in time. Carbon dioxide (as well as O_2) enters the leaf through microscopic pores known as **stomata,** and water vapor escapes from plants via these same openings. In nonsucculent plants, the stomata are open during the day, when light can drive photosynthetic CO_2 fixation, and closed at night. Succulent plants, such as the *Cactaceae* (cacti) and *Crassulaceae,* cannot open their stomata during the heat of day because any loss of precious H_2O in their arid habitats would doom them. Instead, these plants open their stomata to take up CO_2 only at night, when temperatures are lower and water loss is less likely. This carbon dioxide is immediately incorporated into PEP to form OAA by PEP carboxylase; OAA is then reduced to malate by malate dehydrogenase and stored within vacuoles until morning. During the day, the malate is released from the vacuoles and decarboxylated to yield CO_2 and a 3-C product. The CO_2 is then fixed into organic carbon by rubisco and the reactions of the Calvin cycle. Because this process involves the accumulation of organic acids (OAA, malate) and is common to succulents of the *Crassulaceae* family, it is referred to as *crassulacean acid metabolism,* and plants capable of it are called *CAM plants.*

PROBLEMS

1. In photosystem I, P700 in its ground state has an $\mathcal{E}_\circ' = +0.4$ V. Excitation of P700 by a photon of 700-nm light alters the $\mathcal{E}_\circ'$ of P700* to -0.6 V. What is the efficiency of energy capture in this light reaction of P700?

2. What is the $\mathcal{E}_\circ'$ for the light-generated primary oxidant of photosystem II if the light-induced oxidation of water (which leads to O_2 evolution) proceeds with a $\Delta G^{\circ\prime}$ of -25 kJ/mol?

3. Assuming that the concentrations of ATP, ADP, and P_i in chloroplasts are 3 mM, 0.1 mM, and 10 mM, respectively, what is the ΔG for ATP synthesis under these conditions? Photosynthetic electron transport establishes the proton-motive force driving photophosphorylation. What redox potential difference is necessary to achieve ATP synthesis under the foregoing conditions, assuming an electron pair is transferred per molecule of ATP generated?

4. ^{14}C-labeled carbon dioxide is administered to a green plant, and shortly thereafter the following compounds are isolated from the plant: 3-phosphoglycerate, glucose, erythrose-4-phosphate, sedoheptulose-1,7-bisphosphate, ribose-5-phosphate. In which carbon atoms will radioactivity be found?

5. Write a balanced equation for the synthesis of a glucose molecule from ribulose-1,5-bisphosphate and CO_2 that involves the first three reactions of the Calvin cycle and subsequent conversion of the two glyceraldehyde-3-P molecules into glucose.
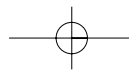
6. If noncyclic photosynthetic electron transport leads to the translocation of 3 H^+/e^- and cyclic photosynthetic electron transport leads to the translocation of 2 H^+/e^-, what is the relative photosynthetic efficiency of ATP synthesis (expressed as the number of photons absorbed per ATP synthesized) for noncyclic *versus* cyclic photophosphorylation? (Assume that the CF_1CF_0 ATP synthase yields 1 ATP/3 H^+.)

7. The photosynthetic CO_2 fixation pathway is regulated in response to specific effects induced in chloroplasts by light. What is the nature of these effects, and how do they regulate this metabolic pathway?

8. The overall equation for photosynthetic CO_2 fixation is

$$6\ CO_2 + 6\ H_2O \longrightarrow C_6H_{12}O_6 + 6\ O_2$$
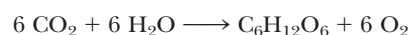
All the O atoms evolved as O_2 come from water; *none* comes from carbon dioxide. But 12 O atoms are evolved as 6 O_2, and only 6 O atoms appear as 6 H_2O in the equation. Also, 6 CO_2 have 12 O atoms, yet there are only 6 O atoms in $C_6H_{12}O_6$. How can you account for these discrepancies? (*Hint:* Consider the partial reactions of photosynthesis: ATP synthesis, $NADP^+$ reduction, photolysis of water, and the overall reaction for hexose synthesis in the Calvin–Benson cycle.)

FURTHER READING

Anderson, J. M., 1986. Photoregulation of the composition, function and structure of the thylakoid membrane. *Annual Review of Plant Physiology* **37:**93–136.

Anderson, J. M., and Andersson, B., 1988. The dynamic photosynthetic membrane and regulation of solar energy conversion. *Trends in Biochemical Sciences* **13:**351–355.

Arnon, D. I., 1984. The discovery of photosynthetic phosphorylation. *Trends in Biochemical Sciences* **9:**258–262. A historical account of photophosphorylation by its discoverer.

Bendall, D. S., and Manasse, R. S., 1995. Cyclic photophosphorylation and electron transport. *Biochimica et Biophysica Acta* **1229:**23–38.

Berry, S., and Rumberg, B., 1996. H^+/ATP coupling ratio at the unmodulated CF_1CF_0–ATP synthase determined by proton flux measurements. *Biochimica et Biophysica Acta* **1276:**51–56.

Blankenship, R. E., and Hartman, H., 1998. The origin and evolution of oxygenic photosynthesis. *Trends in Biochemical Sciences* **23:**94–97.

Burnell, J. N., and Hatch, M. D., 1985. Light-dark modulation of leaf pyruvate, P_i dikinase. *Trends in Biochemical Sciences* **10:**288–291. Regulation of a key enzyme in C4 CO_2 fixation.

Chapman, M. S., et al., 1988. Tertiary structure of plant rubisco: Domains and their contacts. *Science* **241:**71–74. Structural details of rubisco.

Cramer, W. A., et al., 1985. Topography and function of thylakoid membrane proteins. *Trends in Biochemical Sciences* **10:**125–129.

Cramer, W. A., and Knaff, D. B., 1990. *Energy Transduction in Biological Membranes—A Textbook of Bioenergetics.* New York: Springer-Verlag, 545 pp. A textbook on bioenergetics by two prominent workers in photosynthesis.

Cramer, W. A., et al., 1996. Some new structural aspects and old controversies concerning the cytochrome $b_6 f$ complex of oxygenic photosynthesis. *Annual Review of Plant Physiology and Plant Molecular Biology* **47:**477–508.

Deisenhofer, J., and Michel, H., 1989. The photosynthetic reaction center from the purple bacterium *Rhodopseudomonas viridis. Science* **245:**1463–1473. Published version of the Nobel laureate address by the researchers who first elucidated the molecular structure of a photosynthetic reaction center.

Deisenhofer, J., Michel, H., and Huber, R., 1985. The structural basis of light reactions in bacteria. *Trends in Biochemical Sciences* **10:**243–248.

Deisenhofer, J., et al., 1985. Structure of the protein subunits in the photosynthetic reaction center of *Rhodopseudomonas viridis* at 3 Å resolution. *Nature* **318:**618–624; also *The Journal of Molecular Biology* (1984) **180:**385–398. These papers are the original reports of the crystal structure of a photosynthetic reaction center.

Ghanotakis, D. F., and Yocum, C. F., 1990. Photosystem II and the oxygen-evolving complex. *Annual Review of Plant Physiology and Plant Molecular Biology* **41:**255–276.

Glazer, A. N., 1983. Comparative biochemistry of photosynthetic light-harvesting pigments. *Annual Review of Biochemistry* **52:**125–157.

Glazer, A. N., and Melis, A., 1987. Photochemical reaction centers: Structure, organization and function. *Annual Review of Plant Physiology* **38:**11–45.

Golbeck, J. H., 1992. Structure and function of photosystem I. *Annual Review of Plant Physiology and Plant Molecular Biology* **43:**292–324.

Green, B. R., and Durnford, D. G., 1996. The chlorophyll-carotenoid proteins of oxygenic photosynthesis. *Annual Review of Plant Physiology and Plant Molecular Biology* **47:**685–714.

Hankamer, B., Barber, J., and Boekema, E. J., 1997. Structure and membrane organization of photosystem II in green plants. *Annual Review of Plant Physiology and Plant Molecular Biology* **48:**641–671.

Harold, F. M., 1986. *The Vital Force: A Study of Bioenergetics.* Chapter 8: Harvesting the Light. San Francisco: Freeman & Company.

Hatch, M. D., 1987. C_4 photosynthesis: A unique blend of modified biochemistry, anatomy and ultrastructure. *Biochimica et Biophysica Acta* **895:**81–106. A review of C_4 biochemistry by its discoverer.

Hoffman, E., et al., 1996. Structural basis of light harvesting by carotenoids: Peridinin-chlorophyll-protein from *Amphidinium carterae. Science* **272:**1788–1791.

Hoganson, C. W., and Babcock, G. T., 1997. A metalloradical mechanism for the generation of oxygen in photosynthesis. *Science* **277:**1953–1956.

Jagendorf, A. T., and Uribe, E., 1966. ATP formation caused by acid–base transition of spinach chloroplasts. *Proceedings of the National Academy of Sciences, USA* **55:**170–177. The classic paper providing the first experimental verification of Mitchell's chemiosmotic hypothesis.

Knaff, D. B., 1989. The regulatory role of thioredoxin in chloroplasts. *Trends in Biochemical Sciences* **14:**433–434.

Knaff, D. B., 1991. Regulatory phosphorylation of chloroplast antenna proteins. *Trends in Biochemical Sciences* **16:**82–83. Additional discussion of the structure of light-harvesting antenna complexes associated with photosynthetic reaction centers can be found in *Trends in Biochemical Sciences* **11:**414 (1986), **14:**72 (1989), and **16:**181 (1991).

Knight, S., Andersson, I., and Branden, C. I., 1990. Crystallographic analysis of ribulose 1,5-bisphosphate carboxylase from spinach at 2.4 Å resolution. Subunit interactions and active site. *Journal of Molecular Biology* **215:**113–160.

Krauss, N., et al., 1993. Three-dimensional structure of system I of photosynthesis at 6 Å resolution. *Nature* **361:**326–331.

Krauss, N., et al., 1996. Photosystem I at 4 Å resolution represents the first structural model of a joint photosynthetic reaction centre and core antenna system. *Nature Structural Biology* **3:**965–973.

Miziorko, H. M., and Lorimer, G. H., 1983. Ribulose-1,5-bisphosphate carboxylase/oxygenase. *Annual Review of Biochemistry* **52:**507–535. An early review of the enzymological properties of rubisco.

Murata, N., and Miyao, M., 1985. Extrinsic membrane proteins in the photosynthetic oxygen-evolving complex. *Trends in Biochemical Sciences* **10:**122–124.

Nitschke, W., and Rutherford, A. W., 1991. Photosynthetic reaction centers: Variations on a common structural theme. *Trends in Biochemical Sciences* **16:**241–245.

Ogren, W. L., 1984. Photorespiration: Pathways, regulation and modification. *Annual Review of Plant Physiology* **35:**415–442.

Portis, A. R., Jr., 1992. Regulation of ribulose 1,5-bisphosphate carboxylase/oxygenase activity. *Annual Review of Plant Physiology and Plant Molecular Biology* **43:**415–437.

Rögner, M., Boekema, E. J., and Barber, J., 1996. How does photosystem 2 split water? The structural basis of energy conversion. *Trends in Biochemical Sciences* **21:**44–49.

Ting, I. P., 1985. Crassulacean acid metabolism. *Annual Review of Plant Physiology* **36:**595–622.

Con pan y vino se anda el camino.
(With bread and wine you can walk
your road.)

Spanish proverb

*C*hapter 23

Gluconeogenesis, Glycogen Metabolism, and the Pentose Phosphate Pathway
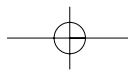
Bread and pasteries on a rack at a French bakery, Paris. Carbohydrates such as these provide a significant portion of human caloric intake. (© Steven Rothfeld/ Tony Stone Images)

As shown in Chapters 18 and 19, the metabolism of sugars is an important source of energy for cells. Animals, including humans, typically obtain significant amounts of glucose and other sugars from the breakdown of starch and glycogen in their diets. Glucose can also be supplied via breakdown of cellular reserves of glycogen (in animals) or starch (in plants). Significantly, glucose also can be synthesized from noncarbohydrate precursors by a process known as *gluconeogenesis*. Each of these important pathways, as well as the synthesis of glycogen from glucose, will be examined in this chapter.

Another pathway of glucose catabolism, the *pentose phosphate pathway,* is the primary source of NADPH, the reduced coenzyme essential to most reductive biosynthetic processes. For example, NADPH is crucial to the biosynthesis of
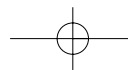
fatty acids (Chapter 25) and amino acids (Chapter 26). The pentose phosphate pathway also results in the production of ribose-5-phosphate, an essential component of ATP, NAD^+, FAD, coenzyme A, and particularly DNA and RNA. This important pathway will also be considered in this chapter.

23.1 • Gluconeogenesis

The ability to synthesize glucose from common metabolites is very important to most organisms. Human metabolism, for example, consumes about 160 ± 20 grams of glucose per day, about 75% of this in the brain. Body fluids carry only about 20 grams of free glucose, and glycogen stores normally can provide only about 180 to 200 grams of free glucose. Thus, the body carries only a little more than a one-day supply of glucose. If glucose is not obtained in the diet, the body must produce new glucose from noncarbohydrate precursors. The term for this activity is **gluconeogenesis,** which means the generation (*genesis*) of new (*neo*) glucose.

Further, muscles consume large amounts of glucose via glycolysis, producing large amounts of pyruvate. In vigorous exercise, muscle cells become anaerobic and pyruvate is converted to lactate. Gluconeogenesis salvages this pyruvate and lactate and reconverts it to glucose.

The Substrates of Gluconeogenesis

In addition to pyruvate and lactate, other noncarbohydrate precursors can be used as substrates for gluconeogenesis in animals. These include most of the amino acids, as well as glycerol and all the TCA cycle intermediates. On the other hand, fatty acids are not substrates for gluconeogenesis in animals, because most fatty acids yield only acetyl-CoA upon degradation, and animals cannot carry out net synthesis of sugars from acetyl-CoA. Lysine and leucine are the only amino acids that are not substrates for gluconeogenesis. These amino acids produce only acetyl-CoA upon degradation. Note also that acetyl-CoA is a substrate for gluconeogenesis when the glyoxylate cycle is operating (Chapter 20).

Nearly All Gluconeogenesis Occurs in the Liver and Kidneys in Animals

Interestingly, the mammalian organs that consume the most glucose, namely, brain and muscle, carry out very little glucose synthesis. The major sites of gluconeogenesis are the liver and kidneys, which account for about 90% and 10% of the body's gluconeogenic activity, respectively. Glucose produced by gluconeogenesis in the liver and kidney is released into the blood and is subsequently absorbed by brain, heart, muscle, and red blood cells to meet their metabolic needs. In turn, pyruvate and lactate produced in these tissues are returned to the liver and kidney to be used as gluconeogenic substrates.
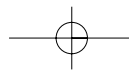
Gluconeogenesis Is Not Merely the Reverse of Glycolysis

In some ways, gluconeogenesis is the reverse, or antithesis, of glycolysis. Glucose is synthesized, not catabolized; ATP is consumed, not produced; and NADH is oxidized to NAD^+, rather than the other way around. However, gluconeogenesis cannot be *merely* the reversal of glycolysis, for two reasons. First, glycolysis is exergonic, with a $\Delta G°'$ of approximately -74 kJ/mol. If gluconeogenesis were merely the reverse, it would be a strongly endergonic process and could not occur spontaneously. Somehow the energetics of the process must be aug-
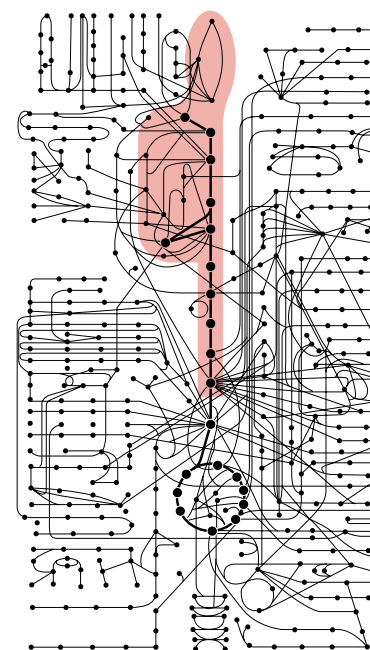
Gluconeogenesis, Glycogen Metabolism, and the Pentose Phosphate Pathway
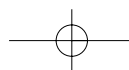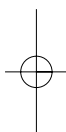
mented so that gluconeogenesis can proceed spontaneously. Second, the processes of glycolysis and gluconeogenesis must be regulated in a reciprocal fashion so that when glycolysis is active, gluconeogenesis is inhibited, and when gluconeogenesis is proceeding, glycolysis is turned off. Both of these limitations are overcome by having unique reactions within the routes of glycolysis and gluconeogenesis, rather than a completely shared pathway.

Gluconeogenesis—Something Borrowed, Something New

The complete route of gluconeogenesis is shown in Figure 23.1, side by side with the glycolytic pathway. Gluconeogenesis employs three different reactions, catalyzed by three different enzymes, for the three steps of glycolysis that are
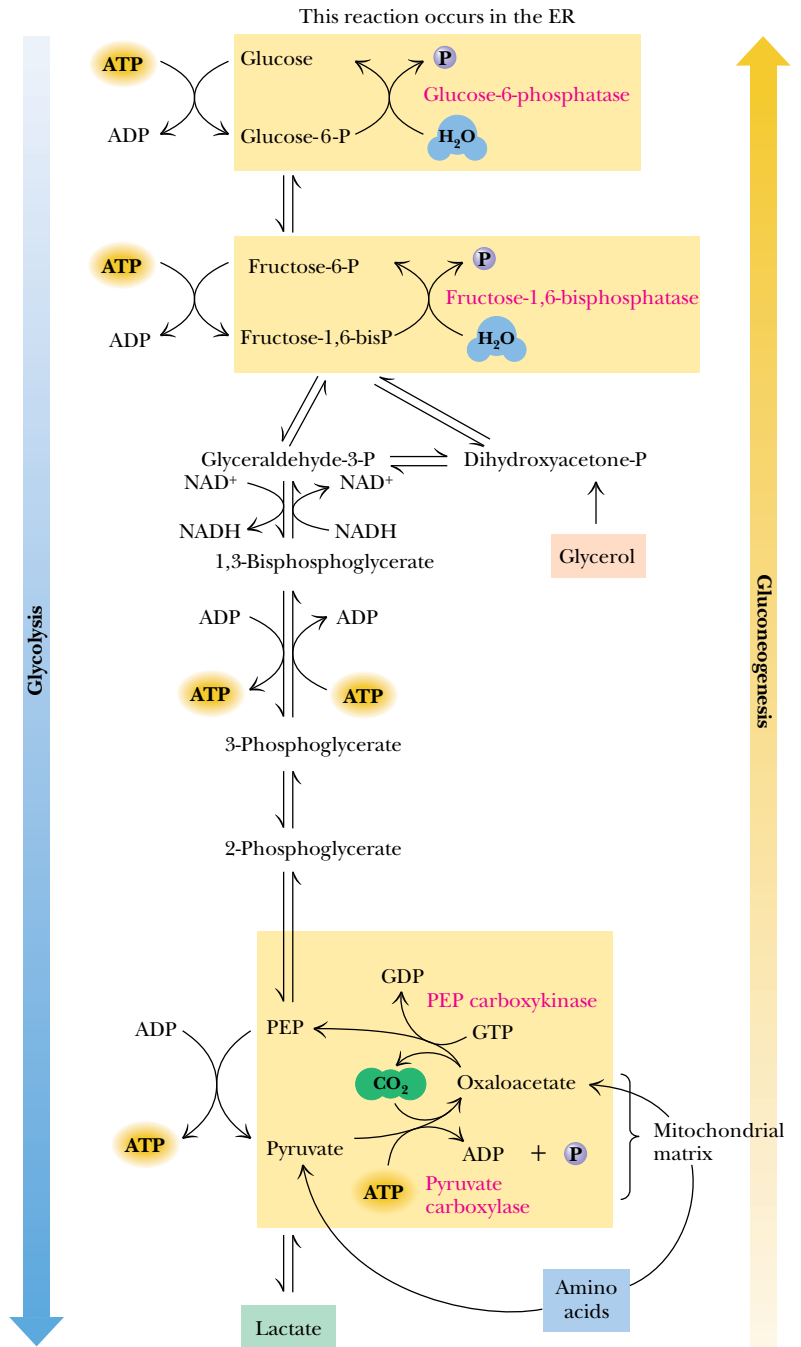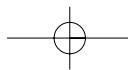
FIGURE 23.1 • The pathways of gluconeogenesis and glycolysis. Species in blue, green, and peach-colored shaded boxes indicate other entry points for gluconeogenesis (in addition to pyruvate).
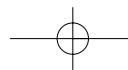
highly exergonic (and highly regulated). In essence, seven of the ten steps of glycolysis are merely reversed in gluconeogenesis. The six reactions between fructose-1,6-bisphosphate and PEP are shared by the two pathways, as is the isomerization of glucose-6-P to fructose-6-P. The three exergonic regulated reactions—the hexokinase (glucokinase), phosphofructokinase, and pyruvate kinase reactions—are replaced by alternative reactions in the gluconeogenic pathway.

The conversion of pyruvate to PEP that initiates gluconeogenesis is accomplished by two unique reactions. **Pyruvate carboxylase** catalyzes the first, converting pyruvate to oxaloacetate. Then, **PEP carboxykinase** catalyzes the conversion of oxaloacetate to PEP. Conversion of fructose-1,6-bisphosphate to fructose-6-phosphate is catalyzed by a specific phosphatase, **fructose-1,6-bis-phosphatase.** The final step to produce glucose, hydrolysis of glucose-6-phosphate, is mediated by **glucose-6-phosphatase.** Each of these steps is considered in detail in the following paragraphs. The overall conversion of pyruvate to PEP by pyruvate carboxylase and PEP carboxykinase has a $\Delta G^{\circ\prime}$ close to zero but is pulled along by subsequent reactions. The conversion of fructose-1,6-bisphosphate to glucose in the last three steps of gluconeogenesis is strongly exergonic with a $\Delta G^{\circ\prime}$ of about -30.5 kJ/mol. This sequence of two phosphatase reactions separated by an isomerization accounts for most of the free energy release that makes the gluconeogenesis pathway spontaneous.

The Unique Reactions of Gluconeogenesis

(1) Pyruvate Carboxylase—A Biotin-Dependent Enzyme

Initiation of gluconeogenesis occurs in the **pyruvate carboxylase reaction**—the conversion of pyruvate to oxaloacetate (Figure 23.2). The reaction takes place in two discrete steps, involves ATP and bicarbonate as substrates, and utilizes biotin as a coenzyme and acetyl-coenzyme A as an allosteric activator. Pyruvate carboxylase is a tetrameric enzyme (with a molecular mass of about 500 kD). Each monomer possesses a biotin covalently linked to the ϵ-amino group of a lysine residue at the active site (Figure 23.3). The first step of the reaction involves nucleophilic attack of a bicarbonate oxygen at the γ-P of ATP to form **carbonylphosphate,** an activated form of CO_2, and ADP (Figure 23.4). Reaction of carbonylphosphate with biotin occurs rapidly to form N-carboxybiotin, liberating inorganic phosphate. The third step involves abstraction of a proton from the C-3 of pyruvate, forming a carbanion which can attack the carbon of N-carboxybiotin to form oxaloacetate.

PYRUVATE CARBOXYLASE IS ALLOSTERICALLY ACTIVATED BY ACYL-COENZYME A
Two particularly interesting aspects of the pyruvate carboxylase reaction are (a) allosteric activation of the enzyme by acyl-coenzyme A derivatives and (b) compartmentation of the reaction in the mitochondrial matrix. The carboxylation of biotin requires the presence (at an allosteric site) of acetyl-coenzyme A or other acylated coenzyme A derivatives. The second half of the carboxylase reaction—the attack by pyruvate to form oxaloacetate—is not affected by CoA derivatives.
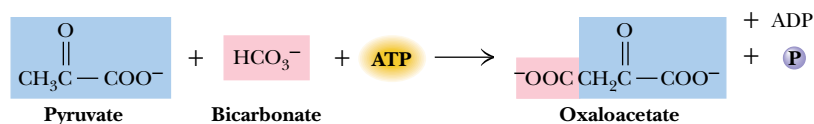
FIGURE 23.2 • The pyruvate carboxylase reaction.
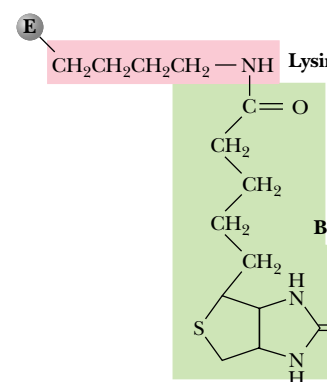
FIGURE 23.3 • Covalent linkage of an active-site lysine in pyruvate carb
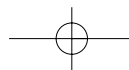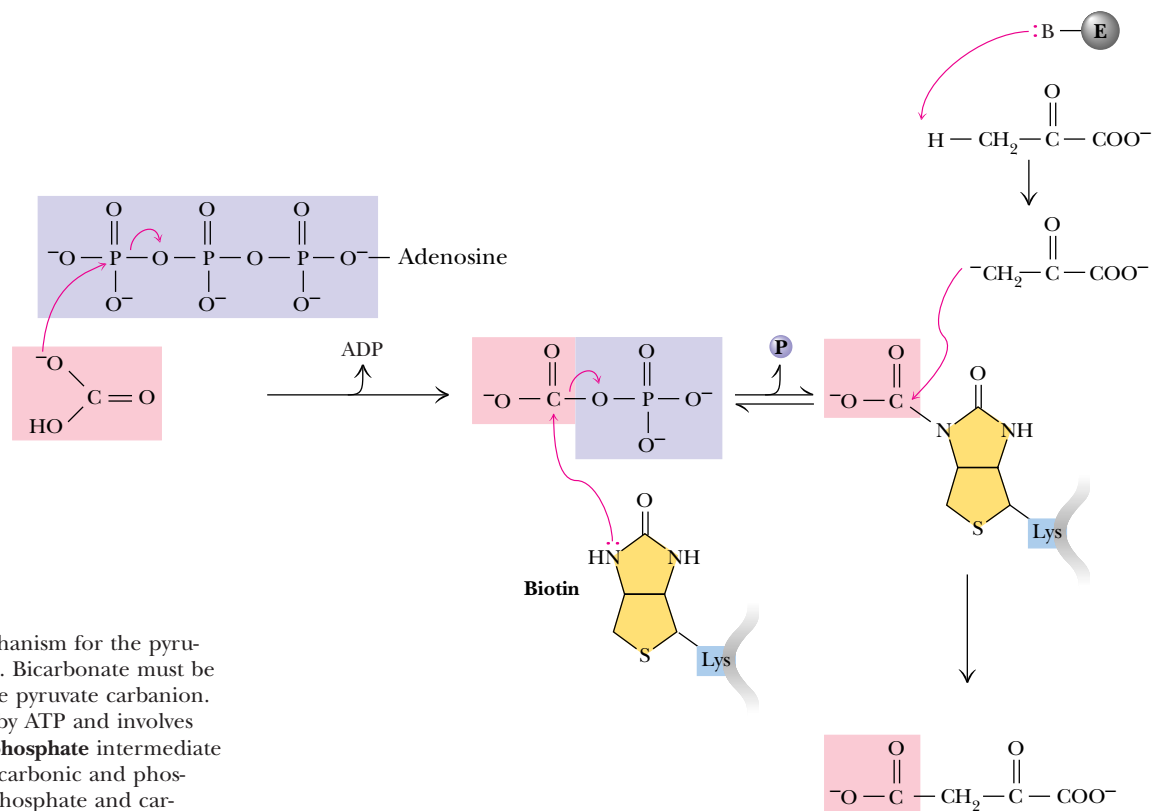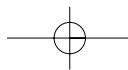
FIGURE 23.4 • A mechanism for the pyruvate carboxylase reaction. Bicarbonate must be activated for attack by the pyruvate carbanion. This activation is driven by ATP and involves formation of a **carbonylphosphate** intermediate —a mixed anhydride of carbonic and phosphoric acids. (Carbonylphosphate and carboxyphosphate are synonyms.)

Activation of pyruvate carboxylase by acetyl-CoA provides an important physiological regulation. Acetyl-CoA is the primary substrate for the TCA cycle, and oxaloacetate (formed by pyruvate carboxylase) is an important intermediate in both the TCA cycle and the gluconeogenesis pathway. If levels of ATP and/or acetyl-CoA (or other acyl-CoAs) are low, pyruvate is directed primarily into the TCA cycle, which eventually promotes the synthesis of ATP. If ATP and acetyl-CoA levels are high, pyruvate is converted to oxaloacetate and consumed in gluconeogenesis. Clearly, high levels of ATP and CoA derivatives are signs that energy is abundant and that metabolites will be converted to glucose (and perhaps even glycogen). If the energy status of the cell is low (in terms of ATP and CoA derivatives), pyruvate is consumed in the TCA cycle. Also, as noted in Chapter 20, pyruvate carboxylase is an important anaplerotic enzyme. Its activation by acetyl-CoA leads to oxaloacetate formation, replenishing the level of TCA cycle intermediates.

COMPARTMENTALIZED PYRUVATE CARBOXYLASE DEPENDS ON METABOLITE CONVERSION AND TRANSPORT   The second interesting feature of pyruvate carboxylase is that it is found only in the *matrix* of the mitochondria. By contrast, the next enzyme in the gluconeogenic pathway, PEP carboxykinase, may be localized in the cytosol or in the mitochondria or both. For example, rabbit liver PEP carboxykinase is predominantly mitochondrial, whereas the rat liver enzyme is strictly cytosolic. In human liver, PEP carboxykinase is found both in the cytosol and in the mitochondria. Pyruvate is transported into the mitochondrial matrix, where it can be converted to acetyl-CoA (for use in the TCA cycle) and then to citrate (for fatty acid synthesis; see Figure 25.1). Alternatively, it may be converted directly to OAA by pyruvate carboxylase and used in glu-

coneogenesis. In tissues where PEP carboxykinase is found only in the mitochondria, oxaloacetate is converted to PEP, which is then transported to the cytosol for gluconeogenesis (Figure 23.6). However, in tissues that must convert some oxaloacetate to PEP in the cytosol, a problem arises. Oxaloacetate cannot be transported directly across the mitochondrial membrane. Instead, it must first be transformed into malate or aspartate for transport across the mitochondrial inner membrane (Figure 23.5). Cytosolic malate and aspartate must be reconverted to oxaloacetate before continuing along the gluconeogenic route.

(2) PEP Carboxykinase

The second reaction in the gluconeogenic pyruvate-PEP bypass is the conversion of oxaloacetate to PEP. Production of a high-energy metabolite such as PEP requires energy. The energetic requirements are handled in two ways here. First, the CO_2 added to pyruvate in the pyruvate carboxylase step is removed in the PEP carboxykinase reaction. Decarboxylation is a favorable process and helps to drive the formation of the very high-energy enol phosphate in PEP. This decarboxylation drives a reaction that would otherwise be highly endergonic. Note the inherent metabolic logic in this pair of reactions: pyruvate carboxylase consumed an ATP to drive a carboxylation, so that the PEP carboxykinase could use the decarboxylation to facilitate formation of PEP. Second, as shown in Figure 23.6, another high-energy phosphate is consumed by the carboxykinase. Mammals and several other species use GTP in this reaction, rather than ATP. The use of GTP here is equivalent to the consumption of an ATP, due to the activity of the **nucleoside diphosphate kinase** (see Figure 20.4). The substantial free energy of hydrolysis of GTP is crucial to the synthesis of PEP in this step. The overall ΔG for the pyruvate carboxylase and PEP carboxykinase reactions under physiological conditions in the liver is -22.6 kJ/mol. Once PEP is formed in this way, the phosphoglycerate mutase, phosphoglycerate kinase, glyceraldehyde-3-P dehydrogenase, aldolase, and triose phosphate isomerase reactions act to eventually form fructose-1,6-bisphosphate, as in Figure 23.1.

(3) Fructose-1,6-Bisphosphatase

The hydrolysis of fructose-1,6-bisphosphate to fructose-6-phosphate (Figure 23.7), like all phosphate ester hydrolyses, is a thermodynamically favorable (exergonic) reaction under standard-state conditions ($\Delta G°' = -16.7$ kJ/mol). Under physiological conditions in the liver, the reaction is also exergonic ($\Delta G = -8.6$ kJ/mol). **Fructose-1,6-bisphosphatase** is an allosterically regulated enzyme. Citrate stimulates bisphosphatase activity, but *fructose-2,6-bisphosphate* is a potent allosteric inhibitor. AMP also inhibits the bisphosphatase; the inhibition by AMP is enhanced by fructose-2,6-bisphosphate.

Pyruvate

Pyruvate

Oxaloacetate

NADH

NAD⁺

Malate

Malate

NAD⁺

NADH

Oxaloacetate

Gluconeogenesis

FIGURE 23.5 • Pyruvate carboxyl compartmentalized reaction. Pyruvate verted to oxaloacetate in the mitoch Because oxaloacetate cannot be tran across the mitochondrial membrane reduced to malate, transported to the and then oxidized back to oxaloaceta gluconeogenesis can continue.

FIGURE 23.6 • The PEP carboxykinase reaction. GTP formed in this reaction can be converted to ATP by nucleoside diphosphate kinase, although liver cells in some species may not contain this enzyme.

Fructose-1,6-bisphosphate + H_2O $\xrightarrow{\text{Fructose-1,6-bisphosphatase}}$ **Fructose-6-phosphate** + P

$$\Delta G^{\circ\prime} = -16.7 \text{ kJ/mol}$$
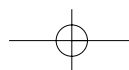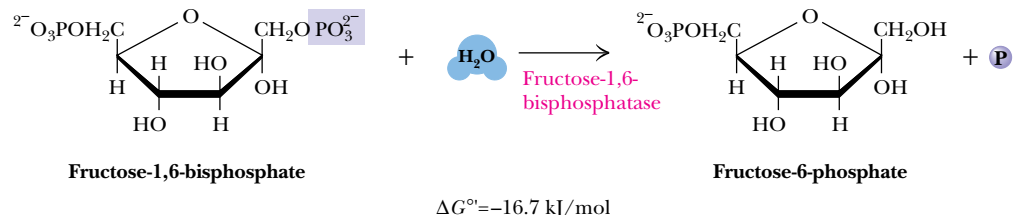
FIGURE 23.7 • The fructose-1,6-bisphosphatase reaction.

(4) Glucose-6-Phosphatase

The final step in the gluconeogenesis pathway is the conversion of glucose-6-phosphate to glucose by the action of **glucose-6-phosphatase.** This enzyme is present in the membranes of the endoplasmic reticulum of liver and kidney cells, but is absent in muscle and brain. For this reason, gluconeogenesis is not carried out in muscle and brain. Its membrane association is important to its function because (Figure 23.8) the substrate is hydrolyzed as it passes into the endoplasmic reticulum itself. Vesicles form from the endoplasmic reticulum membrane and diffuse to the plasma membrane and fuse with it, releasing their glucose contents into the bloodstream. The glucose-6-phosphatase reaction involves a phosphorylated enzyme intermediate, which may be a phosphohistidine (Figure 23.9). The ΔG for the glucose-6-phosphatase reaction in liver is -5.1 kJ/mol.

COUPLING WITH HYDROLYSIS OF ATP AND GTP DRIVES GLUCONEOGENESIS The net reaction for the conversion of pyruvate to glucose in gluconeogenesis is

$$2 \text{ Pyruvate} + 4 \text{ ATP} + 2 \text{ GTP} + 2 \text{ NADH} + 2 \text{ H}^+ + 6 \text{ H}_2\text{O}$$
$$\downarrow$$
$$\text{glucose} + 4 \text{ ADP} + 2 \text{ GDP} + 6 \text{ P}_i + 2 \text{ NAD}^+$$
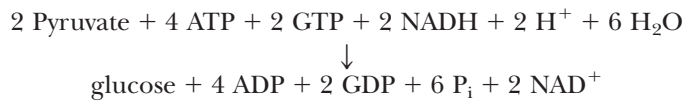
The net free energy change, $\Delta G^{\circ\prime}$, for this conversion is -37.7 kJ/mol. The consumption of a total of six nucleoside triphosphates drives this process forward. If glycolysis were merely reversed to achieve the net synthesis of glucose from pyruvate, the net reaction would be

$$2 \text{ Pyruvate} + 2 \text{ ATP} + 2 \text{ NADH} + 2 \text{ H}^+ + 2 \text{ H}_2\text{O}$$
$$\downarrow$$
$$\text{glucose} + 2 \text{ ADP} + 2 \text{ P}_i + 2 \text{ NAD}^+$$
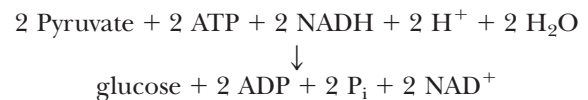
and the overall $\Delta G^{\circ\prime}$ would be about $+74$ kJ/mol. Such a process would be highly endergonic, and therefore thermodynamically unfeasible. Hydrolysis of four additional high-energy phosphate bonds makes gluconeogenesis thermodynamically favorable. Under physiological conditions, however, gluconeogenesis is somewhat less favorable than at standard state, with an overall ΔG of -15.6 kJ/mol for the conversion of pyruvate to glucose.

FIGURE 23.8 • Glucose-6-phosphatase is localized in the endoplasmic reticulum membrane. Conversion of glucose-6-phosphate to glucose occurs during transport into the ER.
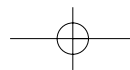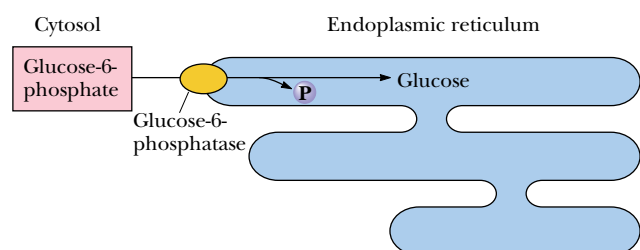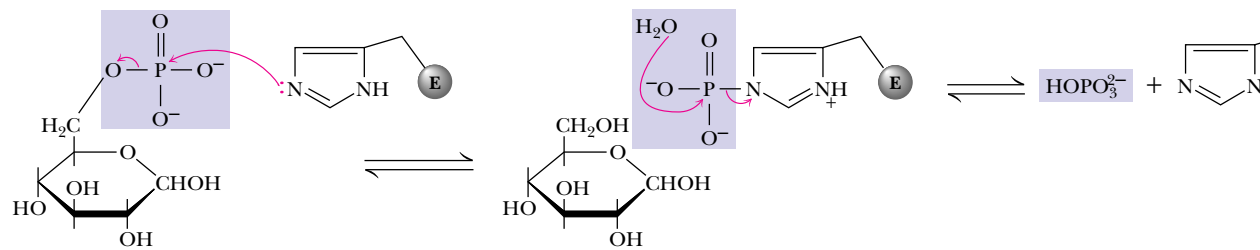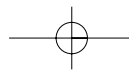
FIGURE 23.9 • The glucose-6-pho
reaction involves formation of a pho
dine intermediate.

LACTATE FORMED IN MUSCLES IS RECYCLED TO GLUCOSE IN THE LIVER   A final point on the redistribution of lactate and glucose in the body serves to emphasize the metabolic interactions between organs. Vigorous exercise can lead to oxygen shortage (anaerobic conditions), and energy requirements must be met by increased levels of glycolysis. Under such conditions, glycolysis converts NAD^+ to NADH, yet O_2 is unavailable for regeneration of NAD^+ via cellular respiration. Instead, large amounts of NADH are reoxidized by the reduction of pyruvate to lactate. The lactate thus produced can be transported from muscle to the liver, where it is reoxidized by liver lactate dehydrogenase to yield pyruvate, which is converted eventually to glucose. In this way, the liver shares in the metabolic stress created by vigorous exercise. It exports glucose to muscle, which produces lactate, which can be processed by the liver into new glucose. This is referred to as the **Cori cycle** (Figure 23.10). Liver, with a typically high NAD^+/NADH ratio (about 700), readily produces more glucose than it can use. Muscle that is vigorously exercising will enter anaerobiosis and show a decreasing NAD^+/NADH ratio, which favors reduction of pyruvate to lactate.
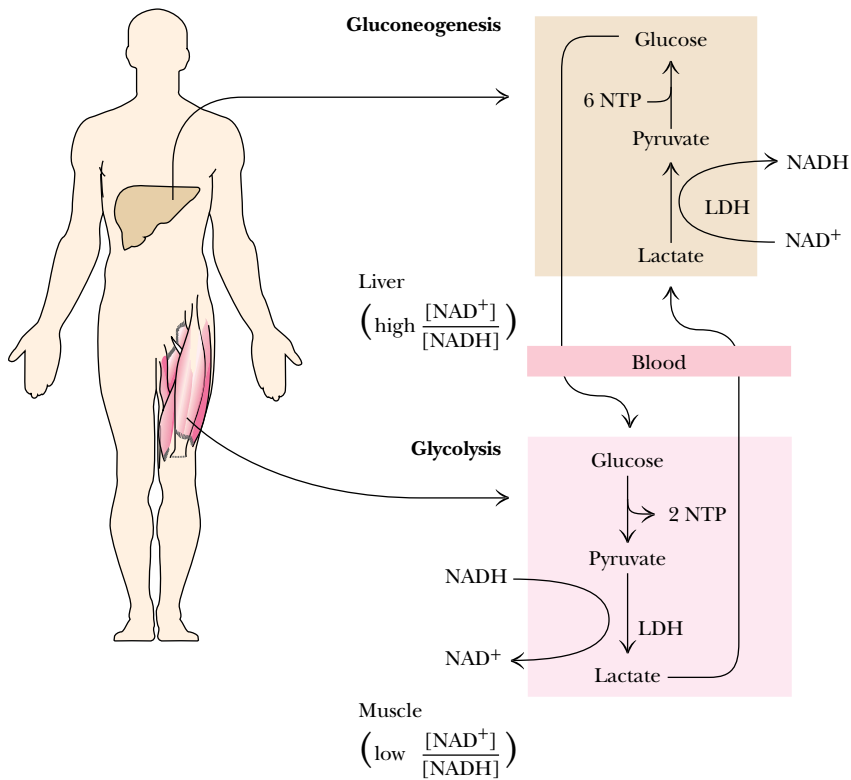
FIGURE 23.10 • The Cori cycle.
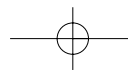
CRITICAL DEVELOPMENTS IN BIOCHEMISTRY

The Pioneering Studies of Carl and Gerty Cori

The Cori cycle is named for Carl and Gerty Cori, who received the Nobel Prize in physiology or medicine in 1947 for their studies of glycogen metabolism and blood glucose regulation. Carl Ferdinand Cori and Gerty Theresa Radnitz were both born in Prague (then in Austria). They earned medical degrees from the German University of Prague in 1920 and were married later that year. They joined the faculty of the Washington University School of Medicine in St. Louis in 1931. Their remarkable collaboration resulted in many fundamental advances in carbohydrate and glycogen metabolism. They were credited with the discovery of glucose-1-phosphate, also known at the time as the "Cori ester."

They also showed that glucose-6-phosphate was produced from glucose-1-P by the action of phosphoglucomutase. They isolated and crystallized glycogen phosphorylase and elucidated the pathway of glycogen breakdown. In 1952, they showed that absence of glucose-6-phosphatase in the liver was the enzymatic defect in *von Gierke's disease,* an inherited glycogen-storage disease. Six eventual Nobel laureates received training in their laboratory. Gerty Cori was the first American woman to receive a Nobel prize. Carl Cori said of their remarkable collaboration: "Our efforts have been largely complementary and one without the other would not have gone so far. . . ."

23.2 • Regulation of Gluconeogenesis

Nearly all of the reactions of glycolysis and gluconeogenesis take place in the cytosol. If metabolic control were not exerted over these reactions, glycolytic degradation of glucose and gluconeogenic synthesis of glucose could operate simultaneously, with no net benefit to the cell and with considerable consumption of ATP. This is prevented by a sophisticated system of **reciprocal control,** so that glycolysis is inhibited when gluconeogenesis is active, and vice versa. Reciprocal regulation of these two pathways depends largely on the energy status of the cell. When the energy status of the cell is low, glucose is rapidly degraded to produce needed energy. When the energy status is high, pyruvate and other metabolites are utilized for synthesis (and storage) of glucose.

In glycolysis, the three regulated enzymes are those catalyzing the strongly exergonic reactions: hexokinase (glucokinase), phosphofructokinase, and pyruvate kinase. As noted, the gluconeogenic pathway replaces these three reactions with corresponding reactions that are exergonic in the direction of glucose synthesis: glucose-6-phosphatase, fructose-1,6-bisphosphatase, and the pyruvate carboxylase–PEP carboxykinase pair, respectively. These are the three most appropriate sites of regulation in gluconeogenesis.

Gluconeogenesis Is Regulated by Allosteric and Substrate-Level Control Mechanisms

The mechanisms of regulation of gluconeogenesis are shown in Figure 23.11. Control is exerted at all of the predicted sites, but in different ways. Glucose-6-phosphatase is not under allosteric control. However, the K_m for the substrate, glucose-6-phosphate, is considerably higher than the normal range of substrate concentrations. As a result, glucose-6-phosphatase displays a near-linear dependence of activity on substrate concentrations and is thus said to be under **substrate-level control** by glucose-6-phosphate.

Acetyl-CoA is a potent allosteric effector of glycolysis and gluconeogenesis. It allosterically inhibits pyruvate kinase (as noted in Chapter 19) and activates pyruvate carboxylase. Because it also allosterically inhibits pyruvate dehydrogenase (the enzymatic link between glycolysis and the TCA cycle), the cellular fate of pyruvate is strongly dependent on acetyl-CoA levels. A rise in
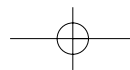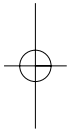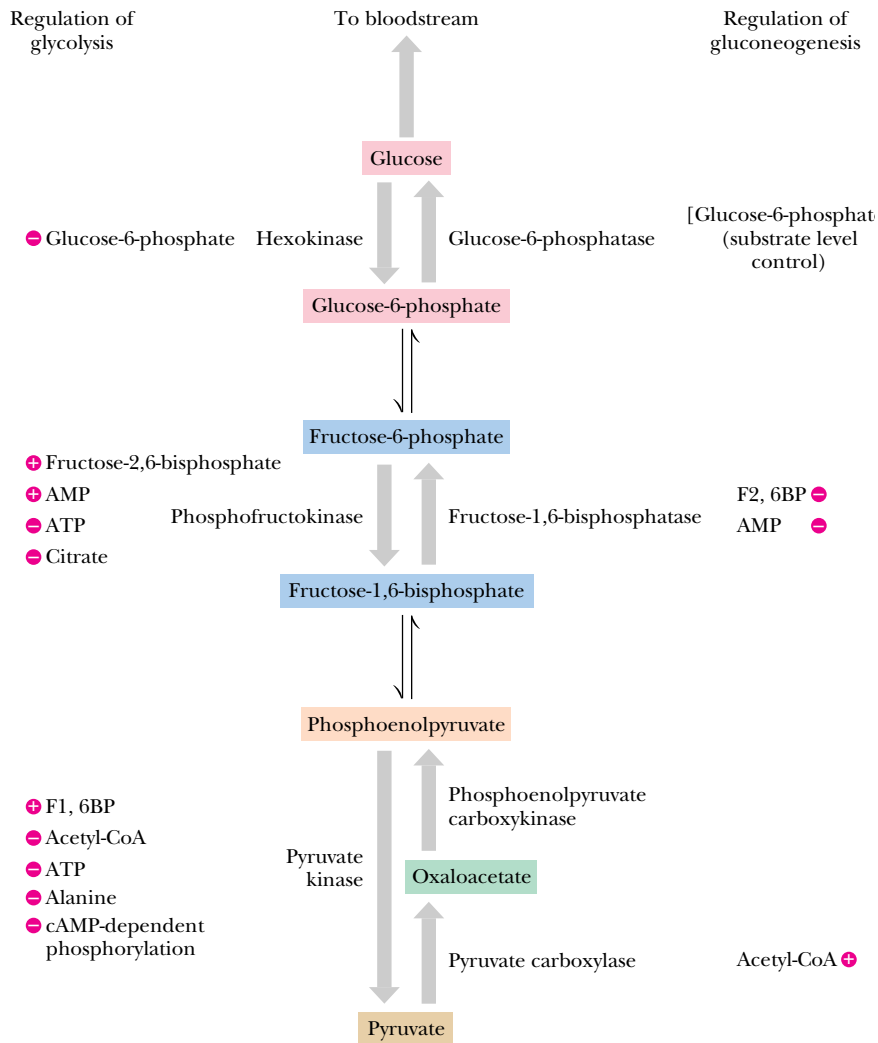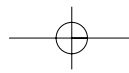
FIGURE 23.11 • The principal re
mechanisms in glycolysis and glucon
Activators are indicated by plus sign
inhibitors by minus signs.

[acetyl-CoA] indicates that cellular energy levels are high and that carbon metabolites can be directed to glucose synthesis and storage. When acetyl-CoA levels drop, the activities of pyruvate kinase and pyruvate dehydrogenase increase and flux through the TCA cycle increases, providing needed energy for the cell.

Fructose-1,6-bisphosphatase is another important site of gluconeogenic regulation. This enzyme is inhibited by AMP and activated by citrate. These effects by AMP and citrate are the opposites of those exerted on phosphofructokinase in glycolysis, providing another example of reciprocal regulatory effects. When AMP levels increase, gluconeogenic activity is diminished and glycolysis is stimulated. An increase in citrate concentration signals that TCA cycle activity can be curtailed and that pyruvate should be directed to sugar synthesis instead.

Fructose-2,6-Bisphosphate—Allosteric Regulator of Gluconeogenesis

As described in Chapter 19, Emile Van Schaftingen and Henri-Géry Hers demonstrated in 1980 that fructose-2,6-bisphosphate is a potent stimulator of phosphofructokinase. Cognizant of the reciprocal nature of regulation in glycolysis and gluconeogenesis, Van Schaftingen and Hers also considered the

Fructose-2,6-biphosphate
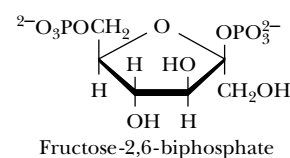
possibility of an opposite effect—inhibition—for fructose-1,6-bisphosphatase. In 1981 they reported that fructose-2,6-bisphosphate was indeed a powerful inhibitor of fructose-1,6-bisphosphatase (Figure 23.12). Inhibition occurs in either the presence or absence of AMP, and the effects of AMP and fructose-2,6-bisphosphate are synergistic.

Cellular levels of fructose-2,6-bisphosphate are controlled by **phospho-fructokinase-2 (PFK-2),** an enzyme distinct from the phosphofructokinase of the glycolytic pathway, and by **fructose-2,6-bisphosphatase (F-2,6-BPase).** Remarkably, these two enzymatic activities are both found in the same protein molecule, which is an example of a **bifunctional,** or **tandem, enzyme** (Figure 23.13). The opposing activities of this bifunctional enzyme are themselves regulated in two ways. First, fructose-6-phosphate, the substrate of phosphofructokinase and the product of fructose-1,6-bisphosphatase, allosterically activates PFK-2 and inhibits F-2,6-BPase. Second, the phosphorylation by **cAMP-dependent protein kinase** of a single Ser residue on the 49-kD subunit of this dimeric enzyme exerts reciprocal control of the PFK-2 and F-2,6-BPase activities. Phosphorylation then inhibits PFK-2 activity (by increasing the K_m for fructose-6-phosphate) and stimulates F-2,6-BPase activity.

Substrate Cycles Provide Metabolic Control Mechanisms

If fructose-1,6-bisphosphatase and phosphofructokinase acted simultaneously, they would constitute a **substrate cycle** in which fructose-1,6-bisphosphate and fructose-6-phosphate became interconverted with net consumption of ATP:

$$\text{Fructose-1,6-bisP} + H_2O \longrightarrow \text{fructose-6-P} + P_i$$
$$\underline{\text{Fructose-6-P} + ATP \longrightarrow \text{fructose-1,6-bisP} + ADP}$$
$$Net: \qquad ATP + H_2O \longrightarrow ADP + P_i$$
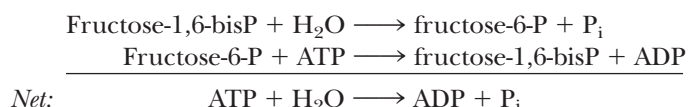
Because substrate cycles such as this appear to operate with no net benefit to the cell, they were once regarded as metabolic quirks and were referred to as *futile cycles.* More recently, substrate cycles have been recognized as important devices for controlling metabolite concentrations.
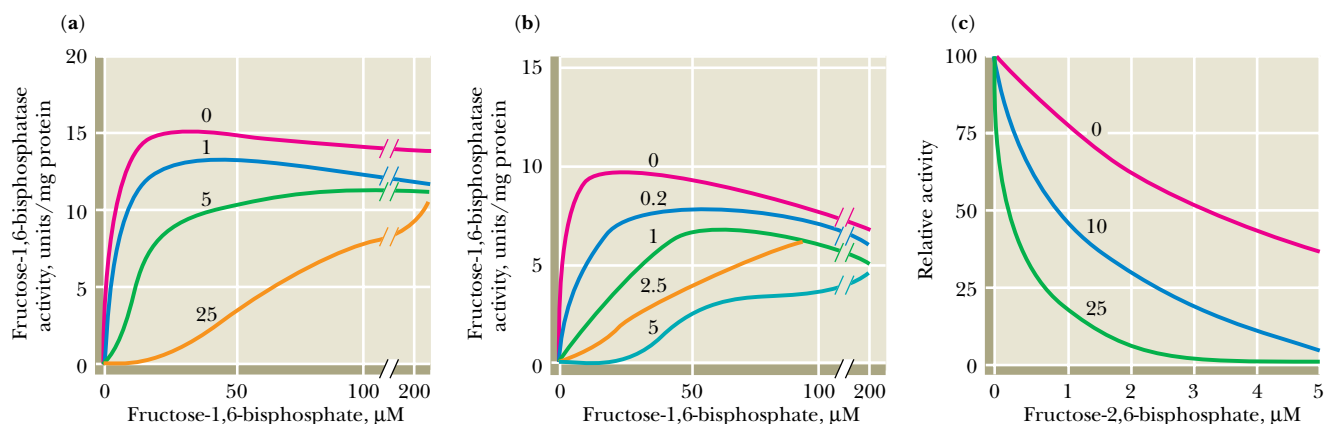
FIGURE 23.12 • Inhibition of fructose-1,6-bisphosphatase by fructose-2,6-bisphosphate in the (a) absence and (b) presence of 25 μM AMP. In (a) and (b), enzyme activity is plotted against substrate (fructose-1,6-bisphosphate) concentration. Concentrations of fructose-2,6-bisphosphate (in μM) are indicated above each curve. (c) The effect of AMP (0, 10, and 25 μM) on the inhibition of fructose-1,6-bisphosphatase by fructose-2,6-bisphosphate. Activity was measured in the presence of 10 μM fructose-1,6-bisphosphate. *(Adapted from Van Schaftingen, E., and Hers, H.-G., 1981. Inhibition of fructose-1,6-bisphosphatase by fructose-2,6-bisphosphate. Proceedings of the National Academy of Science, USA **78:**2861–2863.)*
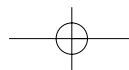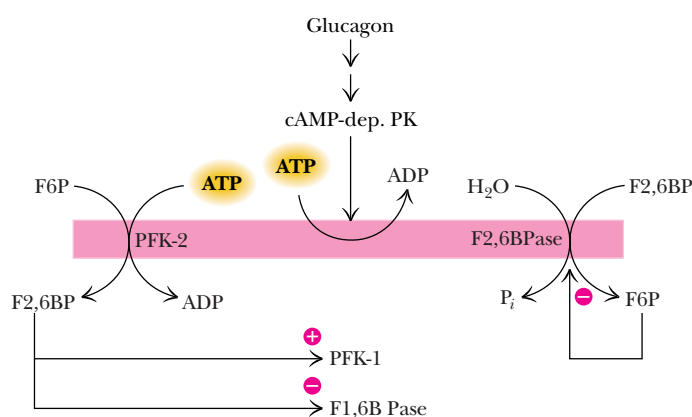
FIGURE 23.13 • Synthesis and de
of fructose-2,6-bisphosphate are cata
the same bifunctional enzyme.

The three steps in glycolysis and gluconeogenesis that differ constitute three such substrate cycles, each with its own particular metabolic *raison d'être*. Consider, for example, the regulation of the fructose-1,6-bisP–fructose-6-P cycle by fructose-2,6-bisphosphate. As already noted, fructose-1,6-bisphosphatase is subject to allosteric inhibition by fructose-2,6-bisphosphate, whereas phospho-fructokinase is allosterically activated by fructose-2,6-bisP. The combination of these effects should permit *either* phosphofructokinase *or* fructose-1,6-bisphos-phatase (but not both) to operate at any one time and should thus prevent futile cycling. For instance, in the **fasting state,** when food (i.e., glucose) intake is zero, phosphofructokinase (and therefore glycolysis) is inactive due to the low concentration of fructose-2,6-bisphosphate. In the liver, gluconeogenesis operates to provide glucose for the brain. However, in the fed state, up to 30% of fructose-1,6-bisphosphate formed from phosphofructokinase is recycled back to fructose-6-P (and then to glucose). Because the dependence of fruc-tose-1,6-bisphosphatase activity on fructose-1,6-bisphosphate is sigmoidal in the presence of fructose-2,6-bisphosphate (Figure 23.12), substrate cycling occurs only at relatively high levels of fructose-1,6-bisphosphate. Substrate cycling in this case prevents the accumulation of excessively high levels of fructose-1,6-bisphosphate.

23.3 • Glycogen Catabolism

Dietary Glycogen and Starch Breakdown

As noted earlier, well-fed adult human beings normally metabolize about 160 g of carbohydrates each day. A balanced diet easily provides this amount, mostly in the form of starch, with smaller amounts of glycogen. If too little carbohy-drate is supplied by the diet, glycogen reserves in liver and muscle tissue can also be mobilized. The reactions by which ingested starch and glycogen are digested are shown in Figure 23.14. The enzyme known as **α-amylase** is an important component of saliva and pancreatic juice. (**β-Amylase** is found in plants. The α- and β-designations for these enzymes serve only to distinguish the two, and do not refer to glycosidic linkage nomenclature.) α-Amylase is an *endoglycosidase* that hydrolyzes α-(1 → 4) linkages of amylopectin and glycogen at random positions, eventually producing a mixture of maltose, maltotriose [with three α-(1 → 4)-linked glucose residues], and other small oligosaccha-rides. α-Amylase can cleave on either side of a glycogen or amylopectin branch point, but activity is reduced in highly branched regions of the polysaccharide and stops four residues from any branch point.
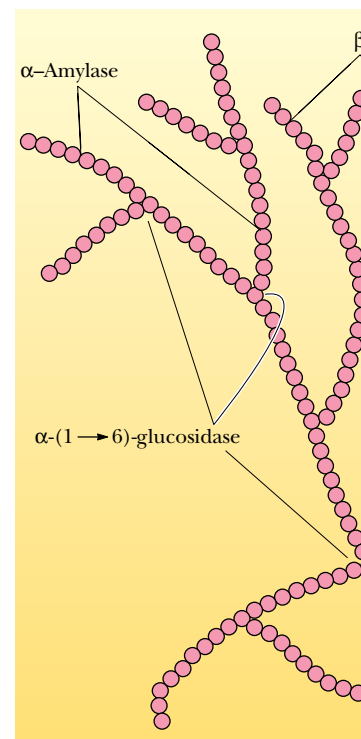
FIGURE 23.14 • Hydrolysis of glyc
starch by α-amylase and β-amylase.
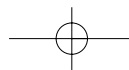
The highly branched polysaccharides that are left after extensive exposure to α-amylase are called **limit dextrins.** These structures can be further degraded by the action of a **debranching enzyme,** which carries out two distinct reactions. The first of these, known as **oligo(α1,4 → α1,4) glucantransferase** activity, removes a trisaccharide unit and transfers this group to the end of another, nearby branch (Figure 23.15). This leaves a single glucose residue in α-(1 → 6) linkage to the main chain. The **α-(1 → 6) glucosidase** activity of the debranching enzyme then cleaves this residue from the chain, leaving a polysaccharide chain with one branch fewer. Repetition of this sequence of events leads to complete degradation of the polysaccharide.

β-Amylase is an *exoglycosidase* that cleaves maltose units from the free, nonreducing ends of amylopectin branches, as in Figure 23.14. Like α-amylase, however, β-amylase does not cleave either the α-(1 → 6) bonds at the branch points or the α-(1 → 4) linkages near the branch points.

Metabolism of Tissue Glycogen

Digestion itself is a highly efficient process in which almost 100% of ingested food is absorbed and metabolized. Digestive breakdown of starch and glycogen is an unregulated process. On the other hand, tissue glycogen represents an important reservoir of potential energy, and it should be no surprise that the reactions involved in its degradation and synthesis are carefully controlled and regulated. Glycogen reserves in liver and muscle tissue are stored in the cytosol as granules exhibiting a molecular weight range from 6×10^6 to 1600×10^6. These granular aggregates contain the enzymes required to synthesize and catabolize the glycogen, as well as all the enzymes of glycolysis.

FIGURE 23.15 • The reactions of glycogen debranching enzyme. Transfer of a group of three α-(1 → 4)-linked glucose residues from a limit branch to another branch is followed by cleavage of the α-(1 → 6) bond of the residue that remains at the branch point.

Limit branch

Limit dextrin

Glycogen debranching enzyme

α–(1→6)-glucosidase activity of debranching enzyme cleaves this residue

Further cleavage by α-amylase
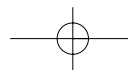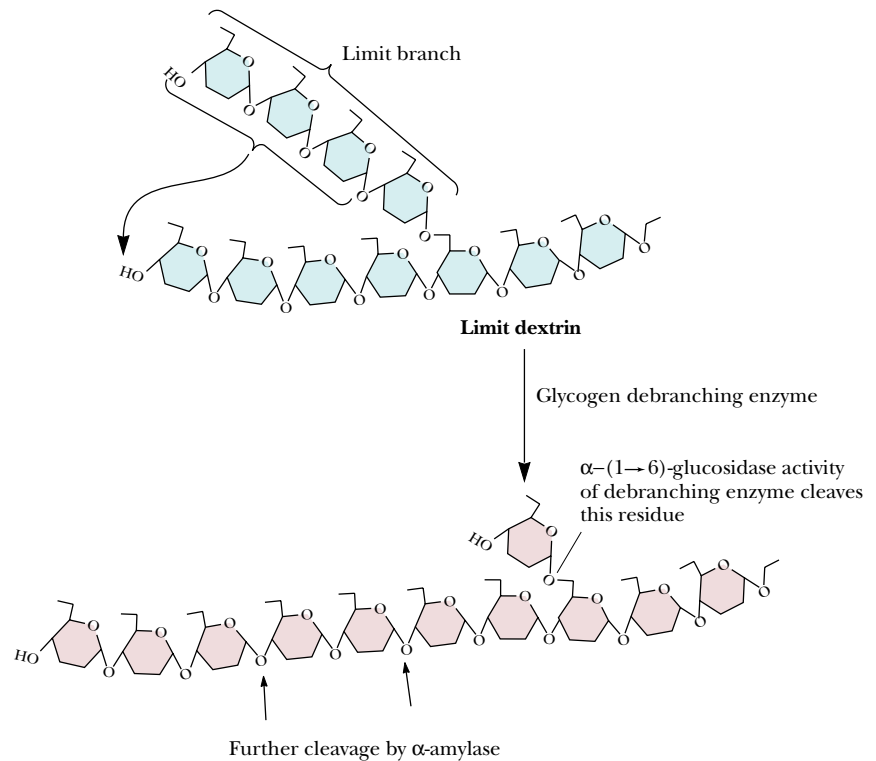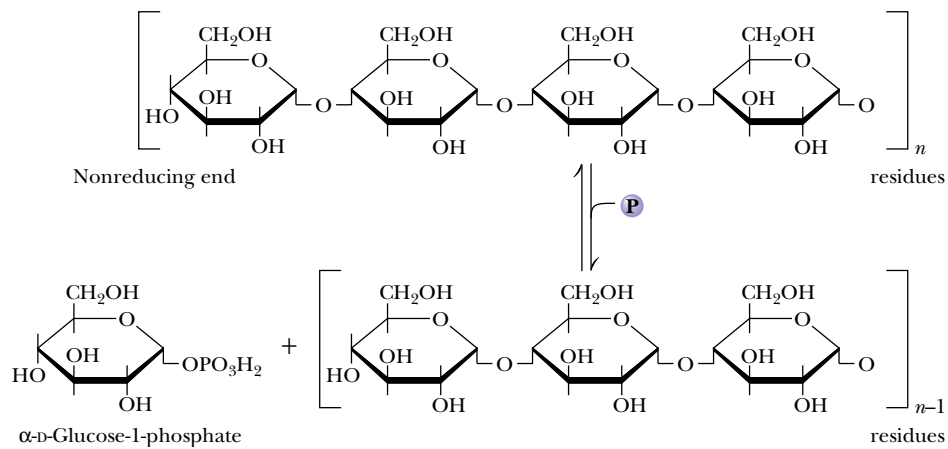
FIGURE 23.16 • The glycogen phosphorylase reaction.

The principal enzyme of glycogen catabolism is **glycogen phosphorylase,** a highly regulated enzyme that was discussed extensively in Chapter 15. The glycogen phosphorylase reaction (Figure 23.16) involves phosphorolysis at a nonreducing end of a glycogen polymer. The standard-state free energy change for this reaction is +3.1 kJ/mol, but the intracellular ratio of $[P_i]$ to [glucose-1-P] approaches 100, and thus the actual ΔG *in vivo* is approximately -6 kJ/mol. There is an energetic advantage to the cell in this phosphorolysis reaction. If glycogen breakdown were hydrolytic and yielded glucose as a product, it would be necessary to phosphorylate the product glucose (with the expenditure of a molecule of ATP) to initiate its glycolytic degradation.

The glycogen phosphorylase reaction degrades glycogen to produce limit dextrins, which are further degraded by debranching enzyme, as already described.

23.4 • Glycogen Synthesis

Animals synthesize and store glycogen when glucose levels are high, but the synthetic pathway is not merely a reversal of the glycogen phosphorylase reaction. High levels of phosphate in the cell favor glycogen breakdown and prevent the phosphorylase reaction from synthesizing glycogen *in vivo,* in spite of the fact that $\Delta G^{\circ\prime}$ for the phosphorylase reaction actually favors glycogen synthesis. Hence, another reaction pathway must be employed in the cell for the net synthesis of glycogen. In essence, this pathway must activate glucose units for transfer to glycogen chains.

Glucose Units Are Activated for Transfer by Formation of Sugar Nucleotides

We are familiar with several examples of chemical activation as a strategy for group transfer reactions. Acetyl-CoA is an activated form of acetate, biotin and tetrahydrofolate activate one-carbon groups for transfer, and ATP is an activated form of phosphate. Luis Leloir, a biochemist in Argentina, showed in the 1950s that glycogen synthesis depended upon **sugar nucleotides,** which may be

**Uridine diphosphate glucose
(UDPG)**
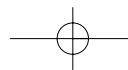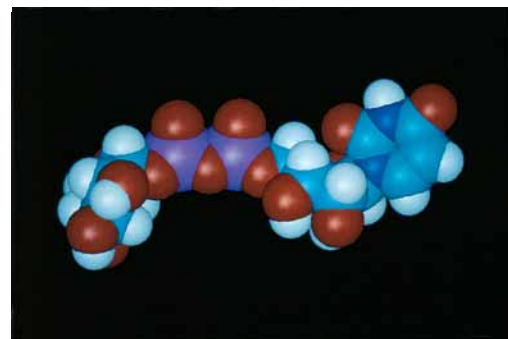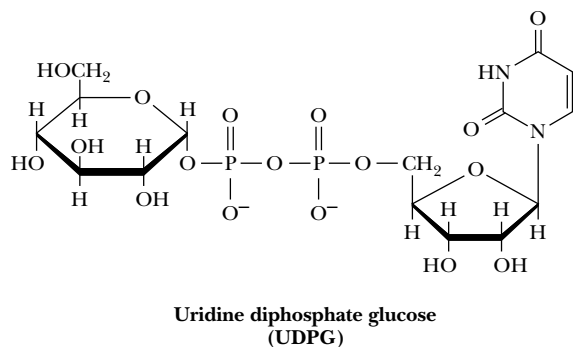
FIGURE 23.17 • The structure of UDP-glucose, a sugar nucleotide.

thought of as activated forms of sugar units (Figure 23.17). For example, formation of an ester linkage between the C-1 hydroxyl group and the β-phosphate of UDP activates the glucose moiety of **UDP-glucose.**

UDP-Glucose Synthesis Is Driven by Pyrophosphate Hydrolysis

Sugar nucleotides are formed from sugar-1-phosphates and nucleoside triphosphates by specific **pyrophosphorylase** enzymes (Figure 23.18). For example, **UDP-glucose pyrophosphorylase** catalyzes the formation of UDP-glucose from glucose-1-phosphate and uridine 5′-triphosphate:

$$\text{Glucose-1-P} + \text{UTP} \longrightarrow \text{UDP-glucose} + \text{pyrophosphate}$$

FIGURE 23.18 • The UDP-glucose pyrophosphorylase reaction is a phosphoanhydride exchange, with a phosphoryl oxygen of glucose-1-P attacking the α-phosphorus of UTP to form UDP-glucose and pyrophosphate.
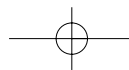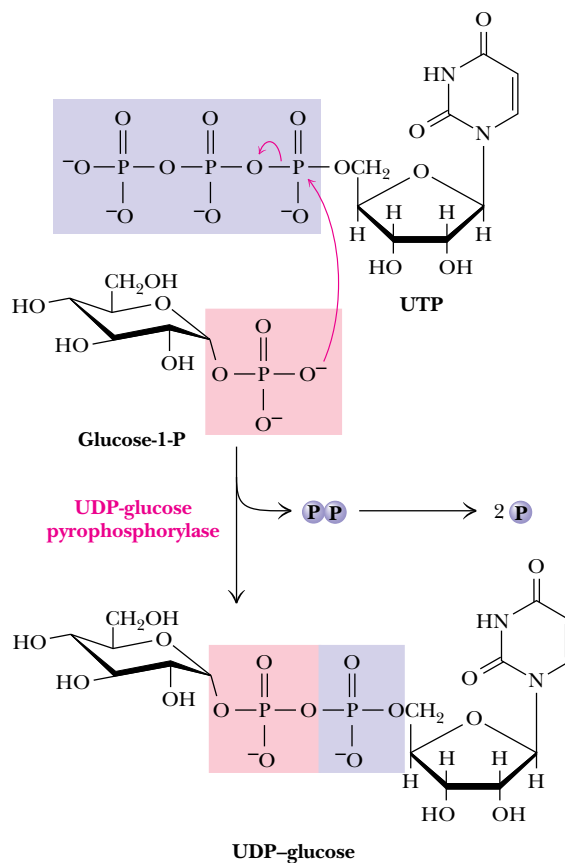
The reaction proceeds via attack by a phosphate oxygen of glucose-1-phosphate on the α-phosphorus of UTP, with departure of the pyrophosphate anion. The reaction is a reversible one, but—as is the case for many biosynthetic reactions—it is driven forward by subsequent hydrolysis of pyrophosphate:

$$\text{Pyrophosphate} + \text{H}_2\text{O} \longrightarrow 2\ \text{P}_i$$
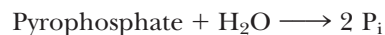
The net reaction for sugar nucleotide formation (combining the preceding two equations) is thus

$$\text{Glucose-1-P} + \text{UTP} + \text{H}_2\text{O} \longrightarrow \text{UDP-glucose} + 2\ \text{P}_i$$
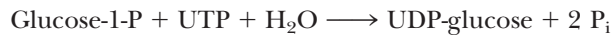
Sugar nucleotides of this type act as donors of sugar units in the biosynthesis of oligo- and polysaccharides. In animals, UDP-glucose is the donor of glucose units for glycogen synthesis, but ADP-glucose is the glucose source for starch synthesis in plants.

Glycogen Synthase Catalyzes Formation of α-(1 → 4) Glycosidic Bonds in Glycogen

The very large glycogen polymer is built around a tiny protein core. The first glucose residue is covalently joined to the protein **glycogenin** via an acetal linkage to a tyrosine–OH group on the protein. Sugar units are added to the glycogen polymer by the action of **glycogen synthase.** The reaction involves transfer of a glucosyl unit from UDP-glucose to the C-4 hydroxyl group at a nonreducing end of a glycogen strand. The mechanism proceeds by cleavage of the C—O bond between the glucose moiety and the β-phosphate of UDP-glucose, leaving an oxonium ion intermediate, which is rapidly attacked by the C-4 hydroxyl oxygen of a terminal glucose unit on glycogen (Figure 23.19). The reaction is exergonic and has a $\Delta G^{\circ\prime}$ of -13.3 kJ/mol.
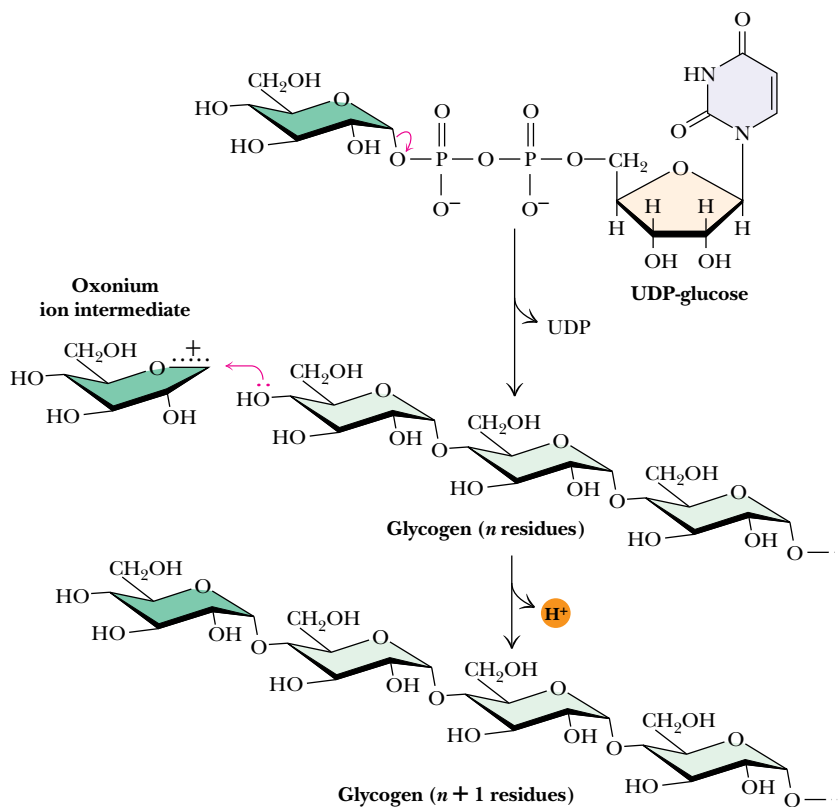
FIGURE 23.19 • The glycogen syn
tion. Cleavage of the C—O bond of
cose yields an oxonium intermediat
the hydroxyl oxygen of the termina
a glycogen molecule completes the

(1 →4)-terminal
chains of glycogen

Branching
enzyme
cuts here...

...and transfers
a seven residue
terminal segment
to a C(6)–OH
group
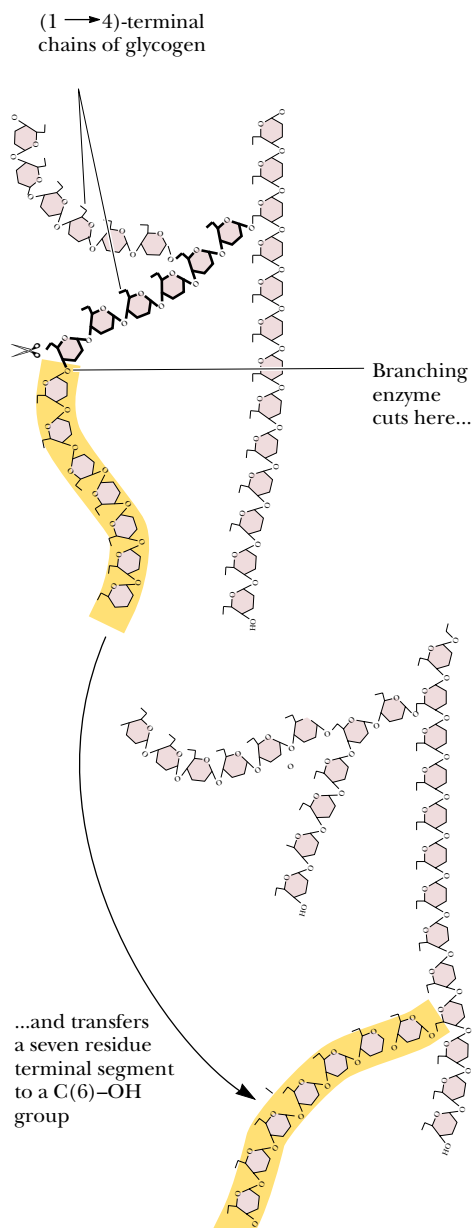
FIGURE 23.20 • Formation of glycogen branches by the branching enzyme. Six- or seven-residue segments of a growing glycogen chain are transferred to the C-6 hydroxyl group of a glucose residue on the same or a nearby chain.

Glycogen Branching Occurs by Transfer of Terminal Chain Segments

Glycogen is a branched polymer of glucose units. The branches arise from α-$(1 \rightarrow 6)$ linkages which occur every 8 to 12 residues. As noted in Chapter 7, the branches provide multiple sites for rapid degradation or elongation of the polymer and also increase its solubility. Glycogen branches are formed by **amylo-(1,4 → 1,6)-transglycosylase,** also known as *branching enzyme*. The reaction involves the transfer of a six- or seven-residue segment from the nonreducing end of a linear chain at least 11 residues in length to the C-6 hydroxyl of a glucose residue of the same chain or another chain (Figure 23.20). For each branching reaction, the resulting polymer has gained a new terminus at which growth can occur.

23.5 • Control of Glycogen Metabolism

Glycogen Metabolism Is Highly Regulated

Synthesis and degradation of glycogen must be carefully controlled so that this important energy reservoir can properly serve the metabolic needs of the organism. Glucose is the principal metabolic fuel for the brain, and the concentration of glucose in circulating blood must be maintained at about 5 mM for this purpose. Glucose derived from glycogen breakdown is also a primary energy source for muscle contraction. Control of glycogen metabolism is effected via reciprocal regulation of glycogen phosphorylase and glycogen synthase. Thus, activation of glycogen phosphorylase is tightly linked to inhibition of glycogen synthase, and vice versa. Regulation involves both allosteric control and covalent modification, with the latter being under hormonal control. The regulation of glycogen phosphorylase is discussed in detail in Chapter 15.

Regulation of Glycogen Synthase by Covalent Modification

Glycogen synthase also exists in two distinct forms which can be interconverted by the action of specific enzymes: active, dephosphorylated **glycogen synthase I** (glucose-6-P-independent) and less active phosphorylated **glycogen synthase D** (glucose-6-P-dependent). The nature of phosphorylation is more complex with glycogen synthase. As many as nine serine residues on the enzyme appear to be subject to phosphorylation, each site's phosphorylation having some effect on enzyme activity.
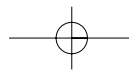
Dephosphorylation of both glycogen phosphorylase and glycogen synthase is carried out by **phosphoprotein phosphatase 1.** The action of phosphoprotein phosphatase 1 inactivates glycogen phosphorylase and activates glycogen synthase.

Hormones Regulate Glycogen Synthesis and Degradation

Storage and utilization of tissue glycogen, maintenance of blood glucose concentration, and other aspects of carbohydrate metabolism are meticulously regulated by hormones, including *insulin, glucagon, epinephrine,* and the *glucocorticoids.*

Insulin Is a Response to Increased Blood Glucose

The primary hormone responsible for conversion of glucose to glycogen is **insulin** (Figure 6.36). Insulin is secreted by special cells in the pancreas called the **islets of Langerhans.** *Secretion of insulin is a response to increased glucose in the*

A DEEPER LOOK

Carbohydrate Utilization in Exercise

Animals have a remarkable ability to "shift gears" metabolically during periods of strenuous exercise or activity. Metabolic adaptations allow the body to draw on different sources of energy (all of which produce ATP) for different types of activity. During periods of short-term, high-intensity exercise (e.g., a 100-m dash), most of the required energy is supplied directly by existing stores of ATP and creatine phosphate (Figure, part a). Long-term, low-intensity exercise (a 10-km run or a 42.2-km marathon) is fueled almost entirely by aerobic metabolism. Between these extremes is a variety of activities (an 800-m run, for example) that rely on anaerobic glycolysis—conversion of glucose to lactate in the muscles and utilization of the Cori cycle.

For all these activities, breakdown of muscle glycogen provides much of the needed glucose. The rate of glycogen con-

sumption depends upon the intensity of the exercise (... b). By contrast, glucose derived from gluconeogenesis ... small contributions to total glucose consumed duri ... During prolonged mild exercise, gluconeogenesis a ... only about 8% of the total glucose consumed. During ... cise, this percentage becomes even lower.

Choice of diet has a dramatic effect on glycogen r ... lowing exhaustive exercise. A diet consisting mainly ... and fat results in very little recovery of muscle gly ... after 5 days (Figure, part c). On the other hand, a hi ... drate diet provides faster restoration of muscle glycog ... this case, however, complete recovery of glycogen ... about 2 days.

(a) Contributions of the various energy sources to muscle activity during mild exercise. (b) Consumption of glycogen stores in fast-twitch muscles during light, moderate, and heavy exercise. (c) Rate of glycogen replenishment following exhaustive exercise. *(a and c adapted from Rhodes and Pflanzer, 1992. Human Physiology. Philadelphia: Saunders College Publishing; b adapted from Horton and Terjung, 1988. Exercise, Nutrition and Energy Metabolism. New York: Macmillan.)*
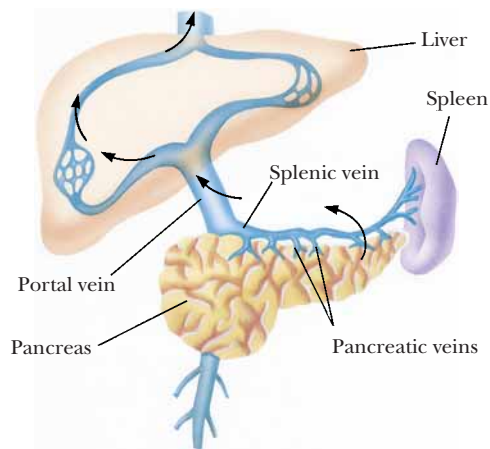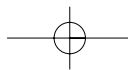
FIGURE 23.21 • The portal vein system carries pancreatic secretions such as insulin and glucagon to the liver and then into the rest of the circulatory system.

blood. When blood glucose levels rise (after a meal, for example), insulin is secreted from the pancreas into the *pancreatic vein,* which empties into the **portal vein system** (Figure 23.21), so that insulin traverses the liver before it enters the systemic blood supply. Insulin acts to rapidly lower blood glucose concentration in several ways. Insulin stimulates glycogen synthesis and inhibits glycogen breakdown in liver and muscle.

Several other physiological effects of insulin also serve to lower blood and tissue glucose levels (Figure 23.22). Insulin stimulates the active transport of glucose (and amino acids) across the plasma membranes of muscle and adipose tissue. Insulin also increases cellular utilization of glucose by inducing the synthesis of several important glycolytic enzymes, namely, glucokinase, phosphofructokinase, and pyruvate kinase. In addition, insulin acts to inhibit several enzymes of gluconeogenesis. These various actions enable the organism to respond quickly to increases in blood glucose levels.

Glucagon and Epinephrine Stimulate Glycogen Breakdown

Catabolism of tissue glycogen is triggered by the actions of the hormones **epinephrine** and **glucagon** (Figure 23.23). *In response to decreased blood glucose,* glucagon is released from the α cells in pancreatic islets of Langerhans. This peptide hormone travels through the blood to specific receptors on liver cell membranes. (Glucagon is active in liver and adipose tissue, but not in other tissues.) Similarly, signals from the central nervous system cause release of *epinephrine* (Figure 23.24)—also known as adrenaline—from the adrenal glands into the bloodstream. Epinephrine acts on liver and muscles. When either hormone binds to its receptor on the outside surface of the cell membrane, a cascade is initiated that activates glycogen phosphorylase and inhibits glycogen synthase. The result of these actions is *tightly coordinated stimulation of glycogen breakdown and inhibition of glycogen synthesis.*
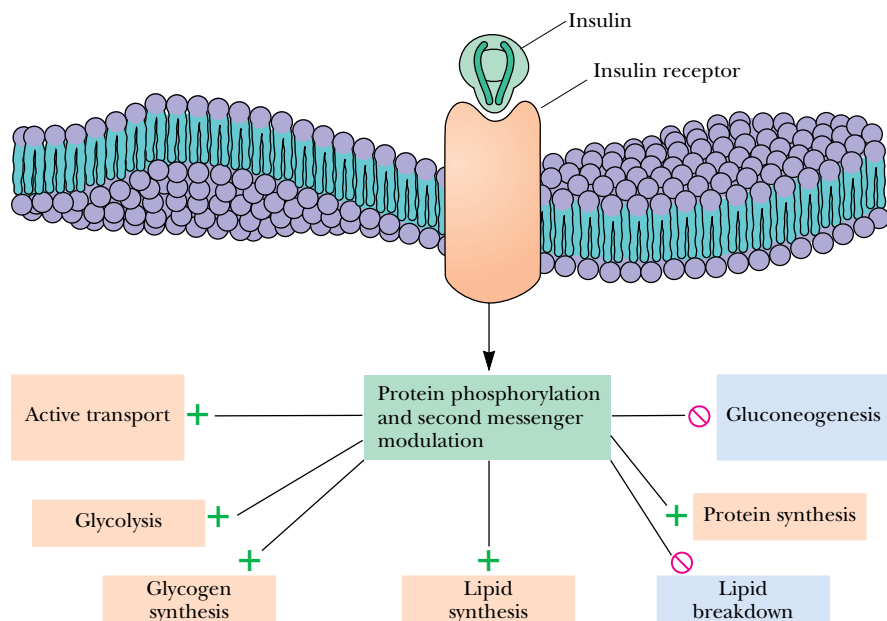
FIGURE 23.22 • The metabolic effects of insulin. As described in Chapter 34, binding of insulin to membrane receptors stimulates the protein kinase activity of the receptor. Subsequent phosphorylation of target proteins modulates the effects indicated.
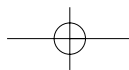
The Phosphorylase Cascade Amplifies the Hormonal Signal

Stimulation of glycogen breakdown involves consumption of molecules of ATP at three different steps in the hormone-sensitive adenylyl cyclase cascade (Figure 15.19). Note that the cascade mechanism is a means of chemical amplification, because the binding of just a few molecules of epinephrine or glucagon results in the synthesis of many molecules of cyclic AMP, which, through the action of cAMP-dependent protein kinase, can activate many more molecules of phosphorylase kinase and even more molecules of phosphorylase. For example, an extracellular level of 10^{-10} to 10^{-8} M epinephrine prompts the formation of 10^{-6} M cyclic AMP, and for each protein kinase activated by cyclic AMP, approximately 30 phosphorylase kinase molecules are activated; these in turn activate some 800 molecules of phosphorylase. Each of these catalyzes the formation of many molecules of glucose-1-P.

The Difference Between Epinephrine and Glucagon

Although both epinephrine and glucagon exert glycogenolytic effects, they do so for quite different reasons. Epinephrine is secreted as a response to anger or fear and may be viewed as an alarm or danger signal for the organism. Called the "fight or flight" hormone, it prepares the organism for mobilization of large amounts of energy. Among the many physiological changes elicited by epinephrine, one is the initiation of the enzyme cascade, as in Figure 15.19, which leads to rapid breakdown of glycogen, inhibition of glycogen synthesis, stimulation of glycolysis, and production of energy. The burst of energy produced is the result of a 2000-fold amplification of the rate of glycolysis. Because a fear or anger response must include generation of energy (in the form of glucose) —both immediately in localized sites (the muscles) and eventually throughout the organism (as supplied by the liver)—epinephrine must be able to activate glycogenolysis in both liver and muscles.

Glucagon is involved in the long-term maintenance of steady-state levels of glucose in the blood and other tissues. It performs this function by stimulating the liver to release glucose from glycogen stores into the bloodstream. To further elevate glucose levels, glucagon also activates liver gluconeogenesis. It is important to note, however, that stabilization of blood glucose levels is managed almost entirely by the liver. Glucagon does not activate the phosphorylase cascade in muscle (muscle membranes do not contain glucagon receptors). Muscle glycogen breakdown occurs only in response to epinephrine release, and muscle tissue does not participate in maintenance of steady-state glucose levels in the blood.

Cortisol and Glucocorticoid Effects on Glycogen Metabolism

Glucocorticoids are a class of steroid hormones that exert distinct effects on liver, skeletal muscle, and adipose tissue. The effects of cortisol, a typical glucocorticoid, are best described as *catabolic* because cortisol promotes protein breakdown and decreases protein synthesis in skeletal muscle. In the liver, however, it stimulates gluconeogenesis and increases glycogen synthesis. Cortisol-induced gluconeogenesis results primarily from increased conversion of amino acids into glucose (Figure 23.25). Specific effects of cortisol in the liver include increased gene expression of several of the enzymes of the gluconeogenic pathway, activation of enzymes involved in amino acid metabolism, and stimulation of the urea cycle, which disposes of nitrogen liberated during amino acid catabolism (Chapter 27).

H_3^+N —His — Ser — Glu — Gly —Th

Tyr — Lys — Ser — Ty
Leu
|
Asp
Ser —Arg — Arg —Ala

Leu — Trp — Gl
Met
|
Asn
Thr — COO⁻
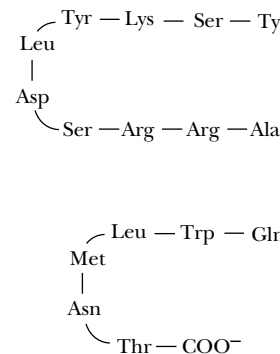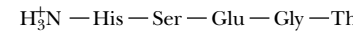
FIGURE 23.23 • The amino acid glucagon.
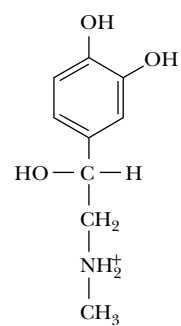
FIGURE 23.24 • Epinephrine
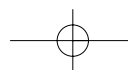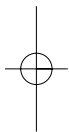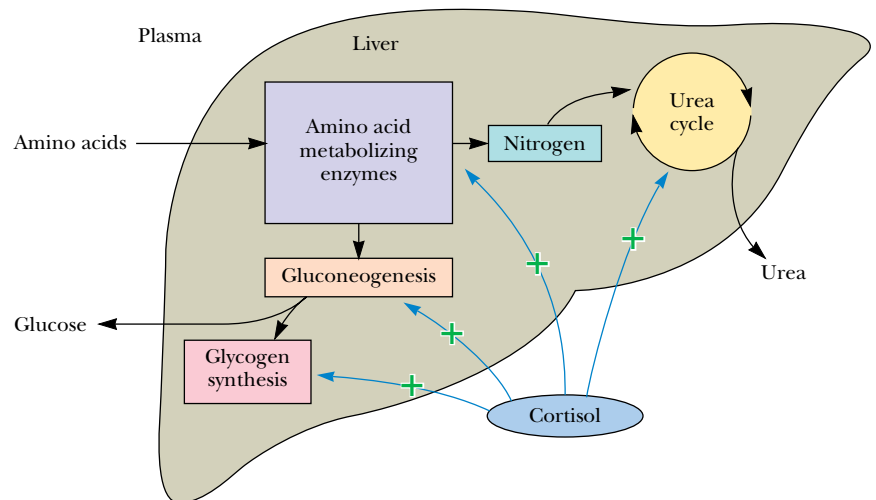
FIGURE 23.25 • The effects of cortisol on carbohydrate and protein metabolism in the liver.

23.6 • The Pentose Phosphate Pathway

Cells require a constant supply of NADPH for reductive reactions vital to biosynthetic purposes. Much of this requirement is met by a glucose-based metabolic sequence variously called the **pentose phosphate pathway,** the **hexose monophosphate shunt,** or the **phosphogluconate pathway.** In addition to providing NADPH for biosynthetic processes, this pathway produces *ribose-5-phosphate,* which is essential for nucleic acid synthesis. Several metabolites of the pentose phosphate pathway can also be shuttled into glycolysis.

An Overview of the Pathway

The pentose phosphate pathway begins with glucose-6-phosphate, a six-carbon sugar, and produces three-, four-, five-, six-, and seven-carbon sugars (Figure 23.26). As we will see, two successive oxidations lead to the reduction of NADP$^+$ to NADPH and the release of CO_2. Five subsequent nonoxidative steps produce a variety of carbohydrates, some of which may enter the glycolytic pathway. The enzymes of the pentose phosphate pathway are particularly abundant in the cytoplasm of liver and adipose cells. These enzymes are largely absent in muscle, where glucose-6-phosphate is utilized primarily for energy production via glycolysis and the TCA cycle. These pentose phosphate pathway enzymes are located in the cytosol, which is the site of fatty acid synthesis, a pathway heavily dependent on NADPH for reductive reactions.

The Oxidative Steps of the Pentose Phosphate Pathway

(1) Glucose-6-Phosphate Dehydrogenase

The pentose phosphate pathway begins with the oxidation of glucose-6-phosphate. The products of the reaction are a cyclic ester (the lactone of phosphogluconic acid) and NADPH (Figure 23.27). **Glucose-6-phosphate dehydrogenase,** which catalyzes this reaction, is highly specific for NADP$^+$. As the first step of a major pathway, the reaction is irreversible and highly regulated. Glucose-6-phosphate dehydrogenase is strongly inhibited by the product coenzyme, NADPH, and also by fatty acid esters of coenzyme A (which are
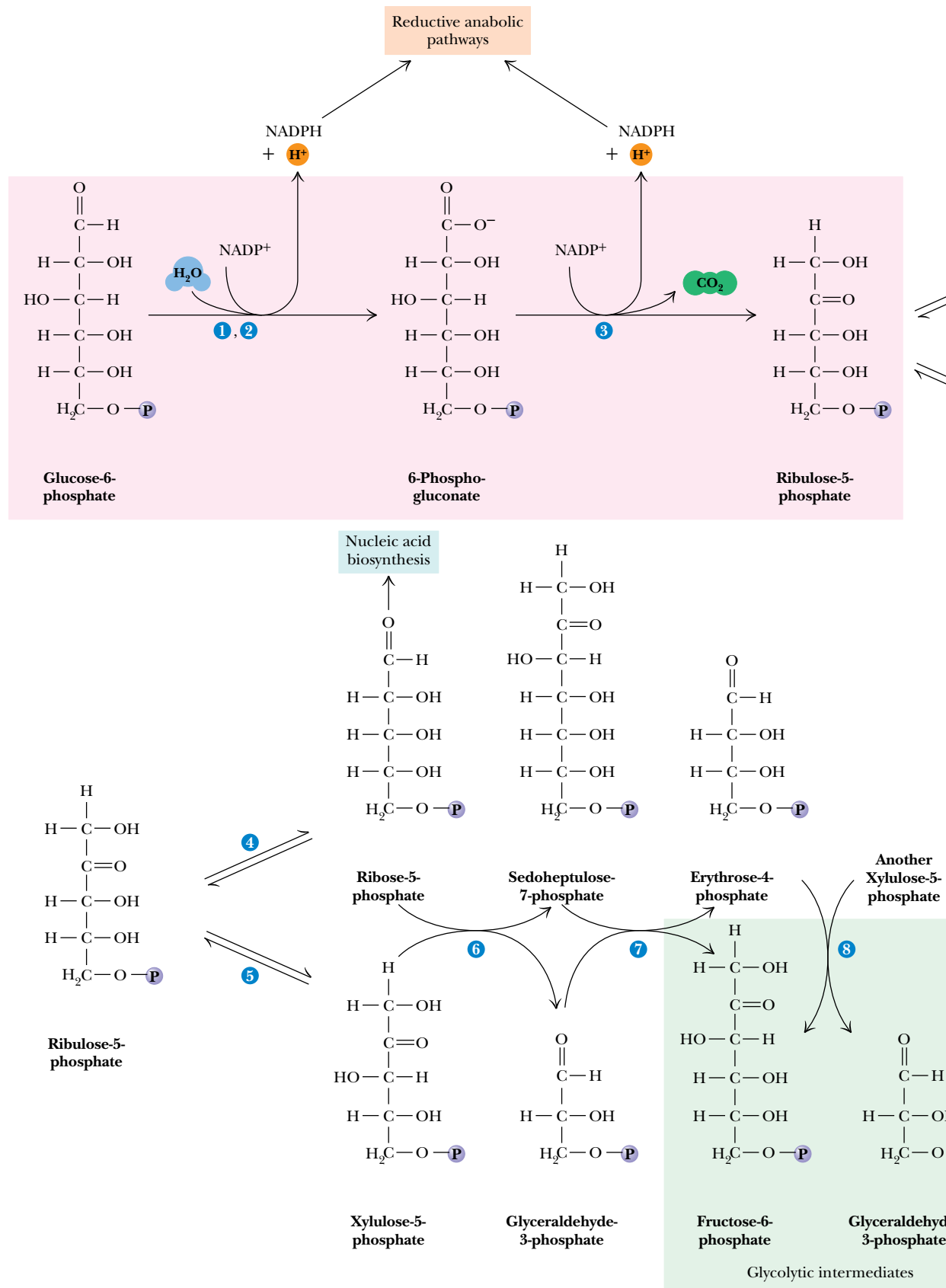
FIGURE 23.26 • The pentose phosphate pathway. The numerals in the blue circles indicate the steps discussed in the text.
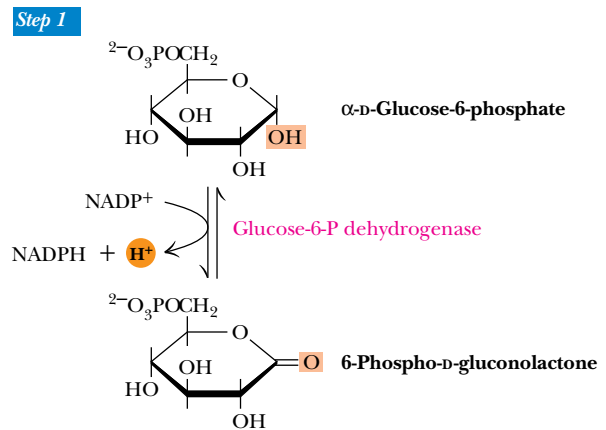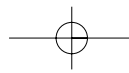
FIGURE 23.27 • The glucose-6-phosphate dehydrogenase reaction is the committed step in the pentose phosphate pathway.

intermediates of fatty acid biosynthesis). Inhibition due to NADPH depends upon the cytosolic $NADP^+/NADPH$ ratio, which in the liver is about 0.015 (compared to about 725 for the $NAD^+/NADH$ ratio in the cytosol).

(2) Gluconolactonase

The gluconolactone produced in step 1 is hydrolytically unstable and readily undergoes a spontaneous ring-opening hydrolysis, although an enzyme, **gluconolactonase,** accelerates this reaction (Figure 23.28). The linear product, the sugar acid 6-phospho-D-gluconate, is further oxidized in step 3.

(3) 6-Phosphogluconate Dehydrogenase

The oxidative decarboxylation of 6-phosphogluconate by **6-phosphogluconate dehydrogenase** yields D-ribulose-5-phosphate and another equivalent of NADPH. There are two distinct steps in this reaction (Figure 23.29): the initial $NADP^+$-dependent dehydrogenation yields a β-keto acid, 3-keto-6-phosphogluconate, which is very susceptible to decarboxylation (the second step). The resulting product, D-ribulose-5-P, is the substrate for the nonoxidative reactions composing the rest of this pathway.

The Nonoxidative Steps of the Pentose Phosphate Pathway

This portion of the pathway begins with an isomerization and an epimerization, and it leads to the formation of either D-ribose-5-phosphate or D-xylulose-5-phosphate. These intermediates can then be converted into glycolytic intermediates or directed to biosynthetic processes.

FIGURE 23.28 • The gluconolactonase reaction.

Step 3

6-P-D-Gluconate   **3-keto-6-P-D-Gluconate**   **D-Ribulose-5-P**
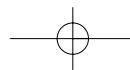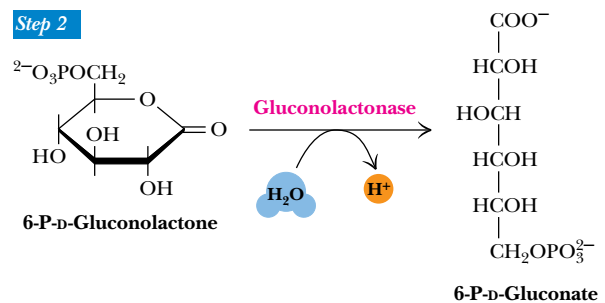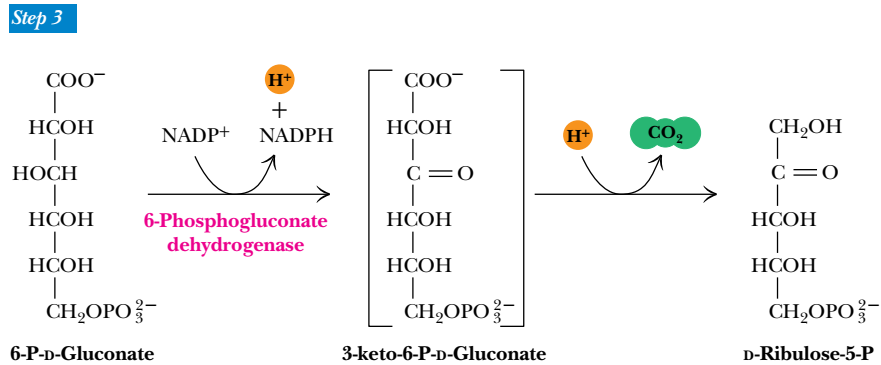
(4) Phosphopentose Isomerase

This enzyme interconverts ribulose-5-P and ribose-5-P via an enediol interme-
diate (Figure 23.30). The reaction (and mechanism) is quite similar to the
phosphoglucoisomerase reaction of glycolysis, which interconverts glucose-6-P
and fructose-6-P. The ribose-5-P produced in this reaction is utilized in the
biosynthesis of coenzymes (including NADH, NADPH, FAD, and B_{12}),
nucleotides, and nucleic acids (DNA and RNA). The net reaction for the first
four steps of the pentose phosphate pathway is

$$\text{Glucose-6-P} + 2\ \text{NADP}^+ \longrightarrow \text{ribose-5-P} + 2\ \text{NADPH} + 2\ \text{H}^+ + \text{CO}_2$$

(5) Phosphopentose Epimerase

This reaction converts ribulose-5-P to another ketose, namely, xylulose-5-P. This
reaction also proceeds by an enediol intermediate, but involves an inversion
at C-3 (Figure 23.31). In the reaction, an acidic proton located α- to a carbonyl
carbon is removed to generate the enediolate, but the proton is added back
to the same carbon from the opposite side. Note the distinction in nomencla-
ture here. Interchange of groups on a single carbon is an epimerization, and
interchange of groups between carbons is referred to as an isomerization.

To this point, the pathway has generated a pool of pentose phosphates.
The $\Delta G^{\circ\prime}$ for each of the last two reactions is small, and the three pentose-5-
phosphates coexist at equilibrium. The pathway has also produced two mole-
cules of NADPH for each glucose-6-P converted to pentose-5-phosphate. The
next three steps rearrange the five-carbon skeletons of the pentoses to produce
three-, four-, six-, and seven-carbon units, which can be used for various meta-
bolic purposes. Why should the cell do this? Very often, the cellular need for
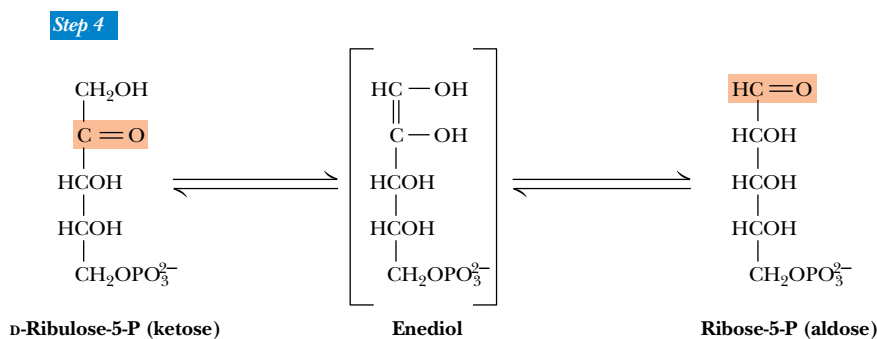
Step 4

D-Ribulose-5-P (ketose)   **Enediol**   **Ribose-5-P (aldose)**

Step 5

Ribulose-5-P   **Enediolate**   **Xylulose-5-P**
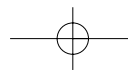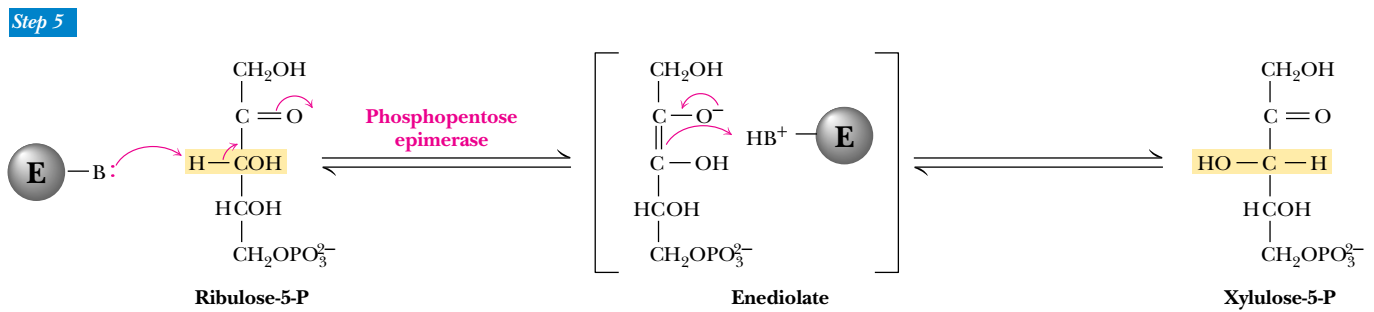
FIGURE 23.31 • The phosphopentose epimerase reaction interconverts ribulose-5-P and xylulose-5-phosphate. The mechanism involves an enediol intermediate and occurs with inversion at C-3.

NADPH is considerably greater than the need for ribose-5-phosphate. The next three steps thus return some of the five-carbon units to glyceraldehyde-3-phosphate and fructose-6-phosphate, which can enter the glycolytic pathway. The advantage of this is that the cell has met its needs for NADPH and ribose-5-phosphate in a single pathway, yet at the same time it can return the excess carbon metabolites to glycolysis.

(6) and (8) Transketolase

The transketolase enzyme acts at both steps 6 and 8 of the pentose phosphate pathway. In both cases, the enzyme catalyzes the transfer of two-carbon units. In these reactions (and also in step 7, the transaldolase reaction, which transfers three-carbon units), the donor molecule is a ketose and the recipient is an aldose. In step 6, xylulose-5-phosphate transfers a two-carbon unit to ribose-5-phosphate to form glyceraldehyde-3-phosphate and sedoheptulose-7-phosphate (Figure 23.32). Step 8 involves a two-carbon transfer from xylulose-5-phosphate to erythrose 4-phosphate to produce another glyceraldehyde-3-phosphate and a fructose-6-phosphate (Figure 23.33). Three of these products enter directly into the glycolytic pathway. (The sedoheptulose-7-phosphate is taken care of in step 7, as we shall see.) Transketolase is a thiamine pyrophosphate–dependent enzyme, and the mechanism (Figure 23.34) involves abstraction of the acidic thiazole proton of TPP, attack by the resulting carbanion at the carbonyl carbon of the ketose phosphate substrate, expulsion of the glyceraldehyde-3-phosphate product, and transfer of the two-carbon unit. Transketolase can process a variety of 2-keto sugar phosphates in a similar manner. It is specific for ketose substrates with the configuration shown, but can accept a variety of aldose phosphate substrates.

FIGURE 23.32 • The transketolase reaction of step 6 in the pentose phosphate pathway.

Step 6

Xylulose-5-P   **Ribose-5-P**   **Glyceraldehyde-3-P**   **Sedoheptulose-7-P**

Step 8

Xylulose-5-P   **Erythrose-4-P**   **Glyceraldehyde-3-P**   **Fructose-6-P**
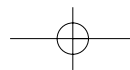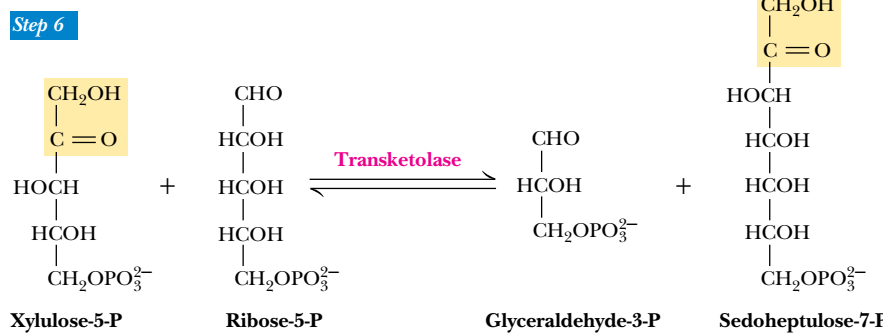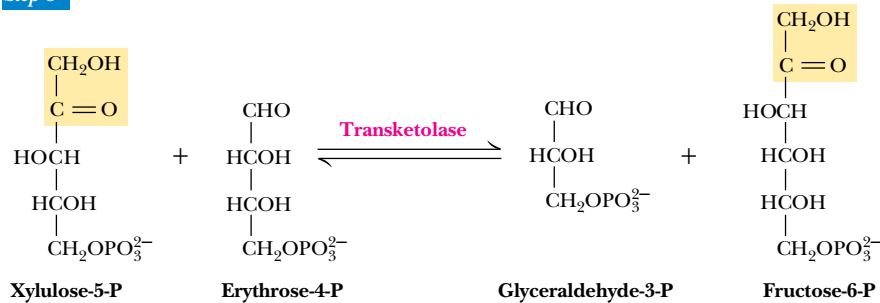
FIGURE 23.33 • The transketolas of step 8 in the pentose phosphate

D–Xylulose-5-P

Glyceraldehyde

D–Ribose-5-P

Sedoheptulose-7-P
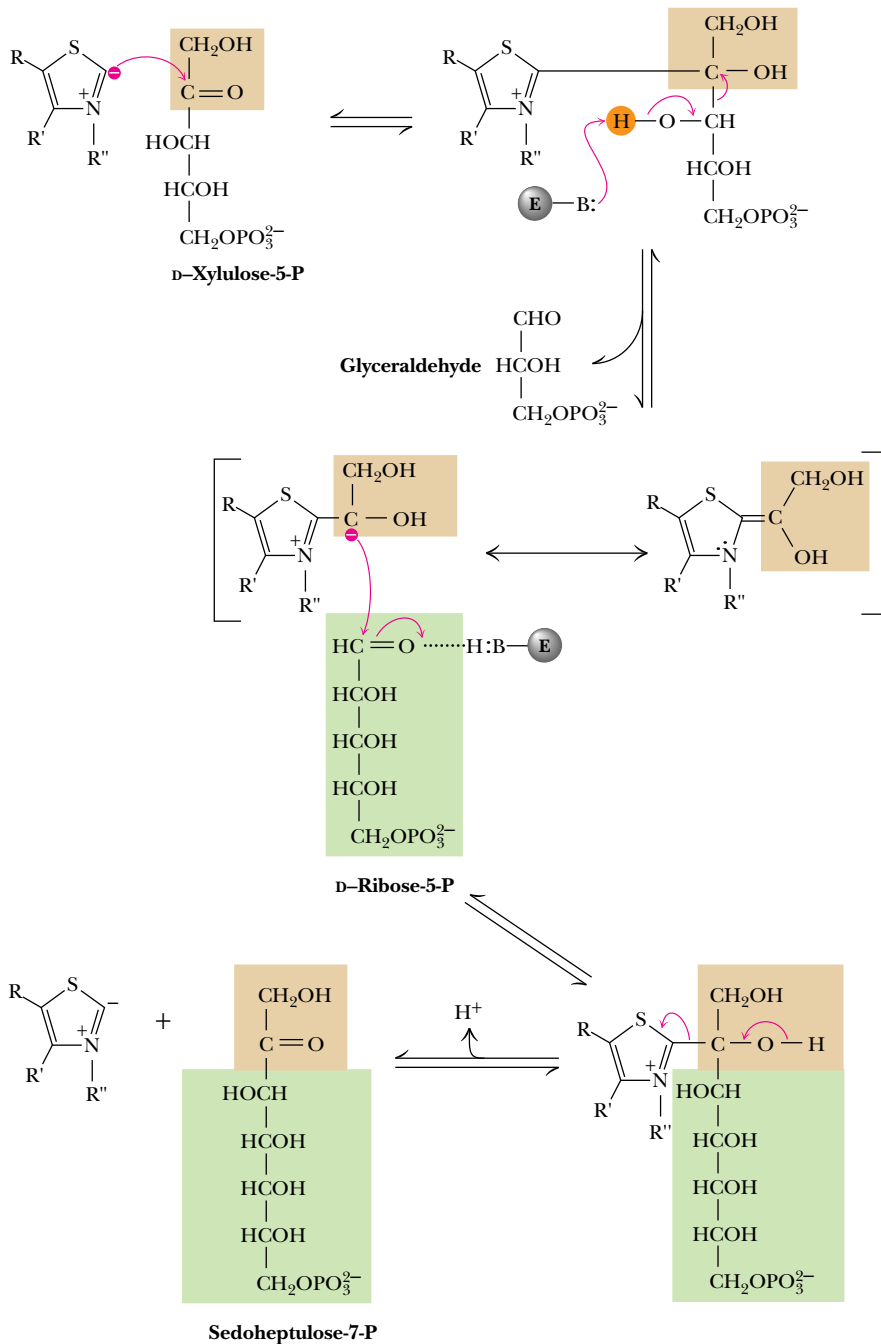
FIGURE 23.34 • The mechanism
dependent transketolase reaction. In
the group transferred in the transke
tion might best be described as an a
whereas the transferred group in th
dolase reaction is actually a ketol. D
irony, these names persist for histor
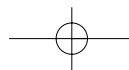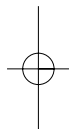
(7) Transaldolase

The transaldolase functions primarily to make a useful glycolytic substrate from the sedoheptulose-7-phosphate produced by the first transketolase reaction. This reaction (Figure 23.35) is quite similar to the aldolase reaction of glycolysis, involving formation of a Schiff base intermediate between the sedoheptulose-7-phosphate and an active-site lysine residue (Figure 23.36). Elimination of the erythrose-4-phosphate product leaves an enamine of dihydroxyacetone, which remains stable at the active site (without imine hydrolysis) until the other substrate comes into position. Attack of the enamine carbanion at the carbonyl carbon of glyceraldehyde-3-phosphate is followed by hydrolysis of the Schiff base (imine) to yield the product fructose-6-phosphate.

Utilization of Glucose-6-P Depends on the Cell's Need for ATP, NADPH, and Ribose-5-P

It is clear that glucose-6-phosphate can be used as a substrate either for glycolysis or for the pentose phosphate pathway. The cell makes this choice on the basis of its relative needs for biosynthesis and for energy from metabolism. ATP can be produced in abundance if glucose-6-phosphate is channeled into glycolysis. On the other hand, if NADPH or ribose-5-phosphate is needed, glucose-6-phosphate can be directed to the pentose phosphate pathway. The molecular basis for this regulatory decision depends on the enzymes that metabolize glucose-6-phosphate in glycolysis and the pentose phosphate pathway. In glycolysis, phosphoglucoisomerase converts glucose-6-phosphate to fructose-6-phosphate, which is utilized by phosphofructokinase (a highly regulated enzyme) to produce fructose-1,6-bisphosphate. In the pentose phosphate pathway, glucose-6-phosphate dehydrogenase (also highly regulated) produces gluconolactone from glucose-6-phosphate. Thus, the fate of glucose-6-phosphate is determined to a large extent by the relative activities of phosphofructokinase and glucose-6-P dehydrogenase. Recall (Chapter 19) that PFK is inhibited when the ATP/AMP ratio increases, and that it is inhibited by citrate but activated by fructose-2,6-bisphosphate. Thus, when the energy charge is high, glycolytic flux decreases. Glucose-6-P dehydrogenase, on the other hand, is inhibited by high levels of NADPH and also by the intermediates of fatty acid biosynthesis. Both of these are indicators that biosynthetic demands have been satisfied. If that is the case, glucose-6-phosphate dehydrogenase and the pen-

FIGURE 23.35 • The transaldolase reaction.
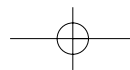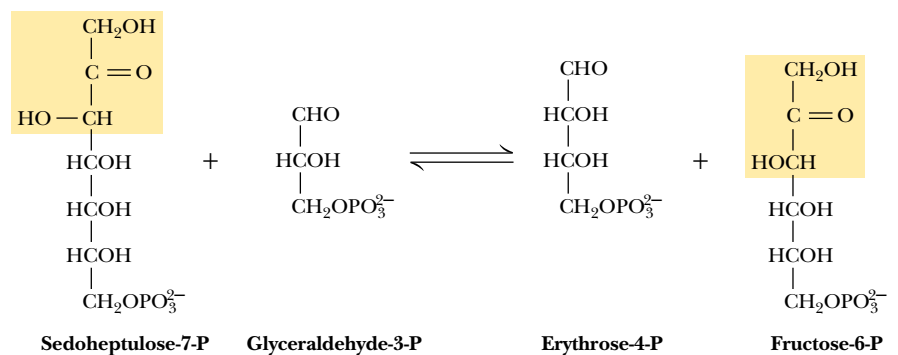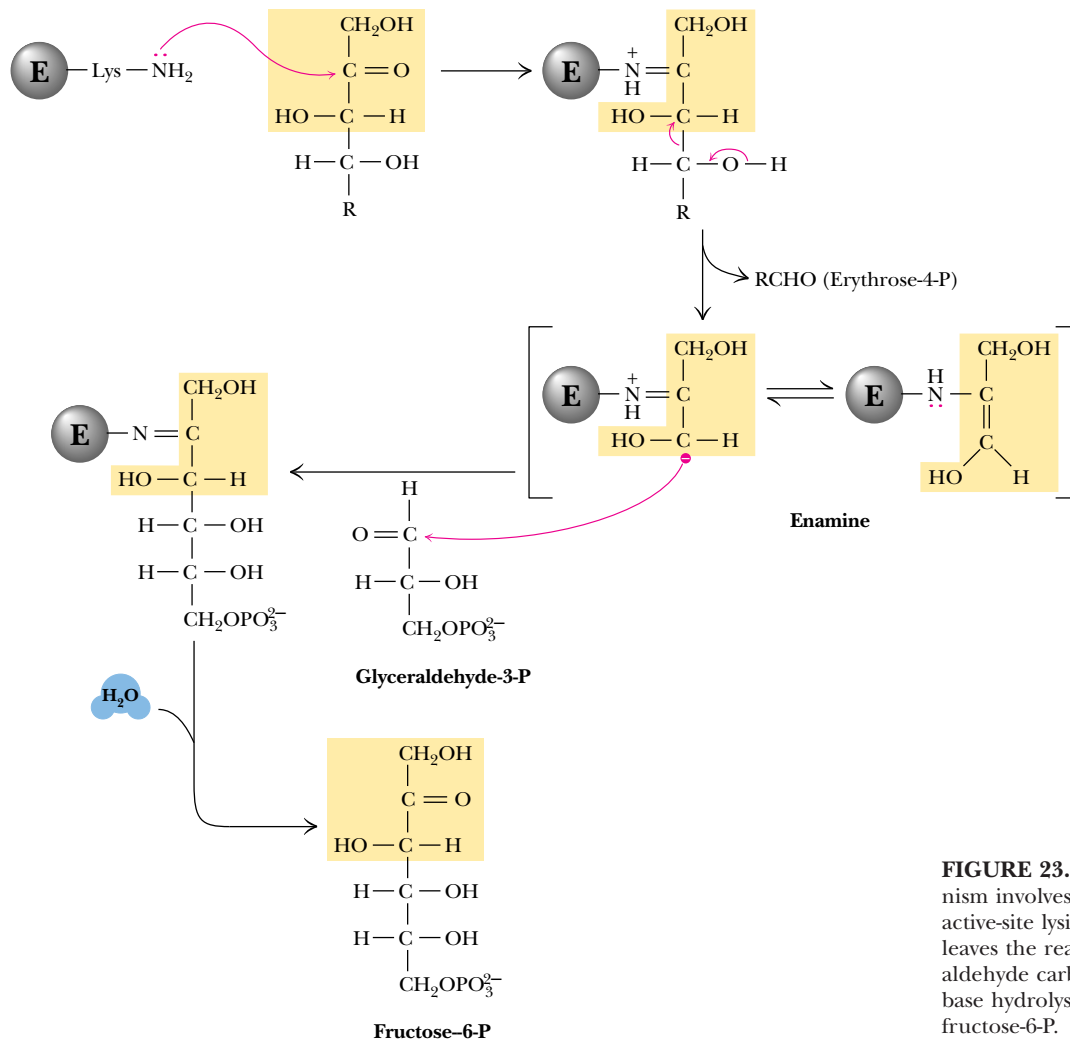
FIGURE 23.36 • The transaldolas[e] nism involves attack on the substrat[e] active-site lysine. Departure of eryth[rose] leaves the reactive enamine, which a[ttacks] aldehyde carbon of glyceraldehyde-[3] base hydrolysis yields the second pr[oduct,] fructose-6-P.

tose phosphate pathway are inhibited. If NADPH levels drop, the pentose phosphate pathway turns on, and NADPH and ribose-5-phosphate are made for biosynthetic purposes.

Even when the latter choice has been made, however, the cell must still be "cognizant" of the relative needs for ribose-5-phosphate and NADPH (as well as ATP). Depending on these relative needs, the reactions of glycolysis and the pentose phosphate pathway can be combined in novel ways to emphasize the synthesis of needed metabolites. There are four principal possibilities.

(1) BOTH RIBOSE-5-P AND NADPH ARE NEEDED BY THE CELL In this case, the first four reactions of the pentose phosphate pathway predominate (Figure 23.37). NADPH is produced by the oxidative reactions of the pathway, and ribose-5-P is the principal product of carbon metabolism. As stated earlier, the net reaction for these processes is

$$\text{Glucose-6-P} + 2\ \text{NADP}^+ + \text{H}_2\text{O} \longrightarrow \text{ribose-5-P} + \text{CO}_2 + 2\ \text{NADPH} + 2\ \text{H}^+$$
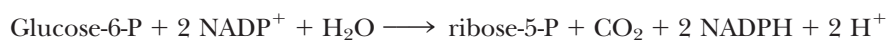
(2) MORE RIBOSE-5-P THAN NADPH IS NEEDED BY THE CELL Synthesis of ribose-5-P can be accomplished without production of NADPH if the oxidative steps of the pentose phosphate pathway are bypassed. The key to this route is the extrac-
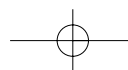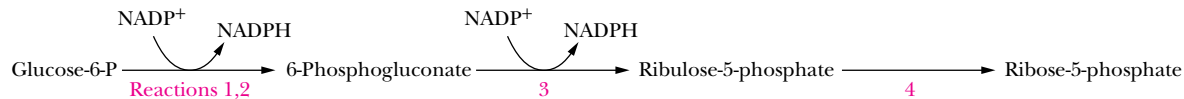
FIGURE 23.37 • When biosynthetic demands dictate, the first four reactions of the pentose phosphate pathway predominate and the principal products are ribose-5-P and NADPH.

tion of fructose-6-P and glyceraldehyde-3-P, but not glucose-6-P, from glycolysis (Figure 23.38). The action of transketolase and transaldolase on fructose-6-P and glyceraldehyde-3-P produces three molecules of ribose-5-P from two molecules of fructose-6-P and one of glyceraldehyde-3-P. In this route, as in case 1, no carbon metabolites are returned to glycolysis. The net reaction for this route is

$$5 \text{ Glucose-6-P} + \text{ATP} \longrightarrow 6 \text{ ribose-5-P} + \text{ADP} + \text{H}^+$$
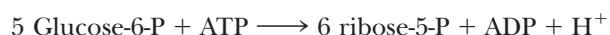
(3) MORE NADPH THAN RIBOSE-5-P IS NEEDED BY THE CELL   Large amounts of NADPH can be supplied for biosynthesis without concomitant production of ribose-5-P, if ribose-5-P produced in the pentose phosphate pathway is recycled to produce glycolytic intermediates. As shown in Figure 23.39, this alternative involves a complex interplay between the transketolase and transaldolase reac-
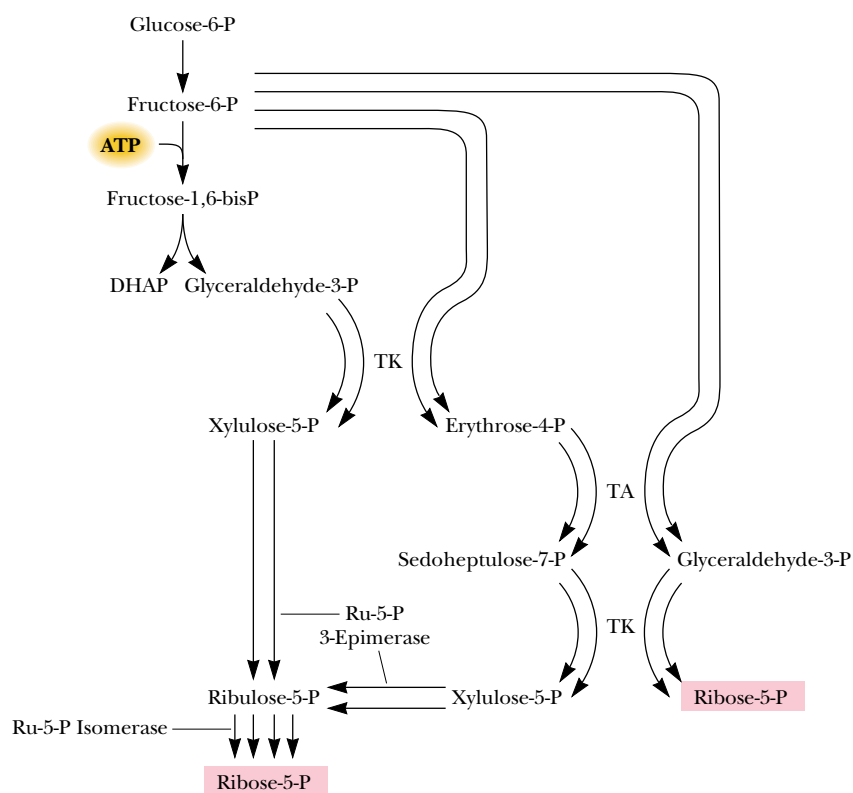
FIGURE 23.38 • The oxidative steps of the pentose phosphate pathway can be bypassed if the primary need is for ribose-5-P.
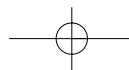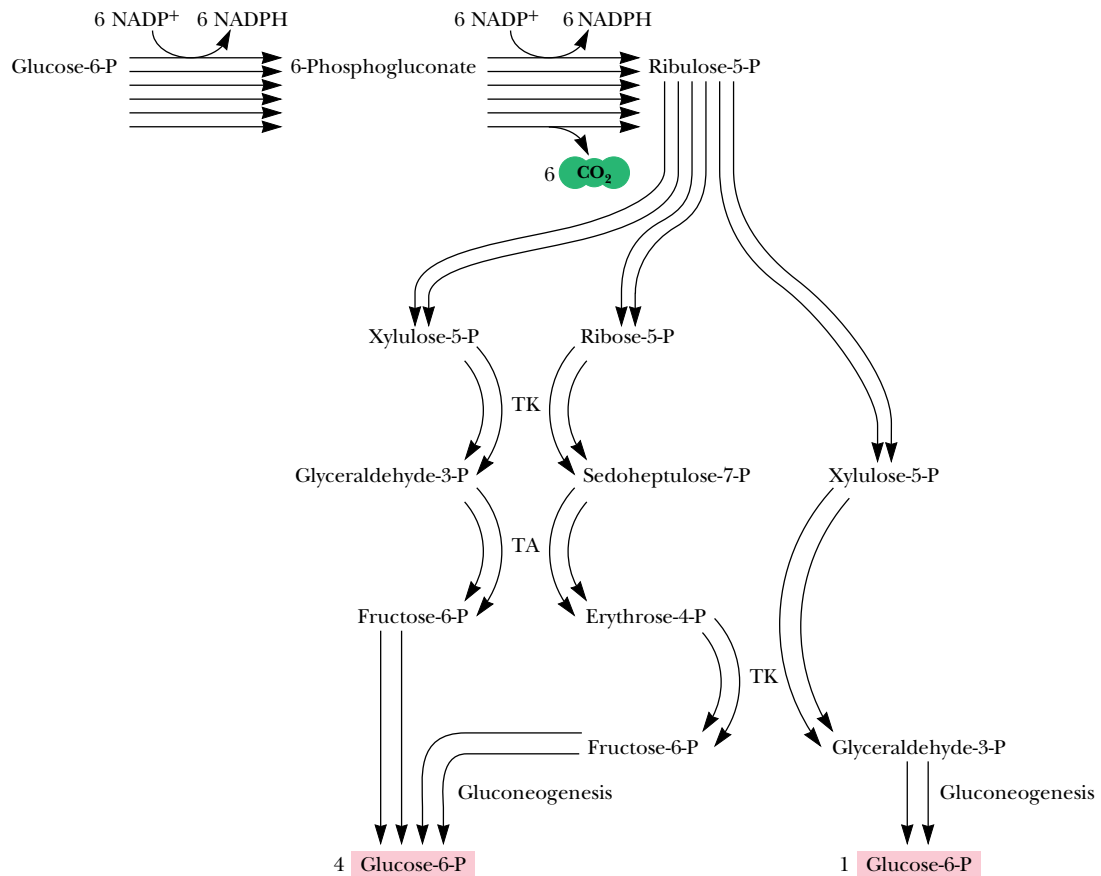
FIGURE 23.39 • Large amounts of NADPH can be produced by the pentose phosphate pathway without significant net production of ribose-5-P. In this version of the pathway, ribose-5-P is recycled to produce glycolytic intermediates.

tions to convert ribulose-5-P to fructose-6-P and glyceraldehyde-3-P, which can be recycled to glucose-6-P via gluconeogenesis. The net reaction for this process is

$$6 \text{ Glucose-6-P} + 12 \text{ NADP}^+ + 6 \text{ H}_2\text{O} \longrightarrow$$
$$6 \text{ ribulose-5-P} + 6 \text{ CO}_2 + 12 \text{ NADPH} + 12 \text{ H}^+$$
$$6 \text{ Ribulose-5-P} \longrightarrow 5\text{-glucose-6-P} + \text{P}_i$$
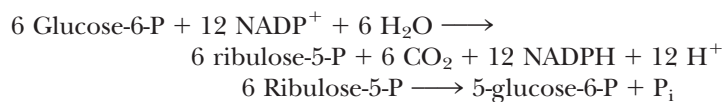
Note that in this scheme, the six hexose sugars have been converted to six pentose sugars with release of six molecules of CO_2, and the six pentoses are reconverted to five glucose molecules.

(4) BOTH NADPH AND ATP ARE NEEDED BY THE CELL, BUT RIBOSE-5-P IS NOT Under some conditions, both NADPH and ATP must be provided in the cell. This can be accomplished in a series of reactions similar to case 3, if the fructose-6-P and glyceraldehyde-3-P produced in this way proceed through glycolysis to produce ATP and pyruvate, which itself can yield even more ATP by continuing on to the TCA cycle (Figure 23.40). The net reaction for this alternative is

$$3 \text{ Glucose-6-P} + 5 \text{ NAD}^+ + 6 \text{ NADP}^+ + 8 \text{ ADP} + 5 \text{ P}_i \longrightarrow$$
$$5 \text{ pyruvate} + 3 \text{ CO}_2 + 5 \text{ NADH} + 6 \text{ NADPH} + 8 \text{ ATP} + 2 \text{ H}_2\text{O} + 8 \text{ H}^+$$
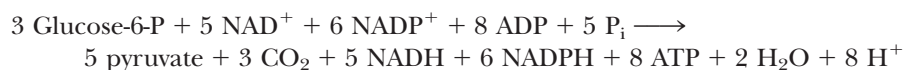
Note that, except for the three molecules of CO_2, all the other carbon from glucose-6-P is recovered in pyruvate.
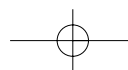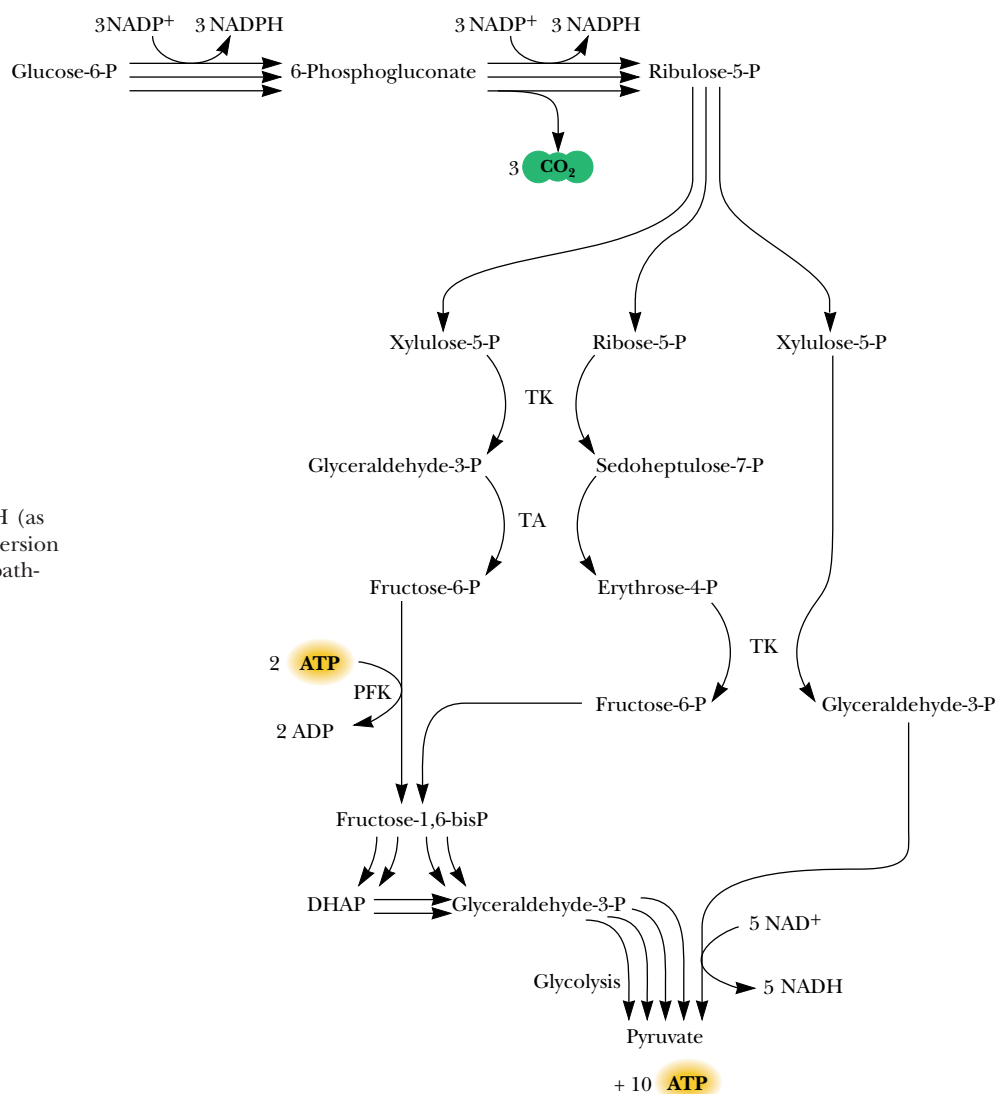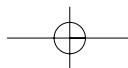
FIGURE 23.40 • Both ATP and NADPH (as well as NADH) can be produced by this version of the pentose phosphate and glycolytic pathways.

PROBLEMS

1. Consider the balanced equation for gluconeogenesis in Section 23.1. Account for each of the components of this equation and the indicated stoichiometry.

2. Calculate $\Delta G°'$ and ΔG for gluconeogenesis in the erythrocyte, using data in Table 19.2 (assume $NAD^+/NADH = 20$, $[GTP] = [ATP]$, and $[GDP] = [ADP]$). See how closely your values match those in Section 23.1.

3. Use the data of Figure 23.12 to calculate the percent inhibition of fructose-1,6-bisphosphatase by 25 μM fructose-2,6-bisphosphate when fructose-1,6-bisphosphate is (a) 25 μM and (b) 100 μM.

4. Suggest an explanation for the exergonic nature of the glycogen synthase reaction ($\Delta G°' = -13.3$ kJ/mol). Consult Chapter 3 to review the energetics of high-energy phosphate compounds if necessary.

5. Using the values in Table 24.1 for body glycogen content and the data in part b of the illustration for A Deeper Look (page 759), calculate the rate of energy consumption by muscles in heavy exercise (in J/sec). Use the data for fast-twitch muscle.

6. What would be the distribution of carbon from positions 1, 3, and 6 of glucose after one pass through the pentose phosphate pathway if the primary need of the organism is for ribose-5-P and the oxidative steps are bypassed (Figure 23.38)?

7. What is the fate of carbon from positions 2 and 4 of glucose-6-P after one pass through the scheme shown in Figure 23.40?

8. Which reactions of the pentose phosphate pathway would be inhibited by $NaBH_4$? Why?

9. Imagine a glycogen molecule with 8000 glucose residues. If branches occur every eight residues, how many reducing ends does the molecule have? If branches occur every 12 residues, how many reducing ends does it have? How many nonreducing ends does it have in each of these cases?

10. Explain the effects of each of the following on the rates of gluconeogenesis and glycogen metabolism:

a. Increasing the concentration of tissue fructose-1,6-bisphosphate

b. Increasing the concentration of blood glucose

c. Increasing the concentration of blood insulin

d. Increasing the amount of blood glucagon

e. Decreasing levels of tissue ATP

f. Increasing the concentration of tissue AMP

g. Decreasing the concentration of fructose-6-phosphate
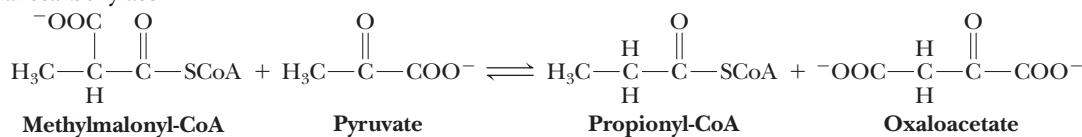
772
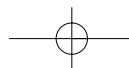
11. The free-energy change of the glycogen phosphorylase reaction is $\Delta G^{\circ\prime} = +3.1$ kJ/mol. If $[P_i] = 1$ mM, what is the concentration of glucose-1-P when this reaction is at equilibrium?

12. Based on the mechanism for pyruvate carboxylase (Figure 23.4), write reasonable mechanisms for the reactions shown below:
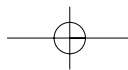

β-Methylcrotonyl-CoA → **β-Methylglutaconyl-CoA**

Geranyl-CoA → **γ-Carboxygeranyl-CoA**

Urea → **N-Carboxyurea**

Transcarboxylase
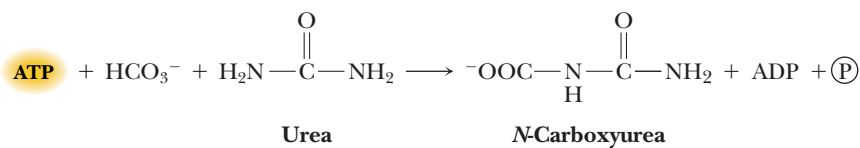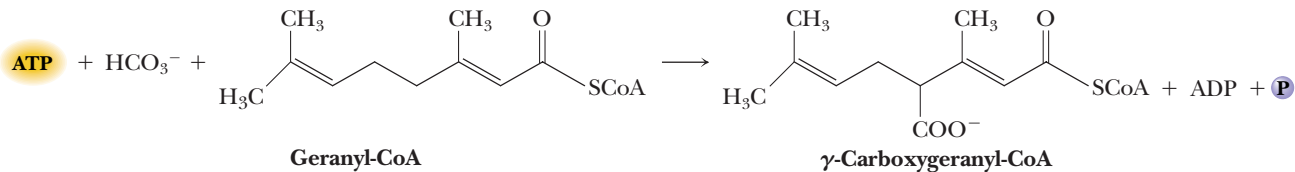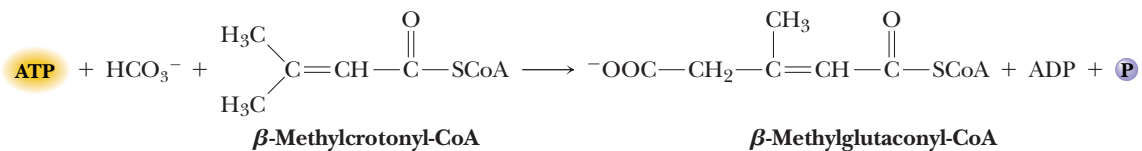
Methylmalonyl-CoA + **Pyruvate** ⇌ **Propionyl-CoA** + **Oxaloacetate**

13. The mechanistic chemistry of the acetolactate synthase and phosphoketolase reactions (shown below) is similar to that of the transketolase reaction (Figure 23.34). Write suitable mechanisms for these reactions.

Acetolactate synthase

Phosphoketolase

Fructose-6-P   **Acetyl-P**   **Erythrose-4-P**
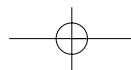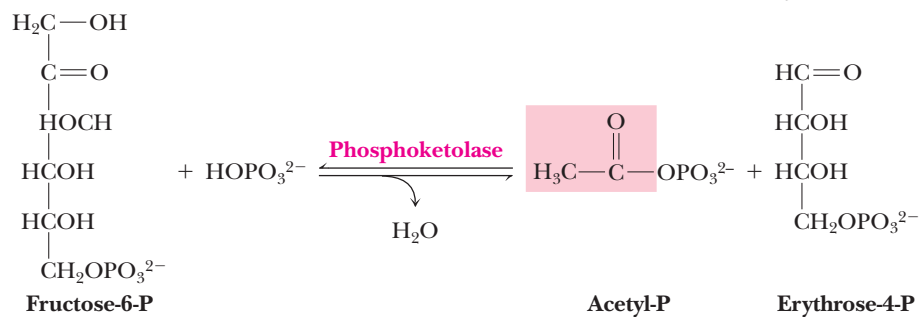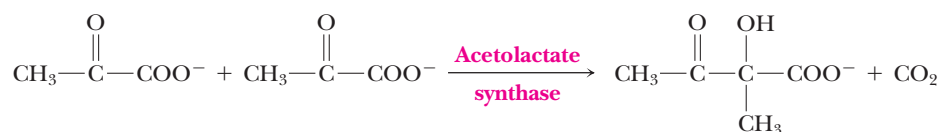
FURTHER READING

Akermark, C., Jacobs, I., Rasmusson, M., and Karlsson, J., 1996. Diet and muscle glycogen concentration in relation to physical performance in Swedish elite ice hockey players. *International Journal of Sport Nutrition* **6:**272–284.

Browner, M. F., and Fletterick, R. J., 1992. Phosphorylase: A biological transducer. *Trends in Biochemical Sciences* **17:**66–71.

Fox, E. L., 1984. *Sports Physiology,* 2nd ed. Philadelphia: Saunders College Publishing.

Hanson, R. W., and Reshef, L., 1997. Regulation of phosphoenolpyruvate carboxykinase (GTP) gene expression. *Annual Review of Biochemistry* **66:**581–611.

Hargreaves, M., 1997. Interactions between muscle glycogen and blood glucose during exercise. *Exercise and Sport Sciences Reviews* **25:**21–39.

Hers, H.-G., and Hue, L., 1983. Gluconeogenesis and related aspects of glycolysis. *Annual Review of Biochemistry* **52:**617–653.

Horton, E. S., and Terjung, R. L., eds. 1988. *Exercise, Nutrition and Energy Metabolism.* New York: Macmillan.

Huang, D., Wilson, W. A., and Roach, P. J., 1997. Glucose-6-P control of glycogen synthase phosphorylation in yeast. *Journal of Biological Chemistry* **272:**22495–22501.

Johnson, L. N., 1992. Glycogen phosphorylase: Control by phosphorylation and allosteric effectors. *FASEB Journal* **6:**2274–2282.

Larner, J., 1990. Insulin and the stimulation of glycogen synthesis: The road from glycogen structure to glycogen synthase to cyclic AMP-dependent protein kinase to insulin mediators. *Advances in Enzymology* **63:**173–231.

Newsholme, E. A., Chaliss, R. A. J., and Crabtree, B., 1984. Substrate cycles: Their role in improving sensitivity in metabolic control. *Trends in Biochemical Sciences* **9:**277–280.

Newsholme, E. A., and Leech, A. R., 1983. *Biochemistry for the Medical Sciences.* New York: Wiley.

Pilkis, S. J., El-Maghrabi, M. R., and Claus, T. H., 1988. Hormonal regulation of hepatic gluconeogenesis and glycolysis. *Annual Review of Biochemistry* **57:**755–783.

Rhoades, R., and Pflanzer, R., 1992. *Human Physiology.* Philadelphia: Saunders College Publishing.

Rolfe, D. F., and Brown, G. C., 1997. Cellular energy utilization and molecular origin of standard metabolic rate in mammals. *Physiological Reviews* **77:**731–758.

Rybicka, K. K., 1996. Glycosomes—The organelles of glycogen metabolism. *Tissue and Cell* **28:**253–265.

Sies, H., ed., 1982. *Metabolic Compartmentation.* London: Academic Press.

Shulman, R. G., and Rothman, D. L., 1996. Nuclear magnetic resonance studies of muscle and applications to exercise and diabetes. *Diabetes* **45:**S93–S98.

Stalmans, W., Cadefau, J., Wera, S., and Bollen, M., 1997. New insight into the regulation of liver glycogen metabolism by glucose. *Biochemical Society Transactions* **25:**19–25.

Sukalski, K. A., and Nordlie, R. C., 1989. Glucose-6-phosphatase: Two concepts of membrane-function relationship. *Advances in Enzymology* **62:**93–117.

Taylor, S. S., et al., 1993. A template for the protein kinase family. *Trends in Biochemical Sciences* **18:**84–89.

Van Schaftingen, E., and Hers, H.-G., 1981. Inhibition of fructose-1,6-bisphosphatase by fructose-2,6-bisphosphate. *Proceedings of the National Academy of Sciences, USA* **78:**2861–2863.

Williamson, D. H., Lund, P., and Krebs, H. A., 1967. The redox state of free nicotinamide–adenine dinucleotide in the cytoplasm and mitochondria of rat liver. *Biochemical Journal* **103:**514–527.

Woodget, J. R., 1991. A common denominator linking glycogen metabolism, nuclear oncogenes, and development. *Trends in Biochemical Sciences* **16:**177–181.
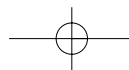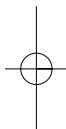
*C*hapter 24

Fatty Acid Catabolism

The hummingbird's tremendous capacity to store and use fatty acids enables it to make migratory journeys of remarkable distances. (Two Hummingbirds Lithograph; The Academy of Natural Sciences of Philadelphia/Corbis Images)
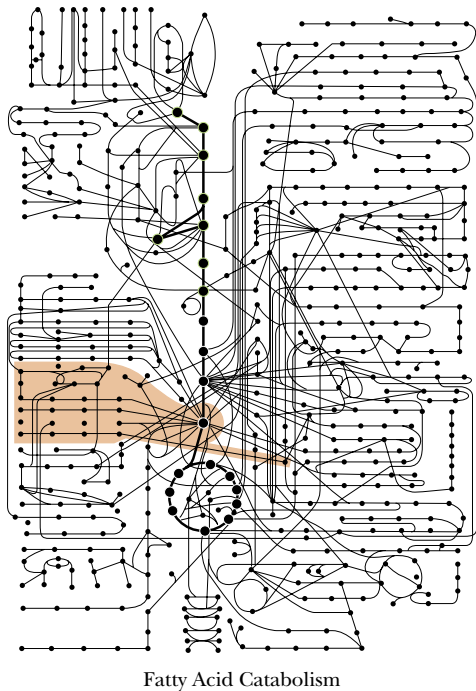
The fat is in the fire.

Proverbs, JOHN HEYWOOD (1497–1580)

Fatty acids represent the principal form of stored energy for many organisms. There are two important advantages to storing energy in the form of fatty acids. (1) The carbon in fatty acids (mostly —CH_2— groups) is almost completely reduced compared to the carbon in other simple biomolecules (sugars, amino acids). Therefore, oxidation of fatty acids will yield more energy (in the form of ATP) than any other form of carbon. (2) Fatty acids are not generally hydrated as mono- and polysaccharides are, and thus can pack more closely in storage tissues. This chapter will be devoted to several important aspects of fatty acid catabolism. Lipid biosynthetic processes will be considered in Chapter 25.
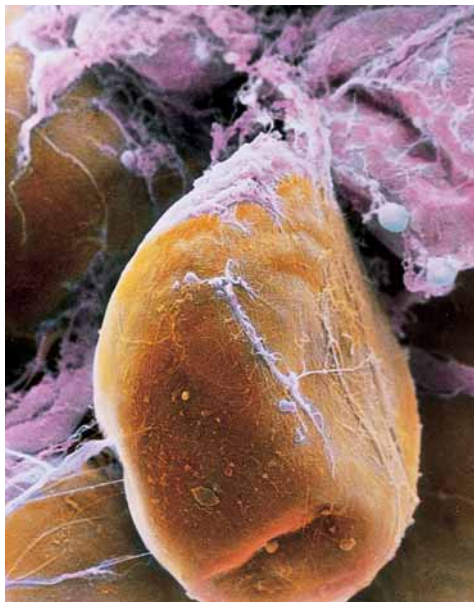
775

Fatty Acid Catabolism

FIGURE 24.1 • Scanning electron micrograph of an adipose cell (fat cell). Globules of triacylglycerols occupy most of the volume of such cells. *(Prof. P. Motta, Dept. of Anatomy, University "La Sapienza," Rome/Science Photo Library/Photo Researchers, Inc.)*

24.1 • Mobilization of Fats from Dietary Intake and Adipose Tissue

Modern Diets Are Often High in Fat

Fatty acids are acquired readily in the diet and can also be made from carbohydrates and the carbon skeletons of amino acids. Fatty acids provide 30% to 60% of the calories in the diets of most Americans. For our caveman and cavewoman ancestors, the figure was probably closer to 20%. Dairy products were apparently not part of their diet, and the meat they consumed (from fast-moving animals) was low in fat. In contrast, modern domesticated cows and pigs are actually bred for high fat content (and better taste). However, woolly mammoth burgers and saber-toothed tiger steaks are hard to find these days—even in the gourmet sections of grocery stores—and so, by default, we consume (and metabolize) large quantities of fatty acids.

Triacylglycerols Are a Major Form of Stored Energy in Animals

Although some of the fat in our diets is in the form of phospholipids, **triacylglycerols** are a major source of fatty acids. Triacylglycerols are also our principal stored energy reserve. As shown in Table 24.1, the energy available in stores of fat in the average person far exceeds the energy available from protein, glycogen, and glucose. Overall, fat accounts for approximately 83% of available energy, partly because more fat is stored than protein and carbohydrate, and partly because of the substantially higher energy yield per gram for fat compared with protein and carbohydrate. Complete combustion of fat yields about 37 kJ/g, compared with about 16 to 17 kJ/g for sugars, glycogen, and amino acids. In animals, fat is stored mainly as triacylglycerols in specialized cells called **adipocytes** or **adipose cells.** As shown in Figure 24.1, triacylglycerols, aggregated to form large globules, occupy most of the volume of adipose cells. Much smaller amounts of triacylglycerols are stored as small, aggregated globules in muscle tissue.

Hormones Signal the Release of Fatty Acids from Adipose Tissue

The pathways for liberation of fatty acids from triacylglycerols, either from adipose cells or from the diet, are shown in Figures 24.2 and 24.3. Fatty acids are mobilized from adipocytes in response to hormone messengers such as adren-

Table 24.1

Stored Metabolic Fuel in a 70-kg Person

Constituent	Energy (kJ/g dry weight)	Dry Weight (g)	Available Energy (kJ)
Fat (adipose tissue)	37	15,000	555,000
Protein (muscle)	17	6,000	102,000
Glycogen (muscle)	16	120	1,920
Glycogen (liver)	16	70	1,120
Glucose (extracellular fluid)	16	20	320
Total			660,360

Sources: Owen, O. E., and Reichard, G. A., Jr., 1971. *Progress in Biochemistry and Pharmacology* **6:**177; Newsholme, E. A., and Leech, A. R., 1983. *Biochemistry for the Medical Sciences.* New York: Wiley.

aline, glucagon, and ACTH (adrenocorticotropic hormone). These signal molecules bind to receptors on the plasma membrane of adipose cells and lead to the activation of adenylyl cyclase, which forms cyclic AMP from ATP. (Second messengers and hormonal signaling are discussed in Chapter 34.) In adipose cells, cAMP activates protein kinase A, which phosphorylates and activates a **triacylglycerol lipase** (also termed **hormone-sensitive lipase**) that hydrolyzes a fatty acid from C-1 or C-3 of triacylglycerols. Subsequent actions of **diacylglycerol lipase** and **monoacylglycerol lipase** yield fatty acids and glycerol. The cell then releases the fatty acids into the blood, where they are carried (in complexes with *serum albumin*) to sites of utilization.

Degradation of Dietary Fatty Acids Occurs Primarily in the Duodenum

Dietary triacylglycerols are degraded to a small extent (via fatty acid release) by lipases in the low-pH environment of the stomach, but mostly pass untouched into the duodenum. Alkaline pancreatic juice secreted into the
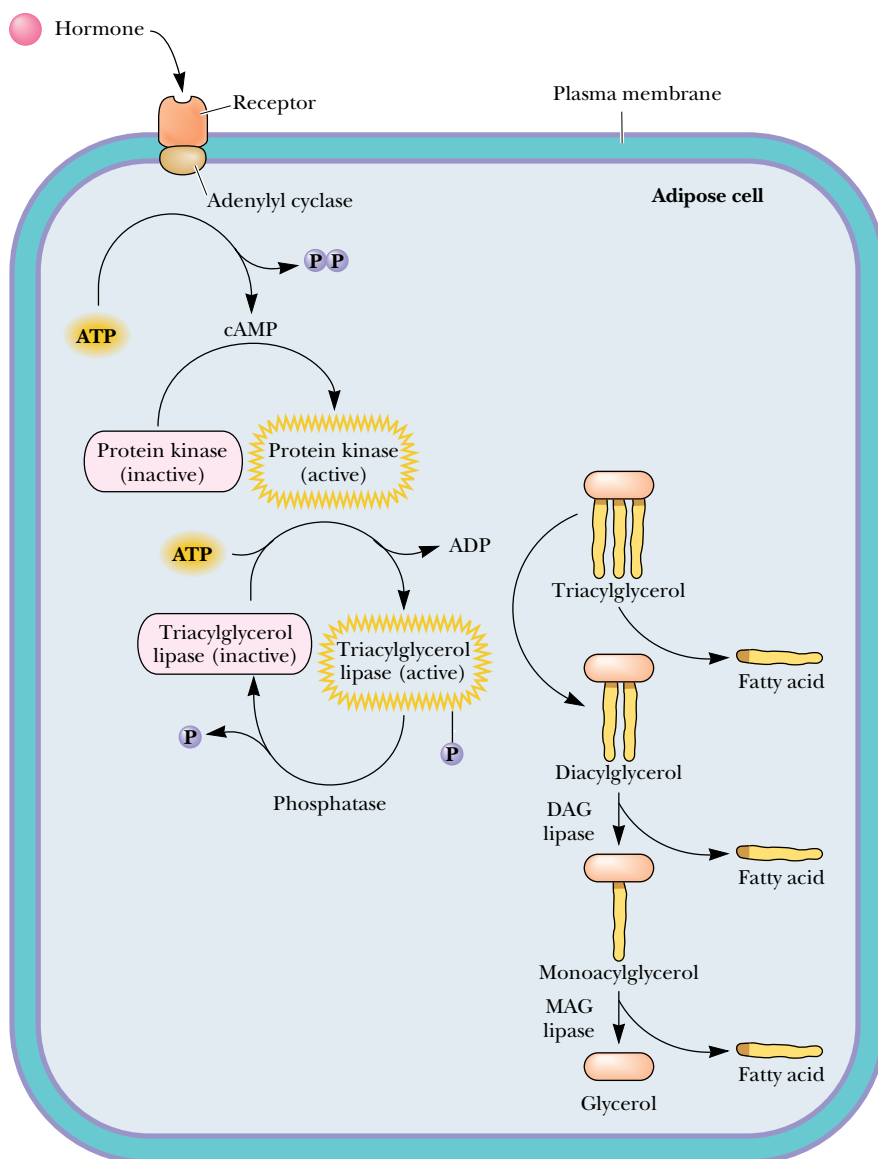

FIGURE 24.2 • Liberation of fatty acids from triacylglycerols in adipose tissue is hormone-dependent.
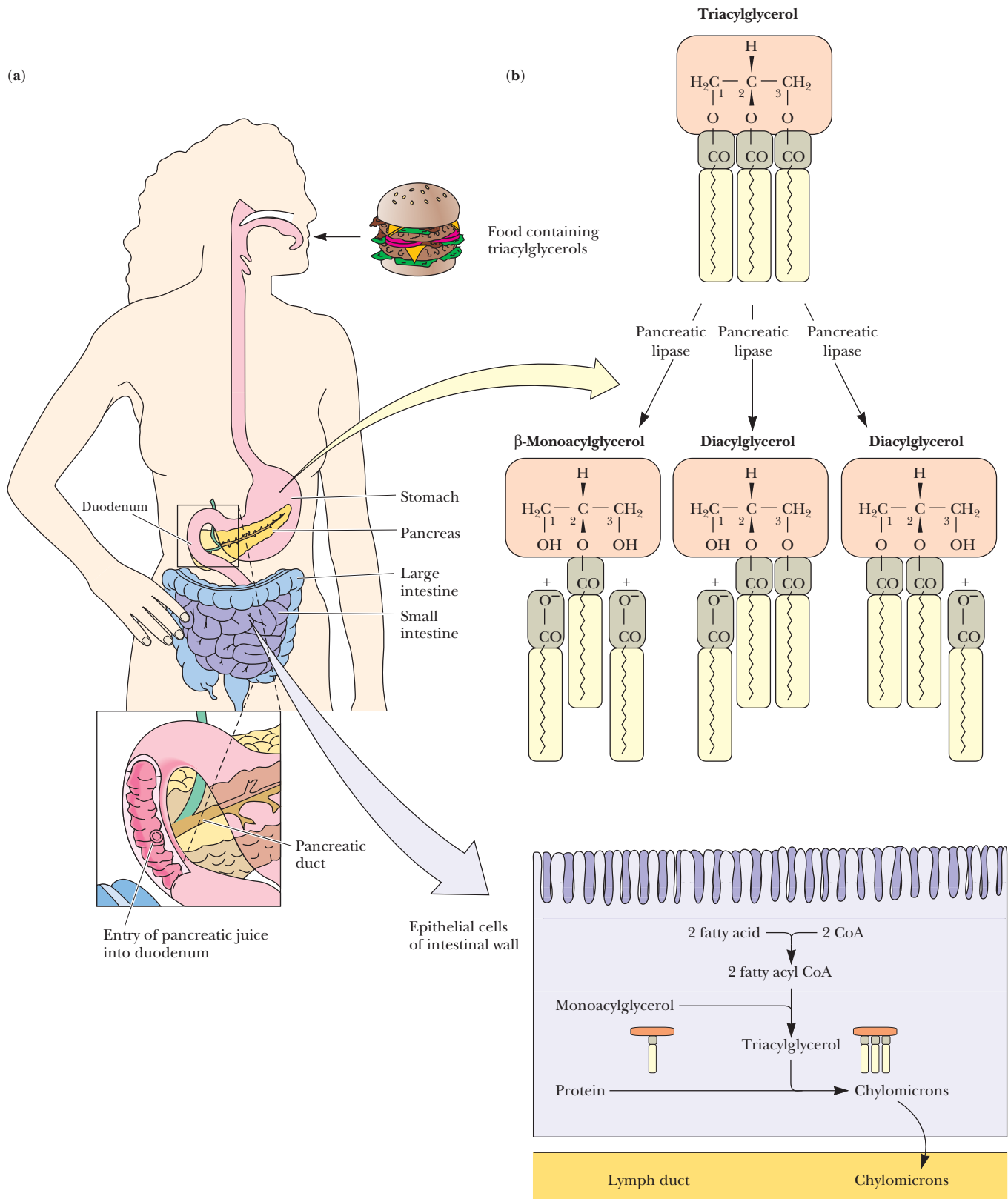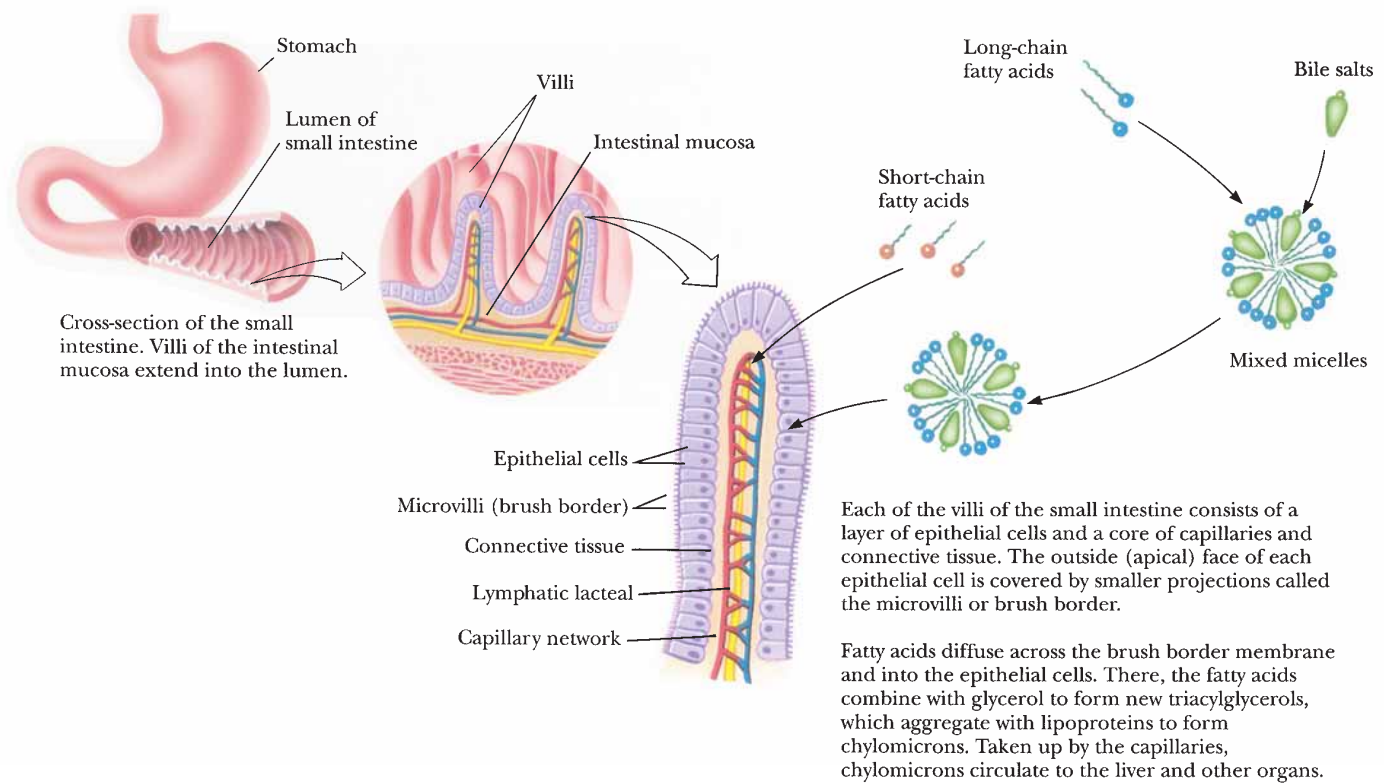
FIGURE 24.3 • (a) A duct at the junction of the pancreas and duodenum secretes pancreatic juice into the duodenum, the first portion of the small intestine. (b) Hydrolysis of triacylglycerols by pancreatic and intestinal lipases. Pancreatic lipases cleave fatty acids at the C-1 and C-3 positions. Resulting monoacylglycerols with fatty acids at C-2 are hydrolyzed by intestinal lipases. Fatty acids and monoacylglycerols are absorbed through the intestinal wall and assembled into lipoprotein aggregates termed *chylomicrons* (discussed in Chapter 25).

Cross-section of the small
intestine. Villi of the intestinal
mucosa extend into the lumen.

Villi

Lumen of
small intestine

Intestinal mucosa

Long-chain
fatty acids

Bile salts

Short-chain
fatty acids

Mixed micelles

Epithelial cells

Microvilli (brush border)

Connective tissue

Lymphatic lacteal

Capillary network

Each of the villi of the small intestine consists of a
layer of epithelial cells and a core of capillaries and
connective tissue. The outside (apical) face of each
epithelial cell is covered by smaller projections called
the microvilli or brush border.

Fatty acids diffuse across the brush border membrane
and into the epithelial cells. There, the fatty acids
combine with glycerol to form new triacylglycerols,
which aggregate with lipoproteins to form
chylomicrons. Taken up by the capillaries,
chylomicrons circulate to the liver and other organs.

duodenum (Figure 24.3a) raises the pH of the digestive mixture, allowing hydrolysis of the triacylglycerols by pancreatic lipase and by nonspecific esterases, which hydrolyze the fatty acid ester linkages. Pancreatic lipase cleaves fatty acids from the C-1 and C-3 positions of triacylglycerols, and other lipases and esterases attack the C-2 position (Figure 24.3b). These processes depend upon the presence of **bile salts,** a family of carboxylic acid salts with steroid backbones (see also Chapter 25). These agents act as detergents to emulsify the triacylglycerols and facilitate the hydrolytic activity of the lipases and esterases. Short-chain fatty acids (10 carbons or less) released in this way are absorbed directly into the villi of the intestinal mucosa, whereas long-chain fatty acids, which are less soluble, form mixed micelles with bile salts, and are carried in this fashion to the surfaces of the epithelial cells that cover the villi (Figure 24.4). The fatty acids pass into the epithelial cells, where they are condensed with glycerol to form new triacylglycerols. These triacylglycerols aggregate with lipoproteins to form particles called **chylomicrons,** which are then transported into the lymphatic system and on to the bloodstream, where they circulate to the liver, lungs, heart, muscles, and other organs (Chapter 25). At these sites, the triacylglycerols are hydrolyzed to release fatty acids, which can then be oxidized in a highly exergonic metabolic pathway known as *β-oxidation*.

FIGURE 24.4 • In the small intestine, fatty acids combine with bile salts in mixed micelles, which deliver fatty acids to epithelial cells that cover the intestinal villi. Triacylglycerols are formed within the epithelial cells.

24.2 • *β*-Oxidation of Fatty Acids

### Franz Knoop and the Discovery of *β*-Oxidation

The earliest clue to the secret of fatty acid oxidation and breakdown came in the early 1900s, when Franz Knoop carried out experiments in which he fed dogs fatty acids in which the terminal methyl group had been replaced with a

phenyl ring (Figure 24.5). Knoop discovered that fatty acids containing an even number of carbon atoms were broken down to yield phenyl acetate as the final product, whereas fatty acids with an odd number of carbon atoms yielded benzoate as the final product (Figure 24.5). From these experiments, Knoop concluded that the fatty acids must be degraded by *oxidation at the β-carbon* (Figure 24.6), followed by cleavage of the C_α—C_β bond. Repetition of this process yielded 2-carbon units, which Knoop assumed must be acetate. Much later, Albert Lehninger showed that this degradative process took place in the mitochondria, and F. Lynen and E. Reichart showed that the 2-carbon unit released

FIGURE 24.5 • The oxidative breakdown of phenyl fatty acids observed by Franz Knoop. He observed that fatty acid analogs with even numbers of carbon atoms yielded phenyl acetate, whereas compounds with odd numbers of carbon atoms produced only benzoate.
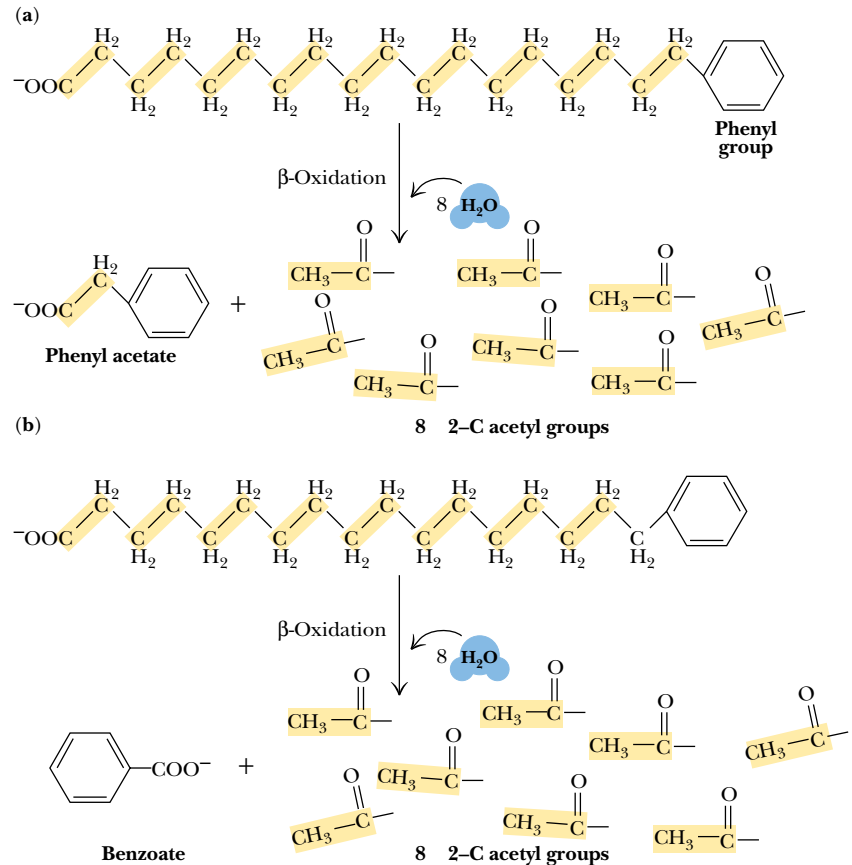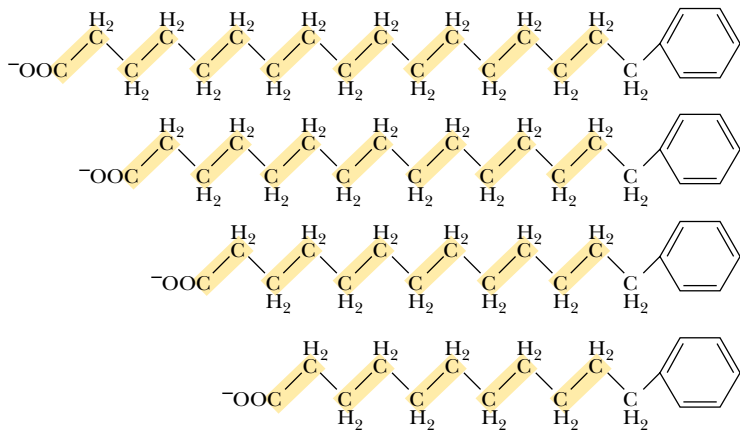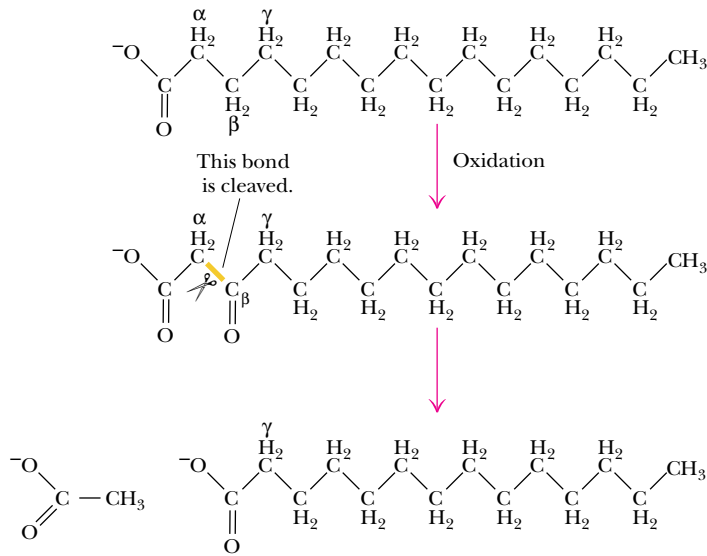
FIGURE 24.6 • Fatty acids are degraded by repeated cycles of oxidation at the β-carbon and cleavage of the C_α—C_β bond to yield acetate units.

is *acetyl-CoA,* not free acetate. Because the entire process begins with oxidation of the carbon that is "β" to the carboxyl carbon, the process has come to be known as **β-oxidation.**

Coenzyme A Activates Fatty Acids for Degradation

The process of β-oxidation begins with the formation of a thiol ester bond between the fatty acid and the thiol group of coenzyme A. This reaction, shown in Figure 24.7, is catalyzed by **acyl-CoA synthetase,** which is also called **acyl-CoA ligase** or **fatty acid thiokinase.** This condensation with CoA activates the fatty acid for reaction in the β-oxidation pathway. For long-chain fatty acids, this reaction normally occurs at the outer mitochondrial membrane, prior to entry of the fatty acid into the mitochondrion, but it may also occur at the surface of the endoplasmic reticulum. Short- and medium-length fatty acids undergo this activating reaction in the mitochondria. In all cases, the reaction is accompanied by the hydrolysis of ATP to form AMP and pyrophosphate. As shown in Figure 24.7, the two combined reactions have a net $\Delta G^{\circ\prime}$ of about -0.8 kJ/mol, so that the reaction is favorable but easily reversible. However, there is more to the story. As we have seen in several similar cases, the pyrophosphate produced in this reaction is rapidly hydrolyzed by inorganic pyrophosphatase to two molecules of phosphate, with a net $\Delta G^{\circ\prime}$ of about -33.6 kJ/mol.

$$\Delta G^{\circ\prime}\text{ for } ATP \longrightarrow AMP + PP = -32.3\ \frac{kJ}{mol}$$

$$\Delta G^{\circ\prime}\text{ for acyl-CoA synthesis} = +31.5\ \frac{kJ}{mol}$$

$$\text{Net }\Delta G^{\circ\prime} = -0.8\ \frac{kJ}{mol}$$

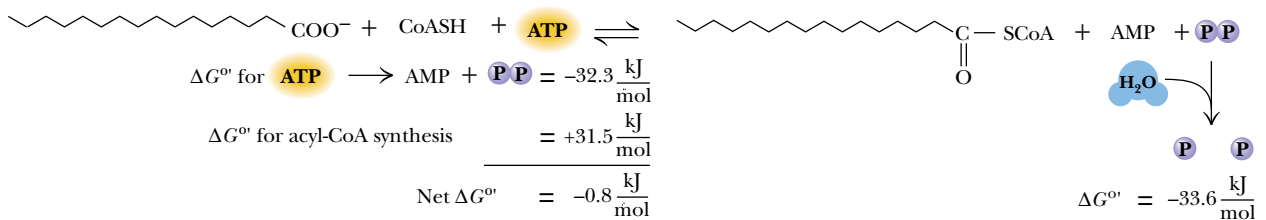$$\Delta G^{\circ\prime} = -33.6\ \frac{kJ}{mol}$$

FIGURE 24.7 • The acyl-CoA synthetase reaction activates fatty acids for β-oxidation. The reaction is driven by hydrolysis of ATP to AMP and pyrophosphate and by the subsequent hydrolysis of pyrophosphate.
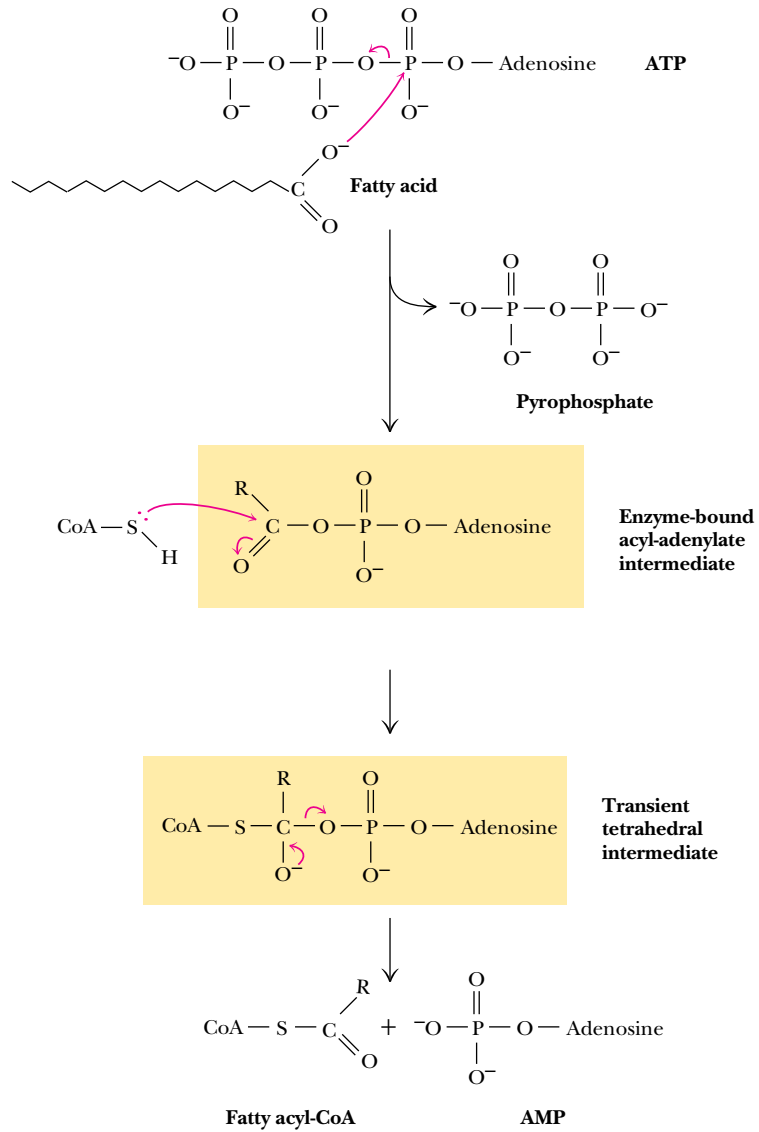
FIGURE 24.8 • The mechanism of the acyl-CoA synthetase reaction involves fatty acid carboxylate attack on ATP to form an acyl-adenylate intermediate. The fatty acyl CoA thioester product is formed by CoA attack on this intermediate.

Thus, pyrophosphate is maintained at a low concentration in the cell (usually less than 1 mM) and the synthetase reaction is strongly promoted. The mechanism of the acyl-CoA synthetase reaction is shown in Figure 24.8 and involves attack of the fatty acid carboxylate on ATP to form an *acyladenylate intermediate,* which is subsequently attacked by CoA, forming a fatty acyl-CoA thioester.

Carnitine Carries Fatty Acyl Groups Across the Inner Mitochondrial Membrane

All of the other enzymes of the β-oxidation pathway are located in the mitochondrial matrix. Short-chain fatty acids, as already mentioned, are transported into the matrix as free acids and form the acyl-CoA derivatives there. However, long-chain fatty acyl-CoA derivatives cannot be transported into the matrix directly. These long-chain derivatives must first be converted to *acylcarnitine* derivatives, as shown in Figure 24.9. **Carnitine acyltransferase I,** located on the outer side of the inner mitochondrial membrane, catalyzes the formation of
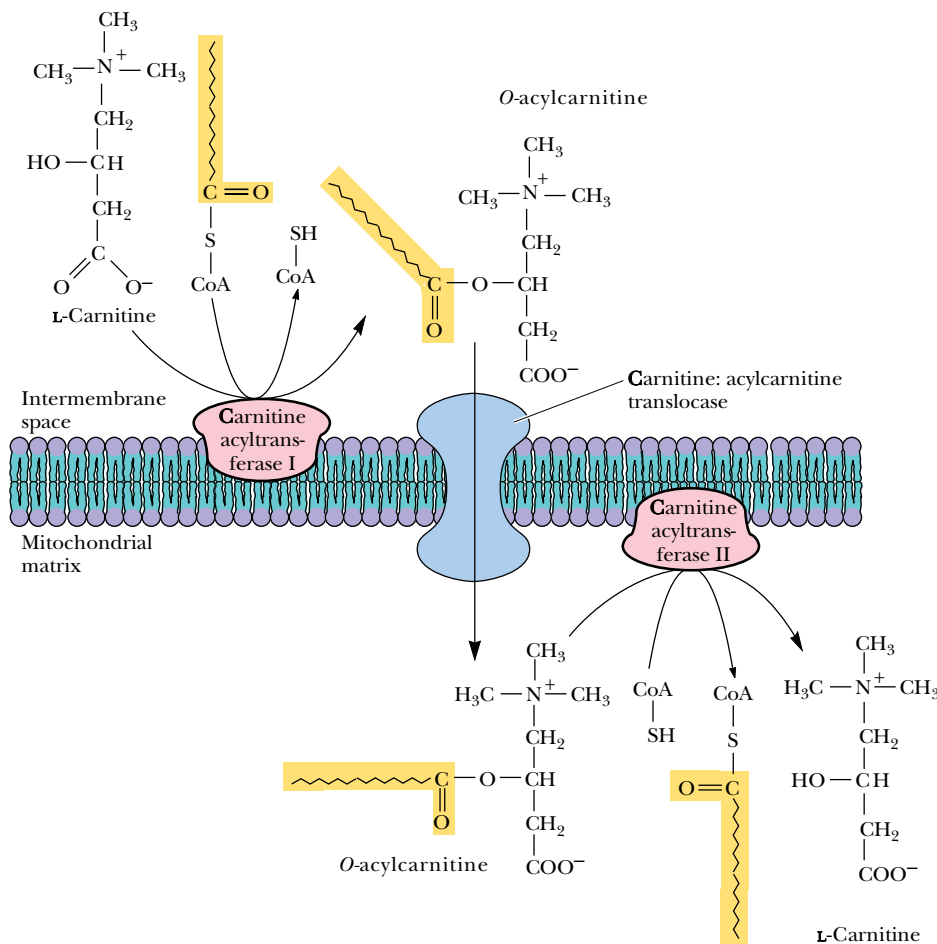
FIGURE 24.9 • The formation of acylcarnitines and their transport across the inner mitochondrial membrane. The process involves the coordinated actions of carnitine acyltransferases on both sides of the membrane and of a translocase that shuttles O-acylcarnitines across the membrane.

the O-acylcarnitine, which is then transported across the inner membrane by a **translocase.** At this point, the acylcarnitine is passed to **carnitine acyltransferase II** on the matrix side of the inner membrane, which transfers the fatty acyl group back to CoA to re-form the fatty acyl-CoA, leaving free carnitine, which can return across the membrane via the translocase.

Several additional points should be made. First, although oxygen esters usually have lower group-transfer potentials than thiol esters, the O—acyl bonds in acylcarnitines have high group-transfer potentials, and the transesterification reactions mediated by the acyltransferases have equilibrium constants close to 1. Second, note that eukaryotic cells maintain separate pools of CoA in the mitochondria and in the cytosol. The cytosolic pool is utilized principally in fatty acid biosynthesis (Chapter 25), and the mitochondrial pool is important in the oxidation of fatty acids and pyruvate, as well as some amino acids.

β-Oxidation Involves a Repeated Sequence of Four Reactions

For saturated fatty acids, the process of β-oxidation involves a recurring cycle of four steps, as shown in Figure 24.10. The overall strategy in the first three steps is to create a carbonyl group on the β-carbon by oxidizing the C_α—C_β bond to form an olefin, with subsequent hydration and oxidation. In essence, this cycle is directly analogous to the sequence of reactions converting succi-
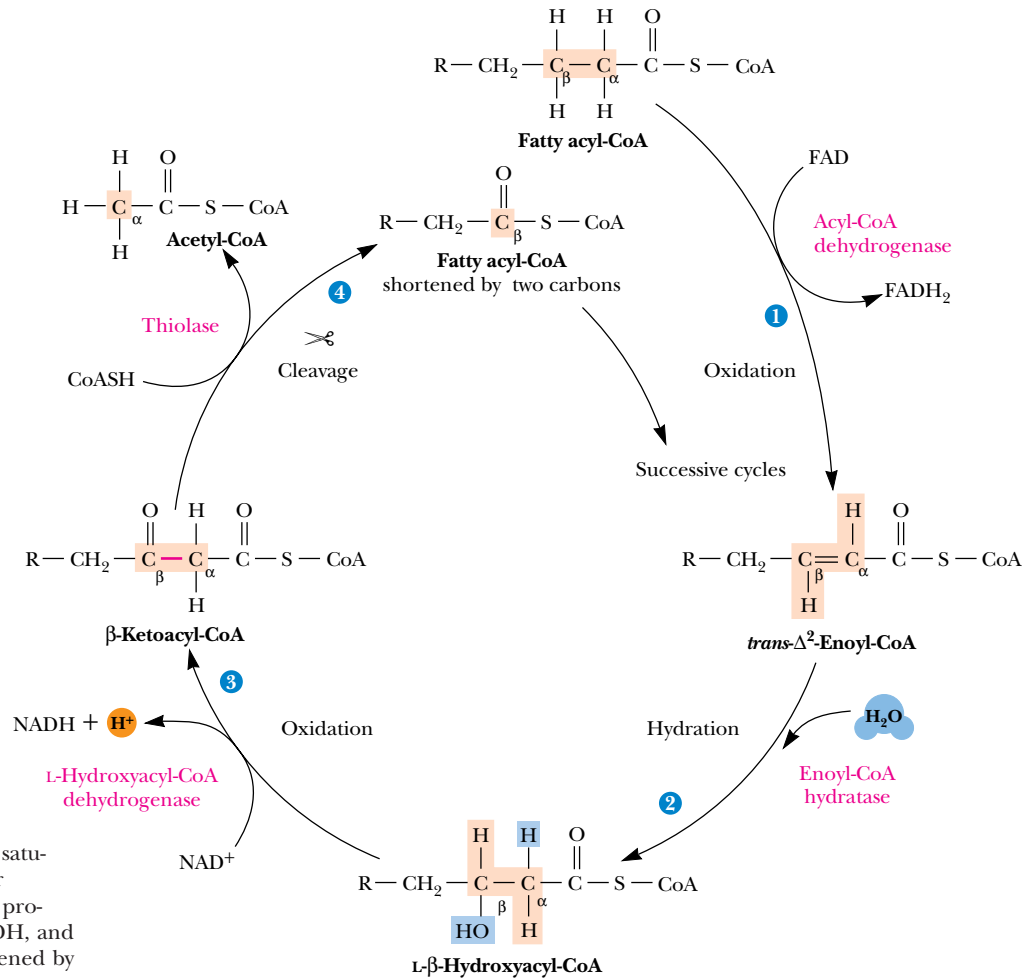
FIGURE 24.10 • The β-oxidation of saturated fatty acids involves a cycle of four enzyme-catalyzed reactions. Each cycle produces single molecules of FADH$_2$, NADH, and acetyl-CoA and yields a fatty acid shortened by two carbons. (The delta [Δ] symbol connotes a double bond, and its superscript indicates the lower-numbered carbon involved.)

nate to oxaloacetate in the TCA cycle. The fourth reaction of the cycle cleaves the β-keto ester in a reverse Claisen condensation, producing an acetate unit and leaving a fatty acid chain that is two carbons shorter than it began. (Recall from Chapter 20 that Claisen condensations involve attack by a nucleophilic agent on a carbonyl carbon to yield a β-keto acid.)

Acyl-CoA Dehydrogenase—The First Reaction of β-Oxidation

The first reaction, the oxidation of the C_α—C_β bond, is catalyzed by **acyl-CoA dehydrogenases,** a family of three soluble matrix enzymes (with molecular weights of 170 to 180 kD), which differ in their specificity for either long-, medium-, or short-chain acyl-CoAs. They carry noncovalently (but tightly) bound FAD, which is reduced during the oxidation of the fatty acid. As shown in Figure 24.11, FADH$_2$ transfers its electrons to an **electron transfer flavoprotein** (ETF). Reduced ETF is reoxidized by a specific oxidoreductase (an iron–sulfur protein), which in turn sends the electrons on to the electron transport chain at the level of coenzyme Q. As always, mitochondrial oxidation of FAD in this way eventually results in the net formation of about 1.5 ATP. The mechanism of the acyl-CoA dehydrogenase (Figure 24.12) involves deprotonation of the fatty acid chain at the α-carbon, followed by hydride transfer from the β-carbon to FAD. The structure of the medium-chain dehydrogenase from pig liver places an FAD molecule in an extended conformation between a bundle of α-helices and a distorted β-barrel (Figure 24.13).
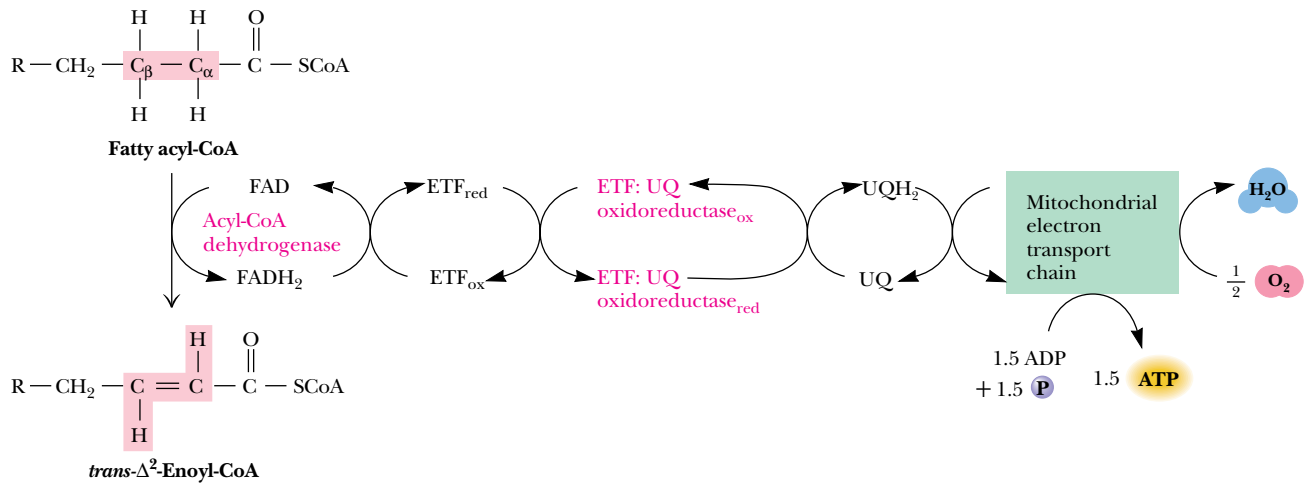
FIGURE 24.11 • The acyl-CoA dehydrogenase reaction. The two electrons removed in this oxidation reaction are delivered to the electron transport chain in the form of reduced coenzyme Q (UQH_2).
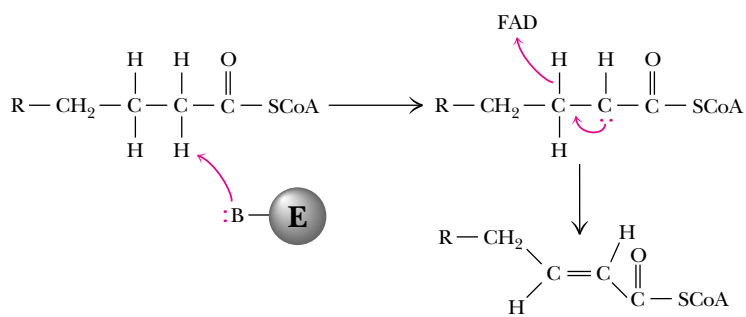

FIGURE 24.12 • The mechanism of acyl-CoA dehydrogenase. Removal of a proton from the α-C is followed by hydride transfer from the β-carbon to FAD.
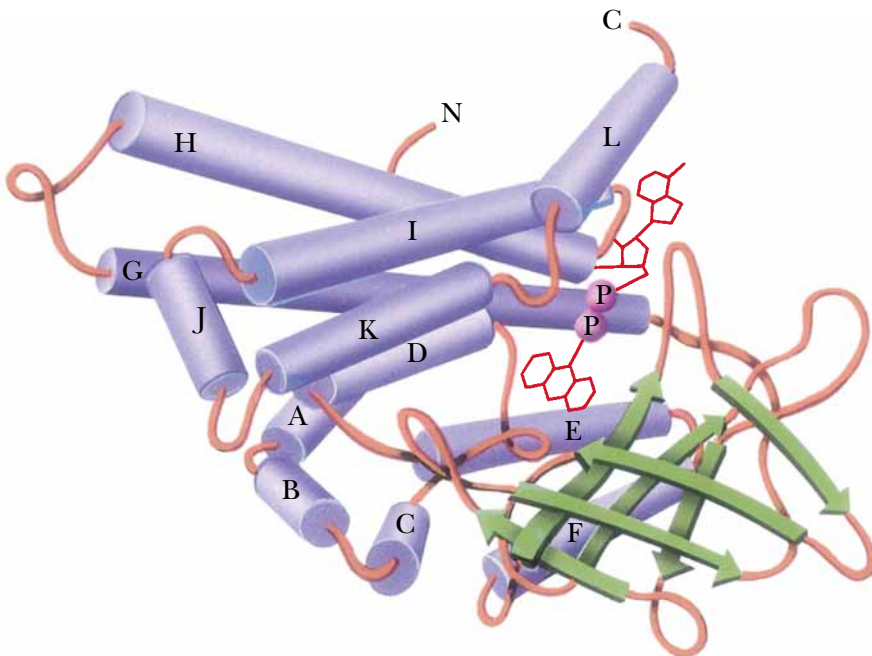

FIGURE 24.13 • The subunit structure of medium chain acyl-CoA dehydrogenase from pig liver mitochondria. Note the location of the bound FAD (red). *(Adapted from Kim, J.-T., and Wu, J., 1988. Structure of the medium-chain acyl-CoA dehydrogenase from pig liver mitochondria at 3-Å resolution. Proceedings of the National Academy of Sciences, USA* **85:**6671–6681.)

𝒜 D E E P E R L O O K

The Akee Tree

The akee (also spelled *ackee*) tree is native to West Africa and was brought to the Caribbean by African slaves. It was introduced to science by William Bligh, captain of the infamous sailing ship the *Bounty,* and its botanical name is (appropriately) *Blighia sapida* (the latter name from the Latin *sapidus* meaning "tasty"). A popular dish in the Caribbean consists of akee and salt fish.

> *"Akee, rice, salt fish are nice,*
> *And the rum is fine any time of year."*
> —*From the song* Jamaica Farewell

(R.R. Head/Earth Scenes/Animals, Animals)

A Metabolite of Hypoglycin from Akee Fruit Inhibits Acyl-CoA Dehydrogenase

The unripened fruit of the **akee tree** contains **hypoglycin,** a rare amino acid (Figure 24.14). Metabolism of hypoglycin yields *methylenecyclopropylacetyl-CoA* (MCPA-CoA). Acyl-CoA dehydrogenase will accept MCPA-CoA as a substrate,

FIGURE 24.14 • The conversion of hypoglycin from akee fruit to a form that inhibits acyl-CoA dehydrogenase.
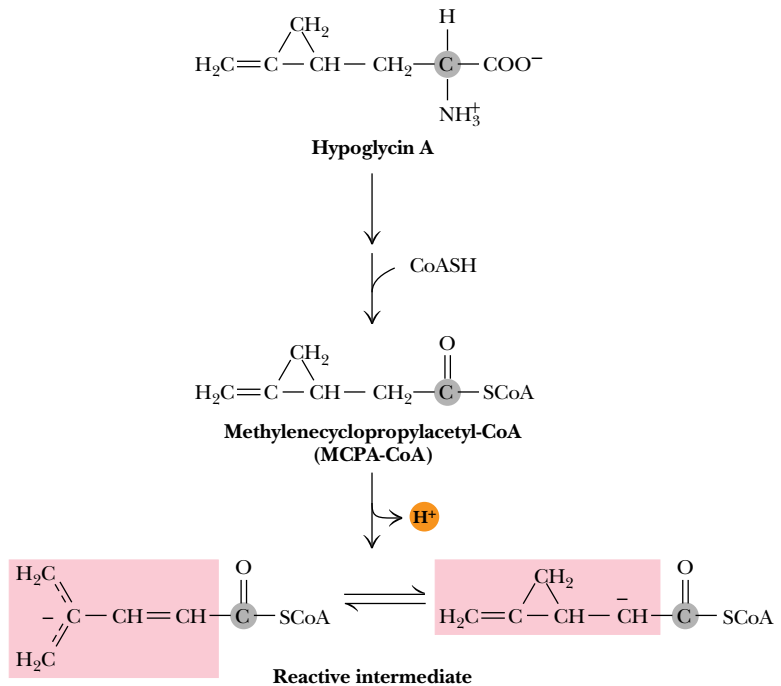
removing a proton from the α-carbon to yield an intermediate that irreversibly inactivates acyl-CoA dehydrogenase by reacting covalently with FAD on the enzyme. For this reason, consumption of unripened akee fruit can lead to vomiting and, in severe cases, convulsions, coma, and death. The condition is most severe in individuals with low levels of acyl-CoA dehydrogenase.

Enoyl-CoA Hydratase Adds Water Across the Double Bond

The next step in β-oxidation is the addition of the elements of H_2O across the new double bond in a stereospecific manner, yielding the corresponding hydroxyacyl-CoA (Figure 24.15). The reaction is catalyzed by **enoyl-CoA hydratase.** At least three different enoyl-CoA hydratase activities have been detected in various tissues. Also called **crotonases,** these enzymes specifically convert *trans*-enoyl-CoA derivatives to L-β-hydroxyacyl-CoA. As shown in Figure 24.15, these enzymes will also metabolize *cis*-enoyl-CoA (at slower rates) to give specifically D-β-hydroxyacyl-CoA. Recently, a novel enoyl-CoA hydratase was discovered, which converts *trans*-enoyl-CoA to D-β-hydroxyacyl-CoA, as shown in Figure 24.15.

L-Hydroxyacyl-CoA Dehydrogenase Oxidizes the β-Hydroxyl Group

The third reaction of this cycle is the oxidation of the hydroxyl group at the β-position to produce a β-ketoacyl-CoA derivative. This second oxidation reaction is catalyzed by **L-hydroxyacyl-CoA dehydrogenase,** an enzyme that requires NAD^+ as a coenzyme. NADH produced in this reaction represents metabolic energy. Each NADH produced in mitochondria by this reaction drives the synthesis of 2.5 molecules of ATP in the electron transport pathway. L-Hydroxyacyl-
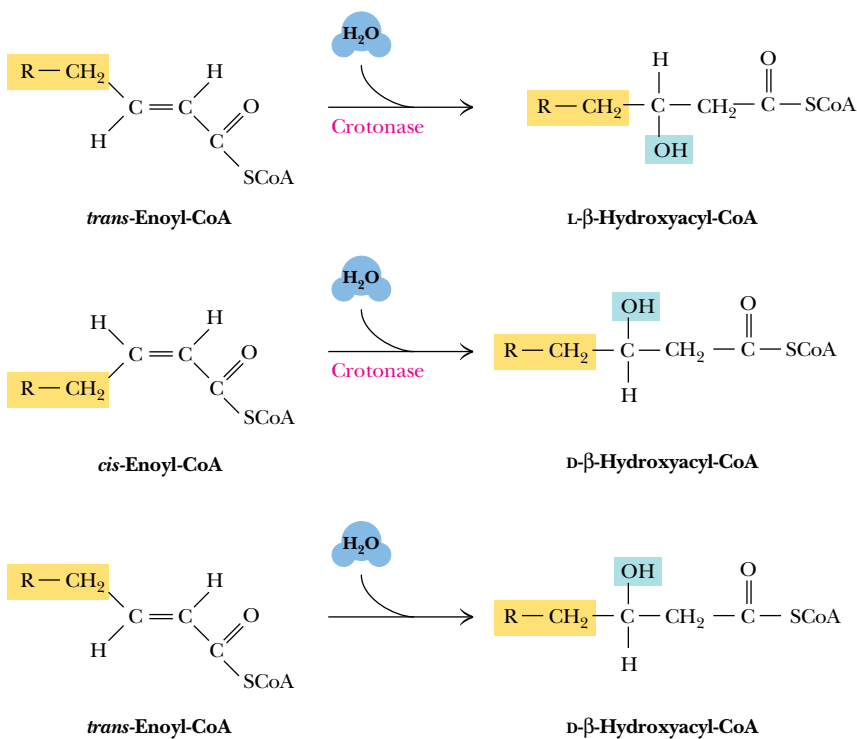

FIGURE 24.15 • The conversion of *trans*- and *cis*-enoyl CoA derivatives to L- and D-β-hydroxyacyl CoA, respectively. These reactions are catalyzed by enoyl-CoA hydratases (also called crotonases), enzymes that vary in their acyl-chain length specificity. A recently discovered enzyme converts *trans*-enoyl-CoA directly to D-β-hydroxyacyl-CoA.

FIGURE 24.16 • The L-β-hydroxyacyl-CoA dehydrogenase reaction.

CoA dehydrogenase shows absolute specificity for the L-hydroxyacyl isomer of the substrate (Figure 24.16). (D-Hydroxyacyl isomers, which arise mainly from oxidation of unsaturated fatty acids, are handled differently.)

β-Ketoacyl-CoA Intermediates Are Cleaved in the Thiolase Reaction

The final step in the β-oxidation cycle is the cleavage of the β-ketoacyl-CoA. This reaction, catalyzed by **thiolase** (also known as **β-ketothiolase**), involves the attack of a cysteine thiolate from the enzyme on the β-carbonyl carbon, followed by cleavage to give the enolate of acetyl-CoA and an enzyme-thioester intermediate (Figure 24.17). Subsequent attack by the thiol group of a second CoA and departure of the cysteine thiolate yields a new (shorter) acyl-CoA. If the reaction in Figure 24.17 is read in reverse, it is easy to see that it is a Claisen condensation—an attack of the enolate anion of acetyl-CoA on a thioester. Despite the formation of a second thioester, this reaction has a very favorable K_{eq}, and it drives the three previous reactions of β-oxidation.
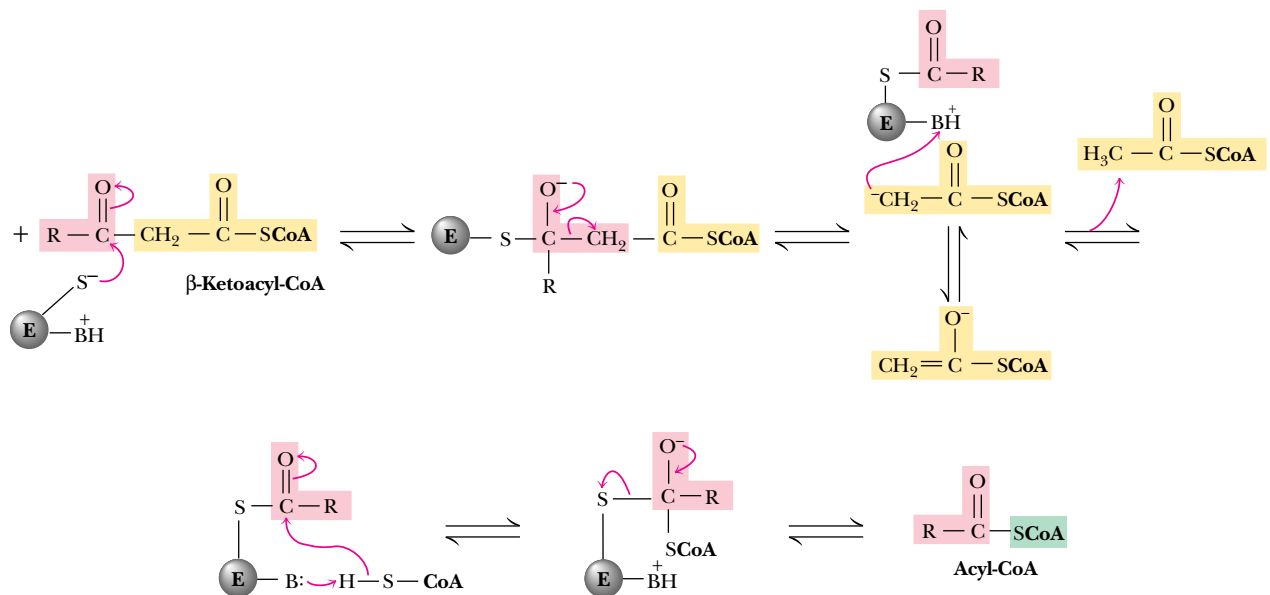

FIGURE 24.17 • The mechanism of the thiolase reaction. Attack by an enzyme cysteine thiolate group at the β-carbonyl carbon produces a tetrahedral intermediate, which decomposes with departure of acetyl-CoA, leaving an enzyme thioester intermediate. Attack by the thiol group of a second CoA yields a new (shortened) acyl-CoA.

Repetition of the *β*-Oxidation Cycle Yields a Succession of Acetate Units

In essence, this series of four reactions has yielded a fatty acid (as a CoA ester) that has been shortened by two carbons, and one molecule of acetyl-CoA. The shortened fatty acyl-CoA can now go through another *β*-oxidation cycle, as shown in Figure 24.10. Repetition of this cycle with a fatty acid with an even number of carbons eventually yields two molecules of acetyl-CoA in the final step. As noted in the first reaction in Table 24.2, complete *β*-oxidation of palmitic acid yields eight molecules of acetyl-CoA as well as seven molecules of $FADH_2$ and seven molecules of NADH. The acetyl-CoA can be further metabolized in the TCA cycle (as we have already seen). Alternatively, acetyl-CoA can also be used as a substrate in amino acid biosynthesis (Chapter 26). As noted in Chapter 23, however, acetyl-CoA cannot be used as a substrate for gluconeogenesis.

Complete *β*-Oxidation of One Palmitic Acid Yields 106 Molecules of ATP

If the acetyl-CoA is directed entirely to the TCA cycle in mitochondria, it can eventually generate approximately 10 high-energy phosphate bonds—that is, 10 molecules of ATP synthesized from ADP (Table 24.2). Including the ATP formed from $FADH_2$ and NADH, complete *β*-oxidation of a molecule of palmitoyl-CoA in mitochondria yields 108 molecules of ATP. Subtracting the two high-energy bonds needed to form palmitoyl-CoA, the substrate for *β*-oxidation, one concludes that *β*-oxidation of a molecule of palmitic acid yields 106 molecules of ATP. The $\Delta G^{\circ\prime}$ for complete combustion of palmitate to CO_2 is -9790 kJ/mol. The hydrolytic energy embodied in 106 ATPs is 106×30.5 kJ/mol $= 3233$ kJ/mol, so the overall efficiency of *β*-oxidation under standard-state conditions is approximately 33%. The large energy yield from fatty acid oxidation is a reflection of the highly reduced state of the carbon in fatty acids. Sugars, in which the carbon is already partially oxidized, produce much less energy, carbon for carbon, than do fatty acids. The breakdown of fatty acids is regulated by a variety of metabolites and hormones. Details of this regulation are described in Chapter 25, following a discussion of fatty acid synthesis.

Table 24.2

Equations for the Complete Oxidation of Palmitoyl-CoA to CO_2 and H_2O

Equation	ATP Yield	Free Energy (kJ/mol) Yield
$CH_3(CH_2)_{14}CO-CoA + 7$ [FAD] $+ 7\ H_2O + 7\ NAD^+ + 7$ CoA $\longrightarrow$ 8 CH_3CO-CoA $+ 7$ [$FADH_2$] $+ 7$ NADH $+ 7\ H^+$		
7 [$FADH_2$] $+ 10.5\ P_i + 10.5$ ADP $+ 3.5\ O_2 \longrightarrow$ 7 [FAD] $+ 17.5\ H_2O + 10.5$ ATP	10.5	320
7 NADH $+ 7\ H^+ + 17.5\ P_i + 17.5$ ADP $+ 3.5\ O_2 \longrightarrow$ 7 $NAD^+ + 24.5\ H_2O + 17.5$ ATP	17.5	534
8-Acetyl-CoA $+ 16\ O_2 + 80$ ADP $+ 80\ P_i \longrightarrow$ 8 CoA $+ 88\ H_2O + 16\ CO_2 + 80$ ATP	80	2440
$CH_3(CH_2)_{14}CO-CoA + 108\ P_i + 108$ ADP $+ 23\ O_2 \longrightarrow$ 108 ATP $+ 16\ CO_2 + 130\ H_2O +$ CoA	108	3294
Energetic "cost" of forming palmitoyl-CoA from palmitate and CoA	-2	-61
	106	3233

(a) Gerbil

(b) Ruby-throated hummingbird

Migratory Birds Travel Long Distances on Energy from Fatty Acid Oxidation

Because they represent the most highly concentrated form of stored biological energy, fatty acids are the metabolic fuel of choice for sustaining the incredibly long flights of many migratory birds. Although some birds migrate over land masses and dine frequently, other species fly long distances without stopping to eat. The American golden plover flies directly from Alaska to Hawaii, a 3300-kilometer flight requiring 35 hours (at an average speed of nearly 60 miles/hr) and more than 250,000 wing beats! The ruby-throated hummingbird, which winters in Central America and nests in southern Canada, often flies nonstop across the Gulf of Mexico. These and similar birds accomplish these prodigious feats by storing large amounts of fatty acids (as triacylglycerols) in the days before their migratory flights. The percentage of dry-weight body fat in these birds may be as high as 70% when migration begins (compared with values of 30% and less for nonmigratory birds).

Fatty Acid Oxidation Is an Important Source of Metabolic Water for Some Animals

Large amounts of metabolic water are generated by β-oxidation (130 H_2O per palmitoyl-CoA). For certain animals—including desert animals, such as gerbils, and killer whales (which do not drink seawater)—the oxidation of fatty acids can be a significant source of dietary water. A striking example is the camel (Figure 24.18), whose hump is essentially a large deposit of fat. Metabolism of fatty acids from this store provides needed water (as well as metabolic energy) during periods when drinking water is not available. It might well be said that "the ship of the desert" sails on its own metabolic water!

(c) Golden plover

(d) Orca

(e) Camels

FIGURE 24.18 • Animals whose existence is strongly dependent on fatty acid oxidation: (a) gerbil, (b) ruby-throated hummingbird, (c) golden plover, (d) orca (killer whale), and (e) camels. *(a, Photo Researchers, Inc.; b, Tom J. Ulrich/Visuals Unlimited; c, S. J. Krasemann/Photo Researchers, Inc.; d, © Francois Gohier/Photo Researchers, Inc.; e, © George Holton/Photo Researchers, Inc.)*

24.3 • β-Oxidation of Odd-Carbon Fatty Acids

β-Oxidation of Odd-Carbon Fatty Acids Yields Propionyl-CoA

Fatty acids with odd numbers of carbon atoms are rare in mammals, but fairly common in plants and marine organisms. Humans and animals whose diets include these food sources metabolize odd-carbon fatty acids via the β-oxidation pathway. The final product of β-oxidation in this case is the 3-carbon propionyl-CoA instead of acetyl-CoA. Three specialized enzymes then carry out the reactions that convert propionyl-CoA to succinyl-CoA, a TCA cycle intermediate. (Because propionyl-CoA is a degradation product of methionine, valine, and isoleucine, this sequence of reactions is also important in amino acid catabolism, as we shall see in Chapter 26.) The pathway involves an initial carboxylation at the α-carbon of propionyl-CoA to produce D-methylmalonyl-CoA (Figure 24.19). The reaction is catalyzed by a biotin-dependent enzyme, **propionyl-CoA carboxylase.** The mechanism involves ATP-driven carboxylation of biotin at N_1, followed by nucleophilic attack by the α-carbanion of propionyl-CoA in a stereo-specific manner.

D-Methylmalonyl-CoA, the product of this reaction, is converted to the L-isomer by **methylmalonyl-CoA epimerase** (Figure 24.19). (This enzyme has often and incorrectly been called "methylmalonyl-CoA racemase." It is not a racemase because the CoA moiety contains five other asymmetric centers.) The epimerase reaction also appears to involve a carbanion at the α-position (Figure 24.20). The reaction is readily reversible and involves a reversible dissociation of the acidic α-proton. The L-isomer is the substrate for methylmalonyl-CoA mutase. Methylmalonyl-CoA epimerase is an impressive catalyst. The pK_a for the proton that must dissociate to initiate this reaction is approximately 21! If binding of a proton to the α-anion is diffusion-limited, with $k_{on} = 10^9$ M^{-1} sec^{-1}, then the initial proton dissociation must be rate-limiting, and the rate constant must be

$$k_{off} = K_a \cdot k_{on} = (10^{-21}\ M) \cdot (10^9\ M^{-1}\ sec^{-1}) = 10^{-12}\ sec^{-1}$$

The turnover number of methylmalonyl-CoA epimerase is 100 sec^{-1}, and thus the enzyme enhances the reaction rate by a factor of 10^{14}.
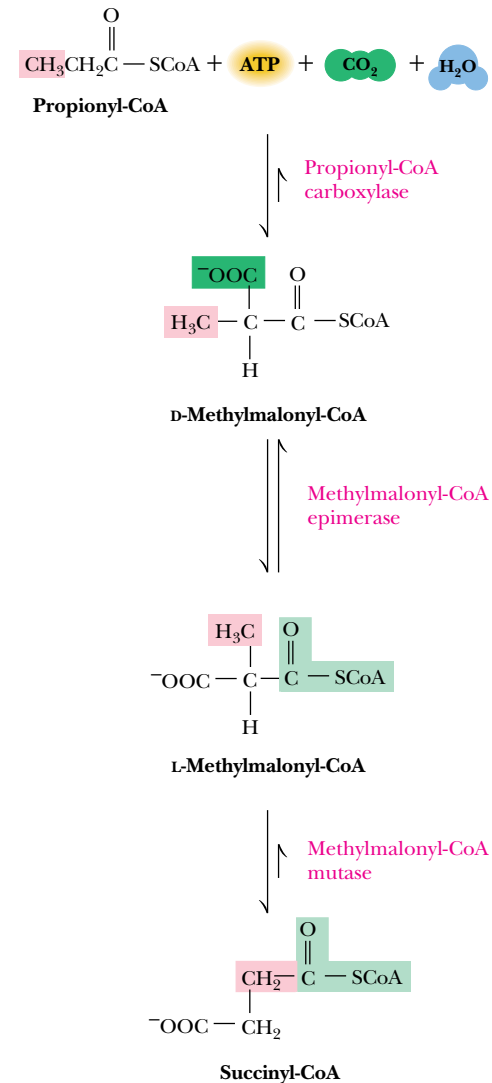

FIGURE 24.19 • The conversion of propionyl-CoA (formed from β-oxidation of odd-carbon fatty acids) to succinyl-CoA is carried out by a trio of enzymes as shown. Succinyl-CoA can enter the TCA cycle or be converted to acetyl-CoA.
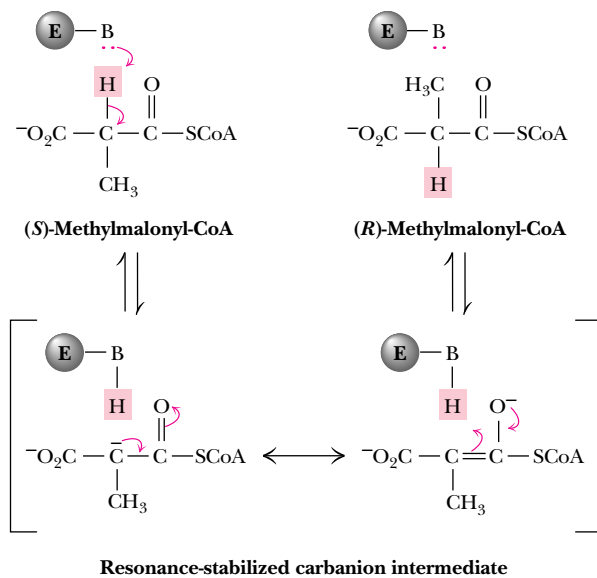

Resonance-stabilized carbanion intermediate

FIGURE 24.20 • The methylmalonyl-CoA epimerase mechanism involves a resonance-stabilized carbanion at the α-position.

A B$_{12}$-Catalyzed Rearrangement Yields Succinyl-CoA from L-Methylmalonyl-CoA

The third reaction, catalyzed by **methylmalonyl-CoA mutase,** is quite unusual because it involves a migration of the carbonyl-CoA group from one carbon to its neighbor (Figure 24.21). The mutase reaction is vitamin B$_{12}$–dependent and begins with **homolytic cleavage** of the Co^{3+}—C bond in cobalamin, reducing the cobalt to Co^{2+}. Transfer of a hydrogen atom from the substrate to the deoxyadenosyl group produces a methylmalonyl-CoA radical, which then can undergo a classic B$_{12}$-catalyzed rearrangement to yield a succinyl-CoA radical. Hydrogen transfer from the deoxyadenosyl group yields succinyl-CoA and regenerates the B$_{12}$ coenzyme.
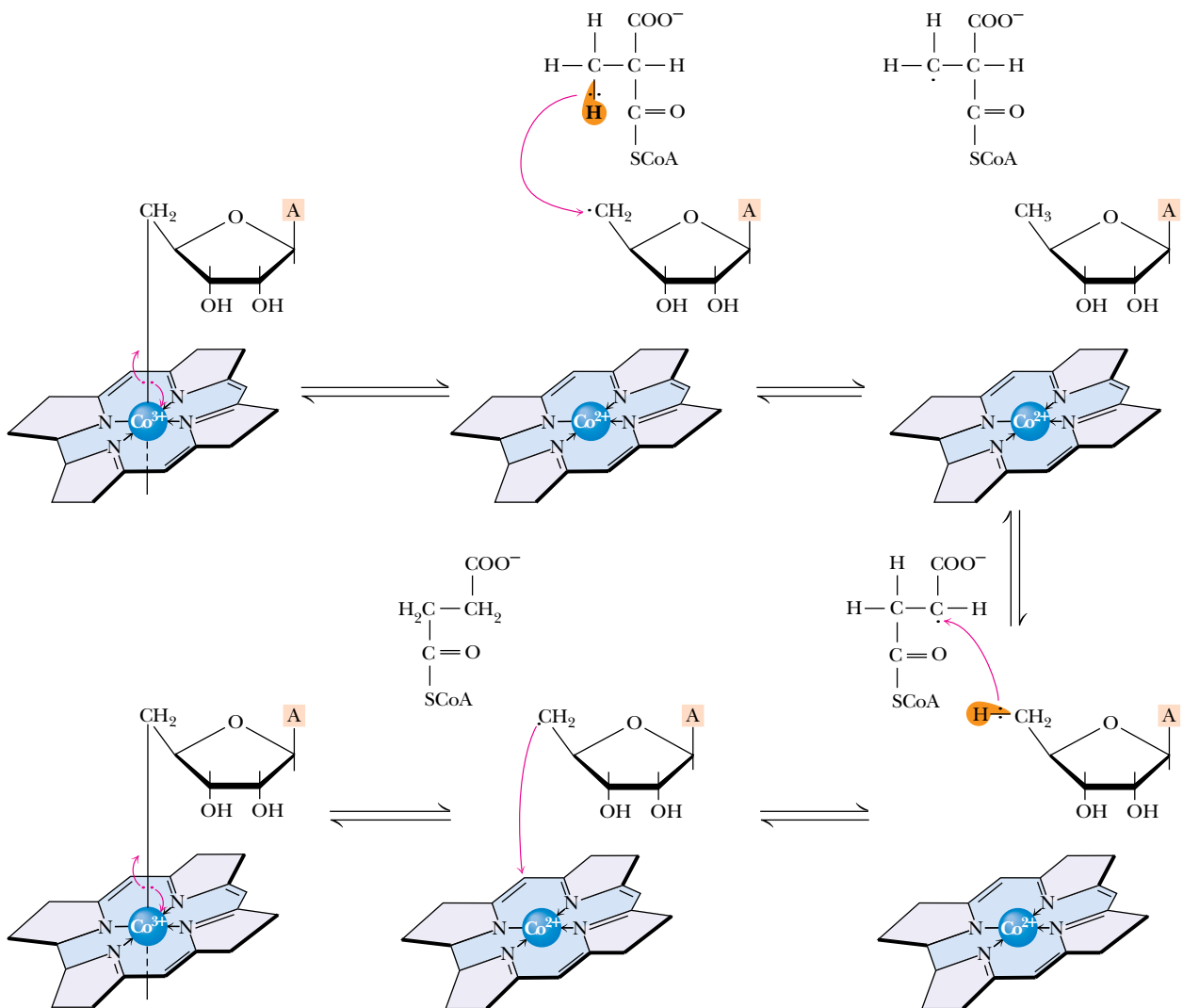

FIGURE 24.21 • A mechanism for the methylmalonyl-CoA mutase reaction. In the first step, Co^{3+} is reduced to Co^{2+} due to homolytic cleavage of the Co^{3+}—C bond in cobalamin. Hydrogen atom transfer from methylmalonyl-CoA yields a methylmalonyl-CoA radical that can undergo rearrangement to form a succinyl-CoA radical. Transfer of an H atom regenerates the coenzyme and yields succinyl-CoA.

The Activation of Vitamin B₁₂

Conversion of inactive *vitamin B₁₂* to active *5′-deoxyadenosylcobalamin* is thought to involve three steps (see figure). Two *flavoprotein reductases* sequentially convert Co^{3+} in cyanocobalamin to the Co^{2+} state and then to the Co^{+} state. Co^{+} is an extremely powerful nucleophile. It attacks the C-5′ carbon of ATP as shown, expelling the triphosphate anion to form 5′-deoxyadenosyl-cobalamin. Because two electrons from Co^{+} are donated to the Co—carbon bond, the oxidation state of cobalt reverts to Co^{3+} in the active coenzyme. This is one of only two known adenosyl transfers (that is, nucleophilic attack on the ribose 5′-carbon of ATP) in biological systems. (The other is the formation of S-adenosylmethionine—see Chapter 26.)
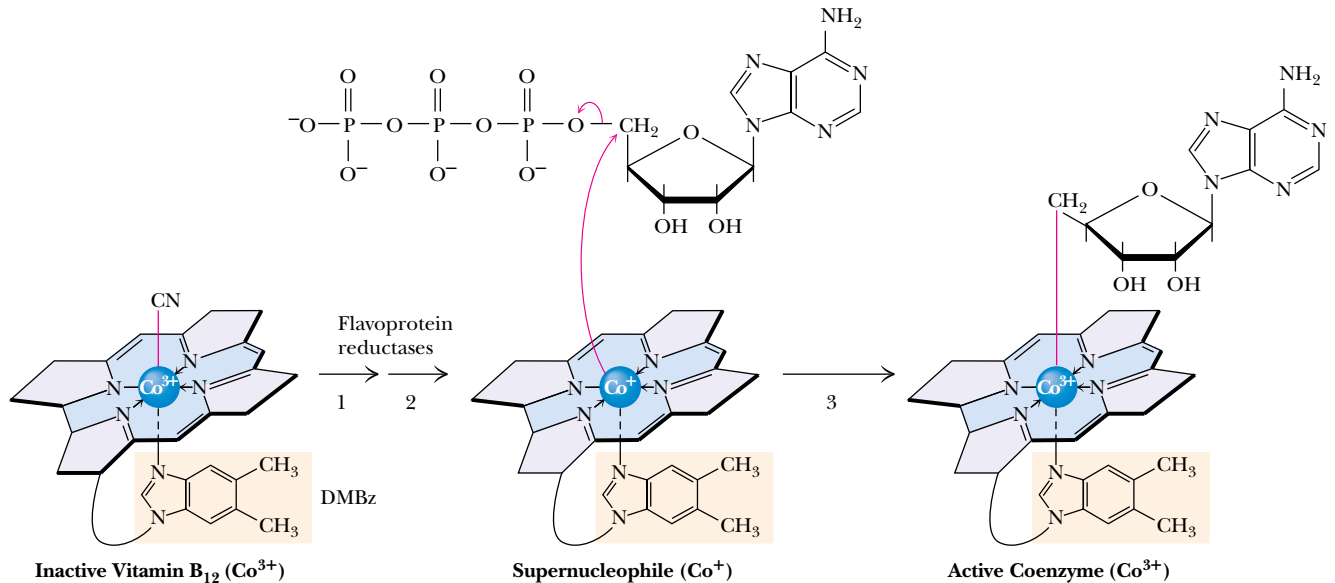
Formation of the active coenzyme 5′-deoxyadenosylcobalamin from inactive vitamin B₁₂ is initiated by the action of flavoprotein reductases. The resulting Co^{+} species, dubbed a supernucleophile, attacks the 5′-carbon of ATP in an unusual adenosyl transfer.

Net Oxidation of Succinyl-CoA Requires Conversion to Acetyl-CoA

Succinyl-CoA derived from propionyl-CoA can enter the TCA cycle. Oxidation of succinate to oxaloacetate provides a substrate for glucose synthesis. Thus, although the acetate units produced in β-oxidation cannot be utilized in gluconeogenesis by animals, the occasional propionate produced from oxidation of odd-carbon fatty acids *can* be used for sugar synthesis. Alternatively, succinate introduced to the TCA cycle from odd-carbon fatty acid oxidation may be oxidized to CO_2. However, all of the 4-carbon intermediates in the TCA cycle are regenerated in the cycle and thus should be viewed as catalytic species. Net consumption of succinyl-CoA thus does not occur directly in the TCA cycle. Rather, the succinyl-CoA generated from β-oxidation of odd-carbon fatty acids must be converted to pyruvate and then to acetyl-CoA (which is completely oxidized in the TCA cycle). To follow this latter route, succinyl-CoA entering the TCA cycle must be first converted to malate in the usual way, and then transported from the mitochondrial matrix to the cytosol, where it is oxida-
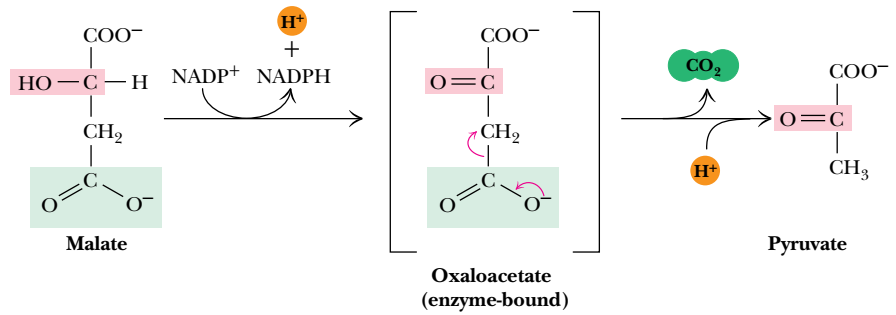
FIGURE 24.22 • The malic enzyme reaction proceeds by oxidation of malate to oxaloacetate, followed by decarboxylation to yield pyruvate.
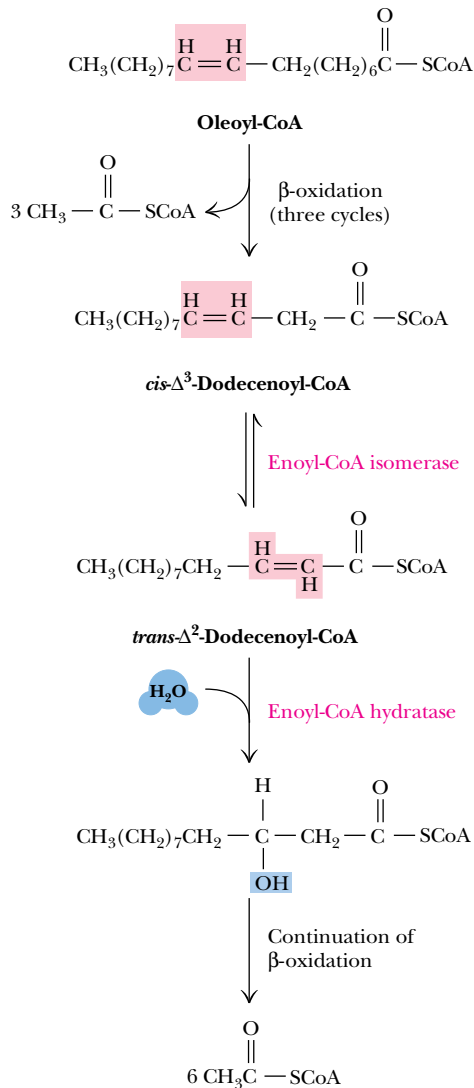

FIGURE 24.23 • β-Oxidation of unsaturated fatty acids. In the case of oleoyl-CoA, three β-oxidation cycles produce three molecules of acetyl-CoA and leave *cis*-Δ^3-dodecenoyl-CoA. Rearrangement of enoyl-CoA isomerase gives the *trans*-Δ^2 species, which then proceeds normally through the β-oxidation pathway.

tively decarboxylated to pyruvate and CO_2 by **malic enzyme,** as shown in Figure 24.22. Pyruvate can then be transported back to the mitochondrial matrix, where it enters the TCA cycle via pyruvate dehydrogenase. Note that malic enzyme plays an important role in fatty acid synthesis (see Figure 25.1).

24.4 • β-Oxidation of Unsaturated Fatty Acids

An Isomerase and a Reductase Facilitate the β-Oxidation of Unsaturated Fatty Acids

Unsaturated fatty acids are also catabolized by β-oxidation, but two additional mitochondrial enzymes—an isomerase and a novel reductase—are required to handle the *cis*-double bonds of naturally occurring fatty acids. As an example, consider the breakdown of oleic acid, an 18-carbon chain with a double bond at the 9,10-position. The reactions of β-oxidation proceed normally through three cycles, producing three molecules of acetyl-CoA and leaving the degradation product *cis*-Δ^3-dodecenoyl-CoA, shown in Figure 24.23. This intermediate is not a substrate for acyl-CoA dehydrogenase. With a double bond at the 3,4-position, it is not possible to form another double bond at the 2,3- (or β) position. As shown in Figure 24.23, this problem is solved by **enoyl-CoA isomerase,** an enzyme that rearranges this *cis*-Δ^3 double bond to a *trans*-Δ^2 double bond. This latter species can proceed through the normal route of β-oxidation.

Degradation of Polyunsaturated Fatty Acids Requires 2,4-Dienoyl-CoA Reductase

Polyunsaturated fatty acids pose a slightly more complicated situation for the cell. Consider, for example, the case of linoleic acid shown in Figure 24.24. As with oleic acid, β-oxidation proceeds through three cycles, and enoyl-CoA isomerase converts the *cis*-Δ^3 double bond to a *trans*-Δ^2 double bond to permit one more round of β-oxidation. What results this time, however, is a *cis*-Δ^4 enoyl-CoA, which is converted normally by acyl-CoA dehydrogenase to a *trans*-Δ^2, *cis*-Δ^4 species. This, however, is a poor substrate for the enoyl-CoA hydratase. This problem is solved by **2,4-dienoyl-CoA reductase,** the product of which depends on the organism. The mammalian form of this enzyme produces a *trans*-Δ^3 enoyl product, as shown in Figure 24.24, which can be converted by an enoyl-CoA isomerase to the *trans*-Δ^2 enoyl-CoA, which can then proceed normally through the β-oxidation pathway. *Escherichia coli* possesses a 2,4-dienoyl-CoA reductase that reduces the double bond at the 4,5-position to yield the *trans*-Δ^2 enoyl-CoA product in a single step.
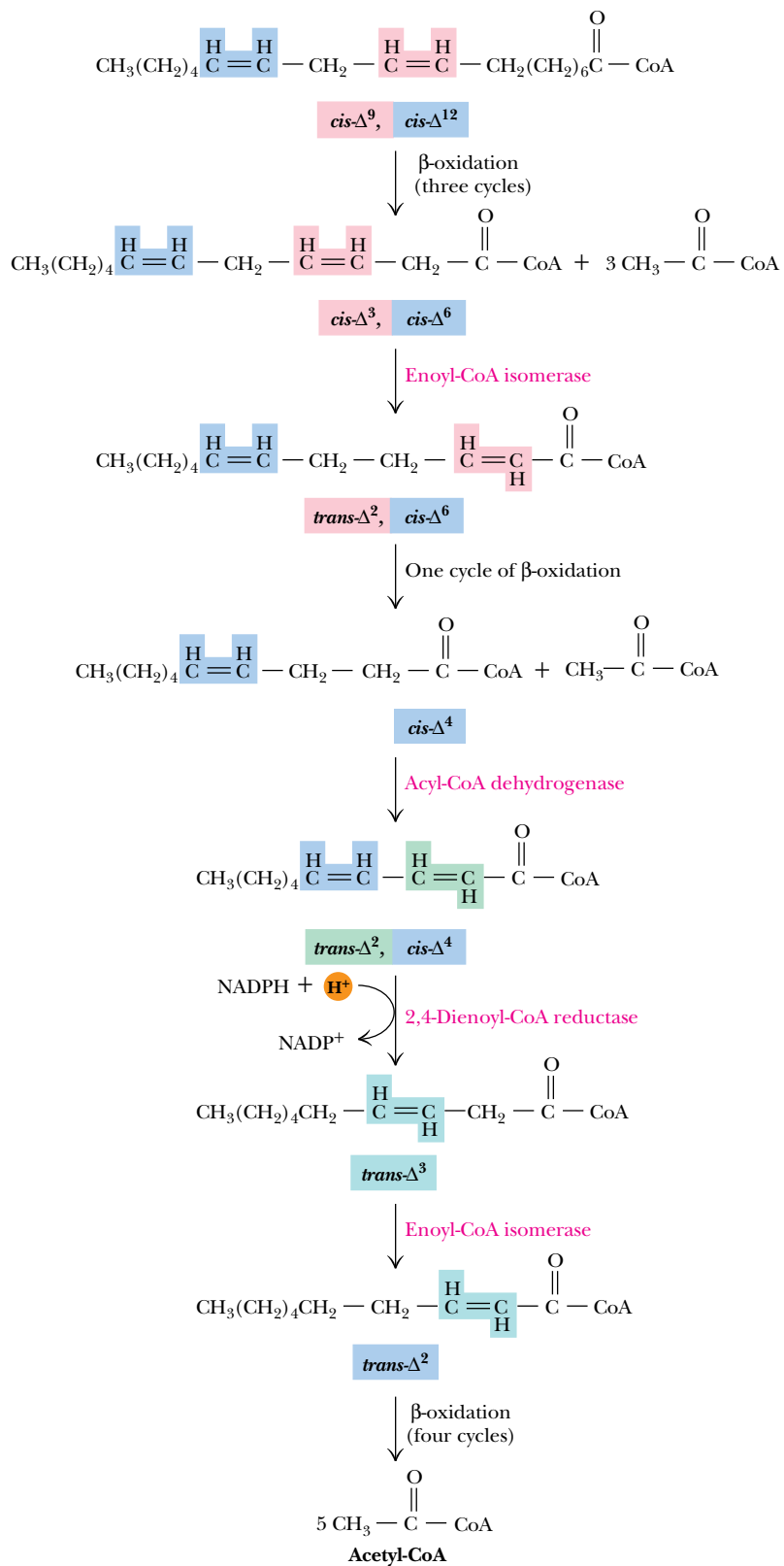
FIGURE 24.24 • The oxidation pathway for polyunsaturated fatty acids, illustrated for linoleic acid. Three cycles of β-oxidation on linoleoyl-CoA yield the *cis*-Δ^3, *cis*-Δ^6 interme-diate, which is converted to a *trans*-Δ^2, *cis*-Δ^6 intermediate. An additional round of β-oxi-dation gives *cis*-Δ^4 enoyl-CoA, which is oxidized to the *trans*-Δ^2, *cis*-Δ^4 species by acyl-CoA dehydrogenase. The subsequent action of 2,4-dienoyl-CoA reductase yields the *trans*-Δ^3 product, which is converted by enoyl-CoA isomerase to the *trans*-Δ^2 form. Normal β-oxida-tion then produces five molecules of acetyl-CoA.
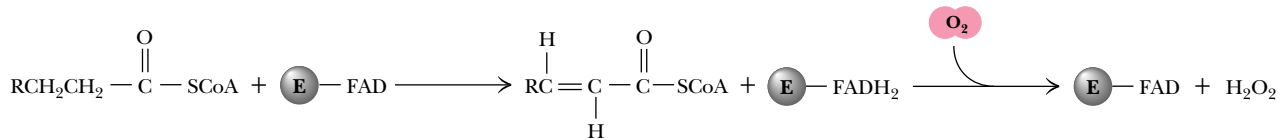
$$RCH_2CH_2 - \overset{\overset{\displaystyle O}{\|}}{C} - SCoA \; + \; \boxed{E} - FAD \; \longrightarrow \; \underset{\underset{\displaystyle H}{|}}{\overset{\overset{\displaystyle H}{|}}{RC}} = C - \overset{\overset{\displaystyle O}{\|}}{C} - SCoA \; + \; \boxed{E} - FADH_2 \; \xrightarrow{\quad O_2 \quad} \; \boxed{E} - FAD \; + \; H_2O_2$$

FIGURE 24.25 • The acyl-CoA oxidase reaction in peroxisomes.

24.5 • Other Aspects of Fatty Acid Oxidation

Peroxisomal β-Oxidation Requires FAD-Dependent Acyl-CoA Oxidase

Although β-oxidation in mitochondria[1] is the principal pathway of fatty acid catabolism, several other minor pathways play important roles in fat catabolism. For example, organelles other than mitochondria carry out β-oxidation processes, including *peroxisomes* and *glyoxysomes*. **Peroxisomes** are so named because they carry out a variety of flavin-dependent oxidation reactions, regenerating oxidized flavins by reaction with oxygen to produce hydrogen peroxide, H_2O_2. Peroxisomal β-oxidation is similar to mitochondrial β-oxidation, except that the initial double bond formation is catalyzed by an FAD-dependent **acyl-CoA oxidase** (Figure 24.25). The action of this enzyme in the peroxisomes transfers the liberated electrons directly to oxygen instead of the electron transport chain. As a result, each 2-carbon unit oxidized in peroxisomes produces fewer ATPs. The enzymes responsible for fatty acid oxidation in peroxisomes are inactive with carbon chains of eight or fewer. Such short-chain products must be transferred to the mitochondria for further breakdown. Similar β-oxidation enzymes are also found in **glyoxysomes**—peroxisomes in plants that also carry out the reactions of the glyoxylate pathway.

Branched-Chain Fatty Acids and α-Oxidation

Although β-oxidation is universally important, there are some instances in which it cannot operate effectively. For example, branched-chain fatty acids with alkyl branches at odd-numbered carbons are not effective substrates for β-oxidation. For such species, **α-oxidation** is a useful alternative. Consider **phytol,** a breakdown product of chlorophyll that occurs in the fat of ruminant animals such as sheep and cows and also in dairy products. Ruminants oxidize phytol to phytanic acid, and digestion of phytanic acid in dairy products is thus an important dietary consideration for humans. The methyl group at C-3 will block β-oxidation, but, as shown in Figure 24.26, **phytanic acid α-hydroxylase** places an —OH group at the α-carbon, and **phytanic acid α-oxidase** decarboxylates it to yield *pristanic acid*. The CoA ester of this metabolite can undergo β-oxidation in the normal manner. The terminal product, isobutyryl-CoA, can be sent into the TCA cycle by conversion to succinyl-CoA.

Refsum's Disease Is a Result of Defects in α-Oxidation

The α-oxidation pathway is defective in **Refsum's disease,** an inherited metabolic disorder that results in defective night vision, tremors, and other neurologic abnormalities. These symptoms are caused by accumulation of phytanic acid in the body. Treatment of Refsum's disease requires a diet free of chloro-

---

[1] Beta oxidation does not occur significantly in plant mitochondria.
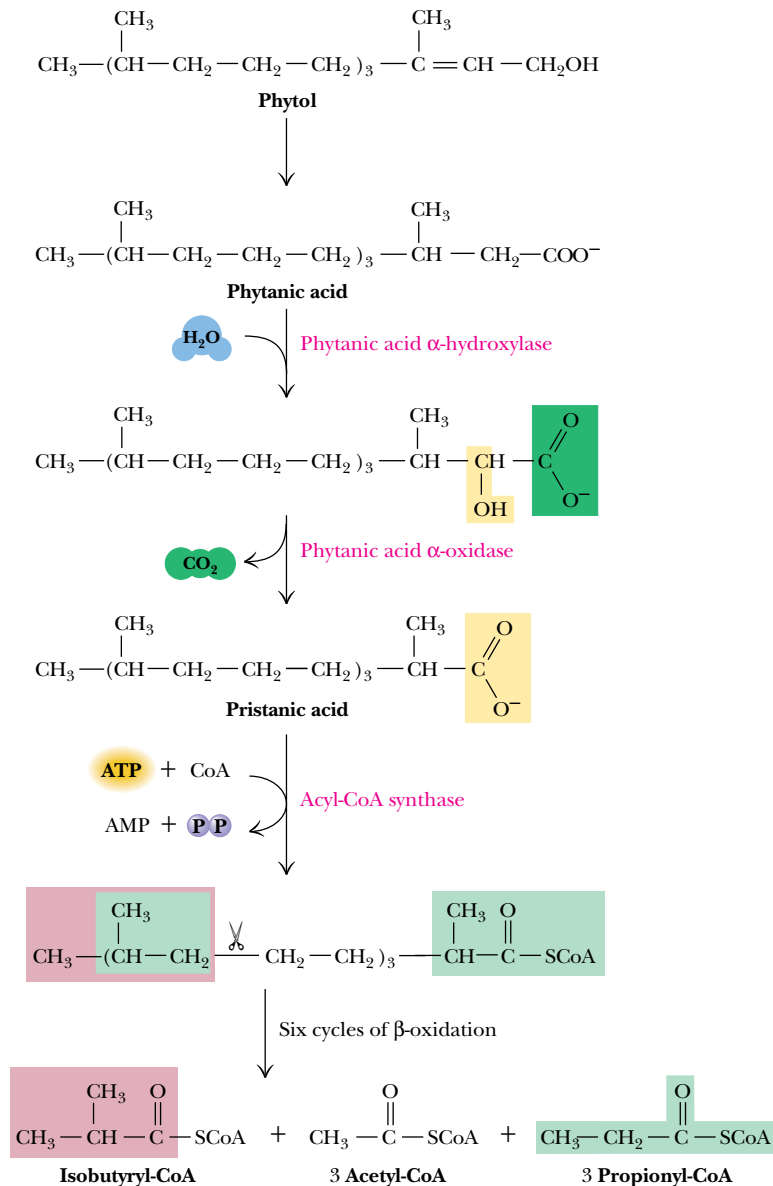
FIGURE 24.26 • Branched-chain fatty acids are oxidized by α-oxidation, as shown for phytanic acid. The product of the phytanic acid oxidase, pristanic acid, is a suitable substrate for normal β-oxidation. Isobutyryl-CoA and propionyl-CoA can both be converted to succinyl-CoA, which can enter the TCA cycle.

phyll, the precursor of phytanic acid. This regimen is difficult to implement because all green vegetables and even meat from plant-eating animals, such as cows, pigs, and poultry, must be excluded from the diet.

ω-Oxidation of Fatty Acids Yields Small Amounts of Dicarboxylic Acids

In the endoplasmic reticulum of eukaryotic cells, the oxidation of the terminal carbon of a normal fatty acid—a process termed ω-oxidation—can lead to the synthesis of small amounts of dicarboxylic acids (Figure 24.27). **Cytochrome P-450,** a monooxygenase enzyme that requires NADPH as a coenzyme and uses O_2 as a substrate, places a hydroxyl group at the terminal carbon. Subsequent oxidation to a carboxyl group produces a dicarboxylic acid. Either end can form an ester linkage to CoA and be subjected to β-oxidation, producing a
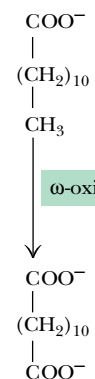

FIGURE 24.27 • Dicarboxylic acids can be formed by oxidation of the methyl group of fatty acids in a cytochrome P-450–dependent reaction.

variety of smaller dicarboxylic acids. (Cytochrome P-450–dependent monooxy-genases also play an important role as agents of **detoxication,** the degradation and metabolism of toxic hydrocarbon agents.)

24.6 • Ketone Bodies

Ketone Bodies Are a Significant Source of Fuel and Energy for Certain Tissues

Most of the acetyl-CoA produced by the oxidation of fatty acids in liver mito-chondria undergoes further oxidation in the TCA cycle, as stated earlier. However, some of this acetyl-CoA is converted to three important metabolites: acetone, acetoacetate, and β-hydroxybutyrate. The process is known as **keto-genesis,** and these three metabolites are traditionally known as **ketone bodies,** in spite of the fact that β-hydroxybutyrate does not contain a ketone function. These three metabolites are synthesized primarily in the liver but are impor-tant sources of fuel and energy for many peripheral tissues, including brain, heart, and skeletal muscle. The brain, for example, normally uses glucose as its source of metabolic energy. However, during periods of starvation, ketone bodies may be the major energy source for the brain. Acetoacetate and 3-hydroxybutyrate are the preferred and normal substrates for kidney cortex and for heart muscle.

Ketone body synthesis occurs only in the mitochondrial matrix. The reac-tions responsible for the formation of ketone bodies are shown in Figure 24.28. The first reaction—the condensation of two molecules of acetyl-CoA to form acetoacetyl-CoA—is catalyzed by **thiolase,** which is also known as **acetoacetyl-CoA thiolase** or **acetyl-CoA acetyltransferase.** This is the same enzyme that car-ries out the thiolase reaction in β-oxidation, but here it runs in reverse. The second reaction adds another molecule of acetyl-CoA to give β-*hydroxy-β-methyl-glutaryl-CoA,* commonly abbreviated HMG-CoA. These two mitochondrial matrix reactions are analogous to the first two steps in cholesterol biosynthe-sis, a cytosolic process, as we shall see in Chapter 25. HMG-CoA is converted to acetoacetate and acetyl-CoA by the action of **HMG-CoA lyase** in a mixed aldol-Claisen ester cleavage reaction. This reaction is mechanistically similar to the reverse of the citrate synthase reaction in the TCA cycle. A membrane-bound enzyme, **β-hydroxybutyrate dehydrogenase,** then can reduce acetoac-etate to β-hydroxybutyrate.

Acetoacetate and β-hydroxybutyrate are transported through the blood from liver to target organs and tissues, where they are converted to acetyl-CoA (Figure 24.29). *Ketone bodies are easily transportable forms of fatty acids that move through the circulatory system without the need for complexation with serum albumin and other fatty acid–binding proteins.*

Ketone Bodies and Diabetes Mellitus

Diabetes mellitus is the most common endocrine disease and the third lead-ing cause of death in the United States, with approximately 6 million diagnosed cases and an estimated 4 million more borderline but undiagnosed cases. Diabetes is characterized by an abnormally high level of glucose in the blood. In **type I diabetes** (representing 10% or fewer of all cases), elevated blood glu-cose results from inadequate secretion of insulin by the islets of Langerhans in the pancreas. **Type II diabetes** (at least 90% of all cases) results from an insen-sitivity to insulin. Type II diabetics produce normal or even elevated levels of insulin, but owing to a shortage of insulin receptors (Chapter 34), their cells
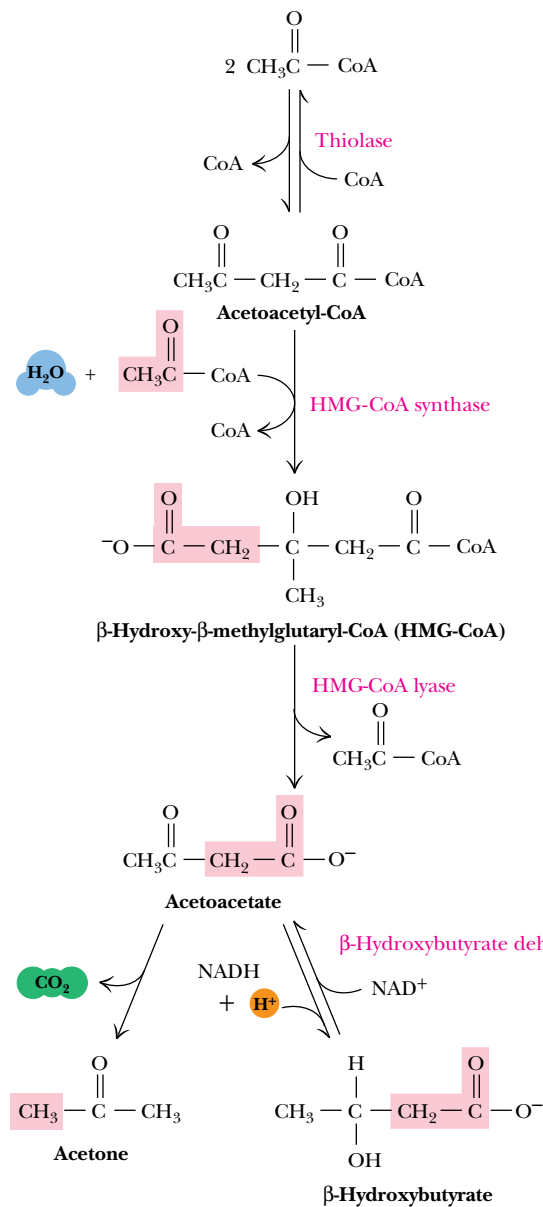
FIGURE 24.28 • The formation of ketone bodies, synthesized primarily in liver mitochondria.

are not responsive to insulin. In both cases, transport of glucose into muscle, liver, and adipose tissue is significantly reduced, and, despite abundant glucose in the blood, the cells are metabolically starved. They respond by turning to increased gluconeogenesis and catabolism of fat and protein. In type I diabetes, increased gluconeogenesis consumes most of the available oxaloacetate, but breakdown of fat (and, to a lesser extent, protein) produces large amounts of acetyl-CoA. This increased acetyl-CoA would normally be directed into the TCA cycle, but, with oxaloacetate in short supply, it is used instead for production of unusually large amounts of ketone bodies. Acetone can often be detected on the breath of type I diabetics, an indication of high plasma levels of ketone bodies.
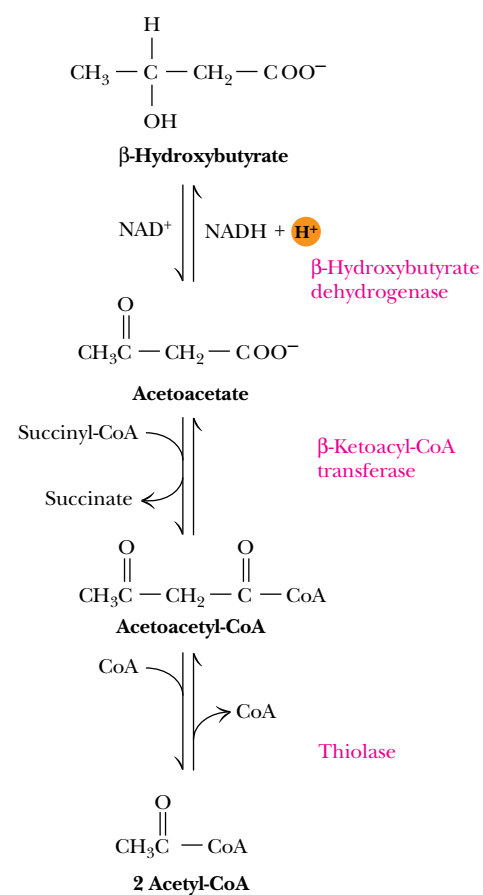

FIGURE 24.29 • Reconversion of ketone bodies to acetyl-CoA in the mitochondria of many tissues (other than liver) provides significant metabolic energy.

PROBLEMS

1. Calculate the volume of metabolic water available to a camel through fatty acid oxidation if it carries 30 lb of triacylglycerol in its hump.

2. Calculate the approximate number of ATP molecules that can be obtained from the oxidation of *cis*-11-heptadecenoic acid to CO_2 and water.

3. Phytanic acid, the product of chlorophyll that causes problems for individuals with Refsum's disease, is 3,7,11,15-tetramethyl hexa-decanoic acid. Suggest a route for its oxidation that is consistent with what you have learned in this chapter. (*Hint:* The methyl group at C-3 effectively blocks hydroxylation and normal β-oxi-dation. You may wish to initiate breakdown in some other way.)

4. Even though acetate units, such as those obtained from fatty acid oxidation, cannot be used for *net* synthesis of carbohydrate in animals, labeled carbon from ^{14}C-labeled acetate *can* be found in newly synthesized glucose (for example, in liver glycogen) in animal tracer studies. Explain how this can be. Which carbons of glucose would you expect to be the first to be labeled by ^{14}C-labeled acetate?

5. What would you expect to be the systemic metabolic effects of consuming unripened akee fruit?

6. Overweight individuals who diet to lose weight often view fat in negative ways because adipose tissue is the repository of excess caloric intake. However, the "weighty" consequences might be even worse if excess calories were stored in other forms. Consider a person who is 10 lb "overweight," and estimate how much more he or she would weigh if excess energy were stored in the form of carbohydrate instead of fat.

7. What would be the consequences of a deficiency in vitamin B_{12} for fatty acid oxidation? What metabolic intermediates might accumulate?

8. Write properly balanced chemical equations for the oxidation to CO_2 and water of (a) myristic acid, (b) stearic acid, (c) α-linolenic acid, and (d) arachidonic acid.

9. How many tritium atoms are incorporated into acetate if a molecule of palmitic acid is oxidized in 100% tritiated water?

10. What would be the consequences of a carnitine deficiency for fatty acid oxidation?

11. Based on the mechanism for the methylmalonyl-CoA mutase (Figure 24.21), write reasonable mechanisms for the reactions shown below.
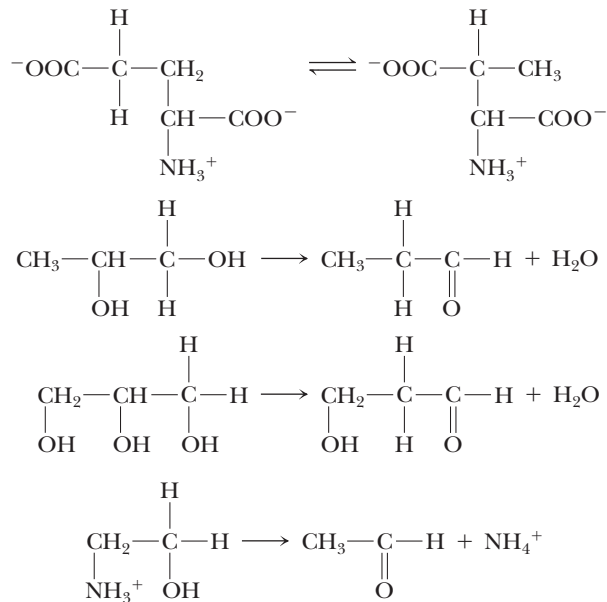
FURTHER READING

Bennett, M. J., 1994. The enzymes of mitochondrial fatty acid oxidation. *Clinica Chimica Acta* **226:**211–224.

Bieber, L. L., 1988. Carnitine. *Annual Review of Biochemistry* **88:**261–283.

Boyer, P. D., ed., 1983. *The Enzymes,* 3rd ed., vol. 16. New York: Academic Press.

Eder, M., Krautle, F., Dong, Y., et al., 1997. Characterization of human and pig kidney long-chain-acyl-CoA dehydrogenases and their role in beta-oxidation. *European Journal of Biochemistry* **245:**600–607.

Grynberg, A., and Demaison, L., 1996. Fatty acid oxidation in the heart. *Journal of Cardiovascular Pharmacology* **28:**S11–S17.

Halpern, J., 1985. Mechanisms of coenzyme B_{12}–dependent rearrangements. *Science* **227:**869–875.

Hiltunen, J. K., Palosaari, P., and Kunau, W.-H., 1989. Epimerization of 3-hydroxyacyl-CoA esters in rat liver. *Journal of Biological Chemistry* **264:**13535–13540.

McGarry, J. D., and Foster, D. W., 1980. Regulation of hepatic fatty acid oxidation and ketone body production. *Annual Review of Biochemistry* **49:**395–420.

Newsholme, E. A., and Leech, A. R., 1983. *Biochemistry for the Medical Sciences.* New York: Wiley.

Pollitt, R. J., 1995. Disorders of mitochondrial long-chain fatty acid oxidation. *Journal of Inherited Metabolic Disease* **18:**473–490.

Romijn, J. A., Coyle, E. F., Sidossis, L. S., et al., 1996. Relationship between fatty acid delivery and fatty acid oxidation during strenuous exercise. *Journal of Applied Physiology* **79:**1939–1945.

Schulz, H., 1987. Inhibitors of fatty acid oxidation. *Life Sciences* **40:**1443–1449.

Schulz, H., and Kunau, W.-H., 1987. β-Oxidation of unsaturated fatty acids: A revised pathway. *Trends in Biochemical Sciences* **12:**403–406.

Scriver, C. R., et al., 1995. *The Metabolic and Molecular Bases of Inherited Disease,* 7th ed. New York: McGraw-Hill.

Sherratt, H. S., 1994. Introduction: The regulation of fatty acid oxidation in cells. *Biochemical Society Transactions* **22:**421–422.

Sherratt, H. S., and Spurway, T. D., 1994. Regulation of fatty acid oxidation in cells. *Biochemical Society Transactions* **22:**423–427.

Srere, P. A., and Sumegi, B., 1994. Processivity and fatty acid oxidation. *Biochemical Society Transactions* **22:**446–450.

Tolbert, N. E., 1981. Metabolic pathways in peroxisomes and glyoxysomes. *Annual Review of Biochemistry* **50:**133–157.

Vance, D. E., and Vance, J. E., eds., 1985. *Biochemistry of Lipids and Membranes.* Menlo Park, CA: Benjamin/Cummings.

Yagoob, P., Newsholme, E. A., and Calder, P. C., 1994. Fatty acid oxidation by lymphocytes. *Biochemical Society Transactions* **22:**116S.

To every thing there is a season, and a time for every purpose under heaven . . . A time to break down, a time to build up.

ECCLESIASTES 3:1–3

Chapter 25

Lipid Biosynthesis

Southern elephant seal, *Mirounga leonina*. *(Gerald Lacz/Peter Arnold, Inc.)*

We turn now to the biosynthesis of lipid structures. We begin with a discussion of the biosynthesis of fatty acids, stressing the basic pathways, additional means of elongation, mechanisms for the introduction of double bonds, and regulation of fatty acid synthesis. Sections then follow on the biosynthesis of glycerophospholipids, sphingolipids, eicosanoids, and cholesterol. The transport of lipids through the body in lipoprotein complexes is described, and the chapter closes with discussions of the biosynthesis of bile salts and steroid hormones.

25.1 • The Fatty Acid Biosynthesis and Degradation Pathways Are Different

We have already seen several cases in which the *synthesis* of a class of biomolecules is conducted differently from degradation (glycolysis versus gluconeogenesis and glycogen or starch breakdown versus polysaccharide synthesis, for

example). Likewise, the synthesis of fatty acids and other lipid components is different from their degradation. Fatty acid synthesis involves a set of reactions that follow a strategy different in several ways from the corresponding degradative process:

1. Intermediates in fatty acid synthesis are linked covalently to the sulfhydryl groups of special proteins, the **acyl carrier proteins.** In contrast, fatty acid breakdown intermediates are bound to the —SH group of coenzyme A.
2. Fatty acid synthesis occurs in the cytosol, whereas fatty acid degradation takes place in mitochondria.
3. In animals, the enzymes of fatty acid synthesis are components of one long polypeptide chain, the **fatty acid synthase,** whereas no similar association exists for the degradative enzymes. (Plants and bacteria employ separate enzymes to carry out the biosynthetic reactions.)
4. The coenzyme for the oxidation–reduction reactions of fatty acid synthesis is $NADP^+$/NADPH, whereas degradation involves the NAD^+/NADH couple.

Lipid Biosynthesis

Formation of Malonyl-CoA Activates Acetate Units for Fatty Acid Synthesis

The design strategy for fatty acid synthesis is this:

a. Fatty acid chains are constructed by the addition of two-carbon units derived from *acetyl-CoA*.
b. The acetate units are activated by formation of *malonyl-CoA* (at the expense of ATP).
c. The addition of two-carbon units to the growing chain is driven by decarboxylation of malonyl-CoA.
d. The elongation reactions are repeated until the growing chain reaches 16 carbons in length (palmitic acid).
e. Other enzymes then add double bonds and additional carbon units to the chain.

## Fatty Acid Biosynthesis Depends on the Reductive Power of NADPH

The net reaction for the formation of palmitate from acetyl-CoA is

$$\text{Acetyl-CoA} + 7 \text{ malonyl-CoA}^- + 14 \text{ NADPH} + 14 \text{ H}^+ \longrightarrow$$
$$\text{palmitoyl-CoA} + 7 \text{ HCO}_3^- + 7 \text{ CoASH} + 14 \text{ NADP}^+ \quad (25.1)$$

(Levels of free fatty acids are very low in the typical cell. The palmitate made in this process is rapidly converted to CoA esters in preparation for the formation of triacylglycerols and phospholipids.)

Providing Cytosolic Acetyl-CoA and Reducing Power for Fatty Acid Synthesis

Eukaryotic cells face a dilemma in providing suitable amounts of substrate for fatty acid synthesis. Sufficient quantities of acetyl-CoA, malonyl-CoA, and NADPH must be generated *in the cytosol* for fatty acid synthesis. Malonyl-CoA is made by carboxylation of acetyl-CoA, so the problem reduces to generating sufficient acetyl-CoA and NADPH.
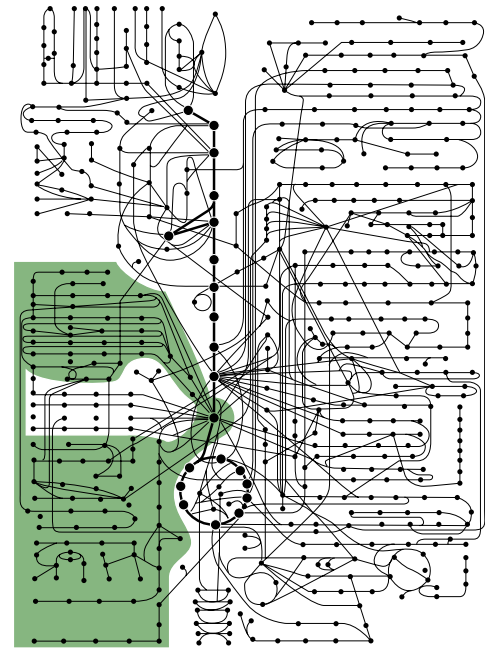
There are three principal sources of acetyl-CoA (Figure 25.1):

1. Amino acid degradation produces cytosolic acetyl-CoA.
2. Fatty acid oxidation produces mitochondrial acetyl-CoA.
3. Glycolysis yields cytosolic pyruvate, which (after transport into the mitochondria) is converted to acetyl-CoA by pyruvate dehydrogenase.

The acetyl-CoA derived from amino acid degradation is normally insufficient for fatty acid biosynthesis, and the acetyl-CoA produced by pyruvate dehydrogenase and by fatty acid oxidation cannot cross the mitochondrial membrane to participate directly in fatty acid synthesis. Instead, acetyl-CoA is linked with oxaloacetate to form citrate, which is transported from the mitochondrial matrix to the cytosol (Figure 25.1). Here it can be converted back into acetyl-CoA and oxaloacetate by **ATP-citrate lyase.** In this manner, mitochondrial acetyl-CoA becomes the substrate for cytosolic fatty acid synthesis. (Oxaloacetate returns to the mitochondria in the form of either pyruvate or malate, which is then reconverted to acetyl-CoA and oxaloacetate, respectively.)
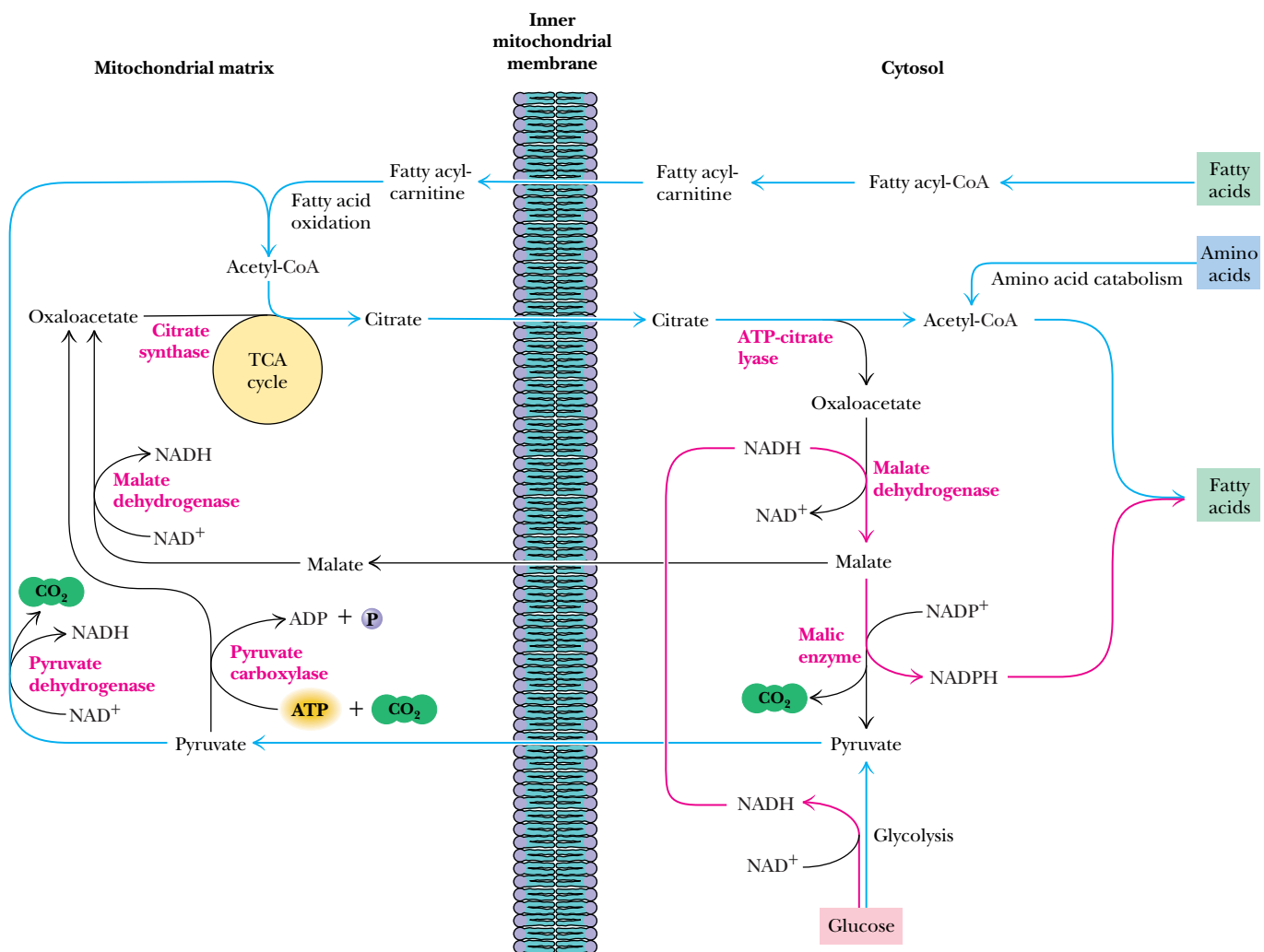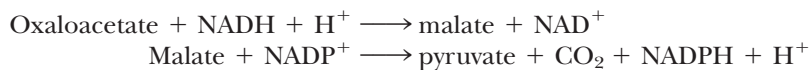

FIGURE 25.1 • The citrate-malate-pyruvate shuttle provides cytosolic acetate units and reducing equivalents (electrons) for fatty acid synthesis. The shuttle collects carbon substrates, primarily from glycolysis but also from fatty acid oxidation and amino acid catabolism. Most of the reducing equivalents are glycolytic in origin. Pathways that provide carbon for fatty acid synthesis are shown in blue; pathways that supply electrons for fatty acid synthesis are shown in red.

NADPH can be produced in the pentose phosphate pathway as well as by malic enzyme (Figure 25.1). Reducing equivalents (electrons) derived from glycolysis in the form of NADH can be transformed into NADPH by the combined action of malate dehydrogenase and malic enzyme:

$$\text{Oxaloacetate} + \text{NADH} + \text{H}^+ \longrightarrow \text{malate} + \text{NAD}^+$$
$$\text{Malate} + \text{NADP}^+ \longrightarrow \text{pyruvate} + \text{CO}_2 + \text{NADPH} + \text{H}^+$$

How many of the 14 NADPH needed to form one palmitate (Eq. 25.1) can be made in this way? The answer depends on the status of malate. Every citrate entering the cytosol produces one acetyl-CoA and one malate (Figure 25.1). Every malate oxidized by malic enzyme produces one NADPH, at the expense of a decarboxylation to pyruvate. Thus, when malate is oxidized, one NADPH is produced for every acetyl-CoA. Conversion of 8 acetyl-CoA units to one palmitate would then be accompanied by production of 8 NADPH. (The other 6 NADPH required [Eq. 25.1] would be provided by the pentose phosphate pathway.) On the other hand, for every malate returned to the mitochondria, one NADPH fewer is produced.

Acetate Units Are Committed to Fatty Acid Synthesis by Formation of Malonyl-CoA
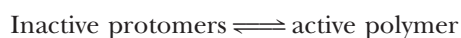
Rittenberg and Bloch showed in the late 1940s that acetate units are the building blocks of fatty acids. Their work, together with the discovery by Salih Wakil that bicarbonate is required for fatty acid biosynthesis, eventually made clear that this pathway involves synthesis of *malonyl-CoA*. The carboxylation of acetyl-CoA to form malonyl-CoA is essentially irreversible and is the **committed step** in the synthesis of fatty acids (Figure 25.2). The reaction is catalyzed by **acetyl-CoA carboxylase,** which contains a biotin prosthetic group. This carboxylase is the only enzyme of fatty acid synthesis in animals that is not part of the multienzyme complex called fatty acid synthase.

Acetyl-CoA Carboxylase Is Biotin-Dependent and Displays Ping-Pong Kinetics

The biotin prosthetic group of acetyl-CoA carboxylase is covalently linked to the ϵ-amino group of an active-site lysine in a manner similar to pyruvate carboxylase (Figure 23.3). The reaction mechanism is also analogous to that of pyruvate carboxylase (Figure 23.4): ATP-driven carboxylation of biotin is followed by transfer of the activated CO_2 to acetyl-CoA to form malonyl-CoA. The enzyme from *Escherichia coli* has three subunits: (1) a **biotin carboxyl carrier protein** (a dimer of 22.5-kD subunits); (2) **biotin carboxylase** (a dimer of 51-kD subunits), which adds CO_2 to the prosthetic group; and (3) **transcarboxylase** (an $\alpha_2\beta_2$ tetramer with 30-kD and 35-kD subunits), which transfers the activated CO_2 unit to acetyl-CoA. The long, flexible biotin–lysine chain (biocytin) enables the activated carboxyl group to be carried between the biotin carboxylase and the transcarboxylase (Figure 25.3).

Acetyl-CoA Carboxylase in Animals Is a Multifunctional Protein

In animals, acetyl-CoA carboxylase (ACC) is a filamentous polymer (4 to 8 $\times 10^6$ D) composed of 230-kD protomers. Each of these subunits contains the biotin carboxyl carrier moiety, biotin carboxylase, and transcarboxylase activities, as well as allosteric regulatory sites. Animal ACC is thus a multifunctional protein. The polymeric form is active, but the 230-kD protomers are inactive. The activity of ACC is thus dependent upon the position of the equilibrium between these two forms:
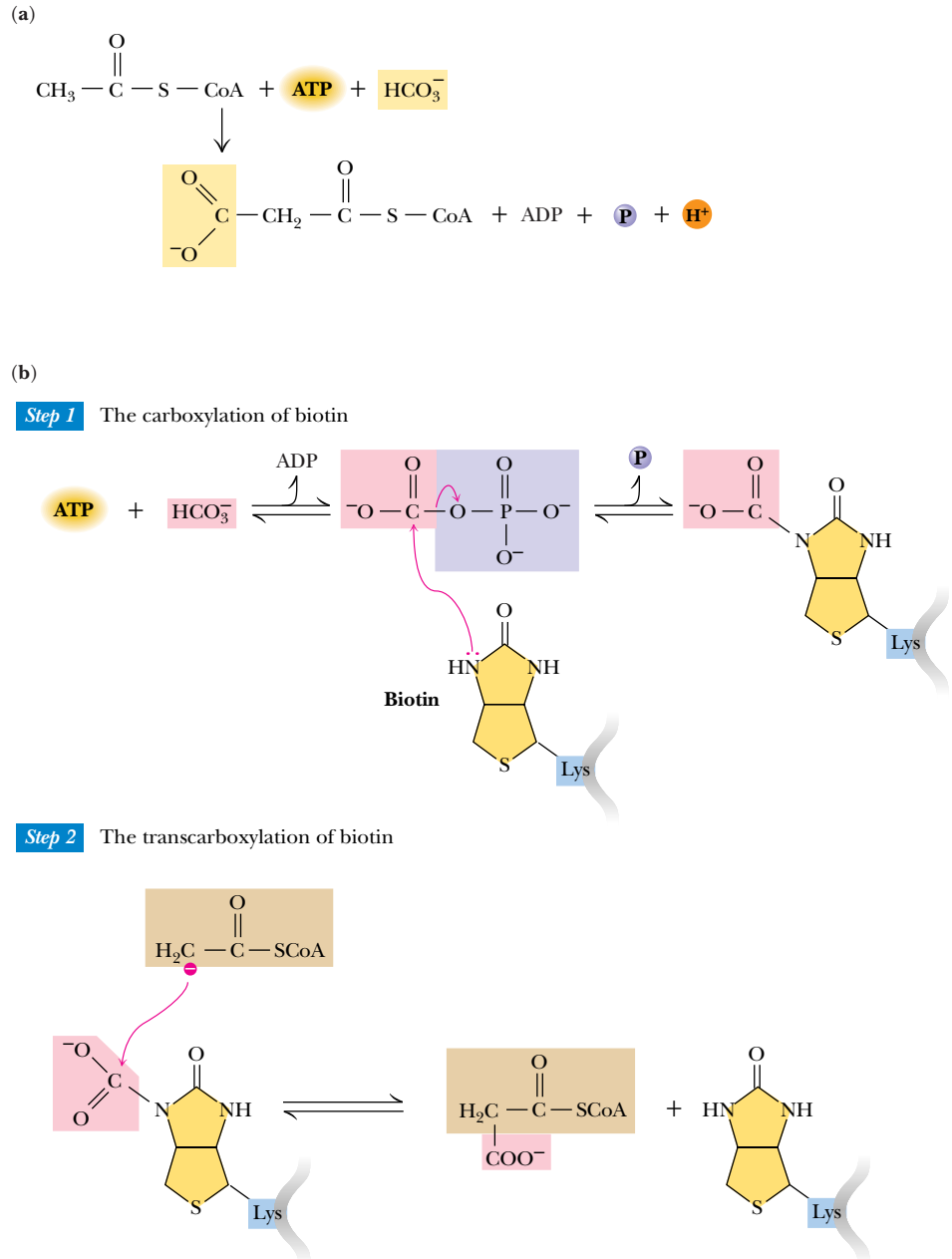
$$\text{Inactive protomers} \rightleftharpoons \text{active polymer}$$

(a)

(b)

Step 1   The carboxylation of biotin

Step 2   The transcarboxylation of biotin

FIGURE 25.2 • (a) The acetyl-CoA carboxylase reaction produces malonyl-CoA for fatty acid synthesis. (b) A mechanism for the acetyl-CoA carboxylase reaction. Bicarbonate is activated for carboxylation reactions by formation of N-carboxybiotin. ATP drives the reaction forward, with transient formation of a carbonylphosphate intermediate (Step 1). In a typical biotin-dependent reaction, nucleophilic attack by the acetyl-CoA carbanion on the carboxyl carbon of N-carboxybiotin—a transcarboxylation—yields the carboxylated product (Step 2).

Because this enzyme catalyzes the committed step in fatty acid biosynthesis, it is carefully regulated. *Palmitoyl-CoA,* the final product of fatty acid biosynthesis, shifts the equilibrium toward the inactive protomers, whereas *citrate,* an important allosteric activator of this enzyme, shifts the equilibrium toward the active polymeric form of the enzyme. Acetyl-CoA carboxylase shows the kinetic behavior of a Monod–Wyman–Changeux V-system allosteric enzyme (Chapter 15).
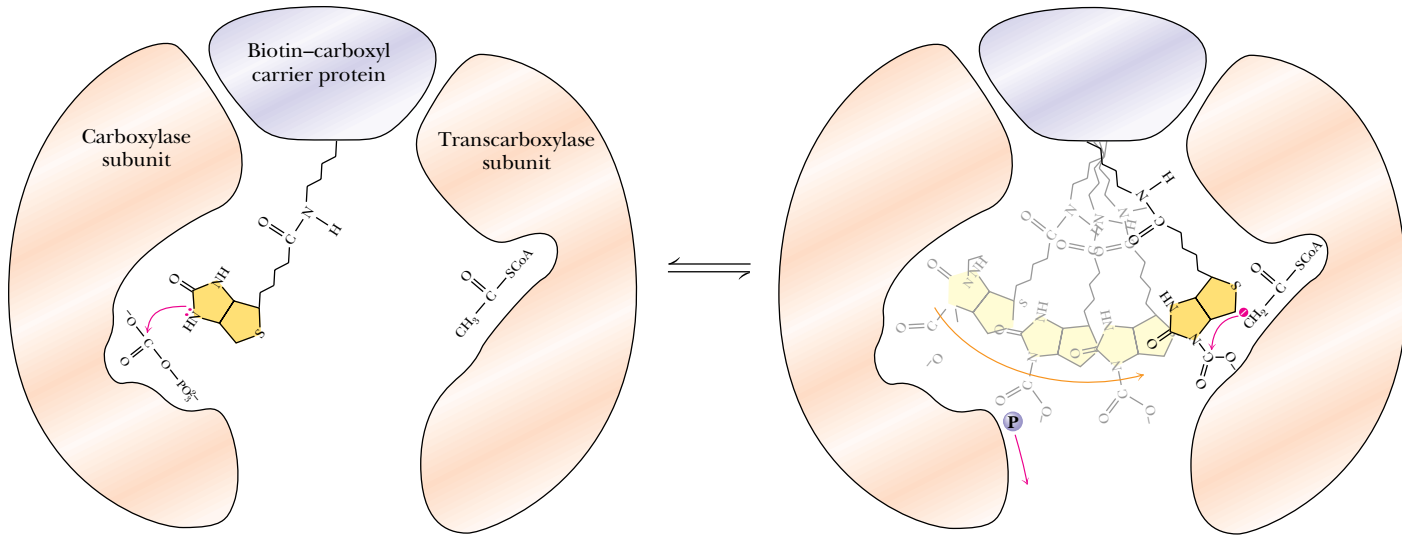
FIGURE 25.3 • In the acetyl-CoA carboxylase reaction, the biotin ring, on its flexible tether, acquires carboxyl groups from carbonylphosphate on the carboxylase subunit and transfers them to acyl-CoA molecules on the transcarboxylase subunits.

Phosphorylation of ACC Modulates Activation by Citrate and Inhibition by Palmitoyl-CoA

The regulatory effects of citrate and palmitoyl-CoA are dependent on the phosphorylation state of acetyl-CoA carboxylase. The animal enzyme is phosphorylated at 8 to 10 sites on each enzyme subunit (Figure 25.4). Some of these sites are reg-
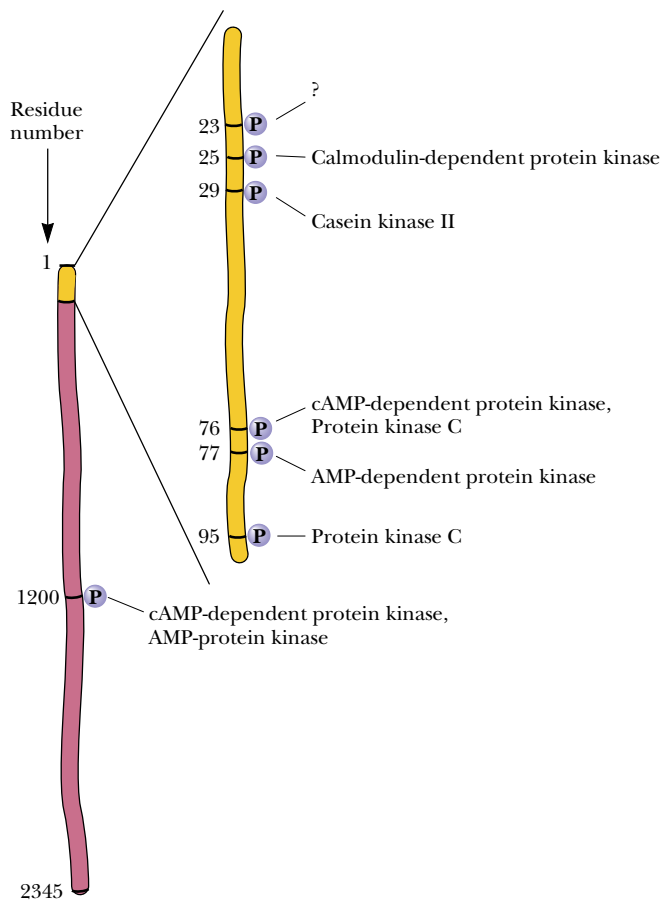

FIGURE 25.4 • Models of the acetyl-CoA carboxylase polypeptide, with phosphorylation sites indicated, along with the protein kinases responsible. Phosphorylation at Ser^{1200} is primarily responsible for decreasing the affinity for citrate.
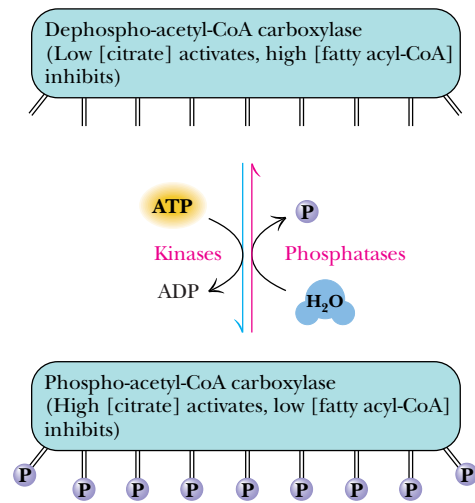
FIGURE 25.5 • The activity of acetyl-CoA carboxylase is modulated by phosphorylation and dephosphorylation. The dephospho form of the enzyme is activated by low [citrate] and inhibited only by high levels of fatty acyl-CoA. In contrast, the phosphorylated form of the enzyme is activated only by high levels of citrate, but is very sensitive to inhibition by fatty acyl-CoA.

ulatory, whereas others are "silent" and have no effect on enzyme activity. Unphosphorylated acetyl-CoA carboxylase binds citrate with high affinity and thus is active at very low citrate concentrations (Figure 25.5). Phosphorylation of the regulatory sites decreases the affinity of the enzyme for citrate, and in this case high levels of citrate are required to activate the carboxylase. The inhibition by fatty acyl-CoAs operates in a similar but opposite manner. Thus, low levels of fatty acyl-CoA inhibit the phosphorylated carboxylase, but the dephosphoenzyme is inhibited only by high levels of fatty acyl-CoA. Specific phosphatases act to dephosphorylate ACC, thereby increasing the sensitivity to citrate.

Acyl Carrier Proteins Carry the Intermediates in Fatty Acid Synthesis

The basic building blocks of fatty acid synthesis are acetyl and malonyl groups, but they are not transferred directly from CoA to the growing fatty acid chain. Rather, they are first passed to **acyl carrier protein** (or simply ACP), discovered by P. Roy Vagelos. This protein consists (in *E. coli*) of a single polypeptide chain of 77 residues to which is attached (on a serine residue) a **phosphopantetheine group,** the same group that forms the "business end" of coenzyme A. Thus, acyl carrier protein is a somewhat larger version of coenzyme A, specialized for use in fatty acid biosynthesis (Figure 25.6).

The enzymes that catalyze formation of acetyl-ACP and malonyl-ACP and the subsequent reactions of fatty acid synthesis are organized quite differently in different organisms. We first discuss fatty acid biosynthesis in bacteria and plants, where the various reactions are catalyzed by separate, independent proteins. Then we discuss the animal version of fatty acid biosynthesis, which involves a single multienzyme complex called **fatty acid synthase.**

Fatty Acid Synthesis in Bacteria and Plants

The individual steps in the elongation of the fatty acid chain are quite similar in bacteria, fungi, plants, and animals. The ease of purification of the separate enzymes from bacteria and plants made it possible in the beginning to sort out each step in the pathway, and then by extension to see the pattern of biosynthesis in animals. The reactions are summarized in Figure 25.7. The elongation reactions begin with the formation of acetyl-ACP and malonyl-ACP, which

Phosphopantetheine group of coenzyme A

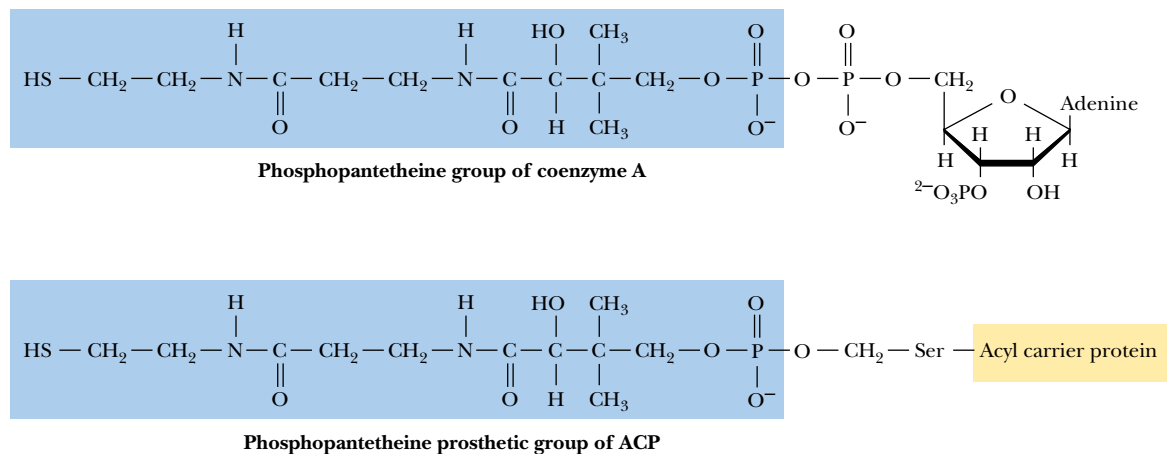**Phosphopantetheine prosthetic group of ACP**

FIGURE 25.6 • Fatty acids are conjugated both to coenzyme A and to acyl carrier protein through the sulfhydryl of phosphopantetheine prosthetic groups.
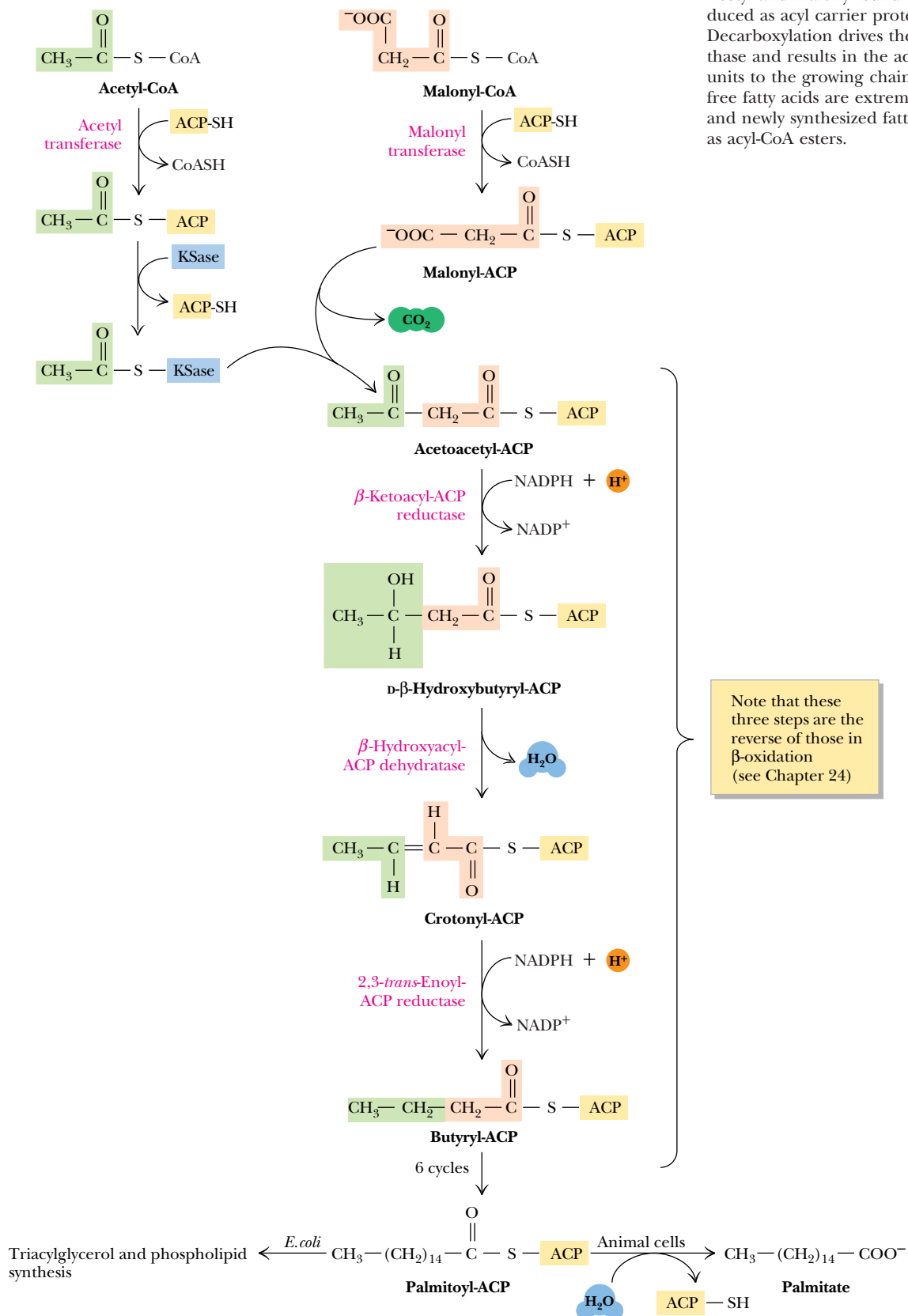
FIGURE 25.7 • The pathway of palmitate synthesis from acetyl-CoA and malonyl-CoA. Acetyl and malonyl building blocks are introduced as acyl carrier protein conjugates. Decarboxylation drives the β-ketoacyl-ACP synthase and results in the addition of two-carbon units to the growing chain. Concentrations of free fatty acids are extremely low in most cells, and newly synthesized fatty acids exist primarily as acyl-CoA esters.

Note that these three steps are the reverse of those in β-oxidation (see Chapter 24)

Choosing the Best Organism for the Experiment

The selection of a suitable and relevant organism is an important part of any biochemical investigation. The studies that revealed the secrets of fatty acid synthesis are a good case in point.

The paradigm for fatty acid synthesis in plants has been the avocado, which has one of the highest fatty acid contents in the plant kingdom. Early animal studies centered primarily on pigeons, which are easily bred and handled and which possess high levels of fats in their tissues. Other animals, richer in fatty tissues, might be even more attractive but more challenging to maintain. Grizzly bears, for example, carry very large fat reserves but are difficult to work with in the lab!

are formed by **acetyl transacylase (acetyl transferase)** and **malonyl transacylase (malonyl transferase),** respectively. The acetyl transacylase enzyme is not highly specific—it can transfer other acyl groups, such as the propionyl group, but at much lower rates. (Fatty acids with odd numbers of carbons are made beginning with a propionyl group transfer by this enzyme.) Malonyl transacylase, on the other hand, is highly specific.

Decarboxylation Drives the Condensation of Acetyl-CoA and Malonyl-CoA

Another transacylase reaction transfers the acetyl group from ACP to **β-keto-acyl-ACP synthase (KSase),** also known as **acyl-malonyl-ACP condensing enzyme.** The first actual elongation reaction involves the condensation of acetyl-ACP and malonyl-ACP by the β-ketoacyl-ACP synthase to form acetoacetyl-ACP (Figure 25.7). *One might ask at this point: Why is the three-carbon malonyl group used here as a two-carbon donor?* The answer is that this is yet another example of a decarboxylation driving a desired but otherwise thermodynamically unfavorable reaction. The decarboxylation that accompanies the reaction with malonyl-ACP drives the synthesis of acetoacetyl-ACP. Note that hydrolysis of ATP drove the carboxylation of acetyl-CoA to form malonyl-ACP, so, indirectly, ATP is responsible for the condensation reaction to form acetoacetyl-ACP. Malonyl-CoA can be viewed as a form of stored energy for driving fatty acid synthesis.

It is also worth noting that the carbon of the carboxyl group that was added to drive this reaction is the one removed by the condensing enzyme. Thus, all the carbons of acetoacetyl-ACP (*and* of the fatty acids to be made) are derived from acetate units of acetyl-CoA.
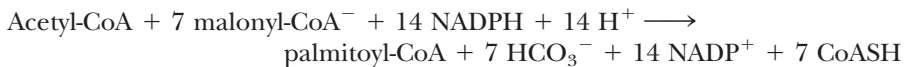
Reduction of the β-Carbonyl Group Follows a Now-Familiar Route

The next three steps—reduction of the β-carbonyl group to form a β-alcohol, followed by dehydration and reduction to saturate the chain (Figure 25.7)—look very similar to the fatty acid degradation pathway in reverse. However, there are two crucial differences between fatty acid biosynthesis and fatty acid oxidation (besides the fact that different enzymes are involved): First, the alcohol formed in the first step has the L configuration rather than the L form seen in catabolism, and, second, the reducing coenzyme is NADPH, although NAD^+ and FAD are the oxidants in the catabolic pathway.
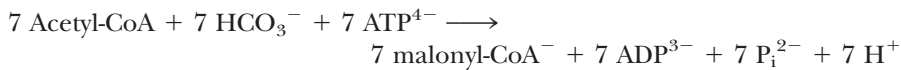
The net result of this biosynthetic cycle is the synthesis of a four-carbon unit, a butyryl group, from two smaller building blocks. In the next cycle of the process, this butyryl-ACP condenses with another malonyl-ACP to make a

six-carbon β-ketoacyl-ACP and CO_2. Subsequent reduction to a β-alcohol, dehydration, and another reduction yield a six-carbon saturated acyl-ACP. This cycle continues with the net addition of a two-carbon unit in each turn until the chain is 16 carbons long (Figure 25.7). The β-ketoacyl-ACP synthase cannot accommodate larger substrates, so the reaction cycle ends with a 16-carbon chain. Hydrolysis of the C_{16}-acyl-ACP yields a palmitic acid and the free ACP.

In the end, seven malonyl-CoA molecules and one acetyl-CoA yield a palmitate (shown here as palmitoyl-CoA):

$$\text{Acetyl-CoA} + 7 \text{ malonyl-CoA}^- + 14 \text{ NADPH} + 14 \text{ H}^+ \longrightarrow$$
$$\text{palmitoyl-CoA} + 7 \text{ HCO}_3^- + 14 \text{ NADP}^+ + 7 \text{ CoASH}$$

The formation of seven malonyl-CoA molecules requires

$$7 \text{ Acetyl-CoA} + 7 \text{ HCO}_3^- + 7 \text{ ATP}^{4-} \longrightarrow$$
$$7 \text{ malonyl-CoA}^- + 7 \text{ ADP}^{3-} + 7 \text{ P}_i^{2-} + 7 \text{ H}^+$$

Thus, the overall reaction of acetyl-CoA to yield palmitic acid is

$$8 \text{ Acetyl-CoA} + 7 \text{ ATP}^{4-} + 14 \text{ NADPH} + 7\text{H}^+ \longrightarrow$$
$$\text{palmitoyl-CoA} + 14 \text{ NADP}^+ + 7 \text{ CoASH} + 7 \text{ ADP}^{3-} + 7\text{P}_i^{2-}$$

Note: These equations are stoichiometric and are charge balanced. See Problem 1 at the end of the chapter for practice in balancing these equations.

Fatty Acid Synthesis in Eukaryotes Occurs on a Multienzyme Complex

In contrast to bacterial and plant systems, the reactions of fatty acid synthesis beyond the acetyl-CoA carboxylase in animal systems are carried out by a special multienzyme complex called **fatty acid synthase (FAS).** In yeast, this 2.4×10^6 D complex contains two different peptide chains, an α subunit of 213 kD and a β subunit of 203 kD, arranged in an $\alpha_6\beta_6$ dodecamer. The separate enzyme activities associated with each chain are shown in Figure 25.8. In animal systems, FAS is a dimer of identical 250-kD *multifunctional polypeptides.* Studies of the action of proteolytic enzymes on this polypeptide have led to a model involving three separate domains joined by flexible connecting sequences (Figure 25.9). The first domain is responsible for the binding of acetyl and malonyl building blocks and for the condensation of these units. This domain includes the acetyl transferase, the malonyl transferase, and the acyl-malonyl-ACP condensing enzyme (the β-ketoacyl synthase). The second domain is primarily responsible for the reduction of the intermediate synthesized in domain 1, and contains the acyl carrier protein, the β-ketoacyl reductase, the dehydratase, and the enoyl-ACP reductase. The third domain contains the thioesterase that liberates the product palmitate when the growing acyl chain reaches its limit length of 16 carbons. The close association of activities in this complex permits efficient exposure of intermediates to one active site and then the next. The presence of all these activities on a single polypeptide ensures that the cell will simultaneously synthesize all the enzymes needed for fatty acid synthesis.

The Mechanism of Fatty Acid Synthase

The first domain of one subunit of the fatty acid synthase interacts with the second and third domains of the other subunit; that is, the subunits are arranged in a head-to-tail fashion (Figure 25.9). The first step in the fatty acid synthase reaction is the formation of an acetyl-O-enzyme intermediate between the acetyl group of an acetyl-CoA and an active-site serine of the acetyl trans-
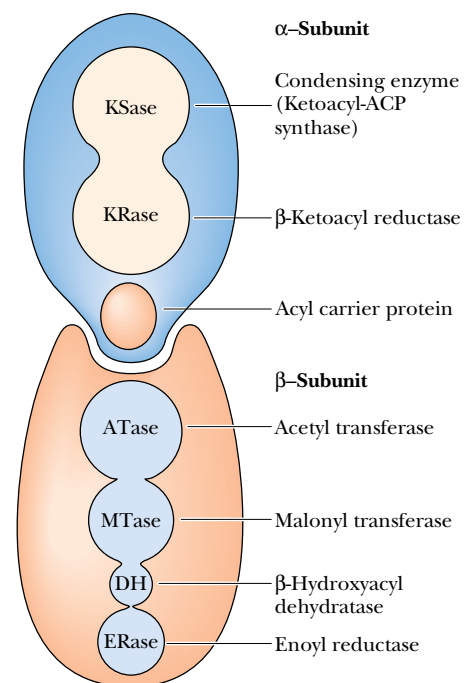

FIGURE 25.8 • In yeast, the functional groups and enzyme activities required for fatty acid synthesis are distributed between α and β subunits.
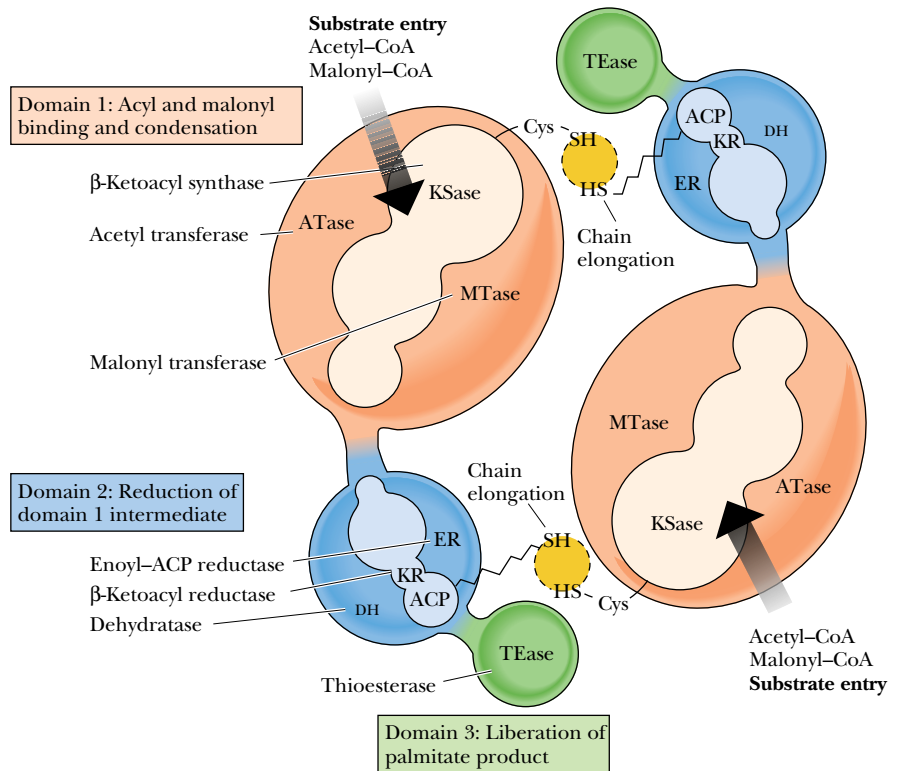
FIGURE 25.9 • Fatty acid synthase in animals contains all the functional groups and enzyme activities on a single multifunctional subunit. The active enzyme is a head-to-tail dimer of identical subunits. *(Adapted from Wakil, S. J., Stoops, J. K., and Joshi, V. C., 1983.* Annual Review of Biochemistry **52:**556.*)*

ferase (Figure 25.10). In a similar manner, a malonyl-O-enzyme intermediate is formed between malonyl-CoA and a serine residue of the malonyl transferase. The acetyl group on the acetyl transferase is then transferred to the —SH group of the acyl carrier protein, as shown in Figure 25.11. The next step is the transfer of the acetyl group to the β-ketoacyl-ACP synthase, or condensing enzyme. This frees the acyl carrier protein to acquire the malonyl group from the malonyl transferase. The next step is the condensation reaction, in which decarboxylation facilitates the concerted attack of the remaining two-carbon unit of the acyl carrier protein at the carbonyl carbon of the acetate group on the condensing enzyme. Note that decarboxylation forms a transient, highly nucleophilic carbanion which can attack the acetate group.

The next three steps—reduction of the carbonyl to an alcohol, dehydration to yield a *trans-α,β* double bond, and reduction to yield a saturated chain— are identical to those occurring in bacteria and plants (Figure 25.7) and
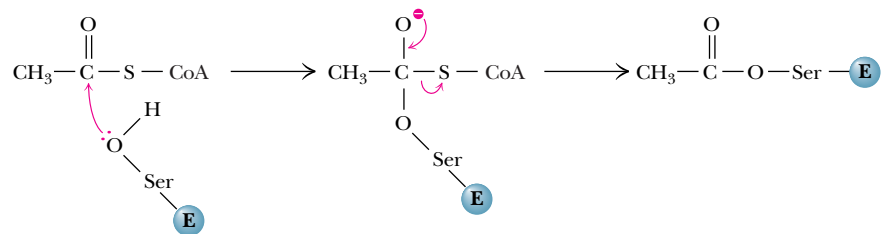

FIGURE 25.10 • Acetyl units are covalently linked to a serine residue at the active site of the acetyl transferase in eukaryotes. A similar reaction links malonyl units to the malonyl transferase.
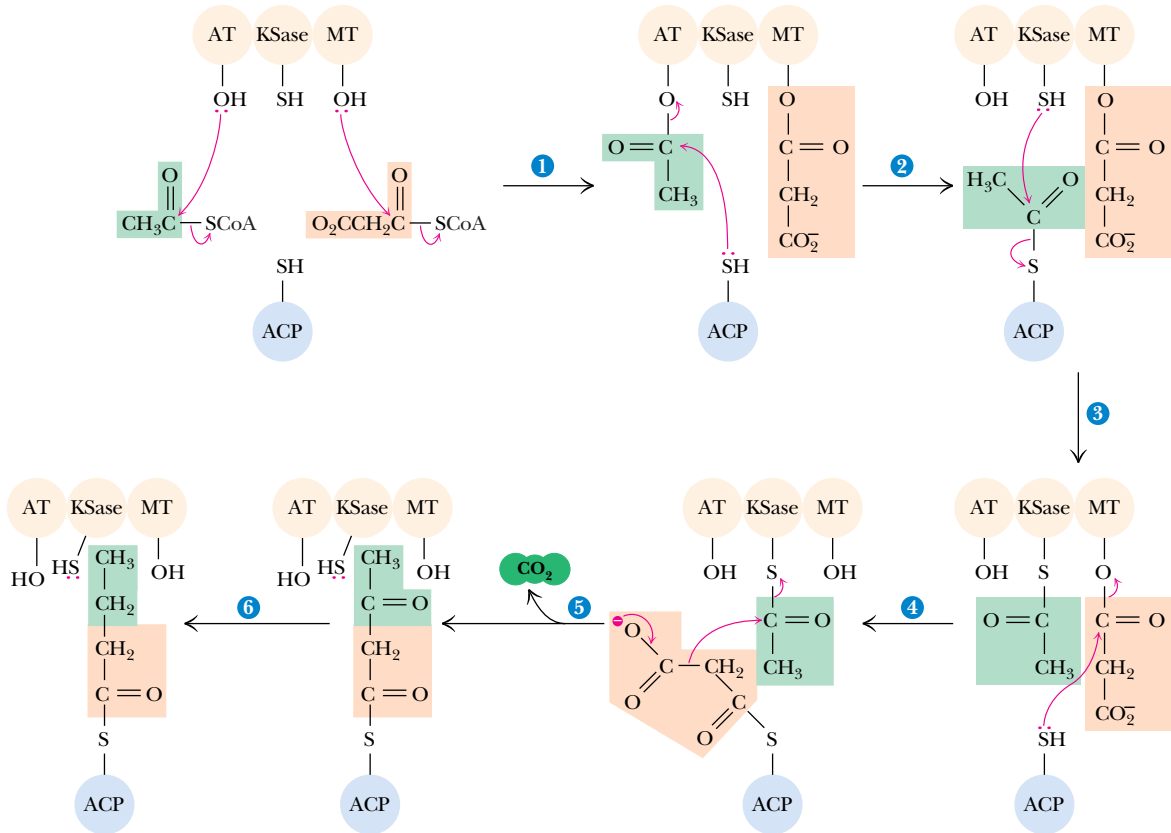
FIGURE 25.11 • The mechanism of the fatty acyl synthase reaction in eukaryotes. (1) Acetyl and malonyl groups are loaded onto acetyl transferase and malonyl transferase, respectively. (2) The acetate unit that forms the base of the nascent chain is transferred first to the acyl carrier protein domain and (3) then to the β-ketoacyl synthase. (4) Attack by ACP on the carbonyl carbon of a malonyl unit on malonyl transferase forms malonyl-ACP. (5) Decarboxylation leaves a reactive, transient carbanion that can attack the carbonyl carbon of the acetyl group on the β-ketoacyl synthase. (6) Reduction of the keto group, dehydration, and saturation of the resulting double bond follow, leaving an acyl group on ACP, and steps 3 through 6 repeat to lengthen the nascent chain.

resemble the reverse of the reactions of fatty acid oxidation (and the conversion of succinate to oxaloacetate in the TCA cycle). This synthetic cycle now repeats until the growing chain is 16 carbons long. It is then released by the thioesterase domain on the synthase. The amino acid sequence of the thioesterase domain is homologous with serine proteases; the enzyme has an active-site serine that carries out nucleophilic attack on the carbonyl carbon of the fatty acyl thioester to be cleaved.

Further Processing of C_{16} Fatty Acids

Additional Elongation

As seen already, palmitate is the primary product of the fatty acid synthase. Cells synthesize many other fatty acids. Shorter chains are easily made if the chain is released before reaching 16 carbons in length. Longer chains are made through special elongation reactions, which occur both in the mitochondria and at the surface of the endoplasmic reticulum. The ER reactions are actually quite similar to those we have just discussed: addition of two-carbon units

at the carboxyl end of the chain by means of oxidative decarboxylations involving malonyl-CoA. As was the case for the fatty acid synthase, this decarboxylation provides the thermodynamic driving force for the condensation reaction. The mitochondrial reactions involve addition (and subsequent reduction) of acetyl units. These reactions (Figure 25.12) are essentially a reversal of fatty acid oxidation, with the exception that NADPH is utilized in the saturation of the double bond, instead of $FADH_2$.

Introduction of a Single **cis** Double Bond

Both prokaryotes and eukaryotes are capable of introducing a single *cis* double bond in a newly synthesized fatty acid. Bacteria such as *E. coli* carry out this process in an O_2-independent pathway, whereas eukaryotes have adopted an O_2-dependent pathway. There is a fundamental chemical difference between the two. The O_2-dependent reaction can occur anywhere in the fatty acid chain,
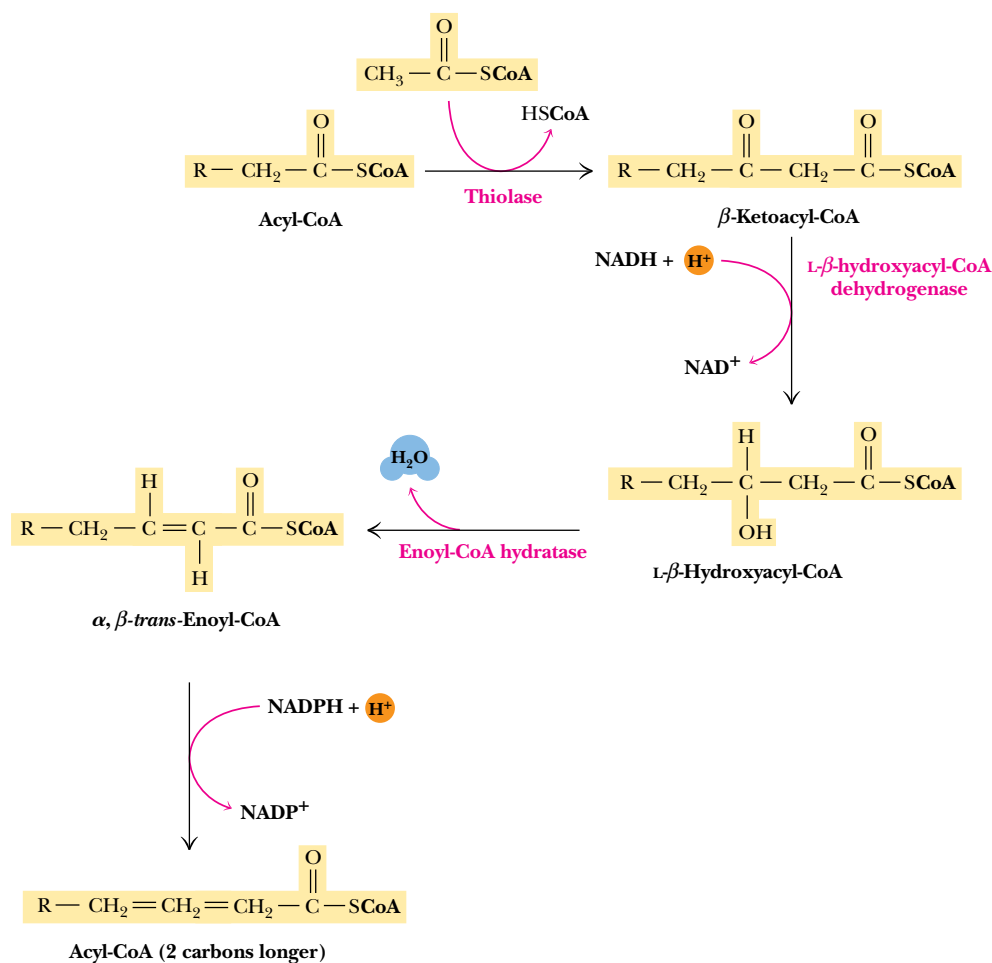

FIGURE 25.12 • Elongation of fatty acids in mitochondria is initiated by the thiolase reaction. The β-ketoacyl intermediate thus formed undergoes the same three reactions (in reverse order) that are the basis of β-oxidation of fatty acids. Reduction of the β-keto group is followed by dehydration to form a double bond. Reduction of the double bond yields a fatty acyl-CoA that is elongated by two carbons. Note that the reducing coenzyme for the second step is NADH, whereas the reductant for the fourth step is NADPH.

with no (additional) need to activate the desired bond toward dehydrogenation. However, in the absence of O_2, some other means must be found to activate the bond in question. Thus, in the bacterial reaction, dehydrogenation occurs while the bond of interest is still near the β-carbonyl or β-hydroxy group and the thioester group at the end of the chain.

In *E. coli,* the biosynthesis of a monounsaturated fatty acid begins with four normal cycles of elongation to form a 10-carbon intermediate, β-hydroxydecanoyl-ACP (Figure 25.13). At this point, **β-hydroxydecanoyl thioester dehydrase** forms a double bond β,γ to the thioester and in the *cis* configuration. This is followed by three rounds of the normal elongation reactions to form *palmitoleoyl-ACP.* Elongation may terminate at this point or may be followed by additional biosynthetic events. The principal unsaturated fatty acid in *E. coli, cis-vaccenic acid,* is formed by an additional elongation step, using palmitoleoyl-ACP as a substrate.

Unsaturation Reactions Occur in Eukaryotes in the Middle of an Aliphatic Chain

The addition of double bonds to fatty acids in eukaryotes does not occur until the fatty acyl chain has reached its full length (usually 16 to 18 carbons). Dehydrogenation of stearoyl-CoA occurs in the middle of the chain despite the absence of any useful functional group on the chain to facilitate activation:

$$CH_3-(CH_2)_{16}CO-SCoA \longrightarrow CH_3-(CH_2)_7CH=CH(CH_2)_7CO-SCoA$$
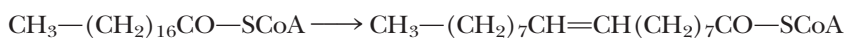
This impressive reaction is catalyzed by **stearoyl-CoA desaturase,** a 53-kD enzyme containing a nonheme iron center. NADH and oxygen (O_2) are required, as are two other proteins: **cytochrome b_5 reductase** (a 43-kD flavoprotein) and **cytochrome b_5** (16.7 kD). All three proteins are associated with the endoplasmic reticulum membrane. Cytochrome b_5 reductase transfers a pair of electrons from NADH through FAD to cytochrome b_5 (Figure 25.14). Oxidation of reduced cytochrome b_5 is coupled to reduction of nonheme Fe^{3+} to Fe^{2+} in the desaturase. The Fe^{3+} accepts a pair of electrons (one at a time in a cycle) from cytochrome b_5 and creates a *cis* double bond at the 9,10-position of the stearoyl-CoA substrate. O_2 is the terminal electron acceptor in this fatty acyl desaturation cycle. Note that two water molecules are made, which means that four electrons are transferred overall. Two of these come through the reaction sequence from NADH, and two come from the fatty acyl substrate that is being dehydrogenated.
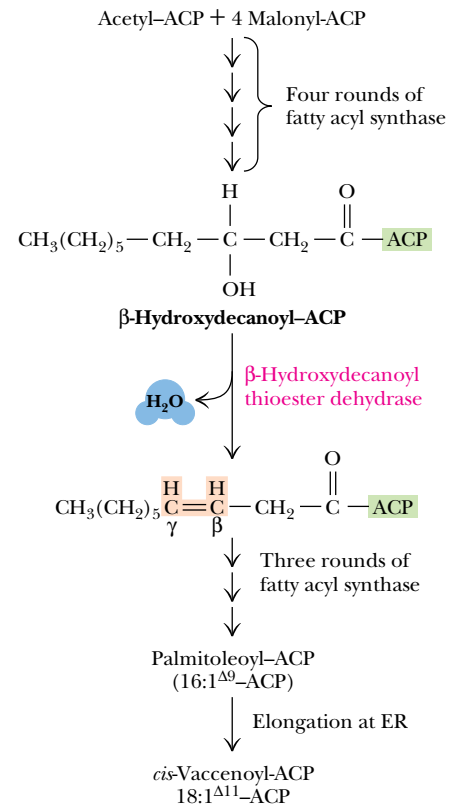

FIGURE 25.13 • Double bonds are introduced into the growing fatty acid chain in *E. coli* by specific dehydrases. Palmitoleoyl-ACP is synthesized by a sequence of reactions involving four rounds of chain elongation, followed by double bond insertion by β-hydroxydecanoyl thioester dehydrase and three additional elongation steps. Another elongation cycle produces *cis*-vaccenic acid.
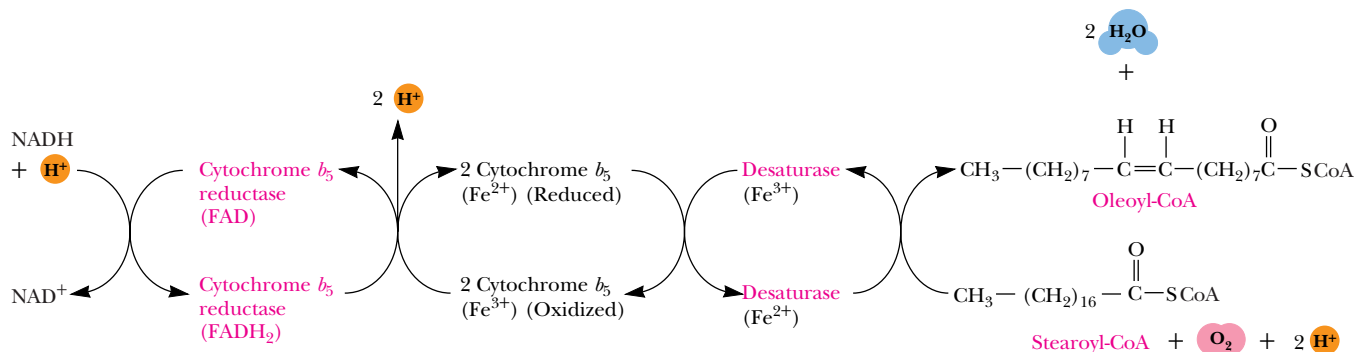

FIGURE 25.14 • The conversion of stearoyl-CoA to oleoyl-CoA in eukaryotes is catalyzed by stearoyl-CoA desaturase in a reaction sequence that also involves cytochrome b_5 and cytochrome b_5 reductase. Two electrons are passed from NADH through the chain of reactions as shown, and two electrons are also derived from the fatty acyl substrate.

The Unsaturation Reaction May Be Followed by Chain Elongation

Additional chain elongation can occur following this single desaturation reaction. The oleoyl-CoA produced can be elongated by two carbons to form a 20:1 cis-Δ^{11} fatty acyl-CoA. If the starting fatty acid is palmitate, reactions similar to the preceding scheme yield palmitoleoyl-CoA (16:1 cis-Δ^9), which subsequently can be elongated to yield cis-vaccenic acid (18:1 cis-Δ^{11}). Similarly, C_{16} and C_{18} fatty acids can be elongated to yield C_{22} and C_{24} fatty acids, such as are often found in sphingolipids.

Biosynthesis of Polyunsaturated Fatty Acids

Organisms differ with respect to formation, processing, and utilization of polyunsaturated fatty acids. *E. coli,* for example, does not have any polyunsaturated fatty acids. Eukaryotes *do* synthesize a variety of polyunsaturated fatty acids, certain organisms more than others. For example, plants manufacture double bonds between the Δ^9 and the methyl end of the chain, but mammals cannot. Plants readily desaturate oleic acid at the 12-position (to give linoleic acid) or at both the 12- and 15-positions (producing linolenic acid). Mammals require polyunsaturated fatty acids, but must acquire them in their diet. As such, they are referred to as **essential fatty acids.** On the other hand, mammals *can* introduce double bonds between the double bond at the 8- or 9-position and the carboxyl group. Enzyme complexes in the endoplasmic reticulum desaturate the 5-position, provided a double bond exists at the 8-position, and form a double bond at the 6-position if one already exists at the 9-position. Thus, oleate can be unsaturated at the 6,7-position to give an 18:2 cis-Δ^6,Δ^9 fatty acid.

Arachidonic Acid Is Synthesized from Linoleic Acid by Mammals

Mammals can add additional double bonds to unsaturated fatty acids in their diets. Their ability to make arachidonic acid from linoleic acid is one example (Figure 25.15). This fatty acid is the precursor for prostaglandins and other biologically active derivatives such as leukotrienes. Synthesis involves formation of a linoleoyl ester of CoA from dietary linoleic acid, followed by introduction of a double bond at the 6-position. The triply unsaturated product is then elongated (by malonyl-CoA with a decarboxylation step) to yield a 20-carbon fatty acid with double bonds at the 8-, 11-, and 14-positions. A second desaturation reaction at the 5-position followed by an **acyl-CoA synthetase** reaction (Chapter 24) liberates the product, a 20-carbon fatty acid with double bonds at the 5-, 8-, 11-, and 14-positions.

Regulatory Control of Fatty Acid Metabolism—An Interplay of Allosteric Modifiers and Phosphorylation–Dephosphorylation Cycles

The control and regulation of fatty acid synthesis is intimately related to regulation of fatty acid breakdown, glycolysis, and the TCA cycle. Acetyl-CoA is an important intermediate metabolite in all these processes. In these terms, it is easy to appreciate the interlocking relationships in Figure 25.16. Malonyl-CoA can act to prevent fatty acyl-CoA derivatives from entering the mitochondria by inhibiting the carnitine acyltransferase that is responsible for this transport. In this way, when fatty acid synthesis is turned on (as signaled by higher levels of malonyl-CoA), β-oxidation is inhibited. As we pointed out earlier, citrate is an important allosteric activator of acetyl-CoA carboxylase, and fatty acyl-CoAs
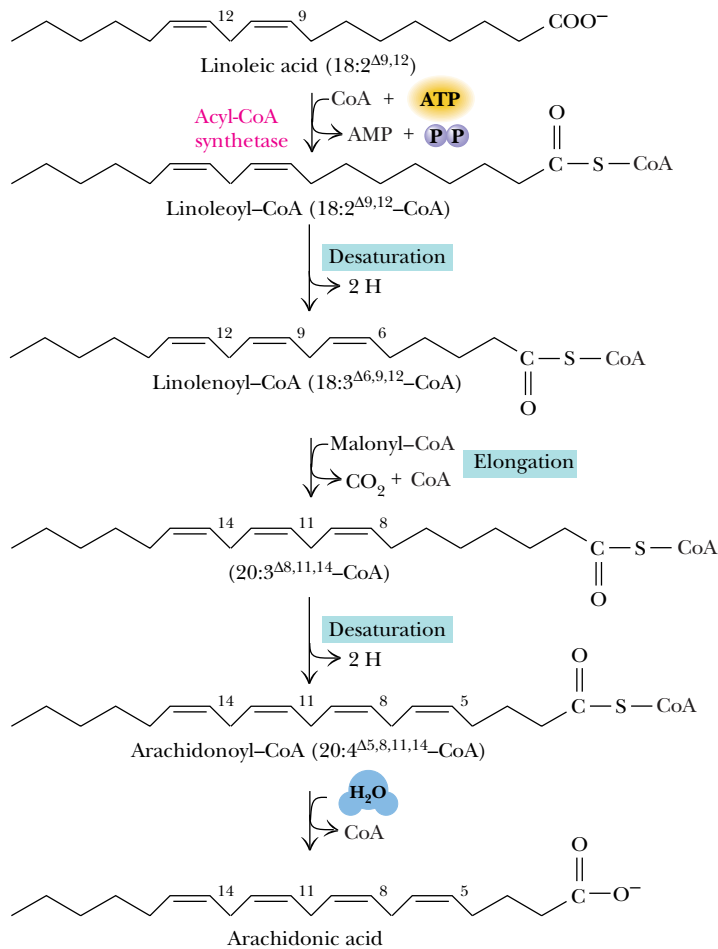
FIGURE 25.15 • Arachidonic acid is synthesized from linoleic acid in eukaryotes. This is the only means by which animals can synthesize fatty acids with double bonds at positions beyond C-9.

are inhibitors. The degree of inhibition is proportional to the chain length of the fatty acyl-CoA; longer chains show a higher affinity for the allosteric inhibition site on acetyl-CoA carboxylase. Palmitoyl-CoA, stearoyl-CoA, and arachidyl-CoA are the most potent inhibitors of the carboxylase.

Hormonal Signals Regulate ACC and Fatty Acid Biosynthesis

As described earlier, citrate activation and palmitoyl-CoA inhibition of acetyl-CoA carboxylase are strongly dependent on the phosphorylation state of the enzyme. This provides a crucial connection to hormonal regulation. Many of the enzymes that act to phosphorylate acetyl-CoA carboxylase (Figure 25.4) are controlled by hormonal signals. Glucagon is a good example (Figure 25.17). As noted in Chapter 23, glucagon binding to membrane receptors activates an intracellular cascade involving activation of adenylyl cyclase. Cyclic AMP produced by the cyclase activates a protein kinase, which then phosphorylates acetyl-CoA carboxylase. Unless citrate levels are high, phosphorylation causes inhibition of fatty acid biosynthesis. The carboxylase (and fatty acid synthesis)
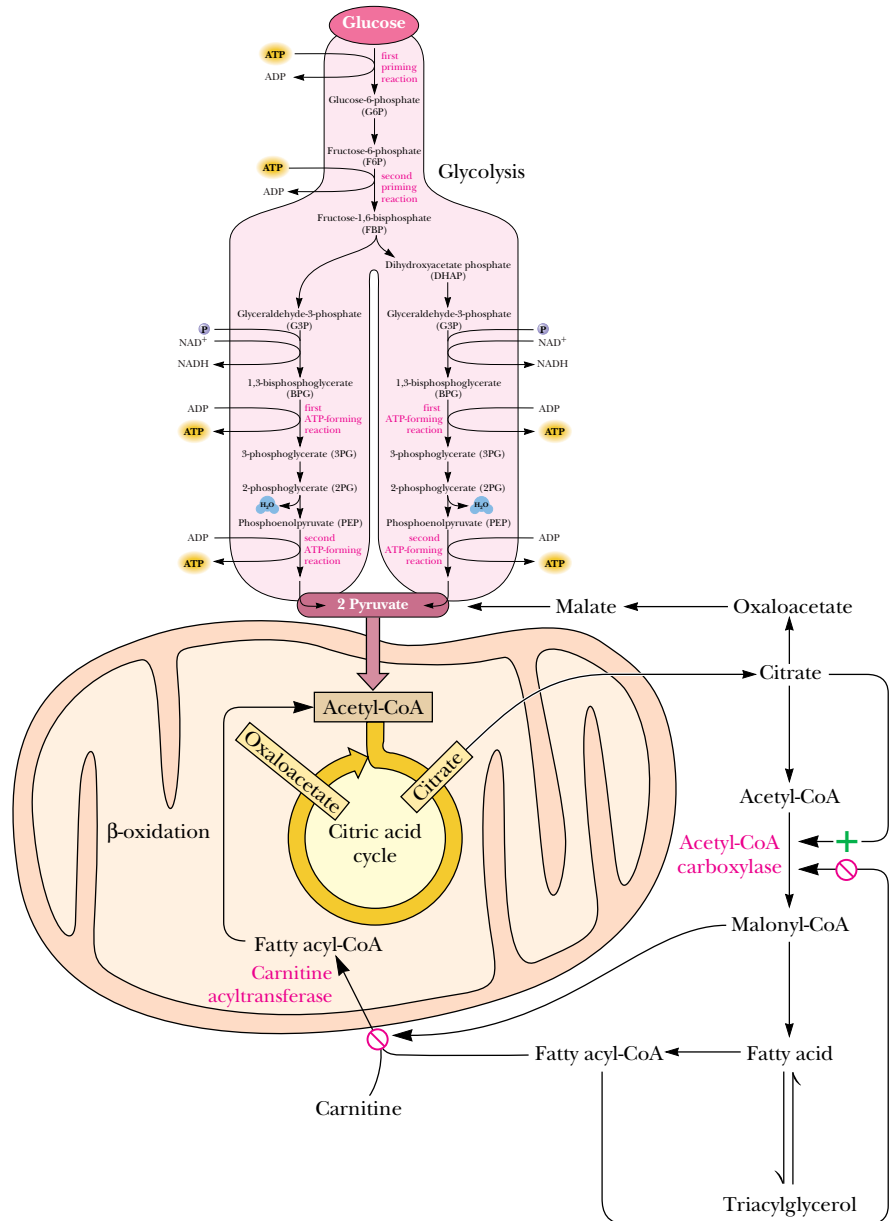
FIGURE 25.16 • Regulation of fatty acid synthesis and fatty acid oxidation are coupled as shown. Malonyl-CoA, produced during fatty acid synthesis, inhibits the uptake of fatty acylcarnitine (and thus fatty acid oxidation) by mitochondria. When fatty acyl CoA levels rise, fatty acid synthesis is inhibited and fatty acid oxidation activity increases. Rising citrate levels (which reflect an abundance of acetyl-CoA) similarly signal the initiation of fatty acid synthesis.

can be reactivated by a specific phosphatase, which dephosphorylates the carboxylase. Also indicated in Figure 25.17 is the simultaneous activation by glucagon of triacylglycerol lipases, which hydrolyze triacylglycerols, releasing fatty acids for β-oxidation. Both the inactivation of acetyl-CoA carboxylase and the activation of triacylglycerol lipase are counteracted by insulin, whose receptor acts to stimulate a phosphodiesterase that converts cAMP to AMP.
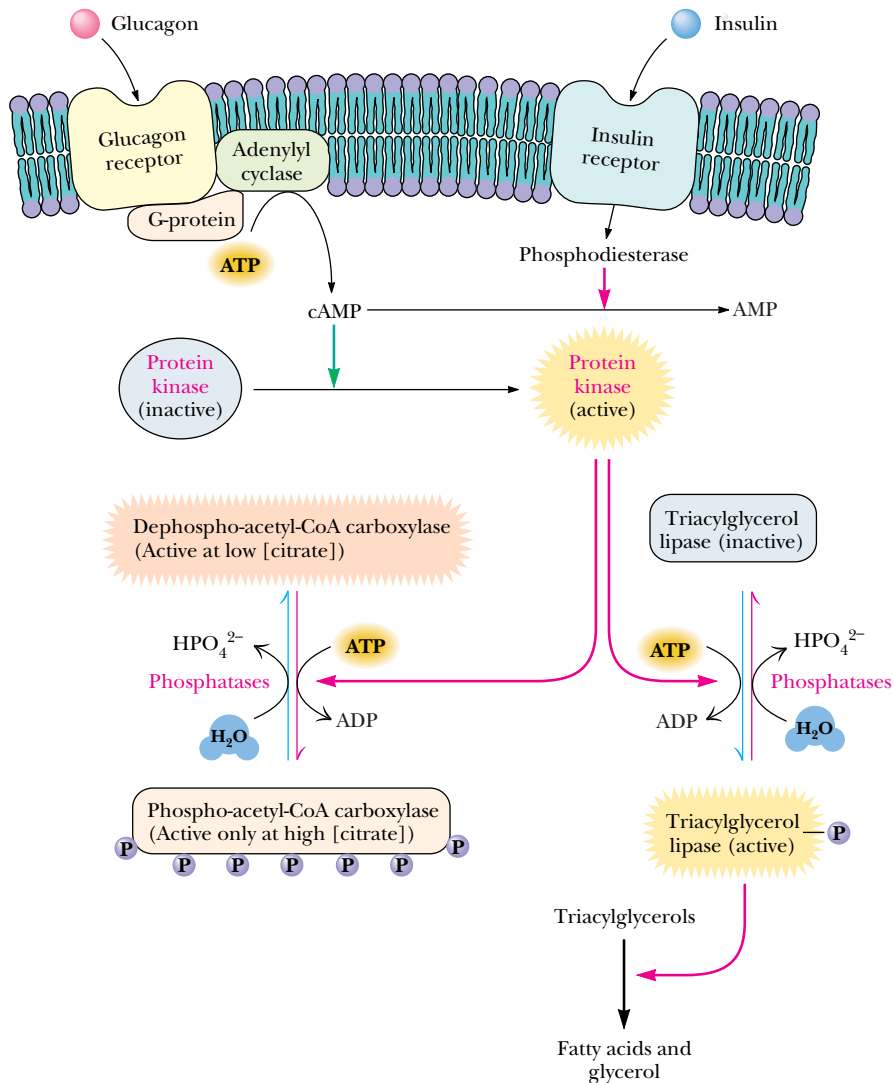
FIGURE 25.17 • Hormonal signals regulate fatty acid synthesis, primarily through actions on acetyl-CoA carboxylase. Availability of fatty acids also depends upon hormonal activation of triacylglycerol lipase.

25.2 • Biosynthesis of Complex Lipids

Complex lipids consist of backbone structures to which fatty acids are covalently bound. Principal classes include the **glycerolipids,** for which glycerol is the backbone, and **sphingolipids,** which are built on a sphingosine backbone. The two major classes of glycerolipids are **glycerophospholipids** and **triacylglycerols.** The **phospholipids,** which include both glycerophospholipids and sphingomyelins, are crucial components of membrane structure. They are also precursors of hormones such as the *eicosanoids* (e.g., *prostaglandins*) and signal molecules, such as the breakdown products of *phosphatidylinositol.*

Different organisms possess greatly different complements of lipids and therefore invoke somewhat different lipid biosynthetic pathways. For example,

sphingolipids and triacylglycerols are produced only in eukaryotes. In contrast, bacteria usually have rather simple lipid compositions. Phosphatidylethanol-amine accounts for at least 75% of the phospholipids in *E. coli,* with phosphatidyl-glycerol and cardiolipin accounting for most of the rest. *E. coli* membranes possess no phosphatidylcholine, phosphatidylinositol, sphingolipids, or choles-terol. On the other hand, some bacteria (such as *Pseudomonas*) can synthesize phosphatidylcholine, for example. In this section and the one following, we consider some of the pathways for the synthesis of glycerolipids, sphingolipids, and the eicosanoids, which are derived from phospholipids.
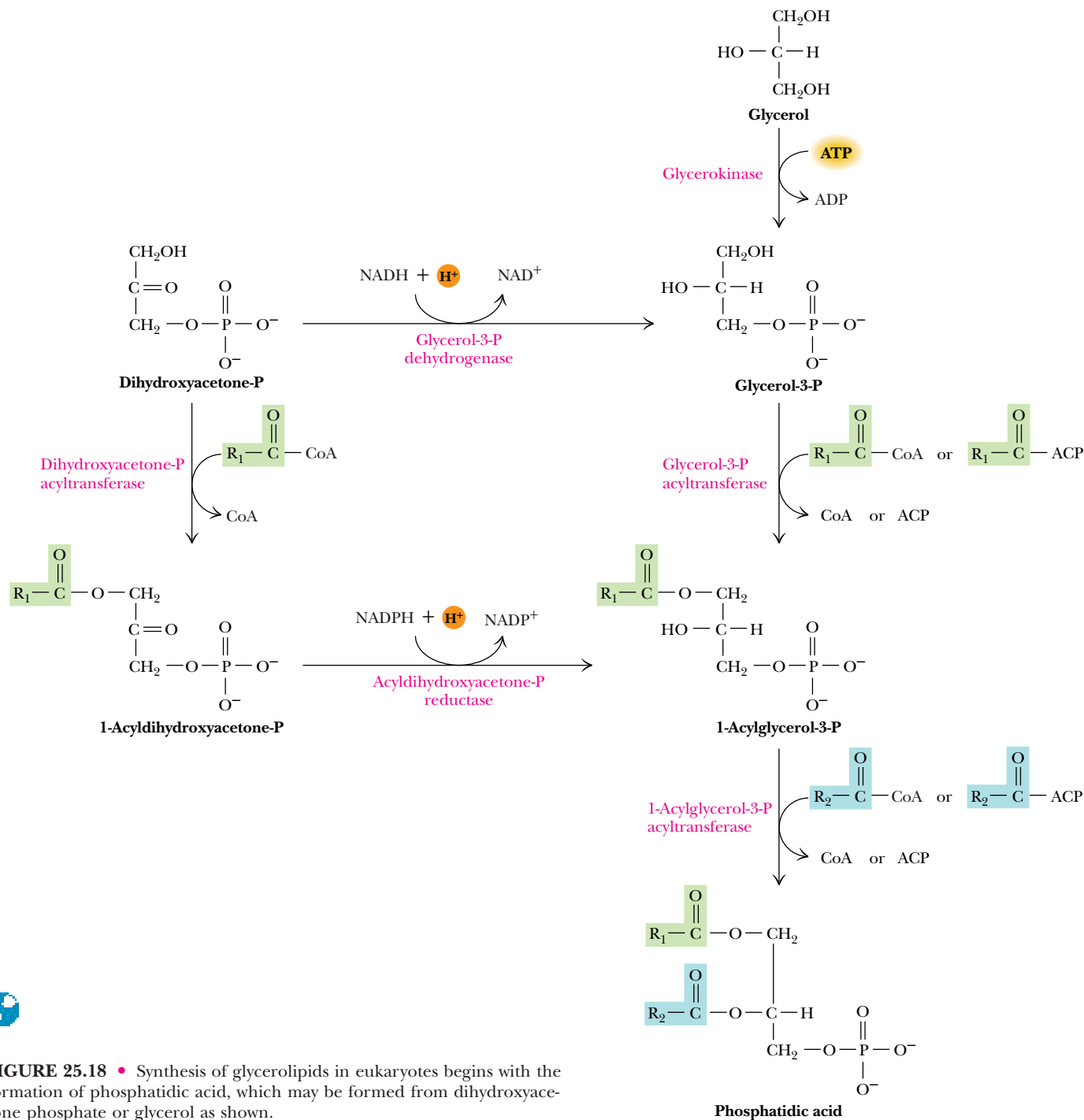

FIGURE 25.18 • Synthesis of glycerolipids in eukaryotes begins with the formation of phosphatidic acid, which may be formed from dihydroxyace-tone phosphate or glycerol as shown.

Glycerolipid Biosynthesis

A common pathway operates in nearly all organisms for the synthesis of **phosphatidic acid,** the precursor to other glycerolipids. **Glycerokinase** catalyzes the phosphorylation of glycerol to form glycerol-3-phosphate, which is then acylated at both the 1- and 2-positions to yield phosphatidic acid (Figure 25.18). The first acylation, at position 1, is catalyzed by **glycerol-3-phosphate acyltransferase,** an enzyme that in most organisms is specific for saturated fatty acyl groups. Eukaryotic systems can also utilize **dihydroxyacetone phosphate** as a starting point for synthesis of phosphatidic acid (Figure 25.18). Again a specific acyltransferase adds the first acyl chain, followed by reduction of the backbone keto group by **acyldihydroxyacetone phosphate reductase,** using NADPH as the reductant. Alternatively, dihydroxyacetone phosphate can be reduced to glycerol-3-phosphate by **glycerol-3-phosphate dehydrogenase.**

Eukaryotes Synthesize Glycerolipids from CDP-Diacylglycerol or Diacylglycerol

In eukaryotes, phosphatidic acid is converted directly either to diacylglycerol or to *cytidine diphosphodiacylglycerol* (or simply *CDP-diacylglycerol;* Figure 25.19). From these two precursors, all other glycerophospholipids in eukaryotes are derived. Diacylglycerol is a precursor for synthesis of triacylglycerol, phosphatidylethanolamine, and phosphatidylcholine. Triacylglycerol is synthesized mainly in adipose tissue, liver, and intestines and serves as the principal energy storage molecule in eukaryotes. Triacylglycerol biosynthesis in liver and adipose tissue occurs via **diacylglycerol acyltransferase,** an enzyme bound to the cytoplasmic face of the endoplasmic reticulum. A different route is used, however, in intestines. Recall (Figure 24.3) that triacylglycerols from the diet are broken down to 2-monoacylglycerols by specific lipases. Acyltransferases then acylate 2-monoacylglycerol to produce new triacylglycerols (Figure 25.20).

Phosphatidylethanolamine Is Synthesized from Diacylglycerol and CDP-Ethanolamine

Phosphatidylethanolamine synthesis begins with phosphorylation of ethanolamine to form phosphoethanolamine (Figure 25.19). The next reaction involves transfer of a cytidylyl group from CTP to form CDP-ethanolamine and pyrophosphate. As always, PP_i hydrolysis drives this reaction forward. A specific **phosphoethanolamine transferase** then links phosphoethanolamine to the diacylglycerol backbone. Biosynthesis of phosphatidylcholine is entirely analogous because animals synthesize it directly. All of the choline utilized in this pathway must be acquired from the diet. Yeast, certain bacteria, and animal livers, however, can convert phosphatidylethanolamine to phosphatidylcholine by methylation reactions involving S-adenosylmethionine (see Chapter 26).

Exchange of Ethanolamine for Serine Converts Phosphatidylethanolamine to Phosphatidylserine

Mammals synthesize phosphatidylserine (PS) in a calcium ion–dependent reaction involving aminoalcohol exchange (Figure 25.21). The enzyme catalyzing this reaction is associated with the endoplasmic reticulum and will accept phosphatidylethanolamine (PE) and other phospholipid substrates. A mitochondrial **PS decarboxylase** can subsequently convert PS to PE. No other pathway converting serine to ethanolamine has been found.
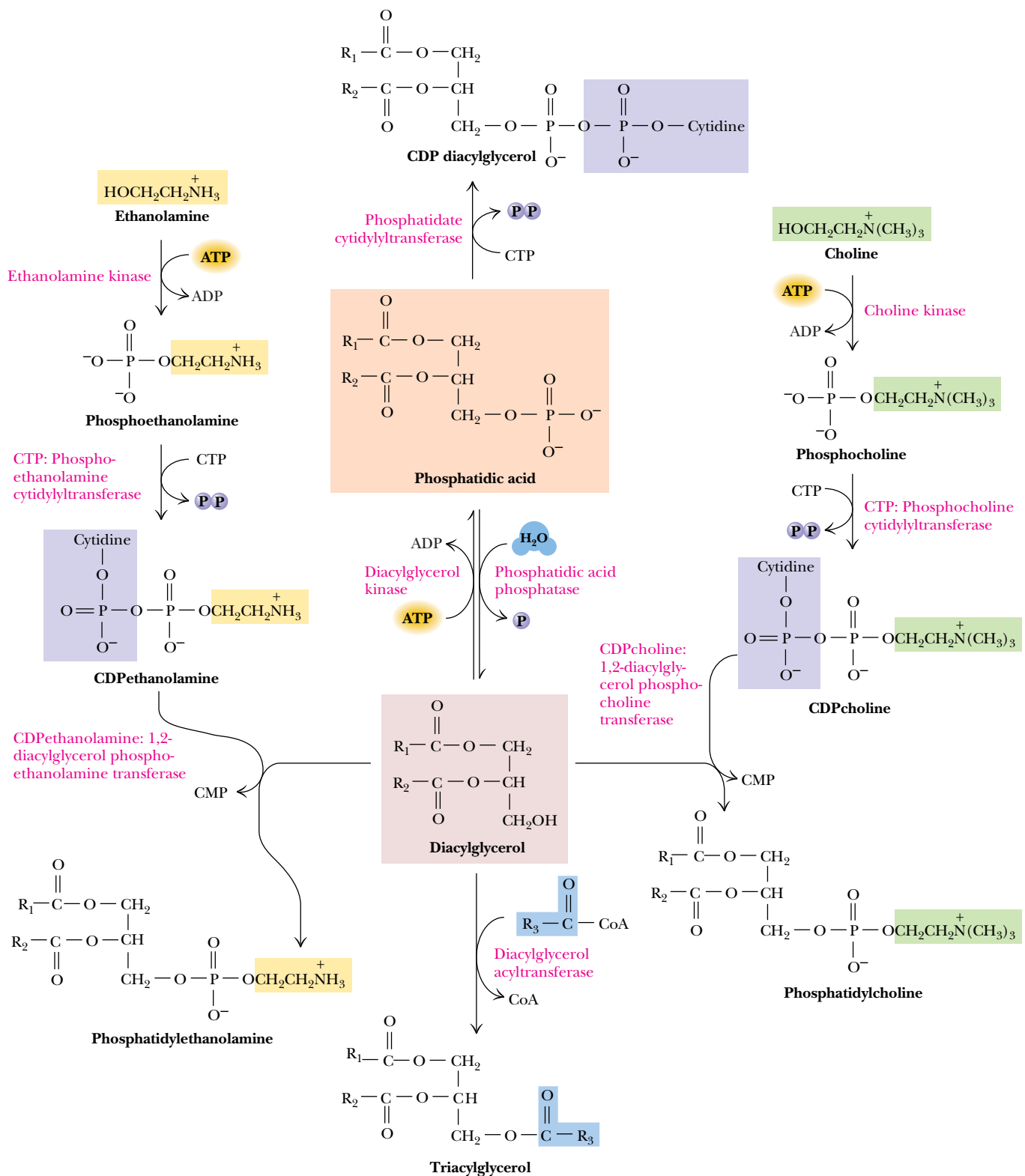
FIGURE 25.19 • Diacylglycerol and CDP-diacylglycerol are the principal precursors of glycerolipids in eukaryotes. Phosphatidylethanolamine and phosphatidylcholine are formed by reaction of diacylglycerol with CDP-ethanolamine or CDP-choline, respectively.

FIGURE 25.20 • Triacylglycerols are formed primarily by the action of acyltransferases on mono- and diacylglycerol. Acyltransferase in *E. coli* is an integral membrane protein (83 kD) and can utilize either fatty acyl-CoAs or acylated acyl carrier proteins as substrates. It shows a particular preference for palmitoyl groups. Eukaryotic acyltransferases use only fatty acyl-CoA molecules as substrates.
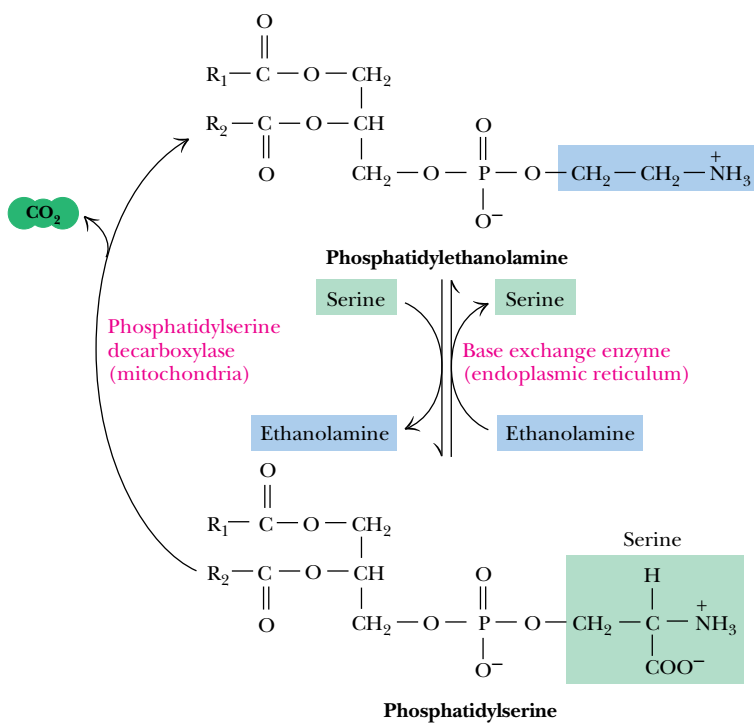

FIGURE 25.21 • The interconversion of phosphatidylethanolamine and phosphatidylserine in mammals.

Eukaryotes Synthesize Other Phospholipids via CDP-Diacylglycerol

Eukaryotes also use CDP-diacylglycerol, derived from phosphatidic acid, as a precursor for several other important phospholipids, including phosphatidyl-inositol (PI), phosphatidylglycerol (PG), and cardiolipin (Figure 25.22). PI accounts for only about 2 to 8% of the lipids in most animal membranes, but breakdown products of PI, including inositol-1,4,5-trisphosphate and diacyl-glycerol, are second messengers in a vast array of cellular signaling processes.

Dihydroxyacetone Phosphate Is a Precursor to the Plasmalogens

Certain glycerophospholipids possess alkyl or alkenyl ether groups at the 1-position in place of an acyl ester group. These glyceroether phospholipids are synthesized from dihydroxyacetone phosphate (Figure 25.23). Acylation of dihydroxyacetone phosphate (DHAP) is followed by an exchange reaction, in which the acyl group is removed as a carboxylic acid and a long-chain alcohol
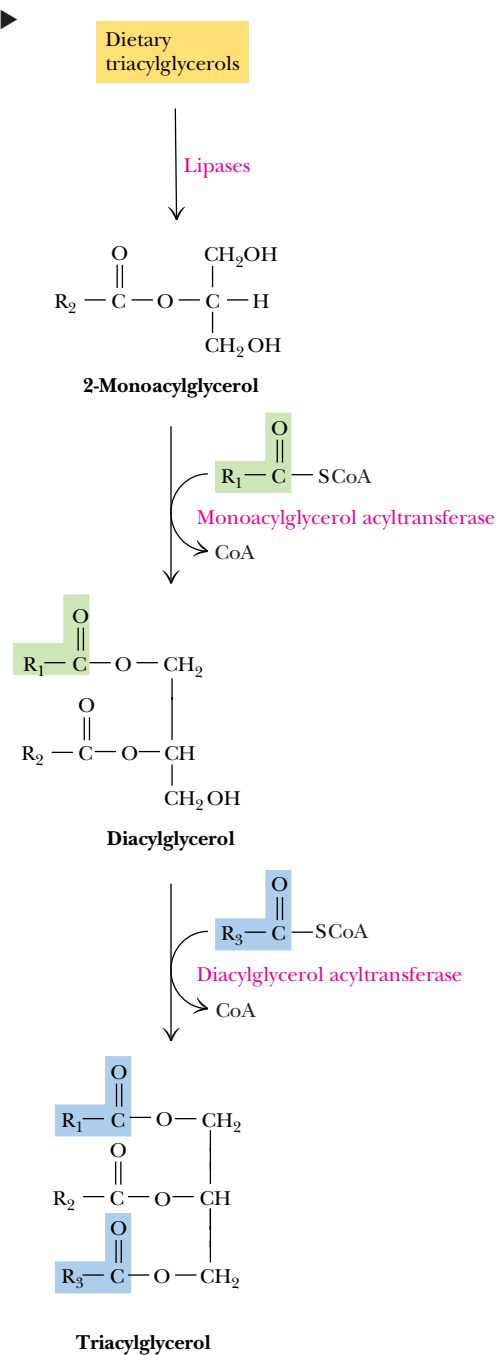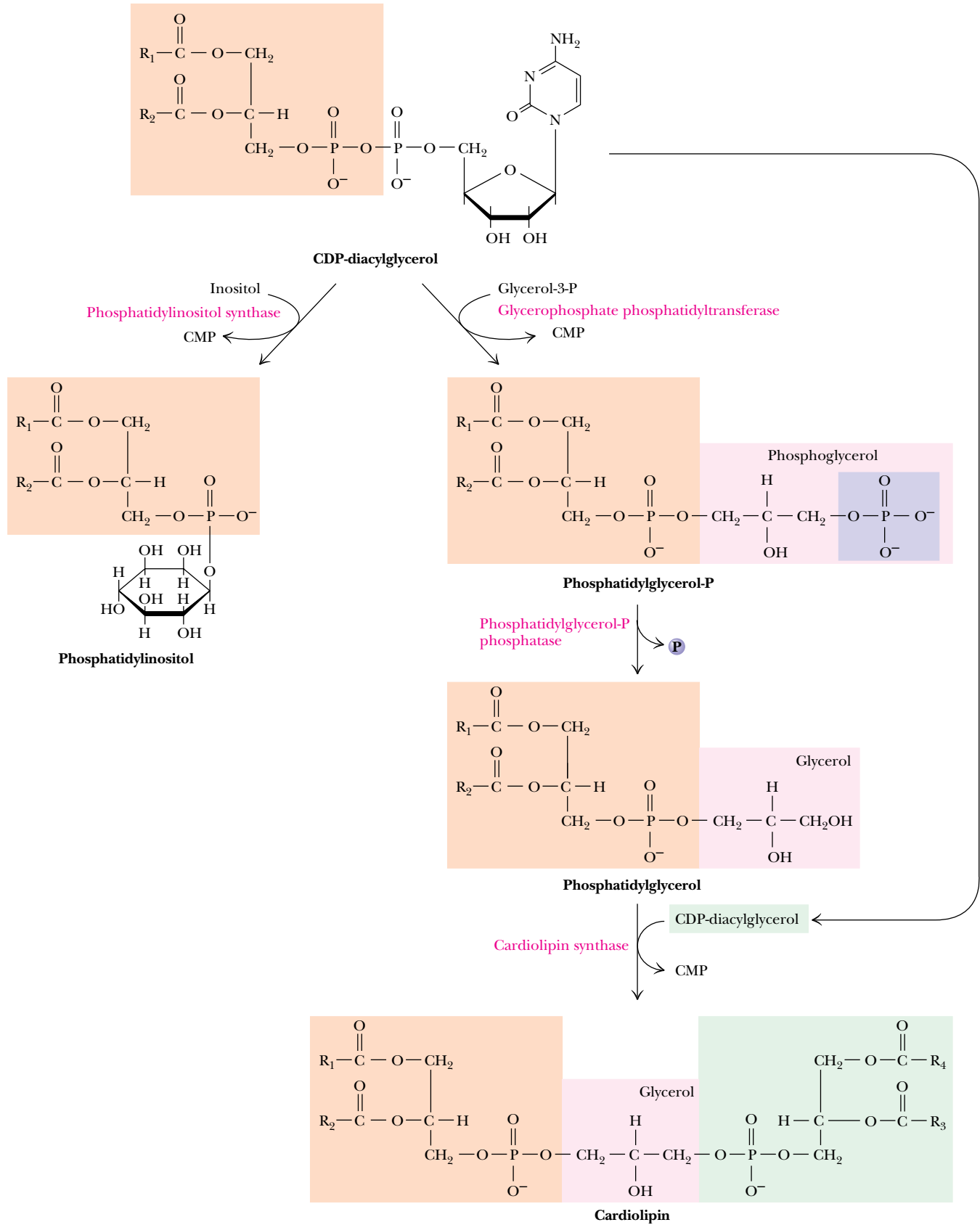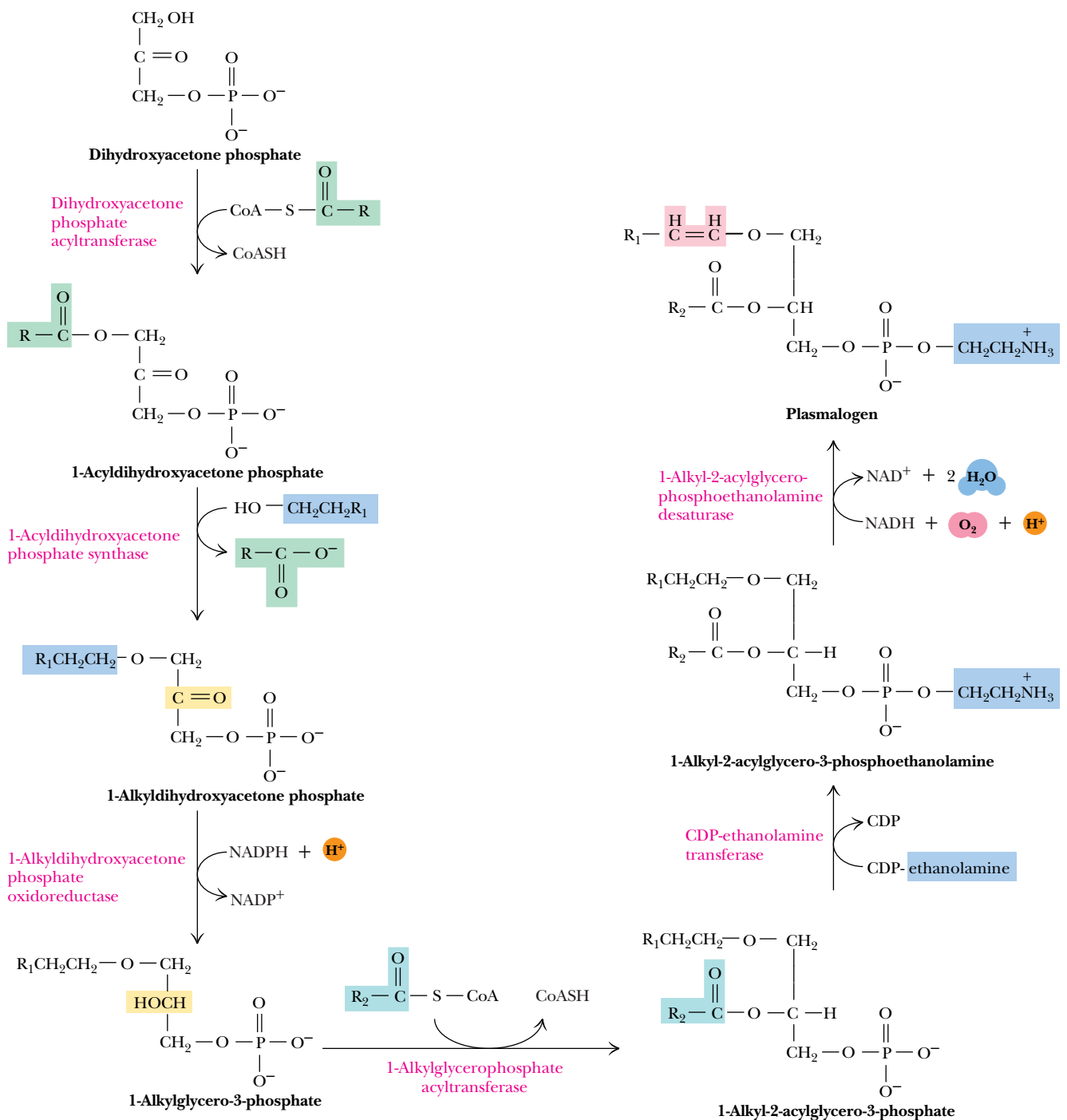
FIGURE 25.22 • CDP-diacylglycerol is a precursor of phosphatidylinositol, phosphatidylglycerol, and cardiolipin in eukaryotes.

FIGURE 25.23 • Biosynthesis of plasmalogens in animals. Acylation at C-1 is followed by exchange of the acyl group for a long-chain alcohol. Reduction of the keto group at C-2 is followed by transferase reactions, which add an acyl group at C-2 and a polar head-group moiety, and a desaturase reaction that forms a double bond in the alkyl chain. The first two enzymes are of cytoplasmic origin, and the last transferase is located at the endoplasmic reticulum.

adds to the 1-position. This long-chain alcohol is derived from the corresponding acyl-CoA by means of an **acyl-CoA reductase** reaction involving oxidation of two molecules of NADH. The 2-*keto* group of the DHAP backbone is then reduced to an alcohol, followed by acylation. The resulting 1-alkyl-2-acylglycero-3-phosphate can react in a manner similar to phosphatidic acid to produce ether analogs of phosphatidylcholine, phosphatidylethanolamine, and so forth (Figure 25.23). In addition, specific **desaturase** enzymes associated with the endoplasmic reticulum can desaturate the alkyl ether chains of these lipids

as shown. The products, which contain α,β-unsaturated ether-linked chains at the C-1 position, are **plasmalogens;** they are abundant in cardiac tissue and in the central nervous system. The desaturases catalyzing these reactions are distinct from but similar to those that introduce unsaturations in fatty acyl-CoAs. These enzymes use cytochrome b_5 as a cofactor, NADH as a reductant, and O_2 as a terminal electron acceptor.

Platelet Activating Factor

A particularly interesting ether phospholipid with unusual physiological properties has recently been characterized. As shown in Figure 25.24, **1-alkyl-2-acetyl-glycerophosphocholine,** also known as **platelet activating factor,** possesses an alkyl ether at C-1 and an acetyl group at C-2. The very short chain at C-2 makes this molecule much more water-soluble than typical glycerolipids. Platelet activating factor displays a dramatic ability to dilate blood vessels (and thus reduce blood pressure in hypertensive animals) and to aggregate platelets.

Sphingolipid Biosynthesis

Sphingolipids, ubiquitous components of eukaryotic cell membranes, are present at high levels in neural tissues. The myelin sheath that insulates nerve axons is particularly rich in sphingomyelin and other related lipids. Prokaryotic organisms normally do not contain sphingolipids. Sphingolipids are built upon sphingosine backbones rather than glycerol. The initial reaction, which involves condensation of serine and palmitoyl-CoA with release of bicarbonate, is catalyzed by **3-ketosphinganine synthase,** a PLP-dependent enzyme (Figure 25.25). Reduction of the ketone product to form *sphinganine* is catalyzed by **3-keto-sphinganine reductase,** with NADPH as a reactant. In the next step, sphinganine is acylated to form N-acyl sphinganine, which is *then* desaturated to form ceramide. Sphingosine itself does not appear to be an intermediate in this pathway in mammals.

FIGURE 25.24 • Platelet activating factor, formed from 1-alkyl-2-lysophosphatidylcholine by acetylation at C-2, is degraded by the action of acetylhydrolase.
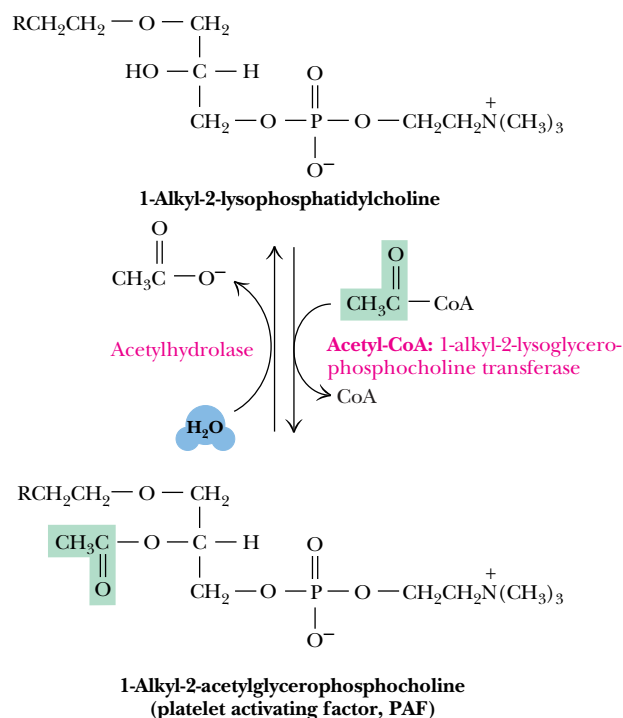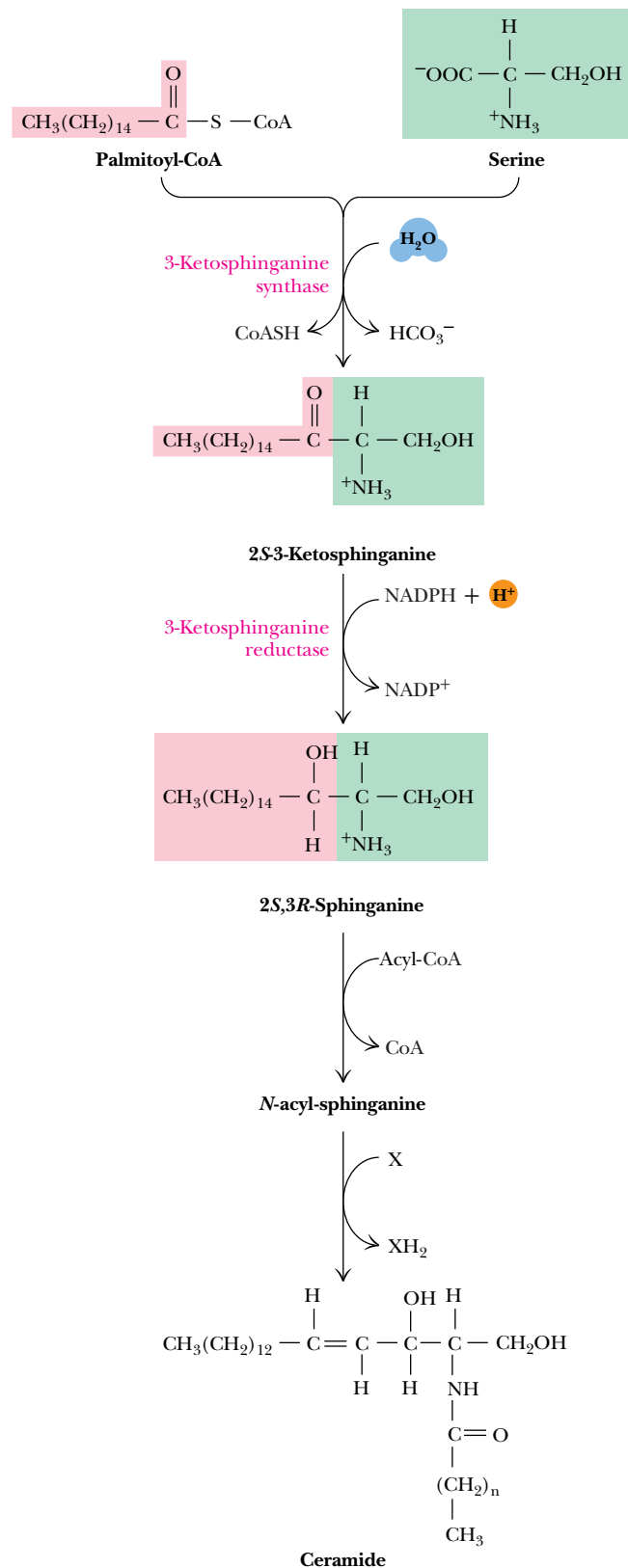
FIGURE 25.25 • Biosynthesis of sphingolipids in animals begins with the 3-ketosphinga-nine synthase reaction, a PLP-dependent condensation of palmitoyl-CoA and serine. Subsequent reduction of the keto group, acylation, and desaturation (via reduction of an electron acceptor, X) form ceramide, the precursor of other sphingolipids.
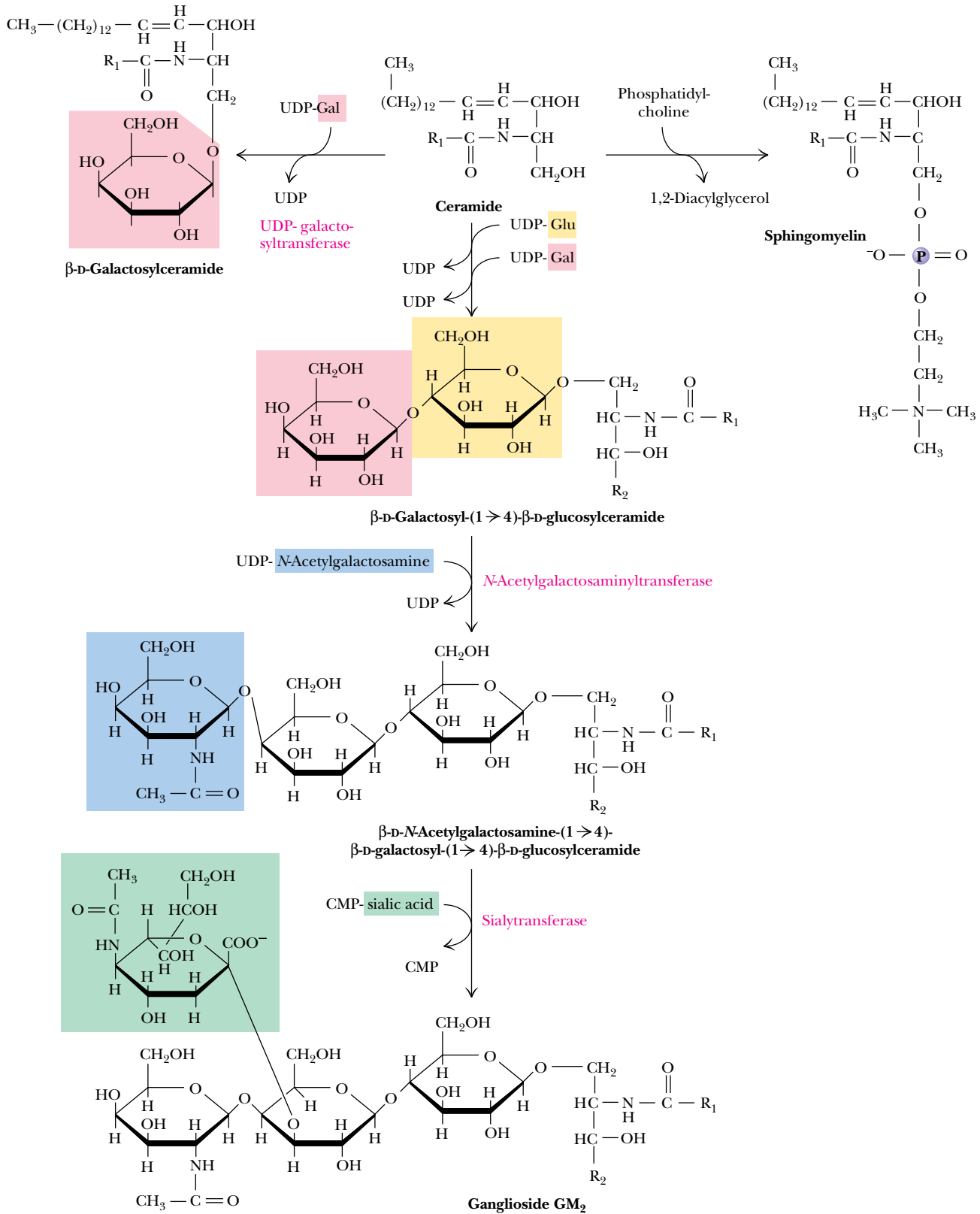
FIGURE 25.26 • Glycosylceramides (such as galactosylceramide), gangliosides, and sphingomyelins are synthesized from ceramide in animals.

Ceramide Is the Precursor for Other Sphingolipids and Cerebrosides

Ceramide is the building block for all other sphingolipids. Sphingomyelin, for example, is produced by transfer of phosphocholine from phosphatidylcholine (Figure 25.26). Glycosylation of ceramide by sugar nucleotides yields **cerebrosides,** such as galactosylceramide, which makes up about 15% of the lipids of myelin sheath structures. Cerebrosides that contain one or more sialic acid (N-acetylneuraminic acid) moieties are called **gangliosides.** Several dozen gangliosides have been characterized, and the general form of the biosynthetic pathway is illustrated for the case of ganglioside GM_2 (Figure 25.26). Sugar units are added to the developing ganglioside from nucleotide derivatives, including UDP-N-acetylglucosamine, UDP-galactose, and UDP-glucose.

25.3 • Eicosanoid Biosynthesis and Function

Eicosanoids, so named because they are all derived from 20-carbon fatty acids, are ubiquitous breakdown products of phospholipids. In response to appropriate stimuli, cells activate the breakdown of selected phospholipids (Figure 25.27). Phospholipase A_2 (Chapter 8) selectively cleaves fatty acids from the C-2 position of phospholipids. Often these are unsaturated fatty acids, among which is arachidonic acid. Arachidonic acid may also be released from phospholipids by the combined actions of phospholipase C (which yields diacylglycerols) and diacylglycerol lipase (which releases fatty acids).

Eicosanoids Are Local Hormones

Animal cells can modify arachidonic acid and other polyunsaturated fatty acids, in processes often involving cyclization and oxygenation, to produce so-called local hormones that (1) exert their effects at very low concentrations and (2) usually act near their sites of synthesis. These substances include the **prostaglandins** (PG) (Figure 25.27) as well as **thromboxanes** (Tx), **leukotrienes,** and other **hydroxyeicosanoic acids.** Thromboxanes, discovered in blood platelets (*thrombo*cytes), are cyclic ethers (TxB_2 is actually a hemiacetal; see Figure 25.27) with a hydroxyl group at C-15.

Prostaglandins Are Formed from Arachidonate by Oxidation and Cyclization

All prostaglandins are cyclopentanoic acids derived from arachidonic acid. The biosynthesis of prostaglandins is initiated by an enzyme associated with the endoplasmic reticulum, called **prostaglandin endoperoxide synthase,** also known as **cyclooxygenase.** The enzyme catalyzes simultaneous oxidation and cyclization of arachidonic acid. The enzyme is viewed as having two distinct activities, cyclooxygenase and peroxidase, as shown in Figure 25.28.

A Variety of Stimuli Trigger Arachidonate Release and Eicosanoid Synthesis

The release of arachidonate and the synthesis or interconversion of eicosanoids can be initiated by a variety of stimuli, including histamine, hormones such as epinephrine and bradykinin, proteases such as thrombin, and even serum albumin. An important mechanism of arachidonate release and eicosanoid syn-
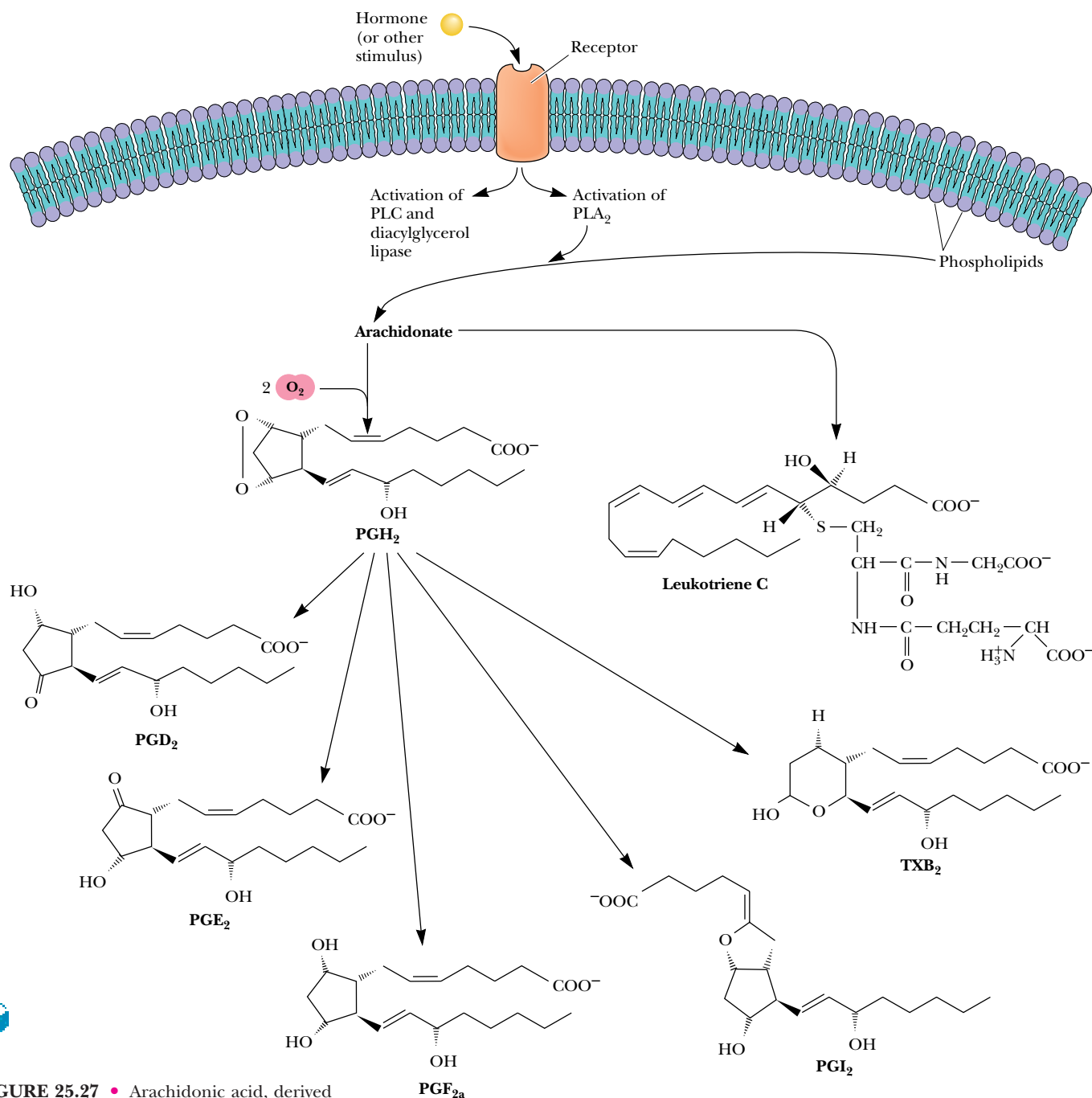
FIGURE 25.27 • Arachidonic acid, derived from breakdown of phospholipids (PL), is the precursor of prostaglandins, thromboxanes, and leukotrienes. The letters used to name the prostaglandins are assigned on the basis of similarities in structure and physical properties. The class denoted PGE, for example, consists of β-hydroxyketones that are soluble in ether, whereas PGF denotes 1,3-diols that are soluble in phosphate buffer. PGA denotes prostaglandins possessing α,β-unsaturated ketones. The number following the letters refers to the number of carbon–carbon double bonds. Thus, PGE_2 contains two double bonds.

thesis involves tissue injury and inflammation. When tissue damage or injury occurs, special inflammatory cells, **monocytes** and **neutrophils,** invade the injured tissue and interact with the resident cells (e.g., smooth muscle cells and fibroblasts). *This interaction typically leads to arachidonate release and eicosanoid synthesis.* Examples of tissue injury in which eicosanoid synthesis has been characterized include heart attack (myocardial infarction), rheumatoid arthritis, and ulcerative colitis.

A DEEPER LOOK

The Discovery of Prostaglandins

The name *prostaglandin* was given to this class of compounds by Ulf von Euler, their discoverer, in Sweden in the 1930s. He extracted fluids containing these components from human semen. Because he thought they originated in the prostate gland, he named them prostaglandins. Actually, they were synthesized in the seminal vesicles, and it is now known that similar substances are synthesized in most animal tissues (both male and female). Von Euler observed that injection of these substances into animals caused smooth muscle contraction and dramatic lowering of blood pressure.

Von Euler (and others) soon found that it is difficult to analyze and characterize these obviously interesting compounds because they are present at extremely low levels. Prostaglandin

$E_{2\alpha}$, or $PGE_{2\alpha}$, is present in human serum at a level of less than 10^{-14} *M!* In addition, they often have half-lives of only 30 seconds to a few minutes, not lasting long enough to be easily identified. Moreover, most animal tissues upon dissection and homogenization rapidly synthesize and degrade a variety of these substances, so the amounts obtained in isolation procedures are extremely sensitive to the methods used and highly variable even when procedures are carefully controlled.

Sune Bergstrom and his colleagues described the first structural determinations of prostaglandins in the late 1950s. In the early 1960s, dramatic advances in laboratory techniques such as NMR spectroscopy and mass spectrometry made further characterization possible.
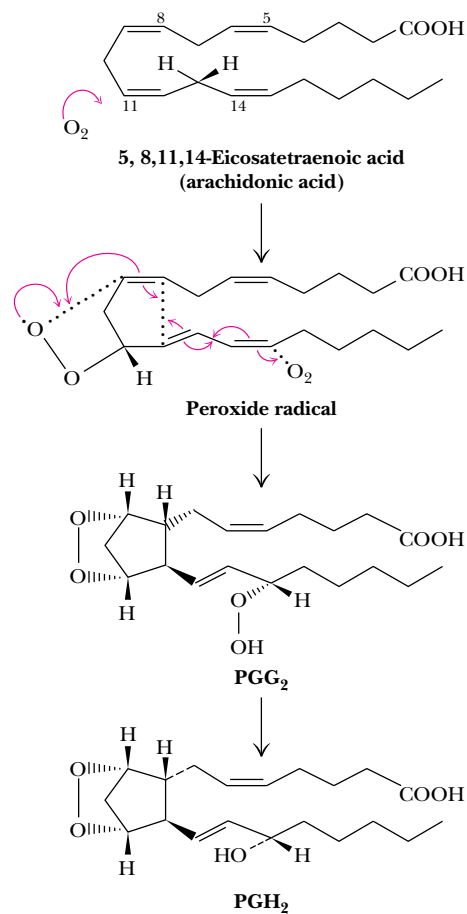

FIGURE 25.28 • Prostaglandin endoperoxide synthase, the enzyme that converts arachidonic acid to prostaglandin PGH_2, possesses two distinct activities: cyclooxygenase (steps 1 and 2) and glutathione (GSSG)–dependent hydroperoxidase (step 3). Cyclooxygenase is the site of action of aspirin and many other analgesic agents.
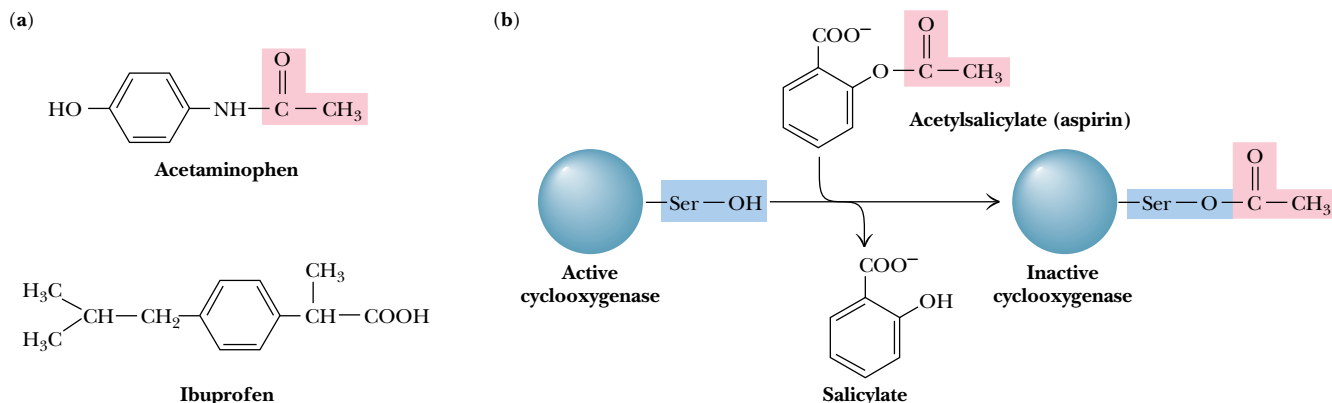
(a)

Acetaminophen

Ibuprofen

(b)

Acetylsalicylate (aspirin)

Active cyclooxygenase

Inactive cyclooxygenase

Salicylate

FIGURE 25.29 • (a) The structures of several common analgesic agents. Acetaminophen is marketed under the tradename Tylenol®. Ibuprofen is sold as Motrin®, Nuprin®, and Advil®. (b) Acetylsalicylate (aspirin) inhibits the cyclooxygenase activity of endoperoxide synthase via acetylation (covalent modification) of Ser[530].

"Take Two Aspirin and . . ." Inhibit Your Prostaglandin Synthesis

In 1971, biochemist John Vane was the first to show that **aspirin** (acetylsalicylate; Figure 25.29) exerts most of its effects by inhibiting the biosynthesis of prostaglandins. Its site of action is prostaglandin endoperoxide synthase. Cyclooxygenase activity is destroyed when aspirin O-acetylates Ser[530] on the enzyme. From this you may begin to infer something about how prostaglandins (and aspirin) function. Prostaglandins are known to enhance inflammation in animal tissues. Aspirin exerts its powerful anti-inflammatory effect by inhibiting this first step in their synthesis. Aspirin does not have any measurable effect on the peroxidase activity of the synthase. Other nonsteroidal anti-inflammatory agents, such as **ibuprofen** (Figure 25.29) and phenylbutazone, inhibit the cyclooxygenase by competing at the active site with arachidonate or with the peroxyacid intermediate (PGG$_2$, Figure 25.28). See A Deeper Look, page 834.

25.4 • Cholesterol Biosynthesis

The most prevalent steroid in animal cells is **cholesterol** (Figure 25.30). Plants contain no cholesterol, but they *do* contain other steroids very similar to cholesterol in structure (see page 256). Cholesterol serves as a crucial component of cell membranes and as a precursor to bile acids (e.g., cholate, glycocholate,
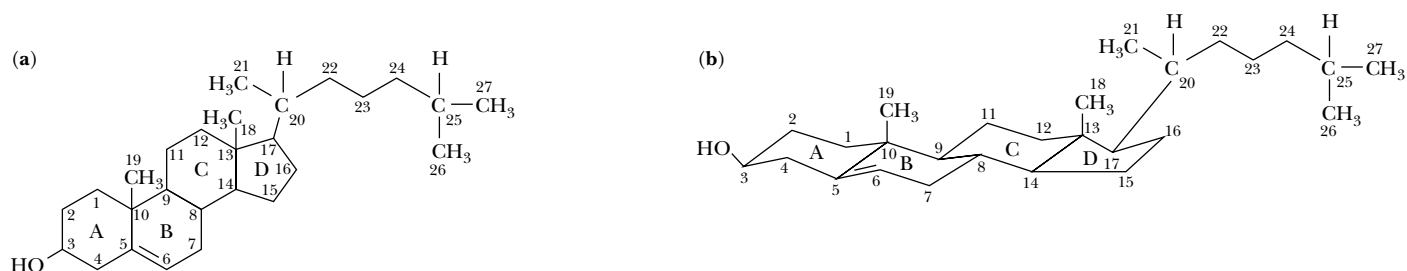
(a)

(b)

FIGURE 25.30 • The structure of cholesterol, drawn (a) in the traditional planar motif and (b) in a form that more accurately describes the conformation of the ring system.

taurocholate) and steroid hormones (e.g., testosterone, estradiol, progesterone). Also, vitamin D_3 is derived from *7-dehydrocholesterol,* the immediate precursor of cholesterol. Liver is the primary site of cholesterol biosynthesis.

Mevalonate Is Synthesized from Acetyl-CoA via HMG-CoA Synthase

The cholesterol biosynthetic pathway begins in the cytosol with the synthesis of mevalonate from acetyl-CoA (Figure 25.31). The first step is the **β-ketothiolase**-catalyzed Claisen condensation of two molecules of acetyl-CoA to form acetoacetyl-CoA. In the next reaction, acetyl-CoA and acetoacetyl-CoA join to form *3-hydroxy-3-methylglutaryl-CoA,* which is abbreviated *HMG-CoA.* The reaction—a second Claisen condensation—is catalyzed by **HMG-CoA synthase.** The third step in the pathway is the rate-limiting step in cholesterol biosynthesis. Here, HMG-CoA undergoes two NADPH-dependent reductions to produce *3R-mevalonate* (Figure 25.32). The reaction is catalyzed by **HMG-CoA reductase,** a 97-kD glycoprotein that traverses the endoplasmic reticulum membrane with its active site facing the cytosol. As the rate-limiting step, HMG-CoA reductase is the principal site of regulation in cholesterol synthesis.
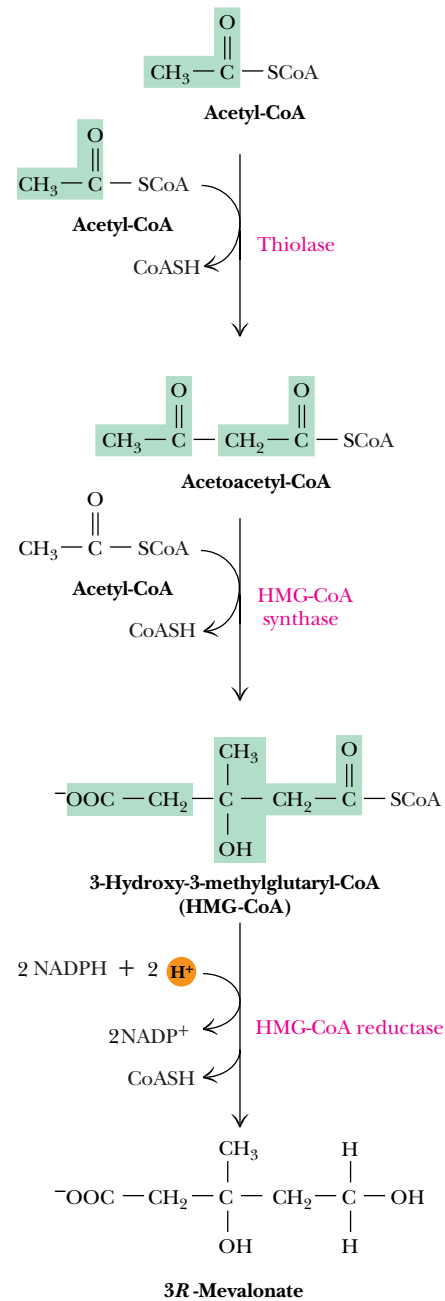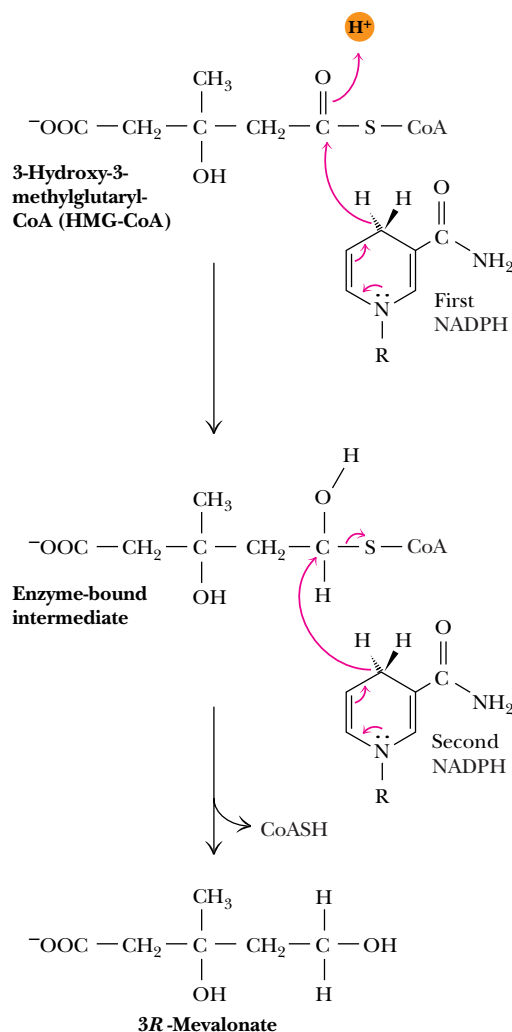

FIGURE 25.31 • The biosynthesis of 3R-mevalonate from acetyl-CoA.

FIGURE 25.32 • A reaction mechanism for HMG-CoA reductase. Two successive NADPH-dependent reductions convert the thioester, HMG-CoA, to a primary alcohol.

The Molecular Basis for the Action of Nonsteroidal Anti-inflammatory Drugs

Prostaglandins are potent mediators of inflammation. The first and committed step in the production of prostaglandins from arachidonic acid is the bis-oxygenation of arachindonate to prostaglandin PGG_2. This is followed by reduction to PGH_2 in a peroxidase reaction. Both these reactions are catalyzed by prostaglandin endoperoxide synthase, also known as PGH_2 synthase or cyclooxygenase, thus abbreviated COX. This enzyme is inhibited by the family of drugs known as nonsteroidal anti-inflammatory drugs, or NSAIDs. Aspirin, ibuprofen, flurbiprofen, and acetaminophen (trade name Tylenol ®) are all NSAIDs.

There are two isoforms of COX in animals: COX-1 (figure a), which carries out normal, physiological production of prostaglandins, and COX-2 (figure b), which is induced by cytokines, mitogens, and endotoxins in inflammatory cells and is responsible for the production of prostaglandins in inflammation.

The enzyme structure shown here is that of residues 33 to 583 of COX-1 from sheep, inactivated by bromoaspirin. These 551 residues comprise three distinct domains. The first of these, residues 33 to 72 (purple), form a small compact module that is similar to epidermal growth factor. The second domain, composed of residues 73 to 116 (yellow), forms a right-handed spiral of four α-helical segments along the base of the protein. These α-helical segments form a membrane-binding motif. The helical segments are amphipathic, with most of the hydrophobic residues (shown in green) facing away from the protein, where they can interact with a lipid bilayer. The third domain of the COX enzyme, the catalytic domain (in blue), is a globular structure that contains both the cyclooxygenase and peroxidase active sites.

The cyclooxygenase active site lies at the end of a long, narrow, hydrophobic tunnel or channel. Three of the α-helices of the membrane-binding domain lie at the entrance to this tunnel. The
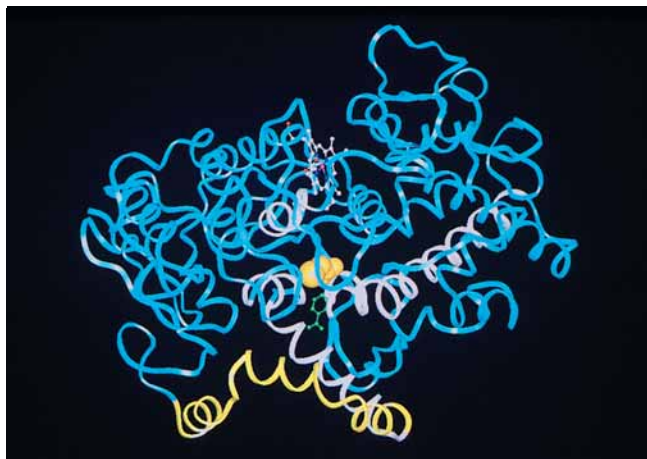
(a)
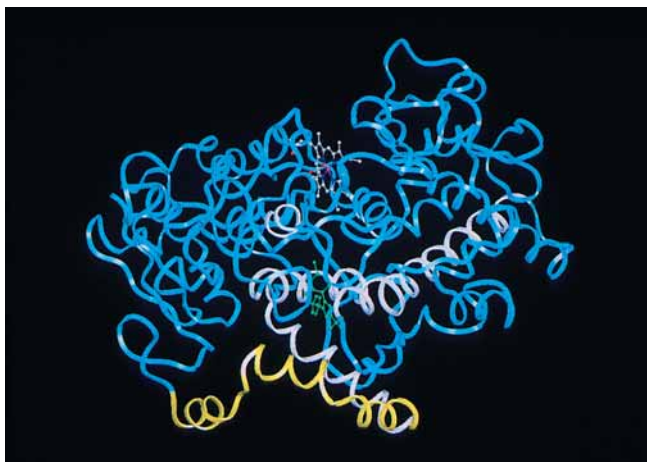
(b)

Three different regulatory mechanisms are involved:

1. Phosphorylation by cAMP-dependent protein kinases inactivates the reductase. This inactivation can be reversed by two specific phosphatases (Figure 25.33).
2. Degradation of HMG-CoA reductase. This enzyme has a half-life of only three hours, and the half-life itself depends on cholesterol levels: high [cholesterol] means a short half-life for HMG-CoA reductase.
3. Gene expression—cholesterol levels control the amount of mRNA. If [cholesterol] is high, levels of mRNA coding for the reductase are reduced. If [cholesterol] is low, more mRNA is made. (Regulation of gene expression is discussed in Chapter 31.)

walls of the tunnel are defined by four α-helices, formed by residues 106 to 123, 325 to 353, 379 to 384, and 520 to 535 (shown in orange).

In this bromoaspirin-inactivated structure, Ser[530], which lies along the wall of the tunnel, is bromoacetylated, and a molecule of salicylate is also bound in the tunnel. Deep in the tunnel, at the far end, lies Tyr[385], a catalytically important residue. Heme-dependent peroxidase activity is implicated in the formation of a proposed Tyr[385] radical, which is required for cyclooxygenase activity. Aspirin and other NSAIDs block the synthesis of prostaglandins by filling and blocking the tunnel, preventing the migration of arachidonic acid to Tyr[385] in the active site at the back of the tunnel.

There are thought to be at least four different mechanisms of action for NSAIDs. Aspirin (and also bromoaspirin) covalently modifies a residue in the tunnel, thus irreversibly inactivating both COX-1 and COX-2. Ibuprofen acts instead by competing in a reversible fashion for the substrate-binding site in the tunnel.

Flurbiprofen and indomethacin, which comprise the third class of inhibitors, cause a slow, time-dependent inhibition of COX-1 and COX-2, apparently via formation of a salt bridge between a carboxylate on the drug and Arg[120], which lies in the tunnel.

The drug SC-558 acts by a fourth mechanism, specifically inhibiting COX-2. It is a weak competitive inhibitor of COX-1 but inhibits COX-2 in a slow, time-dependent process. Specific COX-2 inhibitors will likely be the drugs of the future because they selectively block the inflammation mediated by COX-2, without the potential for stomach lesions and renal toxicity that arise from COX-1 inhibition.
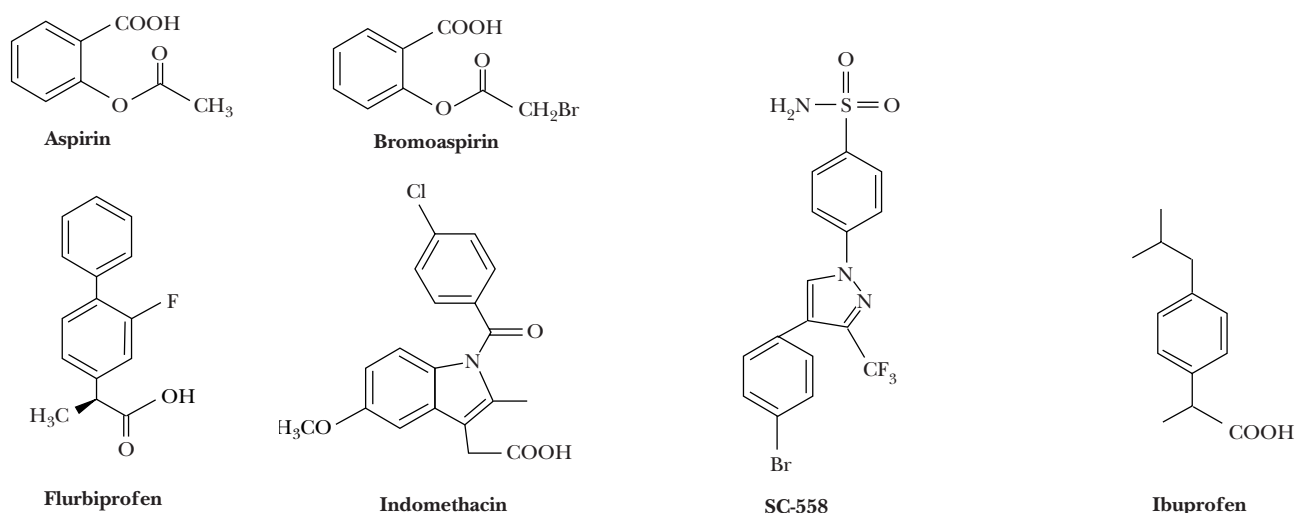
A Thiolase Brainteaser

If acetate units can be condensed by the thiolase reaction to yield acetoacetate in the first step of cholesterol synthesis, why couldn't this same reaction also be used in fatty acid synthesis, avoiding all the complexity of the fatty acyl synthase? The answer is that the thiolase reaction is more or less reversible but slightly favors the cleavage reaction. In the cholesterol synthesis pathway, subsequent reactions, including HMG-CoA reductase and the following kinase reactions, pull the thiolase-catalyzed condensation forward. However, in the case of fatty acid synthesis, a succession of eight thiolase condensations would be distinctly unfavorable from an energetic perspective. Given the necessity of repeated reactions in fatty acid synthesis, it makes better energetic sense to use a reaction that is favorable in the desired direction.
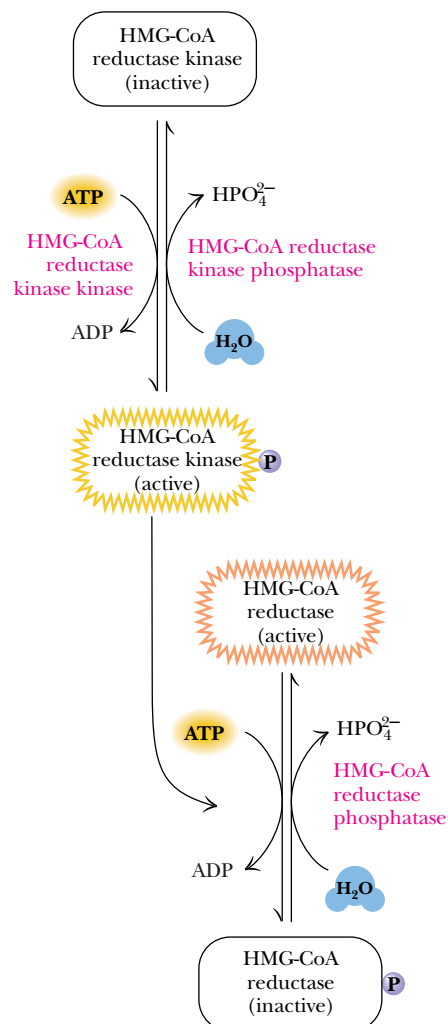
FIGURE 25.33 • HMG-CoA reductase activity is modulated by a cycle of phosphorylation and dephosphorylation.

Squalene Is Synthesized from Mevalonate

The biosynthesis of squalene involves conversion of mevalonate to two key 5-carbon intermediates, *isopentenyl pyrophosphate* and *dimethylallyl pyrophosphate,* which join to yield *farnesyl pyrophosphate* and then squalene. A series of four reactions converts mevalonate to isopentenyl pyrophosphate and then to dimethylallyl pyrophosphate (Figure 25.34). The first three steps each consume an ATP, two for the purpose of forming a pyrophosphate at the 5-position and the third to drive the decarboxylation and double bond formation in the third step. **Pyrophosphomevalonate decarboxylase** phosphorylates the 3-hydroxyl group, and this is followed by *trans* elimination of the phosphate and carboxyl groups to form the double bond in isopentenyl pyrophosphate. Isomerization of the double bond yields the dimethylallyl pyrophosphate. Condensation of these two 5-carbon intermediates produces *geranyl pyrophosphate;* addition of another 5-carbon isopentenyl group gives farnesyl pyrophosphate. Both steps in the production of farnesyl pyrophosphate occur with release of pyrophosphate, hydrolysis of which drives these reactions forward. Note too that the linkage of isoprene units to form farnesyl pyrophosphate occurs in a head-to-
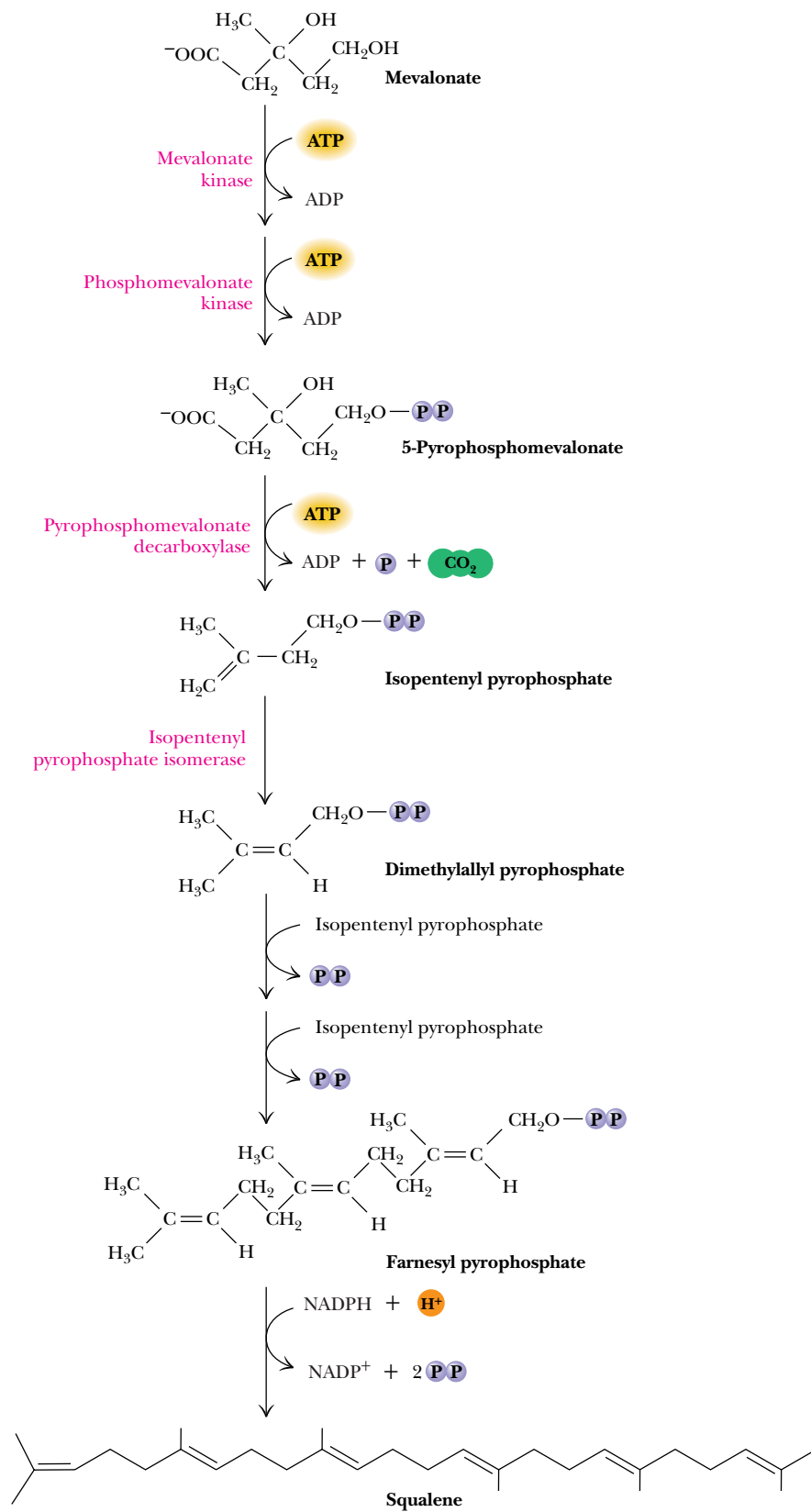
**FIGURE 25.34** • The conversion of mevalonate to squalene.

The Long Search for the Route of Cholesterol Biosynthesis

Heilbron, Kamm, and Owens suggested as early as 1926 that squalene is a precursor of cholesterol. That same year, H. J. Channon demonstrated that animals fed squalene from shark oil produced more cholesterol in their tissues. Bloch and Rittenberg showed in the 1940s that a significant amount of the carbon in the tetracyclic moiety and in the aliphatic side chain of cholesterol was derived from acetate. In 1934, Sir Robert Robinson suggested a scheme for the cyclization of squalene to form cholesterol before the biosynthetic link between acetate and squalene was understood. Squalene is actually a polymer of isoprene units, and Bonner and Arreguin suggested in 1949 that three acetate units could join to form 5-carbon *isoprene* units (see figure, part a).

In 1952, Konrad Bloch and Robert Langdon showed conclusively that labeled squalene is synthesized rapidly from labeled acetate and also that cholesterol is derived from squalene. Langdon, a graduate student of Bloch's, performed the critical experiments in Bloch's laboratory at the University of Chicago, while Bloch spent the summer in Bermuda attempting to demonstrate that radioactively labeled squalene would be converted to cholesterol in shark livers. As Bloch himself admitted, "All I was able to learn was that sharks of manageable length are very difficult to catch and their oily livers impossible to slice" (Bloch, 1987).

In 1953, Bloch, together with the eminent organic chemist R. B. Woodward, proposed a new scheme (see figure, part b) for the cyclization of squalene. (Together with Fyodor Lynen, Bloch received the Nobel Prize in medicine or physiology in 1964 for his work.) The picture was nearly complete, but one crucial question remained: How could isoprene be the intermediate in the

transformation of acetate into squalene? In 1956, Karl Folkers and his colleagues at Merck, Sharpe and Dohme isolated mevalonic acid and also showed that mevalonate was the precursor of isoprene units. The search for the remaining details (described in the text) made the biosynthesis of cholesterol one of the most enduring and challenging bioorganic problems of the forties, fifties, and sixties. Even today, several of the enzyme mechanisms remain poorly understood.

(b)

Squalene

Lanosterol

(Many steps)

Cholesterol

(a)
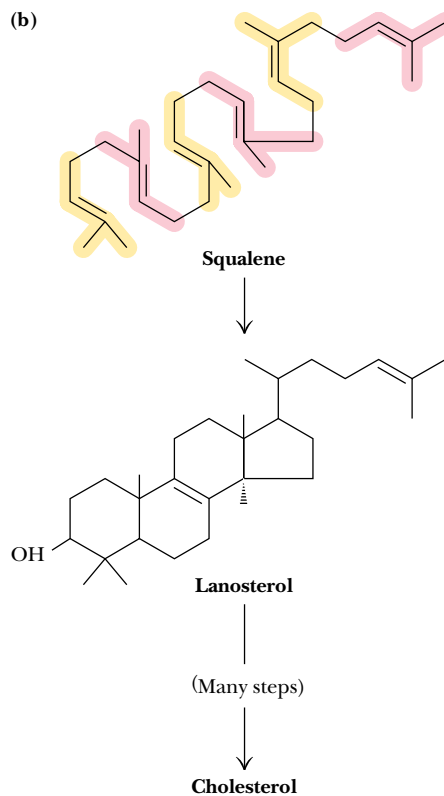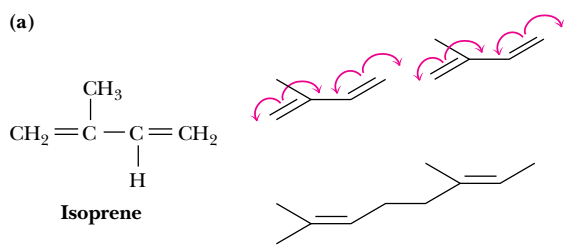
Isoprene

(a) An isoprene unit and a scheme for head-to-tail linking of isoprene units. (b) The cyclization of squalene to form lanosterol, as proposed by Bloch and Woodward.

tail fashion. This is the general rule in biosynthesis of molecules involving isoprene linkages. The next step—the joining of two farnesyl pyrophosphates to produce squalene—is a "tail-to-tail" condensation and represents an important exception to the general rule.

Squalene monooxygenase, an enzyme bound to the endoplasmic reticulum, converts squalene to *squalene-2,3-epoxide* (Figure 25.35). This reaction employs FAD and NADPH as coenzymes and requires O_2 as well as a cytosolic protein called **soluble protein activator.** A second ER membrane enzyme, **2,3-oxidosqualene lanosterol cyclase,** catalyzes the second reaction, which involves a succession of 1,2 shifts of hydride ions and methyl groups.
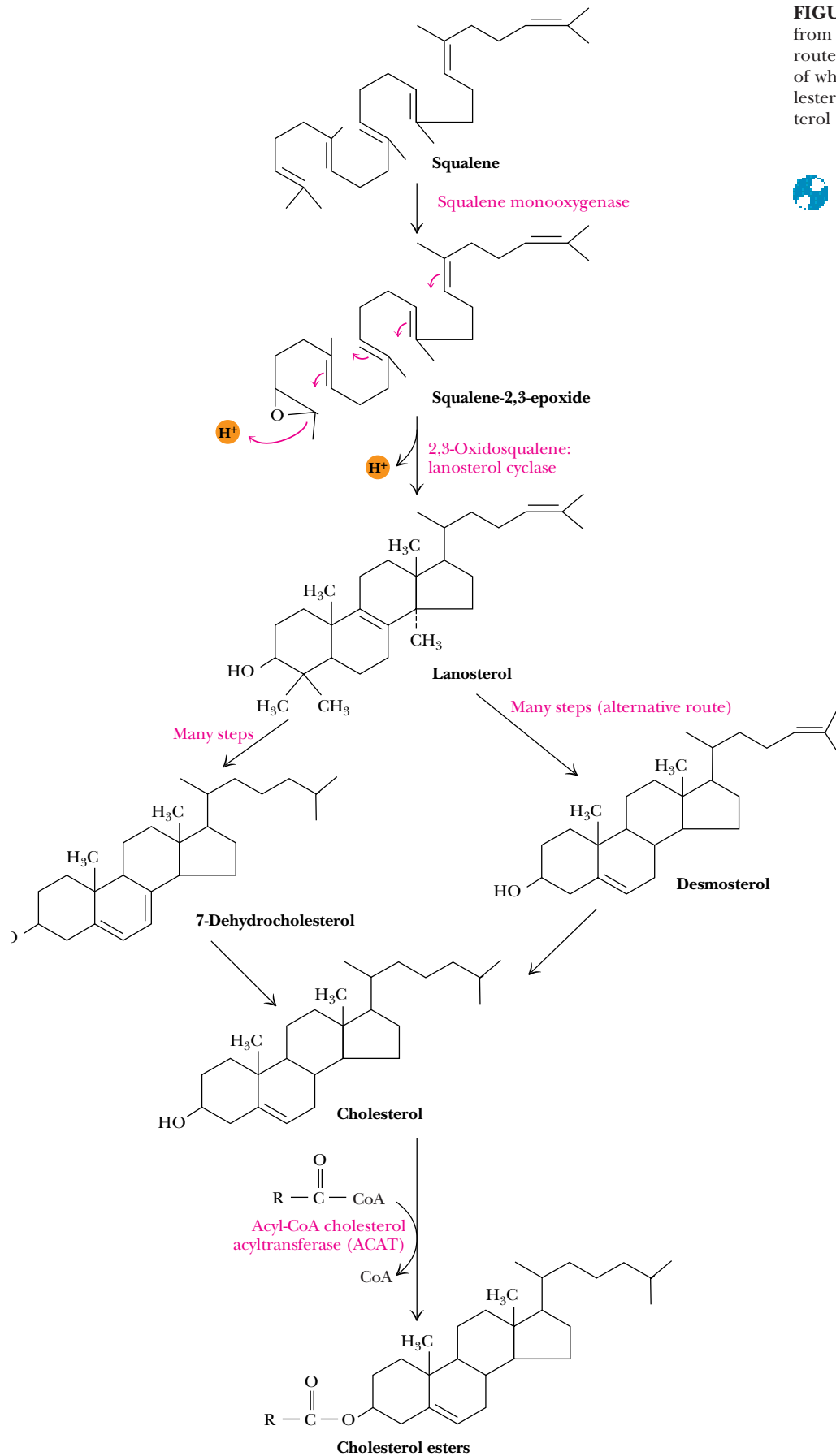
FIGURE 25.35 • Cholesterol is synthesized from squalene via lanosterol. The primary route from lanosterol involves 20 steps, the last of which converts 7-dehydrocholesterol to cholesterol. An alternative route produces desmosterol as the penultimate intermediate.
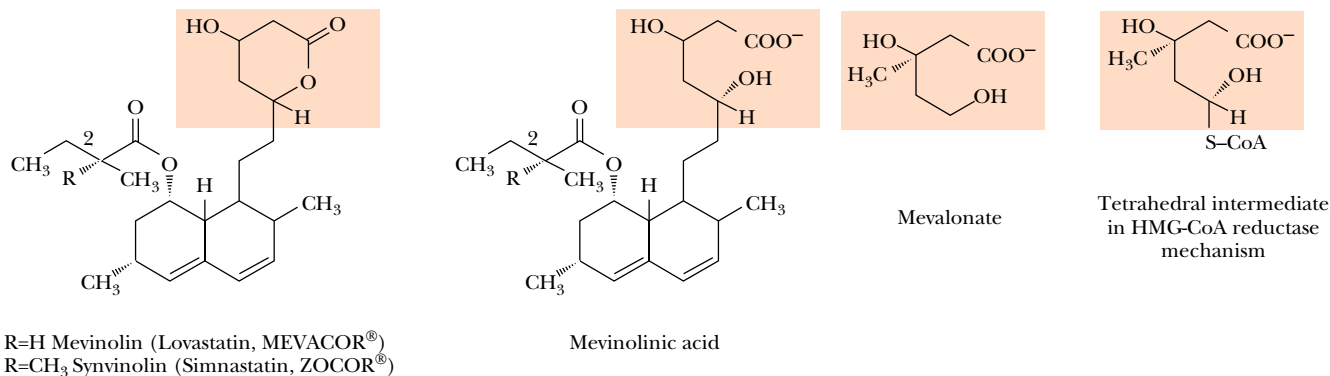
ℋ U M A N B I O C H E M I S T R Y

Lovastatin Lowers Serum Cholesterol Levels

Chemists and biochemists have long sought a means of reducing serum cholesterol levels to reduce the risk of heart attack and cardiovascular disease. Because HMG-CoA reductase is the rate-limiting step in cholesterol biosynthesis, this enzyme is a likely drug target. **Mevinolin,** also known as **lovastatin** (see figure), was isolated from a strain of *Aspergillus terreus* and developed at Merck, Sharpe and Dohme for this purpose. It is now a widely prescribed cholesterol-lowering drug. Dramatic reductions of serum cholesterol are observed at doses of 20 to 80 mg per day.

Lovastatin is administered as an inactive lactone. After oral ingestion, it is hydrolyzed to the active **mevinolinic acid,** a competitive inhibitor of the reductase with a K_I of 0.6 nM. Mevinolinic acid is thought to behave as a transition-state analog (Chapter 16) of the tetrahedral intermediate formed in the HMG-CoA reductase reaction (see figure).

Derivatives of lovastatin have been found to be even more potent in cholesterol-lowering trials. **Synvinolin** lowers serum cholesterol levels at much lower doses than lovastatin.

1 R=H Mevinolin (Lovastatin, MEVACOR®)
2 R=CH₃ Synvinolin (Simnastatin, ZOCOR®)

Mevinolinic acid

Mevalonate

Tetrahedral intermediate in HMG-CoA reductase mechanism

The structures of (inactive) lovastatin, (active) mevinolinic acid, mevalonate, and synvinolin.

Conversion of Lanosterol to Cholesterol Requires 20 Additional Steps

Although lanosterol may appear similar to cholesterol in structure, another *20 steps* are required to convert lanosterol to cholesterol (Figure 25.35). The enzymes responsible for this are all associated with the endoplasmic reticulum. The primary pathway involves *7-dehydrocholesterol* as the penultimate intermediate. An alternative pathway, also composed of many steps, produces the intermediate *desmosterol*. Reduction of the double bond at C-24 yields cholesterol. Cholesterol esters—a principal form of circulating cholesterol—are synthesized by **acyl-CoA:cholesterol acyltransferases (ACAT)** on the cytoplasmic face of the endoplasmic reticulum.

25.5 • Transport of Many Lipids Occurs via Lipoprotein Complexes

When most lipids circulate in the body, they do so in the form of **lipoprotein complexes.** Simple, unesterified fatty acids are merely bound to serum albumin and other proteins in blood plasma, but phospholipids, triacylglycerols, cholesterol, and cholesterol esters are all transported in the form of lipoproteins. At various sites in the body, lipoproteins interact with specific receptors and enzymes that transfer or modify their lipid cargoes. It is now customary to classify lipoproteins according to their densities (Table 25.1). The densities are

Table 25.1

Composition and Properties of Human Lipoproteins

Lipoprotein Class	Density (g/mL)	Diameter (nm)	Composition (% dry weight)			
			Protein	Cholesterol	Phospholipid	Triacylglycerol
HDL	1.063–1.21	5–15	33	30	29	8
LDL	1.019–1.063	18–28	25	50	21	4
IDL	1.006–1.019	25–50	18	29	22	31
VLDL	0.95–1.006	30–80	10	22	18	50
Chylomicrons	<0.95	100–500	1–2	8	7	84

Adapted from Brown, M., and Goldstein, J., 1987. In Braunwald, E., et al., eds., *Harrison's Principles of Internal Medicine,* 11th ed. New York: McGraw-Hill; and Vance, D., and Vance, J., eds., 1985. *Biochemistry of Lipids and Membranes.* Menlo Park, CA: Benjamin/Cummings.

related to the relative amounts of lipid and protein in the complexes. Because most proteins have densities of about 1.3 to 1.4 g/mL, and lipid aggregates usually possess densities of about 0.8 g/mL, the more protein and the less lipid in a complex, the denser the lipoprotein. Thus, there are **high-density lipoproteins** (HDL), **low-density lipoproteins** (LDL), **intermediate-density lipoproteins** (IDL), **very low density lipoproteins** (VLDL), and also **chylomicrons.** Chylomicrons have the lowest protein-to-lipid ratio and thus are the lowest-density lipoproteins. They are also the largest.

The Structure and Synthesis of the Lipoproteins

HDL and VLDL are assembled primarily in the endoplasmic reticulum of the liver (with smaller amounts produced in the intestine), whereas chylomicrons form in the intestine. LDL is not synthesized directly, but is made from VLDL. LDL appears to be the major circulatory complex for cholesterol and cholesterol esters. The primary task of chylomicrons is to transport triacylglycerols. Despite all this, it is extremely important to note that each of these lipoprotein classes contains some of each type of lipid. The relative amounts of HDL and LDL are important in the disposition of cholesterol in the body and in the development of arterial plaques (Figure 25.36). The structures of the various

FIGURE 25.36 • Photograph of an arterial plaque. (*Science Photo Library/Photo Researchers, Inc.*)

lipoproteins are approximately similar, and they consist of a core of mobile triacylglycerols or cholesterol esters surrounded by a single layer of phospholipid, into which is inserted a mixture of cholesterol and proteins (Figure 25.37). Note that the phospholipids are oriented with their polar head groups facing outward to interact with solvent water, and that the phospholipids thus shield the hydrophobic lipids inside from the solvent water outside. The proteins also function as recognition sites for the various lipoprotein receptors throughout the body. A number of different apoproteins have been identified in lipoproteins (Table 25.2), and others may exist as well. The apoproteins are abundant in hydrophobic amino acid residues, as is appropriate for interactions with lipids. A **cholesterol ester transfer protein** also associates with lipoproteins.

Lipoproteins in Circulation Are Progressively Degraded by Lipoprotein Lipase

The livers and intestines of animals are the primary sources of circulating lipids. Chylomicrons carry triacylglycerol and cholesterol esters from the intestines to other tissues, and VLDLs carry lipid from liver, as shown in Figure 25.38. At

(a)

(b)
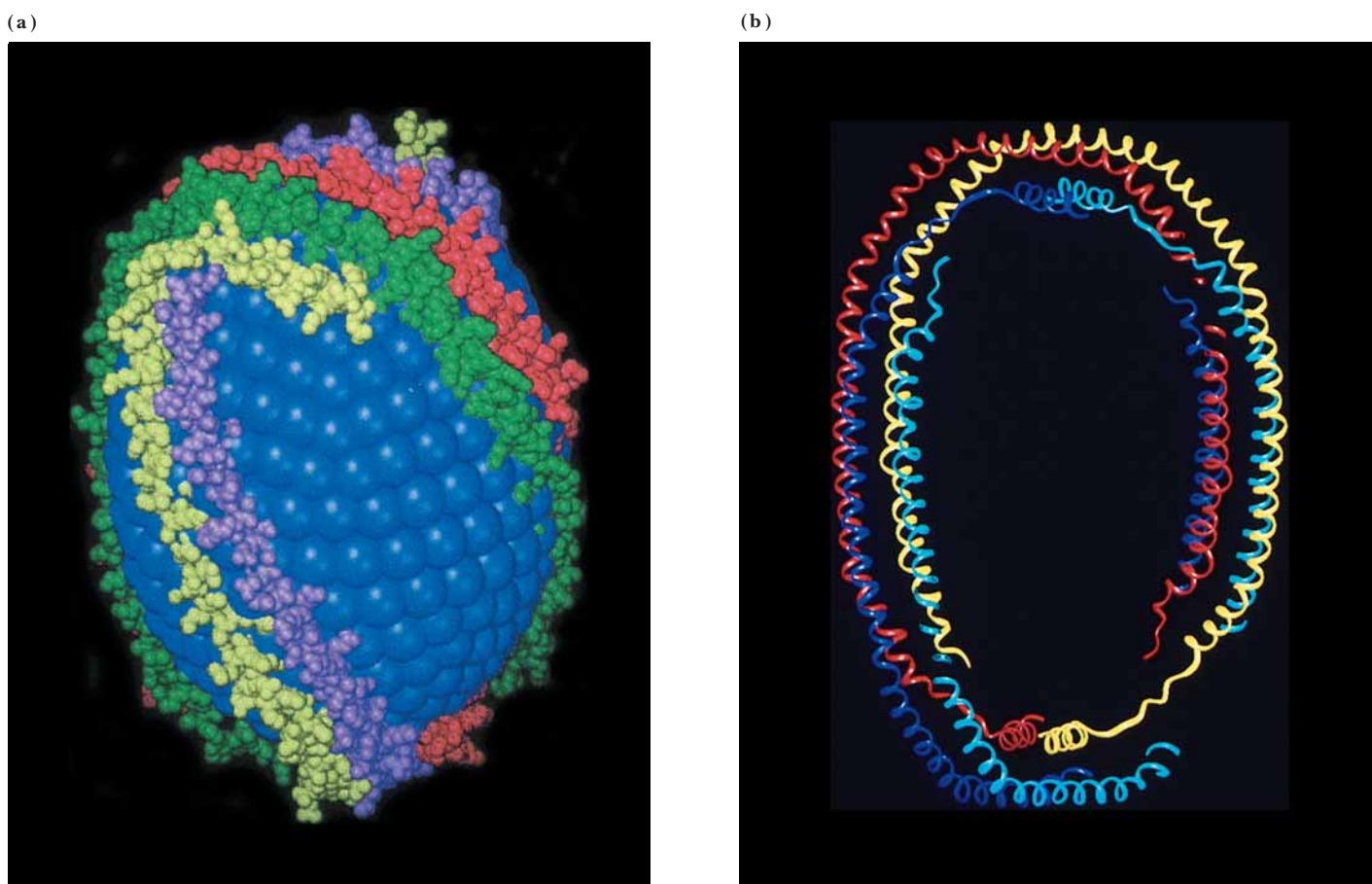
FIGURE 25.37 • A model for the structure of a typical lipoprotein. (a) A core of cholesterol and cholesteryl esters is surrounded by a phospholipid (monolayer) membrane. Apolipoprotein A-I is modeled here as a long amphipathic α-helix, with the nonpolar face of the helix embedded in the hydrophobic core of the lipid particle and the polar face of the helix exposed to solvent. (b) A ribbon diagram of apolipoprotein A-I. (*Adapted from Borhani, D. W., Rogers, D. P., Engler, J. A., and Brouillette, C. G., 1997. Crystal structure of truncated human apolipoprotein A-I suggests a lipid-bound conformation.* Proceedings of the National Academy of Sciences **94:**12291–12296.)

Table 25.2

Apoproteins of Human Lipoproteins

Apoprotein	M_r	Concentration in Plasma (mg/100 mL)	Distribution
A-1	28,300	90–120	Principal protein in HDL
A-2	8,700	30–50	Occurs as dimer mainly in HDL
B-48	240,000	<5	Found only in chylomicrons
B100	500,000	80–100	Principal protein in LDL
C-1	7,000	4–7	Found in chylomicrons, VLDL, HDL
C-2	8,800	3–8	Found in chylomicrons, VLDL, HDL
C-3	8,800	8–15	Found in chylomicrons, VLDL, IDL, HDL
D	32,500	8–10	Found in HDL
E	34,100	3–6	Found in chylomicrons, VLDL, IDL, HDL

Adapted from Brown, M., and Goldstein, J., 1987. In Braunwald, E., et al., eds., *Harrison's Principles of Internal Medicine,* 11th ed. New York: McGraw-Hill; and Vance, D., and Vance, J., eds., 1985. *Biochemistry of Lipids and Membranes,* Menlo Park, CA: Benjamin/Cummings.
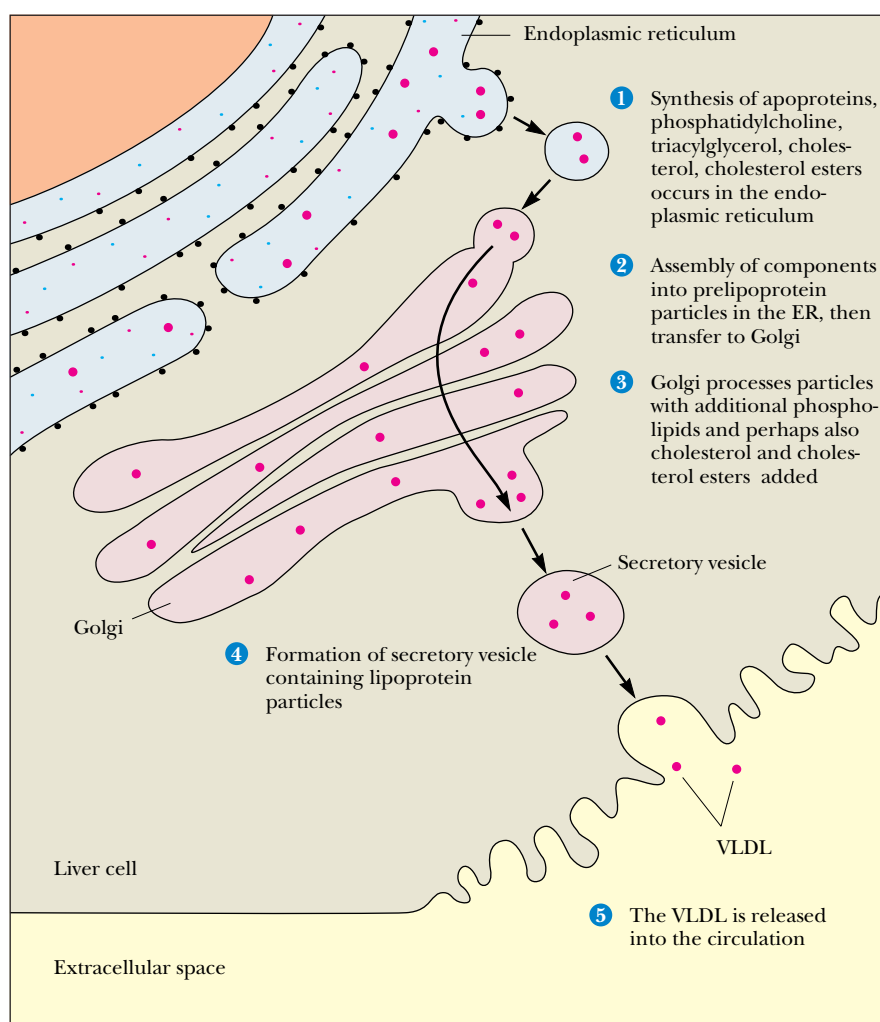

FIGURE 25.38 • Lipoprotein components are synthesized predominantly in the ER of liver cells. Following assembly of lipoprotein particles (*red dots*) in the ER and processing in the Golgi, lipoproteins are packaged in secretory vesicles for export from the cell (via exocytosis) and released into the circulatory system.

Endoplasmic reticulum

❶ Synthesis of apoproteins, phosphatidylcholine, triacylglycerol, cholesterol, cholesterol esters occurs in the endoplasmic reticulum

❷ Assembly of components into prelipoprotein particles in the ER, then transfer to Golgi

❸ Golgi processes particles with additional phospholipids and perhaps also cholesterol and cholesterol esters added

Secretory vesicle

Golgi

❹ Formation of secretory vesicle containing lipoprotein particles

VLDL

Liver cell

❺ The VLDL is released into the circulation
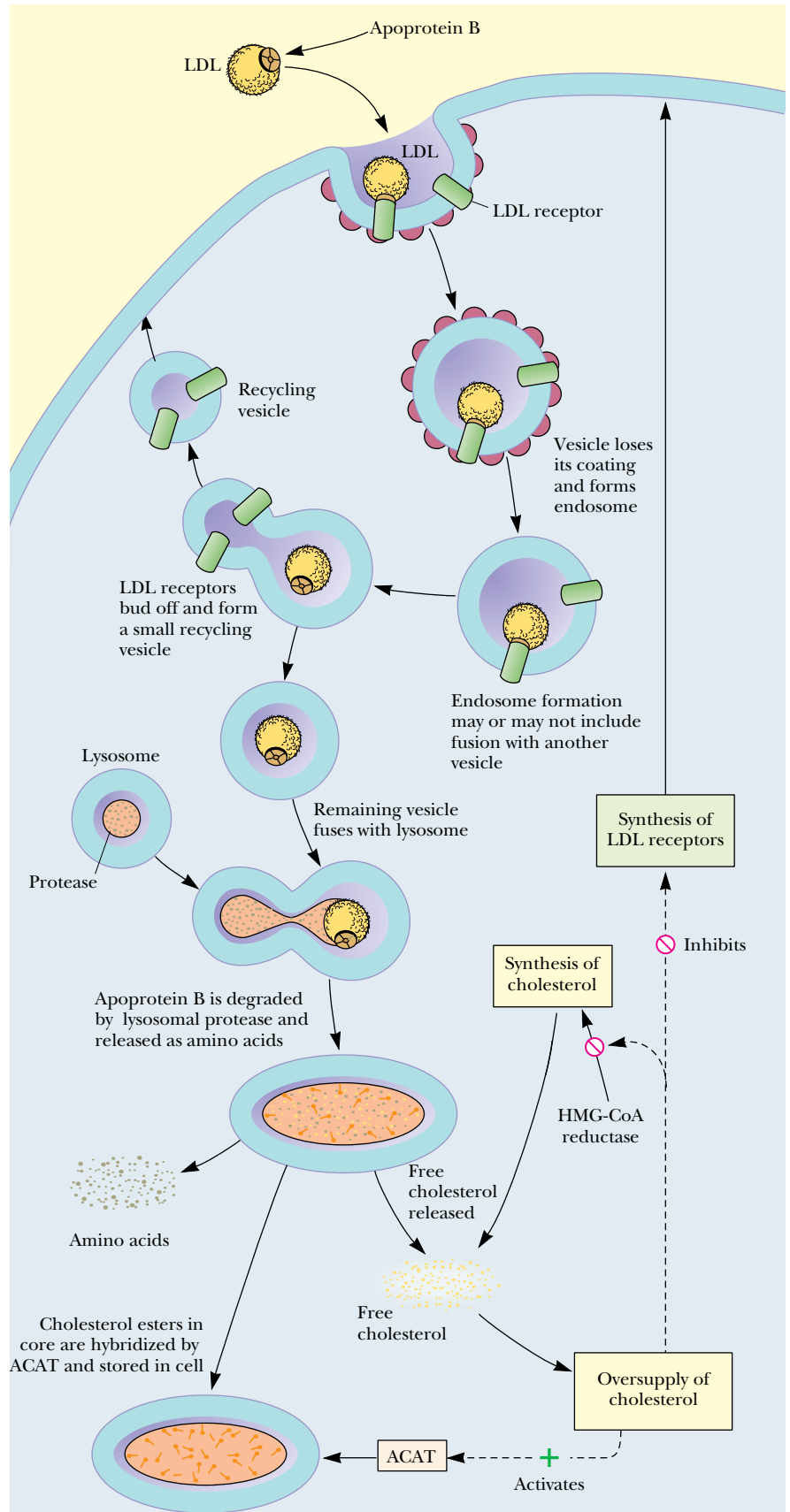
Extracellular space

FIGURE 25.39 • Endocytosis and degradation of lipoprotein particles. (ACAT is acyl-CoA cholesterol acyltransferase.)

various target sites, particularly in the capillaries of muscle and adipose cells, these particles are degraded by **lipoprotein lipase,** which hydrolyzes triacylglycerols. Lipase action causes progressive loss of triacylglycerol (and apoprotein) and makes the lipoproteins smaller. This process gradually converts VLDL particles to IDL and then LDL particles, which are either returned to the liver for reprocessing or redirected to adipose tissues and adrenal glands. Every 24 hours, nearly half of all circulating LDL is removed from circulation in this way. The LDL binds to specific LDL receptors, which cluster in domains of the plasma membrane known as **coated pits** (discussed in subsequent paragraphs). These domains eventually invaginate to form **coated vesicles** (Figure 25.39). Within the cell, these vesicles fuse with lysosomes, and the LDLs are degraded by **lysosomal acid lipases.**

High-density lipoproteins (HDL) have much longer life spans in the body (5 to 6 days) than other lipoproteins. Newly formed HDL contains virtually no cholesterol ester. However, over time, cholesterol esters are accumulated through the action of **lecithin:cholesterol acyltransferase** (LCAT), a 59-kD glycoprotein associated with HDLs. Another associated protein, *cholesterol ester transfer protein,* transfers some of these esters to VLDL and LDL. Alternatively, HDLs function to return cholesterol and cholesterol esters to the liver. This latter process apparently explains the correlation between high HDL levels and reduced risk of cardiovascular disease. (High LDL levels, on the other hand, are correlated with an *increased* risk of coronary artery and cardiovascular disease.)

Structure of the LDL Receptor

The LDL receptor in plasma membranes (Figure 25.40) consists of 839 amino acid residues and is composed of five domains. These domains include an LDL-binding domain of 292 residues, a segment of about 350 to 400 residues containing N-linked oligosaccharides, a 58-residue segment of O-linked oligosaccharides, a 22-residue membrane-spanning segment, and a 50-residue segment extending into the cytosol. The clustering of receptors prior to the formation of coated vesicles requires the presence of this cytosolic segment.

Defects in Lipoprotein Metabolism Can Lead to Elevated Serum Cholesterol

The mechanism of LDL metabolism and the various defects that can occur therein have been studied extensively by Michael Brown and Joseph Goldstein, who received the Nobel Prize in medicine or physiology in 1985. **Familial hypercholesterolemia** is the term given to a variety of inherited metabolic defects that lead to greatly elevated levels of serum cholesterol—much of it in the form of LDL particles. The general genetic defect responsible for familial hypercholesterolemia is the absence or dysfunction of LDL receptors in the body. Only about half the normal level of LDL receptors is found in heterozygous individuals (persons carrying one normal gene and one defective gene). Homozygotes (with two copies of the defective gene) have few if any functional LDL receptors. In such cases, LDLs (and cholesterol) cannot be absorbed, and plasma levels of LDL (and cholesterol) are very high. Typical heterozygotes display serum cholesterol levels of 300 to 400 mg/dL, but homozygotes carry serum cholesterol levels of 600 to 800 mg/dL or even higher. There are two possible causes of an absence of LDL receptors. Either receptor synthesis does not occur at all, or the newly synthesized protein does not successfully reach the plasma membrane, due to faulty processing in the Golgi or faulty transport
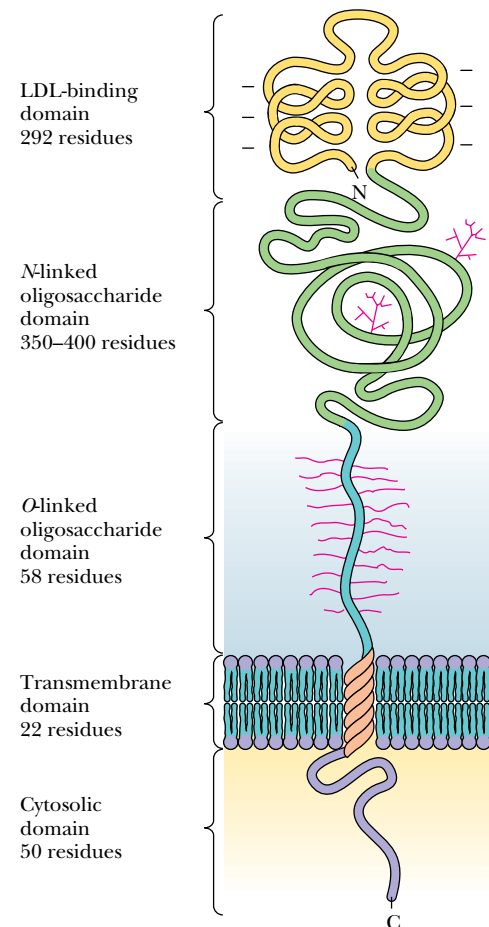
LDL-binding domain
292 residues

N-linked oligosaccharide domain
350–400 residues

O-linked oligosaccharide domain
58 residues

Transmembrane domain
22 residues

Cytosolic domain
50 residues

FIGURE 25.40 • The structure of the LDL receptor. The amino-terminal binding domain is responsible for recognition and binding of LDL apoprotein. The O-linked oligosaccharide-rich domain may act as a molecular spacer, raising the binding domain above the glycocalyx. The cytosolic domain is required for aggregation of LDL receptors during endocytosis.

to the plasma membrane. Even when LDL receptors are made and reach the plasma membrane, they may fail to function for two reasons. They may be unable to form clusters competent in coated pit formation because of folding or sequence anomalies in the carboxy-terminal domain, or they may be unable to bind LDL because of sequence or folding anomalies in the LDL-binding domain.

25.6 • Biosynthesis of Bile Acids

Bile acids, which exist mainly as **bile salts,** are polar carboxylic acid derivatives of cholesterol that are important in the digestion of food, especially the solubilization of ingested fats. The Na$^+$ and K$^+$ salts of *glycocholic acid* and *taurocholic acid* are the principal bile salts (Figure 25.41). Glycocholate and taurocholate are conjugates of *cholic acid* with glycine and taurine, respectively.
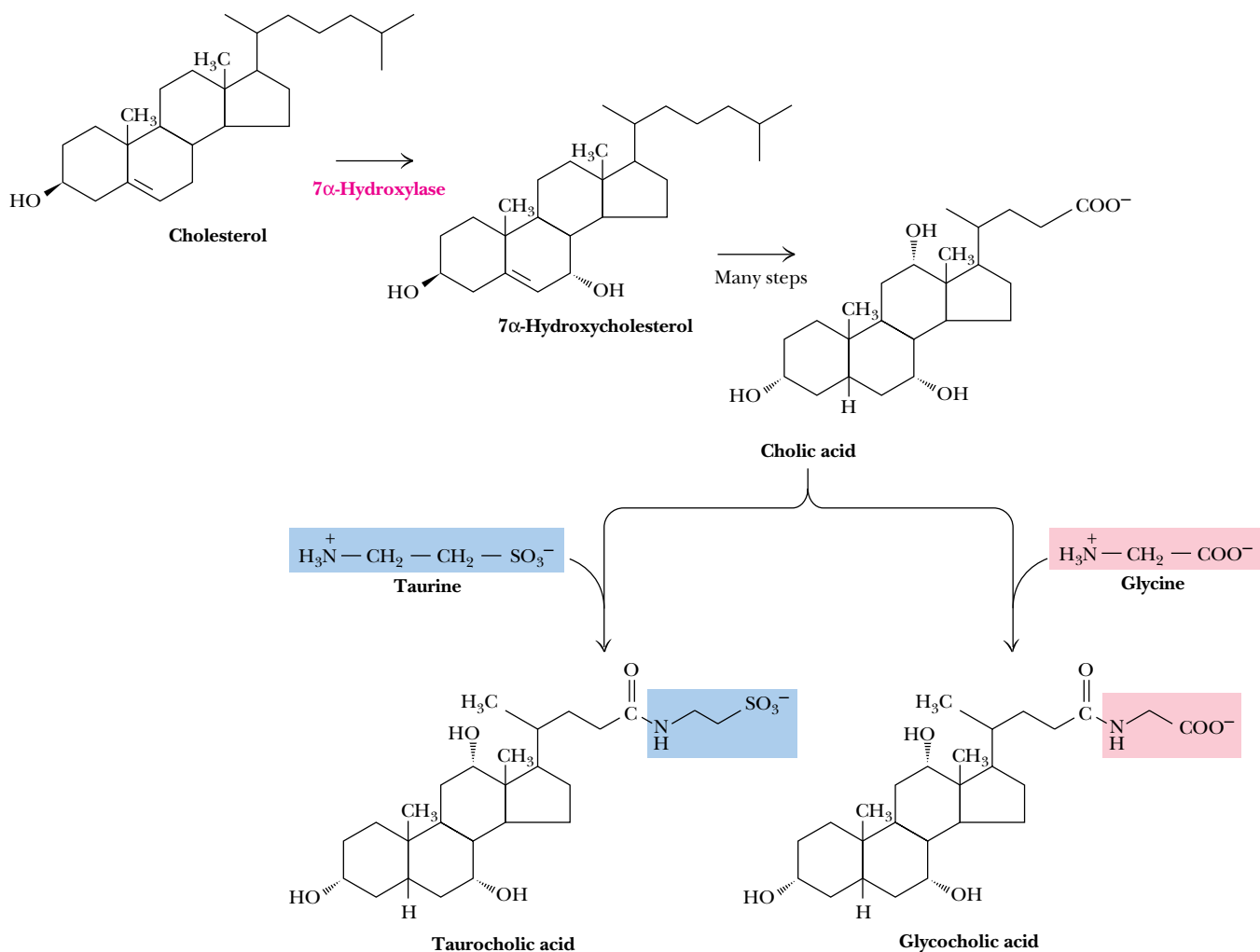

FIGURE 25.41 • Cholic acid, a bile salt, is synthesized from cholesterol via 7α-hydroxycholesterol. Conjugation with taurine or glycine produces taurocholic acid and glycocholic acid, respectively. Taurocholate and glycocholate are freely water-soluble and are highly effective detergents.
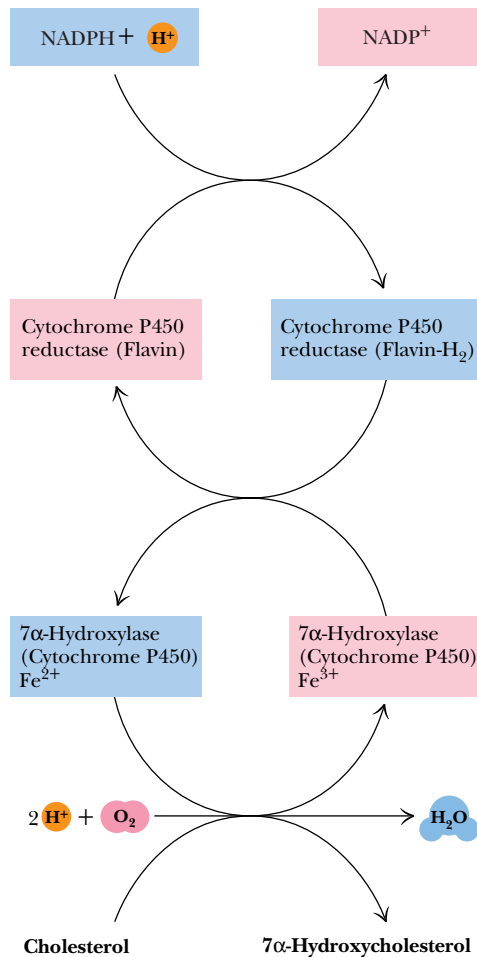
FIGURE 25.42 • The mixed-function oxidase activity of 7α-hydroxylase.

Because they contain both nonpolar and polar domains, these bile salt conjugates are highly effective as detergents. These substances are made in the liver, stored in the gallbladder, and secreted as needed into the intestines.

The formation of bile salts represents the major pathway for cholesterol degradation. The first step involves hydroxylation at C-7 (Figure 25.41). **7α-Hydroxylase,** which catalyzes the reaction, is a mixed-function oxidase involving *cytochrome P450*. **Mixed-function oxidases** use O_2 as substrate. One oxygen atom goes to hydroxylate the substrate, while the other is reduced to water (Figure 25.42). The function of cytochrome P450 is to activate O_2 for the hydroxylation reaction. Such hydroxylations are quite common in the synthetic routes for cholesterol, bile acids, and steroid hormones and also in detoxification pathways for aromatic compounds. Several of these are considered in the next section. 7α-Hydroxycholesterol is the precursor for cholic acid.

25.7 • Synthesis and Metabolism of Steroid Hormones

Steroid hormones are crucial signal molecules in mammals. (The details of their physiological effects are described in Chapter 34.) Their biosynthesis begins with the **desmolase** reaction, which converts cholesterol to preg-
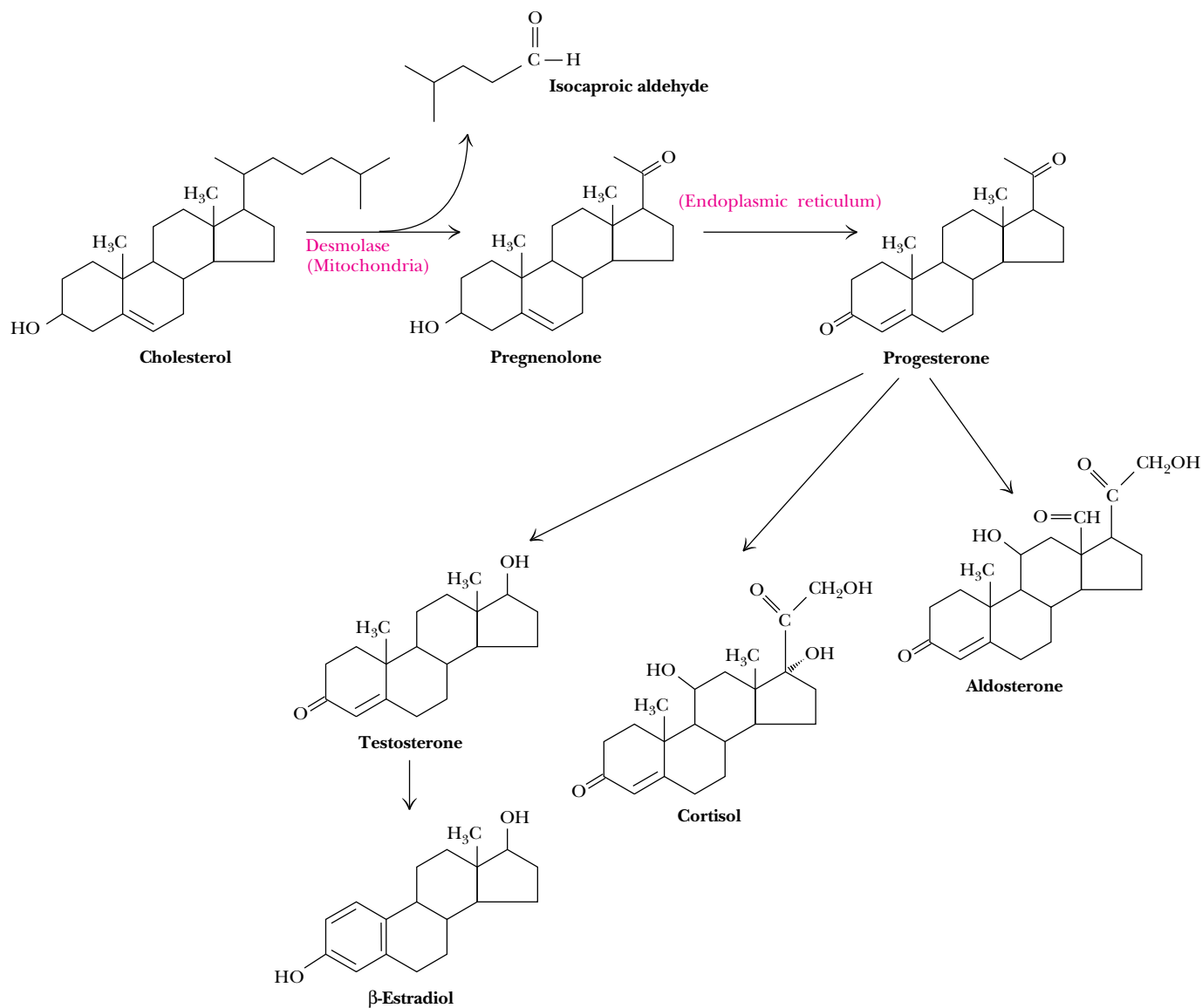
FIGURE 25.43 • The steroid hormones are synthesized from cholesterol, with intermediate formation of pregnenolone and progesterone. Testosterone, the principal male sex hormone steroid, is a precursor to β-estradiol. Cortisol, a glucocorticoid, and aldosterone, a mineralocorticoid, are also derived from progesterone.

nenolone (Figure 25.43). Desmolase is found in the mitochondria of tissues that synthesize steroids (mainly the adrenal glands and gonads). Desmolase activity includes two hydroxylases and utilizes cytochrome P450.

Pregnenolone and Progesterone Are the Precursors of All Other Steroid Hormones

Pregnenolone is transported from the mitochondria to the ER, where a hydroxyl oxidation and migration of the double bond yield progesterone. Pregnenolone synthesis in the adrenal cortex is activated by **adrenocorticotropic hormone** (ACTH), a peptide of 39 amino acid residues secreted by the anterior pituitary gland.

Progesterone is secreted from the corpus luteum during the latter half of the menstrual cycle and prepares the lining of the uterus for attachment of a fertilized ovum. If an ovum attaches, progesterone secretion continues to ensure the successful maintenance of a pregnancy. Progesterone is also the precursor for synthesis of the **sex hormone steroids** and the **corticosteroids.** Male sex hormone steroids are called **androgens,** and female hormones, **estrogens.** Testosterone is an androgen synthesized in males primarily in the testes (and in much smaller amounts in the adrenal cortex). Androgens are necessary for sperm maturation. Even nonreproductive tissue (liver, brain, and skeletal muscle) is susceptible to the effects of androgens.

Testosterone is also produced primarily in the ovaries (and in much smaller amounts in the adrenal glands) of females as a precursor for the estrogens. β-Estradiol is the most important estrogen (Figure 25.43).

Steroid Hormones Modulate Transcription in the Nucleus

Steroid hormones act in a different manner from most hormones we have considered. In many cases, they do not bind to plasma membrane receptors, but rather pass easily across the plasma membrane. Steroids may bind directly to receptors in the nucleus or may bind to cytosolic steroid hormone receptors, which then enter the nucleus. In the nucleus, the hormone-receptor complex binds directly to specific nucleotide sequences in DNA, increasing transcription of DNA to RNA (Chapters 31 and 34).

Cortisol and Other Corticosteroids Regulate a Variety of Body Processes

Corticosteroids, including the *glucocorticoids* and *mineralocorticoids,* are made by the cortex of the adrenal glands on top of the kidneys. **Cortisol** (Figure 25.43) is representative of the **glucocorticoids,** a class of compounds that (1) stimulate gluconeogenesis and glycogen synthesis in liver (by signaling the synthesis of PEP carboxykinase, fructose-1,6-bisphosphatase, glucose-6-phosphatase, and glycogen synthase); (2) inhibit protein synthesis and stimulate protein degradation in peripheral tissues such as muscle; (3) inhibit allergic and inflammatory responses; (4) exert an immunosuppressive effect, inhibiting DNA replication and mitosis and repressing the formation of antibodies and lymphocytes; and (5) inhibit formation of fibroblasts involved in healing wounds and slow the healing of broken bones.

Aldosterone, the most potent of the **mineralocorticoids** (Figure 25.43), is involved in the regulation of sodium and potassium balances in tissues. Aldosterone increases the kidney's capacity to absorb Na^+, Cl^-, and H_2O from the glomerular filtrate in the kidney tubules.

Anabolic Steroids Have Been Used Illegally To Enhance Athletic Performance

The dramatic effects of androgens on protein biosynthesis have led many athletes to the use of *synthetic androgens,* which go by the blanket term **anabolic steroids.** Despite numerous warnings from the medical community about side effects, which include kidney and liver disorders, sterility, and heart disease, abuse of such substances is epidemic. **Stanozolol** (Figure 25.44) was one of the agents found in the blood and urine of Ben Johnson following his record-setting performance in the 100-meter dash in the 1988 Olympic Games. Because use of such substances is disallowed, Johnson lost his gold medal, and Carl Lewis was declared the official winner.
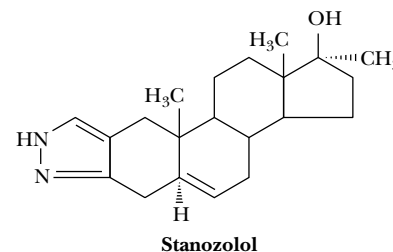

Stanozolol

FIGURE 25.44 • The structure of stanozolol, an anabolic steroid.

PROBLEMS

1. Carefully count and account for each of the atoms and charges in the equations for the synthesis of palmitoyl-CoA, the synthesis of malonyl-CoA, and the overall reaction for the synthesis of palmitoyl-CoA from acetyl-CoA.

2. Use the relationships shown in Figure 25.1 to determine which carbons of glucose will be incorporated into palmitic acid. Consider the cases of both citrate that is immediately exported to the cytosol following its synthesis and citrate that enters the TCA cycle.

3. Based on the information presented in the text and in Figures 25.4 and 25.5, suggest a model for the regulation of acetyl-CoA carboxylase. Consider the possible roles of subunit interactions, phosphorylation, and conformation changes in your model.

4. Consider the role of the pantothenic acid groups in animal fatty acyl synthase and the size of the pantothenic acid group itself, and estimate a maximal separation between the malonyl transferase and the ketoacyl-ACP synthase active sites.

5. Carefully study the reaction mechanism for the stearoyl-CoA desaturase in Figure 25.14, and account for all of the electrons flowing through the reactions shown. Also account for all of the hydrogen and oxygen atoms involved in this reaction, and convince yourself that the stoichiometry is correct as shown.

6. Write a balanced, stoichiometric reaction for the synthesis of phosphatidylethanolamine from glycerol, fatty acyl-CoA, and ethanolamine. Make an estimate of the $\Delta G°'$ for the overall process.

7. Write a balanced, stoichiometric reaction for the synthesis of cholesterol from acetyl-CoA.

8. Trace each of the carbon atoms of mevalonate through the synthesis of cholesterol, and determine the source (i.e., the position in the mevalonate structure) of each carbon in the final structure.

9. Suggest a structural or functional role for the O-linked saccharide domain in the LDL receptor (Figure 25.40).

10. Identify the lipid synthetic pathways that would be affected by abnormally low levels of CTP.

11. Determine the number of ATP equivalents needed to form palmitic acid from acetyl-CoA. (Assume for this calculation that each NADPH is worth 3.5 ATP.)

12. Write a reasonable mechanism for the 3-ketosphinganine synthase reaction, remembering that it is a pyridoxal phosphate-dependent reaction.

FURTHER READING

Athappilly, F. K., and Hendrickson, W. A., 1995. Structure of the biotinyl domain of acetyl-CoA carboxylase determined by MAD phasing. *Structure* **3:**1407.

Bloch, K., 1965. The biological synthesis of cholesterol. *Science* **150:**19–28.

Bloch, K., 1987. Summing up. *Annual Review of Biochemistry* **56:**1–19.

Borhani, D. W., Rogers, D. P., Engler, J. A., and Brouillette, C. G., 1997. Crystal structure of truncated human apolipoprotein A-I suggests a lipid-bound conformation. *Proceedings of the National Academy of Sciences* **94:**12291–12296.

Boyer, P. D., ed., 1983. *The Enzymes,* 3rd ed., Vol. 16. New York: Academic Press.

Carman, G. M., and Henry, S. A., 1989. Phospholipid biosynthesis in yeast. *Annual Review of Biochemistry* **58:**635–669.

Carman, G. M., and Zeimetz, G. M., 1996. Regulation of phospholipid biosynthesis in the yeast *Saccharomyces cerevisiae. Journal of Biological Chemistry* **271:**13292–13296.

Chang, S. I., and Hammes, G. G., 1990. Structure and mechanism of action of a multifunctional enzyme: Fatty acid synthase. *Accounts of Chemical Research* **23:**363–369.

Dunne, S. J., Cornell, R. B., Johnson, J. E., et al., 1996. Structure of the membrane-binding domain of CTP phosphocholine cytidylyltransferase. *Biochemistry* **35:**1975.

Friedman, J. M., 1997. The alphabet of weight control. *Nature* **385:**119–120.

Hansen, H. S., 1985. The essential nature of linoleic acid in mammals. *Trends in Biochemical Sciences* **11:**263–265.

Jackowski, S., 1996. Cell cycle regulation of membrane phospholipid metabolism. *Journal of Biological Chemistry* **271:**20219–20222.

Jeffcoat, R., 1979. The biosynthesis of unsaturated fatty acids and its control in mammalian liver. *Essays in Biochemistry* **15:**1–36.

Kent, C., 1995. Eukaryotic phospholipid biosynthesis. *Annual Review of Biochemistry* **64:**315–343.

Kim, K-H., et al., 1989. Role of reversible phosphorylation of acetyl-CoA carboxylase in long-chain fatty acid synthesis. *The FASEB Journal* **3:**2250–2256.

Lardy, H., and Shrago, E., 1990. Biochemical aspects of obesity. *Annual Review of Biochemistry* **59:**689–710.

Liscum, L., and Underwood, K. W., 1995. Intracellular cholesterol transport and compartmentation. *Journal of Biological Chemistry* **270:**15443–15446.

Lopaschuk, G. D., and Gamble, J., 1994. The 1993 Merck Frosst Award. Acetyl-CoA carboxylase: an important regulator of fatty acid oxidation in the heart. *Canadian Journal of Physiology and Pharmacology* **72:**1101–1109.

McCarthy, A. D., and Hardie, D. G., 1984. Fatty acid synthase—An example of protein evolution by gene fusion. *Trends in Biochemical Sciences* **9:**60–63.

Needleman, P., et al., 1986. Arachidonic acid metabolism. *Annual Review of Biochemistry* **55:**69–102.

Roberts, L. M., Ray, M. J., Shih, T. W., et al., 1997. Structural analysis of apolipoprotein A-I: Limited proteolysis of methionine-reduced and -oxidized lipid-free and lipid-bound human Apo A-I. *Biochemistry* **36:**7615.

Samuelsson, B., et al., 1987. Leukotrienes and lipoxins: Structures, biosynthesis and biological effects. *Science* **237:**1171–1176.

Schewe, T., and Kuhn, H., 1991. Do 15-lipoxygenases have a common biological role? *Trends in Biochemical Sciences* **16:**369–373.

Smith, W. L., Garavito, R. M., and DeWitt, D.L., 1996. Prostaglandin endoperoxide H synthases (cyclooxygenases)-1 and -2. *Journal of Biological Chemistry* **271:**33157–33160.

Tataranni, P. A., and Ravussin, E., 1997. Effect of fat intake on energy balance. *Annals of the New York Academy of Sciences* **819:**37–43.

Vance, D. E., and Vance, J. E., eds., 1985. *Biochemistry of Lipids and Membranes.* Menlo Park, CA: Benjamin/Cummings.

Wakil, S., 1989. Fatty acid synthase, a proficient multifunctional enzyme. *Biochemistry* **28:**4523–4530.

Wakil, S., Stoops, J. K., and Joshi, V. C., 1983. Fatty acid synthesis and its regulation. *Annual Review of Biochemistry* **52:**537–579.